

Dissertation zur Erlangung des Doktorgrades
der Fakultät für Chemie und Pharmazie
der Ludwig-Maximilians-Universität München

**OPTOCHEMICAL CONTROL OF GABA_A
RECEPTORS AND TRP CHANNELS
AND
STUDIES TOWARD LIGHT-DEPENDENT
REGULATION OF Na_v AND mGLUR6**

von

Marco Robert Philip STEIN

aus Ebersberg

2014



ERKLÄRUNG

Diese Dissertation wurde im Sinne von § 7 der Promotionsordnung vom 28. November 2011 von Herrn Professor Dr. Dirk Trauner betreut.

EIDESSTATTLICHE VERSICHERUNG

Diese Dissertation wurde eigenständig und ohne unerlaubte Hilfe erarbeitet.

München, 31. Dezember 2013

.....

Marco Stein

Dissertation eingereicht am 16. Januar 2014

1. Gutachter: Prof. Dr. Dirk Trauner

2. Gutachter: Prof. Dr. Manfred Heuschmann

Mündliche Prüfung am 24. Februar 2014

ACKNOWLEDGMENTS

First and foremost, I am especially grateful to Prof. Dr. Dirk Trauner for accepting me as a PhD student in his group. I want to thank him for trusting in my skills and for providing visionary projects, yet giving me enough space to work on my own ideas. Thank you, Dirk!

I would like to thank the Committee members Prof. Dr. Dirk Trauner, Prof. Dr. Manfred Heuschmann, Prof. Dr. Franz Bracher, Prof. Dr. Konstantin Karaghiosoff, Prof. Dr. Thomas Gudermann and Prof. Dr. Paul Knochel for taking time out of their schedules and carefully reviewing this thesis.

I am especially grateful to Dr. Martin Sumser who introduced me patiently into cell culture works as well as electrophysiology and provided helpful advice.

My special thanks are devoted to my fellow labmates in the Blue Lab, namely Michael Pangerl, Martin Olbrich, Dominik Hager, Maria Matveencko, Giulio Volpin, Nina Vrieling, Shu-An Liu (in chronological order). Especially I would like to thank Martin and Michi for many fun times in the lab and providing decent scientific advice whenever needed („*Ich sehe keinen Grund, warum das nicht klappen sollte...*“). I thank the whole Trauner group for providing a productive working atmosphere.

I would also like to thank Dr. Michael Kienzler for the great time I had during my F-Praktikum in the group and for introducing me to the colorful world of azobenzenes. I am moreover grateful to Pascal Ellerbrock, Martin Olbrich, Dr. Michael Kienzler and Dr. Martin Sumser for proofreading parts of this thesis.

I have to thank Heike Traub who has been a great help in dealing with many organisational tasks. I also want to thank our CTA's Luis de la Osa de la Rosa for keeping the cell culture running, as well as Carrie Louis for her assistance with HPLC separations.

I would like to thank the analytical departments of the LMU for their excellent services, namely Claudia Dubler and Dr. David Stephenson (NMR) and Dr. Werner Spahl (mass spectrometry). I am also thankful to Dr. Peter Mayer for the determination of crystal structures.

I am thankful to Simon J. Middendorp and Prof. Dr. Erwin Sigel (IBMM Bern) as well as Dr. Andreas Breit (Walther-Straub-Institute Munich) for excellent collaborations.

I would also like to acknowledge funding by the *Fonds der Chemischen Industrie* in the form of a PhD scholarship.

I need to thank my parents for their ongoing support throughout my long educational career. Thank you so much for everything!

Last but not least, I wish to thank Charlotte for her love and support through the last couple of years! The hearts you drew on the sash of my fume hood on your first visit in the lab have remained there until the very end and will follow me elsewhere.

Meinen Eltern

TABLE OF CONTENTS

SUMMARY	IX
1 INTRODUCTION	1
1.1 Photoswitches – from Nature to Application	1
1.2 Properties of Azobenzenes and their Use as Photoswitches	2
1.3 Optochemical Genetics	8
1.3.1 The Caged Ligand (CL) Approach	11
1.3.2 The Photochromic Ligand (PCL) Approach	11
1.3.3 The Photoswitchable Tethered Ligand (PTL) Approach	12
1.4 Literature	13
2 PHOTOREGULATION OF GABA_A RECEPTORS	17
2.1 The GABA _A Receptor	17
2.2 Azo-Propofols: Photochromic Potentiators of GABA _A Receptors	19
2.2.1 Original Publication: <u>M. Stein</u> , S. J. Middendorp, V. Carta, E. Pejo, D. E. Raines, S. A. Forman, E. Sigel, D. Trauner, <i>Angew. Chem. Int. Ed.</i> 2012 , <i>51</i> , 10500–10504	20
2.2.2 Supporting Information	25
2.3 Photochromic Potentiation of GABA _A Receptors by Azobenzene Derivatives of Etomidate	81
2.3.1 Azo-Etomidates as Potential Photochromic GABA _A R Potentiators	81
2.3.2 Experimental Procedures and Analytical Data	89
2.3.2.1 General Experimental Details and Instrumentation	89
2.3.2.2 Synthesis of Azo-Etomidates	90
2.3.3 NMR Spectra	106
2.3.4 UV/Vis Spectra of AETD1–5	126
2.3.5 HPLC Chromatograms of AETD2	129
2.4 Literature	131
3 PHOTOCONTROL OF TRP CHANNELS	133
3.1 Transient Receptor Potential Channels	133
3.2 Optical Control of TRPV1 Channels	137

Table of Contents

3.2.1	Original Publication: <u>M. Stein</u> , A. Breit, T. Fehrentz, T. Gudermann, D. Trauner, <i>Angew. Chem. Int. Ed.</i> 2013 , 52, 9845–9848	141
3.2.2	Supporting Information	145
3.3	Azo-Capsazepines in the Retina	208
3.4	The Menthol Receptor TRPM8	209
3.5	Azo-Icilin	210
3.6	Experimental Procedures and Analytical Data	218
3.6.1	General Experimental Details and Instrumentation	218
3.6.2	Synthesis of Azo-Icilins	219
3.6.3	Biological Methods	235
3.7	NMR Spectra	236
3.8	Literature	256
4	PHOTOCHROMIC LIGANDS FOR VOLTAGE-GATED SODIUM CHANNELS	260
4.1	Voltage-gated Sodium Channels	260
4.2	Azo-Lacosamide	261
4.3	Azo-Lamotrigine	266
4.4	Azo-Crobenetine	270
4.5	Attempts toward Photocontrol of Nav 1.7	277
4.6	Experimental Procedures and Analytical Data	280
4.6.1	General Experimental Details and Instrumentation	280
4.6.2	Synthesis of Azo-Lacosamide	281
4.6.3	Synthesis of Azo-Lamotrigine	286
4.6.4	Synthesis of Azo-Crobenetines	291
4.6.5	Synthesis of MS1	305
4.7	NMR Spectra	307
4.8	Literature	340
5	STUDIES TOWARD PHOTOSWITCHABLE MGLUR6 AGONISTS AS A POTENTIAL APPROACH FOR VISION RESTORATION	342
5.1	The Metabotropic Glutamate Receptor 6	342
5.2	Azo-APDC	345
5.3	Azo-3C5HPG	349
5.4	Azo-DCPG	356
5.5	Experimental Procedures and Analytical Data	360

Table of Contents

5.5.1	General Experimental Details and Instrumentation	360
5.5.2	Synthesis of Azo-APDCs	361
5.5.3	Synthesis of Azo-3C5HPGs	369
5.5.4	Synthesis of Azo-DCPG	383
5.6	NMR Spectra	390
5.7	Literature	428
6	MISCELLANEOUS PROJECTS	430
6.1	Development of Azo-SEN12333, a PCL for Nicotinic Acetylcholine Receptors	430
6.2	Development of Red DAD, a Red-shifted, Non-permanently Charged PCL for Voltage-gated Potassium Channels	434
6.3	Development of a New Disulfide Containing Class of PTLs	437
6.4	Synthesis of a PEGylated Photocleavable <i>o</i> -Nitrobenzyl Protecting Group	440
6.5	Experimental Procedures and Analytical Data	443
6.5.1	General Experimental Details and Instrumentation	443
6.5.2	Synthesis of Azo-SEN12333	444
6.5.3	Synthesis of Red DAD	445
6.5.4	Synthesis of MS2 and MS3	449
6.5.5	Synthesis of PEG	454
6.6	NMR Spectra	460
6.7	Literature	482
7	LIST OF ABBREVIATIONS	484

LIST OF PUBLICATIONS

Parts of this thesis have been published or will be submitted for publication (in chronological order):

PUBLICATION	CHAPTER
Azo-Propofols: Photochromic Potentiators of GABA_A Receptors	2.2
<u>M. Stein</u> , S. J. Middendorp, V. Carta, E. Pejo, D. E. Raines, S. A. Forman, E. Sigel, D. Trauner, <i>Angew. Chem. Int. Ed.</i> 2012 , <i>51</i> , 10500–10504; <i>Angew. Chem.</i> 2012 , <i>124</i> , 10652–10656. <i>Highlighted as “Very Important Paper”</i> <i>Highlighted in C&EN</i> 2012 , <i>90</i> , Issue 39, p. 30.	
Optical Control of TRPV1 Channels	3.2
<u>M. Stein</u> , A. Breit, T. Fehrentz, T. Gudermann, D. Trauner, <i>Angew. Chem. Int. Ed.</i> 2013 , <i>52</i> , 9845–9848; <i>Angew. Chem.</i> 2013 , <i>125</i> , 10028–10032. <i>Highlighted as “Hot Paper”</i>	
Lichtschalter für Nervensysteme	
<u>M. Stein</u> , D. Trauner, <i>Nachr. Chem.</i> 2014 , <i>in preparation (invited)</i> .	
A New Photochromic Drug for Vision Restoration	6.2
L. Laprell, <u>M. Stein</u> , M. Sumser, R. H. Kramer, D. Trauner, <i>in preparation</i> .	
Light-dependent Regulation of Slow Inactivation of Na_v Channels	4.2
<u>M. Stein</u> , A. Lampert, D. Trauner, <i>in preparation</i> .	

SUMMARY

The objective of this thesis was to develop new azobenzene-based photochromic ligands (PCLs) for a variety of transmembrane receptors and ion channels. The main targets being GABA_A receptors (chapter 2), which are members of the pentameric ligand-gated ion channel family, and TRP channels (chapter 3), which are nonselective cation channels that are mainly permeable to calcium and sodium ions.

γ -Aminobutyric acid type A (GABA_A) receptors are part of the Cys-loop ligand-gated ion channel superfamily and are activated by γ -aminobutyric acid (GABA), the major inhibitory neurotransmitter in the mammalian brain. Activation of GABA_A receptors by binding of GABA leads to opening of the chloride-selective pore, thus hyperpolarizing the postsynaptic neuron. Therefore, GABA_A receptors are believed to play a major role in anesthesia, although the exact mechanism is not fully understood as of today.

To further interrogate this role, the widely used anesthetics propofol^[a] and etomidate^[b] were converted into photochromic GABA_A potentiators. An azobenzene derivative of propofol (**AP2**, Fig. S.1a) was found to be an effective light-dependent potentiator of GABA-induced currents in *Xenopus* oocytes (Fig. S.1c) and moreover acted as a light-dependent anesthetic in *Xenopus laevis* tadpoles. Illumination of tadpoles with propofol itself resulted in a small rightward shift in the propofol-dependent loss of righting reflex (LORR) dose-response curve (Fig. S.1d). Illumination of tadpoles with **AP2**, however, i.e. switching to *cis*-**AP2**, produced a considerably larger rightward shift, i.e. change in efficacy of **AP2** (Fig. S.1e). The results of this project have been published in *Angewandte Chemie International Edition* (chapter 2.2).^[c]

In addition, the etomidate derivative **AETD2** (Fig. S.1b) was found to act as a potent photochromic potentiator of GABA_A receptors in *Xenopus* oocytes (see chapter 2.3).

^[a] C. Vanlersberghe, F. Camu, *Handb. Exp. Pharmacol.* **2008**, 182, 227–252.

^[b] E. F. Godefroi, P. A. J. Janssen, C. A. M. Van der Eycken, A. H. M. T. Van Heertum, C. J. E. Niemegeers, *J. Med. Chem.* **1965**, 56, 220–223.

^[c] M. Stein, S. J. Middendorp, V. Carta, E. Pejo, D. E. Raines, S. A. Forman, E. Sigel, D. Trauner, *Angew. Chem. Int. Ed.* **2012**, 51, 10500–10504.

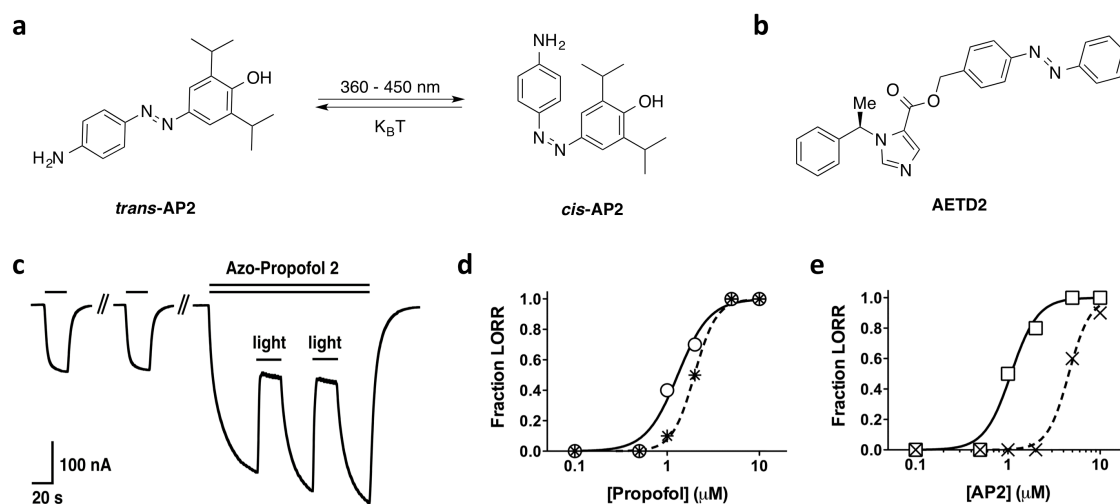


Figure S.1. a) Photoisomerization of AP2, a photochromic GABA_A potentiator; b) molecular structure of AETD2, another PCL for GABA_ARs; c) light-dependent regulation of GABA_A activity (single black bar: application of 1 μM GABA; double black bar: co-application of 1 μM GABA and 1.5 μM AP2); d) and e) dose-response curve of light-dependent anesthesia in tadpoles. Light itself produces only a small rightward shift in the d) propofol-dependent loss of righting reflexes (LORR; circles: dark, stars: λ = 360–370 nm) whereas e) light in the presence of AP2 results in a large rightward shift (squares: dark, crosses: λ = 360–370 nm).

Another PCL project studied transient receptor potential vanilloid channels 1 (TRPV1 channels) which are activated by several chemical and physical stimuli such as heat, voltage, low pH, phosphorylation and endogenous as well as exogenous ligands. Being expressed in different sorts of nociceptive neurons, its activation results in a sensation of burning and pain. Capsaicin, the main ingredient in hot chili peppers, is the most important agonist for TRPV1. Antagonists for this channel are of high interest in efforts to alleviate pain. As such, the TRPV1 antagonists capsazepine^[d] and BCTC^[e] were developed and have been widely used in pharmacological studies. Based on promising SAR studies for these molecules, photoswitchable azobenzene derivatives termed **Azo-Capsazepines (ACs)** and **Azo-BCTC (ABCTC)** were developed in order to control TRPV1 channel activation with light (Fig. S.2a). Upon voltage-activation of the channel, AC4 was found to function as a *trans* antagonist, i. e. blocking more current in the *trans* state than in the *cis* state (Fig. S.2b), whereas ABCTC acted as a *cis* antagonist (Fig. S.2c). With AC4, it was also possible to light-dependently counteract capsaicin (CAP)-induced

^[d] C. S. Walpole, S. Bevan, G. Bovermann, J. Boelsterli, R. Breckenridge, J. W. Davies, G. A. Hughes, I. James, L. Oberer, *J. Med. Chem.* **1994**, *37*, 1942–1954.

^[e] K. J. Valenzano, E. R. Grant, G. Wu, M. Hachicha, L. Schmid, L. Tafesse, Q. Sun, Y. Rotshteyn, J. Francis, J. Limberis, S. Malik, E. R. Whittemore, D. Hodges, *J. Pharmacol. Exp. Ther.* **2003**, *306*, 377–386.

Summary

activation of TRPV1 up to 82% (Fig. S.2d). The results of this project have been published in *Angewandte Chemie International Edition* (chapter 3.2).^[f]

In related work, based on the highly potent synthetic transient receptor potential melastatin channel 8 (TRPM8 channel) agonist icilin,^[g] azobenzene derivatives termed **Azo-Icilins** were developed in order to control TRPM8 with light (Fig. S.2a; chapter 3.5). This channel is also referred to as the “cold receptor” or “menthol receptor”, since cold temperatures and menthol activate TRPM8 and result in the perception of coolness.

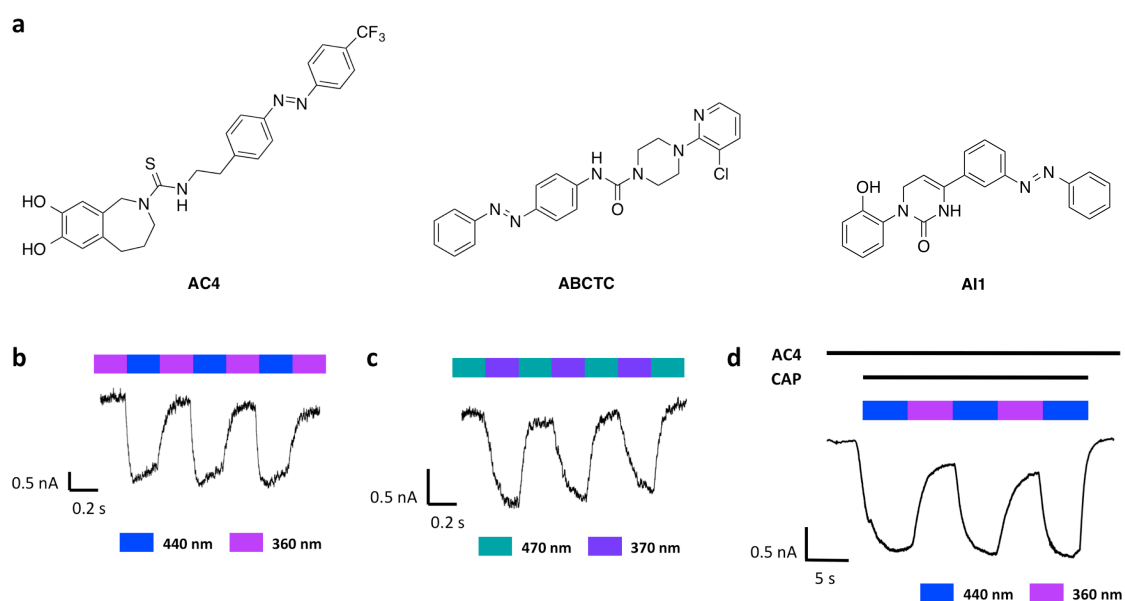


Figure S.2. a) Molecular structures of the photochromic TRPV1 antagonists **AC4**, **ABCTC** and the photochromic TRPM8 agonist **AI1**; b) light-dependent control of voltage activated (at +200 mV) TRPV1 currents upon application of 100 μM **AC4** ($\lambda = 360$ nm: *cis*-**AC4**, $\lambda = 440$ nm: *trans*-**AC4**) and c) 10 μM **ABCTC**, respectively ($\lambda = 370$ nm: *cis*-**ABCTC**, $\lambda = 470$ nm: *trans*-**ABCTC**); d) light-dependent control of CAP-induced activation of TRPV1 with **AC4** (application of 1 μM **AC4** and 100 nM CAP, holding potential -60 mV).

Moreover, PCLs were developed for voltage-gated sodium channels (Na_V channels, chapter 4), the metabotropic glutamate receptor 6 (mGluR6, chapter 5), voltage-gated potassium channels (K_V channels, chapter 6) and nicotinic acetylcholine receptors (nAChRs, chapter 6). For a depiction of all PCLs see figure S.3.

[f] M. Stein, A. Breit, T. Fehrentz, T. Gudermann, D. Trauner, *Angew. Chem. Int. Ed.* **2013**, 52, 9845–9848.

[g] E. T. Wei, D. A. Seid, *J. Pharm. Pharmacol.* **1983**, 35, 110–112.

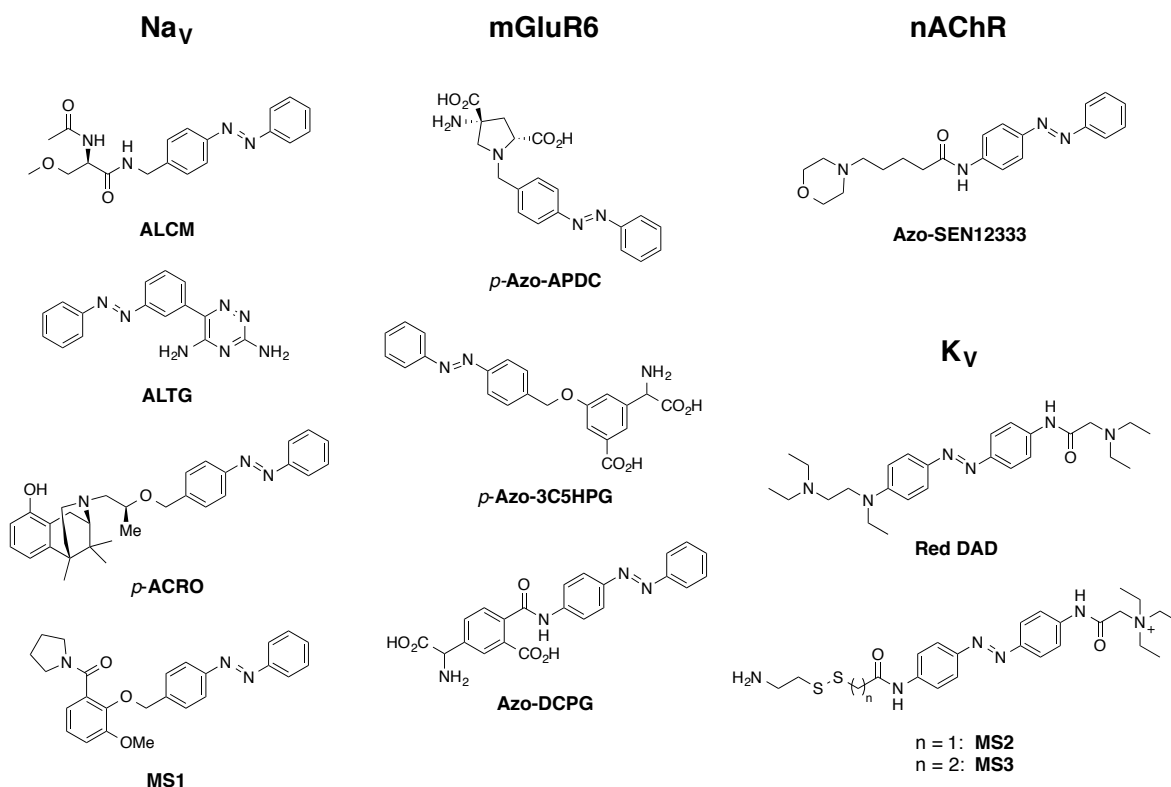


Figure S.3. PCLs developed for Na_v channels, mGluR6, nAChRs and K_v channels.

For Na_v channels, PCL derivatives were made of the known sodium channel blocking drugs lacosamide^[h] (**ALCM**), lamotrigine^[i] (**ALTG**) and crobenetine^[j] (**ACRO**) as well as of a highly potent Na_v 1.7 inhibitor^[k] (**MS1**).

PCLs for mGluR6 comprise azobenzene derivatives of 1-benzyl-APDC (**Azo-APDC**), the only mGluR6-selective agonist known to date,^[l] and the two phenylglycine derivatives 3C5HPG (**Azo-3C5HPG**) and DCPG (**Azo-DCPG**).^[m]

^[h] C. Salome, E. Salome-Grosjean, J. P. Stables, H. Kohn, *J. Med. Chem.* **2010**, *53*, 3756–3771.

^[i] M. Leach, K. Franzmann, D. Riddall, L. Harbige (University of Greenwich), WO/2011/004195 A2, **2011**.

^[j] M. Grauert, W. D. Bechtel, T. Weiser, W. Stransky, H. Nar, A. J. Carter, *J. Med. Chem.* **2002**, *45*, 3755–3764.

^[k] J. Liang, R. M. Brochu, C. J. Cohen, I. E. Dick, J. P. Felix, M. H. Fisher, M. L. Garcia, G. J. Kaczorowski, K. A. Lyons, P. T. Meinke, B. T. Priest, W. A. Schmalhofer, M. M. Smith, J. W. Tarpley, B. S. Williams, W. J. Martinc, W. H. Parsons, *Bioorg. Med. Chem. Lett.* **2005**, *15*, 2943–2947.

^[l] W. Tückmantel, A. P. Kozikowski, S. Wang, S. Pshenichkin, J. T. Wroblewski, *Bioorg. Med. Chem. Lett.* **1997**, *7*, 601–606.

^[m] N. Sekiyama, Y. Hayashi, S. Nakanishi, D. E. Jane, H.-W. Tse, E. F. Birse, J. C. Watkins, *Br. J. Pharmacol.* **1996**, *117*, 1493–1503.

Azo-SEN12333 is a photochromic agonist for $\alpha 7$ nAChRs based on recent SAR studies.^[n] For K_v channels, a red-shifted and non-permanently charged version of QAQ^[o] was developed (**Red DAD**) which has already shown very promising results in our efforts toward vision restoration (see **6.2**). Finally, a new disulfide-containing class of PTLs for K_v channels was developed based on MAQ^[p] in order to hopefully overcome many of the disadvantages related to the use of reactive maleimides in biological systems (**MS2** and **MS3**).

^[n] S. N. Haydar, C. Ghiron, L. Bettinetti, H. Bothmann, T. A. Comery, J. Dunlop, S. La Rosa, I. Micco, M. Pollastrini, J. Quinn, R. Roncarati, C. Scali, M. Valacchi, M. Varrone, R. Zanaletti, *Bioorg. Med. Chem.* **2009**, *17*, 5247–5258.

^[o] A. Mourot, T. Fehrentz, Y. Le Feuvre, C. M. Smith, C. Herold, D. Dalkara, F. Nagy, D. Trauner, R. H. Kramer, *Nat. Meth.* **2012**, *9*, 396–402.

^[p] M. R. Banghart, K. Borges, E. Y. Isacoff, D. Trauner, R. H. Kramer, *Nat. Neurosci.* **2004**, *7*, 1381–1386.

1 INTRODUCTION

1.1 PHOTOSWITCHES – FROM NATURE TO APPLICATION

Photoswitches are small molecules that can undergo photoinduced transformations between two (or more) isoforms. Their stable photostationary states generally have different physicochemical properties such as refractive index, dielectric constant, oxidation/reduction potential, absorption spectra and geometric structure. Therefore, they can be applied to various photonic devices such as erasable optical memory media and optical switch components.^[1] Moreover, photoswitches also play an important role in biological systems, since fundamental biological processes of life such as photosynthesis,^[2] the conversion of light energy into chemical energy (ATP production) and of course vision^[3] are essentially controlled by photoinduction. Probably the most popular biological photoswitch is the bacteriorhodopsin system of halobacteria. Bacteriorhodopsin is a light-driven proton pump that is part of the photosynthetic system of halobacterium, converting light energy into ATP controlled by the specific isomerization of all-*trans*- to 13-*cis*-retinal. It possesses a catalytic cycle period of only 10 ms. Presently, bacteriorhodopsin is the best investigated membrane protein.^[4] Although its molecular assembly is rather simple, it has a high efficiency, is stable toward chemical and thermal degradation and therefore possibly useful for technical applications.

Since light is unsurpassed in terms of spatial and temporal precision, the development of photoswitches for the control of a variety of systems with light has attracted much interest in the scientific community.

Three (main) types of photoswitches exist, classified by their mechanism of function: a) molecules that dimerize upon photoexcitation, such as coumarins **1.1** and anthracenes **1.2**, b) molecules that intramolecularly form bonds upon photoinduction (often cyclization), for example spiropyrans **1.3** or spirooxazines **1.4**,^[5] diarylethenes **1.5**^[6] or fulgides **1.6**,^[7] and c) molecules that exhibit photoisomerization across double bonds, such as stilbenes **1.7**, azobenzenes **1.8**, or indigo **1.9** and thioindigo derivatives **1.10** (Fig. 1.1).^[8]

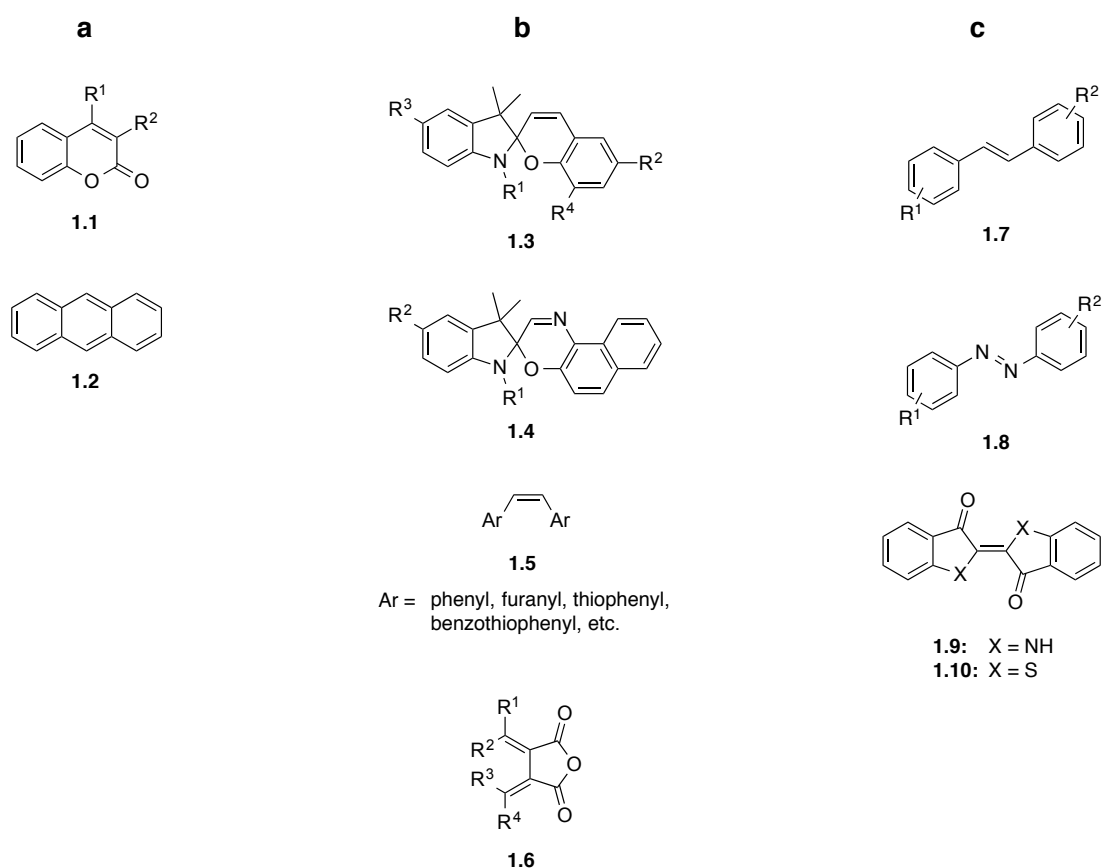


Figure 1.1. Different types of photoswitches, classified by their mechanism upon photoinduction. **a)** Dimerization; **b)** intramolecular bond formation; **c)** isomerization across double bonds.

Within these three types, two subclasses exist: (i) single-cycle photoswitches^[9] are used to deactivate biomaterial by the attachment of a photosensitive chemical protecting group. Light-controlled removal of the protecting group reactivates the biomaterial again. By contrast, (ii) multi-cycle photoswitches are able to switch reversibly between two different states and therefore are considered superior to single-cycle photoswitches in a variety of applications.^[8]

The work of this thesis will focus on azobenzene photoswitches exclusively. Therefore, a brief introduction to azobenzenes, a member of the class of multi-cycle photoswitches, is given in the following chapter.

1.2 PROPERTIES OF AZOBENZENES AND THEIR USE AS PHOTOSWITCHES

Azobenzene (diphenyldiazene) is an aromatic molecule in which a diazo moiety ($-\text{N}=\text{N}-$) joins two phenyl rings. Owing to their elongated π -conjugated system, azobenzenes show strong absorption bands in the UV and/or visible portions of the spectrum. Depending on its substituents, azobenzene derivatives can be tailored to absorb at desired wavelengths. Rau

therefore classified three types of azobenzenes:^[10] a) azobenzene-type molecules, which are similar to the unsubstituted azobenzene, b) aminoazobenzene-type molecules, which are *ortho*- or *para*-substituted with an electron-donating group, and c) pseudo-stilbenes, which are substituted at the 4- and 4'-positions with an electron-donating and electron-withdrawing group, respectively (Fig. 1.2).

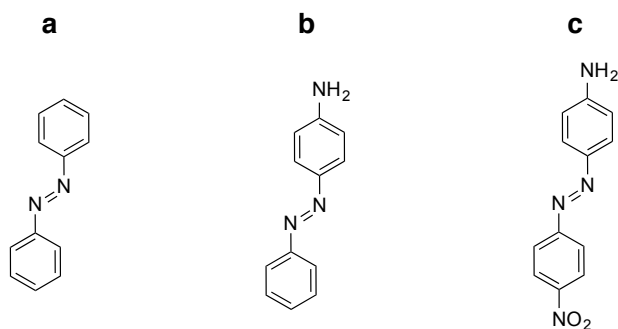
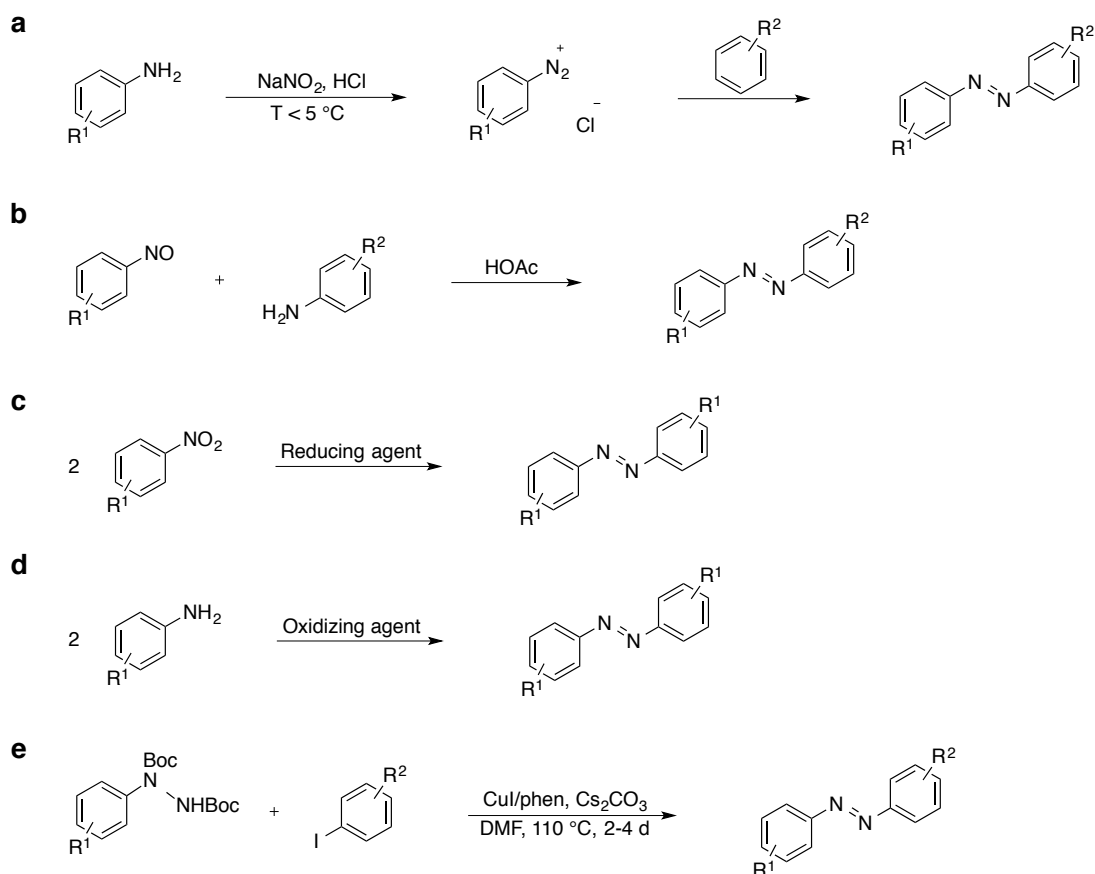


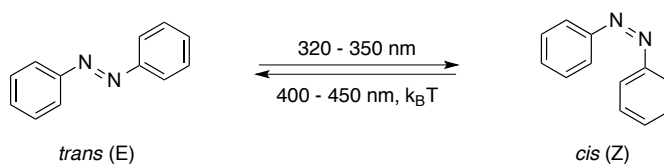
Figure 1.2. Three types of azobenzenes according to Rau. **a)** Azobenzene-type molecules; **b)** aminoazobenzene-type molecules; **c)** pseudo-stilbenes. For each of the three types, a representative example is shown.

There are several methods to synthesize azobenzenes of which the most common are shown in Scheme 1.1.^[11] a) The classic azo coupling is an electrophilic aromatic substitution reaction of aryl diazonium salts (typically generated from the corresponding aniline derivatives with NaNO_2 and HCl) with preferentially electron-rich benzene derivatives.^[12] b) Reaction of aromatic nitroso compounds and anilines in glacial acetic acid (Mills reaction).^[13] The nitroso derivatives are often formed from the corresponding anilines with various oxidants. c) Reductive coupling of aromatic nitro derivatives and d) oxidative coupling of anilines.^[14] However, both methods c) and d) only give access to symmetrical azobenzenes in good yields. e) More recently, one-pot Buchwald-type coupling reactions of Boc-protected aryl hydrazines with aryl iodides and subsequent oxidation was developed as an elegant alternative to obtain azobenzenes.^[15]



Scheme 1.1. Methods for the synthesis of azobenzenes: **a)** Azo coupling; **b)** Mills reaction; **c)** reductive coupling of nitro arenes; **d)** oxidative coupling of anilines; **e)** Buchwald-type cross-coupling.

Since the first observation of the photochemical *trans* \rightleftharpoons *cis* isomerization of azobenzene (Scheme 1.2) by Hartley in 1937,^[16] a huge interest has emerged regarding possible applications of azobenzenes as bistable photoswitches (see below).



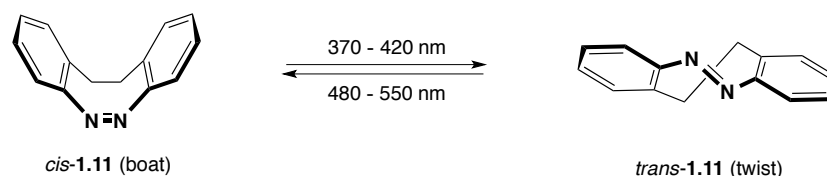
Scheme 1.2. Isomerization of azobenzene between its *trans* and *cis* isomers.

The thermodynamically more stable *trans*-azobenzene (by approximately 50 kJ mol^{-1} ^[17]) isomerizes upon irradiation at $\lambda = 320\text{--}350 \text{ nm}$ to the metastable *cis*-azobenzene. The energy barrier to the photoexcited state is in the order of 200 kJ mol^{-1} .^[18] Although both isomers absorb in this wavelength range (symmetry allowed $\pi \rightarrow \pi^*$), the *trans* isomer has a much higher extinction coefficient than the *cis* isomer.^[19] Either irradiation at $\lambda = 400\text{--}450 \text{ nm}$ (symmetry forbidden $n \rightarrow \pi^*$; higher absorption of the *cis* than of the *trans* isomer) or thermal relaxation

leads back to the *trans* isomer,^[20] whereas in the latter case an activation energy of 90 kJ mol⁻¹ is required for this first-order process.^[21] Lifetimes of *cis* isomers, ranging from less than a second up to several years, strongly depend on the following factors: substituents attached to the azobenzene scaffold, conformational effects in macrocyclic or ring-like compounds, intra- as well as intermolecular interactions, e.g. hydrogen bonds, or even attachment to a surface.^[22]

By fusing the azo moiety into a multiheterocyclic system ("bridged" or "cyclic" azobenzenes), the *cis* isomers become thermodynamically more stable than the *trans* isomers. Although initially prepared in 1910,^[23] 5,6-dihydrodibenzo[*c,g*][1,2]diazocine (**1.11**) has just recently gained increasing interest when Siewertsen *et al.*^[24] discovered its interesting photoisomerization properties in 2009. *cis*-**1.11** can be switched to *trans*-**1.11** with $\lambda = 370\text{--}400$ nm and reverts back to its *cis* form by $\lambda = 480\text{--}550$ nm. The *cis* isomer appears as *cis*-boat conformation, whereas the *trans* isomer can exist as *trans*-chair and *trans*-twist, the latter being the more stable conformation (10.27 kcal mol⁻¹ vs. 7.60 kcal mol⁻¹, referred to the *cis* isomer,^[25] Scheme 1.3).

This *cis*-stability makes diazocines an interesting class of photoswitches for biological applications since often the *trans* isomers are the (more) active ligands. By creating *cis*-stable photoswitches, the desired effect could be triggered by illuminating with light of the respective wavelength ("on switch"). After applying the compound in the dark, the molecule would be in its inactive (less active) form, avoiding constitutively active ligands.

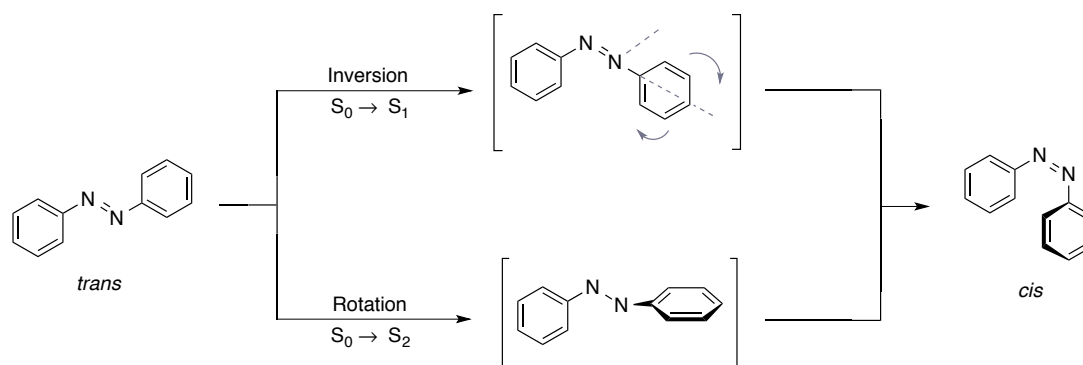


Scheme 1.3. Isomerization of the *cis*-stable bridged azobenzene **1.11**. Only the more stable twist conformation is shown for *trans*-**1.11**.

The extremely efficient photoisomerization of azobenzene is one of the cleanest known,^[9] proceeds very fast (within 1 ps^[26]) and is fully reversible. It is therefore considered to be the most promising artificial mimic of the retinal-rhodopsin photoswitch involved in the process of human vision.^[27]

^[9] Among the few side reactions known, photocyclization to the corresponding benzo[*c*]cinnolines upon irradiation and protonation (e.g. 98% sulphuric acid), complexation (e.g. ferric chloride) or photoreduction upon irradiation in protic solvents, such as alcohols, have been observed.^[19]

Two main mechanisms have been proposed for the isomerization process: by inversion and rotation (Scheme 1.4). The inversion pathway occurs after $n \rightarrow \pi^*$ photoexcitation ($S_0 \rightarrow S_1$) through all-in-plane inversion at one of the two nitrogen atoms ("lateral shift"). One $N=N-C$ angle increases to $\sim 180^\circ$ keeping the $C-N=N-C$ dihedral angle fixed at 0° . This leads to a transition state with a sp hybridized nitrogen atom.^[28] The rotation pathway involves rupture of the $N=N$ double bond to allow free rotation about the $N-N$ single bond. After $\pi \rightarrow \pi^*$ photoexcitation ($S_0 \rightarrow S_2$), the $C-N-N-C$ dihedral angle changes, keeping the $N-N-C$ angle fixed at $\sim 120^\circ$.^[29] Due to steric interactions during the rotation, hindered or constrained molecules strongly prefer isomerization by inversion.^[30] In addition to these two mechanisms, a concerted inversion and an inversion-assisted rotation have also been proposed.^[31]



Scheme 1.4. Isomerization of azobenzenes: Inversion and rotation mechanisms.

Trans-azobenzene adopts a planar structure (C_{2h} symmetry), whereas the two phenyl rings of the *cis* isomer are oriented in an out-of-plane fashion with C_2 symmetry (as correctly drawn in scheme 1.4).^[31] However, for the sake of simplicity, *cis* isomers of azobenzene derivatives are drawn in-plane throughout this thesis.

The $trans \rightleftharpoons cis$ isomerization is accompanied by relatively large changes in molecular properties such as the length of the molecule (distance between the ends of the molecule decreases from 0.99 nm in the *trans* state to 0.55 nm in the *cis* state^[32]) and molecular volume. Depending on the isomerization mechanism (see above), the volume required for isomerization from the *trans* to the *cis* state rises by 0.12 nm^3 in case of an inversion mechanism^[33] and even by 0.28 nm^3 for isomerization by rotation, respectively.^[34] In addition, the dipole moment increases from essentially 0 in the *trans* state to 3.1 D in the *cis* state.^[16]

Because of these remarkable changes of molecular properties, relatively facile syntheses and the many advantages of light-induced reactions, azobenzene derivatives have been and are being used in a great and growing number of applications. Following the observation by Merian in 1966^[35] that a nylon filament fabric dyed with an azobenzene derivative shrank upon irradiation,

the use of azobenzene photoswitches for creating large scale modulations in material properties by essentially amplifying the molecular *trans* \rightleftharpoons *cis* isomerization was proposed and further investigated.

Consequently, azobenzenes have been widely used not only as dyes and pigments, food additives and radical inhibitors, but also as therapeutic agents, electronics and for drug delivery shuttles.^[11] Some examples comprise the application of azobenzene derivatives in liquid crystal (LC) systems, initiating a reversible, isothermal phase transition from an ordered LC state to an isotropic phase by switching from the *trans* to the corresponding *cis* isomers^[27] and thus providing promising features for potential use in display devices, optical memories^[36] and electro-optics.^[37] In order to obtain suitable optical data storage materials, a stable two-state-system is required. Hence, efforts are made to stabilize and thus increase the lifetime of the *cis* isomers. In general, it is found that azobenzene derivatives which are covalently bound to the surface work better than doped ones because this prevents the molecules from aggregating which leads to undesired heterogenous layers and changes in the optical behavior.^[15] Another possible application of azobenzene photoswitches is their use as filters for gases. For example, incorporation of azobenzene derivatives in zeolites can provide light-controlled selective membranes for the permeation of certain gas molecules.^[38] Interestingly, azobenzene-containing liquid-crystalline elastomers (LCE) have been used in efforts to build artificial muscles, since the isomerization process of azobenzenes involves motion and thus the generation of a force.^[r,22] The many advantages of azobenzene photoswitches, including their efficient long-term usage, their high spatial and temporal precision as well as their noninvasive regulation, have made them also very attractive for biological applications.

Following the pioneering work of Erlanger who first introduced the use of azobenzenes as photochromic ligands in biology in the late 1960s (photoregulation of chymotrypsin,^[39] acetylcholine receptors^[40] and acetylcholinesterase^[41]), a vastly increasing number of applications in biological contexts has been developed during the last couple of years, among which only a brief selection is mentioned here. A good compilation of azobenzene photoswitches used for the light-dependent control of biological systems is presented in a recent review article by Beharry and Woolley.^[42]

^[r] AFM measurements estimated the mechanical work by *trans* \rightleftharpoons *cis* isomerization of one molecule of azobenzene to $4.5 \cdot 10^{-20}$ J: a) T. Hugel, N. B. Holland, A. Cattani, L. Moroder, M. Seitz, H. E. Gaub, *Science* **2002**, *296*, 1103–1106; b) N. B. Holland, T. Hugel, G. Neuert, A. Cattani-Scholz, C. Renner, D. Oesterhelt, L. Moroder, M. Seitz, H. E. Gaub, *Macromolecules* **2003**, *36*, 2015–2023.

By attaching azobenzene photoswitches to oligopeptides and proteins (either covalently^[43] in the backbone or as side chains, or by affinity^[39,44]), conformational changes can be induced upon irradiation. Moreover, DNA conformations can be altered by using azobenzene derivatives. Whereas the *trans* isomer intercalates in and stabilizes the DNA duplex, the *cis* isomer disrupts the duplex.^[45] Depending on different interactions with polymerases in the *trans* or *cis* state, gene expression can be photoinduced by introducing azobenzenes in the promotor region of genes.^[46] As already mentioned above, azobenzene containing vesicles or micelles are also interesting approaches to a light-controlled release of drugs at desired spots in the increasingly important field of drug delivery.^[47]

1.3 OPTOCHEMICAL GENETICS

In 2004, Banghart *et al.*^[48] picked up Erlangers pioneering efforts and applied the concept of photochromic ligands to the field of neuroscience by applying azobenzene photoswitches to control voltage-dependent potassium channels, thus ultimately regulating neuronal generation and transduction of action potentials (“*Light-Activated Ion Channels for Remote Control of Neuronal Firing*”). Focussing on the synthesis and application of biologically and photochemically active small molecules rather than genetic engineering, this concept has later been established as “*optochemical genetics*”,^[49] evolving from the rapidly increasing field of *optogenetics*.^[50]

Optogenetical approaches aim for regulation of biological systems down to cellular levels with light by genetic encoding of (artificial) photoreceptors. The first optogenetic construct was “ChARGe”, consisting of rhodopsin, the associated heterotrimeric G protein and arrestin, and was based on the vision cascade of *Drosophila*.^[51] With the discovery of channelrhodopsin-2 (ChR2),^[52] which is a natural photoreceptor isolated from the algae *Chlamydomonas reinhardtii*, a powerful new tool for the optical control of neuronal circuits has been established.^[53] The excitatory, nonspecific cation channel of ChR2 can be controlled with blue light (absorption maximum at $\lambda = 480$ nm) and is based on the naturally occurring photoswitch retinal which is not excised after isomerization (as it is in the mammalian vision cascade). Therefore, ChR2 can be used in multiple cycles to optically induce excitation. Since ChR2, many other mutants and chimeras have been developed. More recently, red-shifted channelrhodopsins have been discovered from the algae *Volvox carteri*, termed VChRs. VChR1 has a peak absorption of $\lambda = 589$ nm and can be used orthogonally to other ChRs.^[54] Beside ChRs, other optogenetic tools have been developed such as *Natromonas pharaonis* halorhodopsin (NpHR) which is an inhibitory chloride pump that reacts to yellow light

(absorption maximum at $\lambda = 570$ nm).^[55] More recently, light-driven proton pumps have also been discovered that are capable of silencing specific genetically targeted neurons with light to investigate their role in neuronal circuits.^[56]

Since the elucidation of the X-ray structure of KcsA, a potassium channel from *Streptomyces lividans* that reacts to changes in pH by MacKinnon in 2002,^[57] many more ion channels and receptors have been crystallized, revealing new insights into structure, selectivity, gating mechanisms and ligand binding at atomic levels. This opens up new possibilities for the rational design of small (photoreactive) molecules that selectively target specific receptors (see PCL concept). Moreover, specific amino acids can be genetically introduced that are in close proximity to the pore region of ion channels or ligand binding sites of receptors in order to anchor (photoreactive) molecules that physically block the channel or position a ligand in close proximity to the binding site, respectively (PTL concept).

Optochemical genetics offers three different strategies to control ion channels and receptors in a light-dependent fashion with photoreactive small molecules: (photochemically) **Caged Ligands (CLs)**, **PhotoChromic Ligands (PCLs)** and **Photoswitchable Tethered Ligands (PTLs)**. These strategies are depicted in Fig. 1.3 and will be briefly introduced in the next section.

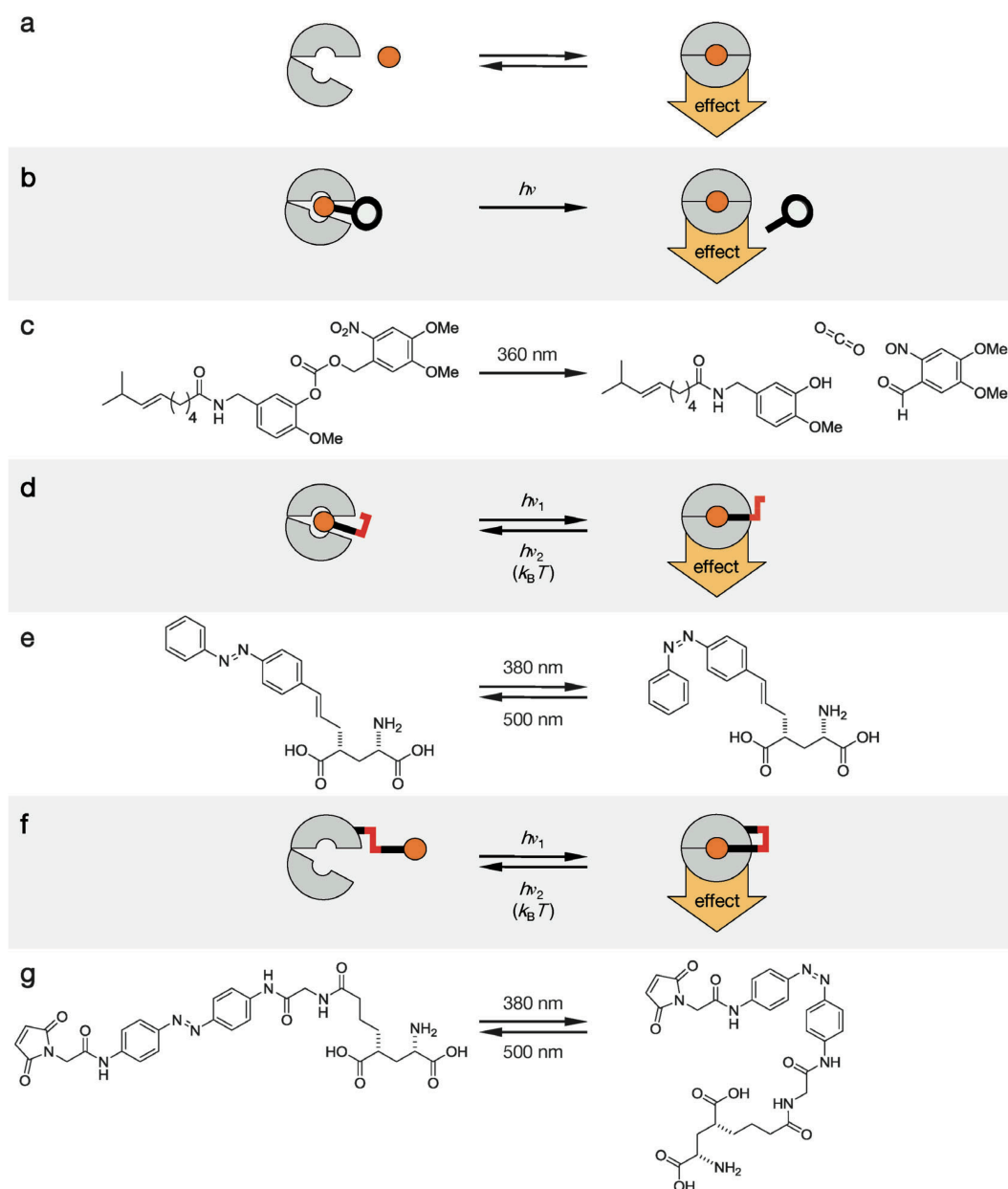


Figure 1.3. **a)** Schematic illustration of receptor-mediated signaling. A ligand (orange) binds to a receptor (grey) and induces an effect; **b)** Caged Ligand (CL) strategy: a caged ligand has no effect on the receptor, whereas the uncaged ligand does. The uncaging event is induced by light; **c)** Example for the CL approach: a caged version of capsaicin (CAP), a TRPV1 agonist; **d)** PhotoChromic Ligand (PCL) approach: a photoswitchable ligand does not exhibit an effect on the receptor in one conformation, but does affect it in another. Both conformations can be interconverted into each other with light of different wavelengths; **e)** 4-GluAzo, a PCL version of glutamate for ionotropic glutamate receptors; **f)** Photoswitchable Tethered Ligand (PTL) approach: a photoswitchable ligand that is covalently attached to the receptor. Only one conformation is in the right proximity to the binding site to induce an effect; **g)** MAG-1, an unconjugated PTL for ionotropic glutamate receptors. A cysteine residue can react with the maleimide moiety of the PTL. Illustration adapted from Trauner *et al.*,^[49] reprinted with permission from John Wiley and Sons. Copyright 2011.

1.3.1 THE CAGED LIGAND (CL) APPROACH

Caged ligands have been used on various receptor types for many years. By attaching a photocleavable protecting group to a ligand that renders it inactive, a desired receptor can be activated with high spatial and temporal precision through irradiation with light (Fig. 1.3b). This concept has been used for example for glutamate receptors,^[58] GABA receptors^[59] and TRPV1 channels (caged capsaicin, see Fig. 1.3c).^[60] However, certain disadvantages are associated with this approach. Most importantly, the uncaging process is an irreversible reaction. Once the protecting group is cleaved, the active ligand is released and cannot be “re-caged”, resulting in sustained receptor action until the ligand diffuses away. Moreover, toxic side products can be released, for example from the remnants of the cleaved protecting group.

To overcome the above mentioned disadvantages, a reversible “caging” process would be desirable which could be achieved by introducing a photoswitchable component onto ligands in order to render them light-sensitive and thus create two isoforms of the ligands with differing efficacies at the receptor. By attaching azobenzene moieties to ligands, two reversible approaches to receptor activation have been created, the PCL and the PTL approach, respectively.

1.3.2 THE PHOTOCROMIC LIGAND (PCL) APPROACH

PCLs combine a biologically active small molecule (agonist, antagonist, allosteric modulator, etc.) with a photoswitchable side chain (in this thesis azobenzenes). By switching between the two isoforms of the molecule *via* irradiation with different wavelengths, the efficacy of the ligand is modulated. Unlike the uncaging event, this approach is fully reversible (Fig. 1.3d). Remarkably, these sometimes rather small changes between the two isoforms have been shown to produce relatively large differences in the action of the ligand on the receptor in complex cellular and neuronal networks. This finding is underpinned by the “all or nothing” concept of action potential (AP) triggering which describes the necessity of reaching a certain threshold for an AP to be triggered. Once this threshold is reached, however, the AP is generated in the same amplitude, irrelevant of the current that has triggered it.

Using the PCL approach, various ligand-gated receptors and ion channels have been successfully rendered light-responsive, thus turning them into artificial light receptors. For voltage-gated potassium channels, photochromic ion channel blockers have been developed by attaching a quaternary ammonium ion to an azobenzene moiety. The cationic ammonium ion blocks the pore of the channel from the cytosolic side in the *trans* state of the molecule, but not in the *cis* state.^[61] Moreover, photochromic blockers of K⁺, Na⁺ and Ca²⁺ channels have been

described to control pain sensation.^[62] 4-GluAzo, a PCL version of glutamate, was used to optically control ionotropic glutamate receptors (iGluRs; Fig. 1.3e)^[63] and ATA-3, a PCL version of AMPA, functions as photochromic agonist for AMPA receptors.^[64]

1.3.3 THE PHOTOSWITCHABLE TETHERED LIGAND (PTL) APPROACH

In contrast to PCLs, PTLs are covalently attached *via* a tether to the receptor by introducing a reactive electrophilic site to the photoswitch, such as acrylate or maleimide, which can react with free cysteine residues on the receptor. Once bound to the receptor, switching between the two isoforms of the molecule leads to a change of the local concentration and/or its efficacy on the receptor (Fig. 1.3f). PTLs can thus overcome the low affinity of a ligand with its high local concentration at the ligand binding site. In principle, they allow for a higher (subtype) selectivity for certain receptors since their point of attachment (a reactive cysteine) can be genetically introduced. Therefore, the PTL concept preferentially is used as a pharmacological tool for the investigation of neuronal circuitries, resembling the original concept of *optogenetics*.

PTL blockers of K^+ , Na^+ and Ca^{2+} channels have been used to control heart beat^[65] and visual responses^[66] in a variety of animals with light. PTL versions of glutamate (e.g. MAG-1, Fig. 1.3g) have also been used to convert ionotropic glutamate receptors (iGluRs) into light-responsive iGluRs. These so-called LiGluRs have been successfully applied *in vitro* and *in vivo*.^[67] More recently, this concept has also been applied to metabotropic glutamate receptors (LimGluRs^[68]) and neuronal nicotinic acetylcholine receptors (nAChR). nAChRs have been rendered light-sensitive with a PTL version of acetylcholine, aiming for new methods to study the physiological and pathological roles of these receptors in the brain and periphery.^[69]

This thesis will focus on new PCL strategies for the optochemical control of ligand-gated receptors and ion channels. A great advantage of PCLs over PTLs is their possible application on wild-type receptors which opens up the opportunity for their use in clinical treatment.

More specifically, new PCLs have been designed, synthesized and successfully applied to the light-dependent regulation of γ -aminobutyric acid type A ($GABA_A$) receptors (see chapter 2) and transient receptor potential (TRP) channels (chapter 3). Moreover, various PCLs have been synthesized for the optical control of voltage-gated sodium channels (Na_V channels, chapter 4) and the metabotropic glutamate receptor 6 (mGluR6; chapter 5). In addition, PCLs for nAChRs and voltage-dependent potassium channels (K_V channels), as well as the synthesis of a photocleavable protecting group are outlined in chapter 6.

1.4 LITERATURE

- [1] M. Irie, *Chem. Rev.* **2000**, *100*, 1683–1684.
- [2] G. Feher, J. P. Allen, M. Okamura, D. C. Rees, *Nature* **1989**, *339*, 111–116.
- [3] L. Stryer, *Ann. Rev. Neurosci.* **1986**, *9*, 87–119.
- [4] a) N. Hampp, *Chem. Rev.* **2000**, *100*, 1755–1776; b) N. Vsevolodov, in *Biomolecular Electronics: An Introduction via photosensitive proteins*, Birkhäuser, Boston, **1998**.
- [5] G. Berkovic, V. Krongauz, V. Weiss, *Chem. Rev.* **2000**, *100*, 1741–1754.
- [6] M. Irie, *Chem. Rev.* **2000**, *100*, 1685–1716.
- [7] Y. Yokoyama, *Chem. Rev.* **2000**, *100*, 1717–1740.
- [8] I. Willner, S. Rubin, *Angew. Chem. Int. Ed. Engl.* **1996**, *35*, 367–385.
- [9] a) A. M. Gurney, H. A. Lester. *Physiol. Rev.* **1987**, *67*, 583–617; b) I. Willner, B. Willner, in *Bioorganic Photochemistry, Vol. 2* (Ed.: H. Morrison), Wiley, Weinheim, New York, **1993**, p. 1.
- [10] H. Rau, in *Photoisomerization of Azobenzenes*, (Ed.: J. Rebek), CRC Press, Boca Raton FL, **1990**.
- [11] E. Merino, *Chem. Soc. Rev.* **2011**, *40*, 3835–3853.
- [12] K. Haghbeen, W. Tan, *J. Org. Chem.* **1998**, *63*, 4503–4505.
- [13] H. H. Davey, R. D. Lee, T. J. Marks, *J. Org. Chem.* **1999**, *64*, 4976–4979.
- [14] S. Wawzoned, T. W. McIntyre, *J. Electrochem. Soc.* **1972**, *119*, 1350–1357.
- [15] K.-Y. Kim, J.-T. Shin, K.-S. Lee, C.-G. Cho, *Tetrahedron Lett.* **2004**, *45*, 117–120.
- [16] G. S. Hartley, *Nature* **1937**, *140*, 281.
- [17] F. W. Schulze, H. J. Petrick, H. K. Cammenga, H. Klinge, *Z. Phys. Chem.* **1977**, *107*, 1–19.
- [18] S. Monti, G. Orlandi, P. Palmieri, *Chem. Phys.* **1982**, *71*, 87–99.
- [19] J. Griffiths, *Chem. Soc. Rev.* **1972**, *1*, 481–493.
- [20] R. Pfister, J. Ihalainen, P. Hamm, C. Kolano, *Org. Biomol. Chem.* **2008**, *6*, 3508–3517.
- [21] P. Haberfield, P. M. Block, M. S. Lux, *J. Am. Chem. Soc.* **1975**, *97*, 5804–5806.
- [22] K. G. Yager, C. J. Barrett, *J. Photochem. Photobiol. A* **2006**, *182*, 250–261.
- [23] H. Duval, *Bull. Soc. Chim. Fr.* **1910**, *7*, 727–732.
- [24] R. Siewertsen, H. Neumann, B. Buchheim-Stehn, R. Herges, C. Näther, F. Renth, F. Temps, *J. Am. Chem. Soc.* **2009**, *131*, 15594–15595.
- [25] H. Sell, C. Näther, R. Herges, *Beilstein J. Org. Chem.* **2013**, *9*, 1–7.
- [26] J. Wachtveitl, T. Nägele, B. Puell, W. Zinth, M. Krüger, S. Rudolph-Böhner, D. Oesterhelt, L. Moroder, *J. Photochem. Photobiol., A* **1997**, *105*, 283–288.
- [27] C. J. Barrett, J.-I. Mamiya, K. G. Yager, T. Ikeda, *Soft Matter* **2007**, *3*, 1249–1261.

- [28] D. Y. Curtin, E. J. Grubbs, C. G. McCarty, *J. Am. Chem. Soc.* **1966**, *88*, 2775–2786.
- [29] J. L. Magee, W. Shand Jr., H. Eyring, *J. Am. Chem. Soc.* **1941**, *63*, 677–688.
- [30] F. Barigelletti, M. Ghedini, D. Pucci, M. La Deda, *Chem. Lett.* **1999**, 297–298.
- [31] H. M. D. Bandara, S. C. Burdette, *Chem. Soc. Rev.* **2012**, *41*, 1809–1825.
- [32] a) J. J. de Lange, J. M. Robertson, I. Woodward, *Proc. Roy. Soc.* **1939**, *A171*, 398–410; b) C. J. Brown, *Acta Crystallogr.* **1966**, *21*, 146–152.
- [33] T. Naito, K. Horie, I. Mita, *Macromolecules* **1991**, *24*, 2907–2911.
- [34] L. Lamarre, C. S. P. Sung, *Macromolecules* **1983**, *16*, 1729–1736.
- [35] E. Merian, *Textile Res. J.* **1966**, *36*, 612–618.
- [36] a) W. M. Gibbons, P. J. Shannon, S.-T. Sun, B. J. Swetlin, *Nature* **1991**, *351*, 49–50; b) T. Ikeda, O. Tsutsumi, *Science* **1995**, *268*, 1873–1875; c) azobenzene functionalized oligopeptides as optical storage: R. H. Berg, S. Hvilsted, P. S. Ramanujam, *Nature* **1996**, *383*, 505–508.
- [37] Y.-Y. Luk, N. L. Abbott, *Science* **2003**, *301*, 623–626.
- [38] K. Weh, M. Noack, K. Hoffmann, K.-P. Schröder, J. Caro, *Microporous Mesoporous Mater.* **2002**, *54*, 15–26.
- [39] H. Kaufmann, S. M. Vratsanos, B. F. Erlanger, *Science* **1968**, *162*, 1487–1489.
- [40] E. Bartels, N. H. Wassermann, B. F. Erlanger, *Proc. Natl. Acad. Sci. USA* **1971**, *68*, 1820–1823.
- [41] J. Bieth, S. M. Vratsanos, N. Wassermann, B. F. Erlanger, *Proc. Natl. Acad. Sci. USA* **1969**, *64*, 1103–1106.
- [42] A. A. Beharry, G. A. Woolley, *Chem. Soc. Rev.* **2011**, *40*, 4422–4437.
- [43] T. Inada, T. Terabayashi, Y. Yamaguchi, K. Kato, K. Kikuchi, *J. Photochem. Photobiol.* **2005**, *175*, 100–107.
- [44] a) D. Fujita, M. Murai, T. Nishioka, H. Miyoshi, *Biochemistry* **2006**, *45*, 6581–6586; b) J. H. Harvey, D. Trauner, *ChemBioChem* **2008**, *9*, 191–193.
- [45] X. Liang, H. Asanuma, H. Kashida, A. Takasu, T. Sakamoto, G. Kawai, M. Komiyama, *J. Am. Chem. Soc.* **2003**, *125*, 16408–16415.
- [46] M. Liu, H. Asanuma, M. Komiyama, *J. Am. Chem. Soc.* **2006**, *128*, 1009–1015.
- [47] a) E. Yoshida, M. Ohta, *Colloid Polym. Sci.* **2005**, *283*, 521–531; b) H. Sakai, A. Matsumura, T. Saji, M. Abe, *Stud. Surf. Sci. Catal.* **2001**, *132*, 505–508; c) X.-M. Liu, B. Yang, Y.-L. Wang, J.-Y. Wang, *Chem. Mater.* **2005**, *17*, 2792–2795; d) X. Tong, G. Wang, A. Soldara, Y. Zhao, *J. Phys. Chem. B* **2005**, *109*, 20281–20287.
- [48] M. R. Banghart, K. Borges, E. Y. Isacoff, D. Trauner, R. H. Kramer, *Nat. Neurosci.* **2004**, *7*, 1381–1386.

- [49] T. Fehrentz, M. Schönberger, D. Trauner, *Angew. Chem. Int. Ed.* **2011**, *50*, 12156–12182.
- [50] a) G. Miesenböck, *Science* **2009**, *326*, 395–399; b) G. Miesenböck, *Annu. Rev. Cell Dev. Biol.* **2011**, *27*, 731–758; c) L. Fenno, O. Yizhar, K. Deisseroth, *Annu. Rev. Cell Dev. Biol.* **2011**, *34*, 389–412.
- [51] B. V. Zemelman, G. A. Lee, M. Ng, G. Miesenböck, *Neuron* **2002**, *33*, 15–22.
- [52] G. Nagel, T. Szellas, W. Huhn, S. Kateriya, N. Adeishvili, P. Berthold, D. Ollig, P. Hegemann, E. Bamberg, *Proc. Natl. Acad. Sci. USA* **2003**, *100*, 13940–13945.
- [53] E. S. Boyden, F. Zhang, E. Bamberg, G. Nagel, K. Deisseroth, *Nat. Neurosci.* **2005**, *8*, 1263–1268.
- [54] F. Zhang, M. Prigge, F. Beyrière, S. P. Tsunoda, J. Mattis, O. Yizhar, P. Hegemann, K. Deisseroth, *Nat. Neurosci.* **2008**, *11*, 631–633.
- [55] F. Zhang, L. P. Wang, M. Brauner, J. F. Liwald, K. Kay, N. Watzke, P. G. Wood, E. Bamberg, G. Nagel, A. Gottschalk, K. Deisseroth, *Nature* **2007**, *446*, 633–639.
- [56] B. Y. Chow, X. Han, A. S. Dobry, X. Qian, A. S. Chuong, M. Li, M. A. Henninger, G. M. Belfort, Y. Lin, P. E. Monahan, E. S. Boyden, *Nature* **2010**, *463*, 98–102.
- [57] D. A. Doyle, J. Morais Cabral, R. A. Pfützner, A. Kuo, J. M. Gulbis, S. L. Cohen, B. T. Chait, R. MacKinnon, *Science* **1998**, *280*, 69–77.
- [58] J. Noguchi, A. Nagaoka, S. Watanabe, G. C. Ellis-Davies, K. Kitamura, M. Kano, M. Matsuzaki, H. Kasai, *J. Physiol.* **2011**, *589*, 2447–2457.
- [59] R. Wieboldt, D. Ramesh, B. K. Carpenter, G. P. Hess, *Biochemistry* **1994**, *33*, 1526–1533.
- [60] B. V. Zemelman, N. Nesnas, G. A. Lee, G. Miesenböck, *Proc. Natl. Acad. Sci. USA* **2003**, *100*, 1352–1357.
- [61] a) M. R. Banghart, A. Mourot, D. L. Fortin, J. Z. Yao, R. H. Kramer, D. Trauner, *Angew. Chem. Int. Ed.* **2009**, *48*, 9097–9101; b) A. Mourot, M. A. Kienzler, M. R. Banghart, T. Fehrentz, F. M. E. Huber, M. Stein, R. H. Kramer, D. Trauner, *ACS Chem. Neurosci.* **2011**, *2*, 536–543.
- [62] A. Mourot, T. Fehrentz, D. Bautista, D. Trauner, R. H. Kramer, *Nat. Meth.* **2012**, *9*, 396–402.
- [63] M. Volgraf, P. Gorostiza, S. Szobota, M. R. Helix, E. Y. Isacoff, D. Trauner, *J. Am. Chem. Soc.* **2007**, *129*, 260–261.
- [64] P. Stawski, M. Sumser, D. Trauner, *Angew. Chem. Int. Ed.* **2012**, *51*, 5748–5751.

- [65] D. L. Fortin, M. R. Banghart, T. D. Dunn, K. Borges, D. A. Wagnaar, Q. Gaudry, M. Karakossian, T. W. Otis, W. B. Kristan, D. Trauner, R. H. Kramer, *Nat. Meth.* **2008**, *5*, 331–338.
- [66] A. Polosukhina, J. Litt, I. Tochitsky, J. Nemargut, Y. Sychev, I. De Kouchkovsky, T. Huang, K. Borges, D. Trauner, R. N. Van Gelder, R. H. Kramer, *Neuron* **2012**, *75*, 271–282.
- [67] a) M. Volgraf, P. Gorostiza, R. Numano, R. H. Kramer, E. Y. Isacoff, D. Trauner, *Nat. Chem. Bio.* **2006**, *1*, 47–52; b) S. Szobota, P. Gorostiza, F. Del Bene, C. Wyart, D. L. Fortin, K. D. Kolstad, O. Tulyathan, M. Volgraf, R. Numano, H. L. Aaron, E. K. Scott, R. H. Kramer, J. Flannery, H. Baier, D. Trauner, E. Y. Isacoff, *Neuron* **2007**, *54*, 535–545; c) P. Gorostiza, M. Volgraf, R. Numano, S. Szobota, D. Trauner, E. Y. Isacoff, *Proc. Natl. Acad. Sci. USA* **2007**, *104*, 10865–10870; d) C. Wyart, F. Del Bene, E. Warp, E. K. Scott, D. Trauner, H. Baier, E. Y. Isacoff, *Nature* **2009**, *461*, 407–410; e) H. Janovjak, S. Szobota, C. Wyart, D. Trauner, E. Y. Isacoff, *Nat. Neurosci.* **2010**, *13*, 1027–1032; f) N. Caporale, K. D. Kolstad, T. Lee, I. Tochitsky, D. Dalkara, D. Trauner, R. H. Kramer, Y. Dan, E. Y. Isacoff, J. G. Flannery, *Mol. Ther.* **2011**, *19*, 1212–1219.
- [68] J. Levitz, C. Pantoja, B. Gaub, H. Janovjak, A. Reiner, A. Hoagland, D. Schoppik, B. Kane, P. Stawski, A. F. Schier, D. Trauner, E. Y. Isacoff, *Nat. Neurosci.* **2013**, *16*, 507–516.
- [69] I. Tochitsky, M. R. Banghart, A. Mourot, J. Z. Zhao, B. Gaub, R. H. Kramer, D. Trauner, *Nat. Chem.* **2012**, *4*, 105–111.

2 PHOTOREGULATION OF GABA_A RECEPTORS

2.1 THE GABA_A RECEPTOR

Most neuronal inhibition in the brain is mediated by γ -aminobutyric acid (GABA)ergic neurons.^[1] They are essential for neuronal oscillations in the β - and γ -bands of the electroencephalogram (EEG) which are believed to underlie a series of cognitive function such as perception, selective attention, working memory and consciousness.^[1] Since GABA_A receptors (GABA_ARs) are involved in a vast number of different signaling circuits, they exist as various subtypes which are encoded by more than a dozen genes. These receptor subtypes vary in their subunit composition, in their cellular expression patterns and subcellular concentrations as well as in their kinetic properties.^[1] The dynamic regulation of receptor function is mediated by highly regulated receptor trafficking, chemical modifications (mostly phosphorylation) as well as by regulation of subunit expression.^[1] Alterations in the subunit composition are often involved in chronic diseases, i.e. epilepsy.^[2]

GABA_ARs are heteropentameric chloride channels and part of the Cys-loop ligand-gated ion channel superfamily. They have a pronounced heterogeneity and consist of numerous subunits which are divided into three main classes based on their sequence homology: α_{1-6} , β_{1-3} , γ_{1-3} . In addition, more specialized and rare subunit forms exist such as δ , ϵ , π , θ , and ρ_{1-3} .^[1] All subunits exhibit a similar topology consisting of a large extracellular N-terminal domain (~200 amino acids), four α -helical transmembrane helices (TM1–4) and a large intracellular loop connecting TM3 and TM4. The extracellular domain consists of mainly β -sheets, whereas the cytoplasmic domain comprises α -helices (Fig. 2.1c). Within the N-terminal domain, a 15 amino acid-long loop linked *via* a disulfide bridge between two cysteine residues exists in all subunits which is characteristic for the Cys-loop superfamily receptors (Fig. 2.1a, left).^[1] The TM2 helices of each of the five subunits form the chloride-selective pore of the channel (Fig. 2.1a, right). Although there is no high-resolution crystal structure of the receptors available to date, the X-ray structure of a soluble acetylcholine binding protein (AChBP) from the snail *Lymnaea stagnalis* obtained in 2001^[3] and a more recent, refined electron microscope structure of nAChR from electric fish at 4.0 Å resolution^[4] serve as templates for the extracellular receptor domains (Fig. 2.1c).

The ligand binding sites are located on the extracellular domains. In the most abundant (~60%) GABA_AR, $\alpha_1\beta_2\gamma_2$, also known as α_1 GABA_AR, the endogenous ligand GABA binds between the interface of α_1 and β_2 subunits, whereas the widely known class of benzodiazepines (BZs), which act as allosteric modulators, bind between the γ_2 and α_1 subunit (Fig. 2.1b). On the

contrary, regulation on the intracellular loop occurs by phosphorylation and receptor associated proteins.^[5]

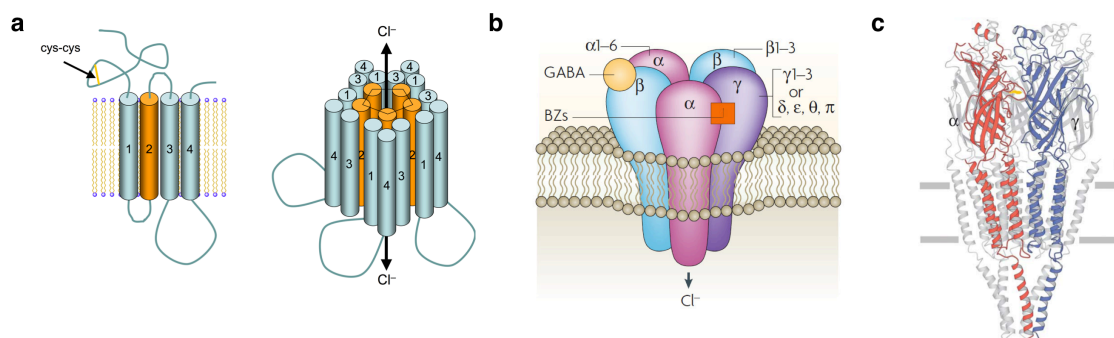


Figure 2.1. a) Schematic illustration of GABA_ARs. Illustration copied from Wikipedia.^[6] b) Model of the GABA_A receptor. Distribution of subunits is shown as well as localization of GABA and benzodiazepine (BZ) binding sites. Illustration copied from Jacob *et al.*,^[7] reprinted with permission from Macmillan Publishers Ltd. Copyright 2008. c) Structure of nAChR from the *Torpedo* electric organ with 4 Å resolution as blueprint for GABA_ARs. The two front subunits are highlighted (α : red; β : blue). The grey lines represent the plasma membrane (E = Extracellular space, I = Intracellular space). Illustration copied from Unwin,^[4] reprinted with permission from Elsevier. Copyright 2005.

The many different GABA_ARs are related to various functions. For instance, $\alpha_4\beta_n\gamma/\delta$ (α_5) GABA_ARs play a crucial role in learning and memory processes.^[1] Sedation is linked to $\alpha_1\beta_2\gamma_2$, whereas α_2 receptors ($\alpha_2\beta_3\gamma_2$) are responsible for mediating anxiolytic effects.^[1] β_3 -containing receptors have been shown to mediate in full the immobilizing action of the two anesthetics etomidate and propofol,^[8] whereas the hypnotic effects of etomidate are mainly mediated by β_2 -containing GABA_ARs.^[9] Interestingly, the heart rate depressant action and to a large part the hypothermic action of propofol and etomidate are linked to other targets.^[10] Consequently, a β_3 -selective drug would probably function as an immobilizing anesthetic without undesired heart rate depressing side effects.^[1]

2.2 AZO-PROPOFOLS: PHOTOCHROMIC POTENTIATORS OF GABA_A RECEPTORS

Propofol is a well-known and clinically widely used anesthetic which functions as a potentiator, that is positive allosteric modulator of GABA-induced chloride currents. The resulting hyperpolarization leads to a silencing of neuronal activity which is thought to be essential for the induction of anesthesia. Propofol recently gained questionable popularity since the famous US singer Michael Jackson died of a propofol intoxication in 2009.

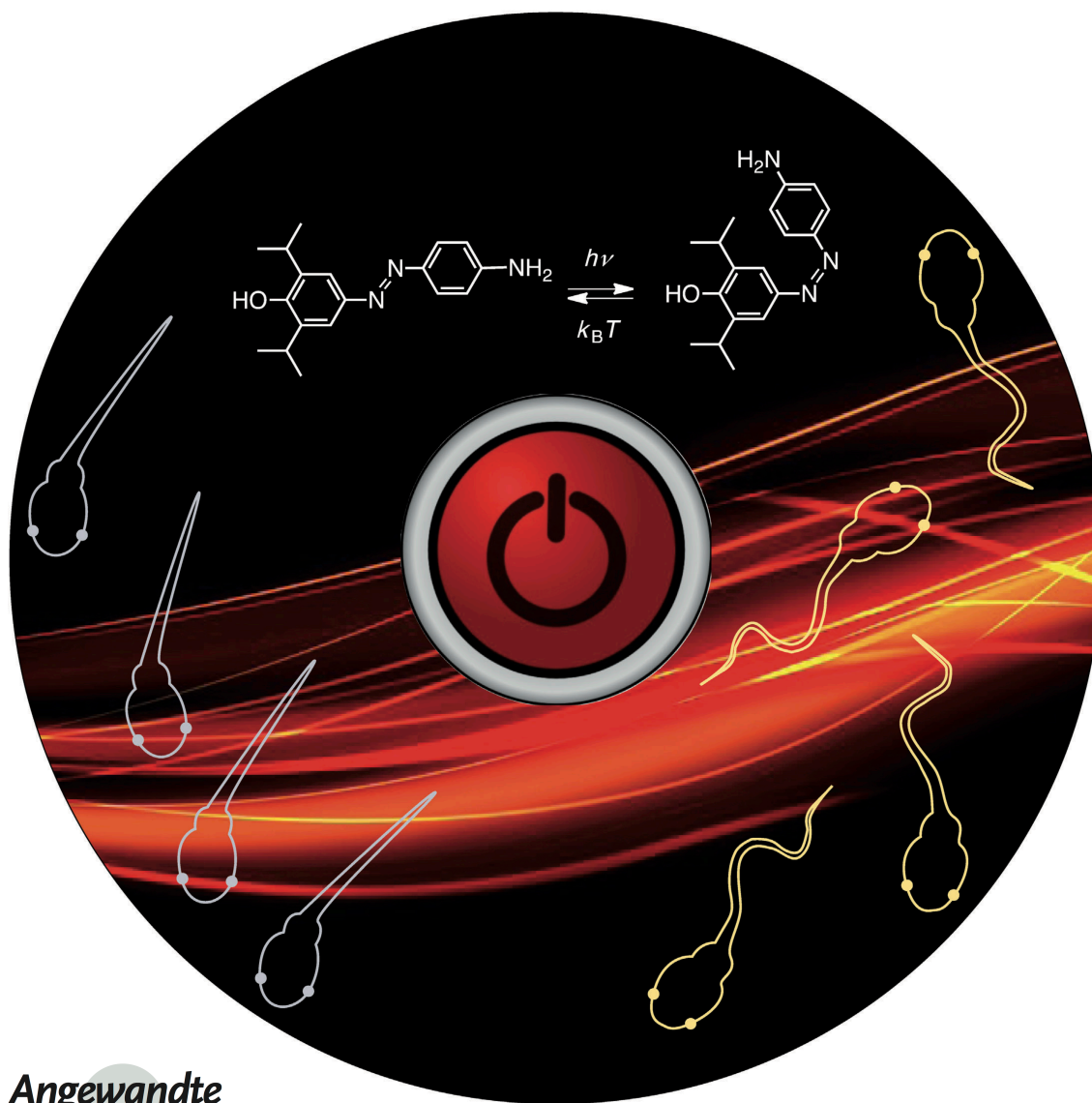
Striving for photocontrol of GABA_A receptors, azobenzene derivatives of propofol were synthesized and tested *in vitro* and *in vivo* for their ability to light-dependently increase or decrease GABA-induced chloride currents, respectively.

In the following, the original publication of this work is presented which was published in *Angewandte Chemie International Edition* in 2012.^[s] Please note that the numbering of schemes, figures as well as compounds in the accompanying *Supporting Information* was adjusted to fit the consecutive numbering of this thesis.

^[s] reprinted with permission from John Wiley and Sons. Copyright 2012.

Azo-Propofols: Photochromic Potentiators of GABA_A Receptors**

Marco Stein, Simon J. Middendorp, Valentina Carta, Ervin Pejo,
Douglas E. Raines, Stuart A. Forman, Erwin Sigel,* and Dirk Trauner*

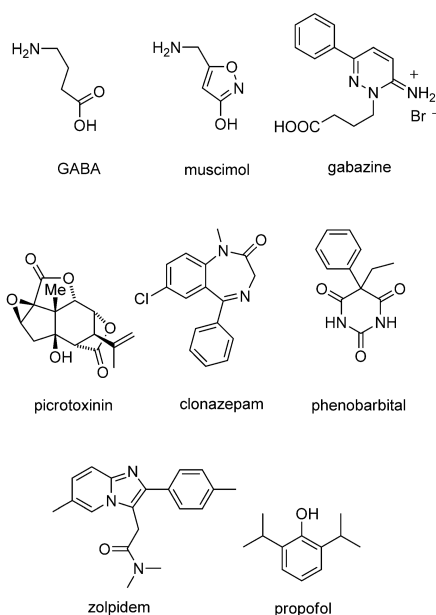


GABA_A receptors are pentameric ligand-gated ion channels that are activated by the major inhibitory neurotransmitter in the mammalian brain, γ -aminobutyric acid (GABA).^[1] Binding of GABA results in the opening of a chloride ion selective pore, thus hyperpolarizing the postsynaptic neuron and decreasing the likelihood of action-potential firing. As such, GABA_A receptors are a prominent target for anesthetic, hypnotic, and anticonvulsant drugs (Scheme 1).^[2,3]

While agonists, antagonists, and blockers of GABA_A receptors, such as muscimol, gabazine, or picrotoxinin, respectively, have proven to be valuable research tools, their impact on human medicine has been limited. Drugs that target these receptors are dominated by allosteric modulators that potentiate, that is, increase, chloride currents elicited by the neurotransmitter. Well-established potentiators include benzodiazepines (e.g. clonazepam), barbiturates (e.g. phenobarbital), the imidazopyridine zolpidem, and the simple phenol propofol.^[2] These drugs bind to distinct allosteric sites on GABA_A receptors, thereby increasing the mean open time or the opening frequency of the channel. However, the analysis of their exact binding sites at a molecular level has been complicated by a lack of detailed structural data.

After its discovery in 1980, propofol has become the most widely used intravenous general anesthetic.^[4] Although its mode of action has not been fully elucidated, it is commonly accepted that the anesthesia induced by this unusually lipophilic drug mostly results from potentiation of GABA-induced currents, as well as a direct activation of the chloride ion channel at high concentrations. Propofol has a rapid onset and offset of action and shows only minimal accumulation upon prolonged use. The intravenous administration of propofol is also associated with reduced postoperative nausea and vomiting.^[5]

While GABA_A receptors respond to a variety of ligands, they are normally not sensitive toward light. It would be fascinating to confer light sensitivity to these ion channels,



Scheme 1. Agonists (GABA, muscimol), antagonists (gabazine), blockers (picrotoxinin), or potentiators (clonazepam, phenobarbital, zolpidem, propofol) of GABA_A receptors.

since light is unsurpassed in terms of the temporal and spatial precision it provides. This light sensitivity could be indirectly achieved by using ligands that act on the receptors but can be optically switched between an active and an inactive form. Photochromic ligands of GABA_A receptors could be agonists, antagonists, or allosteric modulators. In principle, these ligands could be covalently attached as photoswitched tethered ligands (PTLs) or act as soluble photochromic ligands (PCLs).^[6] Indeed, both approaches have been used to convert neuronal^[7] and neuromuscular^[8] nicotinic acetylcholine receptors, another type of pentameric ligand-gated ion channels, as well as ionotropic glutamate receptors^[9] into artificial photoreceptors. Tethered and soluble photochromic blockers of K⁺, Na⁺, and Ca²⁺ ion channels have been described as well and have been used to control heartbeat,^[10] pain sensation^[11] and visual responses^[12] in different animals with light.

We now report photochromic potentiators of GABA currents that change the strength of GABA-induced currents in a light-dependent fashion. Our program was prompted by a recent report on a photoaffinity probe based on propofol, *p*-4-azic5-propofol that underscored that a relatively large substituent in the *para*-position of the phenol would be tolerated and that the propofol pharmacophore would be compatible with photochemistry (Scheme 2a).^[13] Accordingly, we designed a series of azobenzene derivatives of propofol; in these derivatives an aryldiazene unit is directly coupled to the pharmacophore. These molecules, termed azopropofols 1–16 (**API-16**) are shown in Scheme 2a. Their

[*] M. Stein,^[14] D. Trauner
Department of Chemistry, Ludwig-Maximilians-Universität München and Center of Integrated Protein Science 81377 Munich (Germany)
E-mail: dirk.trauner@lmu.de

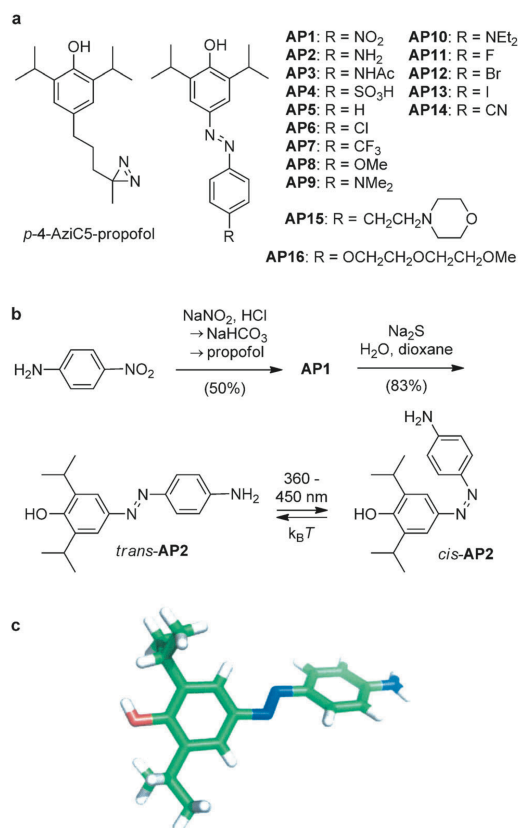
S. J. Middendorp,^[14] V. Carta, E. Sigel
Institute for Biochemistry and Molecular Medicine University of Bern
Bühlstr. 28, CH-3012 Bern (Switzerland)
E-mail: erwin.sigel@ibmm.unibe.ch

E. Pejo, D. E. Raines, S. A. Forman
Department of Anesthesia, Critical Care and Pain Medicine Massachusetts General Hospital
32 Fruit Street, Boston, MA 02114 (USA)

[*] These authors contributed equally to this work.

[**] We thank Dr. Peter Mayer (LMU Munich) for the determination of the X-ray structure. M. S. is grateful to the Fonds der Chemischen Industrie for a Ph.D. fellowship. This work was supported by the Swiss National Science Foundation grants 31003A-132806/1 (E.S.) and the European Science Foundation (ERC grant No 268795 to D.T.) and the National Institutes of Health (GM089745 to S.A.F and GM087316 to D.E.R.). GABA = γ -aminobutyric acid.

Supporting information for this article is available on the WWW under <http://dx.doi.org/10.1002/anie.201205475>.



Scheme 2. a) *p*-4-aziC5-propofol, a photoreactive derivative of propofol, and AP1–16, photoswitchable derivatives of propofol. b) Synthesis of AP1 and AP2, which is shown in its *trans* and *cis* configuration. c) X-ray structure of *trans*-AP2; C green, O red, H white, N blue.

varying substituent in the 4'-position of the azobenzene core determines their pharmacodynamic as well as spectral properties.

Compounds AP1–16 were synthesized using classical diazo-coupling chemistry, as shown in the representative synthesis of AP1 and AP2 (Scheme 2b, also see the Supporting Information).^[14] The X-ray structure of AP2 is displayed in Scheme 2c.^[15] Owing to crystal packing effects, the *trans*-azobenzene is not fully planar in this solid-state structure (see the Supporting Information for a more detailed discussion of these effects).

Although several of the azo-propofols shown in Scheme 2 function as photochromic potentiators, AP2 emerged early on as our most promising candidate owing to its favorable pharmacological and photochemical features. By virtue of its amino substituent, the photoswitch has a red-shifted absorption spectrum, which means that a maximum *cis* content is achieved at irradiation with 404 nm light. However, owing to the broad absorption spectrum, slightly longer or shorter wavelengths could be used effectively (see the Supporting

Information). In addition to this, the substitution of the azobenzene core with electron-donating substituents greatly decreases the thermal stability of the *cis* isomer. Therefore, AP2 quickly reverts to its *trans* form once the light is switched off. Since the absorption spectra of the *cis* and *trans* isomers are very similar (see the Supporting Information), this process cannot be accelerated by irradiation with a different wavelength. Other APs studied have less favorable photophysical properties, show decreased potency (e.g. AP3, AP9, AP10), no activity at all (e.g. AP4),^[14c] or unfavorable solubility and distribution (e.g. AP6).

The effect of AP2 on Cl⁻ currents was investigated with electrophysiology using $\alpha_1\beta_2\gamma_2$ GABA_A receptors expressed in *Xenopus* oocytes (Figure 1).^[16] This receptor subtype represents the most prevalent form in the human brain.^[17] First, the heterologously expressed GABA_A receptors were exposed to GABA at a concentration eliciting 0.3% of the maximal current amplitude in combination with increasing concentrations of propofol or AP2 in the dark to compare the relative effect of the compounds. From the resulting dose-response curves, we extracted an EC₅₀ value of (17.1 ± 2.9) μM for propofol and of (6.1 ± 0.4) μM for AP2 (mean ± standard error of the mean (SEM), *n* = 4; Figure 1a). Thus, AP2 in its dark-adapted *trans* form has a significantly higher affinity than propofol itself, albeit its efficacy is reduced by about twofold when compared with its parent compound.

Having established that AP2, in its dark-adapted form, has an effect on GABA_A receptors, we investigated the light dependency of the current potentiation. UV/Vis light from an Ultrafire 1 Watt UV LED pocket lamp (YonC Trading, Zürich; emission wavelength 390–450 nm) had no effect on the GABA response or the combined GABA/propofol response (data not shown). Figure 1b illustrates the effect of UV/Vis light on currents elicited by the combined application of GABA and AP2. Stimulation of GABA currents by AP2 (1.5 μM) was (159 ± 25)% (mean ± SEM, *n* = 6). Exposure to light decreased the residual stimulation to (18 ± 3)% (mean ± SEM, *n* = 6). Similar observations were made using a UV high power LED pocket lamp, 5 Watt (Uveco GmbH, Bruckmühl, Germany), emission wavelength 355–380 nm equipped with a CHROMA bandpass filter D365/10 ×, to limit light emission to 360–370 nm. The possibility to use these different light sources reflects the broad absorption spectrum of AP2. Owing to redistribution of the hydrophobic compound AP2 into egg yolk, the rate of photoswitching could not be determined in *Xenopus* oocytes. For this purpose, we expressed $\alpha_1\beta_2\gamma_2$ GABA_A receptors in HEK cells and performed experiments using the whole-cell patch-clamp technique. GABA was co-applied with AP2. Subsequently, the perfusion was stopped to prevent arrival of new *trans*-AP2 during the measurement, and the cells were exposed to the light. The current amplitude decreased rapidly and increased again upon turning off the light source. Current traces were fitted with a mono-exponential function. The time constant τ amounted to (1.1 ± 0.4) s (mean ± SD, *n* = 7) for the *trans*-to-*cis* transition and (2.0 ± 0.7) s (mean ± SD, *n* = 6) for the *cis*-to-*trans* transition.

Next, we investigated anesthetic activity and photoreversibility of both propofol and AP2 in a small animal model,

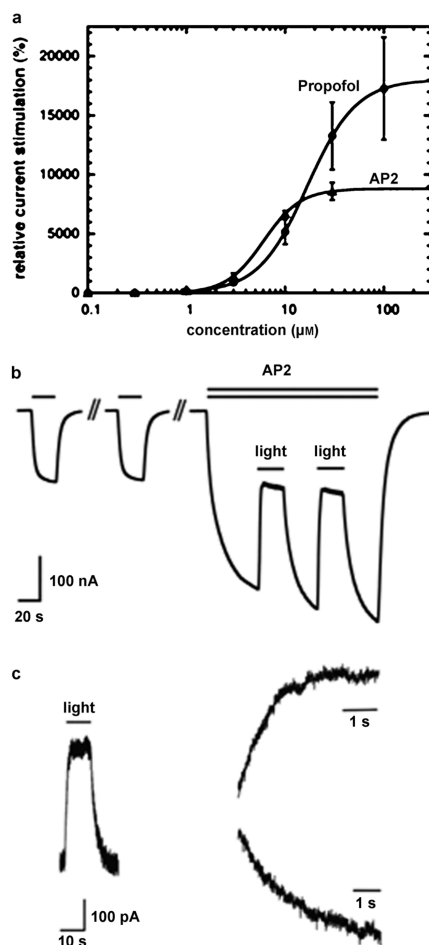


Figure 1. a) $\alpha_1\beta_2\gamma_2$ GABA_A receptors were expressed in *Xenopus* oocytes. Currents were activated with a concentration of GABA eliciting 0.3% of the maximal current amplitude ($EC_{0.3}$) with increasing amounts of either propofol or AP2. Mean \pm SEM of four experiments is shown. b) GABA ($1 \mu\text{M}$) was applied repetitively until a stable current response was observed. Co-application of AP2 ($1.5 \mu\text{M}$) with GABA resulted in current potentiation. During co-application, the oocyte was exposed to a light source emanating 390–450 nm light. As a consequence, current stimulation rapidly decreased until it reached a steady level. When the light-source was turned off, the amplitude increased again. This procedure was repeated. This experiment was repeated independently six times using different oocytes. c) $\alpha_1\beta_2\gamma_2$ GABA_A receptors were expressed in HEK cells. GABA ($0.5 \mu\text{M}$) was co-applied with AP2 ($5 \mu\text{M}$). Subsequently, the perfusion was stopped and the cells were exposed to the light source. The inward current amplitude decreased rapidly and increased again upon turning off the light source (trace left). Current decrease (trace top right) and increase (trace bottom right) were each fitted with a mono-exponential function.

albino *Xenopus laevis* tadpoles. Groups of animals were placed in aqueous solutions containing either propofol or AP2 and tested every five minutes for loss of righting reflexes (LORR), a standard assay for anesthesia.^[13] Steady-state LORR results were observed at 10 min for propofol and 25 min for AP2. After 30 min in drug solution, each animal was exposed for five to ten seconds to 360–370 nm bandpass filtered UV light (details in the Supporting Information) while retesting for LORR. Propofol alone produced LORR with an EC_{50} of $1.3 \mu\text{M}$ (Figure 2a). Illumination induced

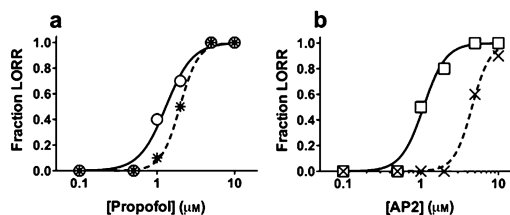


Figure 2. Light-dependent anesthesia in tadpoles. Loss of righting reflexes is plotted against aqueous anesthetic concentration, overlaid with logistic fits. Each point represents data from ten animals. a) 360–370 nm light, an apparently noxious stimulus in *Xenopus* tadpoles, produces a small rightward shift in propofol-dependent loss of righting reflexes (LORR) from $(1.1 \pm 0.1) \mu\text{M}$ (circles) to $(2.0 \pm 0.1) \mu\text{M}$ (stars). b) 360–370 nm light shifts the AP2-dependent LORR curve to the right from $(1.1 \pm 0.1) \mu\text{M}$ (squares) to $4.6 \pm 0.2 \mu\text{M}$ (crosses). This larger shift is due to photoisomerization of AP2.

vigorous swimming activity in unanesthetized tadpoles (thus suggesting that illumination represents a noxious stimulus) and a small rightward shift in the corresponding plot of LORR versus propofol concentration was observed (EC_{50} ca. $2.0 \mu\text{M}$; Figure 2a). AP2 alone produced LORR with an EC_{50} value similar to that of propofol ($1.1 \mu\text{M}$; Figure 2b). However, illumination produced a large rightward shift in the AP2 EC_{50} value to $4.6 \mu\text{M}$ (Figure 2b). All animals recovered from anesthesia when returned to water alone. In an independent set of experiments (see video in the Supporting Information), propofol ($3 \mu\text{M}$) produced LORR in all tadpoles with or without light, whereas in AP2 ($3 \mu\text{M}$), all animals showed LORR without light and all spontaneously righted themselves and swam during illumination with UV light.

The photoreversibility of both AP2-induced GABA_A receptor modulation and its anesthetic action in animals supports the hypothesis that anesthesia caused by AP2 and propofol is largely mediated by GABA_A receptors. However, evidence also implicates other targets, including HCN1 channels (hyperpolarization-activated cation channels),^[18] in propofol's anesthetic actions. The examination of the effects of AP2 on these other targets and the investigation of the photoreversibility of the modulation of these targets might help to further elucidate their roles in the pharmacology of general anesthesia.

In summary, we have developed photoswitchable versions of propofol that allow the indirect optical control of GABA_A receptors. Functionally, our compounds differ from previously introduced PCLs, because they act as photochromic

potentiators rather than photochromic agonists, antagonists, or channel blockers. Application of our lead compound, **AP2**, in the dark potentiates GABA-induced Cl⁻ currents, which can be reversed upon irradiation with violet light. The ability of azo-propofols to control neural systems has been demonstrated, since **AP2** functions as a light-dependent anesthetic in translucent tadpoles. Future work will address the usefulness of azo-propofols in other systems, such as brain slices and retinas lacking innate photoreceptors, wherein photochromic potentiators could restore visual responses through their action on neurons expressing GABA_A receptors.

Received: July 11, 2012

Published online: September 11, 2012

Keywords: azo compounds · GABA receptors · ion channels · photochromism · photopharmacology

- [1] R. L. Macdonald, R. W. Olsen, *Annu. Rev. Neurosci.* **1994**, *17*, 569–602.
- [2] W. Sieghart, *Pharmacol. Rev.* **1995**, *47*, 181–233.
- [3] E. Sigel, B. P. Lüscher, *Curr. Trends Med. Chem.* **2011**, *11*, 241–246.
- [4] C. Vanlersberghe, F. Camu, *Handb. Exp. Pharmacol.* **2008**, *182*, 227–252.
- [5] C. C. Apfel, K. Korttila, M. Abdalla, H. Kerger, A. Turan, I. Vedder, C. Zernak, K. Danner, R. Jokela, S. J. Pocock, S. Trenkler, M. Kredel, A. Biedler, D. I. Sessler, N. Roewer, *N. Engl. J. Med.* **2004**, *350*, 2441–2451.
- [6] T. Fehrentz, M. Schönberger, D. Trauner, *Angew. Chem.* **2011**, *123*, 12362–12390; *Angew. Chem. Int. Ed.* **2011**, *50*, 12156–12182.
- [7] I. Tochitsky, M. R. Banghart, A. Mourot, J. Z. Zhao, B. Gaub, R. H. Kramer, D. Trauner, *Nat. Chem.* **2012**, *4*, 105–111.
- [8] E. Bartels, N. H. Wassermann, B. F. Erlanger, *Proc. Natl. Acad. Sci. USA* **1971**, *68*, 1820–1823.
- [9] a) M. Volgraf, P. Gorostiza, R. Numano, R. H. Kramer, E. Y. Isacoff, D. Trauner, *Nat. Chem. Biol.* **2006**, *2*, 47–52; b) M. Volgraf, P. Gorostiza, S. Szobota, M. R. Helix, E. Y. Isacoff, D. Trauner, *J. Am. Chem. Soc.* **2007**, *129*, 260–261; c) S. Szobota, P. Gorostiza, F. Del Bene, C. Wyart, D. L. Fortin, K. D. Kolstad, O. Tulyathan, M. Volgraf, R. Numano, H. L. Aaron, E. K. Scott, R. H. Kramer, J. Flannery, H. Baier, D. Trauner, E. Y. Isacoff, *Neuron* **2007**, *54*, 535–545; d) P. Gorostiza, M. Volgraf, R. Numano, S. Szobota, D. Trauner, E. Y. Isacoff, *Proc. Natl. Acad. Sci. USA* **2007**, *104*, 10865–10870; e) R. Numano, S. Szobota, A. Y. Laud, P. Gorostiza, M. Volgraf, B. Roux, D. Trauner, E. Y. Isacoff, *Proc. Natl. Acad. Sci. USA* **2009**, *106*, 6814–6819; f) H. Janovjak, S. Szobota, C. Wyart, D. Trauner, E. Y. Isacoff, *Nat. Neurosci.* **2010**, *13*, 1027–1032; g) P. Stawski, H. Janovjak, D. Trauner, *Bioorg. Med. Chem.* **2010**, *18*, 7759–7772; h) N. Caporale, K. D. Kolstad, T. Lee, I. Tochitsky, D. Dalkara, D. Trauner, R. H. Kramer, Y. Dan, E. Y. Isacoff, J. G. Flannery, *Mol. Ther.* **2011**, *19*, 1212–1219.
- [10] D. L. Fortin, M. R. Banghart, T. D. Dunn, K. Borges, D. A. Wagner, Q. Gaudry, M. Karakossian, T. W. Otis, W. B. Kristan, D. Trauner, R. H. Kramer, *Nat. Methods* **2008**, *5*, 331–338.
- [11] A. Mourot, T. Fehrentz, D. Bautista, D. Trauner, R. H. Kramer, *Nat. Methods* **2012**, *9*, 396–402.
- [12] A. Polosukhina, J. Litt, I. Tochitsky, J. Nemargut, Y. Sychev, I. De Kouchkovsky, T. Huang, K. Borges, D. Trauner, R. N. Van Gelder, R. H. Kramer, *Neuron* **2012**, *75*, 271–282.
- [13] D. S. Stewart, P. Y. Savechenkov, Z. Dostalova, D. C. Chiara, R. Ge, D. E. Raines, J. B. Cohen, S. A. Forman, K. S. Bruzik, K. W. Miller, *J. Med. Chem.* **2011**, *54*, 8124–8135.
- [14] a) L. S. Geidysh, G. A. Nikiforov, V. V. Ershov, *Bio. Bull. Acad. Sci. USSR* **1969**, *18*, 2552–2555; b) J. A. Silk, L. A. Summers, *J. Chem. Soc.* **1963**, 3472–3474; c) J. C. Borah, S. Mujtaba, I. Karakikes, L. Zeng, M. Muller, J. Patel, N. Moshkina, K. Morohashi, W. Zhang, G. Gerona-Navarro, R. J. Hajjar, M.-M. Zhou, *Chem. Biol.* **2011**, *18*, 531–541.
- [15] **AP2**: C₁₈H₂₃N₃O, *M_r* = 297.395 g mol⁻¹, red block, 0.14 × 0.25 × 0.30 mm, monoclinic, *P*2₁, *a* = 10.5454(3), *b* = 9.5435(3), *c* = 17.0651(4) Å, α = 90, β = 90.0955(16), γ = 90°, *V* = 1704.28(8) Å³, *Z* = 4, ρ = 1.159 g cm⁻³, μ(MoKα) = 0.073 mm⁻¹, MoKα radiation (λ = 0.71073 Å), *T* = 200 K, 2θ_{max} 55.02°, 13750 refls., 4143 independent, 3271 with *I* ≥ 2σ(*I*), *R*_{int} = 0.042, mean σ(*I*)/*I* = 0.0392, 429 parameters, *R*(*F*_{obs}) = 0.0432, *R_w*(*F*²) = 0.1097, *S* = 1.014, min. and max. residual electron density: -0.21, 0.15 e Å⁻³; data collection by means of a Nonius KappaCCD diffractometer equipped with a rotating anode generator (ω-scans), structure solution by direct methods with SIR97, structure refinement with SHELXL-97, O- and N-bonded H atoms have been refined freely, C-bound H atoms have been added geometrically treated as riding on their parent atoms. CCDC 890176 contains the supplementary crystallographic data for this paper. These data can be obtained free of charge from The Cambridge Crystallographic Data Centre via www.ccdc.cam.ac.uk/data_request/cif.
- [16] E. Sigel, F. Minier, *Mol. Nutr. Food Res.* **2005**, *49*, 228–234.
- [17] R. W. Olsen, W. Sieghart, *Pharmacol. Rev.* **2008**, *60*, 243–260.
- [18] X. Chen, S. Shu, D. A. Bayliss, *J. Neurosci.* **2009**, *29*, 600–609.



Supporting Information

© Wiley-VCH 2012

69451 Weinheim, Germany

Azo-Propofols: Photochromic Potentiators of GABA_A Receptors**

Marco Stein, Simon J. Middendorp, Valentina Carta, Ervin Pejo, Douglas E. Raines, Stuart A. Forman, Erwin Sigel, and Dirk Trauner**

anie_201205475_sm_miscellaneous_information.pdf
anie_201205475_sm_video.m4v

INDEX

Section	Page
General Experimental Details and Instrumentation	27
Synthetic Procedures	28
X-ray Structure Discussion of AP2	46
NMR Spectra	48
UV/Vis Spectra	69
Expression and Functional Characterization in <i>Xenopus</i> Oocytes	78
Expression and Functional Characterization in HEK 293 Cells	79
Anesthetic Effects and Photo-reversibility in <i>Xenopus laevis</i> Tadpoles	80

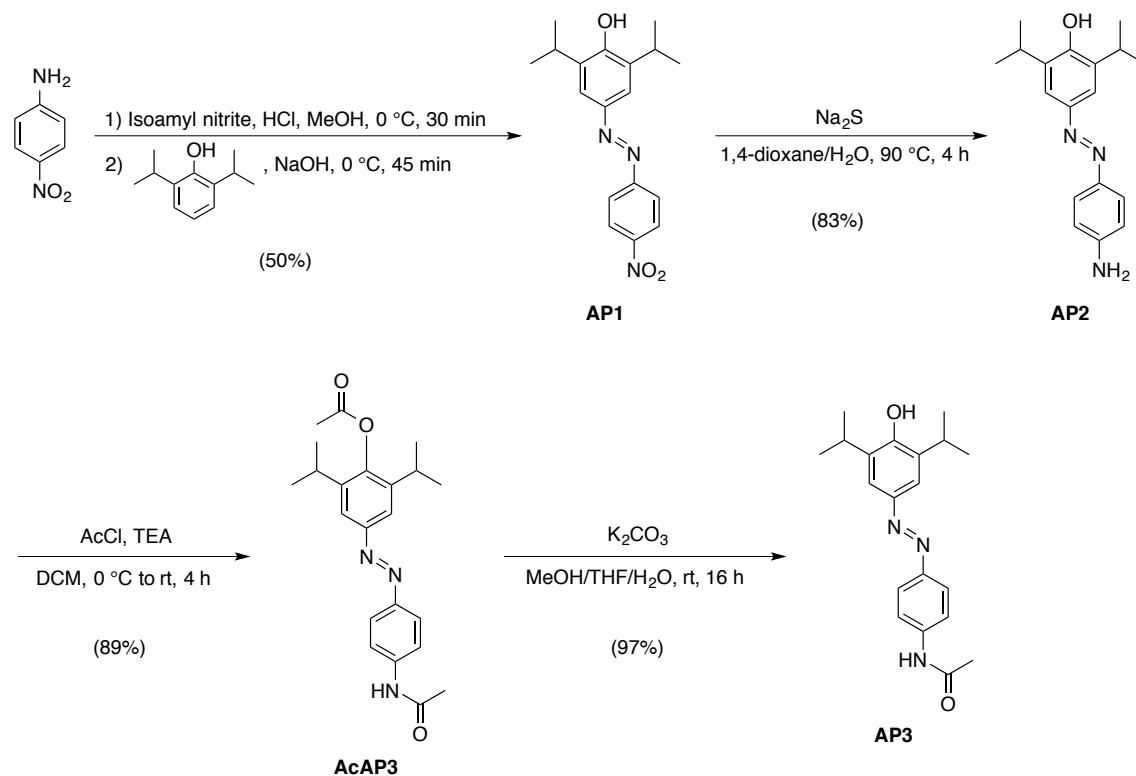
General Experimental Details and Instrumentation

All reactions were carried out with magnetic stirring and if air or moisture sensitive in oven-dried glassware under an atmosphere of nitrogen or argon. Syringes used to transfer reagents and solvents were purged with nitrogen or argon prior to use. Reagents were used as commercially supplied unless otherwise stated. Thin layer chromatography was performed on pre-coated silica gel F₂₅₄ glass backed plates and the chromatogram was visualized under UV light and/or by staining using aqueous acidic vanillin or potassium permanganate, followed by gentle heating with a heat gun. Flash column chromatography was performed using silica gel, particle size 40–63 μm (eluants are given in parenthesis). The diameter of the columns and the amount of silica gel were calculated according to the recommendations of W. C. Still *et al.*^[11] IR spectra were recorded on a Perkin Elmer Spectrum Bx FT-IR instrument as thin films with absorption bands being reported in wave number (cm^{-1}). UV/Vis spectra were obtained using a Varian Cary 50 Scan UV/Vis spectrometer and Helma SUPRASIL precision cuvettes (10 mm light path).

¹H and ¹³C NMR spectra were measured on Varian VNMRS 300, VNMRS 400, INOVA 400 or VNMRS 600 instruments. The chemical shifts are quoted as δ -values in ppm referenced to the residual solvent peak (CDCl_3 : δ_{H} 7.26, δ_{C} 77.2; CD_3OD : δ_{H} 3.31, δ_{C} 49.0).^[12] Multiplicities are abbreviated as follows: s = singlet, d = doublet, t = triplet, q = quartet, quint = quintet, sext = sextet, sept = septet, m = multiplet. High resolution mass spectra (EI, ESI) were recorded by LMU Mass Spectrometry Service using a Thermo Finnigan MAT 95, a Jeol MStation or a Thermo Finnigan LTQ FT Ultra instrument. Melting points were obtained using a Stanford Research Systems MPA120 apparatus and are uncorrected.

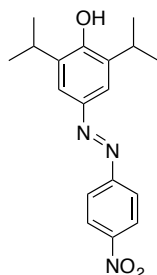
Synthetic Procedures

Synthesis of AP1–3



Scheme 2.1. Synthesis of AP1–3.

Synthesis of 2,6-diisopropyl-4-((4-nitrophenyl)diazenyl)phenol (AP1)

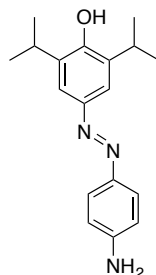


4-Nitroaniline (2.07 g, 15.0 mmol, 1.0 equiv.) was dissolved in MeOH (30 mL) and cooled to 0 °C. Conc. HCl (4 mL) was added and the mixture was stirred for 5 min. Isoamyl nitrite (2.02 mL, 15.0 mmol, 1.0 equiv.) was added slowly in portions and the mixture was stirred for 30 min at 0 °C. Propofol (2.79 mL, 15.0 mmol, 1.0 equiv.) was dissolved in a separate flask in 2 M NaOH (28 mL) and H₂O (2 mL) and cooled to 0 °C. The diazonium salt of 4-nitroaniline was transferred to this solution at 0 °C and the reaction mixture was stirred for 1 h at this temperature. The pH was adjusted to pH = 4–6 with 2 M NaOH and the mixture was extracted

with EtOAc (3 x 30 mL). The combined organic layers were washed with brine (50 mL), dried over MgSO₄ and concentrated *in vacuo*. The crude product was purified by flash silica gel chromatography (hexanes/DCM, gradient from 8:2 to 6:4) to give **AP1** (2.47 g, 7.54 mmol, 50%) as a red solid.

TLC (hexanes/EtOAc, 4:1): $R_f = 0.54$. **M.p.:** 95–98 °C. **¹H NMR (CDCl₃, 400 MHz, 27 °C):** $\delta = 8.39\text{--}8.27$ (m, 2H, ArH), 8.04–7.87 (m, 2H, ArH), 7.82–7.65 (m, 2H, ArH), 5.30 (s, 1H, OH), 3.20 (sept, $J = 6.8$ Hz, 2H, 2 x CH), 1.34 (d, $J = 6.8$ Hz, 12H, 4 x CH₃) ppm. **¹³C NMR (CDCl₃, 100 MHz, 27 °C):** $\delta = 156.2, 154.4, 148.0, 147.0, 134.6, 124.7, 123.0, 119.9, 27.3, 22.5$ ppm. **IR (neat, ATR):** $\tilde{\nu} = 3509$ (w), 2963 (m), 2872 (w), 1590 (m), 1539 (m), 1520 (m), 1461 (m), 1428 (m), 1404 (w), 1385 (w), 1339 (vs), 1288 (m), 1255 (s), 1196 (m), 1145 (m), 1104 (m), 1073 (m), 1007 (w), 940 (m), 906 (w), 861 (m), 848 (m), 817 (w), 754 (w), 733 (w), 716 (w), 691 (w) cm⁻¹. **HRMS (EI⁺):** m/z calcd. for [C₁₈H₂₁N₃O₃]⁺: 327.1583, found: 327.1576 ([M]⁺). **UV/Vis:** $\lambda_{\text{max}} = 388$ nm.

Synthesis of 4-((4-aminophenyl)diazenyl)-2,6-diisopropylphenol (AP2)



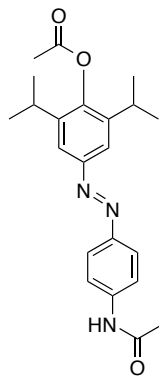
AP1 (1.40 g, 4.28 mmol, 1.0 equiv.) was dissolved in 1,4-dioxane (75 mL) and water (6.5 mL) and Na₂S (999 mg, 12.8 mmol, 3.0 equiv.) was added. The reaction mixture was heated to 90 °C for 3.75 h. A sat. aq. solution of NaHCO₃ (100 mL) was added and the aqueous phase was extracted with EtOAc (2 x 50 mL). The combined organic layers were washed with brine (75 mL), dried over MgSO₄ and the solvent was concentrated *in vacuo*. The crude product was purified by flash silica gel column chromatography (hexanes/EtOAc, gradient from 4:1 to 3:1) to give **AP2** (1.06 g, 3.56 mmol, 83%) as an orange solid.

TLC (hexanes/EtOAc, 3:1): $R_f = 0.32$. **M.p.:** 159–162 °C. **¹H NMR (CD₃OD, 400 MHz, 27 °C):** $\delta = 7.70\text{--}7.63$ (m, 2H, ArH), 7.55 (s, 2H, ArH), 6.79–6.72 (m, 2H, ArH), 3.37 (sept, $J = 6.9$ Hz, 2H, 2 x CH), 1.28 (d, $J = 6.9$ Hz, 12H, 4 x CH₃) ppm. **¹³C NMR (CD₃OD, 100 MHz, 27 °C):** $\delta = 156.9, 154.9, 150.5, 148.5, 139.6, 127.9, 121.3, 117.9, 30.6, 25.9$ ppm. **IR (neat, ATR):** $\tilde{\nu} = 3383$ (m), 2962 (m), 2870 (w), 1619 (m), 1600 (vs), 1507 (m), 1462 (m),

1440 (m), 1280 (m), 1246 (w), 1198 (m), 1160 (m), 1146 (s), 939 (w), 890 (w), 835 (m), 784 (w) cm⁻¹. **HRMS (ESI⁺):** *m/z* calcd. for [C₁₈H₂₄N₃O]⁺: 298.1919, found: 298.1916 ([M+H]⁺).

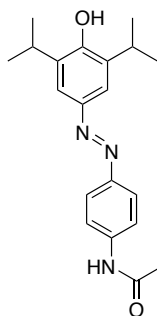
UV/Vis: λ_{max} = 404 nm.

Synthesis of 4-((4-acetamidophenyl)diazenyl)-2,6-diisopropylphenyl acetate (AcAP3)



AP2 (400 mg, 1.35 mmol, 1.0 equiv.) was dissolved in DCM (20 mL) and TEA (0.19 mL, 1.35 mmol, 1.0 equiv.) was added. Acetyl chloride (0.10 mL, 1.4 mmol, 1.0 equiv.) was added dropwise at 0 °C and the reaction mixture was stirred for 1 h at this temperature, before it was warmed to room temperature and stirred for further 3 h. As TLC analysis indicated remaining starting material, another 0.5 equiv. of acetyl chloride (0.050 mL, 0.68 mmol) were added and the mixture was stirred for 3 h. TLC analysis indicated still remaining starting material and another 0.3 equiv. of acetyl chloride (0.030 mL, 0.41 mmol) were added. The mixture was stirred for 12 h at room temperature. H₂O (10 mL) was added and the organic phase was separated and washed with brine (10 mL), dried over MgSO₄ and concentrated *in vacuo*. The crude product was purified by flash silica gel chromatography (DCM/MeOH, gradient from 100:0 to 30:1) to yield bisacetylated **AcAP3** (459 mg, 1.20 mmol, 89%) as an orange solid.

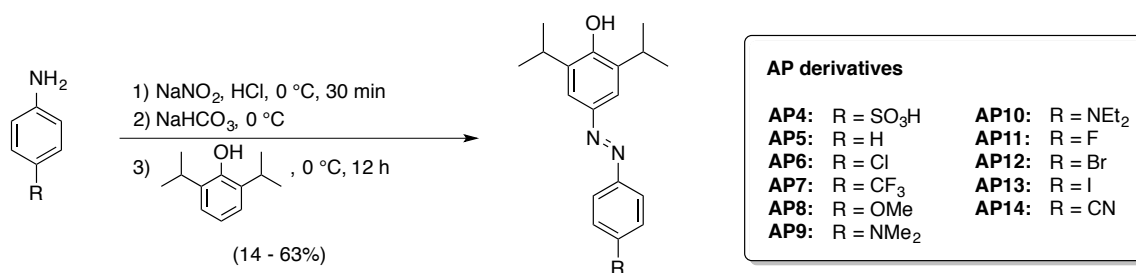
TLC (DCM/MeOH, 20:1): R_f = 0.47. **M.p.:** 247–249 °C. **¹H NMR (CDCl₃, 300 MHz, 27 °C):** δ = 7.86–7.80 (m, 2H, ArH), 7.71 (s, 2H, ArH), 7.60–7.52 (m, 2H, ArH), 2.98 (sept, *J* = 6.8 Hz, 2H, 2 x CH), 2.41 (s, 3H, CH₃), 2.19 (s, 3H, CH₃), 1.27 (d, *J* = 6.8 Hz, 12H, 4 x CH₃) ppm. **¹³C NMR (CDCl₃, 75 MHz, 27 °C):** δ = 169.8, 168.5, 151.1, 149.0, 147.5, 141.4, 140.4, 123.8, 119.5, 118.7, 28.0, 24.6, 23.2, 20.7 ppm. **IR (neat, ATR):** ν̄ = 2964 (m), 1758 (m), 1662 (m), 1597 (m), 1554 (m), 1504 (m), 1462 (w), 1408 (w), 1369 (m), 1323 (m), 1306 (w), 1268 (m), 1200 (vs), 1166 (s), 1149 (m), 1107 (w), 1033 (w), 1006 (w), 909 (m), 853 (m), 757 (m) cm⁻¹. **HRMS (ESI⁺):** *m/z* calcd. for [C₂₂H₂₈N₃O₃]⁺: 382.2131, found: 382.2127 ([M+H]⁺).

Synthesis of *N*-(4-((4-hydroxy-3,5-diisopropylphenyl)diazenyl)phenyl)acetamide (AP3)

AcAP3 (450 mg, 1.18 mmol, 1.0 equiv.) was dissolved in MeOH (15 mL) and THF (15 mL) and K₂CO₃ (945 mg, 6.84 mmol, 5.8 equiv.; dissolved in 5 mL H₂O) was added. The mixture was stirred at room temperature for 16 h. The pH was adjusted to pH = 4–6 with 2 M HCl and the mixture was extracted with EtOAc (2 x 30 mL). The combined organic layers were washed with brine (50 mL), dried over MgSO₄ and concentrated *in vacuo*. The crude product was purified by flash silica gel chromatography (CHCl₃/MeOH, gradient from 100:0 to 40:1), yielding **AP3** (392 mg, 1.15 mmol, 97%) as a deep red oil.

TLC (DCM/MeOH 20:1): R_f = 0.31. **¹H NMR (CDCl₃, 300 MHz, 27 °C):** δ = 8.10 (br s, 1H, NH), 7.92–7.85 (m, 2H, ArH), 7.74–7.63 (m, 4H, ArH), 5.72 (br s, 1H, OH), 3.22 (sept, *J* = 6.9 Hz, 2H, 2 x CH), 2.20 (s, 3H, CH₃), 1.31 (d, *J* = 6.9 Hz, 12H, 4 x CH₃) ppm. **¹³C NMR (CDCl₃, 75 MHz, 27 °C):** δ = 169.0, 153.3, 149.2, 146.8, 139.7, 134.7, 123.4, 120.0, 119.0, 27.3, 24.6, 22.7 ppm. **IR (neat, ATR):** $\tilde{\nu}$ = 3303 (m), 2963 (m), 2870 (w), 1672 (m), 1596 (s), 1538 (s), 1504 (m), 1462 (m), 1441 (m), 1405 (m), 1372 (m), 1315 (m), 1304 (m), 1266 (m), 1195 (m), 1161 (m), 1117 (m), 1014 (w), 965 (w), 939 (w), 902 (w), 847 (m), 795 (w), 756 (m), 700 (w), 668 (w) cm⁻¹. **HRMS (ESI⁺):** *m/z* calcd. for [C₂₀H₂₆N₃O₂]⁺: 340.2025, found: 340.2022 ([M+H]⁺). **UV/Vis:** λ_{max} = 378 nm.

Synthesis of AP4–14

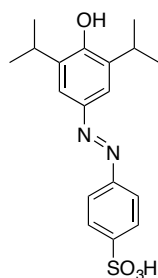


Scheme 2.2. Synthesis of AP4–14.

Typical Procedure (TP) 1: Reaction of propofol with a diazonium salt

The aniline (3.0 mmol, 1.0 equiv.) was dissolved in H₂O (2 mL) and conc. HCl (2 mL) and cooled to 0 °C. If the aniline did not dissolve completely in this mixture, MeOH was added until a clear solution was obtained. A precooled solution of NaNO₂ (228 mg, 3.30 mmol, 1.1 equiv.) in H₂O (2 mL) was added slowly and the mixture stirred for 30 min at 0 °C. The pH was adjusted to pH = 8–9 with a precooled sat. aqu. solution of NaHCO₃. To this mixture, propofol (0.56 mL, 3.0 mmol, 1.0 equiv.) was added dropwise and the mixture stirred at 0 °C for 12 h. The mixture was extracted with CHCl₃ (3 x 20 mL), washed with H₂O (50 mL) and brine (50 mL), dried over MgSO₄ and concentrated *in vacuo*.

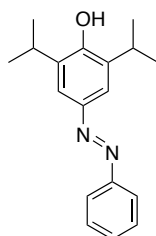
Synthesis of 4-((4-hydroxy-3,5-diisopropylphenyl)diazenyl)benzenesulfonic acid (AP4)



Sulfanilic acid (2.60 g, 15.0 mmol, 1.0 equiv.) was dissolved in 2 M NaOH (9.8 mL) and H₂O (10 mL) and cooled to 0 °C. NaNO₂ (1.04 g, 15.0 mmol, 1.0 equiv.) was added, followed by slow addition of conc. HCl (4.5 mL). The mixture was stirred for 30 min at 0 °C. Propofol (2.79 mL, 15.0 mmol, 1.0 equiv.) was dissolved in 2 M NaOH (28 mL) and H₂O (2 mL) and cooled to 0 °C. The diazonium salt of sulfanilic acid was transferred to this solution at 0 °C and the reaction mixture was stirred for 2 h at this temperature. The solvent was removed *in vacuo* and the crude product was purified by reversed phase flash silica gel chromatography (H₂O/MeOH, gradient from 100:0 to 80:20) to give **AP4** (2.61 g, 7.20 mmol, 48%) as a deep red oil.

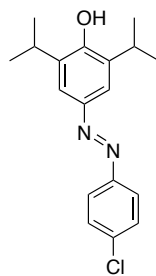
RP-TLC (H₂O/MeOH, 3:1): $R_f = 0.24$. **M.p.:** 145 °C (dec.). **¹H NMR (CD₃OD, 400 MHz, 27 °C):** $\delta = 7.93\text{--}7.89$ (m, 2H, ArH), 7.82–7.77 (m, 2H, ArH), 7.63 (s, 2H, ArH), 3.45 (sept, $J = 6.9$ Hz, 2H, 2 x CH), 3.34 (s, 1H, SO₃H), 1.25 (d, $J = 6.9$ Hz, 12H, 4 x CH₃) ppm. **¹³C NMR (CD₃OD, 100 MHz, 27 °C):** $\delta = 164.9, 154.3, 144.2, 143.2, 137.3, 126.5, 120.9, 119.5, 26.3, 22.2$ ppm. **IR (neat, ATR):** $\tilde{\nu} = 3428$ (m), 2960 (m), 2869 (w), 1653 (m), 1589 (m), 1530 (m), 1456 (m), 1435 (m), 1413 (w), 1384 (w), 1344 (m), 1290 (s), 1197 (s), 1115 (vs), 1034 (s), 1007 (m), 943 (w), 907 (w), 843 (w), 820 (w), 740 (w), 663 (m) cm⁻¹. **HRMS (ESI⁺):** m/z calcd. for [C₁₈H₂₃N₂O₄S]⁺: 363.1379, found: 363.1375 ([M+H]⁺). **UV/Vis:** $\lambda_{\text{max}} = 368, 527$ nm.

Synthesis of 2,6-diisopropyl-4-(phenyldiazenyl)phenol (AP5)



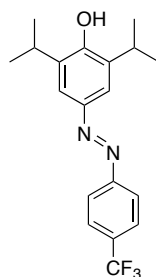
The reaction was carried out using **TPI**. The crude product was purified by flash silica gel chromatography (hexanes/EtOAc, gradient from 50:1 to 20:1) to give **AP5** (195 mg, 0.690 mmol, 23%) as a red oil.

TLC (hexanes/EtOAc, 10:1): $R_f = 0.29$. **¹H NMR (CDCl₃, 300 MHz, 27 °C):** $\delta = 7.92\text{--}7.86$ (m, 2H, ArH), 7.74 (s, 2H, ArH), 7.54–7.43 (m, 3H, ArH), 5.20 (br s, 1H, OH), 3.22 (sept, $J = 6.9$ Hz, 2H, 2 x CH), 1.35 (d, $J = 6.9$ Hz, 12H, 4 x CH₃) ppm. **¹³C NMR (CDCl₃, 75 MHz, 27 °C):** $\delta = 153.2, 152.9, 146.9, 134.4, 130.0, 129.0, 122.4, 119.1, 27.4, 22.6$ ppm. **IR (neat, ATR):** $\tilde{\nu} = 3568$ (w), 3361 (m), 3068 (w), 2962 (m), 2931 (m), 2870 (m), 1654 (w), 1591 (m), 1526 (w), 1463 (s), 1440 (s), 1384 (m), 1364 (m), 1343 (m), 1307 (m), 1278 (s), 1241 (m), 1196 (s), 1147 (s), 1116 (m), 1071 (m), 1020 (w), 962 (w), 938 (m), 904 (m), 864 (w), 840 (w), 816 (w), 796 (m), 763 (vs), 732 (s), 688 (vs) cm⁻¹. **HRMS (ESI⁺):** m/z calcd. for [C₁₈H₂₃N₂O]⁺: 283.1810, found: 283.1807 ([M+H]⁺). **UV/Vis:** $\lambda_{\text{max}} = 362, 450$ nm.

Synthesis of 4-((4-chlorophenyl)diazenyl)-2,6-diisopropylphenol (AP6)

The reaction was carried out using **TP1**. The crude product was purified by flash silica gel chromatography (hexanes/EtOAc, gradient from 20:1 to 10:1) to give **AP6** (437 mg, 1.38 mmol, 46%) as a red oil.

TLC (hexanes/EtOAc, 10:1): $R_f = 0.27$. **¹H NMR (CDCl₃, 300 MHz, 27 °C):** $\delta = 7.89\text{--}7.78$ (m, 2H, ArH), 7.72 (s, 2H, ArH), 7.51–7.41 (m, 2H, ArH), 5.20 (s, 1H, OH), 3.20 (sept, $J = 6.8$ Hz, 2H, 2 x CH), 1.34 (d, $J = 6.8$ Hz, 12H, 4 x CH₃) ppm. **¹³C NMR (CDCl₃, 75 MHz, 27 °C):** $\delta = 153.2, 151.3, 146.8, 135.8, 134.4, 129.2, 123.7, 119.2, 27.4, 22.6$ ppm. **IR (neat, ATR):** $\tilde{\nu} = 3585$ (w), 3421 (w), 2962 (s), 2871 (m), 1589 (m), 1577 (m), 1522 (w), 1483 (m), 1461 (vs), 1440 (s), 1399 (m), 1385 (m), 1364 (m), 1344 (m), 1277 (s), 1246 (m), 1199 (s), 1159 (s), 1117 (m), 1088 (vs), 1010 (m), 960 (w), 938 (m), 902 (m), 868 (w), 835 (s), 799 (w), 768 (w), 727 (m), 710 (w) cm⁻¹. **HRMS (ESI⁺):** m/z calcd. for [C₁₈H₂₂N₂OCl]⁺: 317.1421, found: 317.1416 ([M+H]⁺). **UV/Vis:** $\lambda_{\text{max}} = 369$ nm.

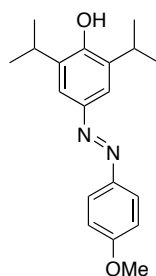
Synthesis of 2,6-diisopropyl-4-((4-(trifluoromethyl)phenyl)diazenyl)phenol (AP7)

The reaction was carried out using **TP1**. The crude product was purified by flash silica gel chromatography (hexanes/EtOAc, gradient from 30:1 to 20:1) to give **AP7** (221 mg, 0.630 mmol, 21%) as a red oil.

TLC (hexanes/EtOAc, 10:1): $R_f = 0.33$. **¹H NMR (CDCl₃, 400 MHz, 27 °C):** $\delta = 7.98\text{--}7.89$ (m, 2H, ArH), 7.77–7.69 (m, 4H, ArH), 5.23 (s, 1H, OH), 3.20 (sept, $J = 6.9$ Hz, 2H, 2 x CH),

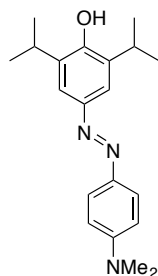
1.34 (d, $J = 6.9$ Hz, 12H, 4 x CH_3) ppm. ^{13}C NMR ($CDCl_3$, 100 MHz, 27 °C): $\delta = 154.7$, 154.0–153.7 (m), 146.7, 134.6, 131.2 (q, $J = 32.2$ Hz), 124.0 (q, $J = 270.6$ Hz), 126.1 (q, $J = 3.8$ Hz), 122.5, 119.6, 27.3, 22.6 ppm. ^{19}F NMR ($CDCl_3$, 376 MHz, 27 °C): $\delta = -62.4$ ppm. **IR (neat, ATR):** $\tilde{\nu} = 3608$ (w), 2964 (m), 2873 (w), 1611 (w), 1590 (m), 1527 (w), 1463 (m), 1441 (m), 1408 (m), 1386 (w), 1364 (w), 1321 (vs), 1280 (m), 1243 (m), 1197 (m), 1164 (m), 1150 (m), 1127 (s), 1102 (m), 1064 (s), 1014 (m), 960 (w), 938 (m), 904 (m), 848 (m), 818 (w), 802 (w), 769 (w), 720 (w), 700 (w) cm^{-1} . **HRMS (ESI⁺):** m/z calcd. for $[C_{19}H_{22}N_2OF_3]^+$: 351.1684, found: 351.1679 ($[M+H]^+$). **UV/Vis:** $\lambda_{max} = 373$ nm.

Synthesis of 2,6-diisopropyl-4-((4-methoxyphenyl)diazenyl)phenol (AP8)



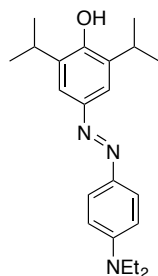
The reaction was carried out using **TP1**. The crude product was purified by flash silica gel chromatography (hexanes/ $CHCl_3$, gradient from 3:1 to 2:8) to give **AP8** (262 mg, 0.840 mmol, 28%) as a red oil.

TLC (hexanes/ $CHCl_3$, 1:1): $R_f = 0.16$. 1H NMR ($CDCl_3$, 300 MHz, 27 °C): $\delta = 7.99$ – 7.92 (m, 2H, ArH), 7.76 (s, 2H, ArH), 7.07– 7.00 (m, 2H, ArH), 5.44 (br s, 1H, OH), 3.88 (s, 3H, CH_3), 3.23 (sept, $J = 6.9$ Hz, 2H, 2 x CH), 1.35 (d, $J = 6.9$ Hz, 12H, 4 x CH_3) ppm. ^{13}C NMR ($CDCl_3$, 75 MHz, 27 °C): $\delta = 161.4$, 152.7, 147.2, 147.0, 134.5, 124.3, 118.7, 114.2, 55.5, 27.4, 22.7 ppm. **IR (neat, ATR):** $\tilde{\nu} = 2961$ (m), 2870 (w), 1600 (m), 1582 (m), 1502 (m), 1460 (m), 1440 (m), 1385 (w), 1363 (w), 1342 (w), 1314 (m), 1279 (m), 1247 (vs), 1195 (m), 1181 (m), 1158 (m), 1143 (s), 1116 (m), 1105 (m), 1075 (w), 1029 (m), 986 (w), 960 (w), 937 (w), 905 (m), 836 (s), 806 (w), 817 (w), 770 (m), 730 (s), 668 (w) cm^{-1} . **HRMS (ESI⁺):** m/z calcd. for $[C_{19}H_{25}N_2O_2]^+$: 313.1916, found: 313.1914 ($[M+H]^+$). **UV/Vis:** $\lambda_{max} = 368$ nm.

Synthesis of 4-((4-(dimethylamino)phenyl)diazenyl)-2,6-diisopropylphenol (AP9)

The reaction was carried out using **TP1**. The reaction mixture was concentrated under reduced pressure and the crude product was purified by flash silica gel chromatography (hexanes/EtOAc, gradient from 20:1 to 10:1) to give **AP9** (615 mg, 1.89 mmol, 63%) as a brownish solid.

TLC (hexanes/EtOAc, 4:1): R_f = 0.52. **M.p.:** 157–160 °C. **¹H NMR (CDCl₃, 300 MHz, 27 °C):** δ = 7.89–7.82 (m, 2H, ArH), 7.65 (s, 2H, ArH), 6.80–6.73 (m, 2H, ArH), 5.06 (s, 1H, OH), 3.19 (sept, J = 6.9 Hz, 2H, 2 x CH), 3.07 (s, 6H, 2 x CH₃), 1.34 (d, J = 6.9 Hz, 12H, 4 x CH₃) ppm. **¹³C NMR (CDCl₃, 75 MHz, 27 °C):** δ = 151.8, 151.7, 147.3, 143.8, 134.1, 124.4, 118.2, 111.6, 40.4, 27.4, 22.7 ppm. **IR (neat, ATR):** $\tilde{\nu}$ = 3337 (m), 2959 (m), 2924 (m), 2864 (m), 2801 (w), 2723 (w), 2648 (w), 1894 (w), 1598 (s), 1564 (m), 1516 (m), 1459 (m), 1440 (s), 1399 (m), 1360 (s), 1343 (m), 1278 (s), 1245 (m), 1224 (m), 1199 (m), 1160 (vs), 1144 (s), 1121 (m), 1107 (m), 1077 (m), 1063 (m), 999 (w), 986 (w), 942 (m), 905 (m), 896 (w), 885 (w), 870 (w), 819 (vs), 801 (m), 753 (s), 726 (w), 668 (w) cm⁻¹. **HRMS (ESI⁺):** m/z calcd. for [C₂₀H₂₈N₃O]⁺: 326.2232, found: 326.2229 ([M+H]⁺). **UV/Vis:** λ_{max} = 417 nm.

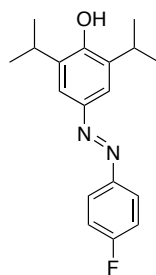
Synthesis of 4-((4-(diethylamino)phenyl)diazenyl)-2,6-diisopropylphenol (AP10)

The reaction was carried out using **TP1**. The reaction mixture was concentrated under reduced pressure and the crude product was purified by reversed-phase flash silica gel chromatography

(H₂O/MeOH, gradient from 5:5 to 2:8) to give **AP10** (477 mg, 1.35 mmol, 45%) as a brownish solid.

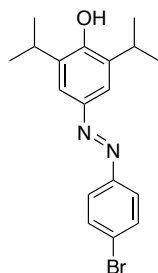
TLC (hexanes/EtOAc, 4:1): R_f = 0.49. **M.p.:** 164–165 °C. **¹H NMR (CDCl₃, 300 MHz, 27 °C):** δ = 7.85–7.78 (m, 2H, ArH), 7.63 (s, 2H, ArH), 6.75–6.68 (m, 2H, ArH), 5.01 (s, 1H, OH), 3.44 (q, J = 7.0 Hz, 4H, 2 x CH₂), 3.19 (sept, J = 6.8 Hz, 2H, 2 x CH), 1.34 (d, J = 6.8 Hz, 12H, 4 x CH₃), 1.22 (t, J = 7.0 Hz, 6H, 2 x CH₃) ppm. **¹³C NMR (CDCl₃, 75 MHz, 27 °C):** δ = 151.5, 149.5, 147.4, 143.3, 134.0, 124.7, 118.1, 111.0, 44.6, 27.4, 22.7, 12.7 ppm. **IR (neat, ATR):** $\tilde{\nu}$ = 3288 (w), 2960 (m), 2930 (w), 1593 (s), 1566 (m), 1516 (m), 1459 (m), 1441 (m), 1397 (m), 1377 (m), 1357 (m), 1269 (m), 1245 (m), 1196 (m), 1163 (m), 1141 (vs), 1094 (m), 1076 (m), 1013 (m), 986 (w), 938 (w), 904 (w), 893 (w), 884 (w), 819 (m), 788 (m), 770 (w), 728 (w), 668 (w) cm⁻¹. **HRMS (ESI⁺):** m/z calcd. for [C₂₂H₃₂N₃O]⁺: 354.2545, found: 354.2542 ([M+H]⁺). **UV/Vis:** λ_{\max} = 425 nm.

Synthesis of 4-((4-fluorophenyl)diazenyl)-2,6-diisopropylphenol (**AP11**)



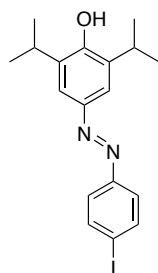
The reaction was carried out using **TP1**. The crude product was purified by flash silica gel chromatography (hexanes/EtOAc, gradient from 50:1 to 25:1) to give **AP11** (249 mg, 0.830 mmol, 28%) as a red oil.

TLC (hexanes/EtOAc, 10:1): R_f = 0.26. **¹H NMR (CDCl₃, 300 MHz, 27 °C):** δ = 7.95–7.87 (m, 2H, ArH), 7.72 (s, 2H, ArH), 7.23–7.14 (m, 2H, ArH), 5.23 (br s, 1H, OH), 3.21 (sept, J = 6.8 Hz, 2H, 2 x CH), 1.35 (d, J = 6.8 Hz, 12H, 4 x CH₃) ppm. **¹³C NMR (CDCl₃, 75 MHz, 27 °C):** δ = 163.9 (q, J = 248 Hz), 153.1, 149.4, 146.8, 134.4, 124.4 (q, J = 8.7 Hz), 119.0, 115.9 (q, J = 22.7 Hz), 27.4, 22.6 ppm. **¹⁹F NMR (CDCl₃, 282 MHz, 27 °C):** δ = -110.9 ppm. **IR (neat, ATR):** $\tilde{\nu}$ = 2962 (m), 2863 (w), 1773 (w), 1670 (w), 1589 (m), 1498 (s), 1460 (s), 1437 (m), 1384 (m), 1362 (m), 1340 (w), 1277 (m), 1223 (s), 1196 (m), 1153 (s), 1133 (s), 1115 (m), 1086 (m), 1007 (w), 937 (m), 904 (m), 839 (vs), 815 (m), 779 (m), 732 (m) cm⁻¹. **HRMS (EI⁺):** m/z calcd. for [C₁₈H₂₁FN₂O]⁺: 300.1638, found: 300.1636 ([M]⁺). **UV/Vis:** λ_{\max} = 363, 450 nm.

Synthesis of 4-((4-bromophenyl)diazenyl)-2,6-diisopropylphenol (AP12)

The reaction was carried out using **TP1**. The crude product was purified by flash silica gel chromatography (hexanes/EtOAc, gradient from 70:1 to 40:1) to give **AP12** (358 mg, 0.990 mmol, 33%) as a deep red oil.

TLC (hexanes/EtOAc, 10:1): $R_f = 0.39$. **¹H NMR (CDCl₃, 300 MHz, 27 °C):** $\delta = 7.79\text{--}7.74$ (m, 2H, ArH), 7.72 (s, 2H, ArH), 7.64–7.60 (m, 2H, ArH), 5.19 (br s, 1H, OH), 3.20 (sept, $J = 6.9$ Hz, 2H, 2 x CH), 1.35 (d, $J = 6.9$ Hz, 12H, 4 x CH₃) ppm. **¹³C NMR (CDCl₃, 75 MHz, 27 °C):** $\delta = 153.3, 151.7, 146.8, 134.4, 132.2, 124.2, 124.0, 119.2, 27.4, 22.6$ ppm. **IR (neat, ATR):** $\tilde{\nu} = 3578$ (w), 3413 (w), 2960 (s), 2928 (m), 2868 (m), 1586 (m), 1573 (m), 1521 (w), 1459 (vs), 1440 (s), 1394 (m), 1384 (m), 1363 (m), 1344 (m), 1276 (m), 1242 (m), 1198 (s), 1159 (s), 1149 (s), 1116 (m), 1066 (m), 1006 (m), 960 (w), 937 (m), 902 (m), 866 (w), 831 (m), 797 (w), 760 (w), 716 (w), 706 (w), 668 (w) cm⁻¹. **HRMS (ESI⁺):** m/z calcd. for [C₁₈H₂₂N₂OBr]⁺: 361.0915, found: 361.0912 ([M+H]⁺). **UV/Vis:** $\lambda_{\text{max}} = 371, 458$ nm.

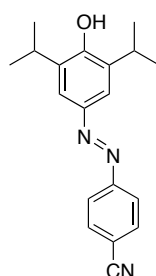
Synthesis of 4-((4-iodophenyl)diazenyl)-2,6-diisopropylphenol (AP13)

The reaction was carried out using **TP1**. The crude product was purified by flash silica gel chromatography (hexanes/EtOAc, gradient from 30:1 to 15:1) to give **AP13** (387 mg, 0.950 mmol, 32%) as a red oil.

TLC (hexanes/EtOAc, 10:1): $R_f = 0.39$. **¹H NMR (CDCl₃, 300 MHz, 27 °C):** $\delta = 7.86\text{--}7.81$ (m, 2H, ArH), 7.72 (s, 2H, ArH), 7.65–7.60 (m, 2H, ArH), 5.21 (br s, 1H, OH), 3.20 (sept,

$J = 6.9$ Hz, 2H, 2 x CH), 1.34 (d, $J = 6.9$ Hz, 12H, 4 x CH_3) ppm. ^{13}C NMR ($CDCl_3$, 75 MHz, 27 °C): $\delta = 153.5, 152.2, 146.8, 138.2, 134.4, 124.1, 119.3, 96.3, 27.4, 22.6$ ppm. IR (neat, ATR): $\tilde{\nu} = 2959$ (m), 2858 (w), 1779 (w), 1670 (w), 1585 (m), 1564 (m), 1515 (m), 1458 (vs), 1437 (s), 1389 (m), 1362 (m), 1343 (m), 1274 (m), 1239 (m), 1195 (s), 1147 (vs), 1115 (s), 1072 (m), 1052 (m), 1002 (s), 937 (m), 902 (s), 827 (vs), 796 (m), 767 (m), 732 (s), 710 (m) cm^{-1} . HRMS (ESI⁺): m/z calcd. for $[C_{18}H_{22}N_2OI]^+$: 409.0777, found: 409.0774 ($[M+H]^+$). UV/Vis: $\lambda_{max} = 374, 460$ nm.

Synthesis of 4-((4-hydroxy-3,5-diisopropylphenyl)diazenyl)benzonitrile (AP14)

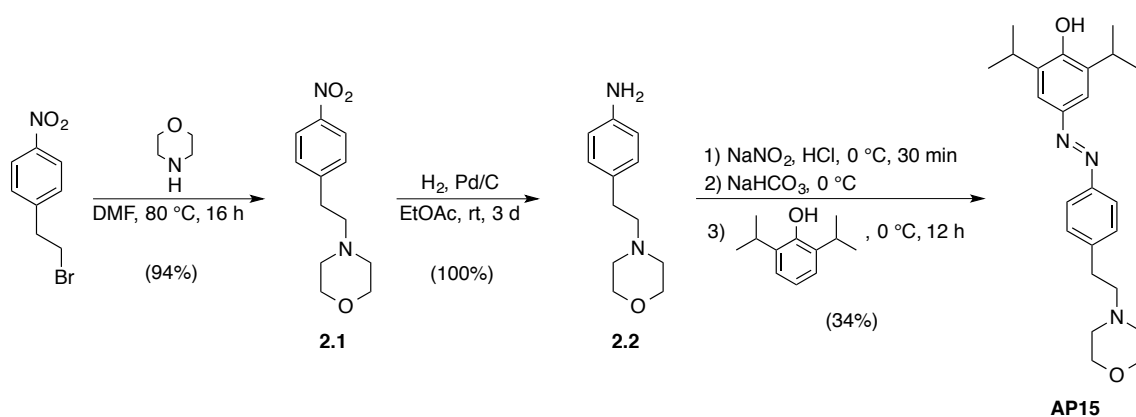


The reaction was carried out using **TP1**. The crude product was purified by flash silica gel chromatography (hexanes/EtOAc, gradient from 20:1 to 5:1) to give **AP14** (132 mg, 0.430 mmol, 14%) as an orange solid.

TLC (hexanes/EtOAc, 10:1): $R_f = 0.21$. **M.p.:** 177–178 °C. 1H NMR ($CDCl_3$, 300 MHz, 27 °C): $\delta = 8.04\text{--}7.86$ (m, 2H, ArH), 7.85–7.67 (m, 4H, ArH), 5.31 (br s, 1H, OH), 3.21 (sept, $J = 6.8$ Hz, 2H, 2 x CH), 1.34 (d, $J = 6.8$ Hz, 12H, 4 x CH_3) ppm. ^{13}C NMR ($CDCl_3$, 75 MHz, 27 °C): $\delta = 154.8, 146.7, 145.8, 134.9, 133.2, 129.8, 129.0, 128.4, 123.5, 122.8, 119.9, 118.7, 116.3, 112.7$ ppm.^[4] IR (neat, ATR): $\tilde{\nu} = 3450$ (m), 2960 (m), 2869 (w), 2229 (m), 1599 (m), 1587 (m), 1527 (m), 1459 (s), 1440 (m), 1424 (m), 1401 (m), 1383 (w), 1372 (w), 1347 (w), 1307 (m), 1289 (m), 1257 (m), 1239 (m), 1191 (m), 1161 (m), 1142 (vs), 1116 (s), 1099 (m), 1073 (m), 1011 (w), 937 (m), 907 (m), 840 (m), 804 (w), 771 (w), 732 (m) cm^{-1} . HRMS (ESI⁺): m/z calcd. for $[C_{19}H_{22}N_3O]^+$: 307.1763, found: 308.1759 ($[M+H]^+$). UV/Vis: $\lambda_{max} = 384$ nm.

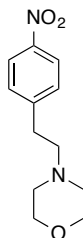
^[4] Additional signals and extensive broadening in the ^{13}C NMR was observed, assumingly due to *cis/trans*-isomerization of **AP14**.

Synthesis of AP15



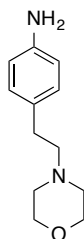
Scheme 2.3. Synthesis of AP15.

Synthesis of 4-(4-nitrophenyl)morpholine (2.1)



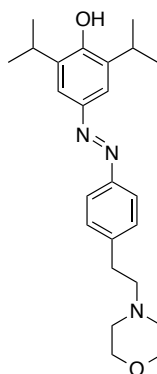
1-(2-Bromoethyl)-4-nitrobenzene (5.18 g, 22.5 mmol, 1.0 equiv.) was dissolved in DMF (40 mL) and morpholine (3.92 mL, 45.0 mmol, 2.0 equiv.) was added. The reaction mixture was heated to 80 °C for 16 h. Water (250 mL) was added and the aqueous phase was extracted with EtOAc (3 x 50 mL). The combined organic phases were washed with water (250 mL) and brine (3 x 250 mL), dried over MgSO₄ and concentrated *in vacuo* to yield tertiary amine **2.1** (5.02 g, 21.2 mmol, 94%) as an orange oil.

TLC (hexanes/EtOAc, 2:1): R_f = 0.34. **¹H NMR (CDCl₃, 300 MHz, 27 °C):** δ = 8.19–8.09 (m, 2H, ArH), 7.40–7.32 (m, 2H, ArH), 3.76–3.68 (m, 4H, 2 x CH₂), 2.94–2.85 (m, 2H, CH₂), 2.66–2.59 (m, 2H, CH₂), 2.56–2.46 (m, 4H, 2 x CH₂) ppm. **¹³C NMR (CDCl₃, 75 MHz, 27 °C):** δ = 148.1, 146.5, 129.5, 123.6, 66.8, 59.7, 53.6, 33.1 ppm. **IR (neat, ATR):** $\tilde{\nu}$ = 2954 (w), 2854 (w), 2808 (w), 1600 (m), 1515 (s), 1457 (w), 1398 (w), 1343 (vs), 1290 (w), 1274 (w), 1257 (w), 1208 (w), 1180 (w), 1135 (m), 1116 (s), 1070 (w), 1036 (w), 1008 (m), 916 (w), 875 (m), 858 (m), 824 (w), 772 (w), 748 (w), 699 (w) cm⁻¹. **HRMS (EI⁺):** m/z calcd. for [C₁₂H₁₆N₂O₃]⁺: 236.1161, found: 236.1103 ([M]⁺).

Synthesis of 4-(2-morpholinoethyl)aniline (2.2)

Nitroarene **2.1** (4.90 g, 20.7 mmol) was dissolved in EtOAc (55 mL) and palladium on charcoal (10%; 500 mg) was added under an argon atmosphere. The flask was purged with H₂ and evacuated (5x). The reaction mixture was then stirred for 3 d under an H₂ atmosphere (1 bar). The mixture was filtered through Celite and the solvent was removed *in vacuo*, furnishing aniline **2.2** (4.26 g, 20.7 mmol, 100%) as an orange solid.

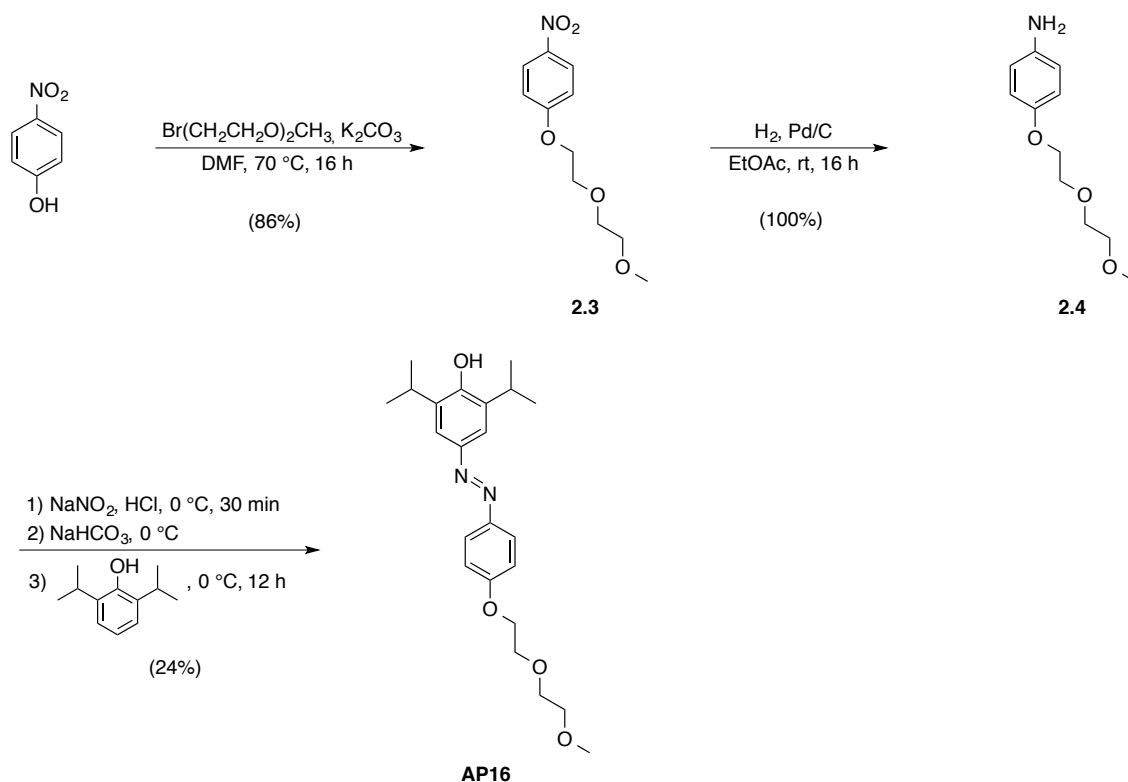
TLC (DCM/MeOH, 10:1): R_f = 0.54. **M.p.:** 81–82 °C. **¹H NMR (CDCl₃, 300 MHz, 27 °C):** δ = 7.04–6.94 (m, 2H, ArH), 6.67–6.56 (m, 2H, ArH), 3.78–3.70 (m, 4H, 2 x CH₂), 3.56 (br s, 2H, NH₂), 2.75–2.65 (m, 2H, CH₂), 2.59–2.46 (m, 6H, 3 x CH₂) ppm. **¹³C NMR (CDCl₃, 75 MHz, 27 °C):** δ = 144.5, 130.0, 129.4, 115.2, 67.0, 61.2, 53.7, 32.4 ppm. **IR (neat, ATR):** $\tilde{\nu}$ = 3376 (m), 3338 (m), 3241 (m), 3002 (w), 2955 (w), 2925 (m), 2896 (m), 2860 (m), 2812 (m), 2765 (w), 1646 (m), 1611 (m), 1516 (s), 1447 (w), 1357 (w), 1336 (w), 1276 (m), 1256 (m), 1210 (w), 1180 (w), 1157 (w), 1136 (m), 1111 (vs), 1070 (m), 1034 (w), 1006 (m), 916 (m), 866 (s), 825 (m), 789 (w), 773 (w), 739 (w) cm⁻¹. **HRMS (EI⁺):** m/z calcd. for [C₁₂H₁₈N₂O]⁺: 206.1419, found: 206.1414 ([M]⁺).

Synthesis of 2,6-diisopropyl-4-((4-(2-morpholinoethyl)phenyl)diazenyl)phenol (AP15)

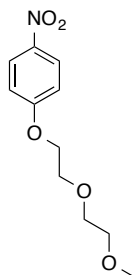
The reaction was carried out using **TP1**. The crude product was purified by flash silica gel chromatography (CHCl₃/MeOH, 100:0 → 100:1) to give **AP15** (409 mg, 1.03 mmol, 34%) as a red solid.

TLC (hexanes/EtOAc, 2:1): R_f = 0.46. **M.p.:** 178–179 °C. **¹H NMR (CDCl₃, 300 MHz, 27 °C):** δ = 7.83–7.78 (m, 2H, ArH), 7.70 (s, 2H, ArH), 7.35–7.30 (m, 2H, ArH), 5.27 (br s, 1H, OH), 3.82–3.73 (m, 4H, 2 x CH₂), 3.21 (sept, J = 6.9 Hz, 2H, 2 x CH), 2.96–2.85 (m, 2H, CH₂), 3.72–2.64 (m, 2H, CH₂), 2.64–2.53 (m, 4H, 2 x CH₂), 1.34 (d, J = 6.9 Hz, 12H, 4 x CH₃) ppm. **¹³C NMR (CDCl₃, 75 MHz, 27 °C):** δ = 152.9, 151.5, 147.0, 134.3, 129.3, 122.6, 118.9, 66.8, 60.4, 53.6, 33.0, 27.4, 22.6 ppm. **IR (neat, ATR):** $\tilde{\nu}$ = 3358 (m), 2961 (m), 2868 (m), 2813 (m), 1654 (w), 1590 (m), 1502 (w), 1461 (s), 1441 (m), 1412 (w), 1385 (w), 1361 (w), 1341 (w), 1305 (w), 1280 (m), 1243 (m), 1199 (m), 1161 (s), 1116 (vs), 1070 (w), 1036 (w), 1005 (w), 939 (w), 906 (m), 871 (m), 847 (w), 824 (w), 802 (w), 771 (w), 733 (m), 682 (w) cm⁻¹. **HRMS (ESI⁺):** m/z calcd. for [C₂₄H₃₄N₃O₂]⁺: 396.2651, found: 396.2643 ([M+H]⁺). **UV/Vis:** λ_{max} = 365, 460 nm.

Synthesis of AP16



Scheme 2.4. Synthesis of AP16.

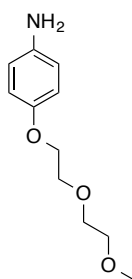
Synthesis of 1-(2-(2-methoxyethoxy)ethoxy)-4-nitrobenzene (**2.3**)

4-Nitrophenol (4.87 g, 35.0 mmol, 1.0 equiv.) was dissolved in DMF (65 mL) and K₂CO₃ (2.28 g, 16.5 mmol, 0.47 equiv.) and 2-(2-methoxyethoxy)ethyl bromide (4.48 mL, 33.3 mmol, 0.95 equiv.) were added. The reaction mixture was heated to 70 °C for 16 h. Water (250 mL) was added and the aqueous phase was extracted with EtOAc (3 x 50 mL). The combined organic phases were washed with water (250 mL), 1 M NaOH (3 x 200 mL), and brine (2 x 250 mL), dried over MgSO₄ and concentrated *in vacuo* to yield PEG ether **2.3** (6.91 g, 28.6 mmol, 86%) as a colorless solid.

TLC (hexanes/EtOAc, 2:1): R_f = 0.48. **M.p.:** 79–80 °C. **¹H NMR (CDCl₃, 300 MHz, 27 °C):** δ = 8.23–8.13 (m, 2H, ArH), 7.02–6.92 (m, 2H, ArH), 4.25–4.20 (m, 2H, CH₂), 3.91–3.86 (m,

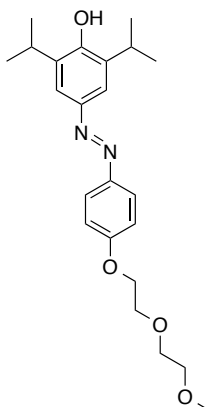
2H, CH₂), 3.73–3.69 (m, 2H, CH₂), 3.59–3.54 (m, 2H, CH₂), 3.38 (s, 3H, CH₃) ppm. ¹³C NMR (CDCl₃, 75 MHz, 27 °C): δ = 163.8, 141.6, 125.8, 114.6, 71.9, 70.9, 69.4, 68.2, 59.1 ppm. IR (neat, ATR): $\tilde{\nu}$ = 3007 (w), 2914 (w), 2897 (m), 2837 (w), 1608 (m), 1592 (m), 1508 (m), 1498 (m), 1479 (m), 1460 (m), 1382 (w), 1360 (w), 1340 (s), 1302 (m), 1292 (m), 1259 (vs), 1191 (m), 1180 (m), 1140 (m), 1124 (m), 1103 (s), 1072 (m), 1052 (m), 1029 (m), 956 (w), 946 (m), 924 (m), 853 (s), 846 (m), 812 (w), 752 (m), 692 (w), 662 (m) cm⁻¹. HRMS (EI⁺): *m/z* calcd. for [C₁₁H₁₅NO₅]⁺: 241.0950, found: 241.0944 ([M]⁺).

Synthesis of 4-(2-(2-methoxyethoxy)ethoxy)aniline (2.4)



Nitroarene **2.3** (6.80 g, 28.2 mmol) was dissolved in EtOAc (75 mL) and palladium on charcoal (10%; 700 mg) was added under an argon atmosphere. The flask was purged with H₂ and evacuated (5x). The reaction mixture was then stirred for 16 h under an H₂ atmosphere (1 bar). The mixture was filtered through Celite and the solvent was removed *in vacuo*, furnishing aniline **2.4** (5.96 g, 28.2 mmol, 100%) as an orange oil.

TLC (hexanes/EtOAc, 2:1): R_f = 0.19. ¹H NMR (CDCl₃, 300 MHz, 27 °C): δ = 6.77–6.68 (m, 2H, ArH), 6.63–6.55 (m, 2H, ArH), 4.03 (dd, *J* = 5.8, 4.1 Hz, 2H, CH₂), 3.78 (dd, *J* = 5.8, 4.1 Hz, 2H, CH₂), 3.72–3.65 (m, 2H, CH₂), 3.58–3.51 (m, 2H, CH₂), 3.46 (s, 2H, NH₂), 3.36 (s, 3H, CH₃) ppm. ¹³C NMR (CDCl₃, 75 MHz, 27 °C): δ = 151.8, 140.2, 116.3, 115.8, 71.9, 70.6, 69.9, 68.1, 59.0 ppm. IR (neat, ATR): $\tilde{\nu}$ = 3428 (w), 3353 (w), 3231 (w), 2919 (w), 2876 (m), 1628 (m), 1509 (vs), 1456 (m), 1375 (w), 1355 (w), 1330 (w), 1274 (w), 1233 (s), 1174 (w), 1102 (s), 1062 (m), 1027 (m), 985 (w), 924 (m), 823 (s), 744 (m), 696 (w) cm⁻¹. HRMS (EI⁺): *m/z* calcd. for [C₁₁H₁₇NO₃]⁺: 211.1208, found: 211.1212 ([M]⁺).

Synthesis of 2,6-diisopropyl-4-((4-(2-(2-methoxyethoxy)ethoxy)phenyl)diazenyl)phenol (AP16)

The reaction was carried out using **TP1**. The crude product was purified by flash silica gel chromatography (hexanes/EtOAc, gradient from 6:1 to 2:1) to give **AP16** (288 mg, 0.720 mmol, 24%) as a red oil.

TLC (hexanes/EtOAc, 2:1): $R_f = 0.46$. **¹H NMR (CDCl₃, 300 MHz, 27 °C):** $\delta = 7.89\text{--}7.82$ (m, 2H, ArH), 7.67 (s, 2H, ArH), 7.04–6.98 (m, 2H, ArH), 5.13 (s, 1H, OH), 4.25–4.17 (m, 2H, CH₂), 3.93–3.87 (m, 2H, CH₂), 3.76–3.70 (m, 2H, CH₂), 3.61–3.57 (m, 2H, CH₂), 3.40 (s, 3H, CH₃), 3.20 (sept, $J = 6.8$ Hz, 2H, 2 x CH), 1.33 (d, $J = 6.8$ Hz, 12H, 4 x CH₃) ppm. **¹³C NMR (CDCl₃, 75 MHz, 27 °C):** $\delta = 160.5, 152.4, 147.3, 147.0, 134.2, 124.1, 118.6, 114.8, 72.0, 70.8, 69.7, 67.7, 59.1, 27.4, 22.6$ ppm. **IR (neat, ATR):** $\tilde{\nu} = 3410$ (m), 2961 (m), 2928 (m), 2872 (m), 1598 (m), 1582 (m), 1501 (m), 1459 (m), 1442 (m), 1384 (w), 1361 (w), 1312 (m), 1281 (m), 1247 (vs), 1199 (m), 1142 (s), 1107 (s), 1062 (m), 938 (w), 902 (w), 838 (m), 780 (w) cm⁻¹. **HRMS (ESI⁺):** m/z calcd. for [C₂₃H₃₃N₂O₄]⁺: 401.2440, found: 401.2435 ([M+H]⁺). **UV/Vis:** $\lambda_{\text{max}} = 370, 470$ nm.

X-ray Structure Discussion of AP2

AP2 crystallizes in the monoclinic $P2_1$ space group with four molecules per unit cell. Azobenzenes usually favor a planar molecular structure due to its gain in aromatization energy.^[13] AP2, however, is twisted around the azo bond with dihedral angles of $-29.0(3)^\circ$ (C5–C4–N1–N2) and $-8.7(3)^\circ$ (N1–N2–C13–C14), respectively (Fig. 2.2).

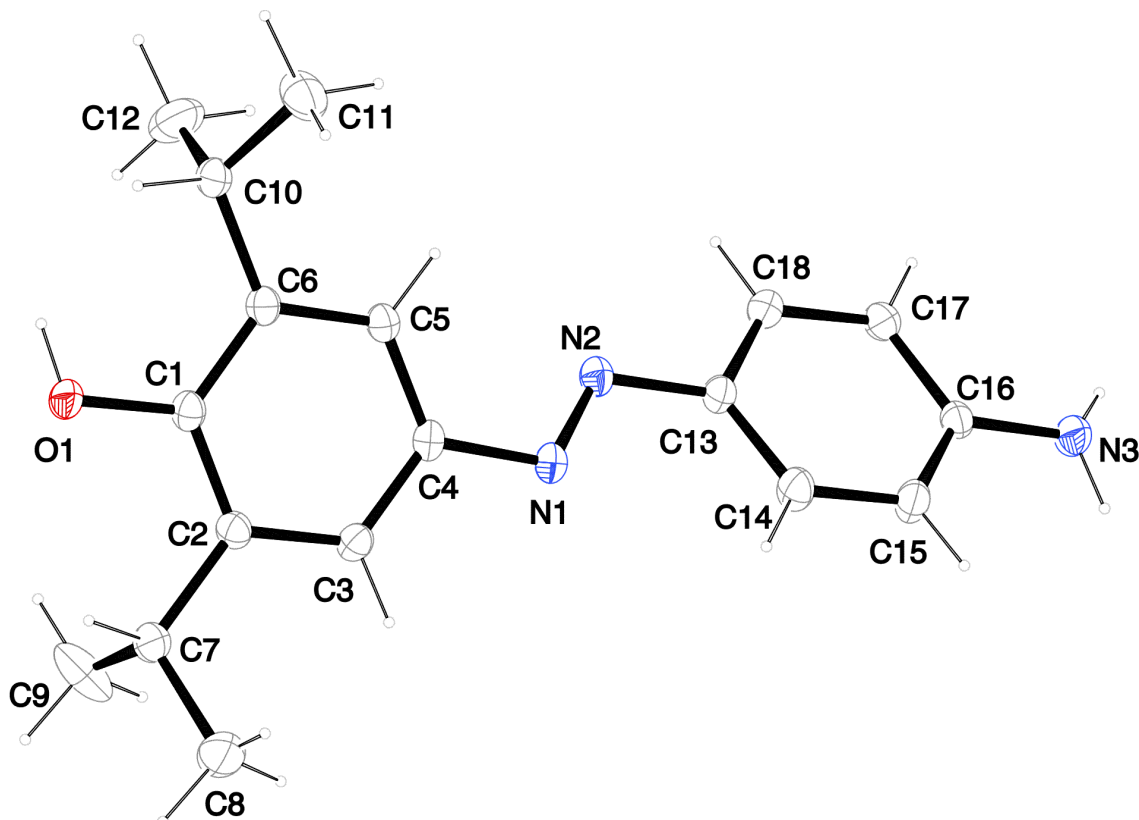


Figure 2.2. X-ray structure of AP2.

The loss of aromaticity is probably overcompensated by the gain of up to six hydrogen bonds per molecule. The molecules are oriented head-to-tail in a lattice fashion, with two neighboring chains aligning antiparallel. The molecules of one chain are connected by hydrogen bonds between the hydroxy and amino groups (N3–H31–O1: D–H 0.86(3) Å, H–A 2.21(3) Å, D–A 3.022(3) Å, D–H–A 158(2) $^\circ$). The orthogonal chains are connected *via* two hydrogen bonds between the amino and hydroxy function to each an azo bond nitrogen of two different chains ((N3–H32–N5: D–H 0.87(3) Å, H–A 2.33(3) Å, D–A 3.194(3) Å, D–H–A 172(2) $^\circ$, and (O1–H1–N2: D–H 0.87(3) Å, H–A 2.40(3) Å, D–A 3.220(3) Å, D–H–A 158(3) $^\circ$, respectively; Fig. 2.3).

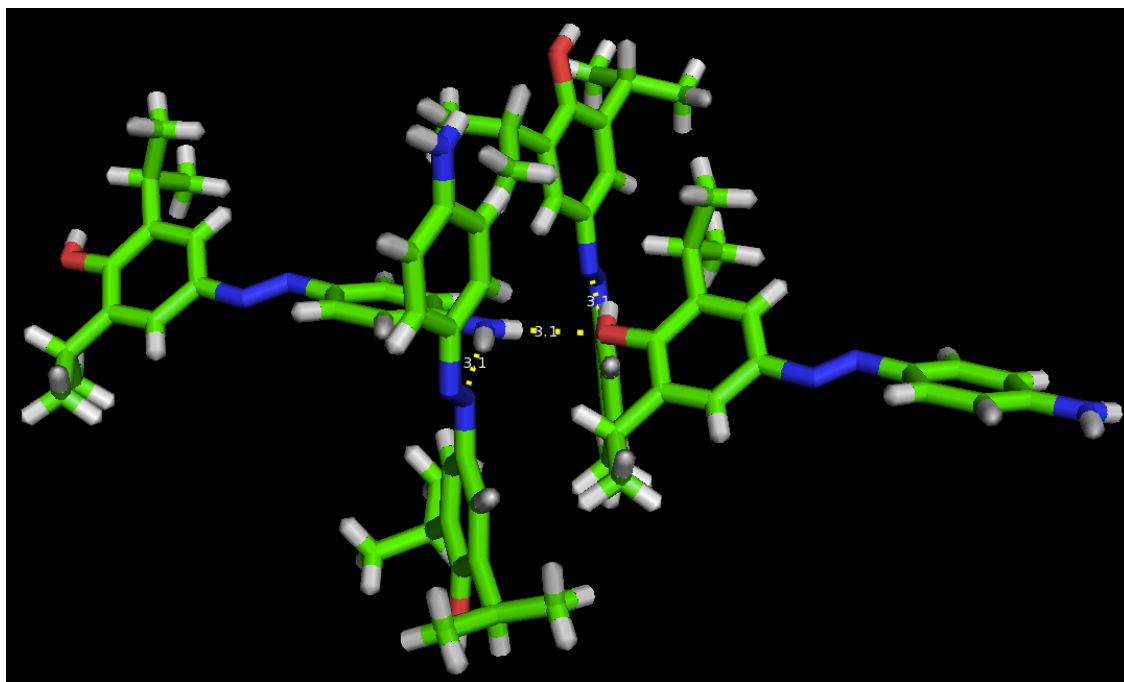
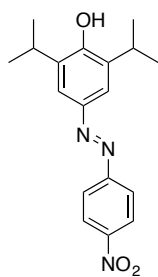
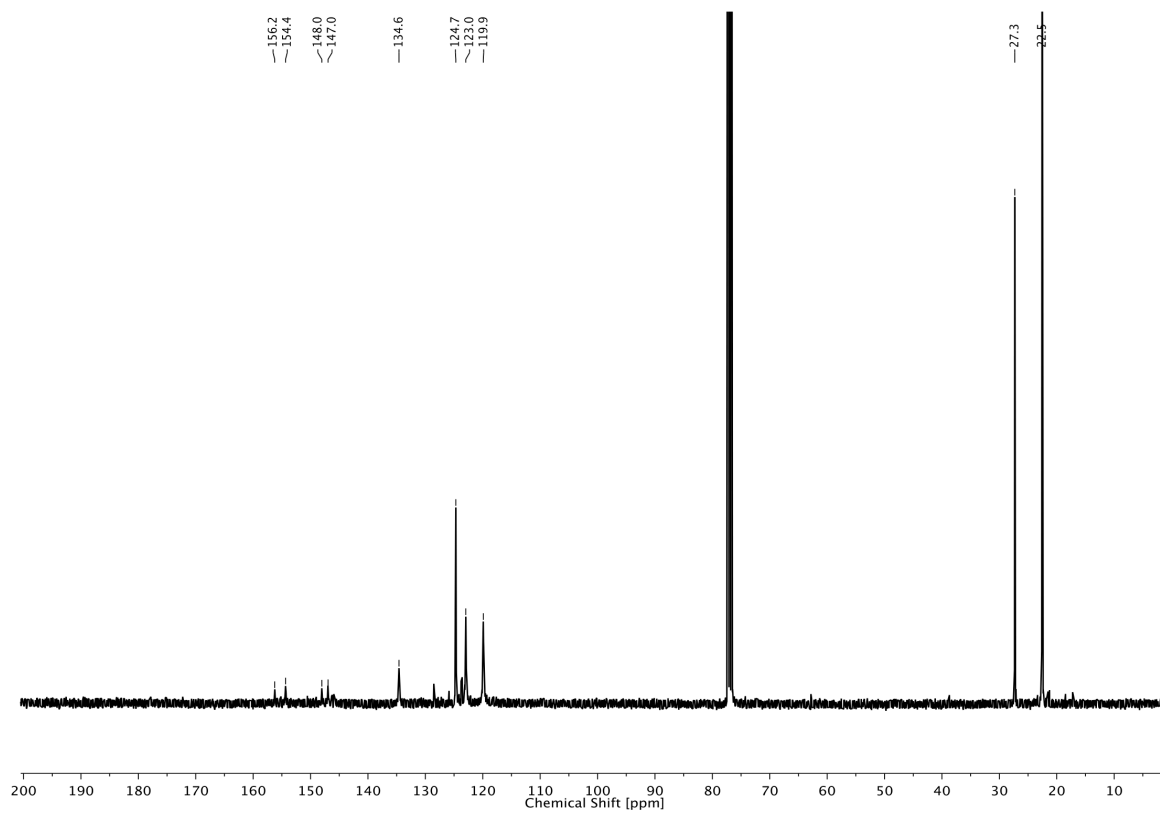
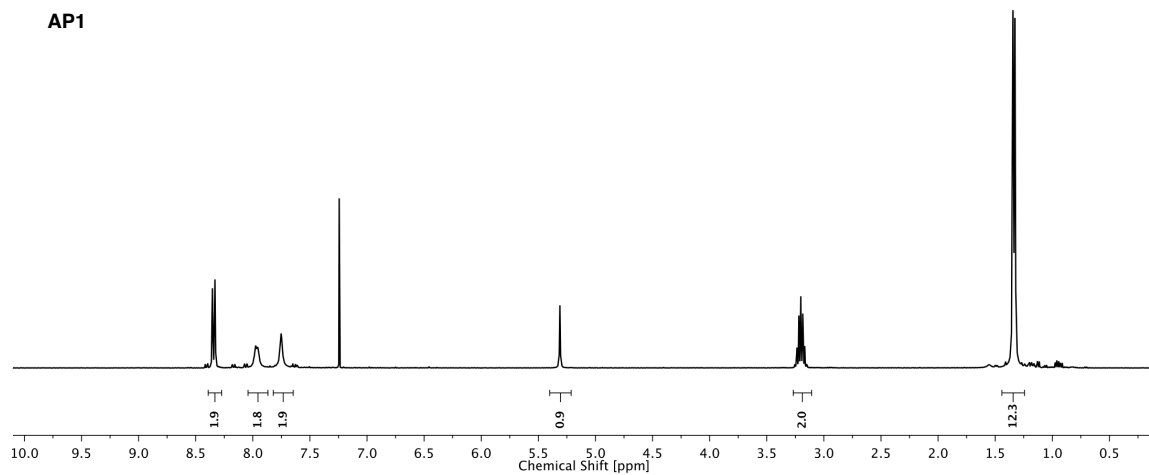


Figure 2.3. Hydrogen bonding network of AP2 in the crystal lattice.

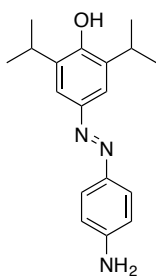
NMR Spectra



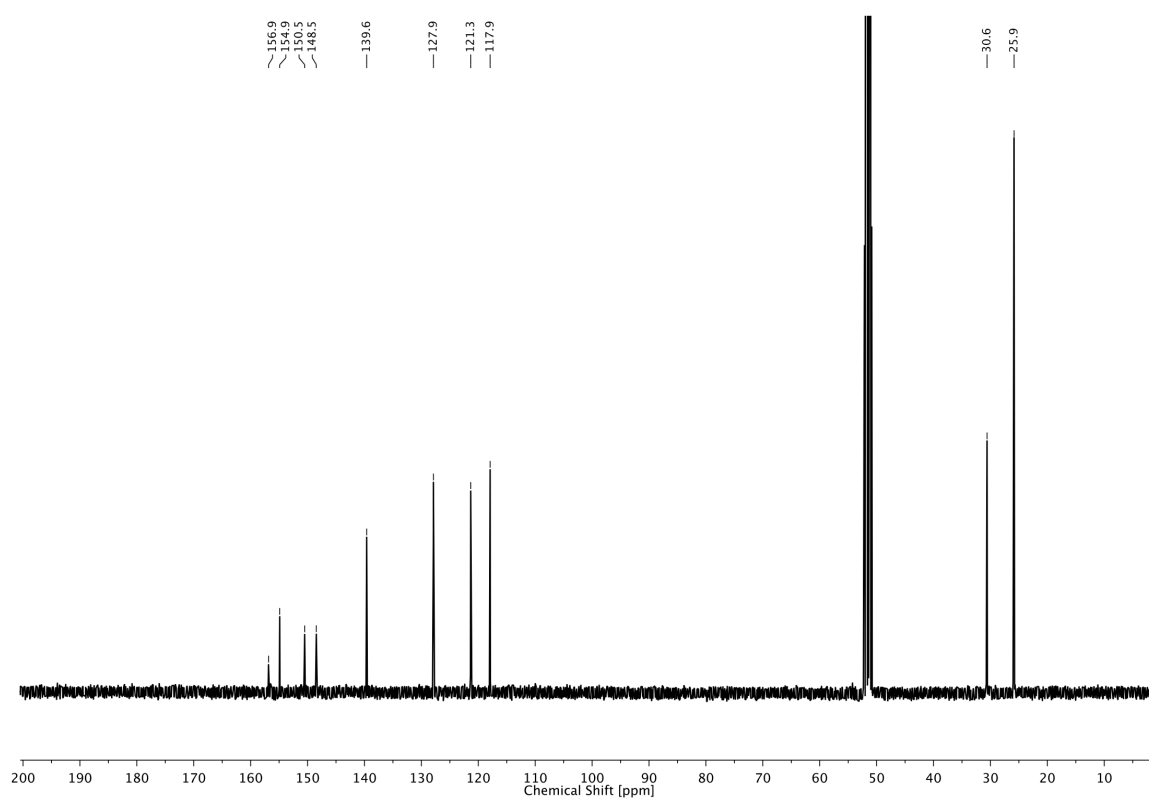
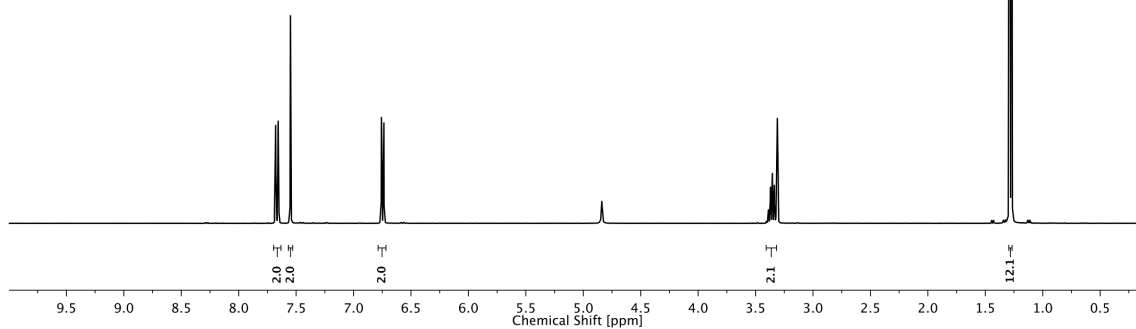
AP1



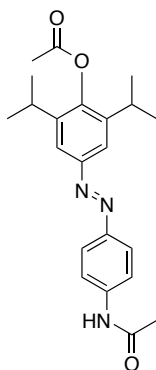
2 PHOTOREGULATION OF GABA_A RECEPTORS



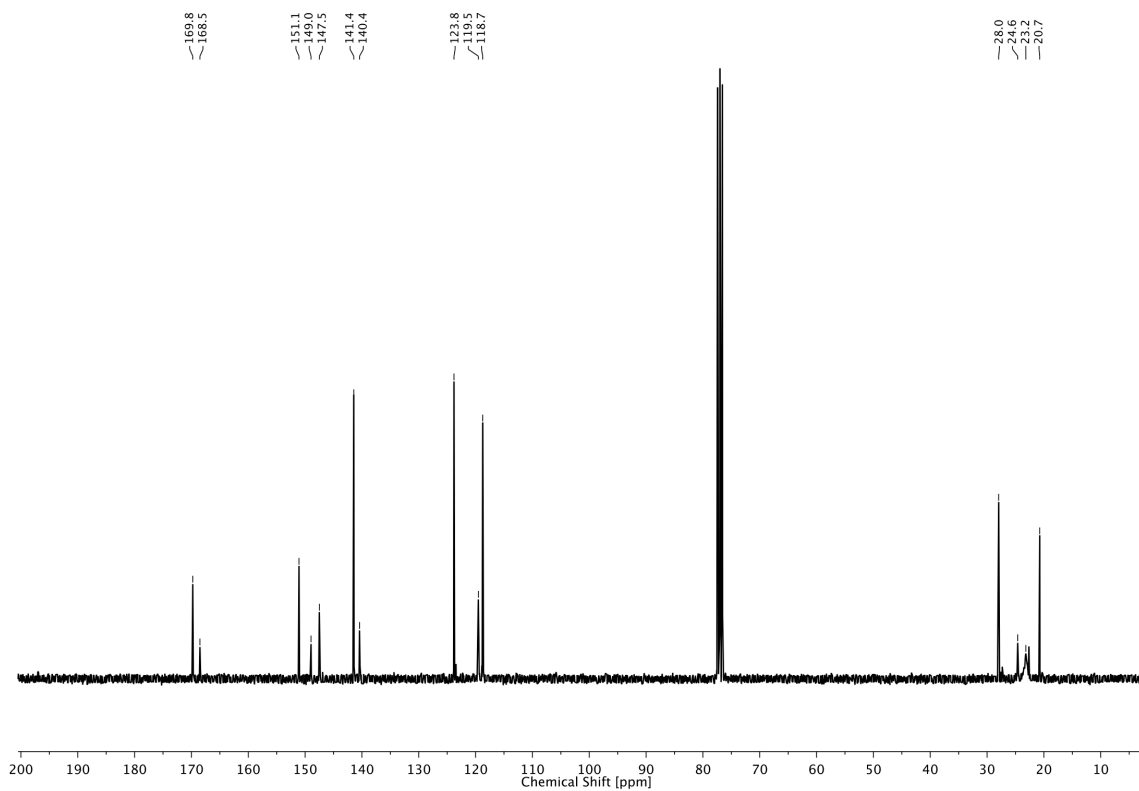
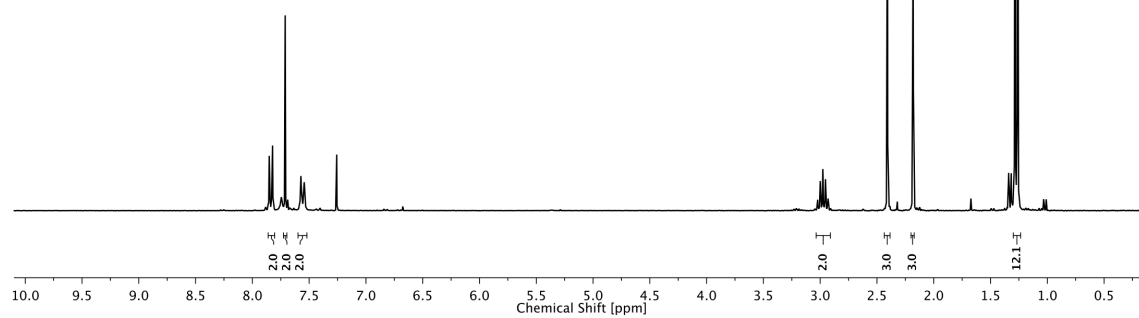
AP2



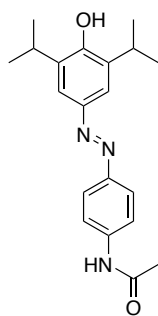
2 PHOTOREGULATION OF GABA_A RECEPTORS



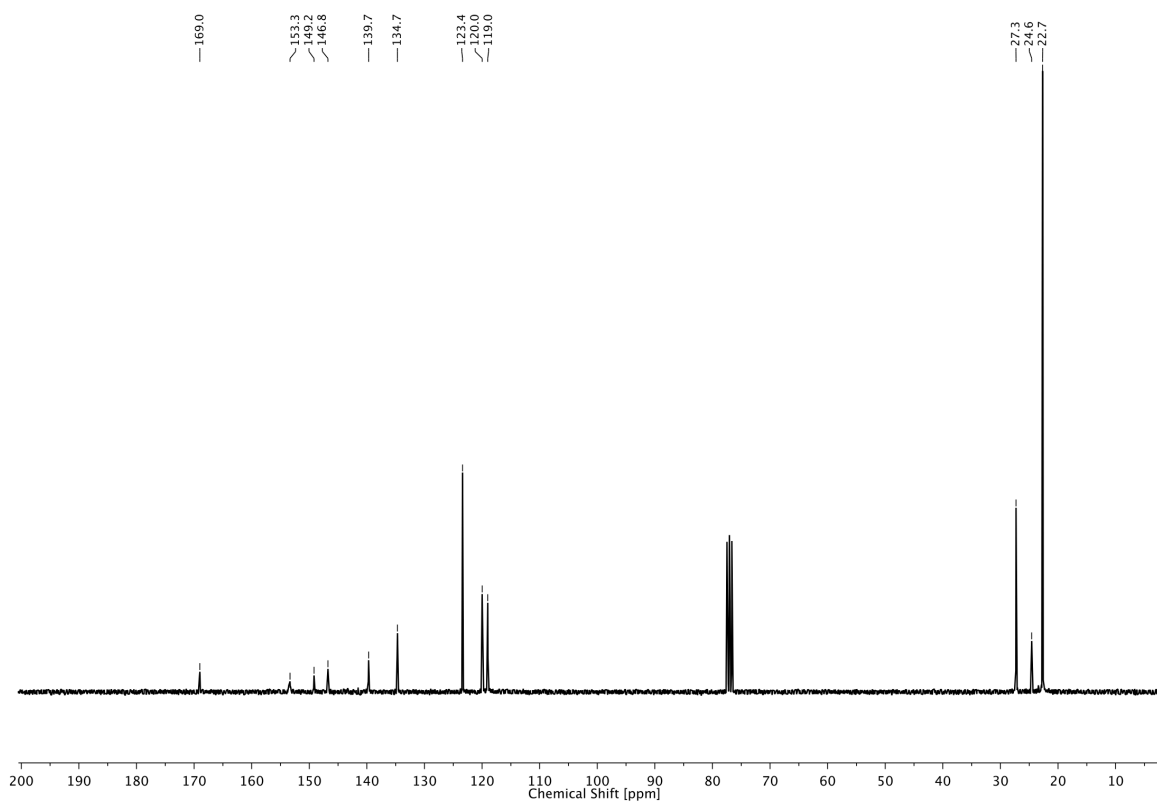
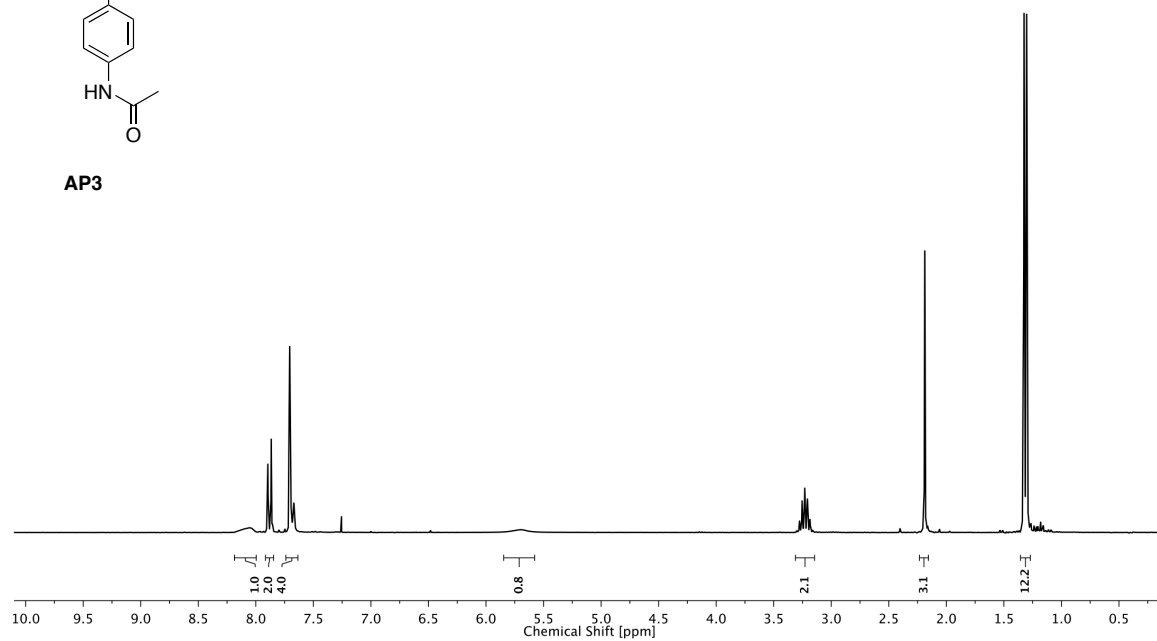
AcAP3



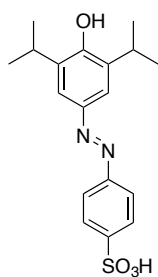
2 PHOTOREGULATION OF GABA_A RECEPTORS



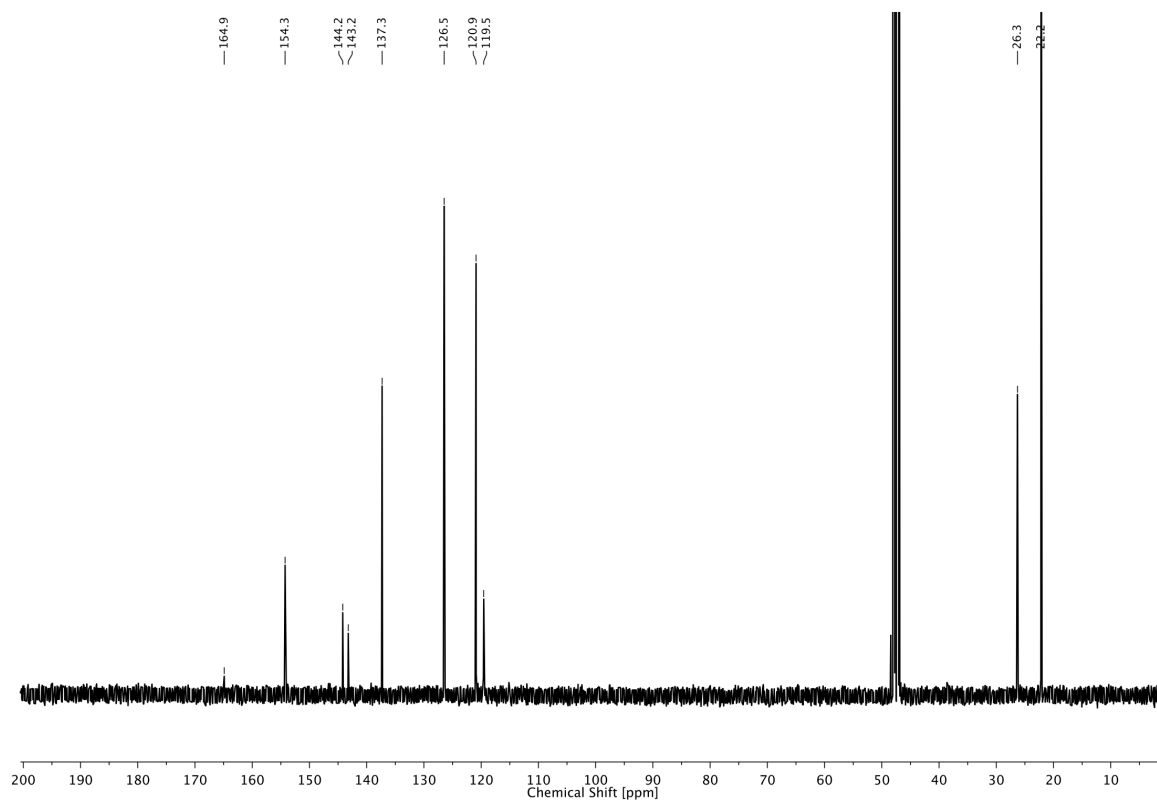
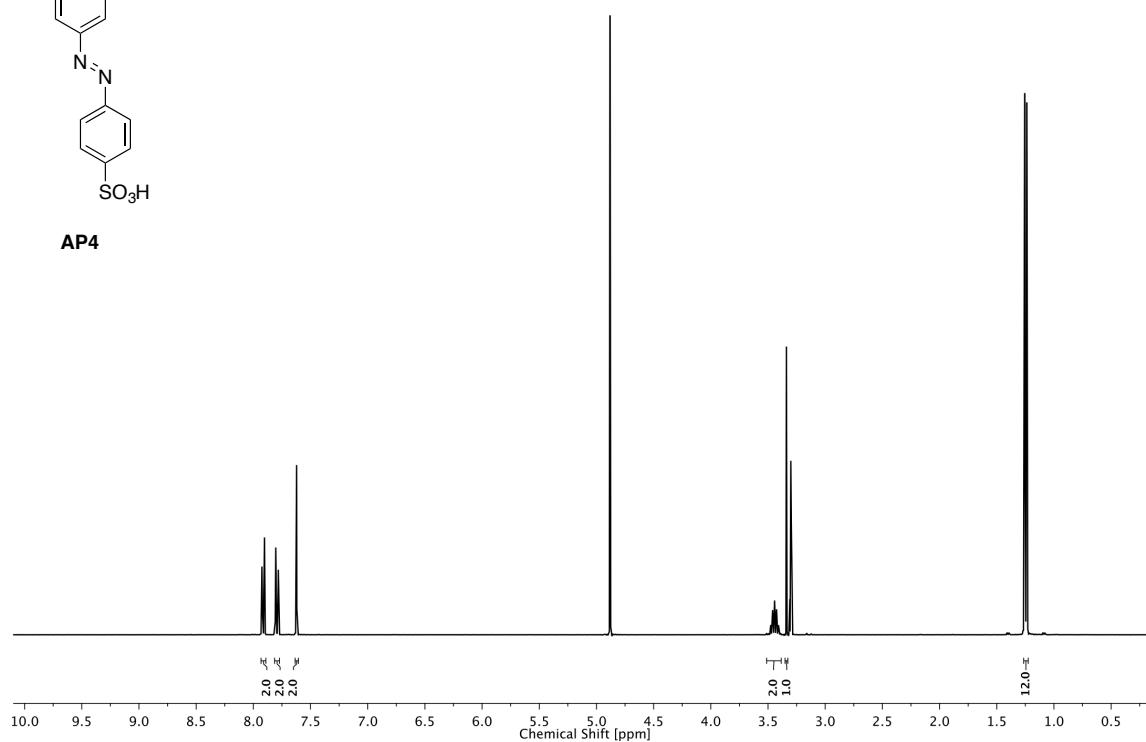
AP3



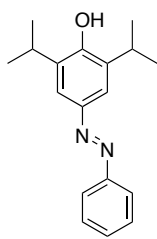
2 PHOTOREGULATION OF GABA_A RECEPTORS



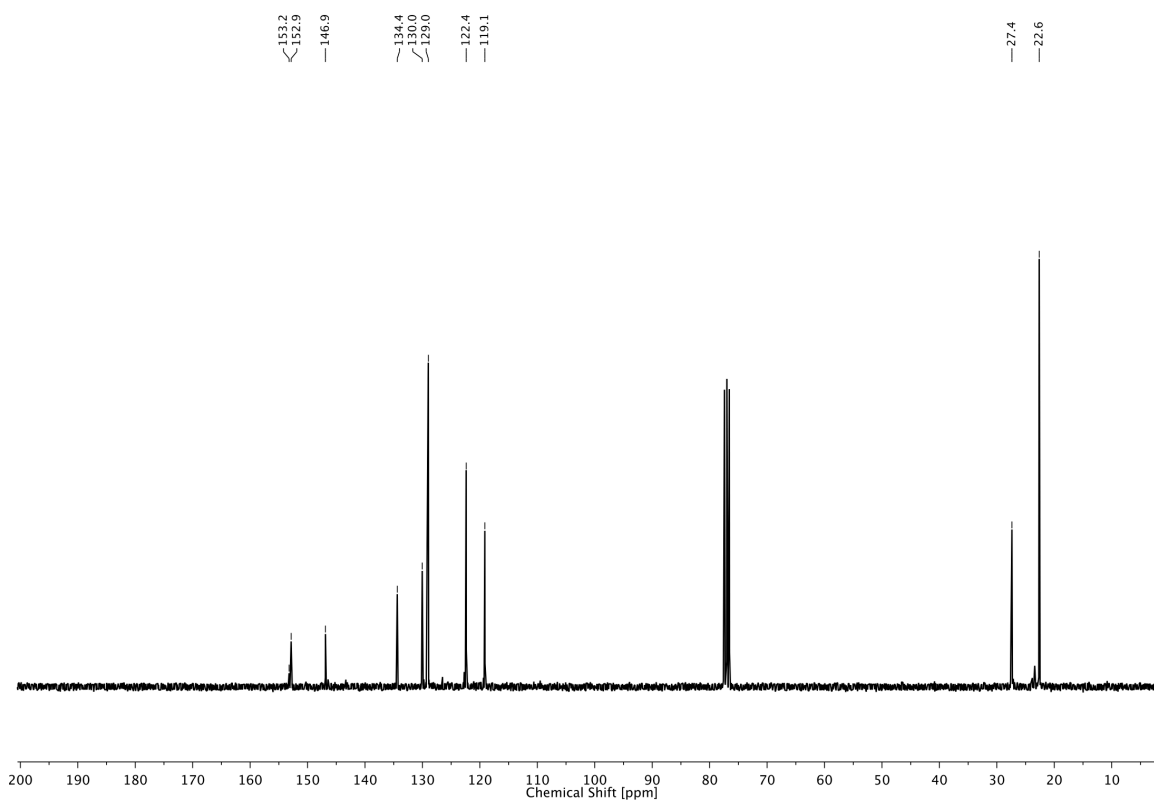
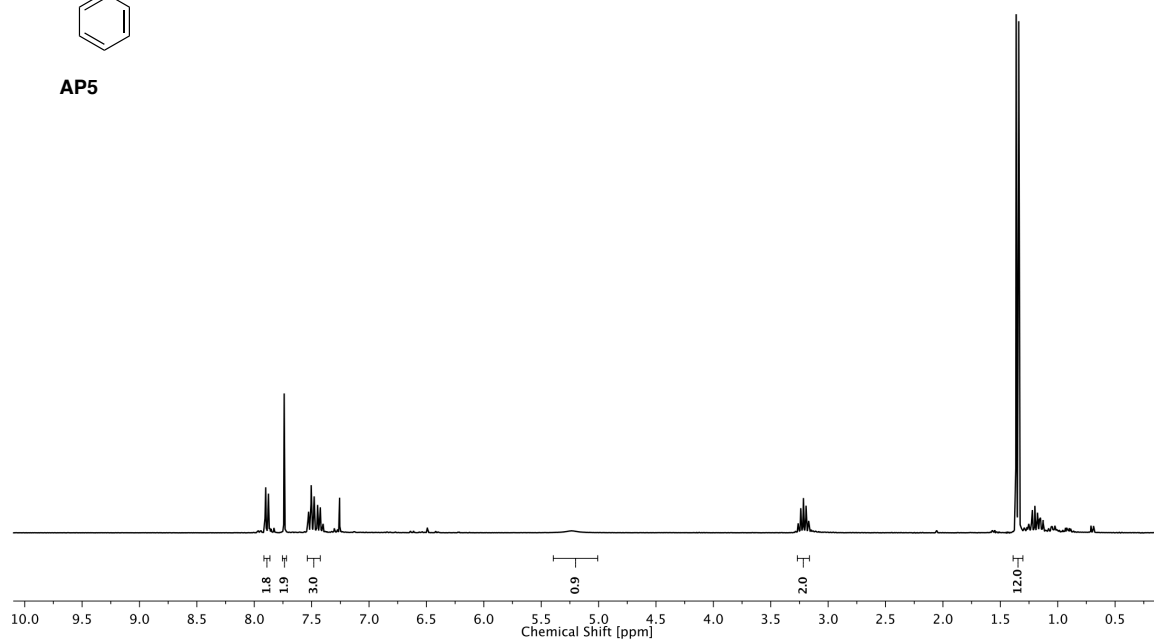
AP4



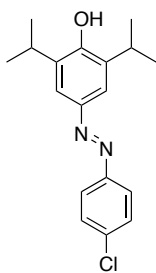
2 PHOTOREGULATION OF GABA_A RECEPTORS



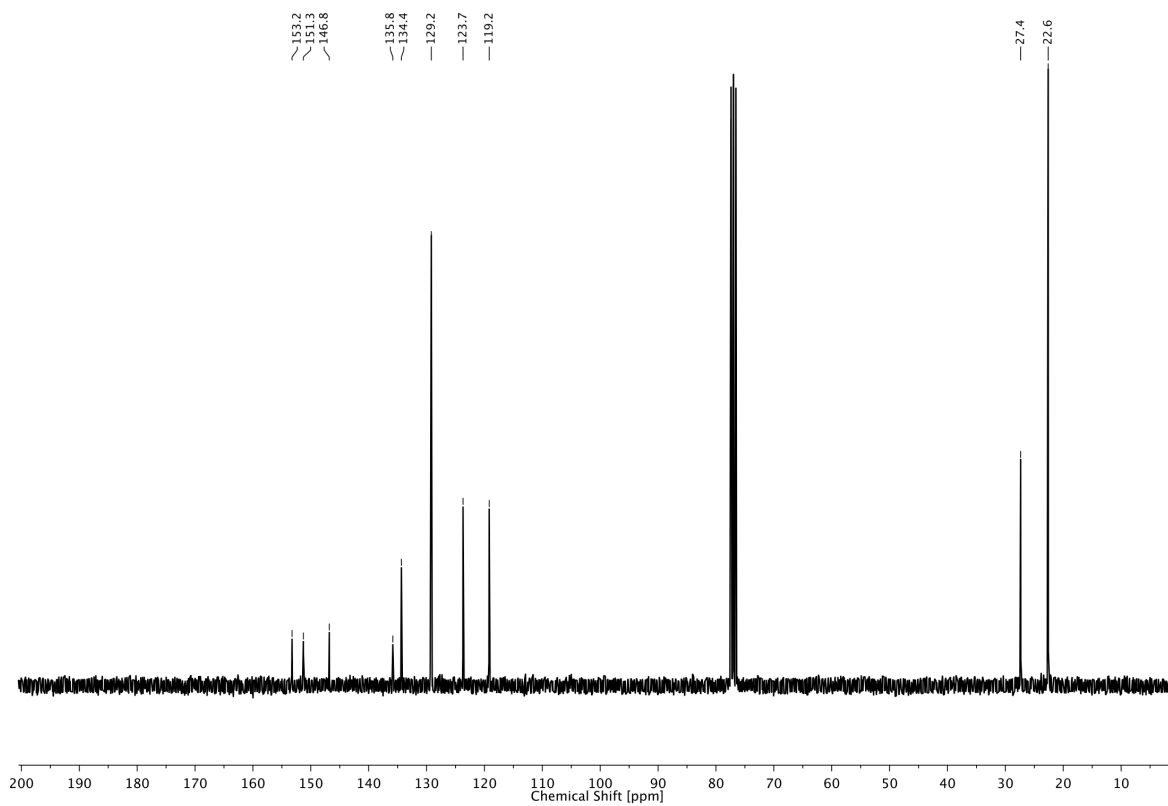
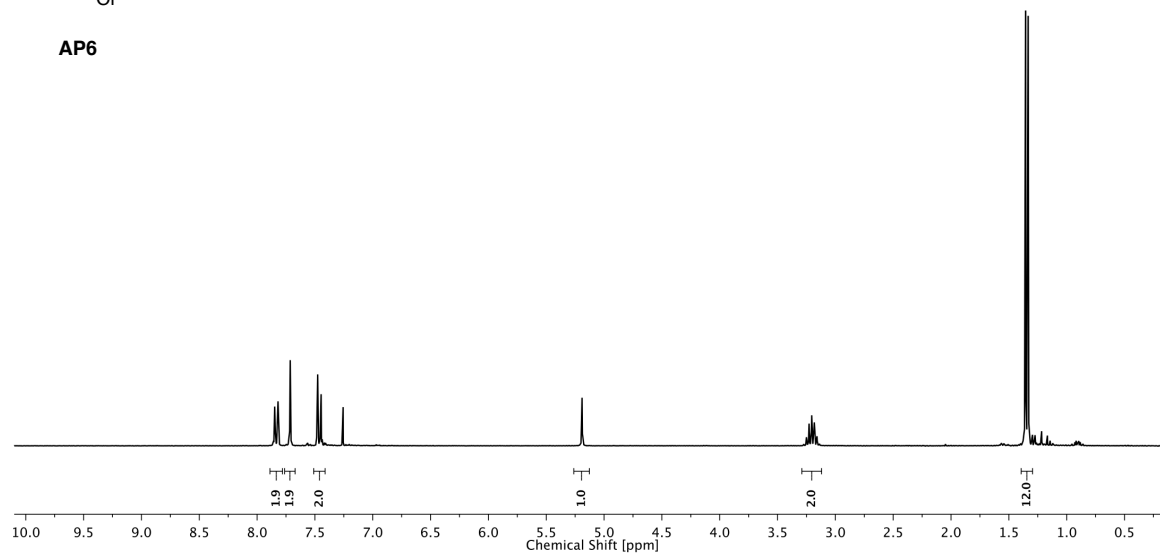
AP5



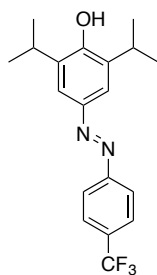
2 PHOTOREGULATION OF GABA_A RECEPTORS



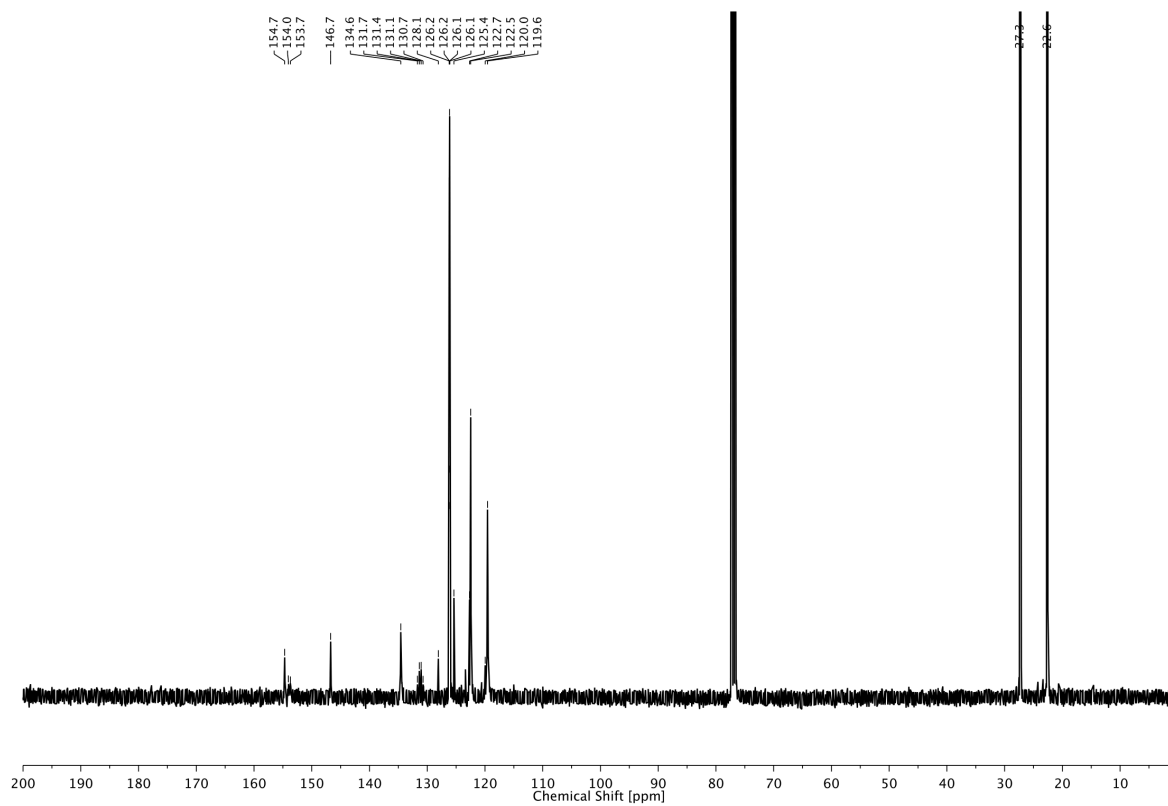
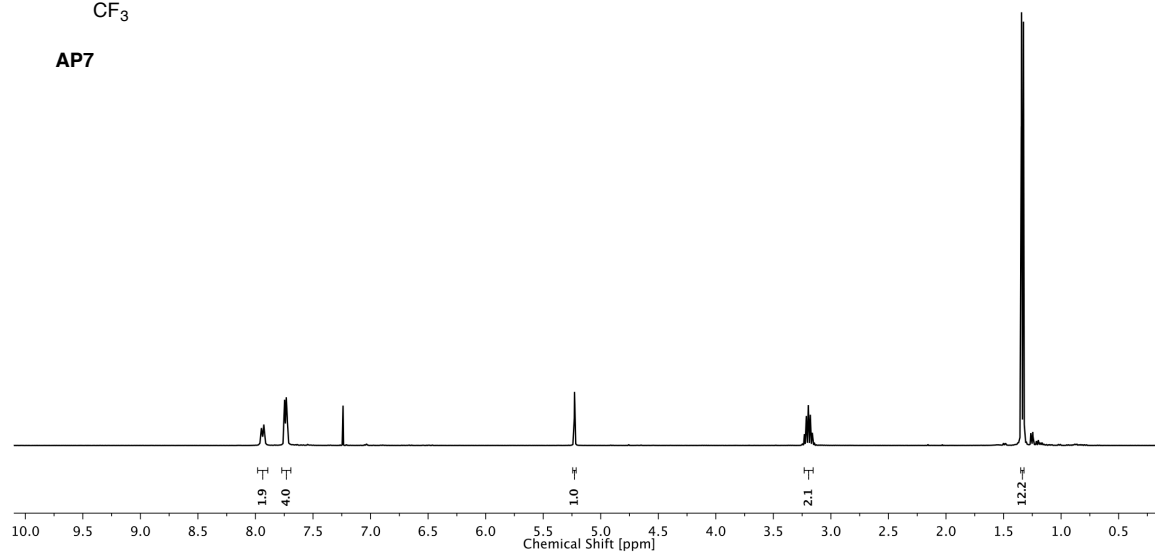
AP6



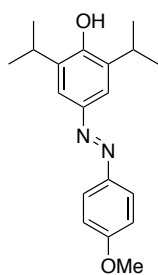
2 PHOTOREGULATION OF GABA_A RECEPTORS



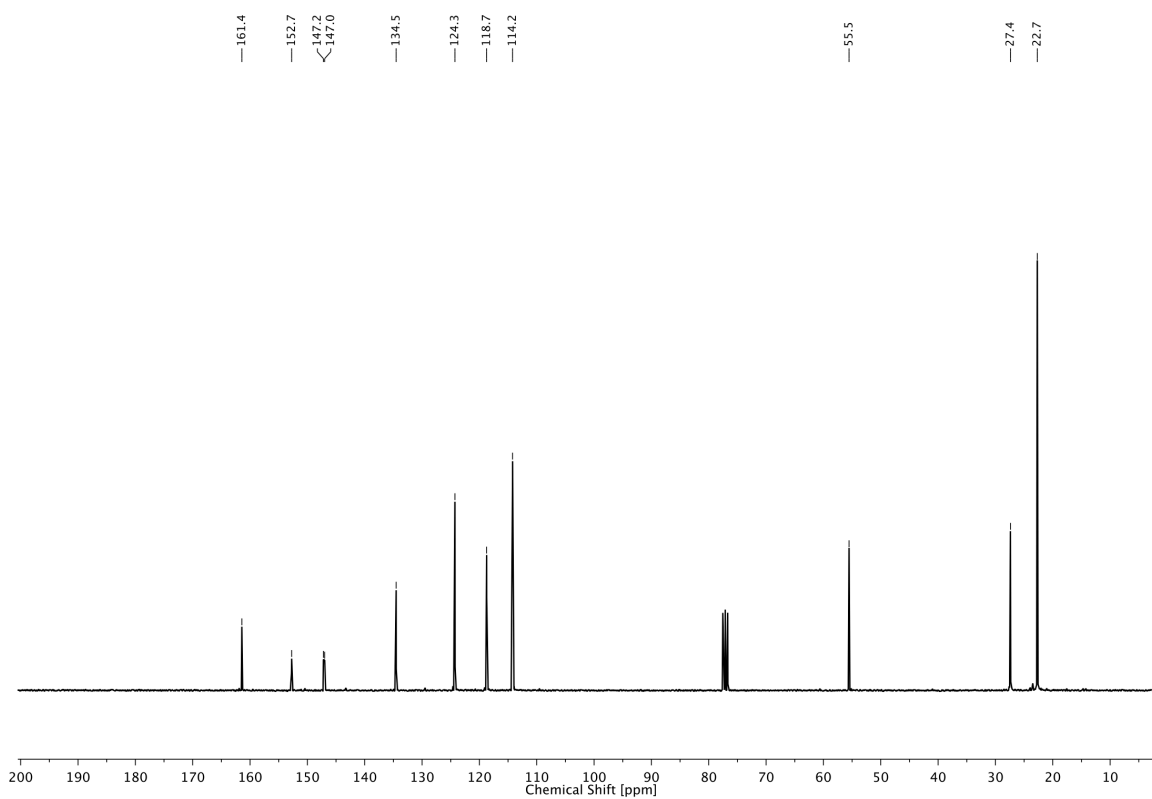
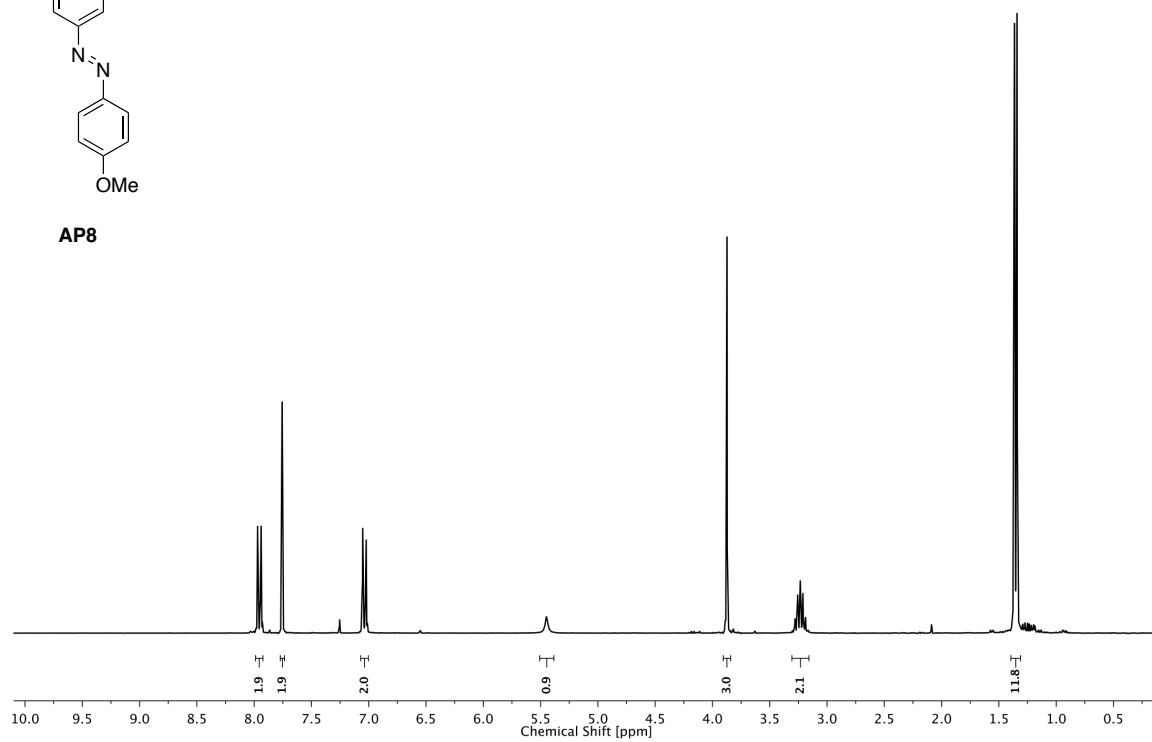
AP7



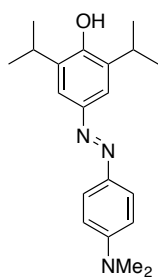
2 PHOTOREGULATION OF GABA_A RECEPTORS



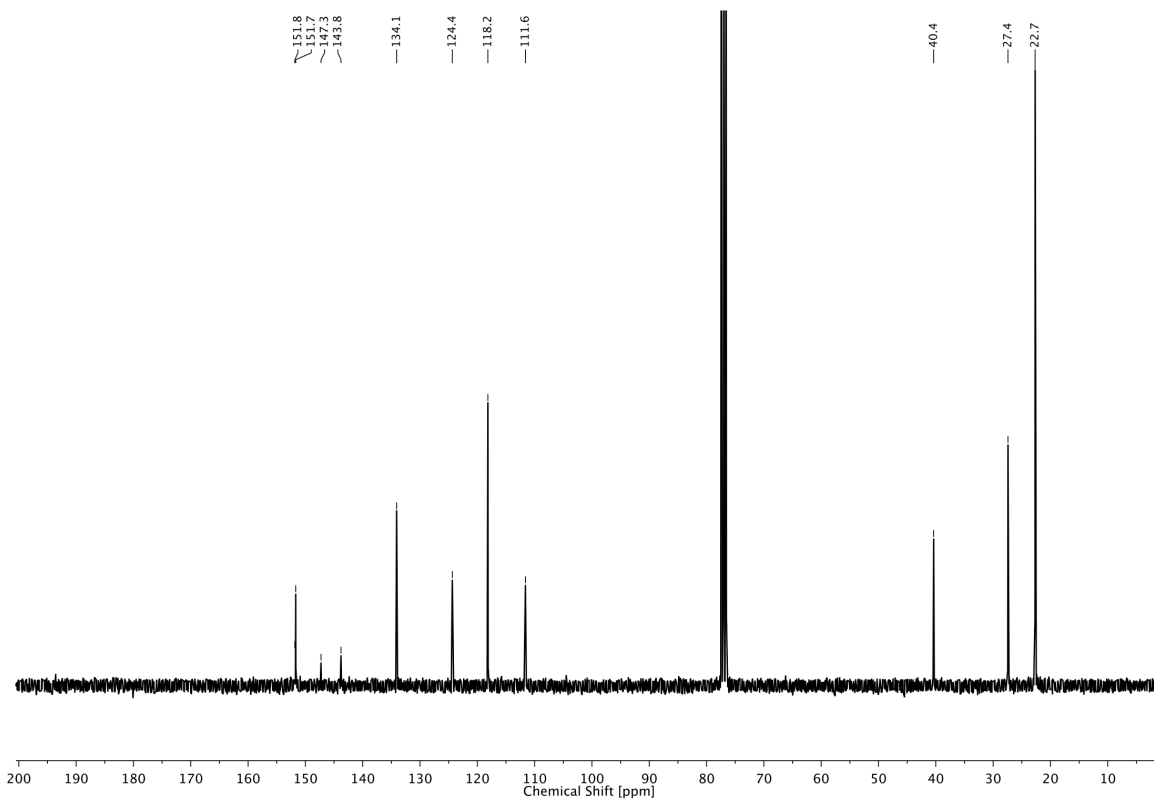
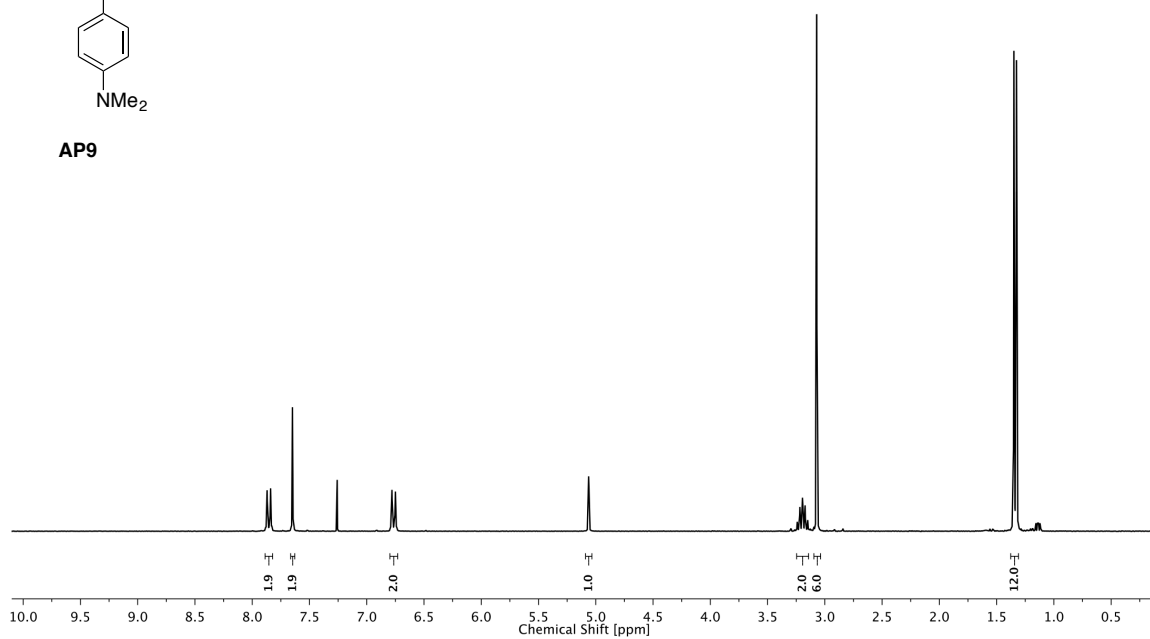
AP8



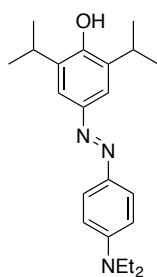
2 PHOTOREGULATION OF GABA_A RECEPTORS



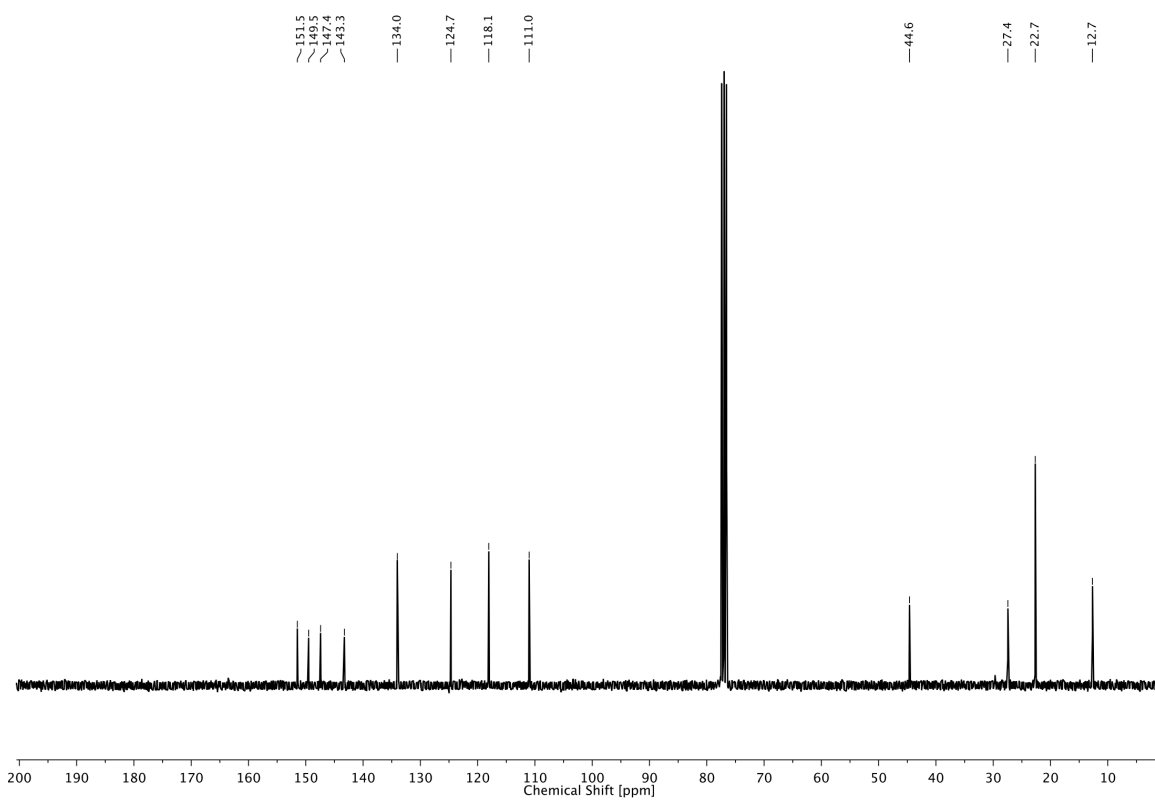
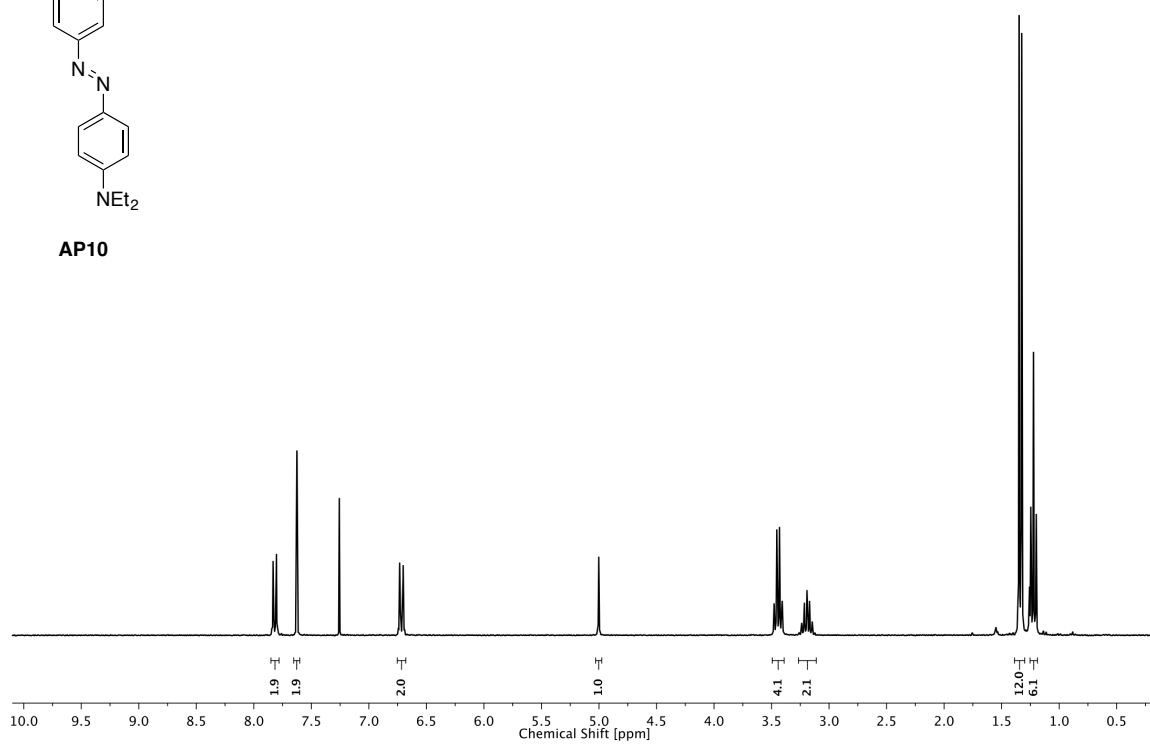
AP9



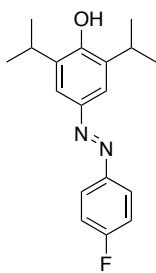
2 PHOTOREGULATION OF GABA_A RECEPTORS



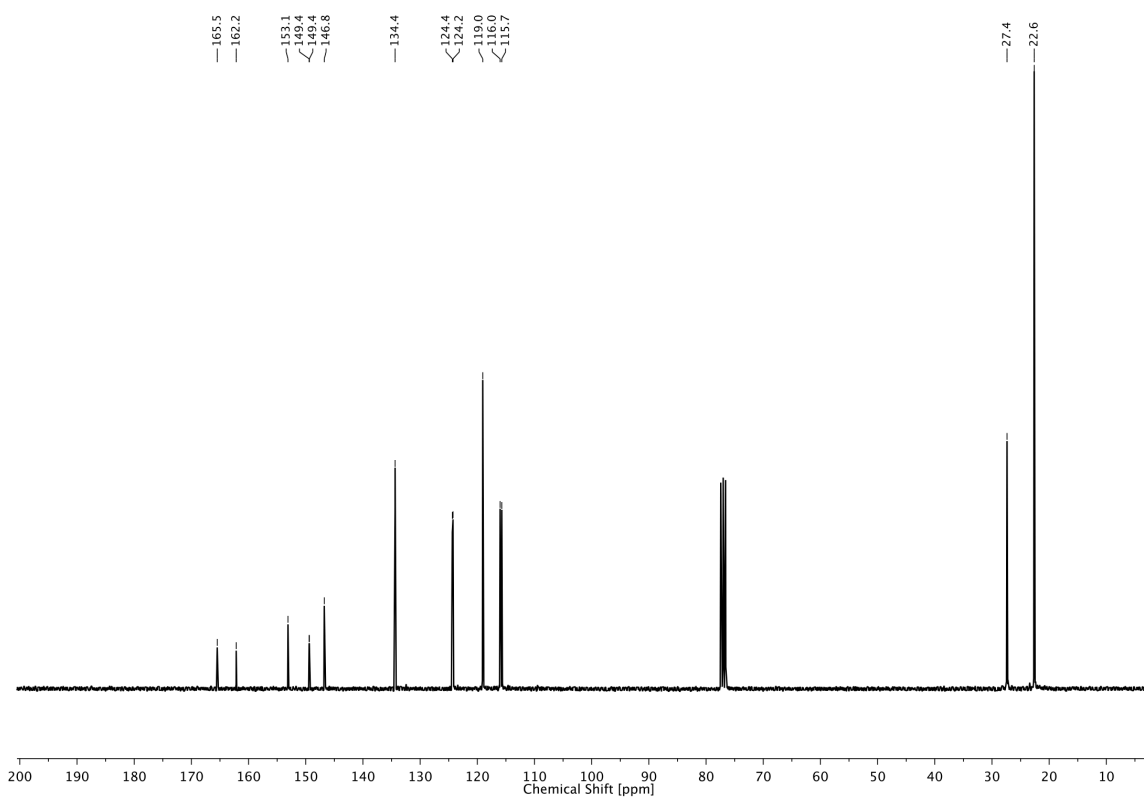
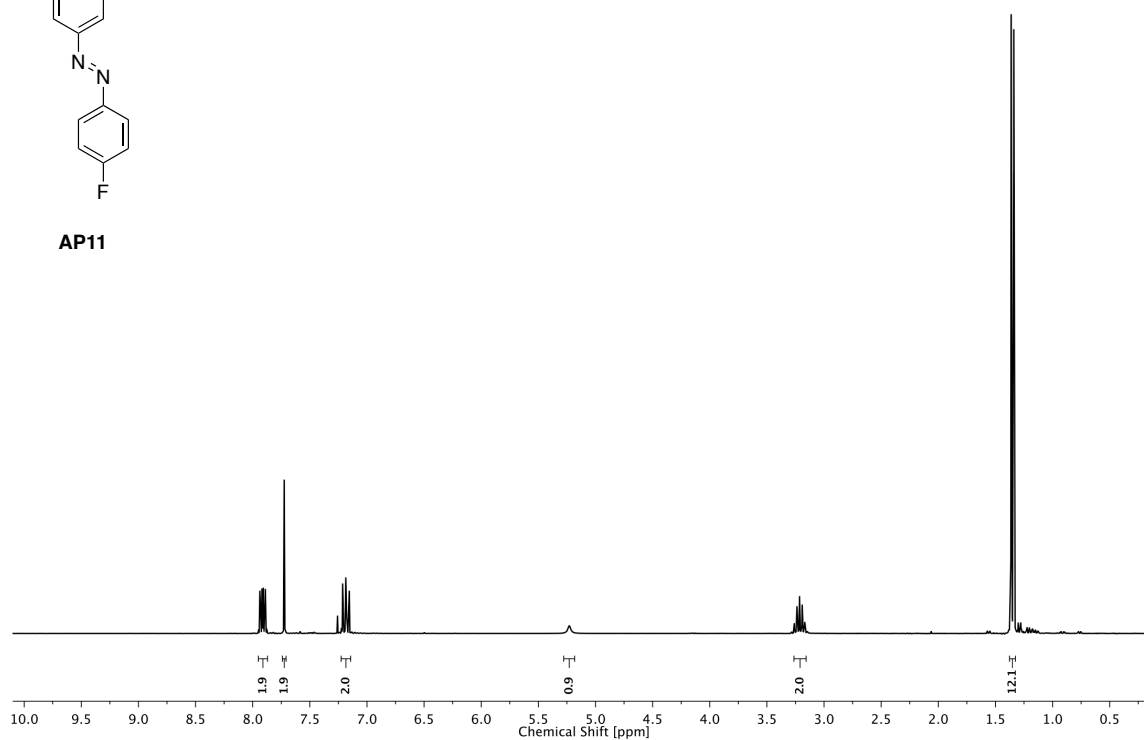
AP10



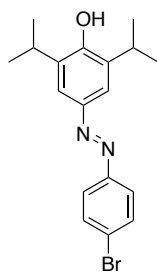
2 PHOTOREGULATION OF GABA_A RECEPTORS



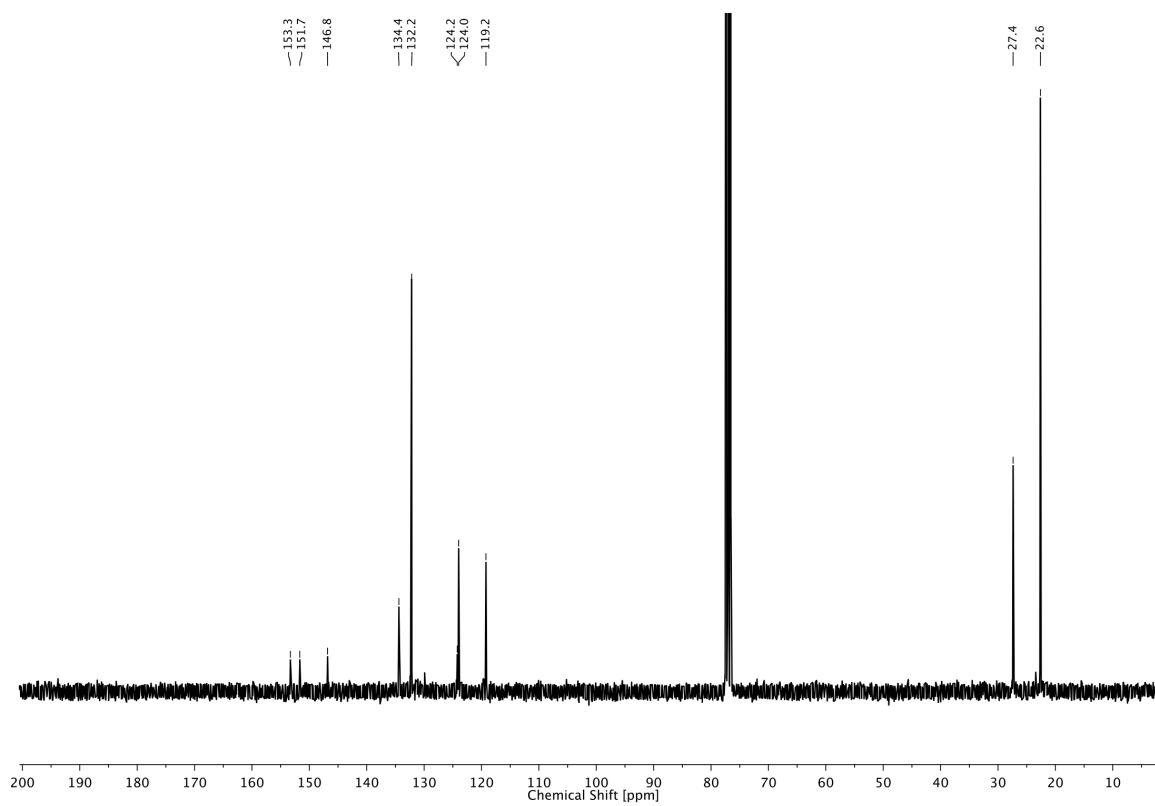
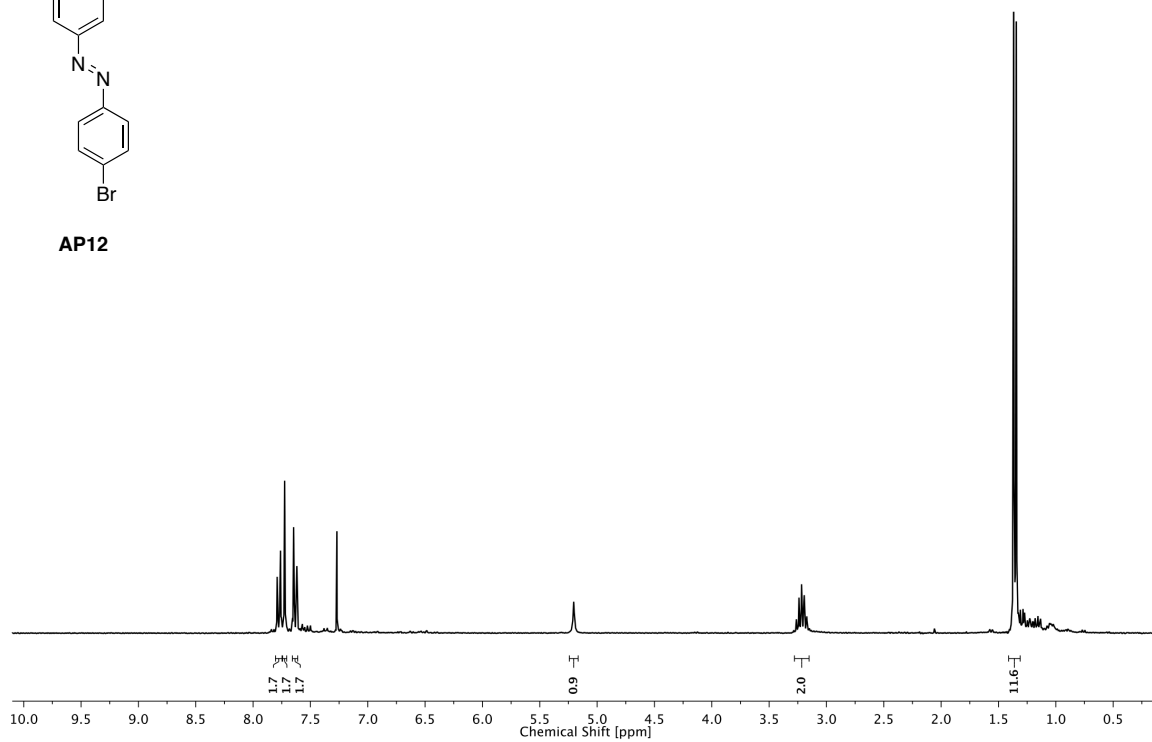
AP11



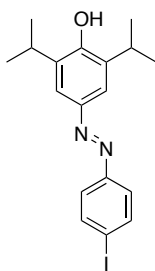
2 PHOTOREGULATION OF GABA_A RECEPTORS



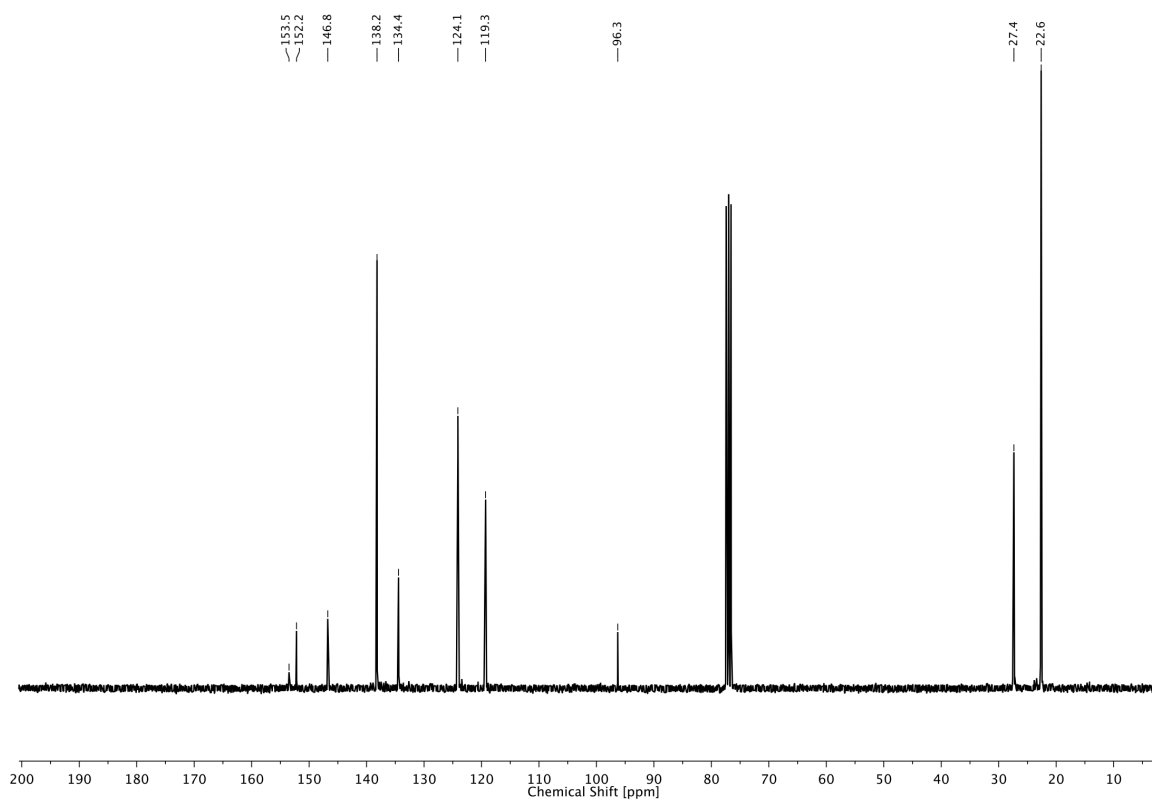
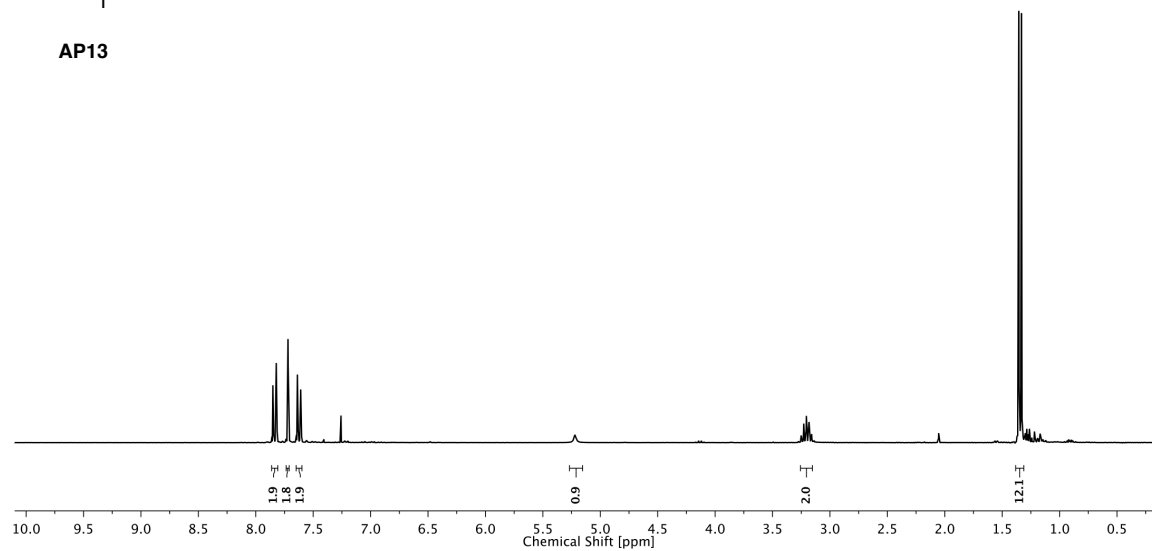
AP12



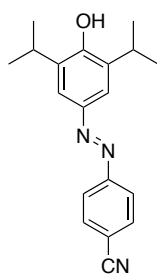
2 PHOTOREGULATION OF GABA_A RECEPTORS



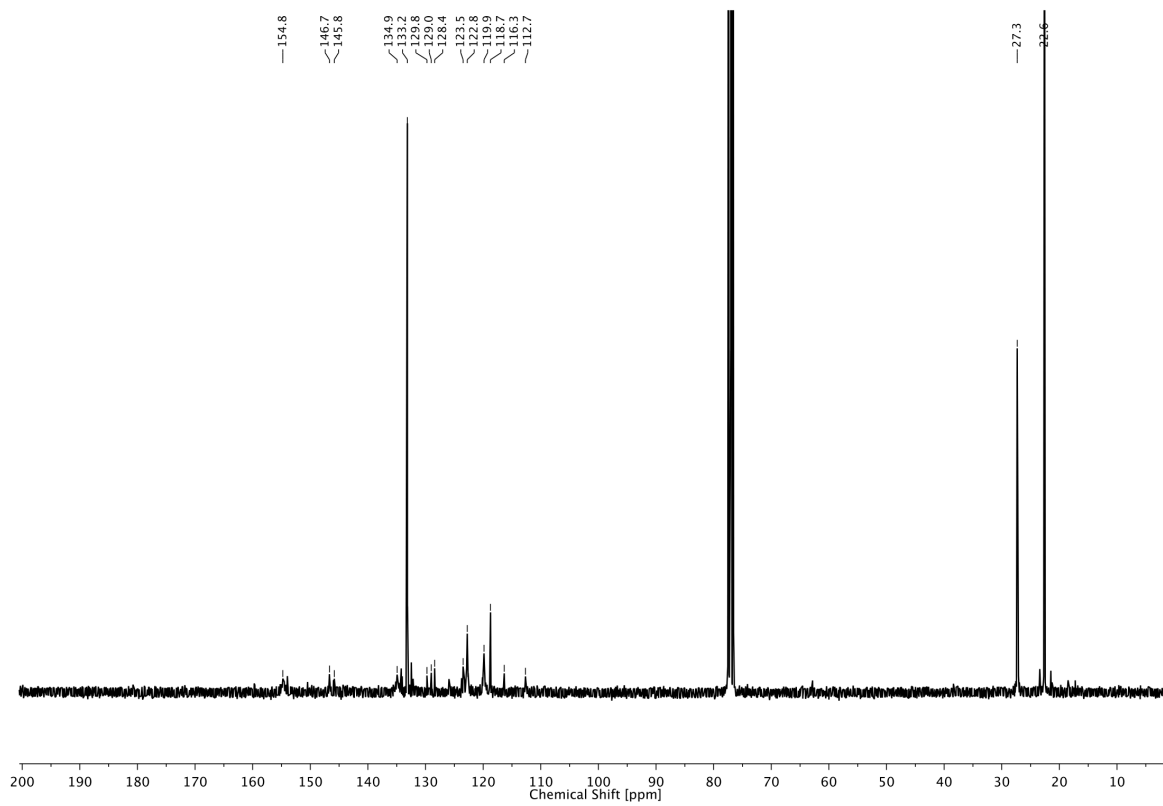
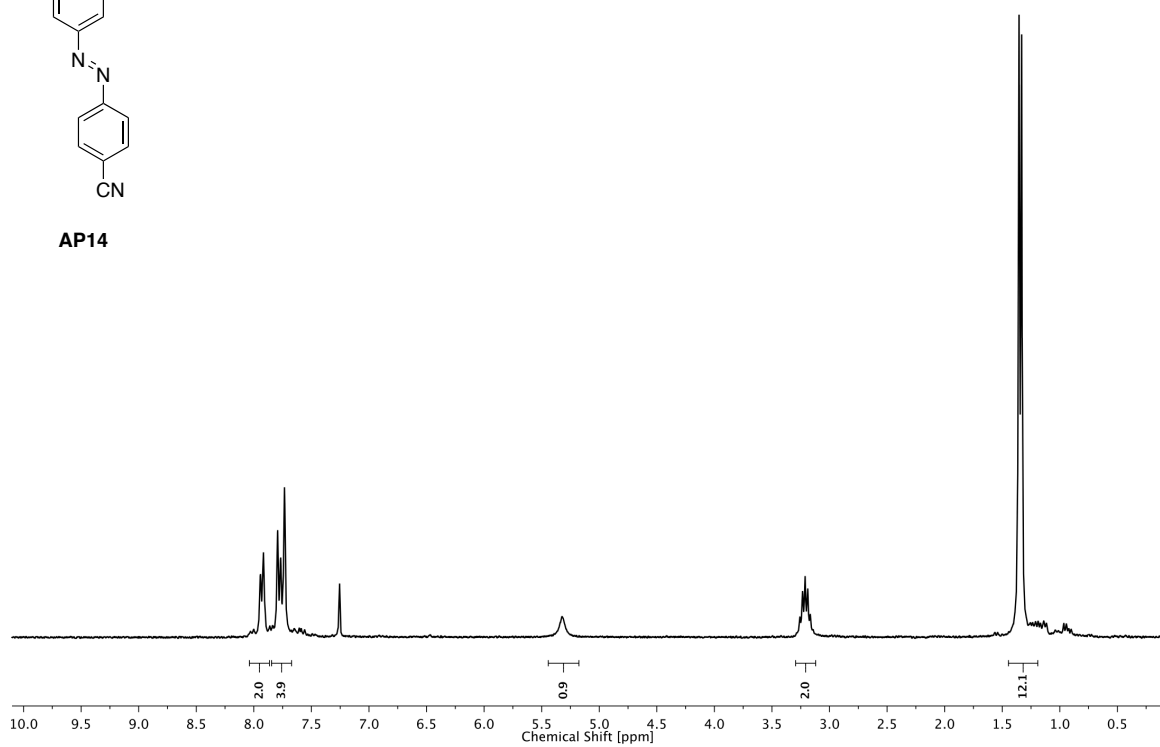
AP13



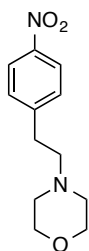
2 PHOTOREGULATION OF GABA_A RECEPTORS



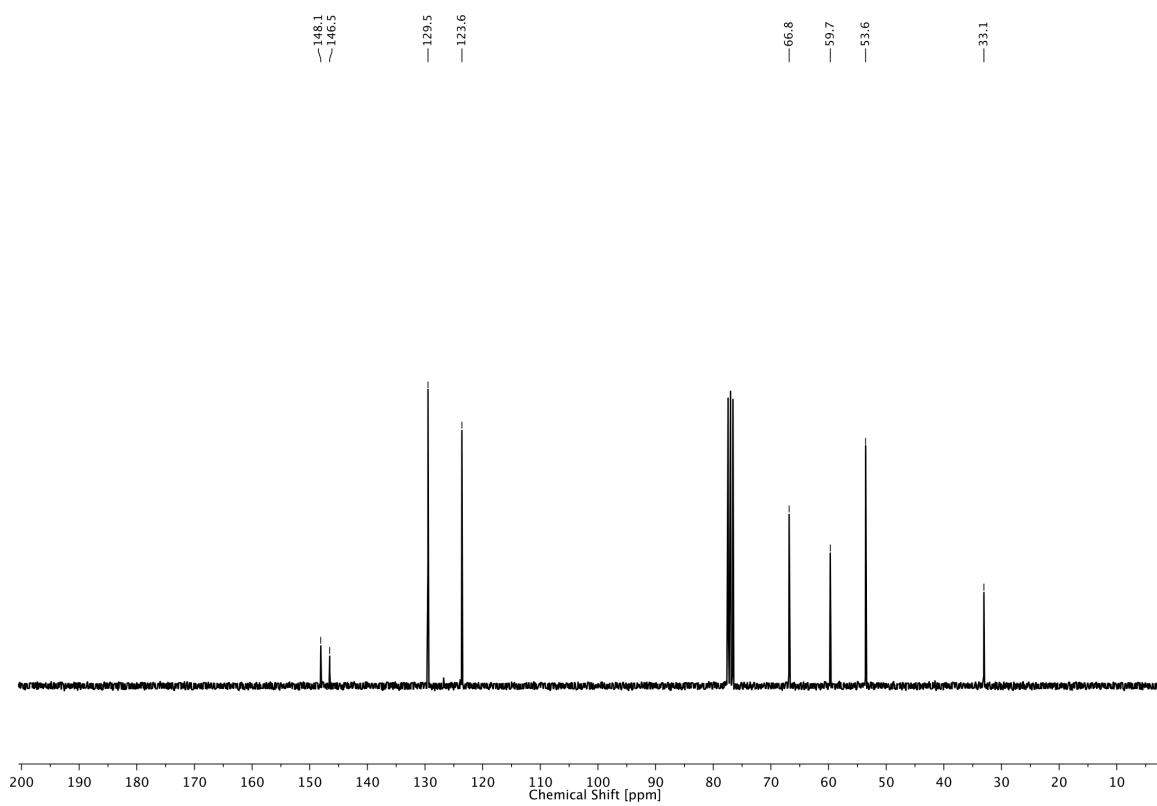
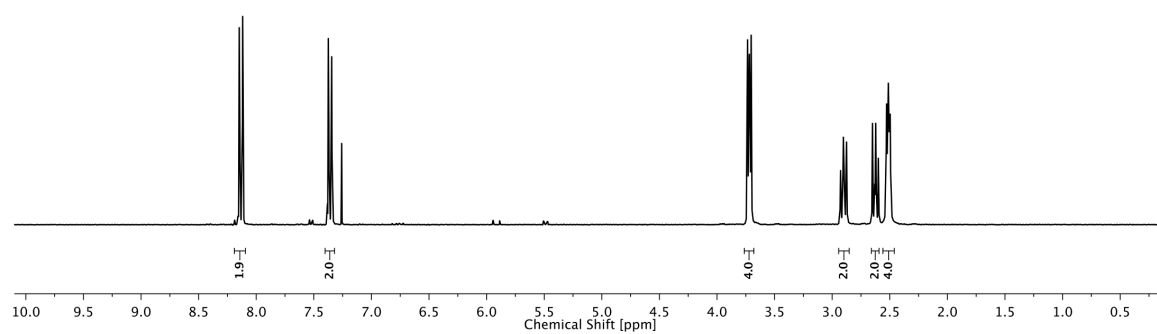
AP14



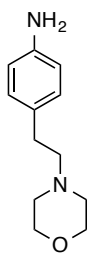
2 PHOTOREGULATION OF GABA_A RECEPTORS



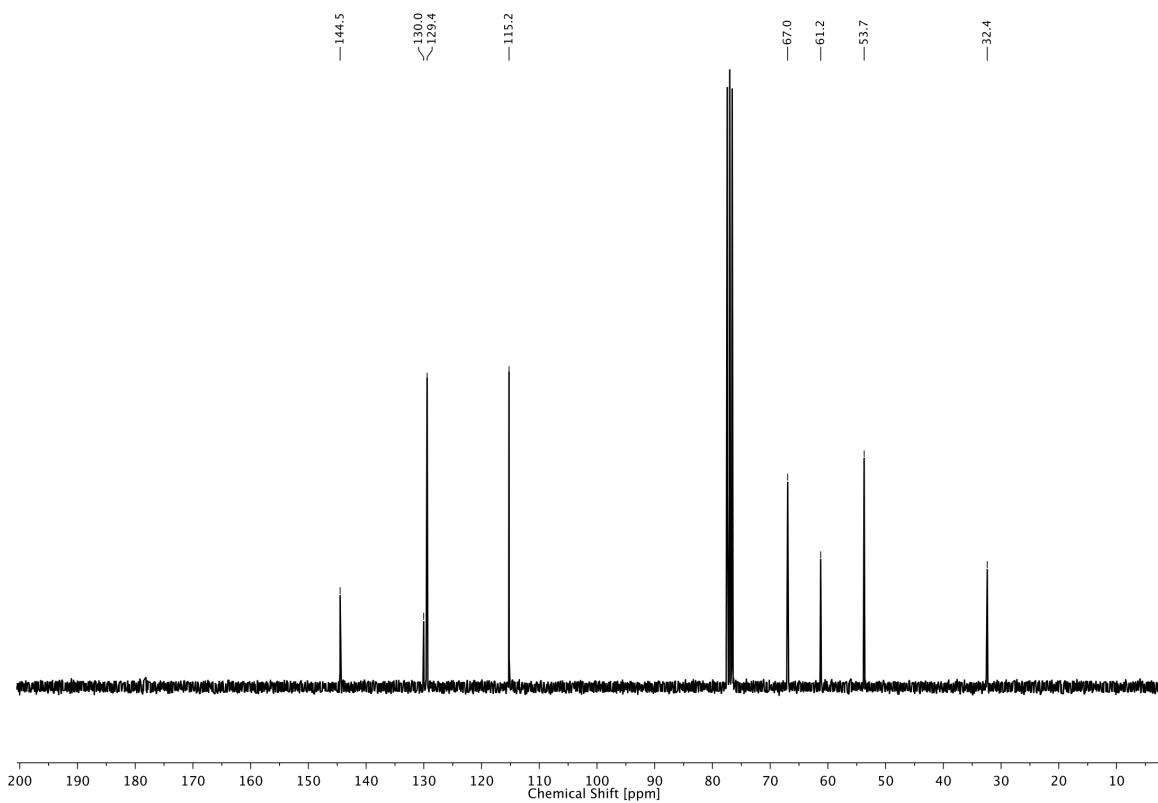
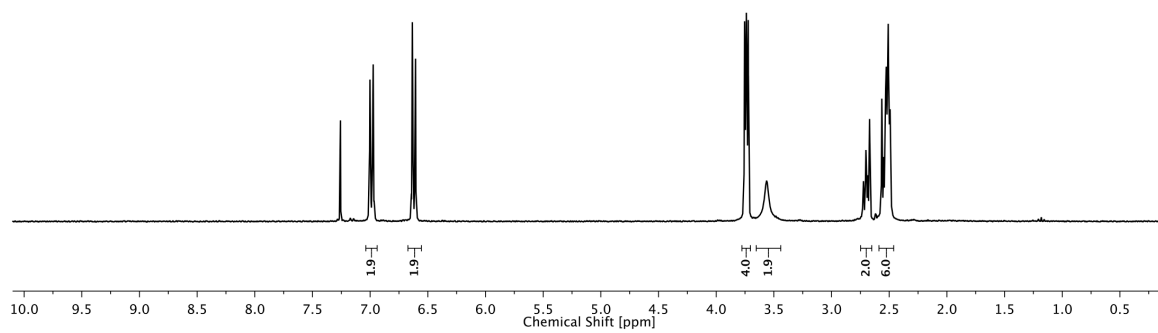
2.1



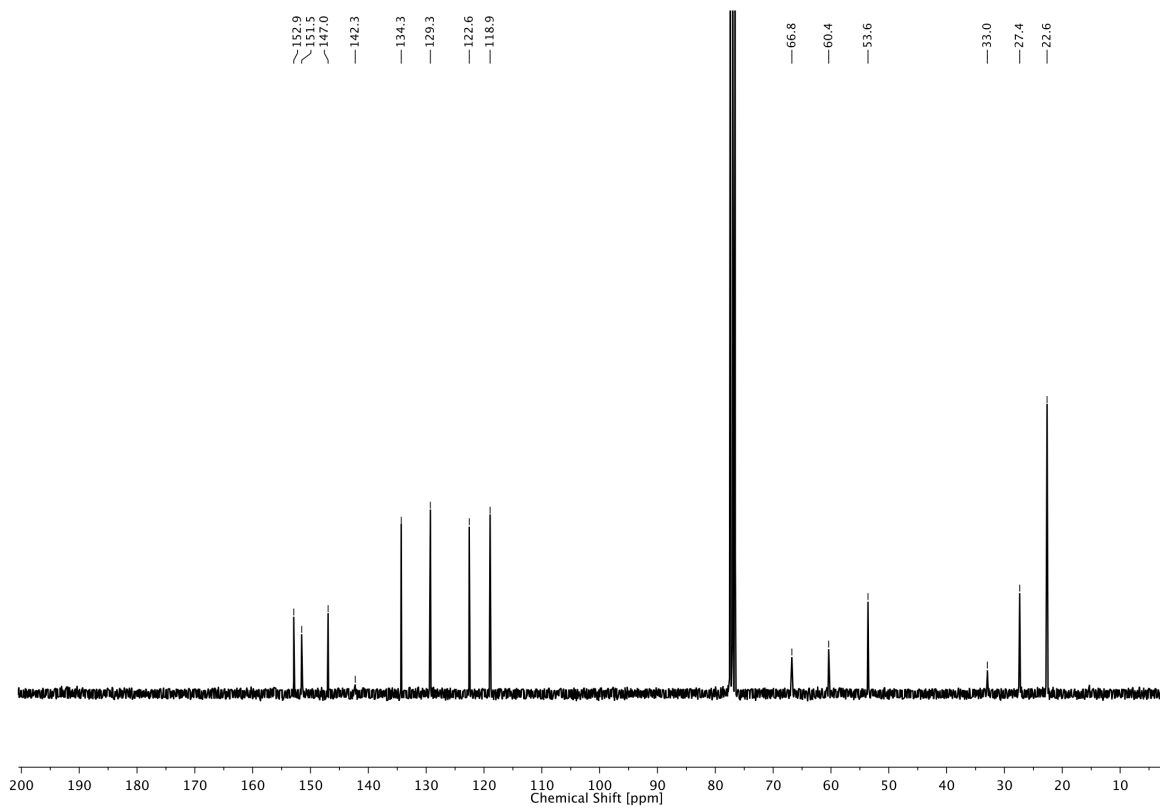
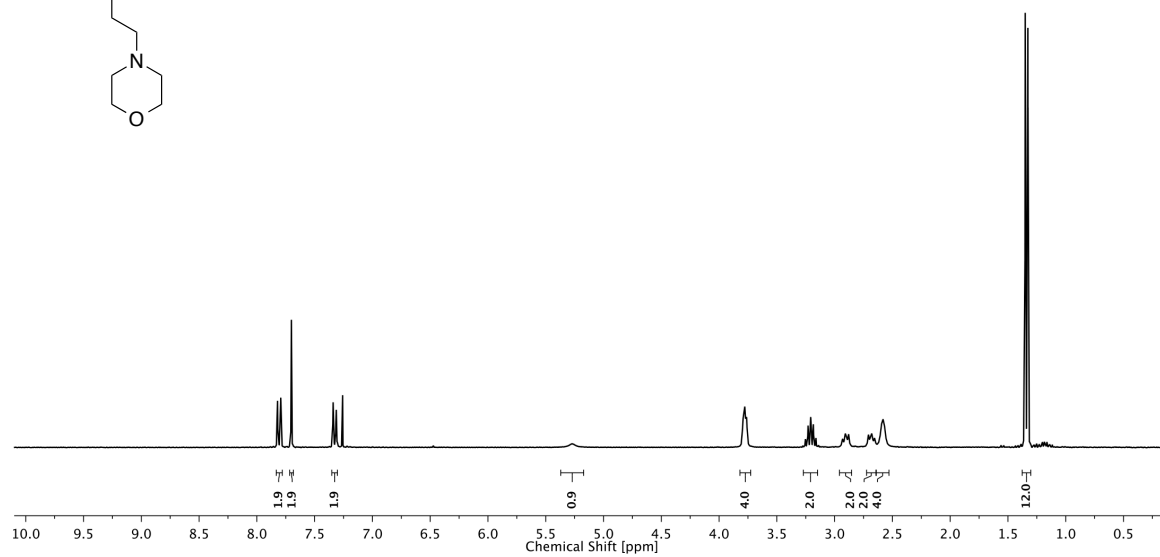
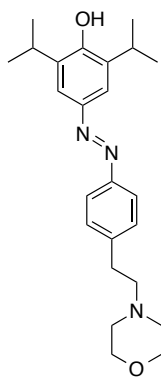
2 PHOTOREGULATION OF GABA_A RECEPTORS



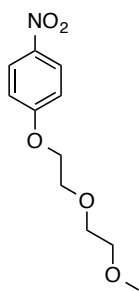
2.2



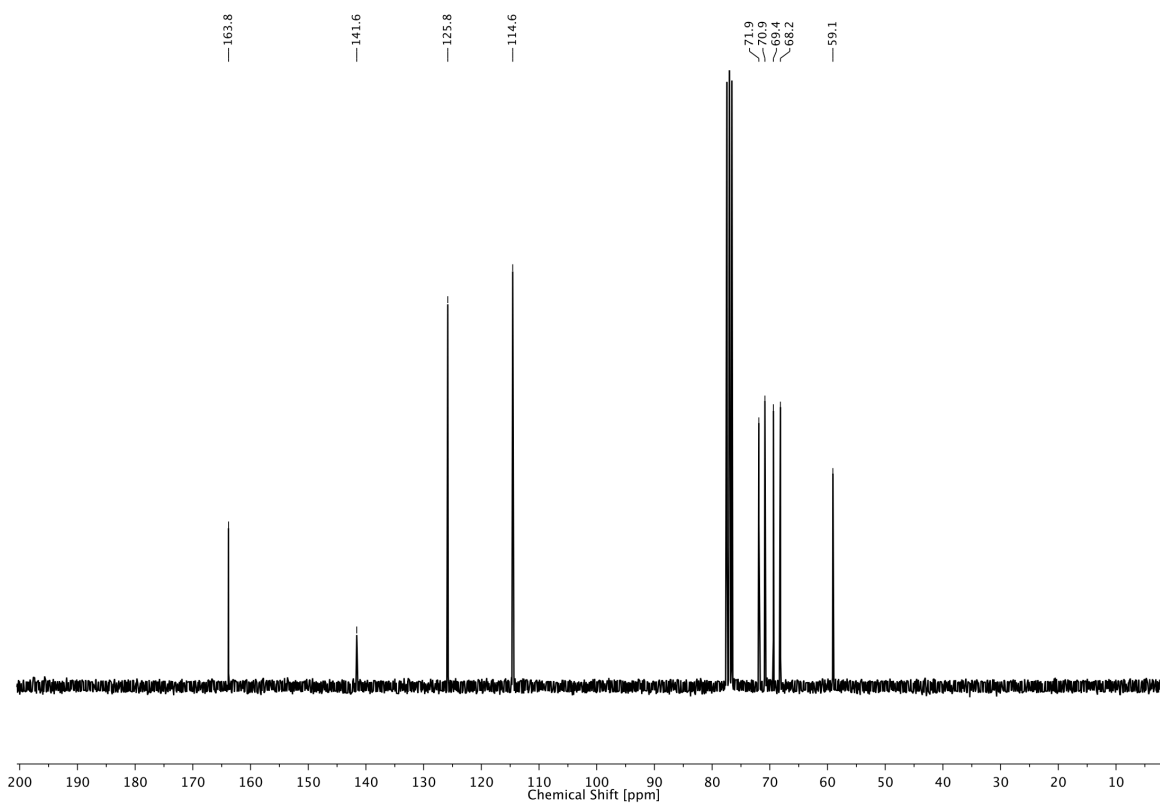
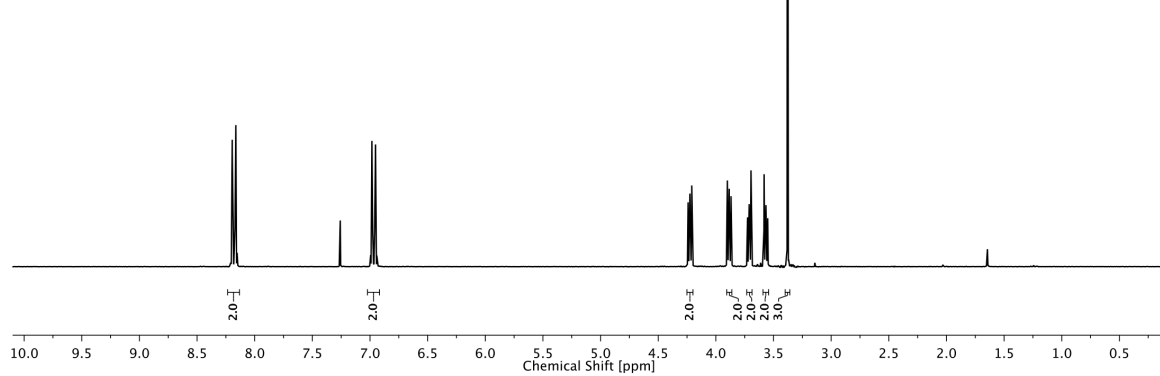
2 PHOTOREGULATION OF GABA_A RECEPTORS



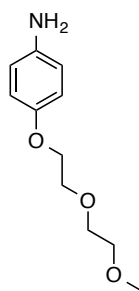
2 PHOTOREGULATION OF GABA_A RECEPTORS



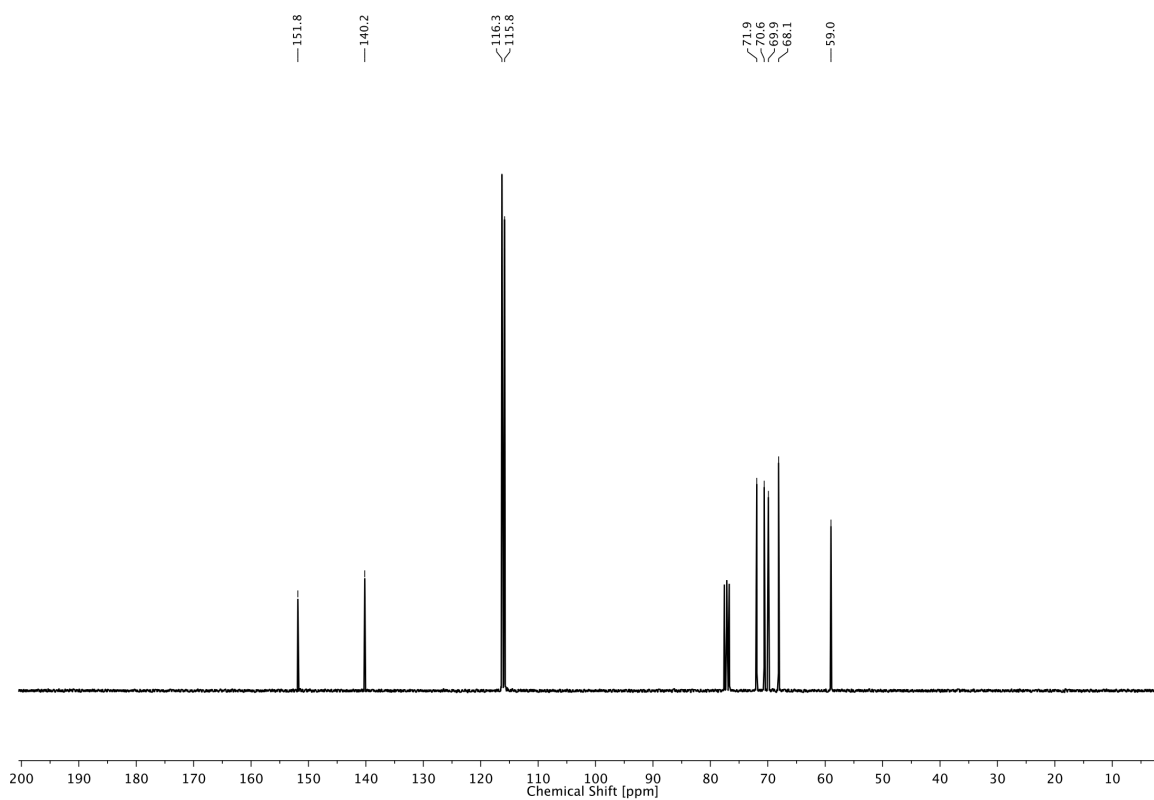
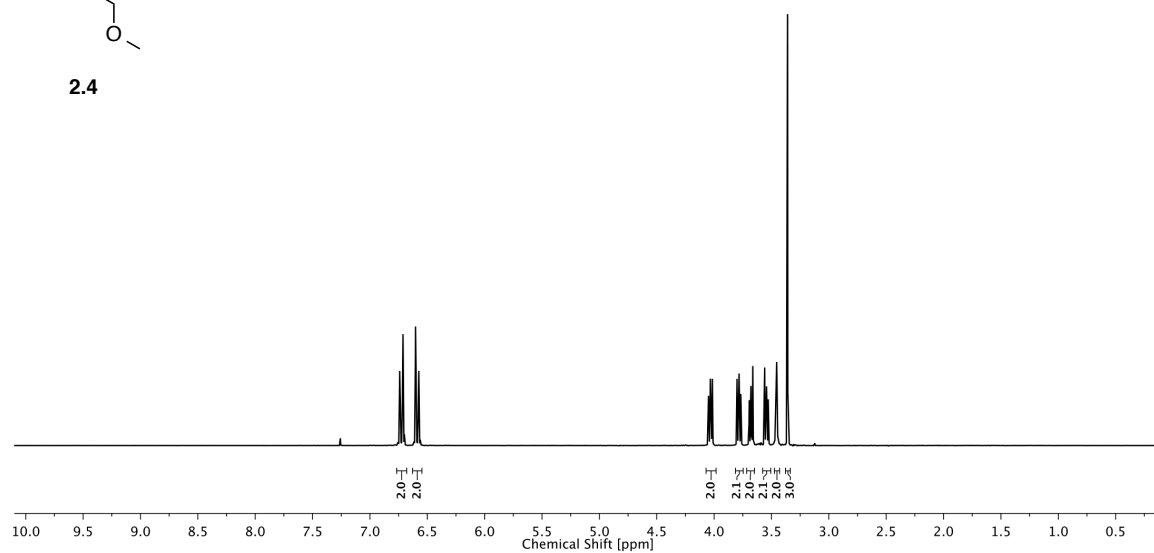
2.3



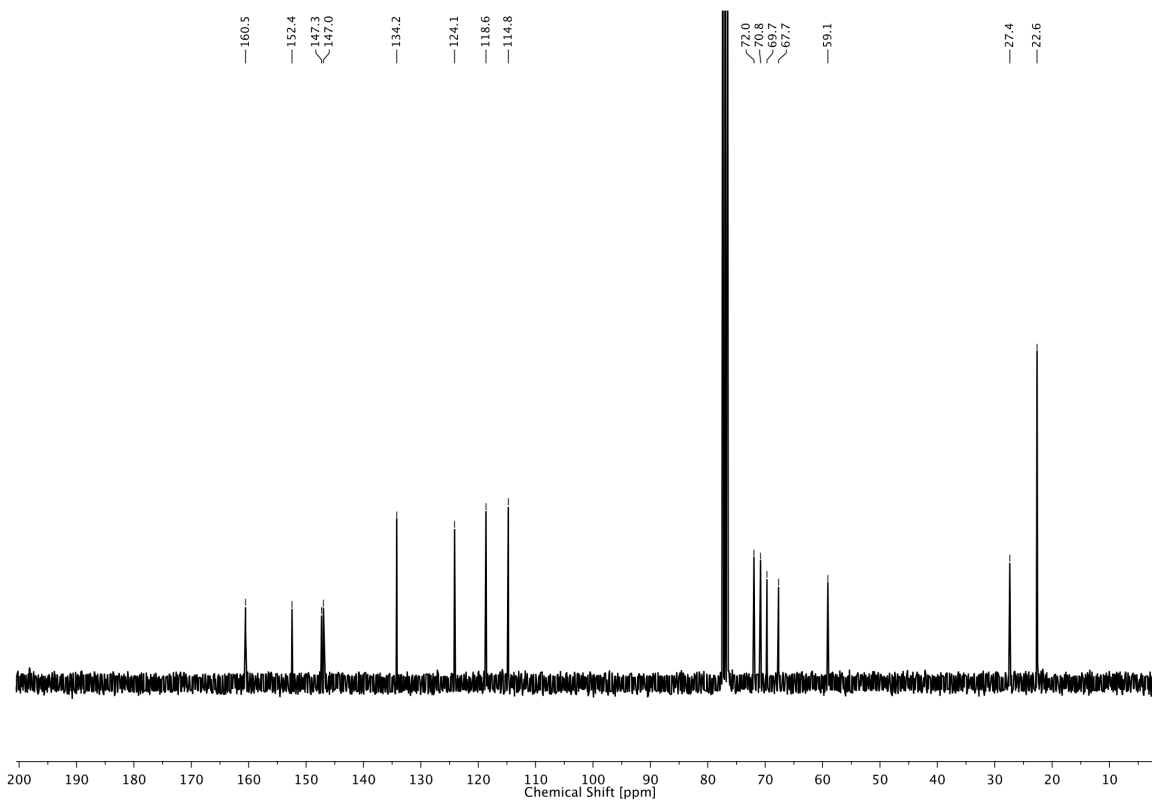
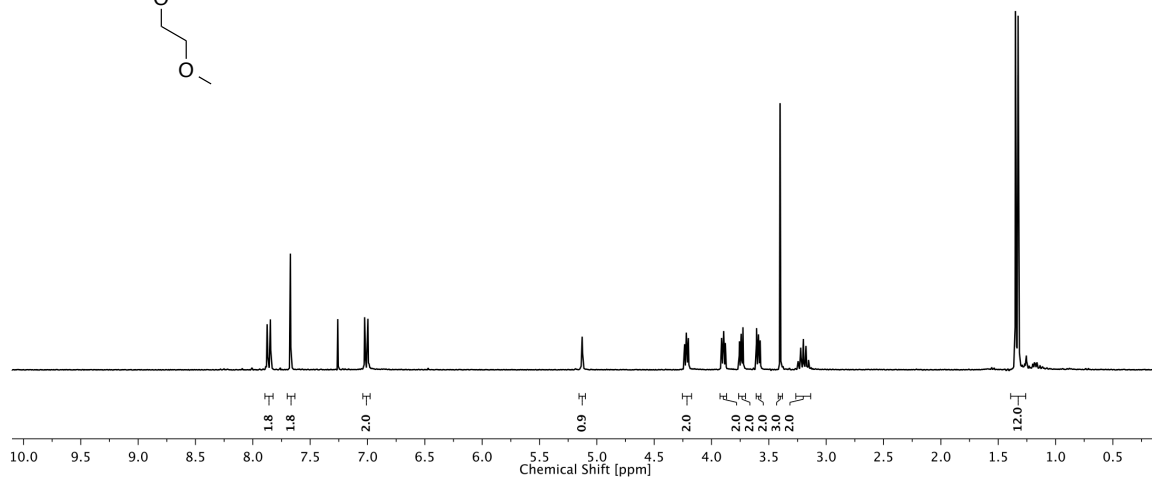
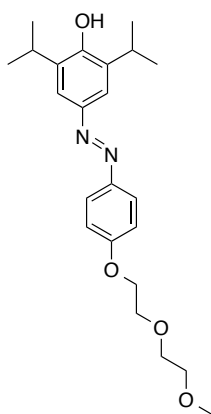
2 PHOTOREGULATION OF GABA_A RECEPTORS



2.4



2 PHOTOREGULATION OF GABA_A RECEPTORS



UV/Vis Spectra

UV/Vis spectra of **AP1–16** were recorded at concentrations of 50 μM in DMSO (**AP2–16**) or CHCl_3 (**AP1**). Spectra were first recorded in the dark, then again after illumination with the absorption maximum wavelength for 1 min unless indicated otherwise.

AP1 shows solvatochromic behavior which is well known for 4-hydroxy-4'-nitro substituted azobenzenes (Fig. 2.3).^[14]

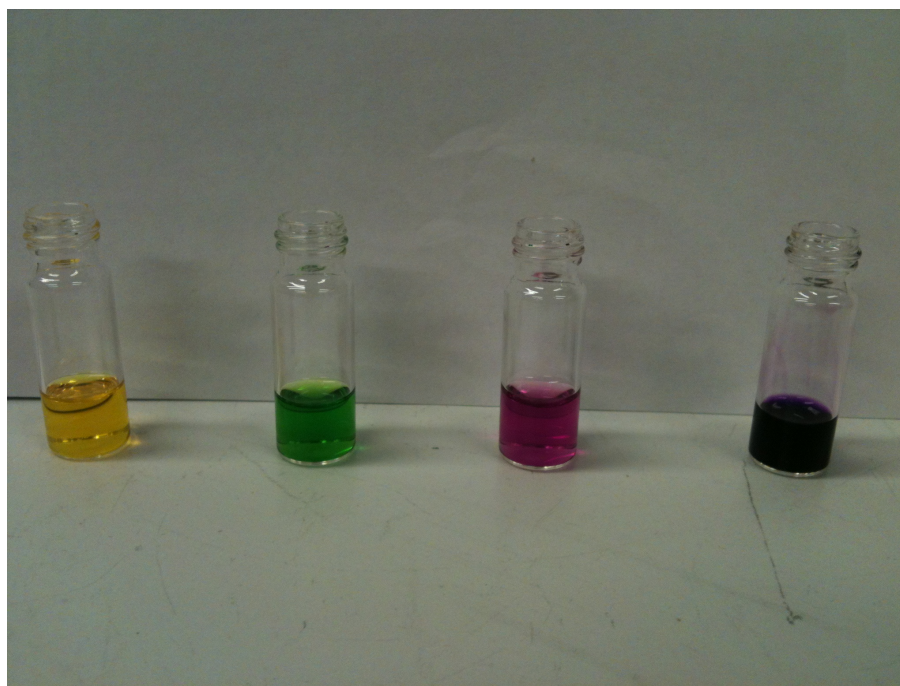
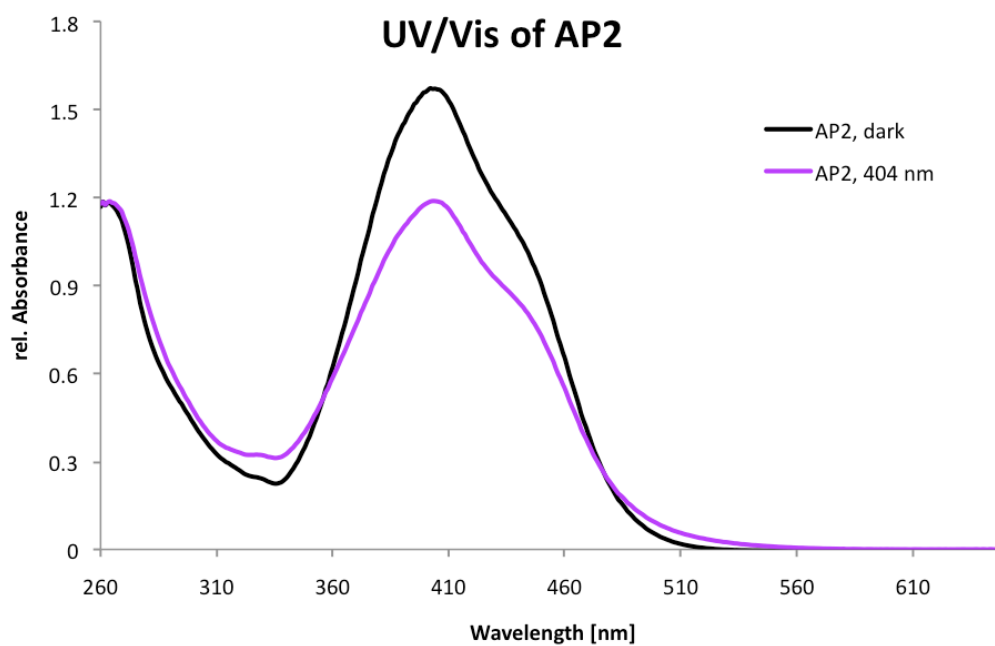
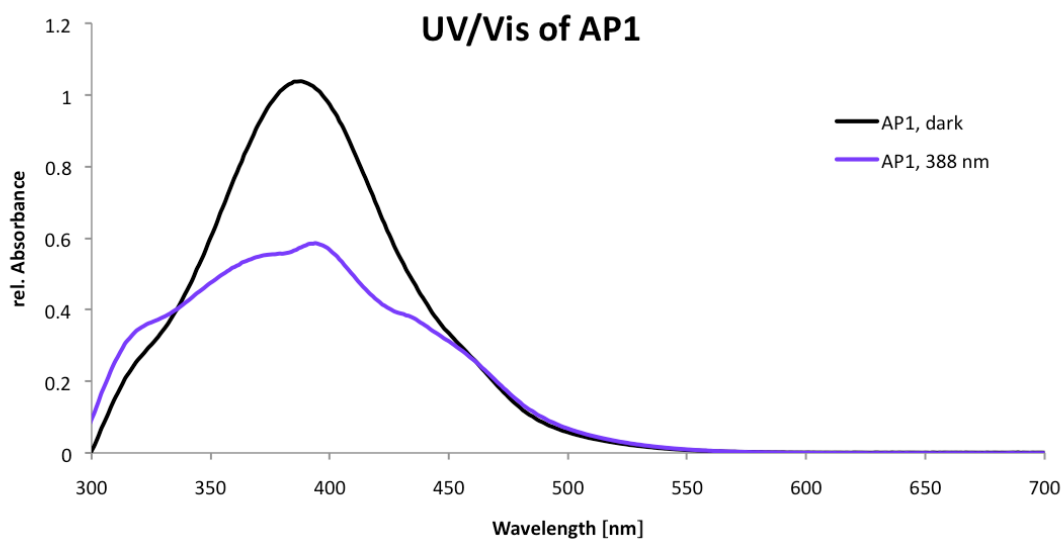
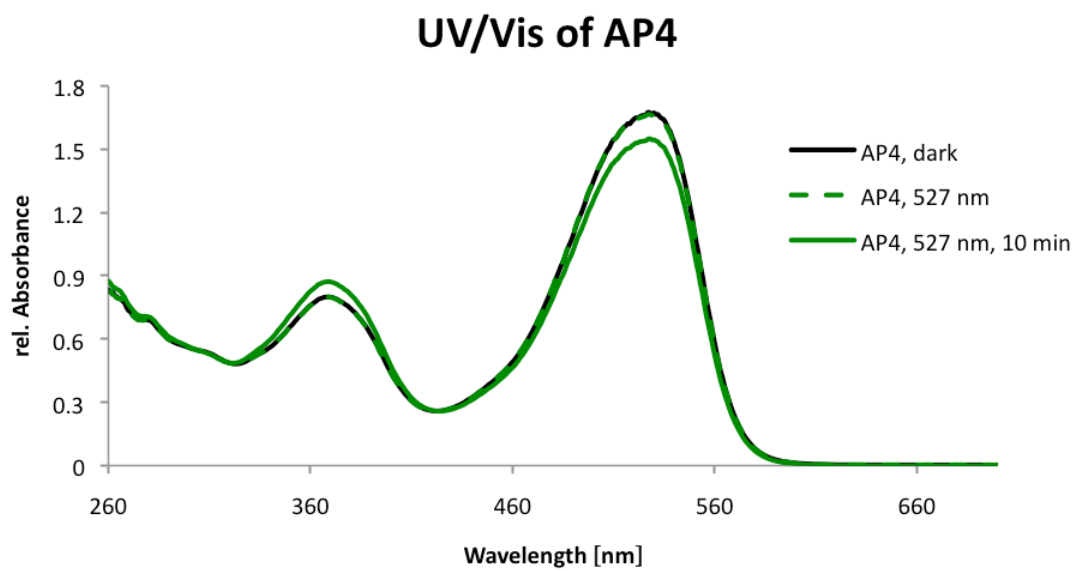
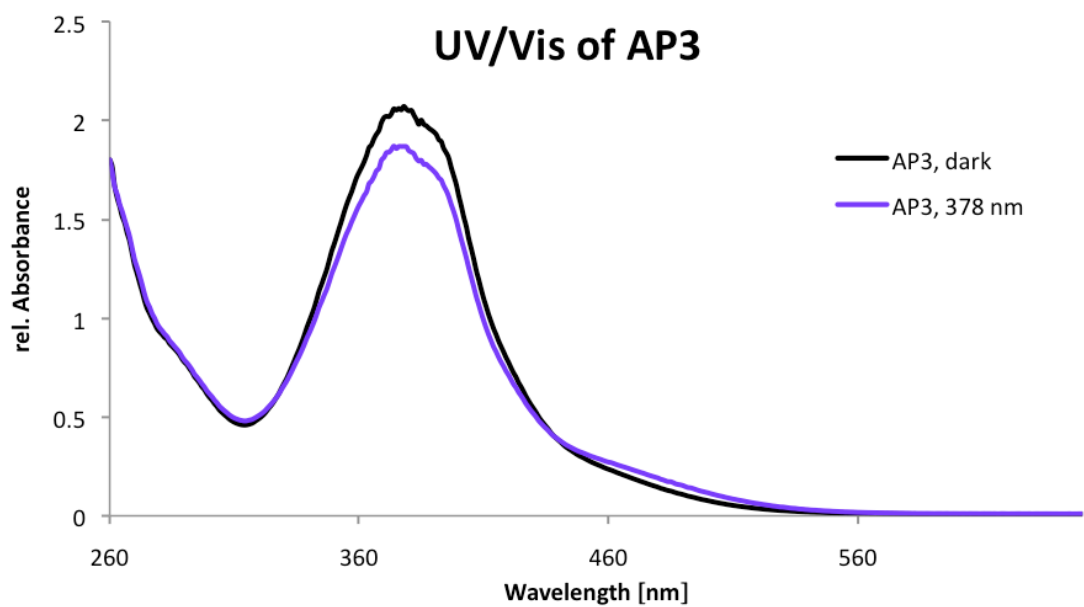
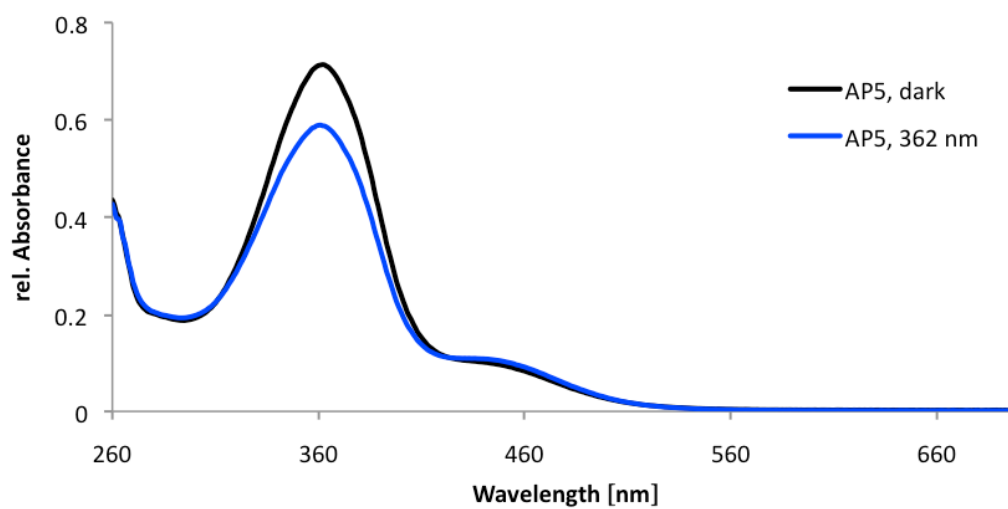


Figure 2.3. Solvatochromic behavior of **AP1**. Solution of **AP1** in from left to right: CHCl_3 , DMSO, 1 M NaOH (each 50 μM **AP1**), 1 M NaOH (500 μM **AP1**).

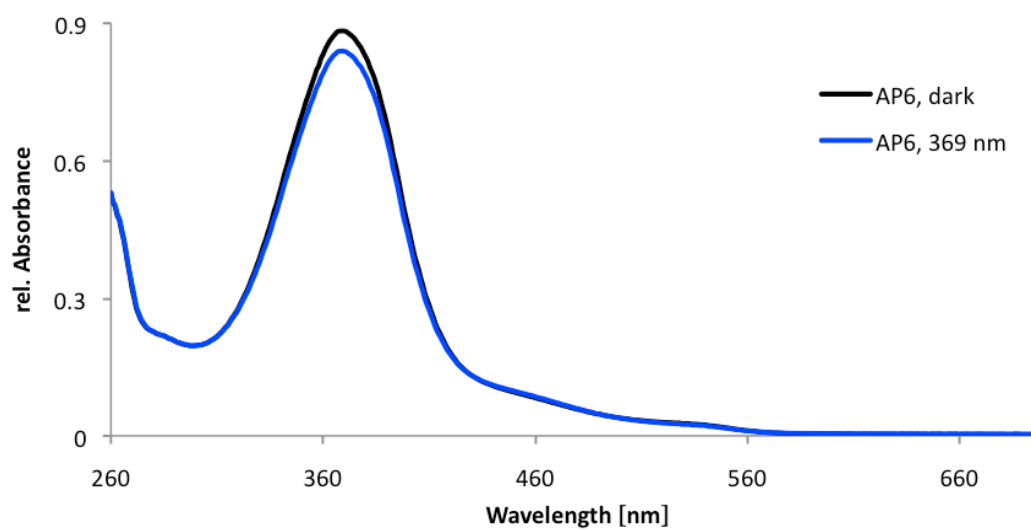




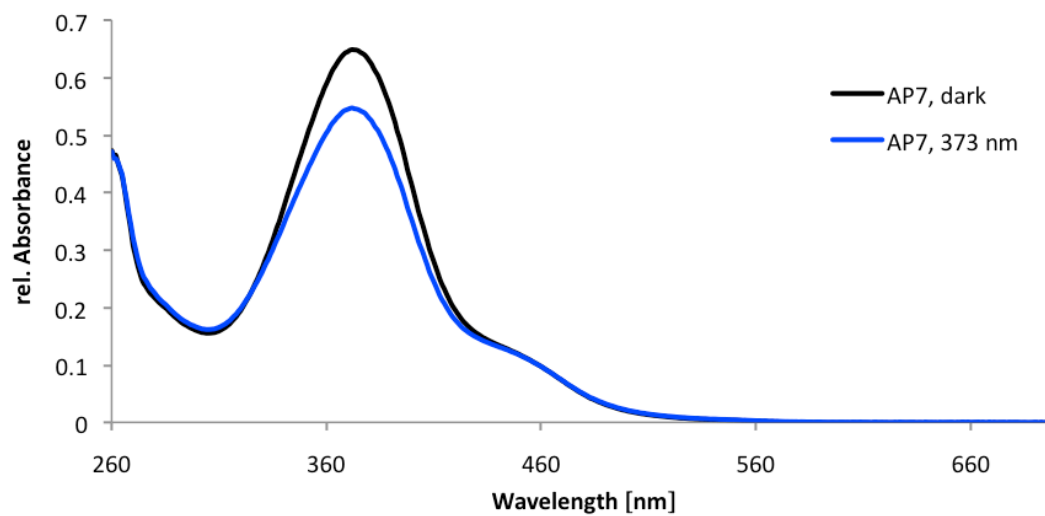
UV/Vis of AP5



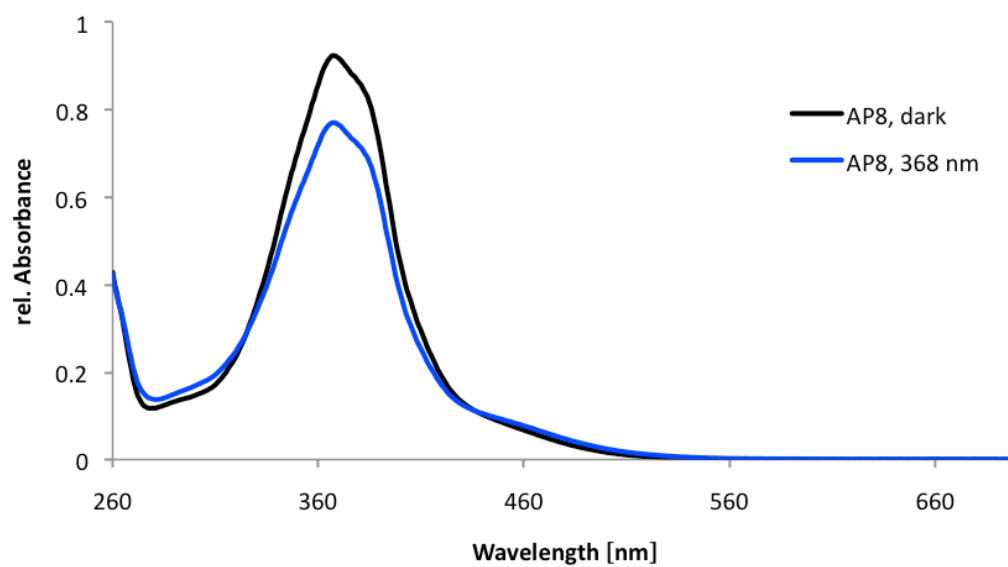
UV/Vis of AP6

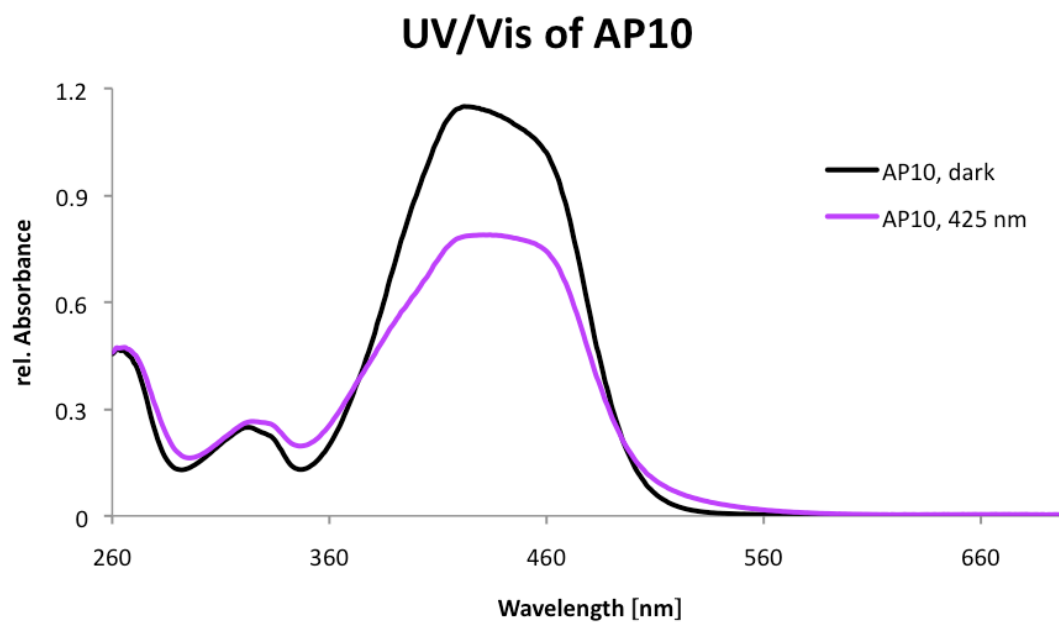
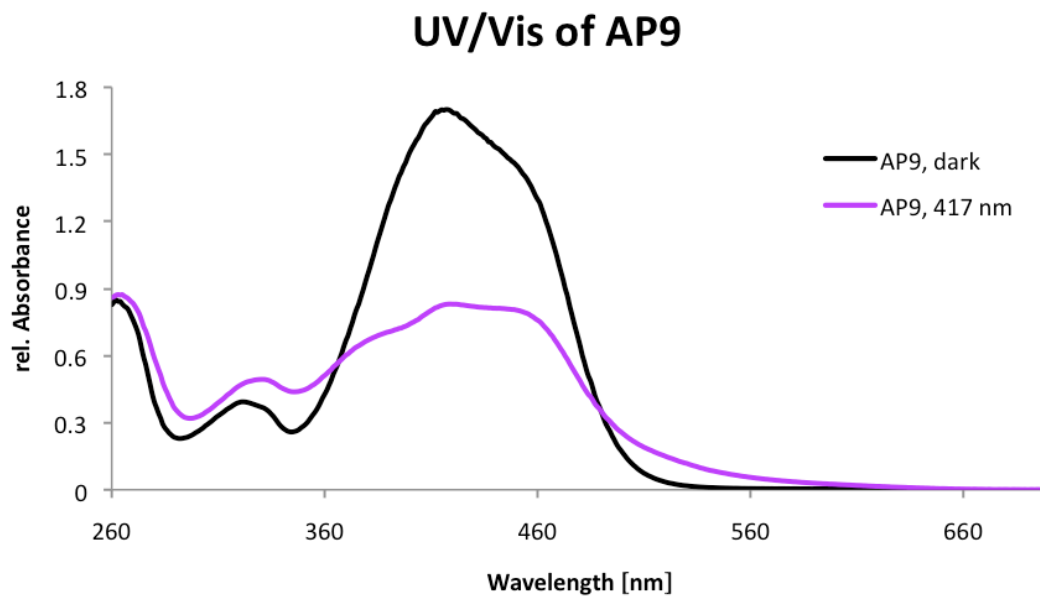


UV/Vis of AP7

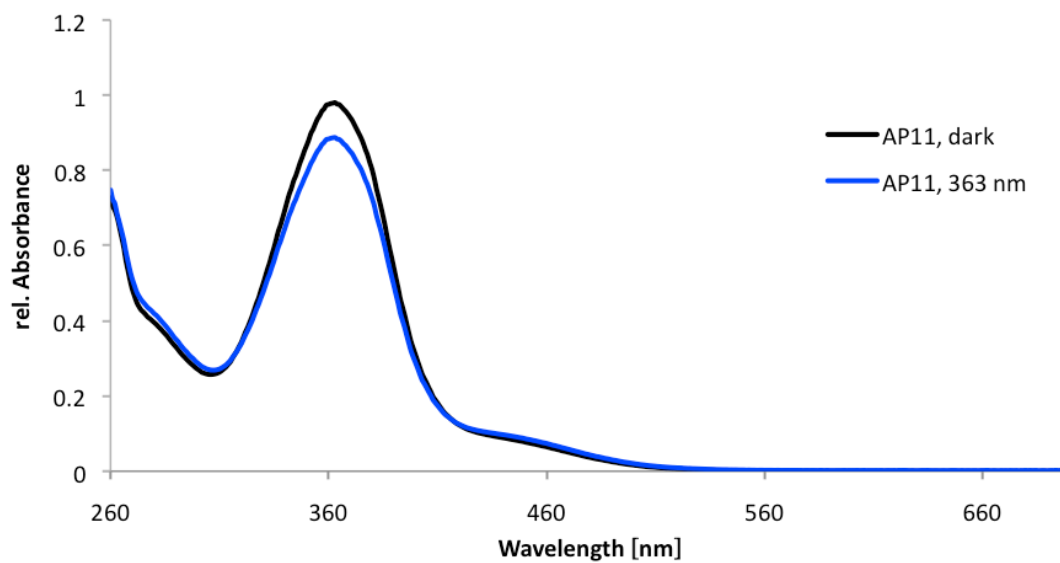


UV/Vis of AP8

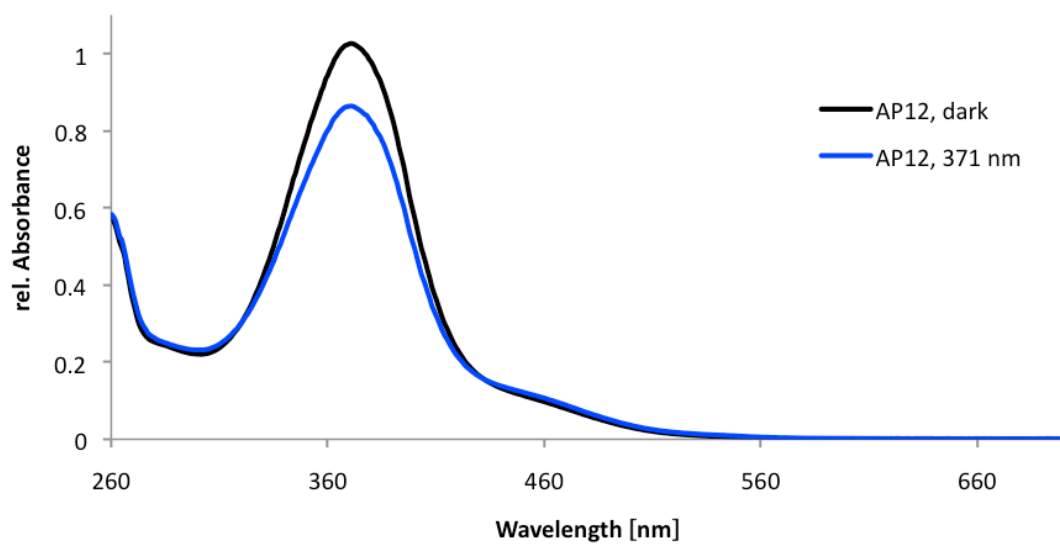




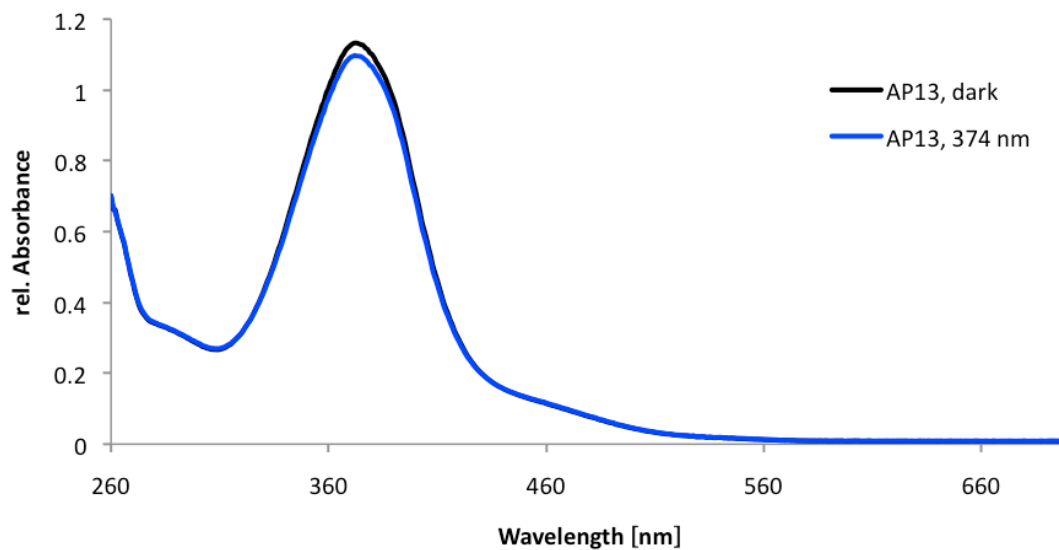
UV/Vis of AP11



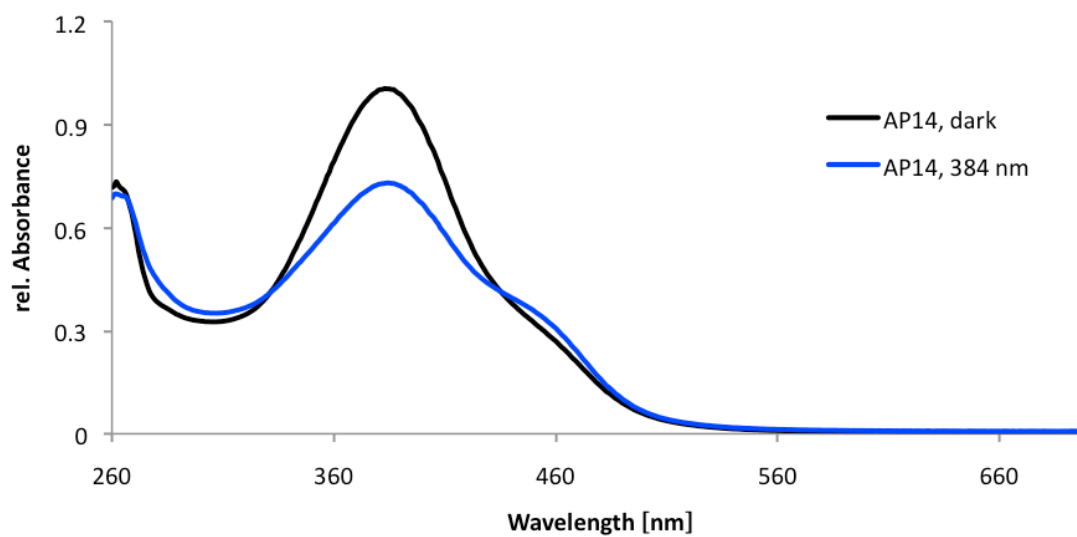
UV/Vis of AP12



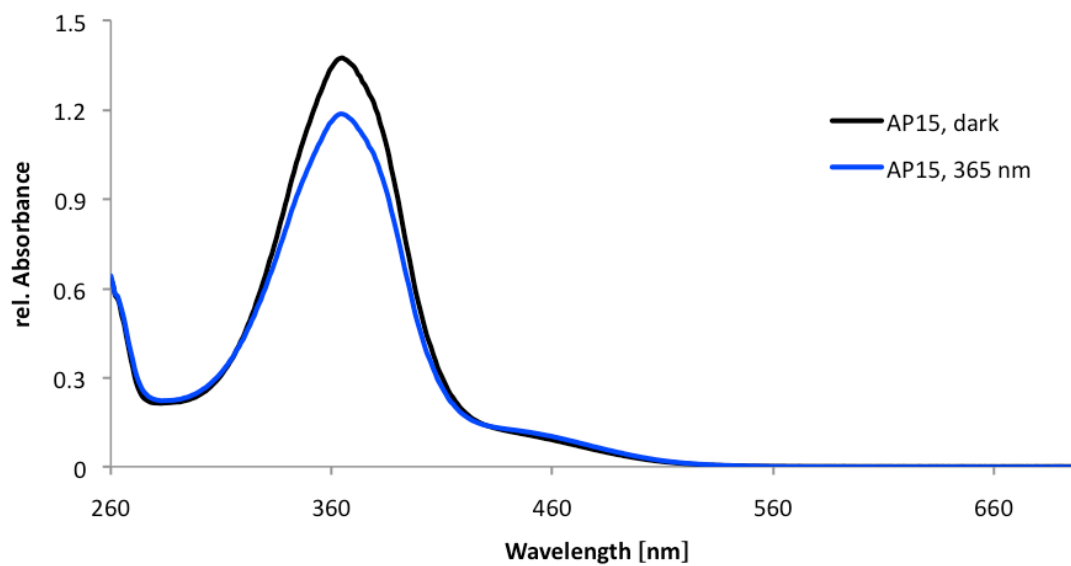
UV/Vis of AP13



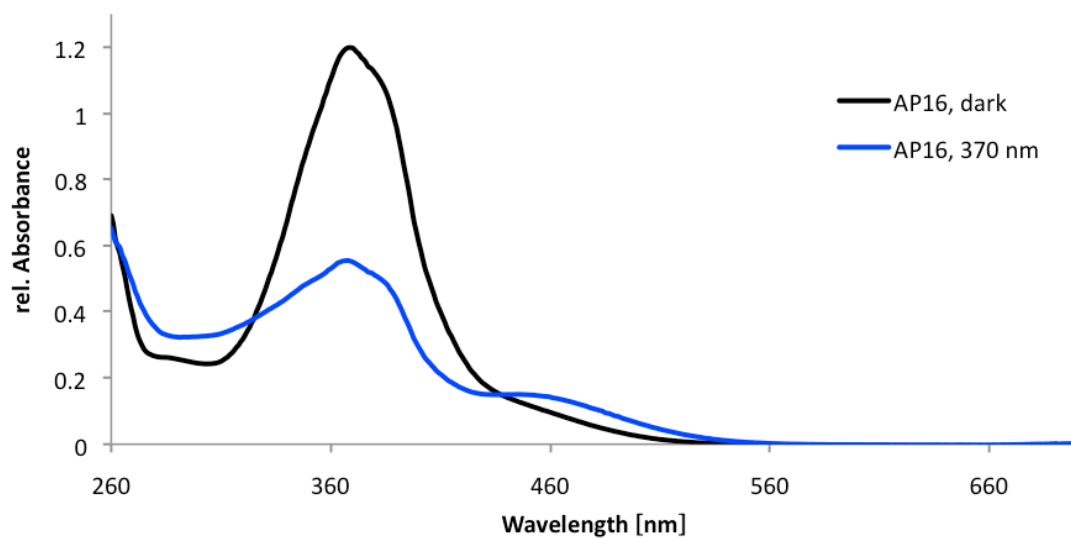
UV/Vis of AP14



UV/Vis of AP15



UV/Vis of AP16



Expression and Functional Characterization in *Xenopus* Oocytes

Capped cRNAs were synthesized (Ambion, Austin, TX, USA) from the linearized plasmids with a cytomegalovirus promotor (pCMV vectors) containing rat α_1 , β_2 , or γ_2 L subunits, respectively. A poly-A tail of about 400 residues was added to each transcript using yeast poly-A polymerase (United States Biologicals, Cleveland, OH, USA). The concentration of the cRNA was quantified on a formaldehyde gel using Radiant Red stain (Bio-Rad) for visualization of the RNA. Known concentrations of RNA ladder (Invitrogen) were loaded as standard on the same gel. cRNAs were precipitated in ethanol/isoamylalcohol 19 : 1, the dried pellet dissolved in water and stored at -80°C . cRNA mixtures were prepared from these stock solutions and stored at -80°C .

Xenopus laevis oocytes were prepared, injected and defolliculated as described previously.^[15,16] They were injected with 50 nL of the cRNA solution containing wild type α_1 , β_2 and γ_2 subunits at a concentration of 10 nM : 10 nM : 50 nM,^[17] and then incubated in modified Barth's solution (10 mM HEPES-NaOH, pH = 7.5, 88 mM NaCl, 1 mM KCl, 2.4 mM NaHCO₃, 0.82 mM MgSO₄, 0.34 mM Ca(NO₃)₂, 0.41 mM CaCl₂, 100 units/mL penicillin, 100 $\mu\text{g}/\text{mL}$ streptomycin) at $+18^{\circ}\text{C}$ for at least 24 h before the measurements.

Electrophysiological experiments were performed by using the two-electrode voltage clamp method at a holding potential of -80 mV. The perfusion medium contained 90 mM NaCl, 1 mM KCl, 1 mM MgCl₂, 1 mM CaCl₂, and 5 mM Na-HEPES (pH = 7.4). Solutions contained a final concentration of 0.5% DMSO to ensure solubility of the compounds.

Concentration-response curves for propofol were measured at a GABA concentration eliciting about 0.3% of the maximal GABA current amplitude ($EC_{0.3}$). GABA was repetitively applied until a constant response was obtained. Subsequently, the oocyte was exposed to the same concentration of GABA in combination with increasing concentrations of propofol or **AP2**. Relative current potentiation by propofol was calculated using the following equation: $[(I_{\text{GABA+Propofol}}/I_{\text{GABA}}) - 1] \times 100\%$. The perfusion system was cleaned between drug applications by flushing with DMSO to avoid contamination.

For photoswitching experiments the oocyte was exposed to an Ultrafire® 1 Watt UV LED pocket lamp (YonC Trading, Zürich; emission wavelength $\lambda = 390\text{--}450$ nm according to the manufacturer) at a distance of ~ 3 cm. The oocytes were continuously perfused at 6 ml/min.

Expression and Functional Characterization in HEK 293 Cells

Human embryonic Kidney 293 cells (HEK 293 cells; American Type Culture Collection-CRL-1573) were maintained in minimum essential medium (Invitrogen) supplemented with 10% fetal calf serum, 2 mM glutamine, 50 units/mL penicillin and 50 µg/mL streptomycin at 37 °C in 5% CO₂–95% air. For electrophysiological experiments (whole-cell patch clamp), cells were plated onto poly-D-lysine (0.01 mg/ml, Sigma) coated culture dishes (Nunc). Equal amounts (total of 3 µg DNA/35 mm dish) of plasmids coding for rat α_1 , β_2 , γ_2 , GABA_A receptor subunits were transfected into HEK 293 cells by the calcium phosphate precipitation method.^[18] As a marker for successfully transfected cells, cDNA encoding green fluorescent protein was co-transfected (0.3 µg DNA/35 mm dish) together with the GABA_A receptor subunits. After overnight incubation, the cells were washed twice with serum free medium and refed with medium.

The kinetics of the action of **AP2** were studied using the patch clamp technique in the whole cell configuration. HEK 293 cells were bathed in an external solution containing (mM): 140 NaCl, 5 KCl, 4 MgCl₂, 1 CaCl₂, 10 HEPES and 5 Glucose; pH adjusted to pH = 7.4 with NaOH. Patch pipettes were pulled from thin-walled borosilicate glass (GC150TF; Harvard Apparatus) using a DMZ universal puller (Zeitz-Instruments). Patch electrodes of a resistance of 2.5–3 M Ω were filled with an internal solution containing (mM): 135 CsCl, 2 MgCl₂, 0.5 EGTA, 10 HEPES, 2 MgATP; pH adjusted to pH = 7.2 with CsOH. This combination of external and internal solution produced a chloride equilibrium potential of ~0 mV. Measurements were performed using an EPC-10 amplifier (HEKA, Lambrecht/Pfalz, Germany). The currents were sampled at 0.5 kHz and filtered with a 0.1 kHz Bessel filter. Cells were voltage-clamped at –60 mV and solutions containing either 0.5 µM GABA or 0.5 µM GABA in combination with 5 µM **AP2** were applied using a perfusion system consisting of glass reservoir connected to a Warner Perfusion solenoid mini valve control system (Harvard Apparatus). The rate of solution exchange time was ~5 s. After bath application of **AP2** for 5 s, the perfusion system was switched off to avoid addition of new *trans*-**AP2**. The cells were exposed to the UV light as described above. The time course of current amplitudes was fitted with a mono-exponential function using the software Kaleidagraph.

Anesthetic Effects and Photo-reversibility in *Xenopus laevis* Tadpoles

Early pre-limb-bud stage albino *Xenopus* tadpoles were purchased from Xenopus One (Ann Arbor, MI, USA). Tadpoles were housed and used in accordance with federal and state guidelines and with the approval of the Massachusetts General Hospital Subcommittee on Research and Animal Care. Loss of righting reflexes (LORR), a standard measure of hypnotic drug effect, was assessed at room temperature (20 to 22 °C) for both propofol and **AP2** at concentrations ranging from 0.1 to 10 μM. A total of 10 animals were tested at each drug concentration by immersion in aqueous solutions of the anesthetics. Control groups of 10 animals were tested in water without drugs. In groups of 5 animals, a fire-polished glass rod was used to gently reposition animals from their normal prone position into a supine position. Animals that did not return to prone position in 5 seconds were deemed to have lost righting reflexes. The drug exposure time until steady-state LORR responses was noted. After immersion in drug for 30 min, $\lambda = 360\text{--}370$ nm illumination was provided using a handheld LED flashlight (5W handheld LED UV torch with $\lambda = 365$ nm peak spectral output, purchased from Uveco GmbH, Bruckmühl, Germany) and a bandpass filter (D365/10x, purchased from Chroma Technology Corp., Bellows Falls, VT, USA) at a distance of approximately 5 cm, while LORR was reassessed. The center of the illumination beam was aimed at individual tadpoles in turn for 5–10 seconds. Following photo-reversal testing, all animals were returned to clean water and observed for one hour to confirm reversibility of drug effects.

Logistic functions of the form $\text{Fraction LORR} = 1/(1+10^{((\text{LogEC}_{50}-\text{LogDrug})\cdot nH)})$ were fitted to results (in the absence *versus* presence of UV light) using GraphPad Prism software (v. 5.0, GraphPad Software, La Jolla, CA, USA). EC_{50} is the half-effect drug concentration for LORR and nH is the Hill slope.

2.3 PHOTOCROMIC POTENTIATION OF GABA_A RECEPTORS BY AZOBENZENE DERIVATIVES OF ETOMIDATE

Etomidate (ETD; also marketed under the name Amidate[®]) was discovered by Janssen Pharmaceutica in 1964.^[19] ETD functions as a short acting intravenous anesthetic and sedative. Due to its rapid onset of action (< 1 min), easy dosing profile and low likelihood of blood pressure decrease it is often used in emergency cases. Like with propofol, induction of anesthesia by ETD is not yet fully understood, but it is believed that the anesthetic effect is also mediated by potentiation of GABA-induced hyperpolarizing chloride currents.

Building up on previous results of Azo-Propofol derivatives (see 2.2), photoswitchable derivatives of ETD were synthesized in order to optochemically control GABA_ARs.

2.3.1 AZO-ETOMIDATES AS POTENTIAL PHOTOCROMIC GABA_AR POTENTIATORS

The pentameric ligand-gated GABA_A receptor is a chloride-selective ion channel that is activated by the major inhibitory neurotransmitter in the mammalian brain, γ -aminobutyric acid (GABA).^[20] GABA-binding leads to hyperpolarization of the postsynaptic neuron, thus decreasing the likelihood of action potential firing. As a consequence, GABA_A receptors are prominent targets for anesthetic, hypnotic, and anticonvulsant drugs.^[21] Most of these drugs, such as benzodiazepines, barbiturates, or the clinically widely used propofol, are allosteric modulators that potentiate GABA-induced chloride currents (Fig. 2.4).^[22] These potentiators bind to distinct allosteric sites on GABA_A receptors and increase the mean open time of the channel or its opening frequency.

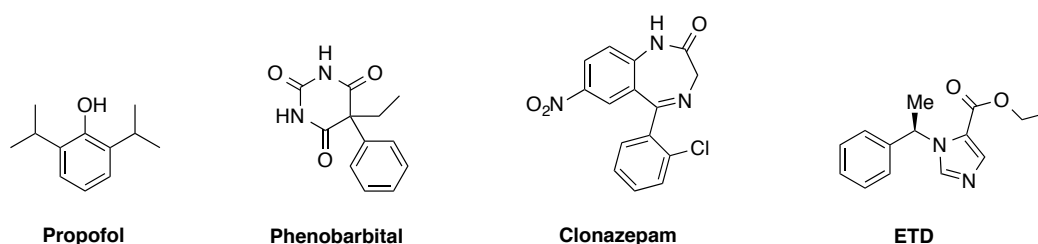


Figure 2.4. Structures of propofol, the barbiturate phenobarbital, the benzodiazepine clonazepam and ETD (positive allosteric modulators of GABA_ARs).

Following the recent studies on photoswitchable propofol derivatives for the optochemical control of GABA_ARs, the pharmacology of ETD, another highly potent allosteric potentiator of GABA_ARs, was investigated in more detail. ETD is a general anesthetic drug in clinical use

which induces anesthesia with a half effective concentration of $\sim 2 \mu\text{M}$.^[23] Due to its easy dosing profile and its ability to quickly induce anesthesia without suppressing ventilation, it is often used in emergency cases.^[24] Moreover, it decreases intracranial pressure while maintaining arterial pressure, thus making it a preferred anesthetic for brain surgery.^[25] ETD not only interacts with GABA_ARs but also with other members of the Cys-loop receptor family, such as glycine, serotonin (5-HT) and acetylcholine (ACh) receptors,^[26] and moreover is a potent inhibitor of 11 β -hydroxylase.^[27] However, GABA_A is the most sensitive receptor to etomidate.^[28] Like propofol, ETD also directly activates GABA_ARs at higher concentrations.^[29] Although propofol and ETD share a lot of features, some differences between the two drugs do exist. ETD mainly acts on GABA_ARs, containing β_2 and β_3 subunits, whereas propofol appears to act on all GABA_ARs, regardless of the β subunit type.^[30]

Inspired by binding studies of diazirine-containing derivatives of etomidate that maintained their action on GABA_ARs,^[29,31] two classes of photoswitchable azobenzene derivatives of ETD were designed (Fig. 2.5). **AETD1** bears the azobenzene moiety on the phenyl portion of ETD, while **AETD2–5** feature the azobenzene on the ester portion of the molecule.

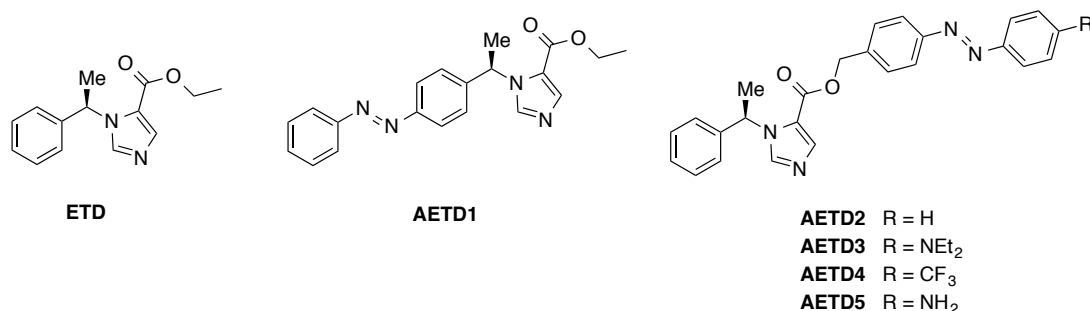
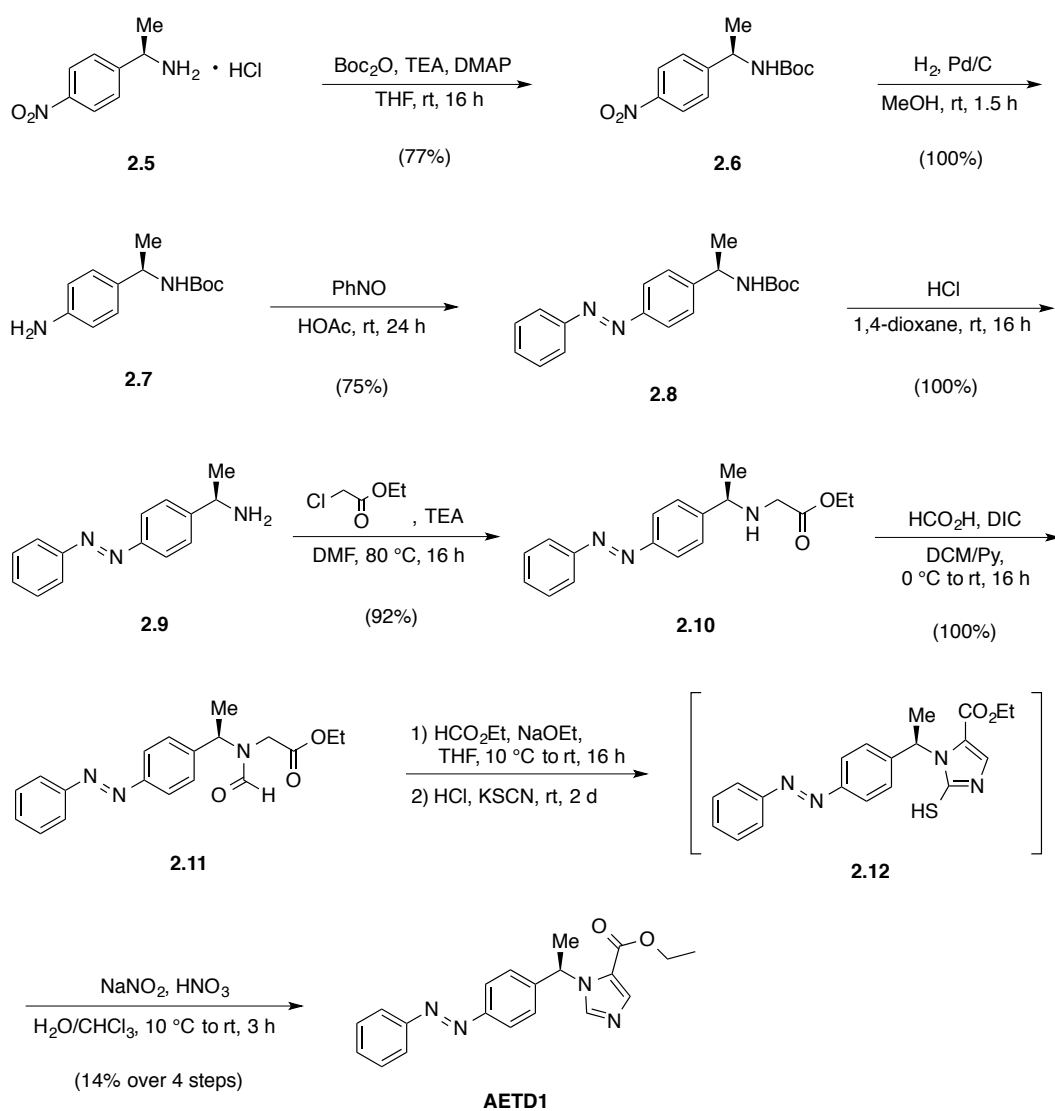


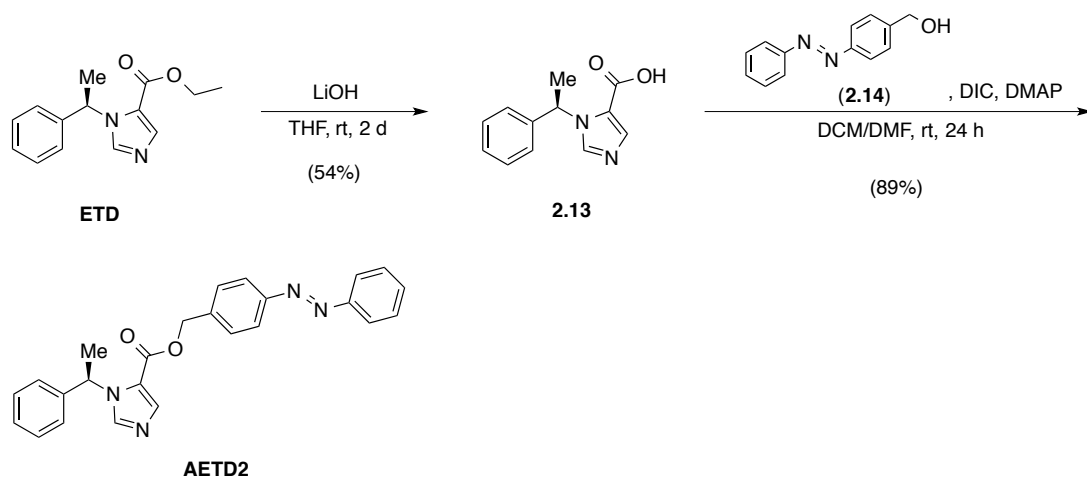
Figure 2.5. Structures of ETD and **AETD1–5**.

AETD1 was synthesized *de novo*, starting from chiral amine **2.5** in analogy to a literature protocol.^[26,29a] Boc protection of the amine gave compound **2.6** in 77% yield which was then reduced quantitatively with hydrogen and palladium on charcoal to aniline **2.7**. Compound **2.7** was subjected to a Mills reaction with nitrosobenzene to afford azobenzene **2.8** in 75% yield. The Boc group was deprotected to give quantitatively primary amine **2.9**, followed by condensation with ethyl chloroacetate to afford secondary amine **2.10** in 92% yield. Formyl protection quantitatively led to **2.11** which was converted in a two-step procedure to mercaptoimidazole **2.12**. Oxidative desulfurization of **2.12** finally yielded **AETD1** (Scheme 2.5).



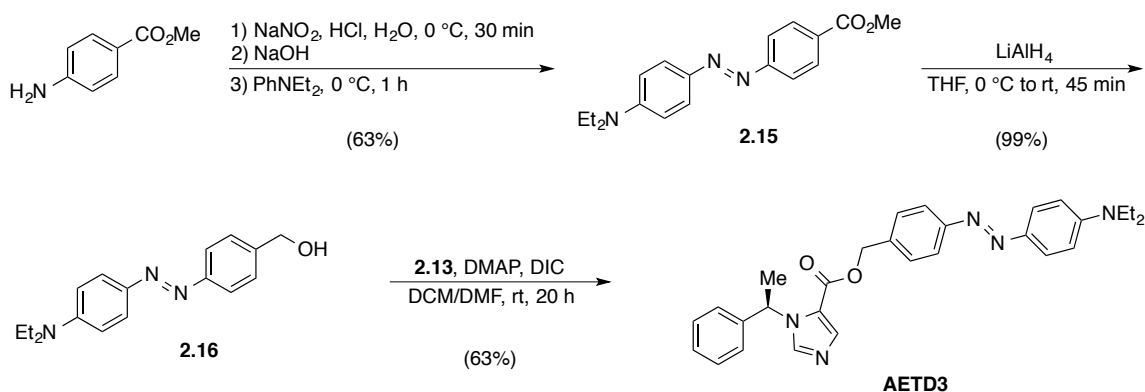
Scheme 2.5. Synthesis of **AETD1**.

By contrast, **AETD2** was synthesized starting from **ETD** itself. Ester hydrolysis under basic conditions afforded carboxylic acid **2.13** in 54% yield which was then reesterified with azobenzene alcohol **2.14** to give **AETD2** (Scheme 2.6).



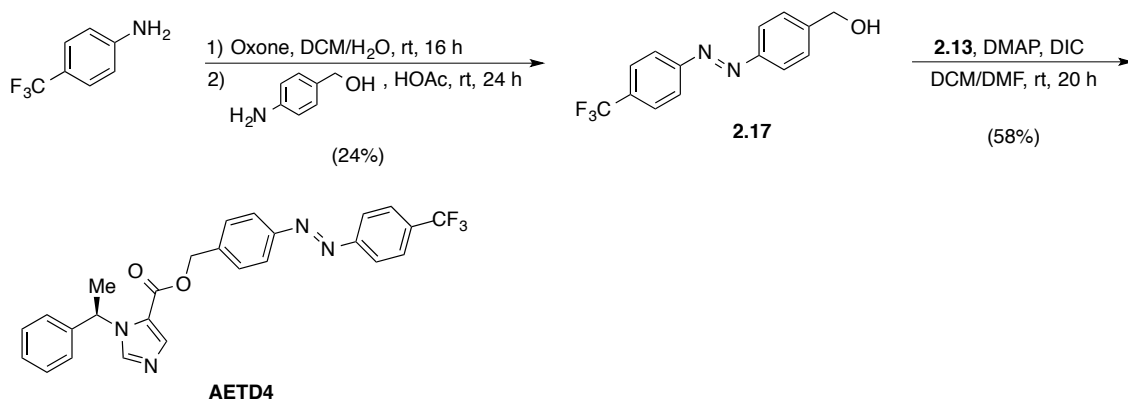
Scheme 2.6. Synthesis of **AETD2**.

AETD3–5 were synthesized accordingly. Methyl 4-aminobenzoate was diazotated and coupled to *N,N*-diethylaniline to give azobenzene **2.15** in 63% yield. Reduction of the ester using LiAlH_4 gave alcohol **2.16** in excellent yield. Esterification with carboxylic acid **2.13** then yielded **AETD3** in 63% (Scheme 2.7).



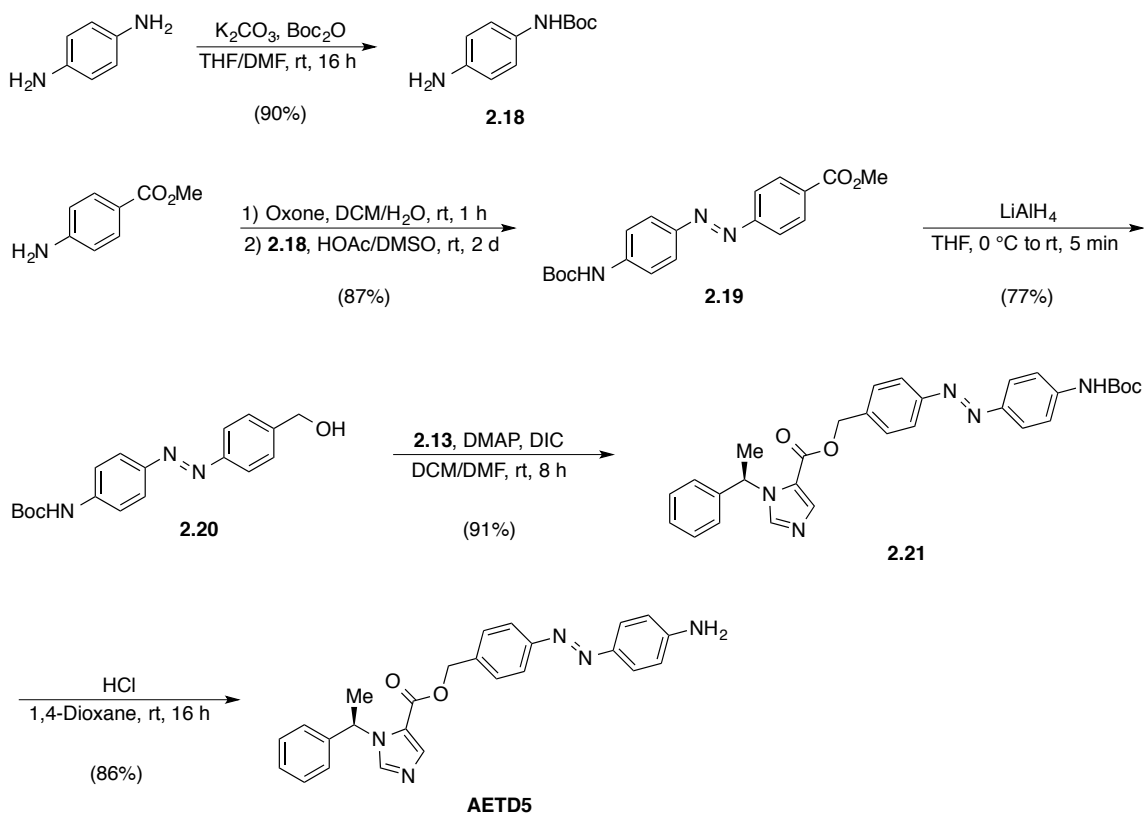
Scheme 2.7. Synthesis of **AETD3**.

For the synthesis of **AETD4**, 4-trifluoromethylaniline was oxidized to the corresponding nitroso derivative and subjected to a Mills reaction with (4-aminophenyl)methanol to give azobenzene **2.17** in 24% yield. Coupling of **2.17** to carboxylic acid **2.13** gave **AETD4** in 58% yield (Scheme 2.8).



Scheme 2.8. Synthesis of **AETD4**.

Finally, the synthesis of **AETD5** commenced with single Boc protection of 1,4-phenylenediamine to give compound **2.18** in 90% yield. Methyl 4-aminobenzoate was then oxidized to the corresponding nitroso derivative using oxone and subsequently reacted with **2.18** to give azobenzene **2.19** in 87% yield. Reduction of the ester function with LiAlH₄ gave alcohol **2.20** which was then coupled to carboxylic acid **2.13** to yield compound **2.21** in 91% yield. Deprotection of the Boc group with HCl afforded **AETD5** in 86% yield (Scheme 2.9).



Scheme 2.9. Synthesis of **AETD5**.

All AETDs were first tested for their ability to potentiate GABA-induced currents mediated by $\alpha_1\beta_2\gamma_2$ receptors expressed in *Xenopus oocytes* (Simon Middendorp, IBMM Bern). Early on, **AETD2** proved to be the best candidate for further biological evaluation. Whereas **AEDT2** showed a current potentiation of >2000% on $\alpha_1\beta_2\gamma_2$ and $\alpha_1\beta_3\gamma_2$ receptors, **AETD3–5** gave potentiations of 400–800% (data not shown) and were therefore not further evaluated.

At low concentrations (corresponding to the therapeutic window of ETD), **AETD2** shows increased potency compared to ETD (Fig. 2.6). The EC₅₀ values for **AETD2** were determined to be 0.29 ± 0.08 and 0.33 ± 0.06 μM acting on $\alpha_1\beta_2\gamma_2$ and $\alpha_1\beta_3\gamma_2$ receptors, respectively, compared to 3.2 ± 0.7 and 3.5 ± 0.4 μM for ETD, respectively (mean \pm SEM, n = 4). However, **AETD2** shows a ~2-fold lower efficacy than ETD. Exchanging the $\beta_{2/3}$ subunit with β_1 resulted in about a 10-fold rightshift of the apparent affinity for ETD which agrees with previously published data.^[30b] Concentration dependent potentiation in $\alpha_1\beta_1\gamma_2$ receptors by ETD was fitted with an EC₅₀ of 35.6 ± 0.7 μM . This fit has to be taken with care as saturation was not reached in this experiment. Interestingly, no strong reduction of the apparent affinity for **AETD2** on $\alpha_1\beta_1\gamma_2$ receptors was observed. The EC₅₀ amounted to 0.49 ± 0.09 μM , efficacy however was reduced by about 4-fold (Fig. 2.6b).

In sharp contrast to the results with **AEDT2–5**, **AETD1** proved to be almost inactive in the potentiation of GABA-induced currents, suggesting a limited space in the binding pocket in that region of the molecule (Fig. 2.6b). Although smaller substituents are tolerated at this position,^[31] the azo phenyl moiety of **AETD1** appears to be too large.

Having established that **AEDT2** functions as a potentiator of GABA currents, it was further investigated if it was possible to control this effect in light-dependent manner. Illumination with $\lambda = 365$ nm, emitted from a UV high power LED pocket lamp (5.2 Watt Uveco GmbH, Bruckmühl, Germany) isomerizes **AETD2** from its *trans* state to the *cis* state. The thermodynamically more stable *trans* isomer is regenerated by thermal relaxation in the dark (Fig. 2.6a; see also 2.3.4 for the UV/Vis spectra of all AETDs). Co-application of 2 μM GABA with 0.2 μM **AETD2** in the absence of light gave a current potentiation of $678 \pm 110\%$ (mean \pm SEM, n = 4) on $\alpha_1\beta_2\gamma_2$ receptors. Illumination with $\lambda = 365$ nm light isomerized **AETD2** to the *cis* form, leading to a reduction of potentiation of ~50 % of the potentiation seen in the dark, resulting in a residual potentiation of $338 \pm 48\%$. Similar observations were made in $\alpha_1\beta_3\gamma_2$ and $\alpha_1\beta_1\gamma_2$ receptors (Fig. 2.6c), whereas ETD did not exhibit any light-dependency in the same experiment (data not shown).

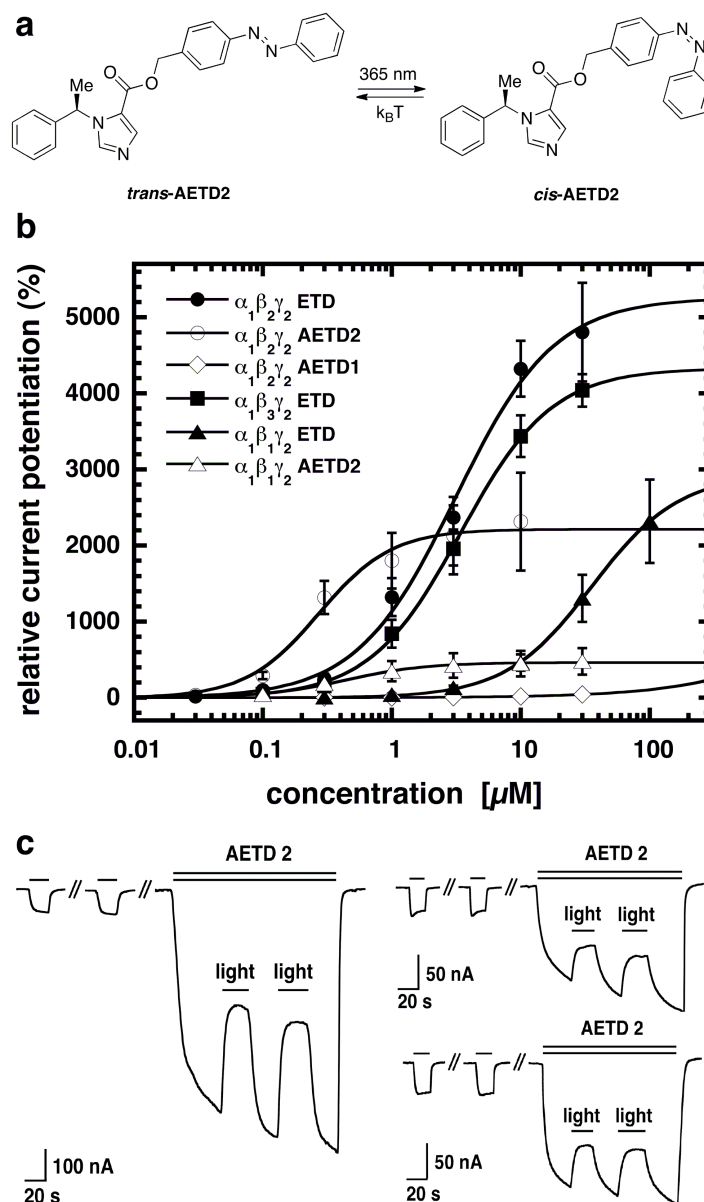


Figure 2.6. a) Photodependent isomerization between *trans*- and *cis*-AETD2, respectively. b) Concentration-dependent potentiation of $\alpha_1\beta_1\gamma_2$, $\alpha_1\beta_2\gamma_2$ and $\alpha_1\beta_3\gamma_2$ receptors by AETD1, AETD2 and ETD. Receptors were expressed in *Xenopus oocytes* and exposed to a GABA concentration eliciting 2% of the maximal current amplitude (EC_2) in combination with increasing concentrations of the drug. Potentiation of GABA currents in $\alpha_1\beta_3\gamma_2$ receptors by AETD2 is not shown as the curve overlaps with the curve obtained in $\alpha_1\beta_2\gamma_2$ receptors. Mean \pm SEM of four experiments is shown. c) Photodependent potentiation of chloride currents in $\alpha_1\beta_2\gamma_2$, (left), $\alpha_1\beta_3\gamma_2$ (top right) and $\alpha_1\beta_1\gamma_2$ receptors (bottom right). First, GABA ($EC_{0.5-2}$) (single bar) was applied alone and then co-applied with either 0.2, 0.1 or 0.3 μM AETD2 in $\alpha_1\beta_2\gamma_2$, $\alpha_1\beta_3\gamma_2$ and $\alpha_1\beta_1\gamma_2$ receptors, respectively. During co-application, the oocyte was exposed to $\lambda = 365 \text{ nm}$ light which resulted in a reduction of potentiation. When the light was turned off, the current amplitude increased again. Experiments were repeated independently four times using different oocytes (Simon Middendorp, IBMM Bern).

Switching off the light re-isomerizes **AETD2** back to its *trans* form, thereby increasing the current again. This process is fully reversible and occurs in the range of seconds.

To determine the kinetics of this light-dependent potentiation of GABA-induced currents by **AETD2**, the GABA_A receptor was expressed in HEK 293 cells. However, no light-dependent change in current potentiation could be observed with none of all AETDs (Simon Middendorp, IBMM Bern, data not shown). As of today, it remains unclear if the reversible, light-dependent current potentiation in oocytes is derived from different affinities of both *trans* and *cis* isomers of **AETD2**, respectively (as shown for Azo-Propofol), or rather from a light-dependent solubility of both isomers, resulting in different local concentrations of either isomer. The latter hypothesis is supported by the qualitative observation of the Tyndall effect when a solution of **AETD2** in aqueous buffer was illuminated with $\lambda = 365$ nm (Prof. Erwin Sigel, IBMM Bern) but could not be proven quantitatively as of today.

In summary, photochromic GABA_A potentiators based on the highly potent anesthetic etomidate (ETD) have been developed. The lead compound **AETD2** has a >10-fold increased affinity at all receptors investigated, when compared to ETD. On all three subtypes, **AETD2** potentiates GABA-induced currents in the dark in the *trans* state and significantly reduces this potentiation upon illumination with light, isomerizing **AETD2** to the *cis* state. This process is fully reversible and could provide a new optochemical tool for investigating the action of etomidate on GABA_ARs.

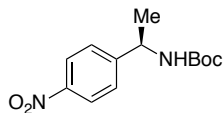
2.3.2 EXPERIMENTAL PROCEDURES AND ANALYTICAL DATA

2.3.2.1 GENERAL EXPERIMENTAL DETAILS AND INSTRUMENTATION

All reactions were carried out with magnetic stirring and if air or moisture sensitive in oven-dried glassware under an atmosphere of nitrogen or argon. Syringes used to transfer reagents and solvents were purged with nitrogen or argon prior to use. Reagents were used as commercially supplied unless otherwise stated. Thin layer chromatography was performed on pre-coated silica gel F₂₅₄ glass backed plates and the chromatogram was visualized under UV light and/or by staining using aqueous acidic vanillin or potassium permanganate, followed by gentle heating with a heat gun. Flash column chromatography was performed using silica gel, particle size 40–63 μm (eluants are given in parenthesis). The diameter of the columns and the amount of silica gel were calculated according to the recommendations of W. C. Still *et al.*^[32] IR spectra were recorded on a Perkin Elmer Spectrum Bx FT-IR instrument as thin films with absorption bands being reported in wave number (cm⁻¹). UV/Vis spectra were obtained using a Varian Cary 50 Scan UV/Vis spectrometer and Helma SUPRASIL precision cuvettes (10 mm light path).

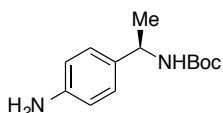
¹H and ¹³C NMR spectra were measured on Varian VNMRS 300, VNMRS 400, INOVA 400 or VNMRS 600 instruments. The chemical shifts are quoted as δ-values in ppm referenced to the residual solvent peak (CDCl₃: δ_H 7.26, δ_C 77.2; CD₃OD: δ_H 3.31, δ_C 49.0).^[12] Multiplicities are abbreviated as follows: s = singlet, d = doublet, t = triplet, q = quartet, quint = quintet, sext = sextet, sept = septet, m = multiplet. High resolution mass spectra (EI, ESI) were recorded by LMU Mass Spectrometry Service using a Thermo Finnigan MAT 95, a Jeol MStation or a Thermo Finnigan LTQ FT Ultra instrument. Melting points were obtained using a Stanford Research Systems MPA120 apparatus and are uncorrected. Optical rotation measurements were performed on a Perkin Elmer 241 polarimeter at 22 °C in a 5 cm cell at concentrations expressed as g/100 mL. Purity >95% was determined by HPLC with an Agilent Technologies 1260 Infinity LC, equipped with an Agilent 1100 Series LC/MSD on a Zorbax XDB-C8 column, eluting with MeCN/H₂O (+ 0.1% formic acid) gradients.

2.3.2.2 SYNTHESIS OF AZO-ETOMIDATES

Synthesis of (*R*)-*tert*-butyl (1-(4-nitrophenyl)ethyl)carbamate (**2.6**)

The HCl salt of amine **2.5** (1.07 g, 5.28 mmol, 1.0 equiv.) was dissolved in THF (20 mL) and TEA (0.88 mL, 6.3 mmol, 1.2 equiv.) was added. The mixture was stirred at room temperature for 15 min. Then, Boc₂O (1.21 g, 5.54 mmol, 1.05 equiv.) and DMAP (65 mg, 0.53 mmol, 0.1 equiv.) were added and the reaction mixture was stirred for 16 h at room temperature. The solvent was removed and the crude product was dissolved in EtOAc (50 mL). The organic layer was washed with water (100 mL) and brine (100 mL), dried over MgSO₄ and concentrated *in vacuo*. The crude product was purified by flash silica gel column chromatography (hexanes/EtOAc, gradient from 10:1 to 3:1) to give Boc-protected amine **2.6** (1.08 g, 4.06 mmol, 77%) as a colorless oil.

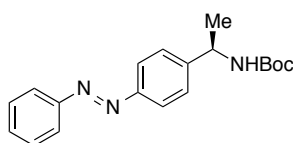
TLC (hexanes/EtOAc, 4:1): $R_f = 0.36$. $[\alpha]_D^{22}$: +47.3 ($c = 1.0$, CHCl₃). **¹H NMR (CDCl₃, 300 MHz, 27 °C):** $\delta = 8.23\text{--}8.15$ (m, 2H, ArH), 7.50–7.41 (m, 2H, ArH), 4.99–4.71 (m, 2H, CH, NH), 1.48–1.34 (m, 12H, CH₃, C(CH₃)₃) ppm. **¹³C NMR (CDCl₃, 75 MHz, 27 °C):** $\delta = 154.9, 151.9, 147.0, 126.5, 123.9, 80.1, 50.0, 28.3, 22.6$ ppm. **IR (neat, ATR):** $\tilde{\nu} = 3331$ (w), 2977 (m), 2930 (w), 1686 (s), 1606 (m), 1515 (s), 1454 (m), 1391 (m), 1365 (m), 1343 (vs), 1316 (m), 1283 (m), 1245 (m), 1164 (s), 1109 (m), 1055 (m), 1014 (m), 1002 (w), 853 (s), 784 (w), 753 (m), 699 (m) cm⁻¹. **HRMS (EI⁺):** m/z calcd. for [C₁₃H₁₈N₂O₄]⁺: 266.1267, found: 266.1267 ([M]⁺).

Synthesis of (*R*)-*tert*-butyl (1-(4-aminophenyl)ethyl)carbamate (**2.7**)

Nitroarene **2.6** (1.06 g, 3.98 mmol) was dissolved in MeOH (20 mL) and palladium on charcoal (10%; 110 mg) was added under an argon atmosphere. The flask was purged with H₂ and subsequently evacuated (5x). The reaction mixture was then stirred for 1.5 h under an H₂ atmosphere (1 bar). The mixture was filtered through Celite and the solvent was removed *in vacuo*, yielding aniline **2.7** (940 mg, 3.98 mmol, 100%) as a colorless oil.

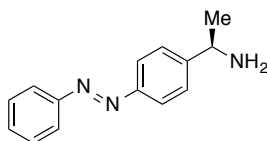
TLC (hexanes/EtOAc, 4:1): $R_f = 0.09$. $[\alpha]_D^{22}$: +76.0 ($c = 1.0$, CHCl_3). $^1\text{H NMR}$ (CDCl_3 , 400 MHz, 27 °C): $\delta = 7.12\text{--}7.05$ (m, 2H, ArH), 6.67–6.61 (m, 2H, ArH), 4.85–4.55 (m, 2H, CH, NH), 3.58 (br s, 2H, NH_2), 1.49–1.33 (m, 12H, CH_3 , $\text{C}(\text{CH}_3)_3$) ppm. $^{13}\text{C NMR}$ (CDCl_3 , 100 MHz, 27 °C): $\delta = 155.1, 145.4, 134.0, 127.0, 115.1, 79.2, 49.6, 28.4, 22.4$ ppm. **IR (neat, ATR):** $\tilde{\nu} = 3352$ (w), 2975 (m), 2930 (w), 1688 (s), 1622 (m), 1516 (s), 1453 (m), 1391 (m), 1365 (m), 1244 (m), 1164 (vs), 1052 (m), 862 (w), 827 (m), 750 (vs), 665 (m) cm^{-1} . **HRMS (ESI⁺):** m/z calcd. for $[\text{C}_{13}\text{H}_{20}\text{N}_2\text{O}_2]^+$: 236.1525, found: 236.1515 ($[\text{M}]^+$).

Synthesis of (*R*)-*tert*-butyl (1-(4-(phenyldiazenyl)phenyl)ethyl)carbamate (**2.8**)



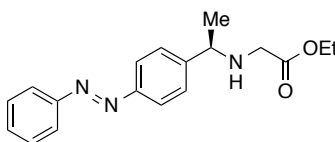
Aniline **2.7** (900 mg, 3.81 mmol, 1.0 equiv.) was dissolved in acetic acid (15 mL) and nitrosobenzene (449 mg, 4.19 mmol, 1.1 equiv.) was added in 3 portions over the course of 10 min. The reaction mixture was stirred for 24 h at room temperature. The mixture was then basified to pH = 8–9 with sat. aqu. NaHCO_3 and extracted with EtOAc (3 x 30 mL). The combined organic layers were washed with sat. aqu. NaHCO_3 (100 mL) and brine (100 mL), then dried over MgSO_4 and concentrated *in vacuo*. The crude product was purified by flash silica gel column chromatography (hexanes/EtOAc, gradient from 10:1 to 5:1) to yield azobenzene **2.8** (929 mg, 2.85 mmol, 75%) as an orange solid.

TLC (hexanes/EtOAc, 4:1): $R_f = 0.47$. **M.p.:** 124–126 °C. $[\alpha]_D^{22}$: +105.2 ($c = 1.0$, CHCl_3). $^1\text{H NMR}$ (CDCl_3 , 300 MHz, 27 °C): $\delta = 8.00\text{--}7.74$ (m, 4H, ArH), 7.56–7.30 (m, 5H, ArH), 4.98–4.64 (m, 2H, CH, NH), 1.54–1.26 (m, 12H, CH_3 , $\text{C}(\text{CH}_3)_3$) ppm. $^{13}\text{C NMR}$ (CDCl_3 , 75 MHz, 27 °C): $\delta = 155.0, 152.7, 151.8, 147.2, 130.9, 129.0, 126.5, 123.1, 122.8, 79.6, 50.1, 28.3, 22.7$ ppm. **IR (neat, ATR):** $\tilde{\nu} = 3372$ (m), 2966 (w), 1682 (s), 1514 (s), 1481 (w), 1444 (m), 1391 (w), 1363 (m), 1341 (w), 1307 (m), 1246 (m), 1167 (s), 1093 (w), 1058 (s), 1002 (m), 922 (w), 861 (w), 846 (s), 771 (s), 737 (w), 686 (vs) cm^{-1} . **HRMS (ESI⁺):** m/z calcd. for $[\text{C}_{19}\text{H}_{24}\text{N}_3\text{O}_2]^+$: 326.1869, found: 326.1864 ($[\text{M}+\text{H}]^+$).

Synthesis of (R)-1-(4-(phenyldiazenyl)phenyl)ethanamine (2.9)

Boc-protected amine **2.8** (880 mg, 2.70 mmol) was dissolved in 1,4-dioxane (25 mL) and a 4 M solution of HCl in dioxane (25 mL) was added. The mixture was stirred for 16 h at room temperature. The solvent was removed under reduced pressure and the residue was taken up in water (50 mL). The aqueous layer was washed with Et₂O (3 x 50 mL) and then basified with sat. aqu. NaHCO₃ to pH = 8–9. The aqueous layer was then extracted with CHCl₃ (2 x 50 mL) and the combined organic layers were washed with brine (70 mL), dried over MgSO₄ and concentrated *in vacuo*. Amine **2.9** (608 mg, 2.70 mmol, 100%) was obtained quantitatively as orange solid.

TLC (DCM/MeOH, 10:1): $R_f = 0.29$. **M.p.:** 64–65 °C. $[\alpha]_D^{22}$: +12.3 ($c = 0.50$, CHCl₃). **¹H NMR (CDCl₃, 300 MHz, 27 °C):** $\delta = 7.95\text{--}7.84$ (m, 4H, ArH), 7.56–7.42 (m, 5H, ArH), 4.22 (q, $J = 6.6$ Hz, 1H, CH), 1.94 (br s, 2H, NH₂), 1.45 (d, $J = 6.6$ Hz, 3H, CH₃) ppm. **¹³C NMR (CDCl₃, 75 MHz, 27 °C):** $\delta = 152.7, 151.7, 150.4, 130.8, 129.0, 126.4, 123.1, 122.8, 51.2, 25.5$ ppm. **IR (neat, ATR):** $\tilde{\nu} = 3377$ (w), 3309 (w), 3040 (w), 2962 (w), 2892 (w), 1599 (m), 1575 (m), 1495 (w), 1482 (w), 1463 (w), 1444 (m), 1414 (m), 1367 (m), 1302 (m), 1272 (w), 1222 (w), 1187 (m), 1153 (s), 1118 (w), 1101 (m), 1069 (m), 1017 (m), 1008 (m), 999 (m), 969 (w), 920 (w), 842 (vs), 808 (m), 772 (vs), 734 (m), 686 (vs) cm⁻¹. **HRMS (EI⁺):** m/z calcd. for [C₁₄H₁₅N₃]⁺: 225.1266, found: 225.1254 ([M]⁺).

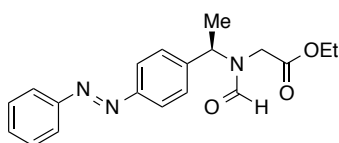
Synthesis of (R)-ethyl 2-((1-(4-(phenyldiazenyl)phenyl)ethyl)amino)acetate (2.10)

Amine **2.9** (577 mg, 2.56 mmol, 1.0 equiv.) was dissolved in DMF (10 mL) and TEA (0.53 mL, 3.8 mmol, 1.5 equiv.) was added, followed by ethyl chloroacetate (0.35 mL, 3.3 mmol, 1.3 equiv.). The mixture was heated to 80 °C for 16 h. To the cooled mixture, EtOAc (50 mL) was added and the organic phase was washed with water (2 x 75 mL) and brine (3 x 75 mL), then dried over MgSO₄ and the solvent removed under reduced pressure. Purification of the

crude product by flash silica gel chromatography (hexanes/EtOAc, gradient from 5:1 to 2:1) afforded secondary amine **2.10** (736 mg, 2.36 mmol, 92%) as a red oil.

TLC (hexanes/EtOAc, 2:1): $R_f = 0.49$. $[\alpha]_D^{22}$: +106.3 ($c = 1.0$, CHCl_3). **$^1\text{H NMR}$ (CDCl_3 , 300 MHz, 27 °C):** $\delta = 7.95\text{--}7.85$ (m, 4H, ArH), 7.55–7.45 (m, 5H, ArH), 4.17 (q, $J = 7.2$ Hz, 2H, CH_2), 3.92 (q, $J = 6.6$ Hz, 1H, CH), 3.34 (d, $J = 17.4$ Hz, 1H, CH), 3.25 (d, $J = 17.4$ Hz, 1H, CH), 2.33 (br s, 1H, NH), 1.44 (d, $J = 6.6$ Hz, 3H, CH_3), 1.25 (t, $J = 7.2$ Hz, 3H, CH_3) ppm. **$^{13}\text{C NMR}$ (CDCl_3 , 75 MHz, 27 °C):** $\delta = 172.2, 152.7, 152.1, 147.5, 130.9, 129.0, 127.5, 123.1, 122.8, 60.8, 57.6, 48.7, 24.1, 14.2$ ppm. **IR (neat, ATR):** $\tilde{\nu} = 3340$ (w), 3049 (w), 2977 (m), 2928 (w), 1735 (vs), 1602 (w), 1582 (w), 1466 (w), 1445 (m), 1416 (w), 1394 (w), 1371 (m), 1344 (w), 1302 (w), 1194 (vs), 1151 (s), 1097 (m), 1072 (m), 1026 (m), 927 (w), 848 (m), 769 (m), 737 (w), 688 (m) cm^{-1} . **HRMS (ESI⁺):** m/z calcd. for $[\text{C}_{18}\text{H}_{22}\text{N}_3\text{O}_2]^+$: 312.1712, found: 312.1705 ($[\text{M}+\text{H}]^+$).

Synthesis of (*R*)-ethyl 2-(*N*-(1-(4-(phenyldiazenyl)phenyl)ethyl)formamido)acetate (**2.11**)

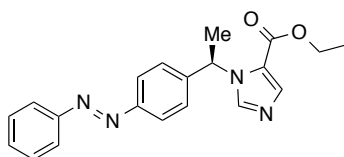


Diisopropylcarbodiimide (50 μL , 0.32 mmol, 2.0 equiv.) was dissolved in DCM (1 mL) and a 2 M solution of formic acid in DCM (0.32 mL, 0.64 mmol, 4.0 equiv.) was added dropwise at 0 °C. The mixture was stirred for 5 min. A precooled to 0 °C solution of glycine ester **2.10** (50 mg, 0.16 mmol, 1.0 equiv.) in pyridine (1 mL) was added to the DIC and formic acid containing solution slowly over a period of 10 min. The mixture was slowly warmed to room temperature and stirred for 16 h. The solvent was removed under reduced pressure and the crude product was purified by flash silica gel chromatography (CHCl_3), giving rise to the *N*-formyl compound **2.11** (55 mg, 0.16 mmol, 100%) as a red oil. Compound **2.11** was obtained as a mixture of two isomers in a ratio of approximately 3:1 with respect to the orientation of the formyl group.

TLC (hexanes/EtOAc, 2:1): $R_f = 0.19$. $[\alpha]_D^{22}$: +66.6 ($c = 1.0$, CHCl_3). **$^1\text{H NMR}$ (CDCl_3 , 300 MHz, 27 °C):** $\delta = 8.48$ (s, 1H, CHO, major isomer), 8.21 (s, 1H, CHO, minor isomer), 7.96–7.86 (m, 4H, ArH, major isomer; 4H, ArH, minor isomer), 7.57–7.41 (m, 5H, ArH; 5H, ArH, minor isomer), 5.90 (q, $J = 7.0$ Hz, 1H, CH, minor isomer), 4.93 (q, $J = 7.0$ Hz, 1H, CH, major isomer), 4.14 (q, $J = 7.2$ Hz, 2H, CH_2 , major isomer), 4.10–4.01 (m, 2H, CH_2 , minor isomer), 3.96 (d, $J = 17.3$ Hz, 1H, CH, major isomer), 3.83–3.77 (m, 1H, CH, major isomer; 1H,

CH, minor isomer), 3.67 (d, $J = 17.7$ Hz, 1H, *CH*, minor isomer), 1.73 (d, $J = 7.0$ Hz, 3H, *CH*₃, major isomer), 1.56 (d, $J = 7.0$ Hz, 3H, *CH*₃, minor isomer), 1.26–1.15 (m, 3H, *CH*₃, major isomer; 3H, *CH*₃, minor isomer) ppm. ¹³C NMR (CDCl₃, 75 MHz, 27 °C): $\delta = 169.6$ (minor isomer), 168.5 (major isomer), 163.7 (minor isomer), 162.5 (major isomer), 152.6 (minor isomer), 152.5 (major isomer), 152.3 (major isomer), 152.1 (minor isomer), 142.3 (major isomer), 142.0 (minor isomer), 131.2 (major isomer), 131.1 (minor isomer), 129.1 (major isomer), 129.1 (minor isomer), 128.5 (minor isomer), 127.7 (major isomer), 123.2 (major isomer), 122.9 (minor isomer), 122.9 (major isomer), 122.9 (minor isomer), 61.7 (minor isomer), 61.3 (major isomer), 56.7 (major isomer), 49.6 (minor isomer), 45.4 (minor isomer), 43.0 (major isomer), 19.0 (major isomer), 16.2 (minor isomer), 14.0 (major isomer), 14.0 (minor isomer) ppm. IR (neat, ATR): $\tilde{\nu} = 2981$ (w), 2938 (w), 1749 (m), 1672 (vs), 1604 (w), 1429 (w), 1402 (m), 1374 (w), 1353 (w), 1302 (w), 1256 (w), 1197 (m), 1161 (m), 1116 (w), 1081 (w), 1029 (w), 1000 (w), 982 (w), 930 (w), 849 (m), 771 (m), 690 (m) cm⁻¹. HRMS (ESI⁺): m/z calcd. for [C₁₉H₂₂N₃O₃]⁺: 340.1661, found: 340.1655 ([M+H]⁺).

Synthesis of (*R*)-ethyl 1-(1-(4-(phenyldiazenyl)phenyl)ethyl)-1*H*-imidazole-5-carboxylate (AETD1)

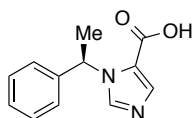


NaOEt (67 μ L, 0.18 mmol, 21% in EtOH, 1.1 equiv.) was dissolved in THF (2 mL) and cooled to 10 °C. Ethyl formate (39 μ L, 0.48 mmol, 3.0 equiv.) was added, followed by a solution of *N*-formyl protected ethyl ester **2.11** (55 mg, 0.16 mmol, 1.0 equiv.) in THF (1.5 mL). The reaction mixture was stirred at room temperature for 16 h. The solvent was removed under reduced pressure and the crude product was immediately used in the next step. The crude product was dissolved in H₂O (1 mL) and MeOH (1 mL) and conc. HCl (0.19 mL) was added. The mixture was heated to 40 °C for 30 min. A solution of KSCN (23 mg, 0.24 mmol, 1.5 equiv.) in H₂O (1 mL) was added to the mixture and heated to 40 °C for 16 h. The crude product was then extracted with CHCl₃ (2 x 10 mL) and the combined organic layers were washed with brine (30 mL), dried over MgSO₄ and the solvent removed under reduced pressure. The crude product was used in the next step without further purification. To a solution of NaNO₂ (0.3 mg, 0.004 mmol, 0.1 equiv.) in H₂O (1 mL) and conc. HNO₃ (0.2 mL), a solution of the crude product in CHCl₃ (1 mL) was added at 10 °C. The reaction mixture was then slowly warmed to room temperature and stirred for 1.5 h. The crude product was extracted with

CHCl₃ (2 x 5 mL) and the combined organic layers were washed with sat. aqu. NaHCO₃ (2 x 15 mL) and brine (20 mL), dried over MgSO₄ and the solvent removed *in vacuo*. The crude product was purified by flash silica gel chromatography (hexanes/EtOAc, 1:1), yielding **AETD1** (8.0 mg, 0.023 mmol, 14% over four steps) as a red oil.

TLC (hexanes/EtOAc, 1:1): $R_f = 0.24$. $[\alpha]_D^{22}$: +48.4 ($c = 0.1$, CHCl₃). **¹H NMR (CDCl₃, 300 MHz, 27 °C):** $\delta = 7.94\text{--}7.84$ (m, 4H, ArH), 7.81 (s, 2H, ArH), 7.56–7.43 (m, 3H, ArH), 7.33–7.27 (m, 2H, ArH), 6.43 (q, $J = 7.2$ Hz, 1H, CH), 4.31–4.21 (m, 2H, CH₂), 1.92 (d, $J = 7.2$ Hz, 3H, CH₃), 1.31 (t, $J = 7.0$ Hz, 3H, CH₃) ppm. **¹³C NMR (CDCl₃, 75 MHz, 27 °C):** $\delta = 160.2, 152.6, 152.1, 144.1, 139.6, 138.3, 131.1, 129.1, 126.9, 123.2, 122.9, 122.7, 60.5, 55.2, 22.2, 14.2$ ppm. **IR (neat, ATR):** $\tilde{\nu} = 2981$ (w), 2914 (w), 1713 (vs), 1604 (w), 1538 (w), 1466 (m), 1391 (w), 1374 (m), 1349 (m), 1304 (w), 1216 (vs), 1156 (w), 1132 (m), 1107 (m), 1052 (m), 1011 (w), 980 (w), 921 (w), 844 (m), 766 (m), 716 (w), 690 (w), 666 (w) cm⁻¹. **HRMS (ESI⁺):** m/z calcd. for [C₂₀H₂₁N₄O₂]⁺: 349.1665, found: 349.1658 ([M+H]⁺). **UV/Vis:** $\lambda_{\max} = 325, 438$ nm.

Synthesis of (*R*)-1-(1-phenylethyl)-1*H*-imidazole-5-carboxylic acid (**2.13**)



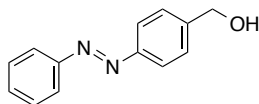
Etomidate (113 mg, 0.460 mmol, 1.0 equiv.) was dissolved in THF (10 mL) and a 1 M solution of LiOH in H₂O (1.38 mL, 1.38 mmol, 3.0 equiv.) was added. The mixture was stirred at room temperature for 16 h. As TLC analysis indicated still remaining starting material, another 3.0 equiv. (1.38 mL, 1.38 mmol) was added and the mixture was stirred for another 8 h. Water (30 mL) was added to the mixture, followed by basification with 1 M NaOH to pH = 12–14. The aqueous phase was washed with EtOAc (2 x 30 mL) and then acidified with 1 M HCl to pH = 4–5 and extracted with EtOAc (5 x 20 mL). The combined organic layers were dried over MgSO₄ and the solvent removed under reduced pressure, affording carboxylic acid **2.13** (55 mg, 0.25 mmol, 54%) as a colorless foam.

TLC (DCM/MeOH, 10:1): $R_f = 0.05$. **¹H NMR (CDCl₃, 300 MHz, 27 °C):** $\delta = 10.51$ (br s, 1H, CO₂H), 7.90–7.82 (m, 2H, ArH), 7.37–7.19 (m, 5H, ArH), 6.56 (q, $J = 7.0$ Hz, 1H, CH), 1.86 (d, $J = 7.0$ Hz, 3H, CH₃) ppm. **¹³C NMR (CDCl₃, 75 MHz, 27 °C):** $\delta = 162.9, 140.4, 138.3, 134.7, 128.9, 128.2, 126.6, 124.5, 55.5, 22.0$ ppm. **IR (neat, ATR):** $\tilde{\nu} = 3126$ (w), 2983 (w), 2470 (m), 1898 (m), 1698 (s), 1532 (m), 1495 (m), 1453 (m), 1354 (m), 1278 (m), 1214

(vs), 1115 (s), 1070 (m), 1028 (m), 980 (m), 922 (w), 852 (w), 750 (vs), 700 (m), 658 (m) cm⁻¹.

HRMS (ESI): *m/z* calcd. for [C₁₂H₁₁N₂O₂]⁻: 215.0821, found: 215.0827 ([M-H]⁻).

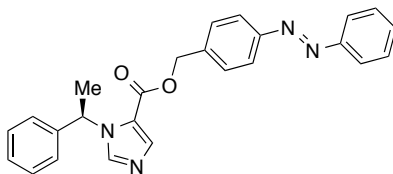
Synthesis of (4-(phenyldiazenyl)phenyl)methanol (**2.14**)



Nitrosobenzene (1.86 g, 17.4 mmol, 1.1 equiv.) was dissolved in a mixture of ethanol (13 mL) and glacial acetic acid (4.7 mL) with careful heating to 45 °C. The clear green solution was cooled to room temperature and 4-aminobenzyl alcohol (1.94 g, 15.8 mmol, 1.0 equiv.) was added in 5 portions over the course of 10 min. The mixture was stirred for another 45 min at room temperature. Et₂O (50 mL) was added and the mixture was washed with sat. aqu. NaHCO₃ (2 x 50 mL; gas evolution!), dried over MgSO₄ and the solvent was removed under reduced pressure. The crude product was dissolved in a small volume of Et₂O and hexanes were added. The mixture was then left in a refrigerator for crystallization. The orange crystals were filtered and washed with hexanes to obtain azobenzene **2.14**. Further crystallization of the mother liquor gave an overall yield of 84% (2.83 g, 13.3 mmol).

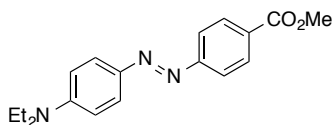
TLC (EtOAc): R_f = 0.80. **M.p.:** 141–142 °C. **¹H NMR (CDCl₃, 300 MHz, 27 °C):** δ = 7.98–7.91 (m, 4H, ArH), 7.58–7.46 (m, 5H, ArH), 4.81 (s, 2H, CH₂), 1.83 (br s, 1H, OH) ppm. **¹³C NMR (CDCl₃, 75 MHz, 27 °C):** δ = 152.7, 152.1, 143.8, 131.0, 129.1, 127.4, 123.1, 122.9, 64.9 ppm. **IR (neat, ATR):** ν̄ = 3308 (m), 2912 (w), 2860 (w), 1442 (m), 1413 (m), 1348 (w), 1302 (m), 1150 (m), 1071 (w), 1026 (vs), 1009 (m), 922 (w), 850 (s), 831 (m), 770 (m), 763 (m), 685 (s), 668 (w) cm⁻¹. **HRMS (ESI⁺):** *m/z* calcd. for [C₁₃H₁₃N₂O]⁺: 213.1028, found: 213.1022 ([M+H]⁺).

Synthesis of (*R*)-4-(phenyldiazenyl)benzyl 1-(1-phenylethyl)-1*H*-imidazole-5-carboxylate (AETD2)



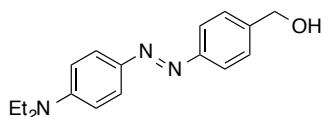
Carboxylic acid **2.13** (42 mg, 0.19 mmol, 1.0 equiv.), benzylic alcohol **2.14** (102 mg, 0.480 mmol, 2.5 equiv.) and DMAP (23 mg, 0.19 mmol, 1.0 equiv.) were dissolved in DCM (3 mL) and DMF (0.3 mL). Diisopropylcarbodiimide (45 μ L, 0.29 mmol, 1.5 equiv.) was added and the mixture was stirred at room temperature for 20 h. The solvent was removed under reduced pressure and the crude product was purified by flash silica gel chromatography (hexanes/EtOAc, gradient from 5:1 to 2:1), yielding **AETD2** (68 mg, 0.17 mmol, 89%) as a red oil as a mixture of *trans* and *cis* isomers.

TLC (hexanes/EtOAc, 2:1): R_f = 0.19. $[\alpha]_D^{22}$: +36.0 (c = 0.5, CHCl_3). **$^1\text{H NMR}$ (CDCl_3 , 600 MHz, 27 $^\circ\text{C}$):** δ = 7.95–7.89 (m, 4H, ArH), 7.88 (s, 1H, ArH), 7.83 (s, 1H, ArH), 7.55–7.46 (m, 5H, ArH), 7.36–7.29 (m, 3H, ArH), 7.20–7.17 (m, 2H, ArH), 6.36 (q, J = 7.2 Hz, 1H, CH), 5.35 (d, J = 12.8 Hz, 1H, CH), 5.30 (d, J = 12.8 Hz, 1H, CH), 1.87 (d, J = 7.2 Hz, 3H, CH_3) ppm. **$^{13}\text{C NMR}$ (CDCl_3 , 150 MHz, 27 $^\circ\text{C}$):** δ = 159.7, 153.3 (*cis* isomer), 153.1 (*cis* isomer), 152.6, 152.4, 140.8, 139.8, 138.4, 137.9, 134.8, 131.1, 129.1, 128.9, 128.9 (*cis* isomer), 128.8 (*cis* isomer), 128.6, 128.3 (*cis* isomer), 128.1, 128.1 (*cis* isomer), 127.5 (*cis* isomer), 126.3, 126.2 (*cis* isomer), 123.1, 122.9, 120.8 (*cis* isomer), 120.4 (*cis* isomer), 65.6, 65.3 (*cis* isomer), 55.7, 22.2 ppm. **IR (neat, ATR):** $\tilde{\nu}$ = 3416 (w), 3062 (w), 3033 (w), 2982 (w), 1712 (s), 1605 (w), 1585 (w), 1534 (m), 1495 (w), 1486 (w), 1468 (m), 1450 (m), 1382 (m), 1349 (m), 1302 (w), 1209 (vs), 1155 (w), 1131 (m), 1103 (s), 1071 (w), 1053 (w), 1028 (w), 1014 (w), 984 (w), 921 (m), 834 (m), 760 (s), 700 (m), 689 (m), 659 (m) cm^{-1} . **HRMS (ESI⁺):** m/z calcd. for $[\text{C}_{25}\text{H}_{23}\text{N}_4\text{O}_2]^+$: 411.1821, found: 411.1814 ($[\text{M}+\text{H}]^+$). **UV/Vis:** λ_{max} = 325, 435 nm.

Synthesis of methyl 4-((4-(diethylamino)phenyl)diazenyl)benzoate (2.15)

Methyl 4-aminobenzoate (1.23 g, 8.12 mmol, 1.0 equiv.) was dissolved in 4 M HCl (50 mL) and cooled to 0 °C. A precooled solution of NaNO₂ (616 mg, 8.93 mmol, 1.1 equiv.) in water (2 mL) was added dropwise and the mixture was stirred for 30 min at 0 °C. The pH was adjusted to pH = 8–10 with an aqu. 10% NaOH solution and *N,N*-diethyl aniline (1.30 mL, 8.21 mmol, 1.0 equiv.) was added. The mixture was stirred for 1 h at 0 °C. The aqueous phase was extracted with EtOAc (3 x 50 mL) and the combined organic layers were washed with sat. aqu. NaHCO₃ (100 mL) and brine (100 mL), dried over MgSO₄ and the solvent was removed under reduced pressure. Purification of the crude product by flash silica gel chromatography (hexanes/EtOAc, gradient from 20:1 to 10:1) afforded azobenzene **2.15** (1.60 g, 5.14 mmol, 63%) as a red solid.

TLC (hexanes/EtOAc, 4:1): R_f = 0.46. **M.p.:** 140–141 °C. **¹H NMR (CDCl₃, 300 MHz, 27 °C):** δ = 8.21–8.08 (m, 2H, ArH), 7.94–7.78 (m, 4H, ArH), 6.82–6.66 (m, 2H, ArH), 3.94 (s, 3H, CH₃), 3.47 (q, J = 7.0 Hz, 4H, 2 x CH₂), 1.24 (t, J = 7.0 Hz, 6H, 2 x CH₃) ppm. **¹³C NMR (CDCl₃, 75 MHz, 27 °C):** δ = 166.8, 156.1, 150.7, 143.3, 130.5, 129.9, 125.8, 122.9, 111.0, 52.1, 44.8, 12.7 ppm. **IR (neat, ATR):** $\tilde{\nu}$ = 2975 (m), 2948 (w), 2897 (w), 2258 (w), 1711 (s), 1595 (s), 1554 (m), 1515 (m), 1483 (w), 1469 (w), 1435 (m), 1421 (m), 1407 (m), 1390 (m), 1377 (m), 1356 (m), 1313 (m), 1270 (vs), 1246 (s), 1192 (m), 1153 (m), 1133 (vs), 1107 (s), 1094 (s), 1079 (m), 1006 (m), 964 (m), 929 (w), 864 (m), 839 (w), 823 (vs), 810 (w), 793 (w), 777 (m), 726 (m), 721 (w), 697 (m) cm⁻¹. **HRMS (ESI⁺):** m/z calcd. for [C₁₈H₂₂N₃O₂]⁺: 312.1712, found: 312.1703 ([M+H]⁺).

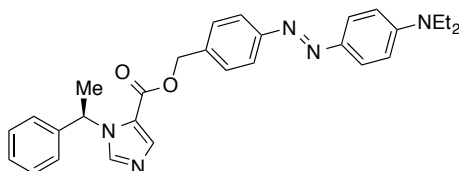
Synthesis of (4-((4-(diethylamino)phenyl)diazenyl)phenyl)methanol (2.16)

Methyl ester **2.15** (500 mg, 1.61 mmol, 1.0 equiv.) was dissolved in THF (20 mL) and LiAlH₄ (110 mg, 2.90 mmol, 1.8 equiv.) was added at 0 °C. The mixture was warmed to room temperature and stirred for 45 min. A sat. aqu. solution of Rochelle's salt (30 mL) was added

and the mixture was stirred vigorously for 15 min. The crude product was extracted with EtOAc (2 x 30 mL) and the combined organic layers were washed with a sat. aqu. solution of Rochelle's salt (50 mL) and brine (100 mL), dried over MgSO₄ and the solvent was removed under reduced pressure. Purification of the crude product by flash silica gel chromatography (hexanes/EtOAc, gradient from 4:1 to 1:1) afforded alcohol **2.16** (450 mg, 1.59 mmol, 99%) as a red solid.

TLC (hexanes/EtOAc, 4:1): R_f = 0.13. **M.p.:** 99–100 °C. **¹H NMR (CDCl₃, 300 MHz, 27 °C):** δ = 7.93–7.75 (m, 4H, ArH), 7.52–7.41 (m, 2H, ArH), 6.79–6.67 (m, 2H, ArH), 4.75 (d, J = 5.7 Hz, 2H, CH₂), 3.46 (q, J = 7.2 Hz, 4H, 2 x CH₂), 1.72 (t, J = 5.7 Hz, 1H, OH), 1.24 (t, J = 7.2 Hz, 6H, 2 x CH₃) ppm. **¹³C NMR (CDCl₃, 75 MHz, 27 °C):** δ = 152.8, 150.1, 143.1, 141.8, 127.5, 125.3, 122.3, 111.0, 65.1, 44.7, 12.7 ppm. **IR (neat, ATR):** $\tilde{\nu}$ = 3408 (w), 2969 (w), 2913 (w), 2869 (w), 1592 (vs), 1556 (m), 1513 (m), 1445 (w), 1424 (w), 1388 (m), 1375 (m), 1346 (s), 1312 (m), 1269 (m), 1250 (m), 1195 (m), 1154 (m), 1136 (vs), 1096 (m), 1078 (m), 1006 (s), 951 (w), 849 (w), 824 (vs), 790 (m), 734 (w), 700 (w) cm⁻¹. **HRMS (ESI⁺):** m/z calcd. for [C₁₇H₂₂N₃O]⁺: 284.1763, found: 284.1755 ([M+H]⁺).

Synthesis of (R)-4-((4-(diethylamino)phenyl)diazenyl)benzyl 1-(1-phenylethyl)-1H-imidazole-5-carboxylate (AETD3)

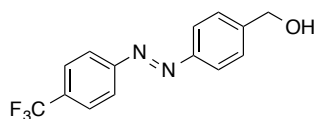


Carboxylic acid **2.13** (42 mg, 0.19 mmol, 1.0 equiv.), primary alcohol **2.16** (136 mg, 0.480 mmol, 2.5 equiv.) and DMAP (23 mg, 0.19 mmol, 1.0 equiv.) were dissolved in DCM (3 mL) and DMF (0.3 mL). Diisopropylcarbodiimide (45 μ L, 0.29 mmol, 1.5 equiv.) was added and the mixture was stirred at room temperature for 20 h. The solvent was removed under reduced pressure and the crude product was purified by flash silica gel chromatography (hexanes/EtOAc, gradient from 4:1 to 1:1), yielding ester **AETD3** (58 mg, 0.12 mmol, 63%) as an orange solid.

TLC (hexanes/EtOAc, 1:1): R_f = 0.28. **M.p.:** 116–117 °C. **$[\alpha]_D^{22}$:** +50.9 (c = 0.5, CHCl₃). **¹H NMR (CDCl₃, 600 MHz, 27 °C):** δ = 7.88–7.83 (m, 3H, ArH), 7.83–7.80 (m, 2H, ArH), 7.74 (s, 1H, ArH), 7.46–7.42 (m, 2H, ArH), 7.36–7.31 (m, 2H, ArH), 7.31–7.27 (m, 1H, ArH), 7.19–7.15 (m, 2H, ArH), 6.75–6.71 (m, 2H, ArH), 6.35 (q, J = 7.2 Hz, 1H, CH), 5.32 (d, J = 12.6 Hz, 1H, CH), 5.27 (d, J = 12.6 Hz, 1H, CH), 3.46 (q, J = 7.1 Hz, 4H, 2 x CH₂), 1.86 (d,

$J = 7.2$ Hz, 3H, CH_3), 1.23 (t, $J = 7.1$ Hz, 6H, 2 x CH_3) ppm. ^{13}C NMR ($CDCl_3$, 150 MHz, 27 °C): $\delta = 160.0, 153.2, 150.2, 143.1, 141.1, 140.0, 138.6, 136.4, 128.8, 128.7, 128.0, 126.2, 125.4, 122.3, 122.3, 111.0, 65.8, 55.4, 44.7, 22.2, 12.7$ ppm. IR (neat, ATR): $\tilde{\nu} = 3124$ (w), 2977 (w), 1690 (m), 1594 (s), 1552 (w), 1514 (m), 1491 (w), 1453 (w), 1424 (w), 1394 (m), 1380 (m), 1344 (s), 1309 (w), 1273 (m), 1251 (w), 1206 (vs), 1160 (m), 1131 (vs), 1106 (s), 1050 (m), 1027 (m), 986 (w), 958 (w), 943 (w), 920 (m), 885 (w), 866 (w), 838 (m), 817 (m), 790 (w), 768 (m), 724 (w), 703 (m), 664 (m) cm^{-1} . HRMS (ESI⁺): m/z calcd. for $[C_{29}H_{32}N_5O_2]^+$: 482.2556, found: 482.2545 ($[M+H]^+$). UV/Vis: $\lambda_{max} = 445$ nm.

Synthesis of (4-((4-(trifluoromethyl)phenyl)diazenyl)phenyl)methanol (**2.17**)



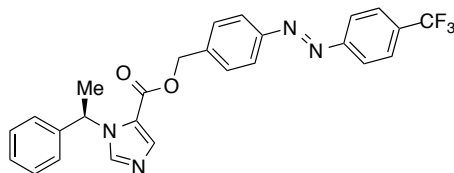
4-(Trifluoromethyl)aniline (0.56 mL, 4.5 mmol, 1.0 equiv.) was dissolved in DCM (20 mL) and oxone (5.47 g, 8.90 mmol, 2.0 equiv.; dissolved in 40 mL of H_2O) was added. The biphasic mixture was stirred vigorously for 16 h at room temperature. The phases were separated, and the aqueous phase was extracted with DCM (20 mL). The combined organic phases were washed with brine (30 mL), dried over $MgSO_4$ and the solvent was removed under reduced pressure. The resulting green solid was immediately dissolved in HOAc (30 mL) and (4-aminophenyl)methanol (548 mg, 4.45 mmol, 1.0 equiv.) was added in 3 portions. The mixture was stirred for 24 h at room temperature. The mixture was basified to pH = 8–10 with 2 M NaOH and the aqueous phase was extracted with EtOAc (2 x 40 mL). The organic phase was washed with sat. aqu. $NaHCO_3$ (100 mL) and brine (100 mL), dried over $MgSO_4$ and concentrated *in vacuo*. The crude product was purified by flash silica gel chromatography (hexanes/EtOAc, gradient from 5:1 to 2:1), affording azobenzene **2.17** (298 mg, 1.06 mmol, 24%) as an orange solid.

TLC (hexanes/EtOAc, 1:1): $R_f = 0.57$. M.p.: 162–163 °C. 1H NMR (CD_3OD , 400 MHz, 27 °C): $\delta = 8.06$ –8.02 (m, 2H, ArH), 7.96–7.92 (m, 2H, ArH), 7.87–7.83 (m, 2H, ArH), 7.58–7.54 (m, 2H, ArH), 4.71 (s, 2H, CH_2) ppm. ^{13}C NMR (CD_3OD , 100 MHz, 27 °C): $\delta = 154.6, 151.6, 146.0, 131.7$ (q, $J = 32.2$ Hz), 127.1, 126.0 (q, $J = 3.9$ Hz), 124.0 (q, $J = 270$ Hz), 122.8, 122.7, 63.2 ppm. ^{19}F NMR ($CDCl_3$, 376 MHz, 27 °C): $\delta = -64.1$ ppm. IR (neat, ATR): $\tilde{\nu} = 3250$ (m), 2923 (w), 1933 (w), 1601 (m), 1503 (w), 1452 (w), 1410 (m), 1308 (m), 1222 (w), 1208 (w), 1169 (s), 1120 (vs), 1101 (s), 1064 (s), 1037 (m), 1019 (m), 1009 (s),

988 (m), 954 (w), 851 (vs), 828 (m), 795 (m), 754 (m), 741 (w), 720 (w), 710 (w), 664 (w) cm⁻¹.

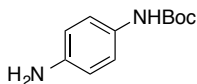
HRMS (ESI⁺): *m/z* calcd. for [C₁₄H₁₂N₂O₂F₃]⁺: 281.0902, found: 281.0893 ([M+H]⁺).

Synthesis of (R)-4-((4-(trifluoromethyl)phenyl)diazenyl)benzyl 1-(1-phenylethyl)-1H-imidazole-5-carboxylate (AETD4)



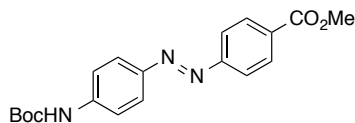
Carboxylic acid **2.13** (42 mg, 0.19 mmol, 1.0 equiv.), primary alcohol **2.17** (135 mg, 0.480 mmol, 2.5 equiv.) and DMAP (23 mg, 0.19 mmol, 1.0 equiv.) were dissolved in DCM (3 mL) and DMF (0.3 mL). Diisopropylcarbodiimide (45 μ L, 0.29 mmol, 1.5 equiv.) was added and the mixture was stirred at room temperature for 20 h. The solvent was removed under reduced pressure and the crude product was purified by flash silica gel chromatography (hexanes/EtOAc, 4:1, increased to 3:1), followed by another reversed-phase flash silica gel chromatography (H₂O/MeOH, gradient from 10:0 to 1:9). Ester **AETD4** was obtained as a red oil (53 mg, 0.11 mmol, 58%).

TLC (hexanes/EtOAc, 1:1): *R_f* = 0.30. [α]_D²²: +46.6 (*c* = 0.1, CHCl₃). **¹H NMR (CD₃OD, 400 MHz, 27 °C):** δ = 8.16 (s, 1H, ArH), 8.07–8.02 (m, 2H, ArH), 7.94–7.90 (m, 2H, ArH), 7.87–7.83 (m, 2H, ArH), 7.80 (s, 1H, ArH), 7.53–7.49 (m, 2H, ArH), 7.32–7.23 (m, 3H, ArH), 7.19–7.15 (m, 2H, ArH), 6.35 (q, *J* = 7.2 Hz, 1H, CH), 5.36–5.30 (m, 2H, CH₂), 1.88 (d, *J* = 7.2 Hz, 3H, CH₃) ppm. **¹³C NMR (CD₃OD, 100 MHz, 27 °C):** δ = 159.4, 154.5, 152.0, 141.6, 140.3, 140.1, 136.9, 131.9 (q, *J* = 32.2 Hz), 128.4, 128.4, 127.5, 126.1 (q, *J* = 3.8 Hz), 125.8, 123.8 (q, *J* = 270 Hz), 122.9, 122.8, 122.5, 65.0, 59.9, 20.9 ppm. **IR (neat, ATR):** $\tilde{\nu}$ = 2928 (w), 1716 (s), 1609 (w), 1535 (w), 1491 (w), 1453 (w), 1409 (w), 1384 (w), 1350 (m), 1323 (vs), 1212 (s), 1168 (m), 1130 (s), 1104 (s), 1064 (m), 1027 (w), 1014 (w), 921 (w), 851 (m), 764 (w), 701 (w), 659 (w) cm⁻¹. **HRMS (ESI⁺):** *m/z* calcd. for [C₂₆H₂₂N₄O₂F₃]⁺: 479.1695, found: 479.1686 ([M+H]⁺). **UV/Vis:** λ_{max} = 318, 435 nm.

Synthesis of *tert*-butyl (4-aminophenyl)carbamate (2.18)

1,4-Phenylenediamine (3.24 g, 30.0 mmol, 3.0 equiv.) was dissolved in THF (30 mL) and DMF (10 mL) and a solution of K₂CO₃ (1.52 g, 11.0 mmol, 1.1 equiv.; dissolved in 5 mL of H₂O) was added, followed by Boc₂O (2.18 g, 10.0 mmol, 1.0 equiv.). The reaction mixture was stirred at room temperature for 16 h. The mixture was then poured onto H₂O (40 mL) and extracted with CHCl₃ (2 x 50 mL). The combined organic layers were dried over MgSO₄ and the solvent was removed under reduced pressure. The crude product was purified by flash silica gel chromatography (DCM/Acetone, 4:1), yielding mono-Boc-protected amine **2.18** (1.88 g, 9.02 mmol, 90%) as a yellow solid.

TLC (DCM/Acetone, 4:1): R_f = 0.89. **M.p.:** 111–112 °C. **¹H NMR (CD₃OD, 400 MHz, 27 °C):** δ = 7.12–7.04 (m, 2H, ArH), 6.67–6.63 (m, 2H, ArH), 1.47 (s, 9H, C(CH₃)₃) ppm. **¹³C NMR (CD₃OD, 100 MHz, 27 °C):** δ = 154.6, 142.8, 130.0, 120.8, 115.6, 79.0, 27.4 ppm. **IR (neat, ATR):** $\tilde{\nu}$ = 3374 (m), 3300 (w), 3213 (w), 2988 (w), 2974 (w), 1689 (m), 1599 (w), 1523 (vs), 1460 (w), 1444 (w), 1429 (m), 1387 (w), 1365 (w), 1306 (m), 1263 (m), 1232 (s), 1158 (vs), 1096 (w), 1055 (m), 1032 (m), 1014 (w), 926 (w), 904 (w), 852 (w), 829 (m), 771 (m), 760 (m), 728 (m), 700 (m) cm⁻¹. **HRMS (EI⁺):** *m/z* calcd. for [C₁₁H₁₆N₂O₂]⁺: 208.1200, found: 208.1212 ([M]⁺).

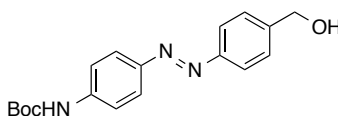
Synthesis of methyl 4-((4-((*tert*-butoxycarbonyl)amino)phenyl)diazenyl)benzoate (2.19)

Methyl 4-aminobenzoate (1.00 g, 6.62 mmol, 1.0 equiv.) was dissolved in DCM (25 mL) and oxone (8.12 g, 13.2 mmol, 2.0 equiv.; dissolved in 50 mL of H₂O) was added. The biphasic mixture was stirred vigorously for 1 h at room temperature. The phases were separated, and the aqueous phase was extracted with DCM (20 mL). The combined organic phases were washed with brine (30 mL), dried over MgSO₄ and the solvent was removed under reduced pressure. The resulting yellow solid was immediately dissolved in HOAc (50 mL) and DMSO (5 mL) and aniline **2.18** (1.31 g, 6.30 mmol, 0.95 equiv.) was added in 2 portions. The mixture was stirred for 2 d at room temperature. The mixture was basified to pH = 8–10 with 2 M NaOH and the

aqueous phase was extracted with DCM (2 x 40 mL). The combined organic layers were washed with sat. aqu. NaHCO₃ (100 mL), dried over MgSO₄ and concentrated *in vacuo*. The crude product was purified by flash silica gel chromatography (hexanes/EtOAc, gradient from 20:1 to 2:1), affording azobenzene **2.19** (1.94 g, 5.46 mmol, 87%) as a red solid.

TLC (hexanes/EtOAc, 4:1): R_f = 0.49. **M.p.:** 185–187 °C. **¹H NMR (CDCl₃, 300 MHz, 27 °C):** δ = 8.20–8.16 (m, 2H, ArH), 7.96–7.89 (m, 4H, ArH), 7.58–7.51 (m, 2H, ArH), 6.75 (s, 1H, NH), 3.96 (s, 3H, CH₃), 1.55 (s, 9H, C(CH₃)₃) ppm. **¹³C NMR (CDCl₃, 75 MHz, 27 °C):** δ = 166.6, 155.3, 152.2, 148.2, 141.8, 131.3, 130.6, 130.4 (*cis* isomer), 130.2 (*cis* isomer), 125.3 (*cis* isomer), 124.5, 122.6 (*cis* isomer), 122.4, 118.2, 81.2, 52.3, 28.3 ppm. **IR (neat, ATR):** $\tilde{\nu}$ = 3336 (m), 2978 (w), 1712 (vs), 1603 (m), 1535 (s), 1508 (m), 1446 (m), 1436 (m), 1414 (m), 1394 (w), 1370 (w), 1329 (w), 1304 (m), 1281 (vs), 1233 (vs), 1189 (m), 1160 (m), 1149 (vs), 1138 (s), 1111 (m), 1051 (m), 1026 (m), 1013 (m), 964 (w), 900 (w), 862 (m), 846 (m), 832 (w), 770 (m), 748 (w), 724 (w), 690 (m), 678 (m) cm⁻¹. **HRMS (ESI):** m/z calcd. for [C₁₉H₂₀N₃O₄]⁻: 354.1454, found: 354.1469 ([M-H]⁻).

Synthesis of *tert*-butyl 4-((4-(hydroxymethyl)phenyl)diazenyl)phenyl)carbamate (**2.20**)

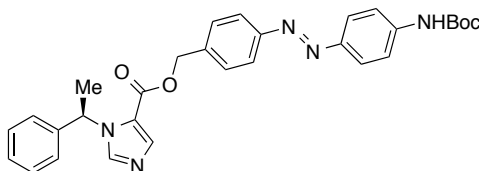


Ester **2.19** (923 mg, 2.60 mmol, 1.0 equiv.) was dissolved in THF (20 mL) and LiAlH₄ (118 mg, 3.12 mmol, 1.2 equiv.) was added at 0 °C. The mixture was warmed to room temperature and stirred for 5 min. A sat. aqu. solution of Rochelle's salt (50 mL) was added and the mixture was stirred for 1 h. The phases were separated and the aqueous phase was extracted with EtOAc (2 x 20 mL). The combined organic layers were washed with brine (50 mL), dried over MgSO₄ and the solvent was removed under reduced pressure. The crude product was purified by flash silica gel chromatography (hexanes/EtOAc, gradient from 3:1 to 1:1), yielding primary alcohol **2.20** (656 mg, 2.00 mmol, 77%) as an orange solid.

TLC (hexanes/EtOAc, 1:1): R_f = 0.55. **M.p.:** 167–168 °C. **¹H NMR (CDCl₃, 400 MHz, 27 °C):** δ = 7.92–7.84 (m, 4H, ArH), 7.54–7.45 (m, 4H, ArH), 6.65 (s, 1H, NH), 4.77 (d, J = 5.9 Hz, 2H, CH₂), 1.75 (t, J = 5.9 Hz, 1H, OH), 1.54 (s, 9H, C(CH₃)₃) ppm. **¹³C NMR (CDCl₃, 100 MHz, 27 °C):** δ = 152.3, 152.2, 148.2, 143.3, 141.0, 127.4, 124.1, 122.8, 118.2, 81.1, 64.9, 28.3 ppm. **IR (neat, ATR):** $\tilde{\nu}$ = 3464 (m), 3434 (m), 3269 (w), 2925 (w), 1723 (m), 1698 (m), 1602 (m), 1524 (s), 1504 (m), 1451 (w), 1431 (w), 1406 (m), 1365 (m), 1319 (m), 1310 (m), 1300 (m), 1268 (w), 1229 (m), 1150 (s), 1110 (m), 1052 (m), 1028 (m), 1014 (m),

995 (m), 898 (w), 845 (vs), 822 (m), 776 (m), 744 (w), 726 (m) cm⁻¹. **HRMS (ESI⁺):** *m/z* calcd. for [C₁₈H₂₂N₃O₃]⁺: 328.1661, found: 328.1656 ([M+H]⁺).

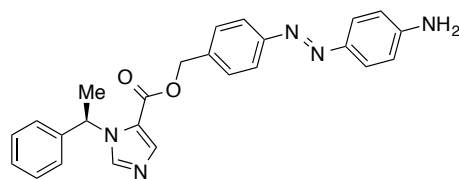
Synthesis of (R)-4-((4-((tert-butoxycarbonyl)amino)phenyl)diazenyl)benzyl 1-(1-phenylethyl)-1H-imidazole-5-carboxylate (2.21)



Carboxylic acid **2.13** (97 mg, 0.45 mmol, 1.0 equiv.), primary alcohol **2.20** (147 mg, 0.450 mmol, 1.0 equiv.) and DMAP (55 mg, 0.45 mmol, 1.0 equiv.) were dissolved in DCM (5 mL) and DMF (0.5 mL). Diisopropylcarbodiimide (0.11 mL, 0.68 mmol, 1.5 equiv.) was added and the mixture was stirred at room temperature for 8 h. The solvent was removed under reduced pressure and the crude product was purified by flash silica gel chromatography (hexanes/EtOAc, gradient from 4:1 to 1:1), followed by another reversed-phase flash silica gel chromatography (H₂O/MeOH, gradient from 20:0 to 1:9), yielding ester **2.21** (215 mg, 0.410 mmol, 91%) as a red solid.

TLC (hexanes/EtOAc, 1:1): *R_f* = 0.44. **[α]_D²²:** +36.0 (*c* = 1.0, CHCl₃). **M.p.:** 179–181 °C. **¹H NMR (CD₃OD, 400 MHz, 27 °C):** δ = 8.13 (s, 1H, ArH), 7.86–7.81 (m, 4H, ArH), 7.78 (s, 1H, ArH), 7.61–7.57 (m, 2H, ArH), 7.48–7.44 (m, 2H, ArH), 7.32–7.24 (m, 3H, ArH), 7.18–7.14 (m, 2H, ArH), 6.34 (q, *J* = 7.2 Hz, 1H, CH), 5.32–5.28 (m, 2H, CH₂), 1.87 (d, *J* = 7.2 Hz, 3H, CH₃), 1.53 (s, 9H, C(CH₃)₃) ppm. **¹³C NMR (CD₃OD, 100 MHz, 27 °C):** δ = 159.5, 153.4, 152.4, 147.7, 142.6, 141.5, 140.2, 138.4, 136.9, 128.4, 128.4, 127.5, 125.7, 123.5, 122.3, 119.8, 118.0, 79.9, 65.2, 55.9, 27.2, 20.9 ppm. **IR (neat, ATR):** $\tilde{\nu}$ = 3371 (w), 2976 (w), 2310 (w), 1715 (s), 1603 (m), 1539 (w), 1506 (m), 1453 (w), 1434 (m), 1387 (vs), 1367 (s), 1304 (m), 1256 (m), 1217 (vs), 1160 (m), 1132 (m), 1119 (s), 1072 (s), 1028 (w), 1012 (w), 983 (w), 930 (w), 887 (w), 864 (w), 846 (m), 832 (m), 762 (m), 774 (m), 742 (w), 725 (w), 708 (w), 694 (w), 660 (w) cm⁻¹. **HRMS (ESI⁺):** *m/z* calcd. for [C₃₀H₃₂N₅O₄]⁺: 526.2454, found: 526.2446 ([M+H]⁺).

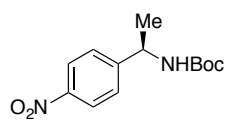
Synthesis of (*R*)-4-((4-aminophenyl)diazenyl)benzyl 1-(1-phenylethyl)-1*H*-imidazole-5-carboxylate (AETD5)



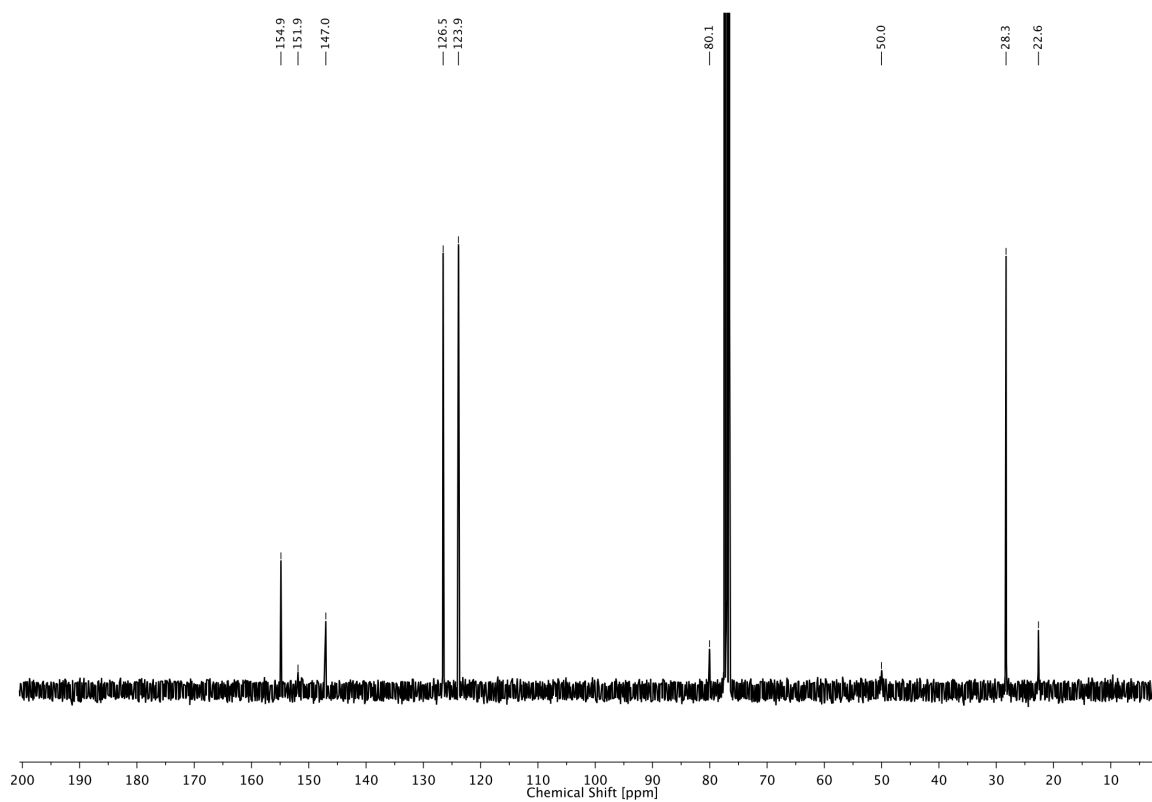
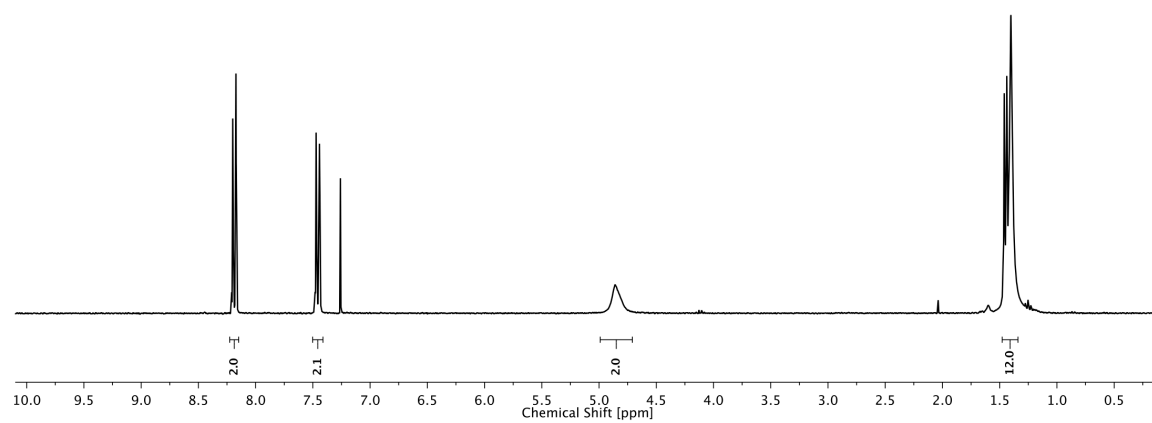
Boc-protected aniline **2.21** (75 mg, 0.14 mmol) was dissolved in 1,4-dioxane (3 mL) and a 4 M solution of HCl in dioxane (3 mL) was added. The mixture was stirred for 16 h at room temperature. 1 M HCl (20 mL) was added and the aqueous phase was washed with EtOAc (20 mL). The aqueous phase then was basified to pH = 8–10 with 2 M NaOH and extracted with CHCl₃ (2 x 20 mL). The combined organic layers were washed with brine (50 mL), dried over MgSO₄ and concentrated *in vacuo*. The crude product was purified by reversed-phase flash silica gel chromatography (H₂O/MeOH, gradient from 10:0 to 2:8), yielding ester **AETD5** (52 mg, 0.12 mmol, 86%) as a orange oil.

TLC (hexanes/EtOAc, 1:1): $R_f = 0.34$. $[\alpha]_D^{22}$: +47.3 ($c = 1.0$, CHCl₃). **¹H NMR (CD₃OD, 400 MHz, 27 °C):** $\delta = 8.11$ (s, 1H, ArH), 7.76–7.68 (m, 5H, ArH), 7.44–7.41 (m, 2H, ArH), 7.33–7.21 (m, 3H, ArH), 7.17–7.13 (m, 2H, ArH), 6.74–6.70 (m, 2H, ArH), 6.33 (q, $J = 7.2$ Hz, 1H, CH), 5.28 (s, 2H, CH₂), 1.86 (d, $J = 7.2$ Hz, 3H, CH₃) ppm. **¹³C NMR (CD₃OD, 100 MHz, 27 °C):** $\delta = 159.5, 152.8, 152.4, 144.2, 141.6, 140.2, 137.1, 136.8, 128.5, 128.4, 127.5, 125.8, 124.9, 122.6, 121.8, 113.7, 65.4, 55.9, 20.9$ ppm. **IR (neat, ATR):** $\tilde{\nu} = 3344$ (m), 3214 (m), 1714 (m), 1621 (m), 1600 (vs), 1537 (w), 1507 (m), 1456 (w), 1430 (w), 1405 (w), 1383 (w), 1350 (m), 1306 (m), 1212 (s), 1137 (s), 1107 (m), 1054 (w), 839 (m), 759 (m), 701 (w), 659 (w) cm⁻¹. **HRMS (ESI⁺):** m/z calcd. for [C₂₅H₂₄N₅O₂]⁺: 426.1930, found: 426.1923 ([M+H]⁺). **UV/Vis:** $\lambda_{\max} = 410$ nm.

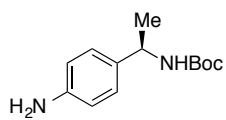
2.3.3 NMR SPECTRA



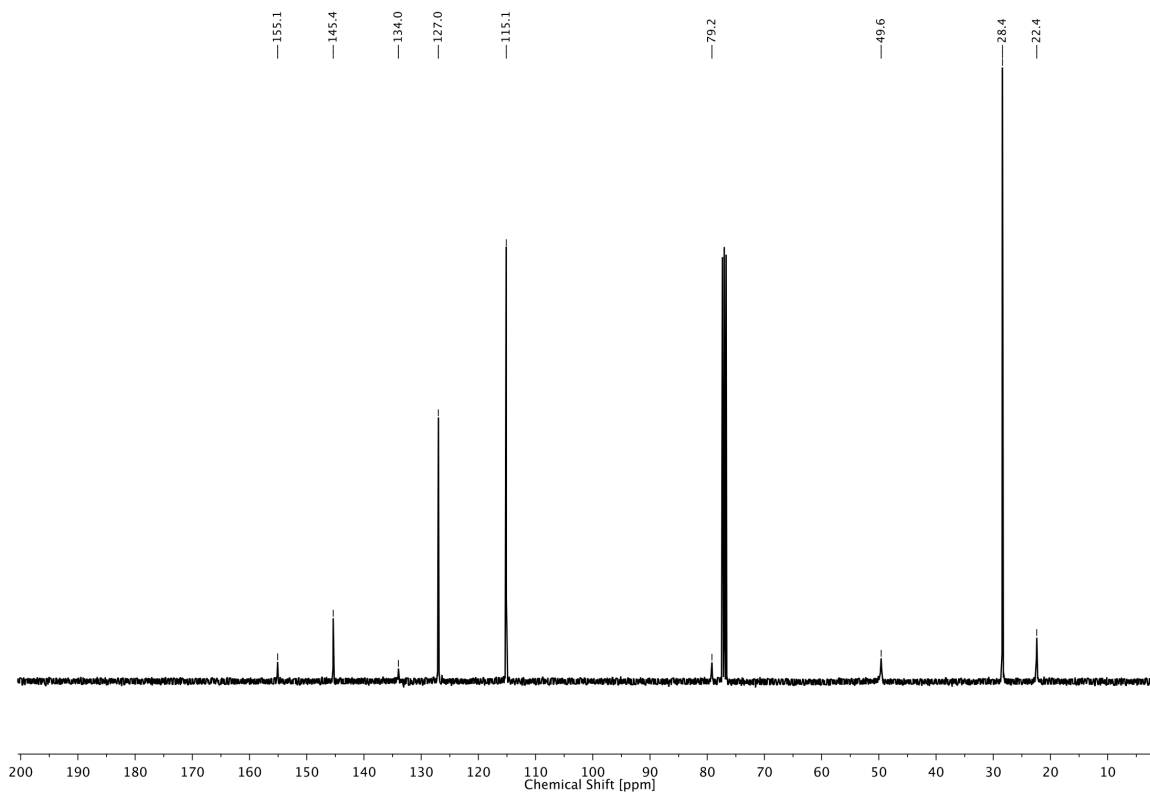
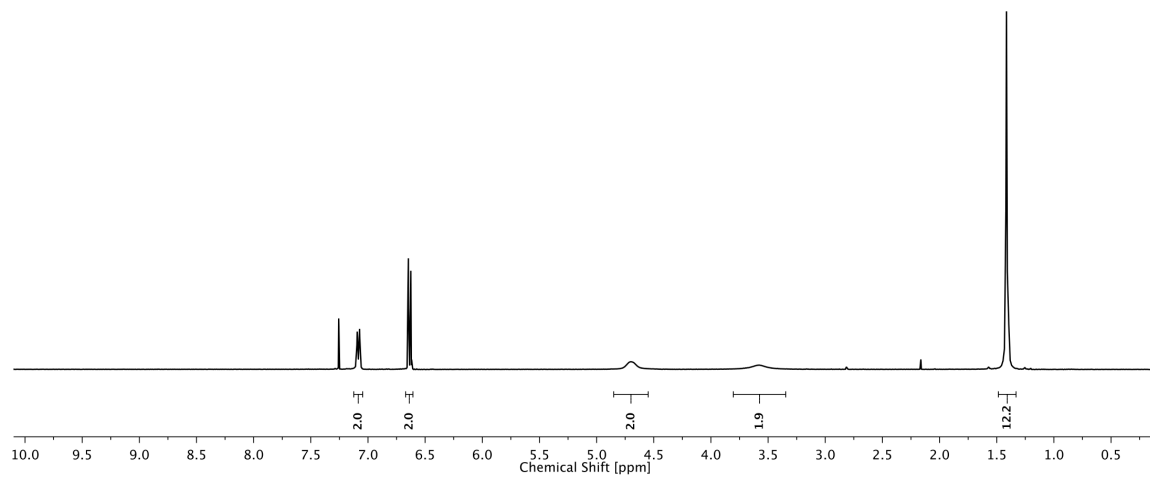
2.6



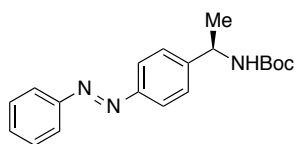
2 PHOTOREGULATION OF GABA_A RECEPTORS



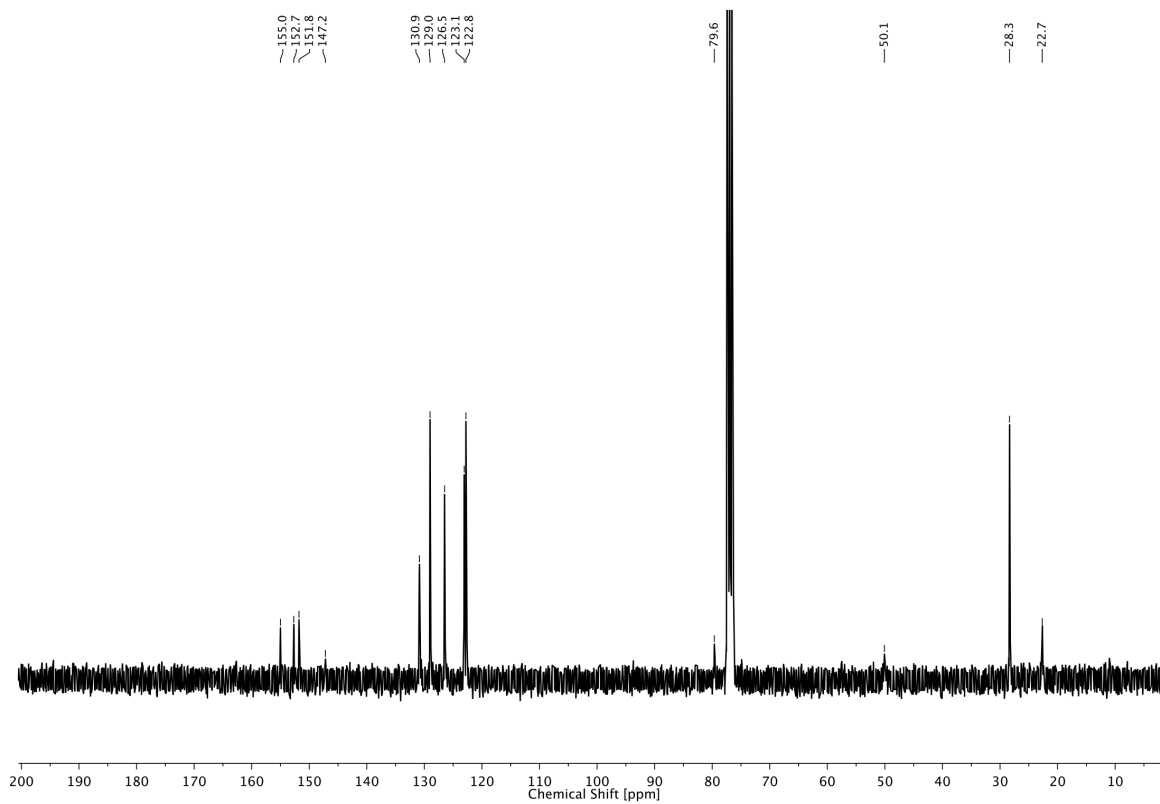
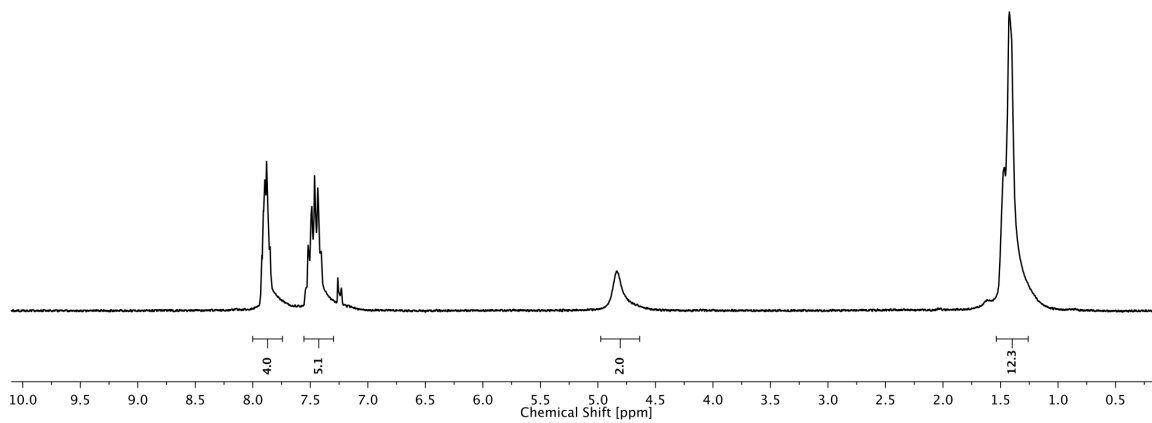
2.7

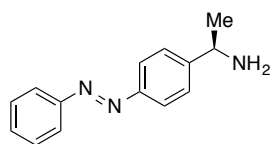


2 PHOTOREGULATION OF GABA_A RECEPTORS

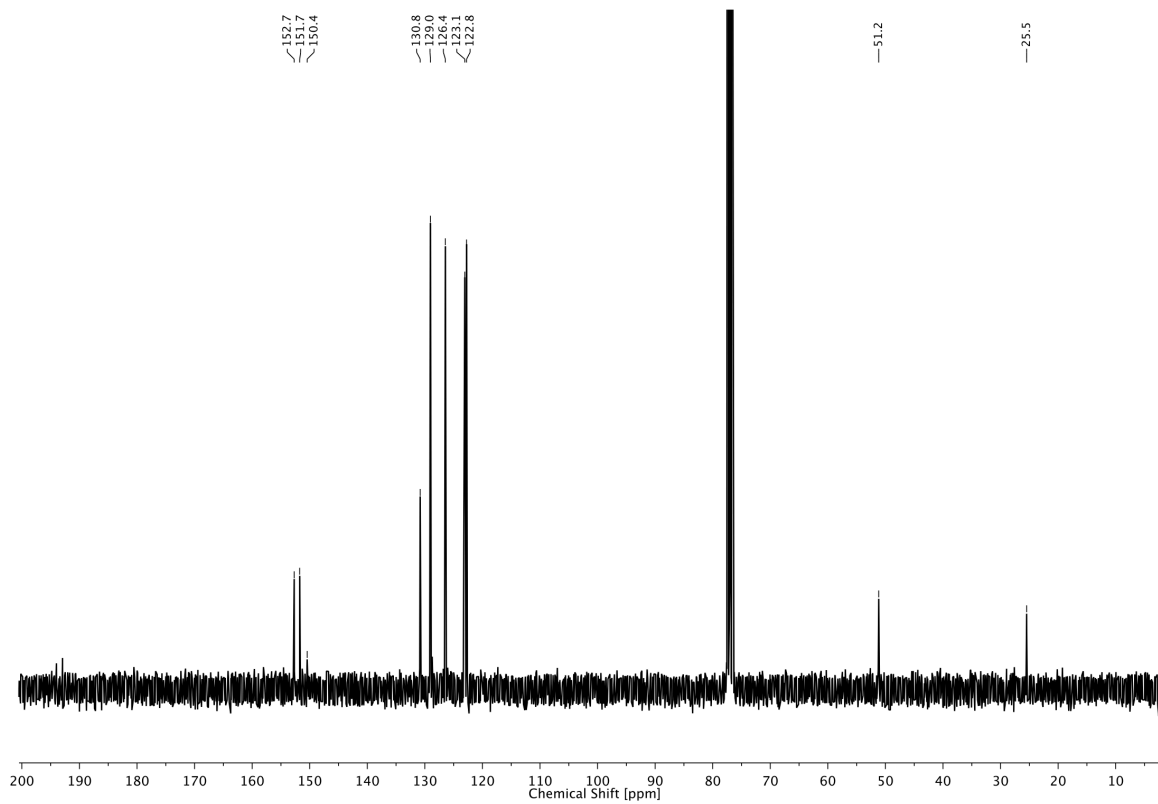
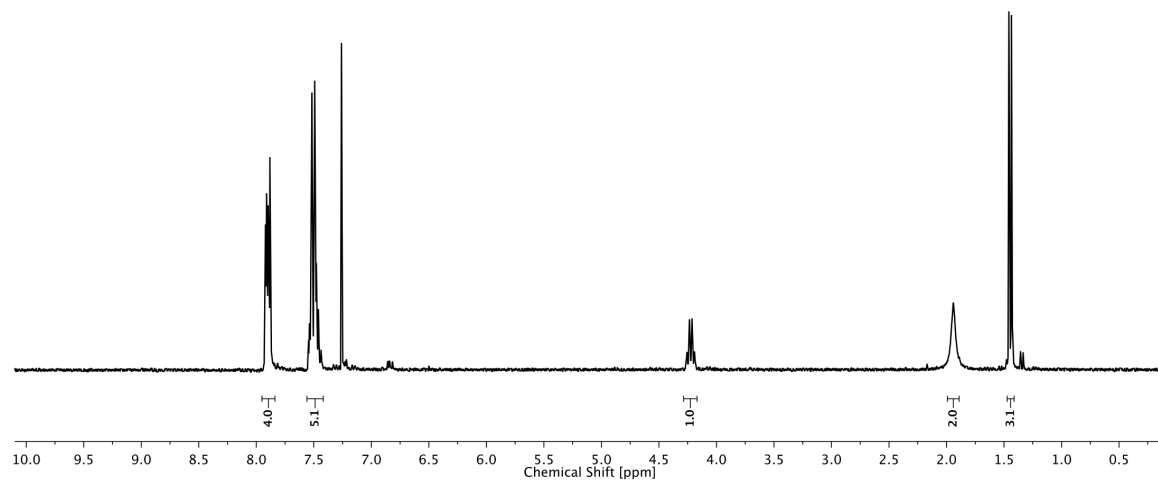


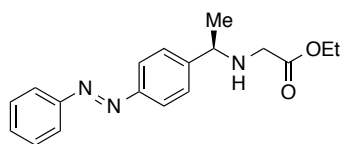
2.8



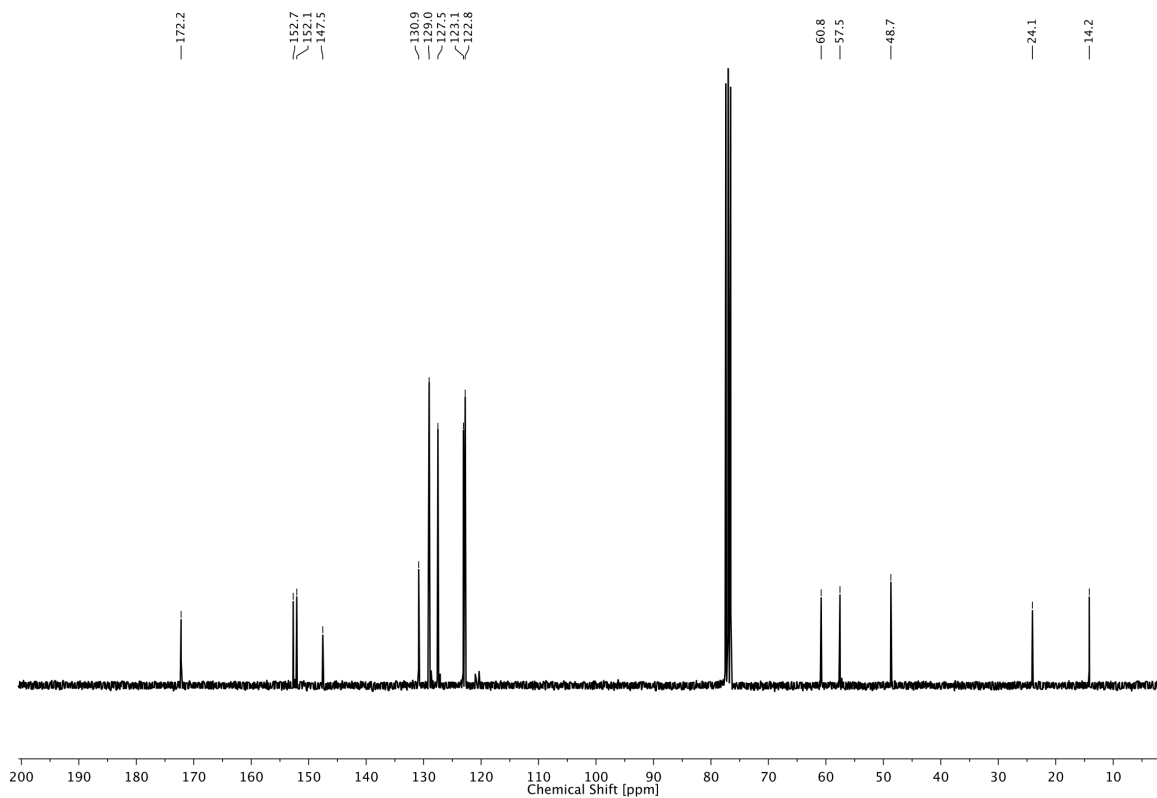
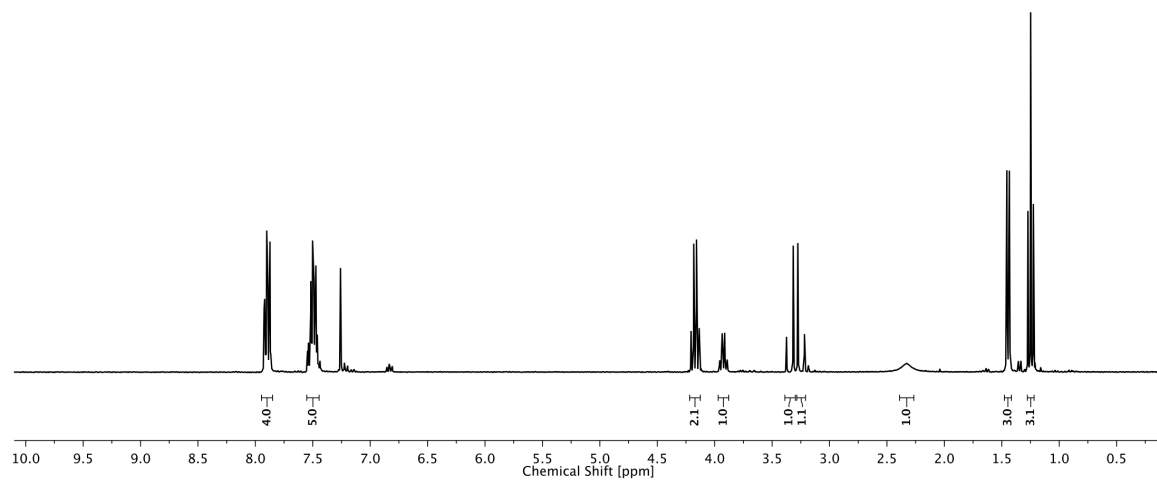


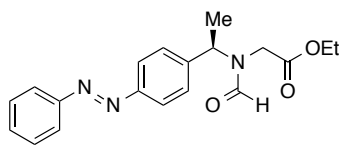
2.9



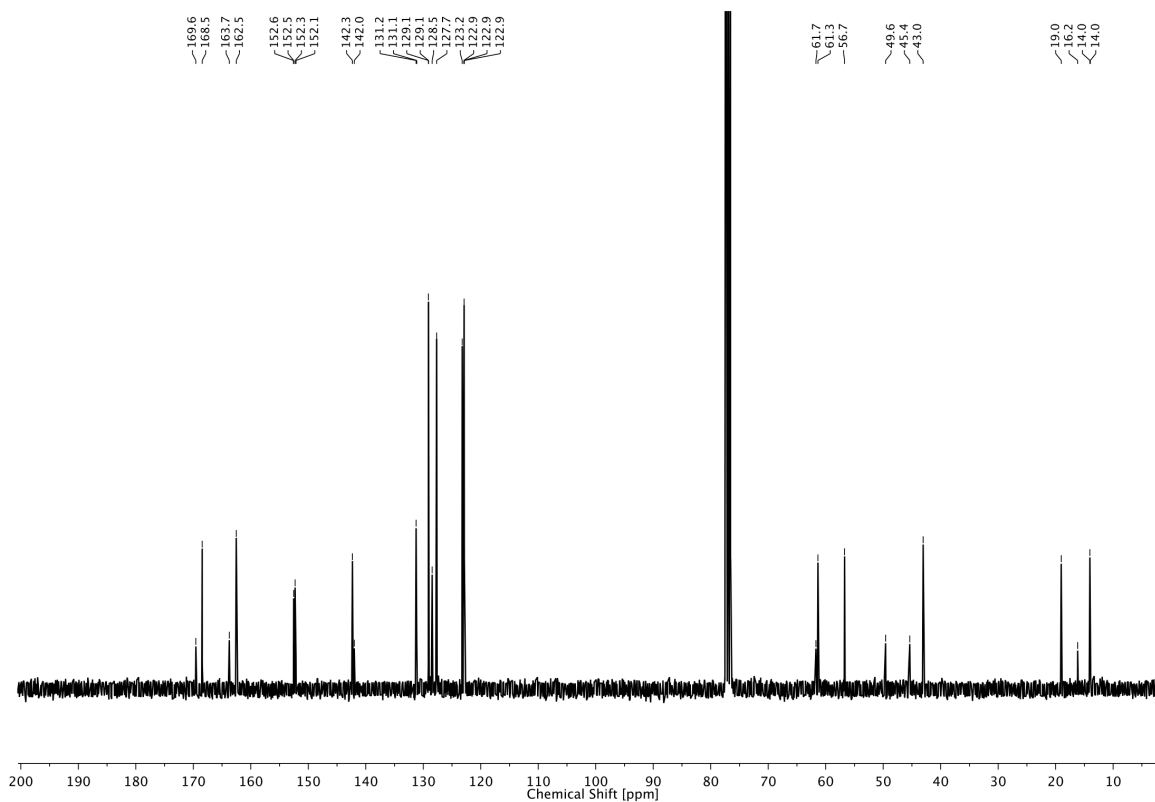
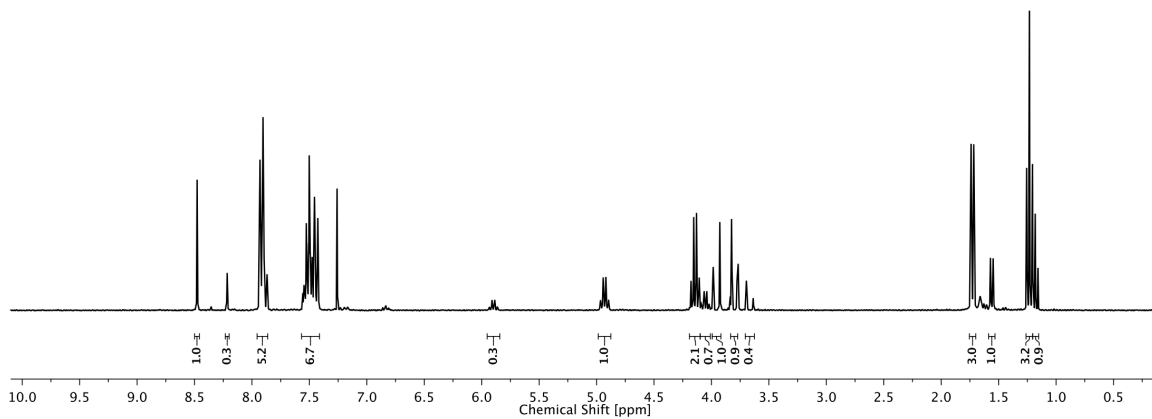


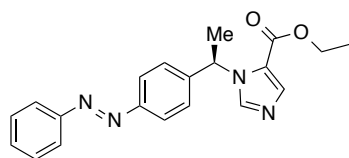
2.10



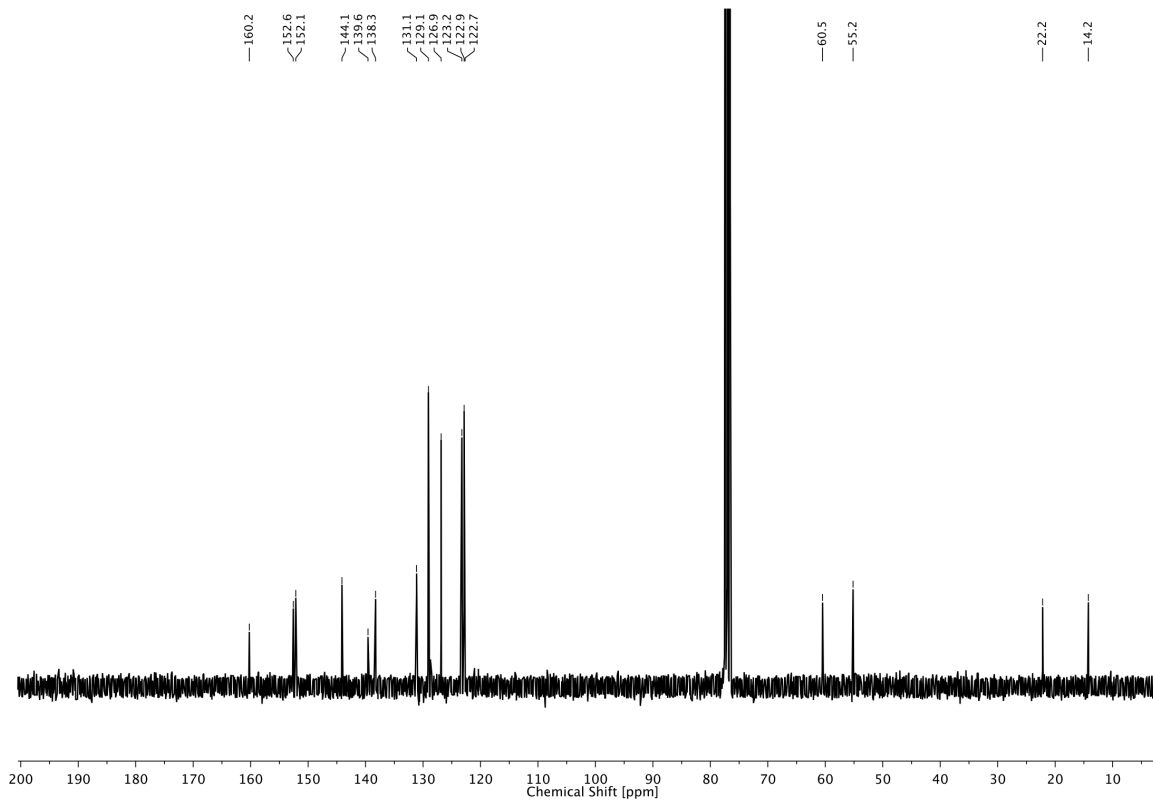
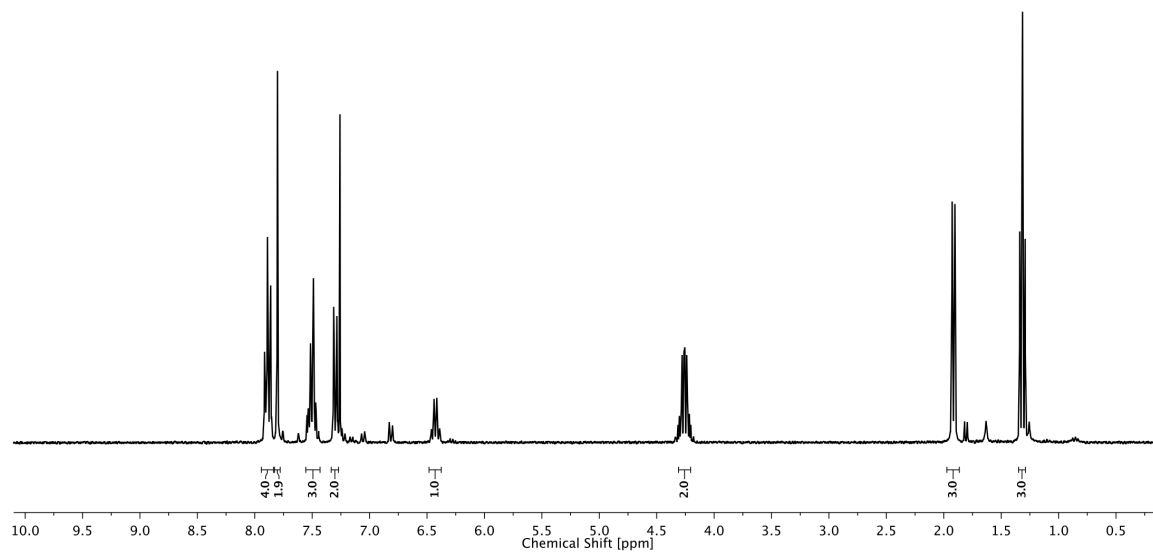


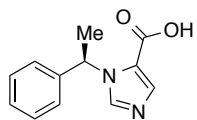
2.11



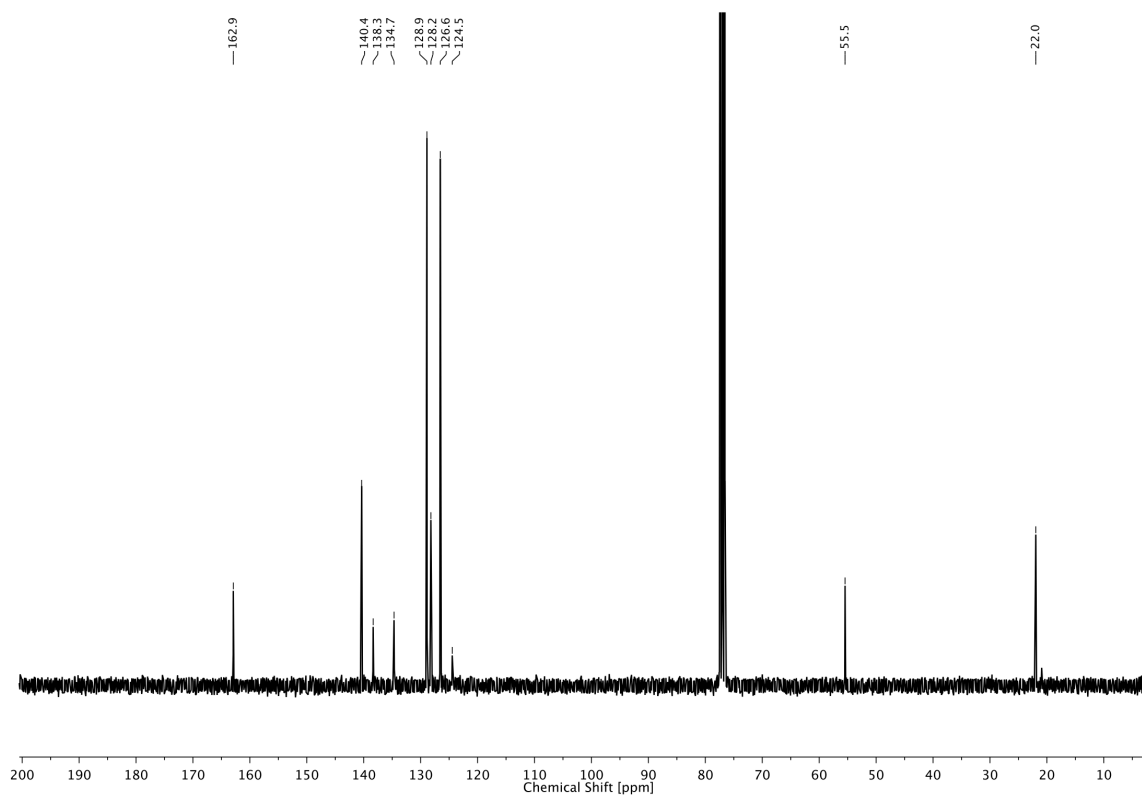
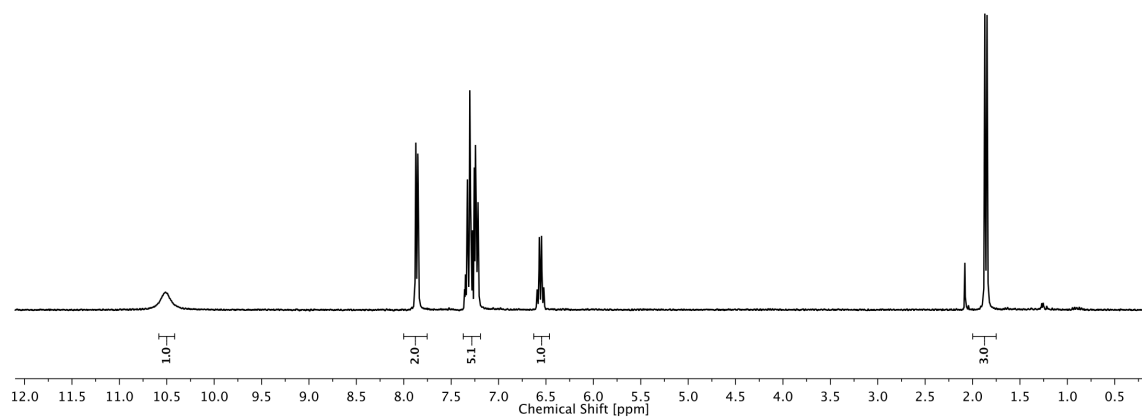


AETD1

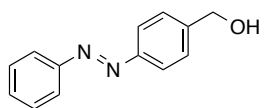




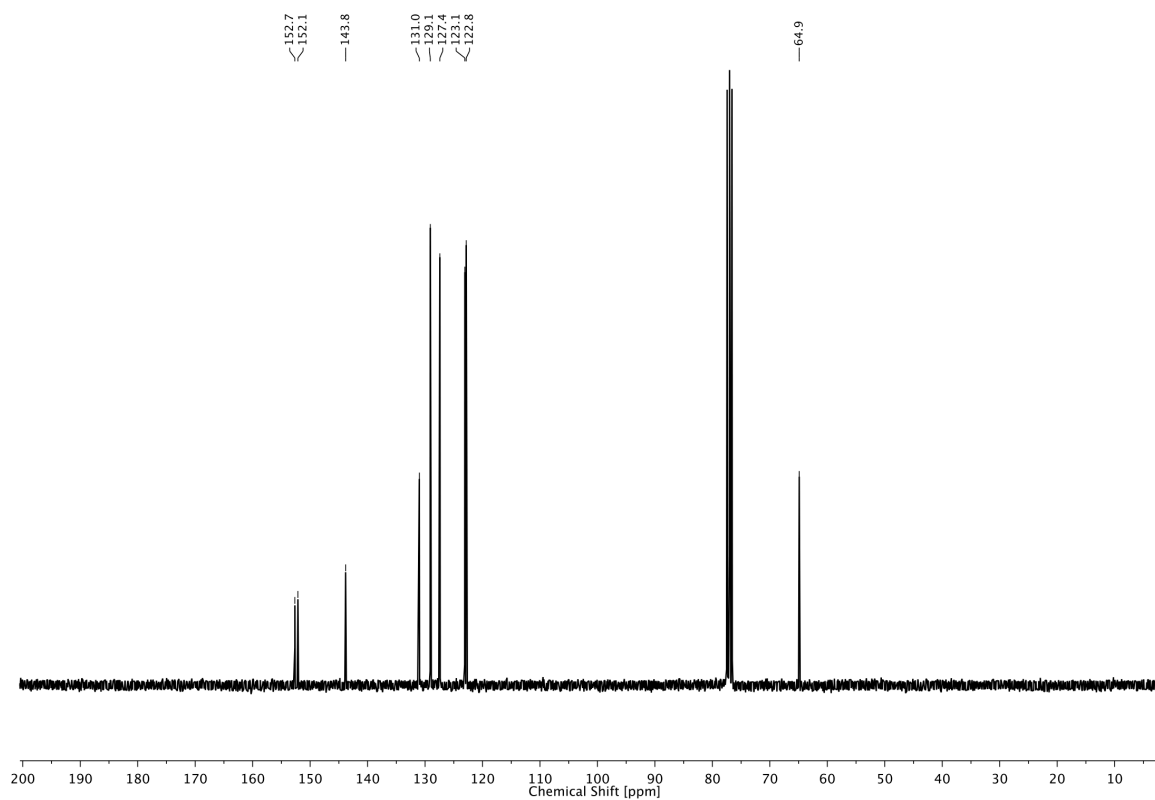
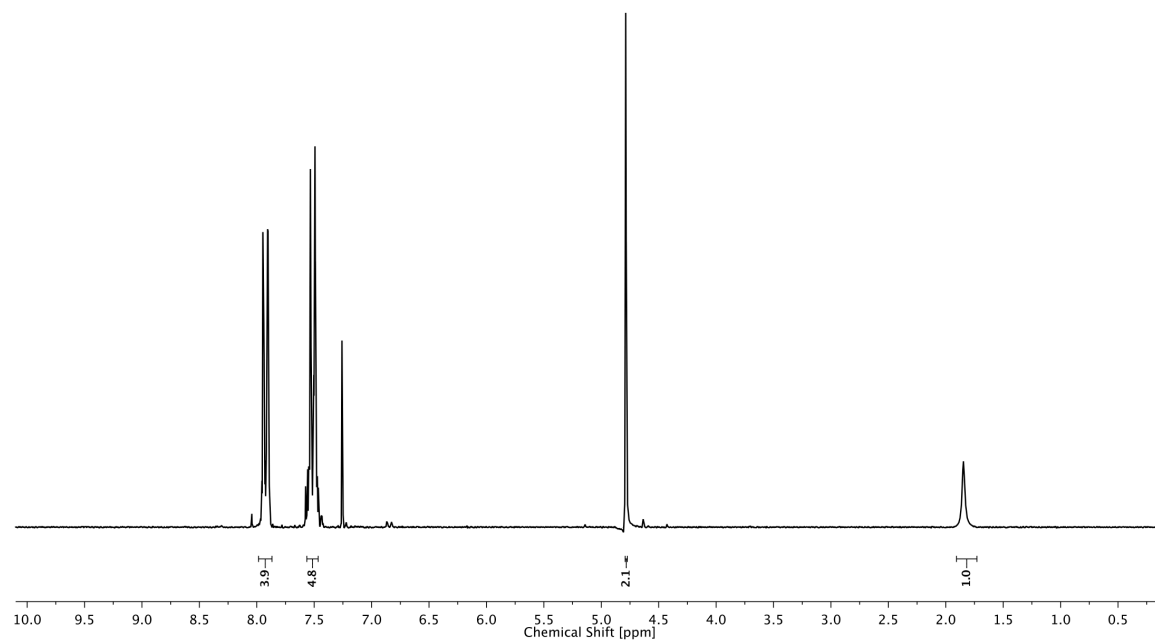
2.13



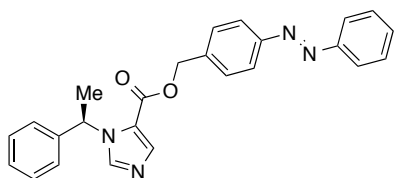
2 PHOTOREGULATION OF GABA_A RECEPTORS



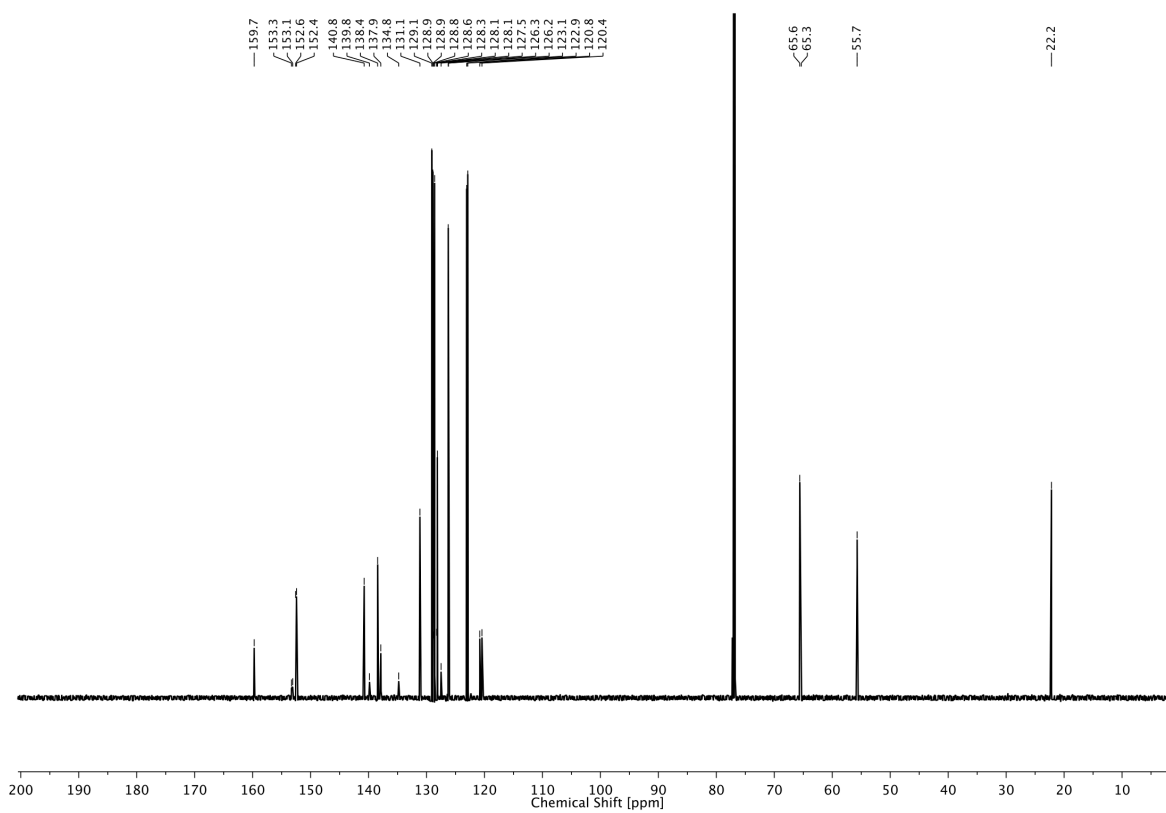
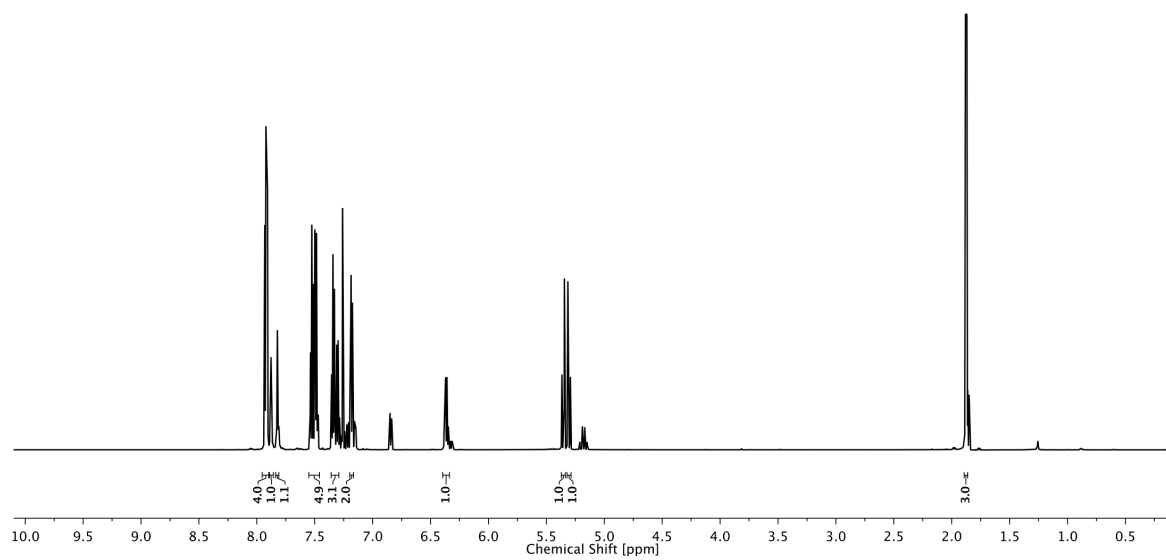
2.14



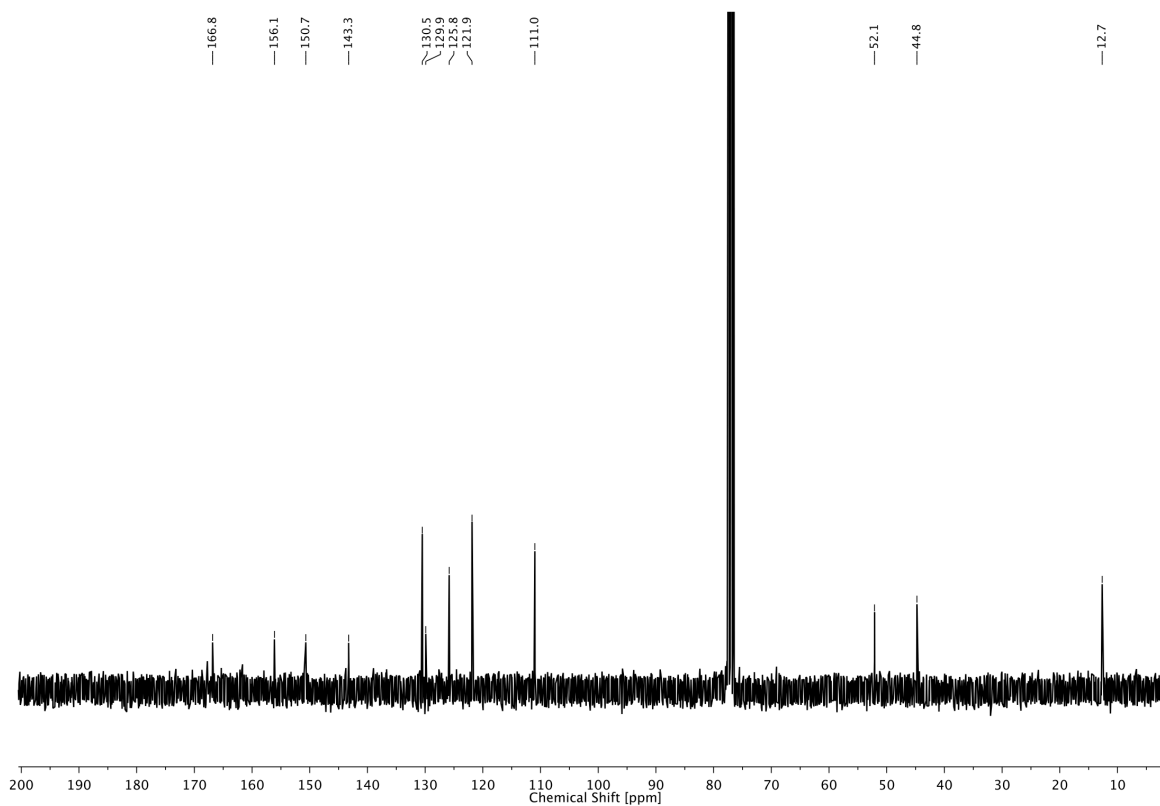
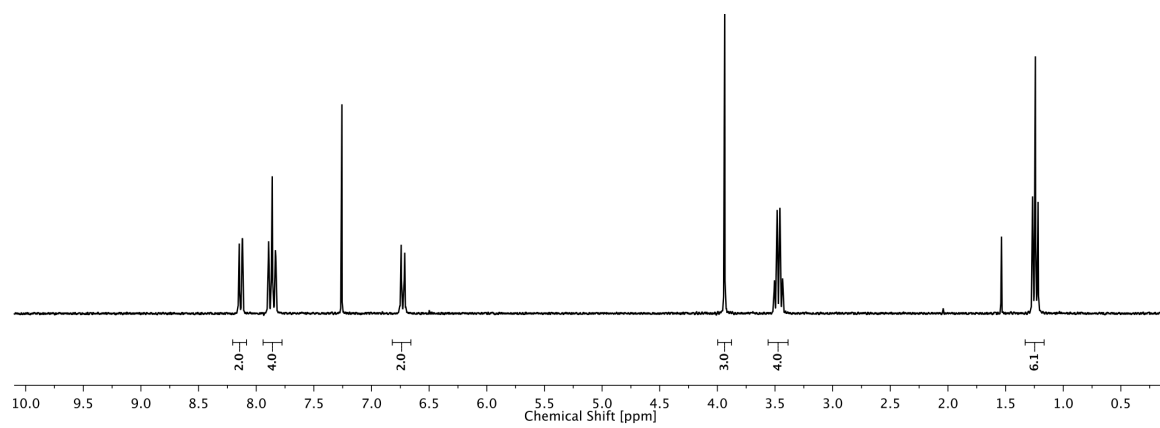
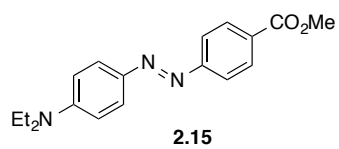
2 PHOTOREGULATION OF GABA_A RECEPTORS



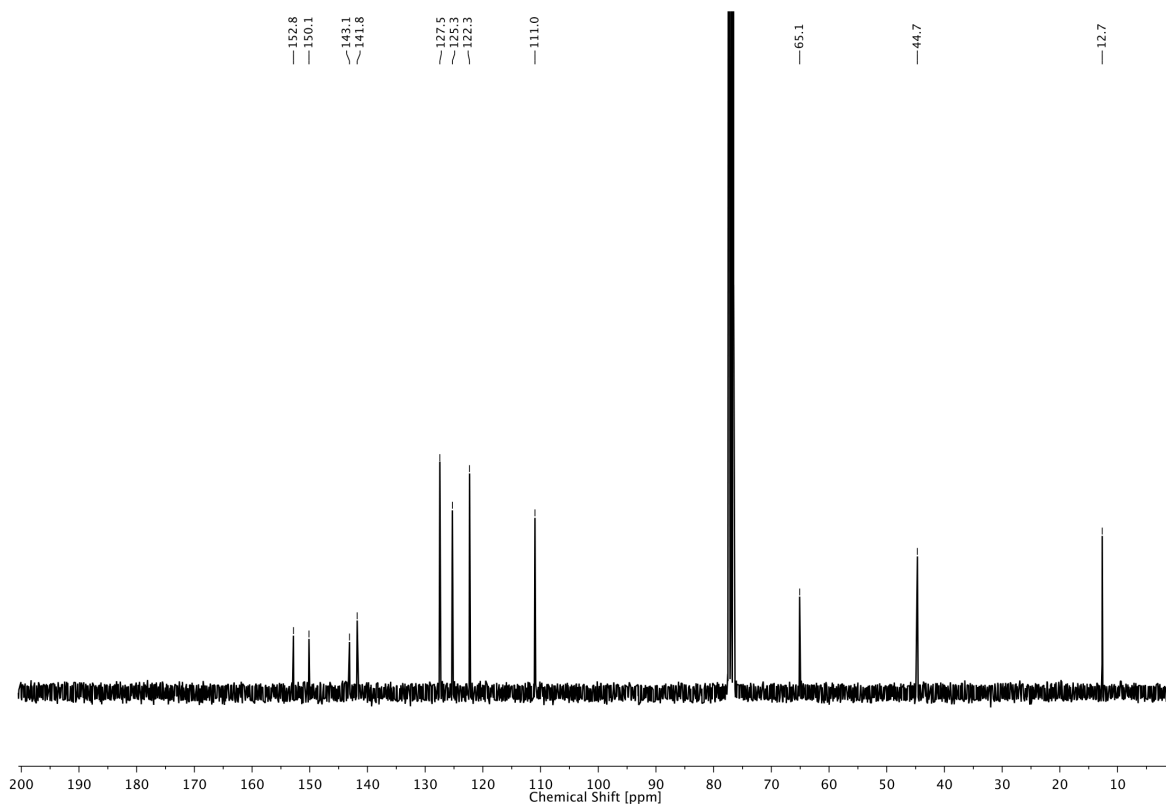
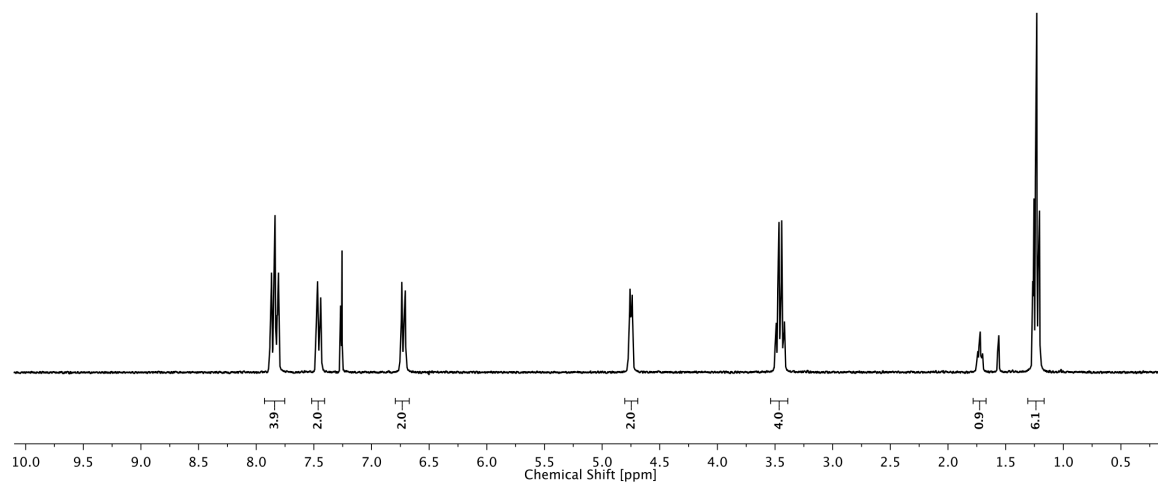
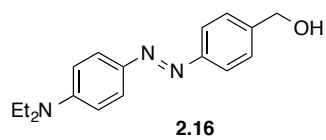
AETD2



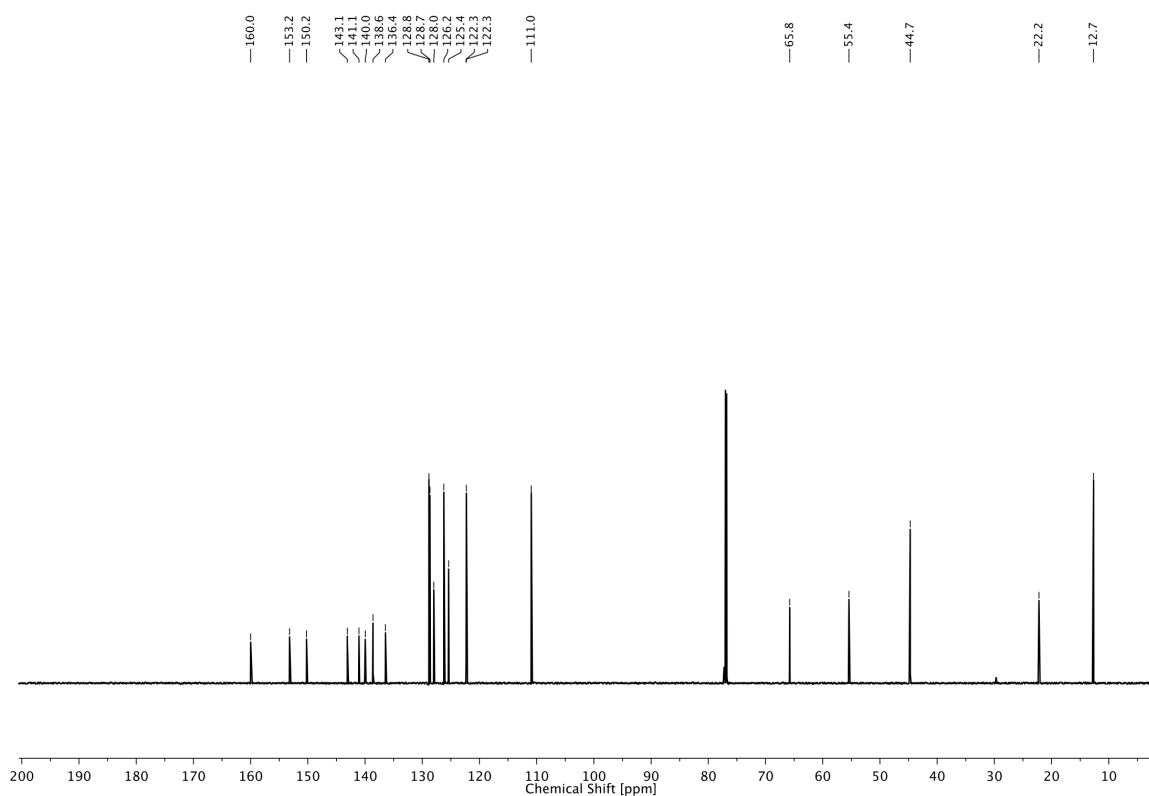
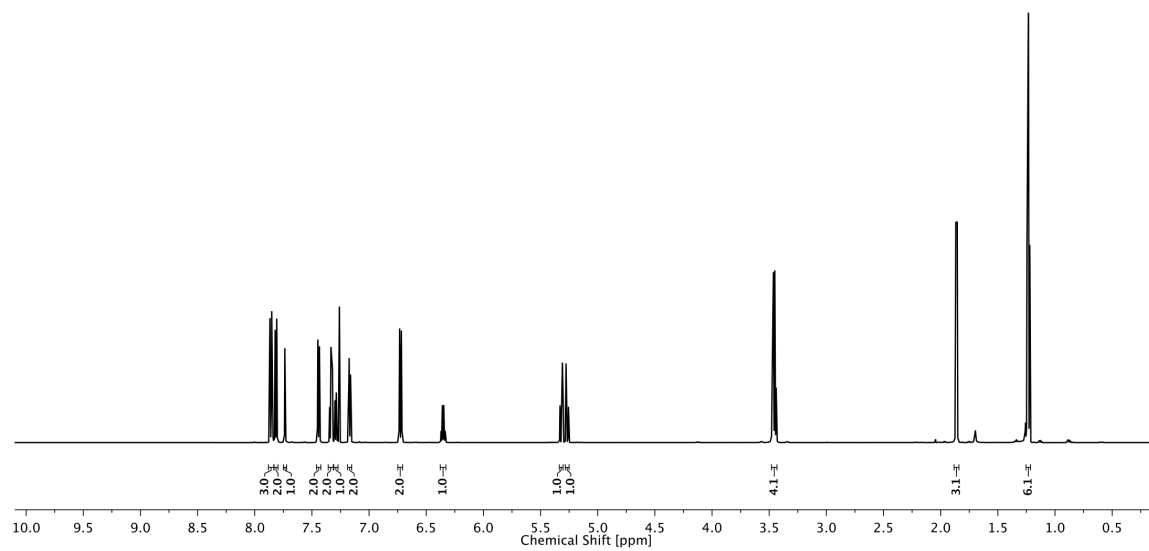
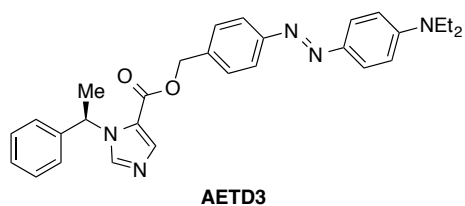
2 PHOTOREGULATION OF GABA_A RECEPTORS



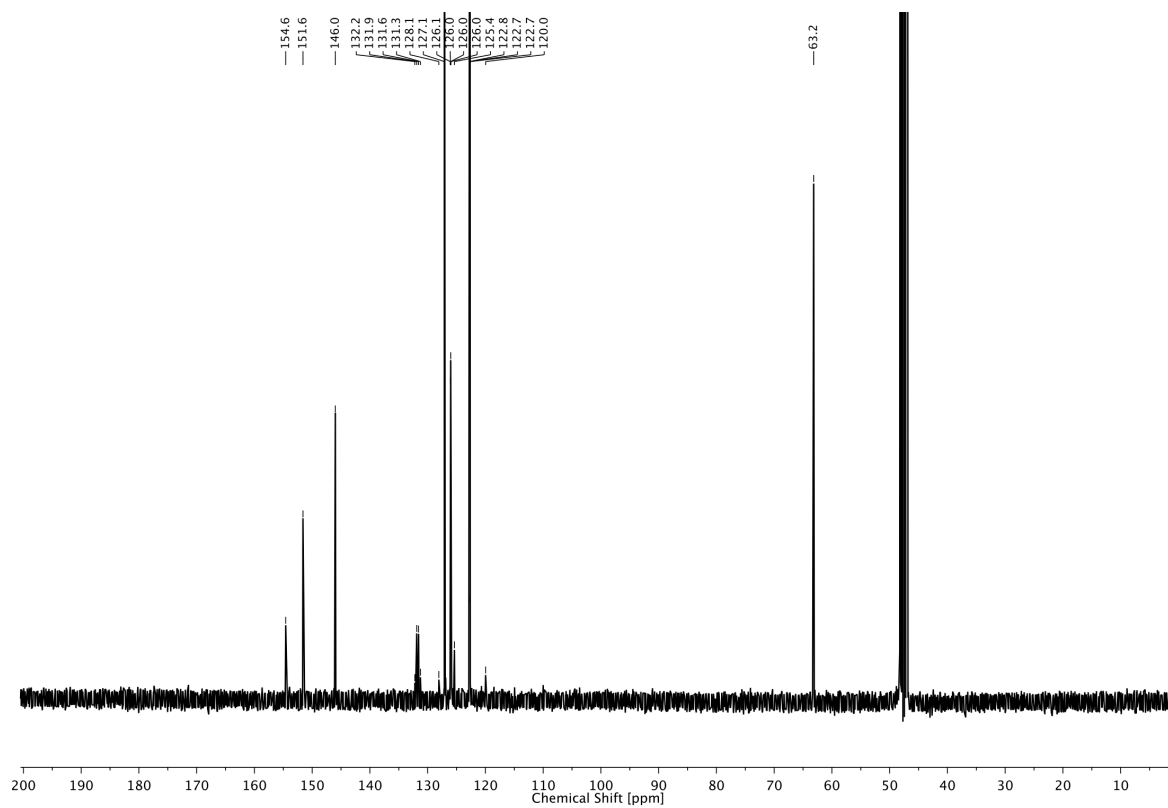
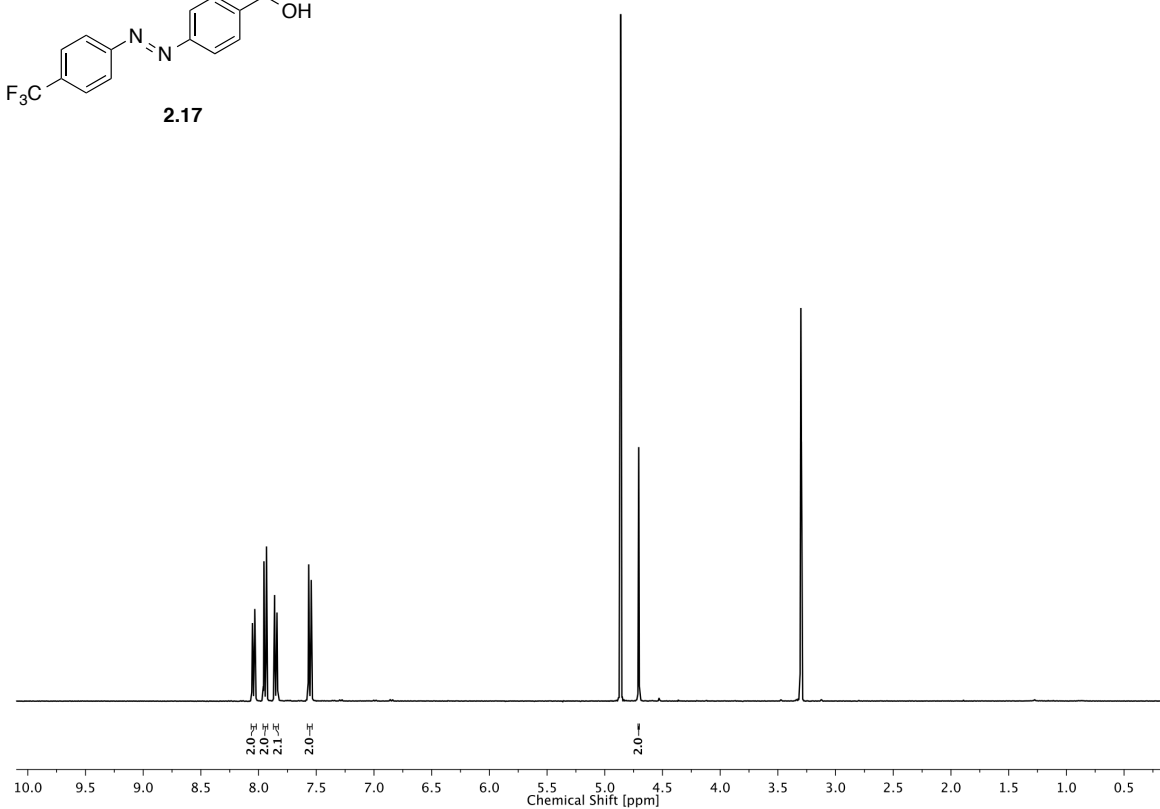
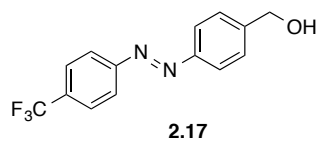
2 PHOTOREGULATION OF GABA_A RECEPTORS

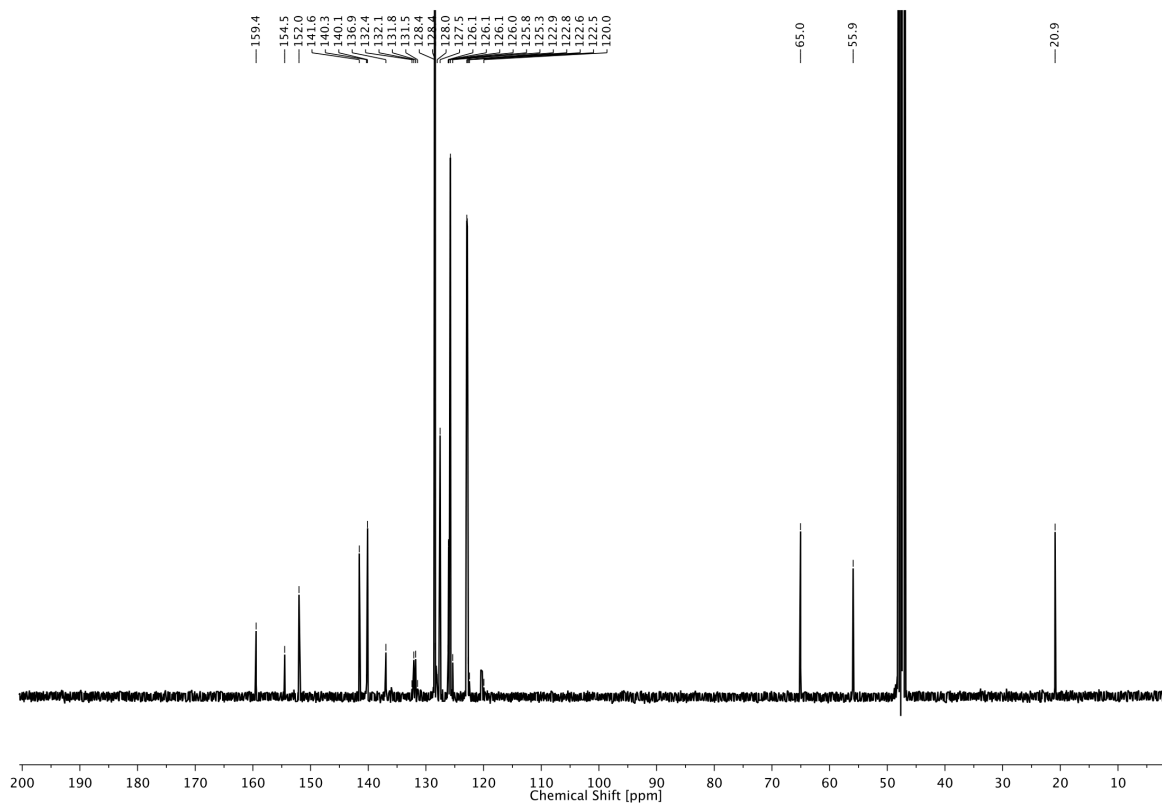
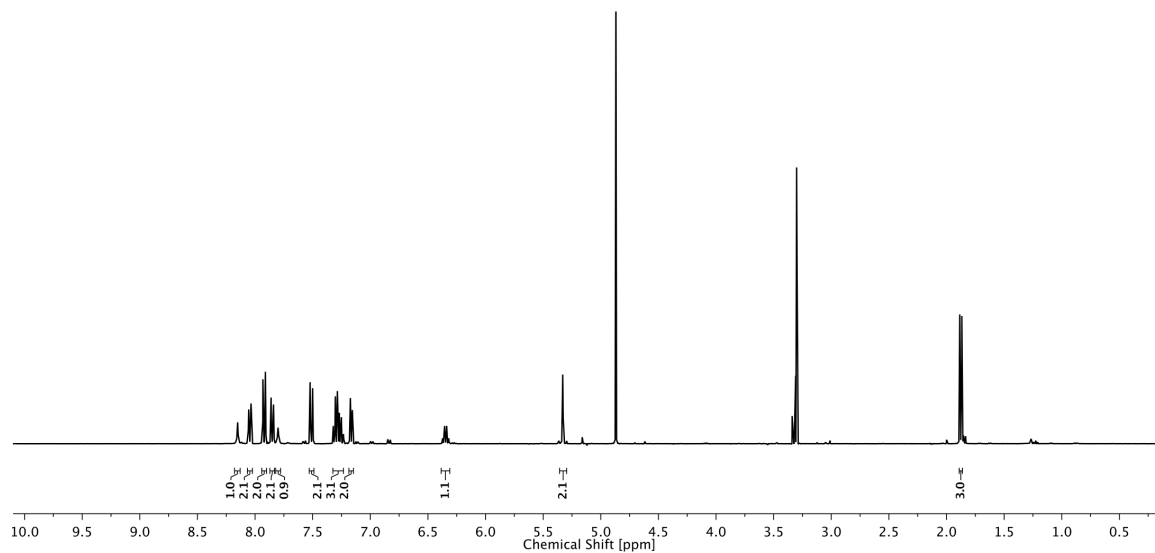
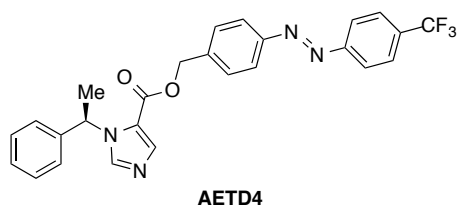


2 PHOTOREGULATION OF GABA_A RECEPTORS

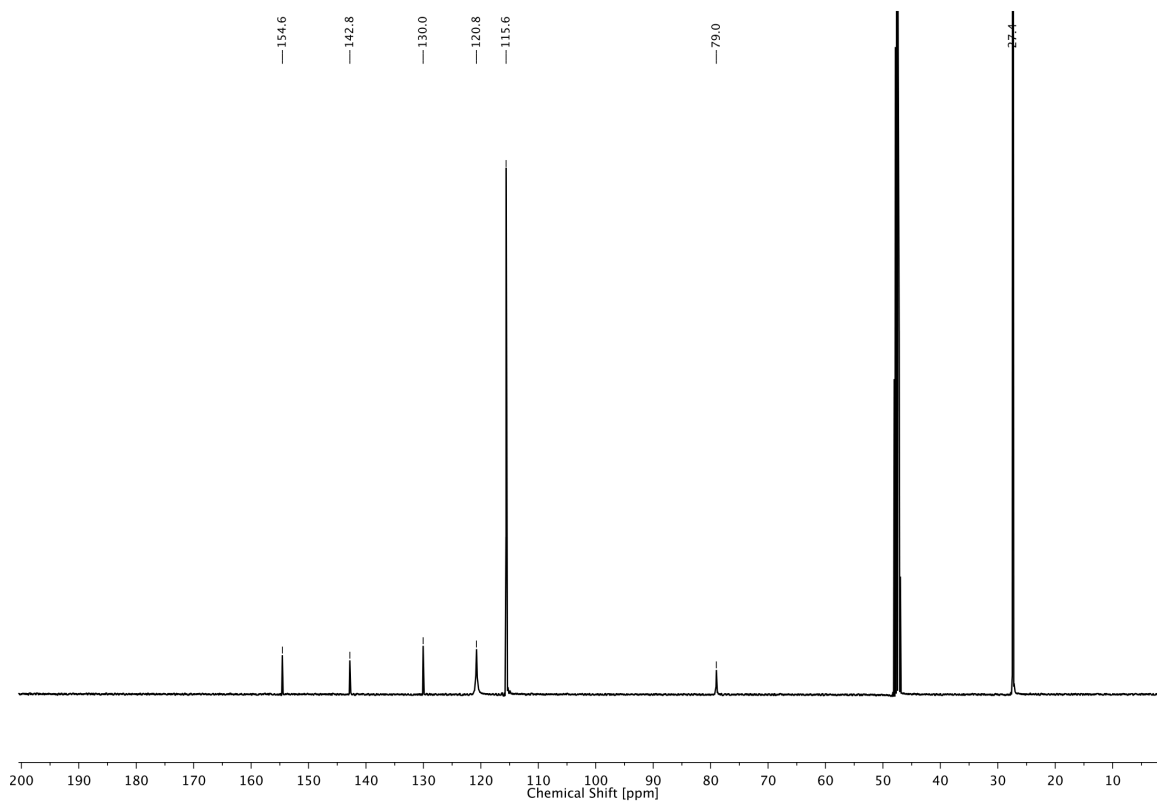
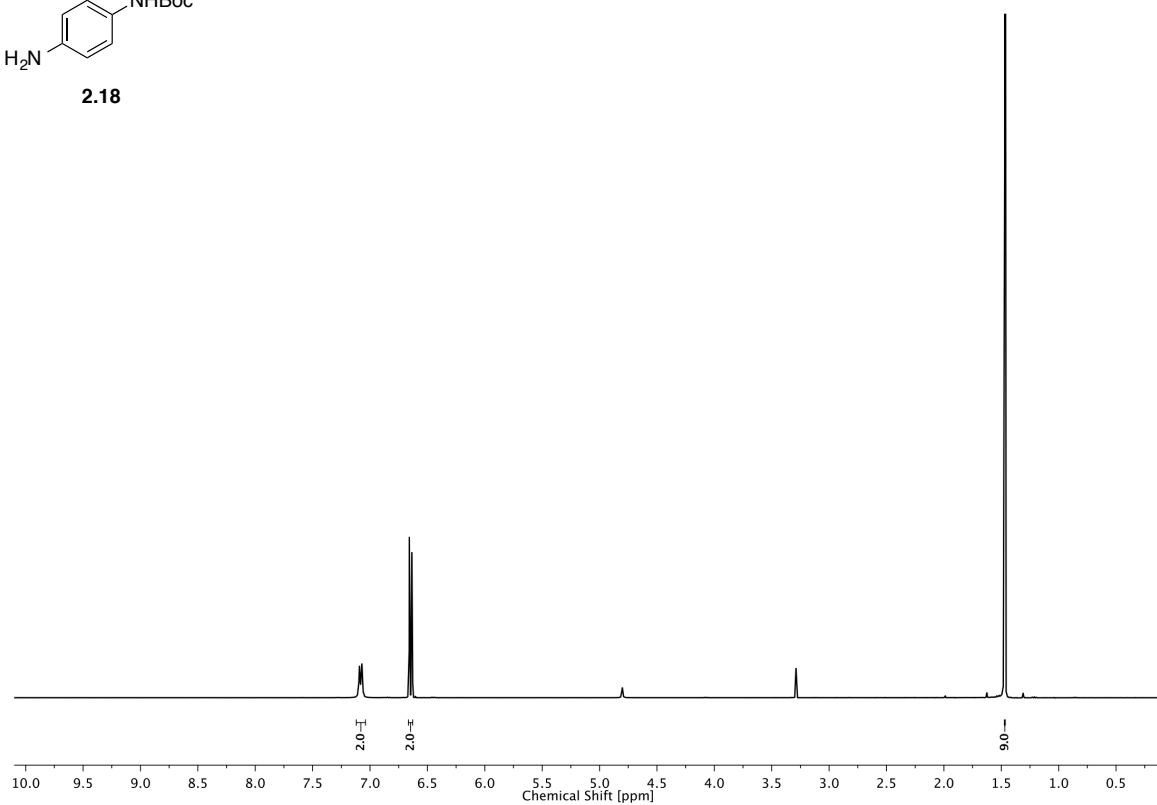
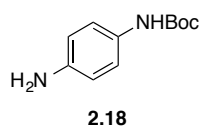


2 PHOTOREGULATION OF GABA_A RECEPTORS

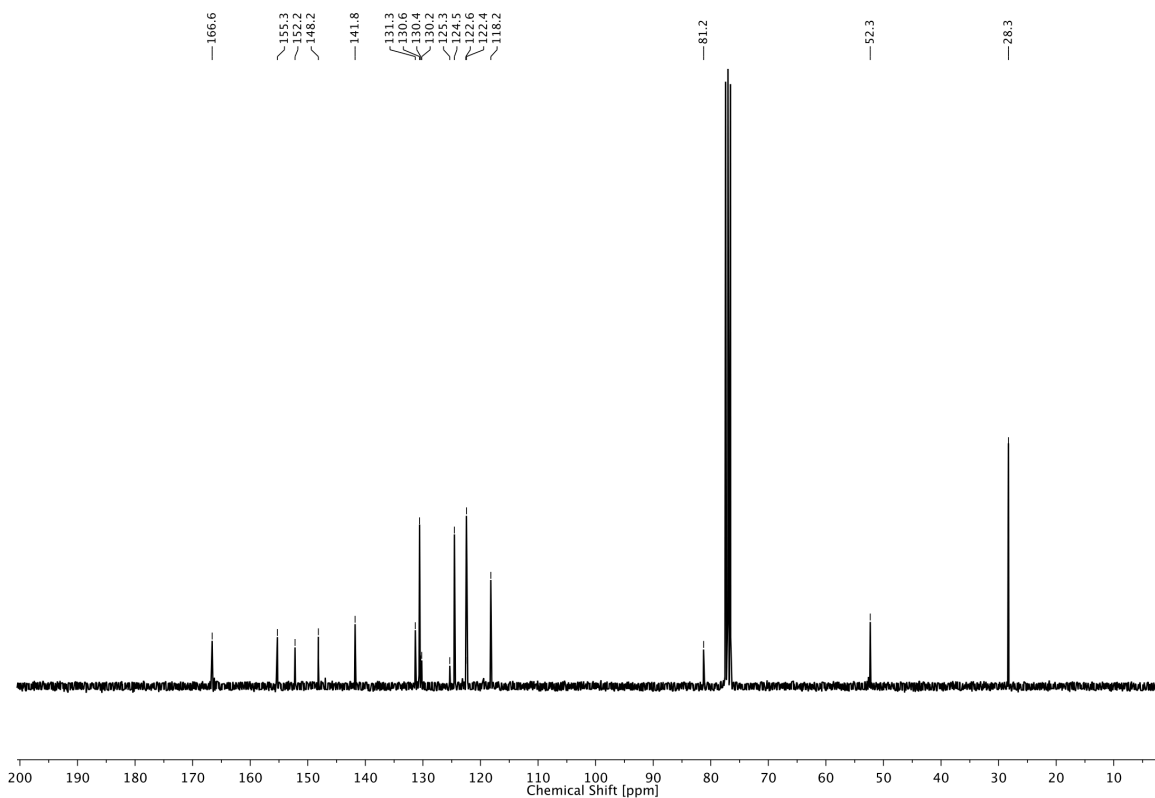
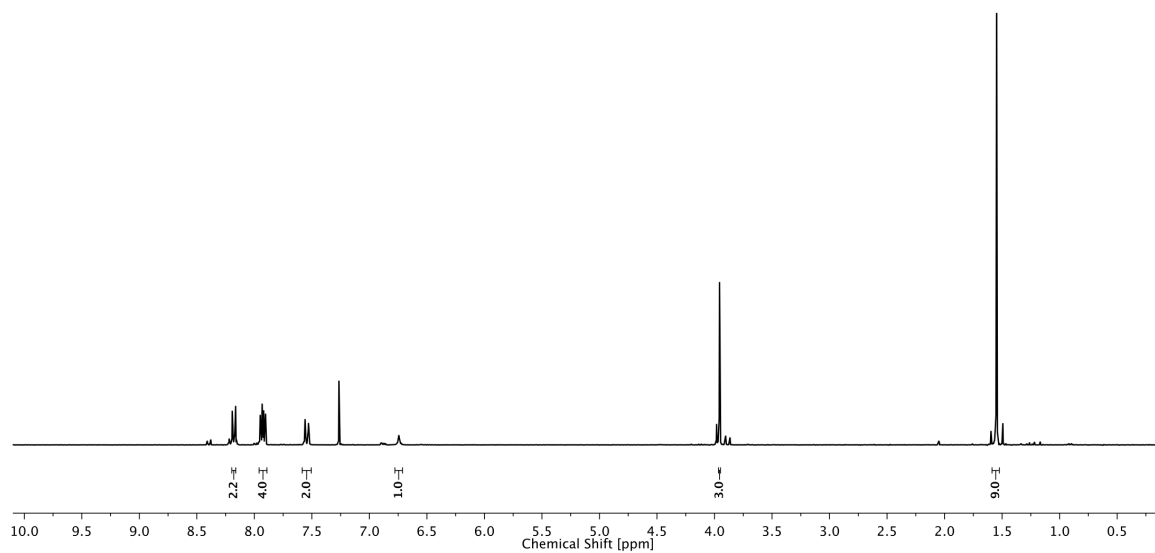
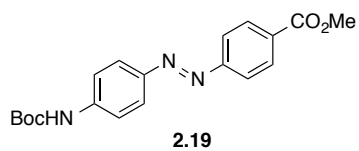




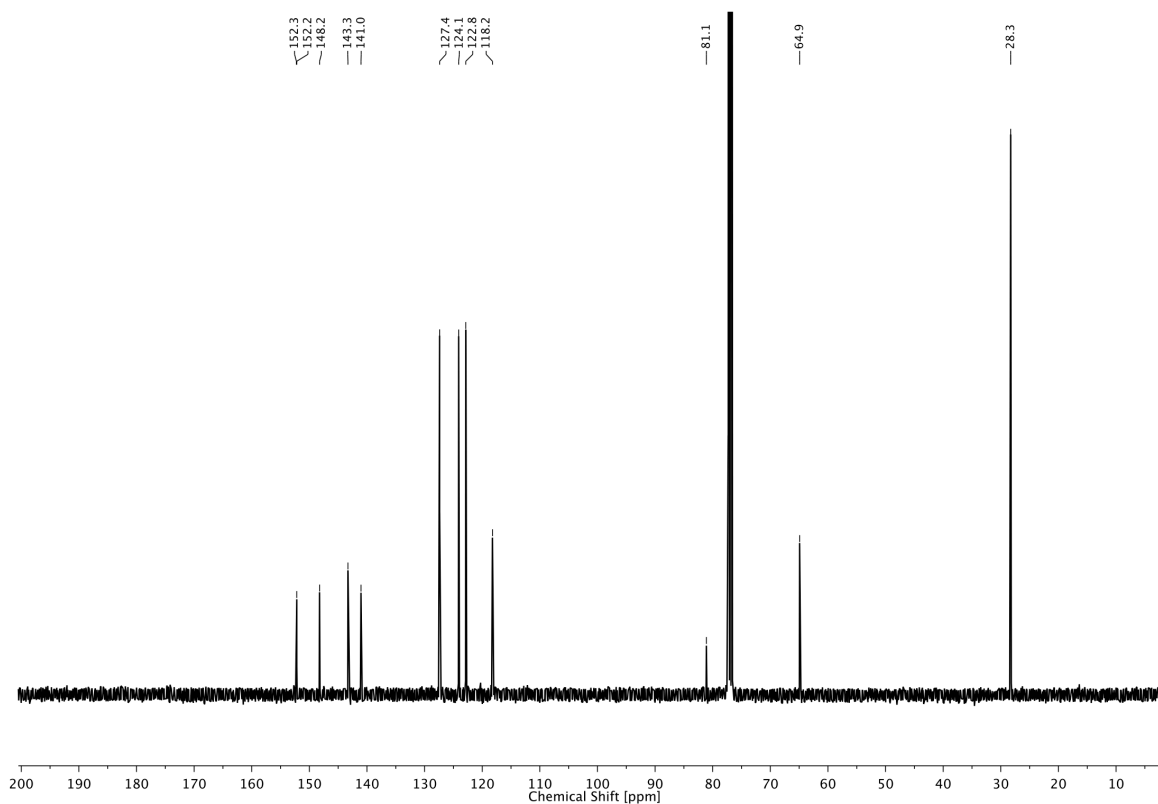
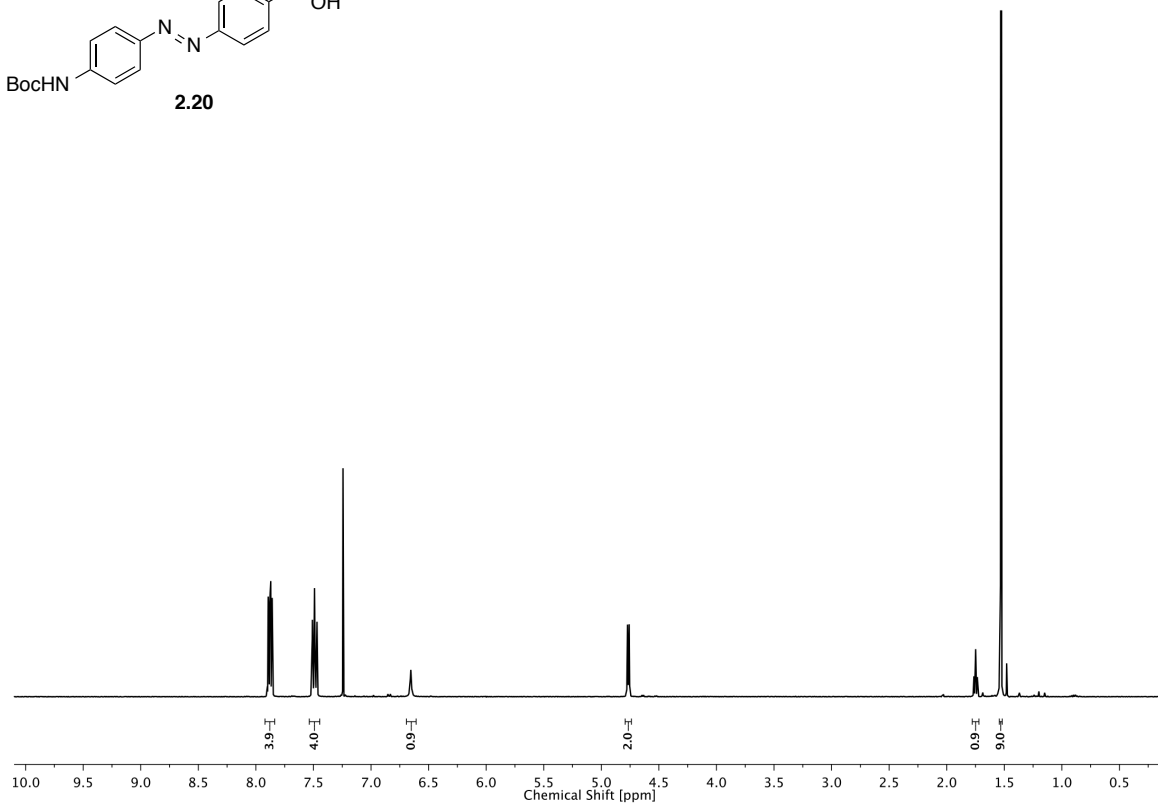
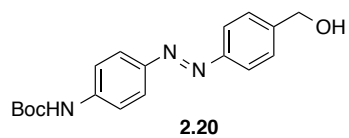
2 PHOTOREGULATION OF GABA_A RECEPTORS

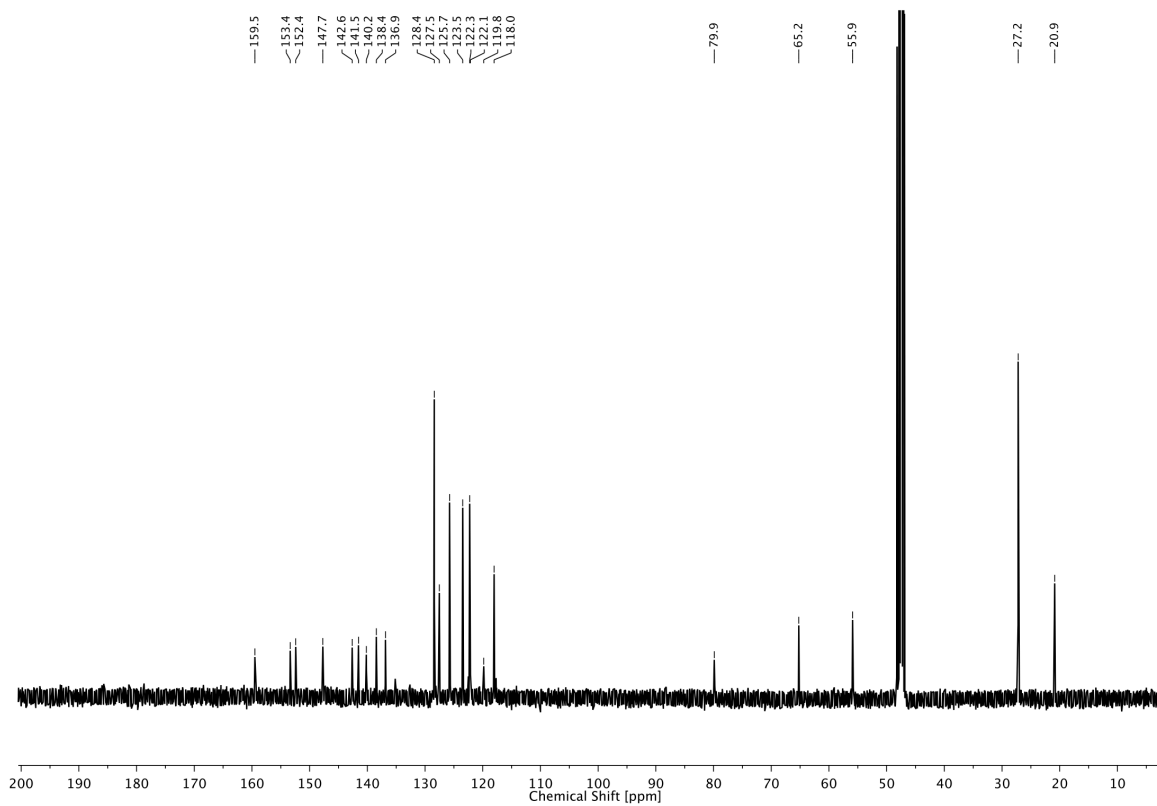
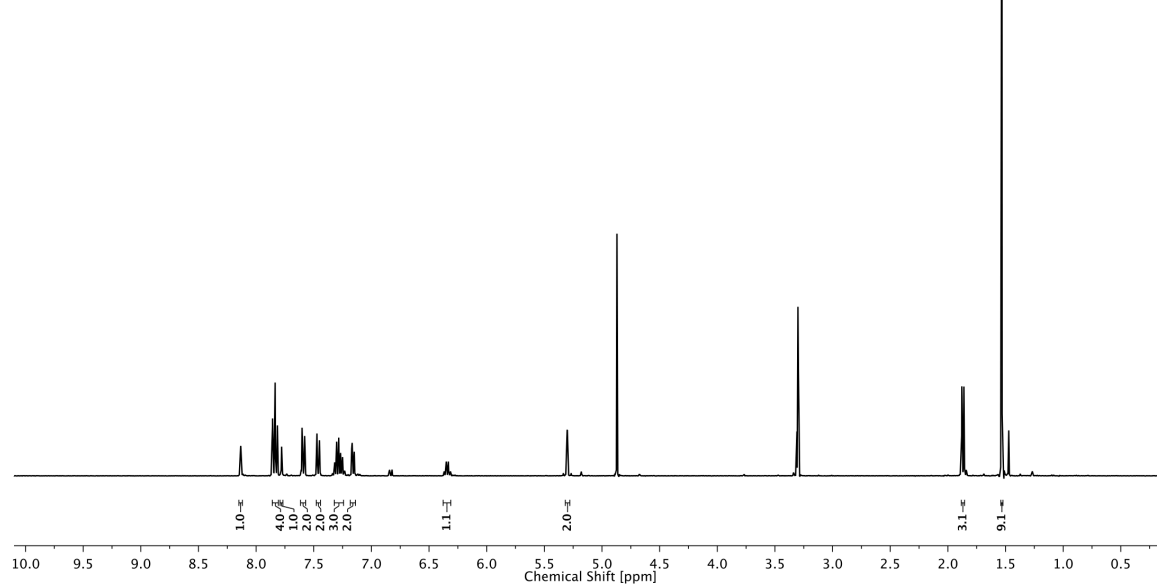
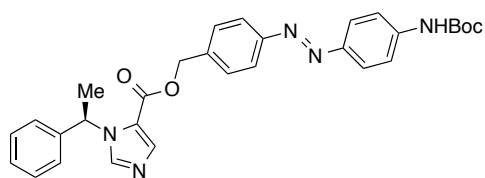


2 PHOTOREGULATION OF GABA_A RECEPTORS

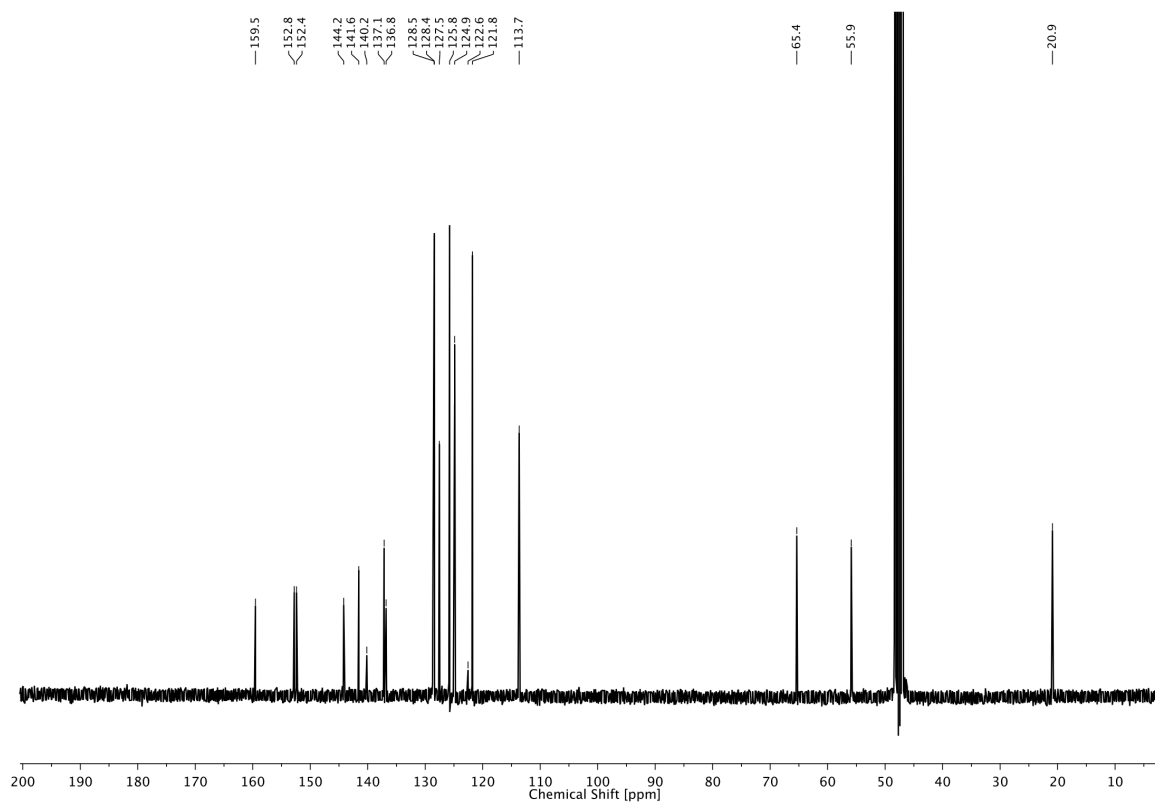
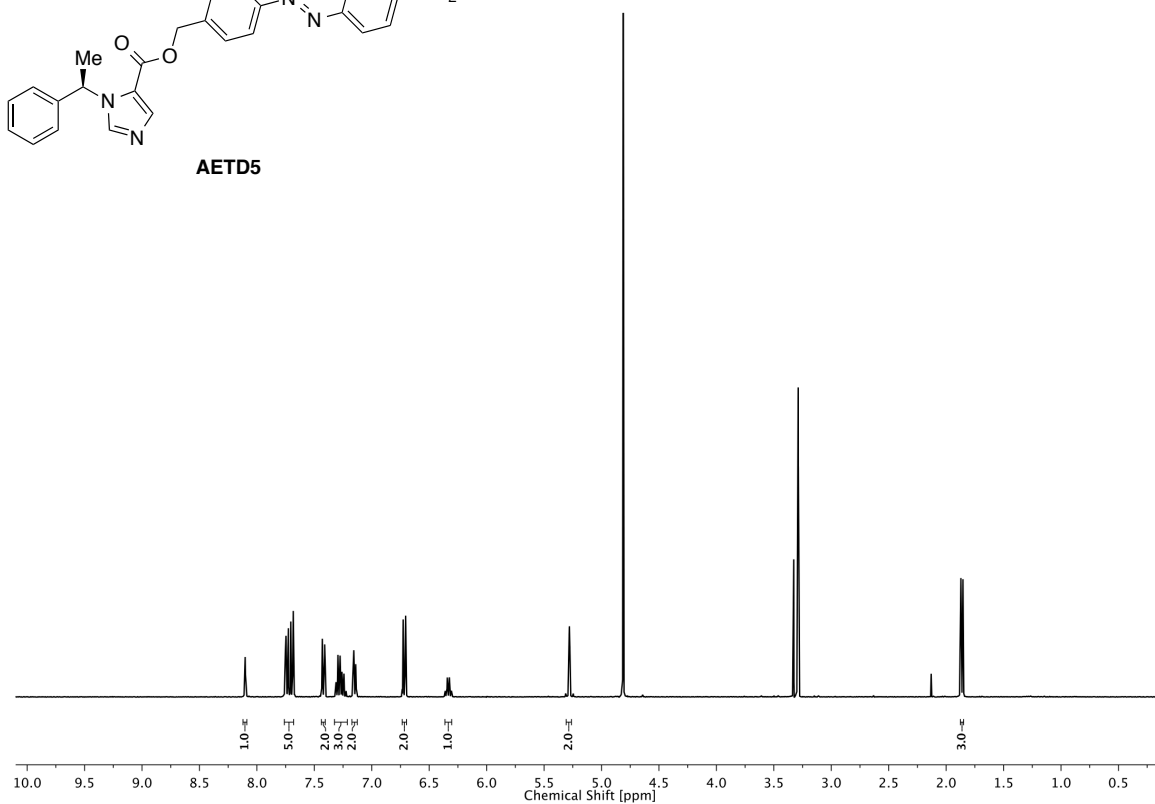
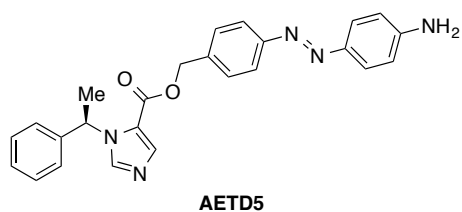


2 PHOTOREGULATION OF GABA_A RECEPTORS



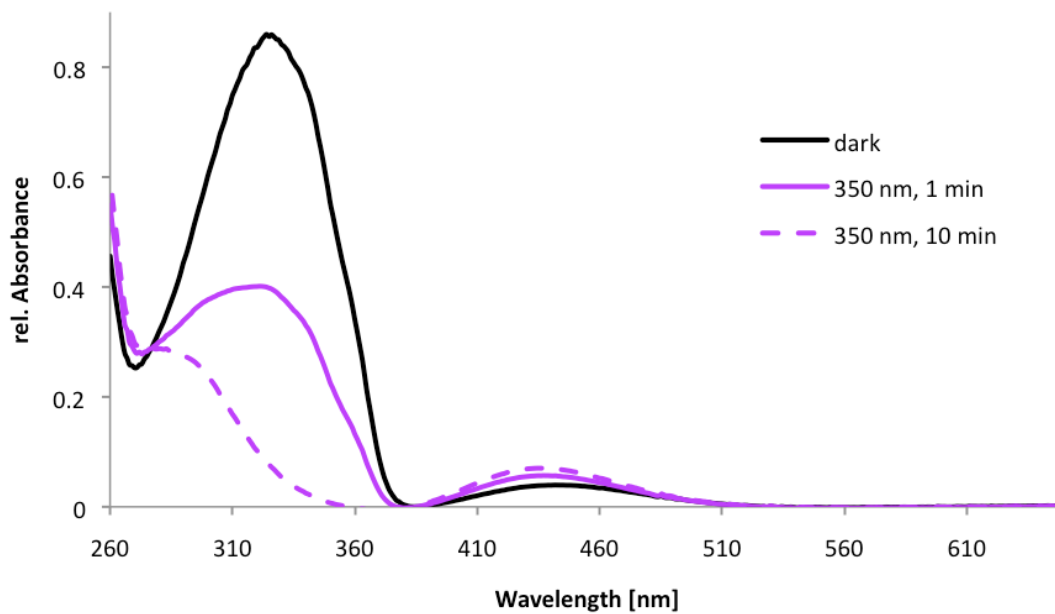


2 PHOTOREGULATION OF GABA_A RECEPTORS

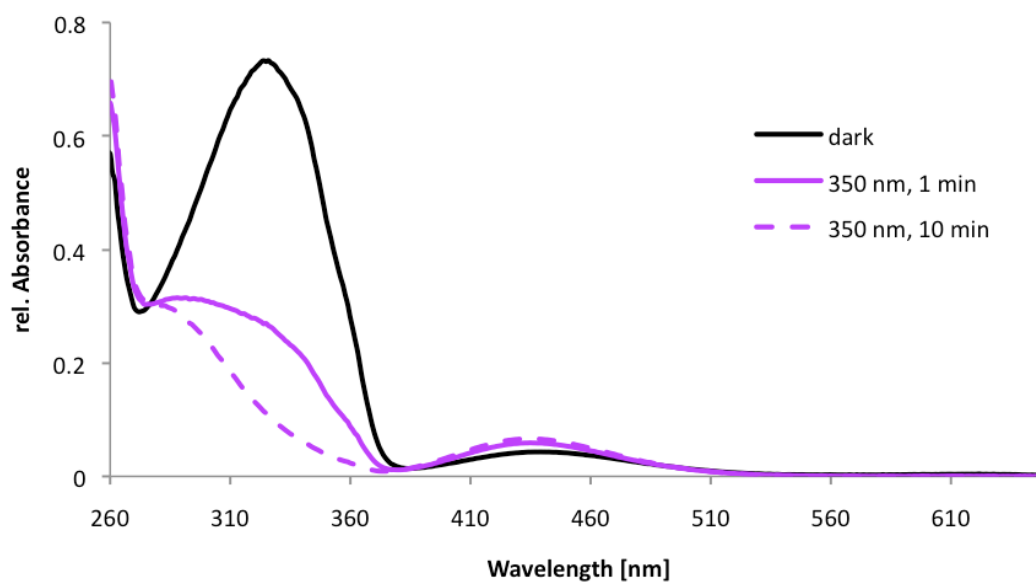


2.3.4 UV/VIS SPECTRA OF AETD1-5

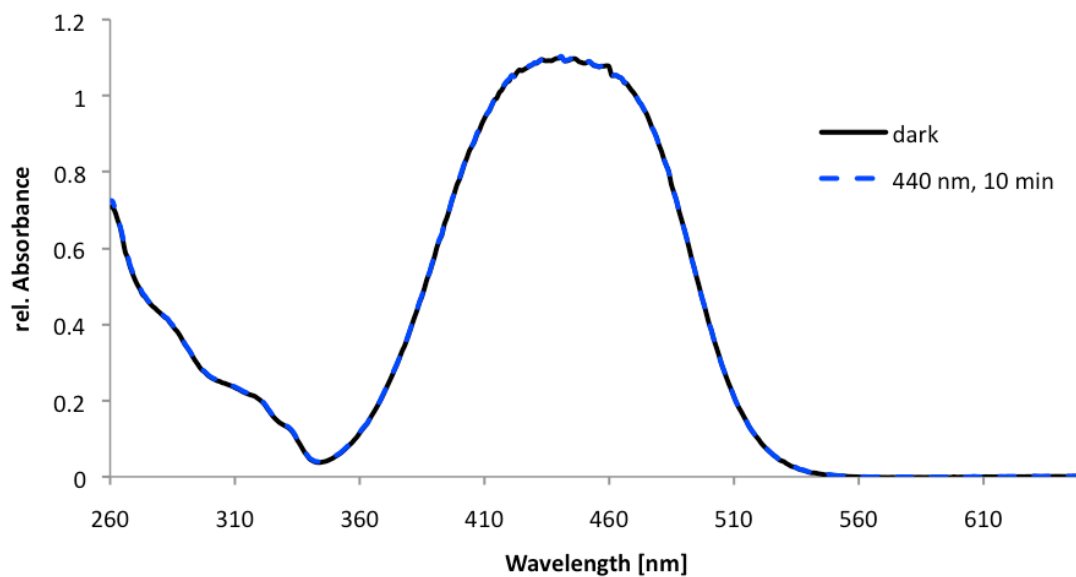
UV/Vis spectrum of AETD1



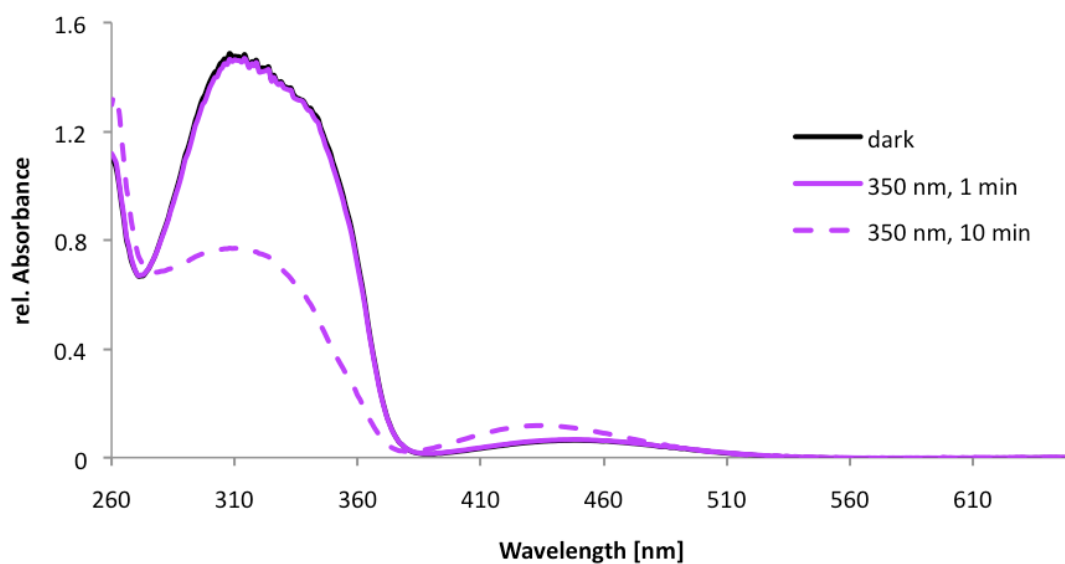
UV/Vis spectrum of AETD2



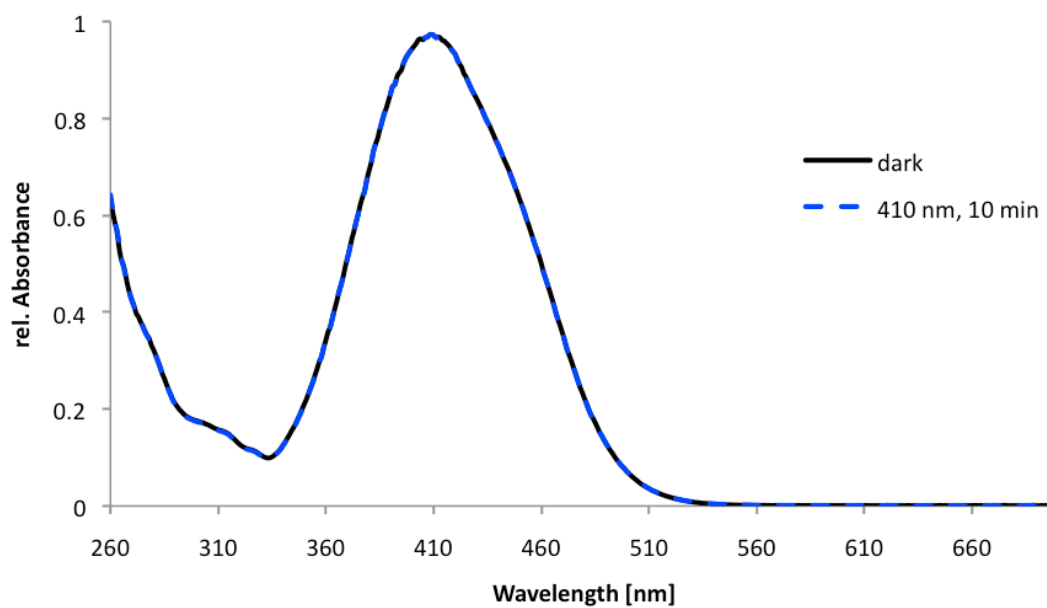
UV/Vis spectrum of AETD3



UV/Vis spectrum of AETD4



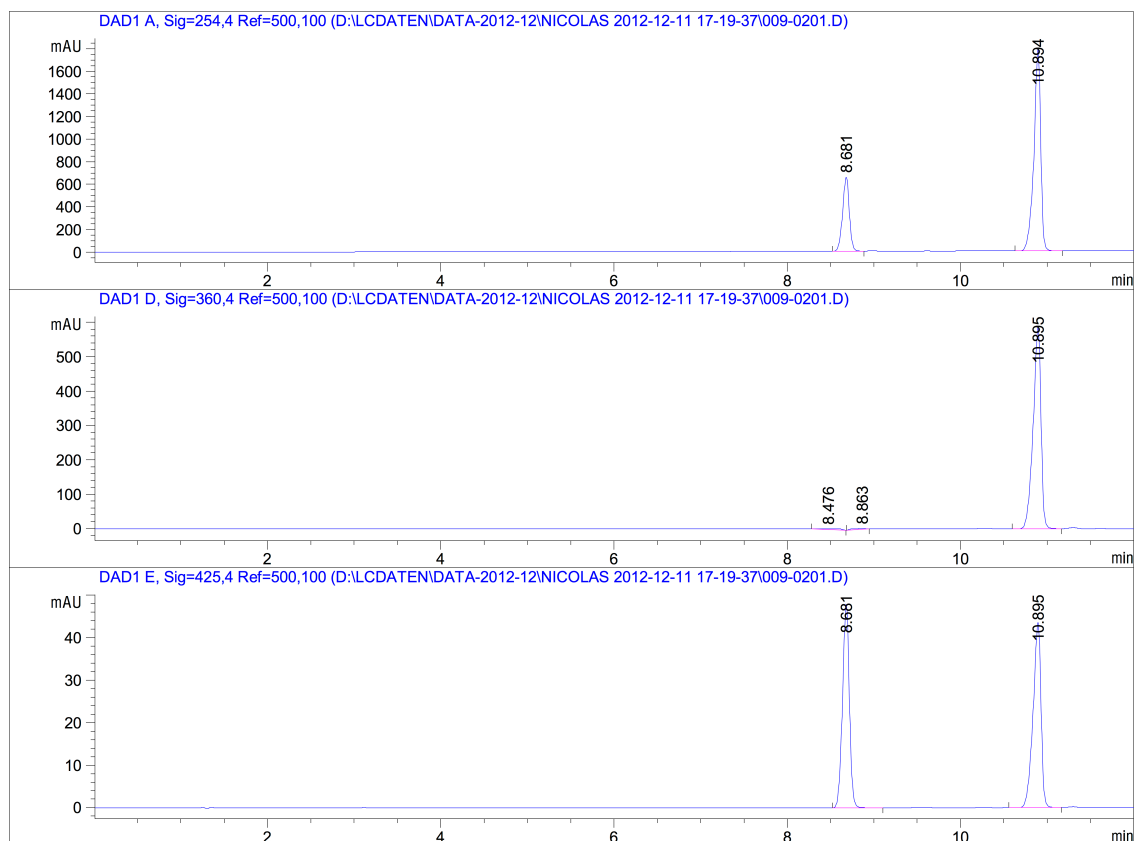
UV/Vis spectrum of AETD5



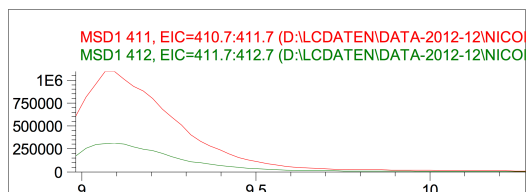
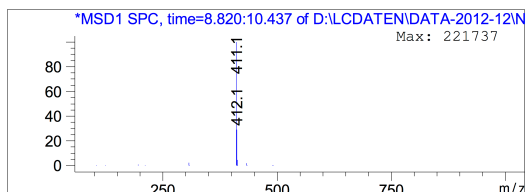
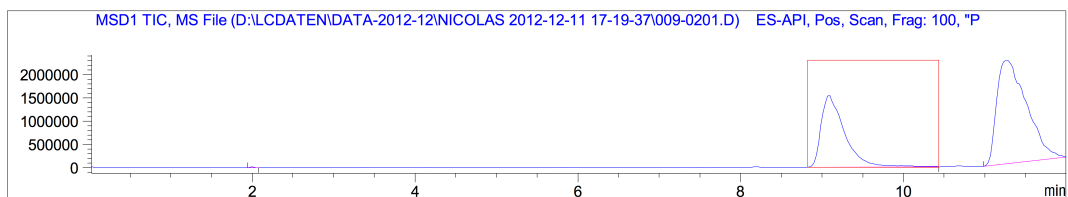
2.3.5 HPLC CHROMATOGRAMS OF AETD2

AETD2

AETD2 was obtained 98.5% pure as a mixture of *trans* ($R_t = 10.89$ min) and *cis* isomers ($R_t = 8.68$ min). As expected from the UV/Vis spectrum (see above), the *cis* isomer has almost no absorption at $\lambda = 360$ nm. Both peaks possess the same mass of 411.1 ($[M+H]^+$).

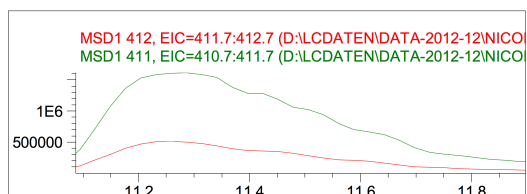
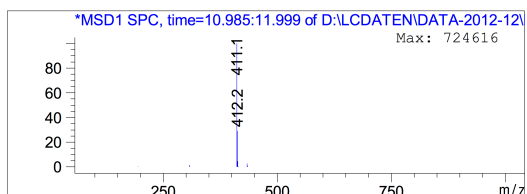
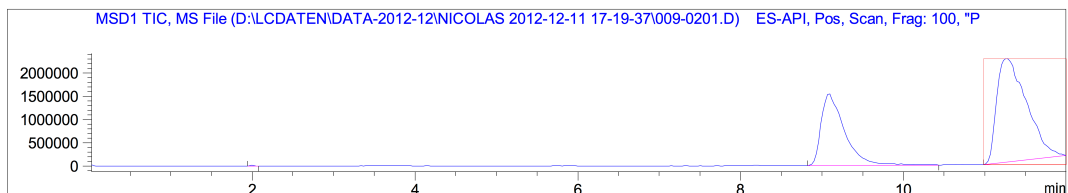


2 PHOTOREGULATION OF GABA_A RECEPTORS



Peak #2 at 9.084 min (8.820 to 10.437 min)
-> The analysis found only one component, indicating a pure peak. <-

Component 1: Peak at Scan 331.7. Top ions are 411 412



Peak #3 at 11.269 min (10.985 to 11.999 min)
-> The analysis found 2 components, indicating an impure peak. <-

Component 1: Peak at Scan 410.9. Top ions are 412

Component 2: Peak at Scan 411.7. Top ions are 411

2.4 LITERATURE

- [1] G. Owsianik, T. Voets, B. Nilius, in *Ion Channels from Structure to Function*, (Eds.: J. N. C. Kew, C. H. Davies), Oxford University Press, New York, **2010**, p. 263
- [2] a) Z. C. Peng, C. S. Huang, B. M. Stell, I. Mody, C. R. Houser, *J. Neurosci.* **2004**, *24*, 8629–8639; b) K. L. Gilby, E. A. Da Silva, D. C. McIntyre, *Epilepsia* **2005**, *46*, 3–9.
- [3] K. Brejc, W. J. van Dijk, R. V. Klaassen, *Nature* **2001**, *411*, 269–276.
- [4] N. Unwin, *J. Mol. Biol.* **2005**, *346*, 967–989.
- [5] a) E. Sigel, *Curr. Top. Med. Chem.* **2002**, *2*, 833–839; b) B. Lüscher, C. A. Keller, *Pharmacol. Ther.* **2004**, *102*, 195–221.
- [6] Illustration from https://upload.wikimedia.org/wikipedia/commons/0/06/GABAA_receptor_schematic.png, last accessed July 9, 2013.
- [7] T. C. Jacob, S. J. Moss, R. Jurd, *Nat. Rev. Neurosci.* **2008**, *9*, 331–343.
- [8] R. Jurd, M. Arras, S. Lambert B. Drexler, R. Siegwart, F. Crestani, M. Zaugg, K. E. Vogt, B. Ledermann, B. Antkowiak, U. Rudolph, *Faseb J.* **2003**, *17*, 250–252.
- [9] D. S. Reynolds, T. W. Rosahl, J. Cirone, G. F. O’Meara, A. Haythornthwaite, R. J. Newman, J. Myers, C. Sur, O. Howell, A. R. Rutter, J. Atack, A. J. Macaulay, K. L. Hadingham, P. H. Hutson, D. Belelli, J. J. Lambert, G. R. Dawson, R. McKernan, P. J. Whiting, K. A. Wafford, *J. Neurosci.* **2003**, *23*, 8608–8617.
- [10] J. Cirone, T. W. Rosahl, D. S. Reynolds, R. J. Newman, G. F. O’Meara, P. H. Hutson, K. A. Wafford, *Anesthesiology* **2004**, *100*, 1438–1445.
- [11] W. C. Still, M. Kahn, A. Mitra, *J. Org. Chem.* **1978**, *43*, 2923–2925.
- [12] H. E. Gottlieb, V. Kotlyar, A. Nudelman, *J. Org. Chem.* **1997**, *62*, 7512–7515.
- [13] F. Hamon, F. Djedaini-Pilard, F. Barbot, C. Len, *Tetrahedron* **2009**, *65*, 10105–10123.
- [14] E. Sawicki, T. W. Winfield, C. R. Sawicki, *Microchem. J.* **1970**, *15*, 294–363.
- [15] E. Sigel, *J. Physiol.* **1987**, *386*, 73–90.
- [16] E. Sigel, F. Minier, *Mol. Nutr. Food Res.* **2005**, *49*, 228–234.
- [17] A. J. Boileau, R. Baur, L. M. Sharkey, E. Sigel, C. Czajkowski, *Neuropharmacol.* **2002**, *43*, 695–700.
- [18] C. Chen, H. Okayama, *Mol. Cell. Biol.* **1987**, *7*, 2745–2752.
- [19] E. F. Godefroi, P. A. J. Janssen, C. A. M. Van der Eycken, A. H. M. T. Van Heertum, C. J. E. Niemegeers, *J. Med. Chem.* **1965**, *56*, 220–223.
- [20] a) R. L. Macdonald, R. W. Olsen, *Annu. Rev. Neurosci.* **1994**, *17*, 569–602; b) E. Sigel, M. E. Steinmann, *J. Biol. Chem.* **2012**, *287*, 40224–40231.
- [21] W. Sieghart, *Pharmacol. Rev.* **1995**, *47*, 181–234.
- [22] E. Sigel, B. P. Lüscher, *Curr. Trends in Med. Chem.* **2011**, *11*, 241–246.

- [23] a) E. F. Godefroi, P. A. J. Janssen, C. A. M. Van Der Eycken, A. H. M. T. Van Heertum, C. J. E. Niemegeers, *J. Med. Chem.* **1965**, *8*, 220–223; b) S. J. Tomlin, A. Jenkins, W. R. Lieb, N. P. Franks, *Anesthesiology* **1998**, *88*, 708–717.
- [24] a) C. M. Hohl, C. H. Kelly-Smith, T. C. Yeug, D. D. Sweet, M. M. Doyle-Waters, M. Schulzer, *Ann. Emerg. Med.* **2012**, *56*, 105–113; b) J. M. Bergen, D. C. Smith, *J. Emerg. Med.* **1998**, *15*, 221–230.
- [25] J. L. Giese, T. H. Stanley, *Pharmacotherapy* **1983**, *3*, 251–258.
- [26] A. K. Hamouda, D. S. Stewart, S. S. Husain, J. B. Cohen, *J. Biol. Chem.* **2011**, *286*, 20466–20477.
- [27] P. Preziosi, M. Vacca, *Life Sci.* **1988**, *42*, 477–489.
- [28] a) J. J. Lambert, D. Belelli, S. Shepard, A.-L. Muntoni, M. Pistis, J. A. Peters, in *The GABA Receptor: An Important Locus for Intravenous Anaesthetic Action. Gases in Medicine: Anaesthesia* (Eds.: E. B. Smith, S. Daniels), Royal Society of Chemistry, Cambridge, **1998**; pp. 121–137; b) P. Charlesworth, C. D. Richards, *Br. J. Pharmacol.* **1995**, *114*, 909–917.
- [29] a) S. S. Husain, M. R. Ziebell, D. Ruesch, F. Hong, E. Arevalo, J. A. Kosterlitz, R. W. Olsen, S. A. Forman, J. B. Cohen, K. W. Miller, *J. Med. Chem.* **2003**, *46*, 1257–1265; b) S. S. Husain, S. Nirthanan, D. Ruesch, K. Solt, Q. Cheng, S. G.-D. Li, E. Arevalo, R. W. Olsen, D. E. Raines, S. A. Forman, J. B. Cohen, K. W. Miller, *J. Med. Chem.* **2006**, *49*, 4818–4825.
- [30] a) E. Sanna, A. Murgia, A. Casula, G. Biggio, *Mol. Pharmacol.* **1997**, *51*, 484–490; b) C. Hill-Venning, D. Belelli, J. A. Peters, J. J. Lambert, *Br. J. Pharmacol.* **1997**, *120*, 749–756; c) B. Drexler, R. Jurd, U. Rudolph, B. Antkowiak, *Neuropharmacol.* **2009**, *57*, 446–455.
- [31] S. S. Husain, D. Stewart, R. Desai, A. K. Hamouda, S. G.-D. Li, E. Kelly, Z. Dostalova, X. Zhou, J. F. Cotten, D. E. Raines, R. W. Olsen, J. B. Cohen, S. A. Forman, K. W. Miller, *J. Med. Chem.* **2010**, *53*, 6432–6444.
- [32] W. C. Still, M. Kahn, A. Mitra, *J. Org. Chem.* **1978**, *43*, 2923–2925.

3 PHOTOCONTROL OF TRP CHANNELS

3.1 TRANSIENT RECEPTOR POTENTIAL CHANNELS

The transient receptor potential (TRP) channels form a large superfamily of versatile channels that are expressed in every cell type in both vertebrates and invertebrates. They are involved in the perception of a broad variety of different physical and chemical stimuli and in the initiation of cellular responses therein.^[1] All TRP family members are homologues of the first characterized *Drosophila* TRP channel which is involved in the response to bright light.^[2] It was found that sustained light induced a transient rather than a normal sustained, plateau-like receptor potential in photoreceptors of *Drosophila* which was then described as the *trp* mutation. Cloning of the *trp* gene revealed that it encodes a Ca²⁺ permeable channel^[3] which functions as receptor-operated channel that is activated downstream of the light-induced phospholipase C (PLC)-mediated hydrolysis of phosphatidylinositol 4,5-bisphosphate (PIP₂).^[4] As of today, it remains to be investigated whether TRP channels open upon reduction of PIP₂ or activation by diacyl glycerol (DAG) or fatty acids derived from DAG.^[5]

Seven subclasses of TRP channels based on their structural homology exist (Fig. 3.1)^[6] and more than 50 TRP channels have been identified.

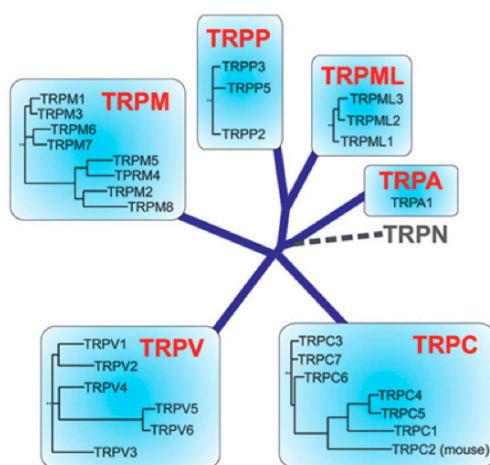


Figure 3.1. TRP Channel subfamilies. Illustration adapted from Voets *et al.*,^[6] reprinted with permission from Macmillan Publishers Ltd. Copyright 2005.

The **TRPC** (*canonical* or *classical*) subfamily members exhibit the highest homology to *Drosophila* TRP channels.^[1] The nomenclature of the other subfamilies originates from their first identified members. The **TRPV** subfamily was named after the vanilloid receptor 1 (TRPV1), the **TRPM** subfamily after the tumor suppressor melastatin (TRPM1), the **TRPA**

subfamily after the protein ankyrin-like with transmembrane domains 1 (ANKTM1, now TRPA1), the **TRPN** subfamily after the *no mechanoreceptor potential C* gene (*nompC*) from *Drosophila*, the **TRPP** subfamily after the polycystic kidney disease-related protein 2 (PKD2, now TRPP2) and the **TRPML** subfamily after mucolipin 1 (TRPML1).^[1]

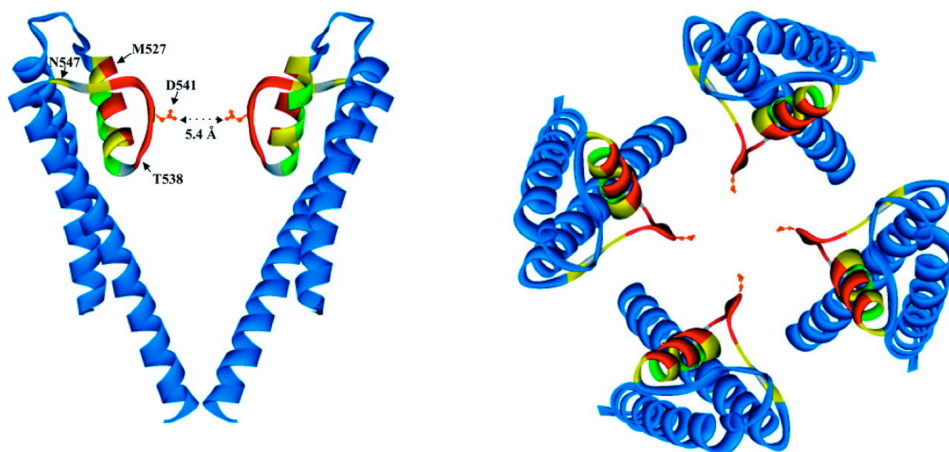


Figure 3.2. Model for the TRPV6 pore region based on the KcsA structure. Views of the structure are shown looking sideways at two opposite subunits (left) or looking down from the extracellular side on the homotetrameric channel. Illustration adapted from Voets *et al.*,^[7] reprinted with permission from the American Society for Biochemistry and Molecular Biology. Copyright 2004.

TRP Channels consist of six transmembrane domains (TM) and a cation-permeable pore region between TM5 and TM6. They function either as homo- or heterotetramers.^[8] Obtaining structural information at the atomic level for any full-length TRP channel is challenging due to difficulties encountered in overexpression.^[9] In 2009, Moiseenkova-Bell *et al.*^[9] were able to obtain a TRPV1 structure at 19 Å resolution from single-particle analysis and electron cryo-microscopy. In 2007, Lishko *et al.*^[10] were successful in crystallizing ankyrin repeats as part of the cytosolic residue of TRPV1. Still, most information about the pore structure has been obtained for members of the TRPV subfamily since the TM5–6 linker region shows significant sequence homology to the selectivity filter of the prokaryotic potassium channel KcsA.^[11] Mutations of negatively charged residues in TRPV1 and TRPV4 strongly reduce the permeabilities of Ca^{2+} and Mg^{2+} and reduce affinity for the TRP channel blocker Ruthenium Red.^[12] Similar to the KcsA crystal structure, residues preceding these negatively charged amino acids show a cyclic pattern of reactivity and thus are believed to form a pore helix.^[11] In TRPV6, the selectivity filter follows the pore helix with a diameter of approximately 5.4 Å (Fig. 3.2).^[7] The narrowest point of the pore is shaped by D541 which contributes to the selectivity filter.^[7]

3 PHOTOCONTROL OF TRP CHANNELS

Very recently, Liao *et al.*^[13] and Cao *et al.*^[14] managed to obtain mammalian TRPV1 structures at a resolution of 3.4 Å by exploiting recent advances in electron cryo-microscopy.

The intracellular amino and carboxy termini vary in their lengths between the different TRP subfamilies and can contain significantly different domains (Fig 3.3).^[15] These cytoplasmic domains play an important role in the regulation and modulation of channel function but mostly remained poorly understood so far.^[1]

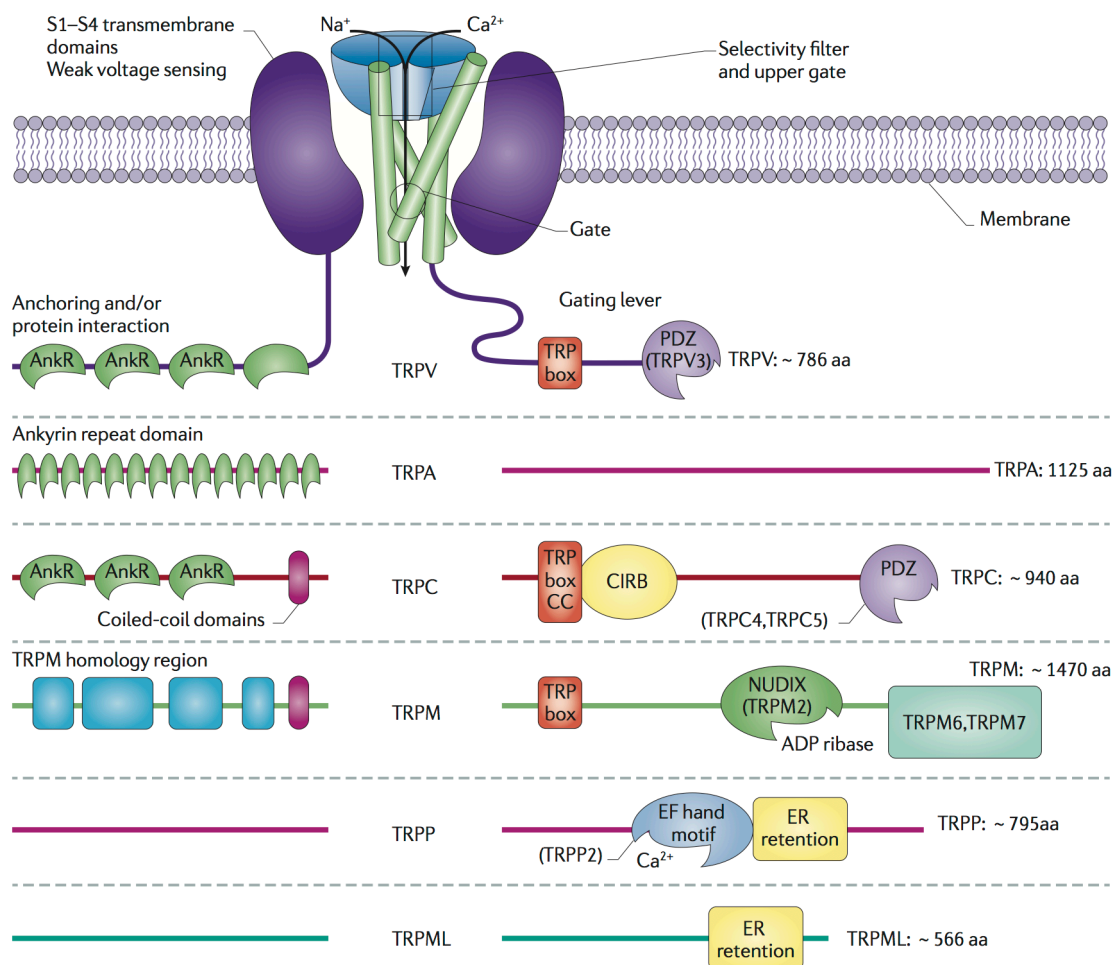


Figure 3.3. Schematic structural composition of TRP channels. The subfamilies differ mostly in their cytosolic N- and C-termini composition. Illustration adapted from Moran *et al.*,^[15] reprinted with permission from Macmillan Publishers Ltd. Copyright 2011.

Certain TRP channels of different subfamilies play an important role in temperature perception, both for heat as well as cooling sensation (Fig. 3.4). Temperatures range from warm (>25 °C for TRPV3,^[16] >31 °C for TRPV4^[17]) to heat (>43 °C for TRPV1^[18]), and noxious heat (>52 °C for TRPV2^[19]). Moreover, TRPM4 and TRPM5^[20] are activated upon heating, whereas TRPM8^[16a,21] and TRPA1^[22] are activated upon cooling. Some of these channels are also

activated by various ligands, such as capsaicin (TRPV1), menthol (TRPM8), camphor (TRPV3) or allyl isothiocyanate (TRPA1).

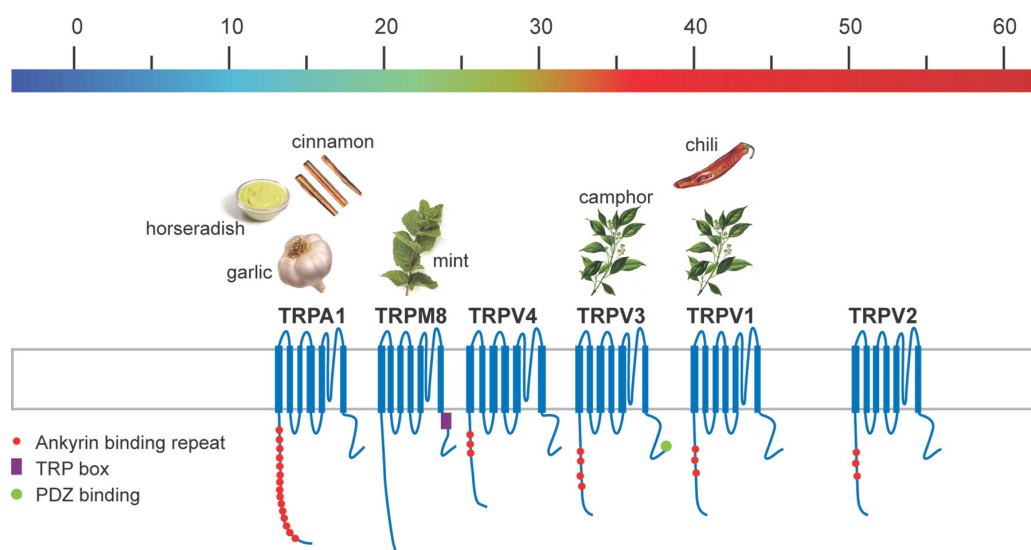


Figure 3.4. Thermosensitive TRP channels. The temperature spectrum ranges from $<8^{\circ}\text{C}$ (TRPA1) to $>52^{\circ}\text{C}$ (TRPV2). Illustration adapted from Dhaka *et al.*,^[23] reprinted with permission from ANNUAL REVIEWS. Copyright 2006.

Several hypotheses have been proposed to explain the temperature sensitivity of TRP channels.^[24] A rather unlikely model proposes that changes in temperature might stimulate generation of an endogenous ligand that in turn activates a particular TRP channel. This model is contradicted by the finding that most thermosensitive TRP channels (except TRPV4) display temperature-sensitivity in cell-free membranes. Another model proposes either a temperature-dependent phase transition of the lipid membrane or a conformational transition of the channel protein which usually happens within a narrow temperature range. A newer hypothesis within the model covers the cold activation of TRPM8 and heat activation of TRPV1.^[25] Both channels are voltage-gated channels that are activated upon membrane depolarization. This voltage-dependent activation could be shifted by changes in temperature from strongly depolarized potentials (voltage for half-maximal activation, $V_{1/2} \approx 150\text{ mV}$) to physiological potential. Thus, temperature-dependent activation would be rather gradual, unlike a single sharp thermal threshold predicted from temperature-induced conformational changes or phase transitions of the lipid membrane.^[25]

Arguably, the pharmacologically most relevant among the TRP channel subfamilies is the capsaicin receptor TRPV1 which plays a major role in nociception and heat sensation. Contrary to TRPV1, the menthol receptor TRPM8 (among others) is responsible for the perception of low

temperatures. These two channels were chosen as target receptors for optochemical control with azobenzene-based photoswitches in this thesis and will be discussed in detail below.

3.2 OPTICAL CONTROL OF TRPV1 CHANNELS

TRPV1 is most abundant in dorsal root ganglion (DRG) and trigeminal ganglion (TG) cells, as well as in spinal and peripheral nerve terminals.^[1] The channel is mostly located in the plasma membrane and in intracellular membranes (e.g. endoplasmic reticulum) where it functions as an intracellular Ca^{2+} release channel.^[26] Assembly of the homotetrameric channel seems to require the putative TRP-box on the C-terminus of each subunit.^[27] Moreover, two calmodulin (CaM) binding domains (CaMBDs) determine the CaM-dependent regulation of TRPV1 activity.^[1] Whereas binding of CaM to the N-terminal CaMBD reduces capsaicin-activated currents,^[28] binding of capsaicin to CaMBD at the C-terminus results in desensitization of these currents.^[29]

TRPV1 is a nonselective cation channel with a rather low discrimination between mono- and divalent cations ($P_{\text{Ca}}/P_{\text{Na}} = 1-10$).^[30] Activation of TRPV1 results in a sensation of burning and pain. There are several chemical and physical stimuli that can activate TRPV1 such as heat, voltage, phosphorylation by protein kinase C (PKC), low pH (TRPV1 is also permeable to H^{+} ^[31]) and endogenous as well as exogenous ligands. Fig. 3.5 gives an overview of some known agonists for TRPV1. Many of these have a vanilline moiety incorporated into their structure which is also responsible for the name of this subfamily of TRP channels: Transient Receptor Potential *Vanilloid* (TRPV) channel.

The most common agonist for TRPV1 is capsaicin, the main ingredient in hot chili peppers.^[18] The *cis* isomer of capsaicin with respect to the double bond also functions as an agonist and is marketed under various names (Zucapsaicin, Civamide, WN-1001).^[32] Allyl isothiocyanate, the pungent compound in mustard, horseradish and wasabi, activates TRPV1 as well as TRPA1.^[33] The complex natural product resiniferatoxin (RTX) was isolated from the cactus *Euphorbia resinifera*^[34] and is an ultra-potent capsaicin analogue that has a rating of 16,000,000,000 on the Scoville Scale,^[u,35] making it one of the highest rated substances known. Piperine, which was isolated from black pepper,^[36] has the two oxygens of vanilline fused into an acetal and is also used as an insecticide. There is evidence that the endocannabinoid anandamide also activates TRPV1.^[37] Although the receptor is mainly found in nociceptive neurons of the peripheral nervous system, these receptors have also been found in the brain where their role is far less

^[u] The Scoville Scale is a measurement of the spicy heat of chili peppers. Capsaicin itself has a value of 16,000,000 SHU (Scoville Heat Units).

understood. In 2010, it was discovered that synaptic activation of TRPV1 triggered a form of long-term depression mediated by the endocannabinoid anandamide in a type 1 cannabinoid receptor-independent manner.^[38]

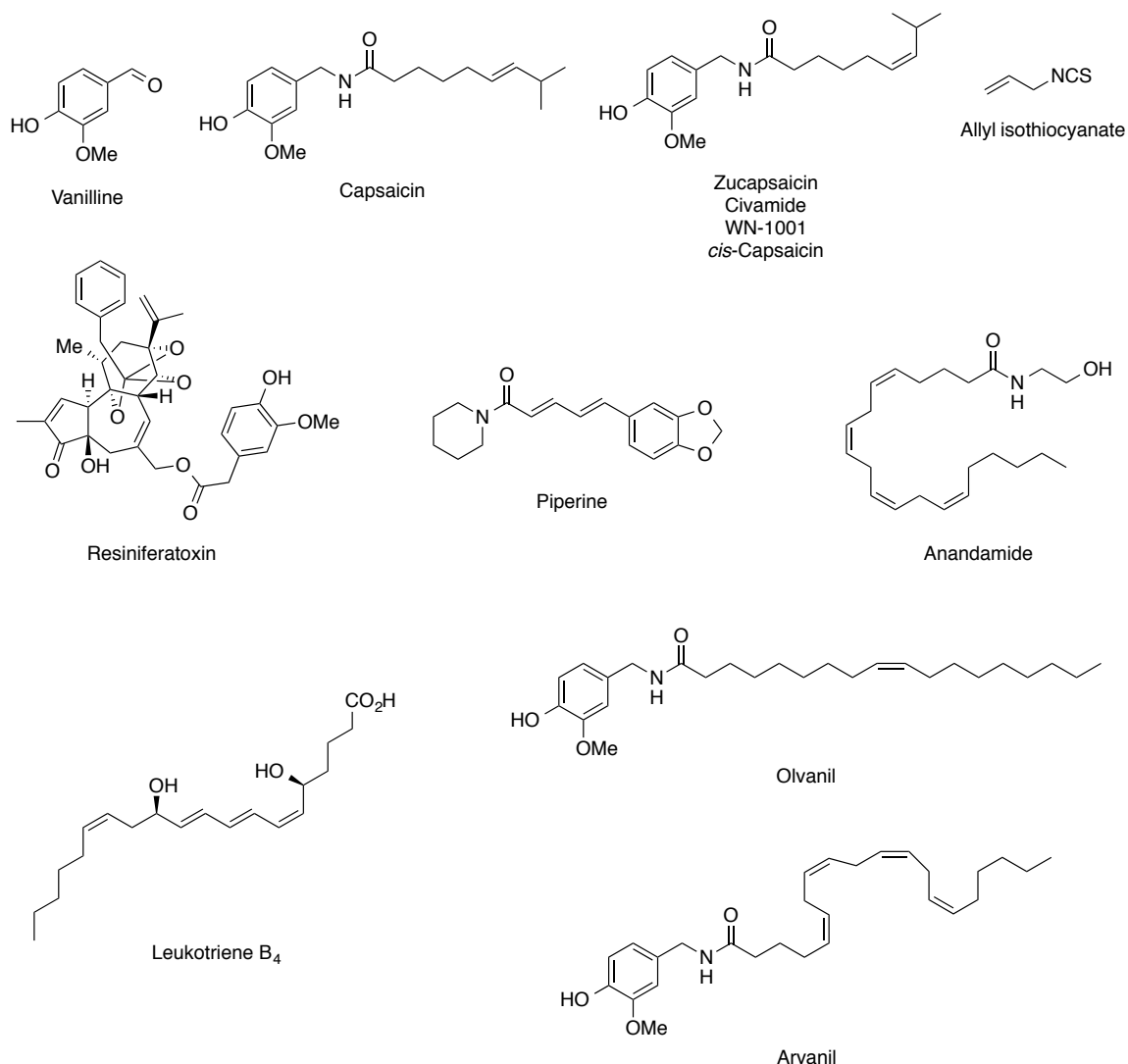


Figure 3.5. Overview of various TRPV1 agonists.

Moreover, leukotriene B₄ was shown to mediate inflammation^[39] and histamine-induced itching^[40] *via* TRPV1. Olvanil was developed as an orally active analgesic and activates TRPV1 at the same or slightly stronger potency as capsaicin, albeit exhibiting only weak pungency which was thought to be caused by the strong lipophilicity of the compound.^[41] Its name originates from the two constitutive parts of the molecule, a *vanilline* core that is esterified with *oleanolic* acid. Arvanil follows the same logic as orvanil with *arachidonic* acid instead of *oleanolic* acid and was just recently shown to induce cell death of high-grade astrocytomas by stimulation of TRPV1.^[42]

The pharmacological relevance of TRPV1 corresponds to the extensive research effort in finding selective antagonists. Fig. 3.6. shows a selection of current highly potent TRPV1 antagonists. Many of these compounds are in clinical trial phases 1 to 3. Subsequently, not much information on them has been published as of today.

Ruthenium Red very effectively blocks all TRPV channels as well as TRPC1/3, TRPM6 and TRPA1.^[1,12] Capsazepine (CPZ) was developed by Sandoz in 1994^[43] and is described as a very specific competitive antagonist for TRPV1. However, it can also inhibit TRPM8 at higher concentrations^[44] and meanwhile was found to also act on nicotinic acetylcholine receptors (nAChRs)^[45] as well as voltage-gated Ca²⁺ channels.^[46] To date, BCTC and thio-BCTC are the most specific blockers for TRPV1.^[44] Both, CPZ and BCTC, will be discussed briefly later (see next section). Moreover, iodination of RTX to form 5-iodoresiniferatoxin (I-RTX; structure not shown here) turns the ultrapotent agonist RTX into a strong competitive antagonist of TRPV1.^[47]

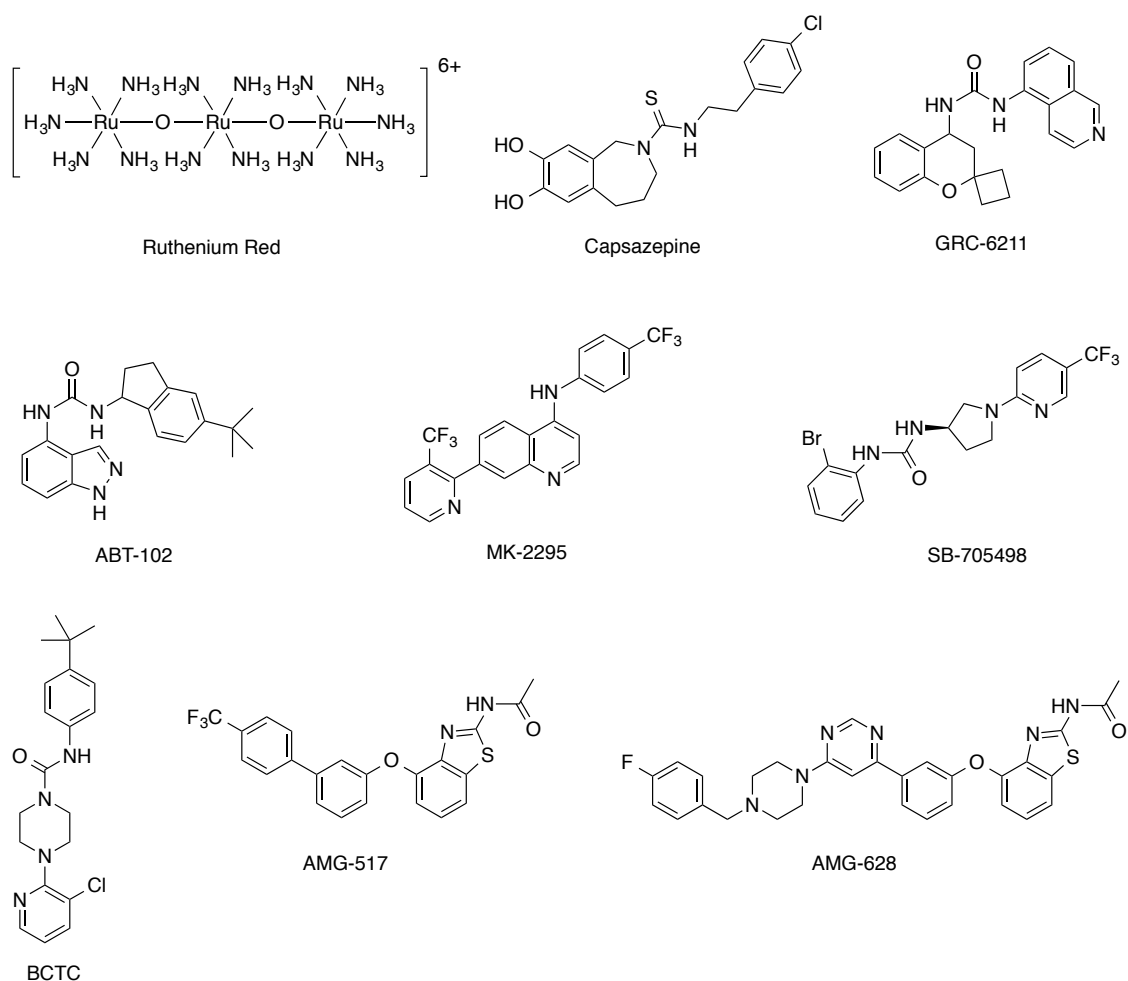


Figure 3.6. Overview of TRPV1 antagonists.

In 2006, Siemens *et al.*^[48] showed that venom from a tarantula that is native to the West Indies contains three inhibitor cysteine knot (ICK) peptides that target TRPV1. Since some vanillotoxins also inhibit voltage-gated potassium channels, potential similarities between TRP and voltage-gated channel structures are supported by this finding. More recently, Bohlen *et al.*^[49] showed that a peptide toxin from the *Earth Tiger tarantula* selectively and irreversibly activates TRPV1. Its high avidity interaction is derived from a unique tandem repeat structure of the toxin that endows it with an antibody-like bivalency. Bohlen *et al.*^[49] found that the ‘double-knot’ toxin traps TRPV1 in the open state by interacting with residues in the presumptive pore-forming region of the channel, highlighting the importance of conformational changes in the outer pore region of TRP channels during activation.^[49]

In order to be able to control this highly interesting channel with light, photoswitchable derivatives of the well-known TRPV1 antagonists CPZ and BCTC were designed and synthesized (see below). Based on their molecular structure and published SAR data, these two antagonists seemed to be the best candidates for the introduction of a photoswitchable azobenzene moiety. On the following pages, the original publication of this work is presented which was published in *Angewandte Chemie International Edition* in 2013.^[v]

Please note that the numbering of schemes and figures in the accompanying *Supporting Information* (but not in the manuscript itself) was adjusted to fit the consecutive numbering of this thesis.

^[v] reprinted with permission from John Wiley & Sons. Copyright 2013.

Photopharmacology
Optical Control of TRPV1 Channels**

Marco Stein, Andreas Breit, Timm Fehrentz, Thomas Gudermann, and Dirk Trauner*

Transient receptor potential channels (TRP channels) constitute one of the largest ion channel families in the human genome and are versatile cellular sensors involved in the perception of pain, warm and cold temperatures, noxious and pungent chemicals, and pressure.^[1] They are also involved in visual processing and might shape the circadian rhythm in mammals.^[2] As such, members of this ion channel family play a key role in sensory physiology, the full extent of which is still unknown. In addition, they are implicated in the regulation of gastrointestinal motility, absorptive and secretory processes, blood flow, and mucosal homeostasis.^[1a] In fact, several human diseases are known that are caused by mutations in TRP channel genes.^[1a] All of this has recently sparked intense research activity in academia and industry, giving rise to various new probes and drug candidates that target TRP channels.

The vanilloid receptor 1 (TRPV1) is one of the most important and best understood representatives of the family.^[1] It is a nonselective cation channel that is, like most TRP channels, permeable to Ca²⁺ ions but shows little discrimination between mono- and divalent cations.^[3] TRPV1 is abundantly expressed in all sorts of nociceptive neurons, such as dorsal root ganglion (DRG) and trigeminal ganglion (TG) neurons, as well as spinal and peripheral nerve terminals and the cornea.^[1c] Usually, the channel is located in the plasma membrane but it is occasionally also found in intracellular membranes (e.g. sarco-/endoplasmic reticulum) where it may function as an intracellular Ca²⁺ release channel.^[4] Activation of TRPV1 results in a sensation of burning and pain, making this channel a promising target for the development of potential analgesics. TRPV1 is activated by several chemical and physical stimuli, such as voltage,^[5] heat,^[6] capsaicin,^[6a] spider toxins,^[7] low pH,^[8] and several fatty acids such as the endocannabinoid anandamide^[9] and is potentiated by phosphorylation.^[10] However, despite its multimodal activation mechanisms, TRPV1 is not known to naturally respond to light.

Over the last decade, we have developed general methods to optically control receptor proteins by either covalently attaching a photoswitchable tethered ligand (PTL), or providing a freely diffusible photochromic ligand (PCL).^[11] We have applied both approaches to voltage-dependent ion channels in order to control heartbeat,^[12] pain sensation,^[13] and visual responses^[14] in a variety of animals. Moreover, we have been able to convert nicotinic acetylcholine receptors,^[15] as well as ionotropic^[16] and metabotropic glutamate receptors^[17] into artificial photoreceptors. Most recently, we succeeded in developing light-switchable anaesthetics based on propofol,^[18] which potentiate GABA-induced chloride currents.

We now report the development of photoswitchable drugs that effectively convert TRPV1 channels into photoreceptors. Our studies were enabled by the highly developed pharmacology of TRPV1, which is outlined in Figure 1. The vanillamine derivative capsaicin (CAP), the pungent ingredient in hot chili peppers, is the best known agonist of TRPV1.^[6a] A much more complex diterpenoid, resiniferatoxin (RTX), isolated from the cactus *Euphorbia resinifera*,^[19] is considered to be the spiciest substance known. The competitive antagonist capsazepine (CPZ) was found by Sandoz in 1994^[20] in an attempt to explore the structure–activity relationship (SAR) of CAP. To date, BCTC and thio-BCTC are the most specific blockers of TRPV1 activity.^[21] BCTC was discovered during SAR studies in 2003^[22] and has become a popular TRPV1 antagonist. It was found to be superior to CPZ in terms of its CAP-antagonizing effects on TRPV1, but also upon activation by low pH.

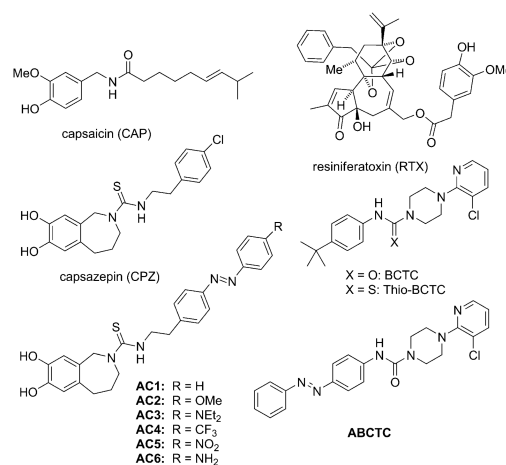


Figure 1. Agonists and antagonists of TRPV1 and their photoswitchable derivatives ABCTC and AC1–6.

[*] M. Sc. M. Stein, Dr. T. Fehrentz, Prof. D. Trauner
Department of Chemistry, Ludwig-Maximilians-University (LMU)
Munich and Center of Integrated Protein Science
Butenandstrasse 5–13, 81377 Munich (Germany)
E-mail: dirk.trauner@lmu.de

Dr. A. Breit, Prof. T. Gudermann
Walther-Straub-Institute for Pharmacology and Toxicology
LMU Munich, Goethestrasse 33, 80336 Munich (Germany)

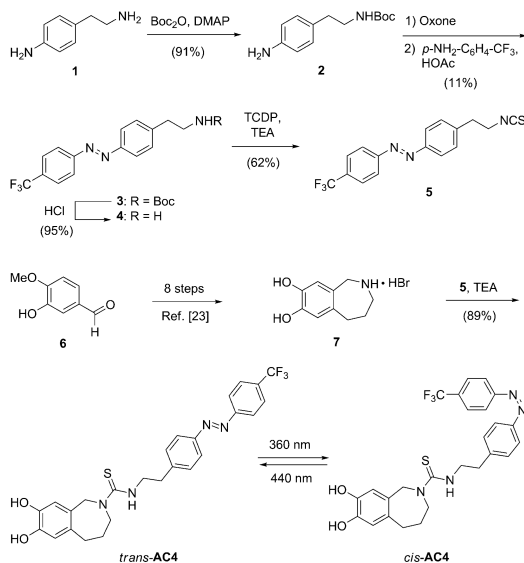
[**] We thank Dr. Peter Mayer (LMU Munich) for the determination of the X-ray structure and Dr. Martin Sumser (LMU Munich) for many helpful discussions. This work was supported by the European Science Foundation (ERC grant no. 268795 to D.T.) and the Fonds der Chemischen Industrie (PhD fellowship to M.S.).

Supporting information for this article is available on the WWW under <http://dx.doi.org/10.1002/anie.201302530>.

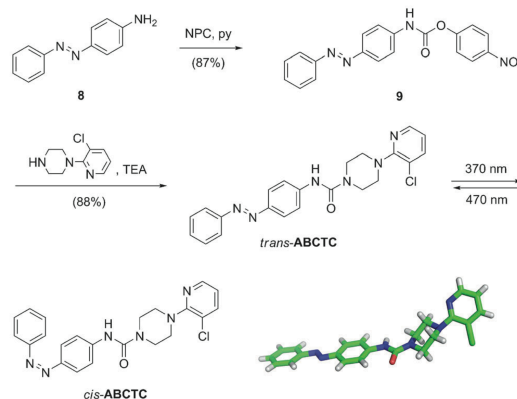
Capsazepine and BCTC contain a phenyl ring with a chloro and *tert*-butyl substituent, respectively, in *para* position with respect to the remainder of the molecule. In both cases, it was known that these substituents could be varied to a certain extent without complete loss of activity.^[20b,22] We thus reasoned that the phenyl rings could be extended to azobenzenes, hoping that the *cis* and *trans* configurations of these moieties would afford antagonists with different efficacies. Based on these considerations, we designed azobenzene derivatives of CPZ and BCTC, termed Azo-Capsazepines 1–6 (**AC1–6**) and Azo-BCTC (**ABCTC**), which cover a range of photophysical and pharmacological properties.

The synthesis of **AC4**, which emerged as our most useful candidate, is depicted in Scheme 1 (for the syntheses of the other AC derivatives, see the Supporting Information). First, amine **1** was protected as a *tert*-butyl carbamate to yield aniline **2**, which was then oxidized to the corresponding nitroso derivative and subsequently coupled to 4-(trifluoromethyl)aniline in a Mills reaction, affording azobenzene **3**. Removal of the Boc group gave free amine **4**, which was converted to the corresponding isothiocyanate **5** using 1,1'-thiocarbonyldi-2(*H*)-pyridone. Compound **5** was then coupled to azepine **7**, which was synthesized from isovanilline **6** in eight steps according to a modified literature protocol^[23] (see the Supporting Information) to afford **AC4**.

The synthesis of **ABCTC** commenced with the coupling of aniline **8** and 4-nitrophenyl chloroformate to give carbamate **9**, which was then treated with 1-(3-chloropyridin-2-yl)piperazine to afford **ABCTC** (Scheme 2). The X-ray structure of



Scheme 1. Synthesis of **AC4**, which isomerizes from its *trans* form to the *cis* state when $\lambda = 360$ nm light is applied and reverts back when $\lambda = 440$ nm light is applied. Boc = *tert*-butyloxycarbonyl, DMAP = 4-dimethylaminopyridine, TCDP = 1,1'-thiocarbonyldi-2(*H*)-pyridone, TEA = triethylamine.



Scheme 2. Synthesis of **ABCTC** and its X-ray structure in the *trans* configuration. The *trans*↔*cis* isomerization occurs with $\lambda = 370$ nm and $\lambda = 470$ nm light, respectively. NPClO = 4-nitrophenyl chloroformate, py = pyridine.

ABCTC illustrates the importance of the *o*-chloro substituent, which forces the pyridine ring out of the average plane of the piperazine ring.^[24]

We next tested our compounds for their ability to act as antagonists using electrophysiology in HEK cells transiently transfected with TRPV1. First, our functional analyses took advantage of the voltage sensitivity of TRPV1.^[5] We found that all six AC derivatives synthesized function as TRPV1 antagonists at concentrations of 5–100 μ M. However, the trifluoromethyl derivative **AC4** emerged as the best photo-switchable antagonist among all Azo-Capsazepines. Under voltage-gating conditions, it functions as a *trans* antagonist, blocking more current at 440 nm, than in the *cis* state at 360 nm (Figure 2a,b). Channel gating by depolarization to +200 mV allows for fast and fully reversible inhibition of TRPV1 currents of > 1 nA when the respective wavelength is applied to 100 μ M **AC4** containing bath solution (Figure 2c).

Conversely, the BCTC derivative **ABCTC** was found to block more TRPV1 current in its *cis* state (at 370 nm) than in its *trans* form (at 470 nm; Figure 2d–f). As such, **ABCTC** functions as a reversible *cis* antagonist. The *I/V* curves of **AC4** and **ABCTC** are similar, with both antagonists blocking > 20% of maximum current in their more active form (*trans*-**AC4** and *cis*-**ABCTC**, respectively).

Since the voltage protocols involve nonphysiological conditions, we next investigated the effect of our photo-switchable TRPV1 antagonists on CAP-induced TRPV1 currents in a Ca^{2+} luminescence assay. Whereas **AC1–3**, **AC5**, and **AC6** showed only low antagonistic effects upon TRPV1 activation with 1 μ M CAP (IC_{50} values > 50 μ M, see the Supporting Information), **AC4** and **ABCTC** exhibited higher activities. We recorded IC_{50} values of (3.1 \pm 0.6) μ M for **AC4** compared to (0.2 \pm 0.06) μ M for CPZ, and (12.8 \pm 0.7) μ M for **ABCTC** compared to (0.2 \pm 0.6) μ M for BCTC, respectively (Figure 3a,b).

We then investigated whether we could regulate CAP-induced TRPV1 currents with light in the presence of either

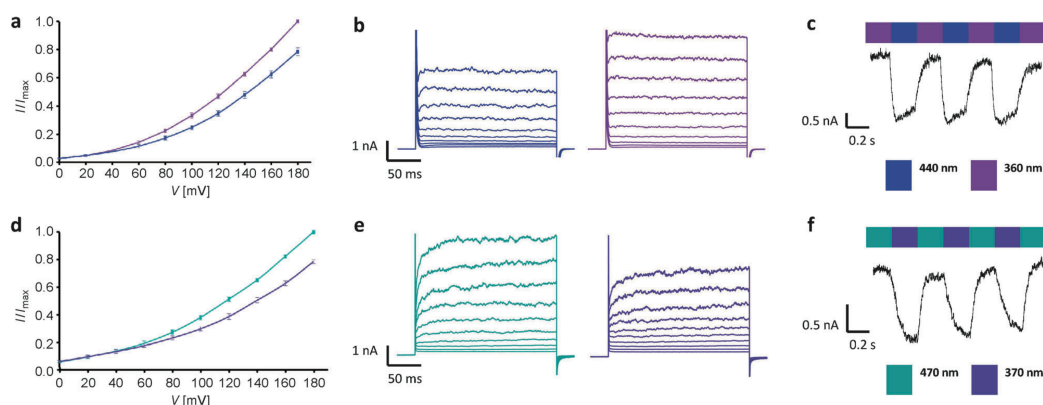


Figure 2. a) I/V curves of voltage-activated TRPV1 channels in 20 mV steps up to +180 mV upon application of $\lambda = 440$ nm light (blue) and $\lambda = 360$ nm light (magenta) to 100 μM of **AC4**, respectively (normalized to I_{max} ; $n = 6$). b) Representative traces from (a). c) Photoswitching cycles by wavelength alternation at +200 mV with 100 μM **AC4**. d)–f) Analogous data for 10 μM **ABCTC** with application of $\lambda = 370$ nm light (purple) and $\lambda = 470$ nm light (turquoise).

AC4 or **ABCTC**. Whereas **ABCTC** gave no change in activity upon irradiation, the antagonistic action of **AC4** could be modulated in this fashion. Puff application of 100 nM CAP to HEK cells, which were transiently transfected with TRPV1 and immersed in a bath solution containing 1 μM **AC4**, resulted in a large current increase that could be reduced by up to 82% upon irradiation with $\lambda = 360$ nm, which isomerizes **AC4** into its *cis* configuration. By applying $\lambda = 440$ nm light, the CAP-induced current could be restored (Figure 3c). This process is fully reversible. Statistical analysis ($n = 8$, $P = 0.01$, Student's *t*-test) revealed a photoswitching index

(determined by the ratio of current increase upon CAP application at $\lambda = 360$ nm and 440 nm, respectively) of 49% (Figure 3d). A control experiment (Figure 3e) showed that the CAP-induced current could not be modulated with light in the absence of the photoswitchable antagonist.

Remarkably, **AC4** acted as a *cis* antagonist of CAP-induced TRPV1 currents, whereas it functioned as *trans* antagonist upon voltage activation. This might appear paradox at first sight but is in good agreement with the observation that agonists interact with TRPV1 channels in a state-dependent fashion and that specific antagonists differ in their ability to block distinct agonists.^[25] Thus, our study may open up new avenues for the development of modality-selective antagonists, which might help to overcome unwanted side effects of analgesics targeting TRPV1.

In conclusion, we have developed a method to optically control TRP channel activity with azobenzene derivatives of the TRPV1 antagonists capsaizepine (CPZ) and BCTC. Six derivatives of CPZ, termed **AC1–6**, have been synthesized, amongst which the trifluoromethyl derivative **AC4** proved to be the most useful and interesting compound. Compound **AC4** functions as *trans* antagonist upon voltage-activation of TRPV1 and as *cis* antagonist upon stimulation with capsaicin (CAP). Another azobenzene, **ABCTC**, was

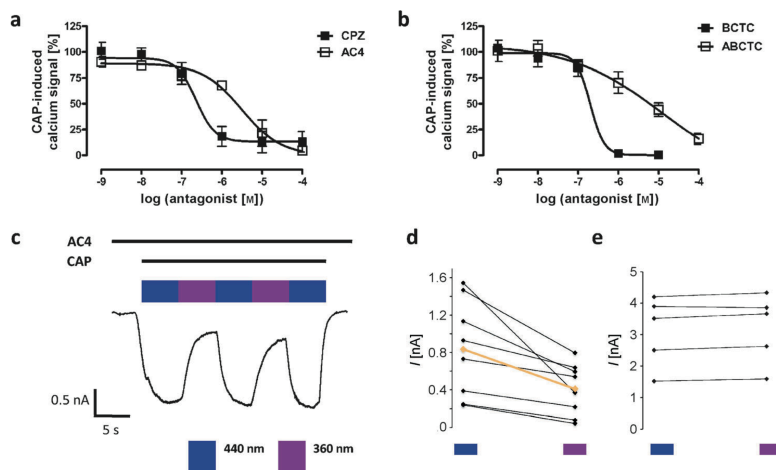


Figure 3. a) Dose–response curve of **AC4**, in comparison with that of CPZ; $n = 5$. b) Dose–response curve of **ABCTC**, in comparison with that of BCTC; $n = 5$. c) CAP-induced currents (100 nM CAP) can be modulated in the presence of **AC4** (1 μM) by switching between $\lambda = 440$ nm and $\lambda = 360$ nm light (holding potential -60 mV). d) Statistical analysis of CAP-induced TRPV1 current photoswitching by **AC4** (orange = median). The difference is significant ($P = 0.01$, Student's *t*-test, $n = 8$). e) No photoswitching of CAP-induced TRPV1 currents was observed in the absence of **AC4** ($n = 5$).

found to act as a *cis* antagonist upon voltage-activation of TRPV1 but did not counteract CAP in a light-dependent fashion. Our photoswitchable compounds add an additional input signal to TRPV1 channels and provide a strategy to stimulate TRP channels with light. As such, they complement the recently described photochemically active molecule “optovin”, which acts on TRPA1 channels and through a different mechanism.^[26] Our lead compound, **AC4**, demonstrates that a photoswitchable antagonist and an agonist can be used in concert. This broadens the scope of photopharmacology and provides a new functional dimension to the optical manipulation of ion channels with synthetic photoswitches. The application of **AC4**, **ABCTC**, and related compounds in sensory physiology is under active investigation and will be reported in due course.

Received: March 26, 2013

Revised: May 9, 2013

Published online: July 19, 2013

Keywords: azobenzenes · capsaicin · capsaizepine · photopharmacology · TRPV1

- [1] a) L.-J. Wu, T.-B. Sweet, D. E. Clapham, *Pharmacol. Rev.* **2010**, *62*, 381–404; b) K. Venkatachalam, C. Montell, *Annu. Rev. Biochem.* **2007**, *76*, 387–417; c) G. Owsianik, T. Voets, B. Nilius in *Ion Channels from Structure to Function* (Eds.: J. N. C. Kew, C. H. Davies), Oxford University Press, New York, **2010**, p. 511.
- [2] a) Y. Shen, M. A. F. Rampino, R. C. Carroll, S. Nawy, *Proc. Natl. Acad. Sci. USA* **2012**, *109*, 8752–8757; b) A. T. Hartwick, J. R. Bramley, J. Yu, K. T. Stevens, C. N. Allen, W. H. Baldrige, P. J. Sollars, G. E. Pickard, *J. Neurosci.* **2007**, *27*, 13468–13480.
- [3] C. D. Benham, J. B. David, A. D. Randall, *Neuropharmacology* **2002**, *42*, 873–888.
- [4] a) H. Turner, A. Fleig, A. Stokes, J.-P. Kinet, R. Penner, *Biochem. J.* **2003**, *371*, 341–350; b) N. Ito, U. T. Rugg, A. Kudo, Y. Miyagoe-Suzuki, S. Takeda, *Nat. Med.* **2013**, *19*, 101–106.
- [5] J. A. Matta, G. P. Ahern, *J. Physiol.* **2007**, *585*, 469–482.
- [6] a) M. J. Caterina, M. A. Schumacher, M. Tominaga, T. A. Rosen, J. D. Levine, D. Julius, *Nature* **1997**, *389*, 816–824; b) E. Cao, J. F. Cordero-Morales, B. Liu, F. Qin, D. Julius, *Neuron* **2013**, *77*, 667–679.
- [7] C. J. Bohlen, A. Priel, S. Zhou, D. King, J. Siemens, D. Julius, *Cell* **2010**, *141*, 834–845.
- [8] M. Tominaga, M. J. Caterina, A. B. Malmberg, T. A. Rosen, H. Gilbert, K. Skinner, B. E. Raumann, A. I. Basbaum, D. Julius, *Neuron* **1998**, *21*, 531–543.
- [9] a) P. M. Zygmunt, J. Petersson, D. A. Andersson, H. Chuang, M. Sorgard, V. Di Marzo, D. Julius, E. D. Hogestatt, *Nature* **1999**, *400*, 452–457; b) S. W. H. Hwang, J. Kwak, S. Y. Lee, C. J. Kang, J. Jung, S. Cho, K. H. Min, Y. G. Suh, D. Kim, U. Oh, *Proc. Natl. Acad. Sci. USA* **2000**, *97*, 6155–6160; c) D. Smart, M. J. Gunthorpe, J. C. Jerman, S. Nasir, J. Gray, A. I. Muir, J. K. Chambers, A. D. Randall, J. B. Davis, *Br. J. Pharmacol.* **2000**, *129*, 227–230.
- [10] D. E. Clapham, *Nature* **2003**, *426*, 517–524.
- [11] T. Fehrentz, M. Schönberger, D. Trauner, *Angew. Chem.* **2011**, *123*, 12362–12390; *Angew. Chem. Int. Ed.* **2011**, *50*, 12156–12182.
- [12] D. L. Fortin, M. R. Banghart, T. D. Dunn, K. Borges, D. A. Wagenaar, O. Gaudry, M. Karakossian, T. W. Otis, W. B. Kristan, D. Trauner, R. H. Kramer, *Nat. Methods* **2008**, *5*, 331–338.
- [13] A. Mourrot, T. Fehrentz, D. Bautista, D. Trauner, R. H. Kramer, *Nat. Methods* **2012**, *9*, 396–402.
- [14] A. Polosukhina, J. Litt, I. Tochitsky, J. Nemargut, Y. Sychev, I. De Kouchkovsky, T. Huang, K. Borges, D. Trauner, R. N. Van Gelder, R. H. Kramer, *Neuron* **2012**, *75*, 271–282.
- [15] I. Tochitsky, M. R. Banghart, A. Mourrot, J. Z. Zhao, B. Gaub, R. H. Kramer, D. Trauner, *Nat. Chem.* **2012**, *4*, 105–111.
- [16] a) M. Volgraf, P. Gorostiza, R. Numano, R. H. Kramer, E. Y. Isacoff, D. Trauner, *Nat. Chem. Biol.* **2006**, *2*, 47–52; b) M. Volgraf, P. Gorostiza, S. Szobota, M. R. Helix, E. Y. Isacoff, D. Trauner, *J. Am. Chem. Soc.* **2007**, *129*, 260–261; c) S. Szobota, P. Gorostiza, F. Del Bene, C. Wyart, D. L. Fortin, K. D. Kolstad, O. Tulyathan, M. Volgraf, R. Numano, H. L. Aaron, E. K. Scott, R. H. Kramer, J. Flannery, H. Baier, D. Trauner, E. Y. Isacoff, *Neuron* **2007**, *54*, 535–545; d) P. Gorostiza, M. Volgraf, R. Numano, S. Szobota, D. Trauner, E. Y. Isacoff, *Proc. Natl. Acad. Sci. USA* **2007**, *104*, 10865–10870; e) R. Numano, S. Szobota, A. Y. Laud, P. Gorostiza, M. Volgraf, B. Roux, D. Trauner, E. Y. Isacoff, *Proc. Natl. Acad. Sci. USA* **2009**, *106*, 6814–6819; f) H. Janovjak, S. Szobota, C. Wyart, D. Trauner, E. Y. Isacoff, *Nat. Neurosci.* **2010**, *13*, 1027–1032; g) P. Stawski, H. Janovjak, D. Trauner, *Bioorg. Med. Chem.* **2010**, *18*, 7759–7772; h) N. Caporale, K. D. Kolstad, T. Lee, I. Tochitsky, D. Dalkara, D. Trauner, R. H. Kramer, Y. Dan, E. Y. Isacoff, J. G. Flannery, *Mol. Ther.* **2011**, *19*, 1212–1219.
- [17] J. Levitz, C. Pantoja, B. Gaub, H. Janovjak, A. Reiner, A. Hoagland, D. Schoppik, B. Kane, P. Stawski, A. F. Schier, D. Trauner, E. Y. Isacoff, *Nat. Neurosci.* **2013**, *16*, 507–516.
- [18] M. Stein, S. J. Middendorp, V. Carta, E. Pejo, D. E. Raines, S. A. Forman, E. Sigel, D. Trauner, *Angew. Chem.* **2012**, *124*, 10652–10656; *Angew. Chem. Int. Ed.* **2012**, *51*, 10500–10504.
- [19] A. Szallasi, P. M. Blumberg, *Neuroscience* **1989**, *30*, 515–520.
- [20] a) C. S. Walpole, S. Bevan, G. Bovermann, J. Boelsterli, R. Breckenridge, J. W. Davies, G. A. Hughes, I. James, L. Oberer, *J. Med. Chem.* **1994**, *37*, 1942–1954; b) M. Berglund, M. F. Dalence-Guzman, S. Skogvall, O. Sterner, *Bioorg. Med. Chem.* **2008**, *16*, 2529–2540.
- [21] H. J. Behrendt, T. Germann, C. Gillen, H. Hatt, R. Jostock, *Br. J. Pharmacol.* **2004**, *141*, 737–745.
- [22] Q. Sun, L. Tafesse, K. Islam, X. Zhou, S. F. Victory, C. Zhang, M. Hachicha, L. A. Schmid, A. Patel, Y. Rotshteyn, K. J. Valenzano, D. J. Kyle, *Bioorg. Med. Chem. Lett.* **2003**, *13*, 3611–3616.
- [23] J. Lee, J. Lee, *Synth. Commun.* **1999**, *29*, 4127–4140.
- [24] X-ray structure of **ABCTC**: C₂₂H₂₁ClN₆O, *M_r* = 420.895 g mol⁻¹, yellow rod, 0.31 × 0.04 × 0.03 mm³, monoclinic, *P2₁/c*, *a* = 5.9574(2), *b* = 21.2314(8), *c* = 15.6580(6) Å; β = 97.353(2)°, *V* = 1964.20(1) Å³, *Z* = 4, ρ = 1.423 g cm⁻³, μ(MoKα) = 0.223 mm⁻¹, MoKα radiation (λ = 0.71073 Å), *T* = 173 K, 2θ_{max} 48.20°, 10388 reflections, 3104 independent, 2064 with *I* ≥ 2σ(*I*), *R_{int}* = 0.0735, mean σ(*I*)/*I* = 0.0625, 274 parameters, *R*(*F_{obs}*) = 0.0446, *R_w*(*F²*) = 0.1092, *S* = 1.038, min. and max. residual electron density: -0.255, 0.199 e Å⁻³; data collection by means of a Nonius KappaCCD diffractometer equipped with a rotating anode generator (ω-scans), structure solution by direct methods with SIR97, structure refinement with SHELXL-97. C-bound H atoms have been added geometrically treated as riding on their parent atoms and N-bound H atoms have been fixed at 0.87(1) Å with *U*(H) = 1.2 *U*(N); CCDC 923926 (**ABCTC**) contains the supplementary crystallographic data for this paper. These data can be obtained free of charge from The Cambridge Crystallographic Data Centre via www.ccdc.cam.ac.uk/data_request/cif.
- [25] H. J. Solinski, S. Zierler, T. Gudermann, A. Breit, *J. Biol. Chem.* **2012**, *287*, 40956–40971, and references therein.
- [26] D. Kokel, C. Y. Cheung, R. Mills, J. Coutinho-Budd, L. Huang, V. Setola, J. Sprague, S. Jin, Y. N. Jin, X. P. Huang, G. Bruni, C. J. Wolf, B. L. Roth, M. R. Hamblin, M. J. Zylka, D. J. Milan, R. T. Peterson, *Nat. Chem. Biol.* **2013**, AOP.



Supporting Information

© Wiley-VCH 2013

69451 Weinheim, Germany

Optical Control of TRPV1 Channels**

*Marco Stein, Andreas Breit, Timm Fehrentz, Thomas Gudermann, and Dirk Trauner**

anie_201302530_sm_miscellaneous_information.pdf

INDEX

Section	Page
General Experimental Details and Instrumentation	147
Synthetic Procedures	148
NMR Spectra	174
UV/Vis Spectra	202
Determination of Antagonistic Potencies of AC1–3 and AC5–6 upon Activation of TRPV1 with CAP	206
Cell Culture	207
Whole-cell Electrophysiology	207
Aequorin-based Calcium Measurements	207

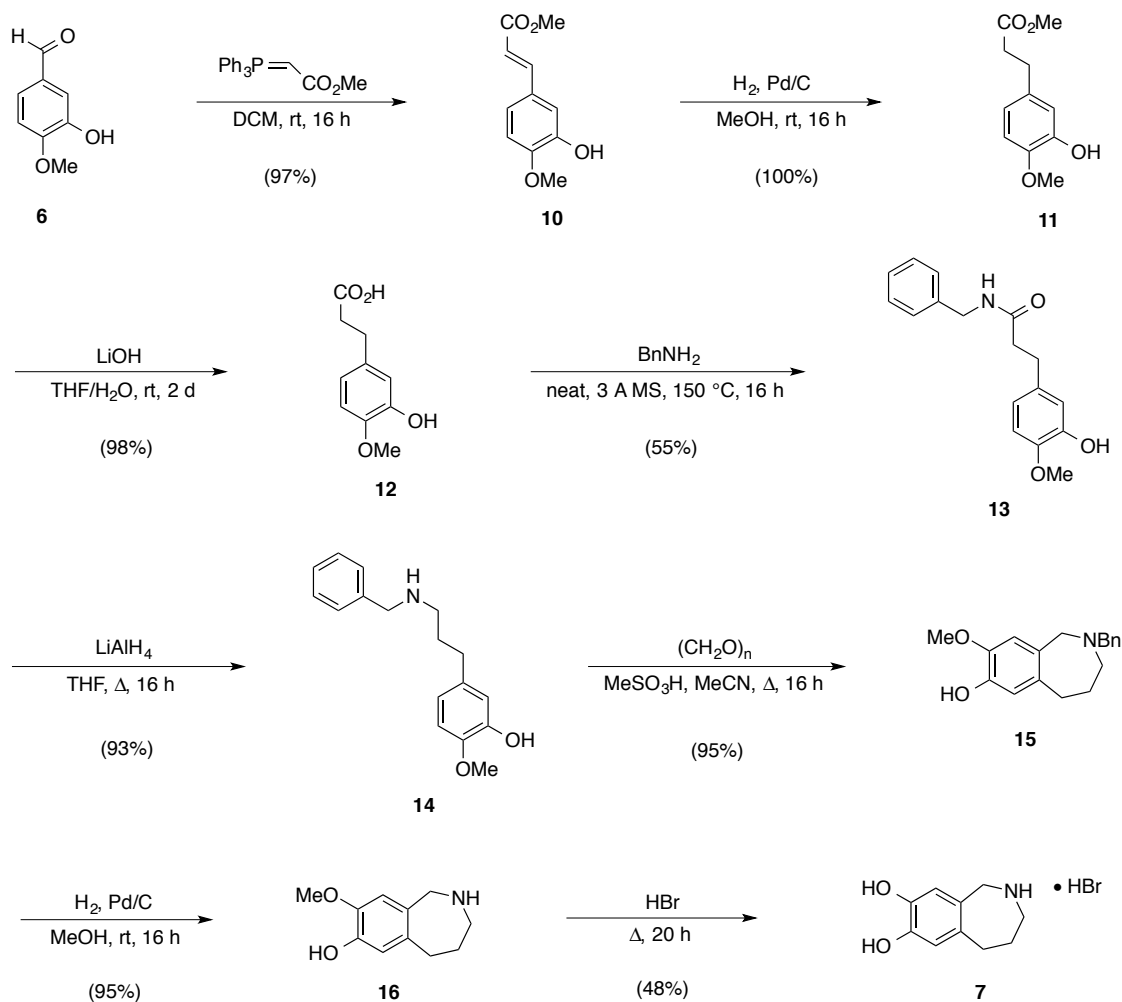
General Experimental Details and Instrumentation

All reactions were carried out with magnetic stirring and if air or moisture sensitive in oven-dried glassware under an atmosphere of nitrogen or argon. Syringes used to transfer reagents and solvents were purged with nitrogen or argon prior to use. Reagents were used as commercially supplied unless otherwise stated. Thin layer chromatography was performed on pre-coated silica gel F₂₅₄ glass backed plates and the chromatogram was visualized under UV light and/or by staining using aqueous acidic vanillin or potassium permanganate, followed by gentle heating with a heat gun. Flash column chromatography was performed using silica gel, particle size 40–63 μm (eluants are given in parenthesis). The diameter of the columns and the amount of silica gel were calculated according to the recommendations of W. C. Still *et al.*^[50] IR spectra were recorded on a Perkin Elmer Spectrum Bx FT-IR instrument as thin films with absorption bands being reported in wave number (cm^{-1}). UV/Vis spectra were obtained using a Varian Cary 50 Scan UV/Vis spectrometer and Helma SUPRASIL precision cuvettes (10 mm light path).

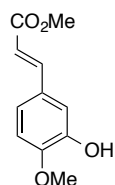
¹H and ¹³C spectra were measured on Varian VNMRS 300, VNMRS 400, INOVA 400 or VNMRS 600 instruments. The chemical shifts are quoted as δ -values in ppm referenced to the residual solvent peak (CDCl_3 : δ_{H} 7.26, δ_{C} 77.2; CD_3OD : δ_{H} 3.31, δ_{C} 49.0; DMSO-d_6 : δ_{H} 2.50, δ_{C} 39.5; acetone- d_6 : δ_{H} 2.05, δ_{C} 29.8, 206.6).^[51] Multiplicities are abbreviated as follows: s = singlet, d = doublet, t = triplet, q = quartet, quint = quintet, sext = sextet, sept = septet, m = multiplet. High resolution mass spectra (EI, ESI) were recorded by LMU Mass Spectrometry Service using a Thermo Finnigan MAT 95, a Jeol MStation, or a Thermo Finnigan LTQ FT Ultra instrument. Melting points were obtained using a Stanford Research Systems MPA120 apparatus and are uncorrected.

Synthetic Procedures

Synthesis of Azepine Core 7 from Isovanilline 6



Scheme 3.1. Synthesis of azepine core 7.

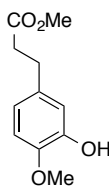
Synthesis of (*E*)-methyl 3-(3-hydroxy-4-methoxyphenyl)acrylate (10)

Isovanillin (**6**; 10.0 g, 65.7 mmol, 1.0 equiv.) and carbomethoxy methylene triphenyl phosphorane (24.2 g, 72.3 mmol, 1.1 equiv.) were dissolved in DCM (220 mL) and stirred at room temperature for 16 h. The mixture was then heated to reflux for 2 h. After cooling, the

solvent was removed *in vacuo* and the crude product was purified by flash silica gel column chromatography (hexanes/EtOAc, 2:1 → 3:2) to yield olefin **10** (13.2 g, 63.5 mmol, 97%) as a colorless solid.

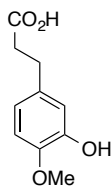
TLC (hexanes/EtOAc, 2:1): $R_f = 0.38$. **M.p.:** 76–78 °C. **$^1\text{H NMR}$ (CDCl_3 , 400 MHz, 27 °C):** $\delta = 7.60$ (d, $J = 15.9$ Hz, 1H, *CH*), 7.14 (d, $J = 2.1$ Hz, 1H, *ArH*), 7.03 (dd, $J = 8.3, 2.1$ Hz, 1H, *ArH*), 6.84 (d, $J = 8.3$ Hz, 1H, *ArH*), 6.29 (d, $J = 15.9$ Hz, 1H, *CH*), 5.63 (s, 1H, *OH*), 3.93 (s, 3H, *OCH*₃), 3.78 (s, 3H, *OCH*₃) ppm. **$^{13}\text{C NMR}$ (CDCl_3 , 100 MHz, 27 °C):** $\delta = 167.7, 148.5, 145.8, 144.6, 128.0, 121.8, 115.8, 112.9, 110.5, 56.0, 51.6$ ppm. **IR (neat, ATR):** $\tilde{\nu} = 3412$ (w), 1698 (m), 1635 (m), 1613 (m), 1583 (m), 1511 (s), 1456 (w), 1439 (m), 1350 (w), 1314 (m), 1264 (vs), 1195 (m), 1172 (m), 1160 (m), 1131 (m), 1025 (m), 980 (m), 925 (w), 856 (w), 805 (m), 762 (w) cm^{-1} . **HRMS (EI^+):** m/z calcd. for $[\text{C}_{11}\text{H}_{12}\text{O}_4]^+$: 208.0736, found: 208.0749 ($[\text{M}]^+$).

Synthesis of methyl 3-(3-hydroxy-4-methoxyphenyl)propanoate (**11**)



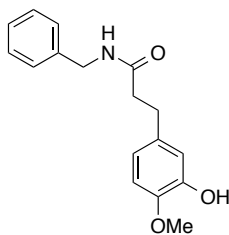
Olefin **10** (13.2 g, 63.4 mmol) was dissolved in MeOH (150 mL) and palladium on charcoal (2.60 g; 10%) was added. The reaction flask was evacuated and repurged with hydrogen (5x) and then stirred at room temperature under a hydrogen atmosphere (1 bar) for 16 h, filtered through Celite and washed thoroughly with DCM. The solvent was removed under reduced pressure, yielding compound **11** quantitatively (13.3 g, 63.3 mmol, 100%) as a colorless solid.

TLC (hexanes/EtOAc, 2:1): $R_f = 0.67$. **M.p.:** 91–93 °C. **$^1\text{H NMR}$ (CDCl_3 , 300 MHz, 27 °C):** $\delta = 7.81$ – 7.76 (m, 2H, *ArH*), 7.72– 7.67 (m, 1H, *ArH*), 5.57 (s, 1H, *OH*), 3.88 (s, 3H, *OCH*₃), 3.69 (s, 3H, *OCH*₃), 2.90– 2.83 (m, 2H, *CH*₂), 2.64– 2.57 (m, 2H, *CH*₂) ppm. **$^{13}\text{C NMR}$ (CDCl_3 , 75 MHz, 27 °C):** $\delta = 173.4, 145.5, 145.0, 133.8, 119.6, 114.5, 110.7, 56.0, 51.6, 35.9, 30.4$ ppm. **IR (neat, ATR):** $\tilde{\nu} = 3427$ (m), 1728 (vs), 1619 (w), 1588 (m), 1514 (m), 1458 (m), 1442 (m), 1422 (w), 1370 (m), 1301 (m), 1269 (s), 1236 (m), 1220 (m), 1195 (m), 1180 (s), 1148 (m), 1127 (m), 1054 (w), 1027 (m), 1013 (m), 979 (w), 959 (w), 894 (w), 874 (w), 816 (m), 810 (m), 786 (w), 762 (w) cm^{-1} . **HRMS (EI^+):** m/z calcd. for $[\text{C}_{11}\text{H}_{14}\text{O}_4]^+$: 210.0892, found: 210.0883 ($[\text{M}]^+$).

Synthesis of 3-(3-hydroxy-4-methoxyphenyl)propanoic acid (12)

Methyl ester **11** (13.2 g, 62.8 mmol) was dissolved in THF (100 mL) and a 2 M solution of LiOH (35 mL) was added. The mixture was stirred for 16 h at room temperature. Since TLC indicated remaining starting material, another 20 mL of 2 M LiOH was added and stirred for another 20 h. The mixture was acidified to pH = 2–3 with 2 M HCl and extracted with EtOAc (3 x 50 mL). The combined organic phases were washed with brine (75 mL), dried over MgSO₄ and concentrated under reduced pressure to yield free acid **12** (12.1 g, 61.7 mmol, 98%) as a colorless solid.

M.p.: 140–141 °C. **¹H NMR (CD₃OD, 400 MHz, 27 °C):** δ = 6.79 (d, *J* = 8.2 Hz, 1H, ArH), 6.66 (d, *J* = 2.1 Hz, 1H, ArH), 6.62 (dd, *J* = 8.2, 2.1 Hz, 1H, ArH), 3.79 (s, 3H, OCH₃), 2.79–2.73 (m, 2H, CH₂), 2.53–2.48 (m, 2H, CH₂) ppm. **¹³C NMR (CD₃OD, 100 MHz, 27 °C):** δ = 175.4, 146.0, 133.7, 120.1, 118.9, 114.9, 111.5, 55.1, 35.6, 30.0 ppm. **IR (neat, ATR):** $\tilde{\nu}$ = 3307 (m), 1684 (vs), 1518 (m), 1456 (m), 1315 (m), 1211 (m), 1079 (m), 967 (w), 938 (w), 808 (w), 766 (w), 732 (w) cm⁻¹. **HRMS (EI⁺):** *m/z* calcd. for [C₁₀H₁₃O₄]⁺: 197.0814, found: 197.0808 ([M+H]⁺).

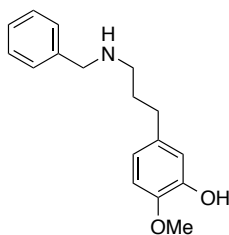
Synthesis of *N*-benzyl-3-(3-hydroxy-4-methoxyphenyl)propanamide (13)

Carboxylic acid **12** (12.1 g, 61.7 mmol, 1.0 equiv.) was heated together with benzyl amine (40.0 mL, 370 mmol, 6.0 equiv.) and 3Å molecular sieves (10.0 g) to 150 °C for 16 h. The mixture was cooled, diluted with DCM (300 mL), washed with 1 M HCl (3 x 150 mL), a sat. aq. solution of NaHCO₃ (2 x 150 mL), water (100 mL) and brine (100 mL). The organic phase was dried over MgSO₄ and the solvent removed *in vacuo*. The crude product was purified by

flash silica gel column chromatography (DCM/MeOH, 98:2 → 95:5) to give benzyl amide **13** (9.65 g, 33.8 mmol, 55%) as a colorless solid.

TLC (DCM/MeOH, 95:5): R_f = 0.38. **M.p.:** 112–114 °C. **^1H NMR (CDCl₃, 400 MHz, 27 °C):** δ = 7.32–7.24 (m, 3H, ArH), 7.17–7.13 (m, 2H, ArH), 6.77 (d, J = 2.1 Hz, 1H, ArH), 6.74 (d, J = 8.2 Hz, 1H, ArH), 6.67 (dd, J = 8.2, 2.1 Hz, 1H, ArH), 5.60 (br m, 2H, OH, NH), 4.39 (d, J = 5.6, 2.1 Hz, 2H, CH₂), 3.86 (s, 3H, OCH₃), 2.93–2.87 (m, 2H, CH₂), 2.49–2.45 (m, 2H, CH₂) ppm. **^{13}C NMR (CDCl₃, 100 MHz, 27 °C):** δ = 171.9, 145.6, 145.1, 138.1, 134.0, 128.6, 127.7, 127.4, 119.8, 114.4, 110.7, 56.0, 43.6, 38.6, 31.1 ppm. **IR (neat, ATR):** $\tilde{\nu}$ = 3290 (m), 1643 (s), 1590 (m), 1512 (vs), 1453 (m), 1440 (m), 1355 (w), 1272 (s), 1240 (m), 1176 (m), 1153 (m), 1130 (m), 1082 (w), 1028 (m), 957 (w), 912 (w), 867 (w), 805 (m), 760 (m), 733 (m), 698 (m) cm⁻¹. **HRMS (EI⁺):** m/z calcd. for [C₁₇H₁₉NO₃]⁺: 285.1365, found: 285.1360 ([M]⁺).

Synthesis of 5-(3-(benzylamino)propyl)-2-methoxyphenol (**14**)

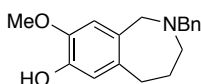


To a solution of amide **13** (9.65 g, 33.8 mmol, 1.0 equiv.) in THF (200 mL) was added slowly a suspension of LiAlH₄ (2.57 g, 67.6 mmol, 2.0 equiv.) in THF (100 mL) at room temperature (gas evolution!). The reaction mixture was heated to reflux for 16 h. A sat. aqu. solution of Rochelle's salt (500 mL) was added and the mixture was stirred vigorously for 1 h. The phases were separated and the aqueous layer was extracted with EtOAc (2 x 200 mL). The combined organic layers were washed with water (200 mL) and brine (200 mL), dried over MgSO₄ and the solvent was removed under reduced pressure. The crude product was purified by flash silica gel column chromatography (DCM/MeOH, gradient from 20:1 to 10:1) to give secondary amine **14** (8.52 g, 31.4 mmol, 93%) as a colorless solid.

TLC (hexanes/EtOAc, 2:1): R_f = 0.67. **M.p.:** 115–117 °C. **^1H NMR (CDCl₃, 300 MHz, 27 °C):** δ = 7.39–7.20 (m, 5H, ArH), 6.79–6.75 (m, 2H, ArH), 6.66 (dd, J = 8.2, 2.1 Hz, 1H, ArH), 3.88 (s, 3H, OCH₃), 3.80 (s, 2H, NCH₂), 2.72–2.65 (m, 2H, CH₂), 2.62–2.55 (m, 2H, CH₂), 1.91–1.77 (m, 2H, CH₂) ppm. **^{13}C NMR (CDCl₃, 75 MHz, 27 °C):** δ = 145.5, 144.8, 140.0, 135.4, 128.4, 128.2, 127.0, 119.6, 114.6, 110.6, 56.0, 53.8, 48.7, 33.0, 31.5 ppm. **IR**

(neat, ATR): $\tilde{\nu}$ = 2932 (m), 2836 (w), 1586 (m), 1509 (s), 1452 (m), 1441 (m), 1349 (w), 1274 (vs), 1243 (s), 1221 (s), 1178 (m), 1154 (m), 1132 (s), 1071 (w), 1028 (m), 961 (w), 908 (w), 867 (w), 802 (m), 737 (m), 698 (s) cm^{-1} . HRMS (EI⁺): m/z calcd. for $[\text{C}_{17}\text{H}_{21}\text{O}_2\text{N}]^+$: 217.1572, found: 271.1568 ($[\text{M}]^+$).

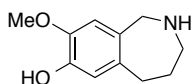
Synthesis of 2-benzyl-8-methoxy-2,3,4,5-tetrahydro-1H-benzo[c]azepin-7-ol (15)



Amine **14** (5.50 g, 20.3 mmol, 1.0 equiv.) and paraformaldehyde (670 mg, 22.3 mmol, 1.1 equiv.) were dissolved in acetonitrile (180 mL) and MeSO_3H (1.45 mL, 22.3 mL, 1.1 equiv.) was added. The mixture was heated to reflux for 16 h. A sat. aqu. solution of NaHCO_3 (200 mL) was added and the phases were separated. The aqueous phase was extracted with DCM (5 x 50 mL) and the combined organic layers were washed with water (150 mL) and brine (150 mL), dried over MgSO_4 and the solvent was removed under reduced pressure. The crude product was purified by flash silica gel column chromatography (DCM/MeOH, 10:1) to give benzazepine **15** (5.47 g, 19.3 mmol, 95%) as a pale yellow solid.

TLC (DCM/MeOH, 10:1): R_f = 0.34. **M.p.:** 115–117 °C. **¹H NMR (CDCl₃, 300 MHz, 27 °C):** δ = 7.34–7.21 (m, 5H, ArH), 6.75 (s, 1H, ArH), 6.42 (s, 1H, ArH), 5.74 (br s, 1H, OH), 3.83 (s, 2H, NCH₂), 3.79 (s, 3H, OCH₃), 3.56 (s, 2H, CH₂), 3.17–3.09 (m, 2H, CH₂), 2.85–2.77 (m, 2H, CH₂), 1.80–1.67 (m, 2H, CH₂) ppm. **¹³C NMR (CDCl₃, 75 MHz, 27 °C):** δ = 144.0, 143.9, 139.2, 136.2, 130.6, 129.1, 128.1, 126.9, 115.6, 113.2, 58.9, 58.6, 57.3, 56.0, 35.4, 25.2 ppm. **IR (neat, ATR):** $\tilde{\nu}$ = 3526 (w), 2926 (m), 2841 (w), 1590 (m), 1513 (m), 1495 (m), 1449 (m), 1332 (m), 1282 (s), 1247 (m), 1205 (m), 1173 (m), 1104 (s), 1079 (w), 1040 (m), 1028 (w), 970 (m), 909 (m), 886 (w), 850 (m), 794 (w), 760 (m), 731 (vs), 698 (m) cm^{-1} . **HRMS (EI⁺):** m/z calcd. for $[\text{C}_{18}\text{H}_{21}\text{O}_2\text{N}]^+$: 283.1572, found: 283.1568 ($[\text{M}]^+$).

Synthesis of 8-methoxy-2,3,4,5-tetrahydro-1H-benzo[c]azepin-7-ol (16)

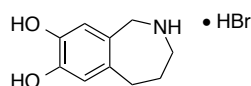


Benzyl protected benzazepine **15** (5.80 g, 20.5 mmol, 1.0 equiv.) was dissolved in MeOH (150 mL) and palladium on charcoal (1.5 g; 10%) was added under an argon atmosphere. The reaction flask was evacuated and repurged with hydrogen (5x) and then stirred at room

temperature overnight under a hydrogen atmosphere (1 bar). The mixture was filtered through Celite, washed with MeOH and concentrated *in vacuo*, affording debenzylated benzazepine **16** (3.76 g, 19.5 mmol, 95%) as a colorless solid. The crude product was sufficiently pure for the next step.

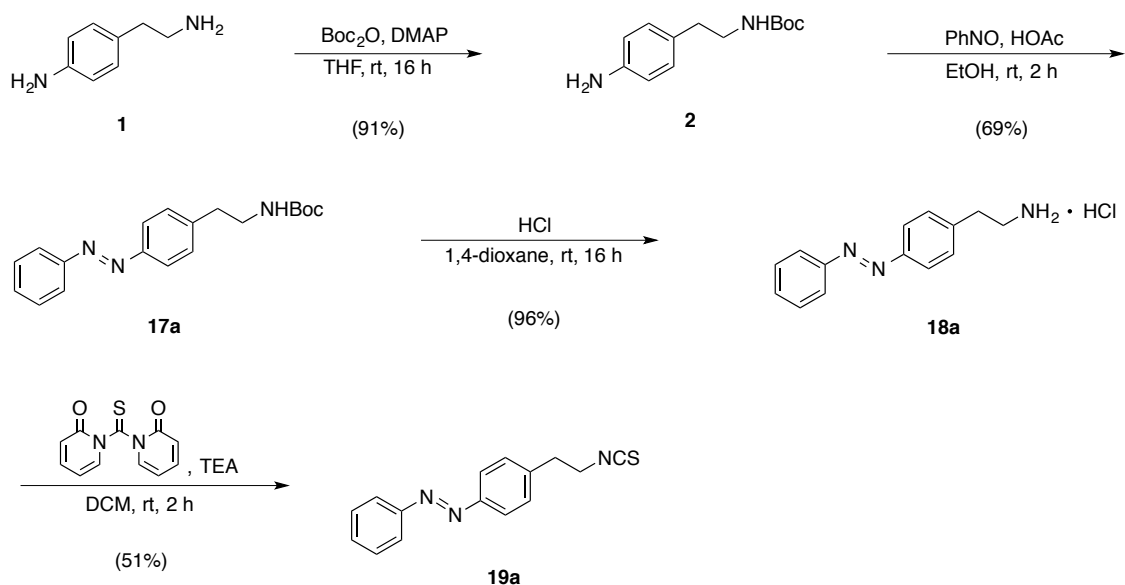
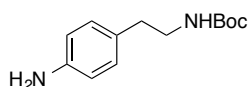
TLC (DCM/MeOH, 10:1): $R_f = 0.09$. **M.p.:** 137–138 °C. **^1H NMR (CD₃OD, 400 MHz, 27 °C):** $\delta = 6.75$ (s, 1H, ArH), 6.62 (s, 1H, ArH), 3.85 (s, 2H, NCH₂), 3.80 (s, 3H, OCH₃), 3.34 (s, 2H, NCH₂), 3.15–3.11 (m, 2H, CH₂), 2.82–2.77 (m, 2H, CH₂), 1.75–1.69 (m, 2H, CH₂) ppm. **^{13}C NMR (CD₃OD, 100 MHz, 27 °C):** $\delta = 145.4, 145.3, 133.7, 130.6, 116.5, 113.2, 55.3, 53.1, 52.2, 34.4, 29.2$ ppm. **IR (neat, ATR):** $\tilde{\nu} = 2933$ (m), 2839 (m), 1592 (m), 1516 (s), 1449 (s), 1334 (m), 1281 (vs), 1243 (m), 1207 (m), 1106 (m), 1079 (w), 1016 (w), 884 (w), 851 (m), 778 (w) cm⁻¹. **HRMS (EI⁺):** m/z calcd. for [C₁₁H₁₅O₂N]⁺: 193.1103, found: 193.1098 ([M]⁺).

Synthesis of 2,3,4,5-tetrahydro-1H-benzo[c]azepine-7,8-diol hydrobromide (**7**)



Methyl ether **16** (1.00 g, 5.17 mmol) was dissolved in aqu. 48% HBr (13 mL) and heated to reflux for 20 h. The cooled solution was concentrated *in vacuo*, resuspended in MeOH (3 mL) and sonicated for 30 min. The suspension was centrifuged and the supernatant was removed. The grey solid was suspended in Et₂O (5 mL), centrifuged and the supernatant was removed again. This procedure was repeated five times and the grey solid obtained was dried under high vacuum to give HBr salt **7** (650 mg, 2.50 mmol, 48%) as a grey solid.

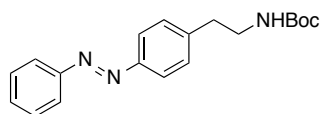
M.p.: 210 °C (dec.). **^1H NMR (DMSO-*d*₆, 400 MHz, 27 °C):** $\delta = 9.03$ (br s, 1H, OH), 8.86 (br s, 1H, OH), 8.57 (br s, 2H, NH₂), 6.74 (s, 1H, ArH), 6.60 (s, 1H, ArH), 4.15–4.02 (m, 2H, NCH₂), 3.28–3.22 (m, 2H, CH₂), 2.78–2.70 (m, 2H, CH₂), 1.82–1.71 (m, 2H, CH₂) ppm. **^{13}C NMR (DMSO-*d*₆, 100 MHz, 27 °C):** $\delta = 145.7, 143.4, 134.4, 123.3, 118.9, 117.4, 50.4, 50.1, 33.0, 25.9$ ppm. **IR (neat, ATR):** $\tilde{\nu} = 3496$ (w), 2971 (m), 2843 (m), 1613 (m), 1570 (m), 1524 (m), 1466 (w), 1440 (w), 1425 (w), 1387 (m), 1358 (w), 1323 (w), 1286 (vs), 1253 (m), 1203 (m), 1170 (m), 1150 (m), 1101 (m), 1071 (m), 1020 (w), 984 (w), 968 (w), 878 (m), 850 (s), 773 (m), 739 (w), 661 (w) cm⁻¹. **HRMS (EI⁺):** m/z calcd. for [C₁₀H₁₃O₂N]⁺: 179.0946, found: 179.0937 ([M-HBr]⁺).

Synthesis of Isothiocyanate **19a**Scheme 3.2. Synthesis of isothiocyanate **19a**.Synthesis of *tert*-butyl 4-aminophenethylcarbamate (**2**)

Aminoaniline **1** (4.40 mL, 34.2 mmol, 1.0 equiv.) was dissolved in THF (110 mL) and Boc_2O (7.92 g, 36.3 mmol, 1.05 equiv.) and DMAP (418 mg, 3.42 mmol, 0.1 equiv.) were added. The mixture was stirred for 16 h at room temperature. The solvent was removed and the crude product was purified by flash silica gel column chromatography (hexanes/EtOAc, 95:5 \rightarrow 6:1, then gradient to 1:1) to give Boc-protected amine **2** (7.37 g, 31.2 mmol, 91%) as a colorless solid.

TLC (hexanes/EtOAc, 2:1): $R_f = 0.25$. **M.p.:** 68–69 °C. **$^1\text{H NMR}$ (CDCl_3 , 300 MHz, 27 °C):** $\delta = 7.01\text{--}6.93$ (m, 2H, ArH), 6.66–6.60 (m, 2H, ArH), 4.52 (br s, 1H, NH), 3.59 (br s, 2H, NH_2), 3.38–3.24 (m, 2H, CH_2), 2.72–2.62 (m, 2H, CH_2), 1.43 (s, 9H, $\text{C}(\text{CH}_3)_3$) ppm. **$^{13}\text{C NMR}$ (CDCl_3 , 75 MHz, 27 °C):** $\delta = 155.9, 144.8, 129.6, 128.8, 115.3, 79.1, 42.0, 35.2, 28.4$ ppm. **IR (neat, ATR):** $\tilde{\nu} = 3351$ (m), 2974 (m), 2934 (w), 1687 (s), 1622 (m), 1581 (w), 1514 (vs), 1451 (m), 1390 (m), 1364 (m), 1248 (m), 1161 (vs), 1047 (m), 958 (m), 864 (m), 823 (m), 774 (m), 756 (m), 678 (w) cm^{-1} . **HRMS (EI^+):** m/z calcd. for $[\text{C}_{13}\text{H}_{20}\text{N}_2\text{O}_2]^+$: 236.1525, found: 236.1519 ($[\text{M}]^+$).

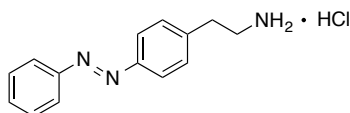
Synthesis of *tert*-butyl 4-(phenyldiazenyl)phenethylcarbamate (**17a**)



Nitrosobenzene (101 mg, 0.940 mmol, 1.1 equiv.) was dissolved in a mixture of ethanol (2.1 mL) and glacial acetic acid (0.76 mL) with careful heating to 50 °C. The clear green solution was cooled to room temperature again and aniline **2** (200 mg, 0.850 mmol, 1.0 equiv.) was added in 3 portions within 5 min. The mixture was stirred for 2 h at room temperature. A sat. aqu. solution of NaHCO₃ was added (20 mL; gas evolution!) and the aqueous phase was extracted with EtOAc (30 mL). The organic phase was carefully washed with sat. aqu. NaHCO₃ (30 mL), and brine (30 mL), then dried over MgSO₄ and concentrated *in vacuo*. The crude product was purified by flash silica gel chromatography (hexanes/EtOAc, gradient from 10:1 to 7:1), affording azobenzene **17a** (192 mg, 0.590 mmol, 69%) as an orange solid.

TLC (hexanes/EtOAc, 4:1): R_f = 0.38. **M.p.:** 116–117 °C. **¹H NMR (CDCl₃, 300 MHz, 27 °C):** δ = 7.94–7.83 (m, 4H, ArH), 7.55–7.44 (m, 3H, ArH), 7.38–7.31 (m, 2H, ArH), 4.54 (br s, 1H, NH), 3.48–3.36 (m, 2H, CH₂), 2.94–2.83 (m, 2H, CH₂), 1.44 (s, 9H, C(CH₃)₃) ppm. **¹³C NMR (CDCl₃, 75 MHz, 27 °C):** δ = 155.8, 152.7, 151.4, 142.4, 130.8, 129.5, 129.0, 123.1, 122.8, 79.4, 41.7, 36.1, 28.4 ppm. **IR (neat, ATR):** $\tilde{\nu}$ = 3379 (m), 2979 (m), 2930 (w), 2877 (w), 1684 (s), 1602 (w), 1521 (vs), 1468 (m), 1443 (m), 1415 (w), 1389 (m), 1366 (m), 1292 (m), 1280 (m), 1244 (s), 1164 (s), 1136 (m), 1108 (m), 1070 (m), 1055 (m), 1040 (m), 1031 (m), 1019 (m), 1012 (m), 1000 (m), 989 (m), 924 (w), 871 (m), 849 (m), 767 (s), 735 (w), 684 (s), 668 (w) cm⁻¹. **HRMS (ESI⁺):** m/z calcd. for [C₁₅H₁₆N₃O₂]⁺: 270.1243, found: 270.1241 ([M-*t*-Bu+2H]⁺).

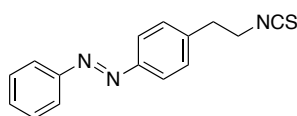
Synthesis of 2-(4-(phenyldiazenyl)phenyl)ethanamine (**18a**)



Boc-protected amine **17a** (81 mg, 0.25 mmol) was dissolved in 1,4-dioxane (1 mL) and a 4 M solution of HCl in dioxane (1 mL) was added. The mixture was stirred for 16 h at room temperature. The orange precipitate was diluted with Et₂O, filtered off and washed thoroughly with Et₂O. Amine **18a** was obtained as its HCl salt (63 mg, 0.24 mmol, 96%) as orange solid.

M.p.: 258 °C (dec.). **¹H NMR (CD₃OD, 400 MHz, 27 °C):** δ = 7.92–7.86 (m, 4H, ArH), 7.56–7.44 (m, 5H, ArH), 3.26–3.20 (m, 2H, CH₂), 3.08–3.02 (m, 2H, CH₂) ppm. **¹³C NMR (CD₃OD, 100 MHz, 27 °C):** δ = 152.5, 151.7, 139.9, 130.9, 129.3, 128.8, 122.9, 122.3, 40.2, 32.9 ppm. **IR (neat, ATR):** $\tilde{\nu}$ = 2990 (m), 2971 (m), 1875 (m), 1605 (m), 1584 (w), 1502 (w), 1475 (m), 1461 (m), 1447 (m), 1418 (w), 1390 (w), 1337 (w), 1307 (w), 1259 (w), 1225 (w), 1158 (w), 1141 (m), 1114 (m), 1072 (w), 1016 (m), 1001 (w), 972 (w), 960 (w), 937 (m), 924 (w), 832 (m), 795 (m), 772 (m), 764 (m), 728 (m), 686 (vs) cm⁻¹. **HRMS (EI⁺):** *m/z* calcd. for [C₁₄H₁₅N₃]⁺: 225.1266, found: 225.1255 ([M-HCl]⁺).

Synthesis of 1-(4-(2-isothiocyanatoethyl)phenyl)-2-phenyldiazene (19a)

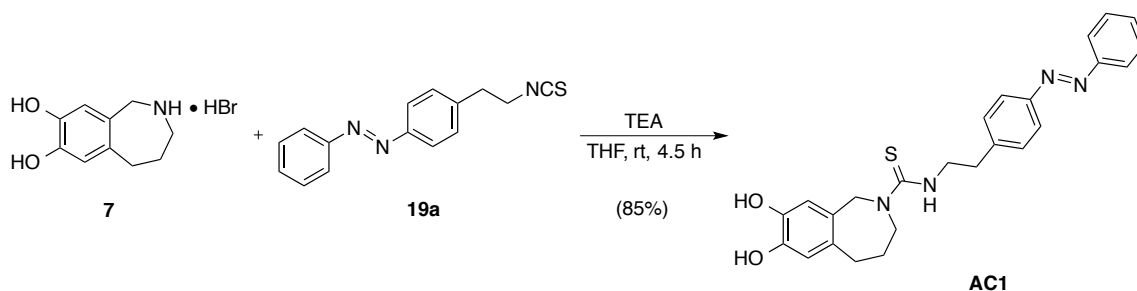


The HCl salt of amine **18a** (139 mg, 0.530 mmol, 1.0 equiv.) was dissolved in DCM (30 mL) and TEA (0.45 mL, 3.2 mmol, 6.0 equiv.) was added. The mixture was stirred for 30 min. 1,1'-Thiocarbonyldi-2(1*H*)-pyridone (123 mg, 0.530 mmol, 1.0 equiv.) was added and the reaction mixture was stirred for 1.5 h. The solvent was removed *in vacuo* and the crude product was purified by flash silica gel column chromatography (hexanes/DCM, gradient from 9:1 to 7:3) to give isothiocyanate **19a** (72 mg, 0.27 mmol, 51%) as orange crystals.

TLC (hexanes/DCM, 7:3): *R_f* = 0.34. **M.p.:** 101–103 °C. **¹H NMR (CDCl₃, 400 MHz, 27 °C):** δ = 7.94–7.86 (m, 4H, ArH), 7.55–7.46 (m, 3H, ArH), 7.40–7.36 (m, 2H, ArH), 3.81–3.76 (m, 2H, CH₂), 3.09–3.05 (m, 2H, CH₂) ppm. **¹³C NMR (CDCl₃, 100 MHz, 27 °C):** δ = 152.6, 151.8, 140.1, 131.0, 129.5, 129.1, 123.3, 122.8, 46.1, 36.4 ppm.^[w] **IR (neat, ATR):** $\tilde{\nu}$ = 2176 (s), 2115 (vs), 1500 (w), 1486 (w), 1436 (m), 1344 (m), 1303 (m), 1185 (w), 1151 (m), 1108 (w), 1071 (w), 1018 (w), 922 (w), 908 (w), 837 (w), 827 (m), 763 (m), 686 (m), 668 (w) cm⁻¹. **HRMS (EI⁺):** *m/z* calcd. for [C₁₅H₁₃N₃S]⁺: 267.0830, found: 267.0821 ([M]⁺).

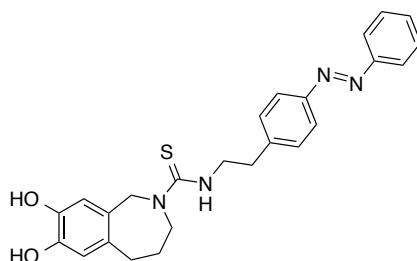
^[w] Due to extensive broadening, the NCS carbon signal could not be observed in the ¹³C NMR spectrum.

Synthesis of AC1



Scheme 3.3. Synthesis of AC1.

Synthesis of 7,8-dihydroxy-N-(4-(phenyldiazenyl)phenethyl)-4,5-dihydro-1H-benzo[c]azepine-2(3H)-carbothioamide (AC1)

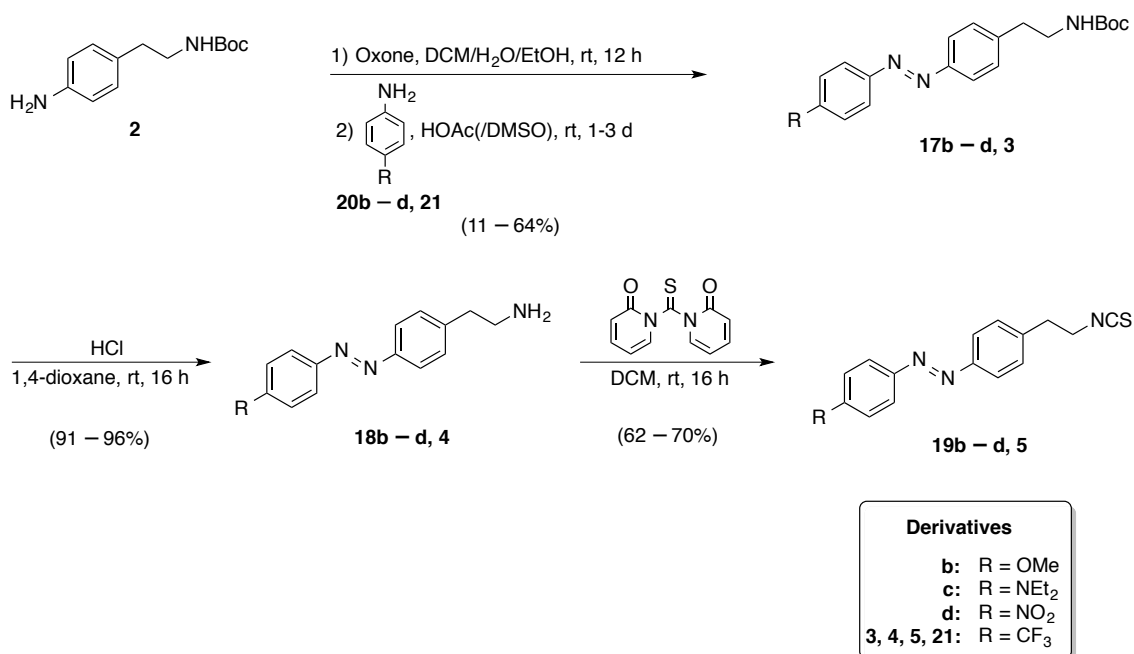


The HBr salt **7** (70 mg, 0.27 mmol, 1.0 equiv.) was suspended in THF (4 mL) and TEA (94 μ L, 0.68 mmol, 2.5 equiv.) was added. The mixture was stirred at room temperature for 30 min. A solution of isothiocyanate **19a** (72 mg, 0.27 mmol, 1.0 equiv.) in THF (3 mL) was added and the reaction mixture was stirred for 4 h. The solution was concentrated *in vacuo* and water (10 mL) was added. The aqueous phase was extracted with EtOAc (3 x 10 mL) and the combined organic layers were washed with brine (25 mL), dried over MgSO₄ and the solvent was removed under reduced pressure. The crude product was purified by flash silica gel column chromatography (hexanes/EtOAc, 1:1), affording thiourea **AC1** (102 mg, 0.230 mmol, 85%) as an orange oil.

TLC (hexanes/EtOAc, 1:1): R_f = 0.29. **M.p.:** 86–88 °C. **¹H NMR (CD₃OD, 600 MHz, 27 °C):** δ = 7.90–7.85 (m, 2H, ArH), 7.82–7.78 (m, 2H, ArH), 7.54–7.50 (m, 2H, ArH), 7.50–7.45 (m, 1H, ArH), 7.34–7.30 (m, 2H, ArH), 6.81 (s, 1H, ArH), 6.59 (s, 1H, ArH), 4.73–4.62 (m, 2H, CH₂), 4.10–3.93 (m, 2H, CH₂), 3.86–3.79 (m, 2H, CH₂), 3.00–2.93 (m, 2H, CH₂), 2.78–2.73 (m, 2H, CH₂), 1.79–1.72 (m, 2H, CH₂) ppm. **¹³C NMR (CD₃OD, 100 MHz, 27 °C):** δ = 179.9, 152.6, 151.1, 143.9, 143.3, 142.3, 132.7, 130.6, 129.4, 128.9, 128.8, 128.6,

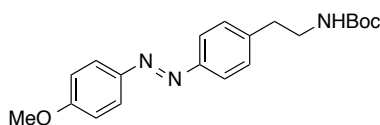
127.4, 122.5, 122.2, 120.6, 120.5, 119.9, 117.0, 116.7, 53.8, 52.7, 46.4, 34.9, 33.3, 27.4 ppm.^[x]
IR (neat, ATR): $\tilde{\nu}$ = 3325 (m), 3287 (m), 3077 (m), 2929 (m), 1696 (m), 1602 (m), 1517 (vs), 1416 (m), 1364 (m), 1314 (s), 1296 (m), 1225 (m), 1161 (m), 1116 (m), 1039 (m), 1022 (m), 969 (w), 824 (w), 766 (w), 737 (w), 695 (m) cm⁻¹. **HRMS (ESI):** m/z calcd. for [C₂₅H₂₅O₂N₄S]⁺: 445.1698, found: 445.1704 ([M-H]⁺). **UV/Vis:** λ_{max} = 332, 436 nm.

Synthesis of Azobenzene Linkers 19b–d and 5 for AC2–AC5



Scheme 3.4. Synthesis of azobenzene linkers **19b–d** and **5** for **AC2–AC5**.

Synthesis of *tert*-butyl 4-((4-methoxyphenyl)diazenyl)phenethylcarbamate (**17b**)



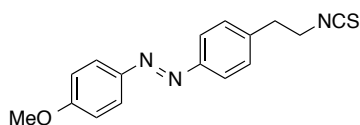
Aniline **2** (2.50 g, 10.6 mmol, 1.0 equiv.) was dissolved in DCM (45 mL) and EtOH (10 mL) and oxone (13.0 g, 21.2 mmol, 2.0 equiv.; dissolved in 100 mL of H₂O) was added. The biphasic mixture was stirred vigorously for 12 h at room temperature. The phases were

^[x] **AC1** was obtained as a mixture of *trans/cis* isomers. Therefore, more signals in the aromatic region were observed in the ¹³C NMR spectrum.

separated and the aqueous phase was extracted with DCM (2 x 50 mL). The combined organic phases were washed with brine (75 mL), dried over MgSO₄ and the solvent was removed under reduced pressure. The resulting green oil was immediately dissolved in HOAc (80 mL) and aniline **20b** (1.31 g, 10.6 mmol, 1.0 equiv.; dissolved in 10 mL of DMSO) was added dropwise. The mixture was stirred for 24 h at room temperature. A sat. aqu. solution of NaHCO₃ was added (300 mL; gas evolution!) and the aqueous phase was extracted with EtOAc (3 x 70 mL). The organic phase was washed with brine (5 x 100 mL) to remove remaining DMSO and the organic phase was then dried over MgSO₄ and concentrated *in vacuo*. The crude product was purified by flash silica gel chromatography (hexanes/EtOAc, gradient from 10:1 to 3:1), affording azobenzene **17b** (1.45 g, 4.08 mmol, 38%) as an orange solid.

TLC (hexanes/EtOAc, 4:1): R_f = 0.27. **M.p.:** 111–112 °C. **¹H NMR (CDCl₃, 300 MHz, 27 °C):** δ = 7.94–7.88 (m, 2H, ArH), 7.84–7.79 (m, 2H, ArH), 7.35–7.28 (m, 2H, ArH), 7.04–6.98 (m, 2H, ArH), 4.58 (br s, 1H, NH), 3.88 (s, 3H, OCH₃), 3.47–3.35 (m, 2H, CH₂), 2.92–2.82 (m, 2H, CH₂), 1.44 (s, 9H, C(CH₃)₃) ppm. **¹³C NMR (CDCl₃, 75 MHz, 27 °C):** δ = 161.9, 155.8, 151.5, 147.0, 141.7, 129.5, 124.7, 122.8, 114.2, 79.3, 55.6, 41.6, 36.0, 28.4 ppm. **IR (neat, ATR):** $\tilde{\nu}$ = 3378 (m), 2968 (m), 2932 (m), 2507 (w), 1684 (s), 1600 (m), 1583 (m), 1524 (s), 1499 (m), 1457 (m), 1443 (m), 1421 (m), 1390 (m), 1366 (m), 1295 (m), 1282 (m), 1243 (vs), 1167 (s), 1153 (s), 1140 (s), 1106 (m), 1054 (w), 1027 (m), 986 (m), 909 (m), 871 (m), 842 (vs), 806 (w), 778 (w), 768 (w), 732 (m) cm⁻¹. **HRMS (ESI⁺):** m/z calcd. for [C₂₀H₂₆N₃O₃]⁺: 356.1974, found: 356.1967 ([M+H]⁺).

Synthesis of 1-(4-(2-isothiocyanatoethyl)phenyl)-2-(4-methoxyphenyl)diazene (**19b**)



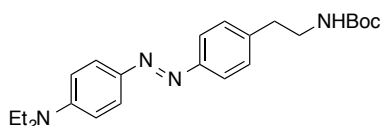
Boc-protected amine **17b** (1.31 g, 3.69 mmol) was dissolved in 1,4-dioxane (20 mL) and a 4 M solution of HCl in 1,4-dioxane (20 mL) was added. The mixture was stirred at room temperature for 16 h. The mixture was basified with 2 M NaOH and the phases were separated. The aqueous phase was extracted with DCM (5 x 30 mL) and the combined organic phases were washed with brine (100 mL), dried over MgSO₄ and the solvent was removed under reduced pressure. Amine **18b** (907 mg, 3.55 mmol, 96%) was obtained as a red oil and used without further purification.

Amine **18b** (200 mg, 0.780 mmol, 1.0 equiv.) was dissolved in DCM (20 mL) and 1,1'-thiocarbonyldi-2(1*H*)-pyridone (193 mg, 0.830 mmol, 1.06 equiv.) was added. The reaction

mixture was stirred for 36 h. The solvent was removed *in vacuo* and the crude product was purified by flash silica gel column chromatography (hexanes/EtOAc, 20:1 → 7:1) to give isothiocyanate **19b** (158 mg, 0.530 mmol, 68%) as an orange solid.

TLC (hexanes/EtOAc, 4:1): $R_f = 0.42$. **M.p.:** 91–92 °C. **$^1\text{H NMR}$ (CDCl_3 , 600 MHz, 27 °C):** $\delta = 7.94\text{--}7.88$ (m, 2H, ArH), 7.87–7.82 (m, 2H, ArH), 7.37–7.31 (m, 2H, ArH), 7.02–6.98 (m, 2H, ArH), 3.88 (s, 3H, OCH_3), 3.78–3.75 (m, 2H, CH_2), 3.07–3.02 (m, 2H, CH_2) ppm. **$^{13}\text{C NMR}$ (CDCl_3 , 150 MHz, 27 °C):** $\delta = 162.1, 151.9, 147.0, 139.4, 131.3, 129.5, 124.7, 123.0, 114.2, 55.7, 46.1, 36.3$ ppm. **IR (neat, ATR):** $\tilde{\nu} = 3007$ (w), 2930 (w), 2837 (w), 2178 (m), 2094 (s), 1600 (m), 1580 (m), 1499 (m), 1454 (m), 1441 (m), 1419 (w), 1411 (w), 1357 (w), 1325 (w), 1299 (w), 1246 (vs), 1181 (w), 1154 (m), 1142 (m), 1107 (m), 1031 (m), 956 (w), 842 (s), 762 (w), 730 (w), 673 (w) cm^{-1} . **HRMS (ESI⁺):** m/z calcd. for $[\text{C}_{16}\text{H}_{16}\text{N}_3\text{OS}]^+$: 298.1014, found: 298.1007 ($[\text{M}+\text{H}]^+$).

Synthesis of *tert*-butyl 4-((4-(diethylamino)phenyl)diazenyl)phenethyl-carbamate (**17c**)

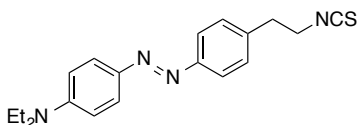


Aniline **2** (2.66 g, 11.3 mmol, 1.0 equiv.) was dissolved in DCM (45) and EtOH (10 mL) and oxone (13.9 g, 22.6 mmol, 2.0 equiv.; dissolved in 100 mL of H_2O) was added. The biphasic mixture was stirred vigorously for 12 h at room temperature. The phases were separated and the aqueous phase was extracted with DCM (5 x 50 mL). The combined organic phases were washed with brine (200 mL), dried over MgSO_4 and the solvent was removed under reduced pressure. The resulting green oil was immediately dissolved in HOAc (80 mL) and aniline **20c** (1.87 mL, 11.3 mmol, 1.0 equiv.) was added dropwise. The mixture was stirred for 3 d at room temperature. A sat. aqu. solution of NaHCO_3 was added (300 mL; gas evolution!) and the aqueous phase was extracted with EtOAc (3 x 70 mL). The organic phase was carefully washed with sat. aqu. NaHCO_3 (150 mL) and brine (150 mL). The organic phase was then dried over MgSO_4 and concentrated *in vacuo*. The crude product was purified by flash silica gel chromatography (hexanes/EtOAc, gradient from 10:1 to 3:1), affording azobenzene **17c** (593 mg, 1.50 mmol, 13%) as a red oil.

TLC (hexanes/EtOAc, 4:1): $R_f = 0.24$. **$^1\text{H NMR}$ (CDCl_3 , 300 MHz, 27 °C):** $\delta = 7.88\text{--}7.81$ (m, 2H, ArH), 7.80–7.74 (m, 2H, ArH), 7.32–7.26 (m, 2H, ArH), 6.76–6.67 (m, 2H, ArH), 4.55 (br s, 1H, NH), 3.51–3.33 (m, 6H, 3 x CH_2), 2.90–2.81 (m, 2H, CH_2), 1.44 (s, 9H, $\text{C}(\text{CH}_3)_3$),

1.22 (t, $J = 6.9$ Hz, 6H, 2 x CH_3) ppm. ^{13}C NMR ($CDCl_3$, 75 MHz, 27 °C): $\delta = 155.8, 152.0, 150.0, 143.1, 140.2, 129.4, 125.2, 122.3, 110.9, 79.3, 44.7, 41.7, 36.0, 28.4, 12.7$ ppm. IR (neat, ATR): $\tilde{\nu} = 3361$ (w), 2975 (m), 2928 (w), 1710 (m), 1600 (vs), 1557 (w), 1515 (s), 1450 (w), 1398 (m), 1357 (m), 1311 (w), 1271 (m), 1250 (m), 1158 (m), 1139 (vs), 1078 (w), 1013 (w), 956 (w), 825 (m), 784 (w) cm^{-1} . HRMS (ESI⁺): m/z calcd. for $[C_{23}H_{33}N_4O_2]^+$: 397.2604, found: 397.2594 ($[M+H]^+$).

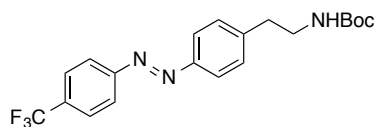
Synthesis of *N,N*-diethyl-4-((4-(2-isothiocyanatoethyl)phenyl)diazenyl)aniline (**19c**)



Boc-protected amine **17c** (550 mg, 1.39 mmol) was dissolved in 1,4-dioxane (10 mL) and a 4 M solution of HCl in 1,4-dioxane (10 mL) was added. The mixture was stirred at room temperature for 16 h. A sat. aqu. solution of $NaHCO_3$ (100 mL) was added and the phases were separated. The aqueous phase was extracted with DCM (2 x 20 mL) and the combined organic phases were washed with sat. aqu. $NaHCO_3$ (30 mL), dried over $MgSO_4$ and the solvent was removed under reduced pressure. Amine **18c** (373 mg, 1.26 mmol, 91%) was obtained as a red oil and used without further purification.

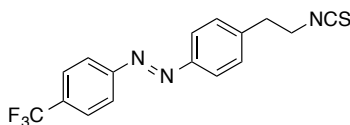
Amine **18c** (100 mg, 0.340 mmol, 1.0 equiv.) was dissolved in DCM (10 mL) and 1,1'-thiocarbonyldi-2(1*H*)-pyridone (86 mg, 0.37 mmol, 1.1 equiv.) was added. The reaction mixture was stirred for 12 h. The solvent was removed *in vacuo* and the crude product was purified by flash silica gel column chromatography (hexanes/EtOAc, 20:1 → 10:1) to give isothiocyanate **19c** (75 mg, 0.22 mmol, 65%) as red crystals.

TLC (hexanes/EtOAc, 4:1): $R_f = 0.34$. 1H NMR ($CDCl_3$, 600 MHz, 27 °C): $\delta = 7.86$ – 7.81 (m, 2H, ArH), 7.81 – 7.77 (m, 2H, ArH), 7.32 – 7.27 (m, 2H, ArH), 6.73 – 6.69 (m, 2H, ArH), 3.77 – 3.72 (m, 2H, CH_2), 3.44 (q, $J = 7.1$ Hz, 4H, 2 x CH_2), 3.06–3.01 (m, 2H, CH_2), 1.23 (q, $J = 7.1$ Hz, 6H, 2 x CH_3) ppm. ^{13}C NMR ($CDCl_3$, 150 MHz, 27 °C): $\delta = 152.5, 150.1, 143.1, 137.9, 131.0, 129.3, 125.3, 122.5, 110.9, 46.2, 44.7, 36.3, 12.7$ ppm. IR (neat, ATR): $\tilde{\nu} = 2974$ (m), 2931 (w), 2899 (w), 2186 (m), 2110 (m), 1598 (vs), 1559 (m), 1514 (m), 1482 (w), 1469 (w), 1447 (w), 1426 (w), 1399 (m), 1377 (m), 1356 (m), 1312 (w), 1271 (m), 1250 (w), 1196 (m), 1156 (m), 1139 (s), 1106 (w), 1096 (w), 1078 (w), 1014 (w), 954 (w), 924 (w), 850 (w), 824 (m), 788 (w), 673 (w) cm^{-1} . HRMS (ESI⁺): m/z calcd. for $[C_{19}H_{23}N_4S]^+$: 339.1643, found: 339.1635 ($[M+H]^+$).

Synthesis of *tert*-butyl 4-((4-(trifluoromethyl)phenyl)diazenyl)phenethylcarbamate (3)

Aniline **2** (1.50 g, 6.35 mmol, 1.0 equiv.) was dissolved in DCM (25 mL) and EtOH (5 mL) and oxone (7.81 g, 12.7 mmol, 2.0 equiv.; dissolved in 50 mL of H₂O) was added. The biphasic mixture was stirred vigorously for 16 h at room temperature. The phases were separated and the aqueous phase was extracted with DCM (2 x 40 mL). The combined organic phases were washed with brine (2 x 75 mL), dried over MgSO₄ and the solvent was removed under reduced pressure. The resulting green oil was immediately dissolved in HOAc (50 mL) and aniline **21** (0.80 mL, 6.35 mmol, 1.0 equiv.; dissolved in 6 mL of DMSO) was added dropwise. The mixture was stirred for 24 h at room temperature. A sat. aqu. solution of NaHCO₃ was added (250 mL; gas evolution!) and the aqueous phase was extracted with DCM (3 x 50 mL). The organic phase was washed with sat. aqu. NaHCO₃ (100 mL), dried over MgSO₄ and concentrated *in vacuo*. The crude product was purified by flash silica gel chromatography (hexanes/EtOAc, gradient from 20:1 to 8:1), affording azobenzene **3** (272 mg, 0.690 mmol, 11%) as an orange solid.

TLC (hexanes/EtOAc, 4:1): R_f = 0.29. **M.p.:** 148–149 °C. **¹H NMR (CDCl₃, 400 MHz, 27 °C):** δ = 8.01–7.96 (m, 2H, ArH), 7.92–7.87 (m, 2H, ArH), 7.80–7.75 (m, 2H, ArH), 7.39–7.34 (m, 2H, ArH), 4.57 (br s, 1H, NH), 3.48–3.39 (m, 2H, CH₂), 2.93–2.86 (m, 2H, CH₂), 1.45 (s, 9H, C(CH₃)₃) ppm. **¹³C NMR (CDCl₃, 150 MHz, 27 °C):** δ = 155.8, 154.4 (m), 151.2, 143.4, 132.1 (q, J = 32.5 Hz), 129.6, 126.3 (q, J = 3.8 Hz), 123.9 (q, J = 406.2 Hz), 123.4, 122.9, 79.4, 41.6, 36.2, 28.4 ppm. **¹⁹F NMR (CDCl₃, 376 MHz, 27 °C):** δ = –62.6 ppm. **IR (neat, ATR):** $\tilde{\nu}$ = 3368 (m), 2977 (w), 2934 (w), 2873 (w), 1679 (vs), 1604 (w), 1527 (s), 1463 (w), 1414 (w), 1392 (w), 1366 (m), 1325 (vs), 1297 (m), 1283 (m), 1251 (m), 1163 (vs), 1125 (vs), 1102 (m), 1065 (m), 1013 (w), 992 (w), 854 (m), 780 (w), 757 (w), 669 (w) cm⁻¹. **HRMS (ESI⁺):** m/z calcd. for [C₂₀H₂₃N₃O₂F₃]⁺: 394.1742, found: 394.1742 ([M+H]⁺).

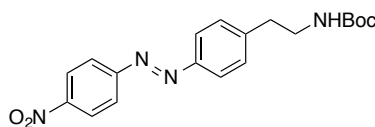
Synthesis of 1-(4-(2-isothiocyanatoethyl)phenyl)-2-(4-(trifluoromethyl)phenyl)diazene (5)

Boc-protected amine **3** (249 mg, 0.630 mmol) was dissolved in 1,4-dioxane (5 mL) and a 4 M solution of HCl in 1,4-dioxane (5 mL) was added. The mixture was stirred at room temperature for 16 h. The mixture was basified with sat. aqu. NaHCO₃ (40 mL; gas evolution!) and the phases were separated. The aqueous phase was extracted with DCM (3 x 10 mL) and the combined organic phases were washed with sat. aqu. NaHCO₃ (25 mL) and brine (25 mL), dried over MgSO₄ and the solvent was removed under reduced pressure. Amine **4** (176 mg, 0.600 mmol, 95%) was obtained as an orange solid and used without further purification.

Amine **4** (176 mg, 0.600 mmol, 1.0 equiv.) was dissolved in DCM (15 mL) and 1,1'-thiocarbonyldi-2(1*H*)-pyridone (153 mg, 0.660 mmol, 1.1 equiv.) was added. The reaction mixture was stirred for 16 h. The solvent was removed *in vacuo* and the crude product was purified by flash silica gel column chromatography (hexanes/EtOAc, 40:1 → 20:1) to give isothiocyanate **5** (124 mg, 0.370 mmol, 62%) as an orange solid.

TLC (hexanes/EtOAc, 4:1): R_f = 0.57. **M.p.:** 106–108 °C. **¹H NMR (CDCl₃, 600 MHz, 27 °C):** δ = 8.01–7.96 (m, 2H, ArH), 7.95–7.91 (m, 2H, ArH), 7.79–7.75 (m, 2H, ArH), 7.41–7.37 (m, 2H, ArH), 3.82–3.77 (m, 2H, CH₂), 3.11–3.06 (m, 2H, CH₂) ppm. **¹³C NMR (CDCl₃, 150 MHz, 27 °C):** δ = 154.4 (m), 151.7, 141.1, 132.2 (q, J = 32.4 Hz), 131.6, 129.7, 129.3 (*cis* isomer), 126.3 (q, J = 3.8 Hz), 123.9 (q, J = 271.2 Hz), 123.6, 123.0, 121.3 (*cis* isomer), 120.3 (*cis* isomer), 46.0, 36.4 ppm. **¹⁹F NMR (CDCl₃, 282 MHz, 27 °C):** δ = –62.6 ppm. **IR (neat, ATR):** $\tilde{\nu}$ = 2927 (w), 2854 (w), 2168 (m), 2111 (m), 1601 (w), 1499 (w), 1436 (m), 1414 (m), 1344 (m), 1318 (vs), 1244 (w), 1220 (m), 1167 (m), 1123 (s), 1108 (s), 1063 (s), 1007 (m), 910 (m), 851 (s), 826 (m), 741 (m), 722 (w), 656 (w) cm⁻¹. **HRMS (ESI⁺):** m/z calcd. for [C₁₆H₁₃N₃F₃S]⁺: 336.0782, found: 336.0771 ([M+H]⁺).

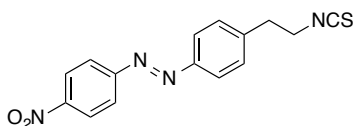
Synthesis of *tert*-butyl 4-((4-nitrophenyl)diazenyl)phenethylcarbamate (**17d**)



4-Nitroaniline **20d** (2.07 g, 15.0 mmol, 1.0 equiv.) was dissolved in DCM (60 mL) and oxone (18.4 g, 30.0 mmol, 2.0 equiv.; dissolved in 120 mL of H₂O) was added. The biphasic mixture was stirred vigorously for 12 h at room temperature. The phases were separated and the aqueous phase was extracted with DCM (70 mL). The combined organic phases were washed with water (75 mL), dried over MgSO₄ and the solvent was removed under reduced pressure. The resulting green oil was immediately dissolved in HOAc (120 mL) and aniline **2** (3.54 g, 15.0 mmol, 1.0 equiv.) was added in 4 portions. The mixture was stirred for 2.5 d at room temperature. Solid Na₂CO₃ and a sat. aqu. solution of NaHCO₃ was added to set the pH to pH = 8–10 (gas evolution!) and the aqueous phase was extracted with EtOAc (2 x 50 mL). The organic phase was washed with sat. aqu. NaHCO₃ (3 x 200 mL), dried over MgSO₄ and concentrated *in vacuo*. The crude product was purified by flash silica gel chromatography (hexanes/EtOAc, gradient from 9:1 to 3:1), affording azobenzene **17d** (3.56 g, 9.61 mmol, 64%) as a red solid.

TLC (hexanes/EtOAc, 4:1): R_f = 0.26. **M.p.:** 149–150 °C. **¹H NMR (CDCl₃, 400 MHz, 27 °C):** δ = 8.36–8.32 (m, 2H, ArH), 8.00–7.96 (m, 2H, ArH), 7.91–7.86 (m, 2H, ArH), 7.38–7.33 (m, 2H, ArH), 4.60 (br s, 1H, NH), 3.46–3.36 (m, 2H, CH₂), 2.92–2.84 (m, 2H, CH₂), 1.42 (s, 9H, C(CH₃)₃) ppm. **¹³C NMR (CDCl₃, 150 MHz, 27 °C):** δ = 155.8, 155.7, 151.1, 148.6, 144.2, 129.7, 124.7, 123.6, 123.3, 79.4, 41.5, 36.3, 28.4 ppm. **IR (neat, ATR):** $\tilde{\nu}$ = 3371 (m), 2979 (w), 2934 (w), 2862 (w), 1677 (s), 1605 (m), 1520 (vs), 1456 (m), 1416 (w), 1391 (w), 1366 (m), 1342 (s), 1277 (m), 1251 (m), 1164 (s), 1107 (m), 1057 (w), 1006 (w), 909 (w), 860 (s), 795 (w), 782 (w), 754 (w), 732 (m), 688 (m), 592 (w) cm⁻¹. **HRMS (ESI⁺):** m/z calcd. for [C₁₅H₁₅N₄O₄]⁺: 315.1093, found: 315.1085 ([M-*t*-Bu+H]⁺).

Synthesis of 1-(4-(2-isothiocyanatoethyl)phenyl)-2-(4-nitrophenyl)diazene (**19d**)



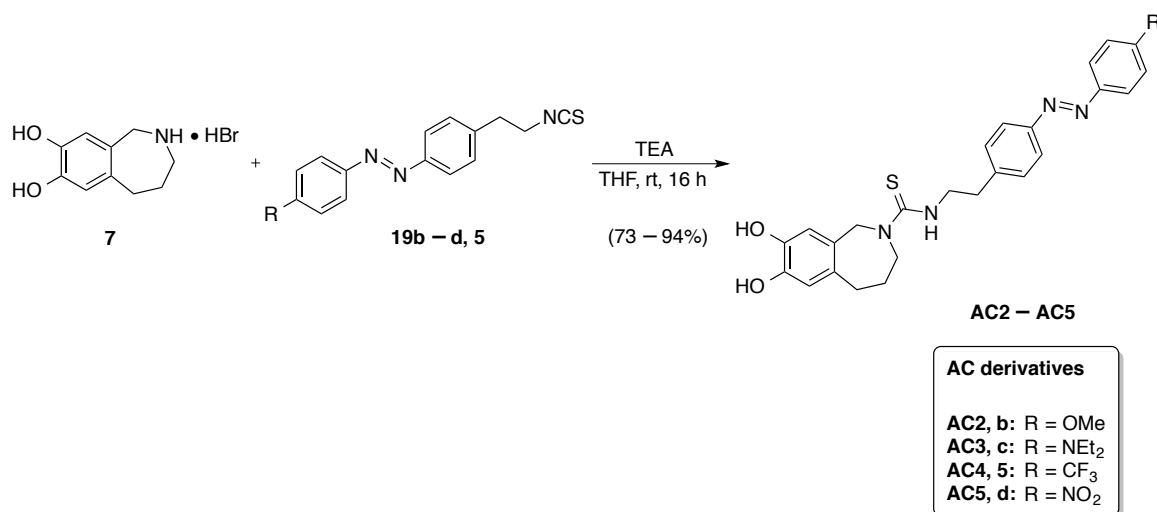
Boc-protected amine **17d** (2.46 g, 6.64 mmol) was dissolved in 1,4-dioxane (40 mL) and a 4 M solution of HCl in 1,4-dioxane (40 mL) was added. The mixture was stirred at room

temperature for 16 h. The mixture was basified with 2 M NaOH and the phases were separated. The aqueous phase was extracted with EtOAc (3 x 30 mL) and the combined organic phases were washed with brine (75 mL), dried over MgSO₄ and the solvent was removed under reduced pressure. Amine **18d** (1.02 g, 3.77 mmol, 57%) was obtained as a red solid and used without further purification.

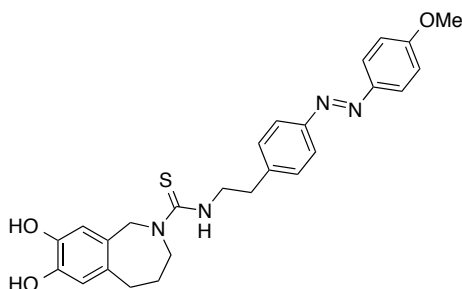
Amine **18d** (600 mg, 2.22 mmol, 1.0 equiv.) was dissolved in DCM (50 mL) and 1,1'-thiocarbonyldi-2(1*H*)-pyridone (567 mg, 2.44 mmol, 1.1 equiv.) was added. The reaction mixture was stirred for 16 h. The solvent was removed *in vacuo* and the crude product was purified by flash silica gel column chromatography (CHCl₃/MeOH, 100:0 → 20:1 → 10:1) to give isothiocyanate **19d** (488 mg, 1.56 mmol, 70%) as an orange solid.

TLC (hexanes/EtOAc, 4:1): R_f = 0.35. **M.p.:** 153–154 °C. **¹H NMR (CDCl₃, 600 MHz, 27 °C):** δ = 8.39–8.35 (m, 2H, ArH), 8.04–8.00 (m, 2H, ArH), 7.97–7.93 (m, 2H, ArH), 7.43–7.38 (m, 2H, ArH), 3.83–3.78 (m, 2H, CH₂), 3.12–3.06 (m, 2H, CH₂) ppm. **¹³C NMR (CDCl₃, 150 MHz, 27 °C):** δ = 155.7, 151.5, 148.7, 141.8, 131.7, 129.8, 124.7, 123.9, 123.4, 46.0, 36.4 ppm. **IR (neat, ATR):** $\tilde{\nu}$ = 2169 (m), 2111 (m), 1609 (m), 1544 (s), 1500 (w), 1483 (w), 1458 (w), 1436 (w), 1415 (w), 1370 (w), 1349 (vs), 1319 (m), 1245 (w), 1218 (w), 1188 (w), 1154 (w), 1110 (m), 1073 (w), 1003 (w), 911 (w), 863 (s), 827 (m), 755 (m), 728 (w), 684 (m), 634 (w) cm⁻¹. **HRMS (EI⁺):** m/z calcd. for [C₁₅H₁₂N₄O₂S]⁺: 312.0681, found: 312.0670 ([M]⁺).

Synthesis of AC2–AC5



Scheme 3.5. Synthesis of AC2–AC5.

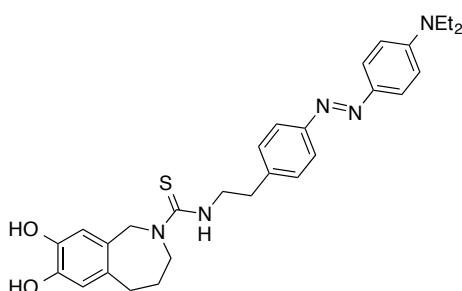
Synthesis of 7,8-dihydroxy-*N*-(4-((4-methoxyphenyl)diazenyl)phenethyl)-4,5-dihydro-1*H*-benzo[*c*]azepine-2(3*H*)-carbothioamide (AC2)

The HBr salt **7** (107 mg, 0.410 mmol, 1.1 equiv.) was suspended in THF (15 mL) and TEA (0.13 mL, 0.93 mmol, 2.5 equiv.) was added. A solution of isothiocyanate **19b** (110 mg, 0.370 mmol, 1.0 equiv.) in THF (5 mL) was added and the reaction mixture was stirred for 16 h. The solution was concentrated *in vacuo* and the crude product was purified by flash silica gel column chromatography (CHCl₃/MeOH, gradient from 100:0 to 80:1), affording thiourea **AC2** (127 mg, 0.270 mmol, 73%) as an orange solid.

TLC (CHCl₃/MeOH, 20:1): R_f = 0.34. **M.p.:** 169–170 °C. **¹H NMR (CD₃OD, 600 MHz, 27 °C):** δ = 7.88–7.85 (m, 2H, ArH), 7.75–7.72 (m, 2H, ArH), 7.30–7.27 (m, 2H, ArH), 7.05–7.03 (m, 2H, ArH), 6.81 (s, 1H, ArH), 6.59 (s, 1H, ArH), 4.75–4.64 (m, 2H, CH₂), 4.10–3.93 (m, 2H, CH₂), 3.86 (s, 3H, OCH₃), 3.84–3.78 (m, 2H, CH₂), 2.98–2.91 (m, 2H, CH₂), 2.78–2.72 (m, 2H, CH₂), 1.77–1.70 (m, 2H, CH₂) ppm. **¹³C NMR (CD₃OD, 100 MHz, 27 °C):**

δ = 179.8, 162.3, 151.2, 146.8, 143.9, 142.4, 142.3, 132.7, 129.3, 127.4, 122.2, 117.0, 116.8, 113.9, 54.7, 53.8, 52.7, 46.5, 34.8, 33.3, 27.4 ppm. **IR (neat, ATR):** $\tilde{\nu}$ = 3292 (m), 2933 (m), 2839 (w), 2503 (w), 2230 (w), 2070 (w), 1600 (m), 1584 (m), 1500 (s), 1463 (m), 1384 (m), 1351 (m), 1292 (s), 1252 (vs), 1179 (m), 1154 (m), 1143 (m), 1103 (m), 1066 (w), 1028 (m), 975 (m), 885 (w), 840 (m), 766 (w), 732 (w), 674 (w) cm^{-1} . **HRMS (ESI⁺):** m/z calcd. for $[\text{C}_{26}\text{H}_{29}\text{O}_3\text{N}_4\text{S}]^+$: 477.1960, found: 477.1958 ($[\text{M}+\text{H}]^+$). **UV/Vis:** λ_{max} = 353, 442 nm.

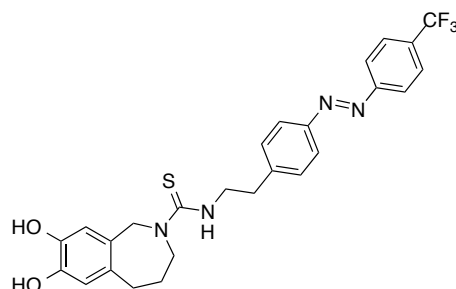
Synthesis of *N*-(4-((4-(diethylamino)phenyl)diazenyl)phenethyl)-7,8-di-hydroxy-4,5-di-hydro-1*H*-benzo[*c*]azepine-2(3*H*)-carbothioamide (AC3)



The HBr salt **7** (49 mg, 0.19 mmol, 1.1 equiv.) was suspended in THF (5 mL) and TEA (60 μL , 0.43 mmol, 2.5 equiv.) was added. The mixture was stirred at room temperature for 30 min. A solution of isothiocyanate **19c** (59 mg, 0.17 mmol, 1.0 equiv.) in THF (5 mL) was added and the reaction mixture was stirred for 12 h. The solution was concentrated *in vacuo* and the crude product was purified by flash silica gel column chromatography ($\text{CHCl}_3/\text{MeOH}$, gradient from 100:0 to 70:1), giving thiourea **AC3** (81 mg, 0.16 mmol, 94%) as a red oil.

TLC ($\text{CHCl}_3/\text{MeOH}$, 20:1): R_f = 0.38. **¹H NMR (CD_3OD , 600 MHz, 27 °C):** δ = 7.80–7.75 (m, 2H, ArH), 7.70–7.64 (m, 2H, ArH), 7.29–7.23 (m, 2H, ArH), 6.80 (s, 1H, ArH), 6.79–6.75 (m, 2H, ArH), 6.60 (s, 1H, ArH), 4.75–4.62 (m, 2H, CH_2), 4.15–3.88 (m, 2H, CH_2), 3.84–3.76 (m, 2H, CH_2), 3.48 (q, J = 7.1 Hz, 4H, 2 x CH_2), 2.97–2.89 (m, 2H, CH_2), 2.81–2.71 (m, 2H, CH_2), 1.81–1.68 (m, 2H, CH_2), 1.21 (t, J = 7.5 Hz, 6H, 2 x CH_3) ppm. **¹³C NMR (CD_3OD , 150 MHz, 27 °C):** δ = 179.8, 151.7, 150.2, 143.9, 142.8, 142.3, 141.0, 132.7, 129.2, 127.4, 124.8, 121.7, 117.0, 116.8, 110.7, 53.8, 52.7, 46.6, 44.2, 34.8, 33.3, 27.4, 11.5 ppm. **IR (neat, ATR):** $\tilde{\nu}$ = 3205 (w), 2973 (m), 2929 (m), 1599 (vs), 1517 (s), 1449 (m), 1422 (m), 1397 (m), 1354 (m), 1314 (m), 1293 (m), 1272 (m), 1194 (m), 1141 (s), 1096 (m), 1077 (m), 1012 (w), 942 (w), 908 (w), 850 (w), 823 (m), 767 (w), 732 (w) cm^{-1} . **HRMS (ESI⁺):** m/z calcd. for $[\text{C}_{29}\text{H}_{36}\text{O}_2\text{N}_5\text{S}]^+$: 518.2590, found: 518.2579 ($[\text{M}+\text{H}]^+$). **UV/Vis:** λ_{max} = 430 nm.

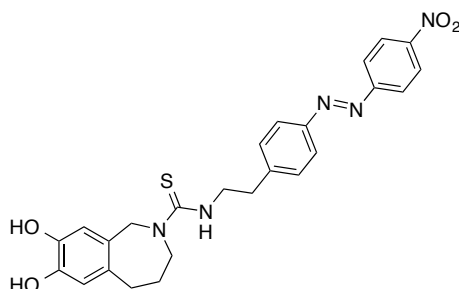
Synthesis of 7,8-dihydroxy-*N*-(4-((4-(trifluoromethyl)phenyl)diazenyl)phenethyl)-4,5-dihydro-1*H*-benzo[*c*]azepine-2(3*H*)-carbothioamide (AC4)



The HBr salt **7** (52 mg, 0.20 mmol, 1.1 equiv.) was suspended in THF (6 mL) and TEA (62 μ L, 0.45 mmol, 2.5 equiv.) was added. A solution of isothiocyanate **5** (60 mg, 0.18 mmol, 1.0 equiv.) in THF (4 mL) was added and the reaction mixture was stirred for 2.5 d. The solution was concentrated *in vacuo* and the crude product was purified by flash silica gel column chromatography (CHCl₃/MeOH, gradient from 100:0 to 50:1), affording thiourea **AC4** (80 mg, 0.16 mmol, 89%) as an orange solid.

TLC (CHCl₃/MeOH, 20:1): R_f = 0.38. **M.p.:** 181–182 °C. **¹H NMR (CD₃OD, 400 MHz, 27 °C):** δ = 8.05–7.97 (m, 2H, ArH), 7.87–7.79 (m, 4H, ArH), 7.36–7.30 (m, 2H, ArH), 6.83 (s, 1H, ArH), 6.60 (s, 1H, ArH), 4.75–4.61 (m, 2H, CH₂), 4.17–3.90 (m, 2H, CH₂), 3.87–3.78 (m, 2H, CH₂), 3.03–2.93 (m, 2H, CH₂), 2.94 (t, J = 7.4 Hz, 2H, CH₂), 2.79–2.72 (m, 2H, CH₂), 1.78–1.68 (m, 2H, CH₂) ppm. **¹³C NMR (CD₃OD, 100 MHz, 27 °C):** δ = 179.8, 154.4 (m), 150.9, 144.3, 144.0, 142.4, 132.7, 131.6 (q, J = 32.3 Hz), 129.5, 129.1 (*cis* isomer), 127.3, 126.0 (q, J = 3.8 Hz), 124.1 (q, J = 270.0 Hz), 122.9, 122.7, 120.8 (*cis* isomer), 120.2 (*cis* isomer), 117.0, 116.8, 53.8, 52.9, 46.3, 34.9, 33.4, 27.4 ppm. **¹⁹F NMR (CD₃OD, 151 MHz, 27 °C):** δ = –64.1 ppm. **IR (neat, ATR):** $\tilde{\nu}$ = 3222 (m), 2939 (w), 1606 (m), 1542 (m), 1520 (m), 1453 (w), 1408 (w), 1385 (w), 1322 (vs), 1297 (m), 1264 (m), 1243 (m), 1212 (m), 1162 (s), 1126 (s), 1101 (m), 1064 (s), 1013 (m), 938 (w), 907 (s), 852 (m), 732 (vs), 668 (w) cm⁻¹. **HRMS (ESI⁺):** m/z calcd. for [C₂₆H₂₆O₂N₄F₃S]⁺: 515.1729, found: 515.1716 ([M+H]⁺). **UV/Vis:** λ_{max} = 334, 437 nm.

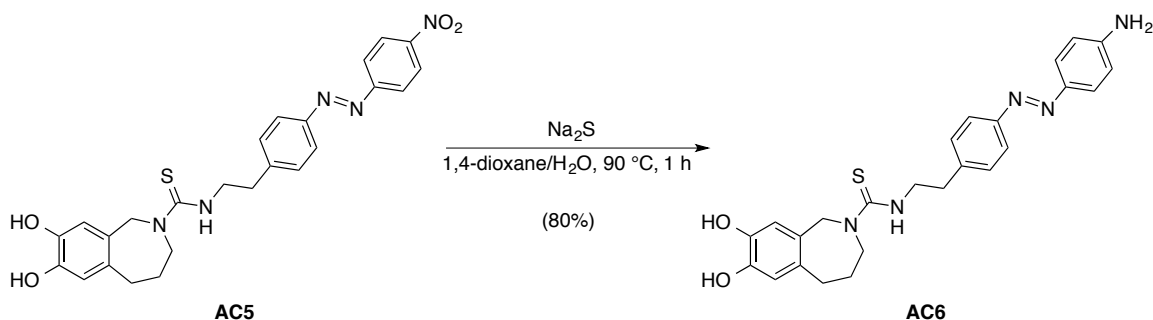
Synthesis of 7,8-dihydroxy-N-(4-((4-nitrophenyl)diazenyl)phenethyl)-4,5-dihydro-1H-benzo-[c]azepine-2(3H)-carbothioamide (AC5)



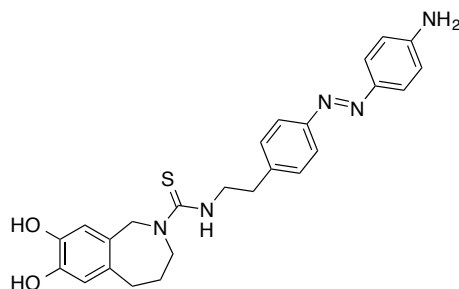
The HBr salt **7** (200 mg, 0.770 mmol, 1.1 equiv.) was suspended in THF (40 mL) and TEA (0.24 mL, 1.8 mmol, 2.5 equiv.) was added. Isothiocyanate **19d** (219 mg, 0.700 mmol, 1.0 equiv.) was added and the reaction mixture was stirred for 16 h. The solution was concentrated *in vacuo* and the crude product was purified by flash silica gel column chromatography (CHCl₃/MeOH, gradient from 100:0 to 50:1), yielding thiourea **AC5** (302 mg, 0.610 mmol, 87%) as an orange solid.

TLC (CHCl₃/MeOH, 20:1): R_f = 0.42. **M.p.:** 195–197 °C. **¹H NMR (Acetone-d₆, 400 MHz, 27 °C):** δ = 8.47–8.40 (m, 2H, ArH), 8.14–8.07 (m, 2H, ArH), 7.93–7.87 (m, 2H, ArH), 7.65 (br s, 2H, 2 x OH), 7.46–7.39 (m, 2H, ArH), 6.91 (s, 1H, ArH), 6.82 (t, J = 5.6 Hz, 1H, NH), 6.67 (s, 1H, ArH), 4.74 (s, 2H, CH₂), 4.12 (br s, 2H, CH₂), 3.92–3.81 (m, 2H, CH₂), 3.07–2.99 (m, 2H, CH₂), 2.80–2.77 (m, 2H, CH₂), 1.80–1.70 (m, 2H, CH₂) ppm. **¹³C NMR (Acetone-d₆, 100 MHz, 27 °C):** δ = 181.1, 155.8, 151.0, 148.8, 145.4, 143.9, 142.4, 133.1, 129.9, 128.2, 124.8, 123.3, 123.3, 117.2, 117.0, 53.5, 53.1, 46.5, 35.1, 33.7, 27.6 ppm. **IR (neat, ATR):** $\tilde{\nu}$ = 3480 (w), 3306 (m), 1700 (w), 1598 (m), 1522 (vs), 1448 (m), 1402 (w), 1344 (s), 1288 (s), 1264 (m), 1232 (m), 1192 (m), 1173 (m), 1153 (m), 1134 (m), 1097 (m), 1013 (w), 969 (m), 944 (m), 886 (m), 860 (s), 852 (m), 797 (m), 767 (m), 755 (m), 726 (w), 688 (m), 649 (w) cm⁻¹. **HRMS (ESI⁺):** *m/z* calcd. for [C₂₅H₂₆O₄N₅S]⁺: 492.1706, found: 492.1694 ([M+H]⁺). **UV/Vis:** λ_{max} = 354, 456 nm.

Synthesis of AC6



Scheme 3.6. Synthesis of AC6.

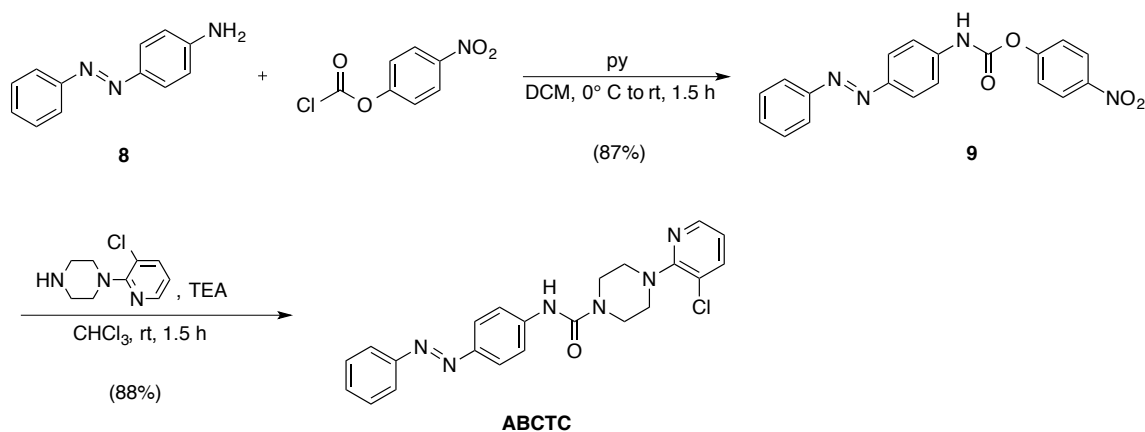
 Synthesis of *N*-(4-((4-aminophenyl)diazenyl)phenethyl)-7,8-dihydroxy-4,5-dihydro-1*H*-benzo[*c*]azepine-2(3*H*)-carbothioamide (AC6)


AC5 (40 mg, 0.081 mmol, 1.0 equiv.) was dissolved in 1,4-dioxane (5 mL) and H₂O (0.5 mL). Sodium sulfide (19 mg, 0.24 mmol, 3.0 equiv.) was added and the reaction mixture was heated to 90 °C for 1 h. A sat. aq. solution of NaHCO₃ (20 mL) was added and the phases were separated. The aqueous phase was extracted with CHCl₃ (3 x 10 mL) and the combined organic layers were washed with brine (30 mL), dried over MgSO₄ and concentrated *in vacuo*. The crude product was purified by flash silica gel column chromatography (CHCl₃/MeOH, gradient from 100:0 to 30:1), yielding aniline AC6 (30 mg, 0.065 mmol, 80%) as an orange solid.

TLC (CHCl₃/MeOH, 20:1): *R_f* = 0.40. **M.p.:** 152–154 °C. **¹H NMR** (CD₃OD, 400 MHz, 27 °C): δ = 7.71–7.64 (m, 4H, ArH), 7.28–7.22 (m, 2H, ArH), 6.80 (s, 1H, ArH), 6.75–6.69 (m, 2H, ArH), 6.59 (s, 1H, ArH), 4.68 (s, 2H, CH₂), 4.02 (br s, 2H, CH₂), 3.82–3.76 (m, 2H, CH₂), 2.96–2.89 (m, 2H, CH₂), 2.78–2.72 (m, 2H, CH₂), 1.77–1.69 (m, 2H, CH₂) ppm. **¹³C NMR** (CD₃OD, 100 MHz, 27 °C): δ = 179.8, 151.9, 151.5, 144.3, 143.9, 142.3, 141.3, 132.7, 129.2, 127.4, 124.6, 121.8, 117.0, 116.8, 113.8, 53.8, 52.7, 46.5, 34.8, 33.3, 27.4 ppm. **IR** (neat, ATR): $\tilde{\nu}$ = 3335 (m), 3210 (w), 2970 (w), 2930 (w), 1598 (s), 1506 (m), 1427 (m), 1402 (m), 1381 (m), 1336 (m), 1291 (s), 1234 (m), 1214 (m), 1139 (s), 1097 (m), 1042 (m), 1066 (w),

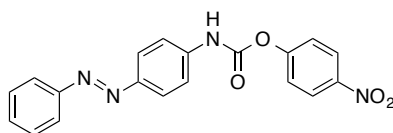
1013 (w), 974 (w), 941 (w), 904 (w), 880 (w), 836 (m), 747 (vs), 665 (m), 644 (m) cm^{-1} . **HRMS (ESI⁺):** m/z calcd. for $[\text{C}_{25}\text{H}_{28}\text{O}_2\text{N}_5\text{S}]^+$: 462.1964, found: 462.1952 ($[\text{M}+\text{H}]^+$). **UV/Vis:** $\lambda_{\text{max}} = 407 \text{ nm}$.

Synthesis of ABCTC



Scheme 3.7. Synthesis of **ABCTC**.

Synthesis of 4-nitrophenyl (4-(phenyldiazenyl)phenyl)carbamate (**9**)

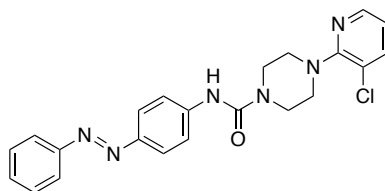


4-Aminoazobenzene (**8**; 250 mg, 1.27 mmol, 1.1 equiv.) was dissolved in DCM (4 mL) and pyridine (1 mL). 4-Nitrophenyl chloroformate (232 mg, 1.15 mmol, 1.0 equiv.) was added at 0 °C. Immediately, precipitate was formed and more DCM (4 mL) was added. The slurry was warmed to room temperature and stirred for 1.5 h. The mixture was diluted with DCM (20 mL) and washed with 0.6 M HCl, 0.02 M HCl, H₂O, and sat. aqu. NaHCO₃ (20 mL each). The organic layer was dried over MgSO₄ and concentrated *in vacuo*. Carbamate **9** (361 mg, 1.00 mmol, 87%) was obtained sufficiently pure for the next step as an orange solid.

TLC (DCM/MeOH/HOAc/H₂O, 90:10:0.6:0.6): $R_f = 0.91$. **M.p.:** 168–169 °C. **¹H NMR (CDCl₃, 600 MHz, 27 °C):** $\delta = 8.33\text{--}8.28$ (m, 2H, ArH), 7.98–7.95 (m, 2H, ArH), 7.93–7.87 (m, 2H, ArH), 7.65–7.58 (m, 2H, ArH), 7.53–7.49 (m, 2H, ArH), 7.49–7.45 (m, 1H, ArH), 7.44–7.39 (m, 2H, ArH), 7.17 (br s, 1H, NH) ppm. **¹³C NMR (CDCl₃, 150 MHz, 27 °C):** $\delta = 155.1, 152.6, 149.8, 149.2, 145.2, 139.0, 130.9, 129.1, 128.9, 125.3, 125.1, 124.2, 122.8,$

122.3, 122.1, 118.9 ppm.^[y] **IR (neat, ATR):** $\tilde{\nu}$ = 3326 (m), 1729 (s), 1601 (m), 1518 (vs), 1488 (m), 1438 (m), 1409 (m), 1342 (m), 1325 (m), 1305 (m), 1197 (vs), 1155 (m), 1108 (m), 840 (w), 857 (m), 841 (s), 769 (m), 749 (m), 719 (w), 687 (m) cm⁻¹. **HRMS (EI⁺):** *m/z* calcd. for [C₁₉H₁₄N₄O₄]⁺: 362.1015, found: 362.1008 ([M]⁺).

Synthesis of 4-(3-chloropyridin-2-yl)-N-(4-(phenyldiazenyl)phenyl)piperazine-1-carboxamide (ABCTC)



Carbamate **9** (200 mg, 0.550 mmol, 1.05 equiv.) and 1-(3-chloropyridin-2-yl)piperazine (103 mg, 0.520 mmol, 1.0 equiv.) were dissolved in CHCl₃ (1 mL) and TEA (0.08 mL, 0.6 mmol, 1.1 equiv) was added at room temperature. The reaction mixture was stirred for 1.5 h and then diluted with CHCl₃ (10 mL) and washed with 2 M K₂CO₃ (2 x 20 mL). The combined aqueous phases were extracted with CHCl₃ (10 mL) and the organic phase was washed with brine (20 mL), dried over MgSO₄ and concentrated *in vacuo*. The crude product was purified by flash silica gel column chromatography (DCM/MeOH, 100:0 → 10:1), yielding **ABCTC** (192 mg, 0.460 mmol, 88%) as an orange solid.

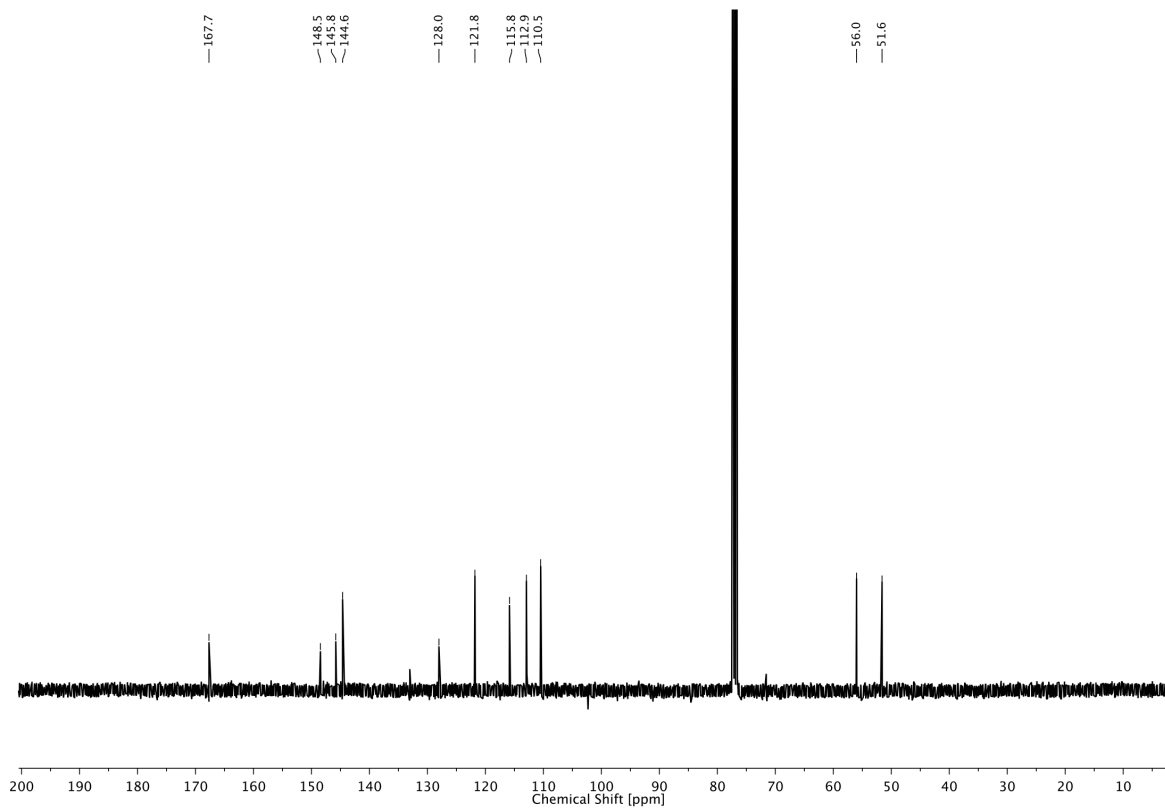
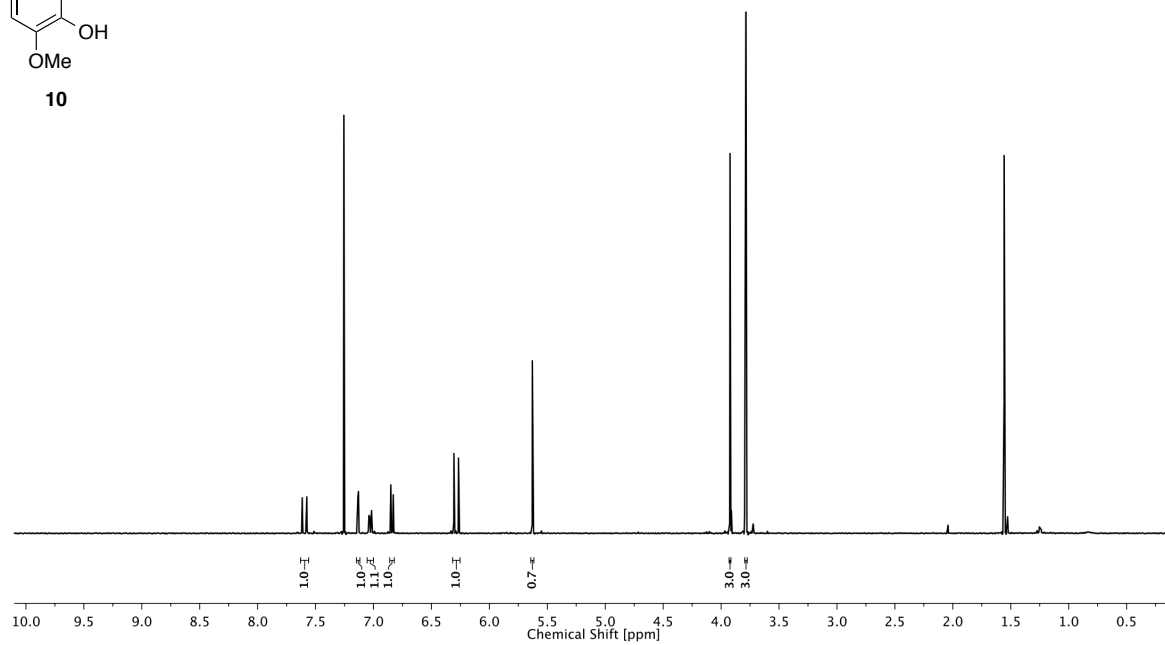
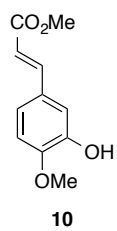
TLC (DCM/MeOH, 10:1): R_f = 0.38. **M.p.:** 176–178 °C. **¹H NMR (CDCl₃, 600 MHz, 27 °C):** δ = 8.19 (dd, *J* = 4.8, 1.2 Hz, 1H, ArH), 7.93–7.86 (m, 4H, ArH), 7.61 (dd, *J* = 7.8, 1.2 Hz, 1H, ArH), 7.56–7.53 (m, 2H, ArH), 7.51–7.47 (m, 2H, ArH), 7.45–7.43 (m, 1H, ArH), 6.88 (dd, *J* = 7.8, 4.8 Hz, 1H, ArH), 6.60 (br s, 1H, NH), 3.71–3.68 (m, 4H, 2 x CH₂), 3.46–3.42 (m, 4H, 2 x CH₂) ppm. **¹³C NMR (CDCl₃, 150 MHz, 27 °C):** δ = 157.9, 154.5, 152.7, 148.3, 145.9, 141.7, 138.9, 130.5, 129.0, 124.0, 122.8, 122.6, 119.4, 119.3, 118.5, 48.7, 44.1 ppm.^[z] **IR (neat, ATR):** $\tilde{\nu}$ = 3308 (w), 3059 (w), 2998 (w), 2893 (w), 2851 (w), 1641 (m), 1592 (m), 1578 (m), 1526 (m), 1505 (m), 1461 (m), 1434 (s), 1414 (s), 1380 (m), 1337 (m), 1300 (m), 1288 (m), 1231 (vs), 1152 (m), 1142 (m), 1123 (m), 1071 (w), 1032 (m), 1019 (w), 995 (m), 937 (m),

^[y] Due to *trans/cis* isomerization, more signals than expected were observed in the ¹³C NMR spectrum.

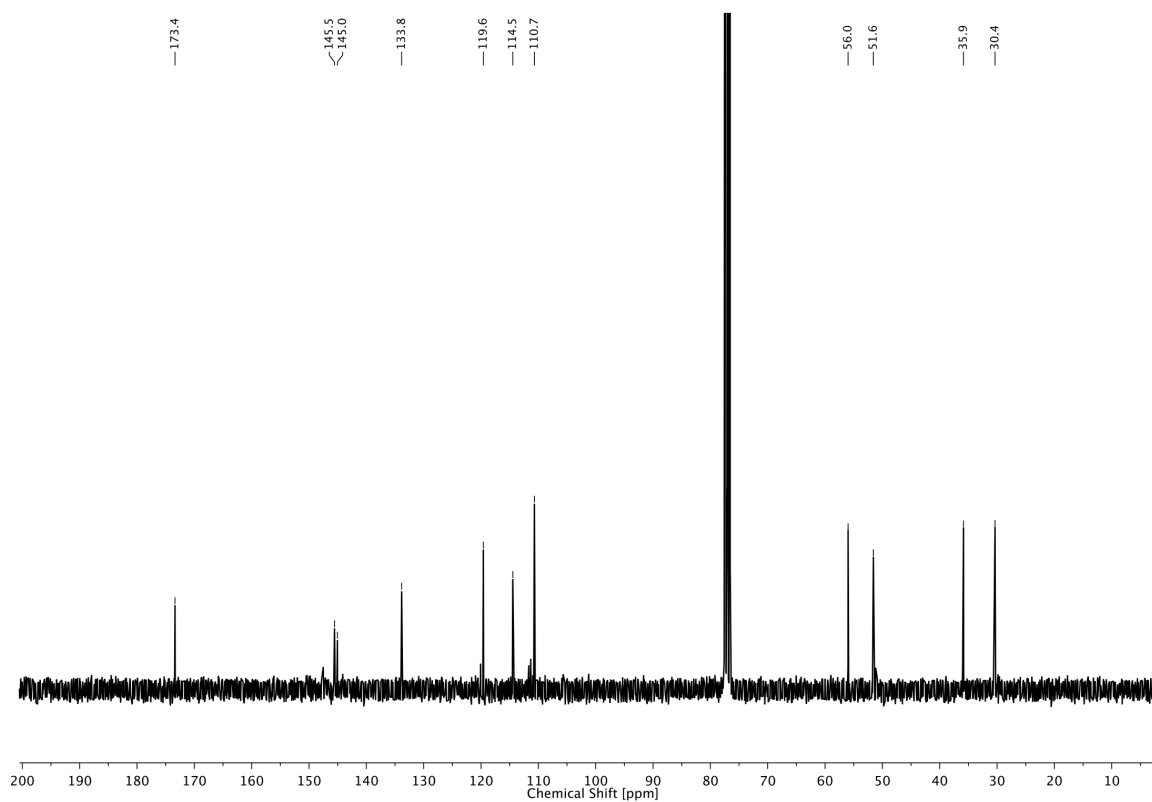
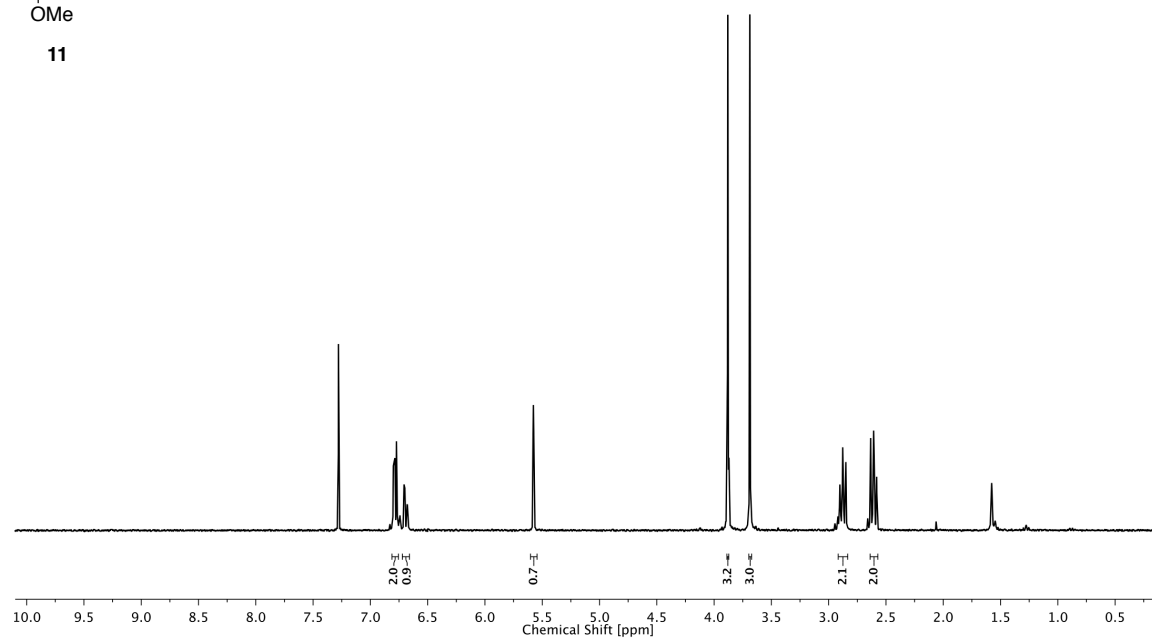
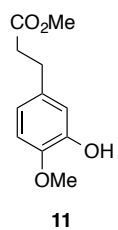
^[z] Due to *trans/cis* isomerization, more signals than expected were observed in the ¹³C NMR spectrum.

842 (m), 789 (w), 753 (s), 722 (w), 688 (m), 666 (w) cm^{-1} . **HRMS (ESI⁺):** m/z calcd. for $[\text{C}_{22}\text{H}_{22}\text{ON}_6\text{Cl}]^+$: 421.1544, found: 421.1540 ($[\text{M}+\text{H}]^+$). **UV/Vis:** $\lambda_{\text{max}} = 370, 446 \text{ nm}$.

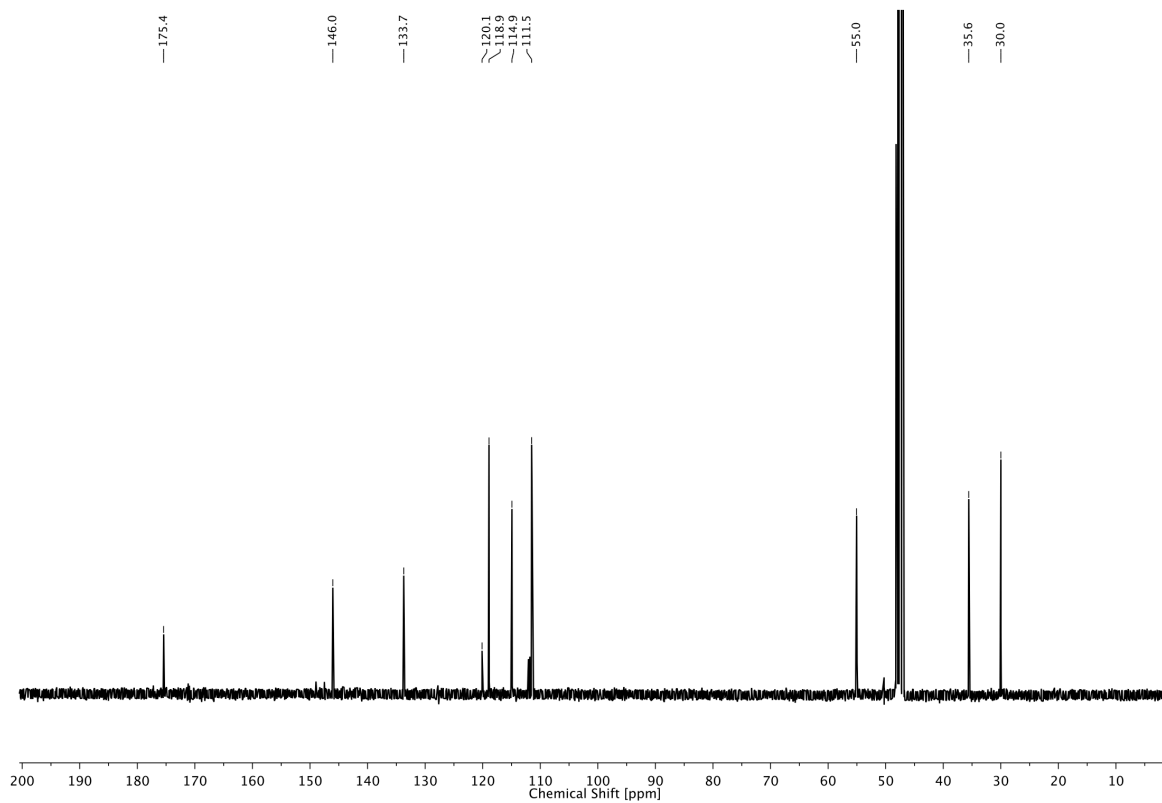
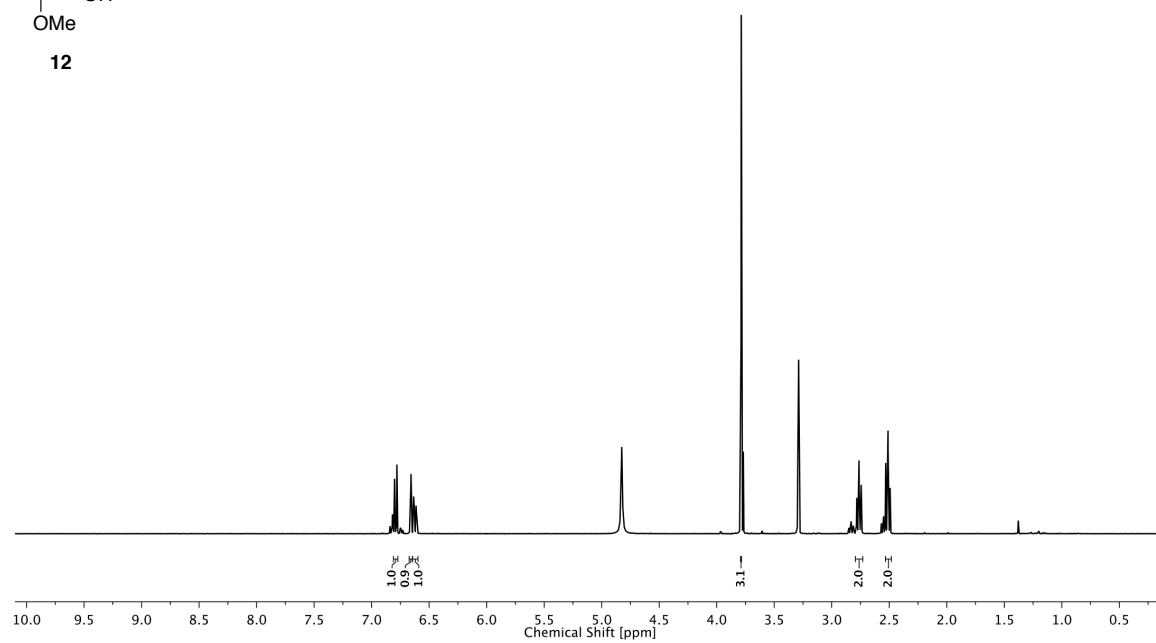
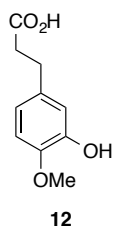
NMR Spectra



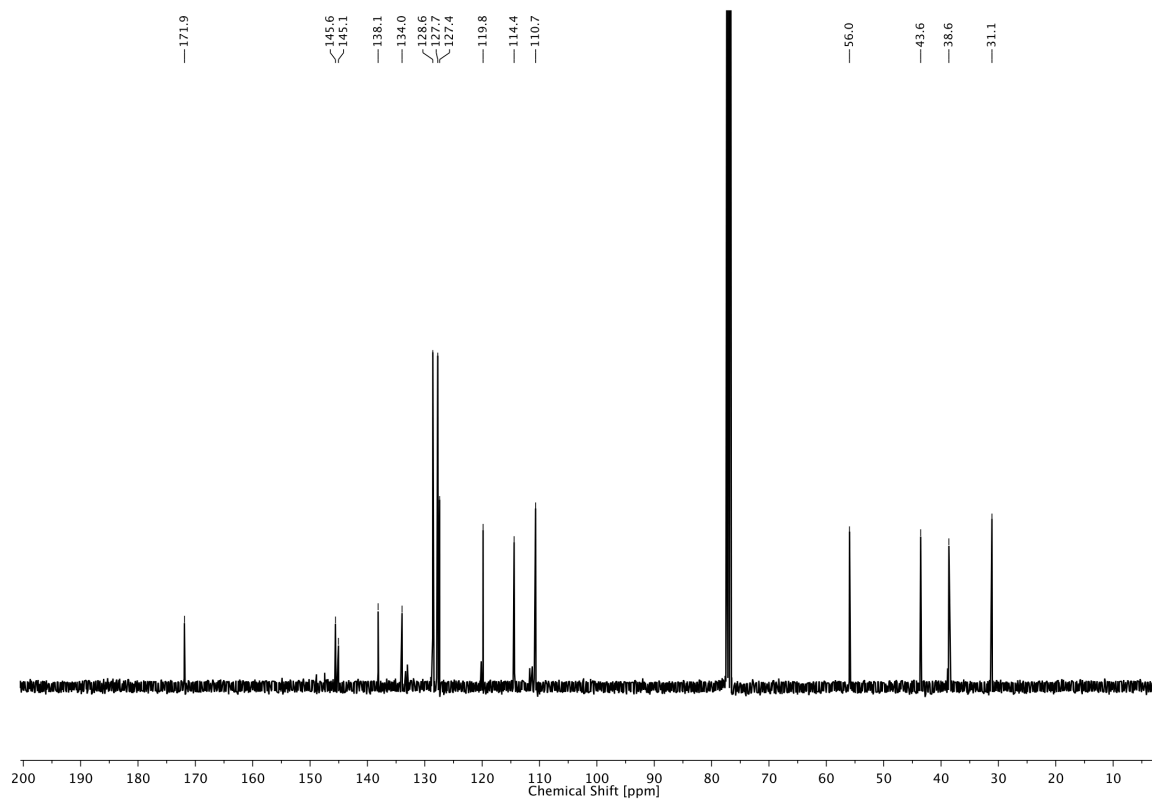
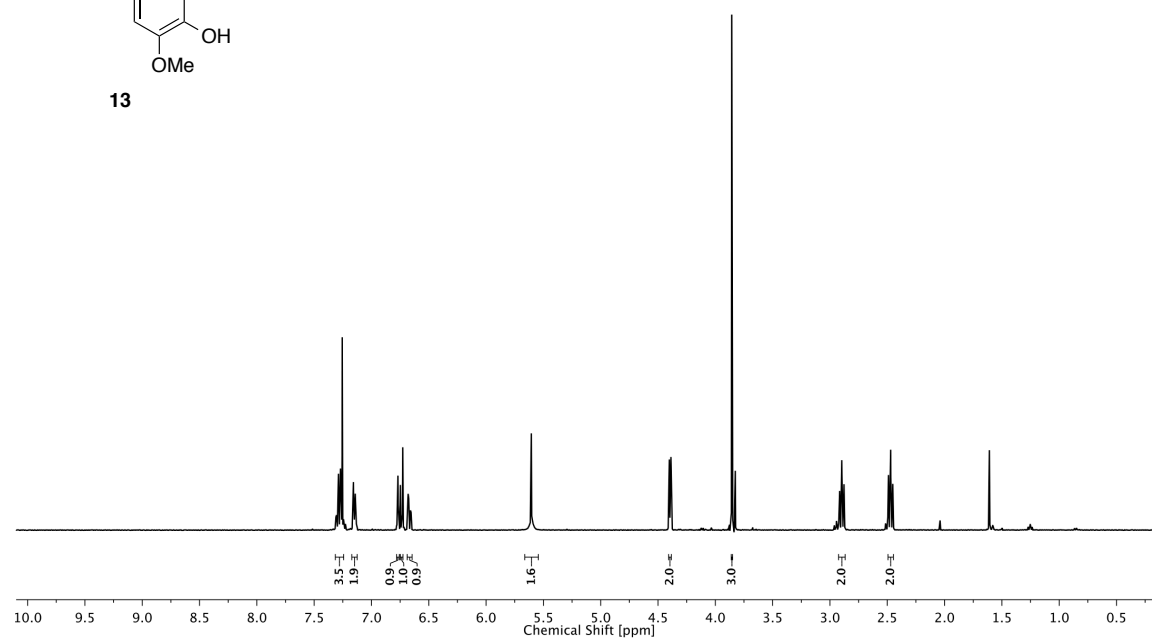
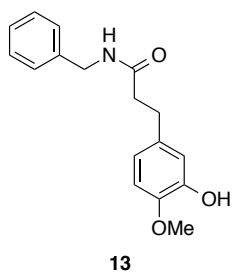
3 PHOTOCONTROL OF TRP CHANNELS



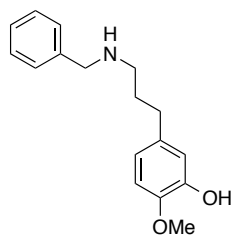
3 PHOTOCONTROL OF TRP CHANNELS



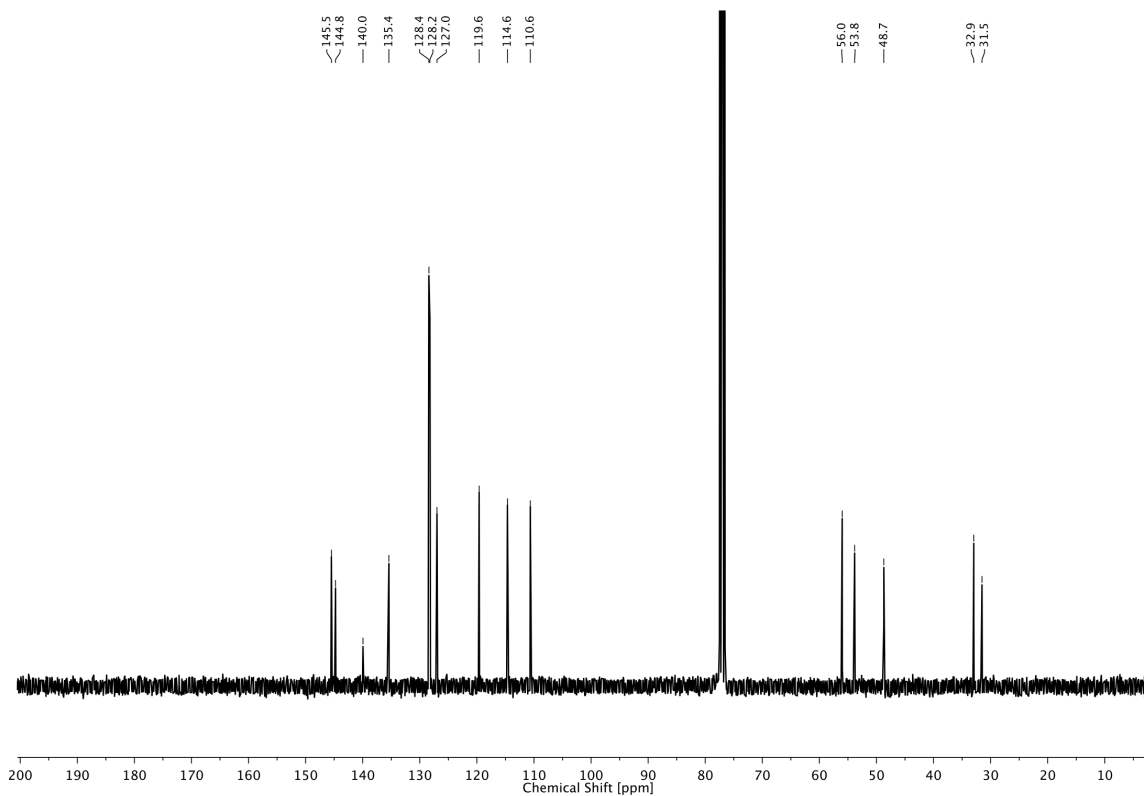
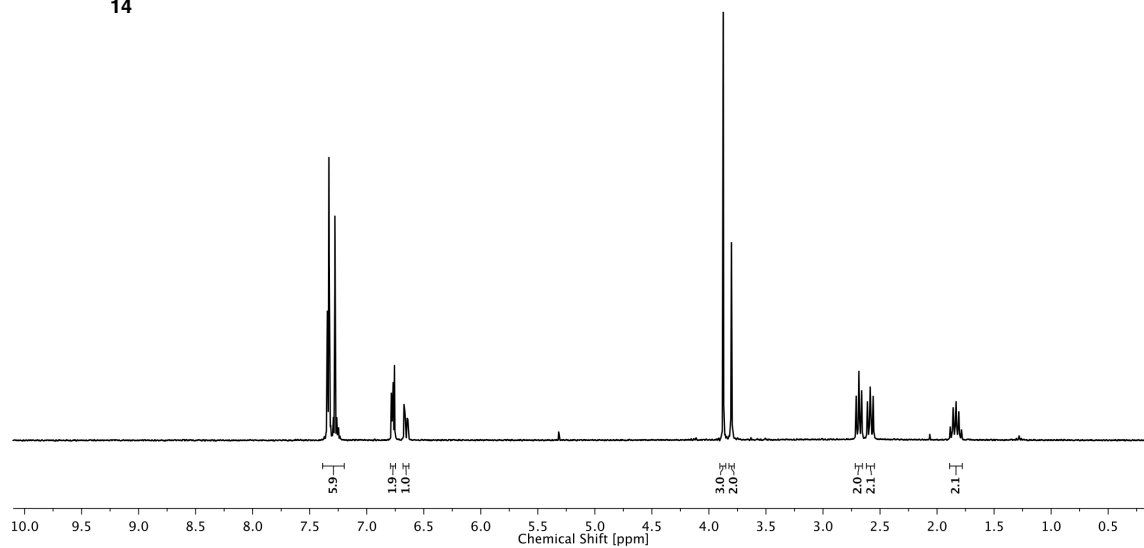
3 PHOTOCONTROL OF TRP CHANNELS



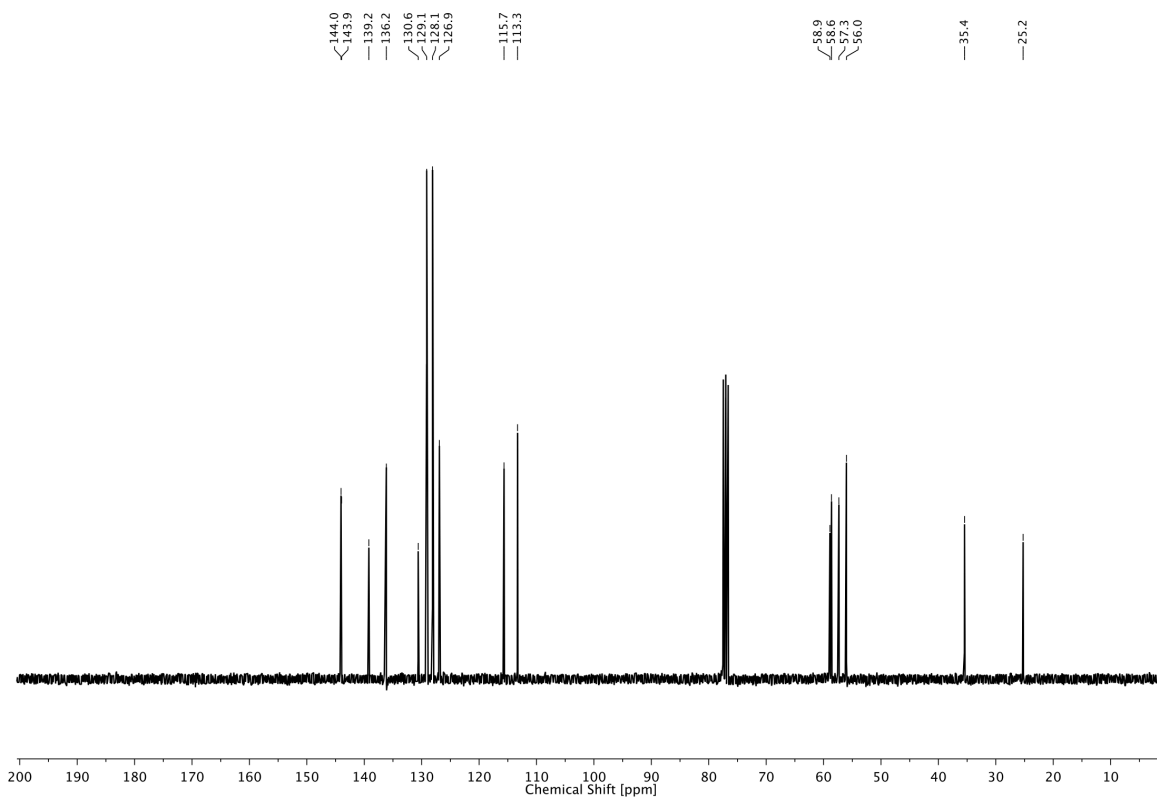
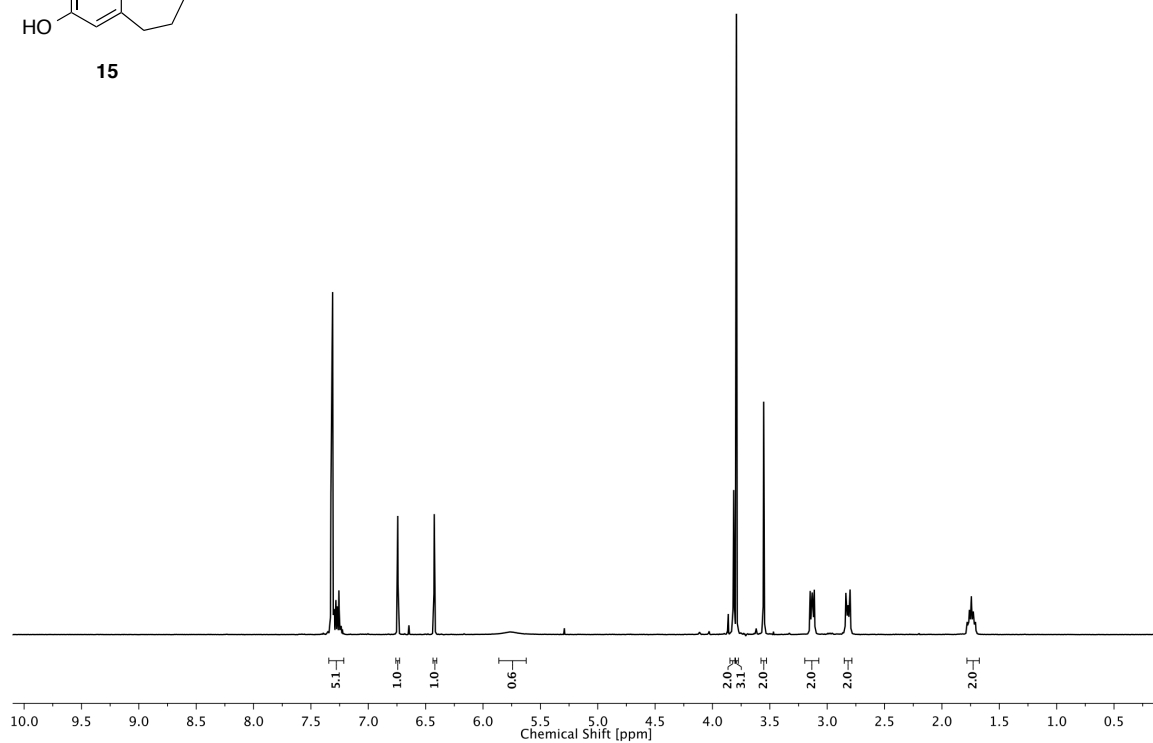
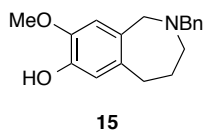
3 PHOTOCONTROL OF TRP CHANNELS



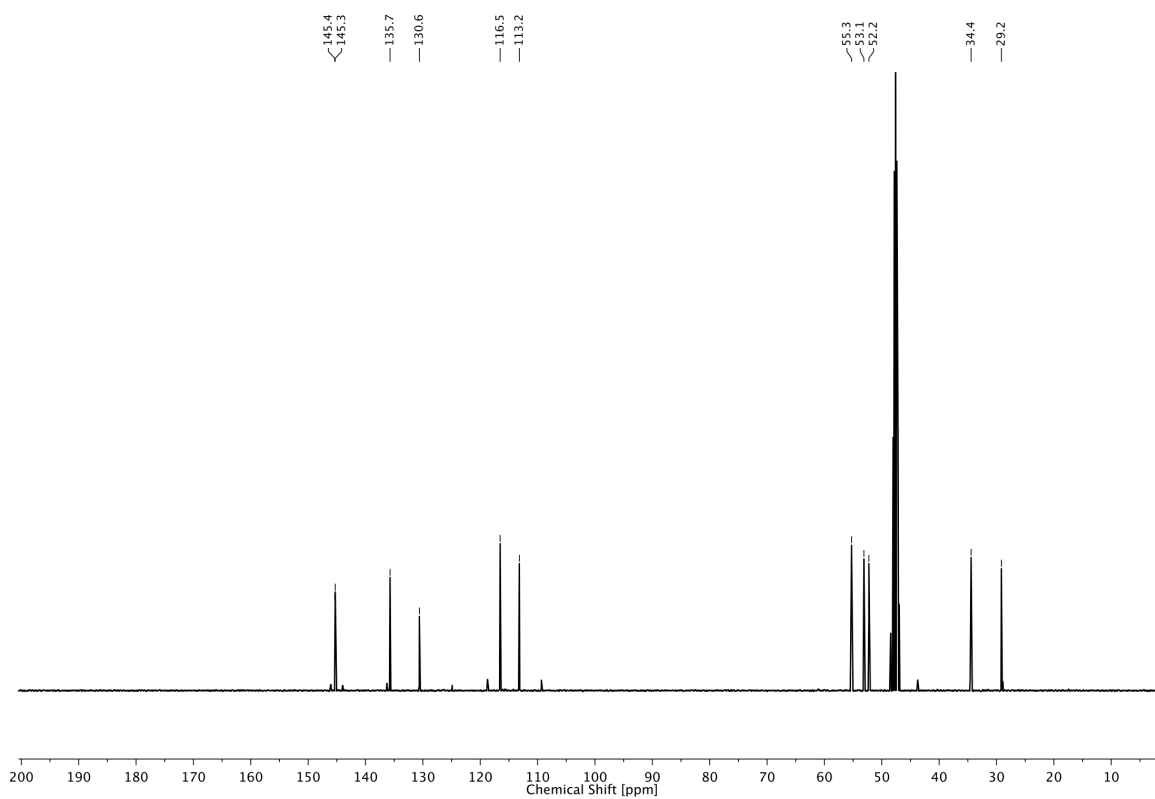
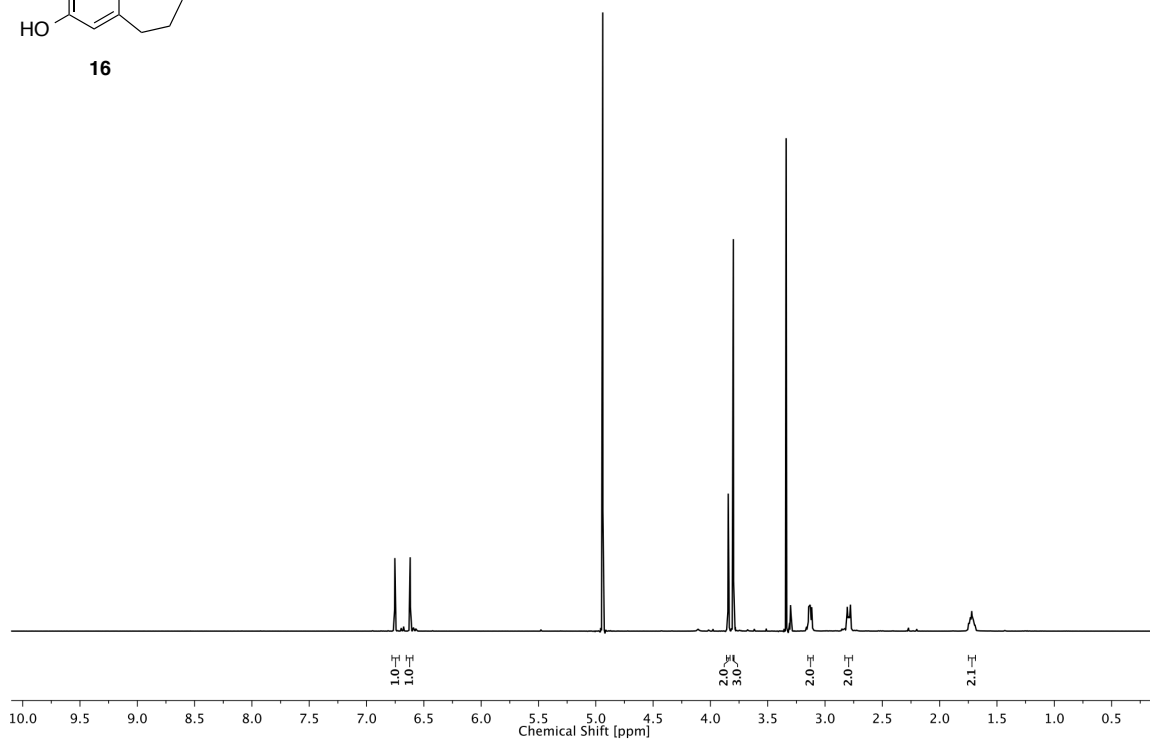
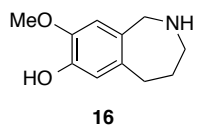
14



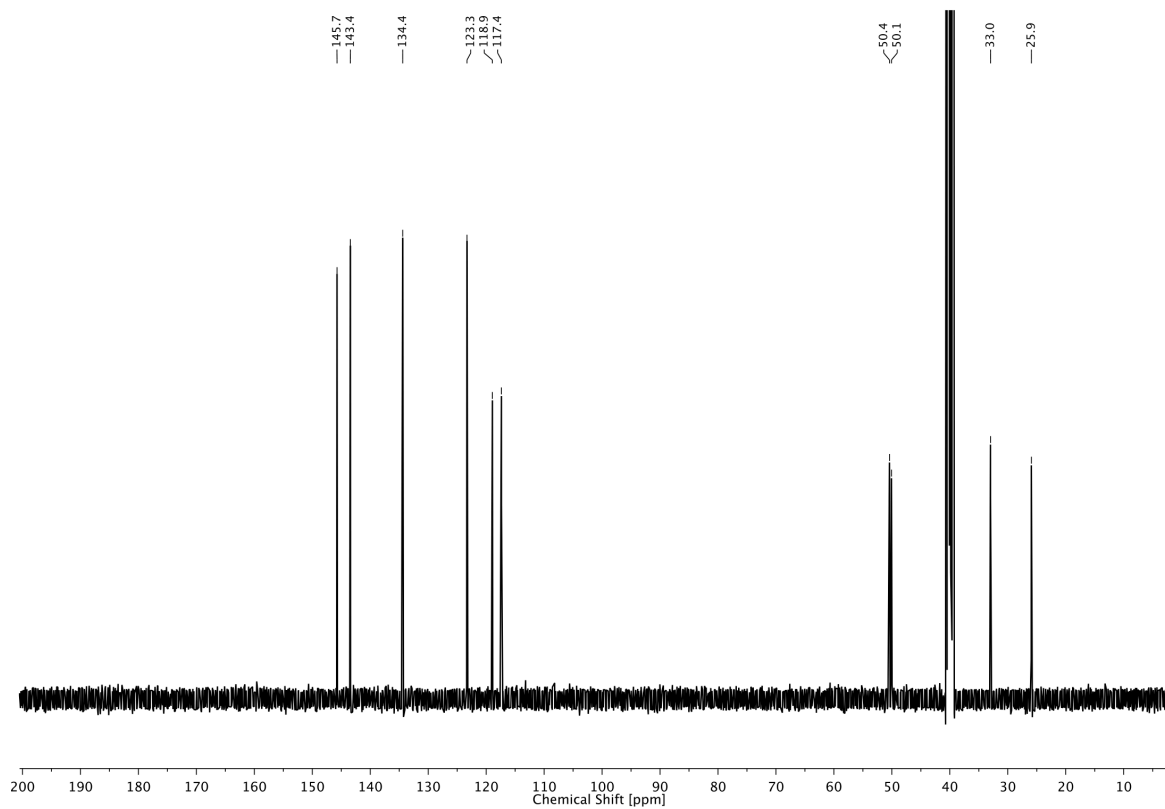
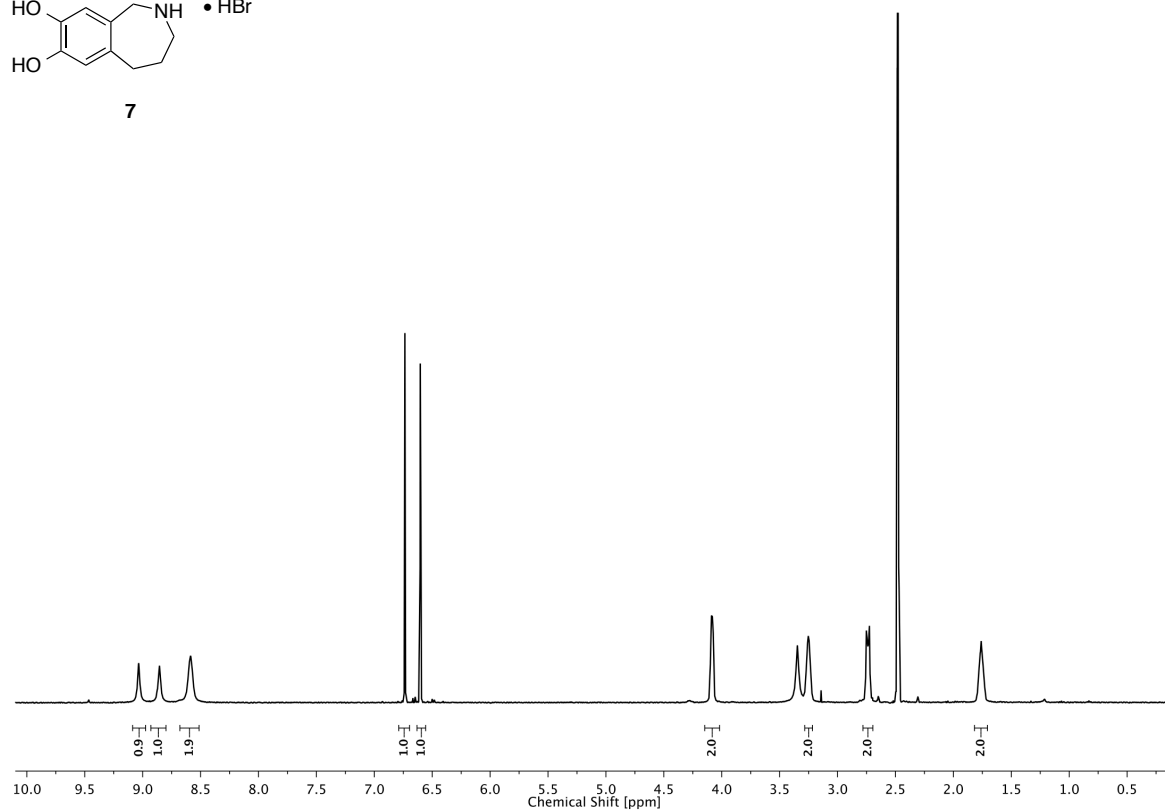
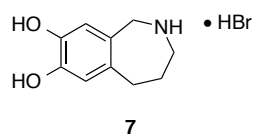
3 PHOTOCONTROL OF TRP CHANNELS



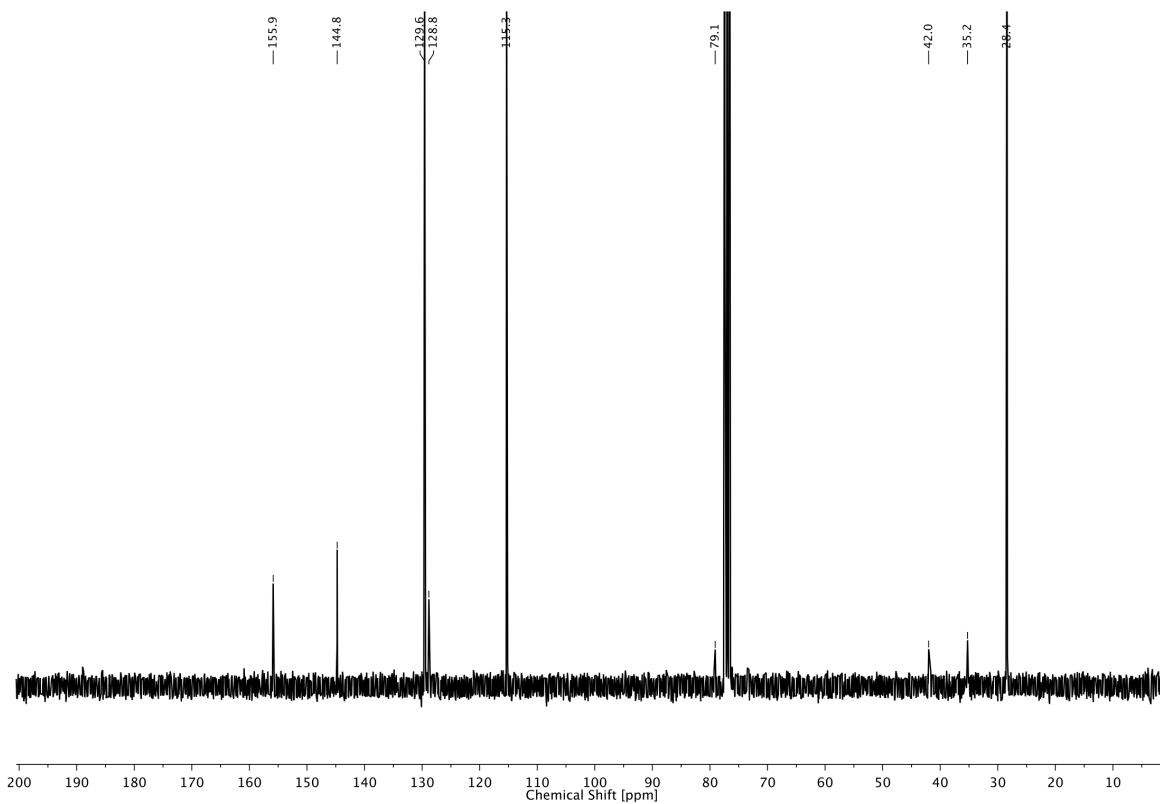
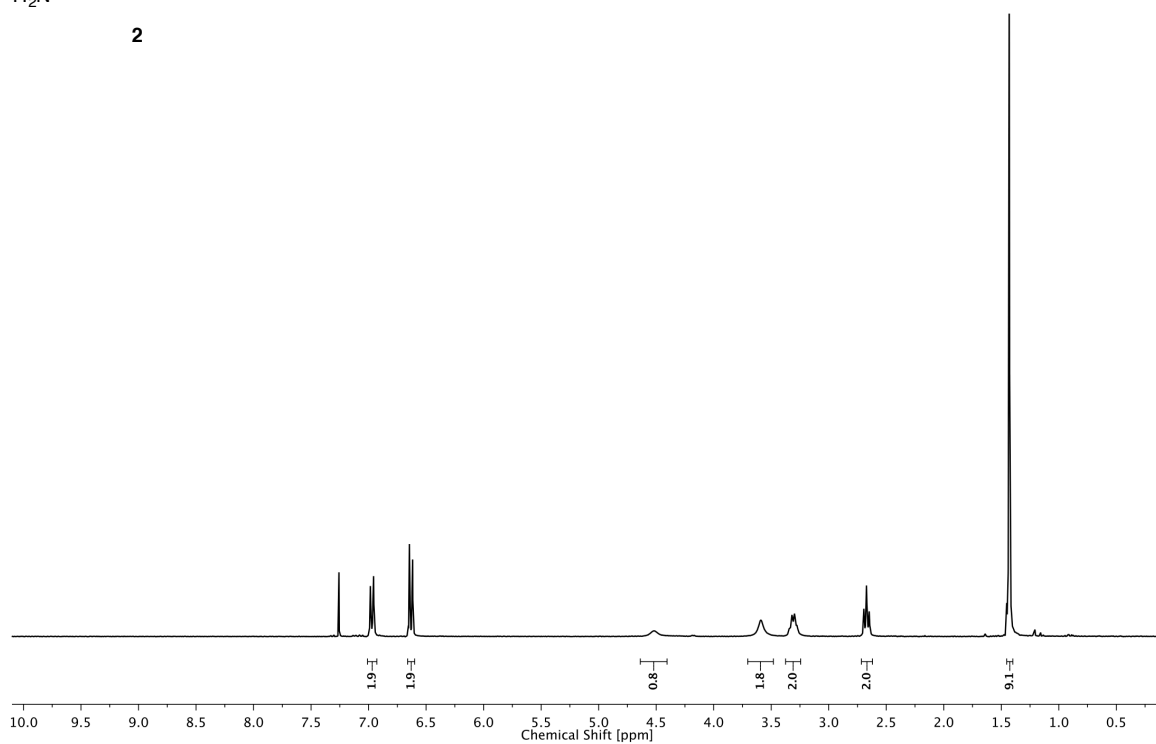
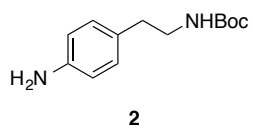
3 PHOTOCONTROL OF TRP CHANNELS



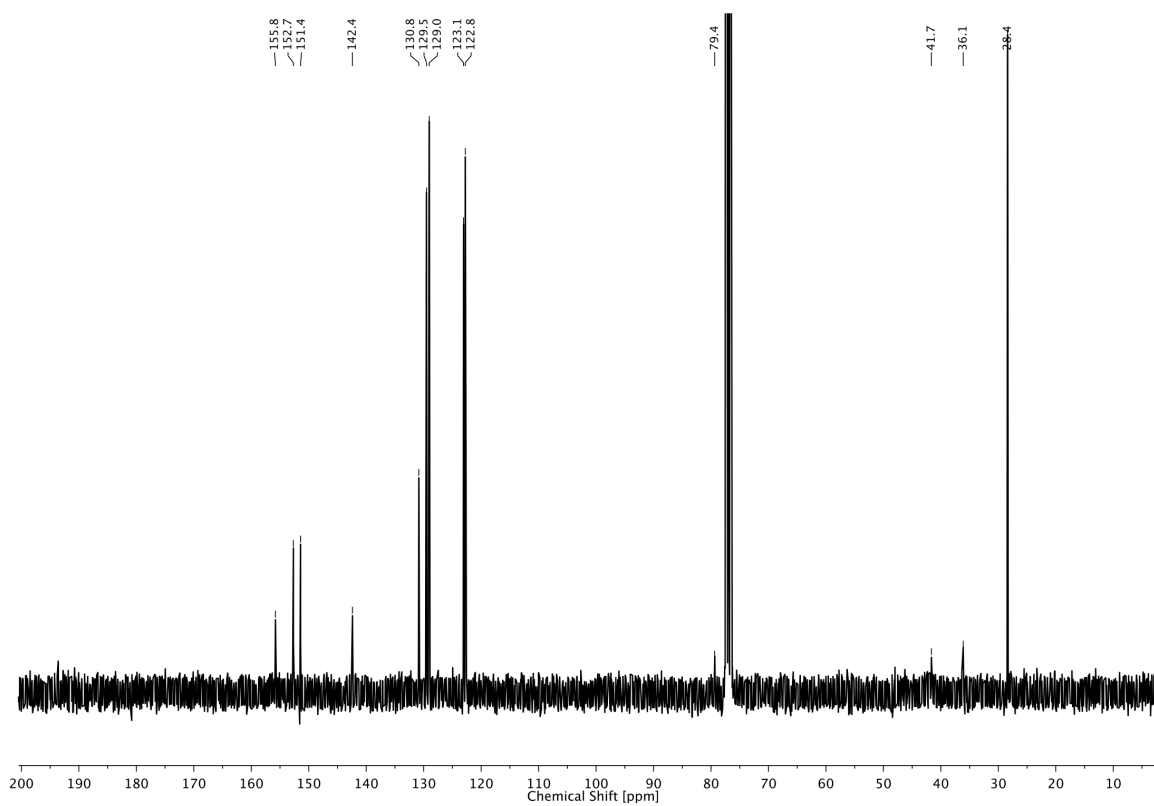
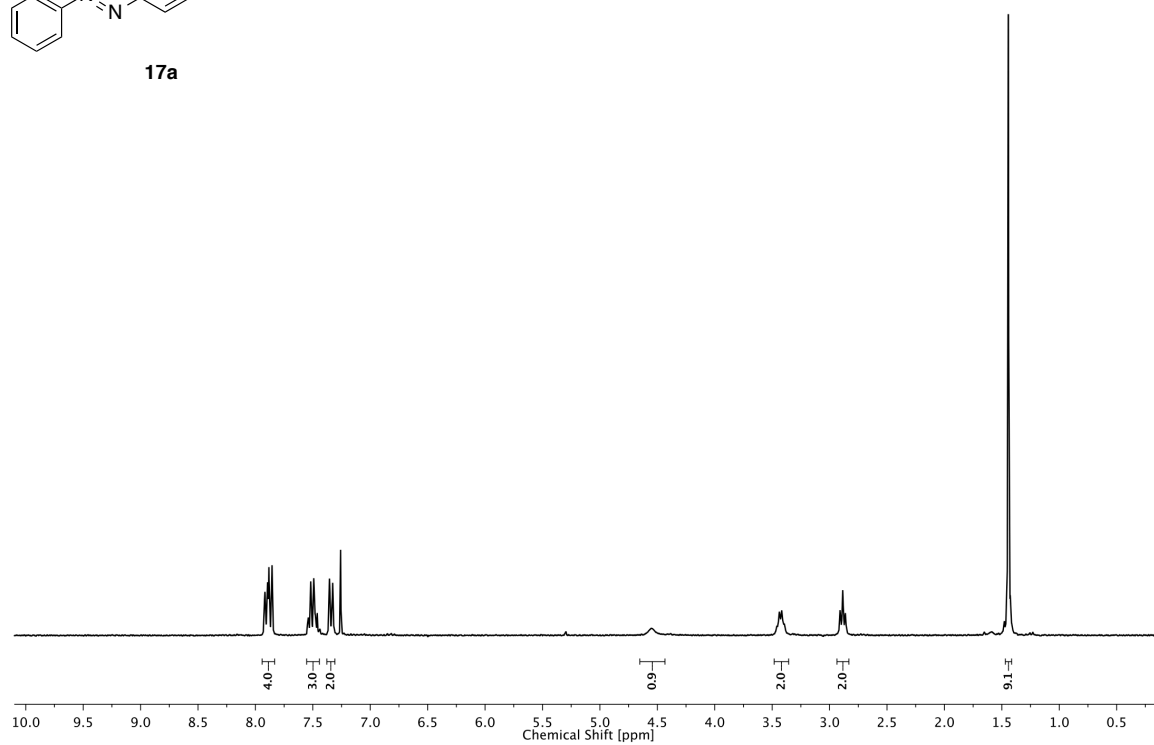
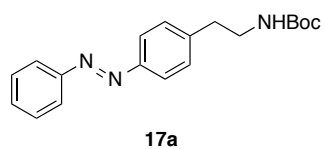
3 PHOTOCONTROL OF TRP CHANNELS



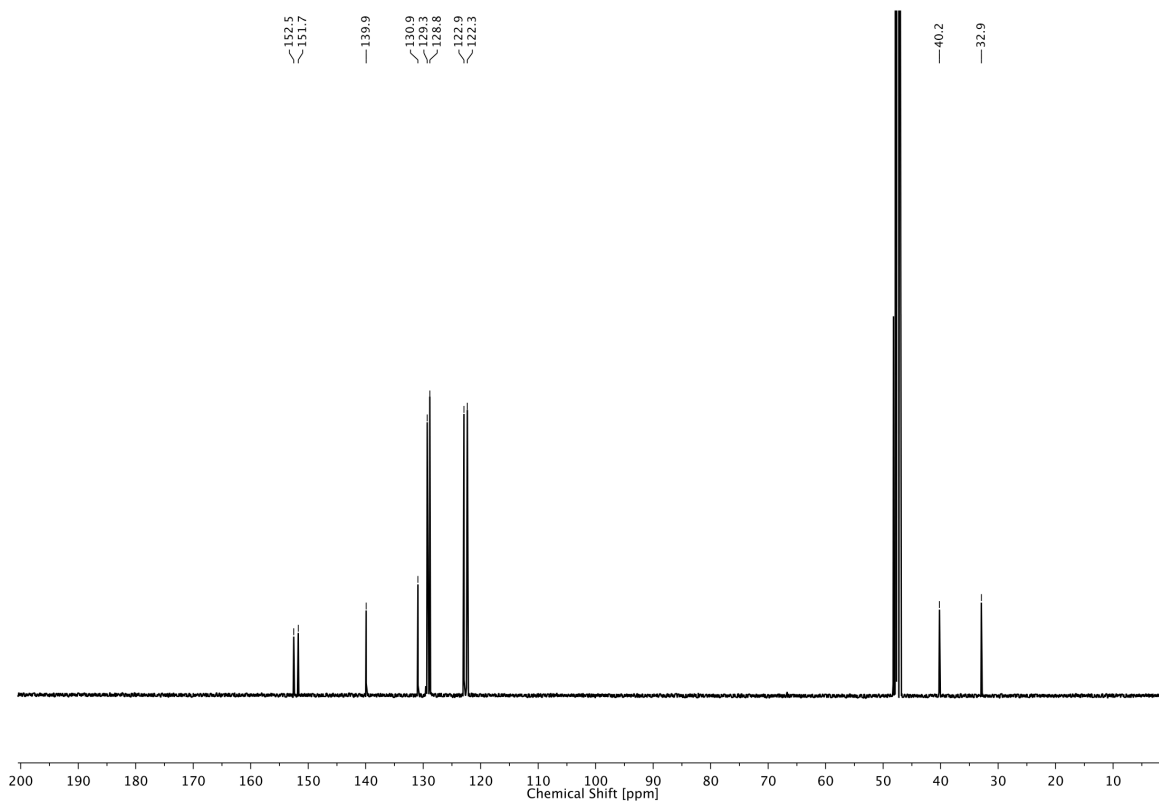
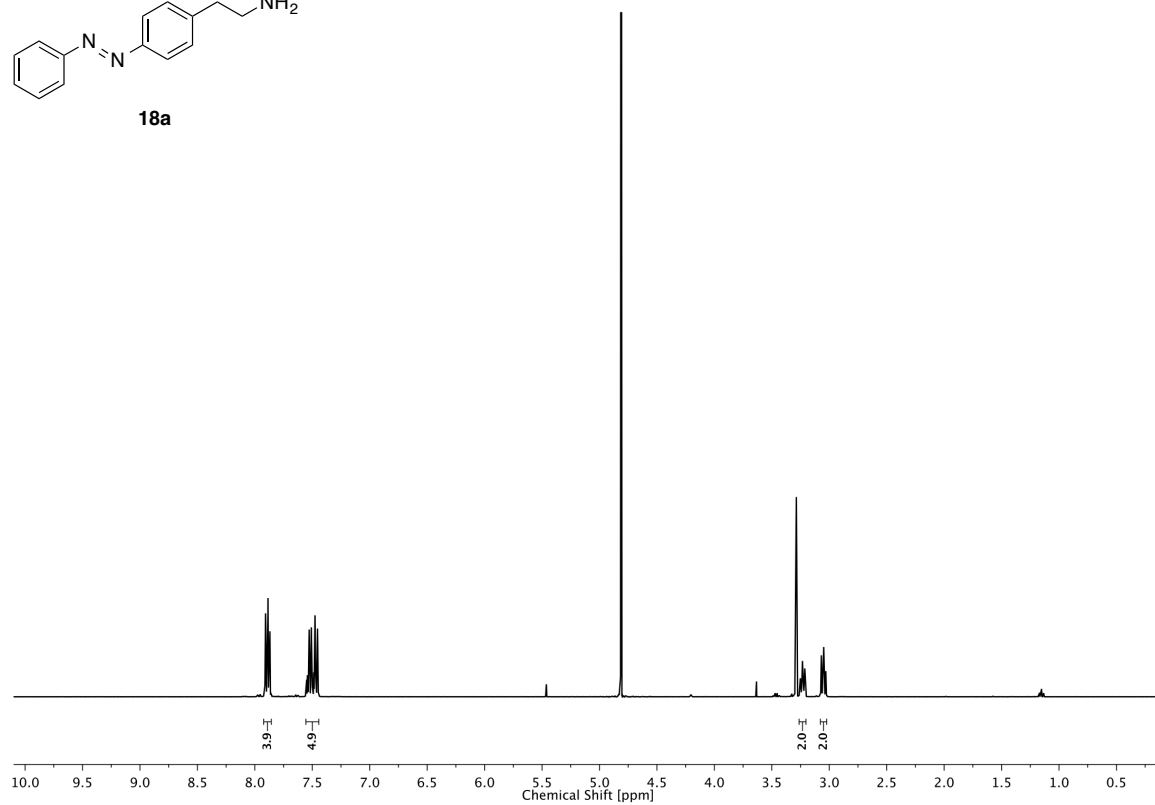
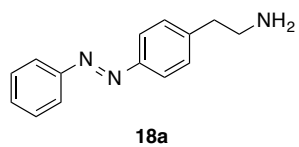
3 PHOTOCONTROL OF TRP CHANNELS



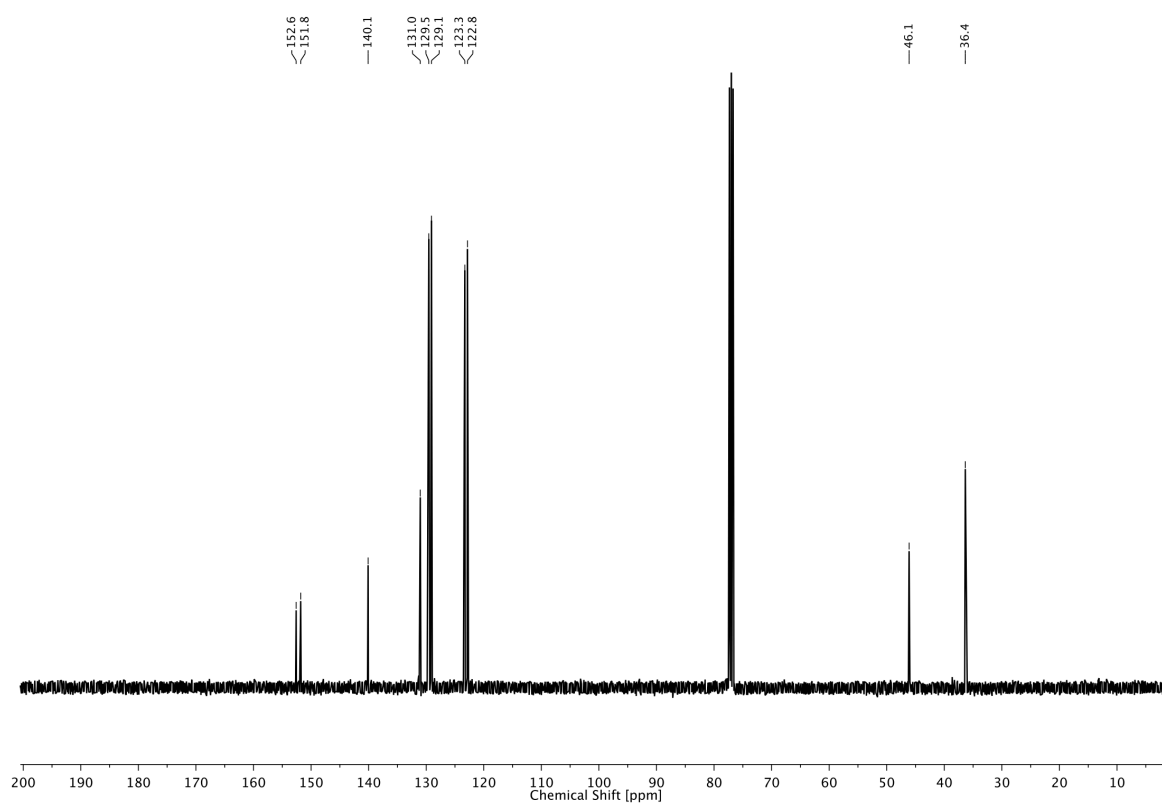
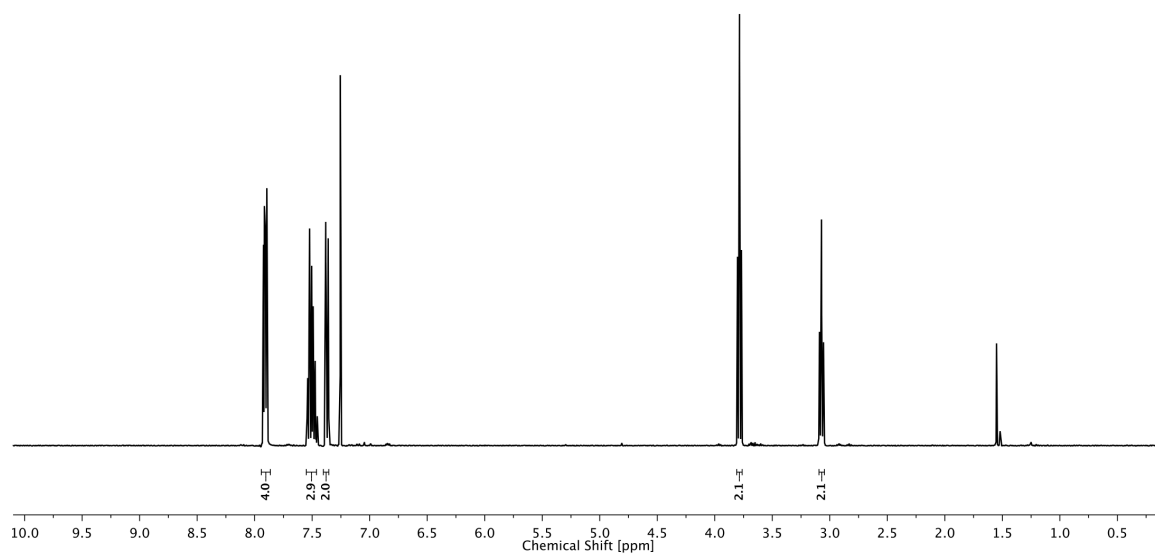
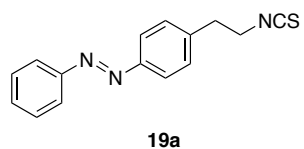
3 PHOTOCONTROL OF TRP CHANNELS



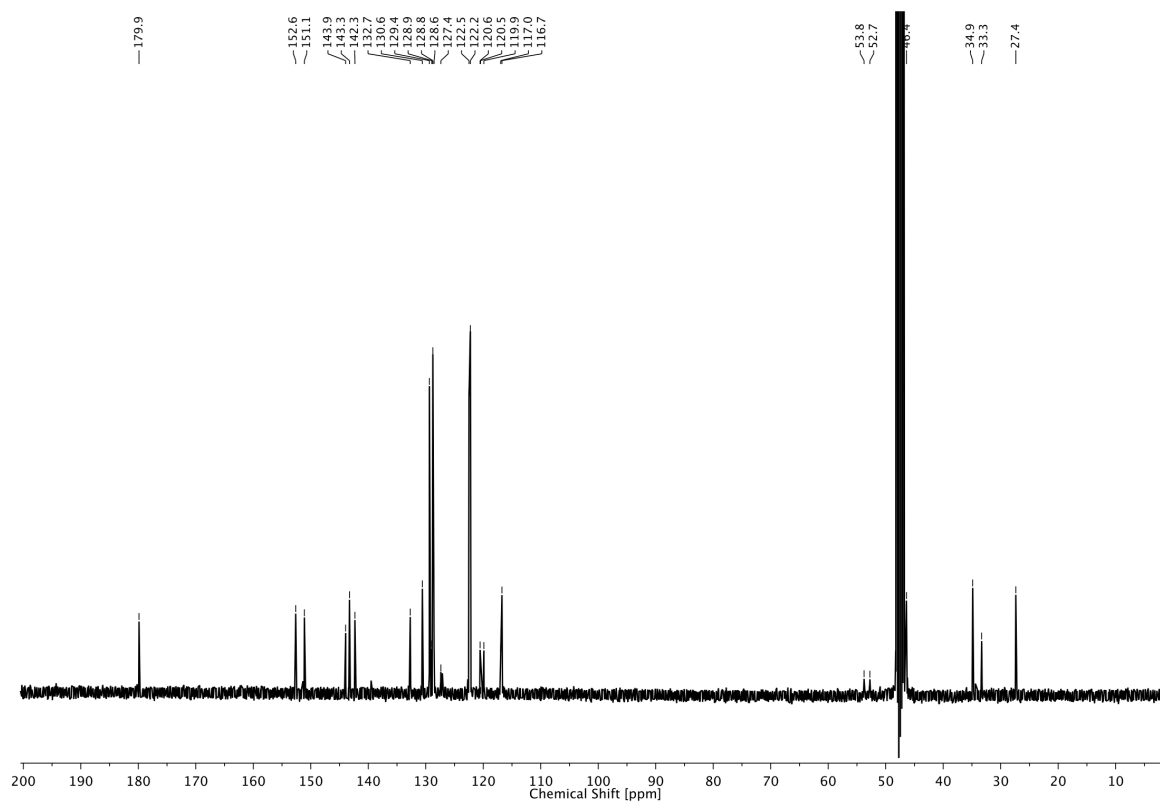
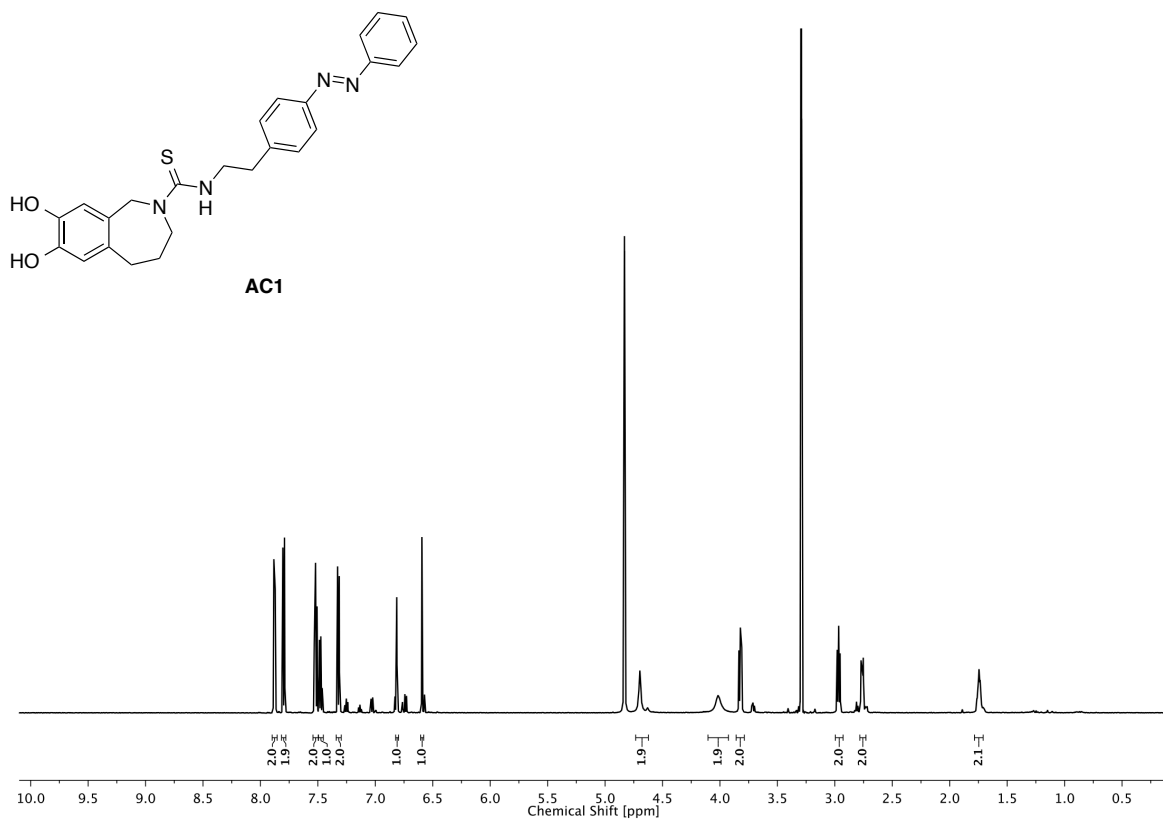
3 PHOTOCONTROL OF TRP CHANNELS



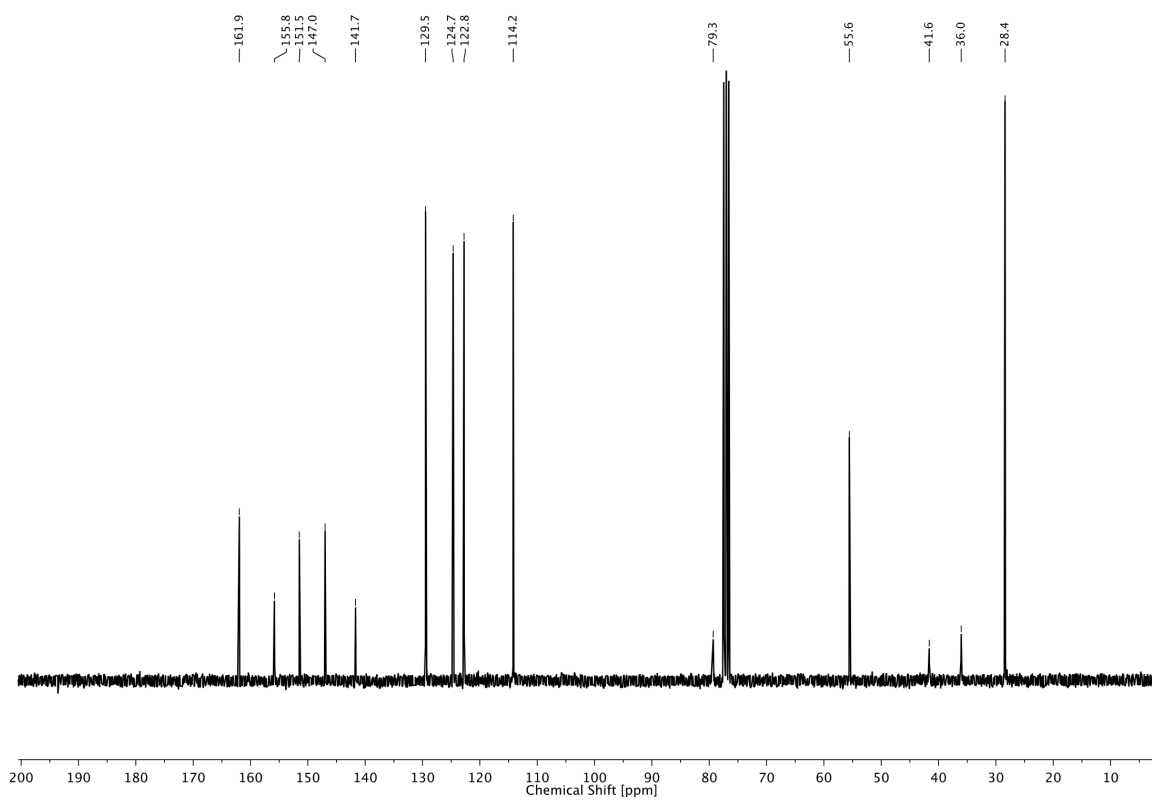
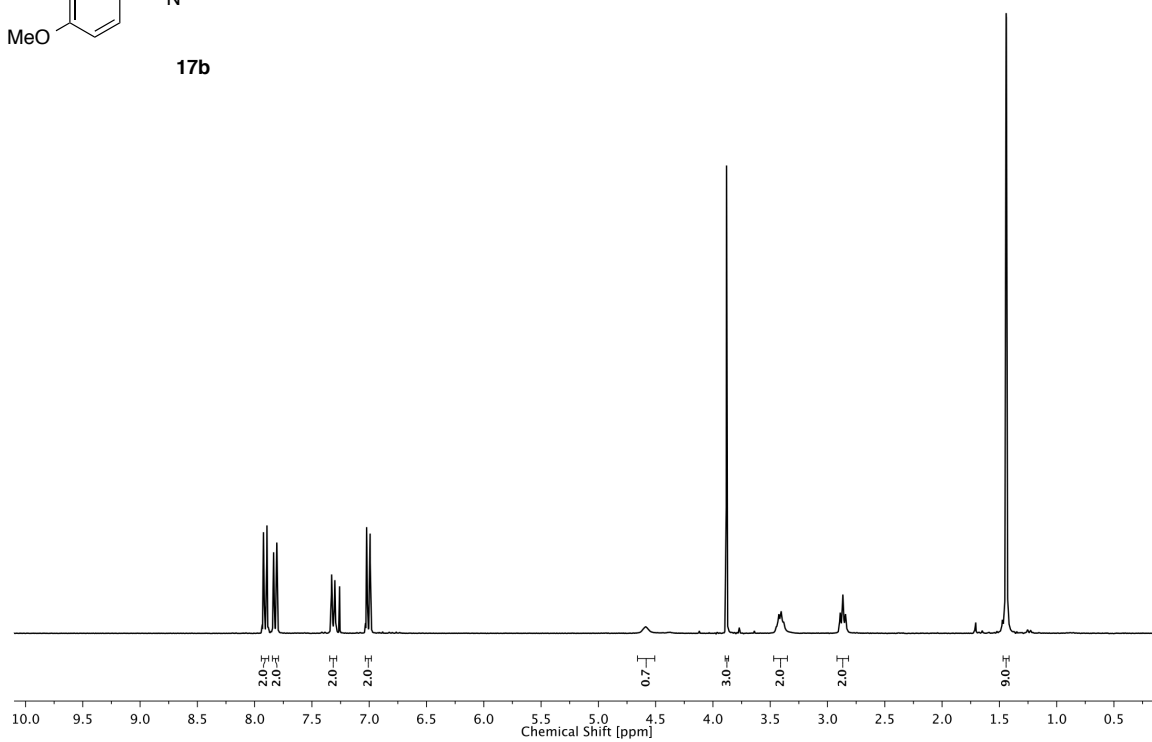
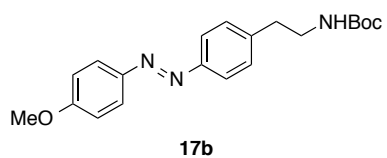
3 PHOTOCONTROL OF TRP CHANNELS



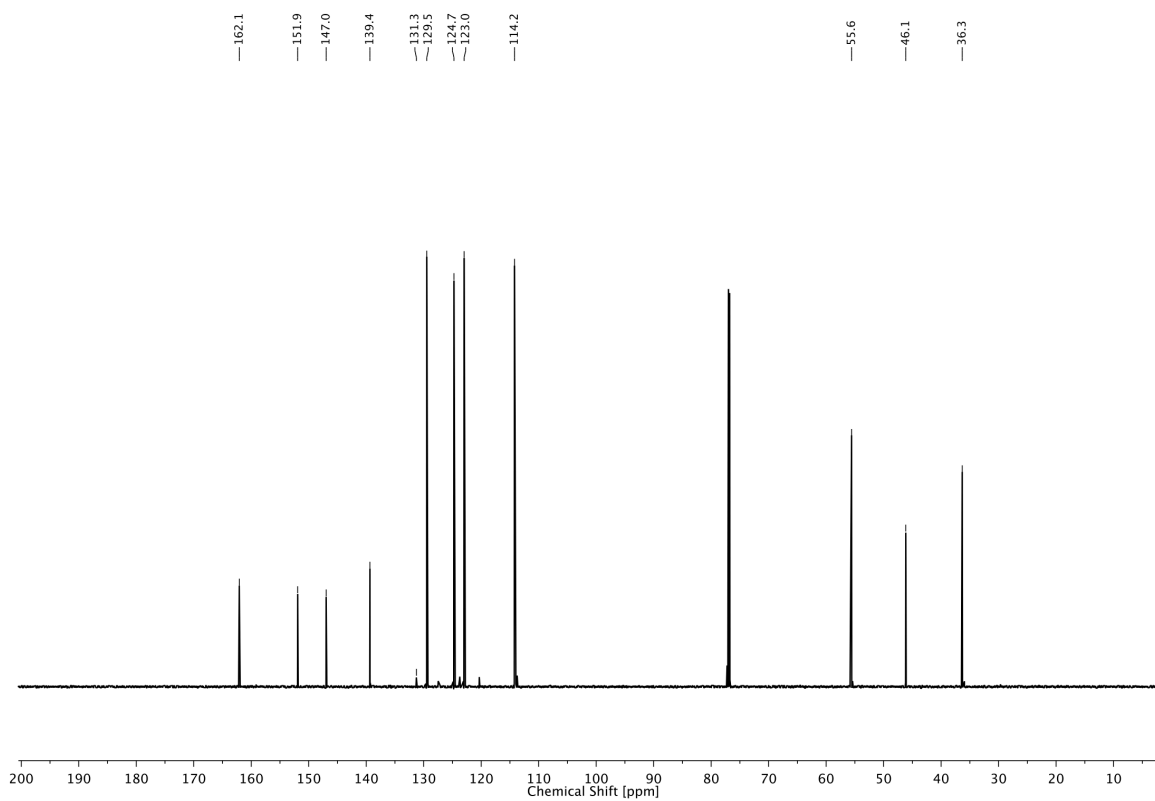
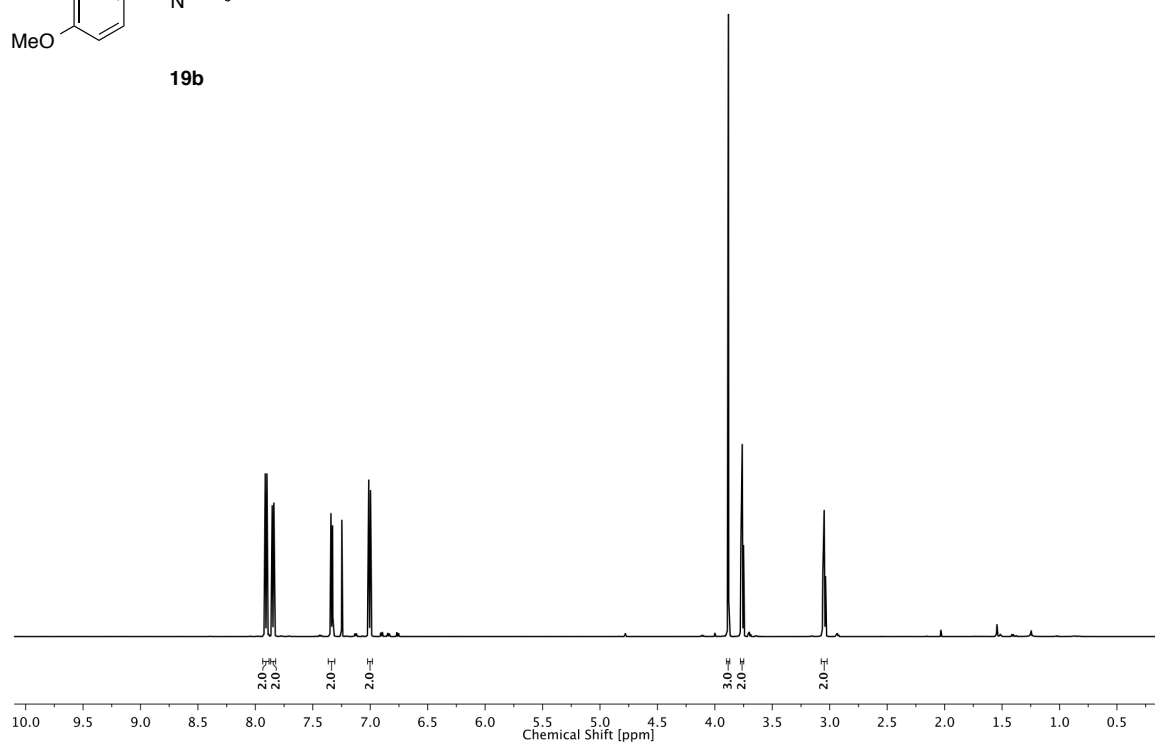
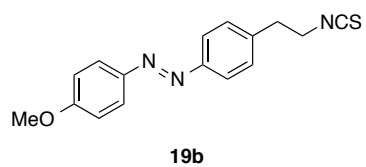
3 PHOTOCONTROL OF TRP CHANNELS



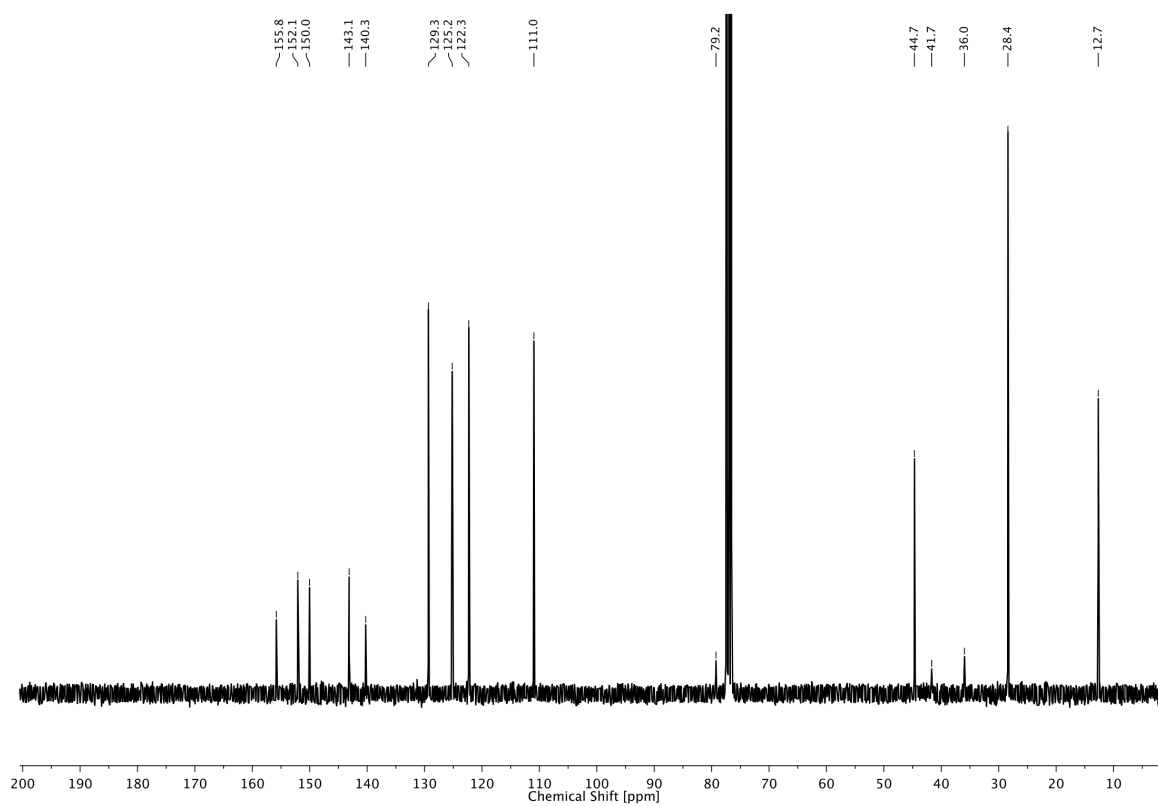
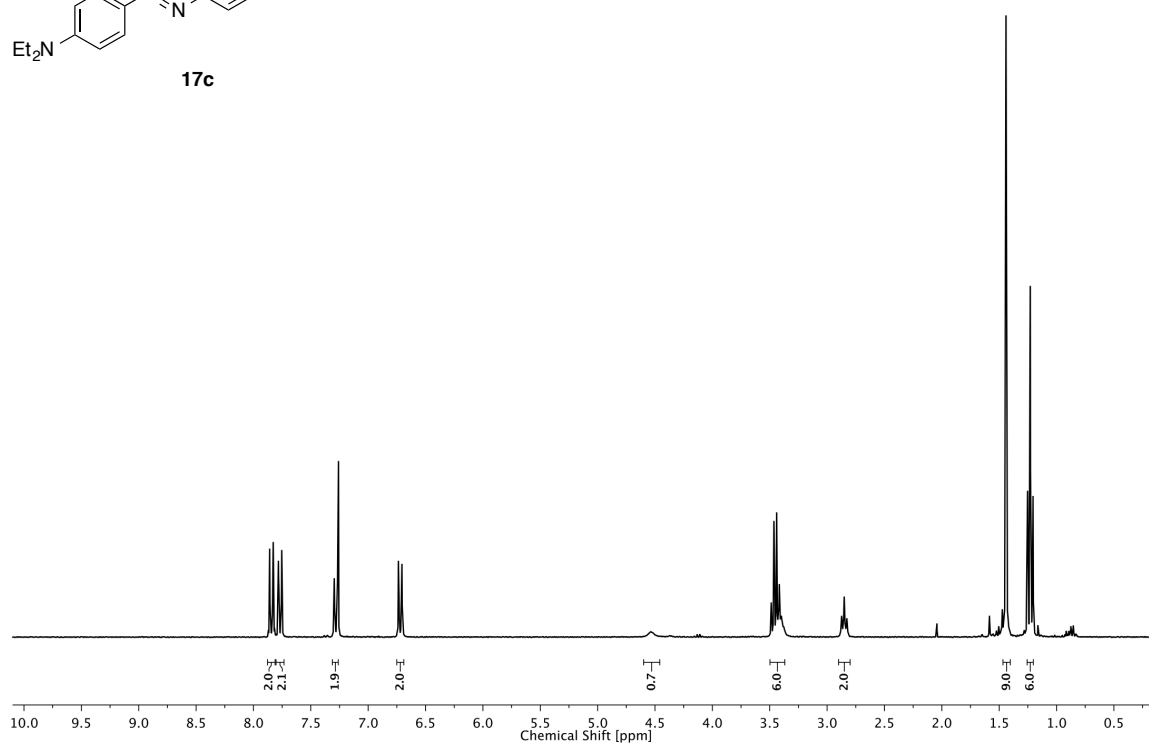
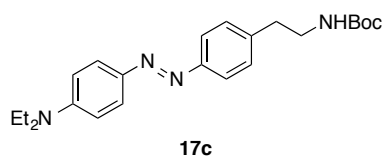
3 PHOTOCONTROL OF TRP CHANNELS



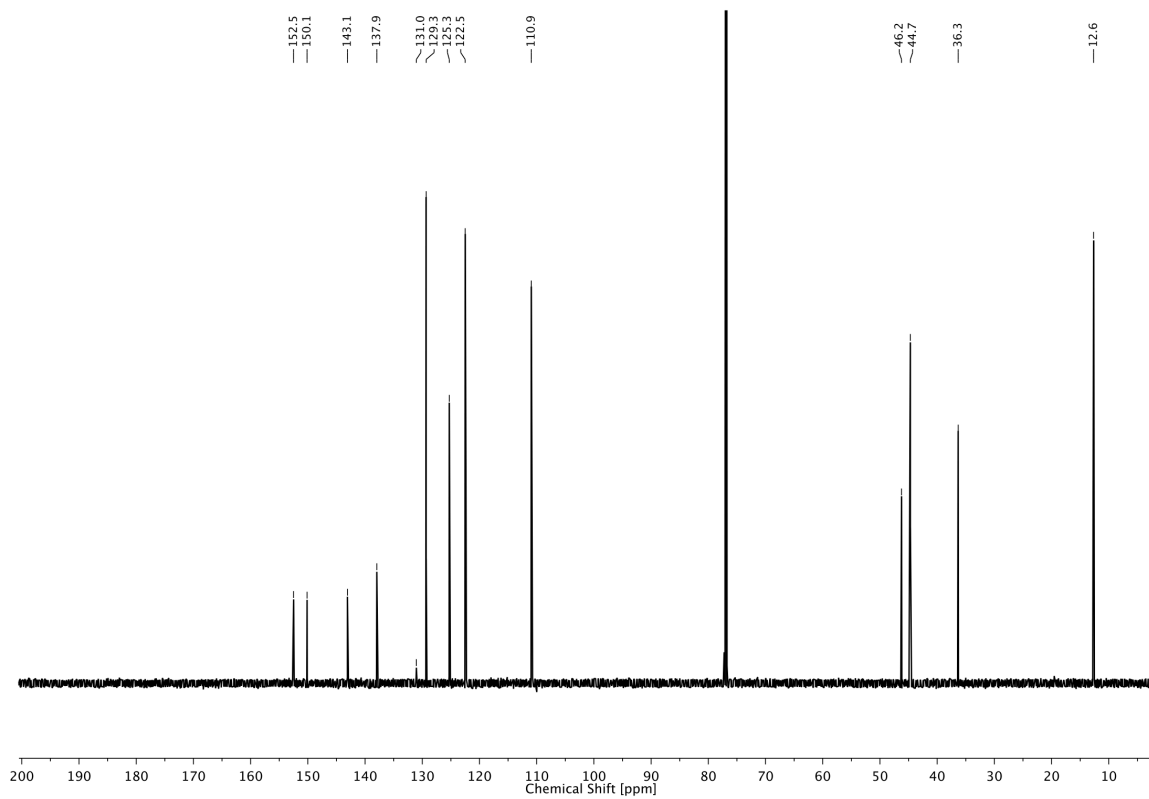
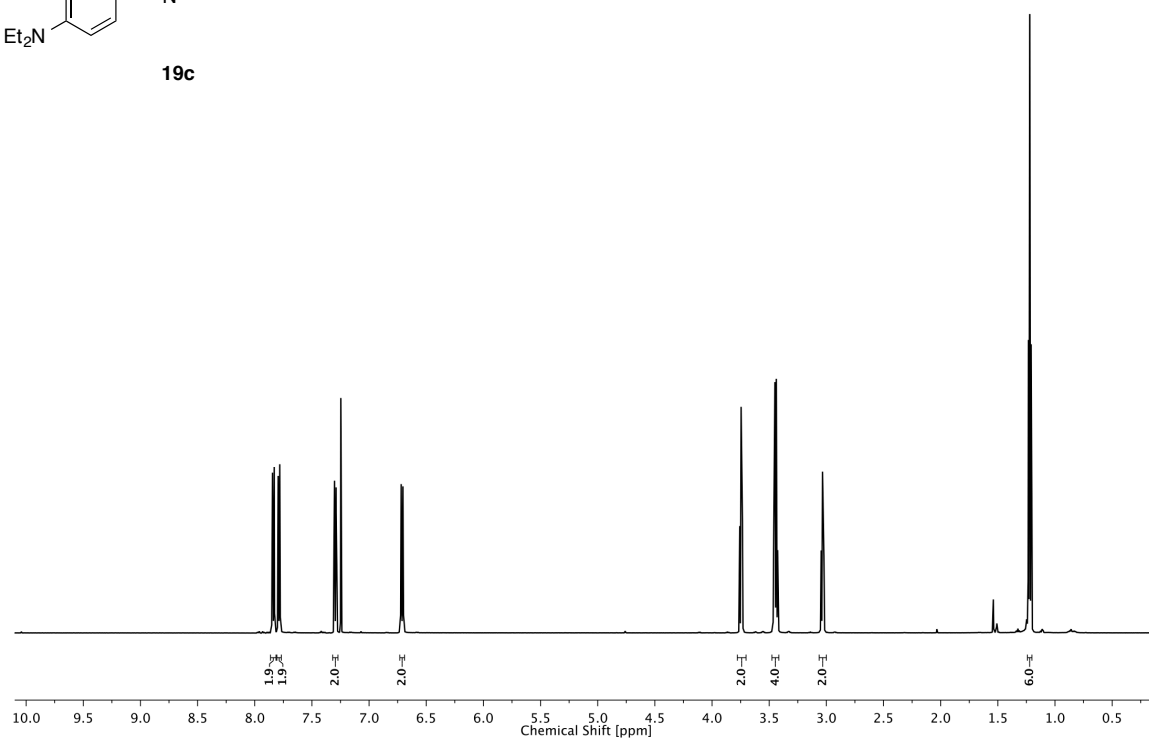
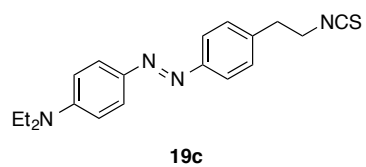
3 PHOTOCONTROL OF TRP CHANNELS



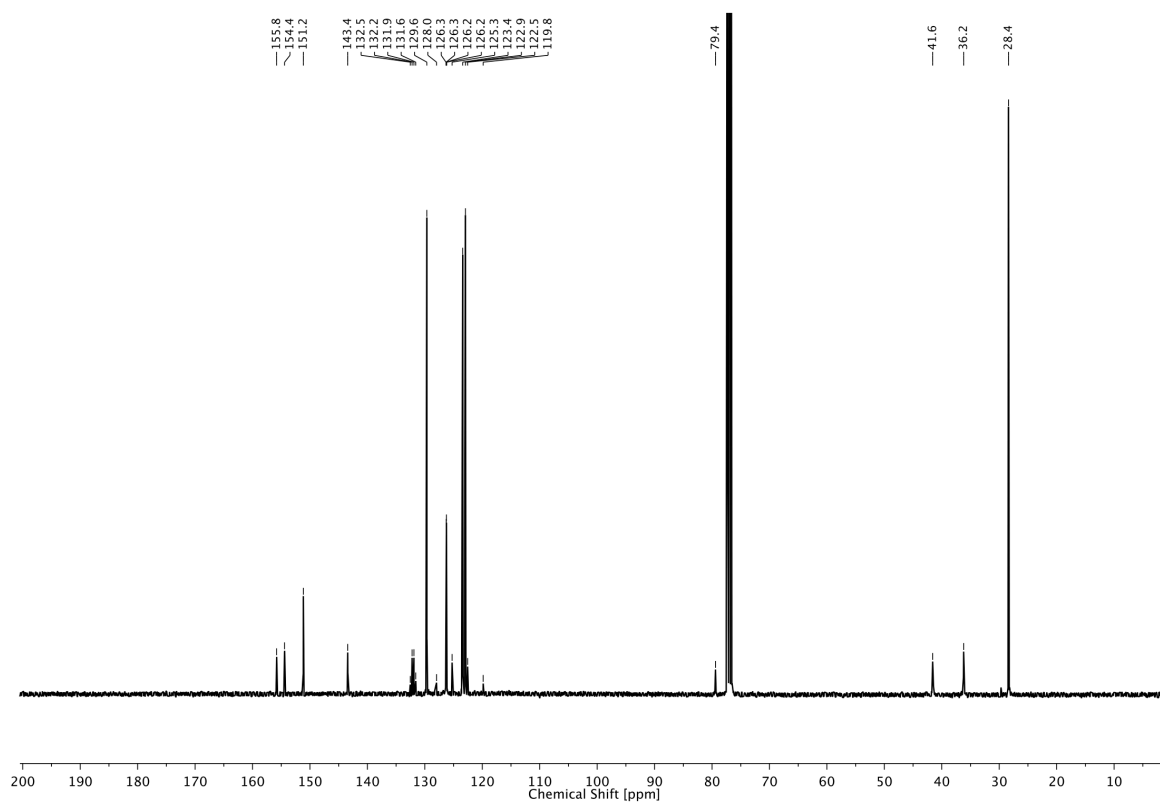
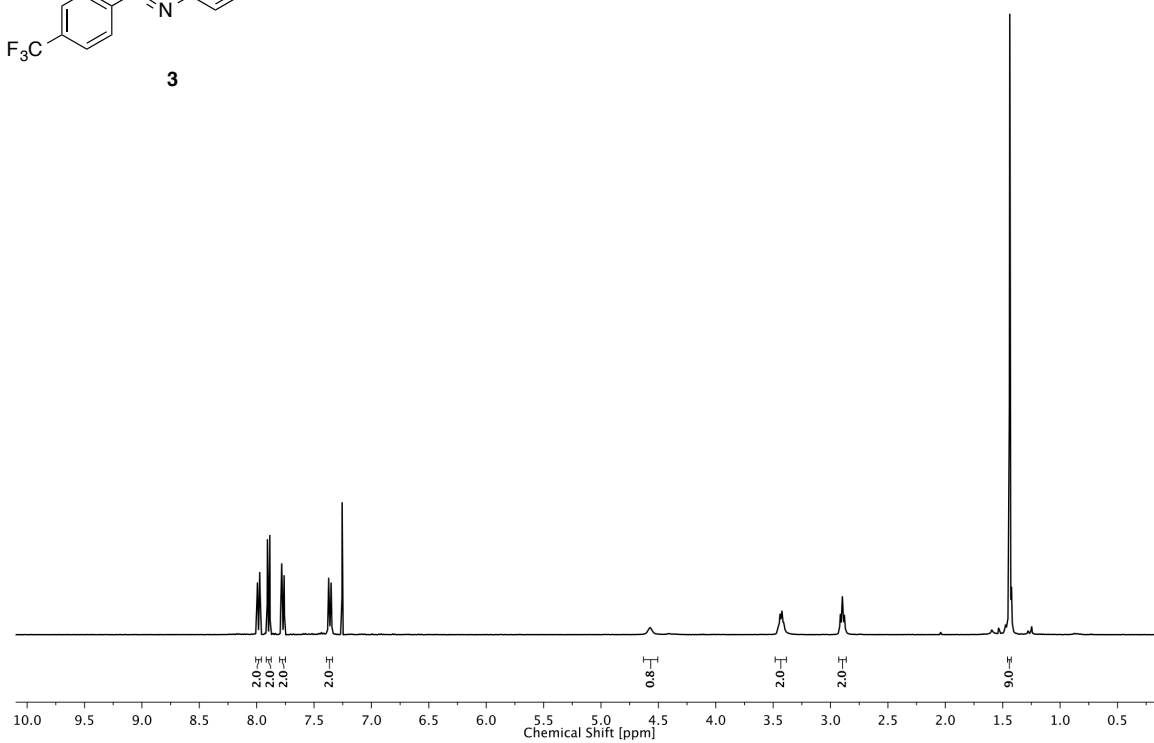
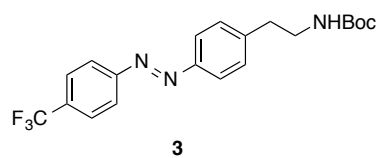
3 PHOTOCONTROL OF TRP CHANNELS



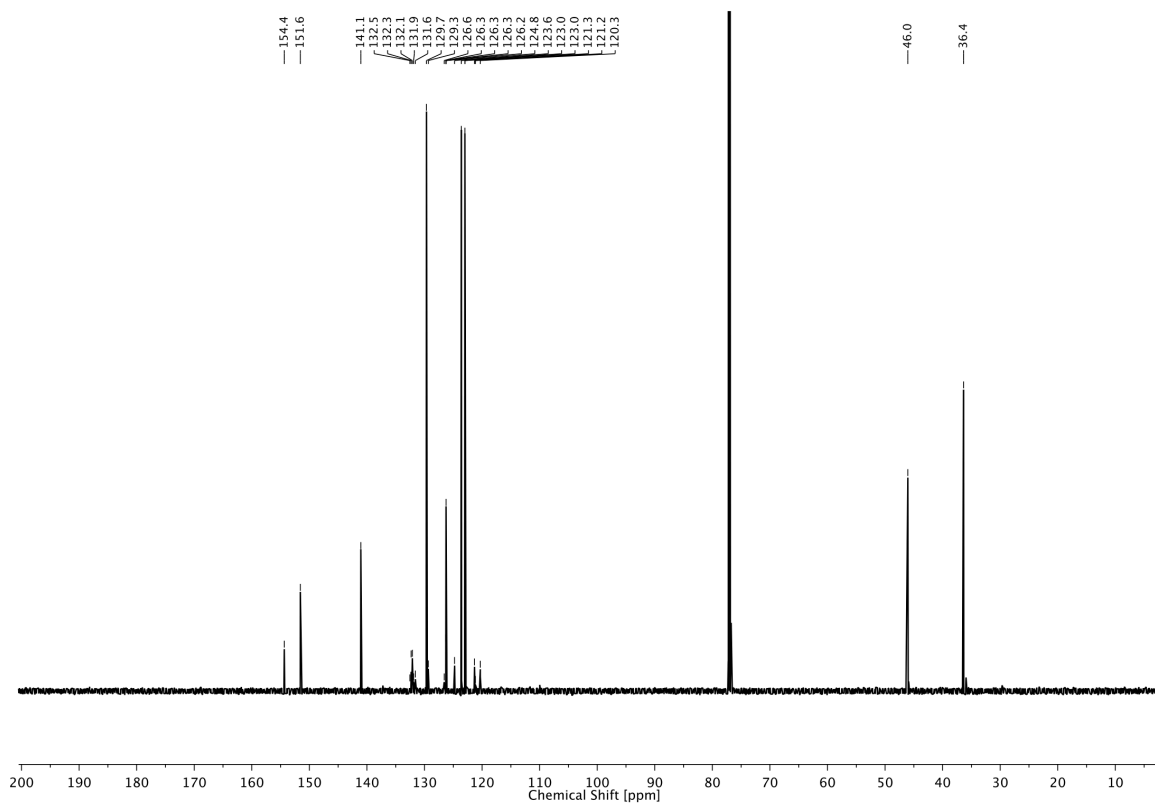
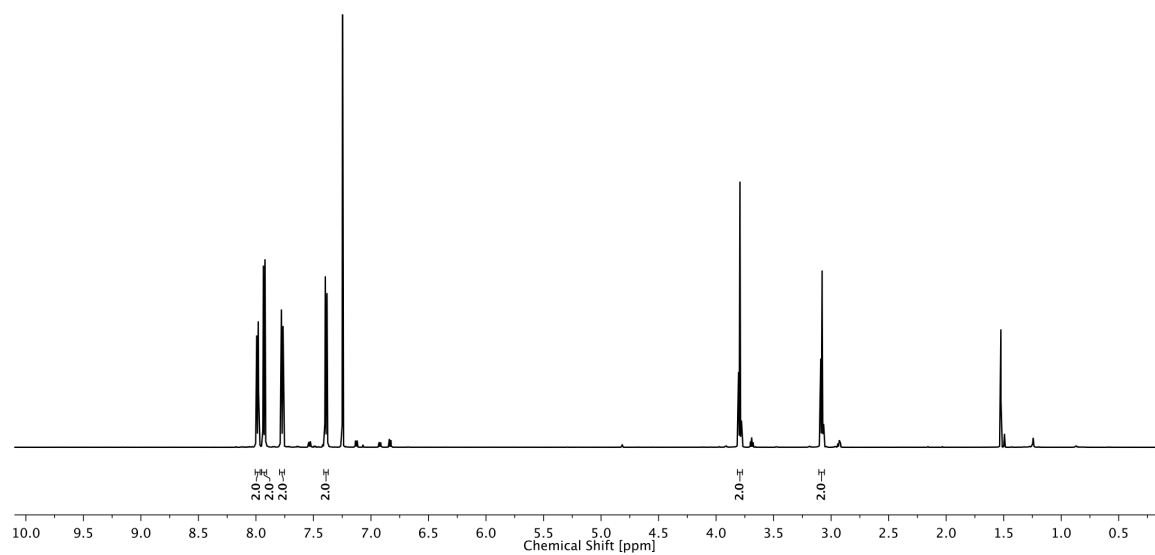
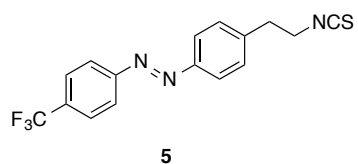
3 PHOTOCONTROL OF TRP CHANNELS



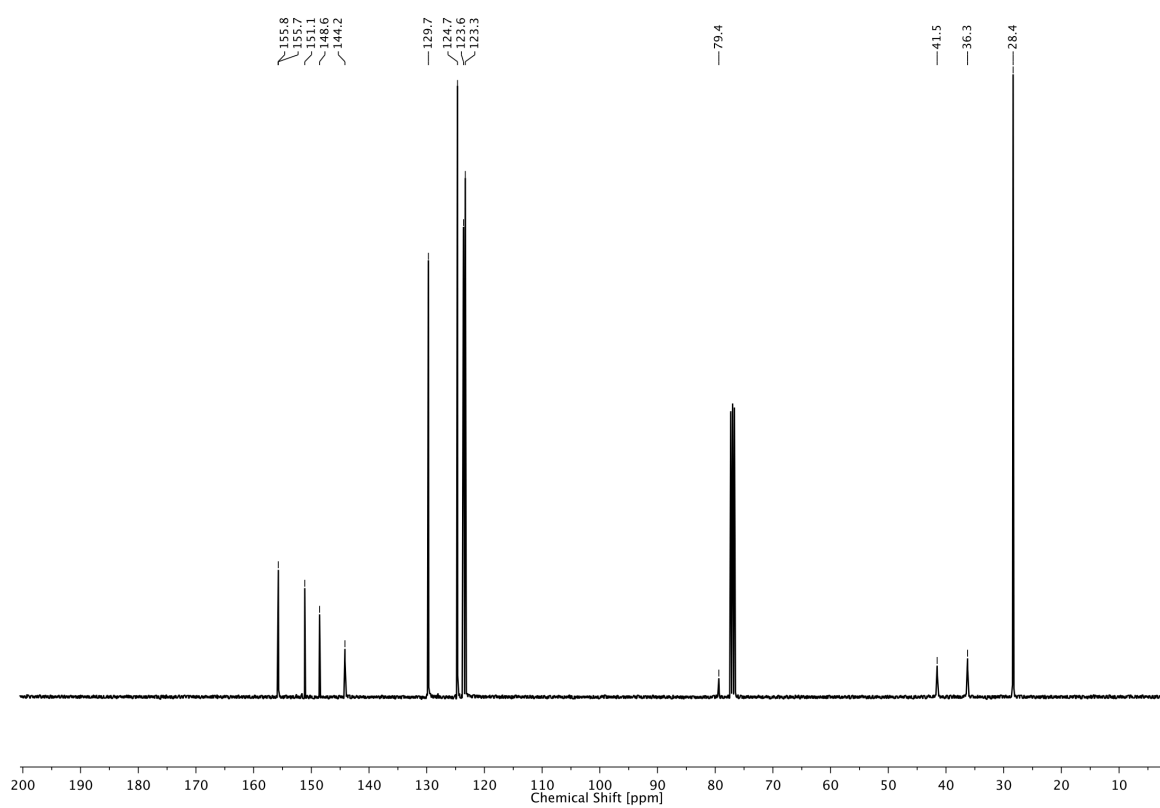
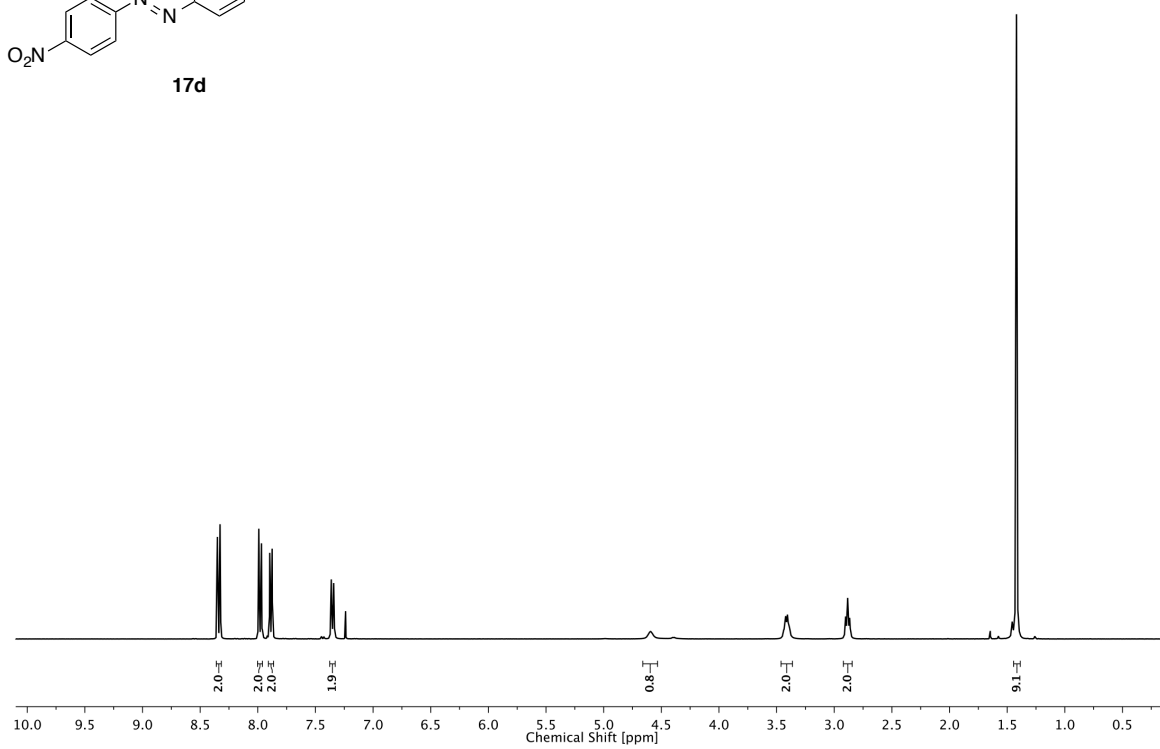
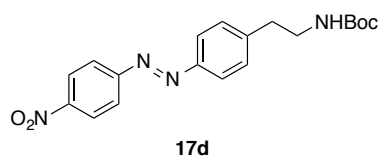
3 PHOTOCONTROL OF TRP CHANNELS



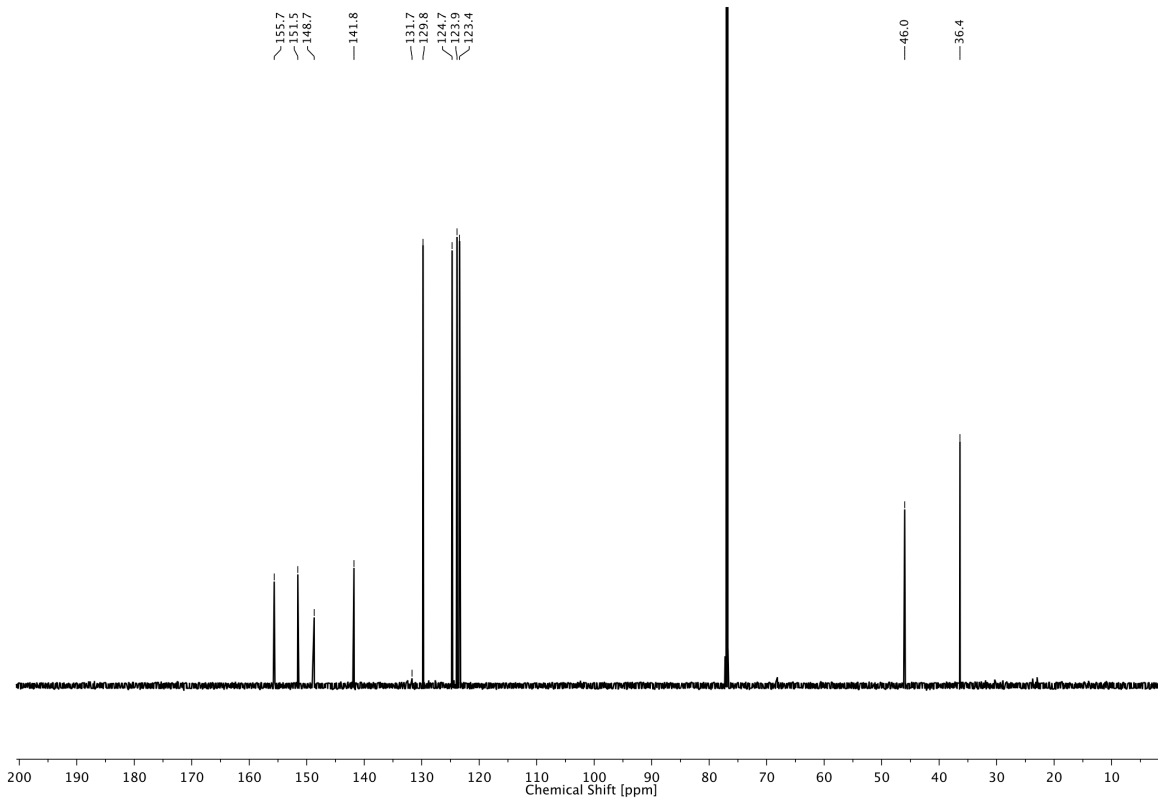
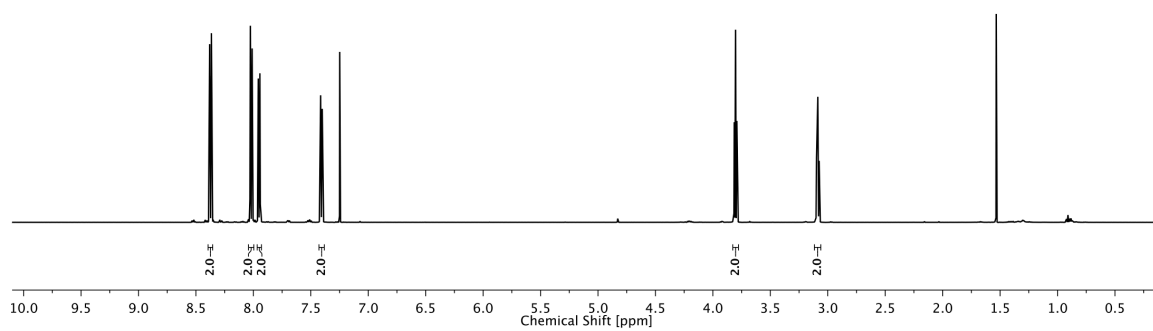
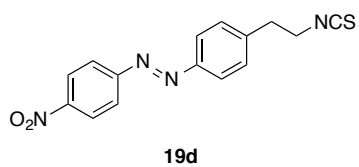
3 PHOTOCONTROL OF TRP CHANNELS



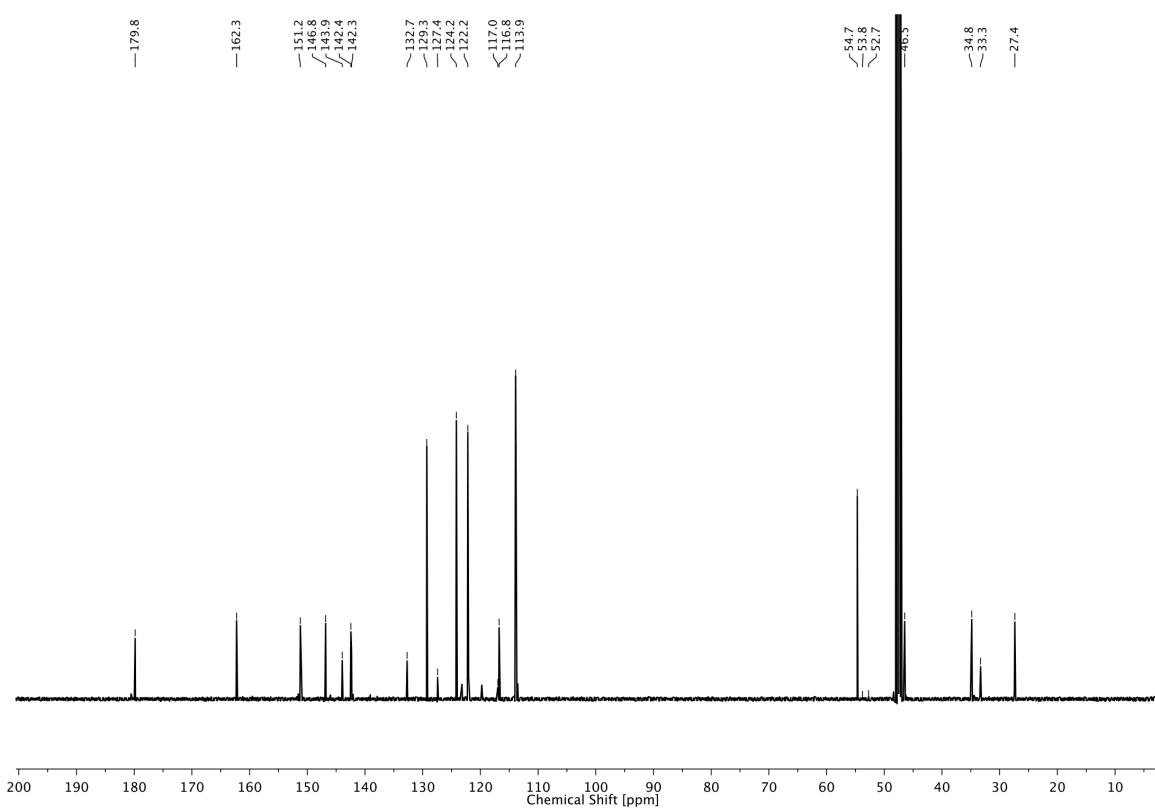
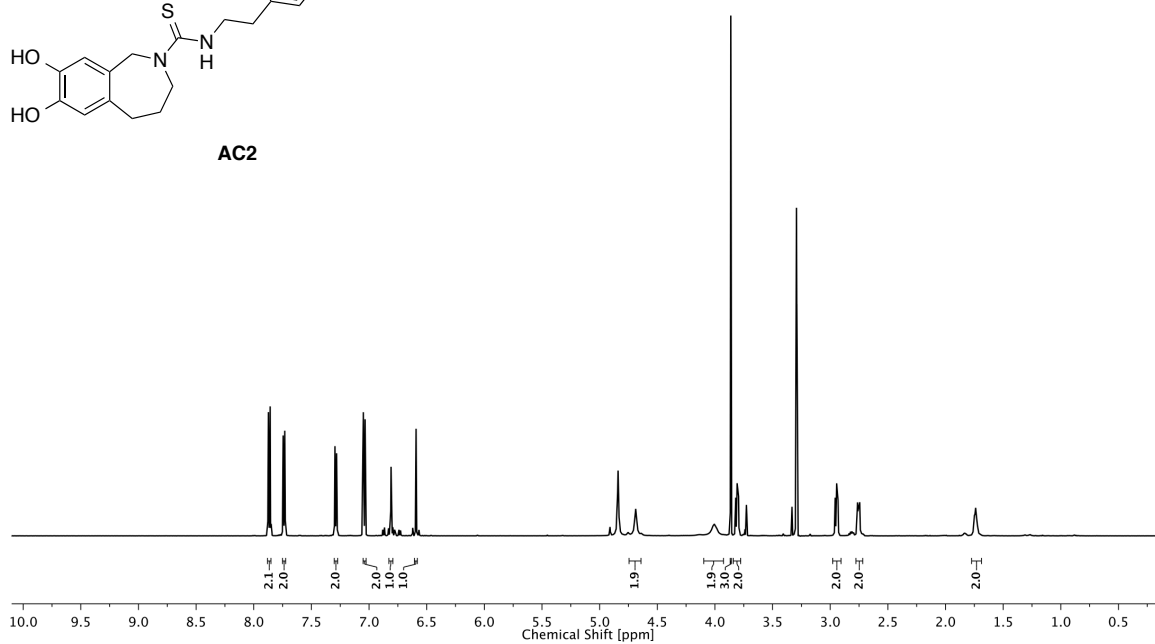
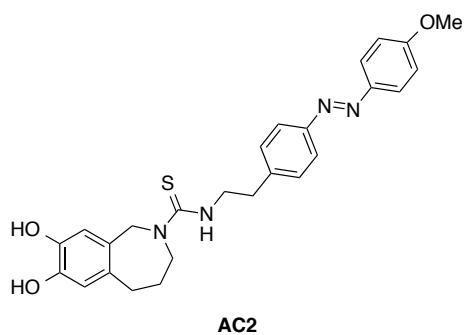
3 PHOTOCONTROL OF TRP CHANNELS



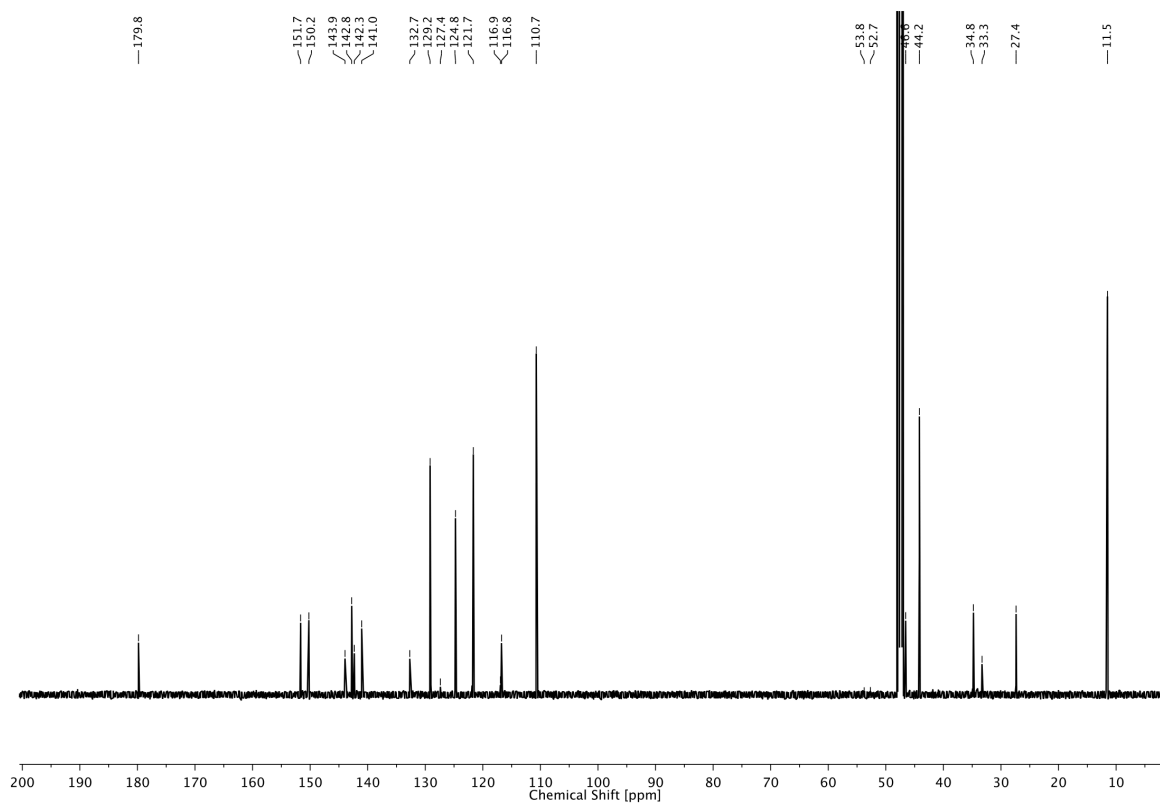
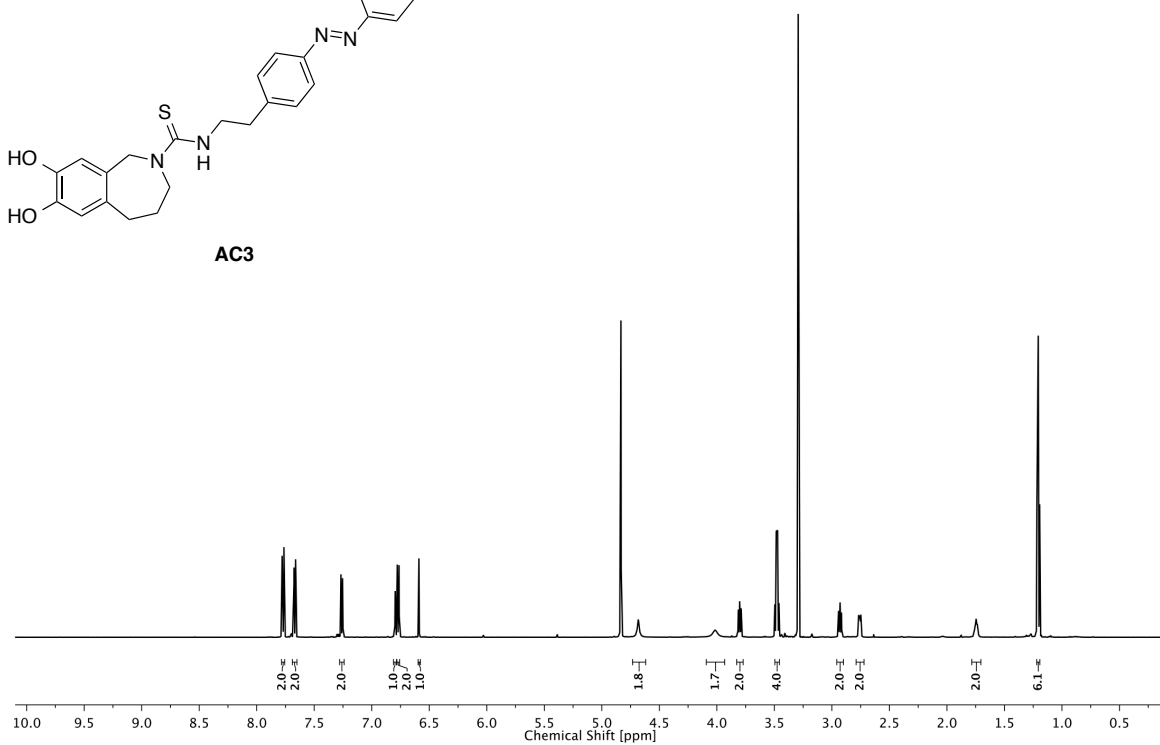
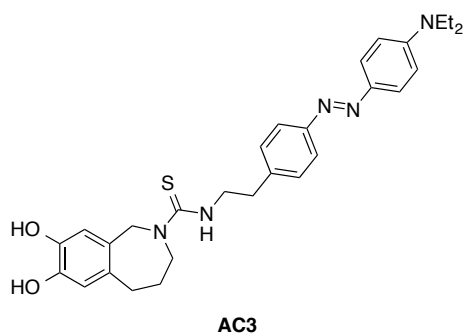
3 PHOTOCONTROL OF TRP CHANNELS



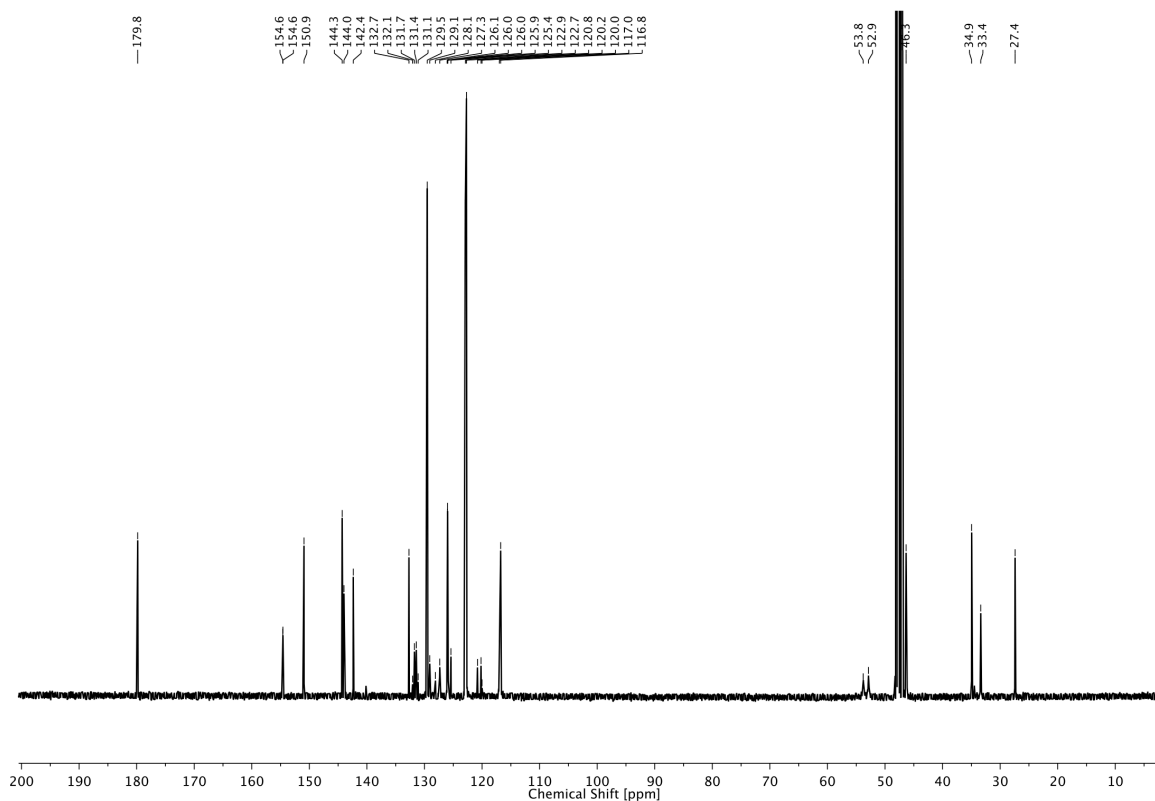
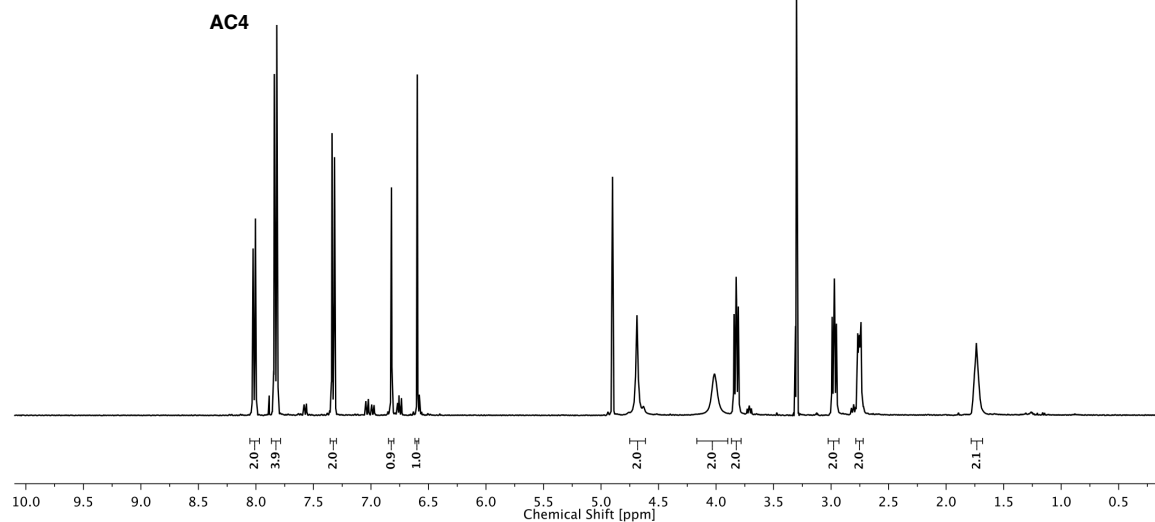
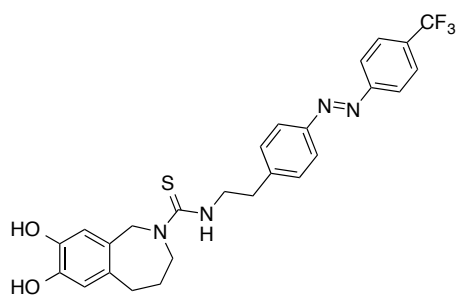
3 PHOTOCONTROL OF TRP CHANNELS



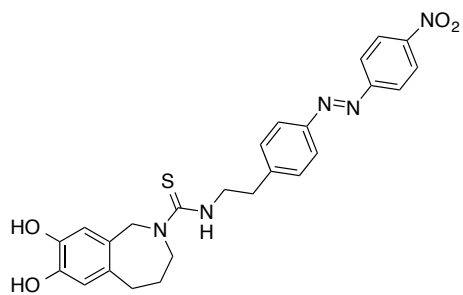
3 PHOTOCONTROL OF TRP CHANNELS



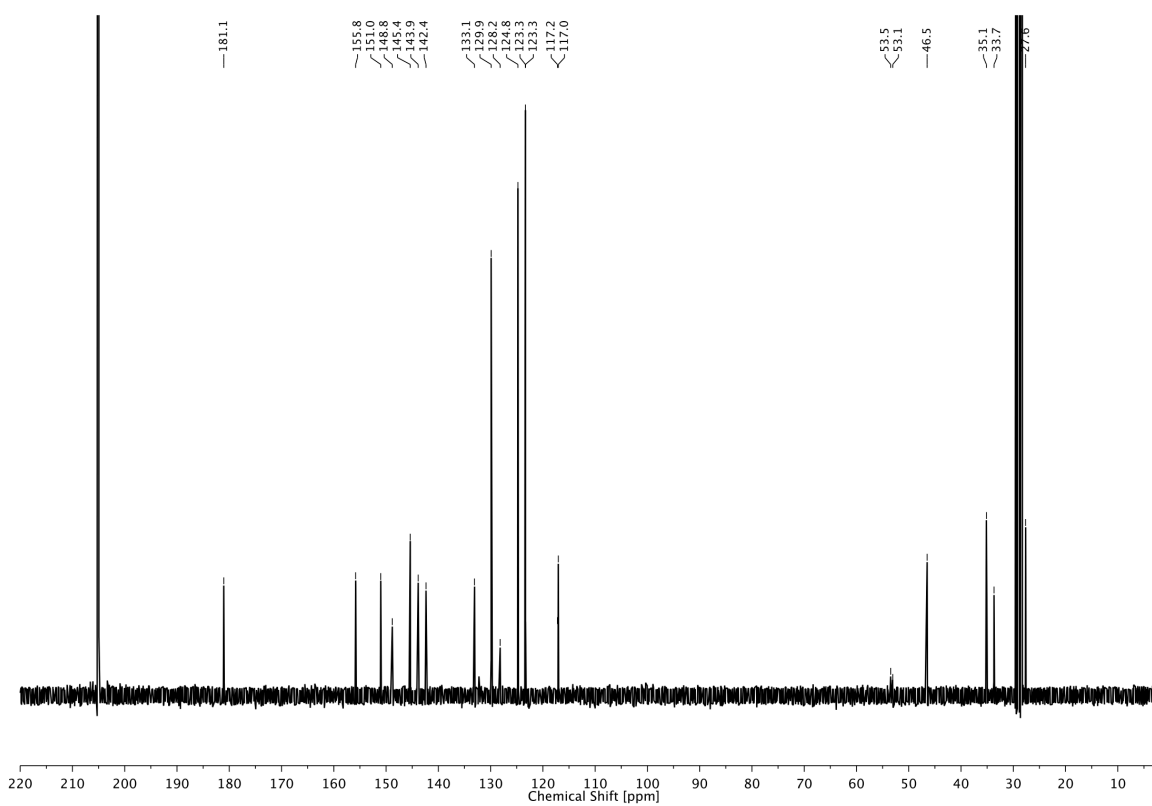
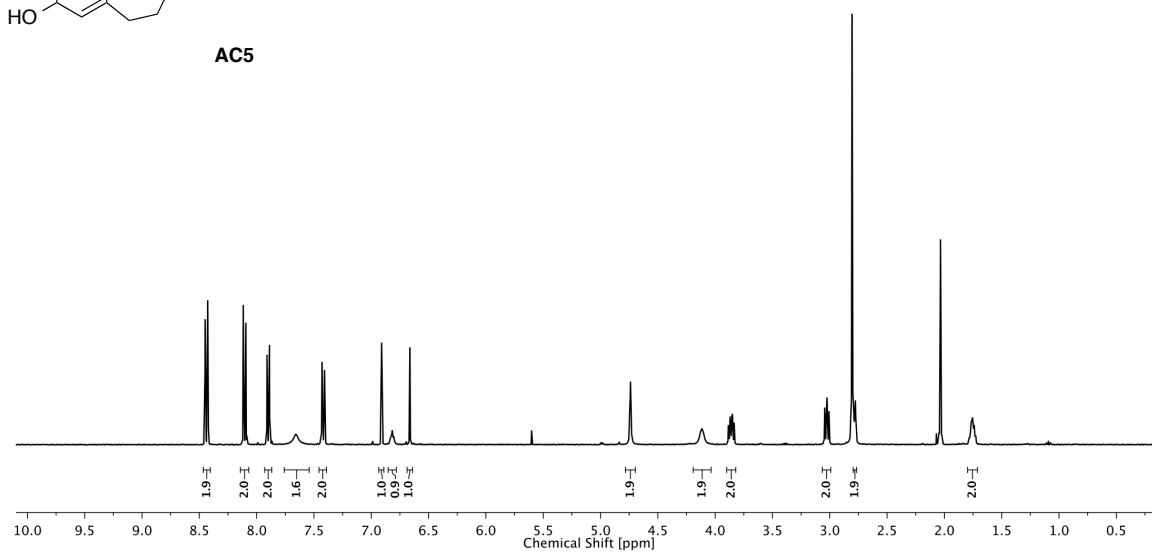
3 PHOTOCONTROL OF TRP CHANNELS



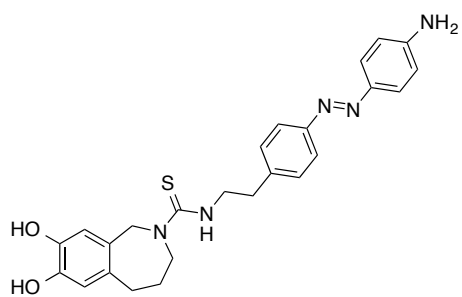
3 PHOTOCONTROL OF TRP CHANNELS



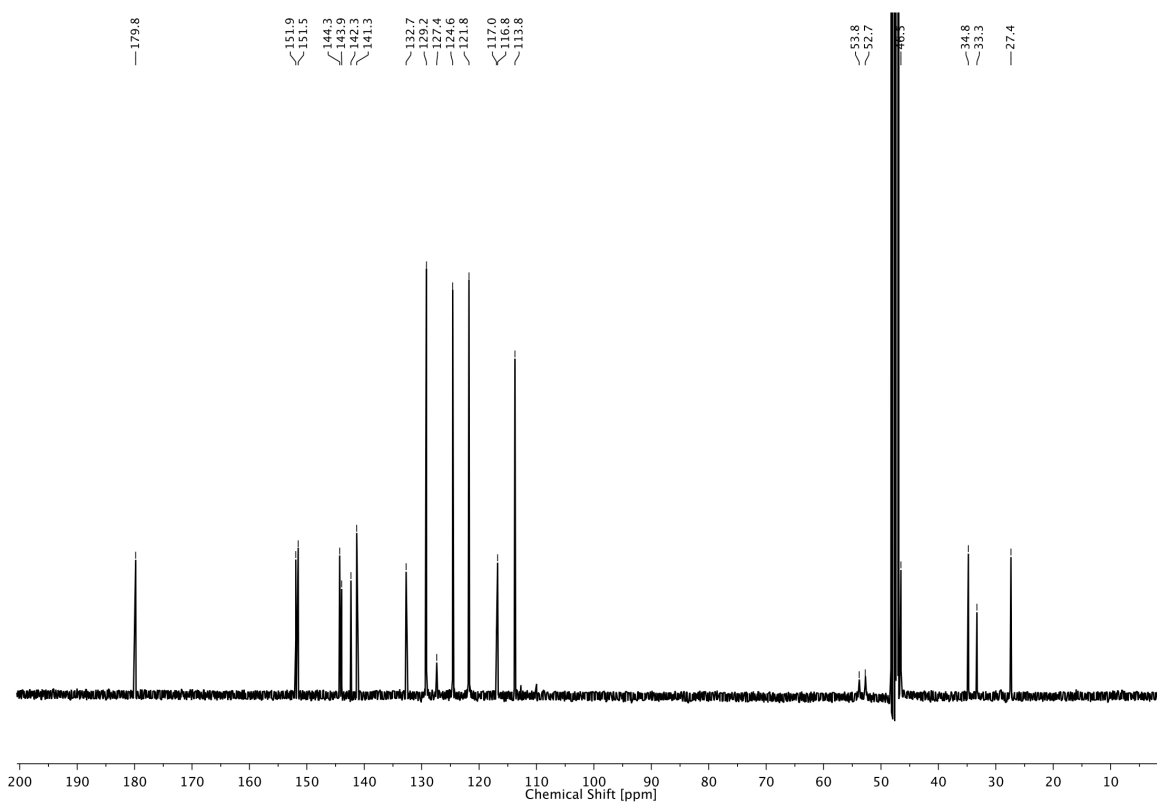
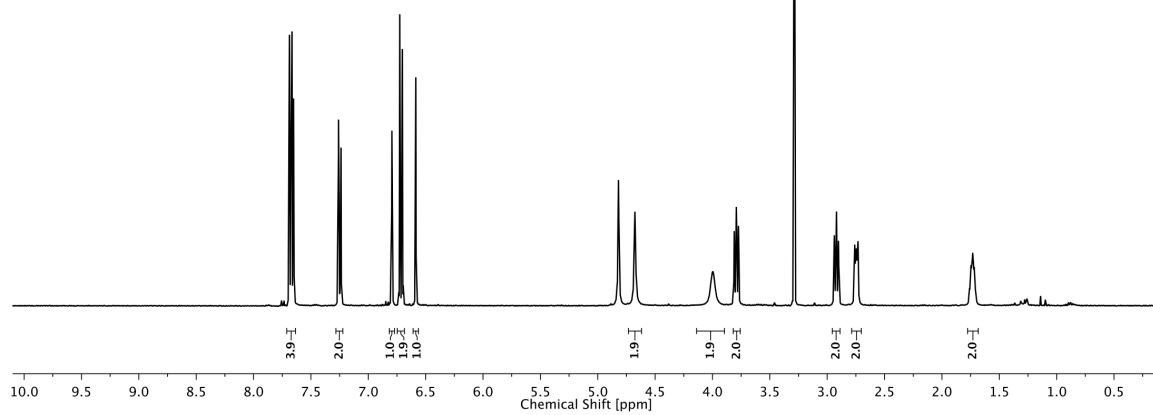
AC5



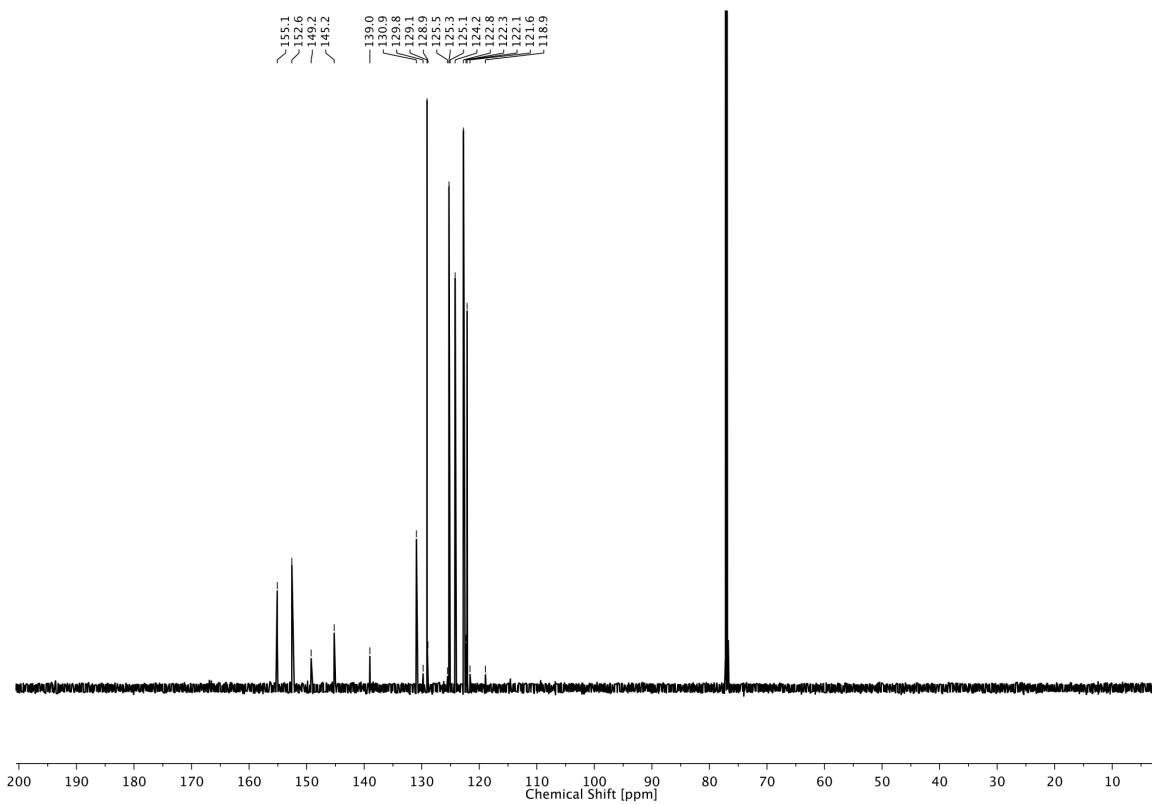
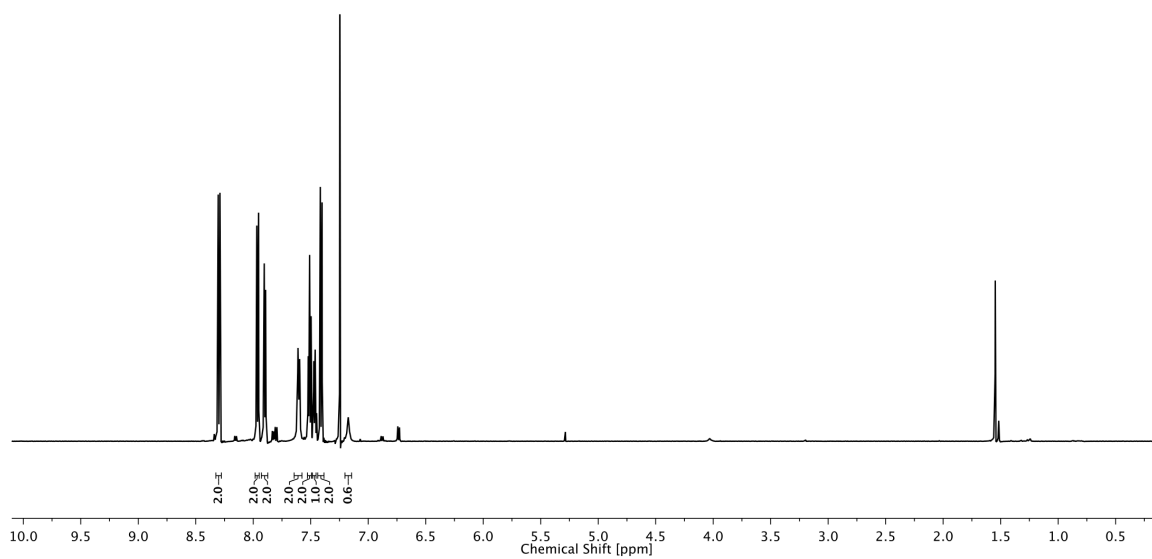
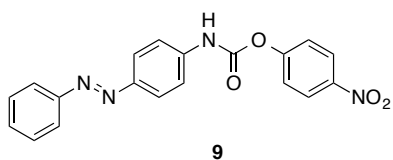
3 PHOTOCONTROL OF TRP CHANNELS



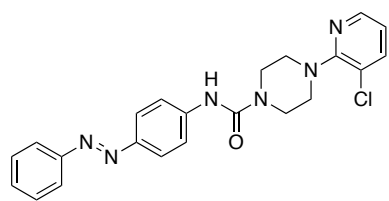
AC6



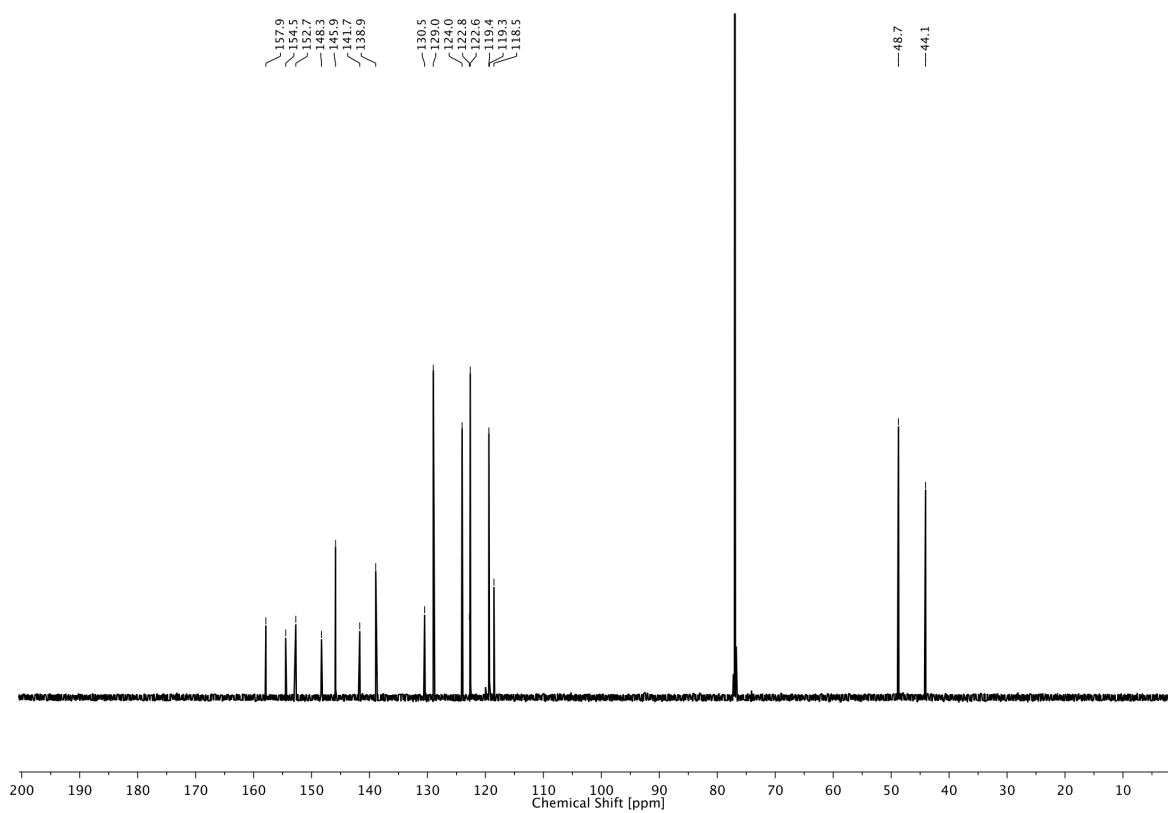
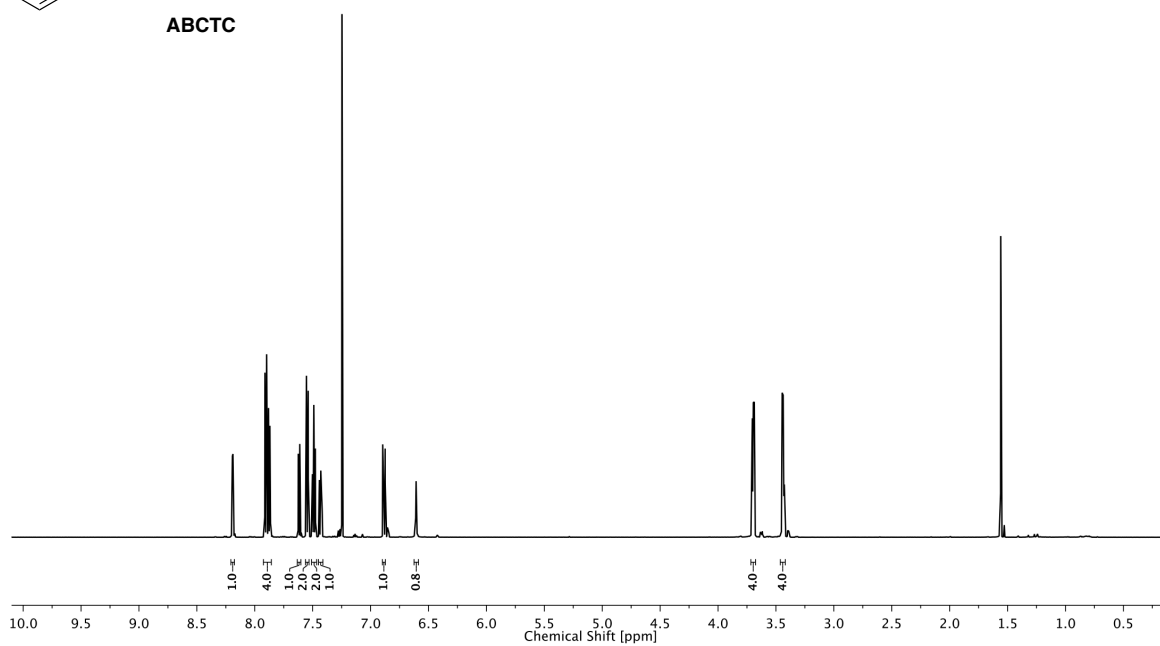
3 PHOTOCONTROL OF TRP CHANNELS



3 PHOTOCONTROL OF TRP CHANNELS

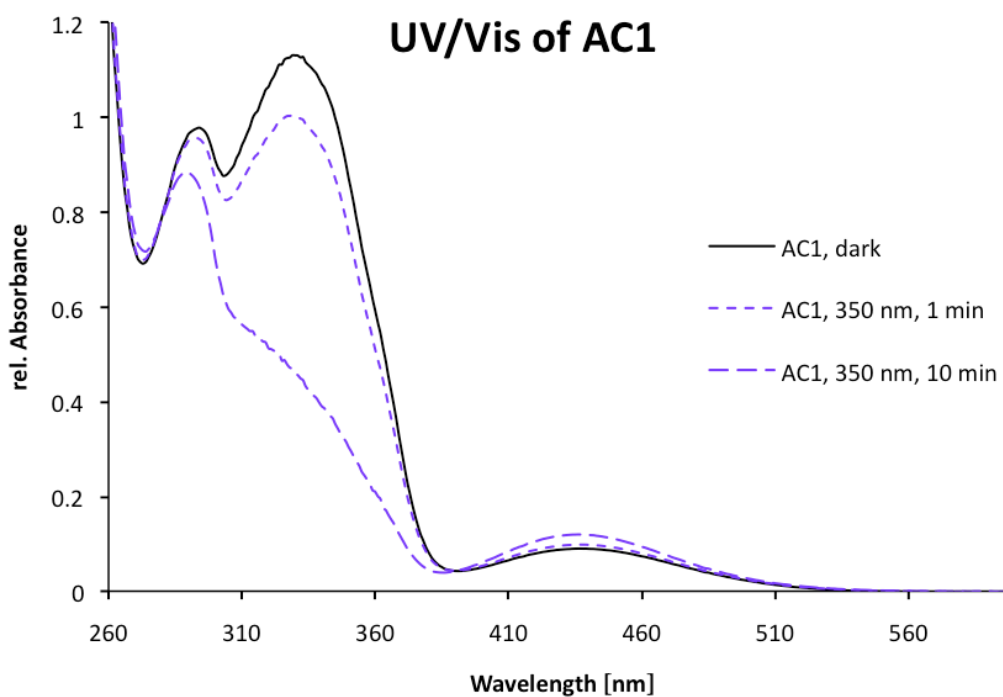


ABCTC

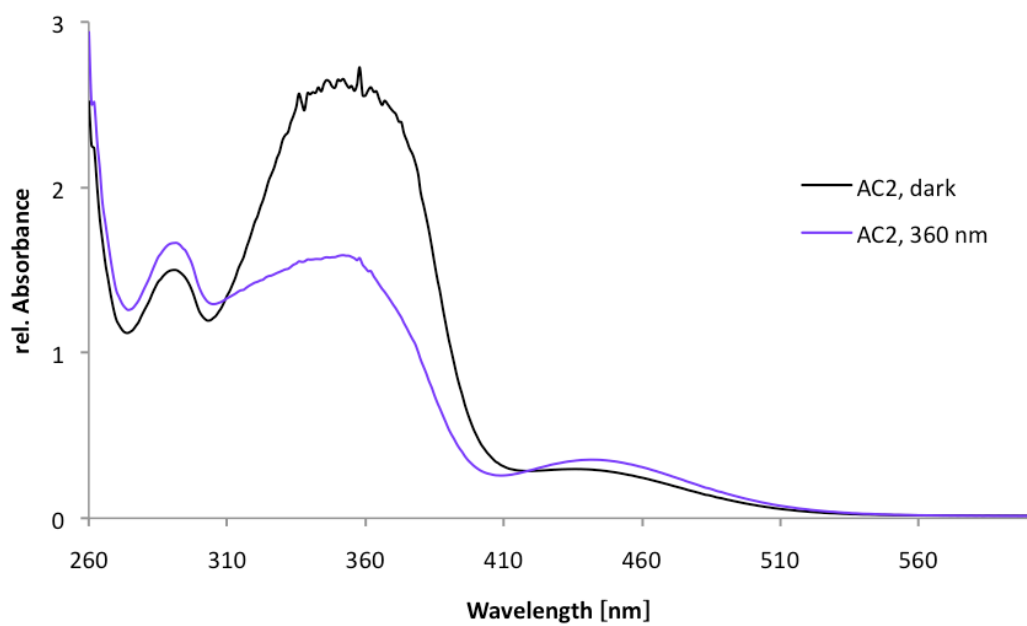


UV/Vis Spectra

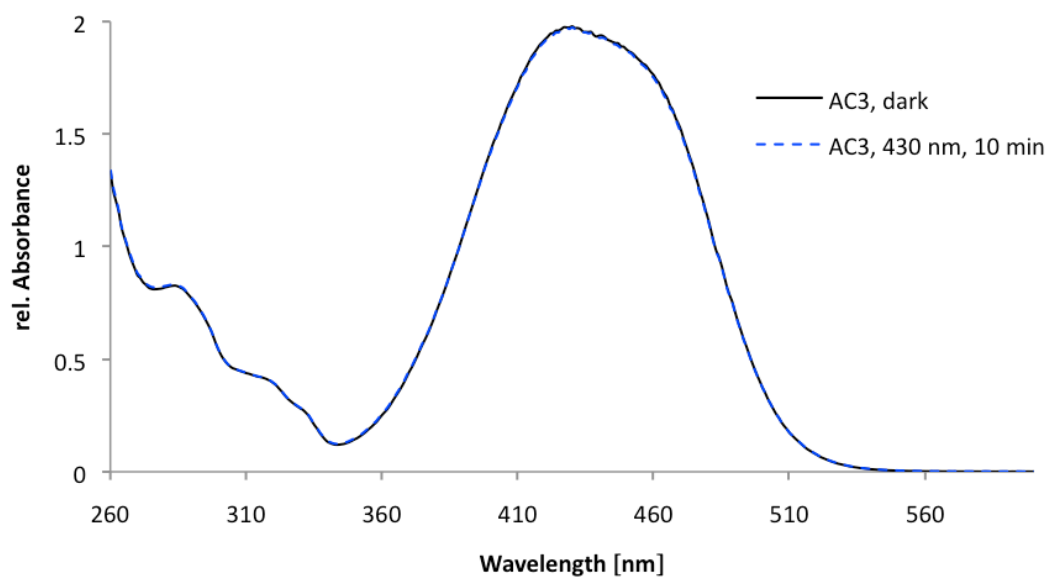
UV/Vis spectra of **AC1–AC6** and **ABCTC** were each recorded at a concentration of 100 μM in DMSO. Spectra were first recorded in the dark, then again after illumination with the absorption maximum wavelength for 1 min (and 10 min in some cases) unless indicated otherwise.



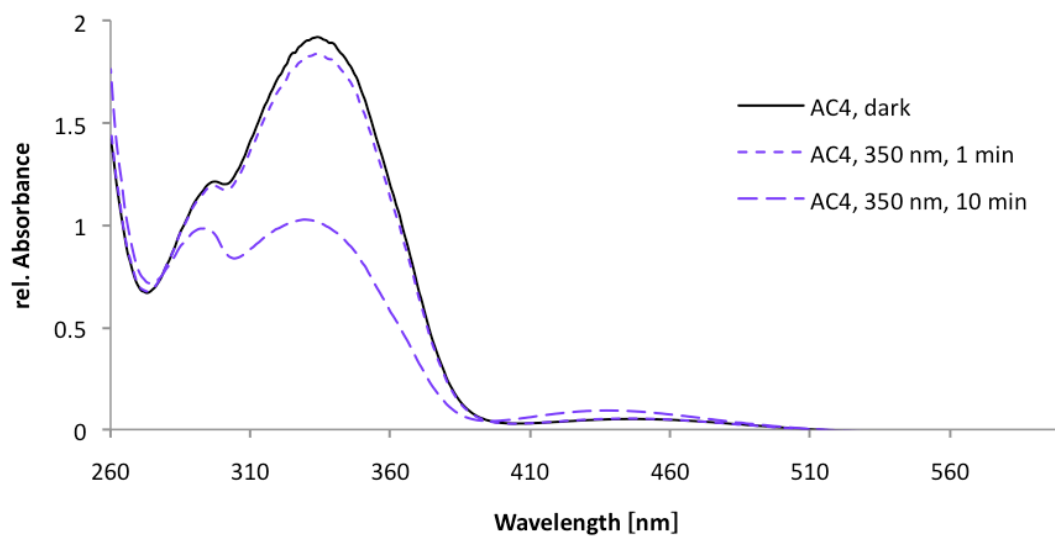
UV/Vis of AC2



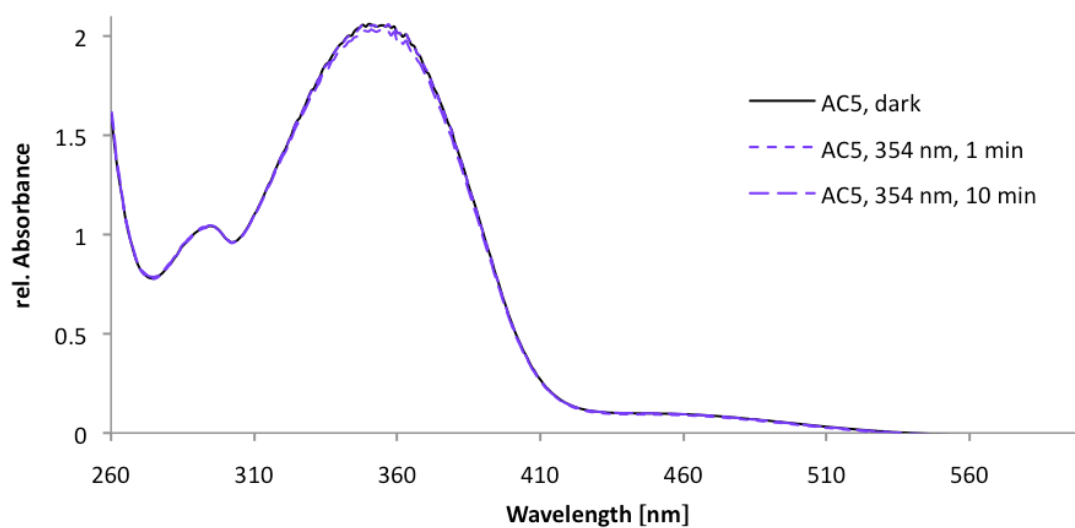
UV/Vis of AC3



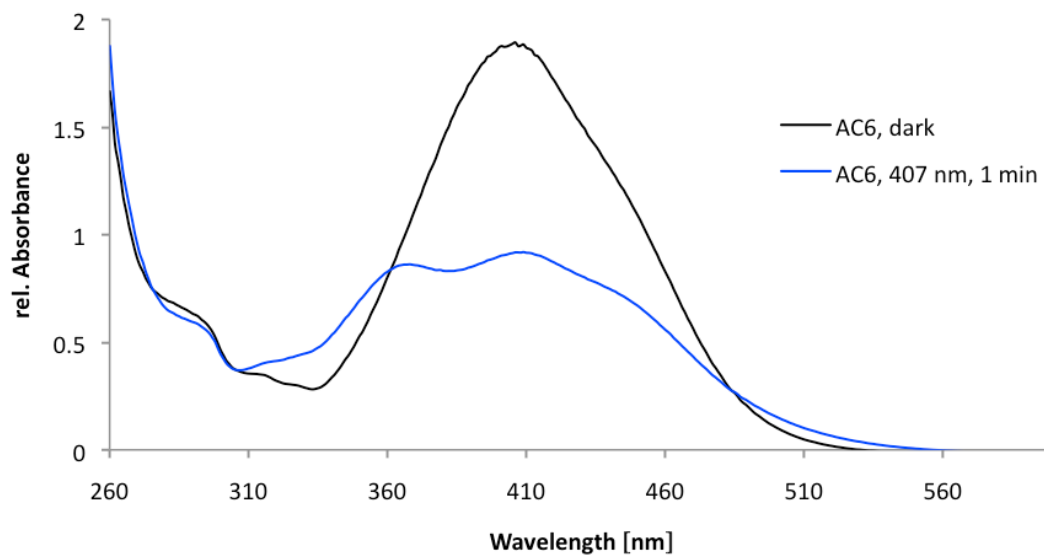
UV/Vis of AC4



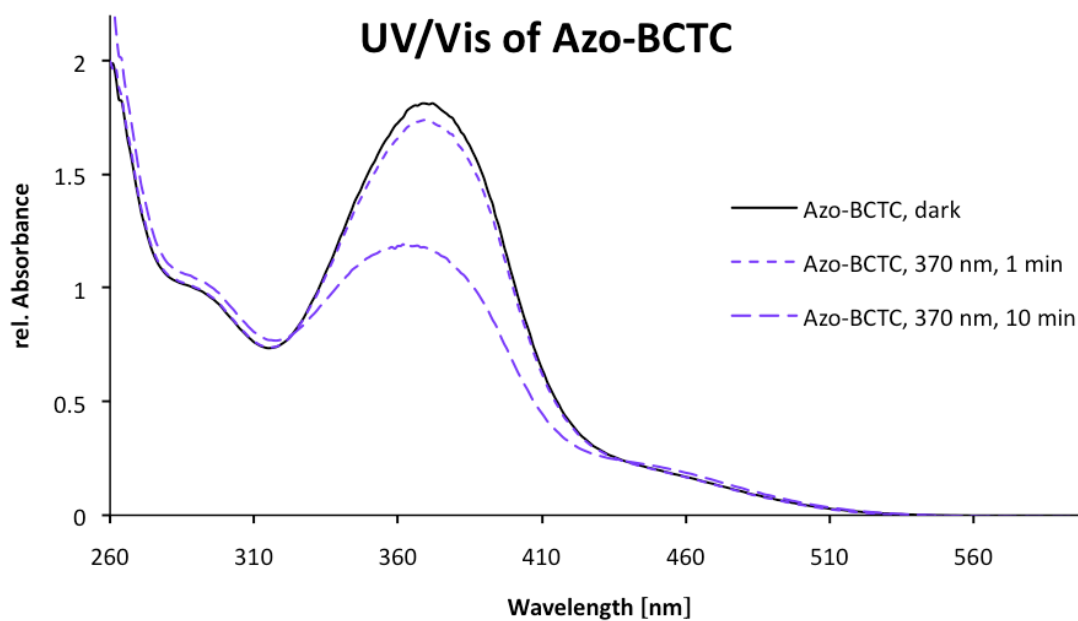
UV/Vis of AC5



UV/Vis of AC6



UV/Vis of Azo-BCTC



Determination of Antagonistic Potencies of AC1–3 and AC5–6 upon Activation of TRPV1 with CAP

Antagonistic potencies were determined by aequorin-based calcium measurements. TRPV1 was activated by addition of 1 μM CAP to increasing concentrations of antagonists. Figure 3.7 displays the dose-response curves of AC1–3 and AC5–6 ($n = 3\text{--}4$). IC_{50} values are summarized in Table 3.1.

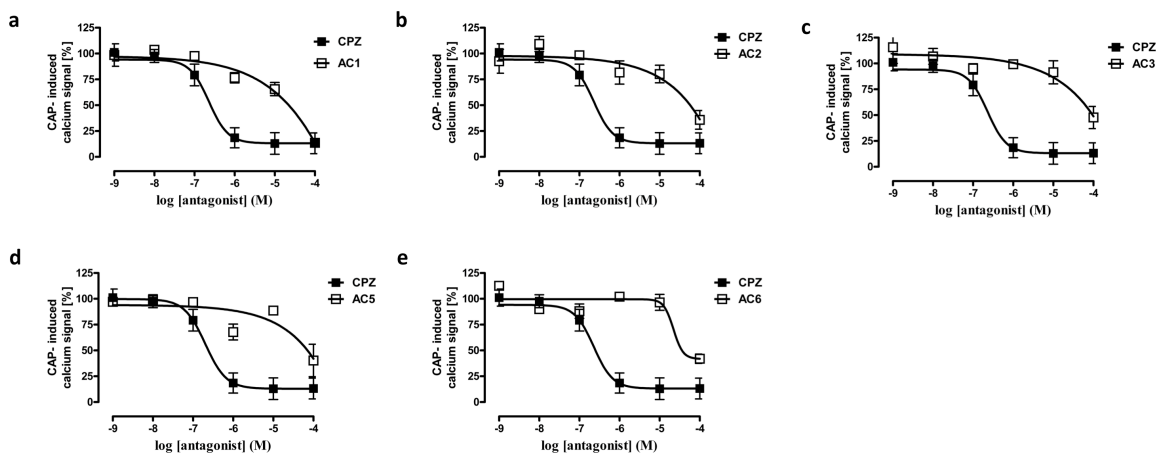


Figure 3.7. Dose-response curves of **a) – c) AC1–3** and **d) – e) AC5–6** upon TRPV1 activation with 1 μM CAP, compared to CPZ ($n = 3\text{--}4$).

Table 3.1. Determination of IC_{50} values of AC derivatives upon TRPV1 activation with 1 μM CAP.

Antagonist	IC_{50} (1 μM CAP)
AC1	> 50 μM
AC2	> 50 μM
AC3	> 50 μM
AC5	> 50 μM
AC6	> 50 μM

Cell Culture

HEK 293T cells were cultured under standard conditions (Dulbecco's modified Eagle medium (DMEM) containing 10% FBS; 37 °C, 10% CO₂). Cells were plated on poly-L-lysine (0.1 mg/ml) treated coverlips in a density of 20,000 cells per cm² for electrophysiological measurements.

HEK 293 cells were transfected with TRPV1-YFP^[52] (kindly provided by Dr. Tim D. Plant, Institute for Pharmacology and Toxicology, Marburg, Germany) using PromoFectin[®] transfection agent according to the manufacturers instructions and measured after 12–24 h.

Whole-cell Electrophysiology

Patch clamp recordings of HEK 293T cells were carried out using a HEKA Patch Clamp EPC10 USB amplifier in whole cell mode and were performed at room temperature. Cells were voltage-clamped at –60 mV. Pipettes (Science Products GB200-F-8P with filament) were pulled with a Narishige PC-10 pipette puller and had resistances of 4–6 MΩ. The Bath solution contained 150 mM NaCl, 6.0 mM CsCl, 1.0 mM MgCl₂, 1.5 mM CaCl₂, 10 mM HEPES and 10 mM glucose, adjusted to pH = 7.4. Pipette solution contained 150 mM NaCl, 3.0 mM MgCl₂, 10.0 mM HEPES and 5.0 mM EGTA, adjusted to pH = 7.2.^[25] Data was recorded using the HEKA PatchMaster software (V2x60). The sampling rate was 20–50 kHz and the currents were digitally filtered at 2.9 kHz. Cells were illuminated with a Polychrome V monochromator (Till Photonics), as described previously.^[53]

Aequorin-based Calcium Measurements

Total luminescence in HEK 293 cells, co-transfected with the aequorin encoding plasmid G5α^[54] and TRPV1-YFP,^[52] was measured using a FLUOstar[®] Omega plate reader at 37 °C after labelling of the cells with coelenterazine H (5 μM) for 30 min at room temperature. HBS as a control was automatically injected 5 s after starting the measurement. In intervals of 1 s total emission was monitored and the area under the curve (AUC) determined. AUC of calcium signals induced by 1 μM CAP in the absence of any antagonist was set to 100% and effects of various antagonist concentrations determined in %. Data were analyzed using Prism4.0 (GraphPad Software Inc., San Diego, CA).

3.3 AZO-CAPSAZEPINES IN THE RETINA

Capsazepine is known to act also as an antagonist on TRPM1 channels^[55] which are involved in the ON-pathway in the vision cascade (see 5.1). Therefore, the most promising of all Azo-Capsazepine derivatives, **AC4**, and the red-shifted **AC3** were tested for light-dependent modulation of retinal activity in dissected blind mouse retinae ($\rho^{-/-}$, $\text{cngA3}^{-/-}$, $\text{opn4}^{-/-}$; Laura Laprell, LMU). Application of both compounds resulted in increased spiking. However, neither **AC3** (20 μM) nor **AC4** (10–20 μM) showed significant pattern changes when illuminated with different wavelengths according to their absorption spectra (**AC3**: dark/480 nm; **AC4**: 360/480 nm).

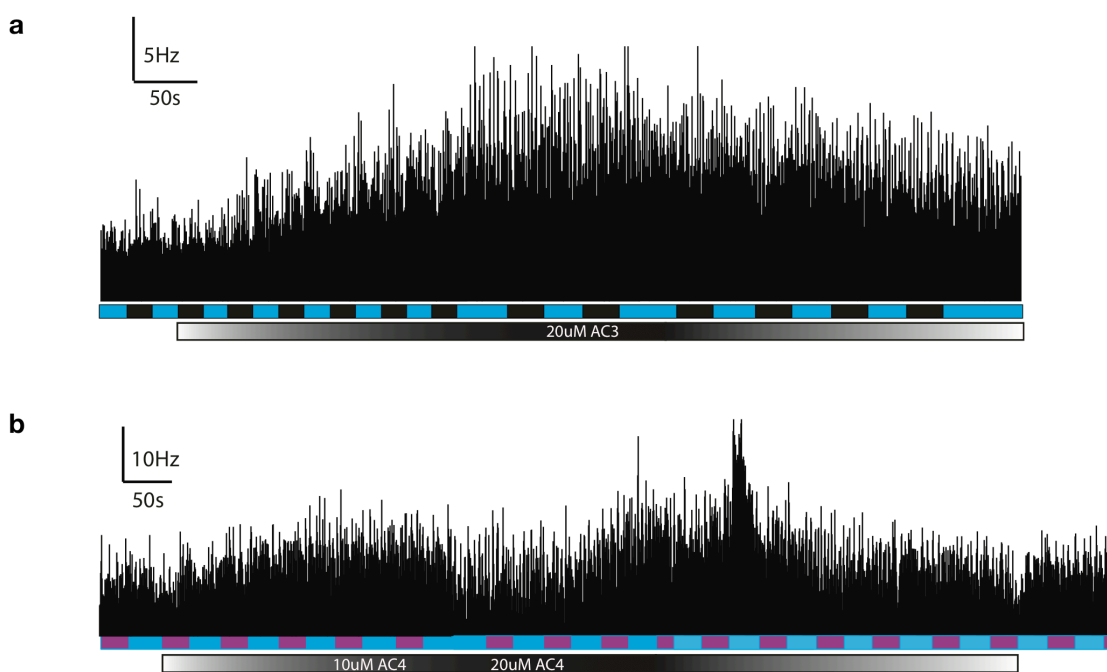


Figure 3.8. No photodependent activity of **a) AC3** (20 μM) and **b) AC4** (10–20 μM) in dissected blind mouse retina recordings (black: darkness; blue: $\lambda = 480$ nm; purple: $\lambda = 360$ nm; Laura Laprell, LMU).

3.4 THE MENTHOL RECEPTOR TRPM8

The functions of TRPM channels are highly diverse and comprise Mg^{2+} homeostasis (TRPM6, TRPM7),^[56] taste detection (TRPM5),^[57] cell proliferation (TRPM7)^[56a] as well as detection of warm temperatures (TRPM5)^[20] and noxious cold (TRPM8).^[21a] TRPM1 was moreover shown to be part of the ON bipolar pathway of the human vision cascade, being involved in the inversion of the mGluR6 signal in ON bipolar cells.^[55] The detailed mechanism of this sign inversion, however, is not yet fully understood. Among all TRP channels, TRPM4 and TRPM5 appear to be the only members of this large family that are impermeable to Ca^{2+} .^[1,58]

The so-called cold or menthol receptor TRPM8 was first discovered by McKemy *et al.* in 2002^[21a] and was found to respond to cold temperatures as well as to the cooling agents menthol and eucalyptol (Fig. 3.9).^[21a,21b]



Figure 3.9. Structures of TRPM8 agonists (-)-menthol and eucalyptol.

TRPM8 was originally identified in prostate cancer, followed by many other non-prostatic tumors.^[59] It is also found in the bladder and in various tissues of the male genital tract.^[60] Attributing to its temperature and pain perception function, TRPM8 is also located in sensory neurons.^[1] The cold activation of TRPM8 is hypothesized to occur – similar to TRPV1 channels – *via* a temperature-dependent shift of the voltage activation of the channel.^[25]

The pleasant perception of coolness is transduced mainly by low-threshold thermoceptors expressing TRPM8 channels, whereas high-threshold nociceptors are responsible for the perception of cold pain. The latter is mediated also by TRPM8 channels and the voltage-gated sodium channel Na_v 1.8. Moreover, TRPA1 channels in sensitized nociceptors may contribute to the perception of noxious cold but their exact role and specific temperature dependence is still under debate (Fig. 3.10).^[61] For example, in a recent study TRPA1 was observed to be insensitive to cold temperatures but cold did amplify agonist evoked TRPA1 currents.^[62] TRPA1 activation is now speculated to lead to cold hypersensitivity, possibly transduced *via* TRPM8.^[61]

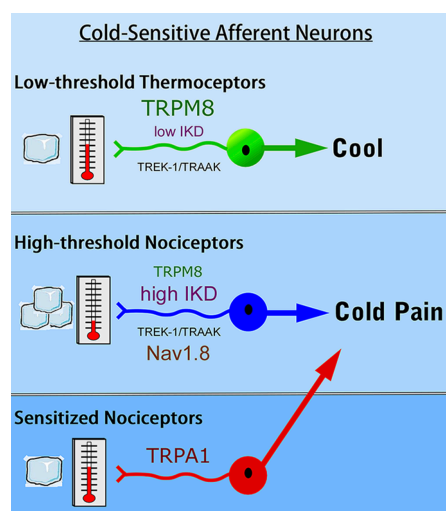


Figure 3.10. TRPM8 mediates the perception of cold temperatures and cold pain, whereas TRPA1 is believed to be related to pain perception only. Illustration copied from McKemy,^[61] reprinted with permission from the American Chemical Society. Copyright 2013.

3.5 AZO-ICILIN

Icilin is a synthetic super-agonist of TRPM8 channels with an EC_{50} value of $0.2 \mu\text{M}$.^[21] Although structurally not related to menthol, it produces an extreme sensation of cold both in humans and animals. It is ~ 200 times more potent than menthol and 2.5 times more efficacious.^[63]

Although there is little information published on the structure–activity relationship of icilin, one derivative bearing a chlorine atom instead of the nitro group is known to retain agonistic effects on TRPM8. Consequently, the *m*-NO₂ group was chosen as an anchor for an azobenzene moiety, leading to the photoswitchable analogue **Azo-Icilin 1 (AI1)**; Fig. 3.11).

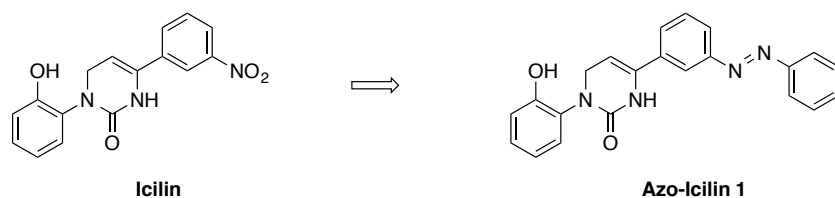
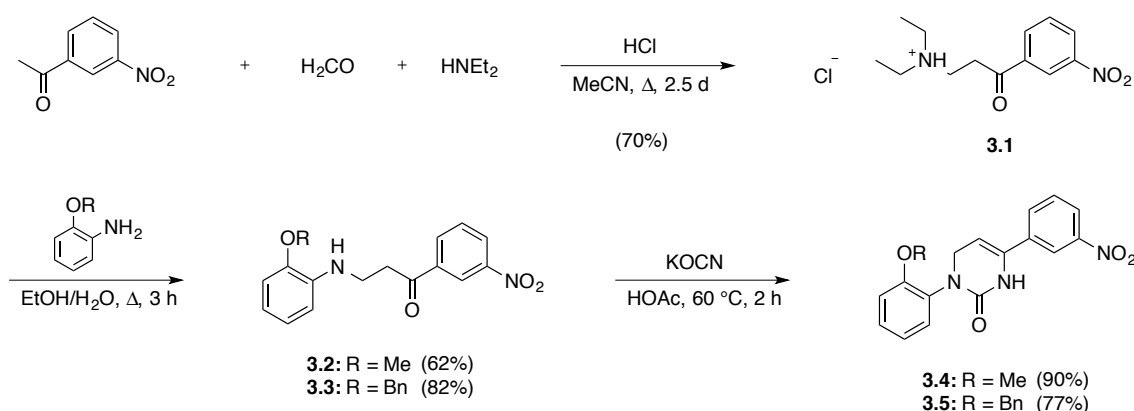


Figure 3.11. Structures of icilin and **AI1**.

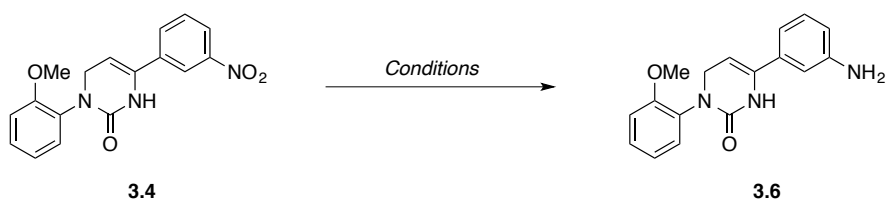
Synthesis of Azo-Icilin 1

The synthesis of **AII** was based on the original synthesis of icilin by Delmar Chemicals Ltd.^[64] Starting from *m*-nitroacetophenone, a Mannich reaction with paraformaldehyde and diethyl amine yielded **3.1** in 70% as the hydrochloride salt.^[65] Unfortunately, using the reported conditions^[64] for the next step, reaction of **3.1** with the unprotected *o*-hydroxy aniline did not lead to the desired substitution product. However, replacing the unprotected phenol with methyl or benzyl protected derivatives led to the desired secondary amines **3.2** and **3.3** in 62% and 82% yield, respectively. Ring closure with potassium cyanate afforded methyl (**3.4**) and benzyl protected icilin (**3.5**) in excellent yields (Scheme 3.8).



Scheme 3.8. Synthesis of phenol protected icilin derivatives **3.4** and **3.5**.

In order to introduce the azobenzene moiety, several attempts to reduce the nitro group of **3.4** to the corresponding aniline **3.6** were undertaken, leading to different results (Scheme 3.9, Table 3.2).

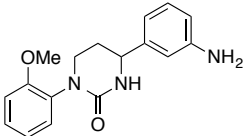


Scheme 3.9. Attempted conditions for the reduction of **3.4** to the aniline **3.6**.

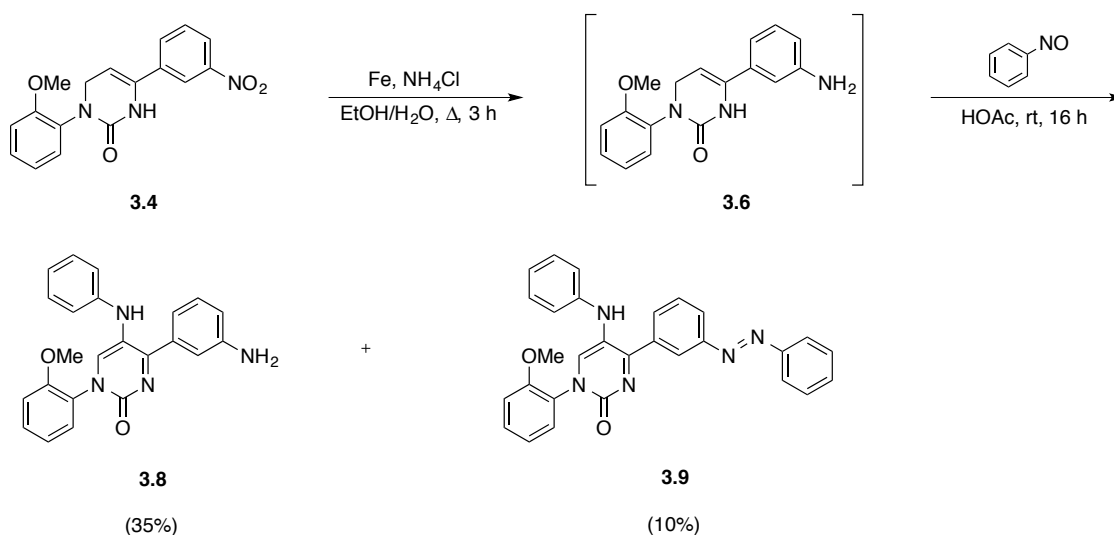
Hydrogen and palladium on charcoal quantitatively yielded **3.7**, in which in addition to the nitro functionality the benzylic double bond was reduced (Table 3.2, entry 1). Attempts with sodium sulfide gave the desired product in 34–40% yield with no other isolated side products (entry 2). Using the rather harsh conditions with tin(II) chloride in concentrated hydrochloric acid led to decomposition of the starting material (entry 3). Zinc in glacial acetic acid afforded **3.6** in 70%

yield (entry 5) but the best results were obtained with iron and ammonium chloride in a refluxing ethanol/water mixture, yielding **3.6** reliably in 80–90% (entry 4).

Table 3.2. Conditions for the reduction of **3.4** to **3.6**.

Entry	Reagent	Conditions	Yield 3.6 [%]	Yield other products [%]
1	H ₂ , Pd/C	MeOH, rt, 1.5 h	0	 3.7 , 100
2	Na ₂ S	1,4-dioxane/H ₂ O, 90 °C, 1 h	34–40	-
3	SnCl ₂ , HCl	rt, 3.5 h	0	-
4	Fe, NH ₄ Cl	EtOH/H ₂ O, Δ, 3 h	80–90	-
5	Zn, HOAc	50 °C, 3 h	70	-

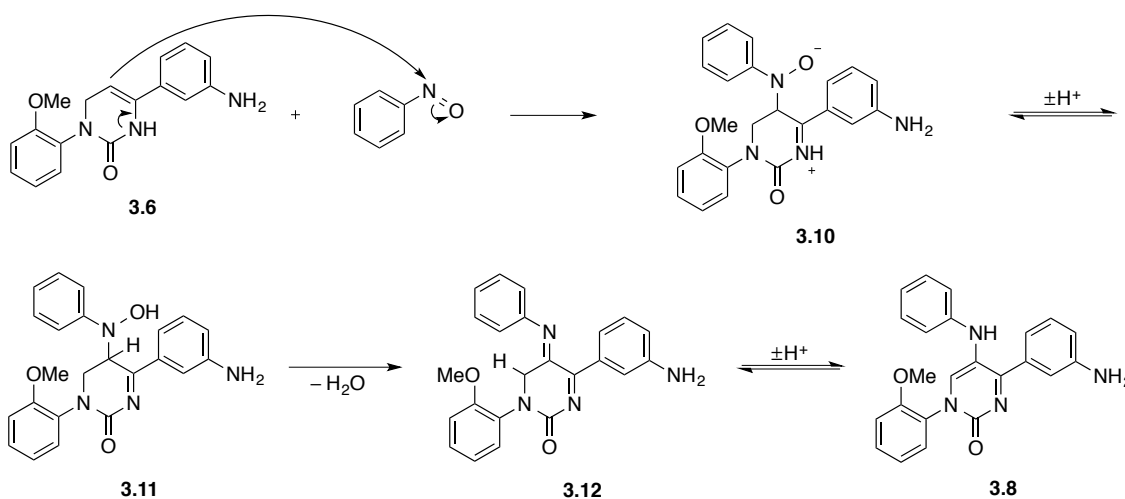
However, since it was not possible to purify **3.6** completely, the so obtained aniline was used crude for the next step (Scheme 3.10). Aniline **3.6** was stirred under Mills conditions with nitrosobenzene, leading to two yellow to orange products which after isolation and characterization turned out to be undesired compounds **3.8** (35% yield) and **3.9** (10%), respectively. The desired Mills product was not observed.



Scheme 3.10 Undesired enamine attack of **3.6** to nitrosobenzene.

A proposed reaction mechanism for the formation of **3.8** is given in Scheme 3.11. The enamine portion of **3.6** nucleophilically attacks the nitrogen of the nitrosobenzene, leading to

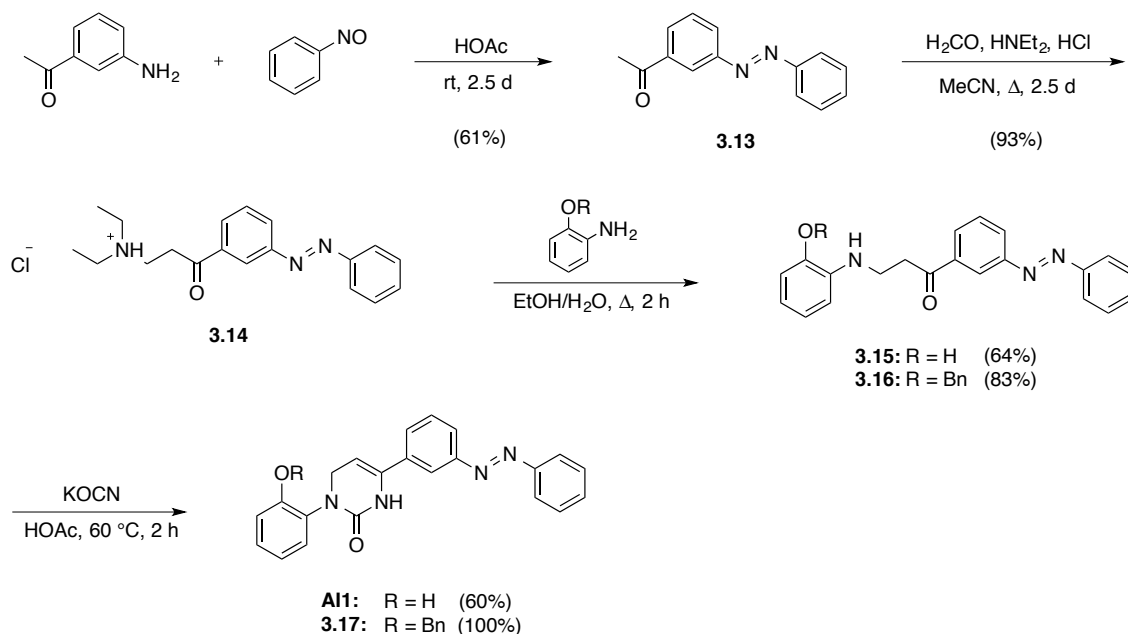
intermediate **3.10** which, after proton transfer, gives hydroxylamine **3.11**. Acid catalyzed dehydration leads to imine **3.12** which is converted into enamine **3.8** through imine-enamine tautomerism. The full aromatization and therefore high stability of **3.8** might be an important feature in this reaction pathway. In a following, second reaction sequence, a regular Mills reaction with a second equivalent of nitrosobenzene then presumably furnishes **3.9**.



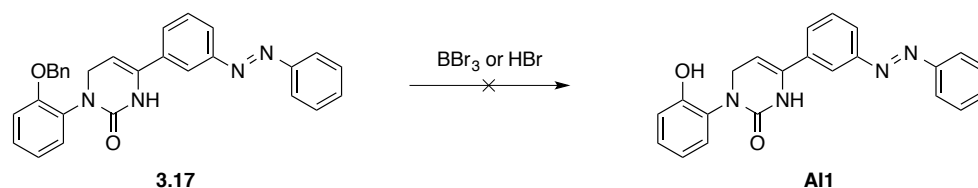
Scheme 3.11. Proposed reaction mechanism of **3.6** and nitrosobenzene to **3.8**.

Subsequently, a new route was developed introducing the azobenzene moiety early on in the synthesis (Scheme 3.12). Mannich precursor **3.13** was synthesized by a Mills reaction of *m*-aminoacetophenone and nitrosobenzene in 61% yield. Ketone **3.13** was then submitted to Mannich conditions (paraformaldehyde, diethylamine, acid catalysis) to provide HCl salt **3.14** in excellent yield (93%). Having obtained poor results with unprotected *o*-hydroxy aniline in the previous route toward **A11**, **3.14** was first condensed with benzyl protected *o*-hydroxy aniline to give **3.16** in 83% yield. Reaction with KOCN yielded benzyl protected Azo-Icilin **3.17** quantitatively. However, attempts to remove the benzyl ether using BBr_3 or HBr in HOAc , respectively, led to decomposition of the starting material (Scheme 3.13).

In another attempt to condense the Mannich product **3.14** with unprotected *o*-hydroxy aniline, the desired product **3.15** was obtained in a good yield of 64%. Formation of the heterocycle with KOCN finally gave rise to **A11** in 60% yield (Scheme 3.12).



Scheme 3.12. Synthesis of Azo-Icilin **1**.



Scheme 3.13. Attempted removal of the benzyl ether of **3.17**.

Biological Evaluation of Azo-Icilin **1**

The absorption maxima of **AII** were determined to be $\lambda = 320$ nm and $\lambda = 435$ nm, respectively (Fig. 3.12a). Subsequent testing in transiently TRPM8 transfected HEK 293 cells was carried out to determine whether **AII** remained an agonist for the channel. Expression of TRPM8 was assured in control experiments by cold activation of the channel with cold buffer solution (not shown). **AII** at various concentrations (0.1–10 μ M) was applied *via* a puff pipette to the cells, leading to a robust inward current, proving the agonistic activity of **AII** (Fig. 3.12b). The current, however, appeared to be steadily increasing, reaching no baseline current which might attribute to the relatively high hydrophobicity of the compound. Application of light of different wavelengths did not lead to light-dependent changes of current. In a different experiment, additional activation of the channel with a voltage step to +200 mV did result in photoswitchable currents when **AII** was applied at a concentration of 5 μ M. Switching between $\lambda = 350$ nm and $\lambda = 440$ nm led to changes in current of >1 nA (Fig. 3.12c).

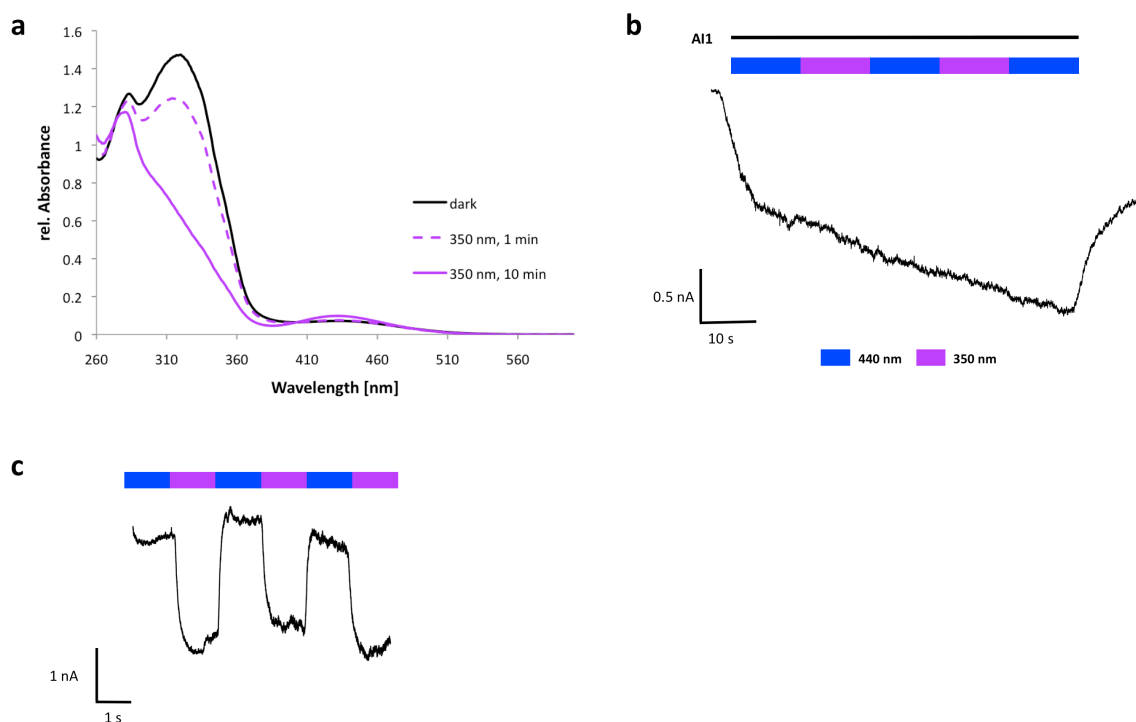
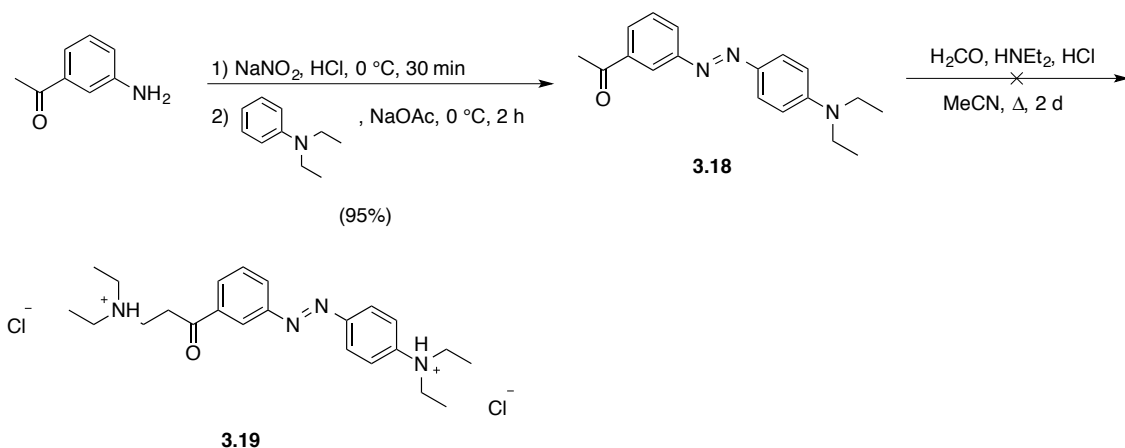


Figure 3.12. **a)** UV/Vis spectrum of **AI1** (DMSO) with peak absorptions at $\lambda = 320$ nm and $\lambda = 435$ nm. **b)** Puff application of **AI1** ($2 \mu\text{M}$) to HEK 293 cells, transiently transfected with TRPM8. The current steadily increased but no changes upon irradiation with either $\lambda = 440$ nm (blue) or $\lambda = 350$ nm (purple) were observed (holding potential -60 mV). **c)** Voltage activation of TRPM8 ($+200$ mV) during application of **AI1** ($5 \mu\text{M}$) resulted in photoswitchable currents of ~ 2 nA.

Taken together, the results obtained with **AI1** proved the tolerance of icilin toward substitution with *meta*-azobenzenes on the dihydropyrimidone moiety, since **AI1** still acts as agonist on TRPM8. The photoswitchable currents upon voltage activation of the channel indicate the potential of photoswitchable icilin derivatives. These findings prompted the development of further azobenzene derivatives of icilin which is described in the following section.

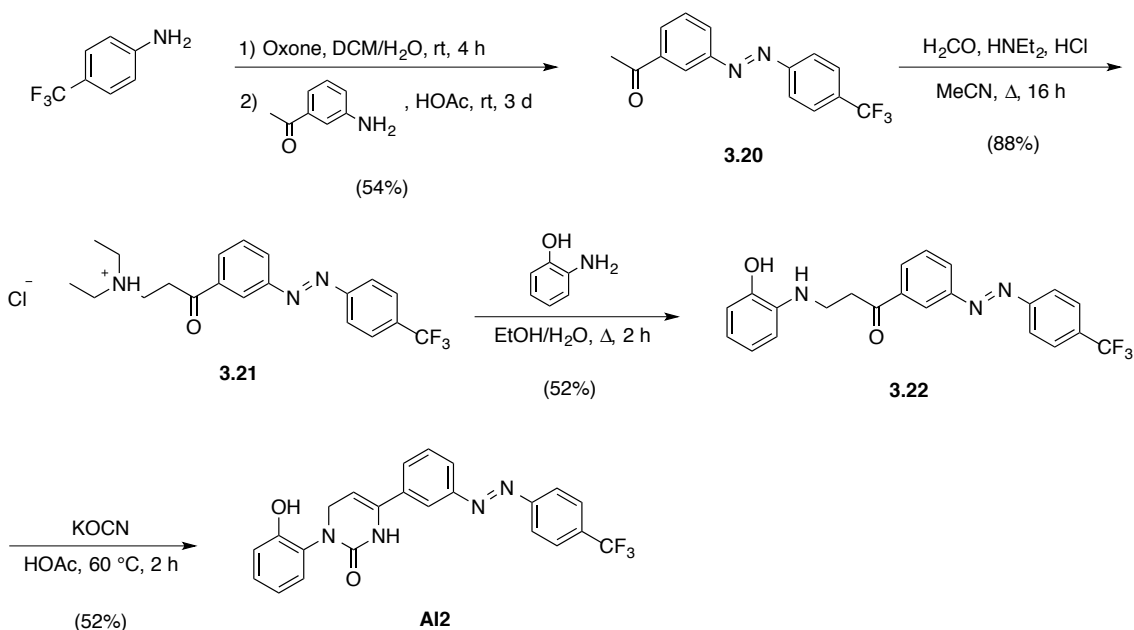
Synthesis of **AI2** and **AI3**

Initial attempts to synthesize a red-shifted, *p*-diethylamino substituted Azo-Icilin derivative failed. Mannich precursor **3.18** was synthesized in 95% yield from 3-aminoacetophenone by diazotization and subsequent coupling to *N,N*-diethylaniline. Ketone **3.18** was then subjected to Mannich conditions as previously established but the desired product **3.19** could not be isolated, probably owing to the influence of the basic nitrogen of the diethylamino group (Scheme 3.14).



Scheme 3.14. Attempted synthesis of a *p*-diethylamino substituted Azo-Icilin derivative.

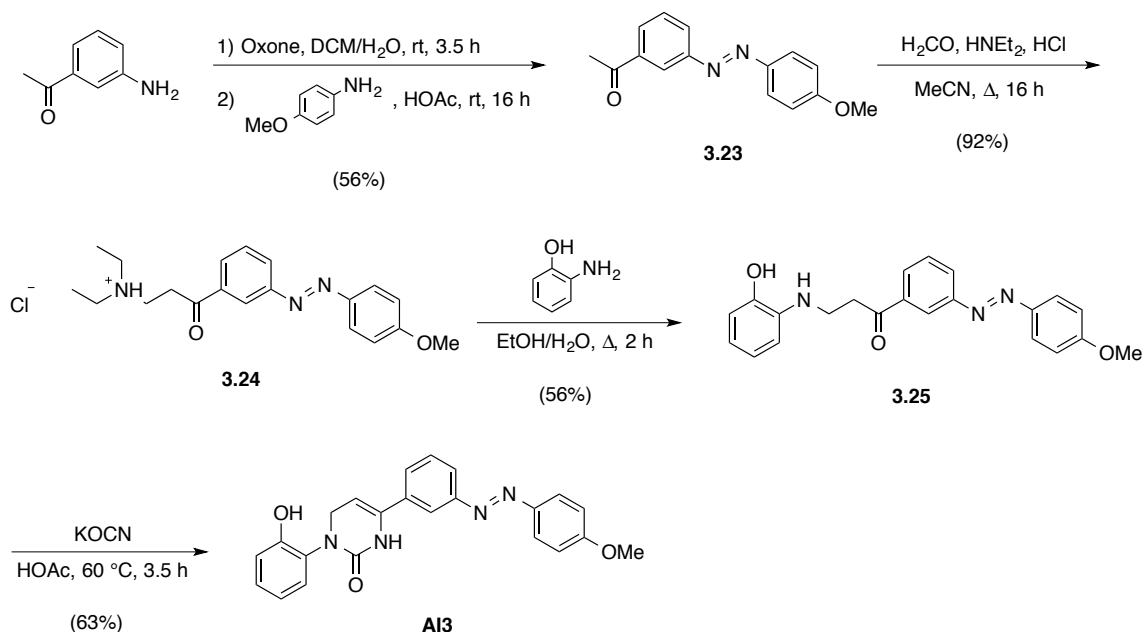
The synthesis of a trifluoromethyl analogue, termed **A12**, was more successful. Firstly, 4-trifluoromethylaniline was oxidized to the corresponding nitroso compound and then condensed with 3-aminoacetophenone in a Mills reaction, furnishing azobenzene **3.20** in 54% yield. A Mannich reaction of **3.20** with paraformaldehyde and diethyl amine under acidic catalysis led to Mannich product **3.21** in 88% yield which was further reacted with 2-hydroxyaniline to yield **3.22** in 52% yield. Finally, formation of the dihydropyrimidone ring was achieved by reaction of **3.22** with potassium cyanate (52% yield; Scheme 3.15).



Scheme 3.15. Synthesis of **A12**.

The synthesis of **A13**, a *p*-methoxy analogue of Azo-Icilin, commenced with oxidation of 3-aminoacetophenone to the corresponding nitroso derivative using oxone, followed by condensation with *p*-anisidine to give azobenzene **3.23** in 56% yield. Reaction of ketone **3.23**

with paraformaldehyde and diethyl amine gave Mannich product **3.24** in 92% yield. Substitution with 2-hydroxyaniline then led to secondary amine **3.25** in 56% yield. Finally, ring closure with potassium cyanate afforded **AI3** in 63% yield (Scheme 3.16).



Scheme 3.16. Synthesis of **AI3**.

The absorption maxima of **AI2** and **AI3** were determined to be at $\lambda = 314$ nm and $\lambda = 428$ nm (**AI2**, Fig. 3.13a), as well as at $\lambda = 355$ nm and $\lambda = 440$ nm (**AI3**, Fig. 3.13b). Both derivatives **AI2** and **AI3** were tested in transiently TRPM8 transfected HEK 293 cells on their ability to directly activate the channel in a light-dependent fashion. However, neither **AI2** nor **AI3** showed direct activation of TRPM8 at concentrations up to 10 μ M (data not shown). Voltage activation of TRPM8 (+200 mV) in the presence of 10 μ M **AI2** resulted in a small photoswitchable current (~40 pA compared to ~2 nA for **AI1**; data not shown).

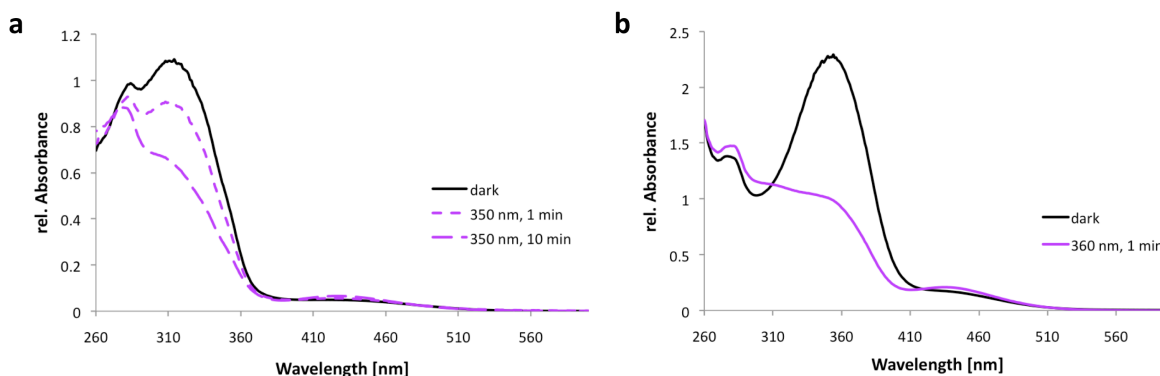


Figure 3.13. UV/Vis spectra of **a) AI2** (DMSO, $\lambda_{\text{max}} = 314$ nm, 428 nm) and **b) AI3** (DMSO, $\lambda_{\text{max}} = 355$ nm, 440 nm).

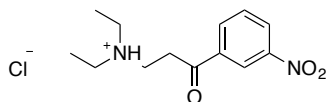
3.6 EXPERIMENTAL PROCEDURES AND ANALYTICAL DATA

3.6.1 GENERAL EXPERIMENTAL DETAILS AND INSTRUMENTATION

All reactions were carried out with magnetic stirring and if air or moisture sensitive in oven-dried glassware under an atmosphere of nitrogen or argon. Syringes used to transfer reagents and solvents were purged with nitrogen or argon prior to use. Reagents were used as commercially supplied unless otherwise stated. Thin layer chromatography was performed on pre-coated silica gel F₂₅₄ glass backed plates and the chromatogram was visualized under UV light and/or by staining using aqueous acidic vanillin or potassium permanganate, followed by gentle heating with a heat gun. Flash column chromatography was performed using silica gel, particle size 40–63 μm (eluants are given in parenthesis). The diameter of the columns and the amount of silica gel were calculated according to the recommendations of W. C. Still *et al.*^[50] IR spectra were recorded on a Perkin Elmer Spectrum Bx FT-IR instrument as thin films with absorption bands being reported in wave number (cm^{-1}). UV/Vis spectra were obtained using a Varian Cary 50 Scan UV/Vis spectrometer and Helma SUPRASIL precision cuvettes (10 mm light path).

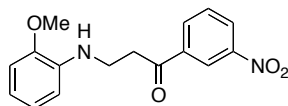
¹H and ¹³C NMR spectra were measured on Varian VNMRS 300, VNMRS 400, INOVA 400 or VNMRS 600 instruments. The chemical shifts are quoted as δ -values in ppm referenced to the residual solvent peak (CDCl_3 : δ_{H} 7.26, δ_{C} 77.2; CD_3OD : δ_{H} 3.31, δ_{C} 49.0; DMSO-d_6 : δ_{H} 2.50, δ_{C} 39.5).^[51] Multiplicities are abbreviated as follows: s = singlet, d = doublet, t = triplet, q = quartet, quint = quintet, sext = sextet, sept = septet, m = multiplet. High resolution mass spectra (EI, ESI) were recorded by LMU Mass Spectrometry Service using a Thermo Finnigan MAT 95, a Jeol MStation or a Thermo Finnigan LTQ FT Ultra instrument. Melting points were obtained using a Stanford Research Systems MPA120 apparatus and are uncorrected.

3.6.2 SYNTHESIS OF AZO-ICILINS

Synthesis of *N,N*-diethyl-3-(3-nitrophenyl)-3-oxopropan-1-aminium chloride (**3.1**)

Diethylamine (3.43 mL, 33.3 mmol, 1.0 equiv.) was dissolved in MeCN (270 mL) and conc. HCl (2.98 mL) was added. Paraformaldehyde (3.00 g, 100 mmol, 3.0 equiv.) was added, followed by *m*-nitroacetophenone (16.5 g, 100 mmol, 3.0 equiv.). The mixture was heated to reflux for 2.5 d. The solvent was removed under reduced pressure and the residue was triturated with Et₂O (2 x 250 mL). The colorless solid was recrystallized from acetone (150 mL) and dried overnight under high vacuum. The HCl salt of Mannich product **3.1** was obtained in 70% yield (6.69 g, 23.3 mmol) as colorless needles.

M.p.: 119–121 °C. **¹H NMR (DMSO-*d*₆, 400 MHz, 27 °C):** δ = 10.46 (br s, 1H, NH), 8.70 (dd, J = 2.0, 2.0 Hz, 1H, ArH), 8.49 (ddd, J = 8.2, 2.4, 1.2 Hz, 1H, ArH), 8.41 (ddd, J = 8.2, 2.4, 1.2 Hz, 1H, ArH), 7.85 (dd, J = 8.2, 8.2 Hz, 1H, ArH), 3.73–3.66 (m, 2H, CH₂), 3.42–3.35 (m, 2H, CH₂), 3.16 (dq, J = 7.2, 2.4 Hz, 4H, 2 x CH₂), 1.22 (t, J = 7.2 Hz, 6H, 2 x CH₃) ppm. **¹³C NMR (DMSO-*d*₆, 100 MHz, 27 °C):** δ = 195.7, 148.5, 137.7, 134.6, 131.1, 128.2, 122.9, 46.8, 45.9, 32.3, 9.0 ppm. **IR (neat, ATR):** $\tilde{\nu}$ = 2444 (m), 1692 (s), 1612 (w), 1530 (s), 1478 (m), 1441 (m), 1387 (w), 1352 (vs), 1213 (m), 1170 (w), 1154 (w), 1109 (w), 1088 (w), 1065 (w), 1046 (w), 1005 (w), 965 (w), 924 (w), 880 (w), 845 (m), 811 (m), 784 (m), 732 (vs), 692 (m), 676 (m) cm⁻¹. **HRMS (ESI⁺):** m/z calcd. for [C₁₃H₁₉N₂O₃]⁺: 251.1396, found: 251.1390 ([M-Cl]⁺).

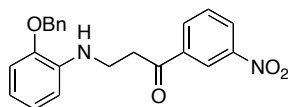
Synthesis of 3-((2-methoxyphenyl)amino)-1-(3-nitrophenyl)propan-1-one (**3.2**)

The HCl salt of amine **3.1** (1.43 g, 5.00 mmol, 1.1 equiv.) and *o*-anisidine (0.51 mL, 4.6 mmol, 1.0 equiv.) were dissolved in ethanol (7.5 mL) and water (7.5 mL) and heated to reflux for 3 h. The mixture was cooled and a sat. aqu. solution of NaHCO₃ was added (50 mL). The aqueous phase was extracted with EtOAc (50 mL). The organic phase was washed with sat. aqu. NaHCO₃ (50 mL) and concentrated under reduced pressure. The crude product was purified by

flash silica gel column chromatography (hexanes/EtOAc, gradient from 6:1 to 4:1) to give secondary amine **3.2** (854 mg, 2.84 mmol, 62%) as a red solid.

TLC (hexanes/EtOAc, 2:1): $R_f = 0.55$. **M.p.:** 95–96 °C. **$^1\text{H NMR}$ (CDCl_3 , 300 MHz, 27 °C):** $\delta = 8.78\text{--}8.73$ (m, 1H, ArH), 8.45–8.36 (m, 1H, ArH), 8.30–8.23 (m, 1H, ArH), 7.66 (dd, $J = 8.0, 8.0$ Hz, 1H, ArH), 6.92–6.84 (m, 1H, ArH), 6.79–6.73 (m, 1H, ArH), 6.72–6.64 (m, 2H, ArH), 4.54 (br s, 1H, NH), 3.81 (s, 3H, CH_3), 3.71–3.65 (m, 2H, CH_2), 3.39–3.31 (m, 2H, CH_2) ppm. **$^{13}\text{C NMR}$ (CDCl_3 , 75 MHz, 27 °C):** $\delta = 196.9, 148.4, 147.1, 138.0, 137.3, 133.5, 129.9, 127.4, 122.9, 121.2, 116.9, 109.7, 109.6, 53.4, 38.3, 38.2$ ppm. **IR (neat, ATR):** $\tilde{\nu} = 3413$ (w), 3081 (w), 2939 (w), 2902 (w), 2869 (w), 2836 (w), 1689 (m), 1613 (m), 1601 (m), 1525 (s), 1511 (vs), 1476 (m), 1456 (m), 1432 (m), 1347 (vs), 1319 (m), 1248 (m), 1221 (vs), 1178 (m), 1128 (m), 1097 (m), 1050 (m), 1027 (m), 1001 (m), 903 (w), 807 (w), 732 (vs), 698 (w), 672 (m) cm^{-1} . **HRMS (ESI $^+$):** m/z calcd. for $[\text{C}_{16}\text{H}_{17}\text{N}_2\text{O}_4]^+$: 301.1188, found: 301.1183 ($[\text{M}+\text{H}]^+$).

Synthesis of 3-((2-(benzyloxy)phenyl)amino)-1-(3-nitrophenyl)propan-1-one (**3.3**)

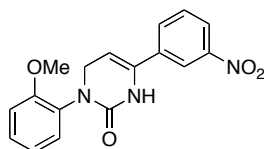


The HCl salt of amine **3.1** (2.00 g, 6.97 mmol, 1.1 equiv.) and 2-benzyloxyaniline (1.26 g, 6.34 mmol, 1.0 equiv.) were dissolved in ethanol (12 mL) and water (12 mL) and heated to reflux for 3 h. The mixture was cooled and a sat. aqu. solution of NaHCO_3 was added (70 mL). The aqueous phase was extracted with EtOAc (2 x 50 mL). The organic phase was washed with sat. aqu. NaHCO_3 (70 mL) and concentrated under reduced pressure. The crude product was purified by flash silica gel column chromatography (hexanes/EtOAc, gradient from 10:1 to 5:1) to give secondary amine **3.3** (1.97 g, 5.23 mmol, 82%) as a red oil.

TLC (Hexane/EtOAc, 2:1): $R_f = 0.64$. **$^1\text{H NMR}$ (CDCl_3 , 600 MHz, 27 °C):** $\delta = 8.77\text{--}8.73$ (m, 1H, ArH), 8.41 (ddd, $J = 7.8, 2.4, 1.2$ Hz, 1H, ArH), 8.25 (ddd, $J = 7.8, 1.8, 1.2$ Hz, 1H, ArH), 7.65 (dd, $J = 7.8, 7.8$ Hz, 1H, ArH), 7.42–7.36 (m, 4H, ArH), 7.35–7.31 (m, 1H, ArH), 6.91 (ddd, $J = 7.8, 7.8, 1.2$ Hz, 1H, ArH), 6.84 (dd, $J = 8.4, 1.2$ Hz, 1H, ArH), 6.72 (dd, $J = 8.4, 1.2$ Hz, 1H, ArH), 6.67 (ddd, $J = 7.8, 7.8, 1.2$ Hz, 1H, ArH), 5.05 (s, 2H, CH_2), 4.66 (br s, 1H, NH), 3.72–3.67 (m, 2H, CH_2), 3.36–3.31 (m, 2H, CH_2) ppm. **$^{13}\text{C NMR}$ (CDCl_3 , 150 MHz, 27 °C):** $\delta = 196.9, 148.4, 146.3, 138.0, 137.6, 137.0, 133.5, 129.9, 128.6, 128.0, 127.5, 127.5, 122.9, 121.7, 116.9, 111.4, 110.1, 70.5, 38.3, 38.2$ ppm. **IR (neat, ATR):** $\tilde{\nu} = 3414$ (w), 3061 (w), 2871 (w), 1689 (m), 1601 (m), 1523 (s), 1511 (s), 1473 (m), 1441 (m), 1378 (m), 1347

(vs), 1314 (m), 1249 (m), 1206 (s), 1162 (w), 1128 (m), 1093 (m), 1015 (m), 918 (w), 853 (w), 808 (w), 731 (vs), 697 (m), 671 (m) cm^{-1} . **HRMS (ESI⁺):** m/z calcd. for $[\text{C}_{22}\text{H}_{21}\text{N}_2\text{O}_4]^+$: 377.1501, found: 377.1494 ($[\text{M}+\text{H}]^+$).

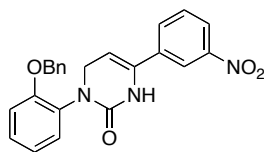
Synthesis of 3-(2-methoxyphenyl)-6-(3-nitrophenyl)-3,4-dihydropyrimidin-2(1H)-one (3.4)



Secondary amine **3.2** (775 mg, 2.30 mmol, 1.0 equiv.) was dissolved in 4 M HCl in 1,4-dioxane (15 mL) and concentrated under reduced pressure. The so obtained HCl salt was then dissolved in glacial acetic acid (20 mL) and potassium cyanate (673 mg, 8.3 mmol, 3.6 equiv.) was added. The mixture was heated to 60 °C for 2 h. Water (20 mL) and sat. aqu. NaHCO_3 (50 mL) were added and the aqueous phase was extracted with CHCl_3 (2 x 30 mL). The combined organic phases were washed with sat. aqu. NaHCO_3 (2 x 30 mL), dried over MgSO_4 and concentrated under reduced pressure, yielding tricycle **3.4** (678 mg, 2.08 mmol, 90%) as a yellow solid. An analytical sample was purified by flash silica gel column chromatography ($\text{CHCl}_3/\text{MeOH}$, gradient from 100:0 to 80:1).

TLC ($\text{CHCl}_3/\text{MeOH}$, 40:1): R_f = 0.23. **M.p.:** 243–245 °C. **¹H NMR (DMSO- d_6 , 400 MHz, 27 °C):** δ = 8.93 (s, 1H, ArH), 8.34 (dd, J = 1.6, 1.6 Hz, 1H, ArH), 8.17 (dd, J = 8.0, 1.6 Hz, 1H, ArH), 7.98 (d, J = 8.4 Hz, 1H, ArH), 7.65 (dd, J = 8.0, 8.0 Hz, 1H, ArH), 7.30–7.21 (m, 2H, ArH), 7.07 (d, J = 7.6 Hz, 1H, ArH), 6.94 (ddd, J = 7.6, 7.6, 1.2 Hz, 1H, ArH), 5.40 (dd, J = 5.7, 3.6 Hz, 1H, CH), 4.22 (d, J = 3.6 Hz, 1H, CH), 3.77 (s, 3H, CH_3) ppm. **¹³C NMR (DMSO- d_6 , 100 MHz, 27 °C):** δ = 155.7, 153.0, 148.3, 135.9, 135.3, 132.2, 130.4, 129.8, 128.9, 123.5, 121.1, 120.5, 112.8, 97.8, 56.0, 49.7 ppm. **IR (neat, ATR):** $\tilde{\nu}$ = 3198 (w), 3085 (w), 2934 (w), 2834 (w), 1653 (vs), 1598 (m), 1525 (m), 1504 (s), 1466 (m), 1345 (m), 1300 (m), 1264 (m), 1230 (m), 1207 (m), 1180 (m), 1164 (w), 1119 (m), 1048 (m), 1026 (m), 976 (m), 927 (w), 890 (w), 862 (w), 845 (w), 800 (m), 757 (s), 743 (s), 730 (m), 664 (m) cm^{-1} . **HRMS (ESI⁺):** m/z calcd. for $[\text{C}_{17}\text{H}_{16}\text{N}_3\text{O}_4]^+$: 326.1141, found: 326.1136 ($[\text{M}+\text{H}]^+$).

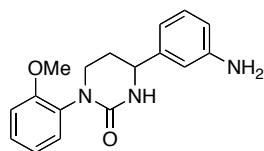
Synthesis of 3-(2-(benzyloxy)phenyl)-6-(3-nitrophenyl)-3,4-dihydropyrimidin-2(1H)-one (3.5)



Secondary amine **3.3** (783 mg, 1.97 mmol, 1.0 equiv.) was dissolved in 4 M HCl in 1,4-dioxane (20 mL) and concentrated under reduced pressure. The so obtained HCl salt was then dissolved in glacial acetic acid (25 mL) and potassium cyanate (799 mg, 9.85 mmol, 5.0 equiv.) was added. The mixture was heated to 60 °C for 2 h. Water (30 mL) and sat. aqu. NaHCO₃ (70 mL) were added and the aqueous phase was extracted with CHCl₃ (2 x 50 mL). The combined organic phases were washed with sat. aqu. NaHCO₃ (2 x 50 mL), dried over MgSO₄ and concentrated under reduced pressure. The crude product was purified by flash silica gel column chromatography (CHCl₃/MeOH, gradient from 100:0 to 70:1) to give tricycle **3.5** (609 mg, 1.52 mmol, 77%) as a yellow solid.

TLC (DCM/MeOH, 10:1): R_f = 0.35. **M.p.:** 69–70 °C. **¹H NMR (CDCl₃, 600 MHz, 27 °C):** δ = 8.32 (dd, J = 1.8, 1.8 Hz, 1H, ArH), 8.18 (ddd, J = 7.8, 1.8, 0.6 Hz, 1H, ArH), 7.80–7.77 (m, 1H, ArH), 7.50 (dd, J = 7.8, 7.8 Hz, 1H, ArH), 7.35–7.27 (m, 6H, ArH), 7.05–7.00 (m, 2H, ArH), 5.27–5.21 (m, 1H, CH), 5.14 (s, 2H, CH₂), 4.55–4.25 (br s, 2H, CH₂) ppm. **¹³C NMR (CDCl₃, 150 MHz, 27 °C):** δ = 154.5, 153.6, 148.5, 136.9, 136.0, 135.2, 130.6, 130.6, 129.8, 129.0, 128.5, 127.8, 127.0, 123.4, 121.5, 120.2, 113.9, 97.2, 70.4, 49.8 ppm. **IR (neat, ATR):** $\tilde{\nu}$ = 3219 (w), 3090 (w), 1656 (s), 1618 (m), 1597 (m), 1528 (m), 1500 (m), 1449 (m), 1378 (w), 1345 (m), 1287 (m), 1214 (m), 1162 (w), 1120 (m), 1046 (w), 1022 (m), 903 (w), 862 (w), 808 (w), 790 (w), 734 (vs), 696 (m), 667 (m) cm⁻¹. **HRMS (ESI⁺):** m/z calcd. for [C₂₃H₂₀N₃O₄]⁺: 402.1454, found: 402.1447 ([M+H]⁺).

Synthesis of 4-(3-aminophenyl)-1-(2-methoxyphenyl)tetrahydropyrimidin-2(1H)-one (3.7)

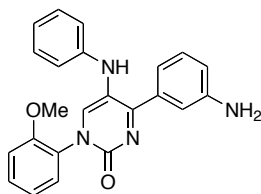


Nitroalkene **3.4** (20 mg, 0.061 mmol) was dissolved in MeOH (3 mL) and palladium on charcoal (10%; 1 spatula) was added under an argon atmosphere. The flask was evacuated and

purged with hydrogen (3x). The mixture was stirred at room temperature for 1.5 h under a hydrogen atmosphere (1 bar). The mixture was filtered over Celite and washed with CHCl_3 . The solvent was removed under reduced pressure, yielding aminoalkane **3.7** (17 mg, 0.058 mmol, 95%) as a colorless solid.

TLC (DCM/MeOH, 10:1): $R_f = 0.38$. **M.p.:** 213–215 °C. **^1H NMR (CDCl_3 , 600 MHz, 27 °C):** $\delta = 7.28\text{--}7.24$ (m, 3H, ArH), 7.16 (dd, $J = 7.8, 7.8$ Hz, 1H, ArH), 6.99–6.94 (m, 2H, ArH), 6.80–6.76 (m, 2H, ArH), 6.63 (ddd, $J = 7.8, 1.8, 0.6$ Hz, 1H, ArH), 4.95 (br s, 1H, NH), 4.65–4.59 (m, 1H, CH), 3.87 (s, 3H, CH_3), 3.80–3.67 (m, 2H, CH_2), 2.34–2.25 (m, 1H, CH), 2.13–2.05 (m, 1H, CH) ppm. **^{13}C NMR (CDCl_3 , 150 MHz, 27 °C):** $\delta = 155.6, 155.5, 146.8, 144.0, 131.7, 129.8, 129.6, 128.4, 120.9, 116.3, 114.4, 112.6, 112.1, 55.7, 55.5, 46.5, 31.1$ ppm. **IR (neat, ATR):** $\tilde{\nu} = 3323$ (w), 3224 (w), 2923 (w), 1653 (vs), 1602 (s), 1557 (m), 1539 (m), 1506 (vs), 1457 (s), 1319 (m), 1299 (m), 1272 (m), 1245 (m), 1180 (w), 1162 (w), 1117 (m), 1046 (w), 1024 (w), 871 (w), 790 (m), 751 (s), 697 (w) cm^{-1} . **HRMS (ESI $^+$):** m/z calcd. for $[\text{C}_{17}\text{H}_{20}\text{N}_3\text{O}_2]^+$: 298.1556, found: 298.1549 ($[\text{M}+\text{H}]^+$).

Synthesis of 4-(3-aminophenyl)-1-(2-methoxyphenyl)-5-(phenylamino)pyrimidin-2(1H)-one (**3.8**)

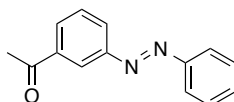


Nitroarene **3.4** (68 mg, 0.17 mmol, 1.0 equiv.) was dissolved in EtOH (3.6 mL) and water (0.9 mL) and Fe (76 mg, 1.4 mmol, 8.0 equiv.) and NH_4Cl (5.0 mg, 0.090 mmol, 0.5 equiv.) were added. The reaction mixture was heated to reflux for 3 h. The cooled solution was filtered over Celite and washed with EtOAc. The organic phase was washed with brine (20 mL), dried over MgSO_4 and concentrated under reduced pressure.

The crude aniline **3.6** was then dissolved in glacial acetic acid (2 mL) and nitrosobenzene (18 mg, 0.17 mmol, 1.0 equiv.) was added. The mixture was stirred at room temperature for 16 h. The mixture was then basified with sat. aqu. NaHCO_3 and extracted with EtOAc (2 x 10 mL). The combined organic layers were washed with sat. aqu. NaHCO_3 (20 mL), brine (20 mL), then dried over MgSO_4 and concentrated *in vacuo*. The crude product was purified by flash silica gel column chromatography ($\text{CHCl}_3/\text{MeOH}$, gradient from 100:0 to 30:1) to yield aromatic enamine **3.8** (23 mg, 0.060 mmol, 35%). As a side product, the double adduct of nitrosobenzene, azo enamine **3.9** (8.0 mg, 0.017 mmol, 10%) was obtained.

TLC (DCM/MeOH, 10:1): $R_f = 0.34$. **^1H NMR (CD_3OD , 400 MHz, 27 °C):** $\delta = 7.90$ (s, 1H, ArH), 7.50 (ddd, $J = 8.4, 7.5, 1.6$ Hz, 1H, ArH), 7.44 (dd, $J = 7.8, 1.6$ Hz, 1H, ArH), 7.23 (dd, $J = 8.4, 1.0$ Hz, 1H, ArH), 7.19 (dd, $J = 2.0, 2.0$ Hz, 1H, ArH), 7.16 (ddd, $J = 7.6, 2.0, 2.0$ Hz, 1H, ArH), 7.13–7.08 (m, 4H, ArH), 6.80 (ddd, $J = 7.9, 2.0, 1.1$ Hz, 1H, ArH), 6.70–6.66 (m, 3H, ArH), 3.90 (s, 3H, CH_3) ppm. **^{13}C NMR (CD_3OD , 100 MHz, 27 °C):** $\delta = 174.7, 155.4, 154.0, 148.3, 147.5, 146.7, 136.3, 130.7, 128.9, 128.4, 128.1, 127.7, 120.6, 120.4, 118.3, 118.2, 117.5, 115.1, 113.5, 112.3, 55.1$ ppm. **IR (neat, ATR):** $\tilde{\nu} = 3338$ (m), 3007 (w), 1654 (vs), 1621 (m), 1599 (s), 1497 (s), 1474 (m), 1436 (m), 1412 (m), 1358 (m), 1305 (m), 1286 (m), 1266 (m), 1220 (w), 1180 (w), 1159 (w), 1119 (w), 1042 (w), 1024 (w), 994 (w), 877 (w), 786 (m), 748 (s), 693 (w), 668 (w) cm^{-1} . **HRMS (ESI⁺):** m/z calcd. for $[\text{C}_{23}\text{H}_{21}\text{N}_4\text{O}_2]^+$: 385.1665, found: 385.1656 ($[\text{M}+\text{H}]^+$).

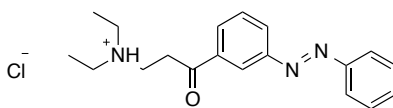
Synthesis of 1-(3-(phenyldiazenyl)phenyl)ethanone (3.13)



3-Aminoacetophenone (6.76 g, 50.0 mmol, 1.0 equiv.) was dissolved in glacial acetic acid (50 mL) and nitrosobenzene (5.36 g, 50.0 mmol, 1.0 equiv.) was added in 5 portions over 10 min. The reaction mixture was stirred at room temperature for 2.5 d and then extracted with CHCl_3 (5 x 20 mL). The combined organic layers were washed with sat. aqu. NaHCO_3 (3 x 50 mL), dried over MgSO_4 and concentrated under reduced pressure. The crude product was purified by flash silica gel column chromatography (CHCl_3 /hexanes, gradient from 2:8 to 5:5) to yield azobenzene **3.13** (6.85 g, 30.5 mmol, 61%) as a red solid.

TLC (CHCl_3 /hexanes, 4:6): $R_f = 0.41$. **M.p.:** 89–90 °C. **^1H NMR (CDCl_3 , 300 MHz, 27 °C):** $\delta = 8.47$ (dd, $J = 1.8, 1.8$, 1H, ArH), 8.14–8.05 (m, 2H, ArH), 7.98–7.92 (m, 2H, ArH), 7.62 (ddd, $J = 7.8, 7.8, 0.6$ Hz, 1H, ArH), 7.58–7.47 (m, 3H, ArH), 2.69 (s, 3H, CH_3) ppm. **^{13}C NMR (CDCl_3 , 75 MHz, 27 °C):** $\delta = 197.5, 152.7, 152.4, 138.1, 131.5, 130.2, 129.4, 129.2, 127.0, 123.0, 122.9, 26.8$ ppm. **IR (neat, ATR):** $\tilde{\nu} = 3064$ (w), 1687 (vs), 1586 (w), 1491 (w), 1473 (w), 1425 (w), 1358 (m), 1309 (w), 1290 (m), 1266 (m), 1208 (m), 1153 (m), 1072 (w), 1017 (w), 998 (w), 956 (w), 926 (w), 898 (w), 801 (m), 768 (m), 726 (w), 689 (s) cm^{-1} . **HRMS (EI⁺):** m/z calcd. for $[\text{C}_{14}\text{H}_{12}\text{N}_2\text{O}]^+$: 224.0950, found: 224.0946 ($[\text{M}]^+$).

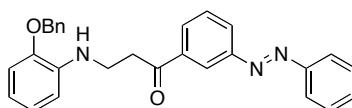
Synthesis of *N,N*-diethyl-3-oxo-3-(3-(phenyldiazenyl)phenyl)propan-1-aminium chloride (3.14)



Diethylamine (1.03 mL, 10.0 mmol, 1.0 equiv.) was dissolved in MeCN (50 mL) and conc. HCl (0.89 mL) was added. Paraformaldehyde (601 mg, 20.0 mmol, 2.0 equiv.) was added, followed by ketone **3.13** (4.49 g, 20.0 mmol, 2.0 equiv.). The mixture was heated to reflux for 2.5 d. The solvent was removed under reduced pressure and the residue was triturated with Et₂O (3 x 50 mL). The colorless solid was recrystallized from acetone (30 mL) and dried under high vacuum. The HCl salt of Mannich product **3.14** was obtained in 93% yield (3.21 g, 9.30 mmol) as a red solid.

M.p.: 129–130 °C. **¹H NMR (DMSO-*d*₆, 400 MHz, 27 °C):** δ = 10.62 (br s, 1H, NH), 8.45 (dd, J = 1.8, 1.8 Hz, 1H, ArH), 8.18 (ddd, J = 7.8, 1.8, 1.2 Hz, 1H, ArH), 8.14 (ddd, J = 7.8, 1.8, 1.2 Hz, 1H, ArH), 7.95–7.88 (m, 2H, ArH), 7.77 (dd, J = 7.8, 7.8 Hz, 1H, ArH), 7.63–7.56 (m, 3H, ArH), 3.77–3.66 (m, 2H, CH₂), 3.44–3.38 (m, 2H, CH₂), 3.21–3.12 (m, 4H, 2 x CH₂), 1.23 (t, J = 7.2 Hz, 6H, 2 x CH₃) ppm. **¹³C NMR (DMSO-*d*₆, 100 MHz, 27 °C):** δ = 196.7, 152.4, 152.2, 137.7, 132.5, 131.0, 130.5, 130.0, 127.0, 123.2, 122.7, 46.8, 46.1, 33.2, 9.0 ppm. **IR (neat, ATR):** $\tilde{\nu}$ = 3360 (w), 2977 (w), 2448 (m), 1687 (s), 1600 (m), 1581 (m), 1477 (m), 1461 (m), 1438 (m), 1397 (m), 1380 (m), 1361 (w), 1311 (m), 1242 (w), 1200 (m), 1169 (w), 1152 (m), 1135 (w), 1115 (w), 1082 (w), 1070 (m), 1012 (m), 979 (w), 964 (w), 930 (w), 906 (w), 864 (w), 842 (w), 802 (m), 778 (m), 693 (vs), 668 (m) cm⁻¹. **HRMS (ESI⁺):** m/z calcd. for [C₁₉H₂₄N₃O]⁺: 310.1919, found: 310.1910 ([M-Cl]⁺).

Synthesis of 3-((2-(benzyloxy)phenyl)amino)-1-(3-(phenyldiazenyl)phenyl)propan-1-one (3.16)

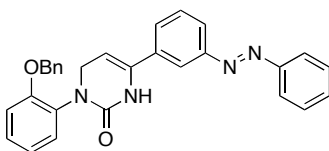


The HCl salt of amine **3.14** (200 mg, 0.580 mmol, 1.1 equiv.) and 2-benzyloxyaniline (106 mg, 0.530 mmol, 1.0 equiv.) were dissolved in ethanol (1 mL) and water (1 mL) and heated to reflux for 2 h. The mixture was cooled and a sat. aqu. solution of NaHCO₃ was added (10 mL). The aqueous phase was extracted with EtOAc (2 x 10 mL). The combined organic phases were

washed with sat. aqu. NaHCO₃ (15 mL) and brine (15 mL) and concentrated under reduced pressure. The crude product was purified by flash silica gel column chromatography (hexanes/EtOAc, gradient from 20:1 to 8:1) to give secondary amine **3.16** (191 mg, 0.440 mmol, 83%) as an orange oil.

TLC (hexanes/EtOAc, 4:1): R_f = 0.50. **¹H NMR (CDCl₃, 400 MHz, 27 °C):** δ = 8.46 (dd, *J* = 1.8, 1.8 Hz, 1H, Ar*H*), 8.11 (ddd, *J* = 7.8, 1.8, 1.2 Hz, 1H, Ar*H*), 8.06 (ddd, *J* = 7.8, 1.8, 1.2 Hz, 1H, Ar*H*), 7.99–7.91 (m, 2H, Ar*H*), 7.66 (dd, *J* = 7.8, 7.8 Hz, 1H, Ar*H*), 8.25 (ddd, *J* = 7.8, 1.8, 1.2 Hz, 1H, Ar*H*), 7.57–7.47 (m, 3H, Ar*H*), 7.44–7.28 (m, 5H, Ar*H*), 6.91 (ddd, *J* = 7.8, 7.8, 1.2 Hz, 1H, Ar*H*), 6.84 (dd, *J* = 7.8, 1.2 Hz, 1H, Ar*H*), 6.75 (dd, *J* = 7.8, 1.2 Hz, 1H, Ar*H*), 6.66 (ddd, *J* = 7.8, 7.8, 1.2 Hz, 1H, Ar*H*), 5.06 (s, 2H, CH₂), 4.75 (br s, 1H, NH), 3.73–3.67 (m, 2H, CH₂), 3.41–3.35 (m, 2H, CH₂) ppm. **¹³C NMR (CDCl₃, 100 MHz, 27 °C):** δ = 198.5, 152.6, 152.4, 146.3, 137.8, 137.1, 131.5, 130.0, 129.4, 129.2, 128.5, 127.9, 127.5, 127.1, 123.0, 122.5, 121.7, 120.4, 116.8, 111.4, 110.2, 70.5, 38.6, 38.1 ppm. **IR (neat, ATR):** $\tilde{\nu}$ = 3726 (w), 3419 (w), 3063 (w), 3035 (w), 2898 (w), 2869 (w), 1684 (s), 1601 (m), 1511 (vs), 1444 (m), 1380 (m), 1344 (w), 1316 (m), 1252 (s), 1207 (s), 1151 (m), 1125 (m), 1072 (w), 1050 (w), 1019 (m), 912 (w), 856 (w), 796 (w), 768 (w), 737 (vs), 691 (vs), 668 (w) cm⁻¹. **HRMS (ESI⁺):** *m/z* calcd. for [C₂₈H₂₆N₃O₂]⁺: 436.2025, found: 436.2015 ([M+H]⁺).

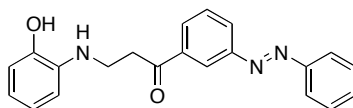
Synthesis of 3-(2-(benzyloxy)phenyl)-6-(3-(phenyldiazenyl)phenyl)-3,4-dihydropyrimidin-2(1*H*)-one (**3.17**)



Secondary amine **3.16** (162 mg, 0.370 mmol, 1.0 equiv.) was dissolved in 4 M HCl in 1,4-dioxane (4 mL) and concentrated under reduced pressure. The so obtained HCl salt was then dissolved in glacial acetic acid (4 mL) and potassium cyanate (150 mg, 1.85 mmol, 5.0 equiv.) was added. The mixture was heated to 60 °C for 2 h. Water (10 mL) and sat. aqu. NaHCO₃ (30 mL) were added and the aqueous phase was extracted with CHCl₃ (2 x 20 mL). The combined organic phases were washed with sat. aqu. NaHCO₃ (2 x 30 mL), dried over MgSO₄ and concentrated under reduced pressure. The crude product was purified by flash silica gel column chromatography (CHCl₃/hexanes, 1:1 → 1:0) to give tricycle **3.17** (172 mg, 0.370 mmol, 100%) as an orange oil.

TLC (hexanes/EtOAc, 1:1): R_f = 0.60. **^1H NMR (CDCl_3 , 400 MHz, 27 °C):** δ = 8.00 (dd, J = 1.8, 1.8 Hz, 1H, ArH), 7.97–7.89 (m, 3H, ArH), 7.57–7.48 (m, 5H, ArH), 7.47–7.42 (m, 2H, ArH), 7.37–7.24 (m, 5H, ArH), 7.05–6.99 (m, 2H, ArH), 6.66 (br s, 1H, NH), 5.23 (td, J = 3.8, 1.9 Hz, 1H, CH), 5.14 (s, 2H, CH_2), 4.49–4.28 (br s, 2H, CH_2) ppm. **^{13}C NMR (CDCl_3 , 100 MHz, 27 °C):** δ = 154.6, 153.5, 152.9, 152.5, 137.0, 136.3, 135.4, 131.3, 131.0, 129.6, 129.4, 129.1, 128.7, 128.5, 127.7, 127.1, 126.9, 124.1, 123.0, 121.6, 118.3, 114.1, 95.8, 70.4, 49.9 ppm. **IR (neat, ATR):** $\tilde{\nu}$ = 3225 (w), 3066 (w), 1657 (vs), 1598 (m), 1502 (m), 1481 (m), 1449 (m), 1382 (w), 1289 (m), 1214 (m), 1159 (w), 1120 (w), 1048 (w), 1023 (w), 908 (w), 841 (w), 801 (w), 750 (m), 692 (m), 668 (w) cm^{-1} . **HRMS (ESI⁺):** m/z calcd. for $[\text{C}_{29}\text{H}_{25}\text{N}_4\text{O}_2]^+$: 461.1978, found: 461.1966 ($[\text{M}+\text{H}]^+$).

Synthesis of 3-((2-hydroxyphenyl)amino)-1-(3-(phenyldiazenyl)phenyl)propan-1-one (3.15)



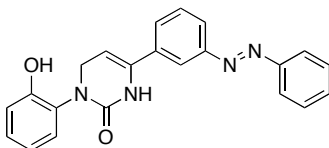
The HCl salt of amine **3.14** (1.50 g, 4.34 mmol, 1.1 equiv.) and 2-hydroxyaniline (431 mg, 3.95 mmol, 1.0 equiv.) were dissolved in ethanol (10 mL) and water (10 mL) and heated to reflux for 2.5 h. The mixture was cooled and a sat. aqu. solution of NaHCO_3 was added (75 mL). The aqueous phase was extracted with EtOAc (2 x 30 mL). The organic phase was washed with sat. aqu. NaHCO_3 (50 mL) and brine (50 mL) and concentrated under reduced pressure. The crude product was purified by flash silica gel column chromatography (hexanes/EtOAc, gradient from 10:1 to 6:1) to give secondary amine **3.15** (869 mg, 2.52 mmol, 64%) as an orange solid.

TLC (hexanes/EtOAc, 2:1): R_f = 0.44. **M.p.:** 137–138 °C. **^1H NMR (CDCl_3 , 400 MHz, 27 °C)^[aa]:** δ = 8.44 (dd, J = 1.7, 1.7 Hz, 1H, ArH), 8.35 (dd, J = 1.7, 1.7 Hz, 0.5H, ArH, *cis* isomer), 8.09 (ddd, J = 7.8, 1.8, 1.2 Hz, 1H, ArH), 8.07–8.03 (m, 1.5H, ArH), 7.98–7.94 (m, 0.5H, ArH, *cis* isomer), 7.94–7.89 (m, 3H, ArH), 7.60 (dd, J = 8.0, 8.0 Hz, 1H, ArH), 7.57–7.47 (m, 5H, ArH), 7.26–7.24 (m, 1H, ArH, *cis* isomer), 6.91–6.70 (m, 5H, ArH), 3.66–3.61 (m, 2H, CH_2), 3.47–3.38 (m, 3H, *trans*- CH_2 , *cis*- CH_2), 3.20–3.13 (m, 1H, CH_2 , *cis* isomer) ppm. **^{13}C NMR (CDCl_3 , 100 MHz, 27 °C)^[aa]:** δ = 198.6, 198.5, 152.6, 152.6, 152.4, 145.6, 137.5, 134.4, 131.5, 131.4, 130.0, 130.0, 129.5, 129.4, 129.1, 129.1, 127.4, 126.9, 123.0, 122.7, 122.5, 121.3, 120.6, 120.1, 115.2, 50.3, 40.7, 37.7, 36.5 ppm. **IR (neat, ATR):** $\tilde{\nu}$ = 3333 (m), 3065

^[aa] In the ^1H and ^{13}C NMR spectrum, a 2:1 mixture of *trans* : *cis* isomers of **3.15** was observed.

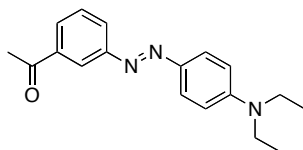
(m), 2683 (vs), 1608 (m), 1513 (m), 1492 (m), 1447 (m), 1391 (w), 1356 (w), 1311 (w), 1260 (m), 1197 (m), 1152 (m), 1116 (w), 1068 (w), 1042 (w), 1019 (w), 996 (w), 911 (w), 839 (w), 797 (w), 743 (m), 690 (s) cm^{-1} . **HRMS (ESI⁺):** m/z calcd. for $[\text{C}_{21}\text{H}_{20}\text{N}_3\text{O}_2]^+$: 346.1556, found: 346.1546 ($[\text{M}+\text{H}]^+$).

Synthesis of 3-(2-hydroxyphenyl)-6-(3-(phenyldiazenyl)phenyl)-3,4-dihydropyrimidin-2(1H)-one (AII)



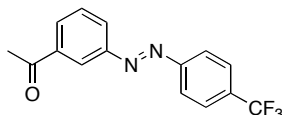
Secondary amine **3.15** (860 mg, 2.49 mmol, 1.0 equiv.) was dissolved in 4 M HCl in 1,4-dioxane (20 mL) and concentrated under reduced pressure. The so obtained HCl salt was then dissolved in glacial acetic acid (40 mL) and potassium cyanate (1.01 g, 12.5 mmol, 5.0 equiv.) was added. The mixture was heated to 60 °C for 2 h. Water (40 mL) and sat. aqu. NaHCO_3 (100 mL) were added and the aqueous phase was extracted with CHCl_3 (2 x 30 mL). The combined organic phases were washed with sat. aqu. NaHCO_3 (3 x 70 mL), dried over MgSO_4 and concentrated under reduced pressure. The crude product was purified by flash silica gel column chromatography ($\text{CHCl}_3/\text{MeOH}$, 100:0) to give **AII** (564 mg, 1.52 mmol, 61%) as an orange solid.

TLC ($\text{CHCl}_3/\text{MeOH}$, 20:1): R_f = 0.43. **M.p.:** 177–178 °C. **¹H NMR (CDCl_3 , 600 MHz, 27 °C):** δ = 7.99 (s, 1H, ArH), 7.96–7.91 (m, 3H, ArH), 7.56–7.49 (m, 5H, ArH), 7.38 (br s, 1H, OH), 7.25–7.23 (m, 1H, ArH), 7.20–7.17 (m, 1H, ArH), 7.07–6.96 (m, 3H, 2 x ArH, NH), 5.33–5.26 (m, 1H, CH), 4.54 (d, J = 3.8 Hz, 2H, CH_2) ppm. **¹³C NMR (CDCl_3 , 150 MHz, 27 °C):** δ = 154.2, 152.9, 152.4, 151.2, 136.0, 134.4, 131.4, 130.4, 129.8, 129.1, 128.1, 127.1, 124.3, 124.2, 123.0, 121.3, 120.1, 118.6, 95.6, 50.3 ppm. **IR (neat, ATR):** $\tilde{\nu}$ = 3241 (m), 1642 (vs), 1597 (m), 1496 (s), 1449 (m), 1333 (w), 1298 (m), 1243 (w), 1212 (w), 1154 (w), 1108 (w), 1056 (w), 1022 (w), 995 (w), 964 (w), 908 (w), 840 (w), 827 (w), 800 (w), 754 (s), 690 (m), 668 (w) cm^{-1} . **HRMS (ESI⁺):** m/z calcd. for $[\text{C}_{22}\text{H}_{19}\text{N}_4\text{O}_2]^+$: 371.1508, found: 371.1498 ($[\text{M}+\text{H}]^+$). **UV/Vis:** λ_{max} = 320, 435 nm.

Synthesis of 1-(3-((4-(diethylamino)phenyl)diazenyl)phenyl)ethanone (3.18)

3-Aminoacetophenone (1.35 g, 10.0 mmol, 1.0 equiv.) was dissolved in 1 M HCl (32 mL) and cooled to 0 °C. A precooled solution of sodium nitrite (720 mg, 10.5 mmol, 1.05 equiv.) in water (5.3 mL) was added dropwise and the resulting mixture was stirred for 30 min at 0 °C. A precooled solution of *N,N*-diethylaniline (1.68 mL, 10.5 mmol, 1.05 equiv.) in 1 M HCl (24 mL) was added slowly, followed by a precooled solution of sodium acetate (5.74 g) in water (40 mL). The reaction mixture was stirred vigorously for 2 h at 0 °C. The mixture was extracted with DCM (2 x 50 mL) and the combined organic layers were washed with sat. aqu. NaHCO₃ (100 mL), dried over MgSO₄ and concentrated under reduced pressure. The crude product was purified by flash silica gel column chromatography (DCM/hexanes, gradient from 1:1 to 100% DCM) to yield azobenzene **3.18** (2.80 g, 9.48 mmol, 95%) as a deep red oil.

TLC (DCM): $R_f = 0.52$. **¹H NMR (CDCl₃, 300 MHz, 27 °C):** $\delta = 8.38$ (dd, $J = 1.8, 1.8$ Hz, 1H, ArH), 8.02 (ddd, $J = 7.8, 1.8, 1.2$ Hz, 1H, ArH), 7.97 (ddd, $J = 7.8, 1.8, 1.2$ Hz, 1H, ArH), 7.92–7.84 (m, 2H, ArH), 7.55 (dd, $J = 7.8, 7.8$ Hz, 1H, ArH), 3.46 (q, $J = 7.1$ Hz, 4H, 2 x CH₂), 2.68 (s, 3H, CH₃), 1.24 (t, $J = 7.1$ Hz, 6H, 2 x CH₃) ppm. **¹³C NMR (CDCl₃, 75 MHz, 27 °C):** $\delta = 197.9, 153.4, 150.5, 143.0, 138.0, 129.2, 128.4, 126.3, 125.6, 122.3, 111.0, 44.8, 26.8, 12.6$ ppm. **IR (neat, ATR):** $\tilde{\nu} = 2971$ (m), 2929 (w), 1684 (s), 1596 (vs), 1561 (m), 1515 (m), 1469 (w), 1446 (w), 1431 (w), 1395 (s), 1353 (s), 1310 (w), 1270 (m), 1240 (m), 1195 (w), 1178 (w), 1153 (m), 1136 (vs), 1093 (w), 1077 (m), 1011 (w), 954 (w), 913 (w), 860 (w), 822 (m), 796 (w), 744 (w), 726 (w), 686 (m) cm⁻¹. **HRMS (ESI⁺):** m/z calcd. for [C₁₈H₂₁N₃O]⁺: 296.1763, found: 296.1759 ([M+H]⁺).

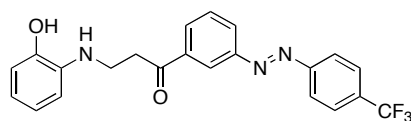
Synthesis of 1-(3-((4-(trifluoromethyl)phenyl)diazenyl)phenyl)ethanone (3.20)

4-(Trifluoromethyl)aniline (1.35 mL, 10.7 mmol, 1.0 equiv.) was dissolved in DCM (25 mL) and oxone (13.2 g, 21.4 mmol, 2.0 equiv.; dissolved in 50 mL of H₂O) was added. The biphasic mixture was stirred vigorously for 4 h at room temperature. The phases were separated and the

aqueous phase was extracted with DCM (30 mL). The combined organic phases were washed with brine (50 mL), dried over MgSO_4 and the solvent was removed under reduced pressure. The resulting green oil was immediately dissolved in HOAc (60 mL) and 3-aminoacetophenone (1.45 g, 10.7 mmol, 1.0 equiv.) was added in small portions over the course of 10 min. The mixture was stirred for 3 d at room temperature. The mixture was basified with 2 M NaOH and extracted with DCM (2 x 30 mL). The combined organic phases were washed with sat. aqu. NaHCO_3 (2 x 50 mL), dried over MgSO_4 and concentrated *in vacuo*. The crude product was purified by flash silica gel column chromatography (DCM/hexanes, gradient from 2:1 to 1:2) to yield azobenzene **3.20** (1.69 g, 5.78 mmol, 54%) in the form of red crystals.

TLC (DCM/hexanes, 1:1): $R_f = 0.35$. **M.p.:** 57–58 °C. **^1H NMR (CDCl_3 , 300 MHz, 27 °C):** $\delta = 8.50$ (dd, $J = 1.8, 1.8$ Hz, 1H, ArH), 8.18–8.09 (m, 2H, ArH), 8.06–8.00 (m, 2H, ArH), 7.83–7.77 (m, 2H, ArH), 7.65 (ddd, $J = 7.8, 7.8, 0.3$ Hz, 1H, ArH), 2.70 (s, 3H, CH_3) ppm. **^{13}C NMR (CDCl_3 , 75 MHz, 27 °C):** $\delta = 197.3, 154.1$ (q, $J = 1.4$ Hz), 152.4, 138.2, 132.7 (q, $J = 32.6$ Hz), 131.0, 129.5, 127.2, 126.4 (q, $J = 3.8$ Hz), 123.8 (q, $J = 270.1$ Hz), 123.2, 123.1, 26.8 ppm. **^{19}F NMR (CDCl_3 , 282 MHz, 27 °C):** $\delta = -62.7$ ppm. **IR (neat, ATR):** $\tilde{\nu} = 1683$ (m), 1609 (w), 1586 (w), 1507 (w), 1472 (w), 1432 (w), 1412 (w), 1358 (m), 1313 (s), 1279 (m), 1261 (m), 1213 (w), 1205 (w), 1165 (m), 1132 (vs), 1101 (s), 1060 (s), 1010 (m), 971 (w), 919 (m), 849 (s), 805 (m), 771 (w), 726 (w), 682 (m), 671 (m) cm^{-1} . **HRMS (ESI $^+$):** m/z calcd. for $[\text{C}_{15}\text{H}_{12}\text{F}_3\text{N}_2\text{O}]^+$: 293.0902, found: 293.0898 ($[\text{M}+\text{H}]^+$).

Synthesis of 3-((2-hydroxyphenyl)amino)-1-(3-((4-(trifluoromethyl)phenyl)diazenyl)phenyl)-propan-1-one (3.22)^[bb]



Diethylamine (0.31 mL, 3.0 mmol, 1.0 equiv.) was dissolved in MeCN (14 mL) and conc. HCl (0.25 mL) was added. Paraformaldehyde (159 mg, 5.30 mmol, 1.75 equiv.) was added, followed by ketone **3.20** (1.55 g, 5.30 mmol, 1.75 equiv.). The mixture was heated to reflux for 16 h. The solvent was removed under reduced pressure and the residue was triturated with Et_2O (3 x 30 mL). The colorless solid was recrystallized from acetone (25 mL) and dried under high

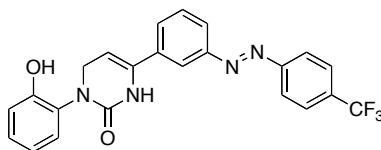
^[bb] Compound **3.22** appeared as a mixture of isomers in the NMR spectra. Even NMR spectra taken at elevated temperatures could not be interpreted due to overlapping signals and isomer peaks.

vacuum. The HCl salt of Mannich product **3.21** was obtained in 88% yield (1.10 g, 2.66 mmol) as orange crystals and directly used in the next step.

The HCl salt of amine **3.21** (1.09 g, 2.63 mmol, 1.1 equiv.) and 2-aminophenol (261 mg, 2.39 mmol, 1.0 equiv.) were dissolved in ethanol (6 mL) and water (6 mL) and heated to reflux for 2 h. The mixture was cooled and a sat. aqu. solution of NaHCO₃ was added (20 mL). The aqueous phase was extracted with EtOAc (2 x 20 mL). The organic phase was washed with sat. aqu. NaHCO₃ (30 mL) and brine (30 mL) and concentrated under reduced pressure. The crude product was purified by flash silica gel column chromatography (hexanes/EtOAc, gradient from 10:1 to 2:1) to give secondary amine **3.22** (515 mg, 1.25 mmol, 52%) as an orange solid.

TLC (hexanes/EtOAc, 2:1): R_f = 0.48. **M.p.:** 124–125 °C. **IR (neat, ATR):** $\tilde{\nu}$ = 2925 (w), 1685 (m), 1598 (w), 1486 (m), 1411 (w), 1370 (w), 1321 (vs), 1253 (w), 1226 (m), 1168 (m), 1126 (s), 1064 (s), 1012 (m), 894 (w), 850 (m), 799 (w), 736 (m), 681 (w) cm⁻¹. **HRMS (ESI⁺):** m/z calcd. for [C₂₂H₁₉N₃O₂F₃]⁺: 414.1429, found: 414.1430 ([M+H]⁺).

Synthesis of 3-(2-hydroxyphenyl)-6-(3-((4-(trifluoromethyl)phenyl)diazenyl)phenyl)-3,4-di-hydropyrimidin-2(1H)-one (AI2)

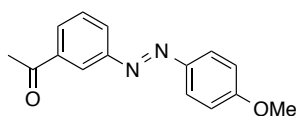


Secondary amine **3.22** (180 mg, 0.440 mmol, 1.0 equiv.) was dissolved in 4 M HCl in 1,4-dioxane (4 mL) and concentrated under reduced pressure. The so obtained HCl salt was then dissolved in glacial acetic acid (7 mL) and potassium cyanate (178 mg, 2.20 mmol, 5.0 equiv.) was added. The mixture was heated to 60 °C for 2.5 h. A sat. aqu. solution of NaHCO₃ in water (20 mL) was added and the aqueous phase was extracted with EtOAc (2 x 20 mL). The combined organic phases were washed with sat. aqu. NaHCO₃ (30 mL) and brine (30 mL), dried over MgSO₄ and concentrated under reduced pressure. The crude product was purified by flash silica gel column chromatography (hexanes/EtOAc, 2:1) to give tricycle **AI2** (100 mg, 0.230 mmol, 52%) as an orange solid.

TLC (hexanes/EtOAc, 2:1): R_f = 0.14. **M.p.:** 199–201 °C. **¹H NMR (DMSO-d₆, 600 MHz, 27 °C):** δ = 9.57 (s, 1H, NH), 8.83 (s, 1H, OH), 8.12 (dd, J = 1.8, 1.8 Hz, 1H, ArH), 8.10–8.07 (m, 2H, ArH), 8.01–7.98 (m, 2H, ArH), 7.93 (ddd, J = 7.8, 1.8, 1.0 Hz, 1H, ArH), 7.81 (ddd, J = 7.8, 1.8, 1.0 Hz, 1H, ArH), 7.65 (dd, J = 7.8, 7.8 Hz, 1H, ArH), 7.19 (dd, J = 7.8, 1.8 Hz, 1H, ArH), 7.13–7.10 (m, 1H, ArH), 6.91 (dd, J = 8.2, 1.4 Hz, 1H, ArH), 6.81 (ddd, J = 7.2, 7.2,

1.2 Hz, 1H, ArH), 5.36 (td, $J = 3.8, 2.0$ Hz, 1H, CH), 4.27 (d, $J = 3.8$ Hz, 2H, CH₂) ppm. ¹³C NMR (DMSO-d₆, 100 MHz, 27 °C): $\delta = 154.4, 153.9, 153.2, 152.3, 136.3, 135.9, 131.4$ (q, $J = 31.2$ Hz), 130.2, 129.9, 129.8, 129.4, 128.5, 127.2 (q, $J = 3.8$ Hz), 124.4 (q, $J = 270.8$ Hz), 123.6, 123.4, 120.1, 119.7, 117.0, 96.7, 49.6 ppm. ¹⁹F NMR (DMSO-d₆, 376 MHz, 27 °C): $\delta = -61.1$ ppm. IR (neat, ATR): $\tilde{\nu} = 3369$ (m), 2411 (m), 2342 (w), 2075 (w), 1682 (w), 1618 (m), 1588 (m), 1576 (m), 1496 (s), 1447 (m), 1412 (w), 1390 (w), 1314 (vs), 1301 (m), 1271 (w), 1225 (w), 1167 (m), 1152 (m), 1108 (s), 1102 (s), 1062 (vs), 1013 (m), 969 (m), 934 (w), 887 (w), 846 (s), 818 (w), 787 (w), 752 (s), 746 (s), 723 (w), 714 (w), 685 (m), 671 (w), 654 (w) cm⁻¹. HRMS (ESI⁺): m/z calcd. for [C₂₃H₁₈N₄O₂F₃]⁺: 439.1382, found: 439.1381 ([M+H]⁺). UV/Vis: $\lambda_{\text{max}} = 314, 428$ nm.

Synthesis of 1-(3-((4-methoxyphenyl)diazenyl)phenyl)ethan-1-one (3.23)

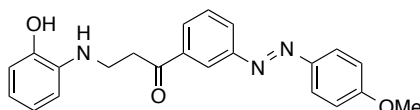


3-Aminoacetophenone (1.35 g, 10.0 mmol, 1.0 equiv.) was dissolved in DCM (25 mL) and oxone (12.3 g, 20.0 mmol, 2.0 equiv.; dissolved in 50 mL of H₂O) was added. The biphasic mixture was stirred vigorously for 3.5 h at room temperature. The phases were separated and the aqueous phase was extracted with DCM (30 mL). The combined organic phases were washed with brine (50 mL), dried over MgSO₄ and the solvent was removed under reduced pressure. The resulting green oil was immediately dissolved in HOAc (50 mL) and *p*-anisidine (1.23 g, 10.0 mmol, 1.0 equiv.) was added in small portions over the course of 10 min. The mixture was stirred for 16 h at room temperature. The mixture was basified with 2 M NaOH and extracted with DCM (3 x 25 mL). The combined organic phases were washed with sat. aqu. NaHCO₃ (2 x 50 mL) and brine (50 mL), dried over MgSO₄ and concentrated *in vacuo*. The crude product was purified by flash silica gel column chromatography (hexanes/EtOAc, gradient from 10:1 to 3:1) to yield azobenzene **3.23** (1.42 g, 5.58 mmol, 56%) as orange solid.

TLC (hexanes/EtOAc, 4:1): $R_f = 0.37$. M.p.: 99–100 °C. ¹H NMR (CDCl₃, 400 MHz, 27 °C): $\delta = 8.45\text{--}8.41$ (m, 1H, ArH), 8.07 (ddd, $J = 7.8, 1.8, 1.2$ Hz, 1H, ArH), 8.04 (ddd, $J = 7.8, 1.8, 1.2$ Hz, 1H, ArH), 7.98–7.92 (m, 2H, ArH), 7.59 (ddd, $J = 7.8, 7.8, 1.2$ Hz, 1H, ArH), 7.06–6.99 (m, 2H, ArH), 7.65 (ddd, $J = 7.8, 7.8, 0.8$ Hz, 1H, ArH), 3.90 (s, 3H, CH₃), 2.69 (s, 3H, CH₃) ppm. ¹³C NMR (CDCl₃, 100 MHz, 27 °C): $\delta = 197.7, 162.5, 152.8, 146.8, 138.0, 129.6, 129.3, 126.8, 125.0, 122.6, 114.3, 55.6, 26.8$ ppm. IR (neat, ATR): $\tilde{\nu} = 1686$ (s), 1600 (m), 1584 (m), 1502 (s), 1454 (w), 1416 (w), 1357 (m), 1313 (w), 1296 (w), 1252 (vs),

1215 (w), 1181 (w), 1152 (m), 1141 (m), 1105 (w), 1028 (m), 956 (w), 913 (w), 839 (m), 805 (w), 787 (w), 724 (w), 685 (m) cm^{-1} . **HRMS (ESI⁺):** m/z calcd. for $[\text{C}_{15}\text{H}_{15}\text{N}_2\text{O}_2]^+$: 255.1134, found: 255.1132 ($[\text{M}+\text{H}]^+$).

Synthesis of 3-((2-hydroxyphenyl)amino)-1-(3-((4-methoxyphenyl)diazenyl)phenyl)propan-1-one (3.25)

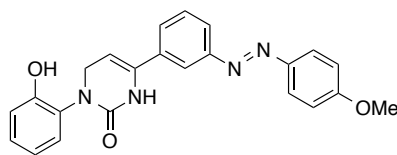


Diethylamine (0.16 mL, 1.6 mmol, 1.0 equiv.) was dissolved in MeCN (15 mL) and conc. HCl (0.13 mL) was added. Paraformaldehyde (83 mg, 2.8 mmol, 1.75 equiv.) was added, followed by ketone **3.23** (700 mg, 2.75 mmol, 1.75 equiv.). The mixture was heated to reflux for 16 h. The solvent was removed under reduced pressure and the residue was triturated with Et₂O (3 x 20 mL). The colorless solid was recrystallized from acetone (20 mL) and dried under high vacuum. The HCl salt of Mannich product **3.24** was obtained in 92% yield (533 mg, 1.42 mmol) as a red solid.

The HCl salt of amine **3.24** (100 mg, 0.270 mmol, 1.0 equiv.) and 2-aminophenol (30 mg, 0.27 mmol, 1.0 equiv.) were dissolved in ethanol (1 mL) and water (1 mL) and heated to reflux for 3 h. The mixture was cooled and a sat. aqu. solution of NaHCO₃ was added (10 mL). The aqueous phase was extracted with EtOAc (2 x 10 mL). The combined organic phases were washed with sat. aqu. NaHCO₃ (20 mL) and brine (20 mL) and concentrated under reduced pressure. The crude product was purified by flash silica gel column chromatography (CHCl₃, 100%) to give secondary amine **3.25** (55 mg, 0.15 mmol, 56%) as an orange solid.

TLC (CHCl₃/MeOH, 19:1): R_f = 0.47. **M.p.:** 132–133 °C. **¹H NMR (CD₃OD, 400 MHz, 27 °C):** δ = 8.36 (dd, J = 1.8, 1.8 Hz, 1H, ArH), 8.02 (dd, J = 7.8, 1.8 Hz, 2H, ArH), 7.92–7.87 (m, 2H, ArH), 7.59 (dd, J = 7.8, 7.8 Hz, 1H, ArH), 7.06–7.03 (m, 2H, ArH), 6.75–6.71 (m, 2H, ArH), 6.69–6.64 (m, 1H, ArH), 6.58–6.51 (m, 1H, ArH), 3.86 (s, 3H, CH₃), 3.58–3.53 (m, 2H, CH₂), 3.39–3.32 (m, 2H, CH₂) ppm. **¹³C NMR (CDCl₃, 100 MHz, 27 °C):** δ = 199.4, 162.8, 152.7, 146.6, 145.2, 137.8, 136.3, 129.3, 129.2, 126.3, 124.6, 121.6, 119.9, 117.8, 114.0, 113.5, 111.8, 54.7, 39.1, 37.6 ppm. **IR (neat, ATR):** $\tilde{\nu}$ = 3395 (w), 1682 (m), 1601 (s), 1584 (m), 1502 (s), 1447 (w), 1415 (w), 1364 (w), 1315 (w), 1297 (w), 1253 (vs), 1205 (w), 1182 (w), 1148 (s), 1119 (w), 1080 (w), 1028 (m), 999 (w), 916 (w), 839 (m), 805 (w), 743 (w), 683 (w) cm^{-1} . **HRMS (ESI⁺):** m/z calcd. for $[\text{C}_{22}\text{H}_{22}\text{N}_3\text{O}_3]^+$: 376.1661, found: 376.1654 ($[\text{M}+\text{H}]^+$).

Synthesis of 3-(2-hydroxyphenyl)-6-(3-((4-methoxyphenyl)diazenyl)phenyl)-3,4-dihydropyrimidin-2(1H)-one (AI3)



Secondary amine **3.25** (119 mg, 0.320 mmol, 1.0 equiv.) was dissolved in 4 M HCl in 1,4-dioxane (10 mL) and concentrated under reduced pressure. The so obtained HCl salt was then dissolved in glacial acetic acid (15 mL) and potassium cyanate (130 mg, 1.60 mmol, 5.0 equiv.) was added. The mixture was heated to 60 °C for 3.5 h. A sat. aqu. solution of NaHCO₃ (50 mL) was added and the aqueous phase was extracted with EtOAc (2 x 20 mL). The combined organic phases were washed with sat. aqu. NaHCO₃ (40 mL) and brine (40 mL), dried over MgSO₄ and concentrated under reduced pressure. The crude product was purified by flash silica gel column chromatography (CHCl₃, 100%) to give **AI3** (80 mg, 0.20 mmol, 63%) as an orange solid.

TLC (CHCl₃/MeOH, 19:1): R_f = 0.34. **M.p.:** 175–176 °C. **¹H NMR (CDCl₃, 600 MHz, 27 °C):** δ = 7.95–7.92 (m, 3H, ArH), 7.90 (ddd, J = 7.2, 1.8, 1.8 Hz, 1H, ArH), 7.55–7.49 (m, 2H, ArH), 7.38 (s, 1H, OH), 7.26–7.24 (m, 1H, ArH), 7.21–7.18 (m, 1H, ArH), 7.07 (dd, J = 7.2, 1.8 Hz, 1H, ArH), 7.03–7.01 (m, 2H, ArH), 6.98 (ddd, J = 7.2, 7.2, 1.8 Hz, 1H, ArH), 6.84 (s, 1H, OH), 5.29 (td, J = 3.9, 2.2 Hz, 1H, CH), 4.55 (d, J = 3.9 Hz, 2H, CH₂), 3.89 (s, 3H, CH₃) ppm. **¹³C NMR (CDCl₃, 150 MHz, 27 °C):** δ = 162.4, 154.1, 153.0, 151.1, 146.8, 136.1, 134.3, 130.4, 129.8, 128.1, 126.4, 125.0, 124.2, 124.1, 121.3, 120.2, 118.1, 114.3, 95.5, 55.6, 50.3 ppm. **IR (neat, ATR):** $\tilde{\nu}$ = 3238 (m), 1643 (s), 1599 (s), 1584 (m), 1500 (vs), 1450 (m), 1416 (w), 1297 (m), 1252 (vs), 1216 (m), 1182 (w), 1146 (m), 1106 (m), 1059 (w), 1029 (m), 964 (w), 902 (w), 839 (m), 803 (w), 752 (vs), 686 (w), 667 (w) cm⁻¹. **HRMS (ESI⁺):** m/z calcd. for [C₂₃H₂₁N₄O₃]⁺: 401.1614, found: 401.1608 ([M+H]⁺). **UV/Vis:** λ_{max} = 355, 440 nm.

3.6.3 BIOLOGICAL METHODS

Cell Culture

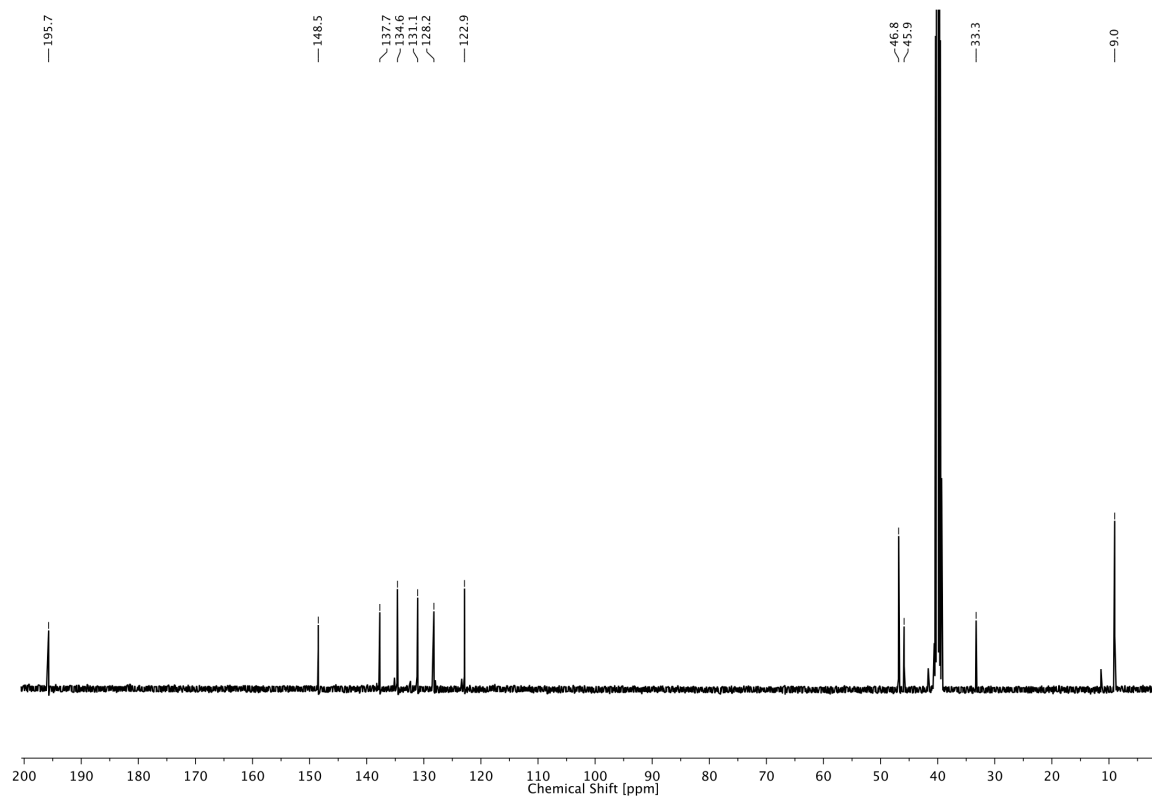
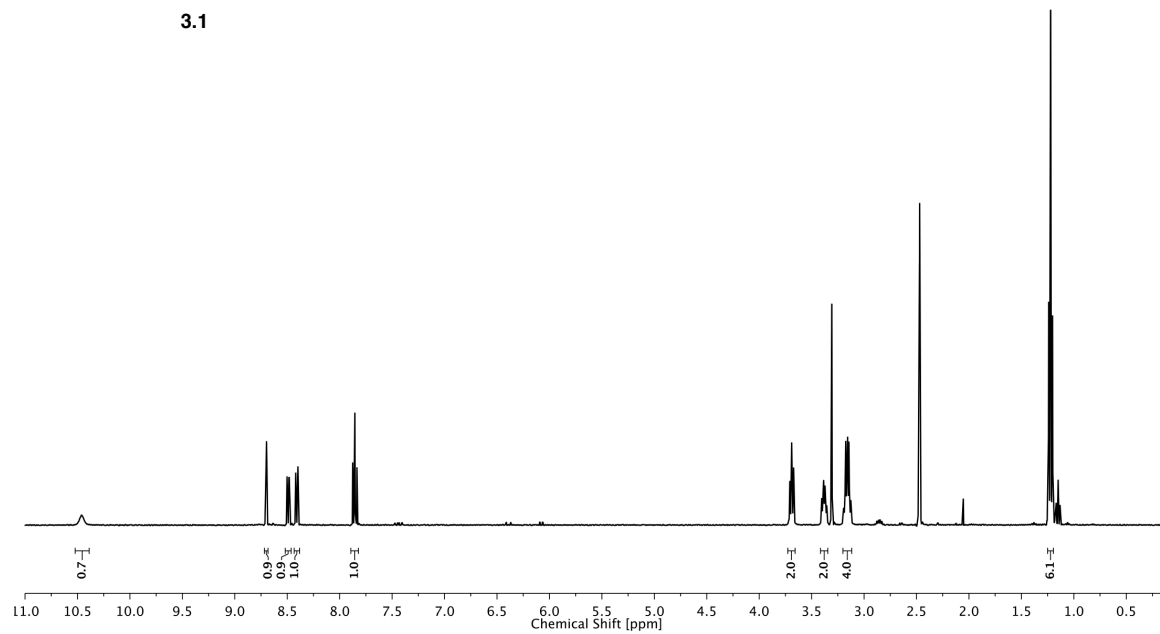
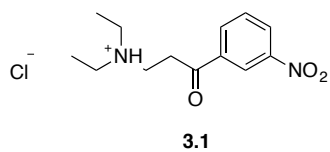
HEK 293T cells were cultured under standard conditions (Dulbecco's modified Eagle medium (DMEM) containing 10% FBS; 37 °C, 10% CO₂). Cells were plated on poly-L-lysine (0.1 mg/ml) treated coverlips in a density of 20,000 cells per cm² for electrophysiological measurements.

HEK 293T cells were transfected with TRPM8 (kindly provided by Dr. V. Chubanov, Walther-Straub-Institute of Pharmacology and Toxicology, Munich) using Lipofectamine[®] transfection agent according to the manufacturers instructions and measured after 12–24 h.

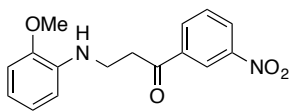
Whole-cell Electrophysiology

Patch clamp recordings of HEK 293T cells were carried out using a HEKA Patch Clamp EPC10 USB amplifier in whole cell mode and were performed at room temperature. Cells were voltage-clamped at –60 mV. Pipettes (Science Products GB200-F-8P with filament) were pulled with a Narishige PC-10 pipette puller and had resistances of 4–6 MΩ. The Bath solution contained 150 mM NaCl, 6.0 mM CsCl, 1.0 mM MgCl₂, 1.5 mM CaCl₂, 10 mM HEPES and 10 mM glucose, adjusted to pH = 7.4. Pipette solution contained 150 mM NaCl, 3.0 mM MgCl₂, 10.0 mM HEPES and 5.0 mM EGTA, adjusted to pH = 7.2.^[25] Data was recorded using the HEKA PatchMaster software (V2x60). The sampling rate was 20–50 kHz and the currents were digitally filtered at 2.9 kHz. Cells were illuminated with a Polychrome V monochromator (Till Photonics), as described previously.^[66]

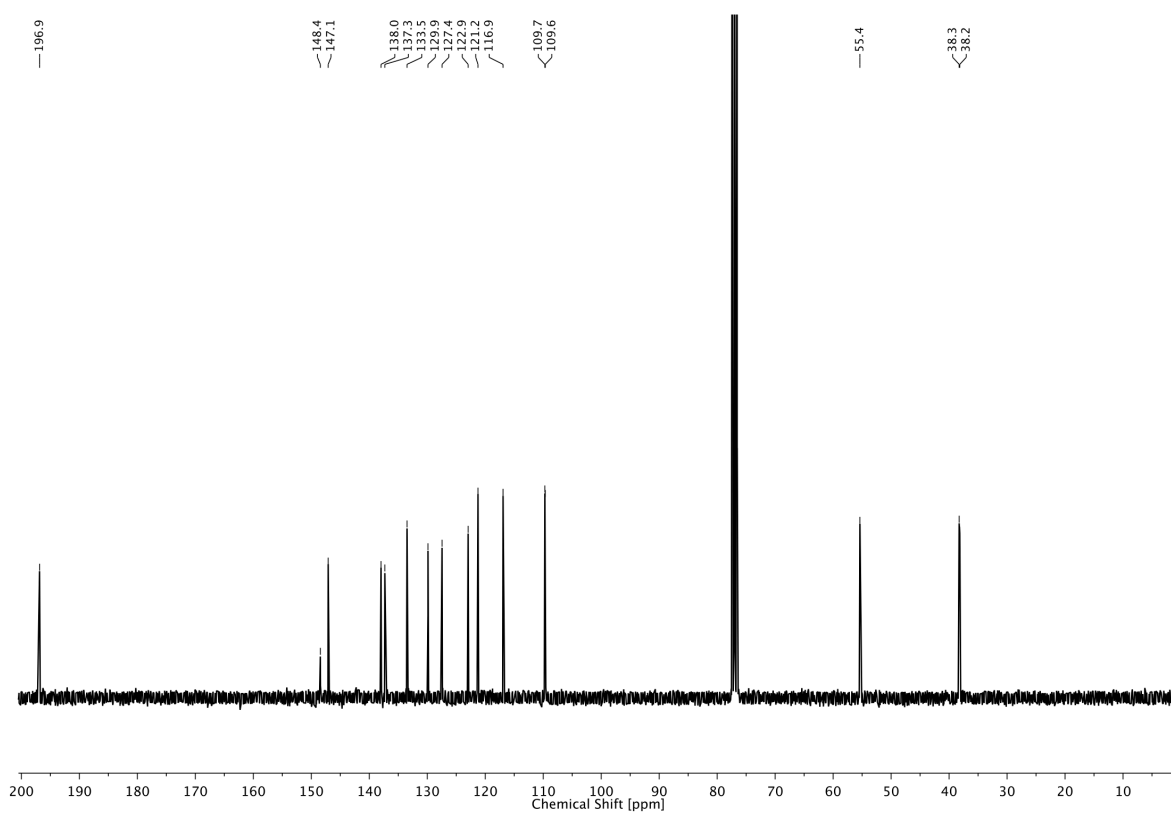
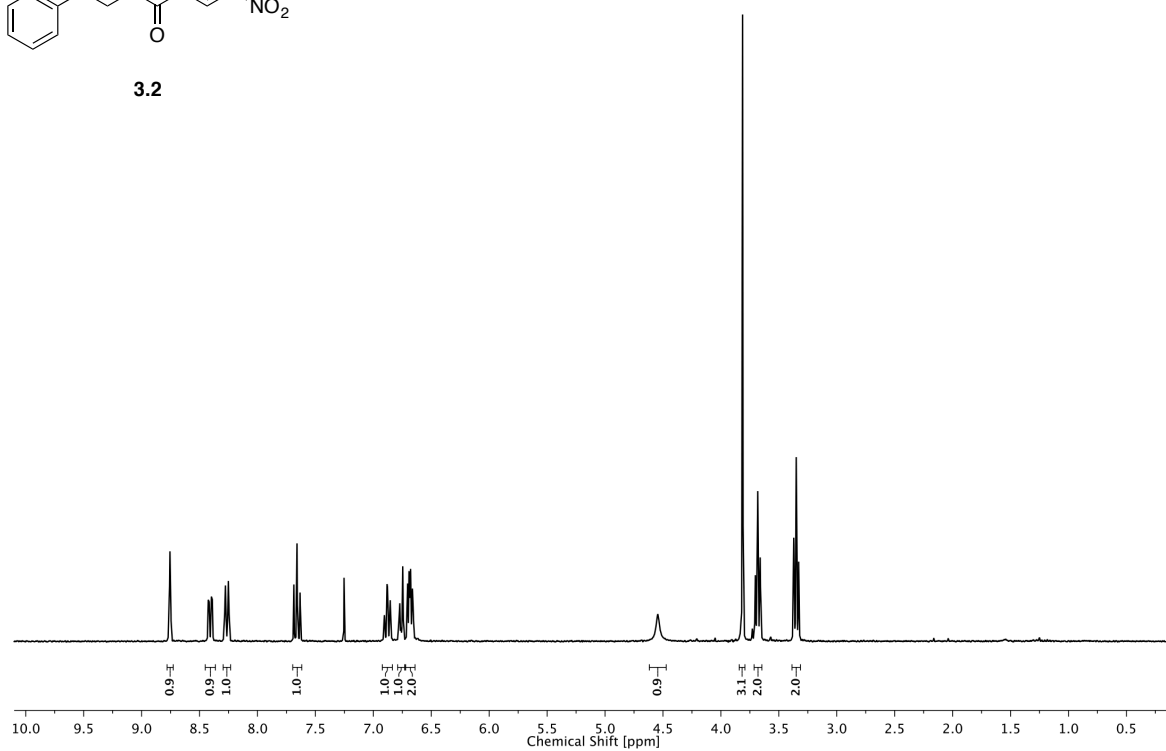
3.7 NMR SPECTRA



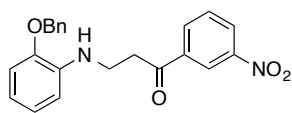
3 PHOTOCONTROL OF TRP CHANNELS



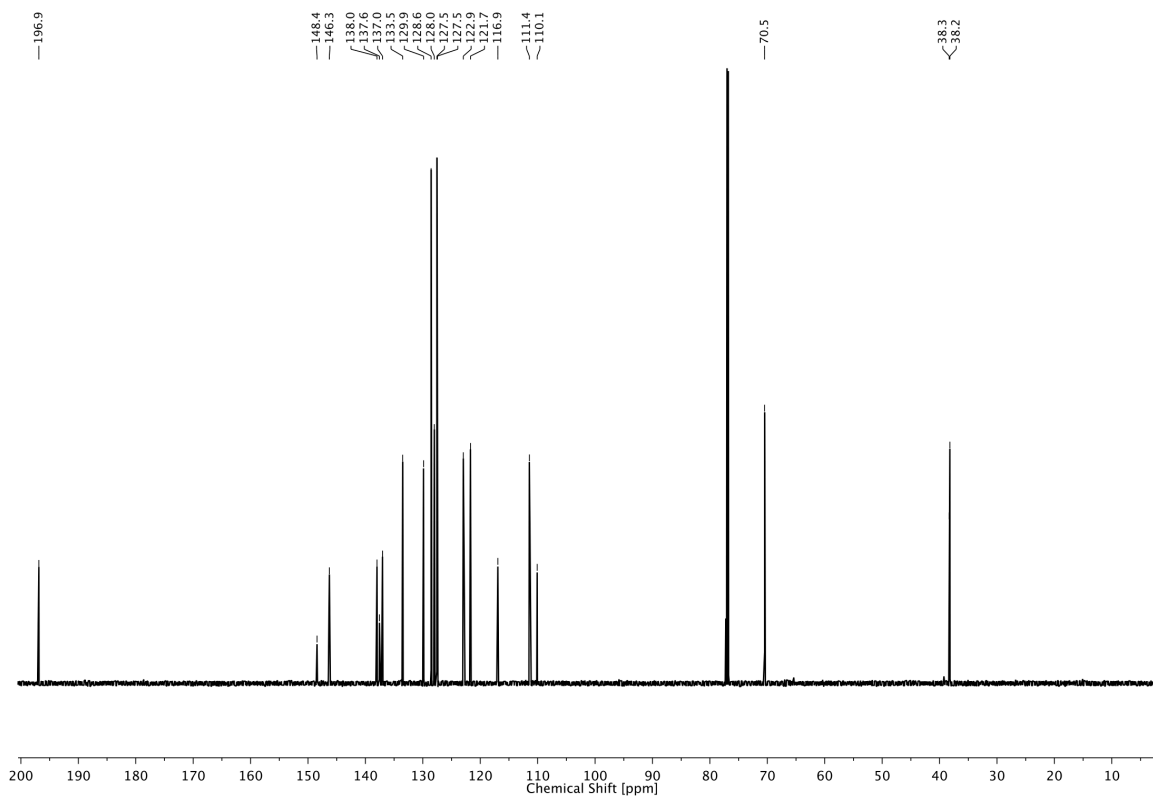
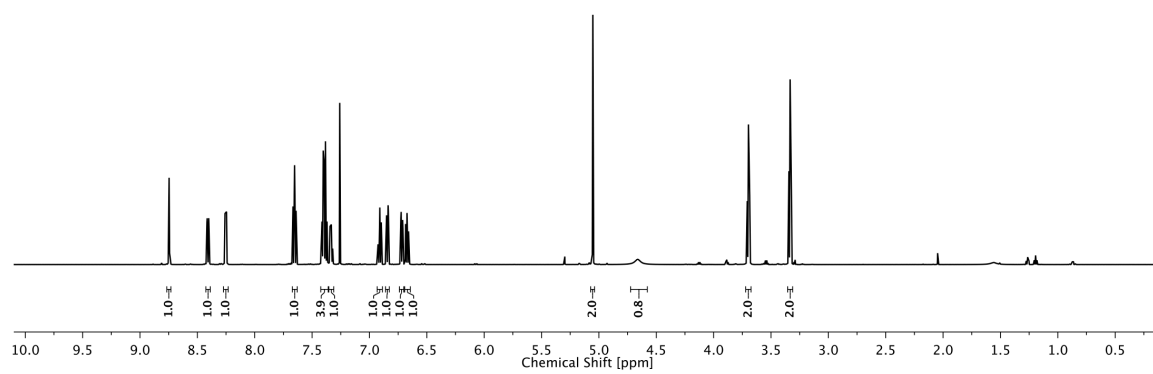
3.2



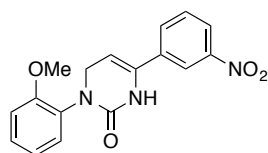
3 PHOTOCONTROL OF TRP CHANNELS



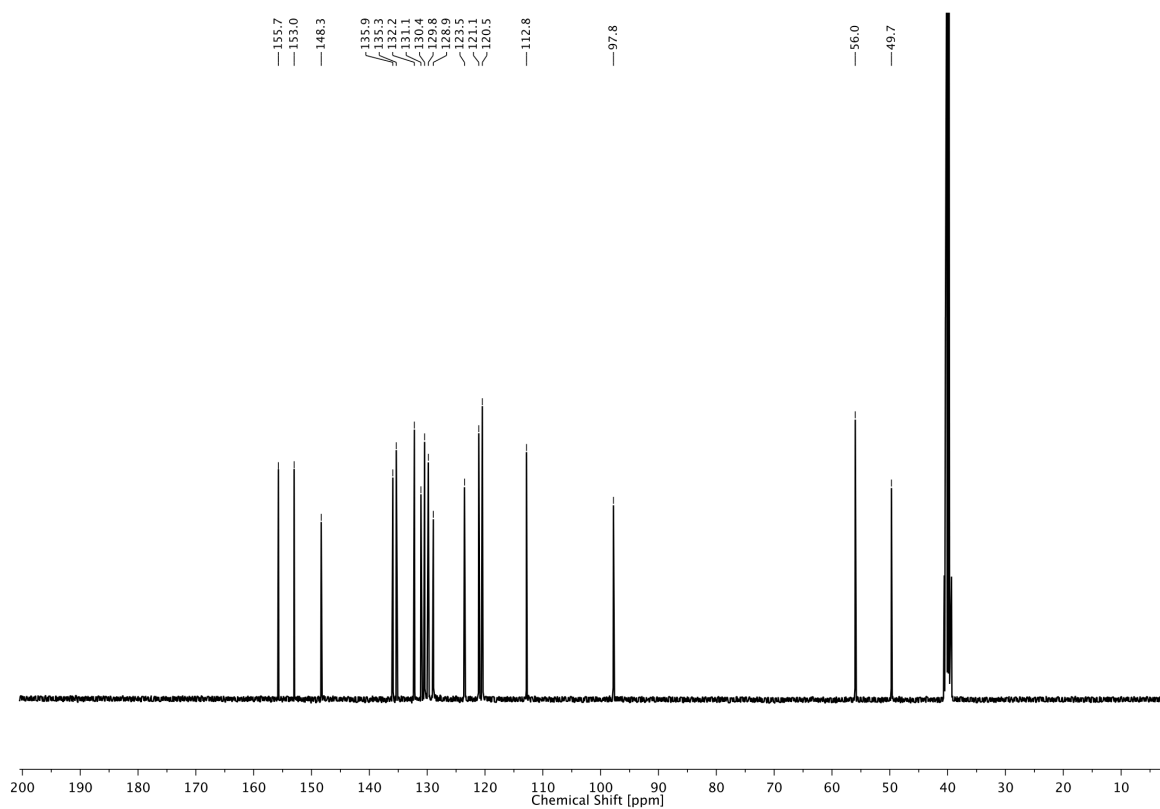
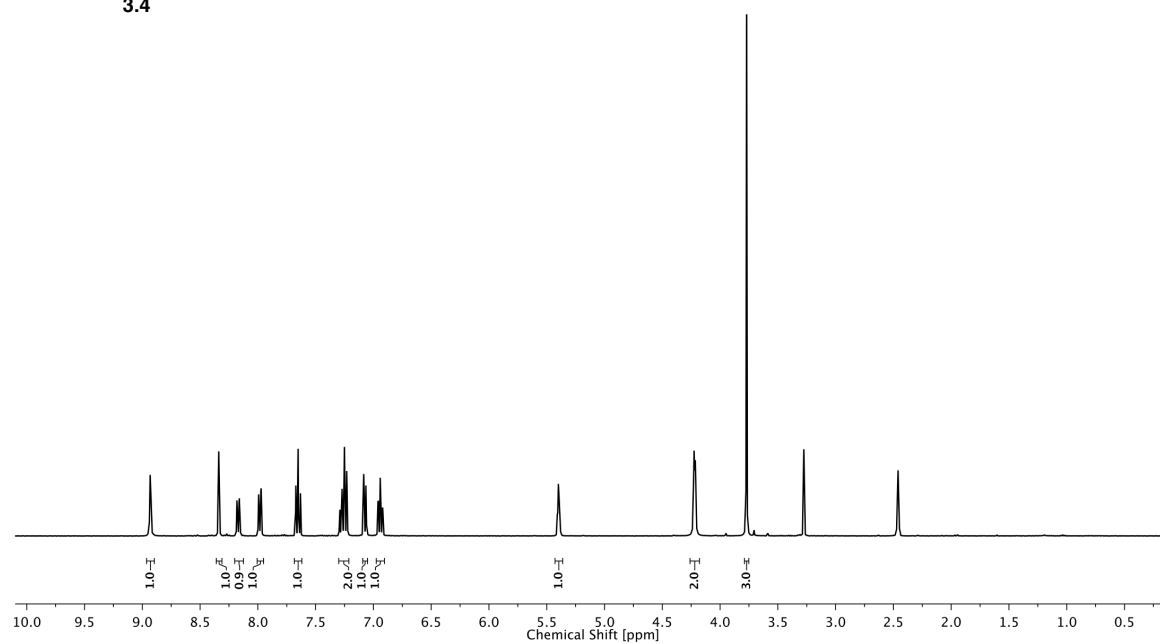
3.3



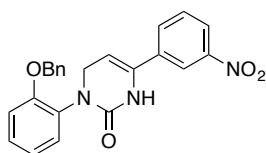
3 PHOTOCONTROL OF TRP CHANNELS



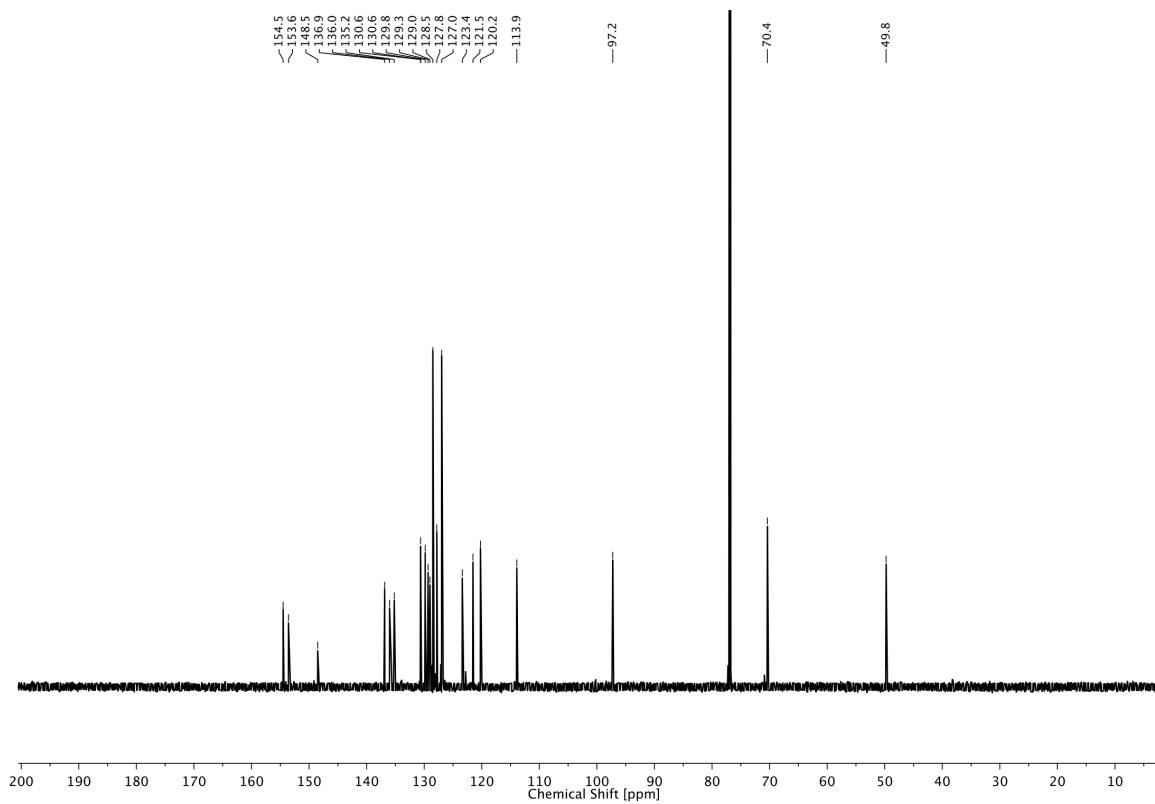
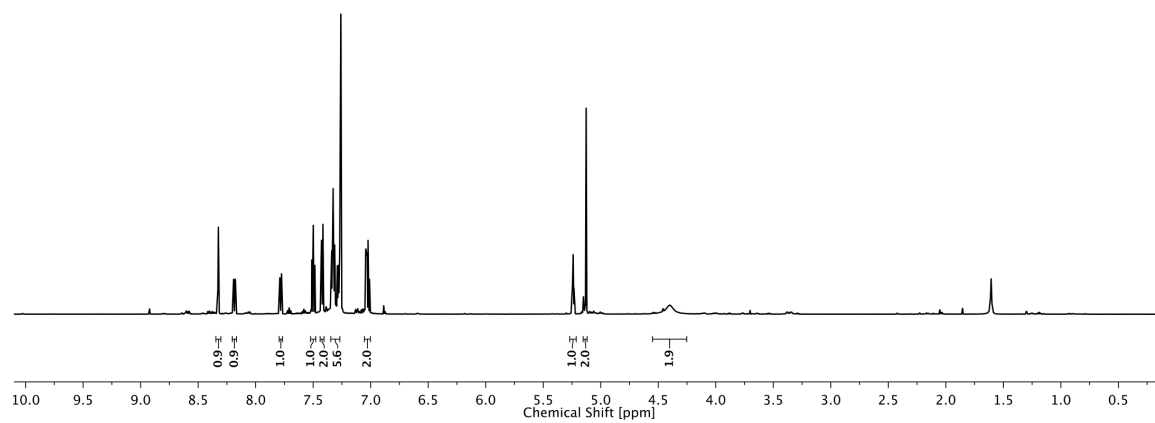
3.4



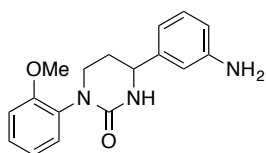
3 PHOTOCONTROL OF TRP CHANNELS



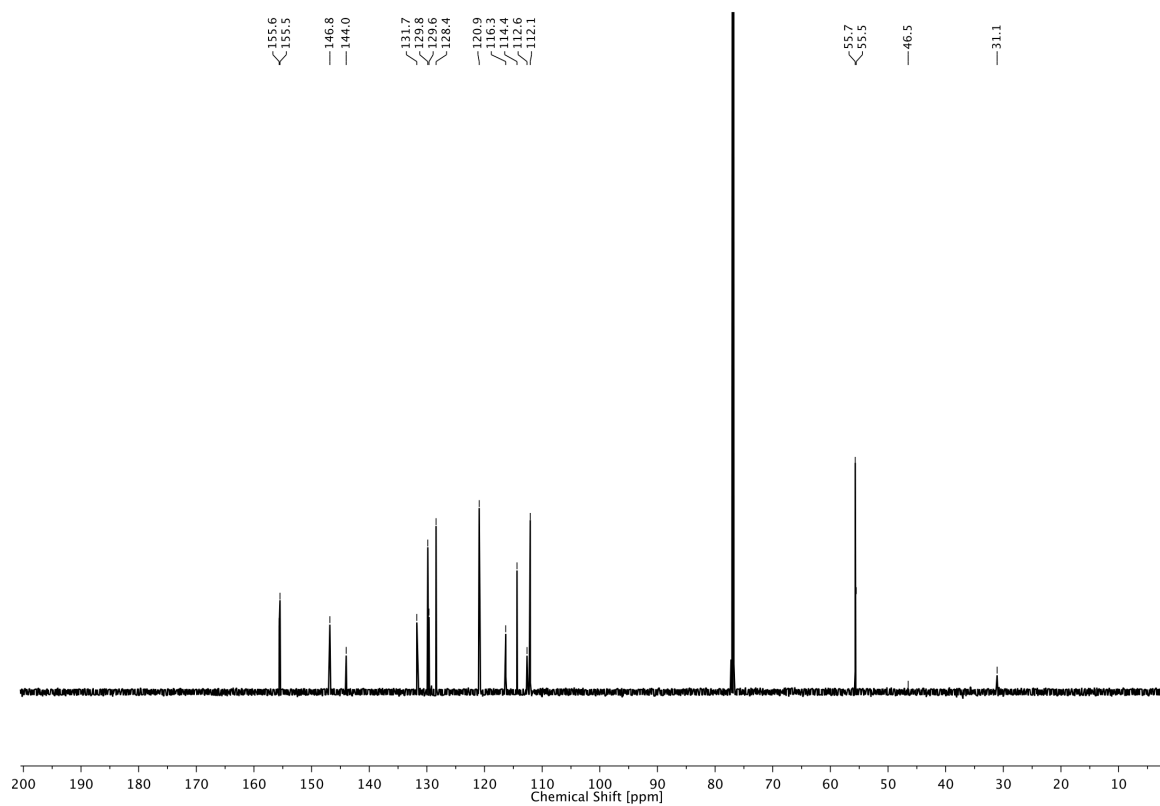
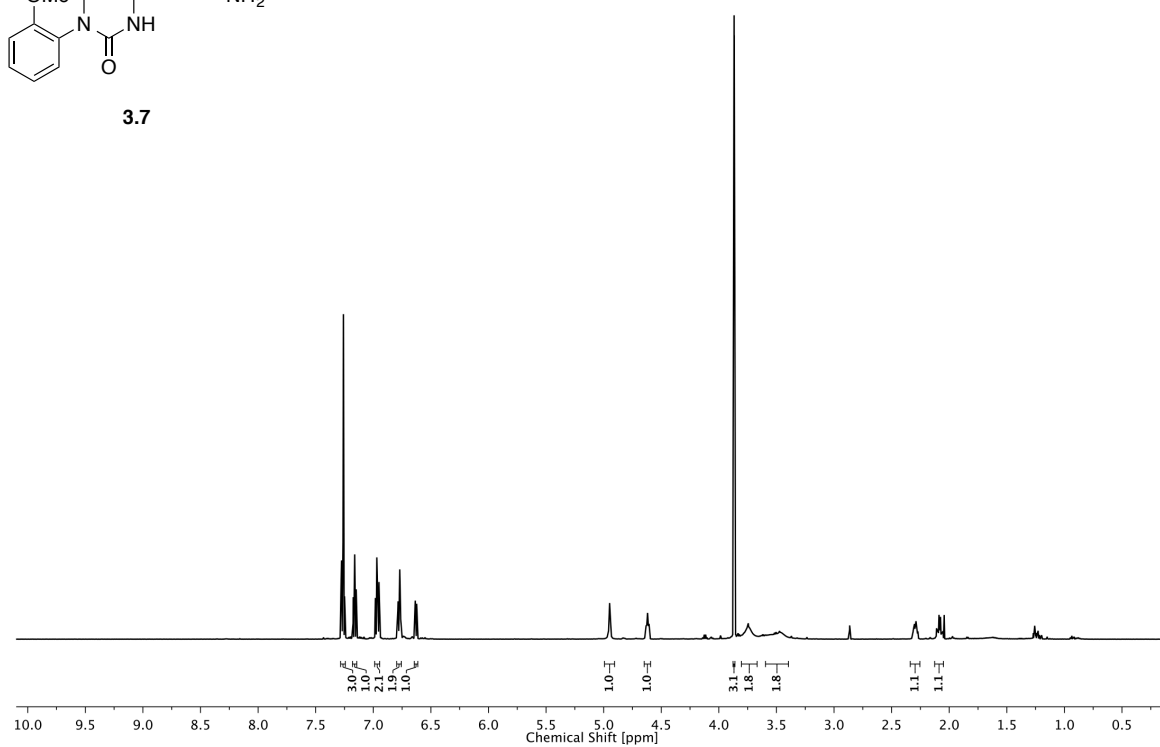
3.5

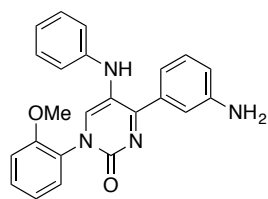


3 PHOTOCONTROL OF TRP CHANNELS

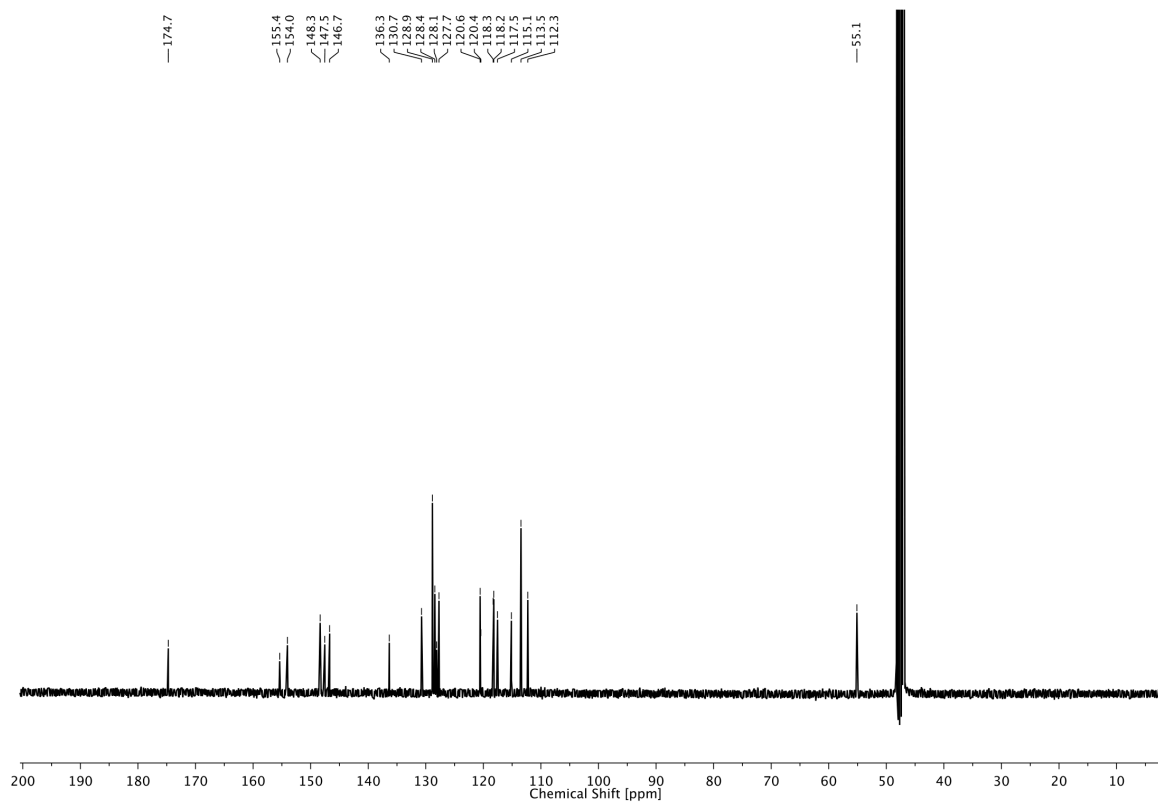
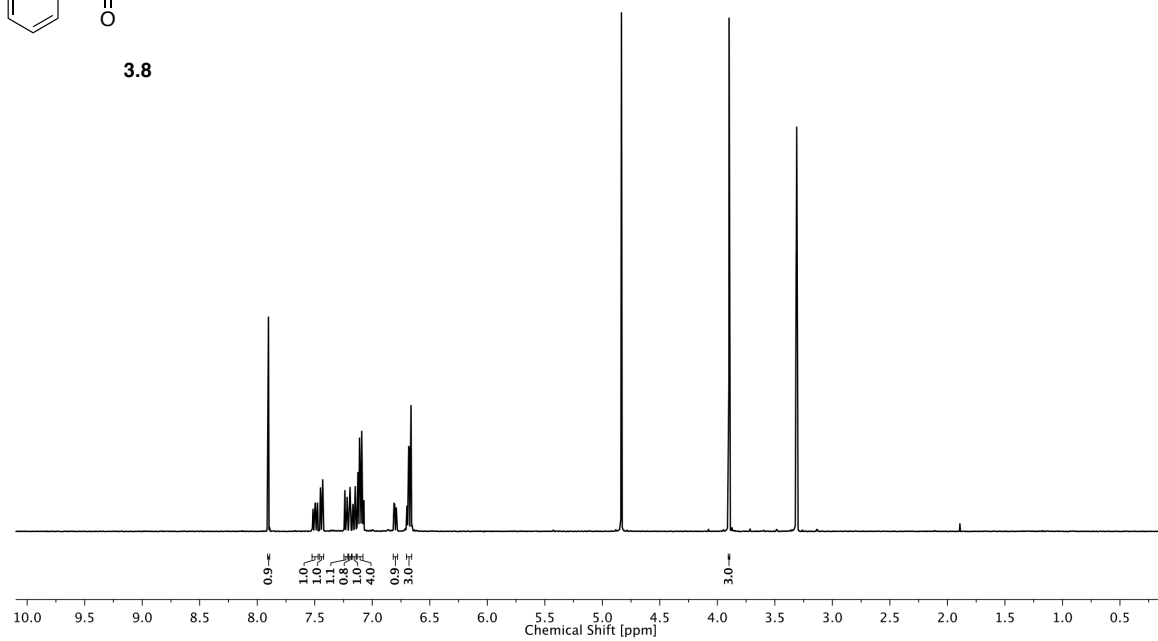


3.7

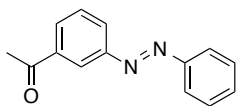




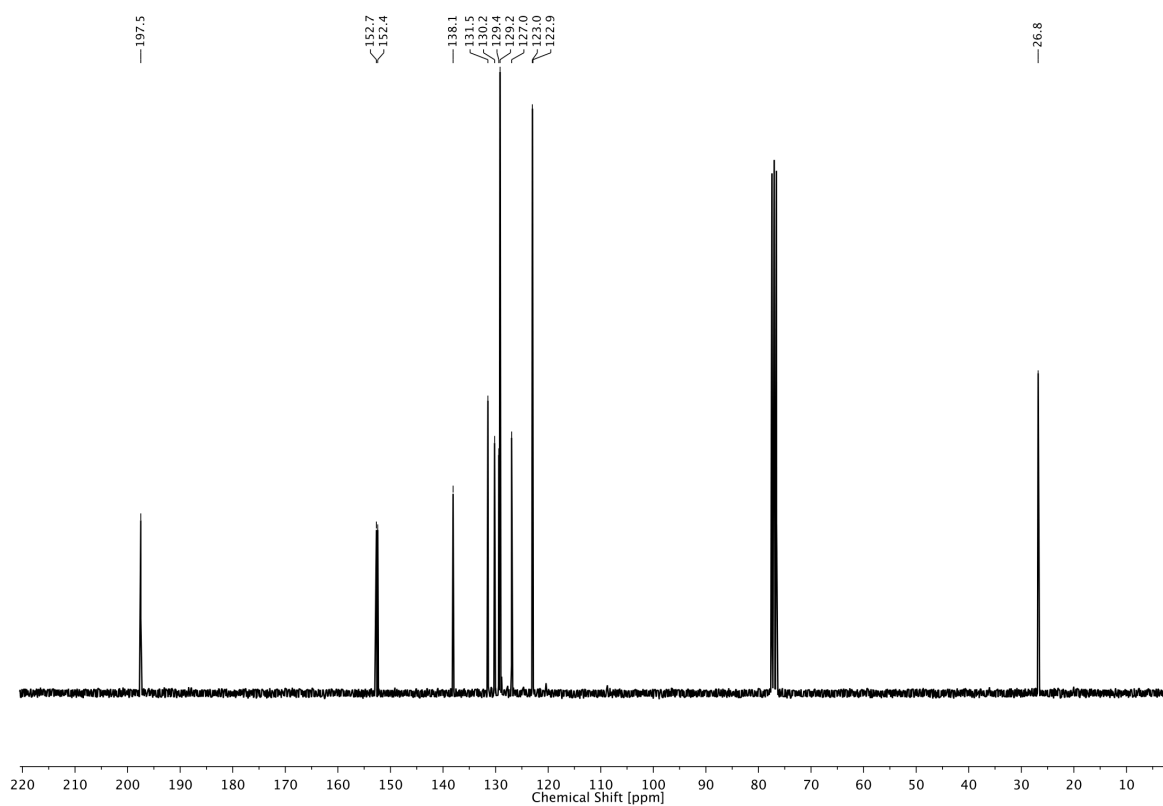
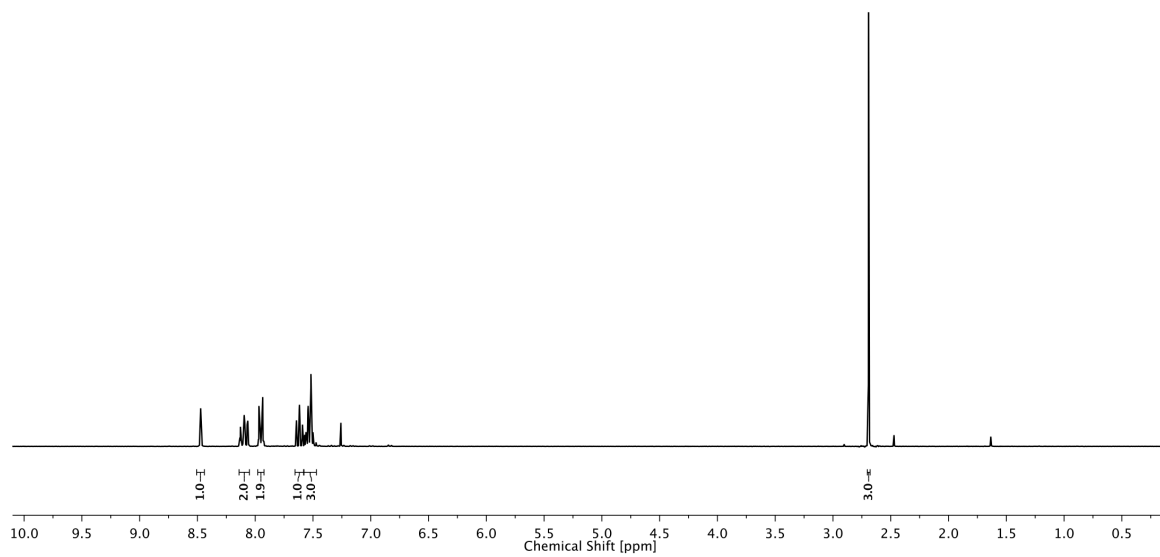
3.8



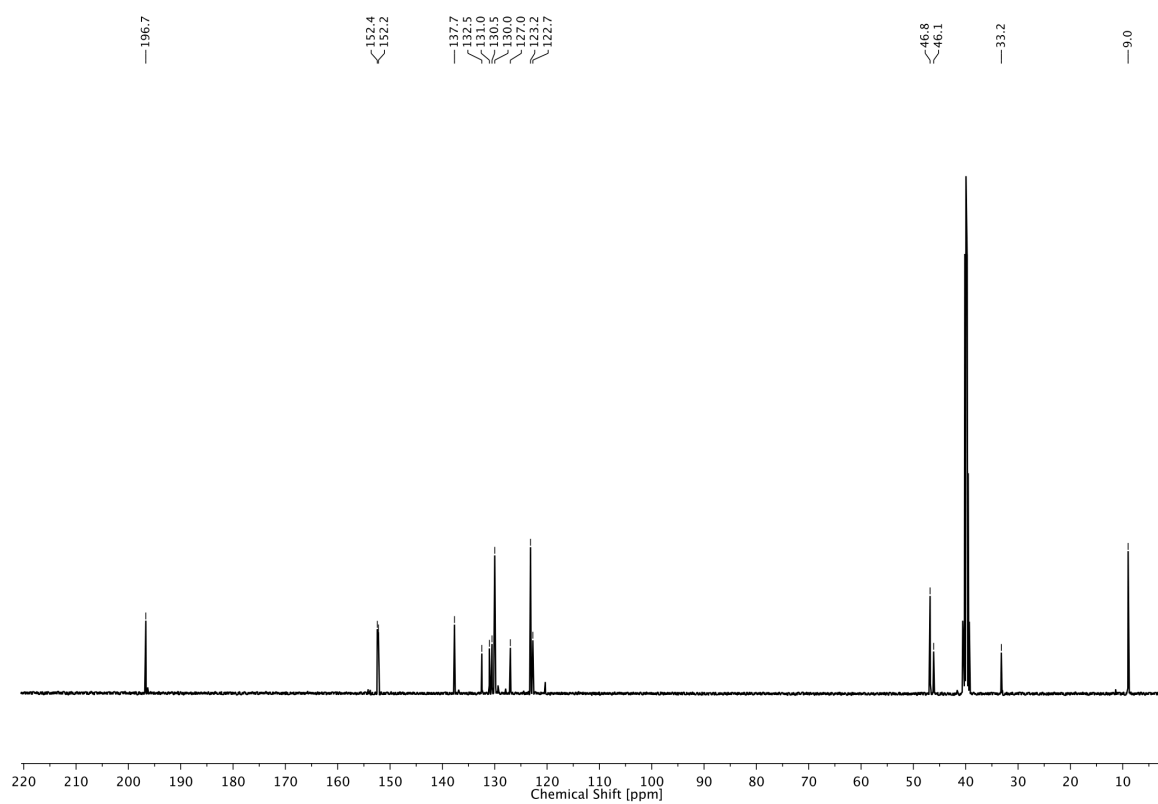
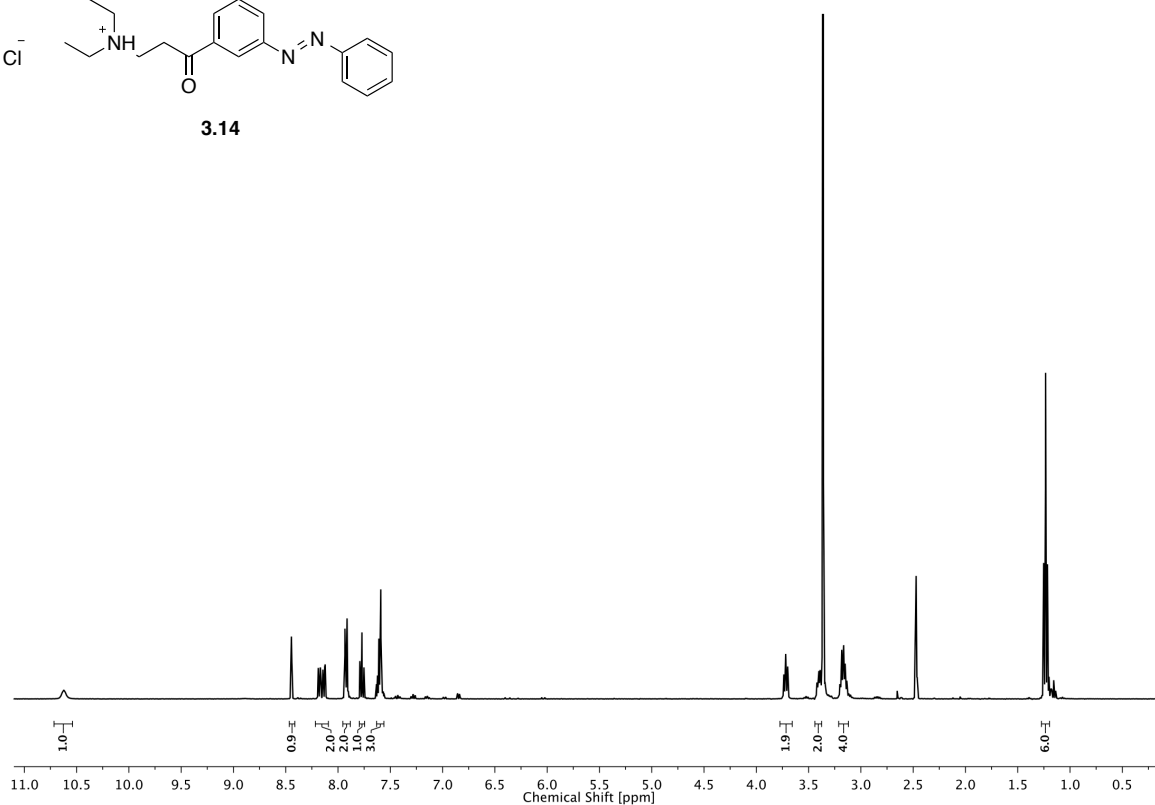
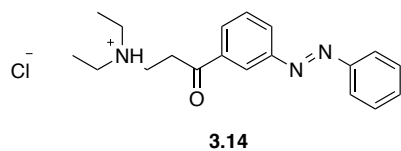
3 PHOTOCONTROL OF TRP CHANNELS



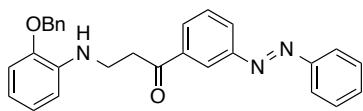
3.13



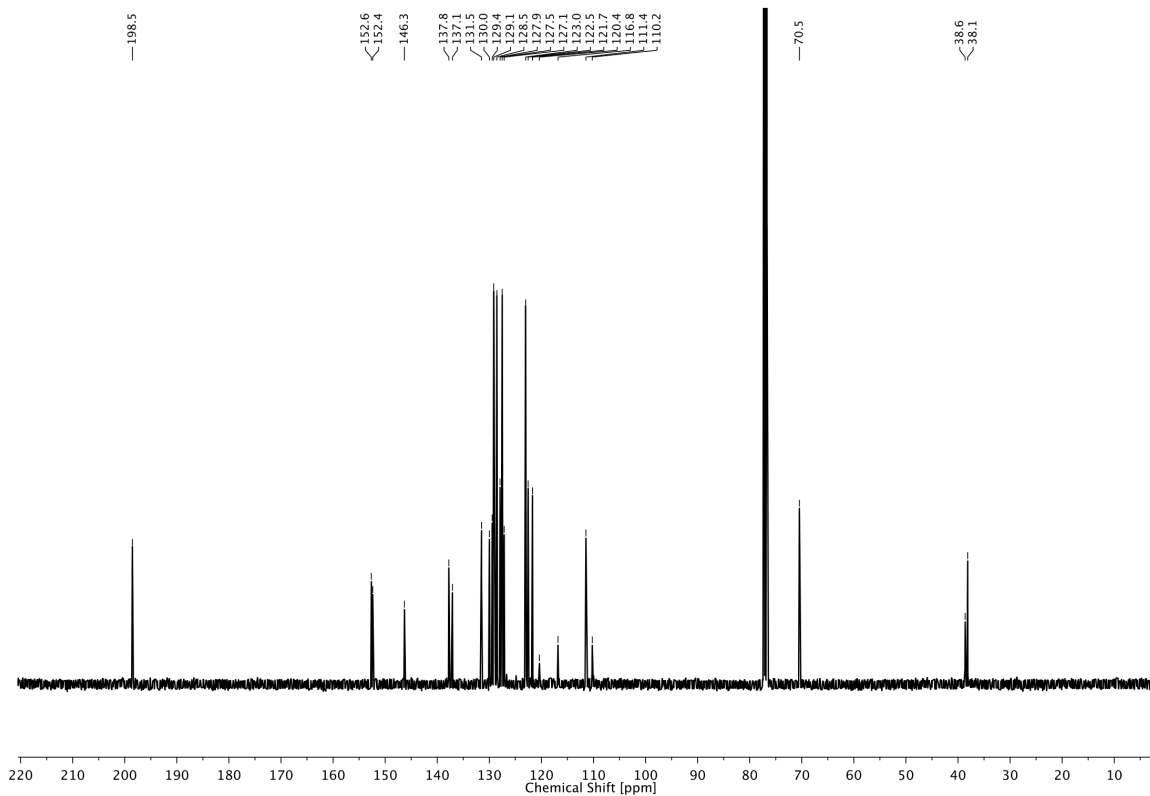
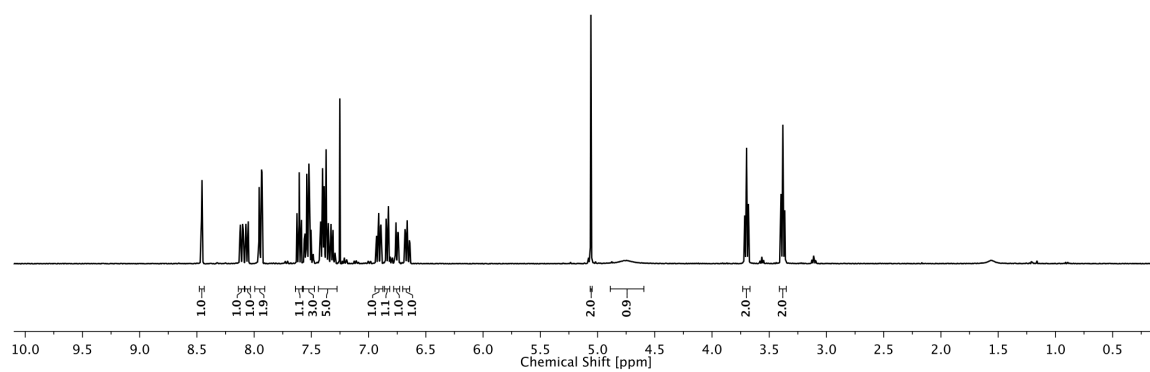
3 PHOTOCONTROL OF TRP CHANNELS

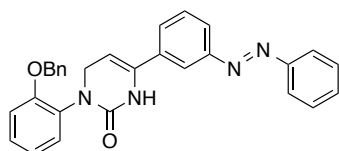


3 PHOTOCONTROL OF TRP CHANNELS

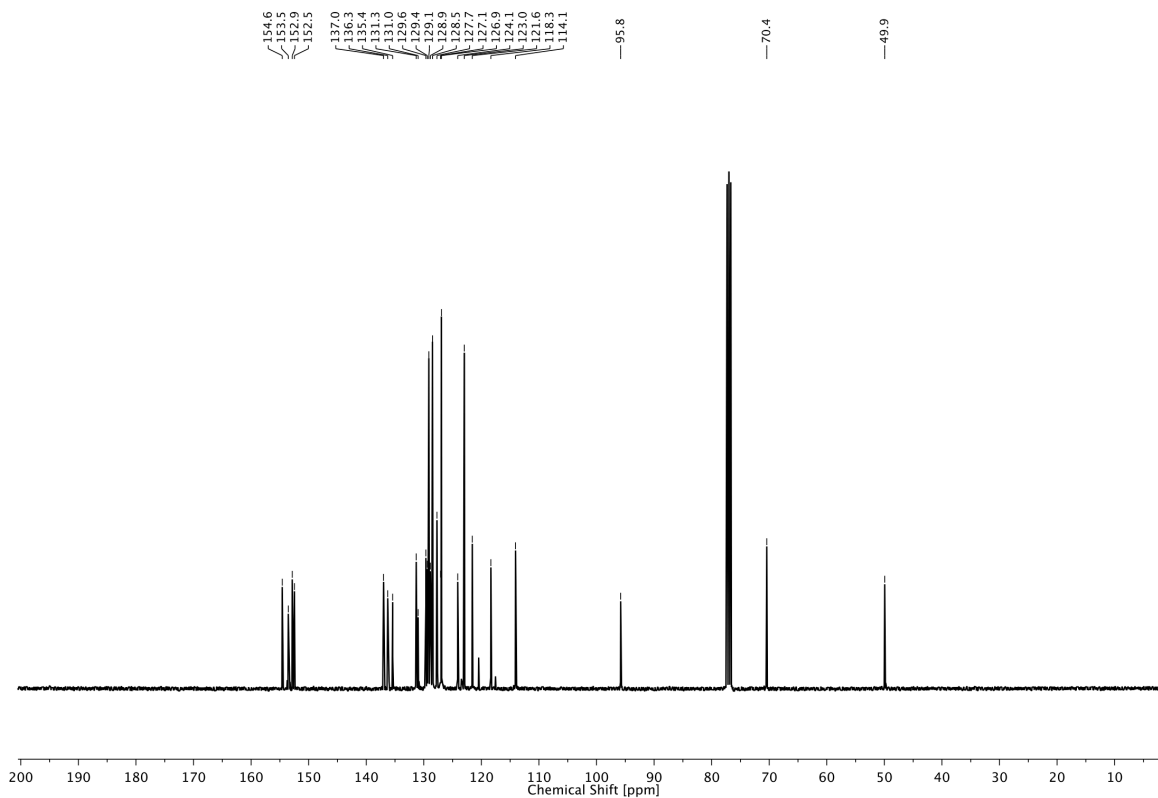
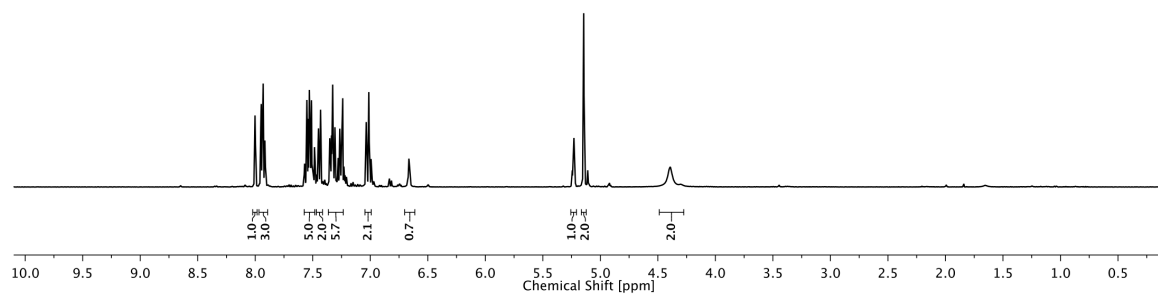


3.16

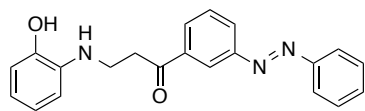




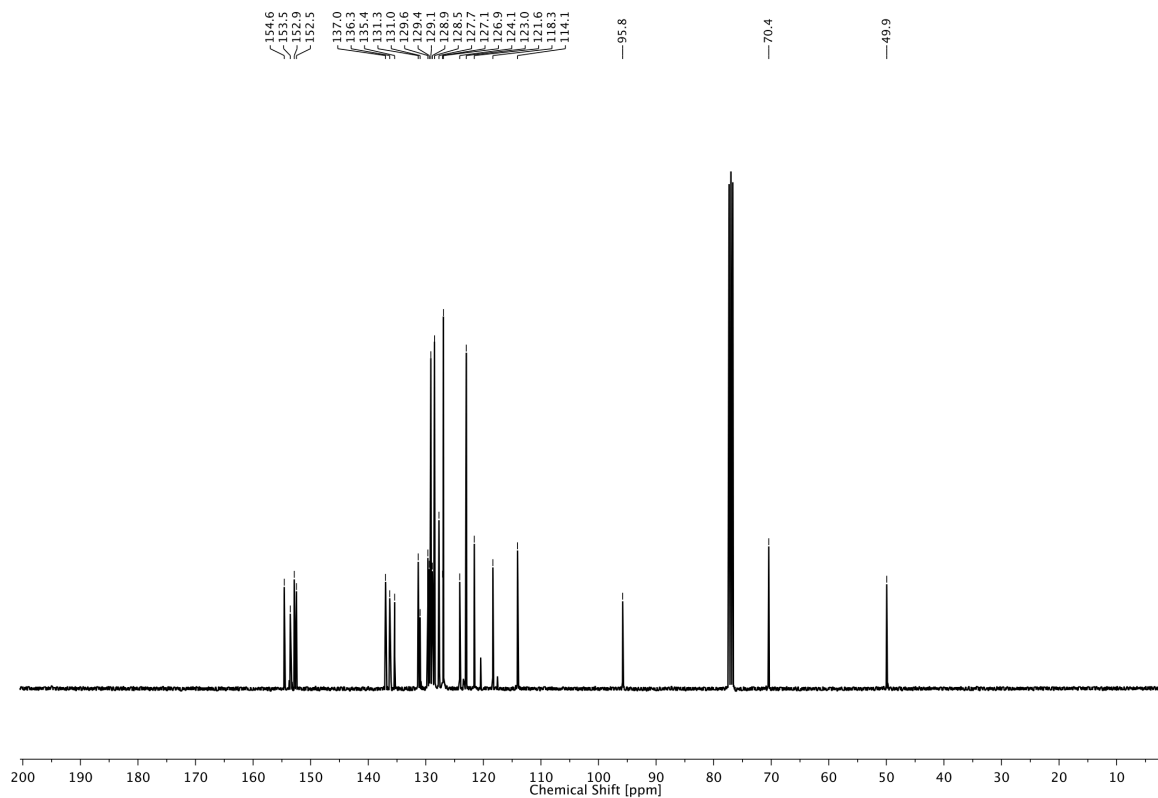
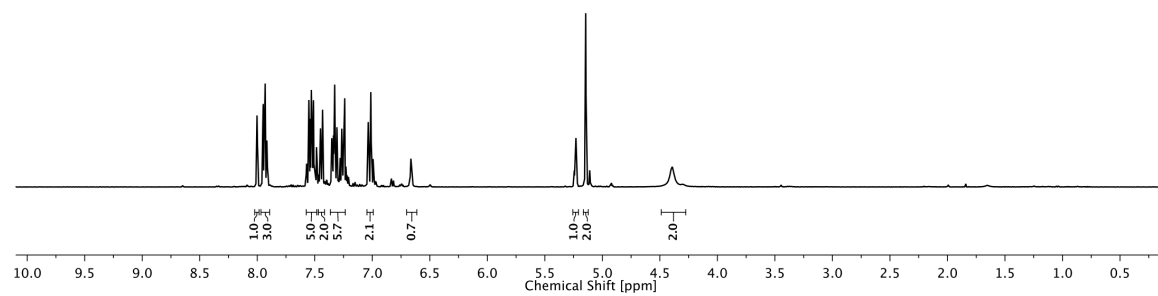
3.17

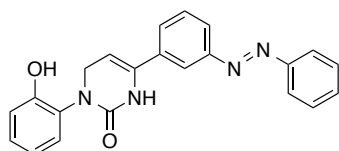


3 PHOTOCONTROL OF TRP CHANNELS

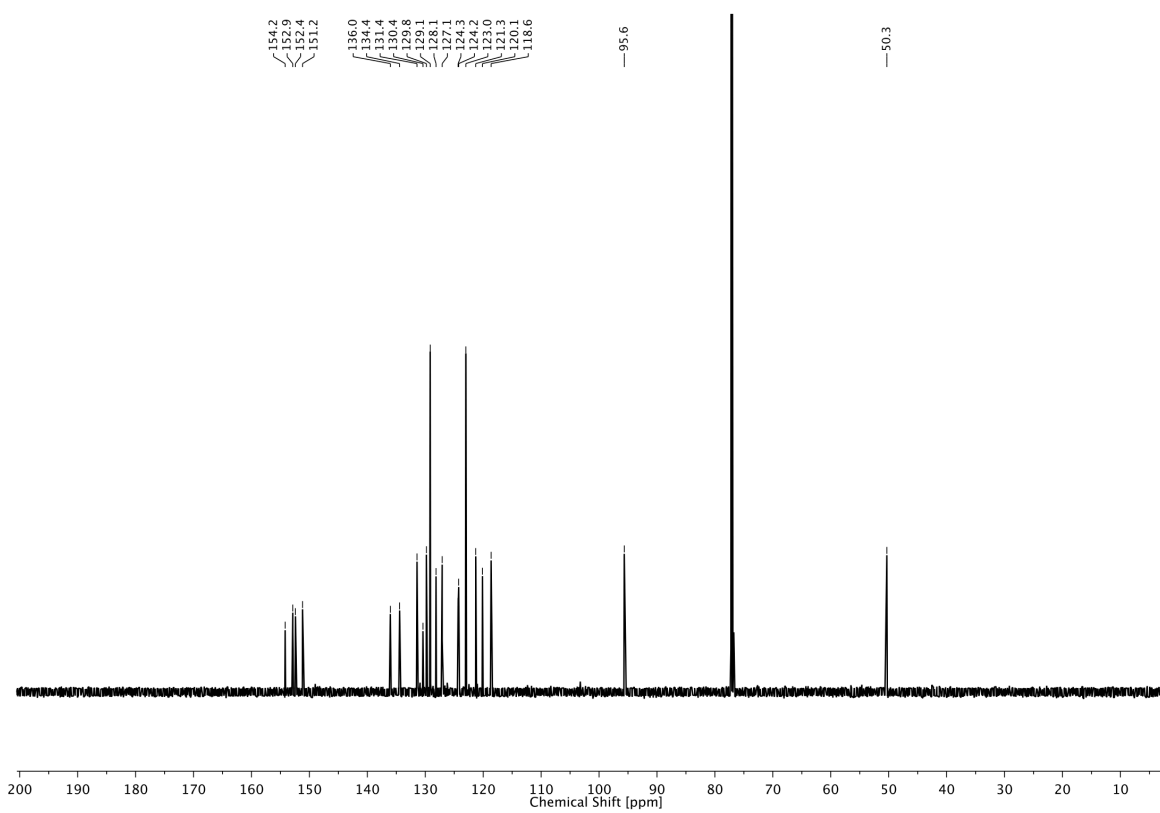
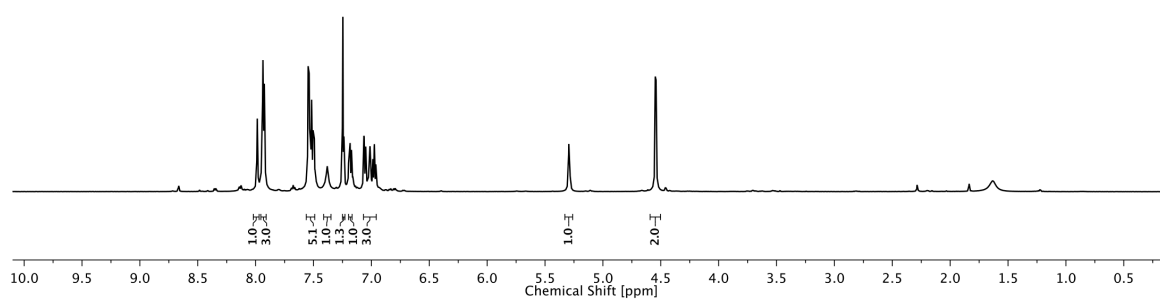


3.15

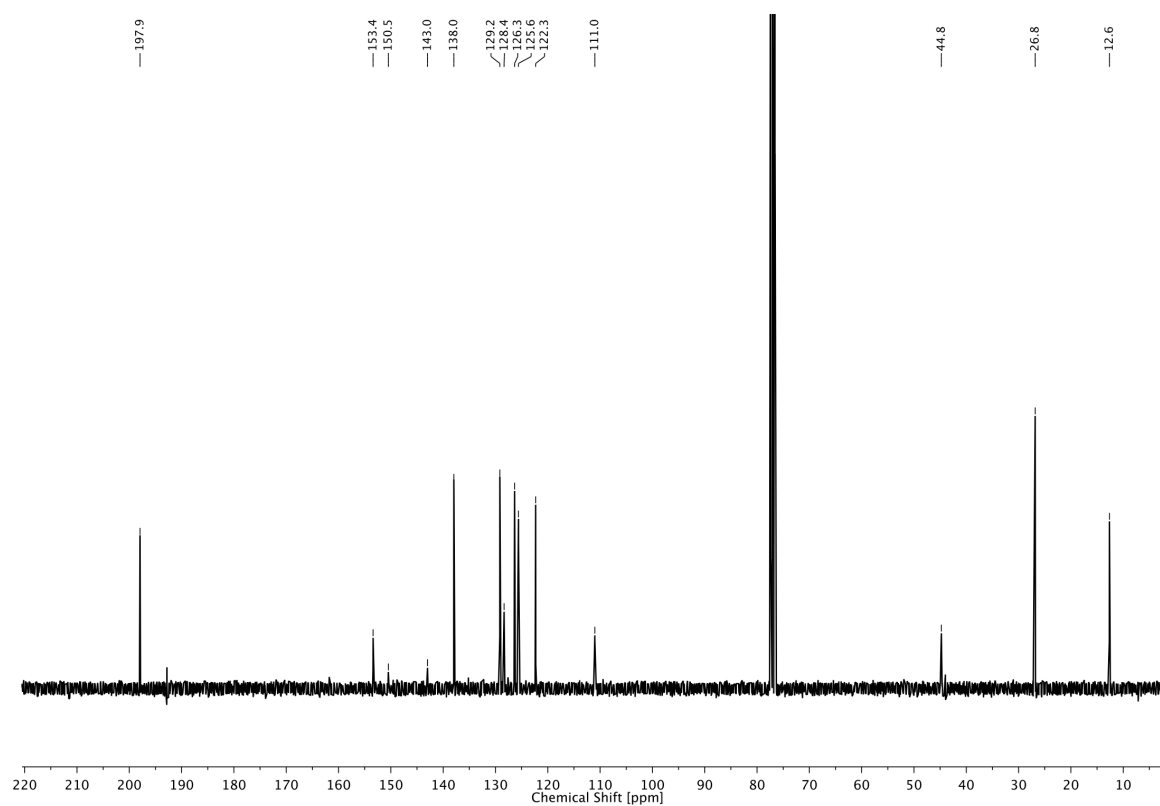
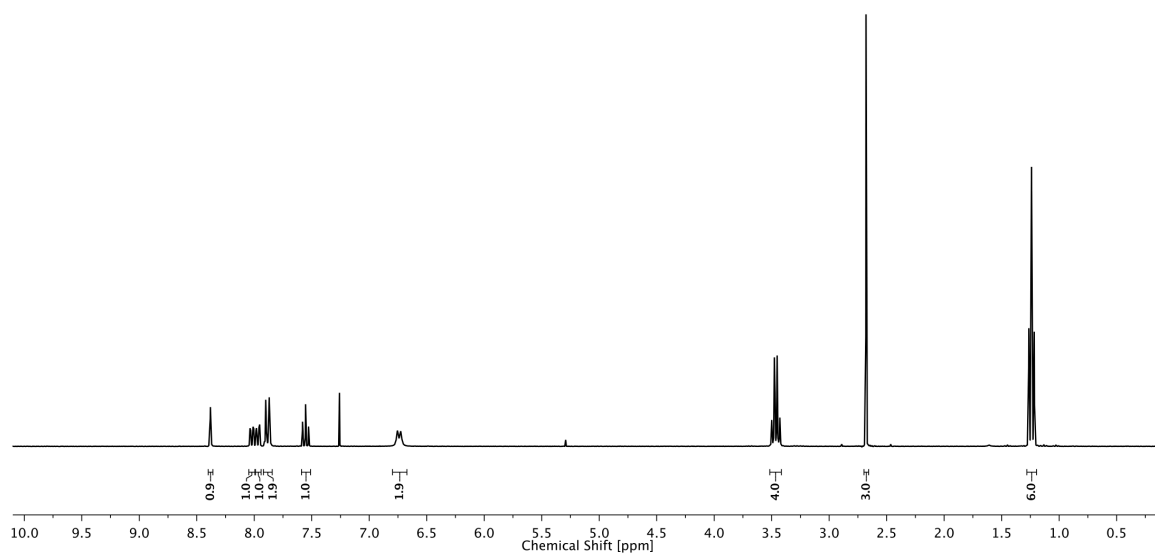
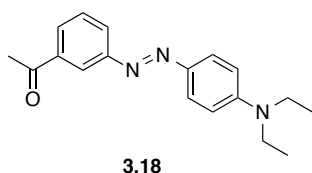




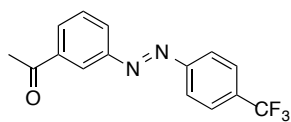
A11



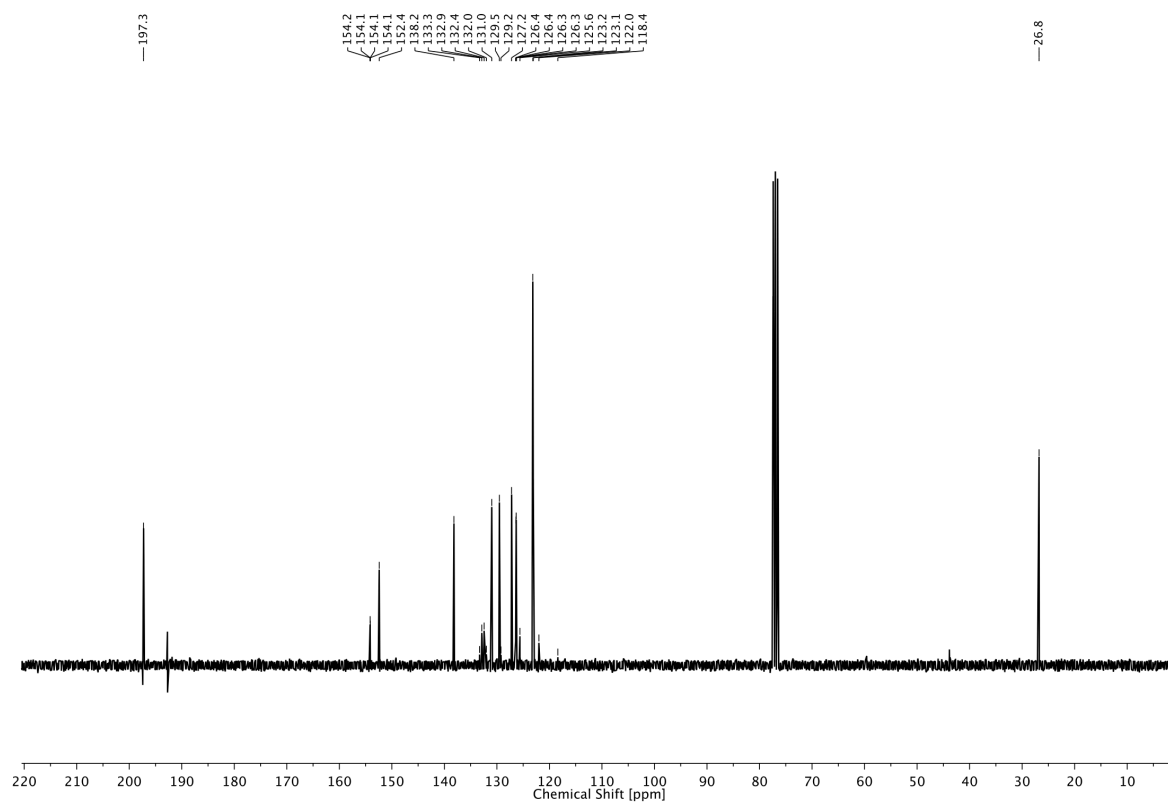
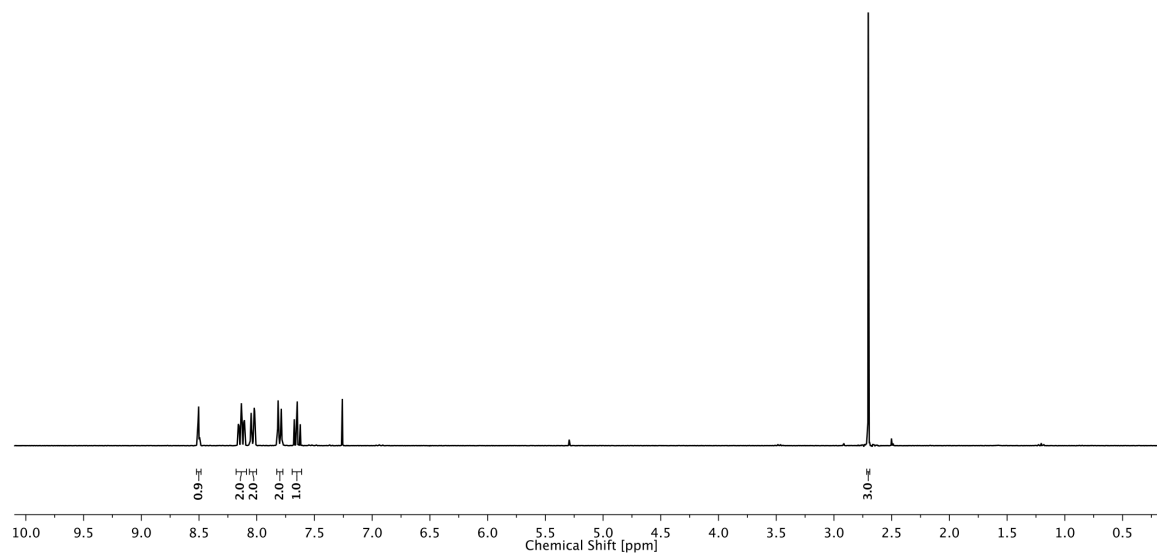
3 PHOTOCONTROL OF TRP CHANNELS



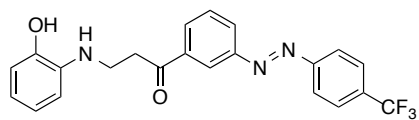
3 PHOTOCONTROL OF TRP CHANNELS



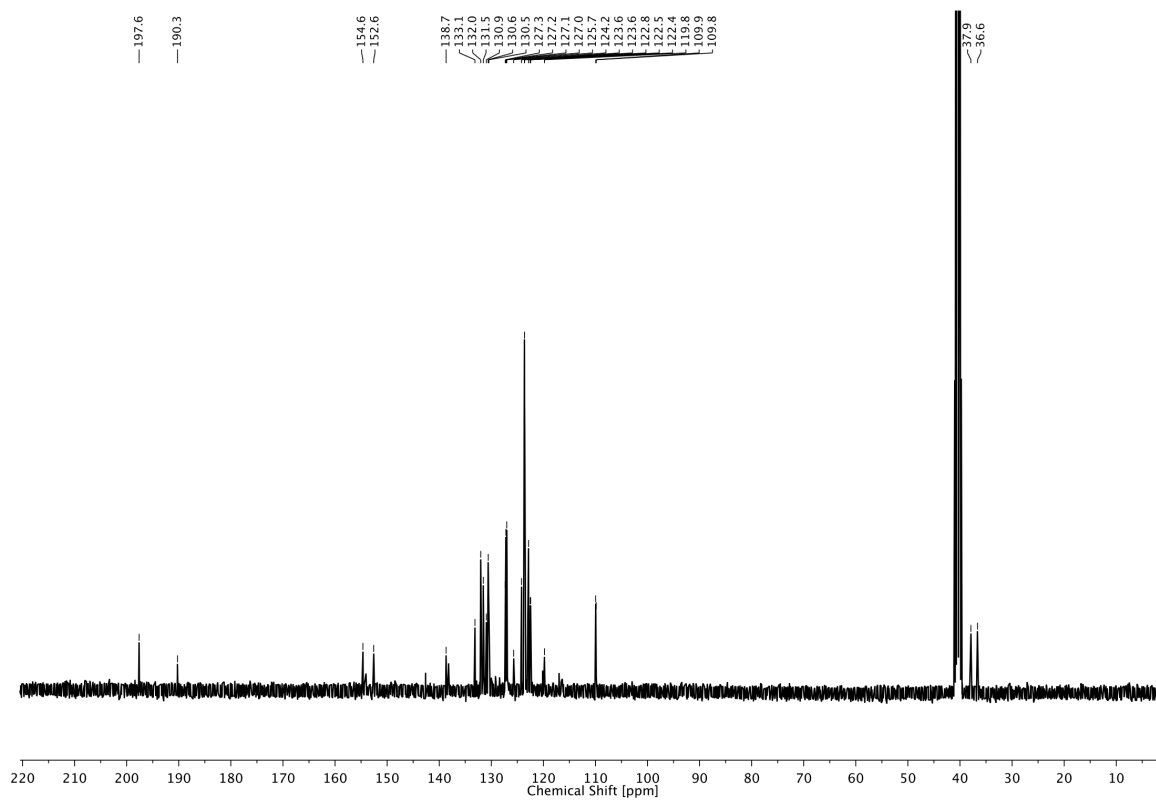
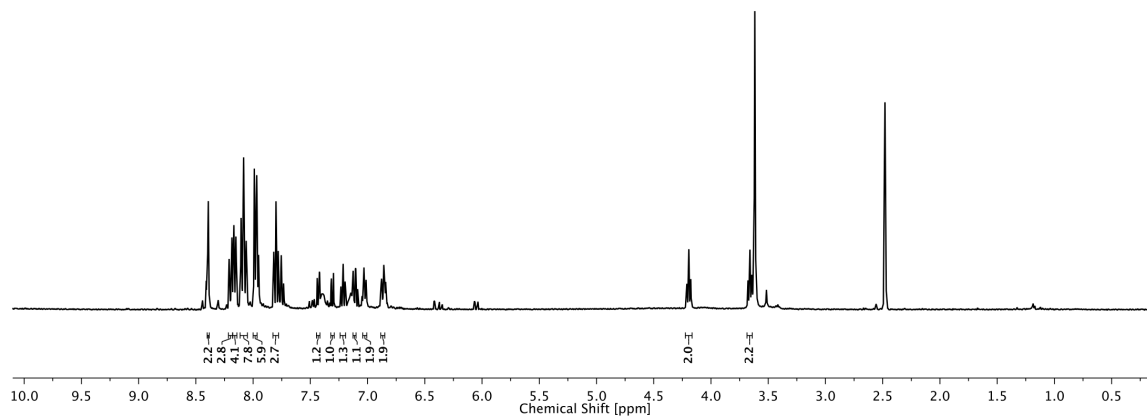
3.20



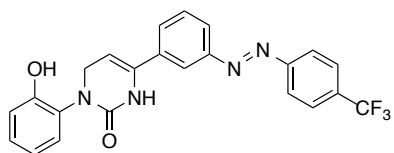
3 PHOTOCONTROL OF TRP CHANNELS



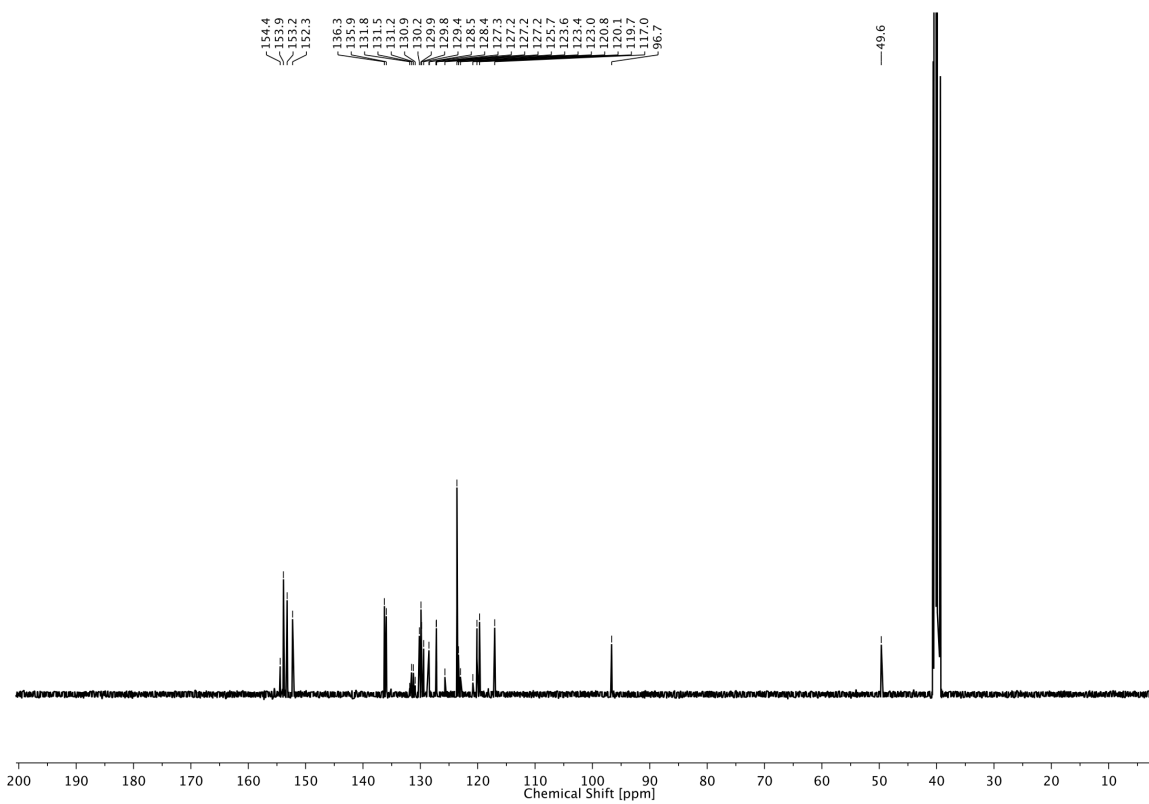
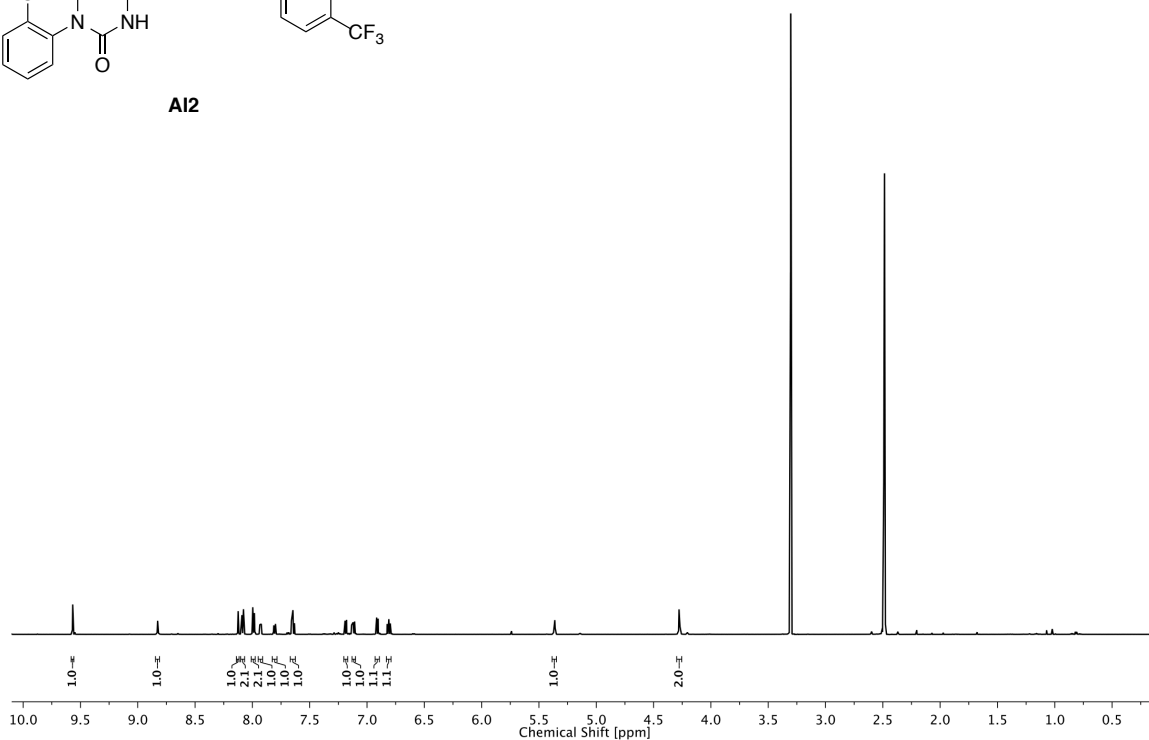
3.22



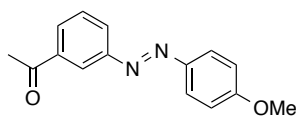
3 PHOTOCONTROL OF TRP CHANNELS



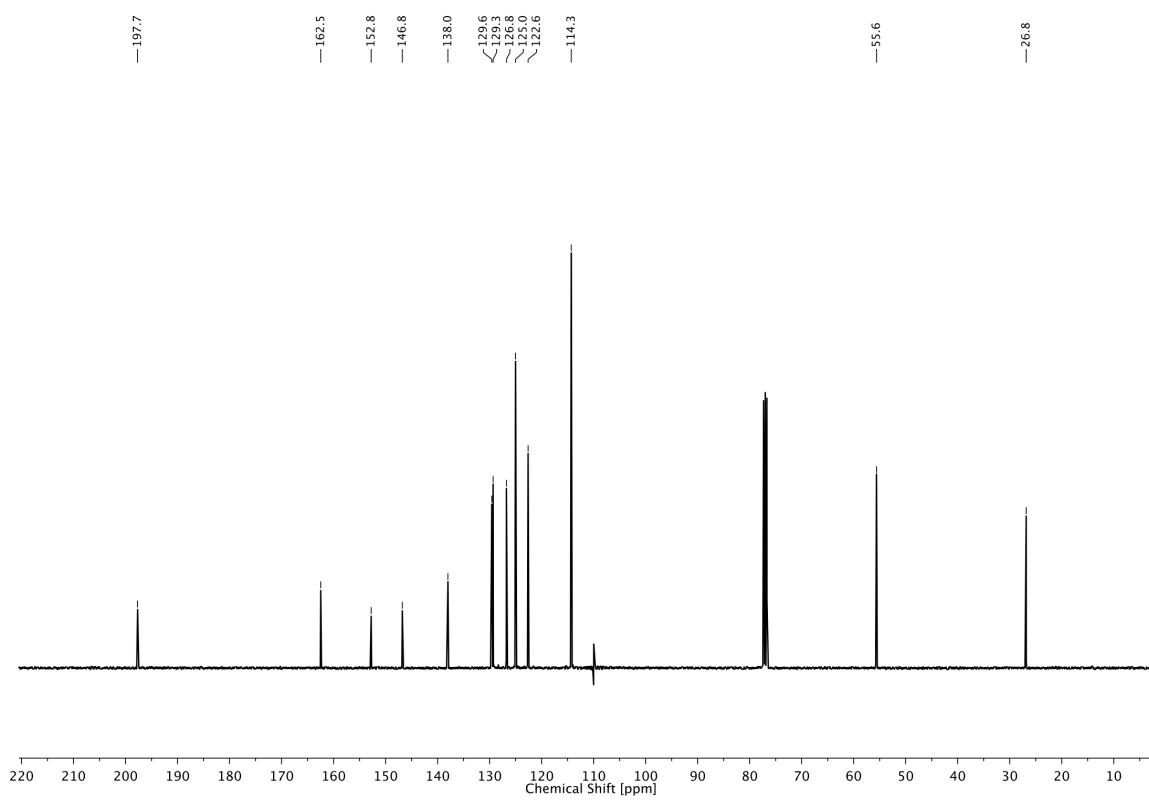
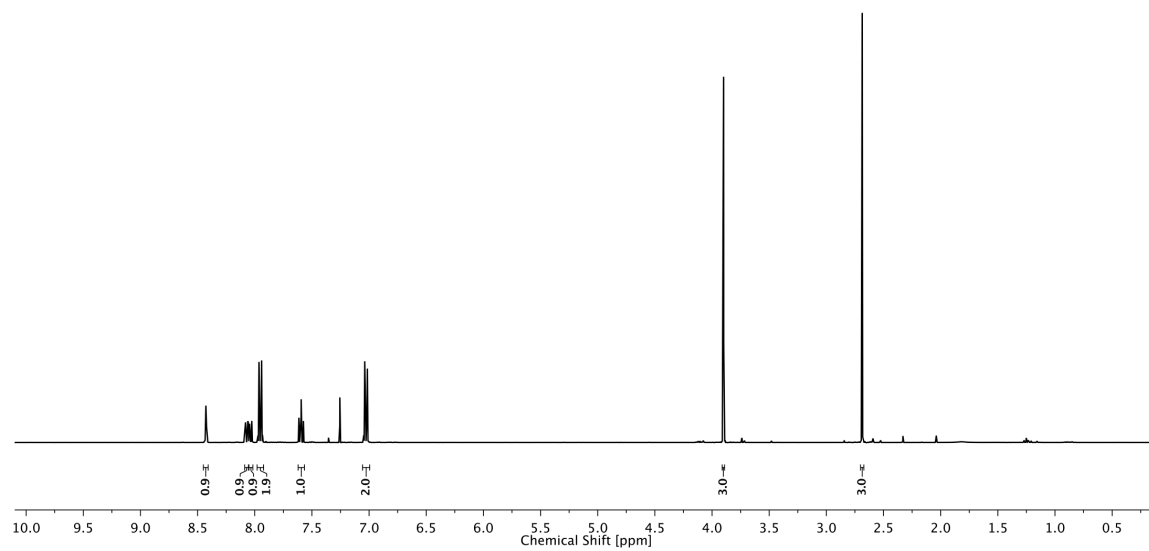
AI2



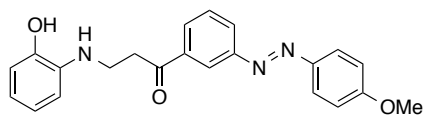
3 PHOTOCONTROL OF TRP CHANNELS



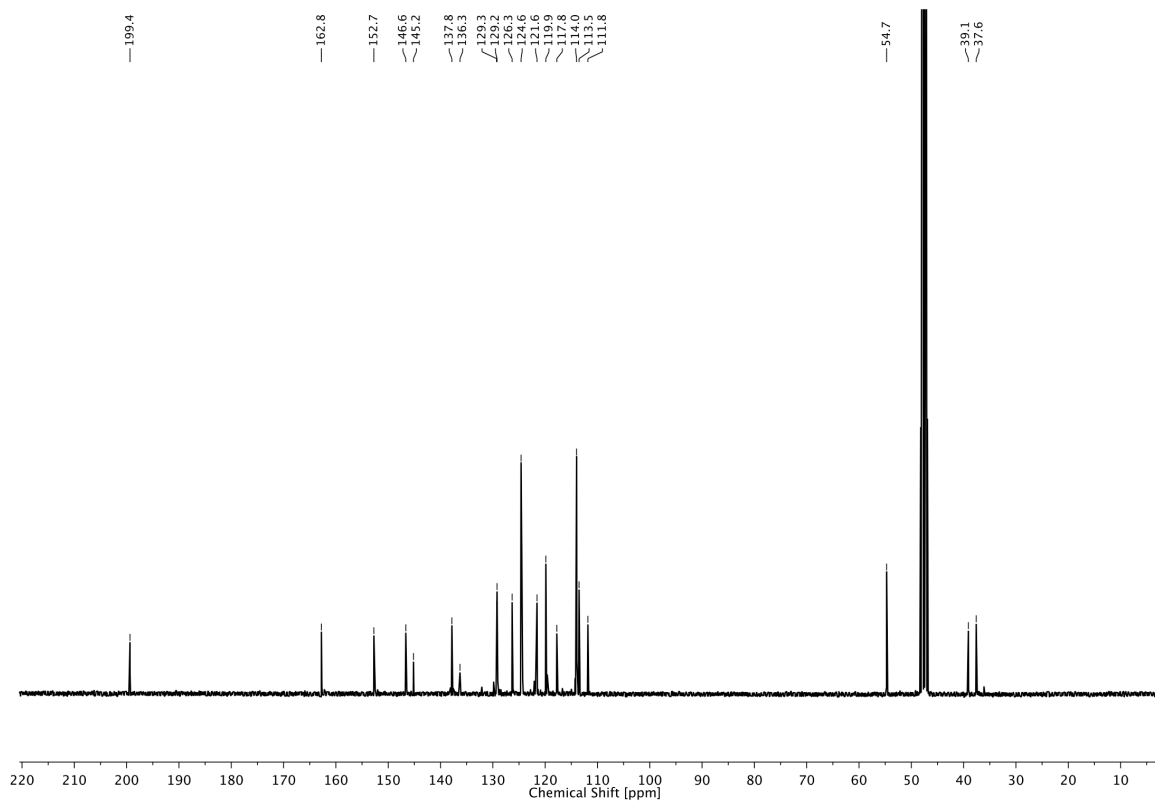
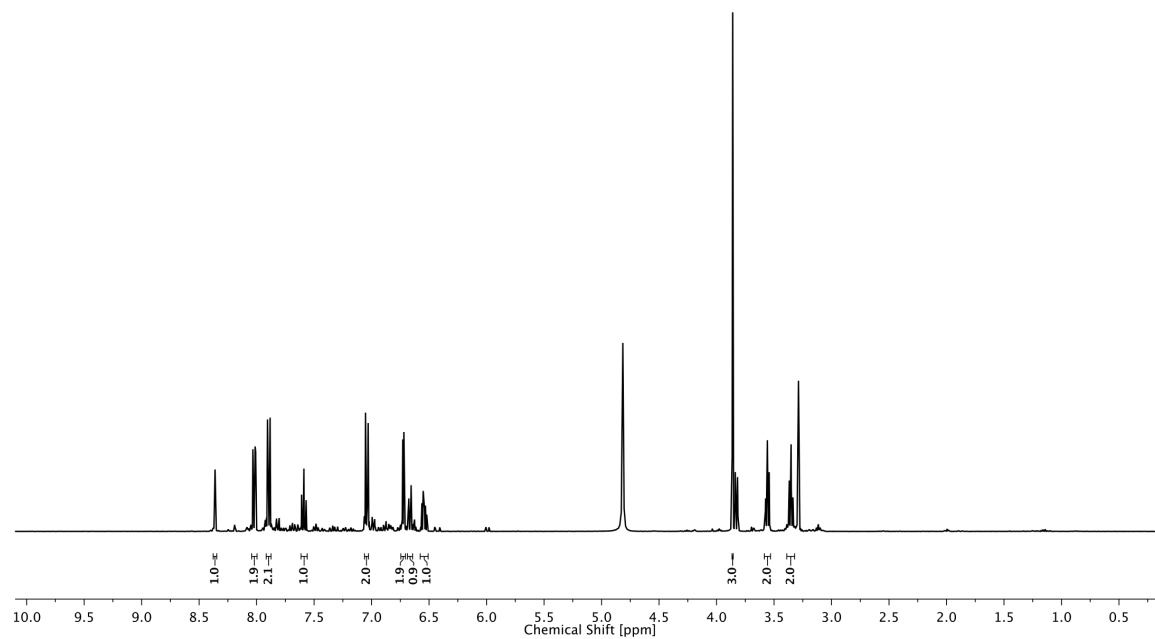
3.23



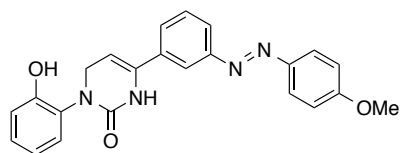
3 PHOTOCONTROL OF TRP CHANNELS



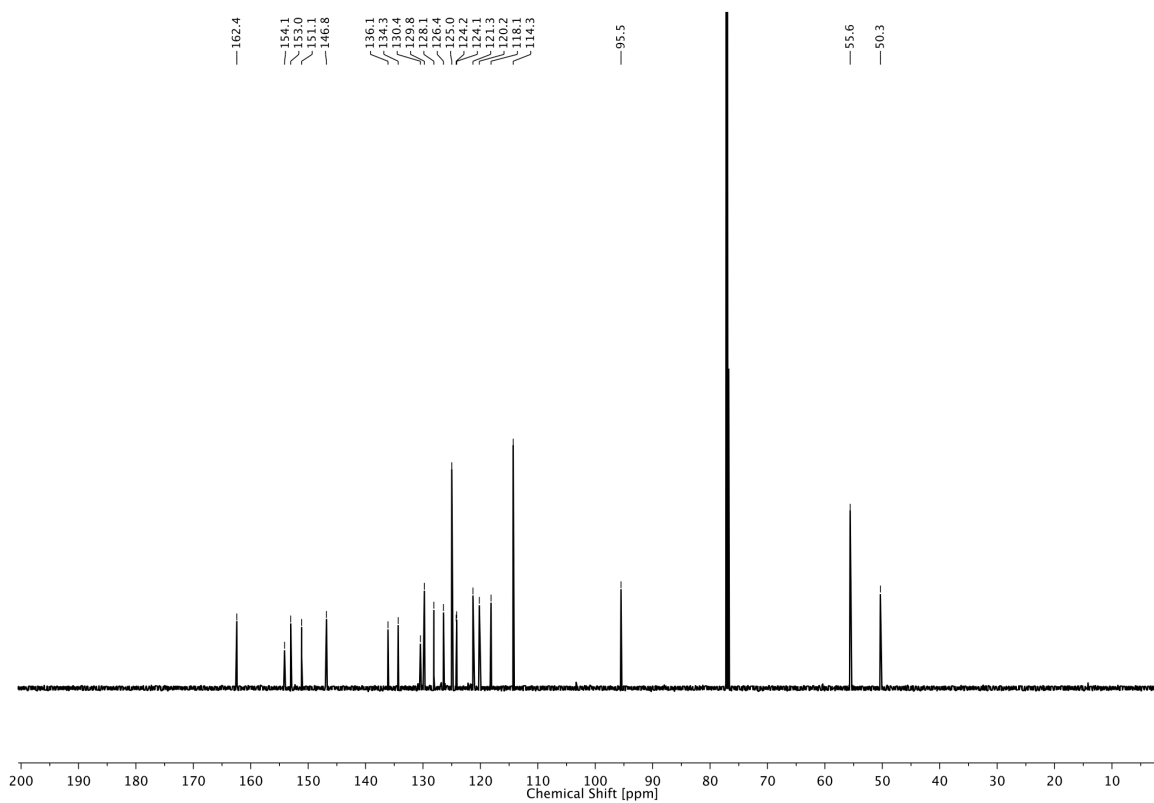
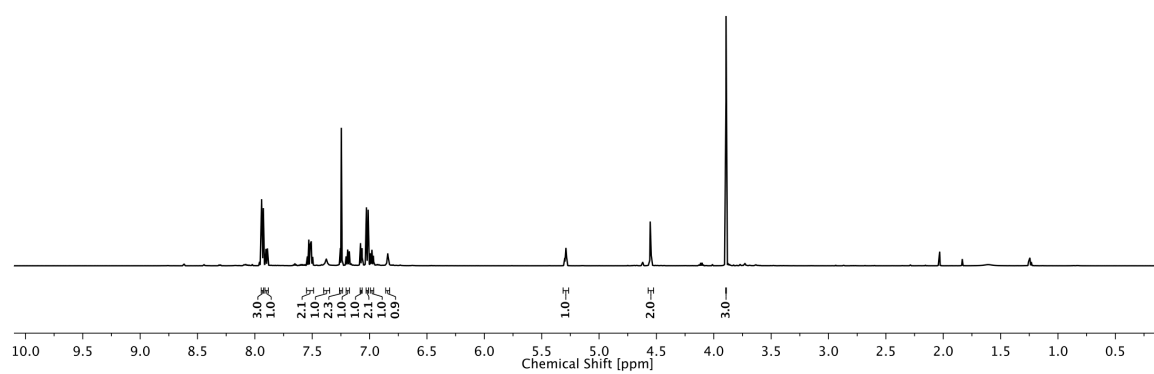
3.25



3 PHOTOCONTROL OF TRP CHANNELS



AI3



3.8 LITERATURE

- [1] G. Owsianik, T. Voets, B. Nilius, in *Ion Channels from Structure to Function*, (Eds.: J. N. C. Kew, C. H. Davies), Oxford University Press, New York, **2010**, p. 511.
- [2] D. J. Cosens, A. Manning, *Nature* **1969**, *224*, 285–187.
- [3] a) C. Montell, G. M. Rubin, *Neuron* **1989**, *2*, 1313–1323; b) R. C. Hardie, B. Minke, *Neuron* **1992**, *8*, 643–651.
- [4] R. C. Hardie, P. Raghu, S. Moore, M. Juusola, R. A. Baines, S. T. Sweeney, *Neuron* **2001**, *30*, 149–159.
- [5] S. Chyb, P. Raghu, R. C. Hardie, *Nature* **1999**, *397*, 255–259.
- [6] T. Voets, K. Talavera, G. Owsianik, *Nat. Chem. Biol.* **2005**, *1*, 85–92.
- [7] T. Voets, A. Janssens, G. Droogmans, B. Nilius, *J. Biol. Chem.* **2004**, *279*, 15223–15230.
- [8] J. G. J. Hoenderop, T. Voets, S. Hoefs, F. Weidema, J. Prenen, B. Nilius, R. J. M. Bindels, *EMBO J.* **2003**, *22*, 776–785.
- [9] V. Y. Moiseenkova-Bell, T. G. Wensel, *J. Gen. Physiol.* **2009**, *133*, 239–244.
- [10] P. V. Lishko, E. Procko, X. Jin, C. B. Phelps, R. Gaudet, *Neuron* **2007**, *54*, 905–918.
- [11] D. A. Doyle, J. Morais Cabral, R. A. Pfützner, A. Kuo, J. M. Gulbis, S. L. Cohen, B. T. Chait, R. MacKinnon, *Science* **1998**, *280*, 69–77.
- [12] C. García-Martínez, C. Morenilla-Palao, R. Planells-Cases R, J. M. Merino, A. Ferrer-Montiel, *J. Biol. Chem.* **2000**, *275*, 32552–32558.
- [13] M. Liao, E. Cao, D. Julius, Z. Cheng, *Nature* **2013**, *504*, 107–112.
- [14] E. Cao, M. Liao, Z. Cheng, D. Julius, *Nature* **2013**, *504*, 113–118.
- [15] M. M. Moran, M. A. McAlexander, T. Biro, A. Szallasi, *Nature Rev. Drug Disc.* **2011**, *10*, 601–620.
- [16] a) A. M. Peier, A. J. Reeve, D. A. Andersson, A. Moqrich, T. J. Earley, A. C. Hergarden, G. M. Story, S. Colley, J. B. Hogenesch, P. McIntyre, S. Bevan, A. Patapoutian, *Science* **2002**, *296*, 2046–2049; b) G. D. Smith, J. Gunthorpe, R. E. Kelsell, P. D. Hayes, P. Reilly, P. Facer, J. E. Wright, J. C. Jerman, J. P. Walhin, L. Ooi, J. Egerton, K. J. Charles, D. Smart, A. D. Randall, P. Anand, J. B. Davies, *Nature* **2002**, *418*, 186–190.
- [17] A. Güler, H. Lee, T. Iida, I. Shimizu, M. Tominaga, M. J. Caterina, *J. Neurosci.* **2002**, *22*, 6408–6414.
- [18] M. J. Caterina, M. A. Schumacher, M. Tominaga, T. A. Rosen, J. D. Levine, D. Julius, *Nature* **1997**, *389*, 816–824.
- [19] M. J. Caterina, T. A. Rosen, M. Tominaga, *Nature* **1999**, *398*, 436–441.

- [20] K. Talavera, K. Yasumatsu, T. Voets, G. Droogmans, N. Shigemura, Y. Ninomiya, R. F. Margolskee, B. Nilius, *Nature* **2005**, *438*, 1022–1025.
- [21] a) D. D. McKemy, W. M. Neuhausser, D. Julius, *Nature* **2002**, *416*, 52–58; b) A. M. Peier, A. Moqrich, A. C. Hergarden, A. J. Reeve, D. A. Andersson, G. M. Story, T. J. Earley, I. Dragoni, P. McIntyre, S. Bevan, A. Patapoutian, *Cell* **2002**, *108*, 705–715.
- [22] G. M. Story, A. M. Peier, A. J. Reeve, S. R. Eid, J. Mosbacher, T. R. Hricik, T. J. Earley, A. C. Hergarden, D. A. Andersson, S. W. Hwang, P. McIntyre, T. Jegla, S. Bevan, A. Patapoutian, *Cell* **2003**, *112*, 819–829.
- [23] A. Dhaka, V. Viswanath, A. Patapoutian, *Annu. Rev. Neurosci.* **2006**, *29*, 135–161.
- [24] D. E. Clapham, *Nature* **2003**, *426*, 517–524.
- [25] T. Voets, G. Droogmans, U. Wissenbach, A. Janssens, V. Flockerzi, B. Nilius, *Nature* **2004**, *430*, 748–754.
- [26] H. Turner, A. Fleig, A. Stokes, J.-P. Kinet, R. Penner, *Biochem. J.* **2003**, *371*, 341–350.
- [27] N. García-Sanz, A. Fernández-Carvajal, C. Morenilla-Palao R. Planells-Cases, E. Fajardo-Sánchez, G. Fernández-Ballester, A. Ferrer-Montiel, *J. Neurosci.* **2004**, *24*, 5307–5314.
- [28] T. Rosenbaum, A. Gordon-Shaag, M. Munari, S. E. Gordon, *J. Gen. Physiol.* **2004**, *123*, 53–62.
- [29] M. Numazaki, T. Tominaga, K. Takeuchi, N. Murayama, H. Toyooka, M. Tominaga, *Proc. Nat. Acad. Sci. USA* **2003**, *100*, 8002–8006.
- [30] C. D. Benham, J. B. David, A. D. Randall, *Neuropharmacol.* **2002**, *42*, 873–888.
- [31] N. Hellwig N, T. D. Plant, W. Janson, M. Schäfer, G. Schultz, M. Schaefer *J. Biol. Chem.* **2004**, *279*, 34553–34561.
- [32] N. Bourne, D. I. Bernstein, L. R. Stanberry, *Antimicrob. Agents Chemother.* **1999**, *43*, 2685–2688.
- [33] W. Everaerts, M. Gees, Y. A. Alpizar, R. Farre, C. Leten, A. Apetrei, I. Dewachter, F. van Leuven, R. Vennekens, D. De Ridder, B. Nilius, T. Voets, K. Talavera, *Curr. Biol.* **2011**, *21*, 316–321.
- [34] A. Szallasi, P. M. Blumberg, *Neurosci.* **1989**, *30*, 515–520.
- [35] T. G. Berke, S. C. Shieh, in *Handbook of Herbs and Spices, Vol. 1*, (Ed.: K. V. Peter), CRC Press LLC, Boca Raton, **2001**, p. 120.
- [36] F. N. McNamara, A. Randall, M. J. Gunthorpe, *Br. J. Pharmacol.* **2005**, *144*, 781–790.
- [37] R. A. Ross, *Br. J. Pharmacol.* **2003**, *140*, 790–801.
- [38] A. E. Chávez, C. Q. Chiu, P. E. Castillo, *Nat. Neurosci.* **2010**, *13*, 1511–1518.

- [39] S. R. Vigna, R. A. Shahid, J. D. Nathan, D. C. McVey, R. A. Liddle, *Pancreas* **2011**, *40*, 708–714.
- [40] W.-S. Shim, M.-H. Tak, M.-H. Lee, M. Kim, M. Kim, J.-Y. Koo, C.-H. Lee, M. Kim, U. Oh, *J. Neurosci.* **2007**, *27*, 2331–2337.
- [41] a) T. Waranabe, K. Kobata, A. Morita, Y. Iwasaki, *Foods Food Ingredients J. Jpn.* **2005**, *210*, 3; b) G. Appendino, L. De Petrocellis, M. Trevisani, *J. Pharmacol. Exp. Ther.* **2005**, *312*, 561–570.
- [42] K. Stock, J. Kumar, M. Synowitz, S. Petrosino, R. Imperatore, E. S. J. Smith, P. Wend, B. Purfürst, U. A. Nuber, U. Gurok, V. Matyash, J.-H. Wälzlein, S. R. Chirasani, G. Dittmar, B. F. Cravatt, S. Momma, G. R. Lewin, A. Ligresti, L. De Petrocellis, L. Cristino, V. Di Marzo, H. Kettenmann, R. Glass, *Nat. Med.* **2012**, *18*, 1232–1238.
- [43] C. S. Walpole, S. Bevan, G. Bovermann, J. Boelsterli, R. Breckenridge, J. W. Davies, G. A. Hughes, I. James, L. Oberer, *J. Med. Chem.* **1994**, *37*, 1942–1954.
- [44] H. J. Behrendt, T. Germann, C. Gillen, H. Hatt, R. Jostock, *Br. J. Pharmacol.* **2004**, *141*, 737–745.
- [45] L. Liu, S. A. Simon, *Neurosci. Lett.* **1997**, *228*, 29–32.
- [46] R. J. Docherty, J. C. Yeats, A. C. Piper, *Br. J. Pharmacol.* **1997**, *121*, 1461–1467.
- [47] P. Wahl, C. Foged, S. Tullin, C. Thomsen, *Mol. Pharmacol.* **2001**, *59*, 9–15.
- [48] J. Siemens, S. Zhou, R. Piskorowski, T. Nikai, E. A. Lumpkin, A. I. Basbaum, D. King, D. Julius, *Nature* **2006**, *444*, 208–212.
- [49] C. J. Bohlen, A. Priel, S. Zhou, D. King, J. Siemens, D. Julius, *Cell* **2010**, *141*, 834–845.
- [50] W. C. Still, M. Kahn, A. Mitra, *J. Org. Chem.* **1978**, *43*, 2923–2925.
- [51] H. E. Gottlieb, V. Kotlyar, A. Nudelman, *J. Org. Chem.* **1997**, *62*, 7512–7515.
- [52] N. Hellwig, N. Albrecht, C. Harteneck, G. Schultz, M. Schaefer, *J. Cell Sci.* **2005**, *118*, 917–928.
- [53] M. R. Banghart, A. Mourot, D. L. Fortin, J. Z. Yao, R. H. Kramer, D. Trauner, *Angew. Chem. Int. Ed.* **2009**, *48*, 9097–9101.
- [54] V. Baubet, H. Le Mouellic, A. K. Campbell, E. Lucas-Meunier, P. Fossier, P. Brûlet, *Proc. Natl. Acad. Sci. USA* **2000**, *97*, 7260–7265.
- [55] Y. Shen, M. A. F. Rampino, R. C. Carroll, S. Nawy, *Proc. Natl. Acad. Sci. USA* **2012**, *109*, 8752–8757.
- [56] a) M. J. Nadler, M. C. Hermosura, K. Inabe, A. L. Perraud, Q. Zhu, A. J. Stokes, T. Kurosaki, J. P. Kinet, R. Penner, A. M. Scharenberg, A. Fleig, *Nature* **2001**, *411*, 590–595; b) K. P. Schlingmann, S. Weber, M. Peters, N. L. Niemann, H. Vitzthum, K.

- Klingel, M. Kratz, E. Haddad, E. Ristoff, D. Dinour, M. Syrrou, S. Nielsen, M. Sassen, S. Waldegger, H. W. Seyberth, M. Konrad, *Nat. Genet.* **2002**, *31*, 166–170.
- [57] C. A. Perez, L. Huang, M. Rong, J. A. Kozak, A. K. Preuss, H. Zhang, M. Max, R. F. Margolskee, *Nat. Neurosci.* **2002**, *5*, 1169–1176.
- [58] T. Hofmann, V. Chubanov, T. Gudermann, C. Montell, *Curr. Biol.* **2003**, *13*, 1153–1158.
- [59] L. Tsavaler, M. H. Shapero, S. Morkowski, R. Laus, *Cancer Res.* **2001**, *61*, 3760–3769.
- [60] R. J. Stein, S. Santos, J. Nagatomi, Y. Hayashi, B. S. Minnery, M. Xavier, A. S. Patel, J. B. Nelson, W. J. Futrell, N. Yoshimura, M. B. Chancellor, F. De Miguel, *J. Urol.* **2004**, *172*, 1175–1178.
- [61] D. D. McKemy, *ACS Chem. Neurosci.* **2013**, *4*, 238–247.
- [62] D. del Camino, S. Murphy, M. Heiry, L. B. Barrett, T. J. Earley, C. A. Cook, M. J. Petrus, M. Zhao, M. D’Amours, N. Deering, G. J. Brenner, M. Costigan, N. J. Hayward, J. A. Chong, C. M. Fanger, C. J. Woolf, A. Patapoutian, M. M. Moran, *J. Neurosci.* **2010**, *30*, 15165–15174.
- [63] E. T. Wei, D. A. Seid, *J. Pharm. Pharmacol.* **1983**, *35*, 110–112.
- [64] C. Podesva, J. do Nascimento (Delmar Chemicals Ltd.), D1 2142385, **1972**.
- [65] C. Mannich, M. Dannehl, *Arch. Pharm.* **1938**, *276*, 206–211.
- [66] M. R. Banghart, A. Mourot, D. L. Fortin, J. Z. Yao, R. H. Kramer, D. Trauner, *Angew. Chem. Int. Ed.* **2009**, *48*, 9097–9101.

4 PHOTOCROMIC LIGANDS FOR VOLTAGE-GATED SODIUM CHANNELS

4.1 VOLTAGE-GATED SODIUM CHANNELS

Voltage-gated sodium (Na_V) channels initiate electrical signaling in neurons through the generation of action potentials. Na_V channels are rapidly activated, have a high selectivity and contribute to a variety of diseases. Mutations of Na_V channels are involved in inherited epilepsy, migraine, periodic paralysis, cardiac arrhythmia and chronic pain syndromes.^[1] Therefore, Na_V channels are a prominent target of drug development in local anesthesia and in the treatment of Na_V channelopathies in the brain, skeletal muscle and heart.^[2] Although many subtypes of voltage-gated sodium channels exist (Na_V 1.1 – Na_V 1.9), their tetrameric structures are highly conserved.

In 2011, Payandeh *et al.* have obtained the first crystal structure of a voltage-gated sodium channel (Na_V of *Arcobacter butzleri*, Na_VAb) at a resolution of 2.7 Å,^[3] shedding light on the structural details of Na_V channels. Each of the four subunits consists of six transmembrane (TM) helices and two additional pore (P) helices. TM1–4 form the voltage-sensing domain (VSD), whereas TM5–6 constitute the pore domain (Fig 4.1a). The selectivity filter of the pore is formed by the four Glu177 residues of the four subunits. Unlike K^+ ions, which pass the selectivity filter of K_V channels without their hydration sphere, Na^+ ions remain fully hydrated at that stage. Having passed the selectivity filter, the hydrophobic inner cavity allows for fast diffusion of ions (Fig. 4.1b+c).^[3]

Interestingly, the crystal structure revealed strong interactions of the channel with the ambient lipid membrane. Four lateral openings allow for lipid penetration into the inner cavity and ion conduction pathway of the channel. Yet, the role of these fenestrations still remains to be investigated but they could play an important role in the delivery of small hydrophobic drugs, as these openings were found to lead to important drug binding sites.^[3]

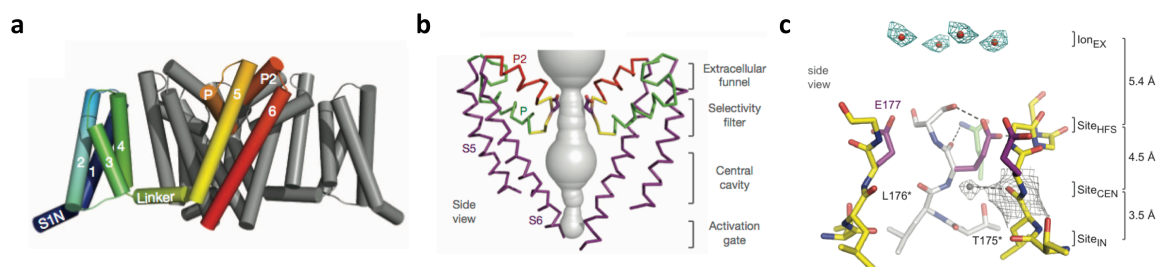


Figure 4.1. **a)** Crystal structure of Na_vAb. Only two of four subunits are shown with one being highlighted. TM1–4 (blue to green) constitute the VSD and TM5–6 (yellow, red) form the pore of the channel. **b)** Architecture of the pore of Na_vAb. The pore volume is shaded in grey, the Glu177 side chains are highlighted in purple. **c)** Side view of the selectivity filter. Four putative cations or molecules of water (red) are shown above the four Glu177 residues and one putative water molecule at Leu176 (grey). Illustrations copied from Payandeh *et al.*,^[3] reprinted with permission from Macmillan Publishers Ltd. Copyright 2011.

As Na_v channels are involved in many neuropathic disorders, strong efforts have been undertaken to develop (subtype-selective) drugs for the treatment of a variety of diseases. Taking advantage of the many published studies including detailed structure–activity relationships, a selection of promising small molecules has been made to develop photochromic ligands for the optical control of voltage-gated sodium channels. These include (but are not limited to) the clinically established drugs lacosamide (UCB) and lamotrigine (GlaxoSmithKline) as well as crobenetine, a drug candidate developed by Boehringer Ingelheim that has made it into clinical trials (see below).

4.2 AZO-LACOSAMIDE

Lacosamide (LCM) is a medication developed by UCB for the adjunctive treatment of partial-onset seizures and diabetic neuropathic pain marketed under the trade name *Vimpat*[®]. LCM is a functionalized amino acid that, like most antiepileptic drugs, acts through Na_v channels.^[4] However, LCM appears to act by enhancing the slow inactivation of Na_v channels rather than stabilizing fast inactivation.^[5] Whereas the latter proceeds via a “ball and chain” mechanism that involves occluding the pore of the channel by binding of a cytoplasmic portion,^[6] the mechanism of slow inactivation is not fully understood yet. It is hypothesized that it results from a structural rearrangement of the pore.^[7]

Extensive SAR studies on LCM with various bulky aromatic substituents for the benzyl group have been carried out.^[8] Lacosamide itself has an ED₅₀ value of 4.5 mg/kg, as determined by maximal electroshock seizure test (MES) on mice.^[8] Fig. 4.2 shows examples of comparably

potent analogues of LCM that strongly resemble azobenzene modifications on the benzyl moiety. Derivatives bearing an ethyl bridge between the two phenyl rings possess an ED₅₀ value between 10 and 30 mg/kg. Several phenyl benzyl ethers or amines are in the same range or possess even lower ED₅₀ values. Linear derivatives bearing a triple bond between the two phenyl rings have an ED₅₀ value between 30 and 100 mg/kg. The most promising, i.e. strongest azobenzene resembling derivative, however, is the stilbene version of LCM, ranging between 30 and 100 mg/kg for its ED₅₀ value.

Lacosamide,
ED₅₀ = 4.5 mg/kg

R	ED ₅₀ [mg/kg] ¹⁾	R	ED ₅₀ [mg/kg] ¹⁾	R	ED ₅₀ [mg/kg] ¹⁾
	10 < X < 30		13		30 < X < 100
	5.9		10 < X < 30		30 < X < 100
	10 < X < 30		5.8		

Figure 4.2. Structure–activity relationship of LCM. ¹⁾ ED₅₀ values were determined by maximal electroshock seizure (MES) test.

Altogether, the flexible substitution pattern on the benzyl moiety of LCM and the pharmacologically established function of the drug prompted the derivatization of LCM into **Azo-Lacosamide (ALCM; Fig. 4.3)**.

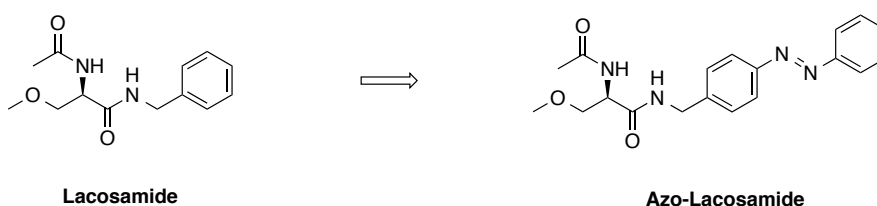
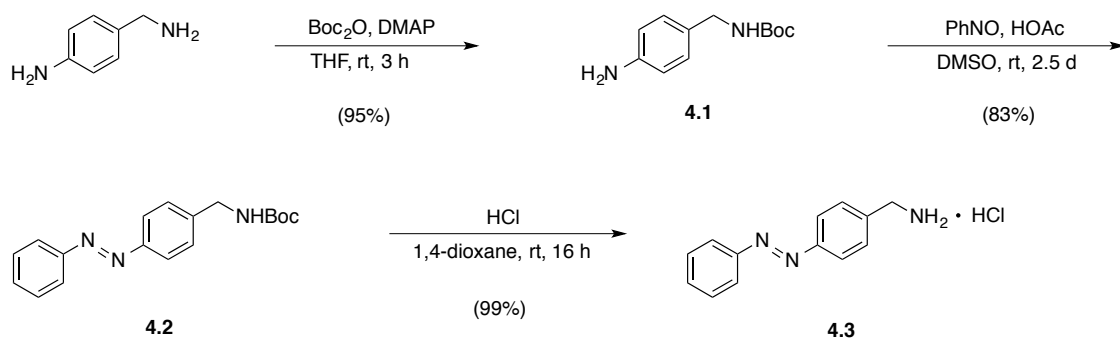


Figure 4.3. Structures of lacosamide and **Azo-Lacosamide**.

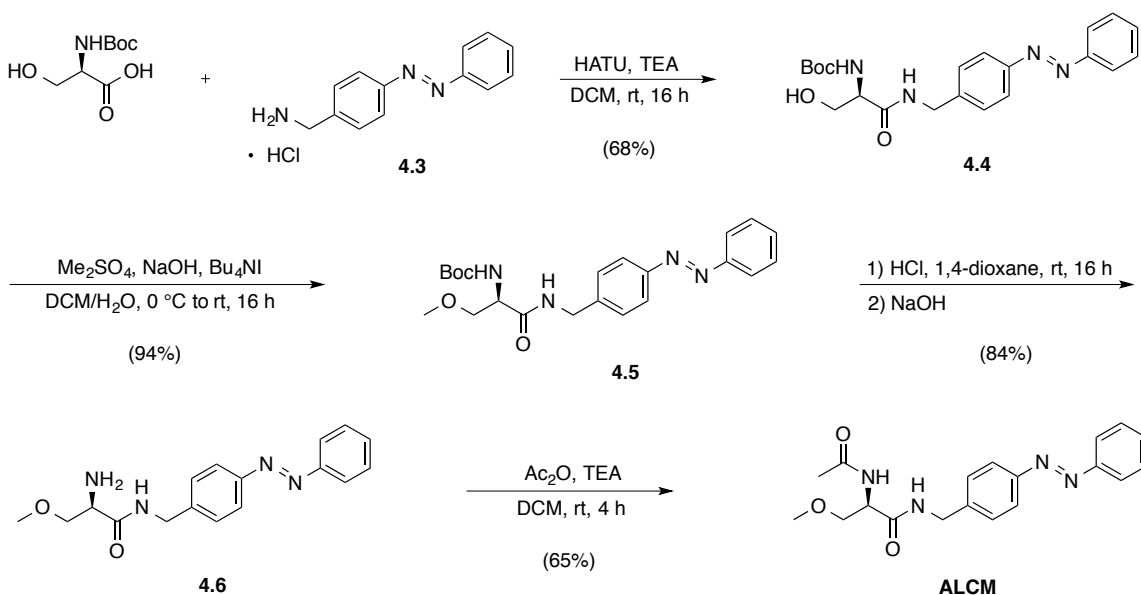
Synthesis of Azo-Lacosamide

Firstly, the azobenzyllic amine **4.1** was synthesized starting from 4-aminobenzylamine which was Boc-protected with Boc_2O and DMAP in 95% yield. Compound **4.1** then underwent a Mills reaction with nitrosobenzene to give azobenzene **4.2** in 83% yield. Deprotection of the Boc group with HCl eventually gave the azobenzyllic amine **4.3** as its hydrochloride salt in 99% yield (Scheme 4.1).



Scheme 4.1. Synthesis of the azobenzyllic amine linker **4.3**.

Compound **4.3** was then reacted with Boc-protected D-serine in a HATU-mediated amide coupling reaction to form amide **4.4** in 68% yield. Methylation of the hydroxy group using dimethyl sulfate furnished **4.5** in 94% yield. Boc deprotection under acidic conditions afforded the free amine **4.6** in 84% yield which was then acetylated using acetic anhydride and triethylamine, giving rise to **ALCM** in 65% yield (Scheme 4.2).



Scheme 4.2. Synthesis of **ALCM**.

The maximum absorption wavelengths of **ALCM** were determined to be at $\lambda = 328$ nm and $\lambda = 440$ nm (Fig. 4.4a). The action of **ALCM** on slow inactivation of Na_V channels was tested using HEK 293 cells, stably transfected with human Na_V 1.7 (h Na_V 1.7; Dr. Angelika Lampert, Friedrich-Alexander University Erlangen-Nürnberg). In order to distinguish the transfected currents from endogenous tetrodotoxin-sensitive (TTXs) sodium channels occurring in HEK 293 cells,^[9] h Na_V 1.7 was mutated to be TTX resistant^[10] and 500 nM TTX was added to the external bath solution to block those endogenous currents.

To assess steady-state slow inactivation, a stimulus protocol was applied (Fig. 4.4b, top) and sodium currents were recorded using whole-cell patch-clamp experiments with and without illumination with light ($\lambda = 340\text{--}380$ nm). The relative current decline due to slow inactivation (calculated as ratio of I_2/I_1) was determined. Exemplary traces of **ALCM** (100 μM ; added to the internal solution) indicate a smaller decrease in relative currents I_2/I_1 after illumination with $\lambda = 340\text{--}380$ nm (blue trace “*post*”) compared to the same experiment in the dark (black trace “*pre*”; Fig. 4.4b, bottom). Statistical analysis ($n = 9$) revealed that *trans*-**ALCM** (100 μM) reduced h Na_V 1.7 currents by slow inactivation in the same range as LCM (100 μM) compared to control experiments with DMSO or EtOH (Fig. 4.4c). Illumination of **ALCM** with $\lambda = 340\text{--}380$ nm light, leading to *cis*-**ALCM**, resulted in significantly increased relative Na^+ currents ($I_2/I_{1\text{light}} = 0.67$) than obtained for *trans*-**ALCM** in the dark ($I_2/I_{1\text{dark}} = 0.58$), indicating that *trans*-**ALCM** is enhancing slow inactivation of h Na_V 1.7 more efficaciously than *cis*-**ALCM**. No light-dependent changes in efficacy were found for LCM (Fig. 4.4c). By comparison of the relative Na^+ currents prior and after illumination with light, a photoswitching index (PI) can be calculated (as determined by the ratio of $(I_2/I_{1\text{light}} - I_2/I_{1\text{dark}}) / I_2/I_{1\text{dark}}$) of $\text{PI} = 16\%$. Further experiments of light-dependent actions of **ALCM** in DRG neurons are currently on the way (Dr. Angelika Lampert, Friedrich-Alexander University Erlangen-Nürnberg).

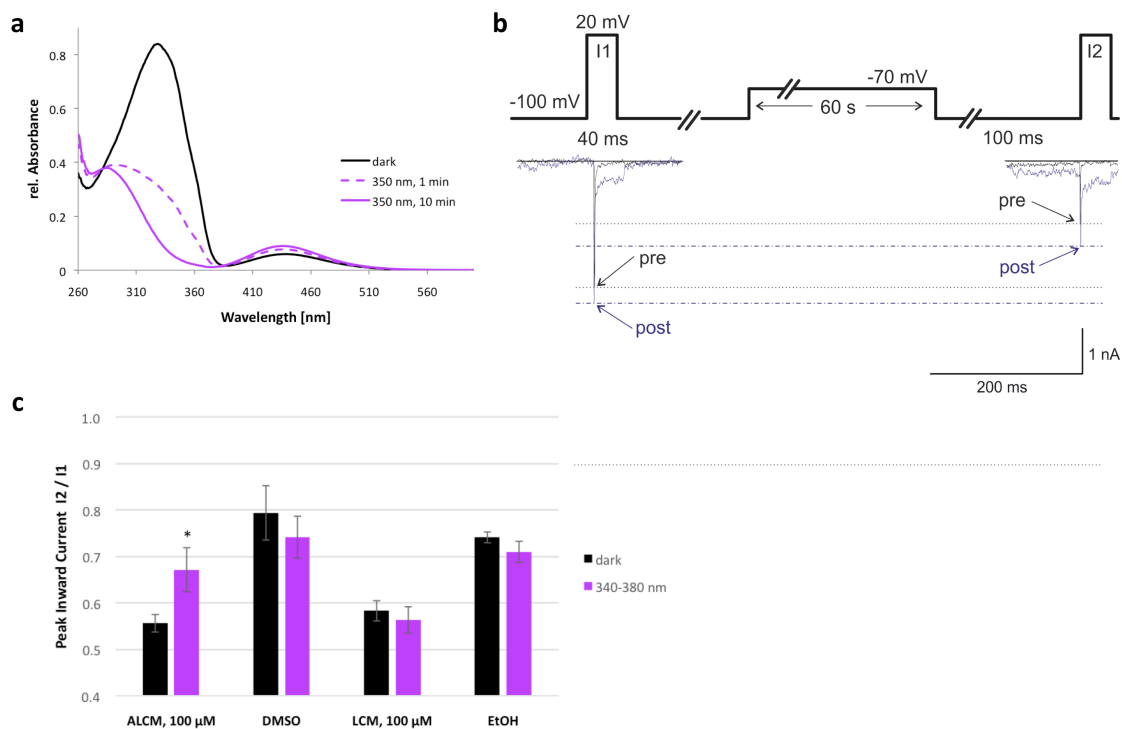


Figure 4.4. **a)** UV/Vis spectrum of **ALCM** (DMSO). The peak absorptions are at $\lambda = 328$ nm and $\lambda = 440$ nm. Photoisomerization from the *trans* to the *cis* form was achieved by applying $\lambda = 350$ nm. **b)** Pulse protocol for slow-type inactivation of hNa_v 1.7 (top) and representative traces of recordings with **ALCM** (100 μM) added to the pipette solution in the dark (*pre*) and after illumination with $\lambda = 340$ –380 nm (*post*). A short depolarizing test pulse (I1) from -100 mV to $+20$ mV was followed by a 60 s pulse to -70 mV, followed by a 100 ms step to -100 mV to remove fast inactivation and a test pulse I2 to $+20$ mV for 40 ms, at which available channels were assessed. This protocol was repeated with (*post*) and without (*pre*) illumination with light ($\lambda = 340$ –380 nm). **c)** Statistical analysis of light-dependent slow-type inactivation of hNa_v 1.7 with **ALCM** (100 μM) and LCM (100 μM, control), respectively. The difference in current change with **ALCM** in the dark *versus* with $\lambda = 340$ –380 nm light is significant. Additional control experiments with DMSO or EtOH revealed no significant light-dependent effects (Dr. Angelika Lampert, Friedrich-Alexander University Erlangen-Nürnberg).

4.3 AZO-LAMOTRIGINE

Lamotrigine (LTG), marketed under the trade name *Lamictal*[®] by GlaxoSmithKline, is an anticonvulsant drug that is used for the treatment of epilepsy, bipolar disorder, depression^[11] and neuropathic pain.^[12] It significantly reduces the frequency of Lennox-Gastaut syndrome seizures, a severe form of epilepsy.^[13] LTG also functions as a mood stabilizer and was the first drug since lithium salts which the U.S. Food and Drug Administration (FDA) has approved for this purpose. It acts presynaptically on Na_v channels and belongs to the class of sodium channel blocking antiepileptic drugs.^[14] Other members of this class of drugs are carbamazepine or phenytoin (Fig. 4.5). Lamotrigine, however, belongs to a different compound class (phenyltriazine) and has a broader spectrum of action. For instance, it is also effective in the treatment of the depressed phase in bipolar disorder, whereas the above-mentioned drugs are not. Belonging to a different class of compounds, it moreover does not share the same side effects as other antiepileptic drugs, thus providing unique properties which can be advantageous in certain treatment cases.^[15] LTG decreases the release of neurotransmitters aspartate and glutamate and inhibits neuronal $\alpha_2\beta_2$ nAChR.^[16] It blocks sustained repetitive firing in cultured mouse spinal cord neurons in a concentration-dependent manner in the treatment of human seizures.^[17] However, it also inhibits voltage-activated calcium channels which might contribute to its broader spectrum of action.^[18]

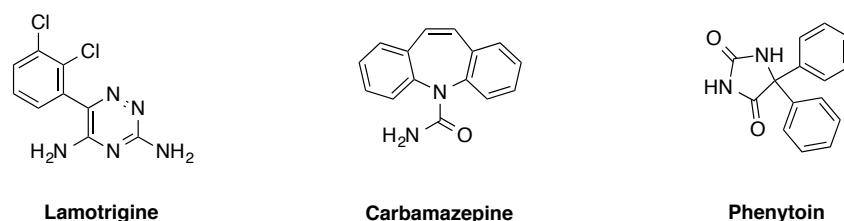


Figure 4.5. Structures of sodium channel blocking antiepileptic drugs.

Extensive SAR have been carried out on LTG, not only investigating its affinity or efficacy on sodium channels, but also other properties such as L-type calcium channel affinity and microsome stability.^[19] Several candidates possess large extended aryl substituents in the 6-position of the triazine core with comparable or even better IC₅₀ values than lamotrigine itself. A composition of benzyloxyphenyl-substituted derivatives is shown in Fig. 4.6 which best resemble the structure of an azobenzene moiety. Substitution of the C6-attached phenyl ring in the *meta* position with respect to the triazine core appears to be superior over *para* substitution.

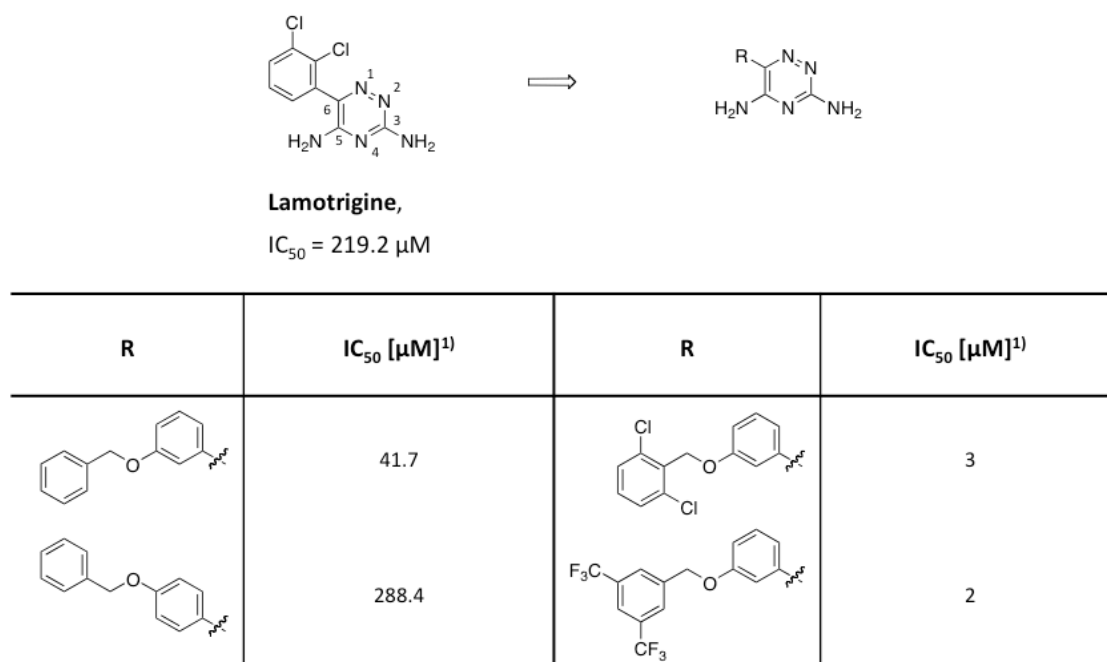


Figure 4.6. Selected examples from SAR studies of LTG.^{[19] 1)} IC₅₀ values were measured with respect to [¹⁴C] guanidine flux as an indicator of sodium channel opening/blockade.

Consequently, **Azo-Lamotrigine (ALTG)**, the *meta*-azobenzene derivative of lamotrigine was chosen as target molecule (Fig. 4.7).

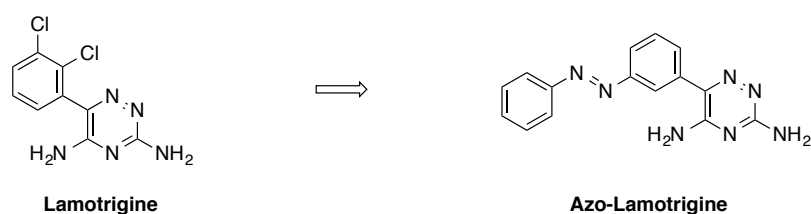
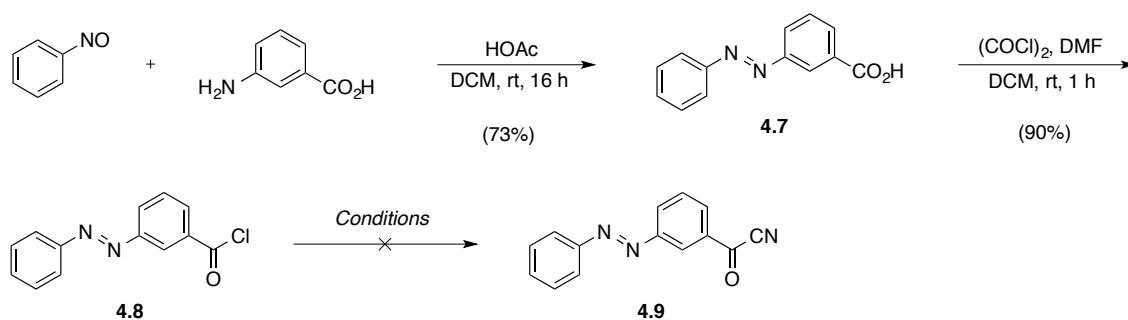


Figure 4.7. Structures of lamotrigine and **Azo-Lamotrigine**.

Synthesis of Azo-Lamotrigine

In the initially planned route, nitrosobenzene was first condensed with 3-aminobenzoic acid in a Mills reaction to give azobenzene **4.7** in 73% yield. The acid was then first converted to the corresponding acid chloride **4.8** with oxalyl chloride and DMF in 90% yield. The acid chloride proved to be very stable, surviving basic workup and even column chromatography. This stability might be the reason for the following problems in the attempted replacement of the chloride with cyanide nucleophiles (Scheme 4.3).



Scheme 4.3. 1st route toward **ALTG**.

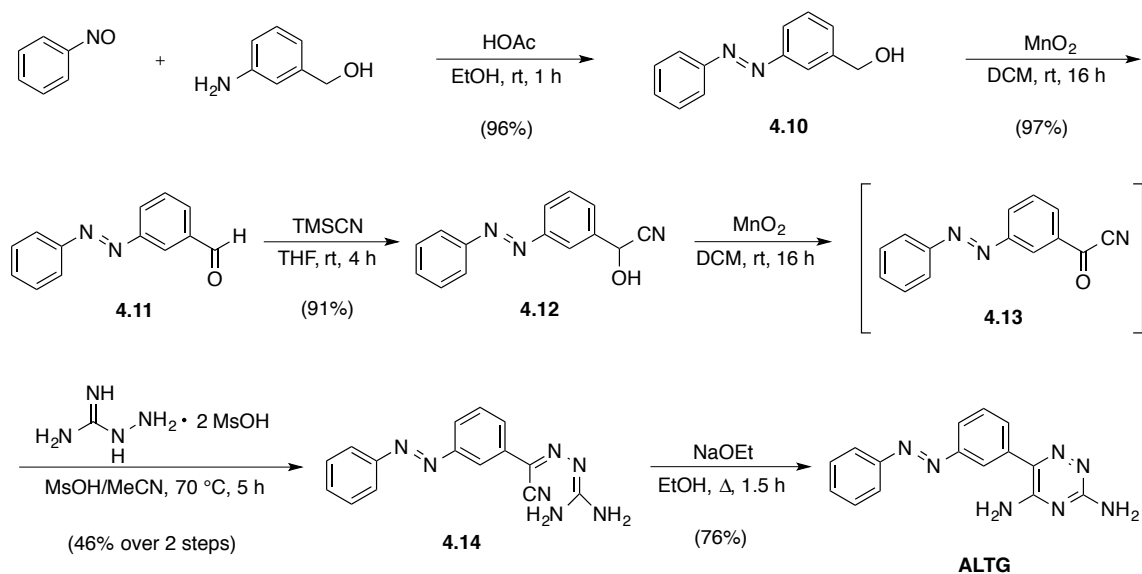
Literature-known methods for this reaction and variations thereof were applied but did not lead to the desired product **4.9** (Table 4.1). Normant's method^[20] comprises refluxing the acid chloride with copper cyanide in acetonitrile (entry 1). However, no traces of **4.9** were observed. Modifications by the addition of Celite (entry 2) or NaI (entry 3) were not successful. Using TMSCN instead (method by Olah^[21]) neither resulted in the formation of **4.9** (entry 4). The addition of SnCl₄ as a Lewis acid resulted in decomposition of the starting material (entry 5).

Table 4.1. Applied conditions for the reaction of acid chloride **4.8** to **4.9**.

Entry	Reagent	Conditions	Yield 4.9 [%]
1	CuCN	MeCN, Δ, 1 h	0
2	CuCN, Celite	MeCN, rt to reflux, 24 h	0
3	CuCN, NaI	MeCN, rt, 16 h	0
4	TMSCN	MeCN, rt, 16 h	0
5	TMSCN, SnCl ₄	MeCN, rt, 16 h	decomp.

As indicated above, due to the surprising stability of acid chloride **4.8**, a new route toward **Azo-Lamotrigine** was designed involving a more reactive aldehyde intermediate for the introduction of the cyanide (Scheme 4.4).

First, azobenzene **4.10** was obtained from a Mills reaction of (3-aminophenyl)methanol and nitrosobenzene in excellent yield. Alcohol **4.10** was oxidized with MnO₂ to the corresponding aldehyde **4.11** in 97% yield. The aldehyde was then reacted with TMSCN in 4 h at room temperature to cyanohydrin **4.12** in excellent yield (91%). Compound **4.12** was oxidized using MnO₂ but the resulting product could not be isolated in pure form. Subsequently, crude **4.13** was reacted with aminoguanidine bismesylate, which had previously been obtained from aminoguanidine bicarbonate and MsOH according to a literature procedure.^[19] Cyanohydrazone **4.14** was obtained in 46% yield over two steps. The triazine ring was finally closed under basic conditions by the addition of NaOEt to an ethanolic solution of **4.14** and heating to reflux for 1.5 h, affording **ALTG** in 76% yield.



Scheme 4.4. Synthesis of **ALTG**: 2nd, successful route.

The photochemical properties of **ALTG** were investigated by UV/Vis spectrometry (Fig. 4.8). The maximum absorption wavelengths of **ALTG** were determined to be $\lambda = 323 \text{ nm}$ and $\lambda = 421 \text{ nm}$, respectively. Its potential as photochromic Na_V blocker is currently investigated in collaboration with Prof. Heinz Beck (Rheinische Friedrich-Wilhelms-University Bonn).

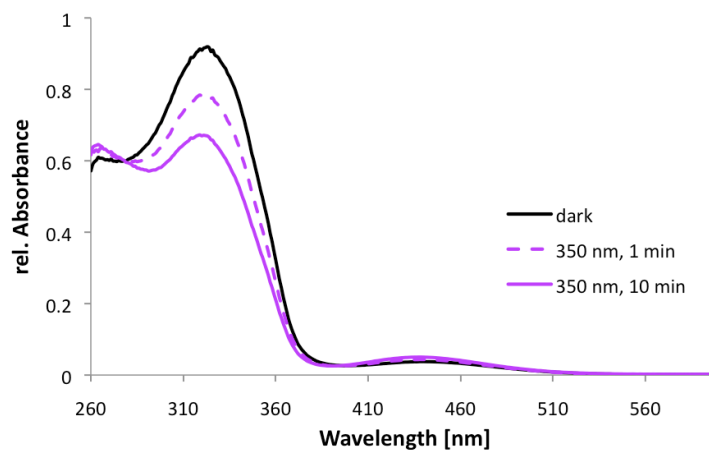


Figure 4.8. UV/Vis spectrum of **ALTG** (DMSO) with maximum absorption wavelengths of $\lambda = 323 \text{ nm}$ and $\lambda = 421 \text{ nm}$.

4.4 AZO-CROBENETINE

Voltage-gated sodium channels are thought to play a key role in excitotoxic damage. Sodium channel blockers could be helpful to protect from excitotoxic damage since they inhibit neuronal depolarization, glutamate release and Na^+ influx, thereby reducing Ca^{2+} influx by means of Ca^{2+} channels.^[22] Crobenetine (BIII 890 CL) was developed by Boehringer Ingelheim from SAR studies of 6,7-benzomorphans^[23] and reported as a potent, selective and highly use-dependent sodium channel blocker to protect brain tissue from ischemia^[24] and function as analgesic.^[25]

It was found that the IC_{50} value of Crobenetine for sodium channels in their inactivated states was much lower ($\text{IC}_{50} = 77 \text{ nM}$) than for sodium channels in the resting state ($\text{IC}_{50} = 18 \text{ }\mu\text{M}$)^[24] which is desired for neuroprotective drugs since they would preferentially block sodium channels in depolarized tissue without inhibiting normal physiological functions.^[24]

Two point mutations (F1764A and Y1771A) in transmembrane segment S6 in domain IV of the α subunit reduced the voltage- and frequency-dependent block which suggests that BIII 890 CL binds to the local anesthetic receptor site in the pore.^[24] Crobenetine crosses the blood–brain barrier in rats and is effective at reversing joint hyperalgesia in rats with adjuvant-induced mono-arthritis and also in decreasing spontaneous pain-related behavioural changes evoked by mono-arthritis.^[25]

Starting from Crobenetine, the syntheses of azo analogues *p*-Azo-Crobenetine (*p*-ACRO) and *m*-Azo-Crobenetine (*m*-ACRO) were planned (Fig. 4.9).

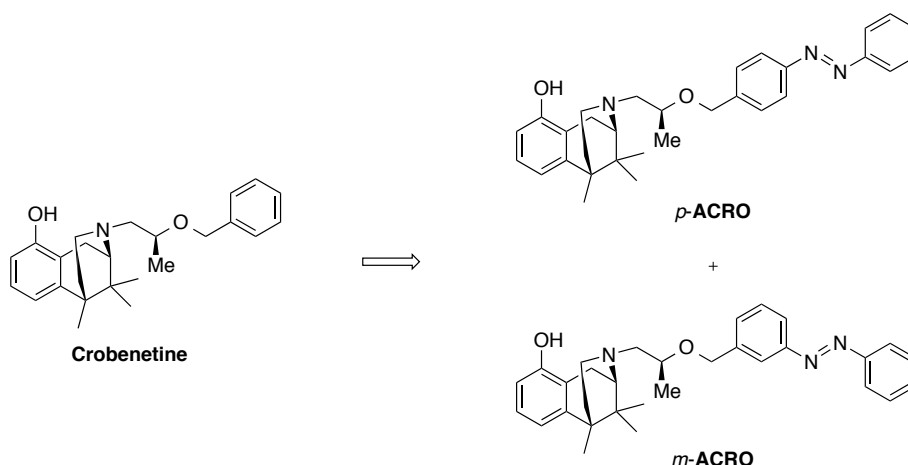
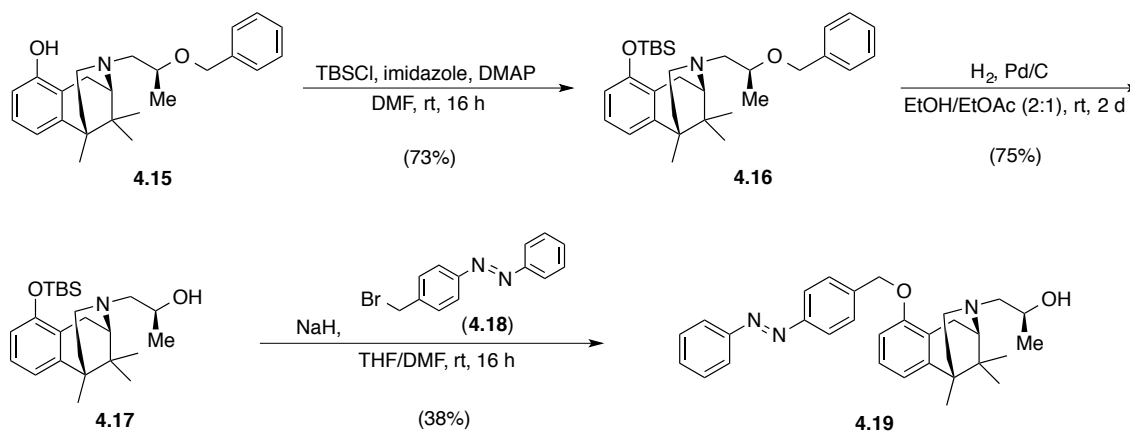


Figure 4.9. Structures of crobenetine and its azo analogues *p*-ACRO and *m*-ACRO.

Synthesis of Azo-Crobenetines

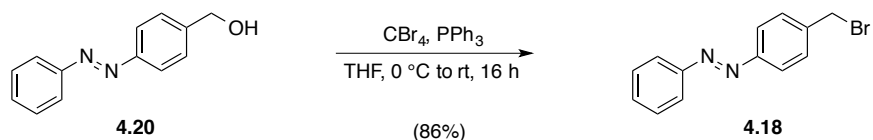
1st Generation Route toward Azo-Crobenetines

Firstly, the phenolic hydroxy group of crobenetine (**4.15**; generously provided by Boehringer Ingelheim) was TBS protected using TBSCl and imidazole, giving rise to **4.16** in 73% yield. The benzyl ether was cleaved by Pd-catalyzed hydrogenation, affording secondary alcohol **4.17** in 75% yield. Unfortunately, in the attempted etherification using bromide **4.18** and NaH as base the phenolic TBS group was cleaved, giving rise to the phenolic ether **4.19** in 38% yield (Scheme 4.5). The reaction was repeated with *meta*-azobromide **4.21** which also led to phenolic ether formation, affording ether **4.22** in 41% yield (Scheme 4.8).

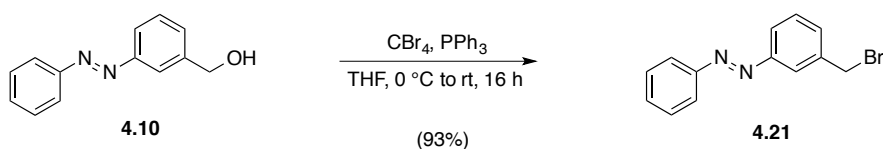


Scheme 4.5. 1st generation route toward *p*-ACRO.

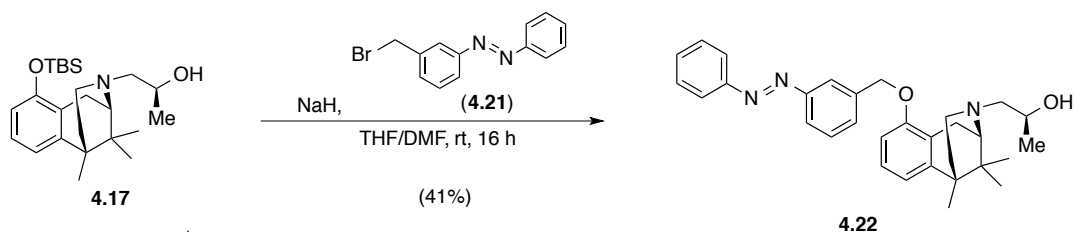
Para-bromide **4.18** was obtained by an Appel reaction from the corresponding *para*-alcohol **4.20** (Scheme 4.6) which has been previously described (compound **10** in chapter 2.3). The corresponding *meta*-bromide **4.21** was synthesized accordingly from *meta*-alcohol **4.10** (Scheme 4.7).



Scheme 4.6. Synthesis of *para*-bromide **4.18**.

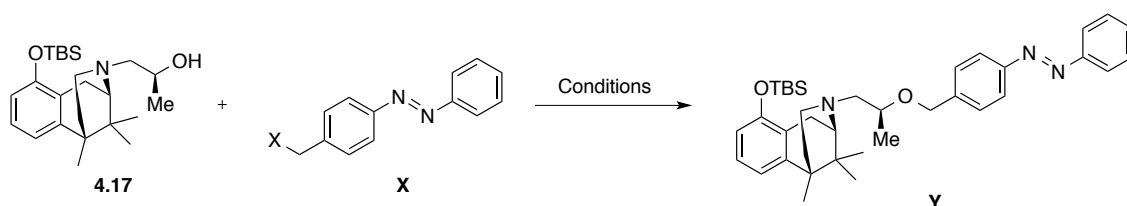


Scheme 4.7. Synthesis of *meta*-bromide **4.21**.



Scheme 4.8. 1st generation route toward *m*-ACRO.

A series of other conditions was investigated to form the desired aliphatic ethers (Scheme 4.9 and Table 4.2).



Scheme 4.9. Attempted etherification of alcohol **4.17** and electrophiles **X** to **Y**.

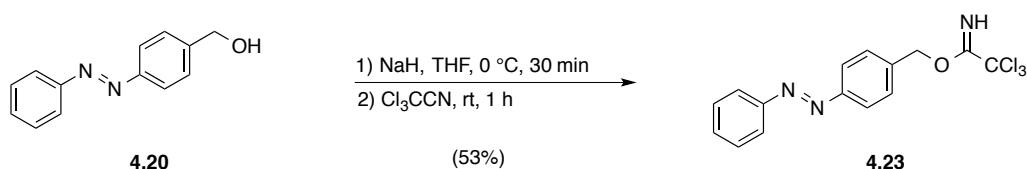
Table 4.2. Ether formation attempts toward *p*-ACRO and *m*-ACRO.

Entry	X	Reagent	Conditions	Equiv. 4.17 / X	Yield Y
1	Br ¹⁾	NaH, Bu ₄ NI	THF/DMF, 0 °C to rt, 16 h	1.0 / 1.25	0% (38% 4.19)
2	Br ¹⁾	Ag ₂ O ²⁾	DCM, rt, 16 h	1.0 / 3.0	0%
3	Br ¹⁾	Ag ₂ O ²⁾	Et ₂ O, Δ, 16 h	1.0 / 2.0	traces
4	Br ¹⁾	Ag ₂ O ²⁾	PhMe, 90 °C, 4 d	1.0 / 5.0	0%
5	Br ¹⁾	KO- <i>t</i> Bu	THF, rt, 16 h	1.0 / 1.6	traces
6	OTf ³⁾	2,6-lutidine	DCM, −78 °C to rt, 16 h	1.0 / 1.1	recovered SM
7	NH(CO)CCl ₃ ¹⁾	BF ₃ • OEt ₂	DCM, −20 °C to rt, 16 h	1.0 / 3.0	recovered SM
8	NH(CO)CCl ₃ ¹⁾	TMSOTf	DCM, 0 °C to rt, 2 d	1.0 / 10	recovered SM
9	OMs ⁴⁾	TEA	THF, 0 °C to rt, 2 h	1.0 / 2.0	0%

¹⁾ isolated and fully characterized. ²⁾ freshly prepared. ³⁾ prepared *in situ* from the corresponding alcohol and Tf₂O, 2,6-lutidine. ⁴⁾ prepared *in situ* from the corresponding alcohol and MsCl, TEA.

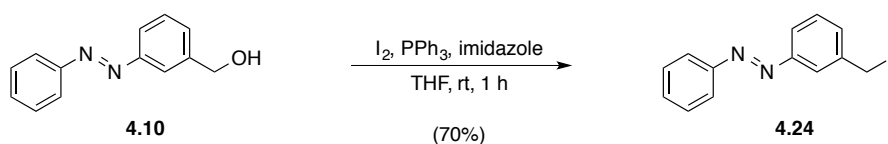
Entry 1 shows the above reported results with undesired phenol alkylation. Exchanging the base for KO-*t*Bu gave only traces of the desired product (entry 5). For etherifications with an

adjacent stereocenter on the alcohol, a common literature protocol is to react the alcohol and the bromide with Ag_2O instead of using a base to generate the alcoholate.^[26] However, only traces of **Y** were obtained by heating **4.17** together with bromide **4.18** and freshly prepared Ag_2O in refluxing Et_2O (Table 4.2, entry 3), whereas stirring the mixture at room temperature in DCM did not yield any product (entry 2). Heating the mixture up to $90\text{ }^\circ\text{C}$ in toluene led to decomposition of the starting material (entry 4). Other than bromide, also the corresponding triflate (entry 6), mesylate (entry 9) and trichloroacetimidate (entries 7 and 8, synthesized from alcohol **4.20** with NaH and trichloroacetone in 53% yield;^[27] see Scheme 4.10) were synthesized as electrophiles. By using the triflate, only starting material could be recovered, whereas the mesylate led to decomposition. No reaction was observed for the trichloroacetimidate **4.23** with the addition of $\text{BF}_3 \cdot \text{OEt}_2$ or TMSOTf as Lewis acids, respectively (entries 7 and 8).



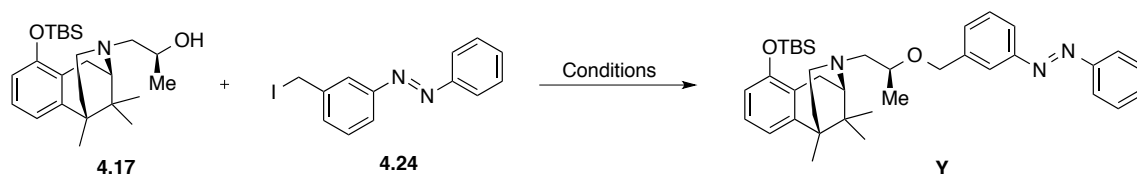
Scheme 4.10. Synthesis of trichloroacetimidate **4.23** from alcohol **4.20**.

In addition to the *para*-substituted azobenzene electrophiles, *meta*-iodide **4.24** was synthesized from alcohol **4.10** under Appel conditions in 70% yield (Scheme 4.11).



Scheme 4.11. Synthesis of iodide **4.24** from alcohol **4.10**.

Alkylation of alcohol **4.17** was also attempted using iodide **4.24** as electrophile (Scheme 4.12 and Table 4.3). Heating at $90\text{ }^\circ\text{C}$ with freshly prepared Ag_2O for 4 d led to decomposition (entry 1). KHMDS at low temperatures allowed for the recovery of the starting material (entry 2), whereas KHMDS with 18-crown-6 at high temperatures led to decomposition (entry 3). With *n*- BuLi as base, no conversion was obtained (entry 4).



Scheme 4.12. Attempted etherification of alcohol **4.17** and iodide **4.24** to **Y**.

Table 4.3. Ether formation attempts of alcohol **4.17** and iodide **4.24**.

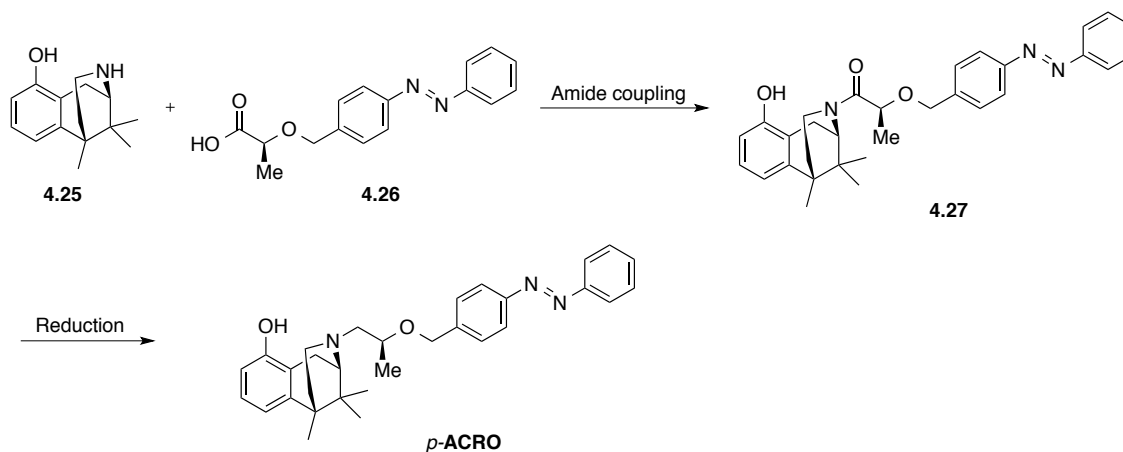
Entry	Reagent	Conditions	Equiv. 4.17 / 4.24	Yield Y
1	Ag ₂ O ¹⁾	PhMe, 90 °C, 4 d	1.0 / 5.0	0%
2	KHMDS	THF, -78 °C to rt, 16 h	1.0 / 2.0	recovered SM
3	KHMDS, 18-crown-6	DME, 0 °C to 90 °C, 16 h	1.0 / 2.0	0%
4	<i>n</i> -BuLi	THF, -78 °C to 50 °C, 16 h	1.0 / 2.0	recovered SM

¹⁾ freshly prepared.

Unfortunately, none of the alkylation attempts of alcohol **4.17** proved successful. Consequently, a new route toward **ACRO** was developed.

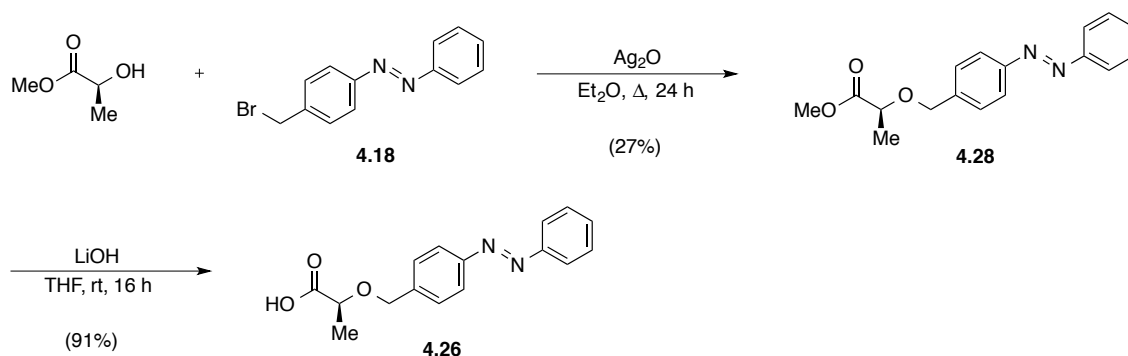
2nd Generation Route toward Azo-Crobenetines

In a new approach toward *p*-**ACRO**, the azolinker was planned to be introduced *via* an amide coupling between amine **4.25** (generously provided by Boehringer Ingelheim) and azo lactate **4.26**. The amide could then be reduced in the next step to the desired *p*-**ACRO** (Scheme 4.13). The same strategy was applied to the synthesis of the corresponding *meta*-derivative *m*-**ACRO**.



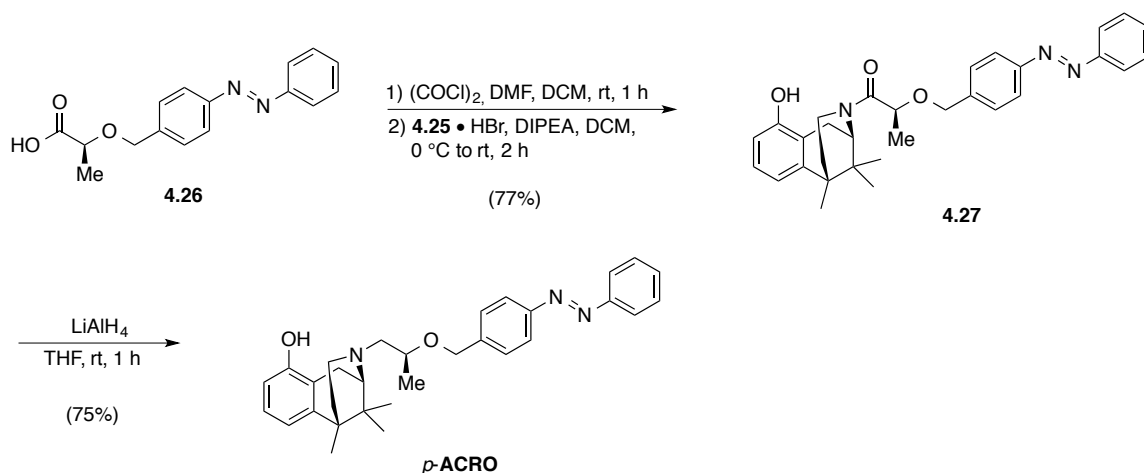
Scheme 4.13. 2nd generation route toward *p*-**ACRO**.

Accordingly, *para*-azo lactate **4.26** was synthesized. Still, ether formation between (–)-methyl L-lactate and bromide **4.18** proved to be challenging, suggesting a strong influence of the neighboring methyl group. Attempts with NaH and the corresponding azo bromide, as well as azo trichloroacetimidate and CSA (no reaction) or TfOH (decomposition), respectively, did not give the desired product. Finally, freshly prepared Ag₂O in refluxing Et₂O furnished ether **4.28** in modest yield (27%). Saponification of the methyl ester with LiOH yielded azo lactate **4.26** in 91% yield (Scheme 4.14).



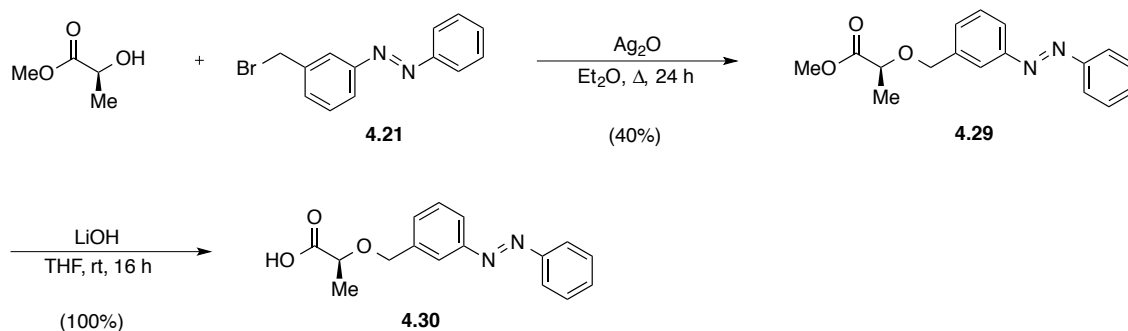
Scheme 4.14. Synthesis of *para*-azo lactate **4.26**.

HATU-mediated coupling of **4.26** and **4.25** provided amide **4.27** in 37% yield, but best results (77% yield) were achieved by converting the acids to the corresponding acid chlorides with oxalyl chloride and catalytic amounts of DMF first, followed by coupling to the secondary amine **4.25**. Amide **4.27** was then reduced with LiAlH_4 in 75% yield to the final product *p*-ACRO (Scheme 4.15).



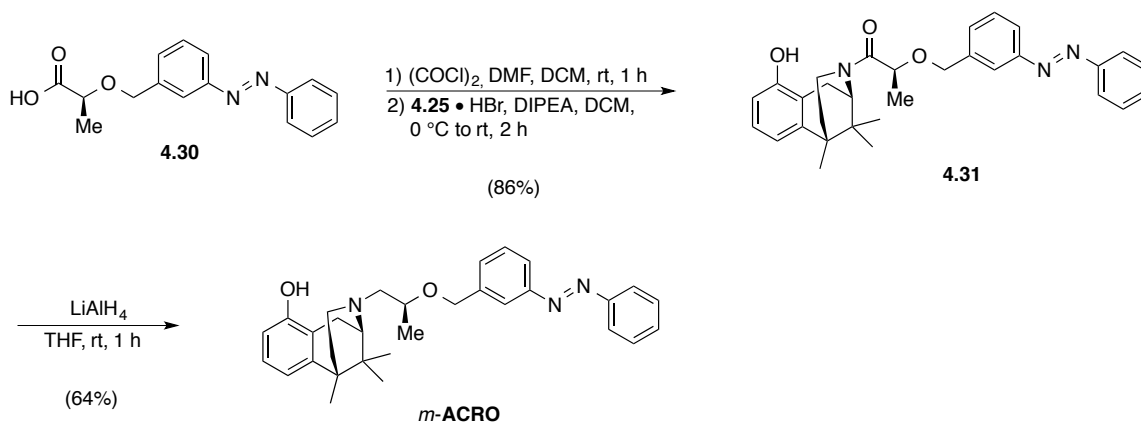
Scheme 4.15. Synthesis of *p*-ACRO from **4.26** and **4.25**.

Following the same protocol, *meta*-azo lactate ester **4.29** was synthesized from (–)-methyl L-lactate and bromide **4.21** with Ag_2O in 40% yield. Basic hydrolysis of the methyl ester with LiOH quantitatively yielded acid **4.30** (Scheme 4.16).



Scheme 4.16. Synthesis of *meta*-azo lactate **4.30**.

Acid **4.30** was converted into the corresponding acid chloride using oxalyl chloride and DMF and then reacted with amine **4.25** to give amide **4.31** in 86% yield. Reduction with LiAlH_4 afforded *m*-ACRO in 64% yield (Scheme 4.17).



Scheme 4.17. Synthesis of *m*-ACRO from **4.30** and **4.25**.

The photochemical properties of both isomers of **Azo-Crobenetine** were investigated using UV/Vis spectrometry. The maximum absorption wavelengths of *p*-ACRO were determined to be $\lambda = 328 \text{ nm}$ and $\lambda = 435 \text{ nm}$, respectively (Fig. 4.10a). As expected, *m*-ACRO differs only slightly from *p*-ACRO with absorption maxima of $\lambda = 325 \text{ nm}$ and $\lambda = 435 \text{ nm}$, respectively (Fig. 4.10b). Its potential as photochromic Na_V blocker is currently investigated in collaboration with Dr. Angelika Lampert (Friedrich-Alexander University Erlangen-Nürnberg).

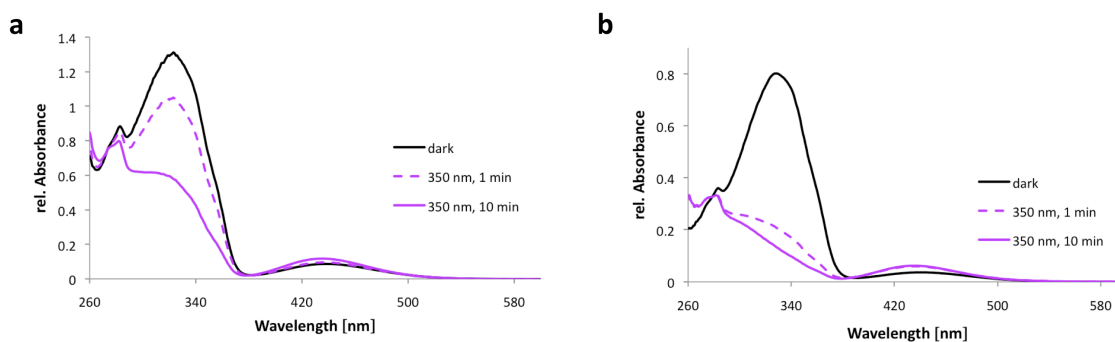


Figure 4.10. UV/Vis spectra (DMSO) of **a)** *p*-ACRO with maximum absorption wavelengths of $\lambda = 328 \text{ nm}$ and $\lambda = 435 \text{ nm}$, and **b)** *m*-ACRO ($\lambda_{max} = 325, 435 \text{ nm}$).

4.5 ATTEMPTS TOWARD PHOTOCNTROL OF Na_V 1.7

The voltage-gated sodium channel type 1.7 is preferentially expressed at high levels in two types of neurons: nociceptive dorsal root ganglion (DRG) neurons and sympathetic ganglion neurons which are part of the involuntary nervous system.^[28] Na_V 1.7 is deployed at the endings of pain-sensing nerves (the nociceptors) close to areas where the impulse is initiated.^[28] The role of Na_V 1.7 as pain sensing channel was discovered from different observations.^[29] Firstly, DRG neurons in animal models of inflammatory pain show increased expression of Na_V 1.7. Secondly, genetically engineered mice lacking Na_V 1.7 expression (specifically in their nociceptors) showed markedly reduced responses to inflammatory pain.^[30]

In 2006, Cox *et al.*^[31] discovered mutations of the Na_V 1.7 encoding gene *SCN9A* that cause a loss of Na_V 1.7 function in three families from Pakistan. Interestingly, the people described in this study have no apparent deficits in non-nociceptive sensory functions, such as the ability to perceive touch, warmth, cold, tickle, pressure, or the position of their limbs (proprioception).^[31] These findings suggest that it may be possible to ameliorate pain by blocking Na_V 1.7 without suffering significant side-effects. Hence, great efforts have been undertaken by the pharmaceutical industry to develop *selective* Na_V 1.7 blockers for the treatment of inflammatory and chronic pain.^[32] However, up to date, to the knowledge of the author no satisfyingly Na_V 1.7 selective small molecule blocker has been developed which might attribute to the great structural resemblance of the Na_V type 1 subfamily. The tarantula venom peptide ProTx-II is one of the rare Na_V 1.7-selective toxins inhibiting Na_V 1.7 with an IC₅₀ value of 0.3 nM, compared with IC₅₀ values of 30 to 150 nM for other heterologously expressed Na_V 1 subtypes.^[33]

In a recent study by Merck, compound **4.32** was discovered as a potent and use-dependent sodium channel blocker for treatment of chronic pain which exhibits a high potency on Na_V 1.7 channels (IC₅₀ = 4.0 μM).^[34] Further development led to the replacement of the azocane moiety with a pyrrolidine ring. Various derivatives of this general structure have been synthesized and tested on their activity on Na_V 1.7 (Fig. 4.11). The *p*-(*t*-butyl)benzyl ether has a slightly increased IC₅₀ value of 9.0 μM, whereas the biphenyl derivative possesses the same IC₅₀ value as **4.32**. By replacing the first phenyl ring with a heterocyclic five-membered ring (i.e. thiazole, 1,2,4-oxadiazole), the IC₅₀ values decrease significantly to 1.3 μM or even 0.86 μM, respectively.

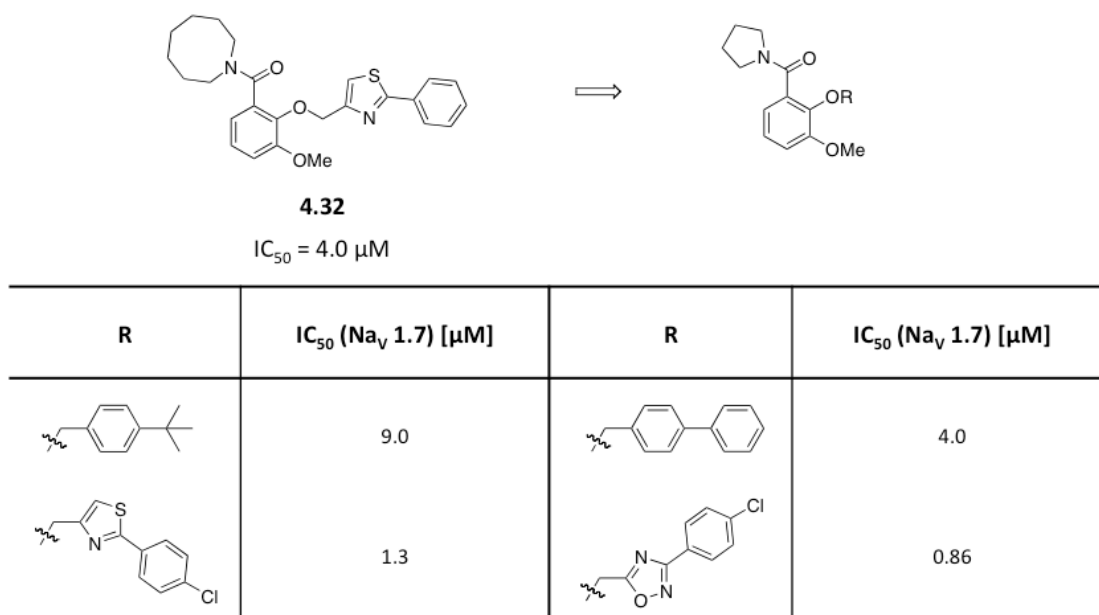


Figure 4.11. Selected examples from structure–activity relationship studies of **4.32**.

Due to its close structural resemblance, the azobenzene derivative **MS1** was designed as a potential photodependent $\text{Na}_V 1.7$ blocker on the basis of **4.33** (Fig. 4.12).

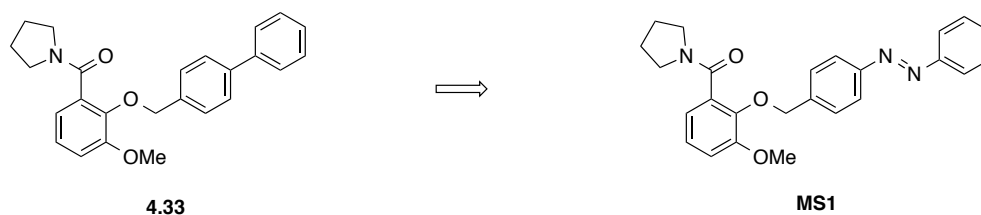
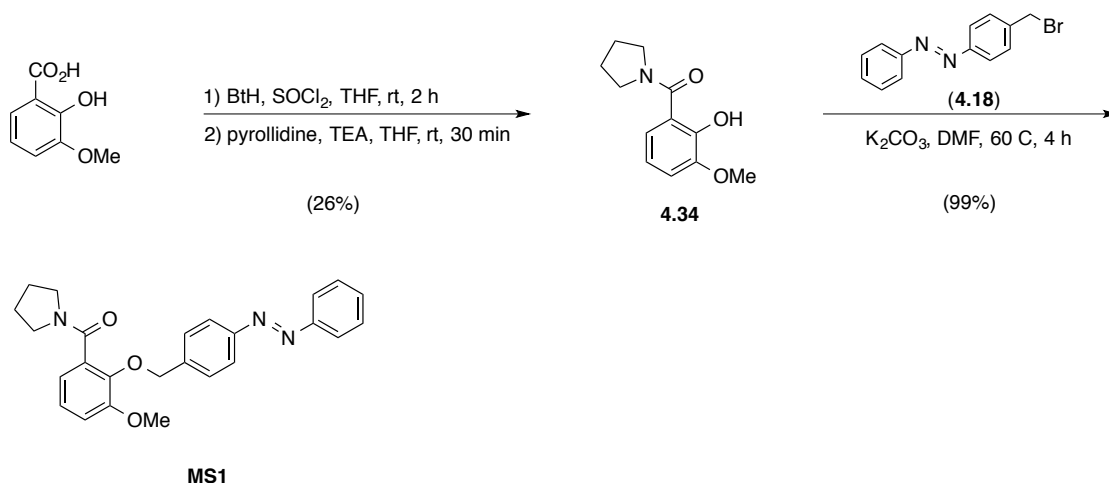


Figure 4.12. Structures of a $\text{Na}_V 1.7$ blocker **4.33** and its azobenzene derivative **MS1**.

Synthesis of MS1

Following a protocol by Katritzky^[35] for direct amide coupling of unprotected *o*-hydroxybenzoic acids, 2-hydroxy-3-methoxybenzoic acid was first converted into its benzotriazole ester using thionyl chloride and benzotriazole. The active ester was then *in situ* reacted with pyrrolidine to yield amide **4.34** in unexpectedly low yield (26%). Next, the azobenzene linker was introduced by etherification of the phenolic hydroxy group under basic conditions with bromide **4.18** to yield **MS1** in 99% yield (Scheme 4.18).



Scheme 4.18. Synthesis of **MS1**, a potential $\text{Na}_V 1.7$ blocker.

The maximum absorption wavelengths of **MS1** were determined by UV/Vis spectrometry to be $\lambda = 328 \text{ nm}$ and $\lambda = 440 \text{ nm}$, respectively (Fig. 4.13). In collaboration with Dr. Angelika Lampert (Friedrich-Alexander University Erlangen-Nürnberg), the selectivity of **MS1** on $\text{Na}_V 1.7$ as well as its light-dependent actions on this subtype of voltage-gated sodium channels are currently investigated.

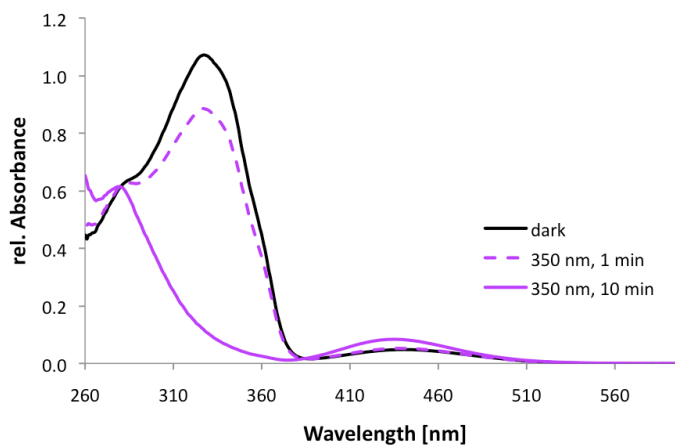


Figure 4.13. UV/Vis spectrum of **MS1** with maximum absorption wavelengths of $\lambda = 328 \text{ nm}$ and $\lambda = 440 \text{ nm}$ (DMSO).

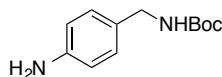
4.6 EXPERIMENTAL PROCEDURES AND ANALYTICAL DATA

4.6.1 GENERAL EXPERIMENTAL DETAILS AND INSTRUMENTATION

All reactions were carried out with magnetic stirring and if air or moisture sensitive in oven-dried glassware under an atmosphere of nitrogen or argon. Syringes used to transfer reagents and solvents were purged with nitrogen or argon prior to use. Reagents were used as commercially supplied unless otherwise stated. Thin layer chromatography was performed on pre-coated silica gel F₂₅₄ glass backed plates and the chromatogram was visualized under UV light and/or by staining using aqueous acidic vanillin or potassium permanganate, followed by gentle heating with a heat gun. Flash column chromatography was performed using silica gel, particle size 40–63 μm (eluants are given in parenthesis). The diameter of the columns and the amount of silica gel were calculated according to the recommendations of W. C. Still *et al.*^[36] IR spectra were recorded on a Perkin Elmer Spectrum Bx FT-IR instrument as thin films with absorption bands being reported in wave number (cm^{-1}). UV/Vis spectra were obtained using a Varian Cary 50 Scan UV/Vis spectrometer and Helma SUPRASIL precision cuvettes (10 mm light path).

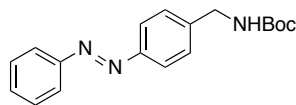
¹H and ¹³C NMR spectra were measured on Varian VNMRS 300, VNMRS 400, INOVA 400 or VNMRS 600 instruments. The chemical shifts are quoted as δ -values in ppm referenced to the residual solvent peak (CDCl_3 : δ_{H} 7.26, δ_{C} 77.2; CD_3OD : δ_{H} 3.31, δ_{C} 49.0; DMSO-d_6 : δ_{H} 2.50, δ_{C} 39.5).^[37] Multiplicities are abbreviated as follows: s = singlet, d = doublet, t = triplet, q = quartet, quint = quintet, sext = sextet, sept = septet, m = multiplet. High resolution mass spectra (EI, ESI) were recorded by LMU Mass Spectrometry Service using a Thermo Finnigan MAT 95, a Jeol MStation or a Thermo Finnigan LTQ FT Ultra instrument. Melting points were obtained using a Stanford Research Systems MPA120 apparatus and are uncorrected. Optical rotation measurements were performed on a Perkin Elmer 241 polarimeter at 22 °C in a 5 cm cell at concentrations expressed as g/100 mL.

4.6.2 SYNTHESIS OF AZO-LACOSAMIDE

Synthesis of *tert*-butyl 4-aminobenzylcarbamate (**4.1**)

4-Aminobenzylamine (4.52 mL, 40.0 mmol, 1.0 equiv.) was dissolved in THF (130 mL) and Boc₂O (9.17 g, 42.0 mmol, 1.05 equiv.) and DMAP (489 mg, 4.00 mmol, 0.100 equiv.) were added. The mixture was stirred for 3 h at room temperature. The solvent was removed *in vacuo* and the crude product was purified by flash silica gel column chromatography (hexanes/EtOAc, gradient from 3:1 to 1:1) to give Boc-protected amine **4.1** (8.40 g, 37.8 mmol, 95%) as a yellowish solid.

TLC (hexanes/EtOAc, 2:1): $R_f = 0.30$. **M.p.:** 82–83 °C. **¹H NMR (CDCl₃, 300 MHz, 27 °C):** $\delta = 7.09\text{--}7.02$ (m, 2H, ArH), 6.66–6.59 (m, 2H, ArH), 4.73 (br s, 1H, NH), 4.17 (d, $J = 5.6$ Hz, 2H, CH₂), 3.60 (br s, 2H, NH₂), 1.45 (s, 9H, C(CH₃)₃) ppm. **¹³C NMR (CDCl₃, 75 MHz, 27 °C):** $\delta = 155.8, 145.7, 128.8, 128.7, 115.1, 79.2, 44.3, 28.4$ ppm. **IR (neat, ATR):** $\tilde{\nu} = 3367$ (m), 1688 (vs), 1623 (m), 1513 (vs), 1457 (m), 1391 (w), 1363 (m), 1325 (w), 1304 (w), 1245 (s), 1161 (s), 1119 (m), 1046 (m), 1027 (m), 937 (w), 931 (w), 864 (w), 821 (m), 784 (w), 758 (w), 666 (w) cm⁻¹. **HRMS (EI⁺):** m/z calcd. for [C₁₂H₁₈N₂O₂]⁺: 222.1368, found: 222.1375 ([M]⁺).

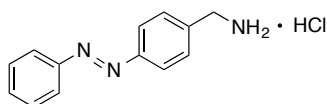
Synthesis of *tert*-butyl 4-(phenyldiazenyl)benzylcarbamate (**4.2**)

Nitrosobenzene (3.94 g, 36.8 mmol, 1.0 equiv.) was dissolved in a mixture of glacial acetic acid (250 mL) and DMSO (10 mL). Aniline **4.1** (8.18 g, 36.8 mmol, 1.0 equiv.) was added in 4 portions within 10 min. The mixture was stirred for 2.5 d at room temperature. Solid Na₂CO₃ was added in portions (gas evolution!), followed by a sat. aqu. solution of NaHCO₃ and the aqueous phase was extracted with DCM (3 x 70 mL). The organic phase was carefully washed with 2 M NaOH (100 mL) and sat. aqu. NaHCO₃ (100 mL), then dried over MgSO₄ and concentrated *in vacuo*. The crude product was purified by flash silica gel chromatography

(hexanes/EtOAc, gradient from 20:1 to 5:1), affording azobenzene **4.2** (9.48 g, 30.4 mmol, 83%) as an orange solid.

TLC (hexanes/EtOAc, 4:1): R_f = 0.40. **M.p.:** 129–130 °C. **^1H NMR (CDCl₃, 600 MHz, 27 °C):** δ = 7.92–7.86 (m, 4H, ArH), 7.53–7.48 (m, 2H, ArH), 7.48–7.44 (m, 1H, ArH), 7.43–7.39 (m, 2H, ArH), 4.93 (br s, 1H, NH), 4.39 (d, J = 5.2 Hz, 2H, CH₂), 1.47 (s, 9H, C(CH₃)₃) ppm. **^{13}C NMR (CDCl₃, 150 MHz, 27 °C):** δ = 155.9, 152.6, 151.9, 142.0, 130.9, 129.0, 128.0, 123.1, 122.8, 79.7, 44.4, 28.4 ppm. **IR (neat, ATR):** $\tilde{\nu}$ = 3324 (m), 2978 (w), 2924 (w), 1682 (vs), 1652 (w), 1602 (w), 1558 (w), 1522 (s), 1485 (w), 1447 (w), 1431 (w), 1391 (m), 1365 (m), 1285 (vs), 1244 (m), 1221 (w), 1167 (m), 1155 (s), 1134 (m), 1106 (w), 1072 (w), 1039 (w), 1021 (m), 1012 (m), 955 (m), 862 (m), 846 (m), 831 (m), 790 (m), 763 (m), 730 (w), 717 (w), 691 (s), 668 (w) cm⁻¹. **HRMS (ESI⁺):** m/z calcd. for [C₁₈H₂₂O₂N₃]⁺: 312.1712, found: 312.1706 ([M+H]⁺).

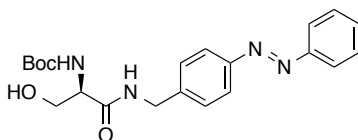
Synthesis of 4-(phenyldiazenyl)phenylmethanaminium chloride (**4.3**)



Boc-protected amine **4.2** (9.36 g, 30.1 mmol) was dissolved in 1,4-dioxane (150 mL) and a 4 M solution of HCl in dioxane (150 mL) was added. The mixture was stirred for 16 h at room temperature. The orange precipitate was filtered off and washed thoroughly with Et₂O (3x). Amine **4.3** was obtained as its HCl salt (7.39 g, 29.8 mmol, 99%) as an orange solid.

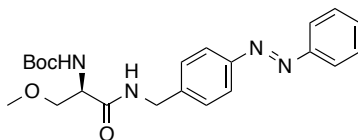
M.p.: 244–247 °C. **^1H NMR (DMSO-d₆, 400 MHz, 27 °C):** δ = 8.55 (br s, 3H, NH₃⁺), 7.92–7.83 (m, 4H, ArH), 7.73–7.66 (m, 2H, ArH), 7.61–7.52 (m, 3H, ArH), 4.10 (s, 2H, CH₂) ppm. **^{13}C NMR (DMSO-d₆, 100 MHz, 27 °C):** δ = 154.1 (*cis* isomer), 153.9 (*cis* isomer), 152.3, 152.1, 137.9, 133.3 (*cis* isomer), 132.2, 130.5, 129.9, 129.9 (*cis* isomer), 129.4 (*cis* isomer), 127.7 (*cis* isomer), 123.0, 123.0, 120.4 (*cis* isomer), 120.2 (*cis* isomer), 42.2 ppm. **IR (neat, ATR):** $\tilde{\nu}$ = 2963 (m), 2880 (m), 2686 (w), 2576 (w), 1593 (m), 1525 (w), 1502 (w), 1480 (s), 1465 (m), 1443 (m), 1419 (w), 1378 (m), 1333 (w), 1301 (w), 1215 (m), 1187 (w), 1157 (w), 1114 (m), 1074 (m), 1018 (m), 969 (m), 955 (m), 930 (w), 917 (w), 881 (m), 847 (s), 837 (s), 774 (m), 756 (s), 726 (m), 681 (vs) cm⁻¹. **HRMS (ESI⁺):** m/z calcd. for [C₁₃H₁₄N₃]⁺: 212.1188, found: 212.1181 ([M-Cl]⁺).

Synthesis of (*R*)-*tert*-butyl (3-hydroxy-1-oxo-1-((4-(phenyldiazenyl)benzyl)-amino)propan-2-yl)carbamate (4.4)



Boc-protected D-serine (257 mg, 1.25 mmol, 1.0 equiv.) was dissolved in DCM (15 mL). The HCl salt of amine **4.3** (372 mg, 1.50 mmol, 1.2 equiv.) and TEA (0.26 mL, 1.9 mmol, 1.5 equiv.) were added, followed by HATU (570 mg, 1.50 mmol, 1.2 equiv.). The reaction mixture was stirred at room temperature for 16 h. The solvent was removed under reduced pressure and the residue was suspended in CHCl₃ (20 mL) and washed with 10% aqu. citric acid (2 x 30 mL). The organic phase was washed with sat. aqu. NaHCO₃ (2 x 30 mL), dried over MgSO₄ and concentrated *in vacuo*. The crude product was purified by flash silica gel chromatography (CHCl₃/MeOH, gradient from 100:0 to 30:1), affording amide **4.4** (339 mg, 0.850 mmol, 68%) as an orange solid.

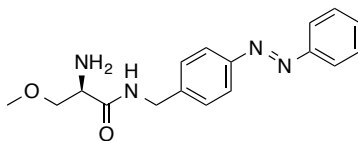
TLC (CHCl₃/MeOH, 20:1): R_f = 0.27. $[\alpha]_D^{22}$: +0.88 (c = 1.0, CHCl₃). **M.p.:** 137–138 °C. **¹H NMR (CDCl₃, 400 MHz, 27 °C):** δ = 7.94–7.82 (m, 4H, ArH), 7.55–7.43 (m, 2H, ArH), 7.48–7.44 (m, 1H, ArH), 7.41–7.36 (m, 2H, ArH), 7.21 (br s, 1H, NH), 5.64 (br s, 1H, NH), 4.62–4.53 (m, 1H, CH), 4.50–4.40 (m, 1H, CH), 4.23–4.11 (m, 2H, 2 x CH), 3.75–3.64 (m, 1H, CH), 3.22 (br s, 1H, OH), 1.43 (s, 9H, C(CH₃)₃) ppm. **¹³C NMR (CDCl₃, 100 MHz, 27 °C):** δ = 171.6, 156.4, 152.6, 152.0, 140.8, 131.0, 129.1, 128.0, 123.2, 122.8, 80.7, 62.7, 54.7, 43.0, 28.3 ppm. **IR (neat, ATR):** $\tilde{\nu}$ = 3325 (m), 2965 (w), 1684 (s), 1627 (vs), 1556 (m), 1530 (vs), 1465 (m), 1444 (m), 1418 (m), 1388 (m), 1363 (m), 1352 (m), 1303 (m), 1243 (s), 1171 (s), 1103 (m), 1069 (m), 1039 (m), 1012 (m), 977 (m), 957 (w), 919 (w), 872 (w), 835 (m), 794 (w), 766 (m), 722 (w), 683 (m), 668 (w) cm⁻¹. **HRMS (ESI⁺):** m/z calcd. for [C₂₁H₂₇N₄O₄]⁺: 399.2032, found: 399.2026 ([M+H]⁺).

Synthesis of (*R*)-*tert*-butyl (3-methoxy-1-oxo-1-((4-(phenyldiazenyl)benzyl)-amino)propan-2-yl)carbamate (4.5**)**

To a solution of alcohol **4.4** (306 mg, 0.770 mmol, 1.0 equiv.) in DCM (10 mL) were added Bu_4NI (55 mg, 0.15 mmol, 0.2 equiv.) and H_2O (1 mL). The solution was cooled to 10 °C and a solution of NaOH (185 mg, 4.62 mmol, 6.0 equiv.) in H_2O (0.2 mL) was added dropwise. Subsequently, Me_2SO_4 (0.32 mL, 3.4 mmol, 4.4 equiv.) was added dropwise at 10 °C and the mixture was stirred at this temperature for 1 h and warmed slowly to room temperature overnight. H_2O (30 mL) was added and the phases were separated. The organic phase was washed with sat. aqu. NaHCO_3 (2 x 30 mL), dried over MgSO_4 and concentrated *in vacuo*. The crude product was purified by flash silica gel chromatography ($\text{CHCl}_3/\text{MeOH}$, gradient from 100:0 to 40:1), affording methyl ether **4.5** (297 mg, 0.720 mmol, 94%) as an orange solid.

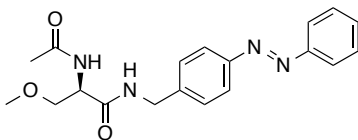
TLC ($\text{CHCl}_3/\text{MeOH}$, 20:1): $R_f = 0.51$. $[\alpha]_D^{22}$: -5.3 ($c = 0.5$, CHCl_3). **M.p.**: 88–89 °C. **$^1\text{H NMR}$** (CDCl_3 , 400 MHz, 27 °C): $\delta = 7.91\text{--}7.83$ (m, 4H, ArH), 7.52–7.42 (m, 3H, ArH), 7.41–7.36 (m, 2H, ArH), 6.84 (t, $J = 5.4$ Hz, 1H, NH), 5.43 (br s, 1H, NH), 4.54 (t, $J = 5.8$ Hz, 2H, CH_2), 4.35–4.23 (m, 1H, CH), 3.84 (dd, $J = 9.2, 3.9$ Hz, 1H, CH), 3.50 (dd, $J = 9.2, 6.2$ Hz, 1H, CH), 3.37 (s, 3H, CH_3), 1.43 (s, 9H, $\text{C}(\text{CH}_3)_3$) ppm. **$^{13}\text{C NMR}$** (CDCl_3 , 100 MHz, 27 °C)^[cc]: $\delta = 170.4, 155.5, 152.6, 151.9, 141.1, 137.4$ (*cis* isomer), 131.0, 129.0, 128.7 (*cis* isomer), 128.0, 127.5 (*cis* isomer), 127.3 (*cis* isomer), 123.1, 122.8, 120.9 (*cis* isomer), 120.3 (*cis* isomer), 80.4, 72.0, 59.1, 54.0, 43.1, 28.2 ppm. **IR** (neat, ATR): $\tilde{\nu} = 3294$ (m), 2931 (w), 1684 (m), 1652 (vs), 1529 (m), 1457 (m), 1391 (m), 1364 (m), 1346 (w), 1312 (m), 1280 (w), 1242 (m), 1165 (s), 1121 (m), 1106 (m), 1082 (m), 1046 (m), 1018 (m), 958 (w), 913 (m), 864 (w), 826 (m), 767 (m), 729 (m), 703 (w), 686 (w) cm^{-1} . **HRMS** (ESI^+): m/z calcd. for $[\text{C}_{22}\text{H}_{29}\text{N}_4\text{O}_4]^+$: 413.2189, found: 413.2182 ($[\text{M}+\text{H}]^+$).

^[cc] Compound **4.5** was obtained as a mixture of *cis/trans* isomers.

Synthesis of (*R*)-2-amino-3-methoxy-*N*-(4-(phenyldiazenyl)benzyl)propanamide (4.6)

Boc-protected amine **4.5** (225 mg, 0.550 mmol) was dissolved in 1,4-dioxane (5 mL) and a 4 M solution of HCl in 1,4-dioxane (5 mL) was added. The reaction mixture was stirred at room temperature for 16 h. A sat. aqu. solution of NaHCO₃ (20 mL) was added and the phases were separated. The aqueous phase was extracted with EtOAc (20 mL) and the combined organic layers were washed with sat. aqu. NaHCO₃ (15 mL), dried over MgSO₄ and concentrated *in vacuo*, affording amine **4.6** (143 mg, 0.460 mmol, 84%) as an orange solid.

TLC (CHCl₃/MeOH, 20:1): R_f = 0.29. [α]_D²²: +5.6 (*c* = 1.0, CHCl₃). **M.p.:** 95–97 °C. **¹H NMR (CDCl₃, 300 MHz, 27 °C):** δ = 7.92–7.86 (m, 4H, ArH), 7.55–7.44 (m, 3H, ArH), 7.43–7.39 (m, 2H, ArH), 4.53 (d, *J* = 6.1 Hz, 2H, CH₂), 3.68–3.60 (m, 3H, CH, CH₂), 3.38 (s, 3H, CH₃), 1.72 (br s, 2H, NH₂) ppm. **¹³C NMR (CDCl₃, 75 MHz, 27 °C):** δ = 172.7, 152.6, 151.9, 141.5, 131.0, 129.0, 128.2, 123.1, 122.8, 74.5, 58.9, 54.9, 42.8 ppm. **IR (neat, ATR):** $\tilde{\nu}$ = 3337 (w), 3269 (m), 2890 (w), 1644 (vs), 1599 (m), 1525 (s), 1483 (m), 1464 (m), 1442 (m), 1412 (w), 1355 (w), 1333 (w), 1302 (w), 1221 (m), 1181 (w), 1152 (m), 1129 (m), 1107 (s), 1070 (m), 1017 (w), 1010 (w), 970 (w), 923 (m), 876 (m), 849 (m), 829 (m), 787 (w), 769 (s), 705 (w), 683 (s), 668 (m) cm⁻¹. **HRMS (ESI⁺):** *m/z* calcd. for [C₁₇H₂₁N₄O₂]⁺: 313.1665, found: 313.1659 ([M+H]⁺).

Synthesis of (*R*)-2-acetamido-3-methoxy-*N*-(4-(phenyldiazenyl)benzyl)propanamide (ALCM)

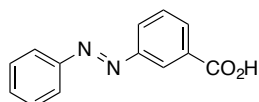
Amine **4.6** (124 mg, 0.400 mmol, 1.0 equiv.) was dissolved in DCM (7 mL) and cooled to 0 °C. TEA (83 μL, 0.60 mmol, 1.5 equiv.) was added, followed by acetyl chloride (34 μL, 0.48 mmol, 1.2 equiv.). The reaction mixture was warmed to room temperature and stirred for 3.5 h. As TLC analysis indicated incomplete reaction, more acetyl chloride (10 μL, 0.14 mmol, 0.35 equiv.) was added and the mixture was stirred for further 15 min. 10% aqu. citric acid (20 mL) was added and the phases were separated. The aqueous layer was extracted with DCM

(20 mL). The combined organic layers were washed with sat. aqu. NaHCO₃ (25 mL), dried over MgSO₄ and concentrated *in vacuo*. The crude product was purified by flash silica gel chromatography (CHCl₃/MeOH, gradient from 100:0 to 40:1), affording **ALCM** (93 mg, 0.26 mmol, 65%) as an orange solid.

TLC (CHCl₃/MeOH, 10:1): $R_f = 0.46$. $[\alpha]_D^{22}$: -15.2 ($c = 0.1$, CHCl₃). **M.p.:** 201–202 °C. **¹H NMR** (CDCl₃, 600 MHz, 27 °C): $\delta = 7.92\text{--}7.86$ (m, 4H, ArH), 7.53–7.44 (m, 3H, ArH), 7.41–7.37 (m, 2H, ArH), 6.88–6.81 (m, 1H, NH), 6.45–6.40 (m, 1H, NH), 4.60–4.50 (m, 3H, CH, CH₂), 3.83 (dd, $J = 9.0, 4.2$ Hz, 1H, CH), 3.47–3.43 (m, 1H, CH), 3.40 (s, 3H, CH₃), 2.04 (s, 3H, CH₃) ppm. **¹³C NMR** (CDCl₃, 150 MHz, 27 °C)^[dd]: $\delta = 170.3, 170.1, 170.0, 152.6, 152.0, 140.9, 140.9, 131.0, 129.1, 128.0, 128.0, 123.2, 122.8, 71.5, 59.1, 52.4, 52.4, 43.2, 43.1, 23.2, 23.2$ ppm. **IR** (neat, ATR): $\tilde{\nu} = 3274$ (m), 3067 (w), 2971 (w), 2923 (w), 2876 (w), 2818 (w), 1783 (w), 1626 (vs), 1544 (s), 1483 (w), 1444 (m), 1371 (m), 1341 (w), 1300 (w), 1278 (w), 1222 (w), 1202 (w), 1138 (m), 1122 (m), 1107 (m), 1055 (w), 1012 (w), 980 (w), 933 (w), 891 (w), 832 (m), 805 (w), 769 (m), 745 (m), 724 (m), 684 (s) cm⁻¹. **HRMS** (ESI⁺): m/z calcd. for [C₁₉H₂₃N₄O₃]⁺: 355.1770, found: 355.1763 ([M+H]⁺). **UV/Vis**: $\lambda_{\max} = 328, 440$ nm.

4.6.3 SYNTHESIS OF AZO-LAMOTRIGINE

Synthesis of 3-(phenyldiazenyl)benzoic acid (4.7)



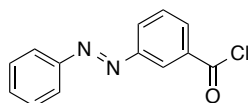
Nitrosobenzene (10.7 g, 100 mmol, 1.0 equiv.) was dissolved in glacial acetic acid (100 mL) and DCM (50 mL). 3-Aminobenzoic acid (13.7 g, 100 mmol, 1.0 equiv.) was added in several portions within 10 min. The mixture was stirred at room temperature for 16 h. The solvent was removed under reduced pressure and residual solvent was coevaporated with toluene (3 x 40 mL). Recrystallization from ethyl acetate afforded azobenzene **4.7** (16.5 g, 72.8 mmol, 73%) as an orange solid.

M.p.: 168–169 °C. **¹H NMR** (CD₃OD, 400 MHz, 27 °C): $\delta = 8.49$ (ddd, $J = 1.6, 1.6, 0.4$ Hz, 1H, ArH), 8.14 (ddd, $J = 8.0, 1.6, 1.2$ Hz, 1H, ArH), 8.12 (ddd, $J = 8.0, 2.0, 1.2$ Hz, 1H, ArH), 7.95–7.90 (m, 2H, ArH), 7.64 (ddd, $J = 8.0, 8.0, 0.4$ Hz, 1H, ArH), 7.57–7.50 (m, 3H,

^[dd] A mixture of rotamers of **ALCM** was observed in the ¹³C NMR.

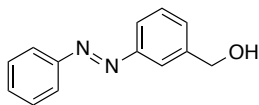
ArH) ppm. ^{13}C NMR (CD_3OD , 100 MHz, 27 °C): δ = 167.6, 152.5, 152.4, 131.9, 131.5, 131.2, 129.1, 128.9, 126.5, 123.3, 122.5 ppm. IR (neat, ATR): $\tilde{\nu}$ = 3353 (s), 2504 (m), 1678 (vs), 1597 (m), 1586 (m), 1472 (w), 1447 (m), 1425 (w), 1354 (m), 1343 (m), 1302 (m), 1274 (w), 1215 (m), 1173 (w), 1159 (w), 1116 (w), 1079 (w), 1019 (w), 996 (w), 923 (w), 821 (w), 765 (m), 682 (m) cm^{-1} . HRMS (ESI): m/z calcd. for $[\text{C}_{13}\text{H}_9\text{N}_2\text{O}_2]^-$: 225.0664, found: 225.0670 ($[\text{M}-\text{H}]^-$).

Synthesis of 3-(phenyldiazenyl)benzoyl chloride (4.8)



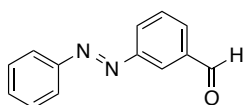
Carboxylic acid **4.7** (200 mg, 0.880 mmol, 1.0 equiv.) was dissolved in DCM (5 mL) and DMF (0.5 mL). Oxalyl chloride (0.71 mL, 1.4 mmol, 1.6 equiv.) was added dropwise within 15 min. The reaction mixture was stirred at room temperature for 1 h, followed by removal of the solvent *in vacuo*. The crude product was purified by flash silica gel chromatography (hexanes/EtOAc, 50:1) to yield acid chloride **4.8** (194 mg, 0.790 mmol, 90%) as an orange solid.

TLC (hexanes/EtOAc, 2:1): R_f = 0.89. M.p.: 69–70 °C. ^1H NMR (CDCl_3 , 300 MHz, 27 °C): δ = 8.65 (ddd, J = 2.1, 2.1, 0.6 Hz, 1H, ArH), 8.25–8.18 (m, 2H, ArH), 8.00–7.94 (m, 2H, ArH), 7.67 (ddd, J = 7.8, 7.8, 0.6 Hz, 1H, ArH), 7.58–7.51 (m, 3H, ArH) ppm. ^{13}C NMR (CDCl_3 , 75 MHz, 27 °C): δ = 168.0, 152.8, 152.3, 134.4, 132.8, 131.9, 129.7, 129.2, 129.0, 125.7, 123.2 ppm. IR (neat, ATR): $\tilde{\nu}$ = 3087 (w), 3060 (w), 1747 (vs), 1673 (w), 1590 (m), 1584 (m), 1489 (m), 1468 (w), 1445 (m), 1415 (w), 1319 (w), 1301 (w), 1279 (w), 1233 (m), 1191 (m), 1169 (w), 1149 (m), 1117 (m), 1082 (w), 1070 (w), 1017 (w), 1000 (w), 970 (w), 921 (w), 912 (m), 889 (m), 816 (s), 767 (s), 694 (s), 684 (vs), 653 (m) cm^{-1} . HRMS (EI $^+$): m/z calcd. for $[\text{C}_{13}\text{H}_9\text{N}_2\text{OCl}]^+$: 244.0403, found: 244.0399 ($[\text{M}]^+$).

Synthesis of 3-(phenyldiazenyl)phenyl)methanol (4.10)

Nitrosobenzene (4.50 g, 42.0 mmol, 1.1 equiv.) was dissolved in a mixture of ethanol (30 mL) and glacial acetic acid (11.4 mL) with careful heating to 45 °C. The clear green solution was cooled to room temperature again and 3-aminobenzyl alcohol (4.71 g, 38.2 mmol, 1.0 equiv.) was added in 5 portions within 10 min. The mixture was stirred for 1 h at room temperature. The solvent was removed under reduced pressure and Et₂O (100 mL) was added. The organic phase was carefully washed with sat. aqu. NaHCO₃ (100 mL; gas evolution!), then dried over MgSO₄ and concentrated *in vacuo*. The crude product was purified by flash silica gel chromatography (hexanes/EtOAc, gradient from 4:1 to 2:1), affording azobenzene **5.11** (7.76 g, 36.6 mmol, 96%) as red crystals.

TLC (hexanes/EtOAc, 2:1): R_f = 0.66. **M.p.:** 35–36 °C. **¹H NMR (CDCl₃, 300 MHz, 27 °C):** δ = 7.98–7.90 (m, 3H, ArH), 7.90–7.84 (dddd, J = 7.2, 1.8, 1.8, 0.3 Hz, 1H, ArH), 7.59–7.45 (m, 5H, ArH), 4.78 (s, 2H, CH₂), 2.25 (br s, 1H, OH) ppm. **¹³C NMR (CDCl₃, 75 MHz, 27 °C):** δ = 152.8, 152.6, 142.1, 131.1, 129.4, 129.3, 129.1, 122.9, 122.6, 120.6, 64.9 ppm. **IR (neat, ATR):** $\tilde{\nu}$ = 3314 (m), 1585 (w), 1447 (m), 1304 (w), 1238 (w), 1195 (w), 1150 (w), 1125 (w), 1019 (m), 922 (w), 884 (w), 838 (w), 793 (s), 768 (s), 690 (vs) cm⁻¹. **HRMS (ESI⁺):** *m/z* calcd. for [C₁₃H₁₃N₂O]⁺: 213.1028, found: 213.1022 ([M+H]⁺).

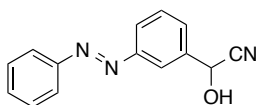
Synthesis of 3-(phenyldiazenyl)benzaldehyde (4.11)

To a solution of alcohol **4.10** (1.89 g, 8.90 mmol, 1.0 equiv.) in DCM (100 mL), MnO₂ (7.74 g, 89.0 mmol, 10 equiv.) was added in one portion. The reaction mixture was stirred at room temperature for 18 h. The mixture was filtered through Celite and washed thoroughly with DCM. The filtrate was concentrated under reduced pressure to give the aldehyde **4.11** (1.82 g, 8.66 mmol, 97%) as a red solid which could be used without further purification. An analytical sample was obtained by preparative TLC (100% CHCl₃).

TLC (hexanes/EtOAc, 2:1): R_f = 0.83. **M.p.:** 62–63 °C. **¹H NMR (CDCl₃, 300 MHz, 27 °C):** δ = 10.14 (s, 1H, CHO), 8.41 (dd, J = 1.8, 1.8 Hz, 1H, ArH), 8.19 (ddd, J = 7.8, 1.8, 1.2 Hz, 1H,

ArH), 7.98–7.93 (m, 2H, ArH), 7.70 (dd, $J = 7.8, 7.8$ Hz, 1H, ArH), 7.59–7.50 (m, 3H, ArH) ppm. ^{13}C NMR (CDCl_3 , 75 MHz, 27 °C): $\delta = 191.7, 153.0, 152.4, 137.3, 131.6, 131.1, 129.8, 129.2, 128.7, 123.8, 123.1$ ppm. IR (neat, ATR): $\tilde{\nu} = 3057$ (w), 2845 (w), 2746 (w), 1688 (vs), 1607 (m), 1580 (m), 1492 (w), 1471 (w), 1435 (m), 1389 (m), 1302 (w), 1271 (w), 1229 (m), 1194 (m), 1143 (m), 1114 (m), 1107 (m), 1070 (m), 1018 (m), 997 (w), 976 (w), 957 (m), 920 (w), 904 (m), 882 (w), 838 (w), 807 (s), 778 (m), 765 (s), 683 (vs), 668 (s) cm^{-1} . HRMS (ESI⁺): m/z calcd. for $[\text{C}_{13}\text{H}_{11}\text{N}_2\text{O}]^+$: 211.0871, found: 211.0865 ($[\text{M}+\text{H}]^+$).

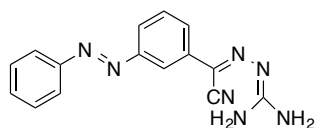
Synthesis of 2-hydroxy-2-(3-(phenyldiazenyl)phenyl)acetonitrile (4.12)



Aldehyde **4.11** (500 mg, 2.38 mmol, 1.0 equiv.) was dissolved in THF (60 mL) and TMSCN (1.20 mL, 9.56 mmol, 9.6 equiv.) was added dropwise. The reaction mixture was stirred at room temperature for 4 h. The solvent was removed under reduced pressure and the crude product was taken up in EtOAc (20 mL). The organic phase was washed with sat. aqu. NaHCO_3 (30 mL) and brine (30 mL), dried over MgSO_4 and concentrated *in vacuo*. Purification of the crude product by flash silica gel chromatography (hexanes/EtOAc, gradient from 20:1 to 2:1) afforded cyanohydrin **4.12** (521 mg, 2.16 mmol, 91%) as an orange oil.

TLC (CHCl_3): $R_f = 0.13$. ^1H NMR (CDCl_3 , 600 MHz, 27 °C): $\delta = 8.05$ (ddd, $J = 1.8, 1.8, 0.6$ Hz, 1H, ArH), 7.97–7.94 (m, 1H, ArH), 7.93–7.90 (m, 2H, ArH), 7.64–7.61 (m, 1H, ArH), 7.58 (dd, $J = 7.8, 7.8$ Hz, 1H, ArH), 7.54–7.49 (m, 3H, ArH), 5.64 (d, $J = 5.4$ Hz, 1H, CH), 3.21 (d, $J = 5.4$ Hz, 1H, OH) ppm. ^{13}C NMR (CDCl_3 , 150 MHz, 27 °C): $\delta = 152.9, 152.3, 136.3, 131.6, 130.0, 129.2, 128.7, 124.6, 123.0, 120.5, 118.5, 63.3$ ppm. IR (neat, ATR): $\tilde{\nu} = 3407$ (m), 3062 (w), 2917 (w), 1700 (w), 1585 (w), 1479 (w), 1448 (m), 1377 (m), 1308 (w), 1215 (w), 1194 (w), 1150 (m), 1129 (w), 1070 (m), 1046 (m), 1000 (w), 927 (w), 899 (w), 851 (w), 803 (m), 766 (m), 692 (vs) cm^{-1} . HRMS (ESI⁺): m/z calcd. for $[\text{C}_{14}\text{H}_{12}\text{N}_3\text{O}]^+$: 238.0980, found: 238.0974 ($[\text{M}+\text{H}]^+$).

Synthesis of (Z)-N'-(diaminomethylene)-3-phenyldiazenyl)benzohydrazonoyl cyanide (4.14)

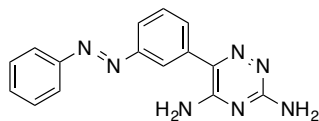


To a solution of cyanohydrin **4.12** (464 mg, 1.96 mmol, 1.0 equiv.) in DCM (35 mL), MnO₂ (1.70 g, 19.6 mmol, 10 equiv.) was added in one portion. The reaction mixture was stirred at room temperature for 16 h. The mixture was filtered through Celite and washed thoroughly with DCM. The filtrate was concentrated under reduced pressure to give compound **4.13** which was directly used in the next step.

To a solution of aminoguanidine bismesylate^[ee] (940 mg, 3.53 mmol, 1.8 equiv.) in MsOH (18 mL) at 70 °C, a solution of compound **4.13** in MeCN (30 mL) was added over 15 min. The reaction mixture was stirred at 70 °C for 5 h. The hot solution was then poured onto ice water and neutralized with 2 M NaOH to pH = 8–9. The aqueous layer was extracted with DCM (3 x 30 mL) and the combined organic layers were washed with sat. aqu. NaHCO₃ (100 mL), brine (100 mL), then dried over MgSO₄ and concentrated *in vacuo*. The crude product was purified by flash silica gel chromatography (DCM/MeOH, 10:0 → 2:1), yielding cyanohydrazone **4.14** (144 mg, 0.490 mmol, 25% over two steps) as a red solid.

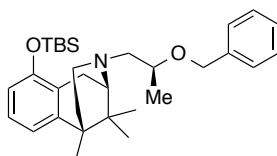
TLC (DCM/MeOH, 10:1): R_f = 0.30. **M.p.:** 178–180 °C. **¹H NMR (DMSO-d₆, 600 MHz, 27 °C):** δ = 8.23 (ddd, *J* = 1.8, 1.8, 0.6 Hz, 1H, ArH), 8.04 (ddd, *J* = 7.8, 1.8, 0.6 Hz, 1H, ArH), 7.92–7.88 (m, 2H, ArH), 7.77 (ddd, *J* = 7.8, 1.8, 0.6 Hz, 1H, ArH), 7.62–7.56 (m, 4H, ArH), 6.75 (br s, 4H, 2 x NH₂) ppm. **¹³C NMR (DMSO-d₆, 150 MHz, 27 °C):** δ = 163.6, 152.7, 152.4, 136.1, 132.1, 130.2, 129.9, 127.6, 123.1, 121.6, 119.4, 117.5, 114.3 ppm. **IR (neat, ATR):** $\tilde{\nu}$ = 3448 (m), 3322 (m), 3185 (m), 2214 (m), 1652 (m), 1609 (m), 1558 (s), 1475 (vs), 1441 (m), 1414 (s), 1314 (m), 1276 (m), 1211 (w), 1150 (s), 1083 (m), 1034 (w), 1018 (s), 998 (w), 972 (m), 926 (w), 915 (w), 887 (m), 867 (w), 798 (m), 762 (m), 740 (w), 678 (vs), 656 (w) cm⁻¹. **HRMS (EI⁺):** *m/z* calcd. for [C₁₅H₁₃N₇]⁺: 291.1232, found: 291.1231 ([M]⁺).

^[ee] Aminoguanidine bismesylate was synthesized from aminoguanidine bicarbonate in quantitative yield according to a literature procedure: M. Leach, K. Franzmann, D. Riddall, L. Harbige (University of Greenwich), WO/2011/004195 A2, 2011.

Synthesis of 6-(3-(phenyldiazenyl)phenyl)-1,2,4-triazine-3,5-diamine (ALTG)

To a solution of cyanohydrazone **4.14** (50 mg, 0.17 mmol, 1.0 equiv.) in EtOH (10 mL), NaOEt (0.25 mL, 21% solution in EtOH) was added in one portion. The reaction mixture was heated to reflux for 1.75 h. The mixture was cooled to room temperature and the solvent was removed under reduced pressure. The crude product was purified by flash silica gel chromatography (DCM/MeOH, gradient from 100:0 to 15:1), affording triazine **ALTG** (39 mg, 0.13 mmol, 76%) as an orange solid.

TLC (DCM/MeOH, 10:1): $R_f = 0.25$. **M.p.:** 225–226 °C. **$^1\text{H NMR}$ (DMSO- d_6 , 600 MHz, 27 °C):** $\delta = 8.02$ (ddd, $J = 1.8, 1.8, 0.6$ Hz, 1H, ArH), 7.92–7.89 (m, 3H, ArH), 7.72 (ddd, $J = 7.8, 1.8, 0.6$ Hz, 1H, ArH), 7.66 (ddd, $J = 7.8, 7.8, 0.6$ Hz, 1H, ArH), 7.61–7.54 (m, 3H, ArH), 6.80 (br s, 2H, NH_2), 6.40 (br s, 2H, NH_2) ppm. **$^{13}\text{C NMR}$ (DMSO- d_6 , 100 MHz, 27 °C):** $\delta = 161.9, 154.8, 152.4, 152.3, 138.9, 137.2, 132.1, 131.4, 130.2, 129.9, 123.0, 122.9, 122.1$ ppm. **IR (neat, ATR):** $\tilde{\nu} = 3488$ (w), 3404 (w), 3319 (m), 3193 (m), 1664 (m), 1624 (s), 1520 (vs), 1432 (m), 1418 (m), 1322 (m), 1307 (w), 1285 (w), 1263 (w), 1209 (w), 1093 (w), 1069 (w), 1020 (w), 915 (w), 901 (m), 858 (w), 808 (m), 759 (m), 722 (m), 699 (m), 683 (s) cm^{-1} . **HRMS (ESI $^+$):** m/z calcd. for $[\text{C}_{15}\text{H}_{14}\text{N}_7]^+$: 292.1311, found: 292.1303 ($[\text{M}+\text{H}]^+$). **UV/Vis:** $\lambda_{\text{max}} = 323, 441$ nm.

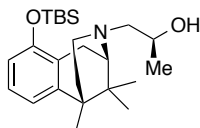
4.6.4 SYNTHESIS OF AZO-CROBENETINES**Synthesis of (2*R*,6*S*)-3-((*S*)-2-(benzyloxy)propyl)-10-((*tert*-butyldimethylsilyl)-oxy)-6,11,11-trimethyl-1,2,3,4,5,6-hexahydro-2,6-methanobenzo[*d*]azocine (4.16)**

To a solution of the HCl salt of crobenetine **4.15** (150 mg, 0.360 mmol, 1.0 equiv.) in DMF (6 mL) were added TBSCl (109 mg, 0.720 mmol, 2.0 equiv.), imidazole (98 mg, 1.4 mmol, 4.0 equiv.) and DMAP (5.0 mg, 0.040 mmol, 0.1 equiv.) at 0 °C. The reaction mixture was

warmed to room temperature and stirred for 16 h. The mixture then was poured into H₂O (100 mL), extracted with Et₂O (3 x 30 mL) and the combined organic layers were washed with H₂O (5 x 100 mL). The combined aqueous layers were again extracted with Et₂O (3 x 30 mL) and the combined organic layers were dried over MgSO₄ and concentrated *in vacuo*. The crude product was used without further purification for the next step. An analytical sample was obtained by flash silica gel chromatography (hexanes/EtOAc, 10:1), affording TBS ether **4.16** (176 mg, 0.360 mmol, 100%) as a colorless oil.

TLC (hexanes/EtOAc, 10:1): $R_f = 0.47$. $[\alpha]_D^{22}$: -81.2 ($c = 0.33$, DCM). **¹H NMR (CDCl₃, 400 MHz, 27 °C):** $\delta = 7.40\text{--}7.30$ (m, 4H, ArH), 7.29–7.26 (m, 1H, ArH), 7.03 (dd, $J = 8.0$, 8.0 Hz, 1H, ArH), 6.91 (dd, $J = 8.0$, 1.2 Hz, 1H, ArH), 6.63 (dd, $J = 8.0$, 1.2 Hz, 1H, ArH), 4.67–4.60 (m, 2H, CH₂), 3.68–3.58 (m, 1H, CH), 2.92 (d, $J = 18.8$ Hz, 1H, CH), 2.71 (dd, $J = 13.2$, 6.0 Hz, 1H, CH), 2.55 (d, $J = 6.0$ Hz, 1H, CH), 2.50–2.42 (m, 2H, 2 x CH), 2.28 (dd, $J = 13.2$, 5.6 Hz, 1H, CH), 2.12 (d, $J = 13.4$ Hz, 1H, CH), 2.06 (d, $J = 13.4$ Hz, 1H, CH), 1.29 (s, 3H, CH₃), 1.28 (s, 3H, CH₃), 1.22 (d, $J = 6.0$ Hz, 3H, CH₃), 1.04 (s, 9H, C(CH₃)₃), 1.02–0.98 (m, 1H, CH), 0.79 (s, 3H, CH₃), 0.23 (s, 3H, SiCH₃), 0.22 (s, 3H, SiCH₃) ppm. **¹³C NMR (CDCl₃, 100 MHz, 27 °C):** $\delta = 151.4$, 145.8, 139.3, 128.6, 128.3, 127.5, 127.3, 126.0, 118.0, 115.3, 73.4, 70.9, 62.5, 61.1, 46.4, 39.0, 37.9, 36.5, 25.9, 23.6, 23.3, 20.7, 20.5, 18.9, 18.4, -4.0 , -4.0 ppm. **IR (neat, ATR):** $\tilde{\nu} = 2958$ (m), 2927 (s), 2856 (m), 1579 (m), 1464 (s), 1389 (m), 1372 (m), 1346 (w), 1313 (w), 1271 (s), 1252 (vs), 1208 (w), 1168 (m), 1102 (m), 1035 (m), 980 (s), 967 (s), 938 (w), 909 (w), 865 (m), 837 (s), 827 (s), 813 (m), 778 (s), 737 (m), 718 (m), 695 (m), 668 (w) cm⁻¹. **HRMS (ESI⁺):** m/z calcd. for [C₃₁H₄₈NO₂Si]⁺: 494.3454, found: 494.3449 ([M+H]⁺).

Synthesis of (S)-1-((2R,6S)-10-((tert-butyl)dimethylsilyloxy)-6,11,11-trimethyl-1,2,5,6-tetrahydro-2,6-methanobenzo[d]azocin-3(4H)-yl)propan-2-ol (4.17)

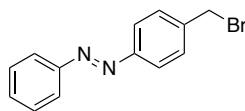


Palladium on charcoal (100 mg, 10%) was added to a solution of crude benzyl ether **4.16** (170 mg, 0.340 mmol, 1.0 equiv.) in EtOH (8 mL) and EtOAc (4 mL) in an autoclave. The autoclave was purged with H₂ (4 bar) and evacuated (5x). The reaction mixture was then stirred for 20 h under an H₂ atmosphere (4 bar). As TLC indicated still remaining starting material, palladium on charcoal (50 mg, 10%) were added and the autoclave was purged again with H₂ (4 bar) and evacuated (5x). The reaction mixture was then stirred for another 7 h under an H₂

atmosphere (4 bar). The mixture was filtered through Celite and the solvent was removed *in vacuo*. The crude product was purified by flash silica gel chromatography (DCM/MeOH, 20:1), giving alcohol **4.17** (126 mg, 0.310 mmol, 91%) as a colorless oil.

TLC (hexanes/EtOAc, 4:1): R_f = 0.48. $[\alpha]_D^{22}$: -41.9 ($c = 0.15$, MeOH). **$^1\text{H NMR}$ (CD_3OD , 600 MHz, 27 °C):** $\delta = 7.03$ (dd, $J = 7.8, 7.8$ Hz, 1H, ArH), 6.93 (dd, $J = 7.8, 1.2$ Hz, 1H, ArH), 6.65 (dd, $J = 7.8, 1.2$ Hz, 1H, ArH), 3.81–3.74 (m, 1H, CH), 2.95–2.86 (m, 1H, CH), 2.59–2.51 (m, 3H, 3 x CH), 2.33–2.29 (m, 2H, 2 x CH), 2.15–2.04 (m, 2H, 2 x CH), 1.31 (s, 6H, 2 x CH_3), 1.13 (d, $J = 6.0$ Hz, 3H, CH_3), 1.05 (s, 9H, $\text{C}(\text{CH}_3)_3$), 1.04–1.02 (m, 1H, CH), 0.82 (s, 3H, CH_3), 0.23 (s, 3H, SiCH_3), 0.22 (s, 3H, SiCH_3) ppm. **$^{13}\text{C NMR}$ (CD_3OD , 100 MHz, 27 °C):** $\delta = 151.3, 145.3, 127.9, 126.0, 117.9, 115.2, 64.4, 63.7, 63.0, 44.4, 38.6, 37.5, 36.3, 24.9, 22.3, 22.2, 21.7, 19.4, 19.1, 17.8, -5.2, -5.3$ ppm. **IR (neat, ATR):** $\tilde{\nu} = 3410$ (m), 2960 (m), 2928 (s), 2857 (m), 1628 (s), 1580 (s), 1465 (vs), 1408 (m), 1390 (m), 1325 (m), 1270 (vs), 1251 (s), 1221 (w), 1190 (w), 1167 (w), 1084 (w), 1036 (w), 981 (m), 967 (m), 941 (w), 864 (m), 838 (s), 827 (s), 814 (m), 780 (m), 719 (w), 668 (w) cm^{-1} . **HRMS (ESI⁺):** m/z calcd. for $[\text{C}_{24}\text{H}_{42}\text{NO}_2\text{Si}]^+$: 404.2985, found: 404.2980 ($[\text{M}+\text{H}]^+$).

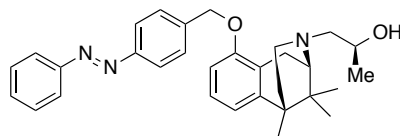
Synthesis of 1-(4-(bromomethyl)phenyl)-2-phenyldiazene (4.18)



To a solution of alcohol **4.20** (1.77 g, 8.30 mmol, 1.0 equiv.) in THF (50 mL) were added CBr_4 (3.18 g, 9.60 mmol, 1.15 equiv.) and PPh_3 (2.52 g, 9.60 mmol, 1.15 equiv.) at 0 °C. The reaction mixture was stirred for 16 h at room temperature and then concentrated *in vacuo*. The crude product was purified by flash silica gel chromatography (hexanes/DCM, gradient from 4:1 to 1:1), affording bromide **4.18** (1.95 g, 7.10 mmol, 86%) as orange crystals.

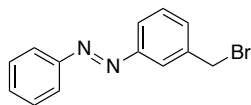
TLC (hexanes/EtOAc, 20:1): R_f = 0.51. **M.p.:** 118–119 °C. **$^1\text{H NMR}$ (CDCl_3 , 400 MHz, 27 °C):** $\delta = 7.95$ –7.87 (m, 4H, ArH), 7.56–7.45 (m, 5H, ArH), 4.55 (s, 2H, CH_2) ppm. **$^{13}\text{C NMR}$ (CDCl_3 , 100 MHz, 27 °C):** $\delta = 152.6, 152.3, 140.5, 131.2, 129.9, 129.1, 123.3, 123.0, 32.8$ ppm. **IR (neat, ATR):** $\tilde{\nu} = 1438$ (w), 1302 (w), 1221 (w), 1194 (w), 1150 (m), 1090 (w), 922 (w), 851 (m), 780 (m), 764 (s), 668 (m), 683 (s) cm^{-1} . **HRMS (ESI⁺):** m/z calcd. for $[\text{C}_{13}\text{H}_{12}\text{BrN}_2]^+$: 275.0184, found: 275.0179 ($[\text{M}+\text{H}]^+$).

Synthesis of (*S*)-1-((2*R*,6*S*)-6,11,11-trimethyl-10-((4-phenyldiazenyl)benzyl)oxy)-1,2,5,6-tetrahydro-2,6-methanobenzo[*d*]azocin-3(4*H*)-yl)propan-2-ol (4.19)



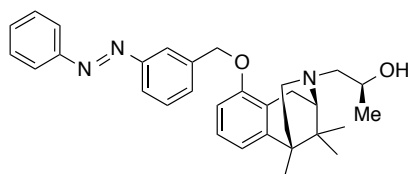
NaH (10 mg, 0.42 mmol, 3.5 equiv.) was suspended in DMF (3 mL) at 0 °C. To this, a solution of alcohol **4.17** (50 mg, 0.12 mmol, 1.0 equiv.) in THF (3 mL) was added and stirred at 0 °C for 1 h. Bu₄NI (4.4 mg, 0.012 mmol, 0.1 equiv.) and bromide **4.18** (66 mg, 0.24 mmol, 2.0 equiv.) were added. The reaction mixture was warmed to room temperature and stirred for 16 h. A sat. aqu. solution of NH₄Cl (10 mL) was added and the mixture was extracted with DCM (2 x 15 mL). The combined organic phases were washed with H₂O (3 x 20 mL), dried over MgSO₄ and the solvent was removed under reduced pressure. The crude product was purified by flash silica gel column chromatography (hexanes/CHCl₃, gradient from 4:1 to 1:1), followed by a second column chromatography (hexanes/EtOAc, 1% TEA, 10:1) to yield phenolic ether **4.19** (22 mg, 0.045 mmol, 38%) as a yellow oil.

TLC (hexanes/EtOAc, 2:1, 1% TEA): R_f = 0.37. [α]_D²²: −48.0 (*c* = 0.10, DCM). **¹H NMR (CDCl₃, 600 MHz, 27 °C):** δ = 7.97–7.94 (m, 2H, ArH), 7.94–7.91 (m, 2H, ArH), 7.61 (d, *J* = 8.6 Hz, 2H, ArH), 7.55–7.51 (m, 2H, ArH), 7.50–7.47 (m, 1H, ArH), 7.16 (dd, *J* = 7.8, 7.8 Hz, 1H, ArH), 6.97 (d, *J* = 7.8 Hz, 1H, ArH), 6.77 (d, *J* = 7.8 Hz, 1H, ArH), 5.18 (s, 2H, OCH₂), 3.88 (br s, 1H, OH), 3.78–3.74 (m, 1H, CH), 2.94 (d, *J* = 19.0 Hz, 1H, CH), 2.72 (dd, *J* = 19.0, 6.1 Hz, 1H, CH), 2.59–2.56 (m, 2H, 2 x CH), 2.46 (dd, *J* = 12.3, 2.9 Hz, 1H, CH), 2.18–2.04 (m, 3H, 3 x CH), 1.34–1.30 (s, 6H, 2 x CH₃), 1.15–1.10 (m, 4H, CH, CH₃), 0.85 (s, 3H, CH₃) ppm. **¹³C NMR (CDCl₃, 150 MHz, 27 °C):** δ = 154.1, 152.6, 152.2, 145.2, 140.5, 131.0, 129.1, 127.7, 126.5, 126.1, 123.0, 122.8, 117.9, 108.2, 69.3, 65.6, 63.9, 62.7, 43.6, 39.0, 37.5, 36.8, 23.6, 23.2, 21.7, 20.4, 19.9 ppm. **IR (neat, ATR):** $\tilde{\nu}$ = 3436 (w), 2966 (m), 2924 (m), 1579 (m), 1468 (m), 1454 (m), 1412 (m), 1374 (m), 1329 (m), 1261 (s), 1248 (s), 1221 (m), 1208 (m), 1190 (m), 1167 (m), 1134 (w), 1102 (m), 1055 (s), 1020 (m), 970 (w), 918 (w), 830 (m), 778 (m), 766 (s), 735 (s), 719 (s), 687 (vs) cm^{−1}. **HRMS (ESI⁺):** *m/z* calcd. for [C₃₁H₃₈N₃O₂]⁺: 484.2964, found: 484.2958 ([M+H]⁺).

Synthesis of 1-(3-(bromomethyl)phenyl)-2-phenyldiazene (4.21)

To a solution of alcohol **4.10** (5.00 g, 23.6 mmol, 1.0 equiv.) in THF (150 mL) were added CBr_4 (9.02 g, 27.2 mmol, 1.15 equiv.) and PPh_3 (7.13 g, 27.2 mmol, 1.15 equiv.) at 0 °C. The reaction mixture was warmed to room temperature and stirred for 16 h. The solvent was removed *in vacuo* and the crude product was purified by flash silica gel chromatography (hexanes/DCM, 5:1 \rightarrow 3:1), yielding bromide **4.21** (6.06 g, 22.0 mmol, 93%) as an orange solid.

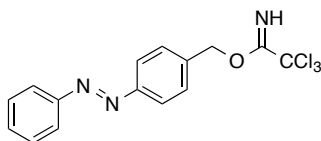
TLC (hexanes/EtOAc, 10:1): R_f = 0.70. **M.p.:** 43–44 °C. **^1H NMR (CDCl_3 , 600 MHz, 27 °C):** δ = 7.97–7.93 (m, 3H, ArH), 7.90–7.86 (m, 1H, ArH), 7.56–7.48 (m, 1H, ArH), 4.59 (s, 2H, CH_2) ppm. **^{13}C NMR (CDCl_3 , 150 MHz, 27 °C):** δ = 152.8, 152.5, 138.9, 131.4, 131.3, 129.6, 129.1, 123.4, 123.0, 122.9, 32.8 ppm. **IR (neat, ATR):** $\tilde{\nu}$ = 1585 (w), 1481 (w), 1444 (m), 1293 (w), 1249 (w), 1212 (m), 1149 (m), 1070 (m), 1020 (w), 999 (w), 922 (m), 903 (m), 796 (m), 762 (s), 688 (vs) cm^{-1} . **HRMS (EI^+):** m/z calcd. for $[\text{C}_{13}\text{H}_{12}\text{BrN}_2]^+$: 274.0105, found: 274.0096 ($[\text{M}]^+$).

Synthesis of (S)-1-((2R,6S)-6,11,11-trimethyl-10-((3-phenyldiazenyl)benzyl)oxy)-1,2,5,6-tetrahydro-2,6-methanobenzo[d]azocin-3(4H)-yl)propan-2-ol (4.22)

NaH (8.5 mg, 0.35 mmol, 3.5 equiv.) was suspended in DMF (2.5 mL) at 0 °C. To this, a solution of alcohol **4.17** (40 mg, 0.099 mmol, 1.0 equiv.) in THF (2.5 mL) was added and stirred at 0 °C for 1 h. Bu_4NI (4.0 mg, 0.010 mmol, 0.1 equiv.) and bromide **4.21** (55 mg, 0.20 mmol, 2.0 equiv.) were added. The reaction mixture was warmed to room temperature and stirred for 16 h. A sat. aqu. solution of NH_4Cl (10 mL) was added and the mixture was extracted with DCM (2 x 15 mL). The combined organic phases were washed with H_2O (3 x 20 mL), dried over MgSO_4 and the solvent was removed under reduced pressure. The crude product was purified by flash silica gel column chromatography (hexanes/EtOAc, 1% TEA, gradient from 10:1 to 1:1), followed by a second column chromatography (hexanes/EtOAc, 1% TEA, gradient from 20:1 to 5:1), affording phenolic ether **4.22** (20 mg, 0.041 mmol, 41%) as a yellow oil.

TLC (hexanes/EtOAc, 2:1, 1% TEA): $R_f = 0.62$. $[\alpha]_D^{22}$: -56.0 ($c = 0.10$, DCM). **$^1\text{H NMR}$ (CDCl_3 , 600 MHz, 27 °C):** $\delta = 8.02$ (s, 1H, ArH), 7.94–7.88 (m, 3H, ArH), 7.59–7.48 (m, 5H, ArH), 7.16 (dd, $J = 8.0, 8.0$ Hz, 1H, ArH), 6.96 (d, $J = 8.0$ Hz, 1H, ArH), 6.78 (d, $J = 8.0$ Hz, 1H, ArH), 5.20 (s, 2H, OCH_2), 3.93 (br s, 1H, OH), 3.78–3.73 (m, 1H, CH), 2.95 (d, $J = 19.0$ Hz, 1H, CH), 2.72 (dd, $J = 19.0, 6.1$ Hz, 1H, CH), 2.61–2.53 (m, 2H, 2 x CH), 2.47 (dd, $J = 12.3, 2.9$ Hz, 1H, CH), 2.20–2.02 (m, 3H, 3 x CH), 1.35–1.31 (m, 6H, 2 x CH_3), 1.15–1.06 (m, 4H, CH, CH_3), 0.84 (s, 3H, CH_3) ppm. **$^{13}\text{C NMR}$ (CDCl_3 , 150 MHz, 27 °C):** $\delta = 154.2, 152.8, 152.6, 145.2, 138.7, 131.2, 129.5, 129.3, 129.1, 126.5, 126.1, 122.8, 122.6, 121.2, 117.9, 108.2, 69.4, 65.6, 63.9, 62.7, 43.6, 39.0, 37.5, 36.8, 23.6, 23.2, 21.7, 20.4, 19.9$ ppm. **IR (neat, ATR):** $\tilde{\nu} = 3431$ (w), 2966 (m), 2924 (m), 2822 (w), 1580 (m), 1468 (m), 1455 (s), 1410 (m), 1374 (m), 1329 (m), 1282 (m), 1262 (s), 1209 (m), 1190 (w), 1167 (m), 1150 (w), 1134 (w), 1076 (m), 1055 (s), 1022 (m), 971 (w), 923 (w), 886 (w), 843 (w), 784 (m), 766 (m), 720 (m), 693 (vs) cm^{-1} . **HRMS (ESI⁺):** m/z calcd. for $[\text{C}_{31}\text{H}_{38}\text{N}_3\text{O}_2]^+$: 484.2964, found: 484.2958 ($[\text{M}+\text{H}]^+$).

Synthesis of 4-(phenyldiazenyl)benzyl 2,2,2-trichloroacetimidate (4.23)

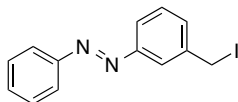


NaH (12.5 mg, 0.520 mmol, 1.1 equiv.) was suspended in THF (10 mL) and cooled to 0 °C. Alcohol **4.20** (100 mg, 0.470 mmol, 1.0 equiv.) was added and the mixture was stirred for 30 min at 0 °C. Trichloroacetonitrile (0.23 mL, 2.4 mmol, 5.0 equiv.) was added and the mixture was warmed to room temperature and stirred for 1 h. A sat. aqu. solution of NH_4Cl (50 mL) was added and the aqueous phase extracted with DCM (3 x 20 mL). The combined organic layers were washed with brine (50 mL), dried over MgSO_4 and concentrated *in vacuo*. The crude product was purified by flash silica gel chromatography (hexanes/DCM, 5:1 → 3:1), affording trichloroacetimidate **4.23** (89 mg, 0.25 mmol, 53%) as orange crystals.

TLC (hexanes/DCM, 2:1): $R_f = 0.29$. **M.p.:** 124–125 °C. **$^1\text{H NMR}$ (CDCl_3 , 600 MHz, 27 °C):** $\delta = 8.44$ (s, 1H, NH), 7.95–7.89 (m, 4H, ArH), 7.60–7.56 (m, 2H, ArH), 7.54–7.43 (m, 2H, ArH), 7.49–7.45 (m, 1H, ArH), 5.42 (s, 2H, CH_2) ppm. **$^{13}\text{C NMR}$ (CDCl_3 , 150 MHz, 27 °C):** $\delta = 162.4, 152.6, 152.4, 138.3, 131.1, 129.1, 128.3, 123.0, 122.9, 91.2, 70.1$ ppm. **IR (neat, ATR):** $\tilde{\nu} = 3340$ (m), 1664 (s), 1489 (w), 1467 (w), 1445 (m), 1409 (m), 1370 (m), 1302 (m), 1290 (m), 1154 (w), 1066 (vs), 1002 (m), 988 (m), 909 (w), 854 (m), 838 (m), 825 (m),

797 (s), 788 (s), 773 (m), 732 (w), 685 (m) cm^{-1} . **HRMS (EI⁺):** m/z calcd. for $[\text{C}_{15}\text{H}_{12}\text{Cl}_3\text{N}_3\text{O}]^+$: 355.0046, found: 355.0048 ($[\text{M}]^+$).

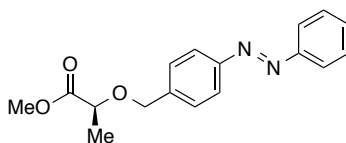
Synthesis of 1-(3-(iodomethyl)phenyl)-2-phenyldiazene (4.24)



PPh_3 (147 mg, 0.560 mmol, 1.2 equiv.) and imidazole (48 mg, 0.71 mmol, 1.5 equiv.) were dissolved in THF (10 mL) and alcohol **4.10** (100 mg, 0.470 mmol, 1.0 equiv.) was added, followed by iodine (142 mg, 0.560 mmol, 1.2 equiv.). The mixture was stirred at room temperature for 1 h. H_2O (100 mL) was added and the aqueous phase extracted with DCM (3 x 20 mL). The combined organic layers were washed with brine (50 mL), dried over MgSO_4 and concentrated *in vacuo*. The crude product was purified by *quick flash silica gel chromatography* (hexanes/DCM, 5:1 \rightarrow 3:1), affording iodide **4.24** (107 mg, 0.330 mmol, 70%) as orange crystals.

TLC (hexanes/DCM, 5:1): $R_f = 0.35$. **M.p.:** 121 $^\circ\text{C}$ (dec.). **$^1\text{H NMR}$ (CDCl_3 , 400 MHz, 27 $^\circ\text{C}$):** $\delta = 7.93\text{--}7.89$ (m, 2H, ArH), 7.87–7.82 (m, 2H, ArH), 7.55–7.47 (m, 5H, ArH), 4.53 (s, 2H, CH_2) ppm. **$^{13}\text{C NMR}$ (CDCl_3 , 100 MHz, 27 $^\circ\text{C}$):** $\delta = 152.6, 151.9, 142.3, 131.1, 129.5, 129.1, 123.3, 122.9, 4.7$ ppm. **IR (neat, ATR):** $\tilde{\nu} = 1596$ (w), 1580 (w), 1498 (w), 1484 (w), 1465 (w), 1441 (w), 1407 (w), 1302 (m), 1222 (w), 1213 (m), 1146 (s), 1116 (m), 1072 (m), 1018 (m), 1008 (w), 922 (w), 850 (s), 822 (m), 779 (m), 764 (s), 730 (m), 682 (vs) cm^{-1} . **HRMS (EI⁺):** m/z calcd. for $[\text{C}_{13}\text{H}_{10}\text{IN}_2]^+$: 320.9889, found: 320.9887 ($[\text{M-H}]^+$).

Synthesis of (S)-methyl 2-((4-(phenyldiazenyl)benzyl)oxy)propanoate (4.28)

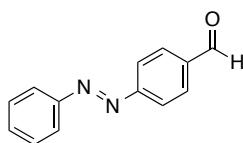


Freshly prepared Ag_2O (840 mg, 3.63 mmol, 2.0 equiv.) was added to a solution of (–)-methyl L-lactate (0.17 mL, 1.8 mmol, 1.0 equiv.) and bromide **4.18** (1.00 g, 3.63 mmol, 2.0 equiv.) in Et_2O (30 mL). The reaction mixture was heated to reflux for 24 h and then filtered through Celite and thoroughly washed with DCM. The solvent was removed under reduced pressure and

the crude product was purified by flash silica gel column chromatography (hexanes/EtOAc, gradient from 50:1 to 10:1), affording ether **4.28** (149 mg, 0.500 mmol, 27%) as a red oil.

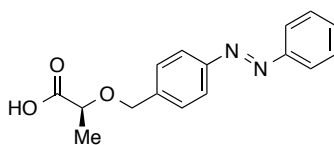
TLC (hexanes/EtOAc, 10:1): $R_f = 0.25$. $[\alpha]_D^{22}$: -78.0 ($c = 0.20$, CHCl_3). **$^1\text{H NMR}$ (CDCl_3 , 400 MHz, 27 °C):** $\delta = 7.94\text{--}7.88$ (m, 4H, ArH), 7.54–7.46 (m, 5H, ArH), 4.77 (d, $J = 12.2$ Hz, 1H, CH), 4.54 (d, $J = 12.2$ Hz, 1H, CH), 4.11 (q, $J = 6.8$ Hz, 1H, CH), 3.77 (s, 3H, OCH_3), 1.48 (d, $J = 6.8$ Hz, 3H, CH_3) ppm. **$^{13}\text{C NMR}$ (CDCl_3 , 100 MHz, 27 °C):** $\delta = 173.5, 152.6, 152.2, 140.6, 131.0, 129.1, 128.4, 122.9, 122.8, 74.2, 71.5, 52.0, 18.7$ ppm. **IR (neat, ATR):** $\tilde{\nu} = 2989$ (w), 2952 (w), 2872 (w), 1748 (vs), 1606 (w), 1485 (w), 1446 (m), 1415 (w), 1392 (w), 1372 (w), 1300 (w), 1274 (w), 1207 (m), 1142 (vs), 1121 (s), 1070 (m), 1014 (m), 975 (w), 924 (w), 831 (m), 767 (m), 688 (m) cm^{-1} . **HRMS (ESI⁺):** m/z calcd. for $[\text{C}_{17}\text{H}_{19}\text{N}_2\text{O}_3]^+$: 299.1396, found: 299.1391 ($[\text{M}+\text{H}]^+$).

Bromide **4.18** was recovered in 48% yield (475 mg, 1.74 mmol) and aldehyde **4.35** was obtained as a side product (63 mg, 0.30 mmol, 16%).



TLC (hexanes/EtOAc, 10:1): $R_f = 0.29$. **M.p.:** 106–108 °C. **$^1\text{H NMR}$ (CDCl_3 , 400 MHz, 27 °C):** $\delta = 10.11$ (s, 1H, CHO), 8.04 (s, 4H, ArH), 7.98–7.95 (m, 2H, ArH), 7.57–7.52 (m, 3H, ArH) ppm. **$^{13}\text{C NMR}$ (CDCl_3 , 100 MHz, 27 °C):** $\delta = 191.6, 155.9, 152.5, 137.4, 132.0, 130.7, 129.2, 123.3, 123.2$ ppm. **IR (neat, ATR):** $\tilde{\nu} = 1699$ (vs), 1598 (m), 1486 (w), 1465 (w), 1442 (w), 1379 (w), 1305 (m), 1263 (w), 1197 (s), 1149 (m), 1071 (m), 1000 (w), 920 (w), 841 (m), 794 (m), 766 (m), 732 (w), 715 (w), 682 (m) cm^{-1} . **HRMS (EI⁺):** m/z calcd. for $[\text{C}_{13}\text{H}_{10}\text{N}_2\text{O}]^+$: 210.1793, found: 210.1791 ($[\text{M}]^+$).

Synthesis of (S)-2-((4-(phenyldiazenyl)benzyl)oxy)propanoic acid (4.26)

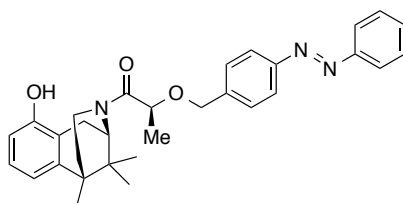


Methyl ester **4.28** (7.0 mg, 0.023 mmol, 1.0 equiv.) was dissolved in THF (0.5 mL) and a 1 M solution of LiOH in H_2O (0.07 mL, 0.07 mmol, 3.0 equiv.) was added. The reaction mixture

was stirred for 16 h at room temperature. The mixture was diluted with H₂O (10 mL) and washed with EtOAc (15 mL). The aqueous phase was then acidified to pH = 2–3 with 1 M HCl and extracted with EtOAc (3 x 10 mL). The combined organic layers were dried over MgSO₄ and concentrated *in vacuo*. Pure carboxylic acid **4.26** was obtained in 91% yield (6.0 mg, 0.021 mmol) as an orange solid.

$[\alpha]_D^{22}$: -85.0 ($c = 0.20$, CHCl₃). ¹H NMR (CDCl₃, 400 MHz, 27 °C): $\delta = 7.97$ – 7.89 (m, 4H, ArH), 7.55–7.46 (m, 5H, ArH), 4.79 (d, $J = 12.0$ Hz, 1H, CH), 4.63 (d, $J = 12.0$ Hz, 1H, CH), 4.16 (q, $J = 6.9$ Hz, 1H, CH), 1.54 (d, $J = 6.9$ Hz, 3H, CH₃) ppm. ¹³C NMR (CDCl₃, 100 MHz, 27 °C): $\delta = 176.3$, 152.6, 152.4, 139.9, 131.1, 129.1, 128.5, 123.0, 122.9, 73.8, 71.6, 18.2 ppm. IR (neat, ATR): $\tilde{\nu} = 2992$ (m), 1731 (s), 1710 (vs), 1457 (w), 1446 (w), 1415 (w), 1333 (w), 1304 (w), 1283 (w), 1219 (m), 1141 (vs), 1118 (m), 1066 (m), 1022 (m), 919 (w), 856 (w), 836 (m), 768 (m), 726 (w), 686 (m), 666 (w) cm⁻¹. HRMS (EI⁺): m/z calcd. for [C₁₆H₁₆N₂O₃]⁺: 284.1161, found: 284.1157 ([M]⁺).

Synthesis of (S)-1-((2R,6S)-10-hydroxy-6,11,11-trimethyl-1,2,5,6-tetrahydro-2,6-methanobenzo[d]azocin-3(4H)-yl)-2-((4-phenyldiazenyl)benzyl)oxy)-propan-1-one (4.27)^[ff]



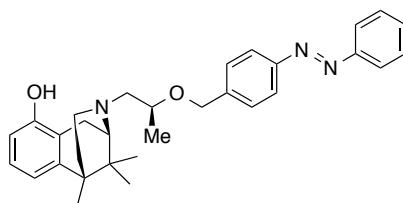
Carboxylic acid **4.26** (75 mg, 0.26 mmol, 1.0 equiv.) was dissolved in DCM (7.5 mL) and oxalyl chloride (0.65 mL, 2 M in DCM, 1.3 mmol, 5.0 equiv.) and DMF (5 drops) were added. The mixture was stirred at room temperature for 1 h and then concentrated *in vacuo*. Residual solvent was coevaporated with toluene (2 x 5 mL) and the residue was dissolved in DCM (7.5 mL) and cooled to 0 °C. This solution was added to a solution of the HBr salt of amine **4.25** (162 mg, 0.520 mmol, 2.0 equiv.) and DIPEA (0.22 mL, 1.3 mmol, 5.0 equiv.) in DCM (7.5 mL) at 0 °C. The reaction mixture was warmed to room temperature and stirred for 2 h. A sat. aq. solution of NH₄Cl (30 mL) was added and the aqueous layer was extracted with EtOAc

^[ff] Compound **4.27** was obtained as an approx. 2:1 mixture of two isomers, probably due to the sterically biased amide bond, as temperature-dependent NMR experiments and the literature (see Grauert *et al.*^[23]) suggested. Thus, two sets of signals were observed in the NMR spectra of **4.27**. Whereas the signals of the major isomer could be clearly assigned in the ¹H NMR spectrum, the ¹³C NMR could not be interpreted. Therefore, all peaks of both isomers are provided.

(3 x 15 mL). The combined organic phases were washed with NH₄Cl (3 x 30 mL) and brine (30 mL), dried over MgSO₄ and the solvent was removed under reduced pressure. The crude product was purified by flash silica gel column chromatography (hexanes/EtOAc, 2:1 → 3:2) to give amide **4.27** (80 mg, 0.16 mmol, 62%) as a mixture of *trans/cis* isomers as a red oil.

TLC (hexanes/EtOAc, 1:1): $R_f = 0.50$. $[\alpha]_D^{22}$: -102.0 ($c = 0.10$, DCM). **¹H NMR (CDCl₃, 600 MHz, 27 °C; major isomer):** $\delta = 7.93\text{--}7.88$ (m, 3H, ArH), 7.87–7.84 (m, 2H, ArH), 7.51–7.49 (m, 3H, ArH), 7.46–7.44 (m, 3H, ArH), 7.08–7.06 (m, 1H, ArH), 6.90–6.88 (m, 1H, ArH), 6.66 (dd, $J = 7.9, 0.9$ Hz, 1H, ArH), 5.51 (br s, 1H, OH), 4.76 (d, $J = 6.7$ Hz, 1H, CH), 4.62 (d, $J = 12.2$ Hz, 1H, CH), 4.54–4.51 (m, 1H, CH), 4.39–4.36 (m, 1H, CH), 3.87 (dd, $J = 14.0, 5.1$ Hz, 1H, CH), 3.06 (dd, $J = 18.7, 6.8$ Hz, 1H, CH), 2.84 (dd, $J = 13.6, 3.8$ Hz, 1H, CH), 2.57–2.54 (m, 1H, CH), 2.02–1.98 (m, 1H, CH), 1.63 (s, 3H, CH₃), 1.44 (d, $J = 6.8$ Hz, 3H, CH₃), 1.11 (s, 3H, CH₃), 1.09–1.06 (m, 1H, CH), 0.87–0.86 (m, 3H, CH₃) ppm. **¹³C NMR (CDCl₃, 150 MHz, 27 °C):** $\delta = 171.3, 170.6, 152.6, 152.2, 152.0, 151.9, 144.1, 143.9, 140.8, 140.7, 131.0, 131.0, 129.1, 129.1, 128.7, 128.5, 128.4, 128.2, 127.1, 127.1, 122.9, 122.9, 122.8, 122.1, 121.9, 120.7, 120.4, 117.6, 117.5, 112.4, 112.3, 75.4, 73.6, 70.7, 70.1, 56.7, 52.5, 40.8, 39.2, 38.9, 38.8, 36.7, 36.2, 36.0, 35.9, 35.7, 28.5, 28.4, 27.3, 23.8, 22.7, 22.5, 22.3, 21.7, 20.8, 20.4, 20.1, 17.9, 17.8, 17.5, 17.3, 14.6, 7.9$ ppm. **IR (neat, ATR):** $\tilde{\nu} = 3261$ (m), 2978 (m), 2928 (m), 1622 (vs), 1584 (s), 1466 (s), 1392 (m), 1374 (m), 1342 (m), 1282 (m), 1257 (m), 1230 (m), 1206 (w), 1154 (m), 1109 (m), 1071 (m), 1014 (w), 982 (w), 970 (w), 947 (w), 922 (w), 833 (m), 787 (m), 766 (m), 735 (m), 689 (m), 668 (w) cm⁻¹. **HRMS (ESI⁺):** m/z calcd. for [C₃₁H₃₆N₃O₃]⁺: 498.2757, found: 498.2750 ([M+H]⁺).

Synthesis of (2*R*,6*S*)-6,11,11-trimethyl-3-((*S*)-2-((4-(phenyldiazenyl)benzyl)oxy)-propyl)-1,2,3,4,5,6-hexahydro-2,6-methanobenzo[*d*]azocin-10-ol (*p*-ACRO)

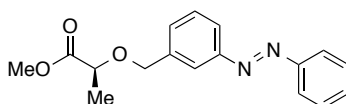


Amide **4.27** (80 mg, 0.16 mmol, 1.0 equiv.) was dissolved in THF (6 mL) and LiAlH₄ (12.1 mg, 0.320 mmol, 2.0 equiv.) was added. The reaction mixture was stirred at room temperature for 1 h. A sat. aqu. solution of Rochelle's salt was added (5 mL) and vigorously stirred for 30 min. The phases were separated and the aqueous layer was extracted with EtOAc (3 x 10 mL). The combined organic phases were washed with brine (20 mL), dried over MgSO₄ and the solvent

was removed under reduced pressure. The crude product was purified by flash silica gel column chromatography (hexanes/EtOAc, 3:1 → 2:1), yielding amine *p*-ACRO (60 mg, 0.12 mmol, 75%) as a red oil.

TLC (hexanes/EtOAc, 1:1): $R_f = 0.76$. $[\alpha]_D^{22}$: -48.0 ($c = 0.10$, DCM). $^1\text{H NMR}$ (CDCl_3 , **600 MHz**, **27 °C**): $\delta = 7.92\text{--}7.88$ (m, 4H, ArH), $7.53\text{--}7.48$ (m, 4H, ArH), $7.48\text{--}7.43$ (m, 1H, ArH), 7.04 (dd, $J = 7.9$, 7.9 Hz, 1H, ArH), 6.89 (d, $J = 7.2$ Hz, 1H, ArH), 6.62 (dd, $J = 7.9$, 1.0 Hz, 1H, ArH), 4.72 (s, 2H, OCH_2), 4.63 (br s, 1H, OH), $3.68\text{--}3.65$ (m, 1H, CH), 2.86 (d, $J = 18.0$ Hz, 1H, CH), 2.71 (dd, $J = 13.3$, 6.6 Hz, 1H, CH), 2.65 (d, $J = 6.0$ Hz, 1H, CH), $2.53\text{--}2.46$ (m, 2H, 2 x CH), 2.35 (dd, $J = 13.3$, 4.8 Hz, 1H, CH), $2.14\text{--}2.07$ (m, 2H, 2 x CH), $1.32\text{--}1.29$ (m, 6H, 2 x CH_3), 1.23 (d, $J = 6.2$ Hz, 3H, CH_3), $1.07\text{--}1.01$ (m, 1H, CH), 0.81 (s, 3H, CH_3) ppm. $^{13}\text{C NMR}$ (CDCl_3 , **150 MHz**, **27 °C**): $\delta = 152.7$, 152.0 , 151.2 , 145.9 , 142.6 , 130.8 , 129.0 , 127.9 , 126.5 , 123.4 , 122.8 , 122.8 , 117.7 , 111.6 , 73.6 , 70.5 , 62.7 , 61.6 , 46.1 , 38.9 , 37.8 , 36.6 , 23.6 , 23.2 , 20.4 , 19.4 , 18.8 ppm. **IR (neat, ATR):** $\tilde{\nu} = 3345$ (m), 2966 (m), 2924 (s), 2814 (m), 1605 (w), 1584 (m), 1485 (w), 1465 (vs), 1415 (w), 1388 (m), 1372 (m), 1338 (m), 1277 (s), 1256 (m), 1220 (m), 1201 (m), 1165 (m), 1153 (m), 1131 (m), 1098 (s), 1072 (vs), 1034 (m), 1014 (m), 972 (w), 944 (w), 921 (w), 909 (m), 829 (m), 786 (m), 766 (m), 731 (m), 720 (m), 688 (m), 668 (w) cm^{-1} . **HRMS (ESI⁺):** m/z calcd. for $[\text{C}_{31}\text{H}_{38}\text{N}_3\text{O}_2]^+$: 484.2964 , found: 484.2959 ($[\text{M}+\text{H}]^+$). **UV/Vis:** $\lambda_{\text{max}} = 328, 435$ nm.

Synthesis of (*S*)-methyl 2-((3-(phenyldiazenyl)benzyl)oxy)propanoate (**4.29**)

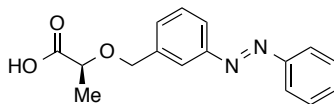


Freshly prepared Ag_2O (0.84 g, 3.6 mmol, 1.0 equiv.) was added to a solution of (–)-methyl L-lactate (0.69 mL, 7.3 mmol, 2.0 equiv.) and bromide **4.21** (1.00 g, 3.63 mmol, 1.0 equiv.) in THF (30 mL). The reaction mixture was heated to 50 °C for 16 h and then filtered through Celite and thoroughly washed with DCM. The solvent was removed under reduced pressure and the crude product was purified by flash silica gel column chromatography (hexanes/EtOAc, gradient from 50:1 to 10:1), affording ether **4.29** (433 mg, 1.45 mmol, 40%) as a red oil.

TLC (hexanes/EtOAc, 10:1): $R_f = 0.26$. $[\alpha]_D^{22}$: -79.0 ($c = 0.20$, CHCl_3). $^1\text{H NMR}$ (CDCl_3 , **300 MHz**, **27 °C**): $\delta = 7.97\text{--}7.83$ (m, 4H, ArH), $7.58\text{--}7.48$ (m, 5H, ArH), 4.83 (d, $J = 12.2$ Hz, 1H, CH), 4.58 (d, $J = 12.2$ Hz, 1H, CH), 4.15 (q, $J = 6.8$ Hz, 1H, CH), 3.80 (s, 3H, OCH_3), 1.50 (d, $J = 6.8$ Hz, 3H, CH_3) ppm. $^{13}\text{C NMR}$ (CDCl_3 , **75 MHz**, **27 °C**): $\delta = 173.6$, 152.8 , 152.6 , 138.8 , 131.0 , 130.3 , 129.2 , 129.1 , 122.9 , 122.5 , 122.0 , 74.3 , 71.6 , 52.0 , 18.7 ppm. **IR (neat,**

ATR): $\tilde{\nu}$ = 1747 (s), 1586 (w), 1447 (m), 1395 (w), 1371 (w), 1272 (m), 1205 (m), 1140 (s), 1118 (s), 1067 (m), 1021 (m), 975 (w), 923 (w), 890 (w), 834 (w), 795 (m), 764 (m), 692 (vs) cm^{-1} . **HRMS (EI⁺):** m/z calcd. for $[\text{C}_{17}\text{H}_{18}\text{N}_2\text{O}_3]^+$: 298.1317, found: 298.1311 ($[\text{M}]^+$).

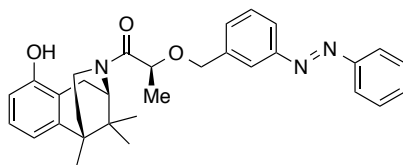
Synthesis of (*S*)-2-((3-(phenyldiazenyl)benzyl)oxy)propanoic acid (**4.30**)



Methyl ester **4.29** (380 mg, 1.27 mmol, 1.0 equiv.) was dissolved in THF (25 mL) and a 1 M solution of LiOH in H₂O (3.81 mL, 3.81 mmol, 3.0 equiv.) was added. The reaction mixture was stirred for 20 h at room temperature. The mixture was diluted with H₂O (10 mL) and washed with EtOAc (15 mL). The aqueous phase was then acidified to pH = 2–3 with 1 M HCl and extracted with EtOAc (3 x 10 mL). The combined organic layers were dried over MgSO₄ and concentrated *in vacuo*. Pure carboxylic acid **4.30** was obtained in 100% yield (361 mg, 1.27 mmol) as a red oil.

$[\alpha]_D^{22}$: -58.0 ($c = 0.20$, CHCl₃). **¹H NMR (CDCl₃, 400 MHz, 27 °C):** δ = 10.10 (br s, 1H, CO₂H), 7.96–7.84 (m, 4H, ArH), 7.56–7.44 (m, 5H, ArH), 4.83 (d, $J = 11.7$ Hz, 1H, CH), 4.63 (d, $J = 11.7$ Hz, 1H, CH), 4.18 (q, $J = 6.9$ Hz, 1H, CH), 1.55 (d, $J = 6.9$ Hz, 3H, CH₃) ppm. **¹³C NMR (CDCl₃, 100 MHz, 27 °C):** δ = 178.0, 152.8, 152.6, 138.3, 131.1, 130.3, 129.3, 129.1, 122.9, 122.7, 122.0, 73.8, 71.7, 18.4 ppm. **IR (neat, ATR):** $\tilde{\nu}$ = 3060 (w), 2987 (w), 2878 (w), 1717 (s), 1462 (w), 1447 (m), 1372 (w), 1327 (w), 1306 (w), 1234 (m), 1197 (w), 1114 (s), 1064 (m), 1020 (m), 909 (m), 795 (m), 764 (m), 731 (m), 691 (vs) cm^{-1} . **HRMS (EI⁺):** m/z calcd. for $[\text{C}_{16}\text{H}_{16}\text{N}_2\text{O}_3]^+$: 284.1161, found: 284.1156 ($[\text{M}]^+$).

Synthesis of (*S*)-1-((2*R*,6*S*)-10-hydroxy-6,11,11-trimethyl-1,2,5,6-tetrahydro-2,6-methano-benzo[*d*]azocin-3(*4H*)-yl)-2-((3-(phenyldiazenyl)benzyl)oxy)propan-1-one (4.31)^[§§]



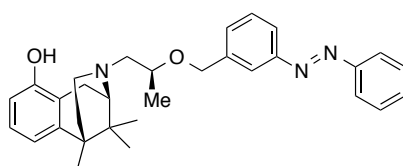
Carboxylic acid **4.30** (100 mg, 0.350 mmol, 1.0 equiv.) was dissolved in DCM (10 mL) and oxalyl chloride (0.88 mL, 2 M in DCM, 1.8 mmol, 5.0 equiv.) and DMF (5 drops) were added. The mixture was stirred at room temperature for 1 h and then concentrated *in vacuo*. The crude residue was coevaporated with toluene (2 x 5 mL), dissolved in DCM (10 mL) and cooled to 0 °C. This solution was added to a solution of the HBr salt of amine **4.25** (219 mg, 0.700 mmol, 2.0 equiv.) and DIPEA (0.30 mL, 1.8 mmol, 5.0 equiv.) in DCM (10 mL) at 0 °C. The reaction mixture was warmed to room temperature and stirred for 2 h. A sat. aqu. solution of NH₄Cl (30 mL) was added and the aqueous layer was extracted with EtOAc (3 x 15 mL). The combined organic phases were washed with NH₄Cl (3 x 30 mL) and brine (30 mL), dried over MgSO₄ and the solvent was removed under reduced pressure. The crude product was purified by flash silica gel column chromatography (hexanes/EtOAc, 2:1 → 3:2) to give amide **4.31** (149 mg, 0.300 mmol, 86%) as a mixture of *trans/cis* isomers as a red oil.

TLC (hexanes/EtOAc, 1:1): $R_f = 0.40$. $[\alpha]_D^{22}$: -90.0 ($c = 0.10$, DCM). **¹H NMR (CDCl₃, 400 MHz, 27 °C; major isomer):** $\delta = 7.93\text{--}7.86$ (m, 4H, ArH), $7.53\text{--}7.46$ (m, 5H, ArH), $7.06\text{--}7.02$ (m, 1H, ArH), $6.90\text{--}6.86$ (m, 1H, ArH), 6.64 (dd, $J = 7.9, 1.0$ Hz, 1H, ArH), 5.63 (s, 1H, OH), 4.78 (d, $J = 6.6$ Hz, 1H, CH), 4.66 (d, $J = 12.2$ Hz, 1H, CH), 4.57 (d, $J = 12.2$ Hz, 1H, CH), $4.41\text{--}4.37$ (m, 1H, CH), 3.85 (dd, $J = 14.4, 5.6$ Hz, 1H, CH), 3.08 (dd, $J = 18.7, 6.7$ Hz, 1H, CH), 2.85 (td, $J = 14.0, 3.6$ Hz, 1H, CH), 2.57 (d, $J = 18.6$ Hz, 1H, CH), $2.05\text{--}1.97$ (m, 1H, CH), 1.66 (s, 1H, CH), 1.45 (d, $J = 6.8$ Hz, 3H, CH₃), 1.13 (s, 3H, CH₃), 0.87 (s, 3H, CH₃) ppm. **¹³C NMR (CDCl₃, 100 MHz, 27 °C):** $\delta = 171.2, 170.6, 152.8, 152.7, 152.6, 152.5, 152.1, 152.0, 144.1, 143.9, 138.9, 138.9, 131.1, 130.4, 129.2, 129.1, 128.8, 128.7, 127.1, 127.0, 122.9, 122.9, 122.6, 122.5, 122.2, 122.1, 122.0, 121.8, 121.8, 120.5, 117.5, 117.5, 112.4, 112.3, 77.2,$

^[§§] Compound **4.31** was obtained as an approx. 2:1 mixture of two isomers, probably due to the sterically biased amide bond, as temperature-dependent NMR experiments and the literature (see Grauert *et al.*^[23]) suggested. Thus, two sets of signals were observed in the NMR spectra of **4.31**. Whereas the signals of the major isomer could be clearly assigned in the ¹H NMR spectrum, the ¹³C NMR could not be interpreted. Therefore, all peaks of both isomers are provided.

75.0, 73.5, 70.7, 70.1, 56.8, 52.5, 39.2, 38.9, 38.8, 36.7, 36.2, 36.0, 35.9, 35.7, 28.5, 27.4, 22.7, 22.5, 22.3, 21.8, 20.4, 20.1, 17.7 ppm. **IR (neat, ATR):** $\tilde{\nu}$ = 3235 (w), 2979 (w), 2935 (w), 1619 (s), 1583 (s), 1466 (s), 1392 (w), 1374 (m), 1342 (m), 1281 (m), 1256 (m), 1230 (m), 1205 (m), 1149 (m), 1105 (m), 1071 (m), 1023 (m), 981 (w), 969 (w), 946 (w), 909 (m), 835 (w), 787 (m), 764 (m), 730 (vs), 693 (vs) cm^{-1} . **HRMS (ESI⁺):** m/z calcd. for $[\text{C}_{31}\text{H}_{36}\text{N}_3\text{O}_3]^+$: 498.2757, found: 498.2749 ($[\text{M}+\text{H}]^+$).

Synthesis of (2*R*,6*S*)-6,11,11-trimethyl-3-((*S*)-2-((3-phenyldiazenyl)benzyl)oxy)-propyl)-1,2,3,4,5,6-hexahydro-2,6-methanobenzo[*d*]azocin-10-ol (*m*-ACRO)



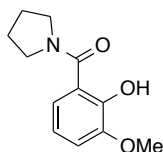
Amide **4.31** (137 mg, 0.280 mmol, 1.0 equiv.) was dissolved in THF (10 mL) and LiAlH_4 (21 mg, 0.56 mmol, 2.0 equiv.) was added. The reaction mixture was stirred at room temperature for 1 h. The mixture was quenched with H_2O and a sat. aqu. solution of Rochelle's salt was added (10 mL) and vigorously stirred for 30 min. The phases were separated and the aqueous layer was extracted with EtOAc (3 x 10 mL). The combined organic phases were washed with brine (20 mL), dried over MgSO_4 and the solvent was removed under reduced pressure. The crude product was purified by flash silica gel column chromatography (hexanes/EtOAc, 3:1 \rightarrow 2:1), yielding amine *m*-ACRO (87 mg, 0.18 mmol, 64%) as a red oil.

TLC (hexanes/EtOAc, 1:1): R_f = 0.73. $[\alpha]_D^{22}$: -46.0 (c = 0.10, DCM). **^1H NMR (CDCl_3 , 400 MHz, 27 °C):** δ = 7.95–7.90 (m, 3H, ArH), 7.86–7.81 (m, 1H, ArH), 7.55–7.45 (m, 5H, ArH), 7.05 (dd, J = 7.9, 7.9 Hz, 1H, ArH), 6.88 (d, J = 6.9 Hz, 1H, ArH), 6.62 (dd, J = 7.9, 1.1 Hz, 1H, ArH), 4.80–4.70 (m, 2H, OCH_2), 3.74–3.67 (m, 1H, CH), 2.87 (d, J = 18.2 Hz, 1H, CH), 2.73 (dd, J = 13.3, 6.7 Hz, 1H, CH), 2.68 (d, J = 5.9 Hz, 1H, CH), 2.54–2.45 (m, 2H, 2 x CH), 2.37 (dd, J = 13.3, 4.7 Hz, 1H, CH), 2.15–2.07 (m, 2H, 2 x CH), 1.34–1.27 (m, 6H, 2 x CH_3), 1.24 (d, J = 6.2 Hz, 3H, CH_3), 1.08–0.99 (m, 1H, CH), 0.80 (s, 3H, CH_3) ppm. **^{13}C NMR (CDCl_3 , 100 MHz, 27 °C):** δ = 152.7, 152.6, 151.3, 145.8, 140.4, 131.0, 130.1, 129.1, 126.5, 123.4, 122.8, 122.0, 121.8, 120.5, 117.6, 111.6, 73.5, 70.6, 62.6, 61.5, 46.2, 38.9, 37.8, 36.5, 23.6, 23.3, 20.4, 19.4, 18.8 ppm. **IR (neat, ATR):** $\tilde{\nu}$ = 3356 (w), 2967 (w), 2925 (w), 1585 (m), 1490 (w), 1465 (m), 1373 (m), 1338 (m), 1269 (s), 1221 (w), 1198 (s), 1154 (s), 1129 (m), 1110 (m), 1098 (m), 1034 (m), 1006 (m), 988 (w), 944 (w), 922 (w), 909 (w), 843 (w), 788

(s), 762 (m), 735 (m), 721 (m), 694 (vs) cm^{-1} . **HRMS (ESI⁺):** m/z calcd. for $[\text{C}_{31}\text{H}_{38}\text{N}_3\text{O}_2]^+$: 484.2964, found: 484.2960 ($[\text{M}+\text{H}]^+$). **UV/Vis:** $\lambda_{\text{max}} = 325, 435 \text{ nm}$.

4.6.5 SYNTHESIS OF MS1

Synthesis of (2-hydroxy-3-methoxyphenyl)(pyrrolidin-1-yl)methanone (4.34)



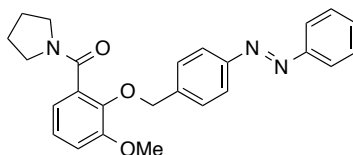
Benzotriazole (1.88 g, 15.8 mmol, 3.15 equiv.) was dissolved in THF (30 mL) and SOCl_2 (0.36 mL, 5.0 mmol, 1.0 equiv.) was added. The mixture was stirred at room temperature for 45 min. A solution of 2-hydroxy-3-methoxybenzoic acid (841 mg, 5.00 mmol, 1.0 equiv.) in THF (20 mL) was added rapidly and the mixture stirred for 2 h at room temperature. In a separate flask, pyrrolidine (0.61 mL, 7.5 mmol, 1.5 equiv.) and TEA (1.04 mL, 7.50 mmol, 1.5 equiv.) were dissolved in THF (5 mL). To this flask was added the supernatant of the 2-hydroxy-3-methoxybenzoic acid benzotriazole amide containing flask rapidly *via* a syringe. The remaining solid was washed with THF (12.5 mL) and the supernatant was again transferred to the reaction flask. The reaction mixture was stirred for 30 min at room temperature. The solvent was removed under reduced pressure and the residue was taken up in EtOAc (30 mL). The organic layer was washed with water (50 mL), 1 M HCl (3 x 50 mL) and brine (50 mL), then dried over MgSO_4 and concentrated under reduced pressure. The crude product was purified by flash silica gel column chromatography (hexanes/EtOAc, gradient from 4:1 to 2:3) to give amide **4.34** (286 mg, 1.29 mmol, 26%) as a colorless oil.

TLC (hexanes/EtOAc, 1:1): $R_f = 0.29$. **¹H NMR (CDCl₃, 300 MHz, 27 °C):** $\delta = 7.05$ (dd, $J = 8.0, 1.5 \text{ Hz}$, 1H, ArH), 6.93 (dd, $J = 8.0, 1.5 \text{ Hz}$, 1H, ArH), 6.78 (dd, $J = 8.0, 8.0 \text{ Hz}$, 1H, ArH), 3.89 (s, 3H, CH₃), 3.71–3.63 (m, 4H, 2 x CH₂), 1.99–1.88 (m, 4H, 2 x CH₂) ppm. **¹³C NMR (CDCl₃, 75 MHz, 27 °C):** $\delta = 169.7, 149.3, 148.6, 119.8, 118.5, 117.8, 113.8, 56.1 \text{ ppm}$.^[hh] **IR (neat, ATR):** $\tilde{\nu} = 3209$ (w), 2966 (w), 2880 (w), 1604 (s), 1576 (s), 1480 (s), 1446 (vs), 1428 (vs), 1361 (w), 1340 (w), 1250 (vs), 1187 (w), 1071 (m), 1033 (w), 973 (w),

^[hh] Due to extensive broadening, the two pyrrolidine carbon atoms of **4.34** could not be observed in the ¹³C NMR spectrum.

948 (w), 913 (w), 838 (w), 819 (w), 793 (w), 749 (w), 720 (w), 664 (w) cm^{-1} . **HRMS (EI⁺):** m/z calcd. for $[\text{C}_{12}\text{H}_{15}\text{NO}_3]^+$: 221.1052, found: 221.1036 ($[\text{M}]^+$).

Synthesis of (3-methoxy-2-((4-(phenyldiazenyl)benzyl)oxy)phenyl)(pyrrolidin-1-yl)-methanone (MS1)

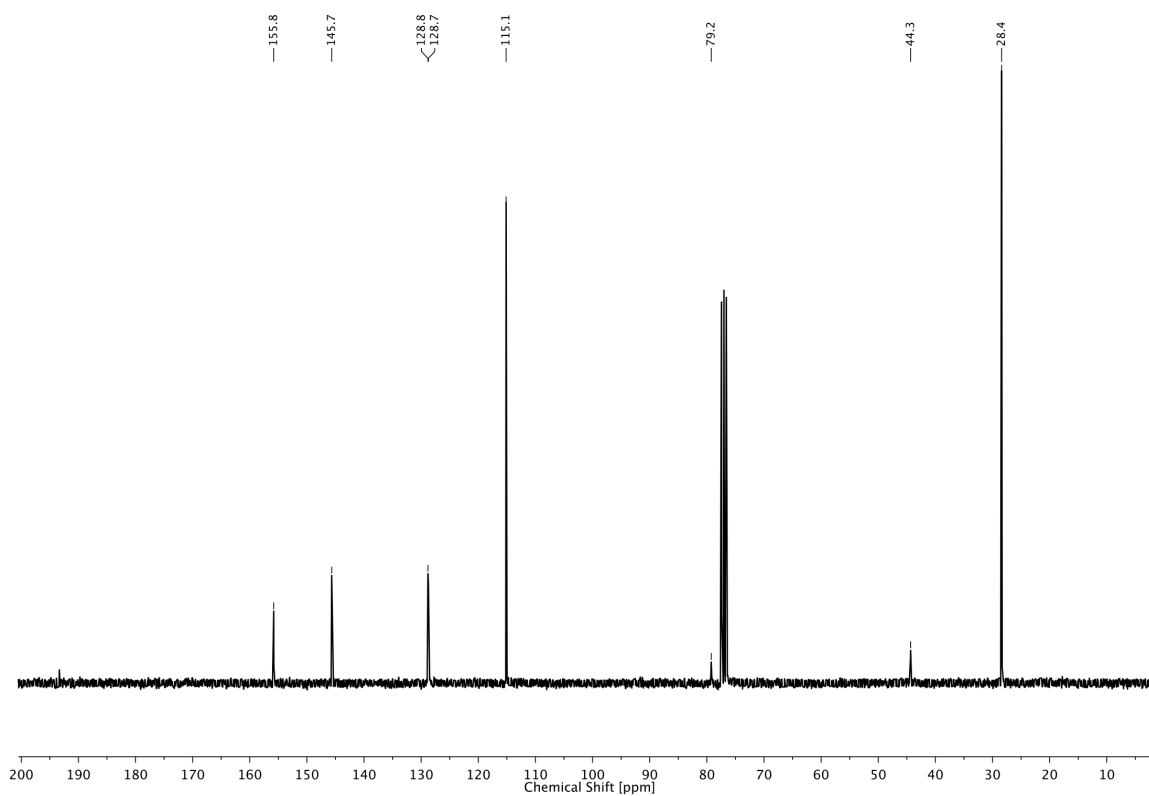
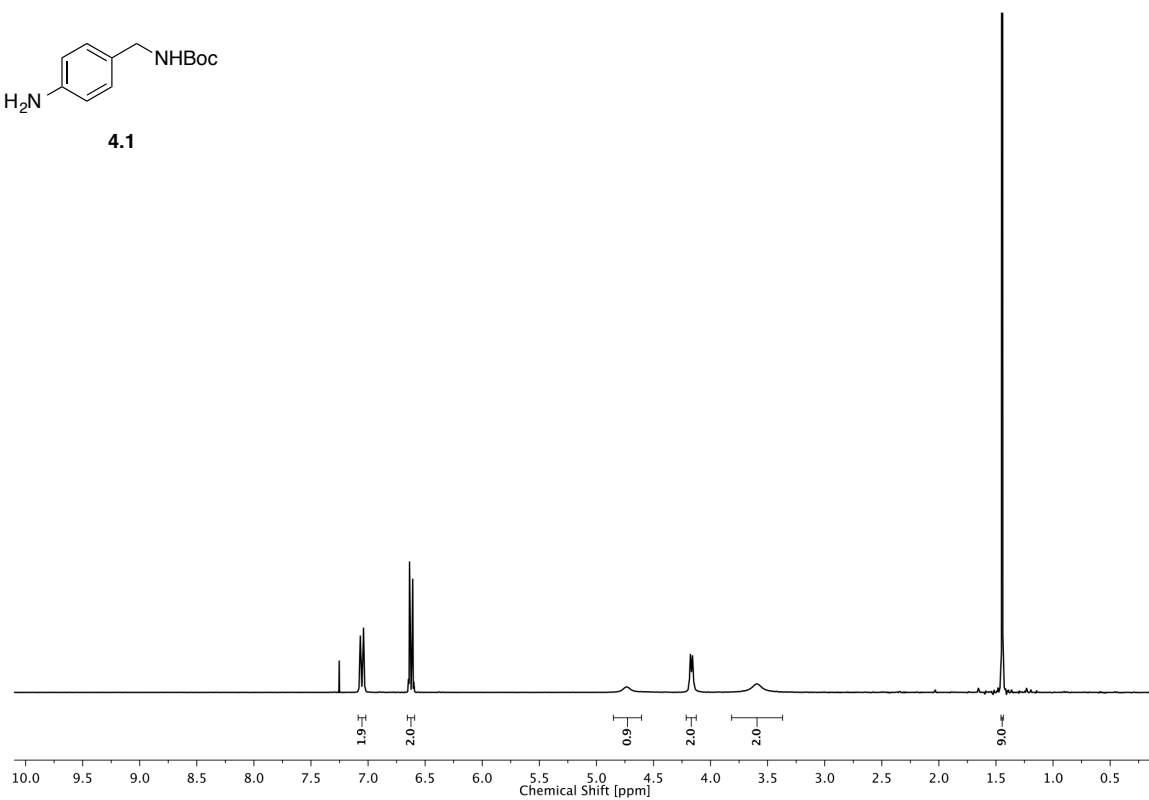
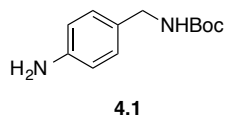


Phenol **4.34** (267 mg, 1.21 mmol, 1.0 equiv.) and K_2CO_3 (669 mg, 4.84 mmol, 4.0 equiv.) were dissolved in DMF (12 mL). Bromide **4.18** (666 mg, 2.42 mmol, 2.0 equiv.) was added and the mixture was stirred for 30 min at room temperature, then heated to 60 °C for 4 h. The solvent was removed *in vacuo* and the residue taken up in DCM (30 mL). The organic layer was washed with water (2 x 50 mL) and brine (3 x 50 mL), then dried over MgSO_4 and concentrated under reduced pressure. The crude product was purified by flash silica gel column chromatography ($\text{CHCl}_3/\text{MeOH}$, 100:0 \rightarrow 100:1) to give **MS1** (500 mg, 1.20 mmol, 99%) as a red oil.

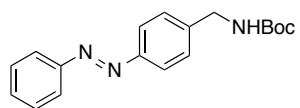
TLC ($\text{CHCl}_3/\text{MeOH}$, 20:1): $R_f = 0.53$. **¹H NMR (CDCl_3 , 400 MHz, 27 °C):** $\delta = 7.93\text{--}7.87$ (m, 4H, ArH), 7.60–7.55 (m, 2H, ArH), 7.53–7.42 (m, 3H, ArH), 7.10 (dd, $J = 8.2, 7.6$ Hz, 1H, ArH), 6.94 (dd, $J = 8.2, 1.4$ Hz, 1H, ArH), 6.90 (dd, $J = 7.6, 1.4$ Hz, 1H, ArH), 5.10 (s, 2H, CH_2), 3.87 (s, 3H, CH_3), 3.60 (t, $J = 7.0$ Hz, 2H, CH_2), 3.28–3.18 (m, 2H, CH_2), 1.90–1.82 (m, 2H, CH_2), 1.77–1.73 (m, 2H, CH_2) ppm.^[ii] **¹³C NMR (CDCl_3 , 100 MHz, 27 °C):** $\delta = 167.2, 152.8, 152.6, 152.2, 143.8, 140.7, 133.3, 130.9, 129.0, 128.7, 125.1, 122.8, 122.8, 119.1, 112.9, 75.4, 55.8, 47.8, 45.6, 25.7, 24.6$ ppm. **IR (neat, ATR):** $\tilde{\nu} = 2971$ (w), 2874 (w), 1670 (w), 1619 (m), 1472 (m), 1442 (m), 1425 (m), 1371 (w), 1340 (w), 1302 (w), 1266 (m), 1214 (m), 1183 (w), 1153 (w), 1103 (w), 1070 (m), 1010 (m), 986 (m), 950 (w), 926 (w), 831 (w), 798 (w), 783 (w), 746 (vs), 687 (m), 663 (m) cm^{-1} . **HRMS (ESI⁺):** m/z calcd. for $[\text{C}_{25}\text{H}_{26}\text{N}_3\text{O}_3]^+$: 416.1974, found: 416.1965 ($[\text{M}+\text{H}]^+$). **UV/Vis:** $\lambda_{\text{max}} = 328, 444$ nm.

^[ii] **MS1** was obtained as a 10:1 mixture of *trans* : *cis* isomers as indicated by ¹H NMR spectrum.

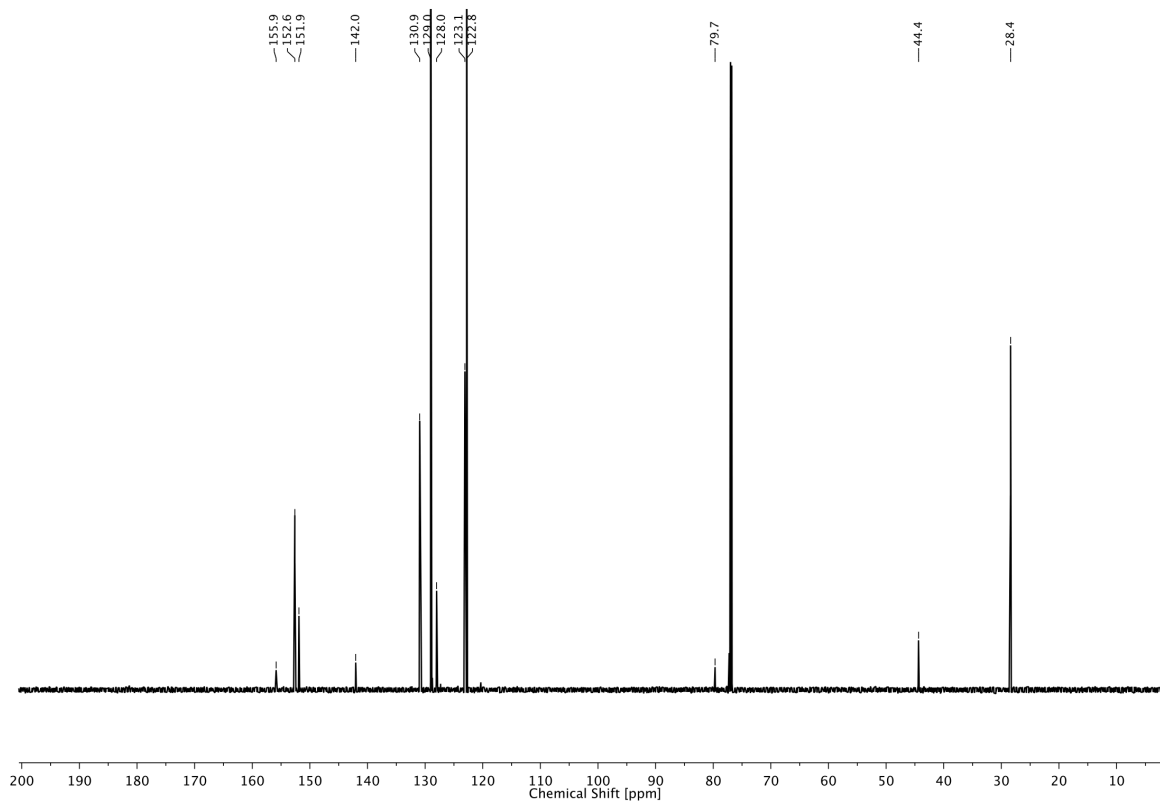
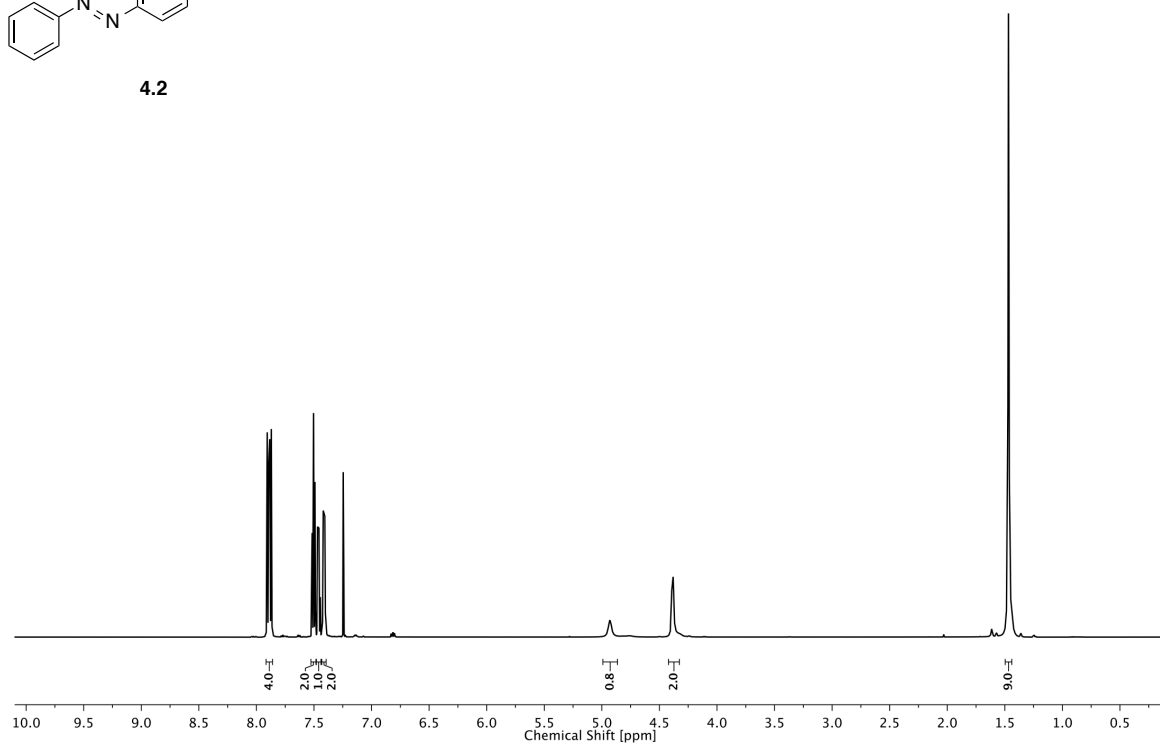
4.7 NMR SPECTRA



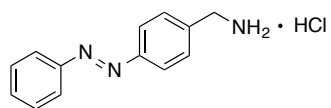
4 PHOTOCROMIC LIGANDS FOR VOLTAGE-GATED SODIUM CHANNELS



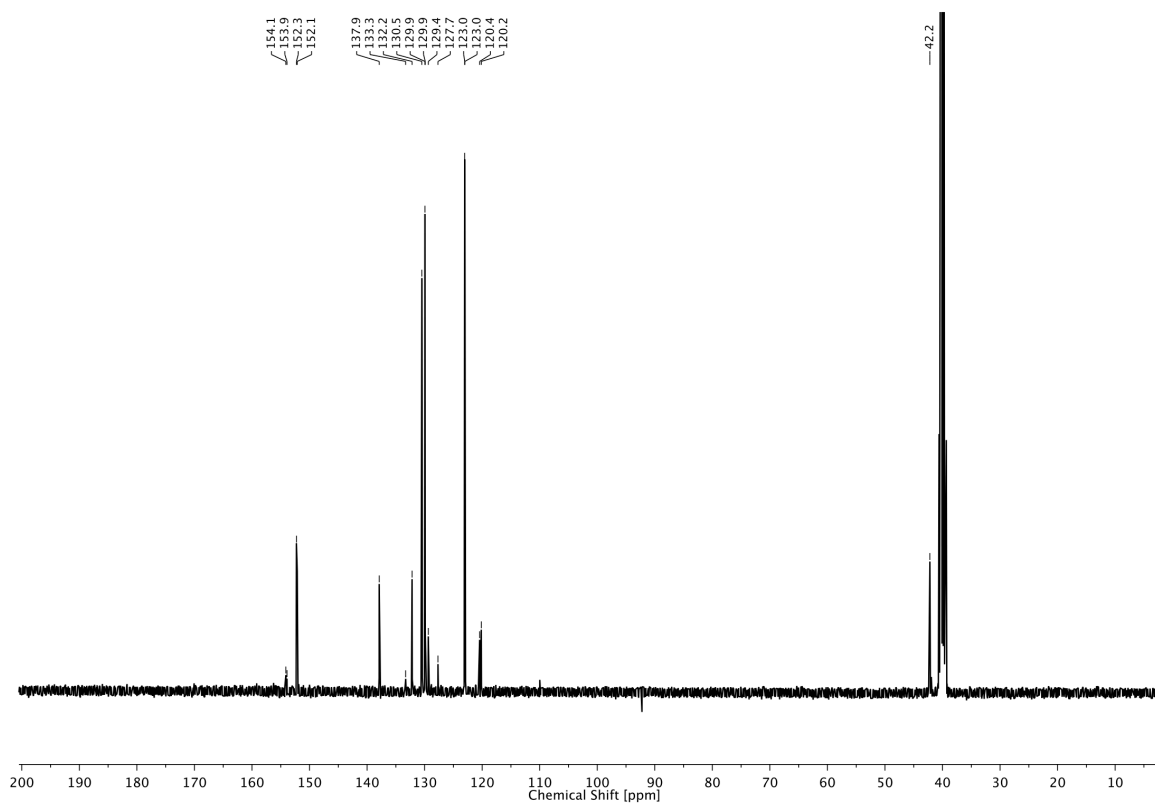
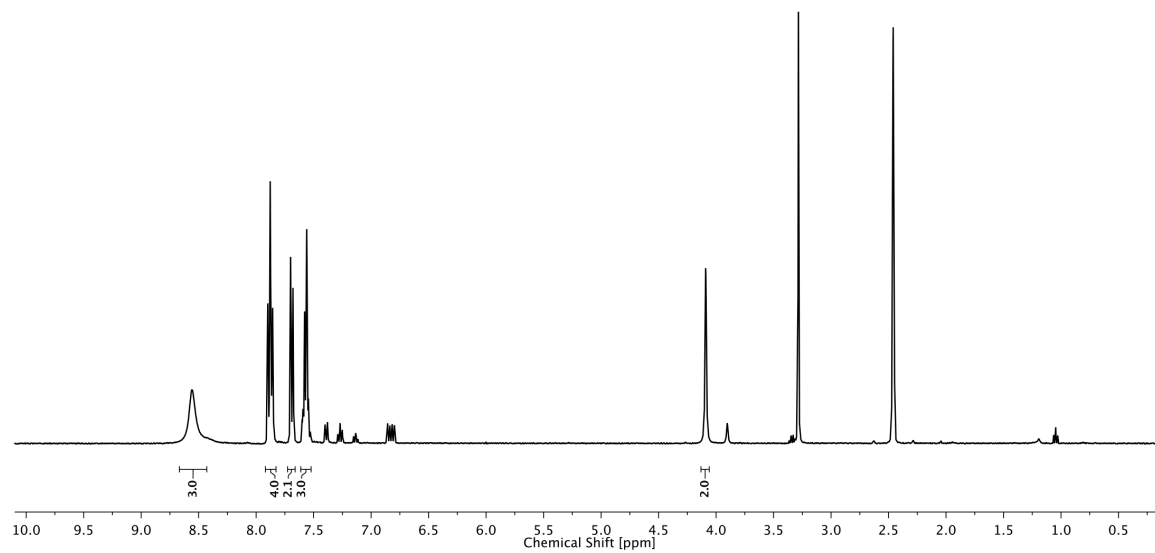
4.2

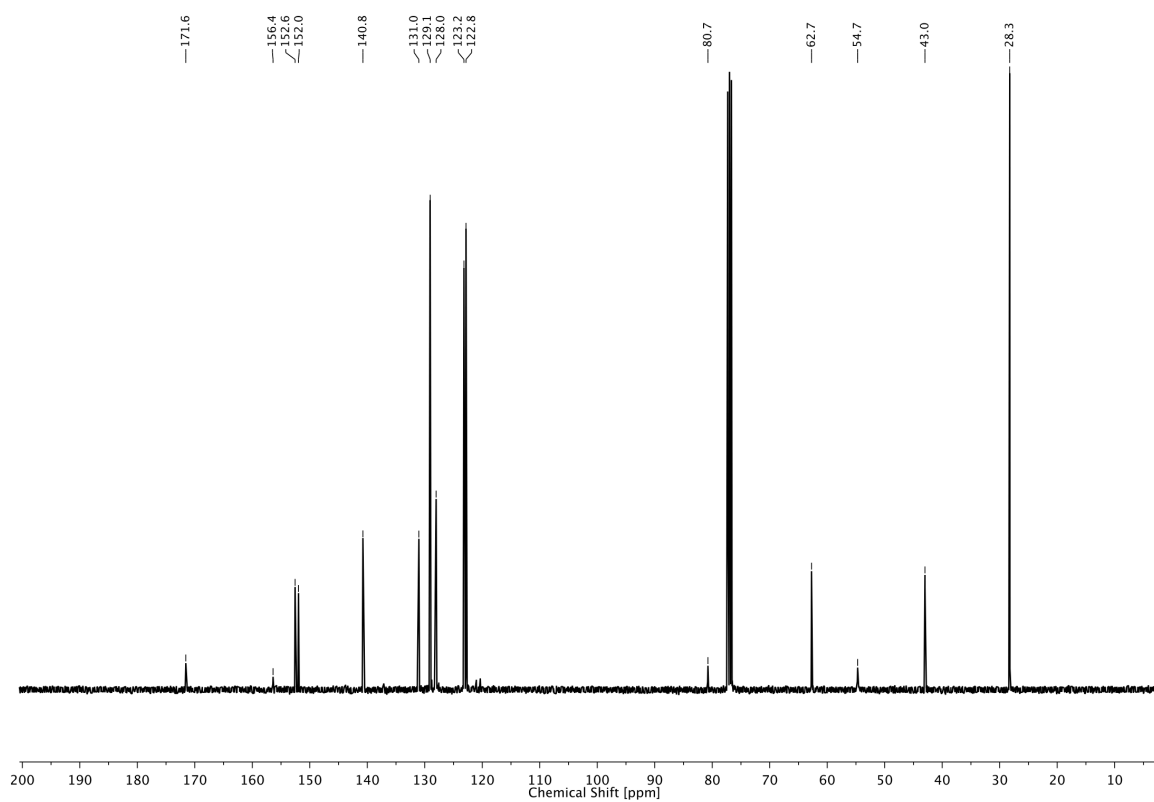
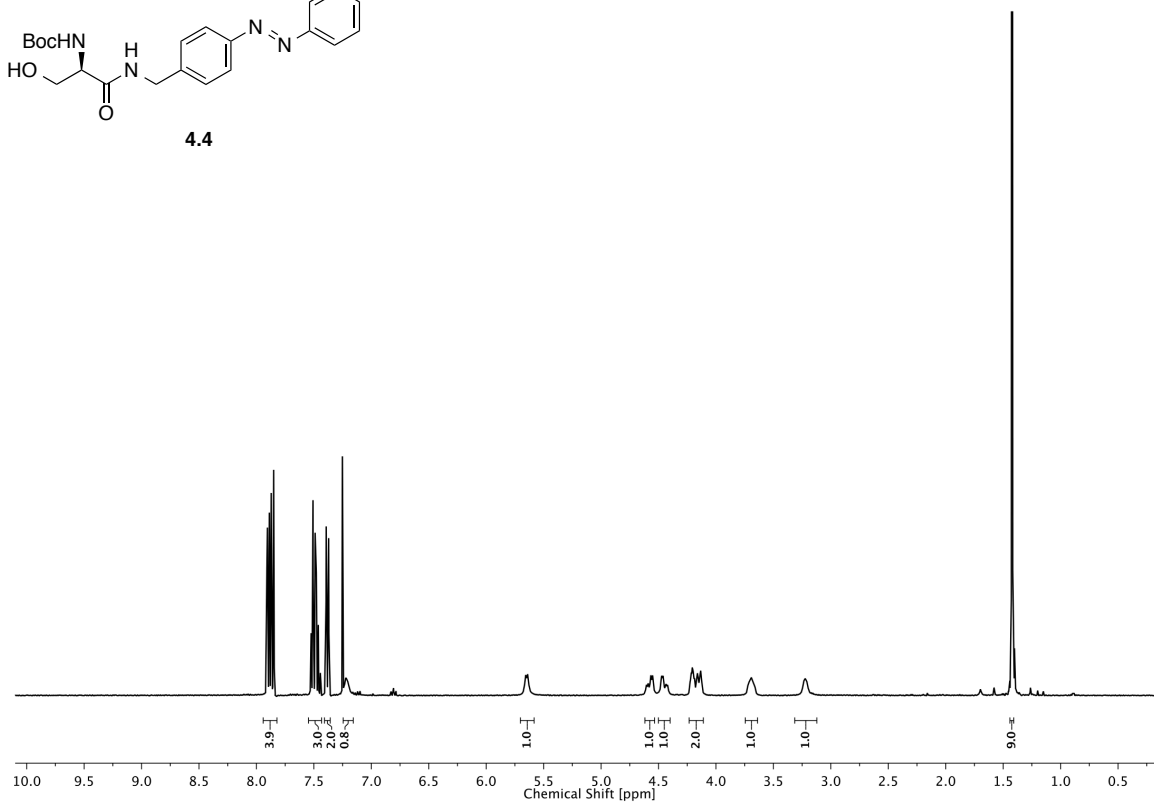
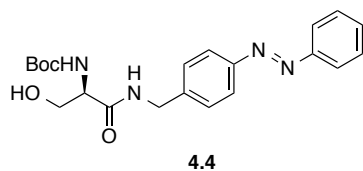


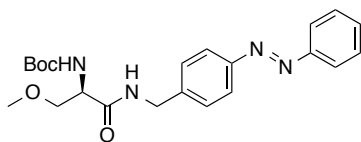
4 PHOTOCROMIC LIGANDS FOR VOLTAGE-GATED SODIUM CHANNELS



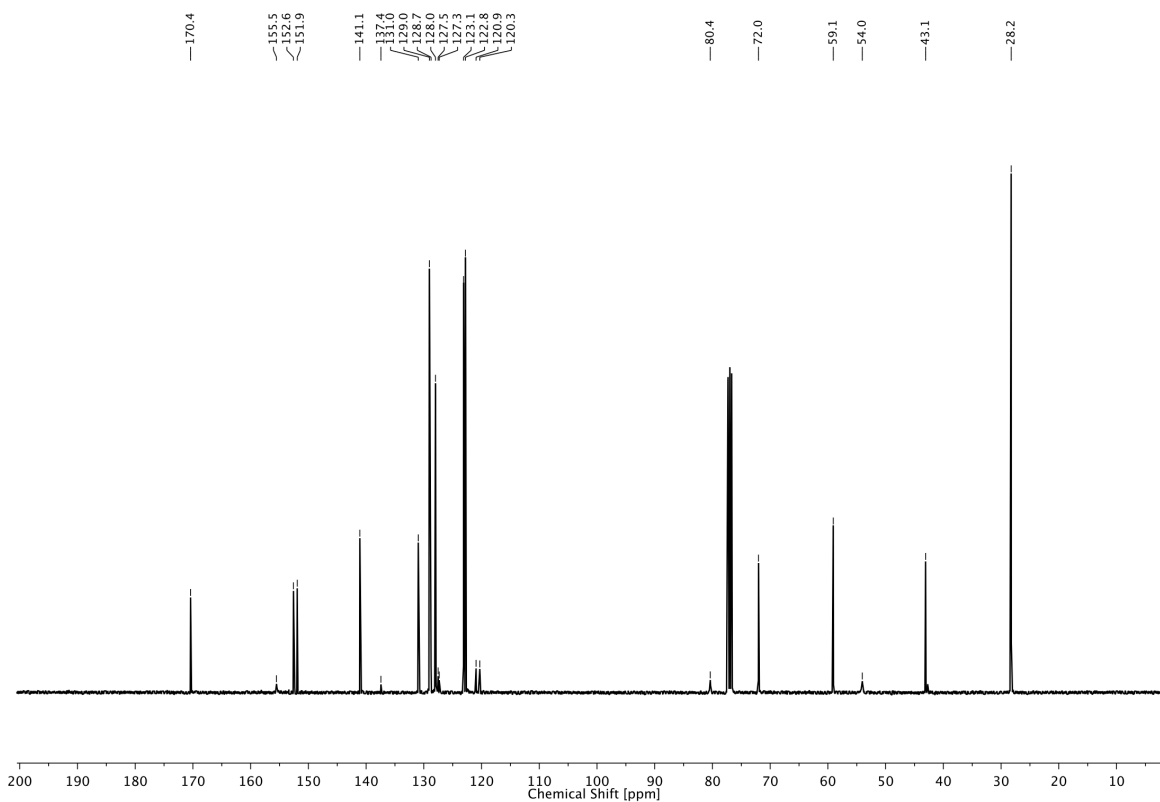
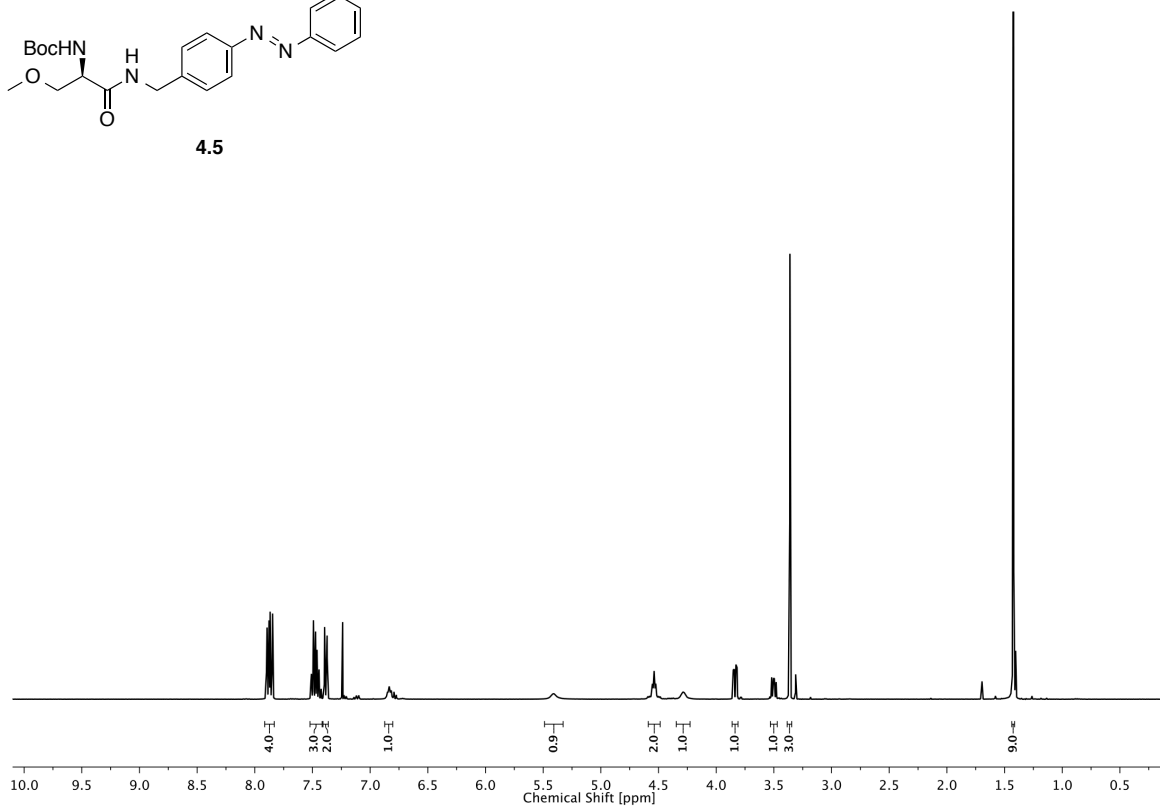
4.3

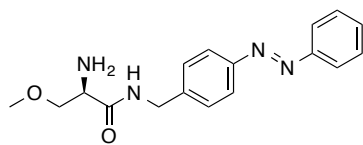




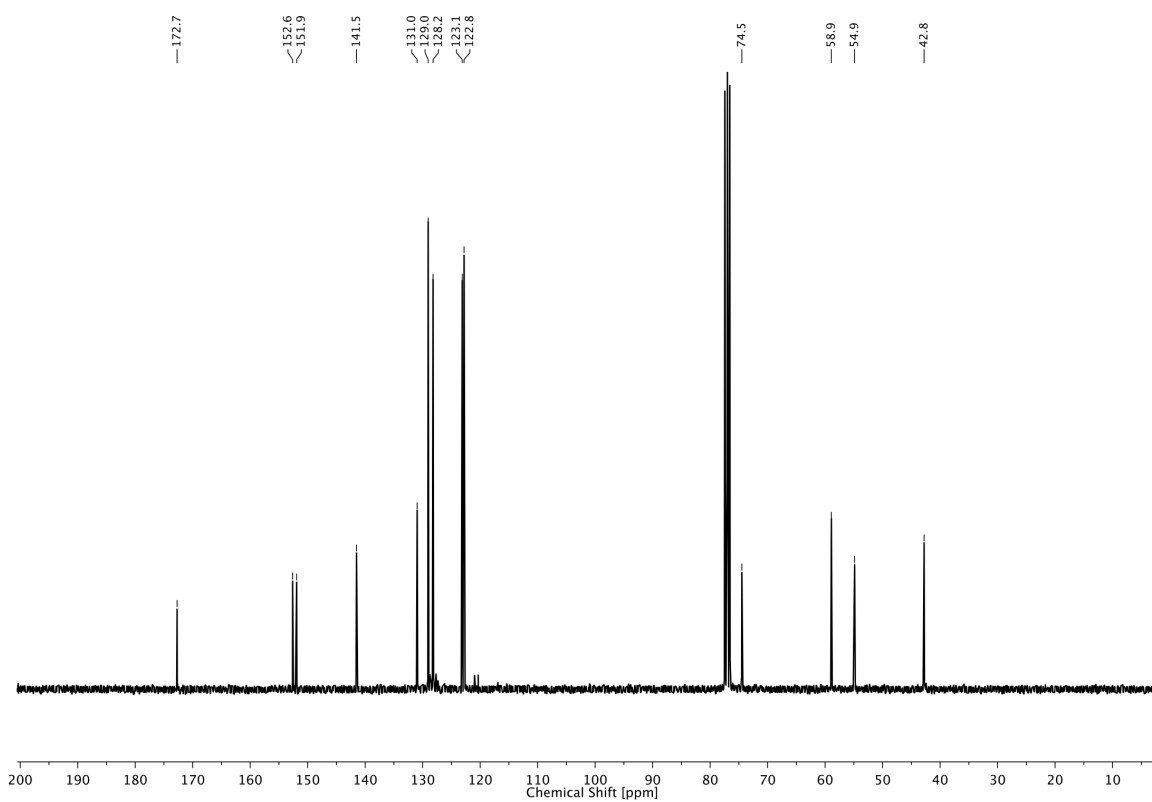
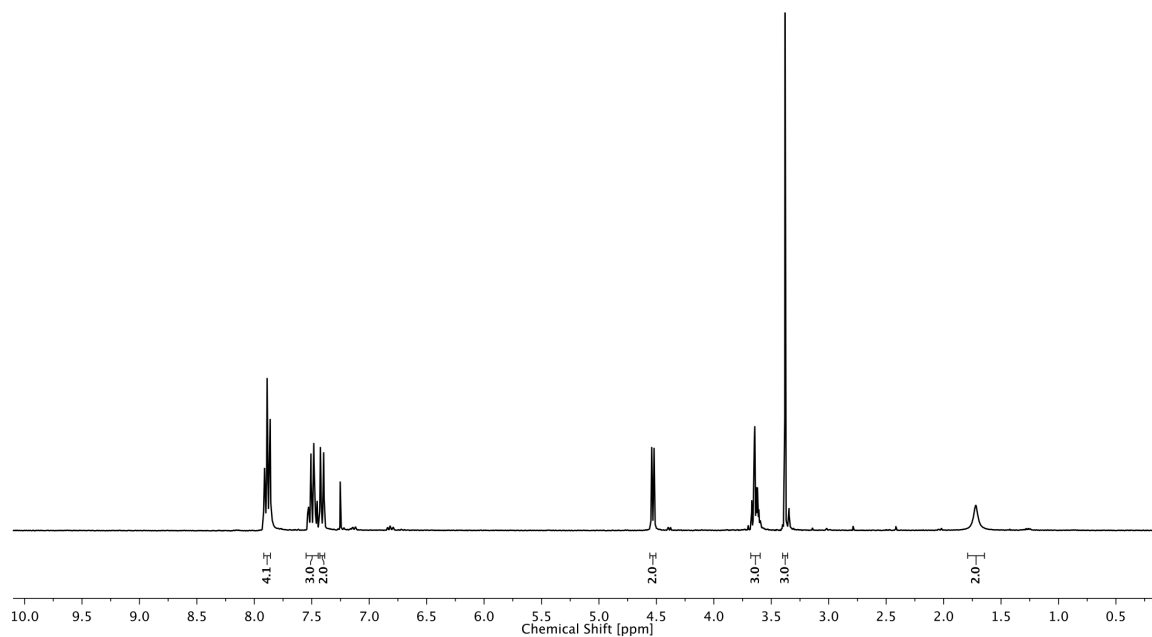


4.5

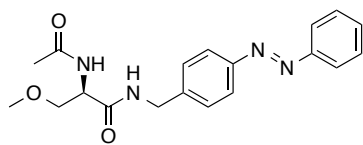




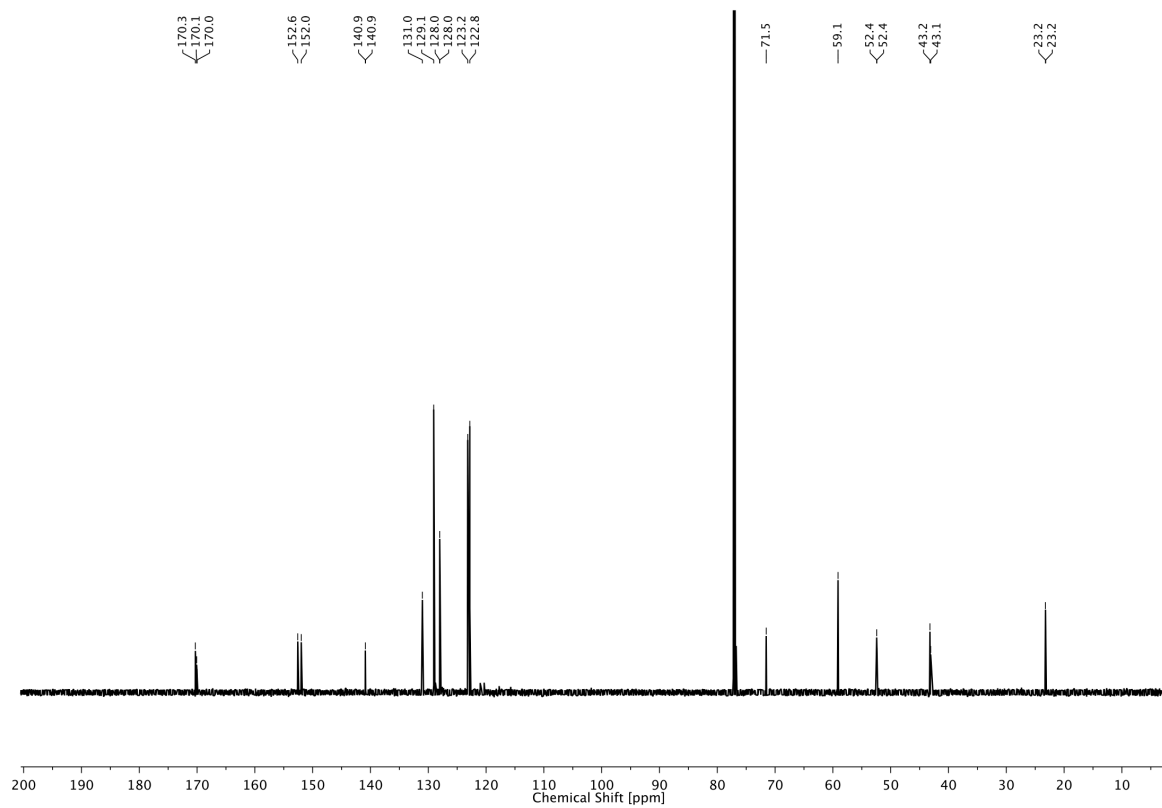
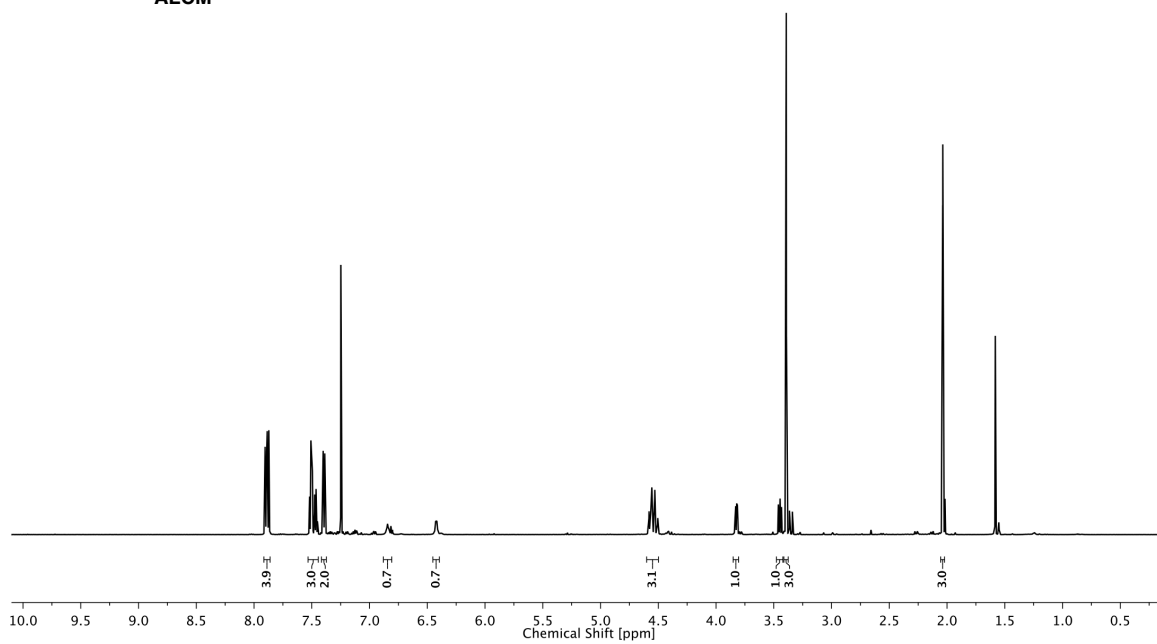
4.6



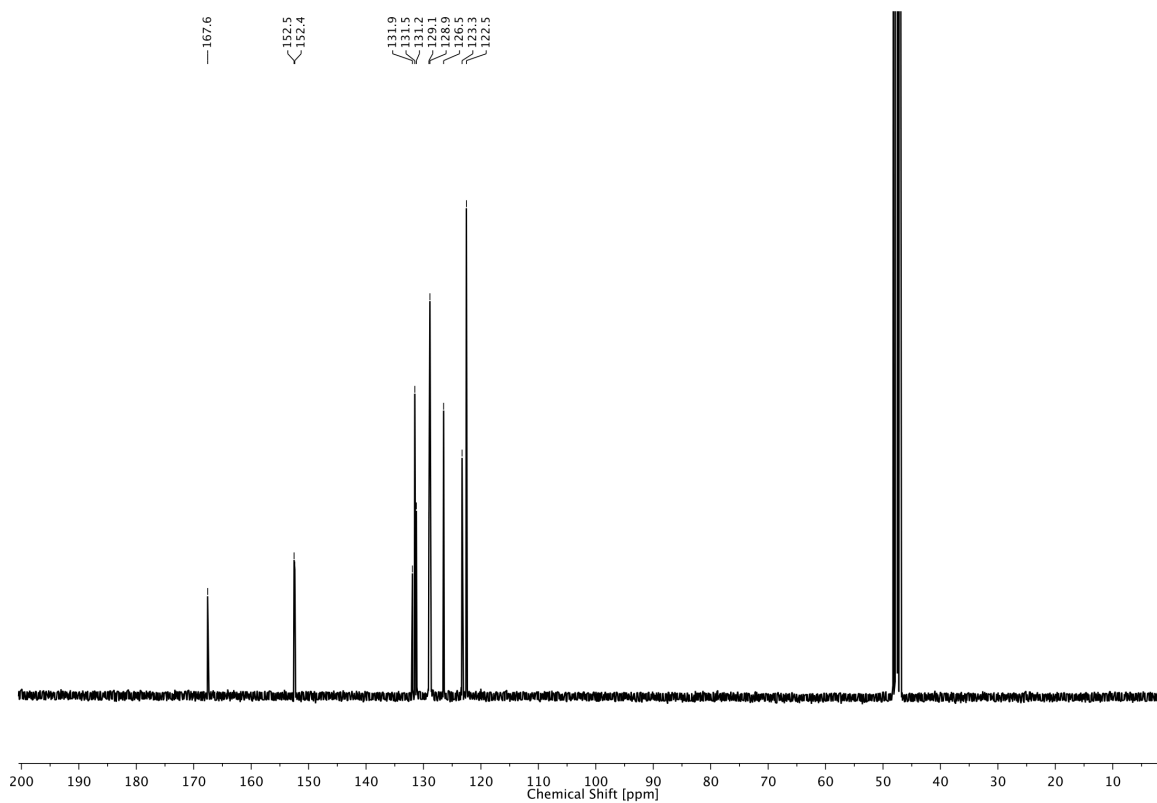
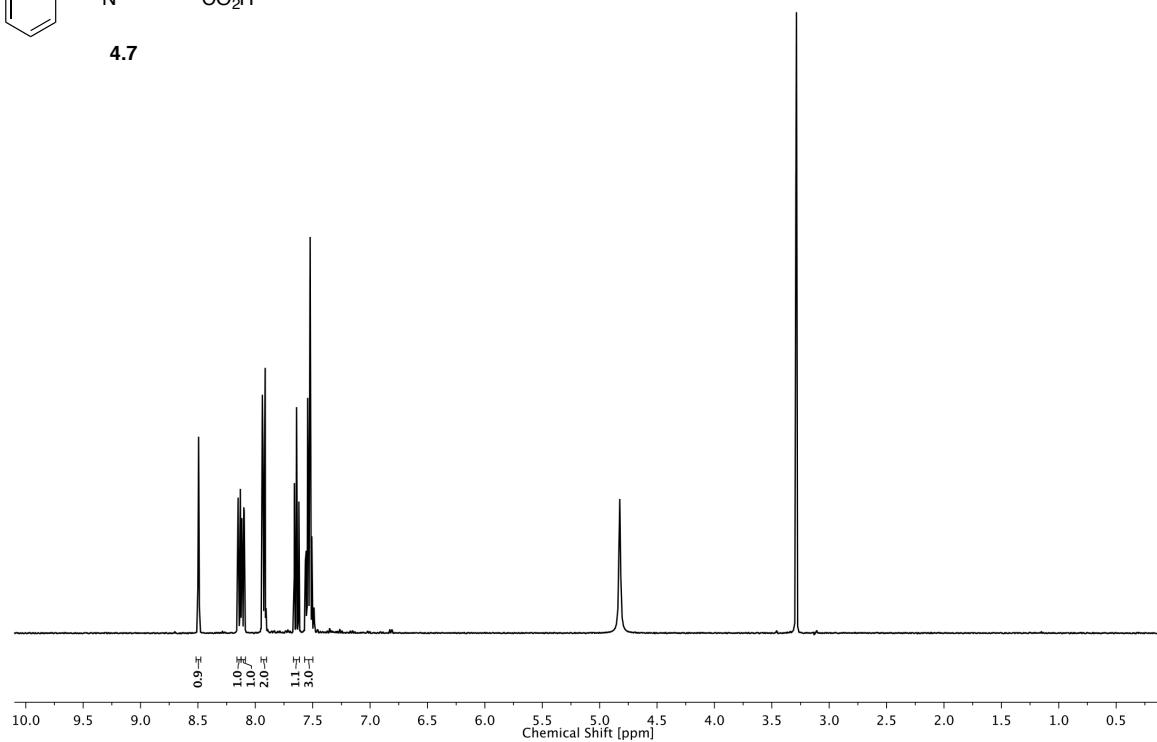
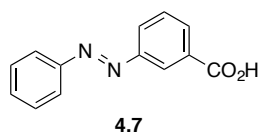
4 PHOTOCROMIC LIGANDS FOR VOLTAGE-GATED SODIUM CHANNELS



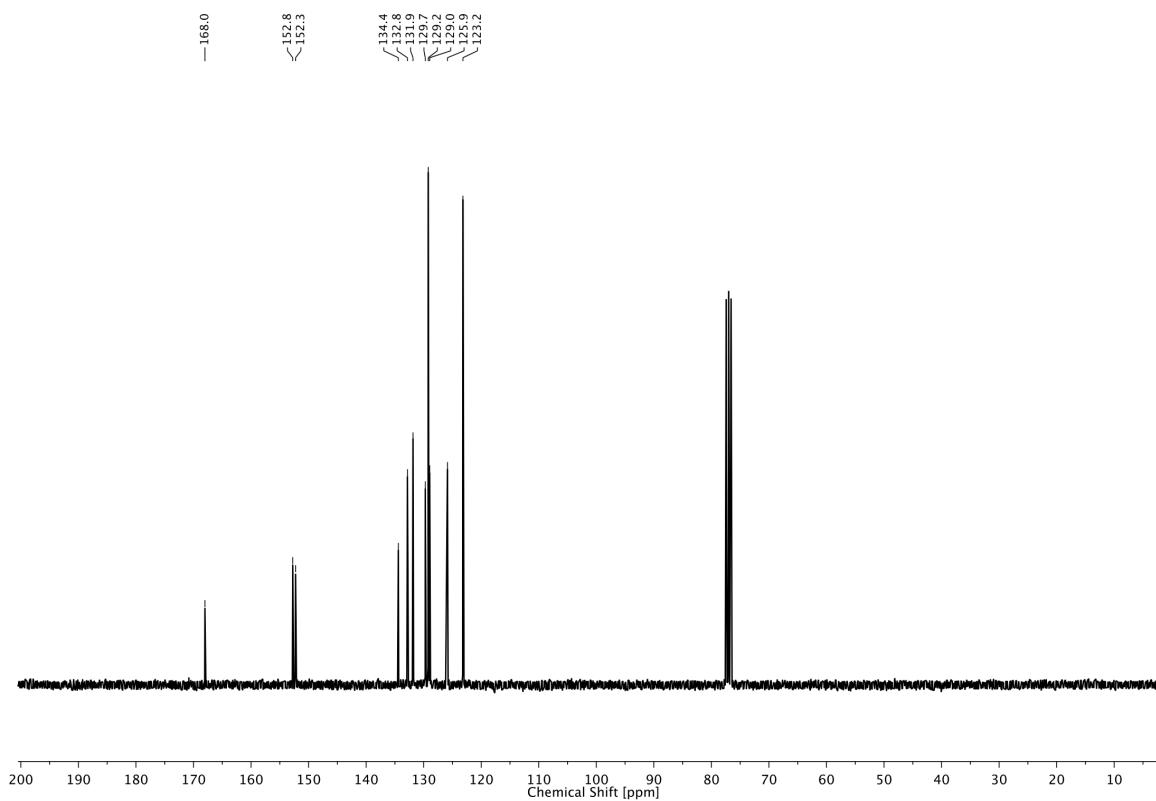
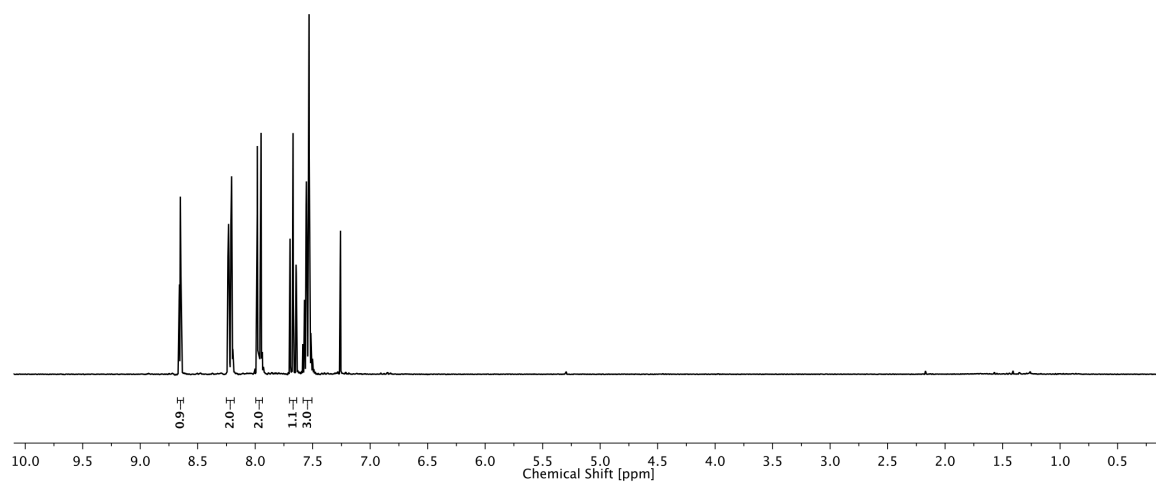
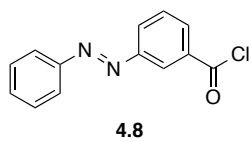
ALCM

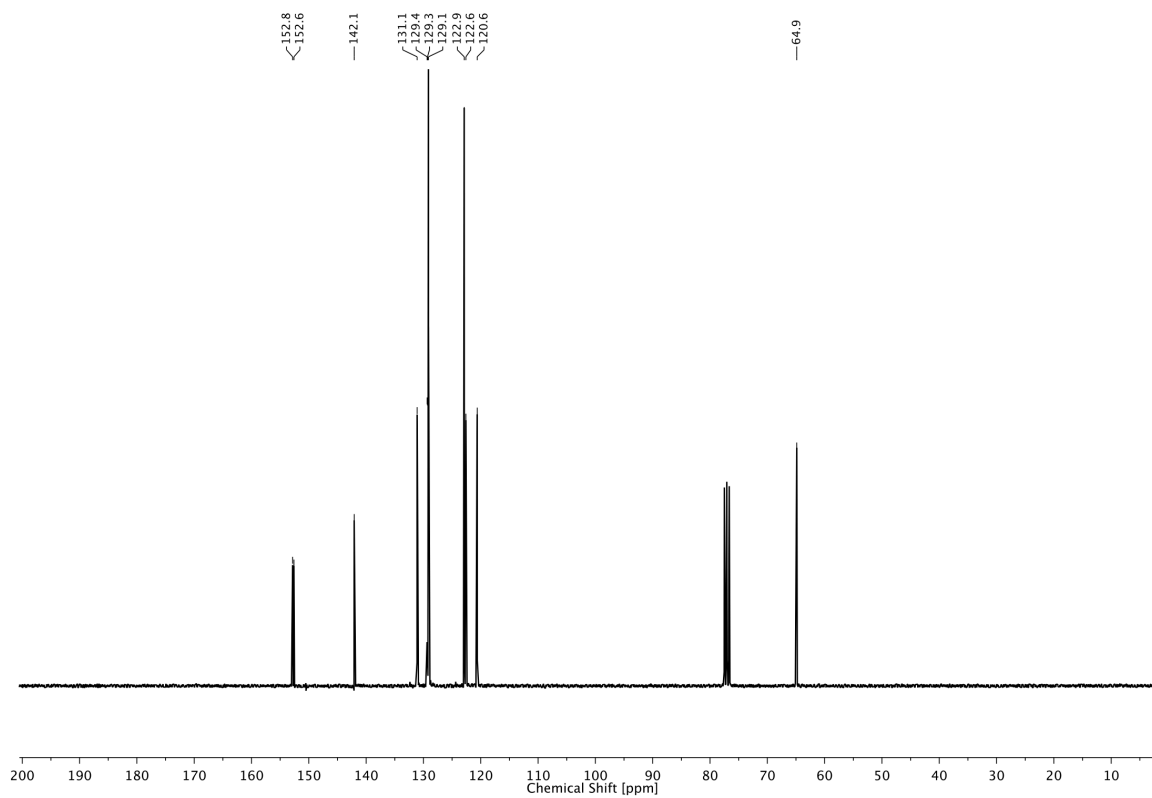
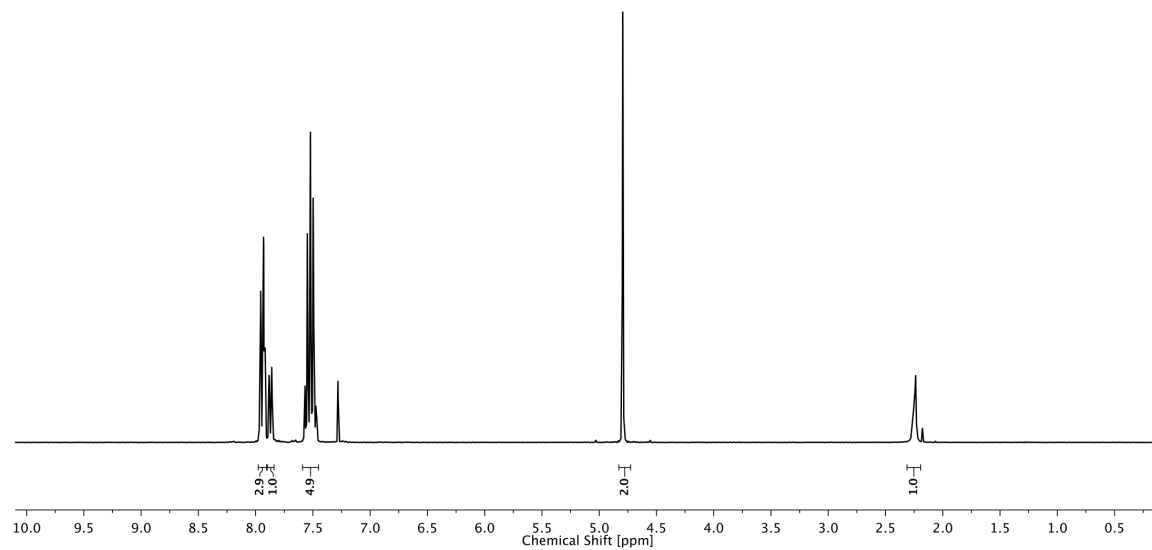
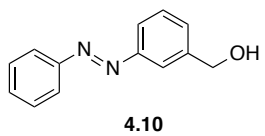


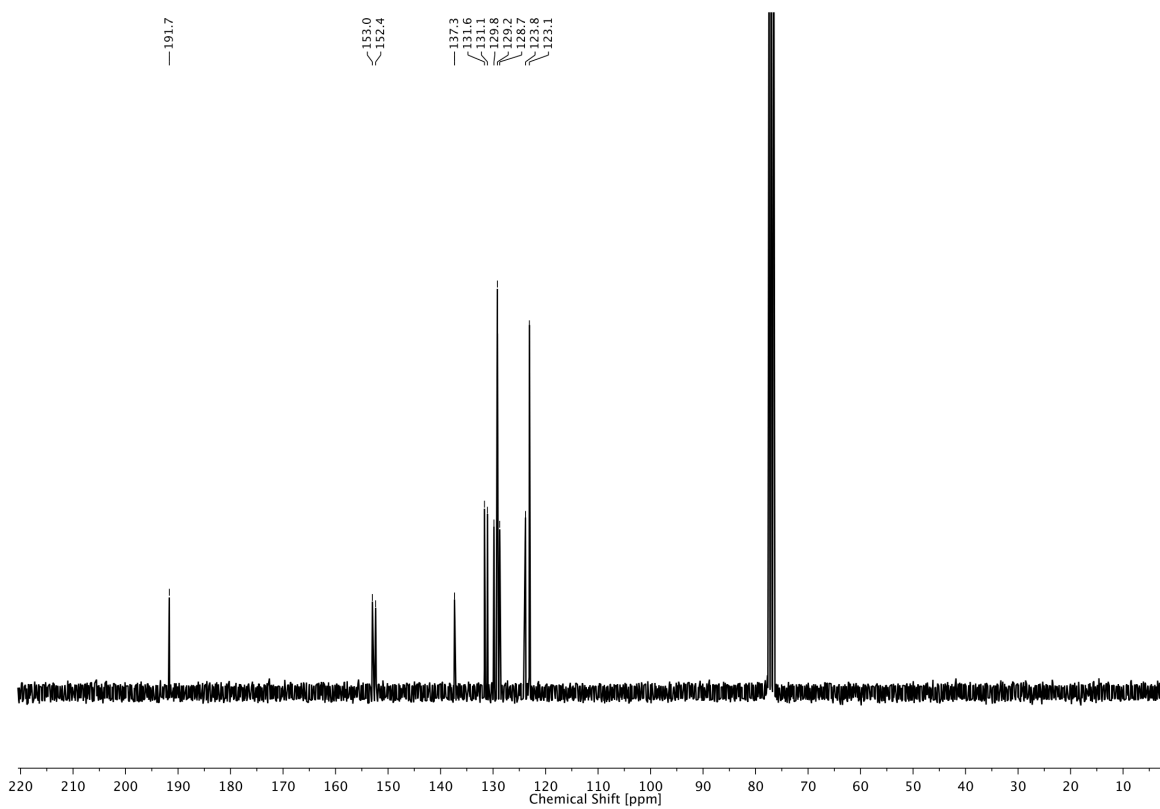
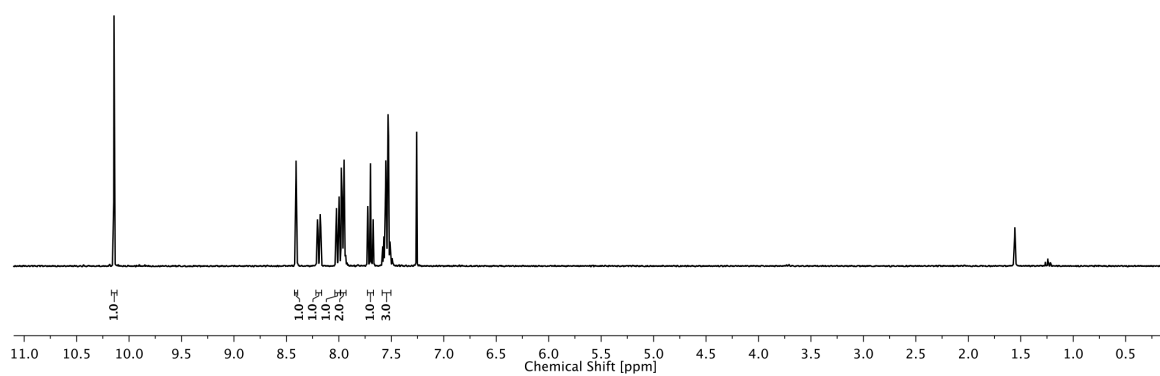
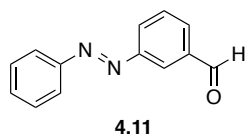
4 PHOTOCROMIC LIGANDS FOR VOLTAGE-GATED SODIUM CHANNELS

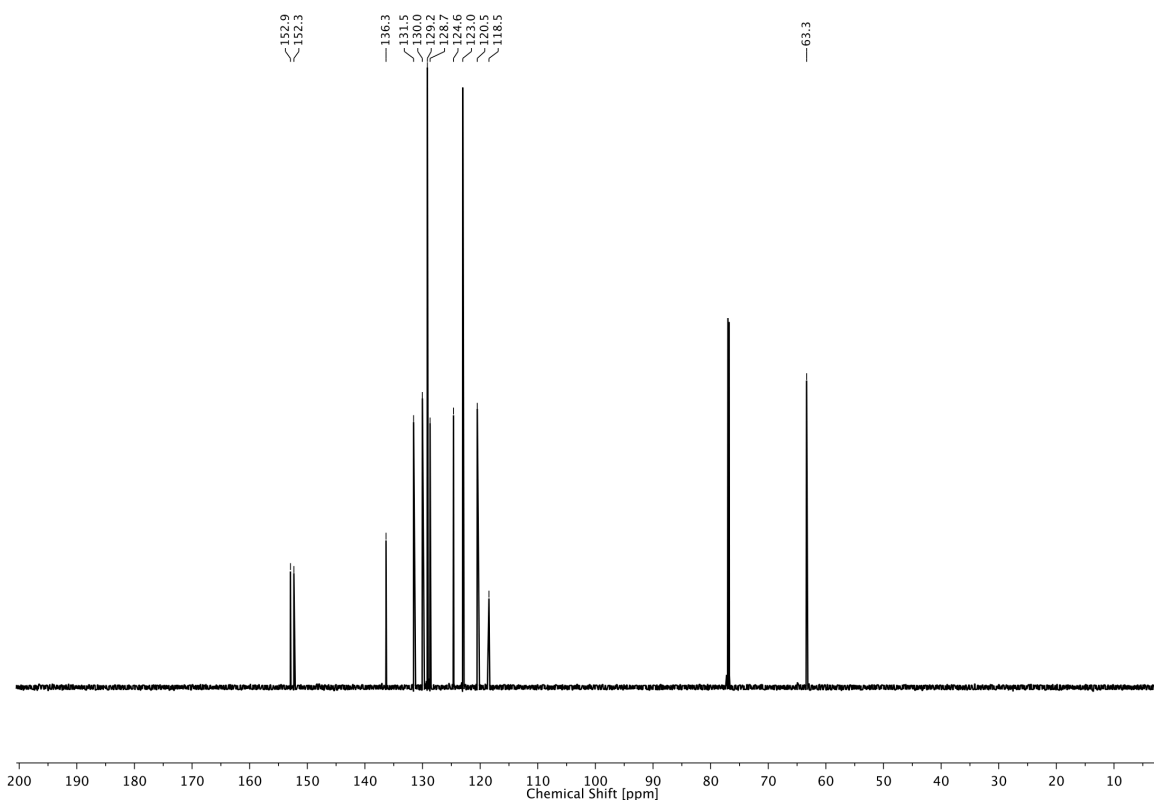
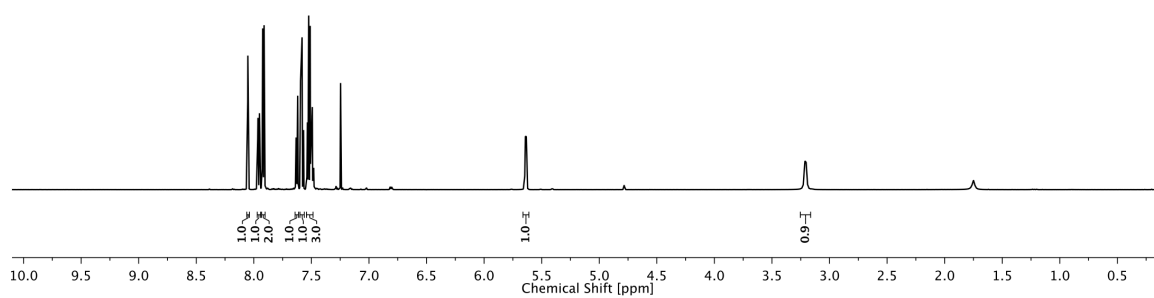
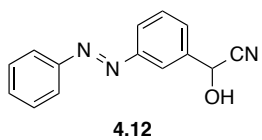


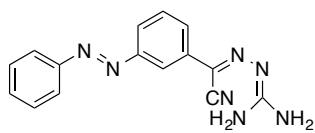
4 PHOTOCROMIC LIGANDS FOR VOLTAGE-GATED SODIUM CHANNELS



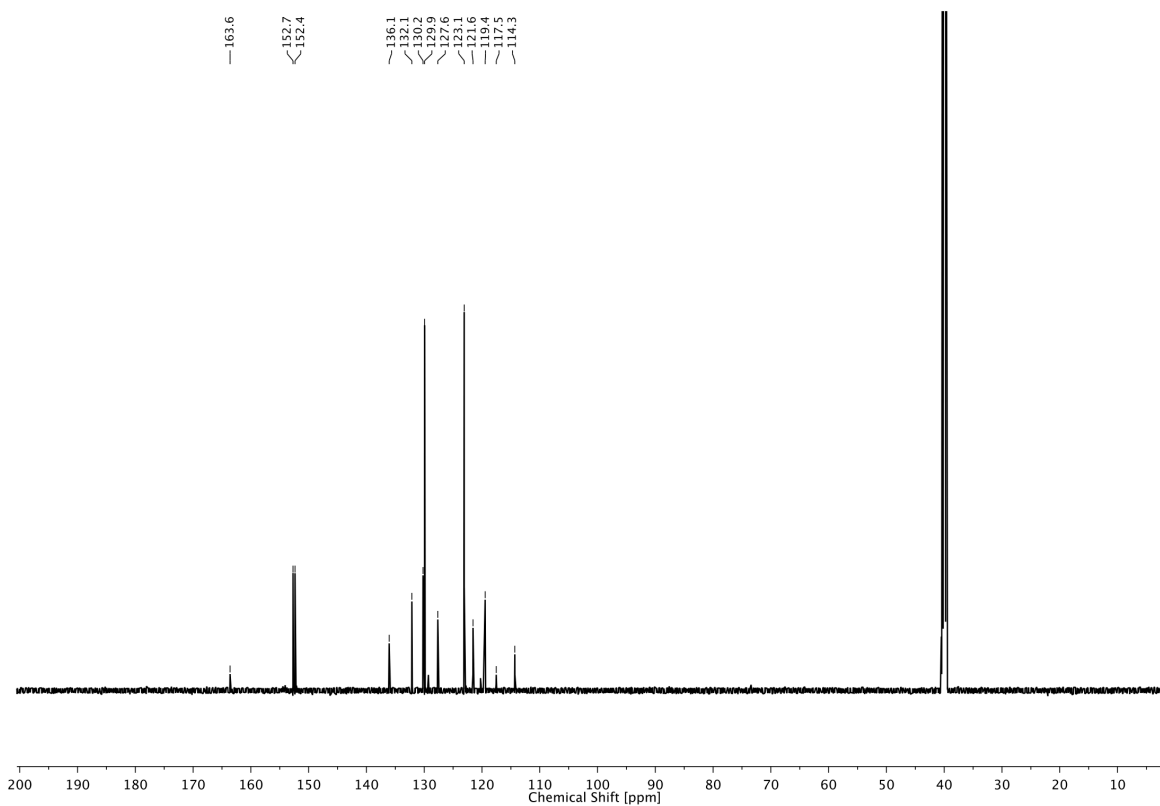
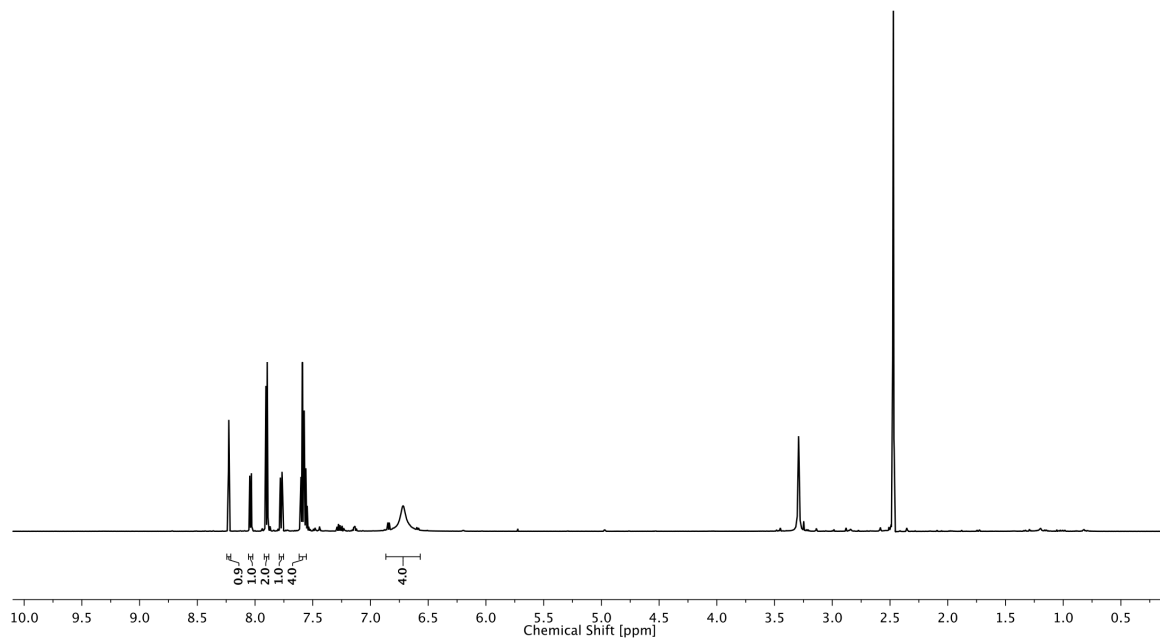




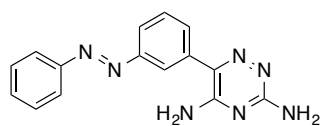




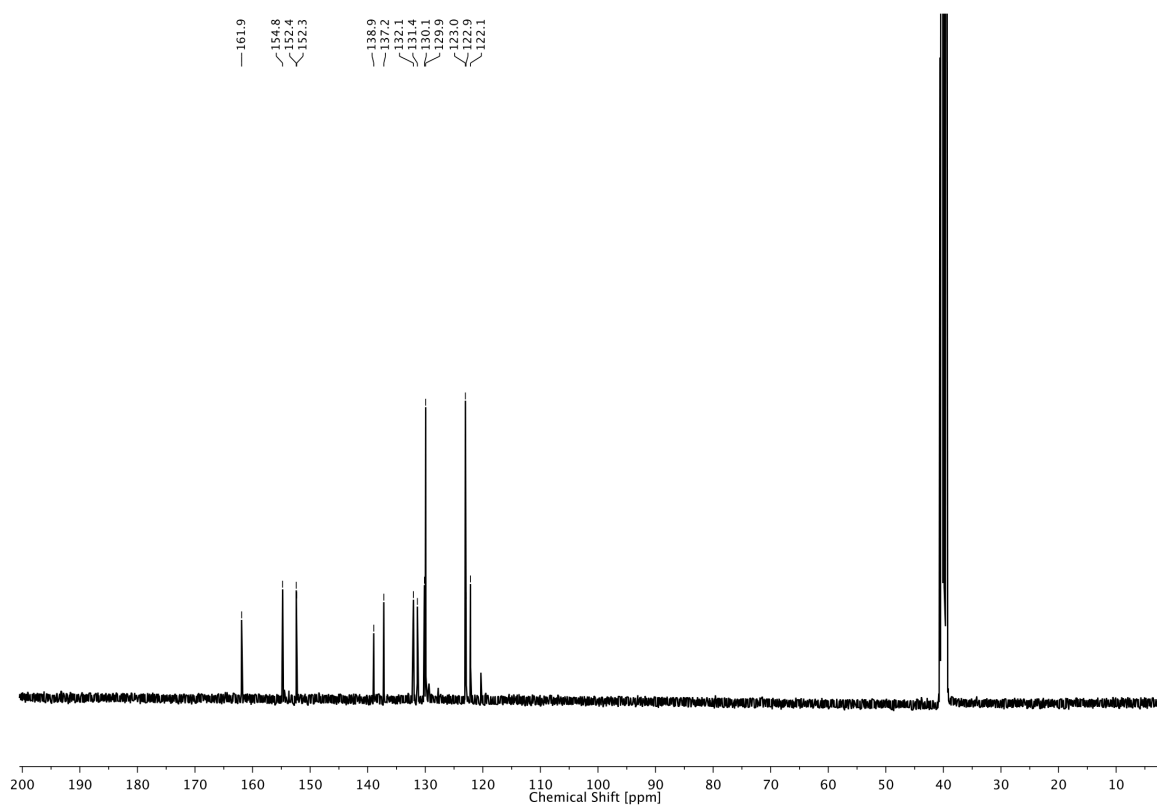
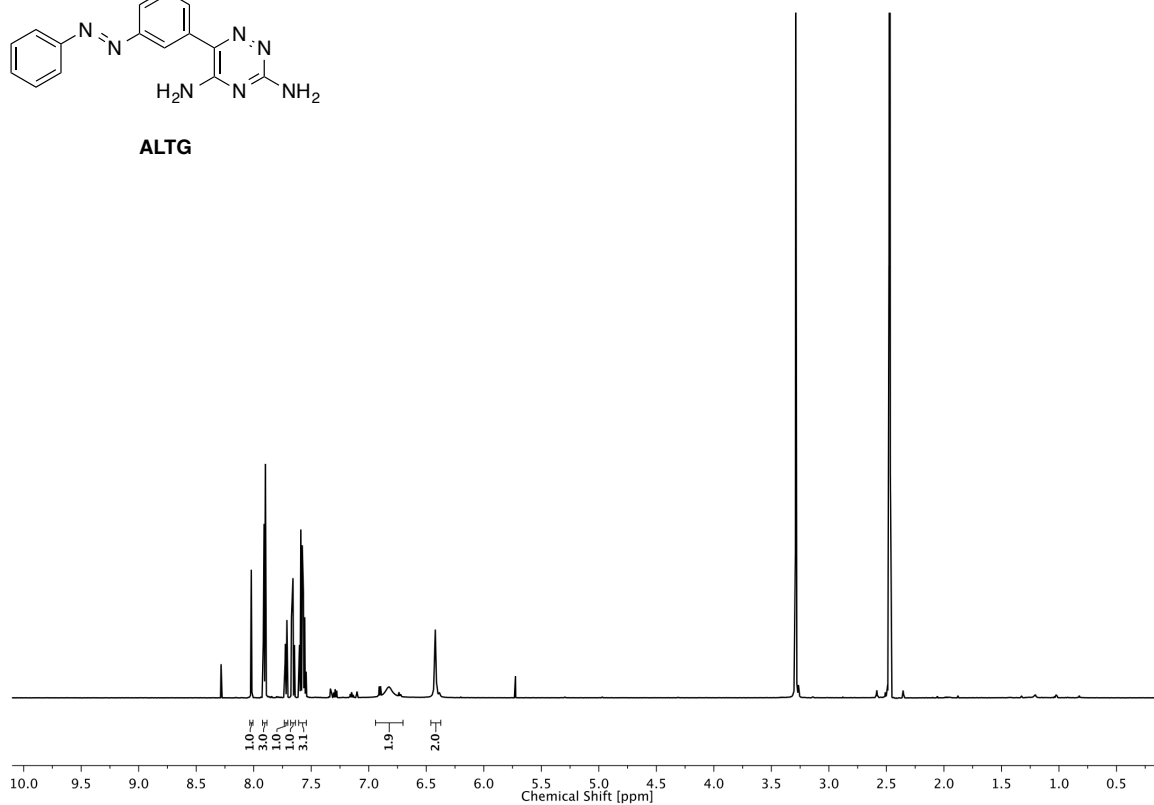
4.14



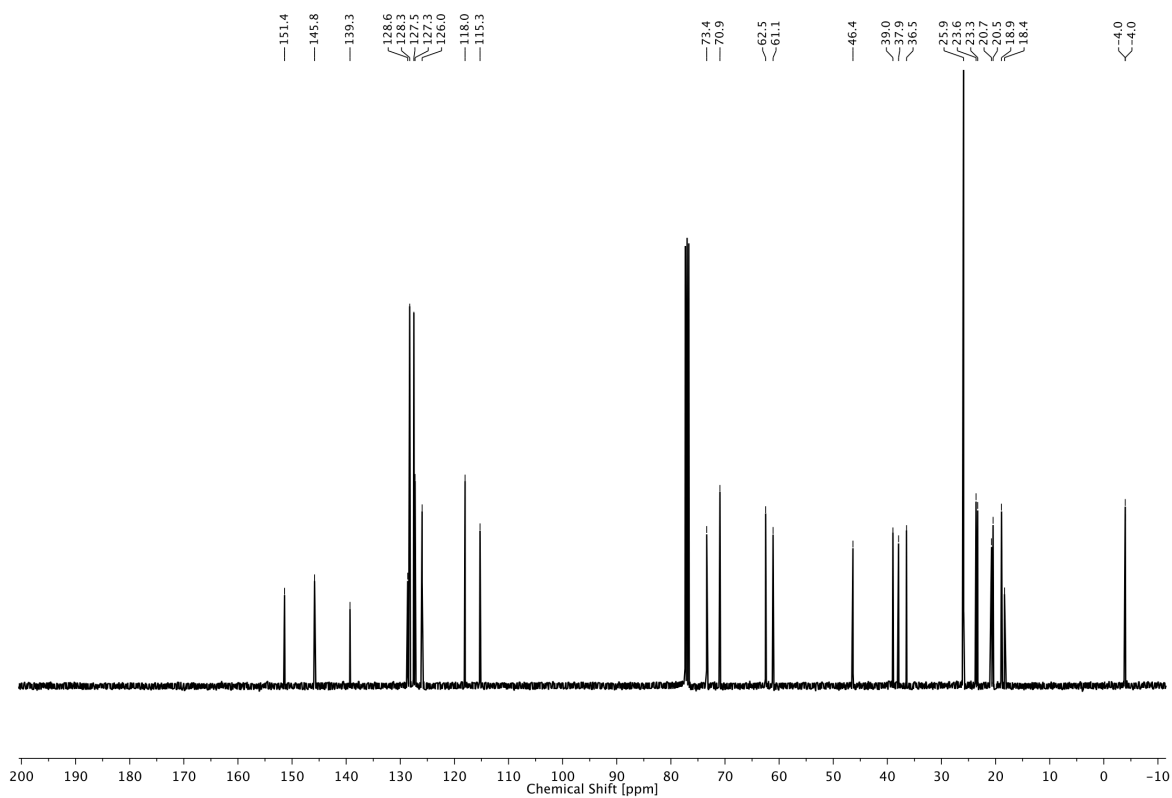
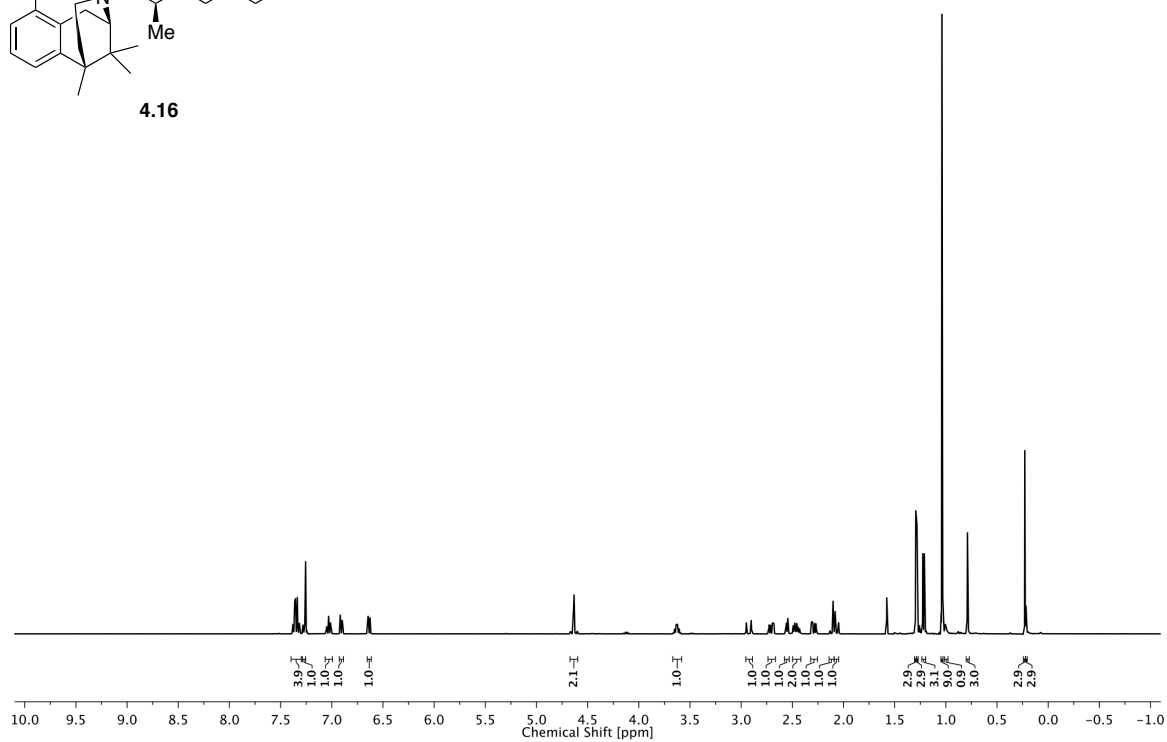
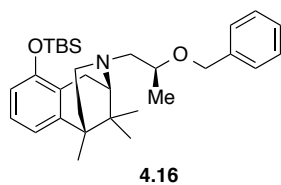
4 PHOTOCROMIC LIGANDS FOR VOLTAGE-GATED SODIUM CHANNELS



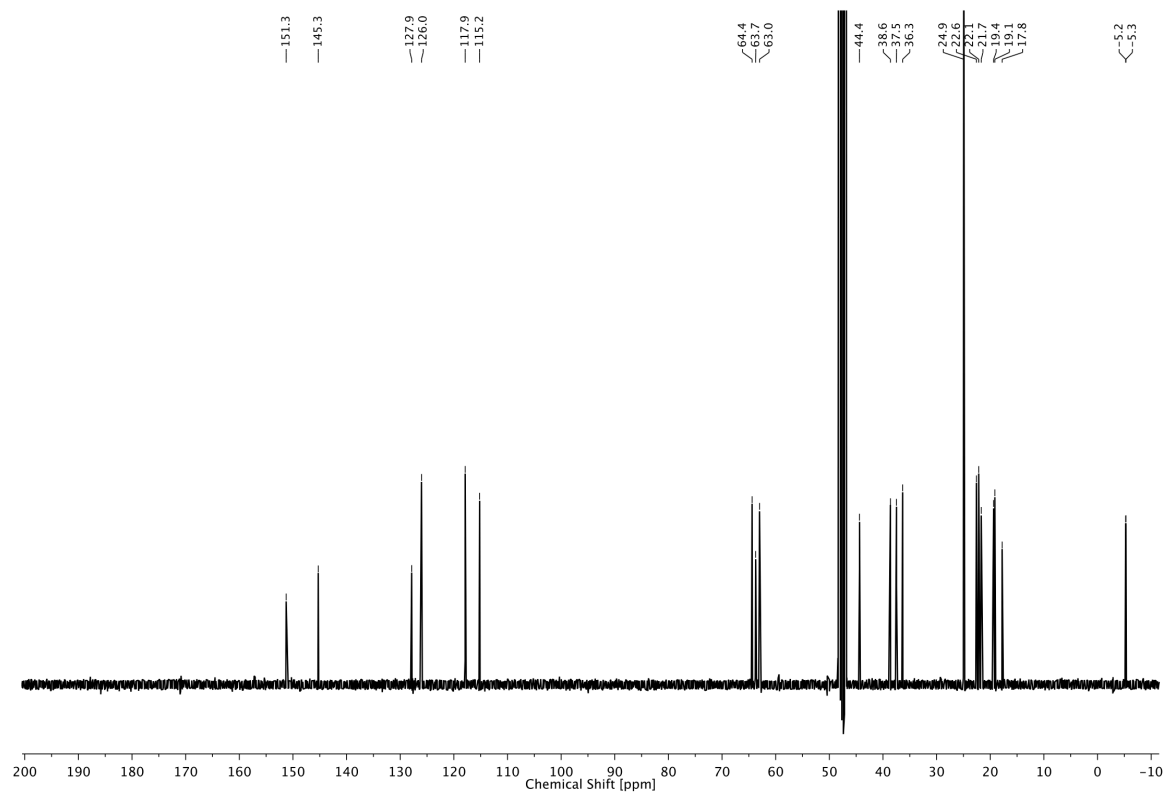
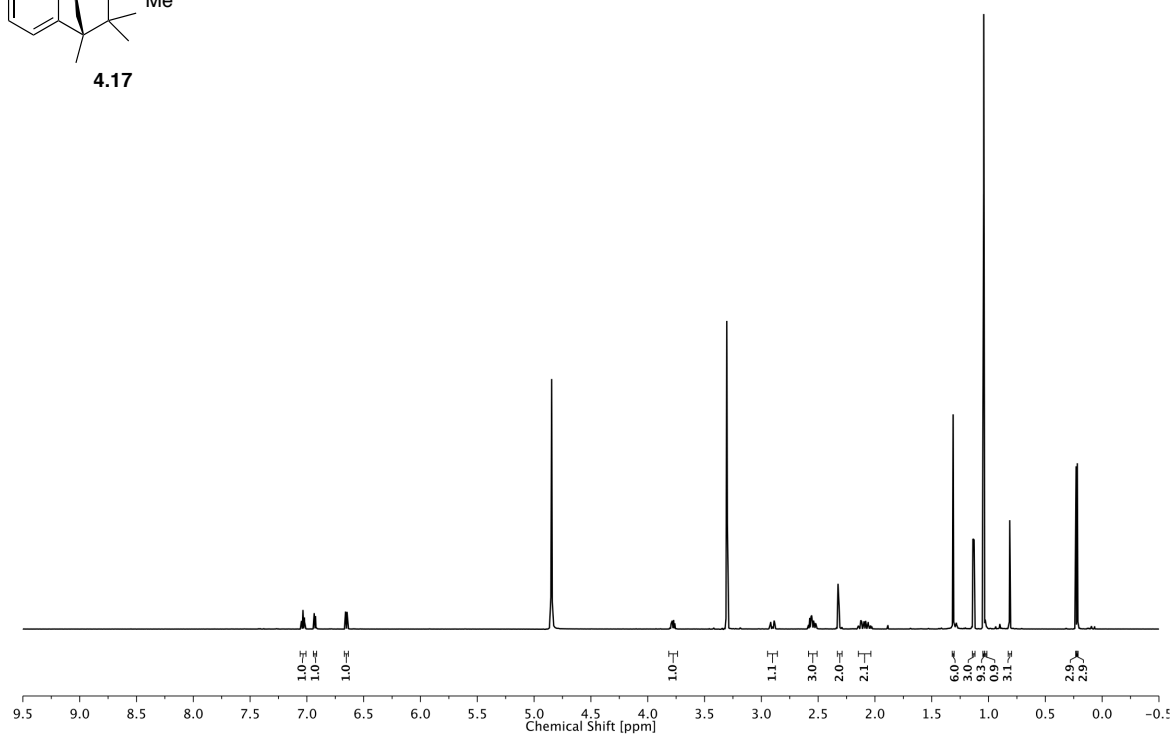
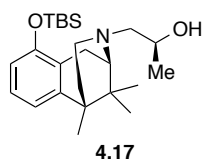
ALTG



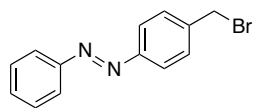
4 PHOTOCROMIC LIGANDS FOR VOLTAGE-GATED SODIUM CHANNELS



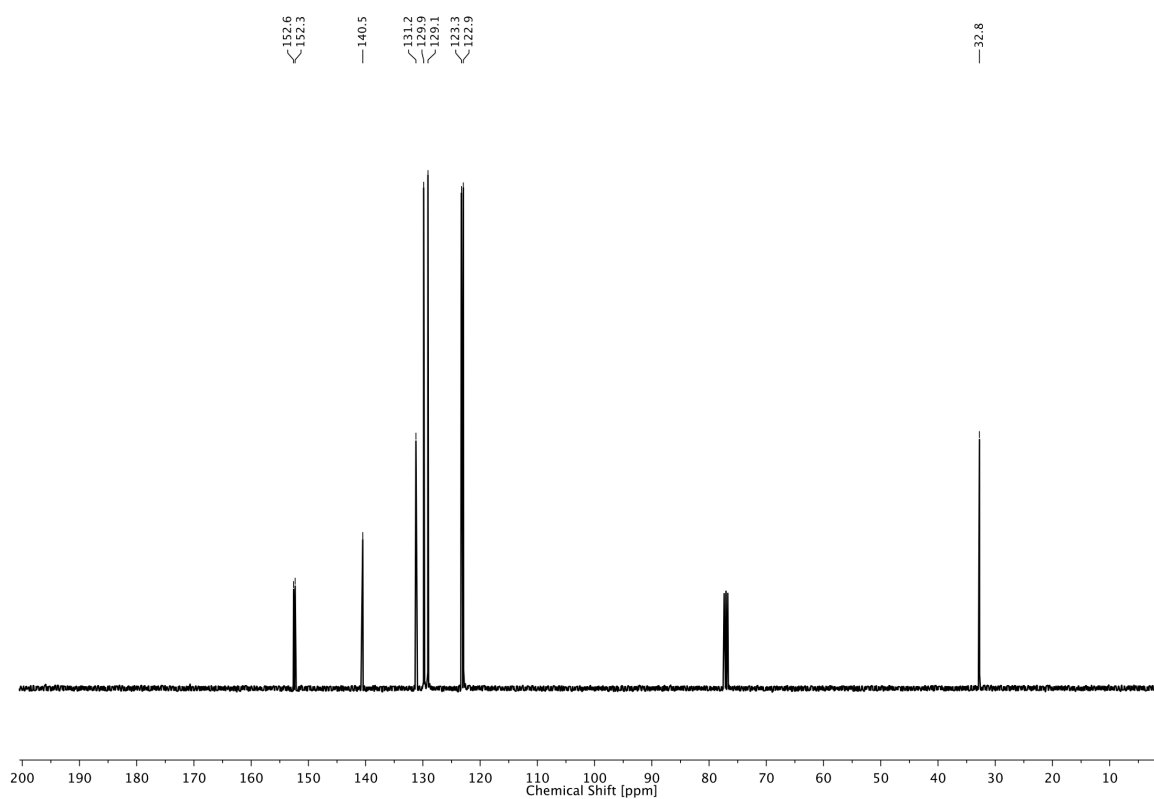
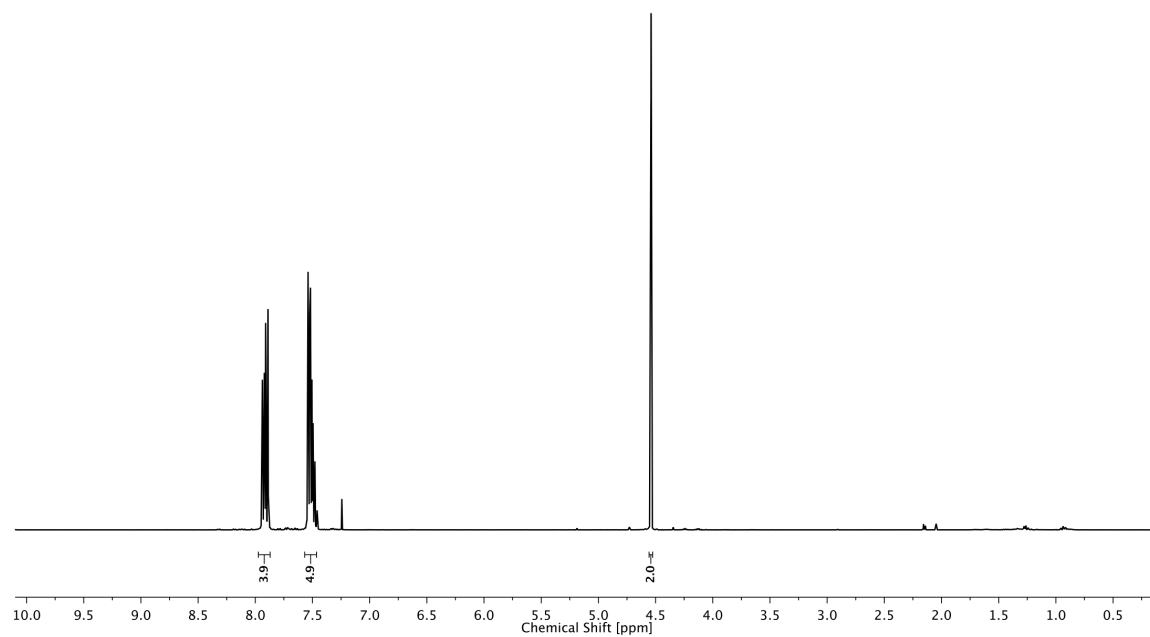
4 PHOTOCROMIC LIGANDS FOR VOLTAGE-GATED SODIUM CHANNELS

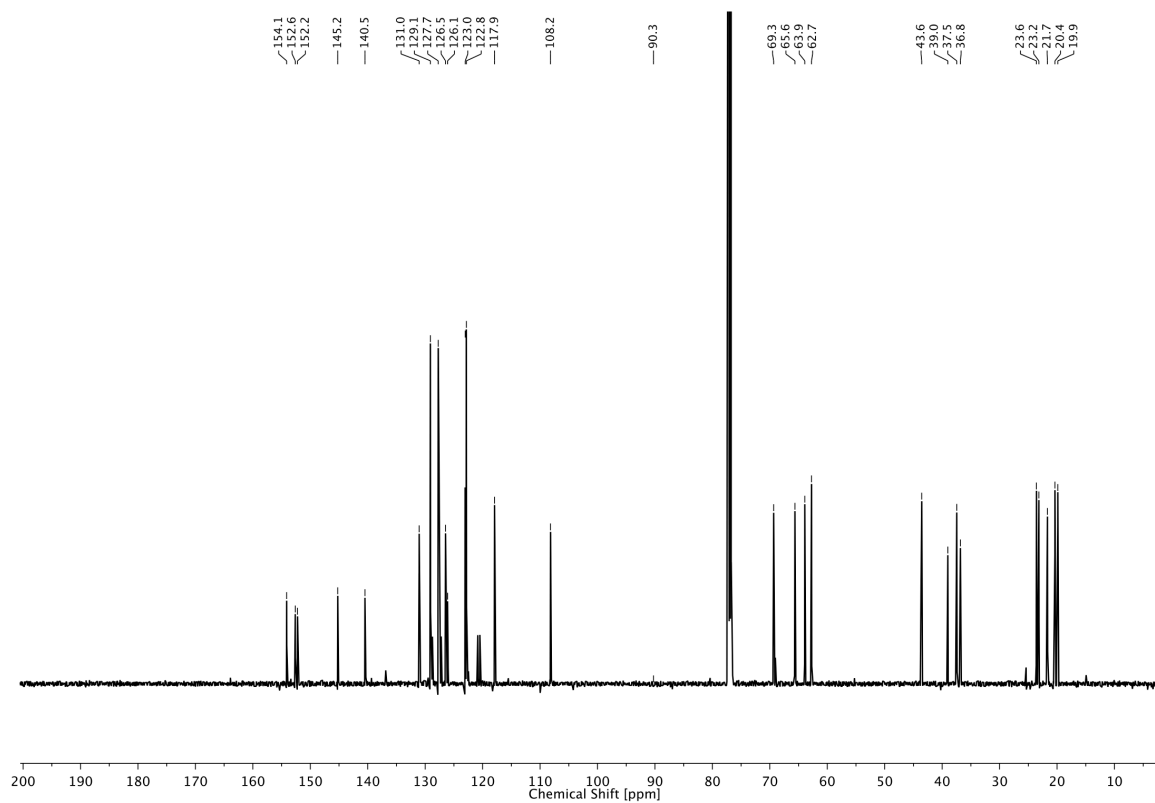
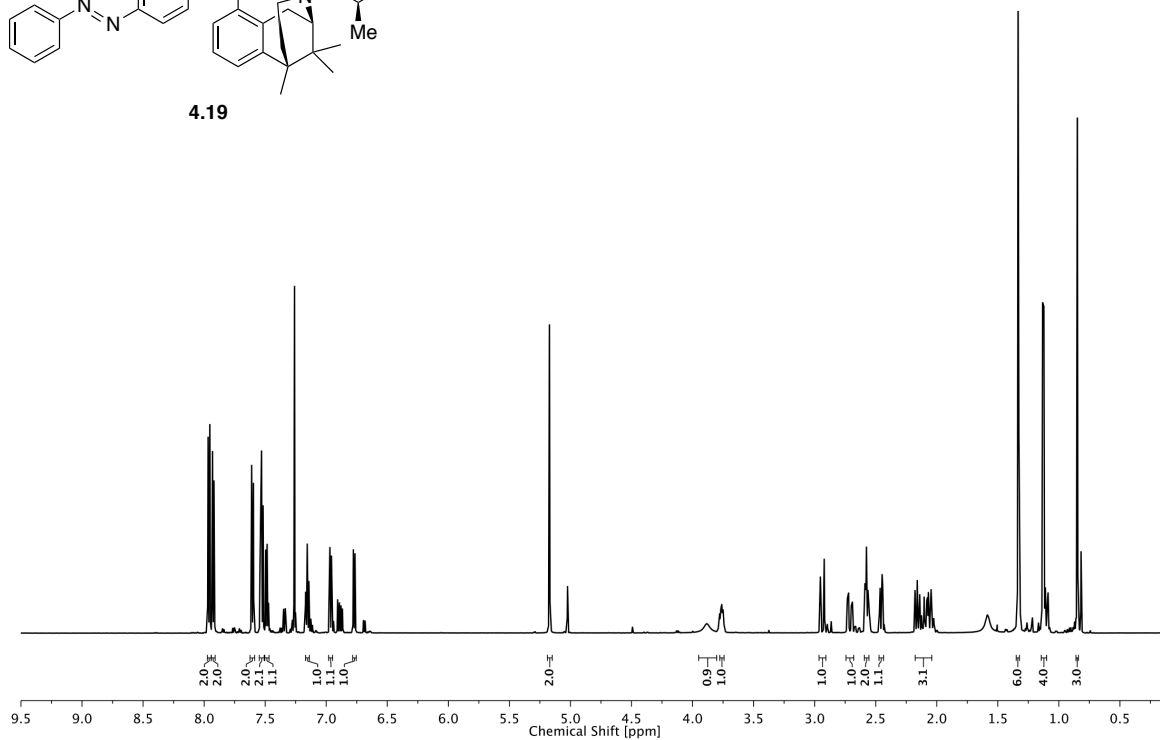
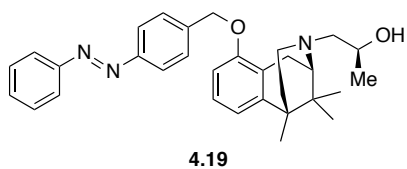


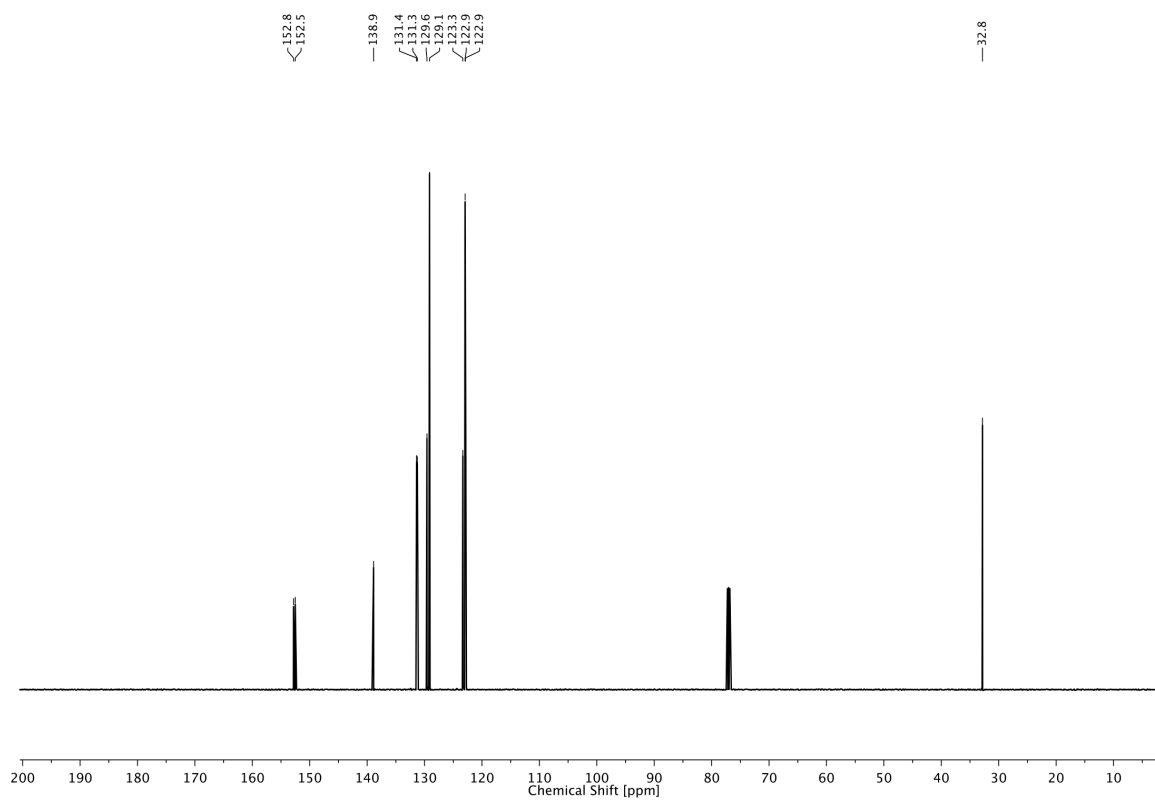
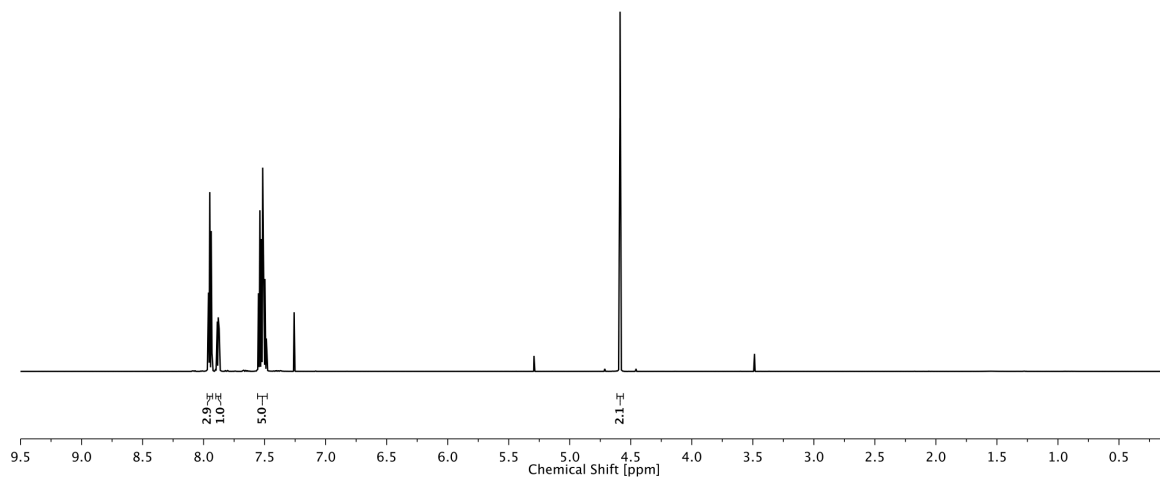
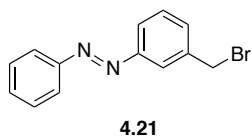
4 PHOTOCROMIC LIGANDS FOR VOLTAGE-GATED SODIUM CHANNELS

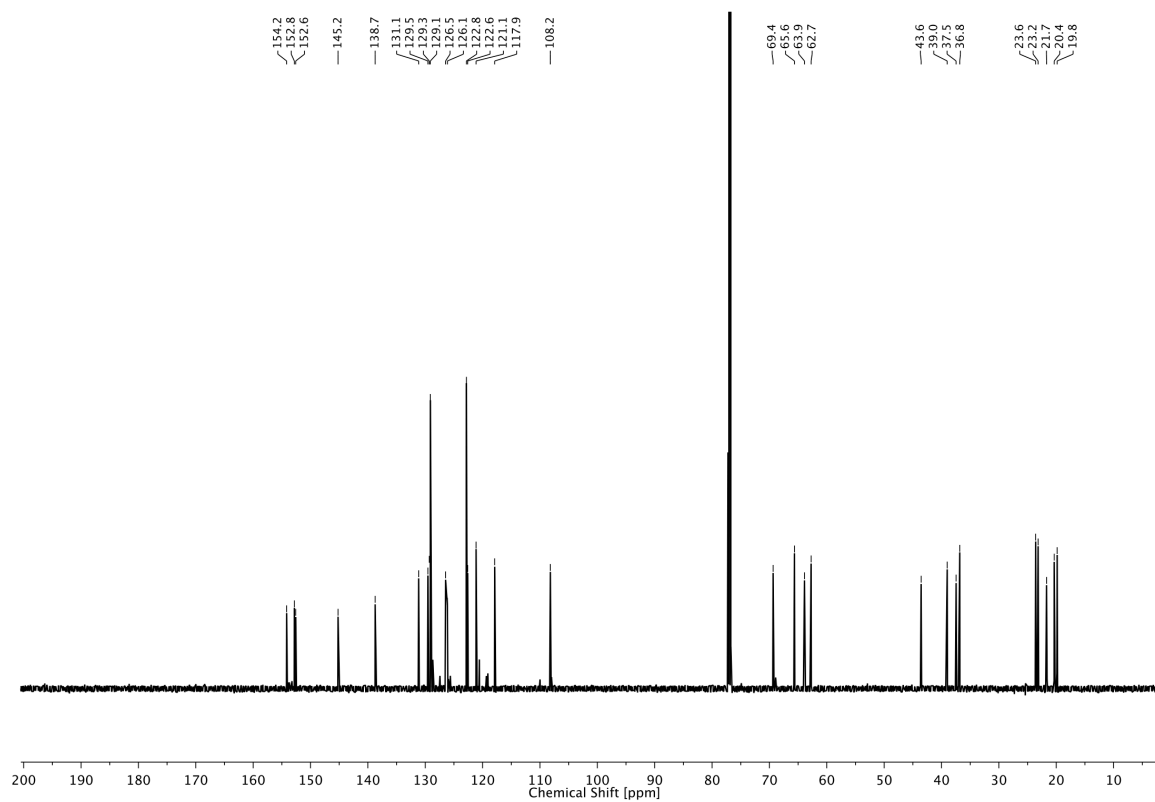
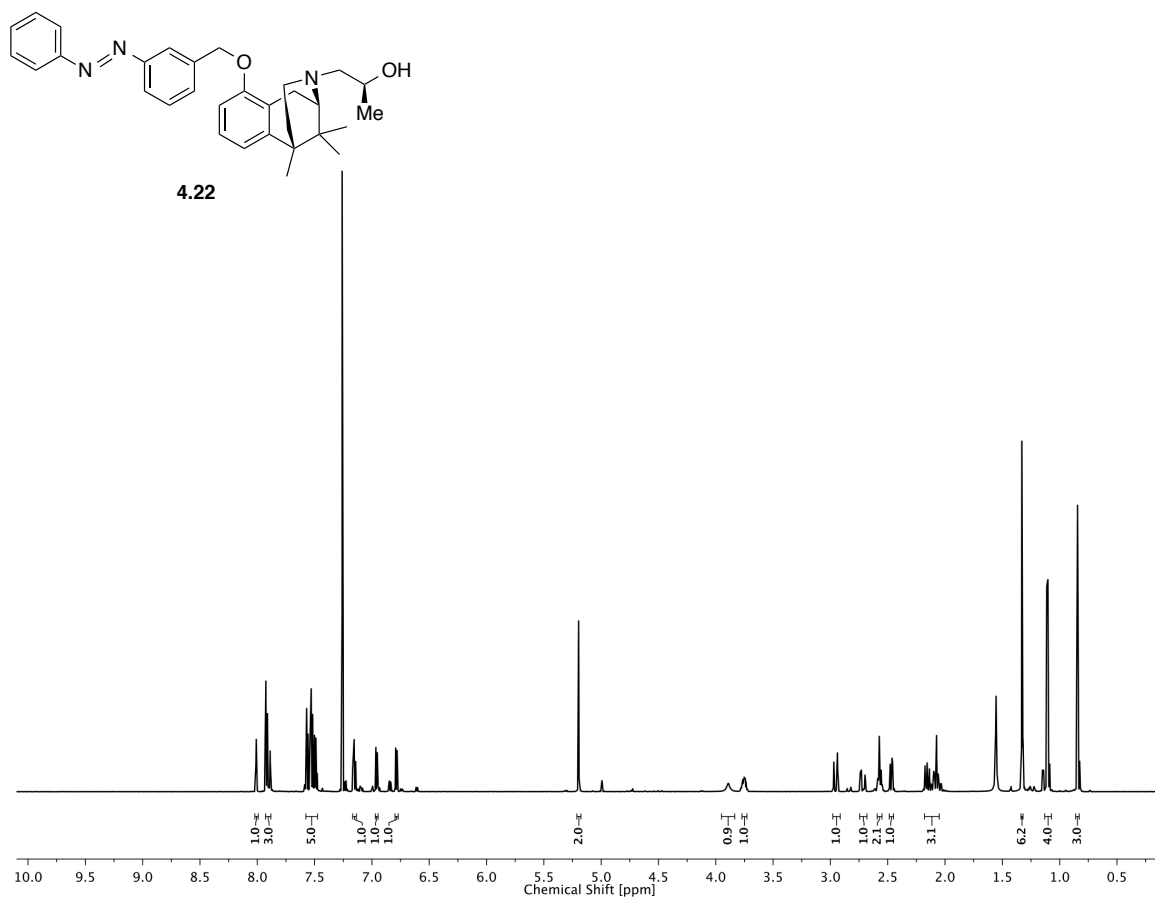


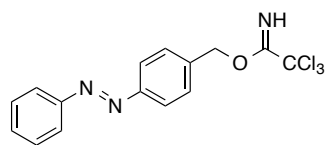
4.18



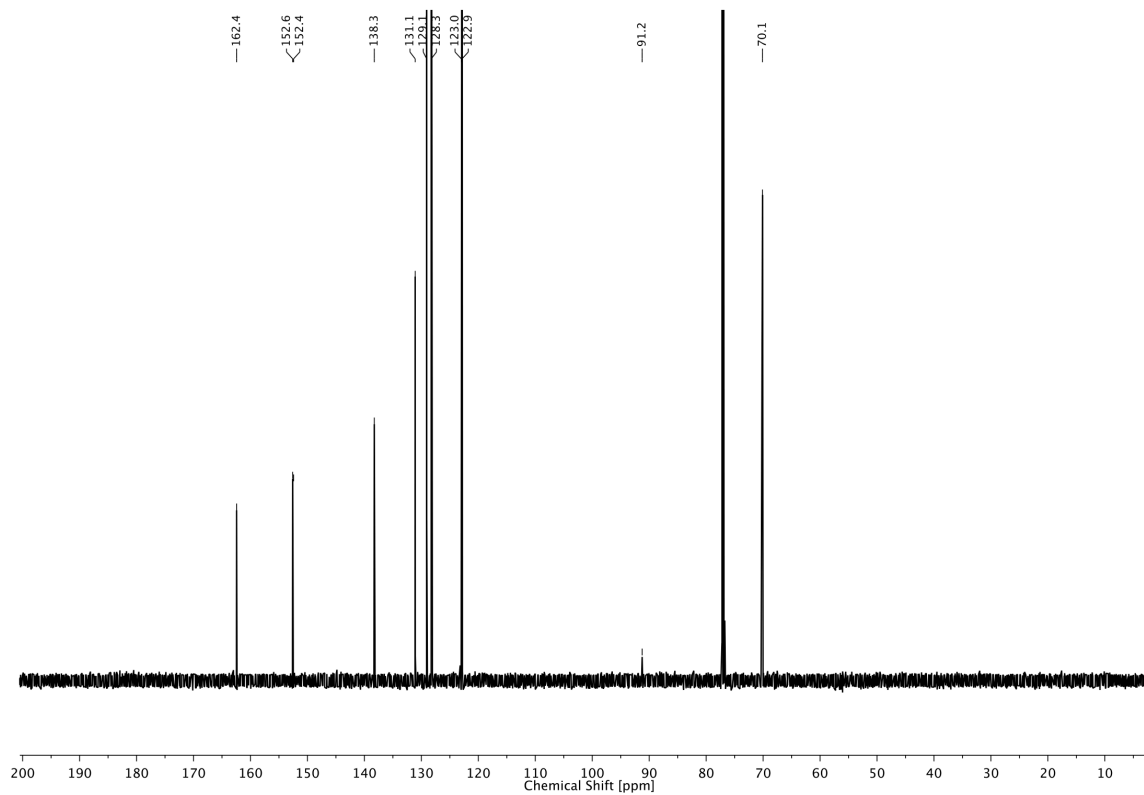
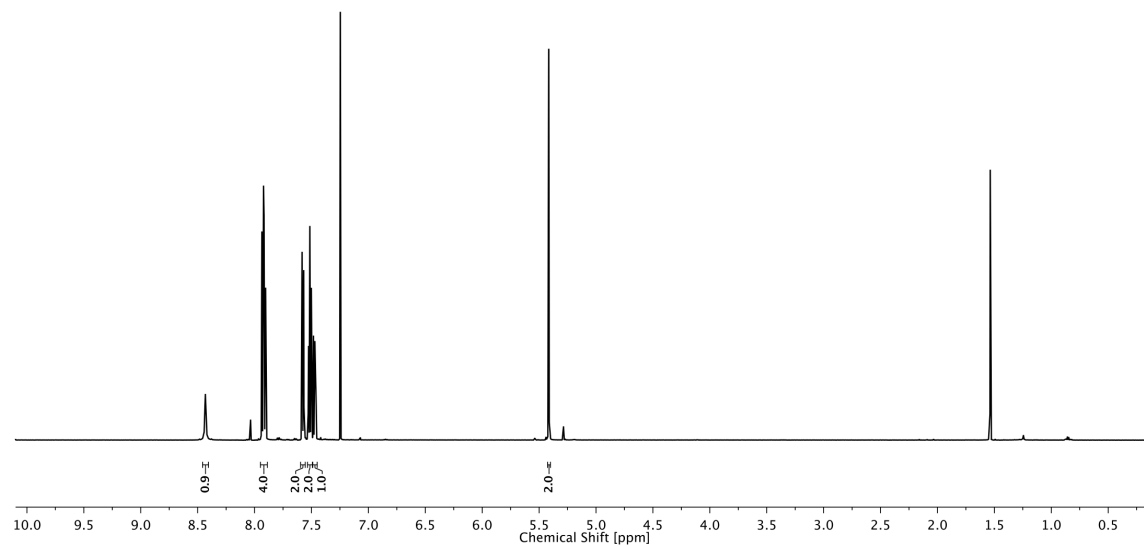




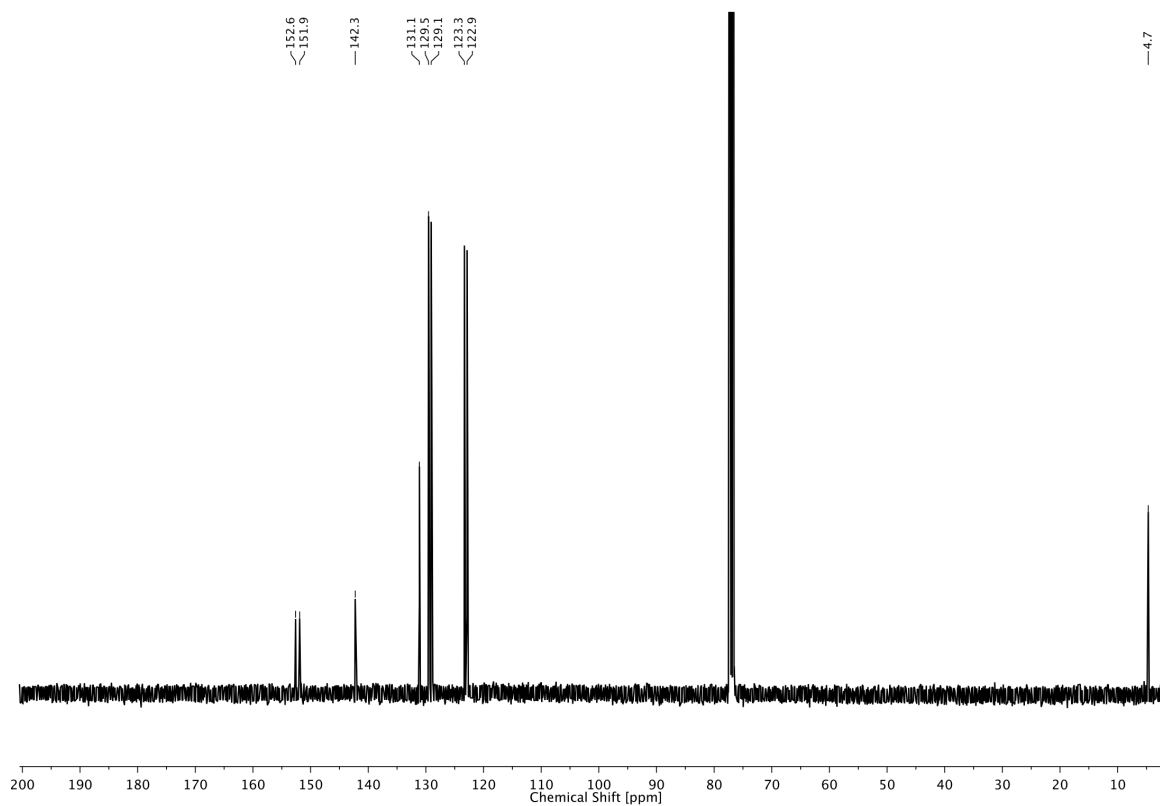
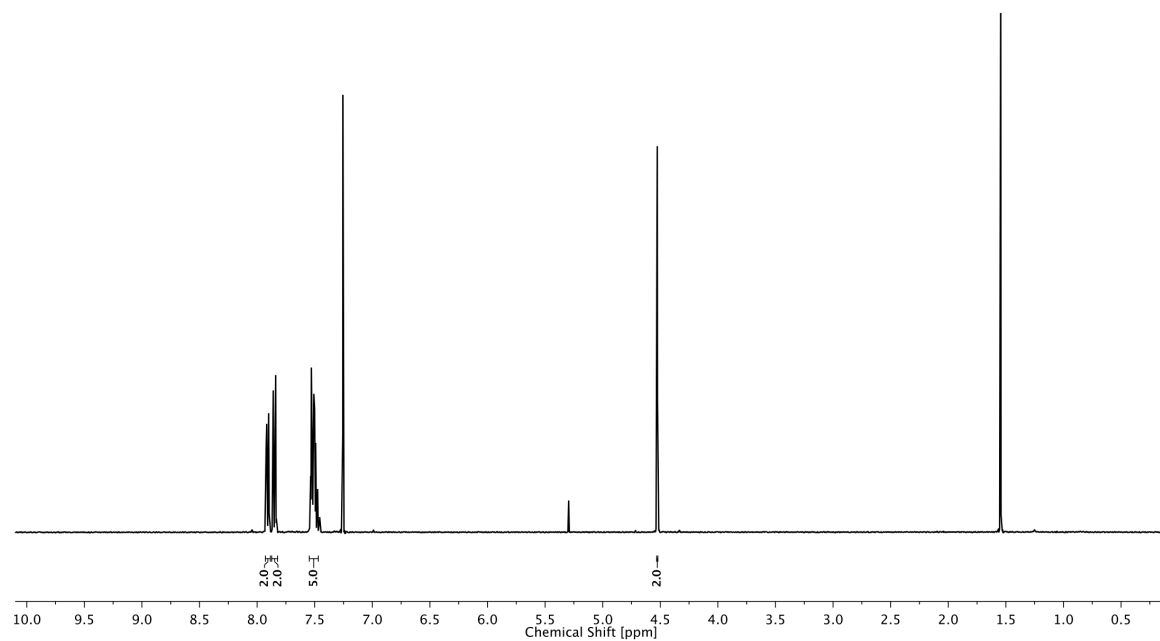
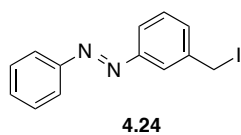


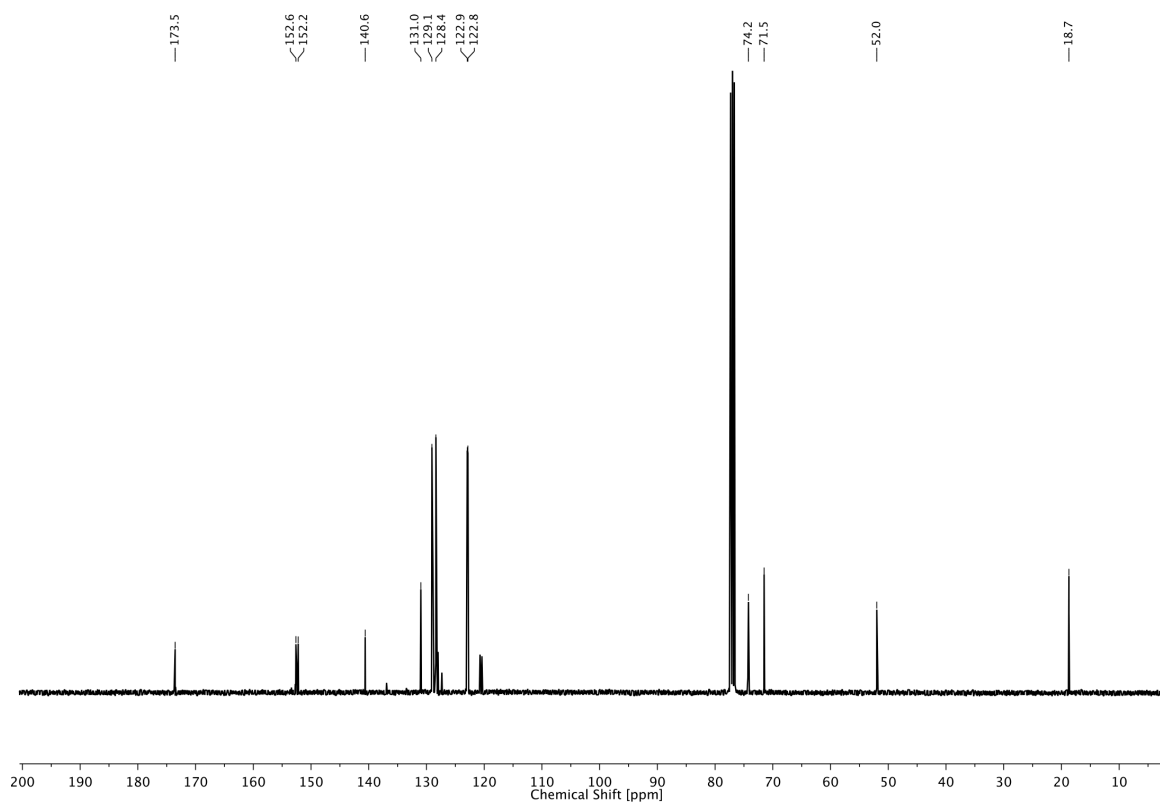
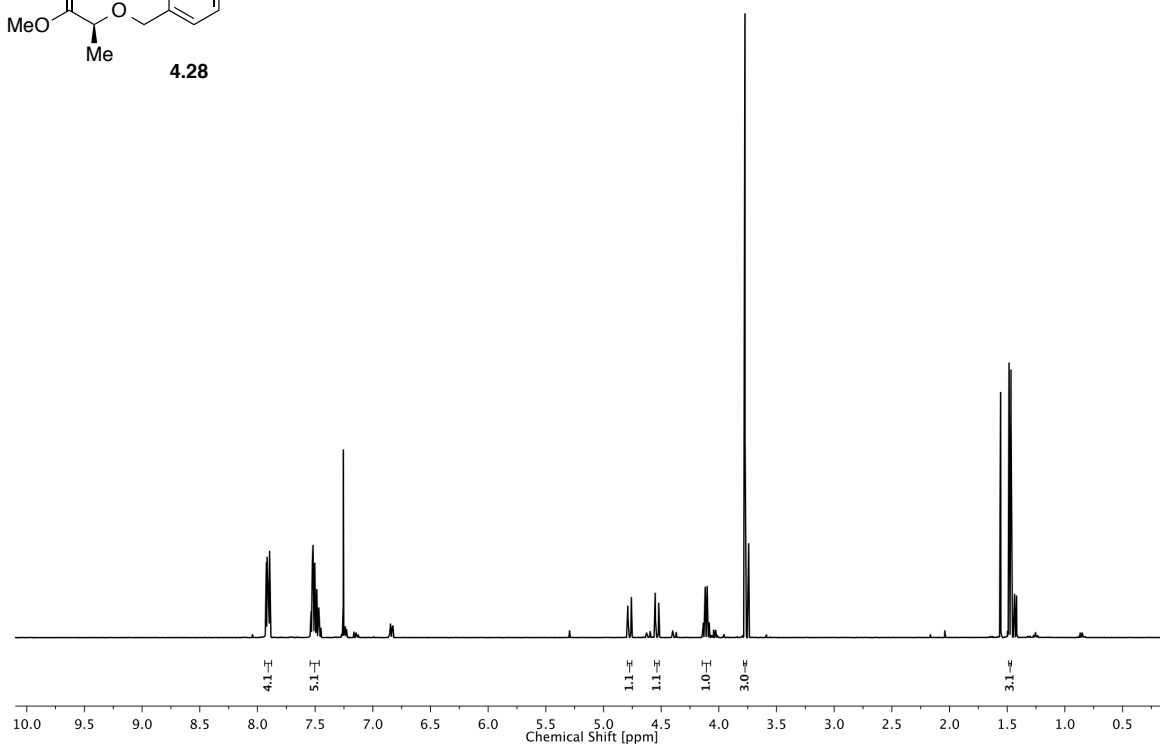
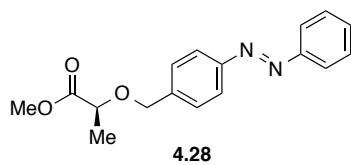


4.23

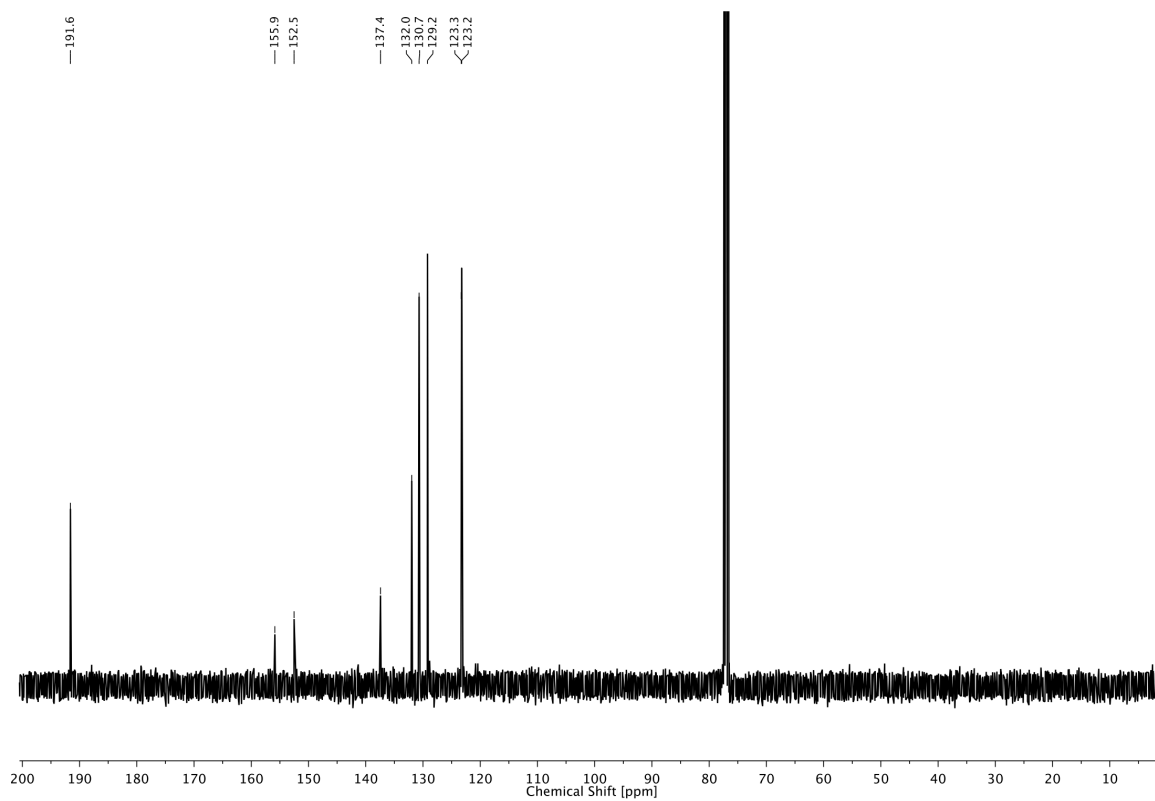
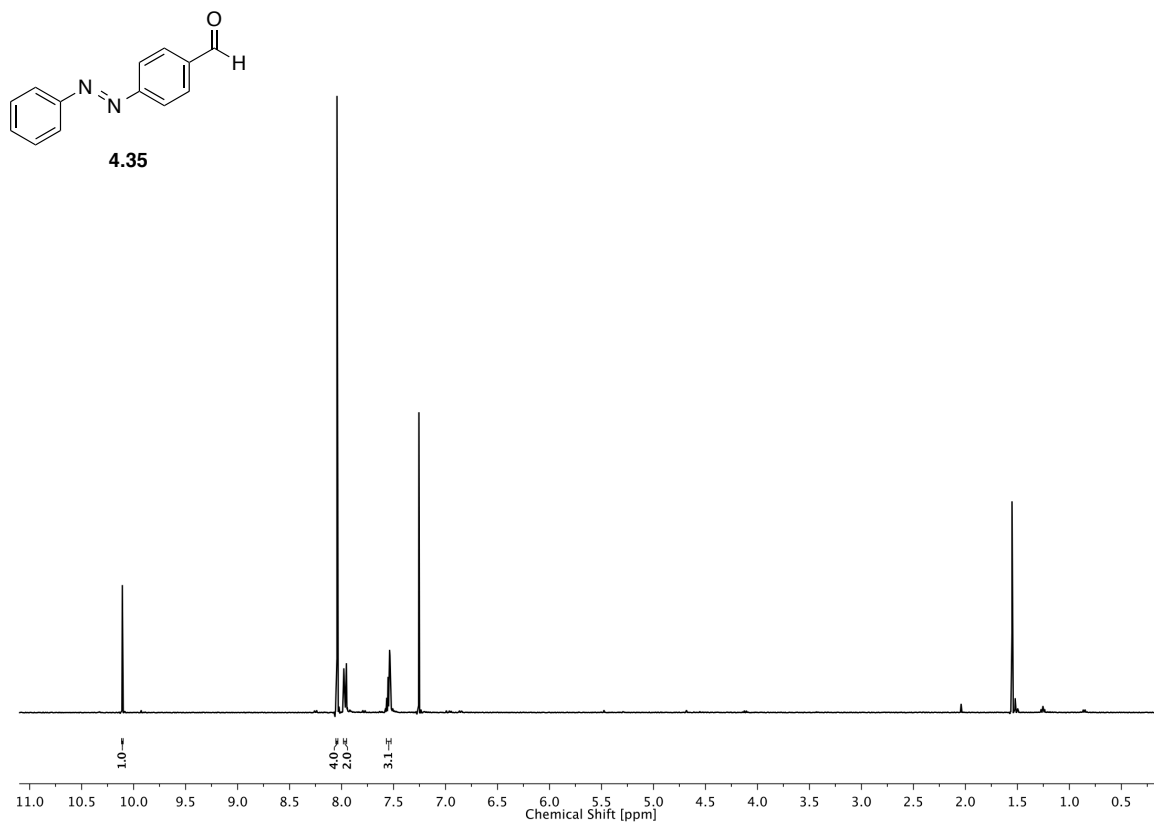


4 PHOTOCROMIC LIGANDS FOR VOLTAGE-GATED SODIUM CHANNELS

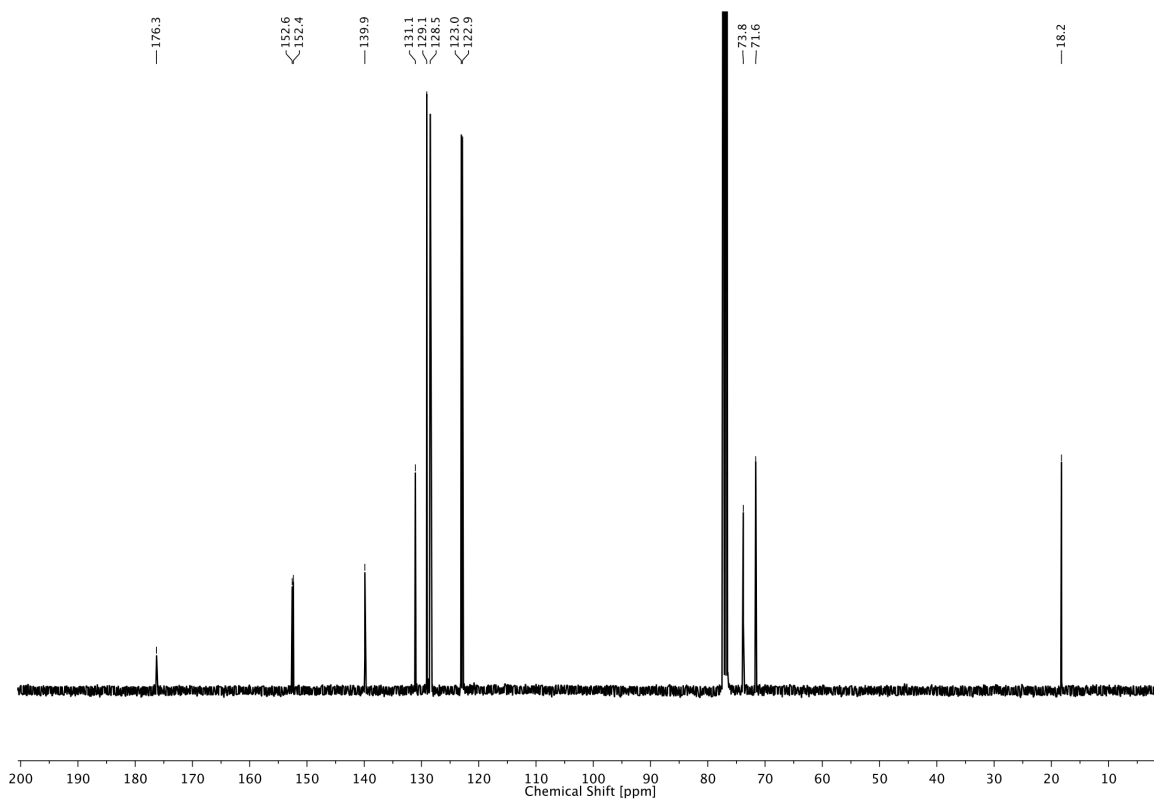
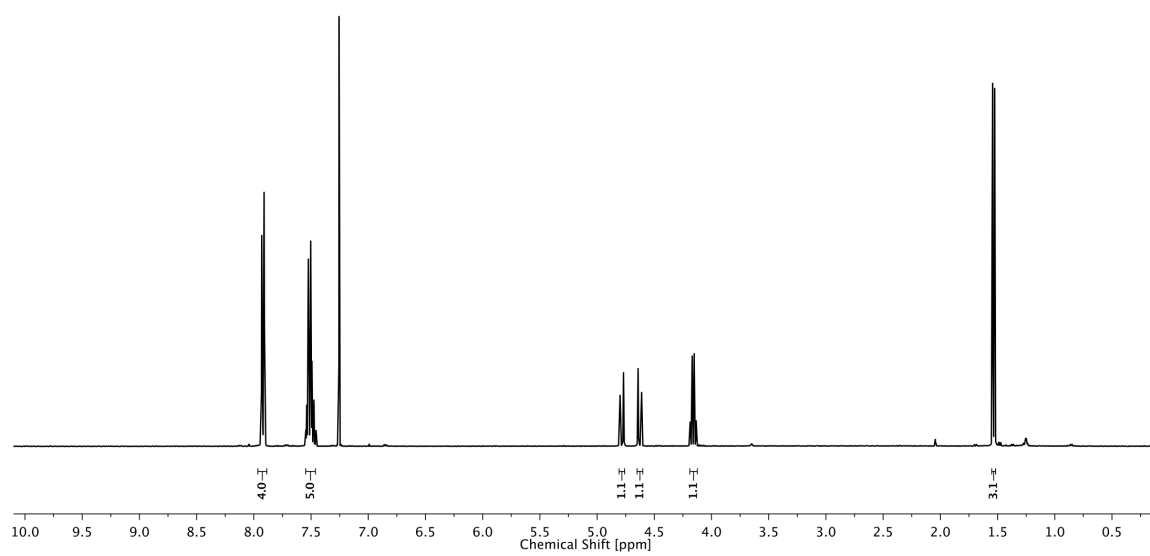
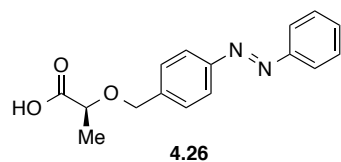


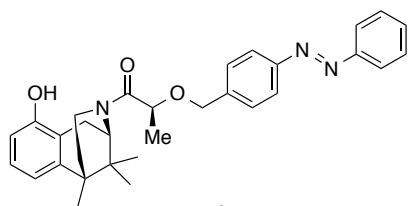


4 PHOTOCROMIC LIGANDS FOR VOLTAGE-GATED SODIUM CHANNELS

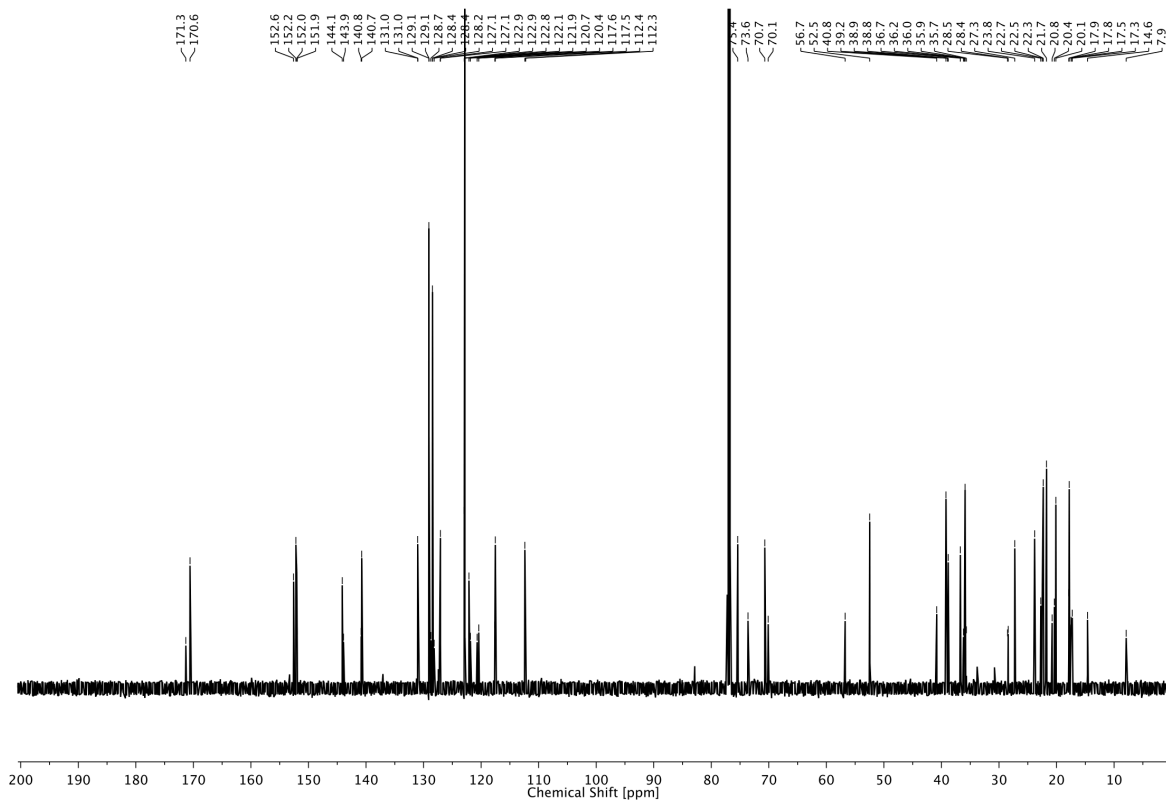
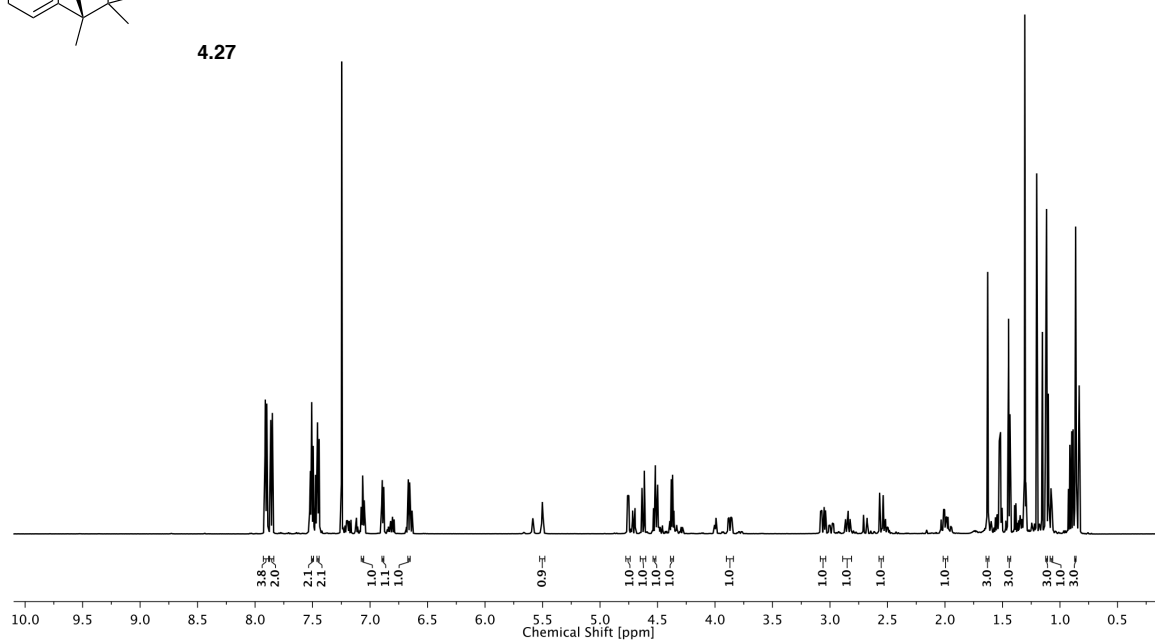


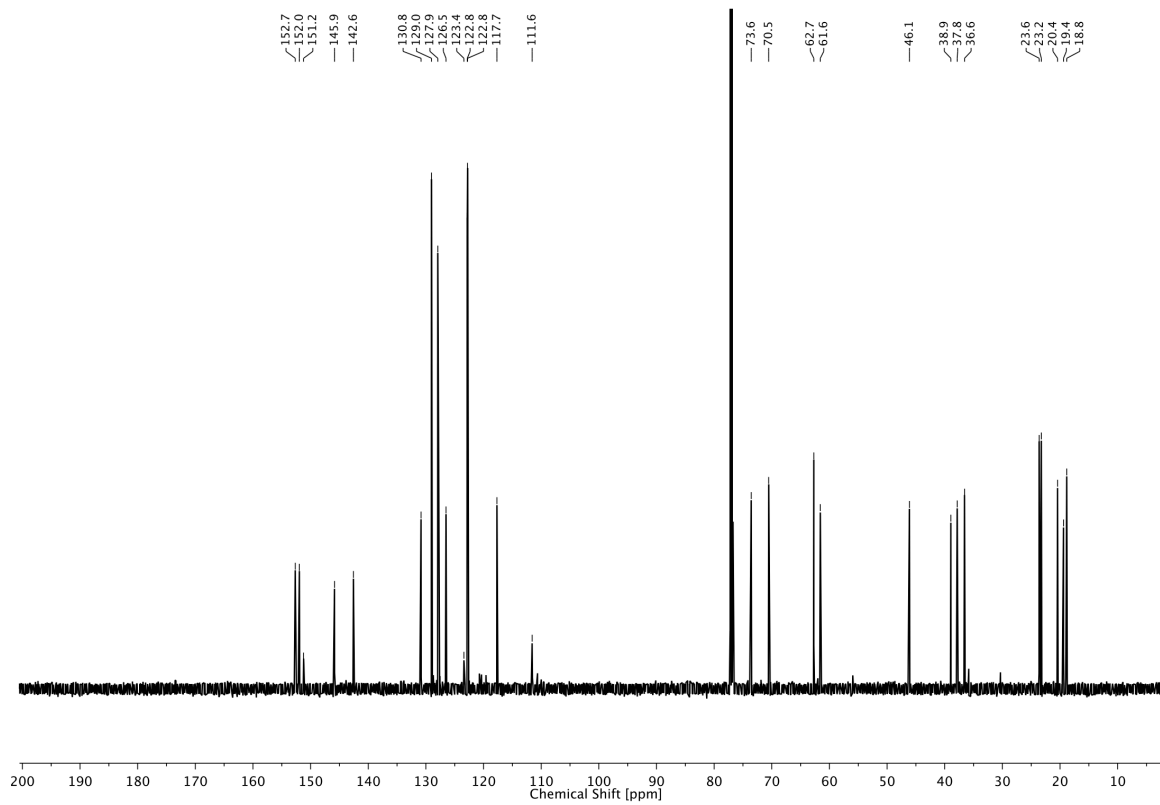
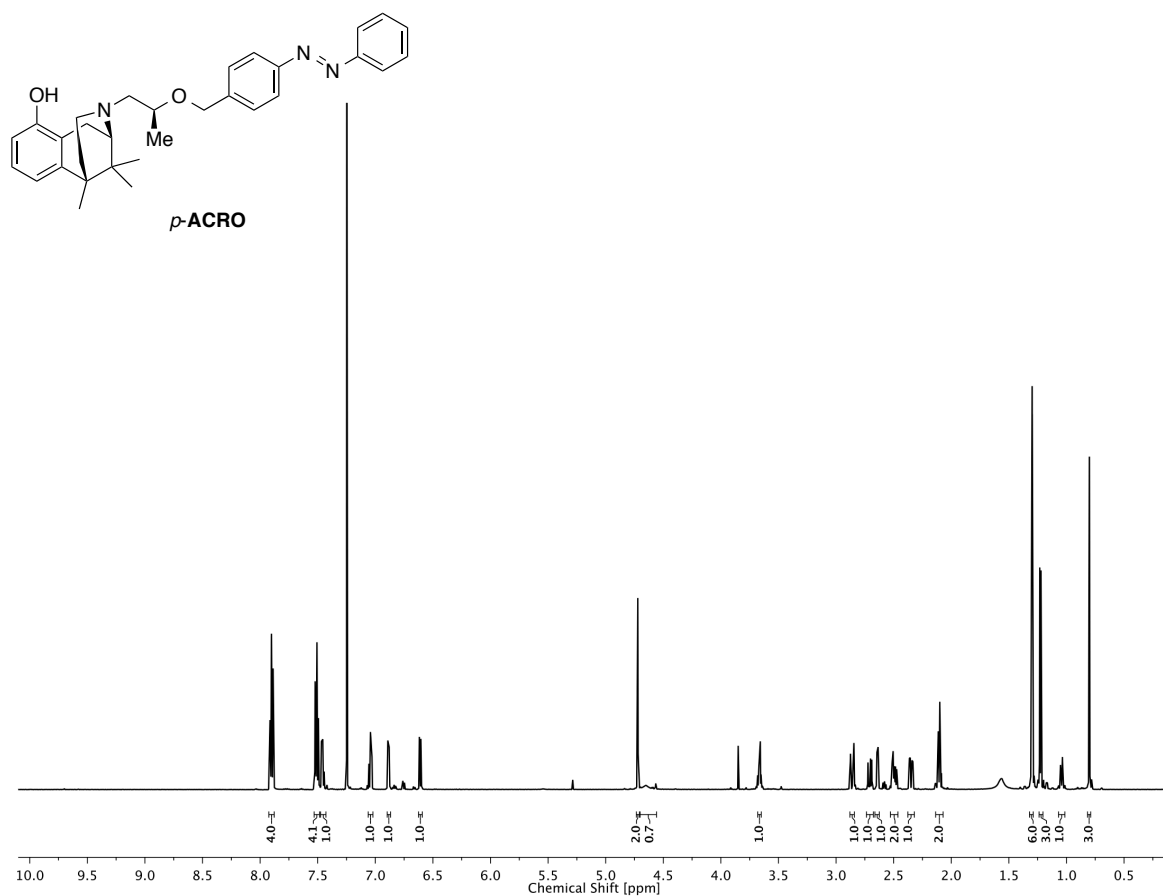
4 PHOTOCROMIC LIGANDS FOR VOLTAGE-GATED SODIUM CHANNELS



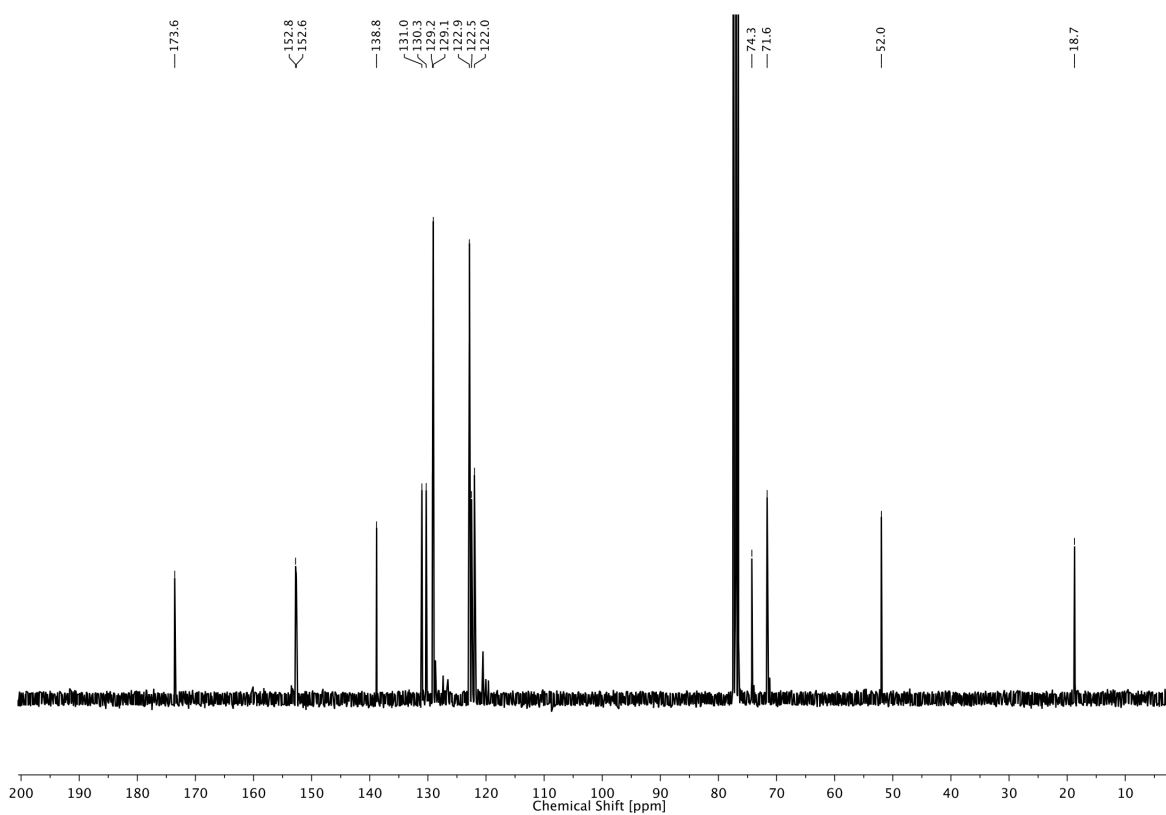
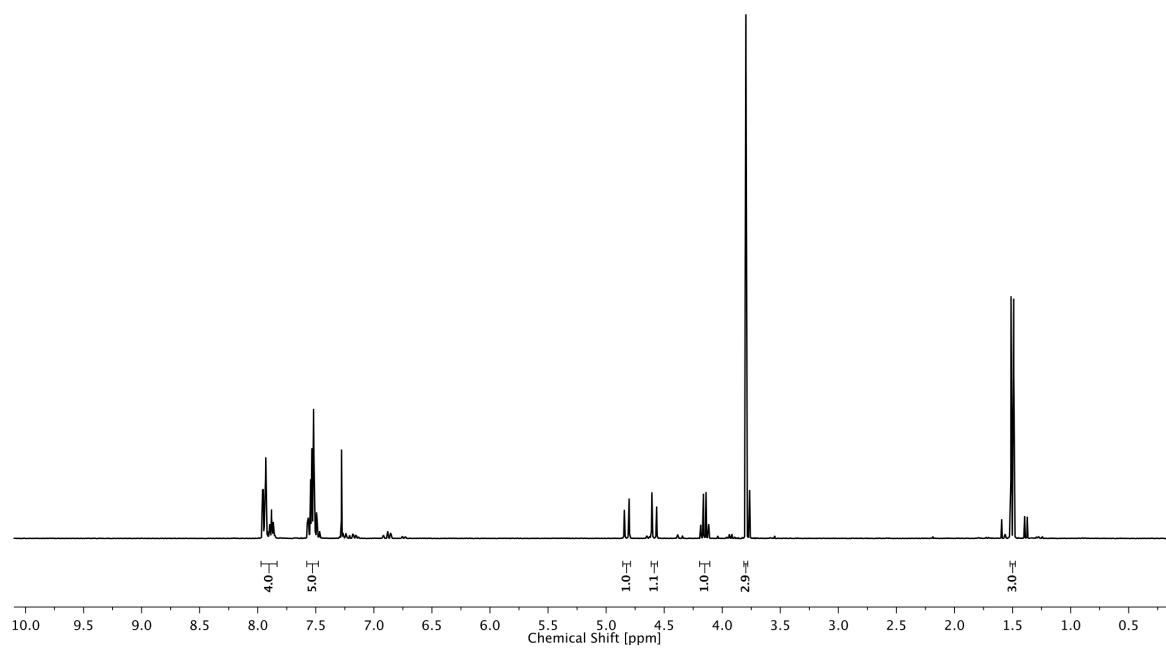
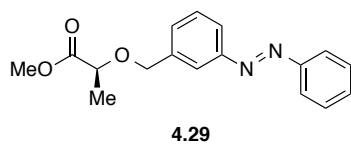


4.27

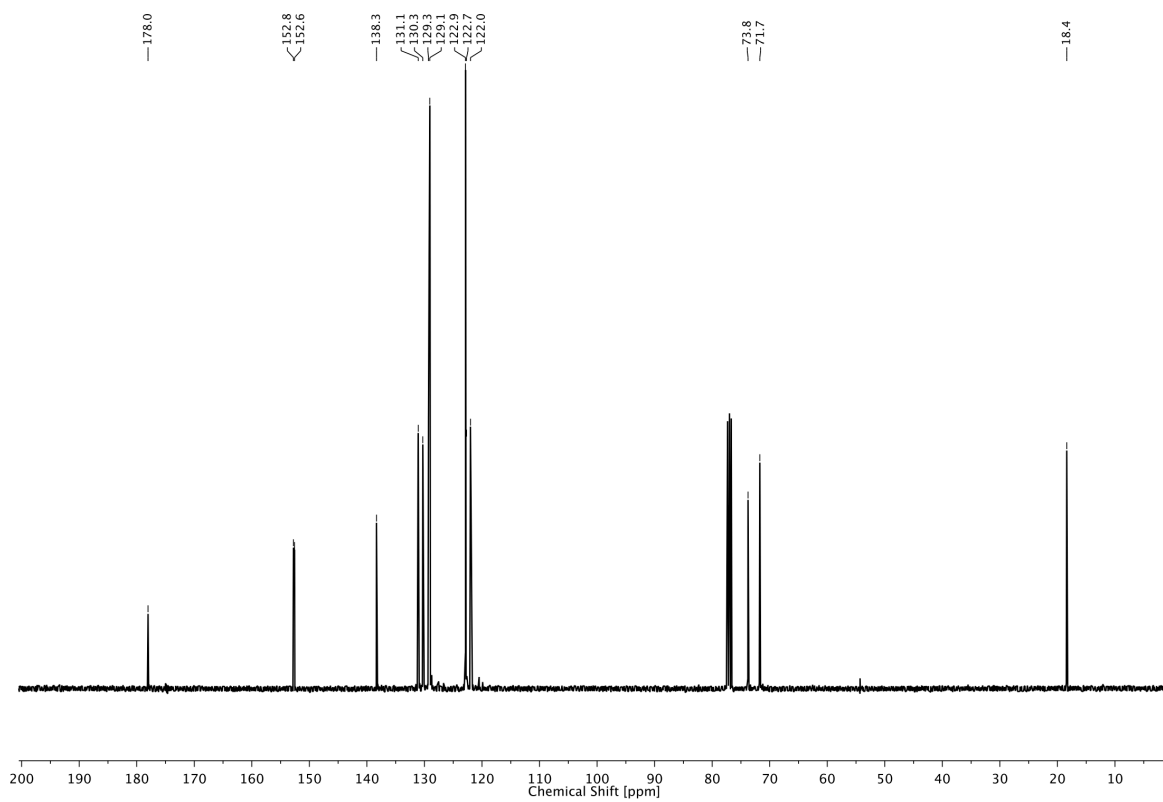
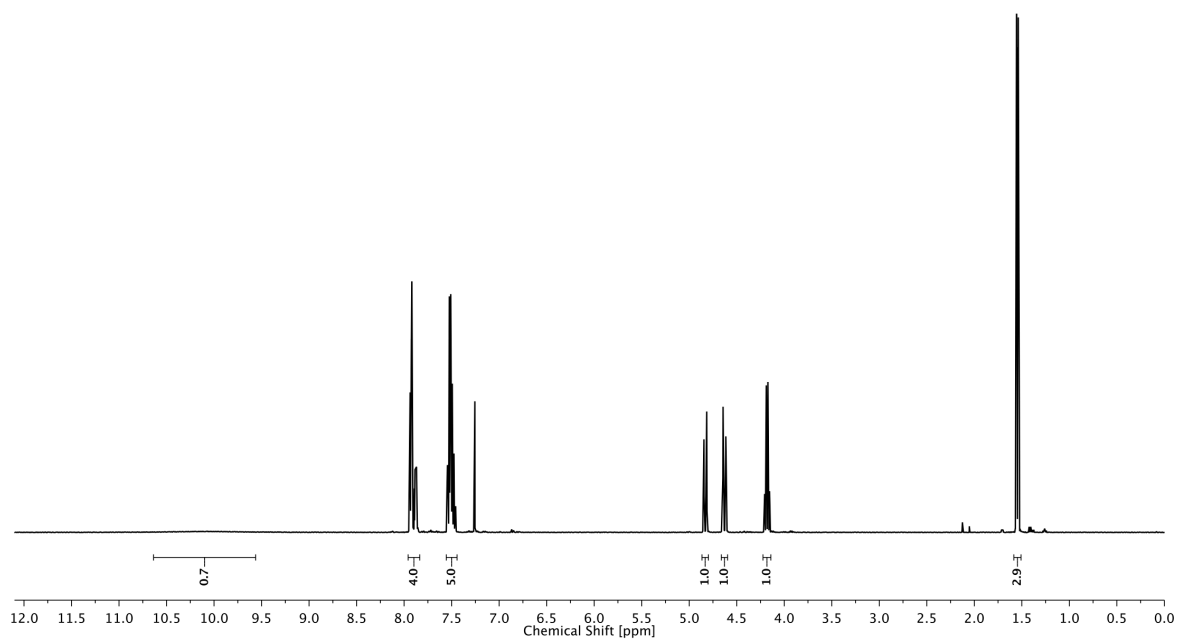
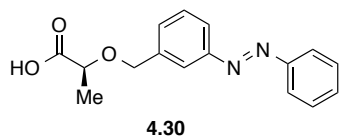


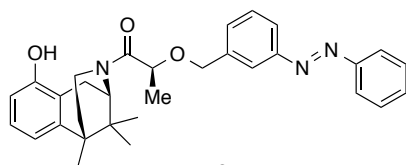


4 PHOTOCROMIC LIGANDS FOR VOLTAGE-GATED SODIUM CHANNELS

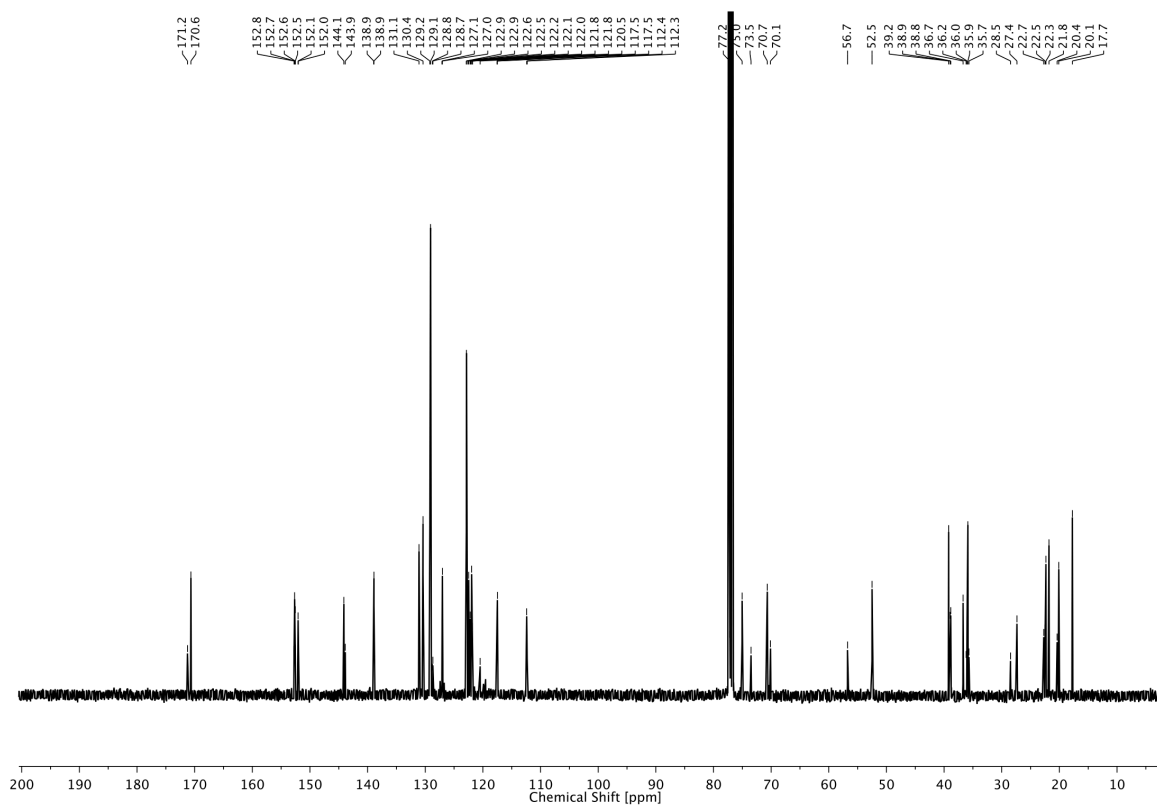
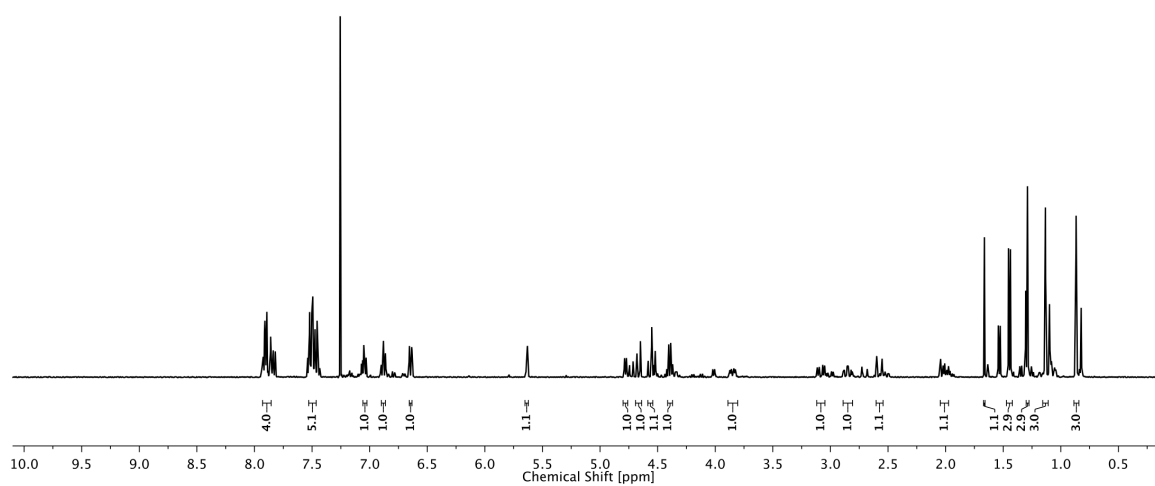


4 PHOTOCROMIC LIGANDS FOR VOLTAGE-GATED SODIUM CHANNELS

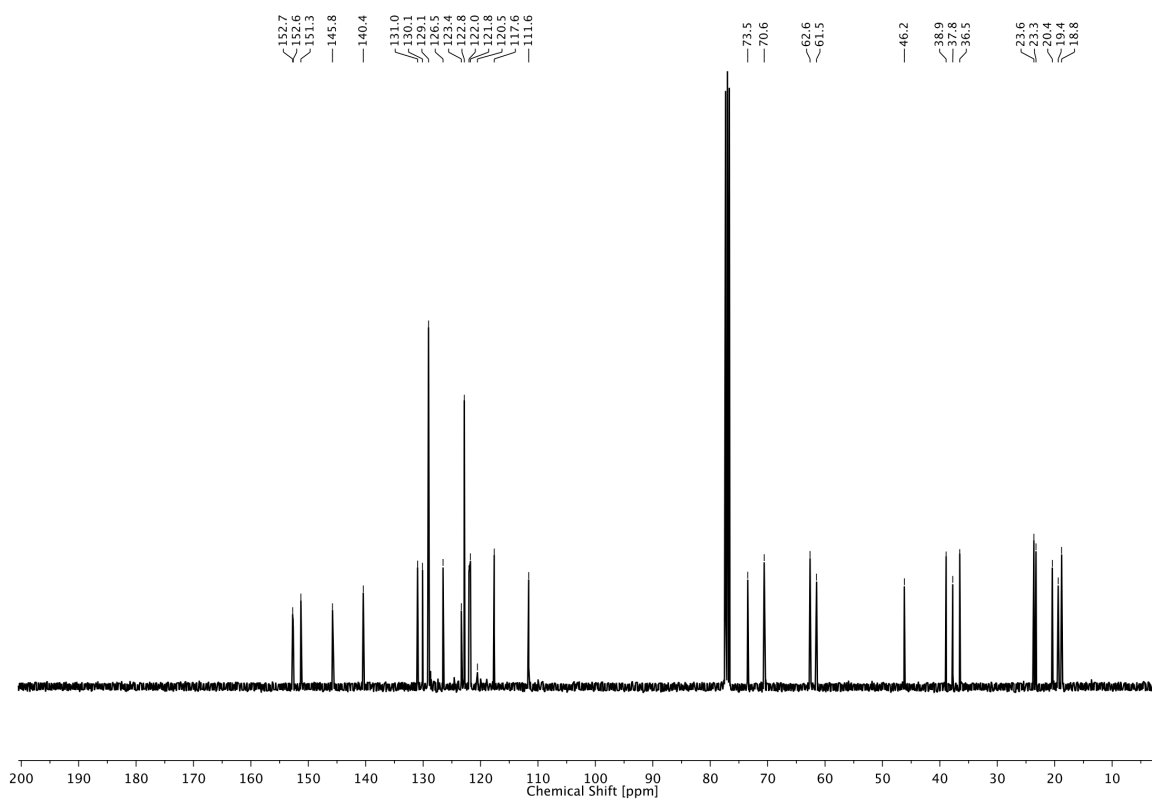
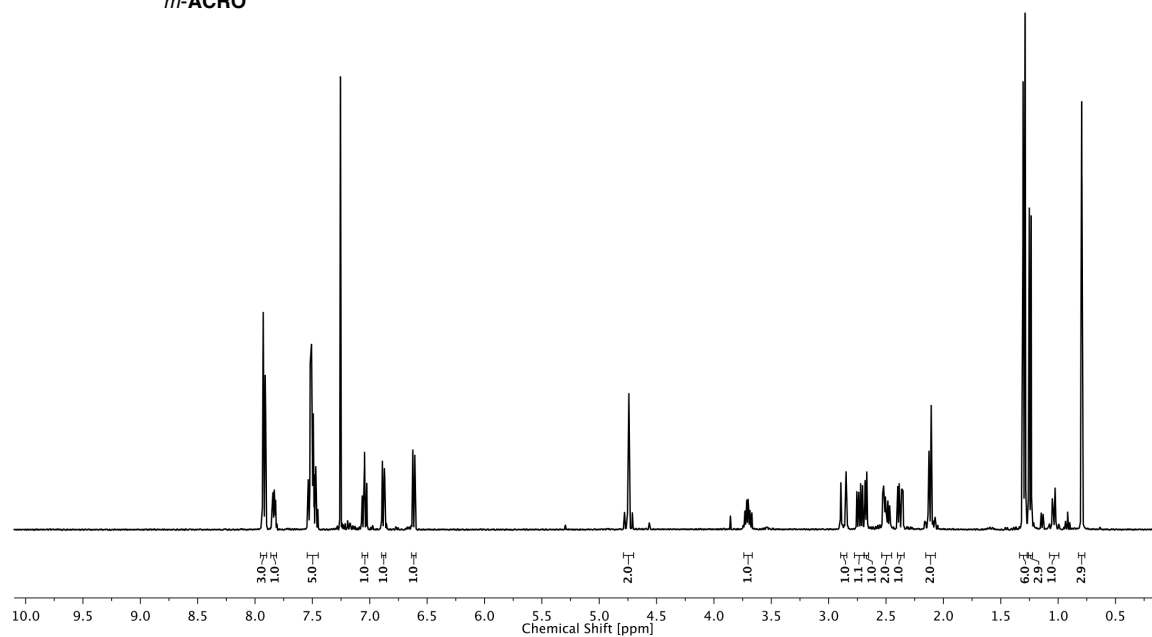
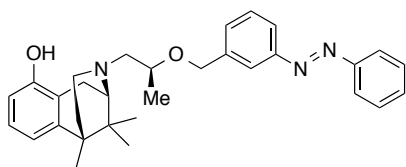




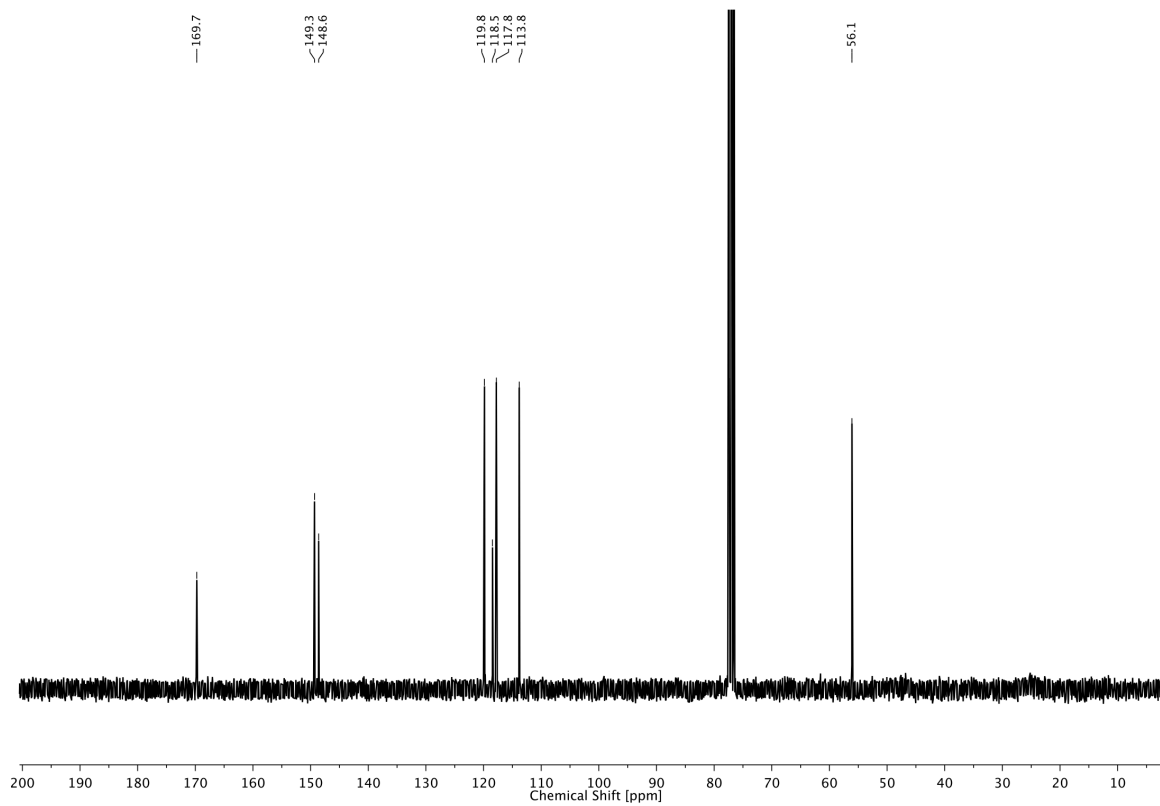
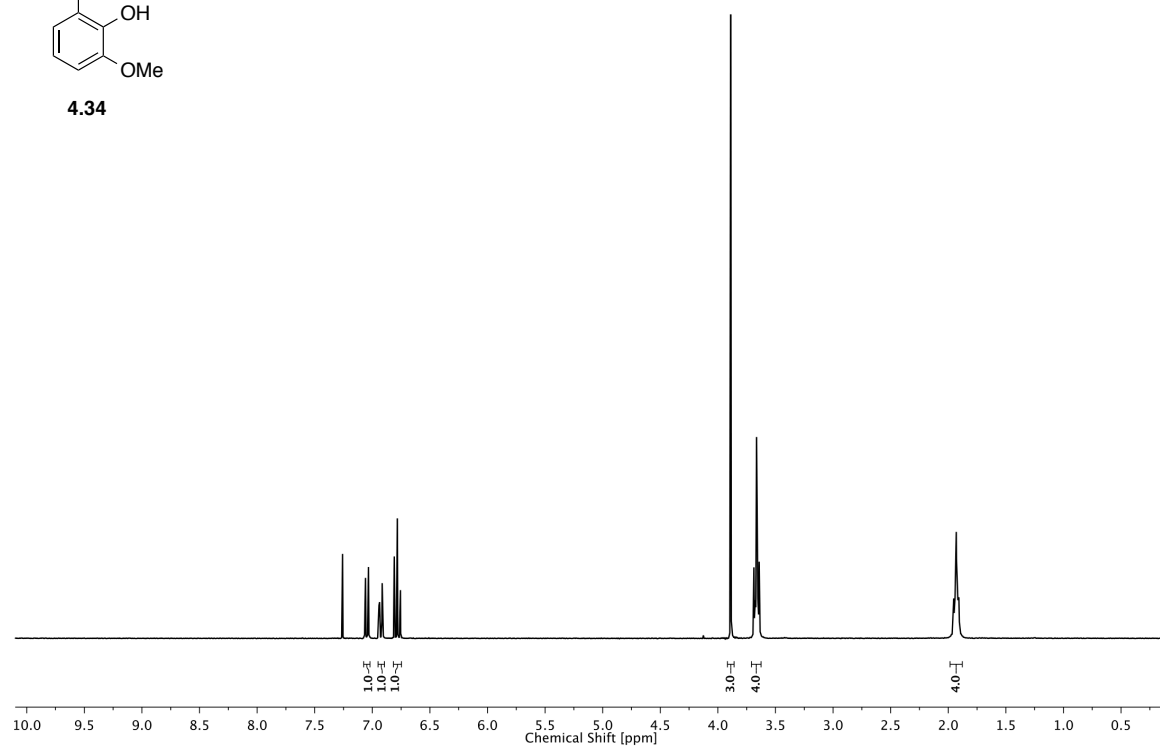
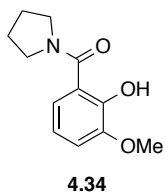
4.31



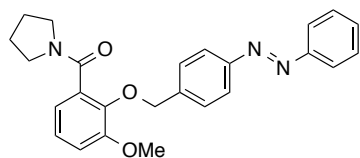
4 PHOTOCROMIC LIGANDS FOR VOLTAGE-GATED SODIUM CHANNELS



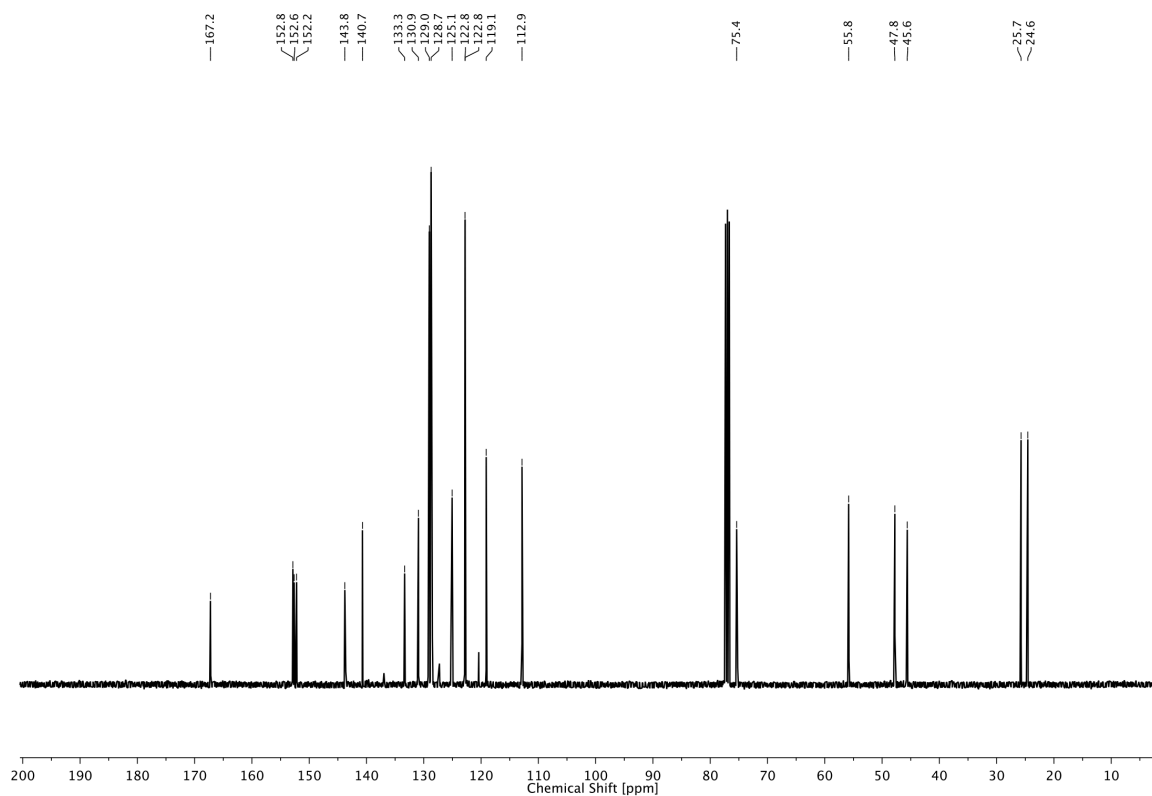
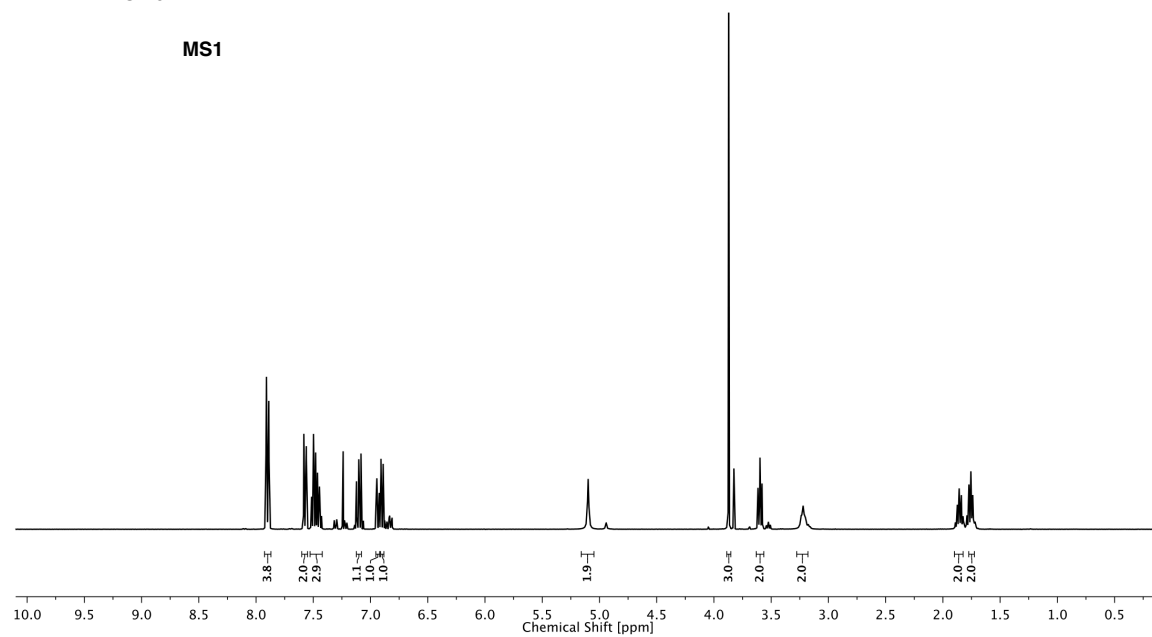
4 PHOTOCROMIC LIGANDS FOR VOLTAGE-GATED SODIUM CHANNELS



4 PHOTOCROMIC LIGANDS FOR VOLTAGE-GATED SODIUM CHANNELS



MS1



4.8 LITERATURE

- [1] D. P. Ryan, L. J. Ptacek, *Neuron* **2010**, *68*, 282–292.
- [2] W. A. Catterall, *Trends Pharmacol. Sci.* **1987**, *8*, 57–65.
- [3] J. Payandeh, T. Scheuer, N. Zheng, W. A. Catterall, *Nature* **2011**, *475*, 353–358.
- [4] M. A. Rogawski, *Epilepsy Res.* **2006**, *69*, 273–294.
- [5] A. C. Errington, T. Stöhr, C. Heers, G. Lees, *Mol. Pharmacol.* **2008**, *73*, 157–169.
- [6] A. L. Goldin, *Curr. Opin. Neurobiol.* **2003**, *13*, 284–290.
- [7] Y. Liu, M. E. Jurman, G. Yellen, *Neuron* **1996**, *16*, 859–867.
- [8] C. Salome, E. Salome-Grosjean, J. P. Stables, H. Kohn, *J. Med. Chem.* **2010**, *53*, 3756–3771.
- [9] T. R. Cummins, J. Zhou, F. J. Sigworth, C. Ukomadu, M. Stephan, L. J. Ptáček, W. S. Agnew, *Neuron* **1993**, *10*, 667–678.
- [10] R. I. Herzog, T. R. Cummins, F. Ghassemi, S. D. Dib-Hajj, S. G. Waxman, *J. Physiol.* **2003**, *551*, 741–750.
- [11] L. Barbosa, M. Berk, M. Vorster, *J. Clin. Psychiatry* **2003**, *64*, 403–407.
- [12] a) M. Pappagallo, *Clin. Ther.* **2003**, *25*, 2506–2538; b) M. Backonja, *Curr. Pain Headache Rep.* **2004**, *8*, 212–216.
- [13] J. A. French, A. M. Kanner, J. Bautista, B. Abou-Khalil, T. Browne, C. L. Harden, W. H. Theodore, C. Bazil, J. Stern, S. C. Schachter, D. Bergen, D. Hirtz, G. D. Montouris, M. Nespeca, B. Gidal, W. J. Marks Jr., W. R. Turk, J. H. Fischer, B. Bourgeois, A. Wilner, R. E. Faught Jr., R. C. Sachdeo, A. Beydoun, T. A. Glauser, *Neurology* **2004**, *62*, 1261–1273.
- [14] M. A. Rogawski, W. Löscher, *Nat. Rev. Neurosci.* **2004**, *5*, 553–564.
- [15] G. Lees, M. J. Leach, *Brain Res.* **1993**, *612*, 190–199.
- [16] C. Zheng, K. Yang, Q. Liu, M. Y. Wang, J. Shen, A. S. Vallés, R. J. Lukas, F. J. Barrantes, J. Wu, *J. Pharmacol. Exp. Ther.* **2010**, *335*, 401–408.
- [17] H. Cheung, D. Kamp, E. Harris, *Epilepsy Res.* **1992**, *13*, 107–112.
- [18] Z.-G. Xiong, X.-P. Chu, J. F. MacDonald, *AJP - JN Physiol.* **2001**, *86*, 2520–2526.
- [19] M. Leach, K. Franzmann, D. Riddall, L. Harbige (University of Greenwich), WO/2011/004195 A2, **2011**.
- [20] J. F. Normant, C. Piechucky, *Bull. Soc. Chim. Fr.* **1972**, *6*, 2402–2403.
- [21] G. A. Olah, M. Arvanaghi, G. K. S. Prakash, *Synthesis* **1983**, 636–637.
- [22] C. P. Taylor, B. S. Meldrum, *Trends Pharmacol. Sci.* **1995**, *16*, 309–316.
- [23] M. Grauert, W. D. Bechtel, T. Weiser, W. Stransky, H. Nar, A. J. Carter, *J. Med. Chem.* **2002**, *45*, 3755–3764.

- [24] A. J. Carter, M. Grauert, U. Pischorn, W. D. Bechtel, C. Bartmann-Lindholm, Y. Qu, T. Scheuer, W. A. Catterall, T. Weiser, *Proc. Natl. Acad. Sci. USA* **2000**, *97*, 4944–4949.
- [25] J. M. A. Laird, A. J. Carter, M. Grauert, F. Cervero, *Br. J. Pharmacol.* **2001**, *134*, 1742–1748.
- [26] A. Solladie-Cavallo, F. Bonne, *Tetrahedron Asym.* **1996**, *7*, 171–180.
- [27] Z. Song, A. DeMarco, M. Zhao, E. G. Corley, A. S. Thompson, J. McNamara, Y. Li, D. Rieger, P. Sohar, D. J. Mathre, D. M. Tschaen, R. A. Reamer, M. F. Huntington, G.-J. Ho, F.-R. Tsay, K. Emerson, R. Shuman, E. J. J. Grabowski, P. J. Reider, *J. Org. Chem.* **1999**, *64*, 1859–1867.
- [28] J. J. Toledo-Aral, B. L. Moss, Z.-J. He, A. G. Koszowski, T. Whisenand, S. R. Levinson, J. J. Wolf, I. Silos-Santiago, S. Halegoua, G. Mandel, *Proc. Natl. Acad. Sci. USA* **1997**, *94*, 1527–1532.
- [29] J. A. Black, S. Liu, M. Tanakaa, T. R. Cummins, S. G. Waxman, *Pain* **2004**, *108*, 237–247.
- [30] M. A. Nassar, L. C. Stirling, G. Forlani, M. D. Baker, E. A. Matthews, A. H. Dickenson, J. N. Wood, *Proc. Natl. Acad. Sci. USA* **2004**, *101*, 12706–12711.
- [31] J. J. Cox, F. Reimann, A. K. Nicholas, G. Thornton, E. Roberts, K. Springell, G. Karbani, H. Jafri, J. Mannan, Y. Raashid, L. Al-Gazali, H. Hamamy, E. M. Valente, S. Gorman, R. Williams, D. P. McHale, J. N. Wood, F. M. Gribble, C. G. Woods, *Nature* **2006**, *444*, 894–898.
- [32] A. Nardi, N. Damann, T. Hertrampf, A. Kless, *ChemMedChem* **2012**, *7*, 1712–1740.
- [33] W. A. Schmalhofer, J. Calhoun, R. Burrows, T. Bailey, M. G. Kohler, A. B. Weinglass, G. J. Kaczorowski, M. L. Garcia, M. Koltzenburg, B. T. Priest, *Mol. Pharmacol.* **2008**, *74*, 1476–1484.
- [34] J. Liang, R. M. Brochu, C. J. Cohen, I. E. Dick, J. P. Felix, M. H. Fisher, M. L. Garcia, G. J. Kaczorowski, K. A. Lyons, P. T. Meinke, B. T. Priest, W. A. Schmalhofer, M. M. Smith, J. W. Tarpley, B. S. Williams, W. J. Martinc, W. H. Parsons, *Bioorg. Med. Chem. Lett.* **2005**, *15*, 2943–2947.
- [35] A. R. Katritzky, S. K. Singh, C. Cai, S. Bobrov, *J. Org. Chem.* **2006**, *71*, 3364–3374.
- [36] W. C. Still, M. Kahn, A. Mitra, *J. Org. Chem.* **1978**, *43*, 2923–2925.
- [37] H. E. Gottlieb, V. Kotlyar, A. Nudelman, *J. Org. Chem.* **1997**, *62*, 7512–7515.

5 STUDIES TOWARD PHOTOSWITCHABLE mGLUR6 AGONISTS AS A POTENTIAL APPROACH TO VISION RESTORATION

5.1 THE METABOTROPIC GLUTAMATE RECEPTOR 6

The metabotropic glutamate receptor 6 (mGluR6) is a G-protein coupled receptor (GPCR) that belongs to the group III mGluRs. It consists of a large (500–600 amino acids) N-terminal extracellular domain, a seven transmembrane (TM) domain and a C-terminal intracellular domain (Fig. 5.1a).^[1] Its natural agonist glutamate binds to the extracellular domain according to the so-called “venus flytrap”-model^[2] and has an EC_{50} value of 20 μ M.^[3] mGluR6 is believed to be expressed solely in ON bipolar cells in the retina, although recent studies revealed that mGluR6 might have different expression patterns in zebrafish.^[4] It is responsible for the synaptic transmission and mediation from the photoreceptors to the ganglion cells of the ON response in the ON pathway of the vertebrate retina. On the contrary, in OFF bipolar cells located AMPA receptors mediate the OFF response. These two pathways respond oppositely to the absorption of light by the photoreceptors which leads to a decrease of glutamate release to the bipolar cells. Whereas this decrease of glutamate leads to less excitation in the AMPA-mediated OFF bipolar pathway, another (yet not fully understood) sign inversion occurs in the mGluR6-mediated ON bipolar cells, leading to an increase in excitation. It is important to note that in the ON pathway the signal of light absorption is transduced with double sign inversion, whereas for the OFF pathway only one inversion occurs. As a consequence, an agonist for mGluR6 would mimic the response to darkness (Fig. 5.1b).^[5] A more detailed plan of the retina and its function can be found elsewhere.^[6]

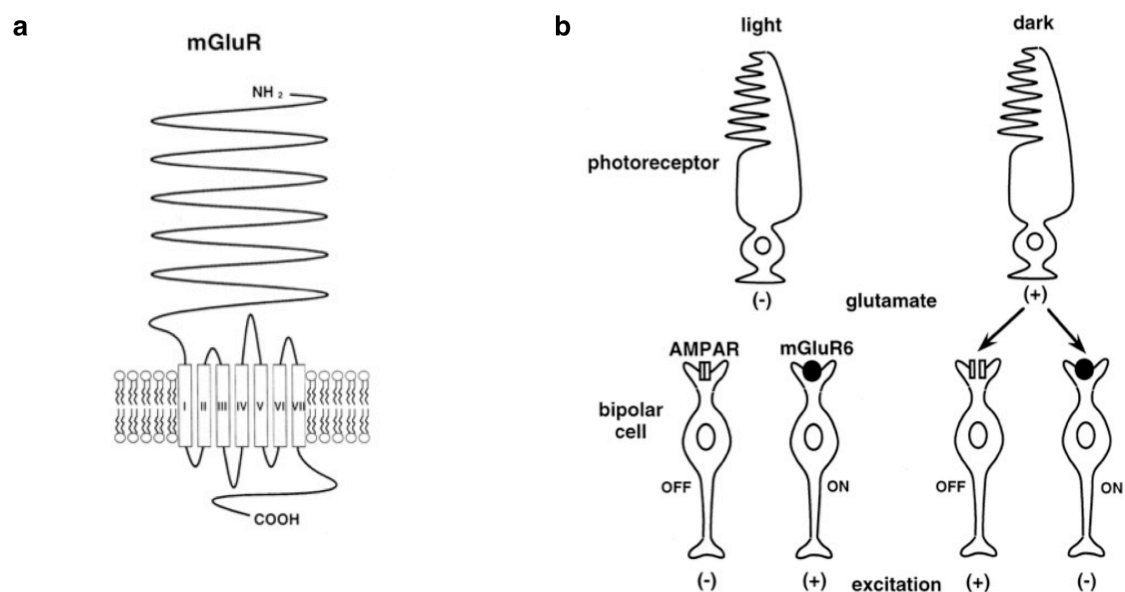


Figure 5.1. Schematic illustration of **a)** the structure of mGluR6 and **b)** signal transduction in the ON- and OFF-pathways in the vertebrate retina, respectively. Illustrations copied from Nakanishi *et al.*,^[5] reprinted with permission from Elsevier. Copyright 1998.

Since mGluR6 is thought to be expressed solely in the retina, it is an ideal target receptor for the photochemical approach toward vision restoration. Undesired side effects could be reduced significantly by naturally avoiding drug distribution problems as well as receptor selectivity problems with an mGluR6-selective photoswitch. To date, no crystal structure of mGluR6 has been published. Hence, a literature search for known agonists and antagonists and their structure–activity relationships was conducted in order to identify promising target molecules which could be turned into possible photoswitches to control mGluR6 by introduction of an azobenzene moiety to the molecules. The azobenzene linkers could in principle be attached not only in the *para*, but also in *meta* or even *ortho* position with respect to the azo moiety. An overview of these is given in figures 5.2 and 5.3 with only the *para*-substituted azobenzenes shown for simplicity reasons. All of these compounds mimic the structure of the endogenous ligand glutamate with slight alterations in the molecule’s geometry (e.g. sp^2 centers, ring fusion) or replacement of a functional group by a similar one (e.g. phosphate). 1-Benzyl-APDC is the most promising compound since it is the only *selective* mGluR6 agonist known and has a EC_{50} value of $20\ \mu M$.^[7] Moreover, some phenylglycine derivatives are known as agonists for mGluR6: the carboxy derivative (*S*)-3,4-DCPG^[8] as well as the hydroxy derivatives 3C5HPG,^[8b] 4Cl-3,5-DHPG,^[8b] and (*S*)-3,5-DHPG.^[8b] As a highly potent agonist, the phosphate derivative L-AP4 was identified ($EC_{50} = 0.2\ \mu M$).^[8b,9]

5 STUDIES TOWARD PHOTOSWITCHABLE mGLUR6 AGONISTS AS A POTENTIAL APPROACH TO VISION RESTORATION

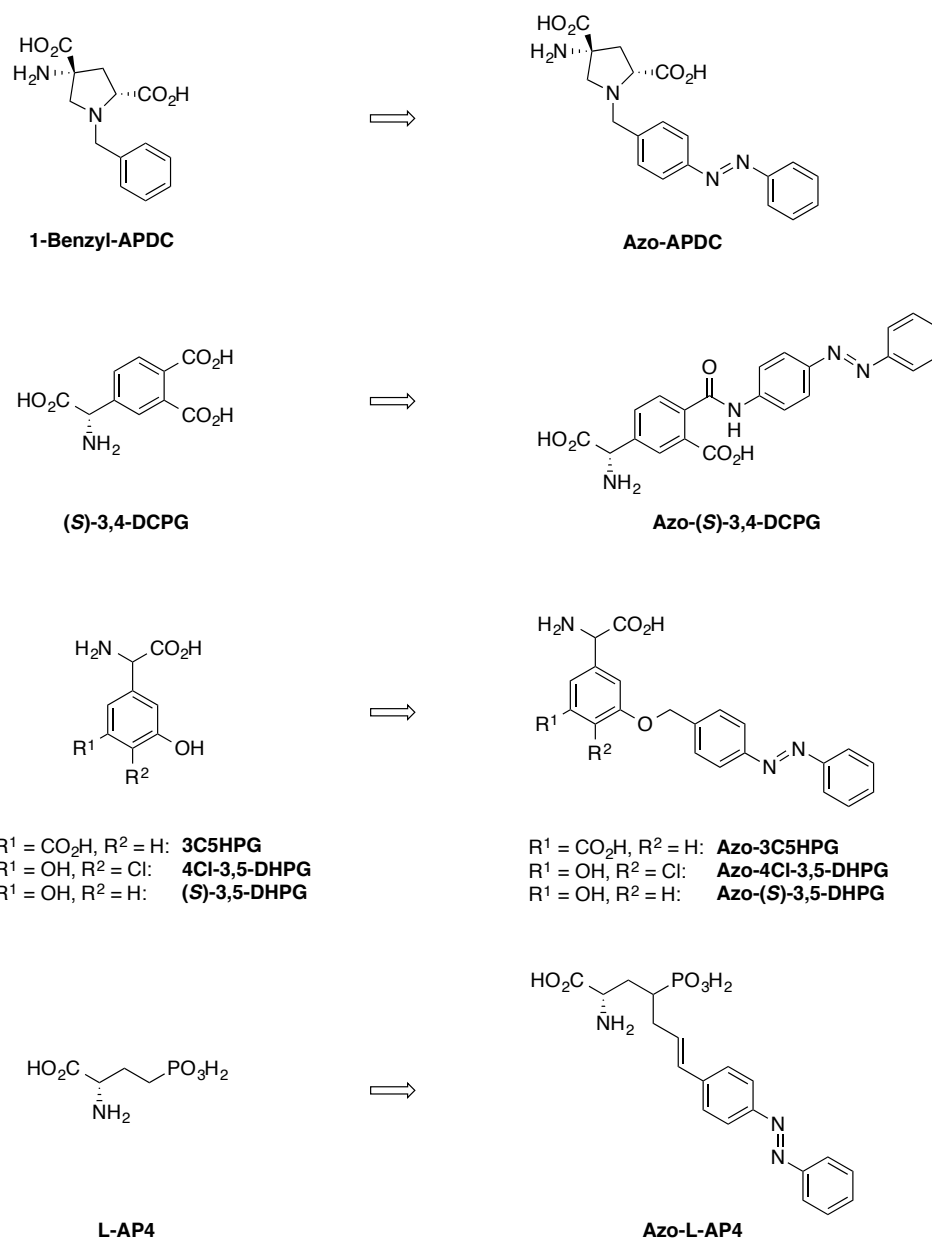


Figure 5.2. Structures of mGluR6 agonists and their possible azobenzene derivatives.

Furthermore, Homo-AMPA ($EC_{50} = 82 \mu\text{M}$),^[10] the elongated analogue of the iGluR agonist AMPA,^[11] could be modified on two positions to introduce the azobenzene unit, either by C-alkylation on the isoxazole ring, or by O-alkylation of the hydroxy group.^[12] More interesting agonists include the cyclopropylphosphate PPCG-2^[13] and the tricarboxylic acid ACPT-I (Fig. 5.3)^[14]

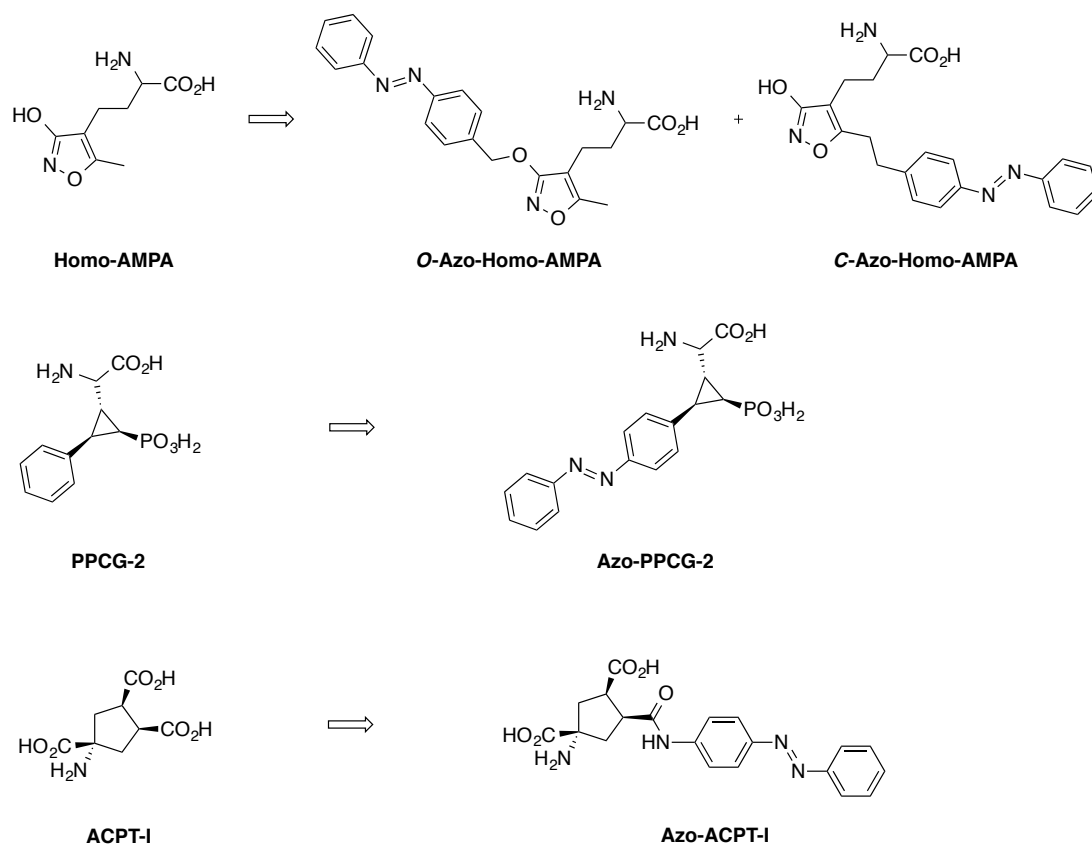


Figure 5.3. Structures of mGluR6 agonists Homo-AMPA, PPCG-2, ACPT-I and their possible azobenzene derivatives.

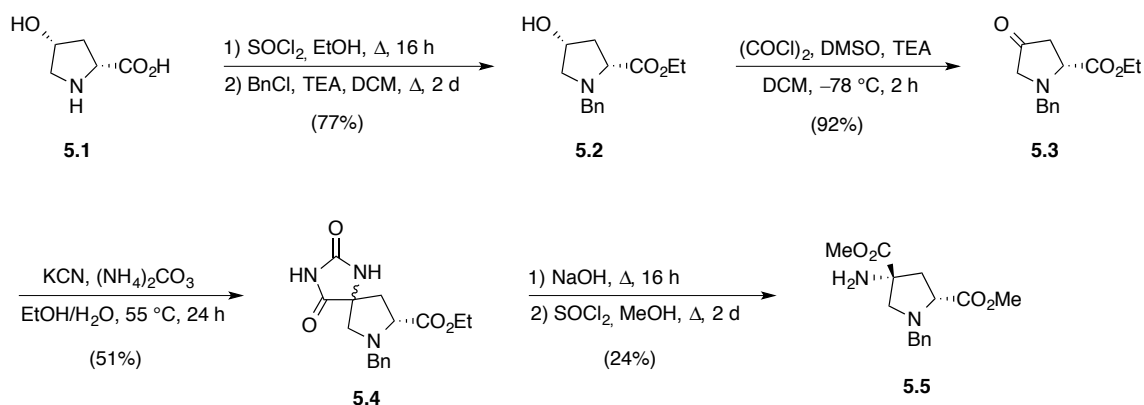
5.2 AZO-APDC

As described above, 1-benzyl-APDC was reported by Tückmantel *et al.*^[7] to be a *selective* agonist for mGluR6. For this reason and in addition for its ideal molecular anchor point for an azobenzene moiety at the pyrrolidine nitrogen atom thereby replacing the benzyl group, it was chosen as the prime candidate for the approach toward photochemical control of mGluR6. Therefore, both *para*- as well as *meta*-Azo-APDC were synthesized and biologically evaluated.

Synthesis of Azo-APDCs

Both Azo-APDC derivatives were synthesized starting from *cis*-4-hydroxy-D-proline (**5.1**) which was first converted to its ethyl ester using thionyl chloride in ethanol, followed by benzyl protection of the secondary amine yielding **5.2** in 77% over two steps. Oxidation of the secondary alcohol under Swern conditions gave ketone **5.3** in 92% yield. A Bucherer-Bergs reaction with potassium cyanide and ammonium carbonate led to hydantoin **5.4** as a mixture of

diastereomers in 51% yield. Hydantoin cleavage with sodium hydroxide, followed by reesterification with thionyl chloride in methanol gave a mixture of two amino diester diastereomers. The desired major diastereomer **5.5** could be separated at that stage and was obtained in 24% yield over two steps (Scheme 5.1).



Scheme 5.1. Synthesis of protected amino acid **5.5** via a Bucherer-Bergs reaction as the key step.

The diastereoselectivity of the Bucherer-Bergs reaction of 4-oxoprolines can be explained by the model studies by Tanaka *et al.*^[15] which are illustrated in Fig 5.4. The hydantoin is formed as a mixture of two diastereomers **A** and **B**. Depending on the steric bulk provided by the ester function shielding the upper face of the molecule, formation of transition state **A** is favored over **B** due to steric interaction of the ester and the imine functions. Whereas the combined yield of **A** and **B** for this reaction stays in the same range (70–75%), the ratio of **A** to **B** steadily increases from 75 : 25 for the sterically less demanding methyl ester up to 96 : 4 for the bulky *tert*-butyl ester.

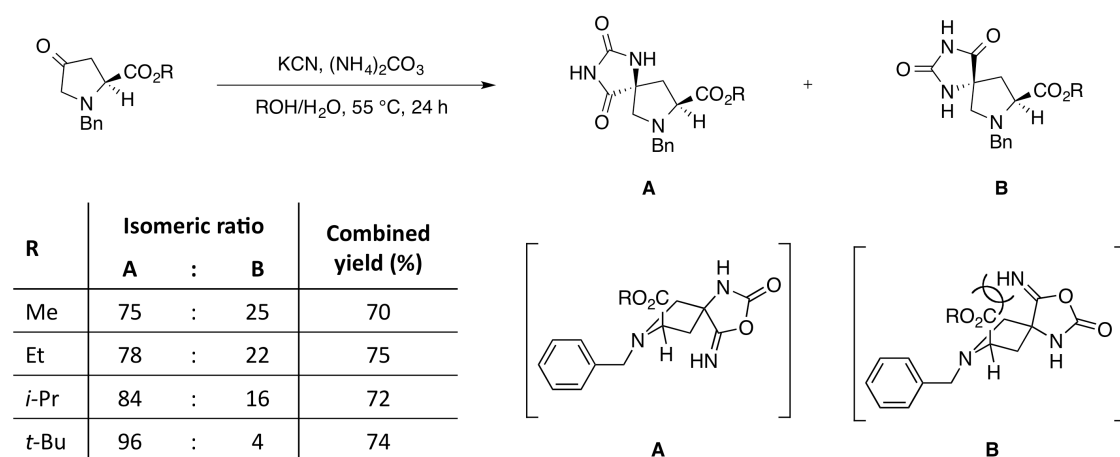
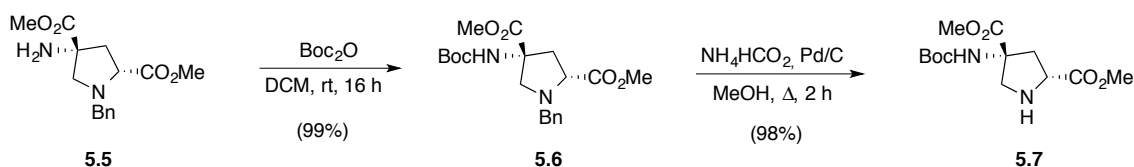


Figure 5.4. Model studies explain the diastereoselectivity of the Bucherer-Bergs reaction of 4-oxoproline derivatives. Bulky ester groups shield the upper face of the molecule and therefore favor hydantoin formation from the bottom face.

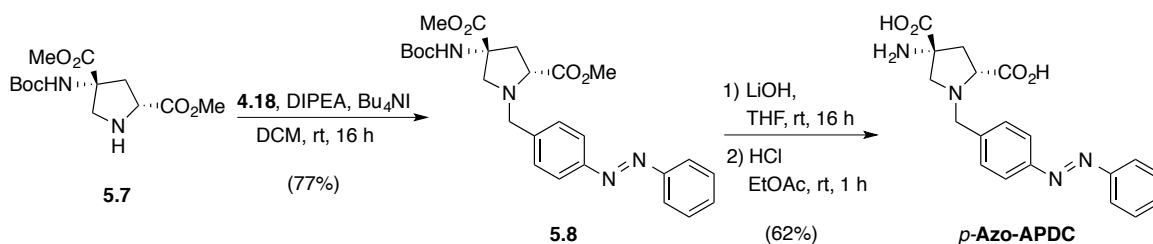
5 STUDIES TOWARD PHOTOSWITCHABLE mGLUR6 AGONISTS AS A POTENTIAL APPROACH TO VISION RESTORATION

Having obtained **5.5**, the primary amino group was Boc protected yielding **5.6** in 99% yield, followed by benzyl deprotection of the tertiary amine using palladium on charcoal and ammonium formate as hydrogen source. Secondary amine **5.7** was obtained in 98% yield (Scheme 5.2).



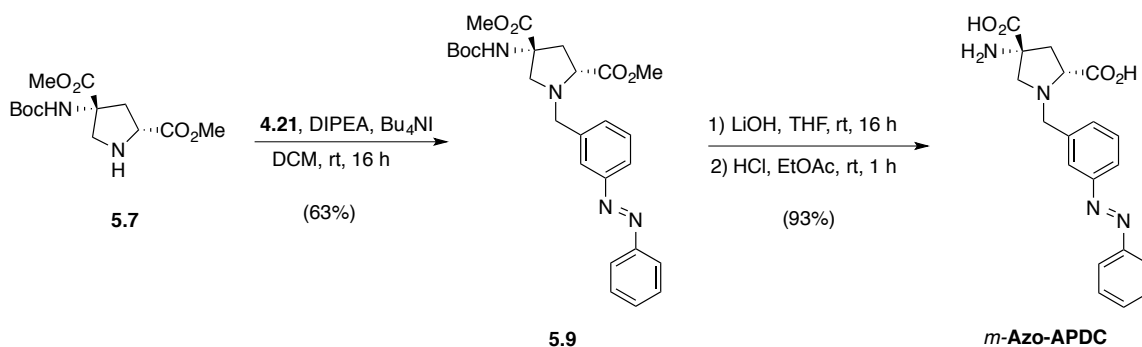
Scheme 5.2. Synthesis of secondary amine **5.7**.

Amine **5.7** was then reacted with bromide **4.18** to give tertiary amine **5.10** in 77% yield. Saponification of the methyl ester using LiOH, followed by deprotection of the Boc group with HCl in ethyl acetate gave *p*-Azo-APDC in 62% over two steps (Scheme 5.3).



Scheme 5.3. Synthesis of *p*-Azo-APDC from amine **5.7** and *para*-azobenzene bromide **4.18**.

Accordingly, **5.9** was synthesized from amine **5.7** and *meta*-bromide **4.21** in 63% yield. Global deprotection afforded *m*-Azo-APDC in 93% yield over two steps (Scheme 5.4).



Scheme 5.4. Synthesis of *m*-Azo-APDC from amine **5.7** and *meta*-azobenzene bromide **4.21**.

Biological Evaluation of Azo-APDCs

The peak absorption wavelengths and photoswitching properties of both Azo-APDCs were determined by UV/Vis spectroscopy in DMSO (Fig. 5.5a+b). Both Azo-APDCs are non-red-shifted azobenzenes and thus show peak absorptions for the *trans*→*cis* transition in the UV range at $\lambda = 323$ nm (*p*-Azo-APDC) and $\lambda = 324$ nm (*m*-Azo-APDC). The *trans*→*cis* transition peaks are found at $\lambda = 420$ nm (*p*-Azo-APDC) and $\lambda = 440$ nm (*m*-Azo-APDC), respectively. The *trans*→*cis* isomerization process appears to proceed faster for *m*-Azo-APDC than for the *para* derivative.

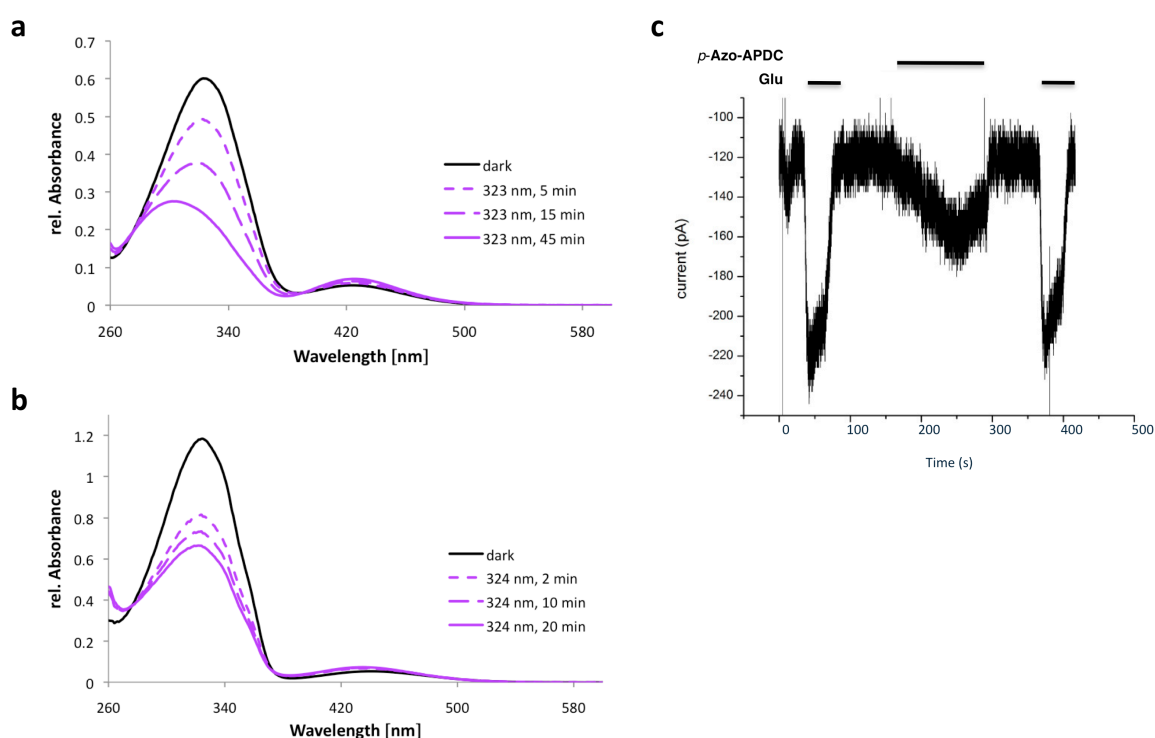


Figure 5.5. **a)** UV/Vis spectrum of *p*-Azo-APDC (DMSO). The absorption maxima are at $\lambda = 323$ and $\lambda = 420$ nm for the *trans*→*cis* and *cis*→*trans* transition, respectively. **b)** UV/Vis spectrum of *m*-Azo-APDC ($\lambda_{\text{max}} = 324, 440$ nm; DMSO). **c)** Electrophysiological trace of GIRK-coupled mGluR6 in HEK 293 cells. Stimulation of saturated glutamate (Glu; 1 mM), followed by 100 μM *p*-Azo-APDC in its *trans* conformation leading to a current increase of ~40% compared to Glu (Benjamin Gaub, University of California, Berkeley).

Figure 5.5c shows an electrophysiological trace of GIRK-coupled mGluR6 in HEK 293 cells (Benjamin Gaub, University of California, Berkeley). 100 μM *p*-Azo-APDC elicits ~40% of saturated glutamate (1mM) current, proving moderate agonist activity of the azo derivative. However, the kinetics were determined to be rather slow compared to glutamate. Moreover, no

significant photoswitching effects could be observed in related experiments (data not shown). The *meta* derivative did not show any agonist activity (no data shown).

5.3 Azo-3C5HPG

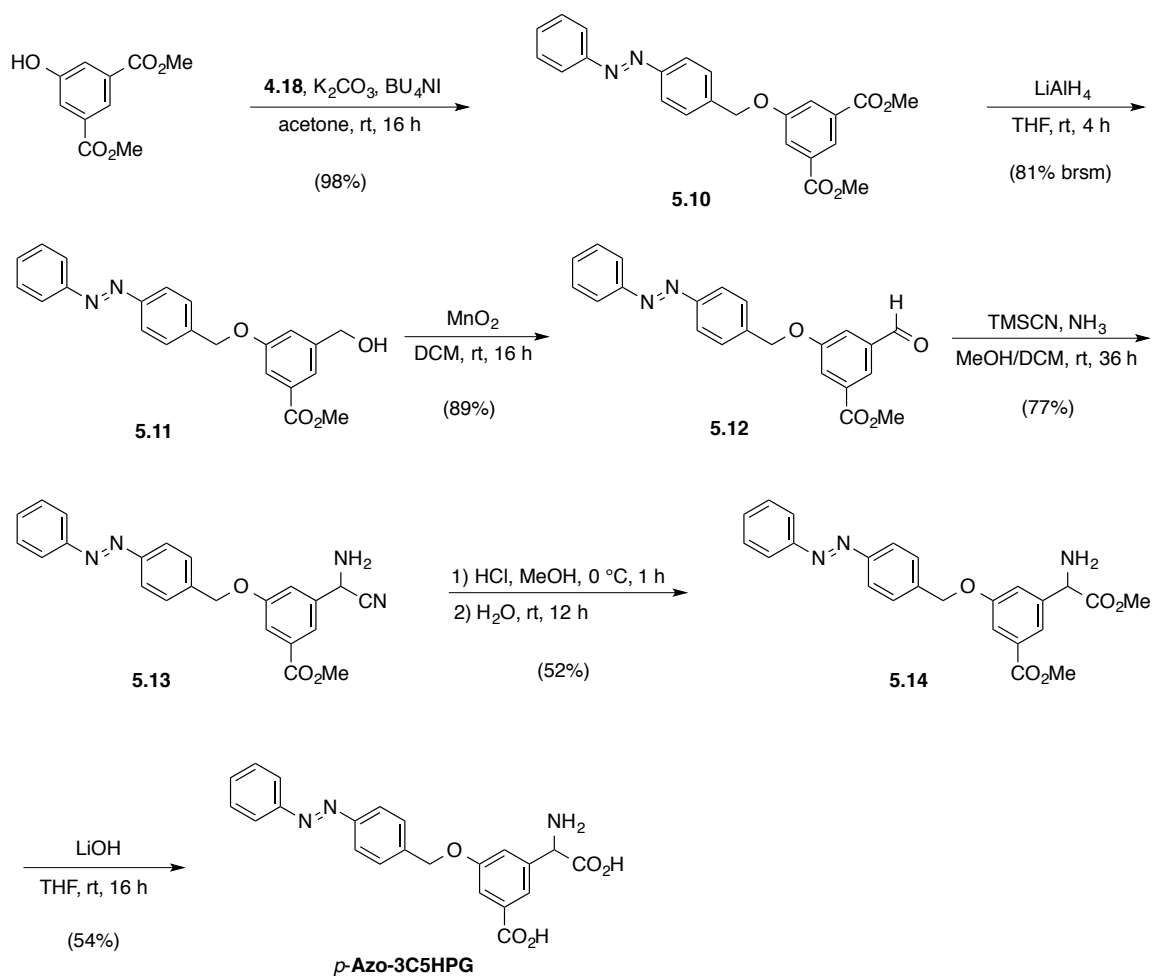
In their structure–activity relationship of different mGluRs, Sekiyama *et al.*^[8b] report (racemic) 3C5HPG as a good agonist for mGluR6 in CHO cells. 3C5HPG (which stands for 3-carboxy-5-hydroxyphenylglycine) has the glutamate backbone incorporated into a benzene ring with an additional hydroxy function that could be used as an anchor point for the attachment of an azobenzene linker. Accordingly, both the *para*- and *meta*-azobenzene derivatives were synthesized and tested for their activity on mGluR6.

Synthesis of Azo-3C5HPGs

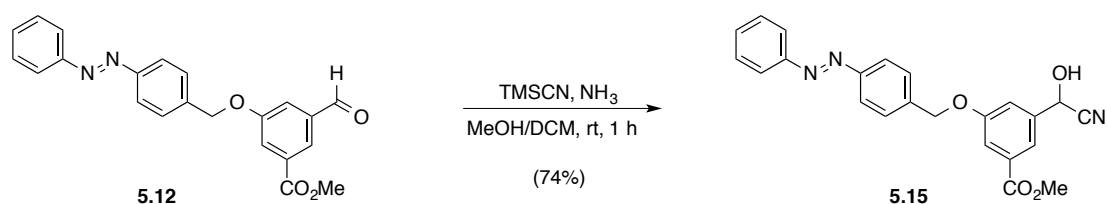
The synthesis of *p*-Azo-3C5HPG is illustrated in Scheme 5.5. The azobenzene linker was introduced early on in the synthesis: Dimethyl 5-hydroxyisophthalate was etherified using azobenzene bromide **4.18** and potassium carbonate, yielding **5.10** in 98% yield. Monoreduction of the symmetric diester **5.10** with LiAlH₄ gave primary alcohol **5.11** in 61% yield (81% brsm), recovering 25% of the starting material (the doubly reduced diol was obtained as a side product in 5%). Benzylic oxidation with MnO₂ gave aldehyde **5.12** in 89% yield which was then converted to aminonitrile **5.13** under Strecker conditions using TMSCN and ammonia in very good yield (77%). Compound **5.13** was then subjected to Pinner conditions affording amino acid methyl ester **5.14** in 52% yield. *p*-Azo-3C5HPG was finally obtained after saponification of the two esters with LiOH in 54% yield.

During this synthesis it was observed that conversion of aldehyde **5.12** into aminonitrile **5.13** required relatively long reaction times. In first attempts the reaction was stopped after 1 h as TLC analysis indicated full conversion of the starting material into a new product which turned out to be cyanohydrin **5.15** which was obtained in 74% yield (Scheme 5.6). Apparently, attack of the cyanide at the carbonyl group is relatively fast but reversible. Hence, the thermodynamic product **5.13** is formed after first reaction of the aldehyde with ammonia to the corresponding imine and subsequent nucleophilic attack of cyanide.

5 STUDIES TOWARD PHOTOSWITCHABLE mGLUR6 AGONISTS AS A POTENTIAL APPROACH TO VISION RESTORATION



Scheme 5.5. Synthesis of *p*-Azo-3C5HPG.



Scheme 5.6. Conversion of aldehyde **5.12** into cyanohydrin **5.15**.

Crucial for the success of the synthesis was the relatively mild conversion of aldehyde **5.12** via aminonitrile **5.13** to the corresponding amino methyl ester **5.14** through a Pinner reaction with HCl in MeOH. Other attempts to install the amino acid moiety requiring harsher conditions (Strecker synthesis, Bucherer-Bergs reaction) failed. Fig. 5.6 gives an overview of classical methods to install amino acid functions. In the classical Strecker synthesis a carbonyl **5.16** is converted to an aminonitrile **5.17** using ammonia and a cyanide source. The nitrile is then hydrolyzed usually with refluxing conc. HCl to give the amino acid **5.18**. Another method

avoiding acidic conditions is the Bucherer-Bergs reaction in which **5.16** is reacted first with ammonium carbonate and cyanide to form hydantoin **5.19** which then can be cleaved using strongly basic conditions and high temperatures to give amino acid **5.18**. The Pinner reaction proceeds over the same aminonitrile **5.17** as in the Strecker synthesis. However, instead of harsh hydrolysis conditions, **5.17** is converted to the so-called Pinner salt with HCl in low concentration in anhydrous alcohols at 0 °C within 30 min.

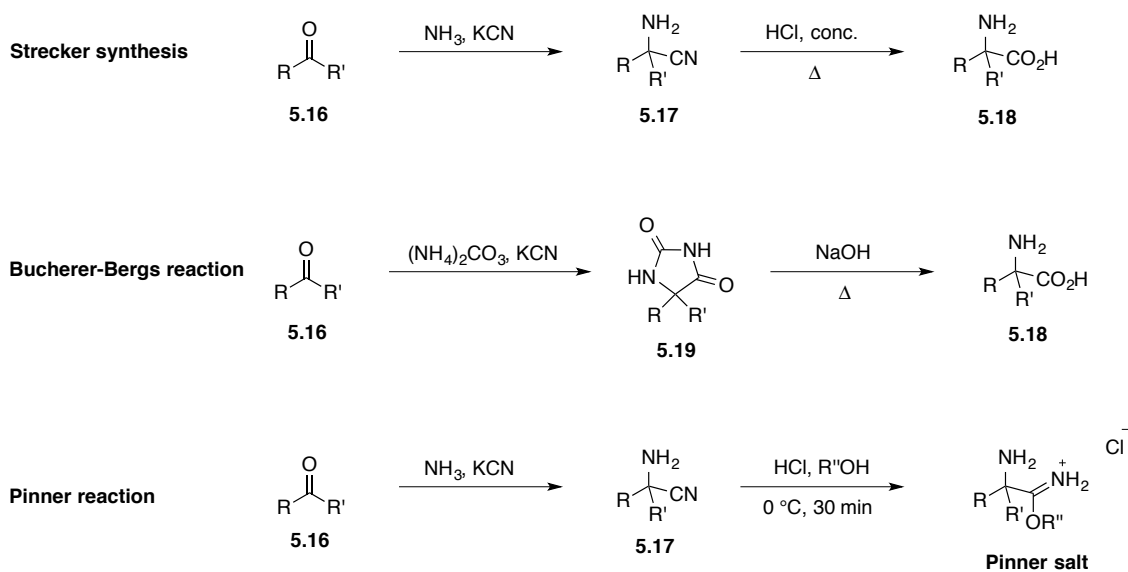


Figure 5.6. Methods for amino acid synthesis: Strecker synthesis, Bucherer-Bergs and Pinner reaction.

The Pinner salt is a versatile starting material to access a variety of functional groups. By adding K_2CO_3 to Pinner salts imidates can be obtained. Hydrolysis gives rise to esters, whereas H_2S and pyridine give thioesters. Addition of ammonia in alcohols leads to the corresponding amidinium salts (Fig. 5.7).

In case of α -amino-substituted Pinner salts oligomerization and eventual dealkylations can occur as side reactions which possibly explains the yields in the range between 50 and 60% reliably obtained in these syntheses.

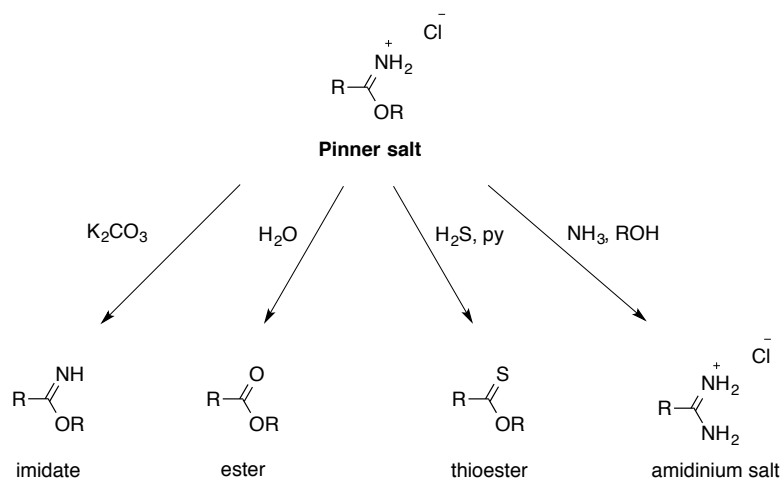
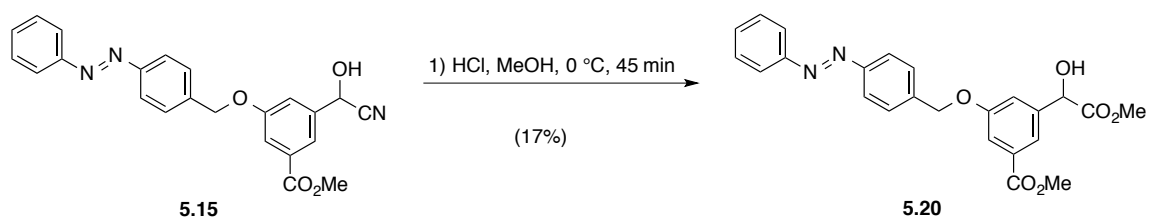


Figure 5.7. Possible reactions of Pinner salts: Syntheses of imidates, esters, thioesters or amidinium salts.

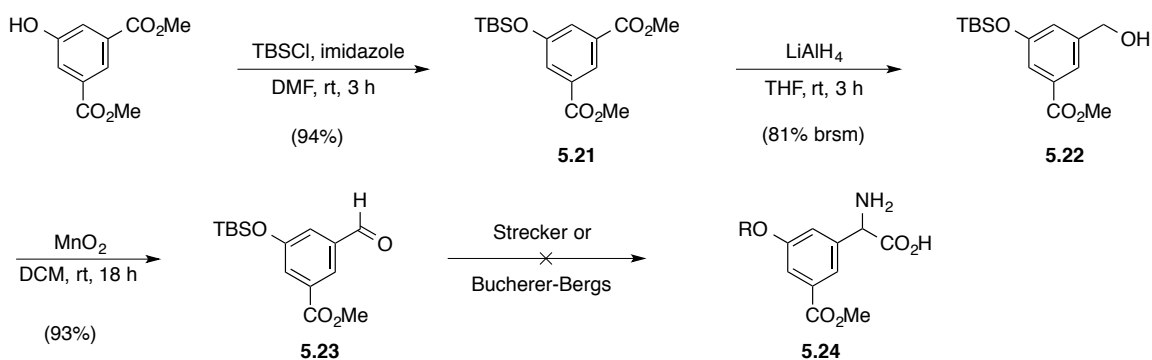
Having obtained cyanohydrin **5.15** accidentally during the synthesis, **5.15** was used as a model system for the Pinner reaction. Compound **5.15** was treated with HCl in methanol at 0 °C for 45 min, followed by aqueous workup to yield methyl ester **5.20** in 17% (Scheme 5.7). Later, the yields of this reaction were improved by prolonged reaction times after the addition of water.



Scheme 5.7. Pinner reaction of model system **5.15**.

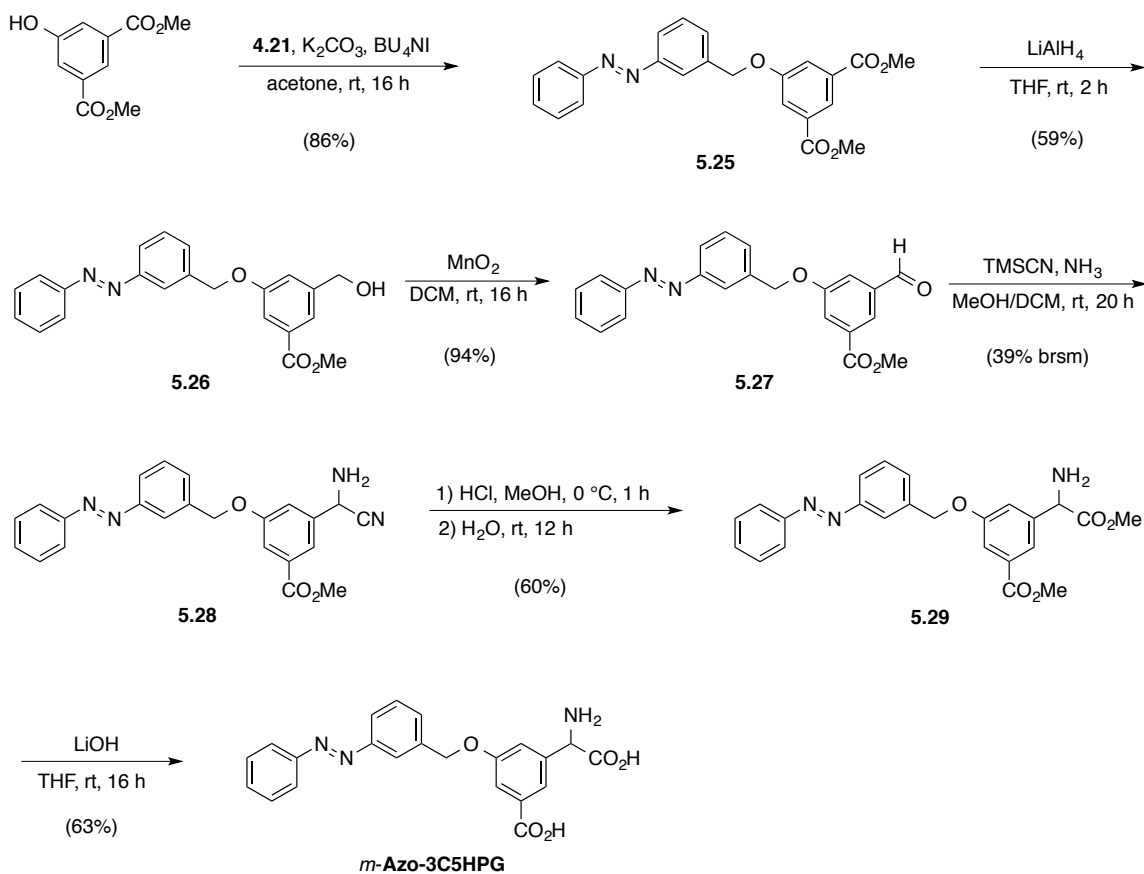
In earlier attempts to install the amino acid function, the simpler aldehyde **5.23** was synthesized (Scheme 5.8). First, dimethyl 5-hydroxyisophthalate was TBS-protected in 94% yield using TBSCl and imidazole. Compound **5.21** was then reduced with LiAlH₄ to alcohol **5.22** in 56% yield (81% brsm). Benzylic oxidation with MnO₂ gave aldehyde **5.23** in 93% yield. However, neither Strecker nor Bucherer-Bergs conditions afforded amino acid derivative **5.24**.

5 STUDIES TOWARD PHOTOSWITCHABLE mGLUR6 AGONISTS AS A POTENTIAL APPROACH TO VISION RESTORATION



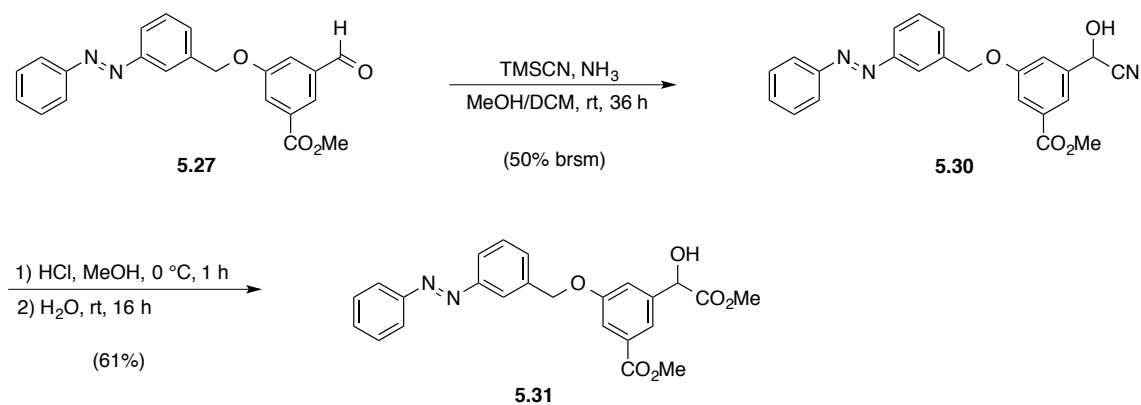
Scheme 5.8. Attempted synthesis of **5.24** by Strecker or Bucherer-Bergs conditions. R = TBS for Bucherer-Bergs reaction, R = H for Strecker reaction.

The *meta*-derivative *m*-Azo-3C5HPG was synthesized according to the route shown above for *p*-Azo-3C5HPG by using the *meta*-azobromide **4.21** instead. Ether formation of bromide **4.21** and dimethyl 5-hydroxyisophthalate yielded **5.25** in 86% yield. Reduction with LiAlH₄ gave alcohol **5.26** in 59% yield, followed by MnO₂-mediated oxidation to aldehyde **5.27** in 94% yield. Aminonitrile **5.28** was synthesized by a Strecker reaction in 31% yield (39% brsm), followed by a Pinner reaction, affording aminoacid methyl ester **5.29** in 60% yield. Saponification using LiOH finally gave rise to *m*-Azo-3C5HPG in 63% yield (Scheme 5.9).



Scheme 5.9. Synthesis of *m*-Azo-3C5HPG.

Again, cyanohydrin **5.30** was obtained as a side product in the conversion of aldehyde **5.27** to aminonitrile **5.28**. Even with 36 h reaction time, **5.30** was obtained in 40% yield (50% brsm). Compound **5.30** was then again used as a model system for a subsequent Pinner reaction, giving the desired product **5.31** reliably in 61% yield (Scheme 5.10).



Scheme 5.10. Synthesis of **5.31**.

Biological Evaluation of Azo-3C5HPGs

The absorption maxima and photoswitching properties of both Azo-3C5HPGs were determined by UV/Vis spectroscopy (Fig. 5.8a+b; *p*-Azo-3C5HPG: $\lambda_{max} = 322, 425$ nm; *m*-Azo-3C5HPG: $\lambda_{max} = 335, 433$ nm). In electrophysiological experiments on GIRK-coupled mGluR6 in HEK 293 cells, application of the *cis* isomer of *p*-Azo-3C5HPG (100 μM ; generated by preillumination of the compound with UV light) lead to 10-20% of the saturated glutamate response (Fig. 5.8c, enlarged window; Benjamin Gaub, University of California, Berkeley). In the same experiment, *m*-Azo-3C5HPG as well as both Azo-APDCs were also tested and did not show significant mGluR6 agonist activity, neither in their *trans* nor in their *cis* configurations.

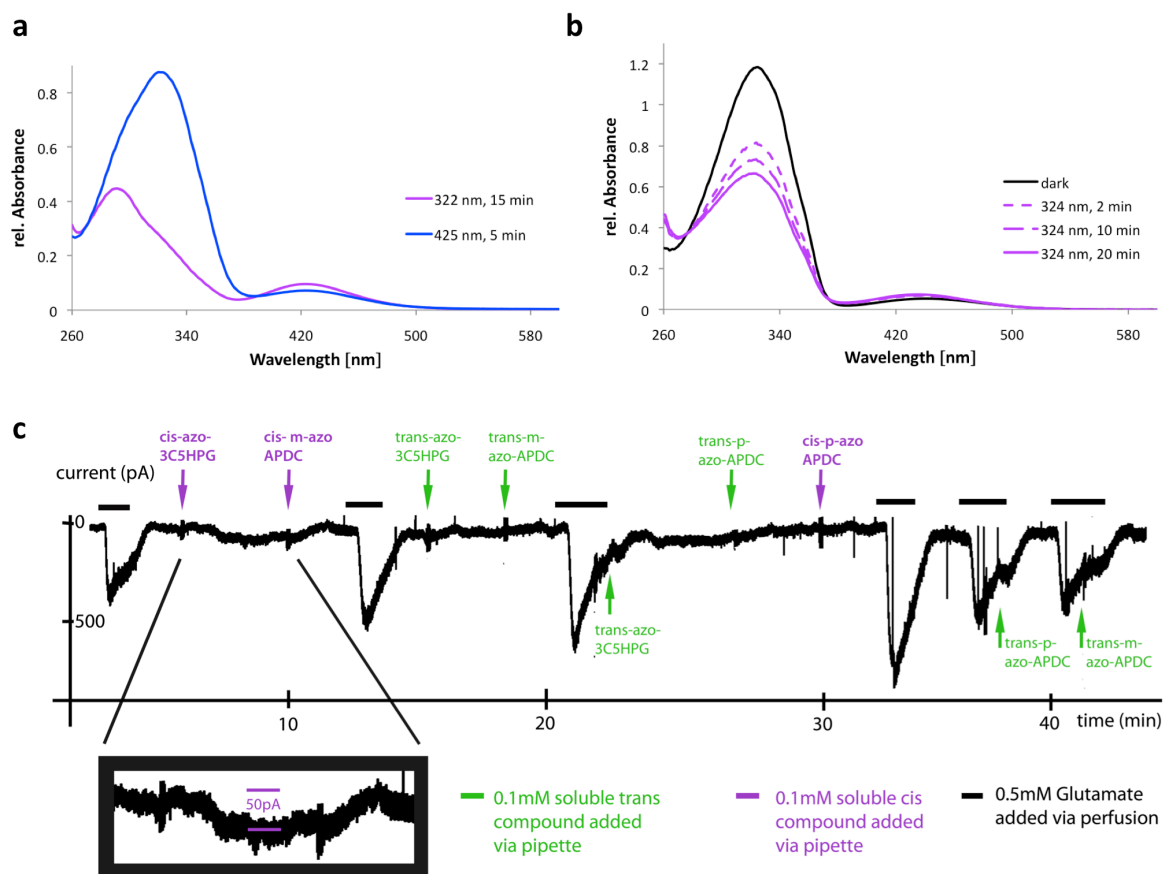
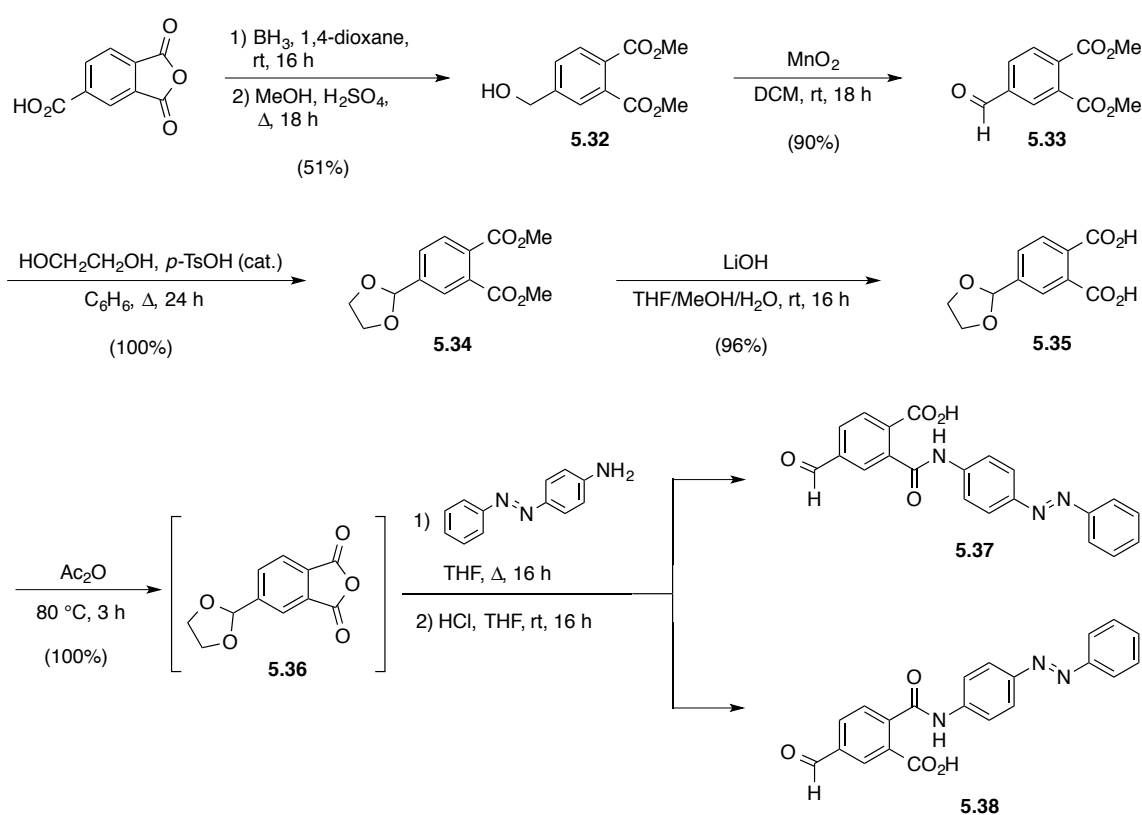


Figure 5.8. a) UV/Vis spectrum of *p*-Azo-3C5HPG with absorption maxima at $\lambda_{max} = 322, 425$ nm (DMSO). The transition between dark and UV light appeared to be relatively slow, therefore switching between $\lambda = 322$ nm and $\lambda = 425$ nm is shown. b) UV/Vis spectrum of *m*-Azo-3C5HPG ($\lambda_{max} = 335, 433$ nm; DMSO). c) Electrophysiological trace of GIRK-coupled mGluR6 in HEK 293 cells (Benjamin Gaub, University of California, Berkeley). Application of both Azo-3C5HPGs as well as both Azo-APDCs is shown. Only *cis-p*-Azo-3C5HPG showed weak agonist activity of 10-20% of sat. Glu (enlarged window).

5.4 Azo-DCPG

Synthesis of Azo-DCPG

Thomas *et al.*^[8a] reported (*S*)-3,4-DCPG as agonist for mGluR6 (and mGluR8a) in 2001. 3,4-DCPG (3,4-dicarboxyphenylglycine) is another phenylglycine derivative which features the glutamate structure fused into a benzene backbone. The additional free 4-carboxy function could be used to install an azobenzene linker *via* an amide.



Scheme 5.11. Synthesis of regioisomers **5.37** and **5.38**.

Firstly, 1,2,4-tricarboxylic anhydride was selectively reduced at the 4-position by borane and subsequently esterified under Fischer conditions with H_2SO_4 in MeOH. This literature known procedure^[16] afforded compound **5.32** in 51% yield over two steps which was then oxidized to aldehyde **5.33** in 90% yield using MnO_2 . The aldehyde was protected at that stage by acetal formation with ethylene glycol and catalytic amounts of *p*-TsOH to afford **5.34** quantitatively. Saponification with LiOH gave dicarboxylic acid **5.35** in 96% yield. Acid **5.35** was then converted quantitatively to its anhydride **5.36** by acetic anhydride and then further reacted with

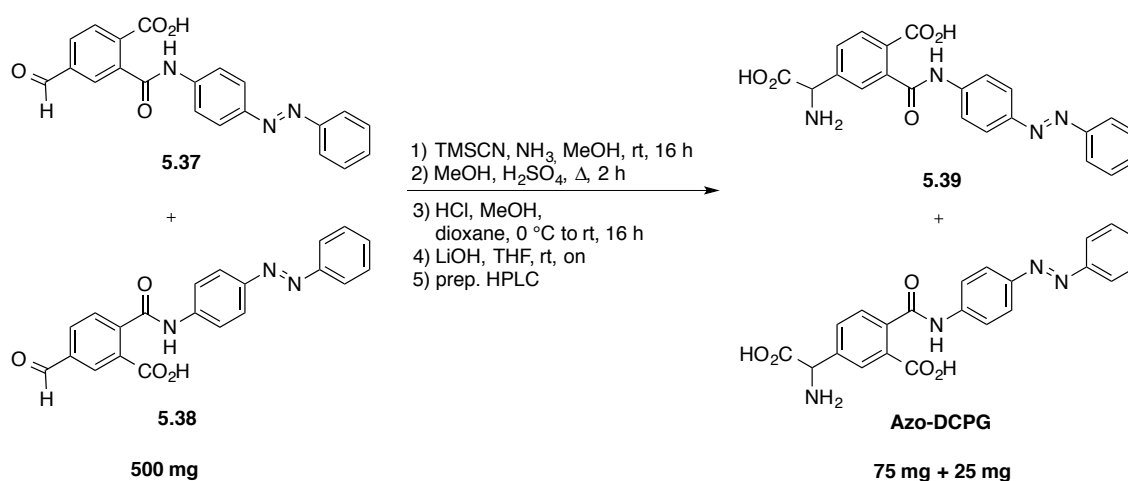
4-aminoazobenzene, followed by acidic acetal deprotection to yield the two regioisomers **5.37** and **5.38** (Scheme 5.11).

Unfortunately, only analytical quantities of the pure regioisomers could be obtained by multiple recrystallization efforts from different solvents. Analysis of the (2D) NMR spectra of both isomers allowed for identification and assignment of the two isomers. In the ^1H NMR spectra, the aldehyde protons A of **5.37** and **5.38** have the same chemical shift of 10.12 ppm. However, the aromatic protons B, C and D can be used to distinguish between the two isomers. For compound **5.38**, B, C and D appear close together between 8.0 and 8.2 ppm (Fig 5.9a. bottom), whereas for **5.37** the singlet of proton B is shifted downfield to 8.40 ppm and the doublet of D is shifted upfield to 7.80 ppm (Fig 5.9a, top). As indicated by the same chemical shifts of proton A, carbon atoms 2 also possess very similar chemical shifts in the ^{13}C NMR spectra (137.0 ppm vs. 138.0 ppm). Carbons 1, 3 and 4, which also share the same direct environment for both regioisomers, appear for both compounds relatively close together a \sim 130 ppm (**5.38**: 129.5 (C1), 130.6 (C3), 130.8 (C4) vs. **5.37**: 129.4 (C4), 131.2 (C1), 132.6 ppm (C3)). Due to the neighboring acid and amide function, respectively, the chemical shifts for C1(**5.37**) and C4(**5.38**), as well as C4(**5.37**) and C1(**5.38**) are very similar. As expected, the biggest differences can be observed for carbon atoms 5 and 6 which are directly attached to the carboxylic acid and amide functions, respectively. C6 next to the carboxylic acid in isomer **5.38** has a chemical shift of 138.7 ppm, whereas the corresponding C5 of isomer **5.37** is significantly downfield shifted (143.5 ppm). The C6 signal for **5.37** unfortunately could not be clearly identified, probably due to extensive broadening as can be seen also for the corresponding C5 signal for compound **5.38** (Fig 5.9b).

5 STUDIES TOWARD PHOTOSWITCHABLE mGLUR6 AGONISTS AS A POTENTIAL APPROACH TO VISION RESTORATION

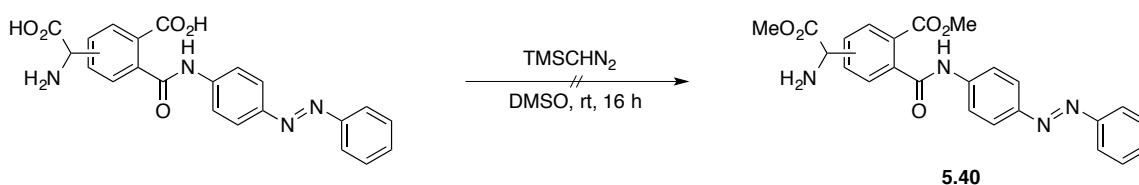


Due to separation problems on large scale (even on HPLC), both regioisomers **5.37** and **5.38** were used as a mixture for all further reactions in order to hopefully be able to separate them at a later stage. 500 mg of the mixture of regioisomeric aldehydes **5.37** and **5.38** were converted to the aminonitriles with TMSCN and ammonia and further reacted to the corresponding methyl ester *via* its Pinner salt using HCl in methanol. Saponification with LiOH gave the final products which at that stage could be separated by preparative HPLC, affording a 3:1 mixture of **Azo-DCPG** and its regioisomer **5.39** (Scheme 5.12).



Scheme 5.12. Synthesis of **Azo-DCPG** and its regioisomer **5.39** from regioisomeric aldehydes **5.37** and **5.38**.

Their identity was confirmed by NMR and HRMS, although unfortunately the regioisomers could not be assigned as no relevant cross peaks were visible in the 2D NMR spectra. Crystallization efforts as well as attempts to convert the major isomer to the dimethyl ester **5.40** with TMSCHN₂ in order to obtain relevant cross peaks in the 2D NMR spectra for structural assignment purposes have failed (Scheme 5.13).



Scheme 5.13. Attempted conversion of major isomer of **Azo-DCPG/5.39** to the dimethyl ester **5.40**.

Nonetheless, the two regioisomers were tested individually in a biological assay similar to the previously described Azo-APDCs and Azo-3C5HPGs on potential activity on mGluR6. Unfortunately, none of the two isomers showed any activity on GIRK-coupled mGluR6 (data not shown).

5.5 EXPERIMENTAL PROCEDURES AND ANALYTICAL DATA

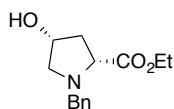
5.5.1 GENERAL EXPERIMENTAL DETAILS AND INSTRUMENTATION

All reactions were carried out with magnetic stirring and if air or moisture sensitive in oven-dried glassware under an atmosphere of nitrogen or argon. Syringes used to transfer reagents and solvents were purged with nitrogen or argon prior to use. Reagents were used as commercially supplied unless otherwise stated. Thin layer chromatography was performed on pre-coated silica gel F₂₅₄ glass backed plates and the chromatogram was visualized under UV light and/or by staining using aqueous acidic vanillin or potassium permanganate, followed by gentle heating with a heat gun. Flash column chromatography was performed using silica gel, particle size 40–63 μm (eluants are given in parenthesis). The diameter of the columns and the amount of silica gel were calculated according to the recommendations of W. C. Still *et al.*^[17] IR spectra were recorded on a Perkin Elmer Spectrum Bx FT-IR instrument as thin films with absorption bands being reported in wave number (cm^{-1}). UV/Vis spectra were obtained using a Varian Cary 50 Scan UV/Vis spectrometer and Helma SUPRASIL precision cuvettes (10 mm light path).

¹H and ¹³C NMR spectra were measured on Varian VNMRS 300, VNMRS 400, INOVA 400 or VNMRS 600 instruments. The chemical shifts are quoted as δ -values in ppm referenced to the residual solvent peak (CDCl_3 : δ_{H} 7.26, δ_{C} 77.2; CD_3OD : δ_{H} 3.31, δ_{C} 49.0; DMSO-d_6 : δ_{H} 2.50, δ_{C} 39.5; D_2O : δ_{H} 4.79).^[18] Multiplicities are abbreviated as follows: s = singlet, d = doublet, t = triplet, q = quartet, quint = quintet, sext = sextet, sept = septet, m = multiplet. High resolution mass spectra (EI, ESI) were recorded by LMU Mass Spectrometry Service using a Thermo Finnigan MAT 95, a Jeol MStation or a Thermo Finnigan LTQ FT Ultra instrument. Melting points were obtained using a Stanford Research Systems MPA120 apparatus and are uncorrected. Optical rotation measurements were performed on a Perkin Elmer 241 polarimeter at 22 °C in a 5 cm cell at concentrations expressed as g/100 mL.

5.5.2 SYNTHESIS OF AZO-APDCs

Synthesis of (2*R*,4*R*)-ethyl 1-benzyl-4-hydroxypyrrolidine-2-carboxylate (**5.2**)

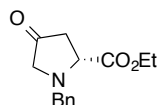


Thionyl chloride (3.34 mL, 46.1 mmol, 1.2 equiv.) was added dropwise to a mixture of *cis*-4-hydroxy-D-proline (**5.1**) (5.00 g, 38.1 mmol, 1.0 equiv.) in ethanol (80 mL) at 0 °C. The solution was heated to reflux for 16 h and cooled to room temperature. The solution was diluted with Et₂O and the resulting white solid was filtered, washed with Et₂O and dried *in vacuo* to yield (2*R*,4*R*)-ethyl 4-hydroxypyrrolidine-2-carboxylate hydrochloride (6.22 g, 31.8 mmol, 83%). This material was directly used for the next reaction without further purification.

Benzyl chloride (5.35 mL, 46.5 mmol, 1.5 equiv.) was added to a mixture of (2*R*,4*R*)-ethyl 4-hydroxypyrrolidine-2-carboxylate hydrochloride (6.22 g, 31.8 mmol, 1.0 equiv.) and TEA (10.0 mL, 71.9 mmol, 2.3 equiv.) in DCM (60 mL). The reaction mixture was heated to reflux for 36 h. After cooling, 1 M NaOH (50 mL) was added and the phases were separated. The aqueous phase was extracted with DCM (2 x 50 mL) and the combined organic phases were washed with brine (100 mL), dried over MgSO₄ and concentrated *in vacuo*. The crude product was purified by silica gel chromatography (hexanes/EtOAc, 1:1) to give the *N*-benzylated ethyl ester **5.2** (7.27 g, 29.2 mmol, 92%; 77% over two steps) as a colorless oil.

TLC (hexanes/EtOAc, 1:1): *R_f* = 0.37. **[α]_D²²:** +57.3 (*c* = 0.37, DCM). **¹H NMR (CDCl₃, 300 MHz, 27 °C):** δ = 7.35–7.21 (m, 5H, ArH), 4.28–4.20 (m, 1H, CH), 4.08 (qd, *J* = 7.2, 2.4 Hz, 2H, CH₂), 3.88 (d, *J* = 13.1 Hz, 1H, CH), 3.70 (d, *J* = 13.1 Hz, 1H, CH), 3.39–3.25 (m, 2H, CH, OH), 3.01 (dt, *J* = 9.8, 1.5 Hz, 1H, CH), 2.63 (dd, *J* = 9.8, 4.1 Hz, 1H, CH), 2.37 (ddd, *J* = 14.1, 9.9, 5.8 Hz, 1H, CH), 2.00–1.88 (m, 1H, CH), 1.22 (t, *J* = 7.2 Hz, 3H, CH₃) ppm. **¹³C NMR (CDCl₃, 75 MHz, 27 °C):** δ = 175.1, 138.1, 129.0, 128.2, 127.2, 70.9, 63.5, 61.8, 61.0, 58.1, 39.1, 14.1 ppm. **IR (neat, ATR):** $\tilde{\nu}$ = 3412 (m), 1728 (s), 1496 (w), 1454 (m), 1376 (m), 1340 (w), 1271 (w), 1194 (vs), 1085 (m), 1050 (m), 1028 (m), 974 (w), 747 (m), 700 (s) cm⁻¹. **HRMS (EI⁺):** *m/z* calcd. for [C₁₄H₁₉NO₃]⁺: 249.1365, found: 249.1364 ([M]⁺).

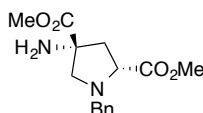
Synthesis of (*R*)-ethyl 1-benzyl-4-oxopyrrolidine-2-carboxylate (**5.3**)



Oxalyl chloride (3.67 mL, 42.8 mmol, 1.5 equiv.) was added dropwise to a solution of DCM (100 mL) and DMSO (4.05 mL, 57.0 mmol, 2.0 equiv.) at -78 °C. The reaction mixture was allowed to equilibrate for 10 min, followed by dropwise addition of a solution of alcohol **5.2** (7.10 g, 28.5 mmol, 1.0 equiv.) in DCM (30 mL). Upon complete addition, the reaction mixture was stirred for 2 h at -78 °C. Then TEA (11.9 mL, 85.5 mmol, 3.0 equiv.) was added dropwise and the reaction mixture was allowed to warm to room temperature. The pH was adjusted to pH = 10 with sat. aqu. NaHCO_3 , the phases were separated and the aqueous phase was extracted with Et_2O (2 x 75 mL). The combined organic phases were washed with brine (100 mL), dried over MgSO_4 and evaporated to dryness. The crude product was purified by silica gel chromatography (hexanes/ EtOAc , 4:1), affording ketone **5.3** (6.50 g, 26.3 mmol, 92%) as an orange oil.

TLC (hexanes/ EtOAc , 4:1): R_f = 0.43. $[\alpha]_D^{22}$: +32.1 (c = 0.75, DCM). **^1H NMR (CDCl_3 , 300 MHz, 27 °C):** δ = 7.37–7.28 (m, 5H, ArH), 4.23 (q, J = 7.1 Hz, 2H, CH_2), 3.98 (d, J = 13.1 Hz, 1H, CH), 3.85 (dd, J = 7.7, 5.7 Hz, 1H, CH), 3.76 (d, J = 13.1 Hz, 1H, CH), 3.38 (d, J = 17.2 Hz, 1H, CH), 3.03 (d, J = 17.2 Hz, 1H, CH), 2.74 (dd, J = 18.0, 7.7 Hz, 1H, CH), 2.57 (dd, J = 18.0, 5.7 Hz, 1H, CH), 1.32 (t, J = 7.2 Hz, 3H, CH_3) ppm. **^{13}C NMR (CDCl_3 , 75 MHz, 27 °C):** δ = 211.0, 172.0, 137.0, 128.8, 128.5, 127.6, 62.3, 61.1, 58.9, 57.4, 41.8, 14.3 ppm. **IR (neat, ATR):** $\tilde{\nu}$ = 1760 (vs), 1729 (s), 1454 (w), 1374 (w), 1345 (w), 1244 (w), 1195 (s), 1176 (s), 1132 (m), 1075 (w), 1029 (m), 753 (w), 700 (m) cm^{-1} . **HRMS (ESI $^+$):** m/z calcd. for $[\text{C}_{14}\text{H}_{18}\text{NO}_3]^+$: 248.1287, found: 248.1281 ($[\text{M}+\text{H}]^+$).

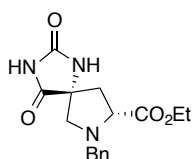
Synthesis of (*2R,4R*)-dimethyl 4-amino-1-benzylpyrrolidine-2,4-dicarboxylate (**5.5**)



KCN (2.64 g, 40.5 mmol, 2.5 equiv.) was added in one portion to a solution of ketone **5.3** (4.00 g, 16.2 mmol, 1.0 equiv.) and ammonium carbonate (4.67 g, 48.6 mmol, 3.0 equiv.) in ethanol (120 mL) and water (120 mL). The resulting reaction mixture was heated to 55 °C for

24 h. The mixture was cooled to room temperature, diluted with water (150 mL) and extracted with EtOAc (3 x 50 mL). The combined organic layers were washed with brine (75 mL), dried over MgSO₄ and the solvent was removed *in vacuo* to yield a mixture of both hydantoin diastereomers (2.63 g, 8.29 mmol, 51%) as colorless gum.

An analytical sample of diastereomeric pure hydantoin **5.4** (main isomer) was obtained by flash silica gel chromatography (CHCl₃/MeOH, 60:1) as colorless gum.



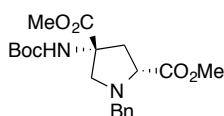
TLC (CHCl₃/MeOH, 50:1): $R_f = 0.16$. $[\alpha]_D^{22}$: +63.5 ($c = 0.40$, DMSO- d_6). **¹H NMR (DMSO- d_6 , 600 MHz, 27 °C):** $\delta = 10.63$ (s, 1H, NH), 8.17 (s, 1H, NH), 7.31–7.25 (m, 4H, ArH), 7.24–7.18 (m, 1H, ArH), 4.10–4.01 (m, 2H, CH₂), 3.93 (d, $J = 13.2$ Hz, 1H, CH), 3.46 (d, $J = 13.2$ Hz, 1H, CH), 3.40 (t, $J = 7.8$ Hz, 1H, CH), 2.89 (d, $J = 10.1$ Hz, 1H, CH), 2.65 (d, $J = 10.1$, 1H, CH), 2.43 (dd, $J = 13.2, 7.8$ Hz, 1H, CH), 2.05 (dd, $J = 13.2, 9.0$ Hz, 1H, CH), 1.25 (t, $J = 7.1$, 3H, CH₃) ppm. **¹³C NMR (DMSO- d_6 , 150 MHz, 27 °C):** $\delta = 178.0, 172.0, 156.6, 138.4, 129.1, 128.6, 127.5, 65.7, 65.0, 61.9, 60.9, 57.8, 40.5, 14.5$ ppm. **IR (neat, ATR):** $\tilde{\nu} = 3242$ (m), 1775 (m), 1712 (vs), 1397 (m), 1286 (m), 1190 (m), 1101 (m), 1028 (m), 749 (s), 700 (m) cm⁻¹. **HRMS (ESI⁺):** m/z calcd. for [C₁₆H₂₀N₃O₄]⁺: 318.1454, found: 318.1446 ([M+H]⁺).

A mixture of both hydantoin diastereomers (2.40 g, 7.56 mmol, 1.0 equiv.) was dissolved in 2 M NaOH (50 mL) and the reaction mixture was heated to reflux for 16 h. The reaction mixture was then cooled to 0 °C, acidified to pH = 1 with conc. HCl and concentrated *in vacuo*. Methanol (50 mL) was added to the crude amino diacid mixture and then concentrated to dryness (5x). The resulting anhydrous amino diacid was then reconstituted in methanol (100 mL), cooled to 0 °C and treated with thionyl chloride (2.20 mL, 30.3 mmol, 4.0 equiv.). Upon complete addition, the reaction mixture was heated to reflux for 36 h. The solids were filtered and the filtrate was concentrated *in vacuo*. The crude product was reconstituted in water (50 mL) and basified to pH = 8 with 1 M NaOH. The aqueous phase was then extracted with EtOAc (3 x 40 mL). The combined organic layers were washed with brine (75 mL), dried over MgSO₄ and evaporated to dryness to give both diastereomers in 59% yield (1.30 g, 4.45 mmol).

The desired diastereomeric pure methyl ester **5.5** was then obtained by flash silica gel chromatography (DCM/MeOH/HOAc/H₂O, 95:5:0.6:0.6 → 90:10:0.6:0.6) in a total yield over two steps of 24% (539 mg, 1.84 mmol) as a colorless gum.

TLC (hexanes/EtOAc, 1:4): $R_f = 0.09$. $[\alpha]_D^{22}$: +68.7 ($c = 0.21$, DCM). **¹H NMR (CDCl₃, 600 MHz, 27 °C):** $\delta = 7.33\text{--}7.27$ (m, 4H, ArH), 7.25–7.22 (m, 1H, ArH), 3.95 (d, $J = 13.2$ Hz, 1H, CH), 3.73 (s, 3H, OCH₃), 3.66 (s, 3H, OCH₃), 3.58 (d, $J = 13.2$ Hz, 1H, CH), 3.46 (dd, $J = 9.6, 5.4$ Hz, 1H, CH), 2.90 (d, $J = 9.0$ Hz, 1H, CH), 2.83 (d, $J = 9.0$ Hz, 1H, CH), 2.77 (dd, $J = 13.2, 9.6$ Hz, 1H, CH), 2.14 (br s, 2H, NH₂), 1.99 (dd, $J = 13.2, 5.4$ Hz, 1H, CH) ppm. **¹³C NMR (CDCl₃, 150 MHz, 27 °C):** $\delta = 174.5, 173.8, 137.8, 129.0, 128.3, 127.3, 64.9, 64.3, 63.0, 58.0, 52.5, 52.0, 42.6$ ppm. **IR (neat, ATR):** $\tilde{\nu} = 3376$ (w), 2952 (w), 1734 (vs), 1496 (w), 1436 (m), 1203 (s), 1119 (m), 1028 (w), 753 (m), 702 (m) cm⁻¹. **HRMS (ESI⁺):** m/z calcd. for [C₁₅H₂₁N₂O₄]⁺: 293.1501, found: 293.1492 ([M+H]⁺).

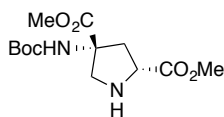
Synthesis of (2*R*,4*R*)-dimethyl 1-benzyl-4-((*tert*-butoxycarbonyl)amino)-pyrrolidine-2,4-dicarboxylate (**5.6**)



Boc₂O (1.15 g, 5.25 mmol, 3.0 equiv.) was added to a solution of amine **5.5** (513 mg, 1.75 mmol, 1.0 equiv.) in DCM (12 mL). The reaction mixture was stirred at room temperature for 16 h. The solvent was removed *in vacuo* and the crude product was purified by flash silica gel chromatography (hexanes/EtOAc, 99:1 → 4:1 → 1:1), affording Boc-protected amine **5.6** (677 mg, 1.73 mmol, 99%) as a colorless solid.

TLC (hexanes/EtOAc, 4:1): $R_f = 0.25$. **M.p.:** 124–125 °C. $[\alpha]_D^{22}$: +29.1 ($c = 0.23$, DCM). **¹H NMR (CDCl₃, 600 MHz, 27 °C):** $\delta = 7.33\text{--}7.24$ (m, 5H, ArH), 5.37 (br s, 1H, NH), 4.01 (br s, 1H, CH), 3.72 (s, 3H, OCH₃), 3.69 (s, 3H, OCH₃), 3.64–3.54 (m, 1H, CH), 3.54–3.45 (m, 1H, CH), 3.07 (br s, 1H, CH), 2.95–2.77 (m, 2H, CH₂), 2.27 (br s, 1H, CH), 1.40 (s, 9H, (CH₃)₃) ppm. **¹³C NMR (CDCl₃, 150 MHz, 27 °C):** $\delta = 173.2, 172.4, 155.1, 137.3, 129.0, 128.4, 127.4, 80.1, 63.8, 63.3, 61.7, 57.9, 52.7, 52.1, 39.8, 28.2$ ppm. **IR (neat, ATR):** $\tilde{\nu} = 3378$ (w), 2953 (w), 1733 (s), 1712 (vs), 1496 (m), 1367 (m), 1251 (s), 1169 (vs), 1075 (m), 749 (w), 702 (w) cm⁻¹. **HRMS (ESI⁺):** m/z calcd. for [C₂₀H₂₉N₂O₆]⁺: 393.2026, found: 393.2018 ([M+H]⁺).

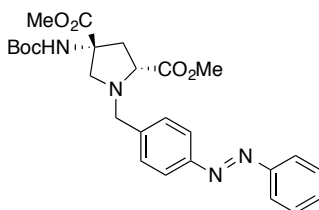
Synthesis of (2*R*,4*R*)-dimethyl 4-((*tert*-butoxycarbonyl)amino)pyrrolidine-2,4-dicarboxylate (**5.7**)



Ammonium formate (523 mg, 8.30 mmol, 5.0 equiv.) was added to a solution of benzyl protected amine **5.6** (650 mg, 1.66 mmol, 1.0 equiv.) and Pd/C (10%, 70 mg) in methanol (17 mL). The resulting reaction mixture was heated to reflux for 2 h. The mixture was cooled to room temperature and filtered through Celite. The filtrate was concentrated *in vacuo* and the residue was purified by flash silica gel chromatography (hexanes/EtOAc, 1:4 → 0:1) to give amine **5.7** (490 mg, 1.62 mmol, 98%) as a colorless gum.

TLC (EtOAc): $R_f = 0.25$. $[\alpha]_D^{22}$: -22.9 ($c = 0.11$, DCM). **$^1\text{H NMR}$ (CDCl_3 , 600 MHz, 27 °C):** $\delta = 5.18$ (br s, 1H, NH), 4.00 (dd, $J = 9.6, 5.4$ Hz, 1H, CH), 3.75 (s, 6H, 2 x OCH_3), 3.65 (br s, 1H, NH), 3.36 (d, $J = 12.0$ Hz, 1H, CH), 3.33–3.27 (m, 1H, CH), 2.76 (dd, $J = 13.8, 9.6$ Hz, 1H, CH), 2.41–2.31 (m, 1H, CH), 1.40 (s, 9H, $(\text{CH}_3)_3$) ppm. **$^{13}\text{C NMR}$ (CDCl_3 , 150 MHz, 27 °C):** $\delta = 173.9, 172.9, 155.0, 80.3, 65.6, 59.7, 57.0, 52.8, 52.5, 40.9, 28.2$ ppm. **IR (neat, ATR):** $\tilde{\nu} = 3360$ (w), 2956 (w), 1732 (vs), 1711 (vs), 1514 (m), 1453 (m), 1392 (w), 1367 (m), 1243 (s), 1165 (vs), 1112 (m), 1074 (m), 1031 (m), 870 (w), 830 (w), 682 (w) cm^{-1} . **HRMS (ESI⁺):** m/z calcd. for $[\text{C}_{13}\text{H}_{23}\text{N}_2\text{O}_6]^+$: 303.1556, found: 303.1549 ($[\text{M}+\text{H}]^+$).

Synthesis of (2*R*,4*R*)-dimethyl 4-((*tert*-butoxycarbonyl)amino)-1-(4-phenyldiazenyl)benzylpyrrolidine-2,4-dicarboxylate (**5.8**)

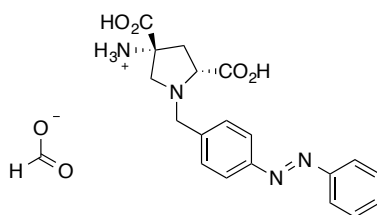


To a solution of amine **5.7** (130 mg, 0.430 mmol, 1.0 equiv.) in DCM (10 mL) were added DIPEA (0.15 mL, 0.85 mmol, 2.0 equiv.) and a solution of bromide **4.18** (233 mg, 0.850 mmol, 2.0 equiv.) in DCM (7 mL). Bu_4NI (159 mg, 0.430 mmol, 1.0 equiv.) was added and the reaction mixture was stirred at room temperature for 16 h. 1 M NaOH (10 mL) was added and the phases were separated. The aqueous phase was extracted with Et_2O (5 x 20 mL) and the

combined organic layers were washed with brine (25 mL), dried over MgSO₄ and concentrated *in vacuo*. The residue was purified by flash silica gel chromatography (hexanes/EtOAc, gradient from 4:1 to 2:1), affording tertiary amine **5.8** (162 mg, 0.330 mmol, 77%) as orange crystals.

TLC (hexanes/EtOAc, 2:1): R_f = 0.38. **M.p.:** 154–155 °C. $[\alpha]_D^{22}$: -18.5 (c = 0.09, DCM). **¹H NMR (CDCl₃, 400 MHz, 27 °C):** δ = 7.93–7.82 (m, 4H, ArH), 7.55–7.43 (m, 5H, ArH), 5.40 (br s, 1H, NH), 4.09 (d, J = 13.2 Hz, 1H, CH), 3.73 (s, 3H, OCH₃), 3.69 (s, 3H, OCH₃), 3.68–3.64 (m, 1H, CH), 3.54 (dd, J = 9.2, 6.0 Hz, 1H, CH), 3.17–3.05 (m, 1H, CH), 2.97–2.80 (m, 2H, 2 x CH), 2.29 (dd, J = 13.2, 5.4 Hz, 1H, CH), 1.39 (s, 9H, (CH₃)₃) ppm. **¹³C NMR (CDCl₃, 100 MHz, 27 °C):** δ = 173.3, 172.5, 155.1, 152.6, 152.0, 140.8, 130.9, 129.6, 129.1, 122.9, 122.8, 80.1, 63.9, 63.3, 61.8, 57.6, 52.7, 52.2, 39.9, 28.2 ppm. **IR (neat, ATR):** $\tilde{\nu}$ = 3394 (w), 1741 (s), 1707 (s), 1508 (m), 1393 (w), 1364 (w), 1301 (m), 1269 (m), 1250 (m), 1168 (vs), 1075 (m), 1050 (m), 829 (w), 765 (w), 685 (w) cm⁻¹. **HRMS (ESI⁺):** m/z calcd. for [C₂₆H₃₃N₄O₆]⁺: 497.2400, found: 497.2391 ([M+H]⁺).

Synthesis of (3*R*,5*R*)-3,5-dicarboxy-1-(4-phenyldiazenyl)benzylpyrrolidin-3-aminium formate (*p*-Azo-APDC)

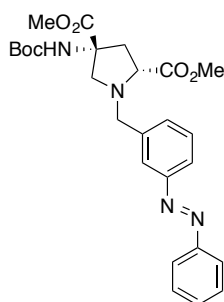


Boc-protected dimethyl ester **5.8** (145 mg, 0.290 mmol) was dissolved in THF (5 mL) and a 2 M solution of LiOH (1 mL) was added. The mixture was stirred at room temperature for 16 h. The phases were separated and the aqueous layer was acidified to pH = 1 with 1 M HCl and then extracted with EtOAc (3 x 5 mL). The combined organic layers were washed with brine (10 mL), dried over MgSO₄ and concentrated under reduced pressure. The crude product was used without further purification in the following step.

The residue was suspended in EtOAc (5 mL) and freshly prepared HCl gas (from NaCl and conc. H₂SO₄) was bubbled through the mixture for 1 h. The solvent was removed *in vacuo* and the residue suspended in Et₂O (10 mL). After centrifugation, the supernatant liquid was removed. The procedure was repeated and the crude product purified by reversed-phase silica gel column chromatography (H₂O/MeOH/HCO₂H, gradient from 100:0:0.1 to 0:100:0.1), yielding *p*-Azo-APDC as its formate salt (67 mg, 0.18 mmol, 62%) as orange crystals.

$[\alpha]_D^{22}$: +9.6 ($c = 0.08$, H₂O). **M.p.**: 78 °C (decomp.). **¹H NMR (D₂O/KOD, 600 MHz, 27 °C)**: $\delta = 7.61\text{--}7.49$ (m, 4H, ArH), 7.41–7.26 (m, 5H, ArH), 3.78 (d, $J = 12.6$ Hz, 1H, CH), 3.23 (d, $J = 12.6$ Hz, 1H, CH), 2.97 (dd, $J = 8.4, 8.4$ Hz, 1H, CH), 2.60 (d, $J = 9.6$ Hz, 1H, CH), 2.54–2.47 (m, 2H, 2 x CH), 1.54–1.48 (m, 1H, CH) ppm. **¹³C NMR (D₂O/KOD, 100 MHz, 25 °C)**: $\delta = 182.0, 180.8, 151.9, 151.0, 141.5, 131.6, 130.6, 130.0, 129.4, 128.9, 128.2, 122.2, 122.2, 120.6, 120.5, 68.9, 65.3, 63.1, 57.7, 43.6$ ppm.^[ii] **IR (neat, ATR)**: $\tilde{\nu} = 3186$ (m), 2916 (s), 2850 (m), 1574 (vs), 1467 (m), 1445 (m), 1386 (s), 1303 (m), 1251 (w), 1155 (w), 1069 (m), 928 (w), 880 (w), 834 (m), 788 (w), 765 (w), 686 (m) cm⁻¹. **HRMS (ESI)**: m/z calcd. for [C₁₉H₁₉N₄O₄]⁻: 367.1406, found: 367.1412 ([M-H]⁻). **UV/Vis**: $\lambda_{\text{max}} = 323, 420$ nm.

Synthesis of (2*R*,4*R*)-dimethyl 4-((*tert*-butoxycarbonyl)amino)-1-(3-(phenyldiazenyl)-benzyl)pyrrolidine-2,4-dicarboxylate (5.9)



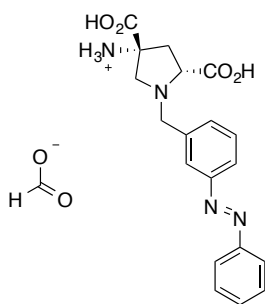
To a solution of amine **5.7** (22 mg, 0.073 mmol, 1.0 equiv.) in DCM (1.5 mL) were added DIPEA (25 μ L, 0.15 mmol, 2.0 equiv.) and a solution of bromide **4.21** (40 mg, 0.15 mmol, 2.0 equiv.) in DCM (1.5 mL). Bu₄NI (27 mg, 0.073 mmol, 1.0 equiv.) was added and the reaction mixture was stirred at room temperature for 16 h. 1 M NaOH (3 mL) was added and the phases were separated. The aqueous phase was extracted with Et₂O (2 x 10 mL) and the combined organic layers were washed with brine (15 mL), dried over MgSO₄ and concentrated *in vacuo*. The residue was purified by flash silica gel chromatography (hexanes/EtOAc, 10:1 \rightarrow 2:1), affording tertiary amine **5.9** (23 mg, 0.046 mmol, 63%) as an orange oil.

TLC (hexanes/EtOAc, 2:1): $R_f = 0.39$. $[\alpha]_D^{22}$: -46.0 ($c = 0.10$, DCM). **¹H NMR (CDCl₃, 300 MHz, 27 °C)**: $\delta = 7.96\text{--}7.94$ (m, 1H, ArH), 7.94–7.92 (m, 1H, ArH), 7.87 (s, 1H, ArH), 7.86–7.81 (m, 1H, ArH), 7.58–7.48 (m, 5H, ArH), 5.41 (br s, 1H, NH), 4.16 (d, $J = 12.9$ Hz,

^[ii] Additional signals in the aromatic region in the ¹³C NMR spectrum were observed due to *cis/trans* isomerization of *p*-Azo-APDC.

1H, CH), 3.75 (s, 3H, OCH₃), 3.73 (s, 3H, OCH₃), 3.72–3.68 (m, 1H, CH), 3.59 (dd, *J* = 9.3, 6.0 Hz, 1H, CH), 3.15 (d, *J* = 10.2 Hz, 1H, CH), 3.00–2.88 (m, 2H, 2 x CH), 2.33 (dd, *J* = 13.8, 6.0 Hz, 1H, CH), 1.41 (s, 9H, (CH₃)₃) ppm. ¹³C NMR (CDCl₃, 150 MHz, 27 °C): δ = 173.3, 172.4, 155.1, 152.7, 152.6, 138.8, 131.5, 131.0, 129.1, 129.1, 123.2, 122.8, 121.9, 80.1, 64.0, 63.4, 61.8, 57.7, 52.7, 52.1, 39.8, 28.2 ppm. IR (neat, ATR): $\tilde{\nu}$ = 3369 (w), 2976 (w), 2951 (w), 2839 (w), 1739 (vs), 1711 (vs), 1586 (w), 1505 (m), 1472 (m), 1448 (m), 1435 (m), 1391 (w), 1366 (m), 1274 (m), 1247 (s), 1200 (s), 1167 (vs), 1075 (m), 1046 (w), 1021 (w), 1000 (w), 915 (w), 871 (w), 830 (w), 799 (w), 766 (m), 734 (m), 694 (s), 668 (w) cm⁻¹. HRMS (ESI⁺): *m/z* calcd. for [C₂₆H₃₃N₄O₆]⁺: 497.2400, found: 497.2393 ([M+H]⁺).

Synthesis of (3*R*,5*R*)-3,5-dicarboxy-1-(3-phenyldiazenyl)benzylpyrrolidin-3-aminium formate (*m*-Azo-APDC)



Boc-protected dimethyl ester **5.9** (23 mg, 0.046 mmol) was dissolved in THF (1 mL) and a 2 M solution of LiOH (0.2 mL) was added. The mixture was stirred at room temperature for 16 h. The phases were separated and the aqueous layer was acidified to pH = 1 with 1 M HCl and then extracted with EtOAc (3 x 2 mL). The combined organic layers were washed with brine (5 mL), dried over MgSO₄ and concentrated under reduced pressure. The crude product was used without further purification in the following step.

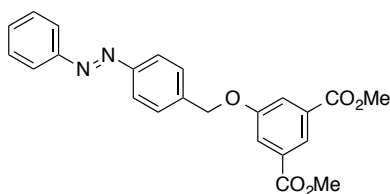
The crude residue was suspended in EtOAc (2 mL) and freshly prepared HCl gas (from NaCl and conc. H₂SO₄) was bubbled through the mixture for 1 h. The solvent was removed *in vacuo* and the crude product was purified by reversed-phase silica gel column chromatography (H₂O/MeOH/HCO₂H, gradient from 100:0:0.1 to 30:70:0.1), yielding *m*-Azo-APDC as its formate salt (16 mg, 0.043 mmol, 93%) as an orange solid.

[α]_D²²: -36.0 (*c* = 0.05, DMSO). M.p.: 183 °C (decomp.). ¹H NMR (DMSO-*d*₆, 600 MHz, 27 °C): δ = 8.24 (s, 1H, HCO₂⁻), 7.92–7.86 (m, 2H, ArH), 7.80 (s, 1H, ArH), 7.76–7.71 (m, 1H, ArH), 7.60–7.52 (m, 3H, ArH), 7.52–7.47 (m, 2H, ArH), 3.92 (d, *J* = 13.2 Hz, 1H, CH), 3.78 (d, *J* = 13.2 Hz, 1H, CH), 3.33 (d, *J* = 9.0 Hz, 1H, CH), 2.97 (d, *J* = 8.4 Hz, 1H, CH), 2.81 (d,

$J = 8.4$ Hz, 1H, *CH*), 2.44–1.37 (m, 1H, *CH*), 1.81 (d, $J = 12.6$ Hz, 1H, *CH*) ppm. ^{13}C NMR (DMSO- d_6 , 150 MHz, 27 °C): $\delta = 176.8, 171.0, 164.3, 152.4, 152.4, 141.3, 132.2, 131.9, 129.9, 129.5, 123.1, 123.0, 121.4, 68.3, 64.9, 61.6, 57.5, 39.5$ ppm. IR (neat, ATR): $\tilde{\nu} = 2978$ (m), 1652 (m), 1614 (s), 1506 (m), 1477 (m), 1439 (m), 1398 (m), 1380 (m), 1334 (s), 1283 (m), 1260 (m), 1224 (w), 1194 (m), 1137 (m), 1092 (w), 1031 (w), 973 (w), 911 (w), 888 (w), 823 (m), 796 (s), 772 (m), 717 (w), 692 (vs) cm^{-1} . HRMS (ESI): m/z calcd. for $[\text{C}_{19}\text{H}_{19}\text{N}_4\text{O}_4]^-$: 367.1406, found: 367.1409 ($[\text{M}-\text{H}]^-$). UV/Vis: $\lambda_{\text{max}} = 324, 440$ nm.

5.5.3 SYNTHESIS OF AZO-3C5HPGS

Synthesis of dimethyl 5-((4-(phenyldiazenyl)benzyl)oxy)isophthalate (5.10)

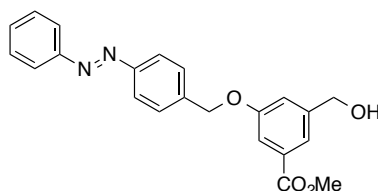


Dimethyl 5-hydroxyisophthalate (1.27 g, 6.06 mmol, 1.0 equiv.) was dissolved in acetone (175 mL) at room temperature and K_2CO_3 (1.67 g, 12.1 mmol, 2.0 mmol) and Bu_4NI (2.24 g, 6.06 mmol, 1.0 equiv.) were added, followed by bromide **4.18** (2.00 g, 7.27 mmol, 1.2 equiv.). The mixture was stirred for 16 h at room temperature. The solvent was removed *in vacuo* and DCM (100 mL) was added and the mixture was washed with water (200 mL). The aqueous layer was extracted with DCM (2 x 50 mL) and the combined organic layers were dried over MgSO_4 and concentrated *in vacuo*. The crude product was purified by flash silica gel chromatography (hexanes/DCM, gradient from 3:1 to 1:9), giving rise to azobenzene ether **5.10** (2.39 g, 5.91 mmol, 98%) as orange crystals. Moreover, bromide **4.18** (204 mg, 0.740 mmol, 10%) was recovered.

TLC (hexanes/DCM, 1:4): $R_f = 0.78$. M.p.: 179–181 °C. ^1H NMR (CDCl_3 , 300 MHz, 27 °C): $\delta = 8.34$ (t, $J = 1.5$ Hz, 1H, *ArH*), 8.01–7.92 (m, 4H, *ArH*), 7.90 (s, 1H, *ArH*), 7.89 (s, 1H, *ArH*), 7.64 (m, 1H, *ArH*), 7.61 (m, 1H, *ArH*), 7.58–7.50 (m, 3H, *ArH*), 5.26 (s, 2H, CH_2), 3.97 (s, 6H, 2 x OCH_3) ppm. ^{13}C NMR (CDCl_3 , 75 MHz, 27 °C): $\delta = 166.1, 158.6, 152.6, 152.5, 139.0, 131.9, 131.1, 129.1, 128.0, 123.4, 123.2, 122.9, 120.2, 70.0, 52.5$ ppm. IR (neat, ATR): $\tilde{\nu} = 1725$ (vs), 1596 (m), 1454 (m), 1429 (m), 1344 (m), 1316 (m), 1250 (vs), 1114 (m),

1052 (m), 1004 (m), 877 (w), 827 (w), 757 (m), 682 (w) cm^{-1} . **HRMS (ESI⁺):** m/z calcd. for $[\text{C}_{23}\text{H}_{21}\text{N}_2\text{O}_5]^+$: 405.1450, found: 405.1444 ($[\text{M}+\text{H}]^+$).

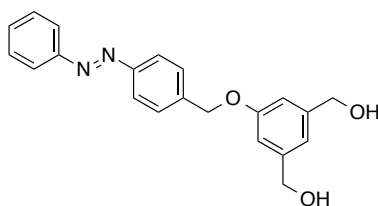
Synthesis of methyl 3-(hydroxymethyl)-5-((4-(phenyldiazenyl)benzyl)oxy)benzoate (5.11)



Dimethyl ester **5.10** (2.00 g, 4.95 mmol, 1.0 equiv.) was dissolved in THF (200 mL) and LiAlH_4 (94 mg, 2.5 mmol, 0.5 equiv.) was added. The mixture was stirred for 4 h at room temperature. H_2O was added (0.10 mL), followed by aq. NaOH (10%, 0.20 mL) and H_2O (0.30 mL). The mixture was stirred for 1 h and then filtered. The filtrate was concentrated *in vacuo*. The crude product was purified by flash silica gel chromatography (hexanes/EtOAc, 2:1 \rightarrow 1:1), affording alcohol **5.11** (1.13 g, 3.00 mmol, 61%) as orange crystals.

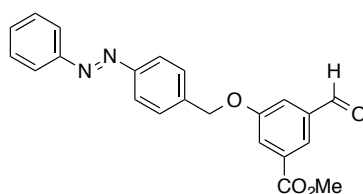
TLC (hexanes/EtOAc, 2:1): R_f = 0.26. **M.p.:** 131–132 °C. **¹H NMR (CDCl₃, 300 MHz, 27 °C):** δ = 7.96–7.90 (m, 4H, ArH), 7.66–7.64 (m, 1H, ArH), 7.60–7.57 (m, 3H, ArH), 7.54–7.46 (m, 3H, ArH), 7.25–7.23 (m, 1H, ArH), 5.20 (s, 2H, CH₂), 4.73 (s, 2H, CH₂), 3.92 (s, 3H, OCH₃), 1.74 (br s, 1H, OH) ppm. **¹³C NMR (CDCl₃, 75 MHz, 27 °C):** δ = 166.7, 158.8, 152.6, 152.3, 142.9, 139.4, 131.7, 131.1, 129.1, 128.0, 123.1, 122.9, 120.6, 118.3, 114.4, 69.7, 64.6, 52.3 ppm. **IR (neat, ATR):** $\tilde{\nu}$ = 3493 (w), 1715 (s), 1598 (m), 1450 (m), 1435 (m), 1377 (w), 1307 (s), 1234 (vs), 1158 (m), 1108 (m), 1049 (s), 1011 (m), 988 (m), 954 (w), 906 (w), 853 (m), 838 (w), 825 (w), 798 (w), 770 (vs), 733 (w), 714 (w), 691 (s), 669 (w) cm^{-1} . **HRMS (ESI⁺):** m/z calcd. for $[\text{C}_{22}\text{H}_{21}\text{N}_2\text{O}_4]^+$: 377.1501, found: 377.1494 ($[\text{M}+\text{H}]^+$).

Moreover, unreacted dimethyl ester **5.10** (500 mg, 1.25 mmol, 25%) was recovered and the doubly reduced diol **5.41** (84 mg, 0.24 mmol, 5%) was obtained as orange crystals.



TLC (hexanes/EtOAc, 1:3): R_f = 0.33. **M.p.:** 108 °C (dec.). **^1H NMR (CDCl₃, 600 MHz, 27 °C):** δ = 7.95–7.91 (m, 4H, ArH), 7.59 (s, 1H, ArH), 7.57 (s, 1H, ArH), 7.54–7.51 (m, 2H, ArH), 7.50–7.46 (m, 1H, ArH), 6.98 (s, 1H, ArH), 6.95 (s, 2H, ArH), 5.17 (s, 2H, CH₂), 4.68 (s, 4H, 2 x CH₂), 1.64 (br s, 2H, 2 x OH) ppm. **^{13}C NMR (CDCl₃, 150 MHz, 27 °C):** δ = 159.2, 152.6, 152.3, 142.9, 139.9, 131.1, 129.1, 127.9, 123.1, 122.9, 117.9, 112.5, 69.5, 65.1 ppm. **IR (neat, ATR):** $\tilde{\nu}$ = 3311 (m), 1600 (m), 1454 (m), 1298 (m), 1165 (m), 1019 (s), 832 (s), 769 (m), 709 (w), 692 (m), 668 (w) cm⁻¹. **HRMS (ESI⁺):** m/z calcd. for [C₂₁H₂₁N₂O₃]⁺: 349.1552, found: 349.1546 ([M+H]⁺).

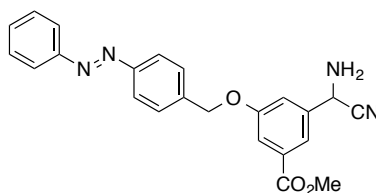
Synthesis of methyl 3-formyl-5-((4-(phenyldiazenyl)benzyl)oxy)benzoate (5.12)



To a solution of alcohol **5.11** (1.12 g, 2.98 mmol, 1.0 equiv.) in DCM (65 mL), MnO₂ (2.59 g, 29.8 mmol, 10 equiv.) was added in one portion. The reaction mixture was stirred at room temperature for 18 h. The mixture was filtered through Celite and the residue washed thoroughly with DCM. The filtrate was concentrated under reduced pressure to give aldehyde **5.12** (990 mg, 2.64 mmol, 89%) as an orange solid.

TLC (hexanes/EtOAc, 2:1): R_f = 0.67. **M.p.:** 147–148 °C. **^1H NMR (CDCl₃, 300 MHz, 27 °C):** δ = 10.04 (s, 1H, CHO), 8.17 (dd, J = 1.4, 1.4 Hz, 1H, ArH), 8.02–7.91 (m, 5H, ArH), 7.70 (dd, J = 2.7, 1.4 Hz, 1H, ArH), 7.63 (s, 1H, ArH), 7.60 (s, 1H, ArH), 7.58–7.50 (m, 3H, ArH), 5.26 (s, 2H, CH₂), 3.99 (s, 3H, OCH₃) ppm. **^{13}C NMR (CDCl₃, 75 MHz, 27 °C):** δ = 191.1, 165.7, 159.2, 152.6, 152.5, 138.7, 138.0, 132.6, 131.2, 129.1, 128.1, 124.8, 123.2, 122.9, 122.2, 117.7, 70.0, 52.6 ppm. **IR (neat, ATR):** $\tilde{\nu}$ = 1732 (s), 1699 (s), 1595 (m), 1461 (m), 1436 (m), 1394 (m), 1339 (m), 1302 (m), 1227 (vs), 1149 (m), 1110 (m), 1048 (m), 999 (w), 866 (w), 832 (w), 802 (w), 764 (m), 684 (m), 668 (w) cm⁻¹. **HRMS (EI⁺):** m/z calcd. for [C₂₂H₁₉N₂O₄]⁺: 375.1345, found: 375.1340 ([M+H]⁺).

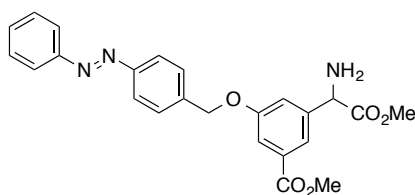
Synthesis of methyl 3-(amino(cyano)methyl)-5-((4-(phenyldiazenyl)benzyl)-oxy)benzoate (5.13)



To a solution of aldehyde **5.12** (678 mg, 1.81 mmol, 1.0 equiv.) in DCM (13 mL), a 7 M solution of NH_3 in MeOH (13 mL) was added. The mixture was stirred for 10 min and TMSCN (0.36 mL, 2.9 mmol, 1.6 equiv.) was added dropwise. The reaction mixture was stirred for 36 h at room temperature, followed by removal of the solvent *in vacuo*. The crude product was purified by flash silica gel chromatography (hexanes/EtOAc, gradient from 4:1 to 1:1), affording aminonitrile **5.13** (557 mg, 1.39 mmol, 77%) as a red viscous oil. As a side product, cyanohydrin **5.15** (111 mg, 0.280 mmol) was obtained in 15% yield.

TLC (hexanes/EtOAc, 2:1): $R_f = 0.28$. **$^1\text{H NMR}$ (CDCl_3 , 400 MHz, 27 °C):** $\delta = 7.96\text{--}7.94$ (m, 1H, ArH), 7.93–7.90 (m, 3H, ArH), 7.82 (ddd, $J = 1.6, 1.6, 0.8$ Hz, 1H, ArH), 7.65 (dd, $J = 2.4, 0.6$ Hz, 1H, ArH), 7.59 (s, 1H, ArH), 7.56 (s, 1H, ArH), 7.52–7.46 (m, 3H, ArH), 7.38 (ddd, $J = 2.4, 1.6, 0.8$ Hz, 1H, ArH), 5.18 (s, 2H, CH_2), 4.91 (s, 1H, CH), 3.91 (s, 3H, OCH_3), 2.05 (br s, 2H, NH_2) ppm. **$^{13}\text{C NMR}$ (CDCl_3 , 100 MHz, 27 °C):** $\delta = 166.1, 159.0, 152.6, 152.4, 139.0, 138.3, 132.4, 131.2, 129.1, 128.0, 123.2, 122.9, 120.5, 120.4, 118.3, 115.7, 69.8, 52.5, 46.9$ ppm. **IR (neat, ATR):** $\tilde{\nu} = 1710$ (vs), 1657 (w), 1596 (m), 1485 (w), 1434 (m), 1361 (m), 1331 (m), 1299 (vs), 1221 (vs), 1154 (m), 1106 (w), 1042 (m), 1012 (w), 1000 (w), 859 (w), 830 (m), 765 (vs), 688 (s) cm^{-1} . **HRMS (ESI⁺):** m/z calcd. for $[\text{C}_{23}\text{H}_{21}\text{N}_4\text{O}_3]^+$: 401.1614, found: 401.1608 ($[\text{M}+\text{H}]^+$).

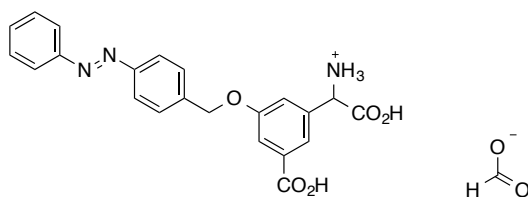
Synthesis of methyl 3-(1-amino-2-methoxy-2-oxoethyl)-5-((4-(phenyl-diazenyl)benzyl)-oxy)benzoate (5.14)



Aminonitrile **5.13** (154 mg, 0.385 mmol) was dissolved in MeOH (4 mL) and cooled to 0 °C. A 4 M solution of HCl in dioxane (4 mL) was added slowly. The solution was stirred for 1 h at 0 °C. H₂O (0.08 mL) was added and the mixture was warmed to room temperature and stirred for 16 h. The mixture was diluted with EtOAc (20 mL) and washed with NaHCO₃ (3 x 20 mL; gas evolution!). The organic layers were dried over MgSO₄ and concentrated *in vacuo*. The crude product was purified by flash silica gel chromatography (DCM/MeOH/HOAc/H₂O, 90:10:0.6:0.6), affording dimethyl ester **5.14** (87 mg, 0.20 mmol, 52%) as a red oil.

TLC (DCM/MeOH/HOAc/H₂O, 90:10:0.6:0.6): R_f = 0.42. **¹H NMR (CDCl₃, 600 MHz, 27 °C):** δ = 7.96–7.95 (m, 1H, ArH), 7.95–7.94 (m, 1H, ArH), 7.94–7.93 (m, 1H, ArH), 7.93–7.92 (m, 1H, ArH), 7.70 (dd, *J* = 1.2, 1.2 Hz, 1H, ArH), 7.61 (dd, *J* = 2.4, 1.2 Hz, 1H, ArH), 7.59 (s, 1H, ArH), 7.58 (s, 1H, ArH), 7.54–7.47 (m, 3H, ArH), 7.26–7.25 (m, 1H, ArH), 5.19 (s, 2H, CH₂), 4.66 (s, 1H, CH), 3.92 (s, 3H, OCH₃), 3.70 (s, 3H, OCH₃), 1.95 (br s, 2H, NH₂) ppm. **¹³C NMR (CDCl₃, 150 MHz, 27 °C):** δ = 173.8, 166.5, 158.8, 152.6, 152.4, 142.1, 139.3, 132.0, 131.1, 129.1, 128.0, 123.1, 122.9, 120.9, 118.7, 114.8, 69.8, 58.4, 52.6, 52.3 ppm. **IR (neat, ATR):** $\tilde{\nu}$ = 3369 (w), 2951 (w), 1720 (s), 1596 (m), 1539 (w), 1485 (w), 1435 (m), 1333 (m), 1299 (vs), 1226 (vs), 1154 (m), 1106 (m), 1037 (m), 1013 (m), 929 (w), 875 (w), 830 (m), 807 (w), 767 (s), 710 (w), 687 (s), 668 (w) cm⁻¹. **HRMS (ESI⁺):** *m/z* calcd. for [C₂₄H₂₄N₃O₅]⁺: 434.1716, found: 434.1710 ([M+H]⁺).

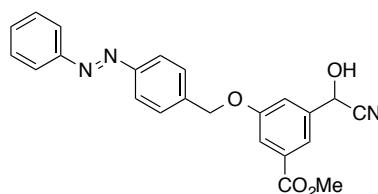
Synthesis of carboxy(3-carboxy-5-((4-(phenyldiazenyl)benzyl)oxy)phenyl)methanaminium formate (*p*-Azo-3C5HPG)



Dimethyl ester **5.14** (59 mg, 0.14 mmol) was dissolved in THF (3 mL) and a 2 M solution of LiOH in water (0.5 mL) was added. The solution was stirred for 16 h at room temperature. The pH was adjusted to pH = 1 with 2 M HCl and the solvent was removed *in vacuo*. The crude product was purified by reversed-phase silica gel column chromatography (H₂O/MeOH/HCO₂H, gradient from 100:0:0.1 to 20:80:0.1), yielding *p*-Azo-3C5HPG as its formate salt (33 mg, 0.073 mmol, 54%) as orange solid.

M.p.: 201 °C (dec.). **¹H NMR (CD₃OD/KOD/D₂O, 600 MHz, 27 °C):** δ = 7.80–7.75 (m, 4H, ArH), 7.62–7.60 (m, 1H, ArH), 7.55 (s, 1H, ArH), 7.54 (s, 1H, ArH), 7.51–7.48 (m, 1H, ArH), 7.47–7.43 (m, 3H, ArH), 7.18 (dd, *J* = 2.4, 2.4 Hz, 1H, ArH), 5.15 (s, 2H, CH₂), 4.39 (s, 1H, CH) ppm. **¹³C NMR (CD₃OD/KOD/D₂O, 150 MHz, 27 °C):** δ = 179.6, 173.7, 169.1, 158.2, 152.2, 151.8, 145.0, 140.4, 139.3, 129.4, 128.5, 128.4, 127.5, 122.8, 122.6, 122.3, 122.1, 69.2, 61.1 ppm. **IR (neat, ATR):** $\tilde{\nu}$ = 3595 (w), 3084 (m), 2013 (w), 1675 (s), 1653 (m), 1611 (s), 1594 (s), 1559 (w), 1500 (s), 1472 (m), 1399 (m), 1337 (m), 1302 (s), 1257 (s), 1167 (m), 1117 (w), 1106 (w), 1062 (m), 1035 (w), 1013 (w), 961 (w), 930 (w), 900 (w), 872 (w), 834 (m), 812 (w), 777 (m), 723 (w), 710 (w), 688 (vs), 668 (w) cm⁻¹. **HRMS (ESI):** *m/z* calcd. for [C₂₂H₁₈N₃O₅]⁻: 404.1246, found: 404.1250 ([M-H]⁻). **UV/Vis:** λ_{max} = 322, 425 nm.

Synthesis of methyl 3-(cyano(hydroxy)methyl)-5-((4-(phenyldiazenyl)benzyl)-oxy)benzoate (5.15)

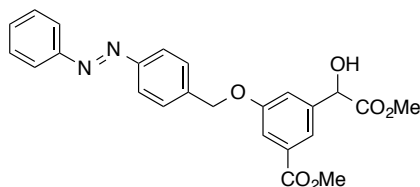


To a solution of aldehyde **5.12** (100 mg, 0.270 mmol, 1.0 equiv.) in DCM (2 mL), a 7 M solution of NH₃ in MeOH (2 mL) was added. The mixture was stirred for 10 min at room

temperature and TMSCN (54 μ L, 0.43 mmol, 1.6 equiv.) was added dropwise. The reaction mixture was stirred for 1 h at room temperature, followed by removal of the solvent *in vacuo*. The crude product was purified by flash silica gel chromatography (hexanes/EtOAc, 4:1), affording cyanohydrin **5.15** (82 mg, 0.20 mmol, 74%) as a red oil.

TLC (hexanes/EtOAc, 2:1): R_f = 0.50. **$^1\text{H NMR}$ (CDCl_3 , 400 MHz, 27 $^\circ\text{C}$):** δ = 7.96–7.94 (m, 1H, ArH), 7.94–7.92 (m, 2H, ArH), 7.92–7.90 (m, 1H, ArH), 7.79–7.77 (m, 1H, ArH), 7.67 (dd, J = 2.5, 1.3 Hz, 1H, ArH), 7.59 (s, 1H, ArH), 7.56 (s, 1H, ArH), 7.55–7.48 (m, 3H, ArH), 7.37 (dd, J = 1.8, 1.8 Hz, 1H, ArH), 5.56 (d, J = 6.4 Hz, 1H, CH), 5.19 (s, 2H, CH_2), 3.92 (s, 3H, OCH_3), 3.53 (d, J = 6.4 Hz, 1H, OH) ppm. **$^{13}\text{C NMR}$ (CDCl_3 , 100 MHz, 27 $^\circ\text{C}$):** δ = 166.2, 159.1, 152.5, 152.4, 138.8, 137.2, 132.4, 131.2, 129.1, 128.0, 123.2, 122.9, 120.3, 118.3, 118.0, 116.5, 69.9, 63.0, 52.6 ppm. **IR (neat, ATR):** $\tilde{\nu}$ = 3418 (m), 1721 (s), 1598 (m), 1436 (m), 1335 (s), 1302 (vs), 1232 (m), 1155 (m), 1111 (m), 1044 (m), 831 (w), 766 (m), 689 (m) cm^{-1} . **HRMS (ESI $^+$):** m/z calcd. for $[\text{C}_{23}\text{H}_{20}\text{N}_3\text{O}_4]^+$: 402.1454, found: 402.1448 ($[\text{M}+\text{H}]^+$).

Synthesis of methyl 3-(1-hydroxy-2-methoxy-2-oxoethyl)-5-((4-(phenyldiazenyl)-benzyl)-oxy)benzoate (5.20)

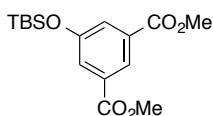


Cyanohydrin **5.15** (29 mg, 0.072 mmol) was dissolved in MeOH (4 mL) and freshly prepared HCl gas (from the addition of conc. H_2SO_4 to NaCl) was bubbled through the solution for 45 min at room temperature. The mixture was diluted with EtOAc (20 mL) and washed with NaHCO_3 (2 x 25 mL; gas evolution!). The organic layers were dried over MgSO_4 and concentrated *in vacuo*. The crude product was purified by flash silica gel chromatography (hexanes/EtOAc, 4:1 \rightarrow 2:1) to yield dimethyl ester **5.20** (5.0 mg, 0.012 mmol, 17%) as a red oil.

TLC (hexanes/EtOAc, 2:1): R_f = 0.38. **$^1\text{H NMR}$ (CDCl_3 , 600 MHz, 27 $^\circ\text{C}$):** δ = 7.96–7.95 (m, 1H, ArH), 7.95–7.94 (m, 1H, ArH), 7.94–7.93 (m, 1H, ArH), 7.92–7.91 (m, 1H, ArH), 7.74 (dd, J = 1.5, 1.5 Hz, 1H, ArH), 7.63 (dd, J = 2.5, 1.4 Hz, 1H, ArH), 7.59 (s, 1H, ArH), 7.58 (s, 1H, ArH), 7.54–7.47 (m, 3H, ArH), 7.29 (dd, J = 1.8, 1.8 Hz, 1H, ArH), 5.21–5.19 (m, 3H, CH, CH_2), 3.92 (s, 3H, OCH_3), 3.76 (s, 3H, OCH_3), 3.52 (d, J = 5.1 Hz, 1H, OH) ppm. **$^{13}\text{C NMR}$**

(CDCl₃, 150 MHz, 27 °C): δ = 173.6, 166.5, 158.7, 152.6, 152.4, 140.1, 139.2, 131.9, 131.1, 129.1, 128.0, 123.1, 122.9, 120.7, 118.2, 115.3, 72.3, 69.8, 53.3, 52.3 ppm. **IR (neat, ATR):** $\tilde{\nu}$ = 3467 (w), 1720 (vs), 1596 (m), 1435 (m), 1331 (m), 1300 (vs), 1223 (s), 1153 (m), 1108 (m), 1046 (m), 1012 (m), 831 (w), 769 (m), 689 (m) cm⁻¹. **HRMS (ESI⁺):** m/z calcd. for [C₂₄H₂₃N₂O₆]⁺: 435.1556, found: 435.1552 ([M+H]⁺).

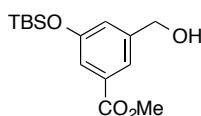
Synthesis of dimethyl 5-((*tert*-butyldimethylsilyl)oxy)isophthalate (**5.21**)



To a solution of dimethyl 5-hydroxyisophthalate (2.00 g, 9.52 mmol, 1.0 equiv.) in DMF (50 mL), imidazole (2.59 g, 38.1 mmol, 4.0 equiv.) and TBSCl (3.59 g, 23.8 mmol, 2.5 equiv.) were added. The reaction mixture was stirred at room temperature for 3 h. The mixture was diluted with H₂O (100 mL) and extracted with Et₂O (3 x 50 mL). The combined organic phases were washed with H₂O (7 x 75 mL) and brine (75 mL) and then dried over MgSO₄. The solvent was removed *in vacuo* and the crude product was purified by flash silica gel chromatography (hexanes/EtOAc, 20:1) to give TBS protected alcohol **5.21** (2.90 g, 8.94 mmol, 94%) as colorless crystals.

TLC (hexanes/EtOAc, 4:1): R_f = 0.69. **M.p.:** 68–70 °C. **¹H NMR (CDCl₃, 300 MHz, 27 °C):** δ = 8.31 (t, J = 1.5 Hz, 1H, ArH), 7.69 (d, J = 1.5 Hz, 2H, ArH), 3.95 (s, 6H, 2 x OCH₃), 1.03 (s, 9H, C(CH₃)₃), 0.26 (s, 6H, 2 x SiCH₃) ppm. **¹³C NMR (CDCl₃, 75 MHz, 27 °C):** δ = 166.1, 155.9, 131.8, 125.4, 123.7, 52.4, 25.6, 18.2, -4.5 ppm. **IR (neat, ATR):** $\tilde{\nu}$ = 2953 (m), 2931 (w), 2859 (w), 1727 (vs), 1593 (m), 1434 (m), 1336 (s), 1236 (s), 1190 (w), 1111 (m), 1024 (m), 1005 (m), 938 (w), 902 (w), 874 (w), 835 (s), 783 (m), 760 (m), 721 (w), 668 (w) cm⁻¹. **HRMS (EI⁺):** m/z calcd. for [C₁₆H₂₄O₅Si]⁺: 324.1393, found: 324.1386 ([M]⁺).

Synthesis of methyl 3-((*tert*-butyldimethylsilyl)oxy)-5-(hydroxymethyl)benzoate (**5.22**)

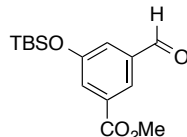


Diester **5.21** (2.85 g, 8.78 mmol, 1.0 equiv.) was dissolved in THF (300 mL) and LiAlH₄ (167 mg, 4.39 mmol, 0.5 equiv.) was added. The mixture was stirred for 3 h at room

temperature. H₂O was added (0.17 mL), followed by aqu. NaOH (10%, 0.34 mL) and H₂O (0.51 mL). The mixture was stirred for 1 h and then filtered. The filtrate was concentrated *in vacuo*. The crude product was purified by flash silica gel chromatography (hexanes/EtOAc, 4:1), affording alcohol **5.22** (1.46 g, 4.93 mmol, 56%) as a colorless oil. Diester **5.21** was recovered in 31% yield (870 mg, 2.68 mmol).

TLC (hexanes/EtOAc, 4:1): $R_f = 0.24$. **¹H NMR (CDCl₃, 300 MHz, 27 °C):** $\delta = 7.65$ (ddt, $J = 1.4, 1.4, 0.6$ Hz, 1H, ArH), 7.44–7.41 (m, 1H, ArH), 7.08 (ddt, $J = 2.3, 1.4, 0.6$ Hz, 1H, ArH), 4.70 (d, $J = 0.6$ Hz, 2H, CH₂), 3.92 (s, 3H, OCH₃), 1.81 (br s, 1H, OH), 1.02 (s, 9H, C(CH₃)₃), 0.24 (s, 6H, 2 x SiCH₃) ppm. **¹³C NMR (CDCl₃, 75 MHz, 27 °C):** $\delta = 166.8, 156.0, 142.8, 131.6, 123.1, 120.8, 120.1, 64.7, 52.2, 25.6, 18.2, -4.4$ ppm. **IR (neat, ATR):** $\tilde{\nu} = 3430$ (w), 2952 (w), 2930 (w), 2885 (w), 2858 (w), 1724 (m), 1595 (m), 1448 (m), 1434 (m), 1390 (w), 1362 (w), 1323 (s), 1253 (m), 1230 (m), 1190 (w), 1153 (m), 1106 (m), 1025 (m), 980 (w), 939 (w), 895 (w), 836 (vs), 817 (w), 782 (m), 772 (m), 739 (w), 684 (w), 671 (w) cm⁻¹. **HRMS (EI⁺):** m/z calcd. for [C₁₅H₂₄O₄Si]⁺: 296.1444, found: 296.1446 ([M]⁺).

Synthesis of methyl 3-((*tert*-butyldimethylsilyloxy)-5-formylbenzoate (**5.23**)

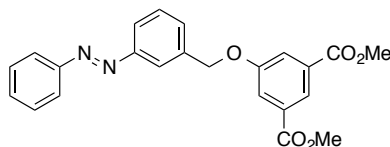


To a solution of alcohol **5.22** (1.40 g, 4.72 mmol, 1.0 equiv.) in DCM (100 mL), MnO₂ (4.10 g, 47.2 mmol, 10 equiv.) was added in one portion. The reaction mixture was stirred at room temperature for 18 h. The mixture was filtered through Celite and the residue was washed thoroughly with DCM. The filtrate was concentrated under reduced pressure to give aldehyde **5.23** (1.29 g, 4.38 mmol, 93%) as a colorless solid.

TLC (hexanes/EtOAc, 4:1): $R_f = 0.65$. **M.p.:** 32–33 °C. **¹H NMR (CDCl₃, 300 MHz, 27 °C):** $\delta = 10.02$ (s, 1H, CHO), 8.14 (dd, $J = 1.5, 1.5$ Hz, 1H, ArH), 7.76 (dd, $J = 2.5, 1.5$ Hz, 1H, ArH), 7.53 (dd, $J = 2.5, 1.5$ Hz, 1H, ArH), 3.97 (s, 3H, OCH₃), 1.02 (s, 9H, C(CH₃)₃), 0.26 (s, 6H, 2 x SiCH₃) ppm. **¹³C NMR (CDCl₃, 75 MHz, 27 °C):** $\delta = 191.1, 165.8, 156.6, 138.0, 132.5, 127.0, 124.8, 123.4, 52.5, 25.6, 18.2, -4.5$ ppm. **IR (neat, ATR):** $\tilde{\nu} = 2953$ (w), 2931 (w), 2886 (w), 2858 (w), 1728 (m), 1704 (s), 1594 (m), 1458 (m), 1440 (m), 1386 (m), 1362 (w), 1323 (s), 1232 (s), 1190 (w), 1145 (m), 1106 (w), 1024 (m), 1005 (w), 939 (w), 898 (m), 834

(vs), 783 (m), 770 (m), 738 (w), 689 (w), 677 (w) cm^{-1} . **HRMS (EI⁺):** m/z calcd. for $[\text{C}_{15}\text{H}_{22}\text{O}_4\text{Si}]^+$: 294.1287, found: 294.1272 ($[\text{M}]^+$).

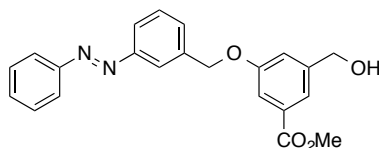
Synthesis of dimethyl 5-((3-(phenyldiazenyl)benzyl)oxy)isophthalate (5.25)



Dimethyl 5-hydroxyisophthalate (1.27 g, 6.06 mmol, 1.0 equiv.) was dissolved in acetone (175 mL) at room temperature and K_2CO_3 (1.67 g, 12.1 mmol, 2.0 mmol) and Bu_4NI (2.24 g, 6.06 mmol, 1.0 equiv.) were added, followed by bromide **4.21** (2.00 g, 7.27 mmol, 1.2 equiv.). The mixture was stirred for 16 h at room temperature. The solvent was removed *in vacuo* and EtOAc (100 mL) was added. The organic phase was washed with H_2O (200 mL) and dried over MgSO_4 and concentrated *in vacuo*. The crude product was purified by flash silica gel chromatography (hexanes/DCM, gradient from 3:1 to 1:9) to yield azobenzene ether **5.25** (2.12 g, 5.24 mmol, 86%) as a red oil.

TLC (hexanes/EtOAc, 10:1): R_f = 0.13. **¹H NMR (CDCl₃, 300 MHz, 27 °C):** δ = 8.33 (dd, J = 1.5, 1.5 Hz, 1H, ArH), 8.05–8.01 (m, 1H, ArH), 7.98–7.90 (m, 3H, ArH), 7.89 (d, J = 1.5 Hz, 2H, ArH), 7.60–7.49 (m, 5H, ArH), 5.26 (s, 2H, CH_2), 3.95 (s, 6H, 2 x OCH_3) ppm. **¹³C NMR (CDCl₃, 75 MHz, 27 °C):** δ = 166.0, 158.7, 152.9, 152.6, 137.3, 131.9, 131.2, 129.7, 129.4, 129.1, 123.4, 122.9, 122.9, 121.5, 120.2, 70.0, 52.4 ppm. **IR (neat, ATR):** $\tilde{\nu}$ = 2950 (w), 1720 (s), 1594 (m), 1454 (m), 1432 (m), 1336 (m), 1312 (m), 1239 (vs), 1189 (w), 1150 (w), 1116 (m), 1103 (w), 1040 (m), 1003 (m), 910 (w), 882 (w), 875 (w), 791 (m), 756 (s), 721 (m), 693 (m), 672 (w) cm^{-1} . **HRMS (EI⁺):** m/z calcd. for $[\text{C}_{23}\text{H}_{20}\text{N}_2\text{O}_5]^+$: 404.1372, found: 404.1376 ($[\text{M}]^+$).

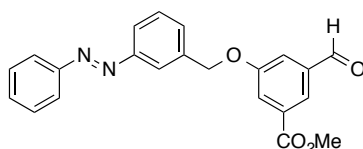
Synthesis of methyl 3-(hydroxymethyl)-5-((3-(phenyldiazenyl)benzyl)oxy)benzoate (5.26)



Dimethyl ester **5.25** (1.98 g, 4.90 mmol, 1.0 equiv.) was dissolved in THF (200 mL) and LiAlH₄ (93 mg, 2.5 mmol, 0.5 equiv.) was added. The mixture was stirred for 2 h at room temperature. H₂O was added (0.10 mL), followed by aqu. NaOH (10%, 0.20 mL) and H₂O (0.30 mL). The mixture was stirred for 30 min and then filtered. The filtrate was concentrated *in vacuo*. The crude product was purified by flash silica gel chromatography (hexanes/EtOAc, 3:1 → 2:1), affording alcohol **5.26** (1.09 g, 2.90 mmol, 59%) as a red oil.

TLC (hexanes/EtOAc, 2:1): R_f = 0.35. **¹H NMR (CDCl₃, 600 MHz, 27 °C):** δ = 8.00–7.97 (m, 1H, ArH), 7.94–7.90 (m, 2H, ArH), 7.88 (ddd, *J* = 6.4, 2.4, 2.4 Hz, 1H, ArH), 7.65 (s, 1H, ArH), 7.59 (dd, *J* = 2.4, 1.5 Hz, 1H, ArH), 7.55–7.46 (m, 5H, ArH), 7.24–7.23 (m, 1H, ArH), 5.20 (s, 2H, CH₂), 4.71 (s, 2H, CH₂), 3.90 (s, 3H, OCH₃), 1.87 (br s, 1H, OH) ppm. **¹³C NMR (CDCl₃, 150 MHz, 27 °C):** δ = 166.7, 158.8, 152.8, 152.5, 142.9, 137.7, 131.7, 131.1, 129.7, 129.4, 129.1, 122.9, 122.8, 121.5, 120.6, 118.3, 114.3, 69.7, 64.6, 52.2 ppm. **IR (neat, ATR):** $\tilde{\nu}$ = 3414 (m), 2949 (w), 2873 (w), 1716 (s), 1595 (m), 1447 (m), 1433 (m), 1329 (m), 1301 (vs), 1224 (s), 1150 (m), 1106 (m), 1044 (m), 998 (m), 924 (w), 887 (m), 796 (m), 785 (m), 767 (s), 732 (w), 692 (vs), 657 (w) cm⁻¹. **HRMS (ESI⁺):** *m/z* calcd. for [C₂₂H₂₁N₂O₄]⁺: 377.1501, found: 377.1496 ([M+H]⁺).

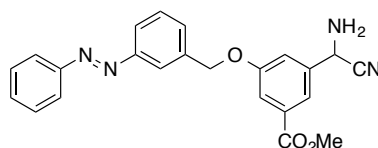
Synthesis of methyl 3-formyl-5-((3-(phenyldiazenyl)benzyl)oxy)benzoate (5.27)



To a solution of alcohol **5.26** (990 mg, 2.63 mmol, 1.0 equiv.) in DCM (60 mL), MnO₂ (2.29 g, 26.3 mmol, 10 equiv.) was added in one portion. The reaction mixture was stirred at room temperature for 2 d. The mixture was filtered through Celite and the residue was washed thoroughly with DCM. The filtrate was concentrated under reduced pressure to give aldehyde **5.27** (920 mg, 2.46 mmol, 94%) as a red oil.

TLC (hexanes/EtOAc, 2:1): $R_f = 0.81$. $^1\text{H NMR}$ (CDCl_3 , 600 MHz, 27 °C): $\delta = 10.01$ (s, 1H, CHO), 8.13 (dd, $J = 1.4, 1.4$ Hz, 1H, ArH), 8.00 (s, 1H, ArH), 7.95–7.88 (m, 4H, ArH), 7.68 (dd, $J = 2.7, 1.4$ Hz, 1H, ArH), 7.57–7.54 (m, 2H, ArH), 7.53–7.46 (m, 3H, ArH), 5.25 (s, 2H, CH_2), 3.95 (s, 3H, OCH_3) ppm. $^{13}\text{C NMR}$ (CDCl_3 , 150 MHz, 27 °C): $\delta = 191.0, 165.7, 159.2, 152.9, 152.5, 137.9, 137.0, 132.6, 131.2, 129.7, 129.5, 129.1, 124.6, 123.0, 122.9, 122.1, 121.5, 117.7, 70.1, 52.5$ ppm. **IR (neat, ATR):** $\tilde{\nu} = 1722$ (m), 1698 (s), 1593 (m), 1458 (m), 1447 (m), 1433 (m), 1334 (m), 1304 (vs), 1223 (s), 1195 (w), 1146 (m), 1106 (m), 1041 (m), 991 (m), 951 (w), 906 (m), 883 (m), 787 (m), 765 (s), 730 (m), 691 (vs), 671 (m) cm^{-1} . **HRMS (EI⁺):** m/z calcd. for $[\text{C}_{22}\text{H}_{19}\text{N}_2\text{O}_4]^+$: 375.1345, found: 375.1340 ($[\text{M}+\text{H}]^+$).

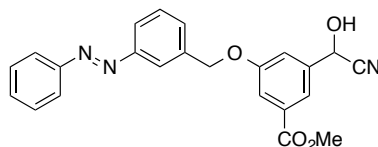
Synthesis of methyl 3-(amino(cyano)methyl)-5-((3-(phenyldiazenyl)benzyl)oxy)benzoate (5.28)



To a solution of aldehyde **5.27** (819 mg, 2.19 mmol, 1.0 equiv.) in DCM (16 mL), a 7 M solution of NH_3 in MeOH (16 mL) was added at 0 °C. The mixture was stirred for 10 min and TMSCN (0.46 mL, 3.5 mmol, 1.6 equiv.) was added dropwise. The reaction mixture was slowly warmed to room temperature and stirred for 20 h, followed by removal of the solvent *in vacuo*. The crude product was purified by flash silica gel chromatography (hexanes/EtOAc, gradient from 10:1 to 1:1), affording aminonitrile **5.28** (274 mg, 0.680 mmol, 31%) as a red oil.

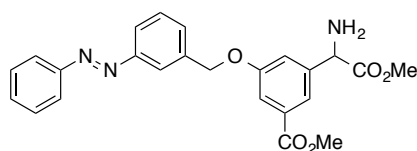
TLC (hexanes/EtOAc, 2:1): $R_f = 0.57$. $^1\text{H NMR}$ (CDCl_3 , 400 MHz, 27 °C): $\delta = 8.02$ –7.99 (m, 1H, ArH), 7.95–7.89 (m, 3H, ArH), 7.84–7.82 (m, 1H, ArH), 7.69 (dd, $J = 2.3, 1.4$ Hz, 1H, ArH), 7.57–7.49 (m, 5H, ArH), 7.41 (ddd, $J = 2.3, 1.7, 0.7$ Hz, 1H, ArH), 5.23 (s, 2H, CH_2), 4.93 (s, 1H, CH), 3.93 (s, 3H, OCH_3), 1.98 (br s, 2H, NH_2) ppm. $^{13}\text{C NMR}$ (CDCl_3 , 100 MHz, 27 °C): $\delta = 166.1, 159.1, 152.9, 152.5, 138.2, 137.3, 132.4, 131.2, 129.8, 129.5, 129.1, 122.9, 122.9, 121.5, 120.4, 120.4, 118.4, 115.7, 69.9, 52.4, 46.9$ ppm. **IR (neat, ATR):** $\tilde{\nu} = 3382$ (w), 1716 (s), 1596 (m), 1447 (m), 1433 (m), 1332 (m), 1304 (s), 1227 (s), 1195 (w), 1152 (m), 1110 (w), 1084 (w), 1042 (m), 999 (w), 907 (w), 888 (w), 798 (m), 786 (m), 767 (m), 731 (m), 693 (vs) cm^{-1} . **HRMS (ESI⁺):** m/z calcd. for $[\text{C}_{23}\text{H}_{21}\text{N}_4\text{O}_3]^+$: 401.1614, found: 401.1609 ($[\text{M}+\text{H}]^+$).

Moreover, aldehyde **5.27** was recovered in 20% yield (162 mg, 0.430 mmol) and cyanohydrin **5.30** was obtained as a side product in 40% yield (354 mg, 0.880 mmol) as a red oil.



TLC (hexanes/EtOAc, 2:1): R_f = 0.70. **^1H NMR (CDCl_3 , 400 MHz, 27 °C):** δ = 7.97–7.94 (m, 1H, ArH), 7.92–7.85 (m, 3H, ArH), 7.75 (ddd, J = 1.6, 1.6, 0.6 Hz, 1H, ArH), 7.64 (dd, J = 2.4, 1.4 Hz, 1H, ArH), 7.53–7.45 (m, 5H, ArH), 7.35 (ddd, J = 2.4, 1.6, 0.6 Hz, 1H, ArH), 5.53 (d, 1H, J = 6.9 Hz, CH), 5.16 (s, 2H, CH_2), 3.96 (d, J = 6.9 Hz, 1H, OH), 3.88 (s, 3H, OCH_3) ppm. **^{13}C NMR (CDCl_3 , 100 MHz, 27 °C):** δ = 166.3, 159.1, 152.8, 152.5, 137.3, 137.2, 132.2, 131.2, 129.8, 129.5, 129.1, 122.9, 122.9, 121.5, 120.3, 118.5, 118.0, 116.4, 69.9, 62.9, 52.6 ppm. **IR (neat, ATR):** $\tilde{\nu}$ = 3410 (w), 1719 (m), 1596 (m), 1447 (m), 1434 (m), 1381 (w), 1334 (m), 1301 (s), 1226 (s), 1195 (w), 1151 (m), 1110 (m), 1040 (m), 999 (m), 908 (m), 787 (m), 765 (s), 730 (m), 710 (w), 692 (vs) cm^{-1} . **HRMS (ESI $^+$):** m/z calcd. for $[\text{C}_{23}\text{H}_{20}\text{N}_3\text{O}_4]^+$: 402.1454, found: 402.1448 ($[\text{M}+\text{H}]^+$).

Synthesis of methyl 3-(1-amino-2-methoxy-2-oxoethyl)-5-((3-(phenyldiazenyl)benzyl)oxy)benzoate (5.29)

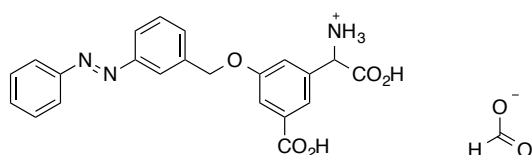


Aminonitrile **5.28** (174 mg, 0.430 mmol) was dissolved in MeOH (4.5 mL) and cooled to 0 °C. A 4 M solution of HCl in dioxane (4.5 mL) was added slowly. The solution was stirred for 1 h at 0 °C. H_2O (0.09 mL) was added and the mixture was warmed to room temperature and stirred for 16 h. The mixture was diluted with EtOAc (25 mL) and washed with NaHCO_3 (2 x 25 mL; gas evolution!). The organic layers were dried over MgSO_4 and concentrated *in vacuo*. The crude product was purified by flash silica gel chromatography (hexanes/EtOAc (+1% TEA), gradient from 1:1 to 1:3), yielding dimethyl ester **5.29** (111 mg, 0.260 mmol, 60%) as a red oil.

TLC (hexanes/EtOAc (+1% TEA), 1:3): R_f = 0.42. **^1H NMR (CDCl_3 , 300 MHz, 27 °C):** δ = 8.05–8.00 (m, 1H, ArH), 7.97–7.90 (m, 3H, ArH), 7.73 (dd, J = 1.4, 1.4 Hz, 1H, ArH), 7.65 (dd, J = 2.5, 1.4 Hz, 1H, ArH), 7.59–7.49 (m, 5H, ArH), 7.31–7.28 (m, 1H, ArH), 5.23 (s, 2H, CH_2), 4.67 (s, 1H, CH), 3.93 (s, 3H, OCH_3), 3.72 (s, 3H, OCH_3), 1.91 (br s, 2H, NH_2) ppm. **^{13}C NMR (CDCl_3 , 75 MHz, 27 °C):** δ = 173.8, 166.5, 158.9, 152.9, 152.6, 142.2, 137.6, 132.0,

131.2, 129.8, 129.4, 129.1, 122.9, 122.8, 121.6, 120.9, 118.7, 114.7, 69.8, 58.4, 52.6, 52.3 ppm. **IR (neat, ATR):** $\tilde{\nu}$ = 2949 (w), 1721 (vs), 1594 (m), 1446 (m), 1434 (m), 1372 (w), 1331 (m), 1301 (s), 1228 (s), 1164 (m), 1109 (w), 1043 (w), 998 (w), 879 (w), 792 (w), 768 (m), 694 (m) cm^{-1} . **HRMS (ESI⁺):** m/z calcd. for $[\text{C}_{24}\text{H}_{24}\text{N}_3\text{O}_5]^+$: 434.1716, found: 434.1709 ($[\text{M}+\text{H}]^+$).

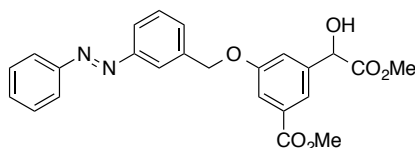
**Synthesis of carboxy(3-carboxy-5-((3-(phenyldiazenyl)benzyl)oxy)phenyl)methan-
aminium formate (*m*-Azo-3C5HPG)**



Dimethyl ester **5.29** (82 mg, 0.19 mmol) was dissolved in THF (4 mL) and a 2 M solution of LiOH in water (0.67 mL) was added. The solution was stirred for 16 h at room temperature. The pH was adjusted to pH = 1 with 2 M HCl and the solvent was removed *in vacuo*. The crude product was purified by reversed-phase silica gel column chromatography ($\text{H}_2\text{O}/\text{MeOH}$ (+0.1% HCO_2H), gradient from 10:0 to 4:6), giving rise to *m*-Azo-3C5HPG as its formate salt (54 mg, 0.12 mmol, 63%) as an orange solid.

RP-TLC ($\text{H}_2\text{O}/\text{MeOH}$, 1:1): R_f = 0.19. **M.p.:** 154 °C (dec.). **¹H NMR (DMSO-*d*₆, 600 MHz, 27 °C):** δ = 7.98–7.96 (m, 1H, ArH), 7.90–7.87 (m, 2H, ArH), 7.85 (ddd, J = 7.6, 1.7, 1.7 Hz, 1H, ArH), 7.64–7.55 (m, 6H, ArH), 7.47 (dd, J = 2.5, 1.3 Hz, 1H, ArH), 7.36–7.34 (m, 1H, ArH), 5.27 (s, 2H, CH_2), 4.31 (s, 1H, CH) ppm. **¹³C NMR (DMSO-*d*₆, 150 MHz, 27 °C):** δ = 167.8, 167.5, 163.9, 158.4, 154.1, 154.0, 152.5, 152.3, 139.9, 138.9, 132.1, 130.8, 130.1, 129.9, 123.0, 122.8, 121.5, 120.2, 113.9, 69.4, 58.3 ppm. **IR (neat, ATR):** $\tilde{\nu}$ = 3055 (w), 2907 (w), 2607 (w), 1689 (m), 1596 (s), 1483 (m), 1394 (m), 1332 (m), 1301 (m), 1243 (m), 1173 (m), 1060 (m), 972 (w), 922 (w), 883 (w), 790 (m), 767 (m), 690 (vs) cm^{-1} . **HRMS (ESI):** m/z calcd. for $[\text{C}_{22}\text{H}_{18}\text{N}_3\text{O}_5]^-$: 404.1246, found: 404.1252 ($[\text{M}-\text{H}]^-$). **UV/Vis:** λ_{max} = 323, 433 nm.

Synthesis of methyl 3-(1-hydroxy-2-methoxy-2-oxoethyl)-5-((3-(phenyldiazenyl)benzyl)-oxy)benzoate (5.31)

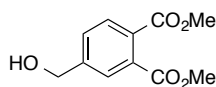


Cyanohydrin **5.30** (60 mg, 0.15 mmol) was dissolved in MeOH (1.5 mL) and cooled to 0 °C. A 4 M solution of HCl in dioxane (1.5 mL) was added slowly. The solution was stirred for 1 h at 0 °C. H₂O (0.03 mL) was added and the mixture was warmed to room temperature and stirred for 16 h. The mixture was diluted with EtOAc (20 mL) and washed with NaHCO₃ (2 x 20 mL; gas evolution!). The organic layers were dried over MgSO₄ and concentrated *in vacuo*. The crude product was purified by flash silica gel chromatography (hexanes/EtOAc, 4:1 → 2:1), affording dimethyl ester **5.31** (40 mg, 0.092 mmol, 61%) as an orange oil.

TLC (hexanes/EtOAc, 2:1): R_f = 0.35. **¹H NMR (CDCl₃, 600 MHz, 27 °C):** δ = 8.00–7.98 (m, 1H, ArH), 7.94–7.88 (m, 3H, ArH), 7.73 (ddd, J = 1.5, 1.5, 0.6 Hz, 1H, ArH), 7.64 (dd, J = 2.5, 1.4 Hz, 1H, ArH), 7.55–7.47 (m, 5H, ArH), 7.30–7.28 (m, 1H, ArH), 5.21–5.18 (m, 3H, CH, CH₂), 3.91 (s, 3H, OCH₃), 3.75 (s, 3H, OCH₃), 3.53 (d, J = 5.4 Hz, 1H, OH) ppm. **¹³C NMR (CDCl₃, 150 MHz, 27 °C):** δ = 173.6, 166.5, 158.8, 152.8, 152.5, 140.1, 137.5, 131.8, 131.1, 129.8, 129.1, 128.7, 122.9, 122.8, 121.6, 120.6, 118.2, 115.2, 72.3, 69.8, 53.3, 52.3 ppm. **IR (neat, ATR):** $\tilde{\nu}$ = 3467 (w), 2951 (w), 1719 (s), 1595 (m), 1380 (w), 1334 (m), 1331 (m), 1300 (vs), 1223 (vs), 1150 (m), 1111 (m), 1044 (m), 999 (m), 913 (m), 797 (m), 768 (m), 733 (w), 693 (s) cm⁻¹. **HRMS (ESI⁺):** m/z calcd. for [C₂₄H₂₃N₂O₆]⁺: 435.1556, found: 435.1551 ([M+H]⁺).

5.5.4 SYNTHESIS OF AZO-DCPG

Synthesis of dimethyl 4-(hydroxymethyl)phthalate (5.32)



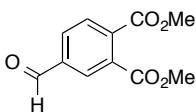
1,2,4-Benzenetricarboxylic anhydride (10.0 g, 52.0 mmol, 1.0 equiv.) was dissolved in 1,4-dioxane (160 mL). BH₃ · THF (1 M solution; 52.0 mL, 52.0 mmol, 1.0 equiv.) was added

dropwise *via* a dropping funnel over a period of 1.5 h at room temperature. The reaction mixture was stirred for 16 h and then poured into a mixture of sat. aqu. NH₄Cl (120 mL) and DCM (200 mL). The phases were separated and the aqueous layer was extracted with DCM (2 x 50 mL). The combined organic layers were dried over MgSO₄ and the solvent was removed under reduced pressure. The crude product was used in the next step without further purification.

The residue was dissolved in methanol (200 mL) and conc. H₂SO₄ (1 mL) was added dropwise. The reaction mixture was heated under reflux for 18 h. After cooling to room temperature, the mixture was poured into a mixture of H₂O (100 mL) and Et₂O (200 mL). The two phases were separated and the aqueous layer was extracted with Et₂O (2 x 100 mL). The combined organic layers were washed with brine (100 mL), dried over MgSO₄ and concentrated *in vacuo*. The crude product was purified by flash silica gel column chromatography (hexanes/EtOAc, gradient from 4:1 to 1:1) to give alcohol **5.32** (5.92 g, 26.4 mmol, 51% over two steps) as a colorless oil.

TLC (hexanes/EtOAc, 1:1): R_f = 0.38. **¹H NMR (CDCl₃, 300 MHz, 27 °C):** δ = 7.65 (d, *J* = 7.8 Hz, 1H, *ArH*), 7.62–7.58 (m, 1H, *ArH*), 7.48–7.42 (m, 1H, *ArH*), 4.69 (s, 2H, CH₂), 3.87 (s, 6H, 2 x OCH₃), 3.38 (br s, 1H, OH) ppm. **¹³C NMR (CDCl₃, 75 MHz, 27 °C):** δ = 168.4, 167.9, 145.0, 132.3, 130.2, 129.2, 128.8, 126.6, 63.8, 52.7, 52.6 ppm. **IR (neat, ATR):** $\tilde{\nu}$ = 3432 (w), 1717 (vs), 1610 (w), 1435 (m), 1283 (vs), 1197 (s), 1126 (s), 1070 (s), 977 (m), 959 (m), 913 (w), 845 (w), 821 (w), 786 (m), 764 (m), 732 (w), 707 (w) cm⁻¹. **HRMS (ESI⁺):** *m/z* calcd. for [C₁₁H₁₃O₅]⁺: 225.0763, found: 225.0757 ([M+H]⁺).

Synthesis of dimethyl 4-formylphthalate (**5.33**)

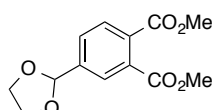


To a solution of alcohol **5.32** (5.75 g, 25.6 mmol, 1.0 equiv.) in DCM (300 mL), MnO₂ (22.3 g, 256 mmol, 10 equiv.) was added in one portion. The reaction mixture was stirred at room temperature for 18 h. The mixture was filtered through Celite and the residue was washed thoroughly with DCM. The filtrate was concentrated under reduced pressure to give aldehyde **5.33** (5.11 g, 23.0 mmol, 90%) as a colorless oil.

TLC (hexanes/EtOAc, 1:1): R_f = 0.71. **¹H NMR (CDCl₃, 300 MHz, 27 °C):** δ = 10.11 (s, 1H, CHO), 8.30 (dd, *J* = 1.8, 0.6 Hz, 1H, *ArH*), 8.08 (dd, *J* = 7.8, 1.8 Hz, 1H, *ArH*), 7.85 (ddd,

$J = 7.8, 0.6, 0.6$ Hz, 1H, ArH), 3.97 (s, 6H, 2 x OCH₃) ppm. ¹³C NMR (CDCl₃, 75 MHz, 27 °C): $\delta = 190.4, 167.4, 166.5, 137.7, 137.5, 132.1, 131.8, 130.5, 129.5, 53.0, 53.0$ ppm. IR (neat, ATR): $\tilde{\nu} = 1729$ (vs), 1707 (s), 1608 (m), 1437 (m), 1289 (s), 1198 (m), 1181 (m), 1125 (m), 1070 (m), 959 (w), 901 (w), 849 (w), 822 (w), 805 (w), 771 (w), 710 (w) cm⁻¹. HRMS (EI⁺): m/z calcd. for [C₁₁H₁₀O₅]⁺: 222.0528, found: 222.0530 ([M]⁺).

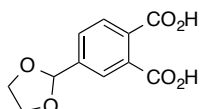
Synthesis of dimethyl 4-(1,3-dioxolan-2-yl)phthalate (5.34)



Aldehyde **5.33** (535 mg, 2.41 mmol, 1.0 equiv.) was dissolved in benzene (10 mL) and ethylene glycol (0.66 mL, 12 mmol, 4.9 equiv.) and a catalytic amount of *p*-TsOH monohydrate (20 mg, 0.11 mmol, 0.05 equiv) were added. The mixture was heated to reflux for 18 h in a Dean-Stark apparatus. After cooling, the solvent was removed *in vacuo* and the crude product was purified by flash silica gel column chromatography (hexanes/EtOAc, gradient from 5:1 to 2:1) to give 1,3-dioxolane **5.34** (642 mg, 2.41 mmol, 100%) as a colorless oil.

TLC (hexanes/EtOAc, 1:1): $R_f = 0.73$. ¹H NMR (CDCl₃, 300 MHz, 27 °C): $\delta = 7.87$ (ddd, $J = 1.7, 0.5, 0.5$ Hz, 1H, ArH), 7.76 (d, $J = 8.0$ Hz, 1H, ArH), 7.65 (ddd, $J = 8.0, 1.7, 0.5$ Hz, 1H, ArH), 5.88 (s, 1H, CH), 4.13–4.06 (m, 4H, 2 x OCH₂), 3.94 (s, 3H, OCH₃), 3.93 (s, 3H, OCH₃) ppm. ¹³C NMR (CDCl₃, 75 MHz, 27 °C): $\delta = 167.8, 167.7, 141.6, 132.5, 132.1, 129.1, 129.0, 127.0, 102.4, 65.4, 52.7, 52.7$ ppm. IR (neat, ATR): $\tilde{\nu} = 1721$ (vs), 1434 (m), 1273 (s), 1206 (s), 1124 (m), 1085 (s), 1069 (s), 1026 (m), 989 (m), 959 (m), 942 (m), 851 (m), 821 (m), 791 (m), 767 (m), 723 (w), 709 (w), 692 (w), 664 (w) cm⁻¹. HRMS (EI⁺): m/z calcd. for [C₁₃H₁₃O₆]⁺: 265.0712, found: 265.0705 ([M-H]⁺).

Synthesis of 4-(1,3-dioxolan-2-yl)phthalic acid (5.35)

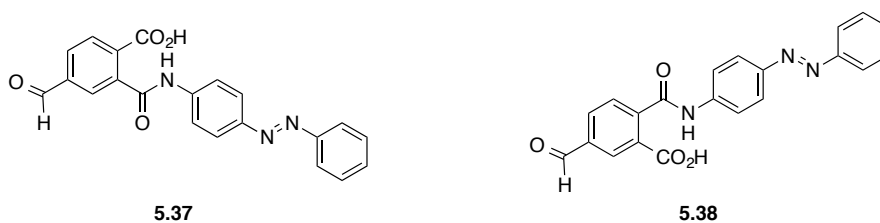


Dimethyl ester **5.34** (300 mg, 1.13 mmol, 1.0 equiv.) was dissolved in a mixture of THF (6 mL) and MeOH (2 mL). LiOH (108 mg, 4.52 mmol, 4.0 equiv.) in H₂O (2 mL) was added and the reaction mixture was stirred for 4 h at room temperature. The mixture was diluted with H₂O

(20 mL) and extracted with EtOAc (15 mL) to remove unreacted starting material. The aqueous phase was then acidified to pH = 1 with 1 M HCl and extracted with CHCl₃/*i*-PrOH (1:1; 3 x 20 mL). The combined organic layers were washed with H₂O (30 mL), dried over MgSO₄ and concentrated *in vacuo*. The crude product was purified by flash silica gel column chromatography (DCM/MeOH/HOAc/H₂O, 90:10:0.6:0.6 → 80:20:0.6:0.6) to give dicarboxylic acid **5.35** (167 mg, 0.700 mmol, 62%) as a colorless solid.

TLC (DCM/MeOH/HOAc/H₂O, 90:10:0.6:0.6): R_f = 0.03. **M.p.:** 148 °C (dec.). **¹H NMR (CDCl₃, 300 MHz, 27 °C):** δ = 10.63–10.17 (br s, 2H, 2 x CO₂H), 8.01 (d, *J* = 1.7, 1H, ArH), 7.91 (d, *J* = 8.0 Hz, 1H, ArH), 7.76 (dd, *J* = 8.0, 1.7 Hz, 1H, ArH), 5.94 (s, 1H, CH), 4.18–4.04 (m, 4H, 2 x OCH₂) ppm. **¹³C NMR (CDCl₃, 75 MHz, 27 °C):** δ = 173.4, 173.3, 142.5, 131.6, 131.4, 129.8, 129.6, 127.5, 102.2, 65.4 ppm. **IR (neat, ATR):** ν̄ = 2891 (m), 1693 (s), 1575 (m), 1495 (m), 1359 (m), 1260 (vs), 1205 (s), 1143 (m), 1090 (vs), 1074 (s), 1024 (m), 986 (m), 943 (m), 912 (w), 849 (m), 796 (s), 770 (m), 729 (w), 695 (w), 682 (w), 654 (w) cm⁻¹. **HRMS (EI⁺):** *m/z* calcd. for [C₁₁H₉O₆]⁺: 237.0399, found: 237.0392 ([M-H]⁺).

Synthesis of 4-formyl-2-((4-(phenyldiazenyl)phenyl)carbamoyl)benzoic acid (**5.37**) and 5-formyl-2-((4-(phenyldiazenyl)phenyl)carbamoyl)benzoic acid (**5.38**)



Dicarboxylic acid **5.35** (1.82 g, 7.64 mmol, 1.0 equiv.) was dissolved in Ac₂O (18 mL) and heated to 80 °C for 3 h. The reaction mixture was cooled to room temperature and the solvent was removed *in vacuo* to give quantitatively the crude anhydride **5.36** (1.31, 7.64 mmol) as a colorless solid.

Without further purification, **5.36** (1.31 g, 5.95 mmol, 1.0 equiv.) was dissolved in THF (60 mL) and 4-aminoazobenzene (1.17 g, 5.95 mmol, 1.0 equiv.) was added. The mixture was heated under reflux for 16 h. The solvent was evaporated under reduced pressure and the crude product purified by a quick flash silica gel column chromatography (DCM/MeOH/HOAc/H₂O, 98:2:0.6:0.6) to give a mixture of the two regioisomers **5.37** and **5.38** (2.48 g, 5.94 mmol, 100%) as a red solid.

This crude mixture was then dissolved in THF (120 mL) and 1 M HCl (11.9 mL, 2.0 equiv.) was added. The reaction mixture was stirred for 16 h at room temperature. 2 M NaOH (5.95 mL, 2.0 equiv.) was added and the organic layer was washed with brine (75 mL), dried over MgSO₄ and concentrated under reduced pressure. The crude product was purified by flash silica gel column chromatography (DCM/MeOH/HOAc/H₂O, 98:2:0.6:0.6), obtaining analytical samples of both regioisomers.

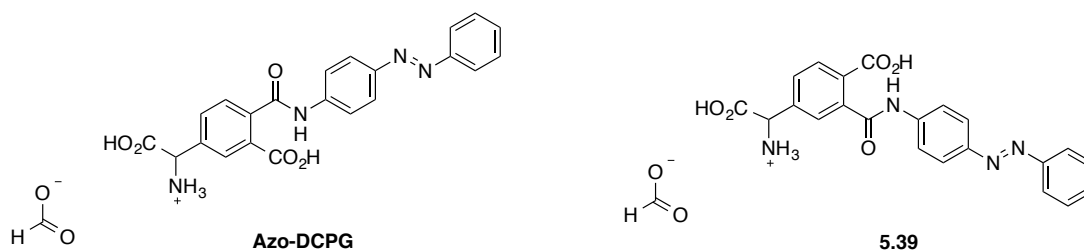
4-Formyl-2-((4-(phenyldiazenyl)phenyl)carbamoyl)benzoic acid (5.37):

TLC (DCM/MeOH/HOAc/H₂O, 90:10:0.6:0.6): R_f = 0.35. **¹H NMR (DMSO-d₆, 400 MHz, 27 °C):** δ = 13.96–12.96 (br s, 1H, CO₂H), 10.88 (s, 1H, NH), 10.12 (s, 1H, CHO), 8.40 (d, J = 1.2 Hz, 1H, ArH), 8.15 (dd, J = 8.0, 1.2 Hz, 1H, ArH), 7.91–7.88 (m, 4H, ArH), 7.87–7.84 (m, 2H, ArH), 7.80 (d, J = 8.0 Hz, 1H, ArH), 7.57–7.54 (m, 2H, ArH), 7.53 (dd, J = 1.6, 1.6 Hz, 1H, ArH) ppm. **¹³C NMR (DMSO-d₆, 100 MHz, 27 °C):** δ = 192.9, 167.3, 166.9, 152.5, 148.2, 143.5, 142.8, 137.0, 132.6, 131.5, 131.2, 131.2, 129.9, 129.4, 124.1, 122.8, 120.2 ppm. **IR (neat, ATR):** $\tilde{\nu}$ = 3313 (m), 3057 (m), 1677 (s), 1663 (s), 1597 (vs), 1545 (vs), 1505 (m), 1464 (w), 1441 (w), 1408 (m), 1313 (s), 1263 (s), 1184 (m), 1154 (m), 1071 (m), 965 (w), 895 (w), 841 (s), 758 (m), 721 (w), 680 (m), 667 (w) cm⁻¹. **HRMS (ESI):** m/z calcd. for [C₂₁H₁₄O₄N₃]⁻: 372.0984, found: 372.0999 ([M-H]⁻).

5-Formyl-2-((4-(phenyldiazenyl)phenyl)carbamoyl)benzoic acid (5.38):

TLC (DCM/MeOH/HOAc/H₂O, 90:10:0.6:0.6): R_f = 0.28. **¹H NMR (DMSO-d₆, 400 MHz, 27 °C):** δ = 11.12 (s, 1H, NH), 10.12 (s, 1H, CHO), 8.14 (d, J = 1.2 Hz, 1H, ArH), 8.08 (dd, J = 8.0, 1.2 Hz, 1H, ArH), 8.04 (d, J = 8.0 Hz, 1H, ArH), 7.93–7.91 (m, 4H, ArH), 7.88–7.85 (m, 2H, ArH), 7.58–7.55 (m, 2H, ArH), 7.54 (dd, J = 1.6, 1.6 Hz, 1H, ArH) ppm. **¹³C NMR (DMSO-d₆, 100 MHz, 27 °C):** δ = 192.9, 167.7, 167.0, 152.5, 148.2, 142.8, 138.7, 138.0, 136.7, 131.5, 130.8, 130.6, 129.9, 129.5, 124.1, 122.8, 120.2 ppm. **IR (neat, ATR):** $\tilde{\nu}$ = 3293 (m), 3059 (m), 1700 (vs), 1595 (s), 1539 (vs), 1499 (m), 1439 (w), 1407 (m), 1325 (m), 1262 (m), 1188 (m), 1153 (m), 1070 (w), 1020 (w), 844 (m), 767 (m), 688 (m), 668 (w) cm⁻¹. **HRMS (ESI):** m/z calcd. for [C₂₁H₁₄O₄N₃]⁻: 372.0984, found: 372.1003 ([M-H]⁻).

Synthesis of carboxy(3-carboxy-4-((4-(phenyldiazenyl)phenyl)carbamoyl)phenyl)methanaminium formate (Azo-DCPG) and carboxy(4-carboxy-3-((4-(phenyldiazenyl)phenyl)carbamoyl)phenyl)methanaminium formate (5.39)



A mixture of both regioisomeric aldehydes **5.37** and **5.38** (525 mg, 1.41 mmol, 1.0 equiv.) was dissolved in 7 M NH₃ in MeOH (27 mL) and TMSCN (0.28 mL, 2.3 mmol, 1.6 equiv.) was added. The mixture was stirred at room temperature for 20 h. The solvent was removed under reduced pressure and the crude product was used without further purification in the next step.

The crude residue was dissolved in MeOH (70 mL) and conc. H₂SO₄ (2 mL) was added dropwise. The reaction mixture was then heated to reflux for 3 h. After cooling to room temperature, the solvent was removed *in vacuo* and the residue was taken up in EtOAc (50 mL). The organic phase was washed with sat. aqu. NaHCO₃ (2 x 50 mL) and brine (50 mL), dried over MgSO₄ and concentrated *in vacuo*. The crude product was purified by a quick flash silica gel column chromatography (DCM/MeOH/HOAc/H₂O, 100:0:0:0 → 98:2:0.6:0.6) to yield a mixture of two isomers which was used directly in the next step.

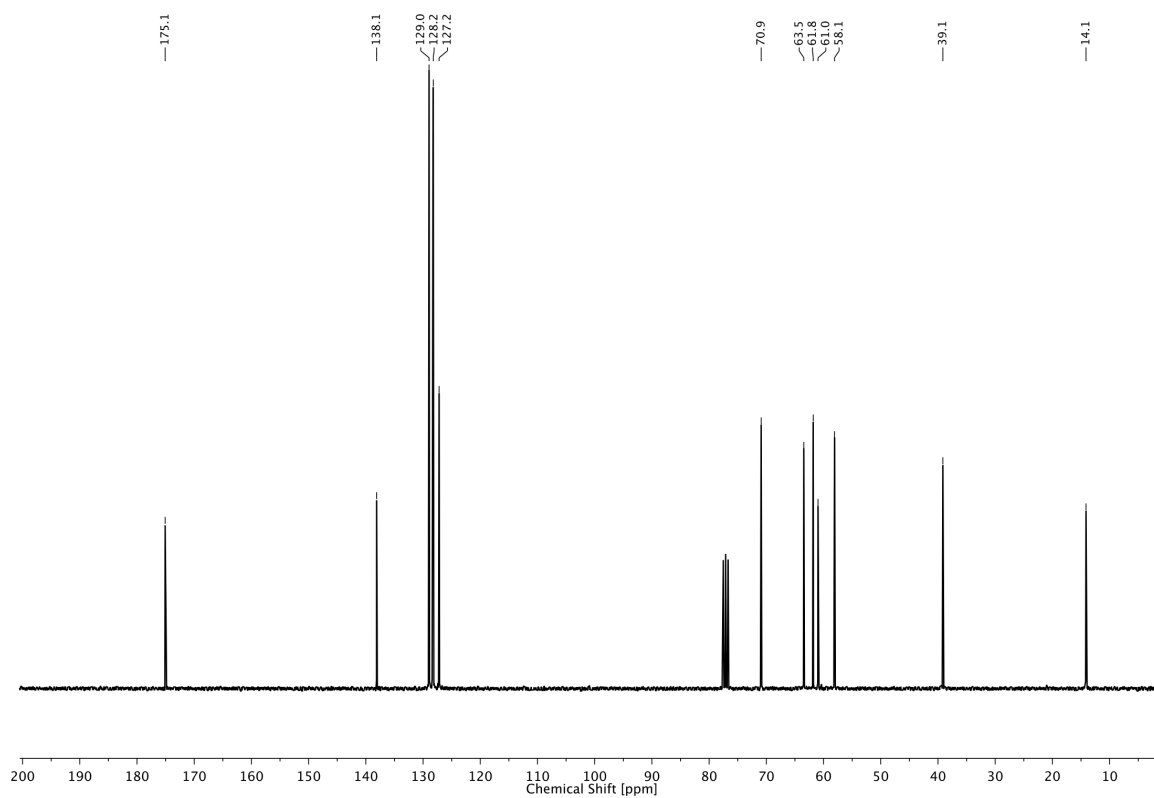
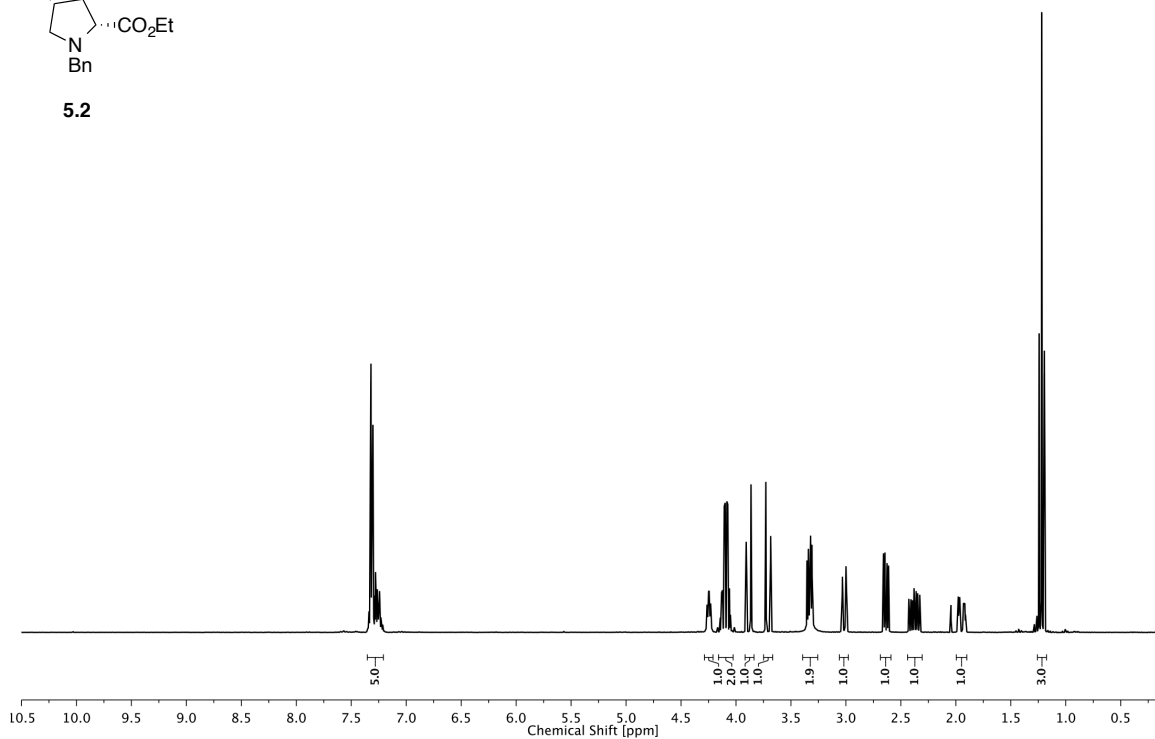
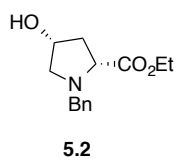
The crude products were dissolved in MeOH (9 mL) and cooled to 0 °C. A 4 M solution of HCl in dioxane (9 mL) was added slowly. The solution was stirred for 1 h at 0 °C. H₂O (0.10 mL) was added and the mixture was warmed to room temperature and stirred for 16 h. The mixture was washed with sat. aqu. NaHCO₃ (25 mL; gas evolution!) and extracted with EtOAc (3 x 20 mL). The combined organic layers were washed with brine (50 mL), dried over MgSO₄ and concentrated *in vacuo*.

The crude product was then dissolved in THF (24 mL) and a 2 M solution of LiOH (4 mL) was added. The mixture was stirred at room temperature for 2 d. 2 M HCl (5 mL) was added and the solvent was removed under reduced pressure. The crude product was purified by reversed-phase flash silica gel column chromatography (H₂O/MeOH, 0.1% HCO₂H, gradient from 100:0 to 50:50), affording a mixture of both regioisomers **Azo-DCPG** and **5.39**. The two regioisomers were then separated by HPLC (H₂O/MeOH, 0.1% HCO₂H, gradient from 95:5 to 30:70) to yield the two products in 75 mg (0.18 mmol, 13% over 4 steps; R_t = 50 min) and 25 mg (0.060 mmol, 4% over 4 steps; R_t = 52 min) both as orange solids. Their identity was confirmed by HRMS and NMR but it was not possible to assign the corresponding structure to each compound.

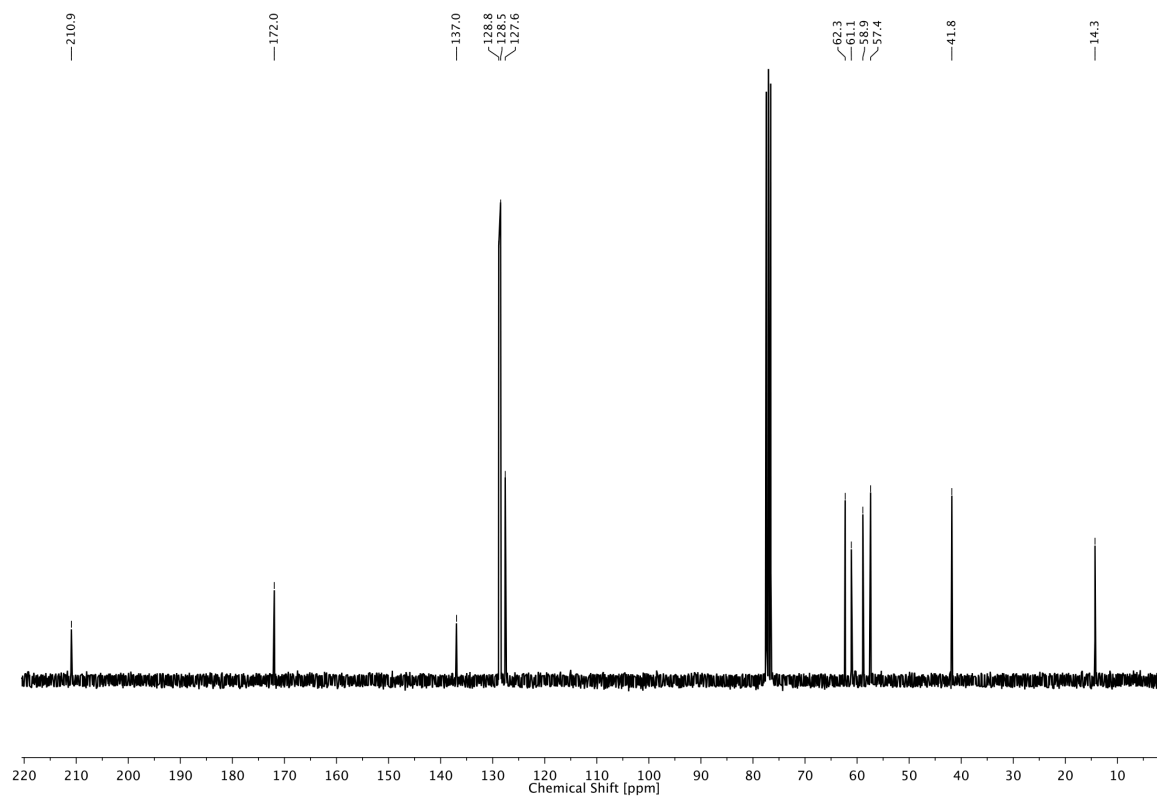
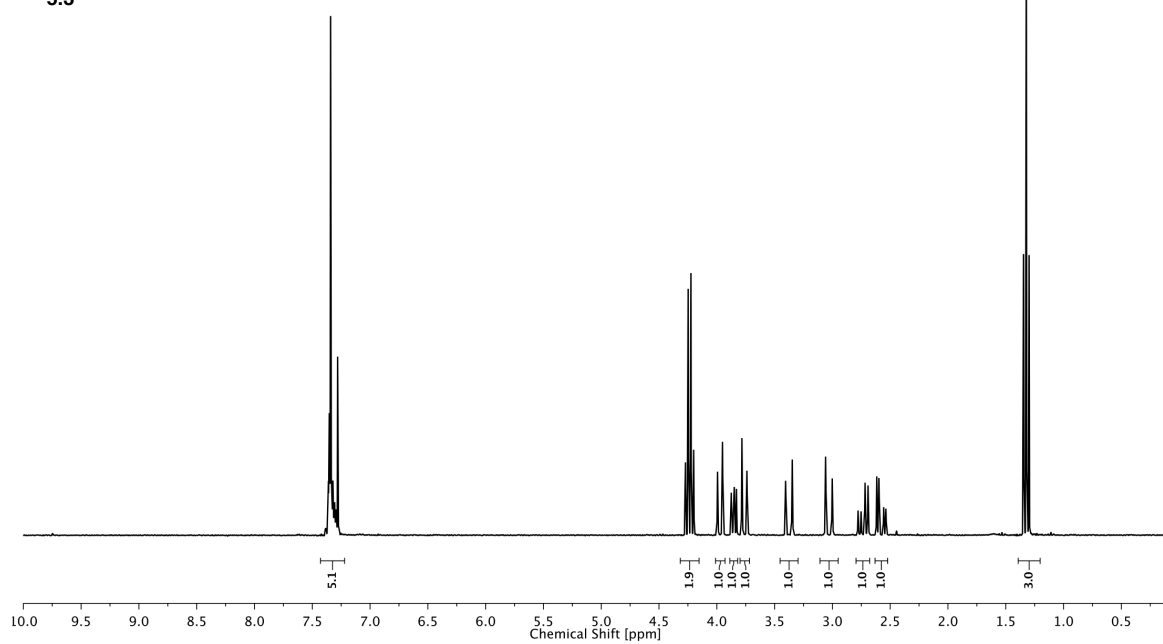
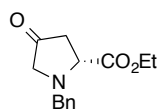
R_t = 50 min: **¹H NMR (CD₃OD, 400 MHz, 27 °C):** δ = 8.07–8.01 (m, 1H, ArH), 7.93–7.83 (m, 6H, ArH), 7.70–7.65 (m, 2H, ArH), 7.54–7.47 (m, 3H, ArH), 4.74 (s, 1H, CH) ppm. **¹³C NMR (CD₃OD, 100 MHz, 27 °C):** δ = 171.0, 169.0, 152.7, 148.9, 141.6, 139.3, 130.6, 130.5, 128.8, 128.7, 127.0, 124.7, 123.3, 122.2, 121.6, 120.1, 113.7, 57.9 ppm. **HRMS (ESI):** *m/z* calcd. for [C₂₂H₁₇O₅N₄]⁻: 417.1199, found: 417.1202 ([M-H]⁻).

R_t = 52 min: **¹H NMR (DMSO-d₆, 600 MHz, 27 °C):** δ = 11.04 (br s, 1H, CO₂H), 7.93–7.92 (m, 1H, ArH), 7.91–7.87 (m, 4H, ArH), 7.86–7.85 (m, 1H, ArH), 7.85–7.84 (m, 1H, ArH), 7.63–7.60 (m, 1H, ArH), 7.58–7.57 (m, 1H, ArH), 7.56–7.54 (m, 2H, ArH), 7.54–7.51 (m, 1H, ArH), 4.75 (s, 1H, CH) ppm. **¹³C NMR (DMSO-d₆, 150 MHz, 27 °C):** δ = 167.9, 167.8, 152.5, 147.9, 143.3, 139.4, 131.4, 129.8, 129.6, 128.8, 128.3, 124.1, 124.1, 122.8, 122.1, 120.1, 120.0, 58.1 ppm. **HRMS (ESI):** *m/z* calcd. for [C₂₂H₁₇O₅N₄]⁻: 417.1199, found: 417.1202 ([M-H]⁻).

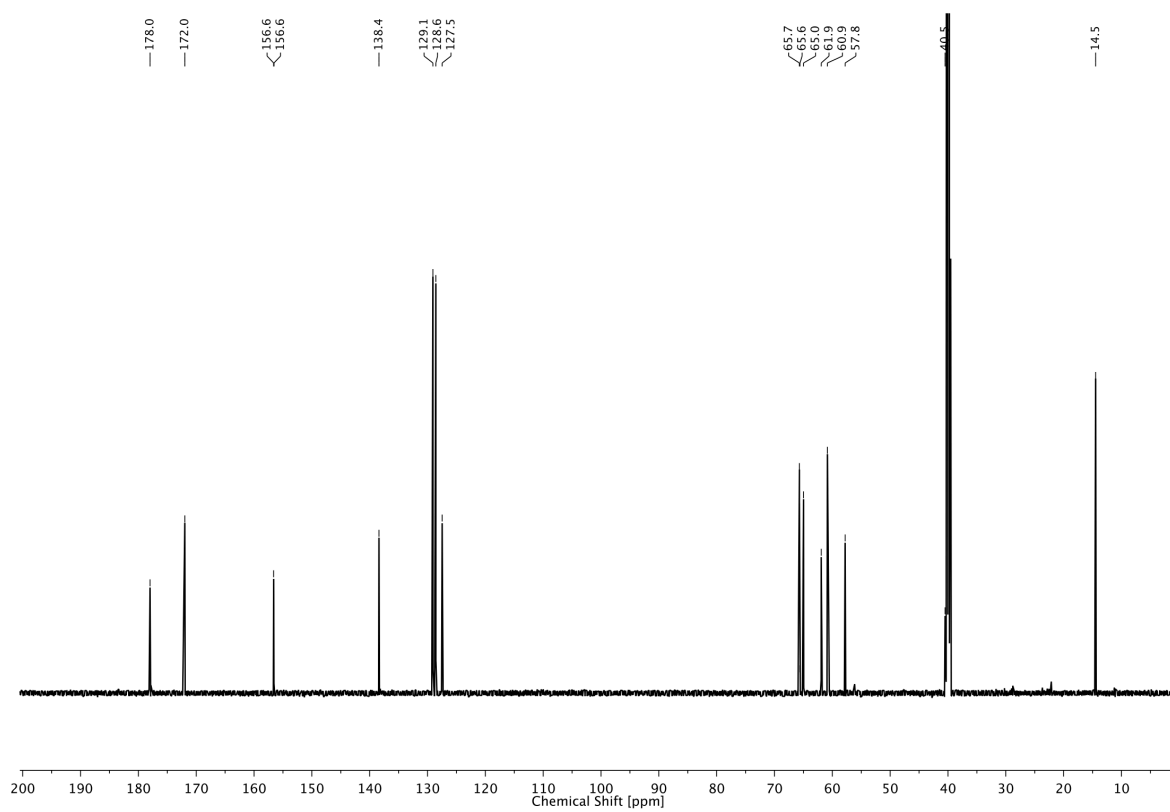
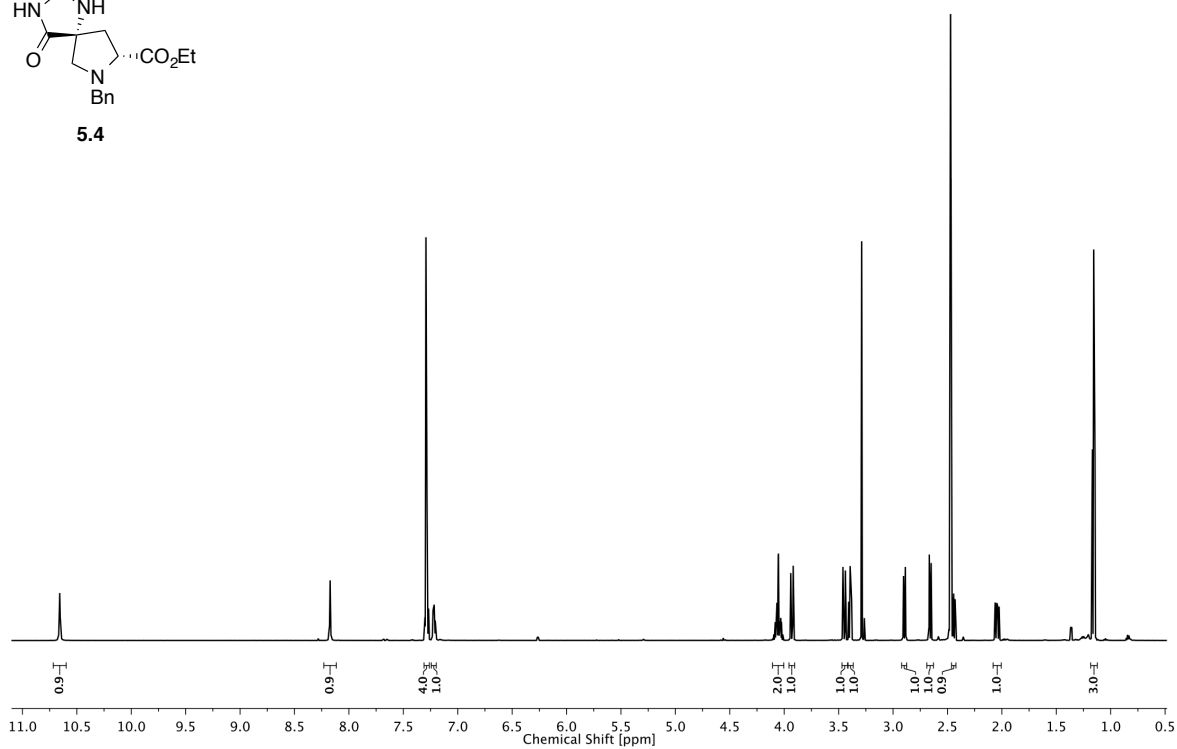
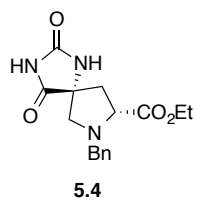
5.6 NMR SPECTRA



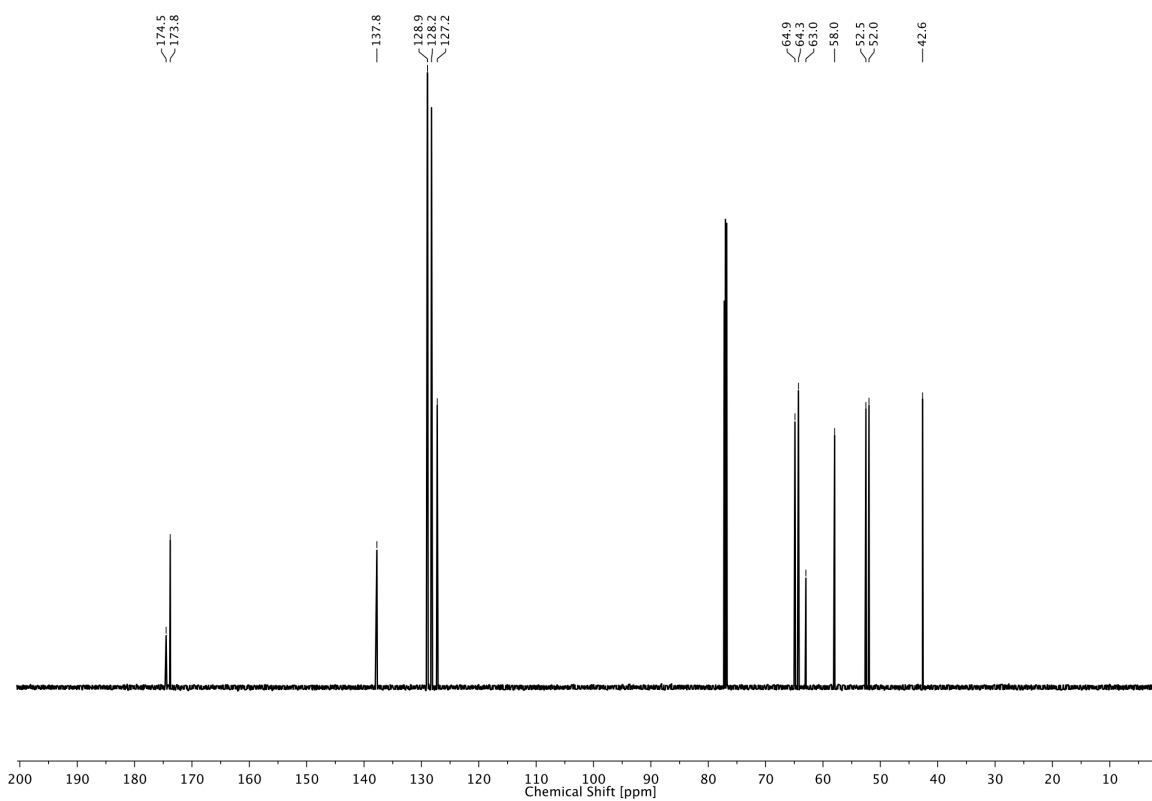
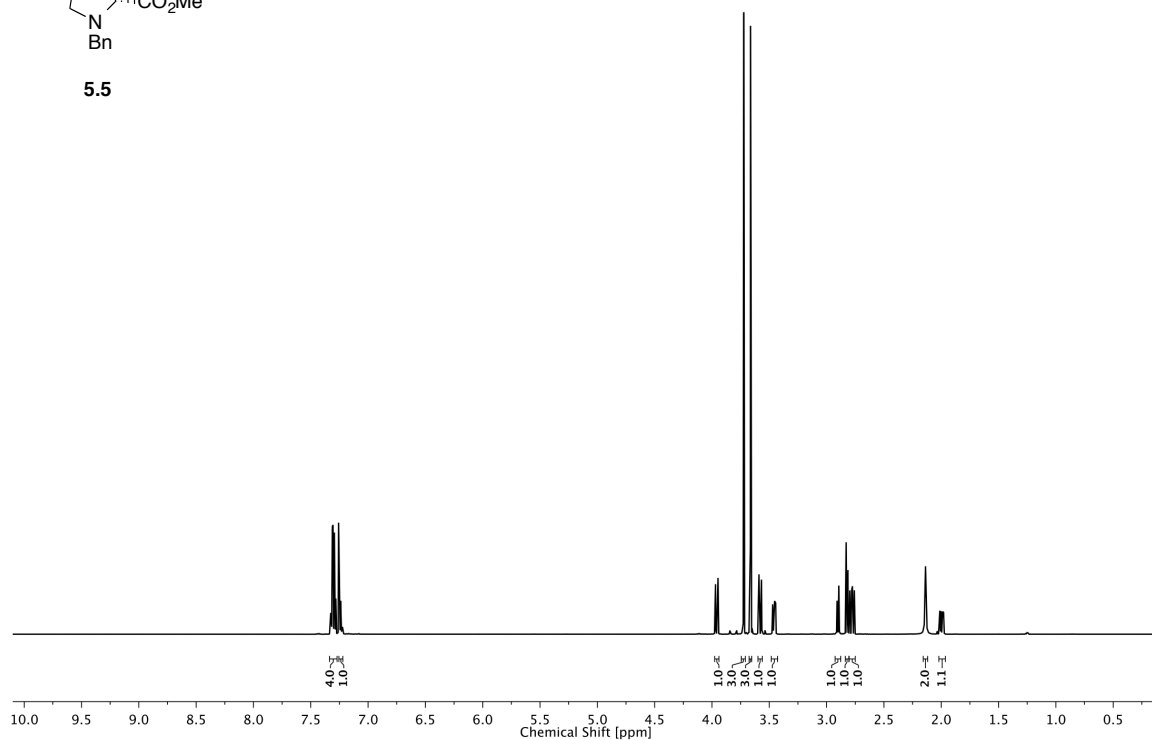
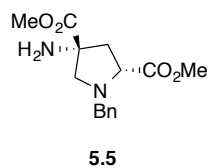
5 STUDIES TOWARD PHOTOSWITCHABLE mGLUR6 AGONISTS AS A POTENTIAL APPROACH TO VISION RESTORATION



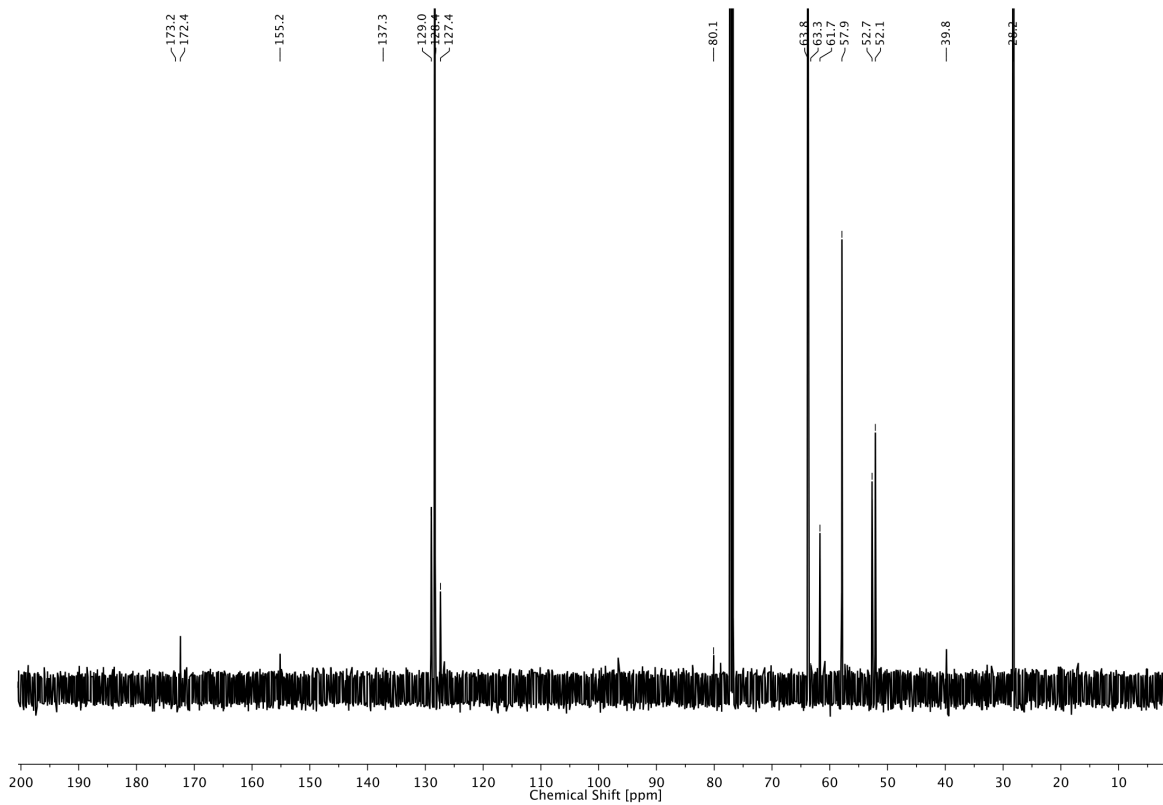
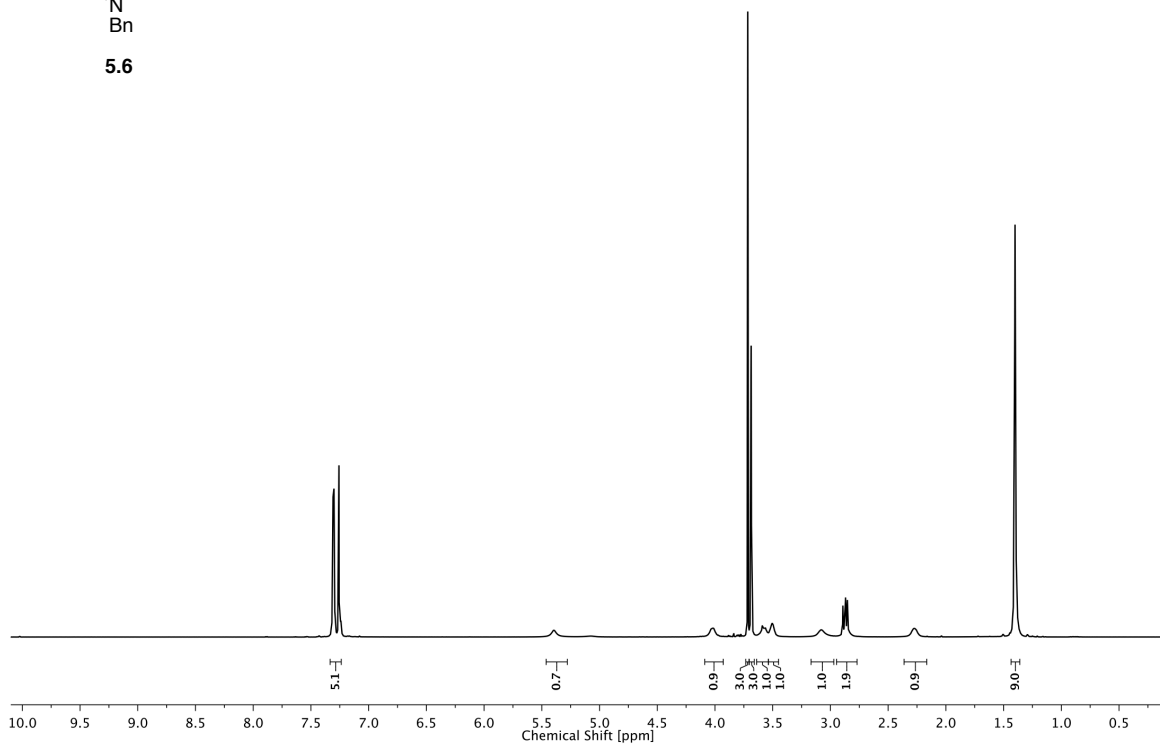
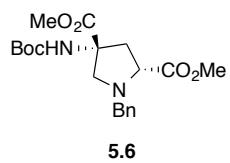
5 STUDIES TOWARD PHOTOSWITCHABLE mGLUR6 AGONISTS AS A POTENTIAL APPROACH TO VISION RESTORATION



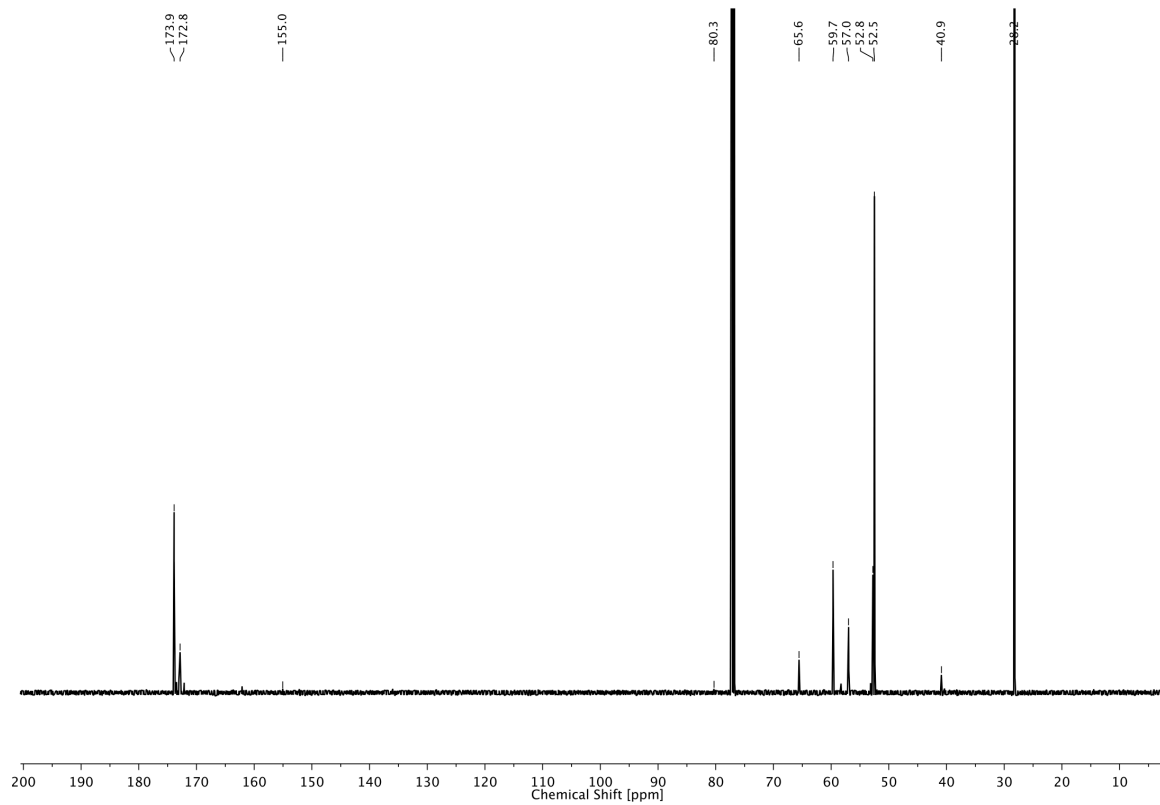
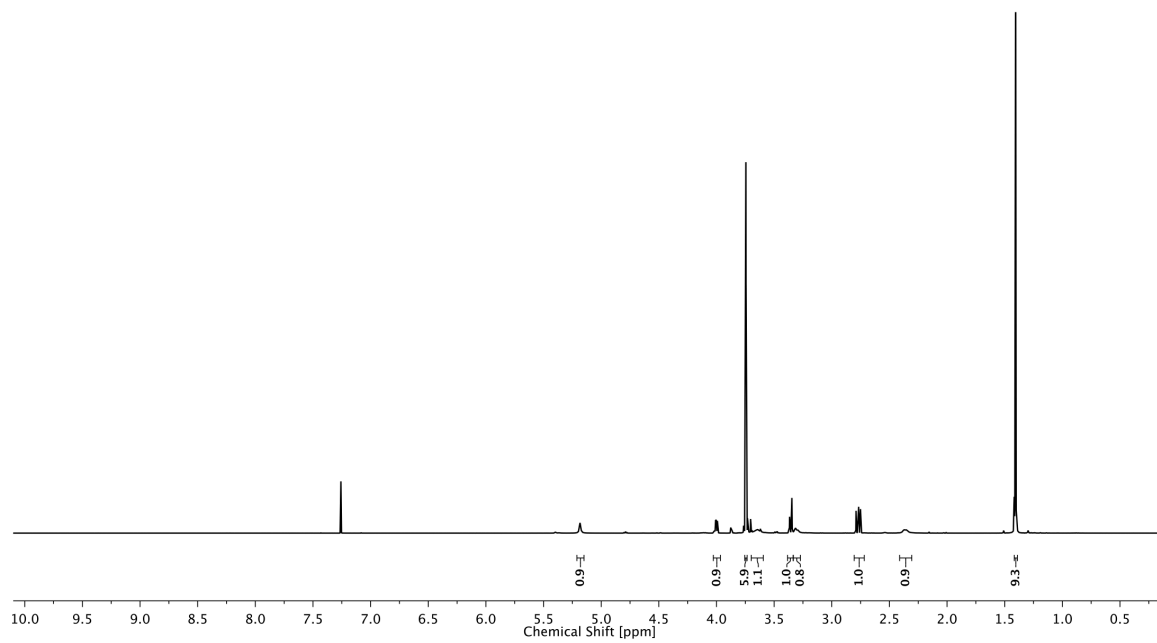
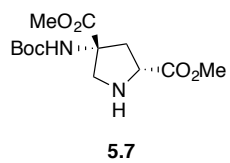
5 STUDIES TOWARD PHOTOSWITCHABLE mGLUR6 AGONISTS AS A POTENTIAL APPROACH TO VISION RESTORATION



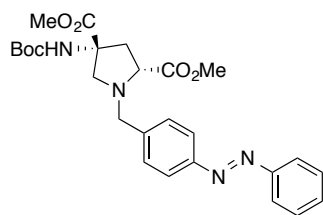
5 STUDIES TOWARD PHOTOSWITCHABLE mGLUR6 AGONISTS AS A POTENTIAL APPROACH TO VISION RESTORATION



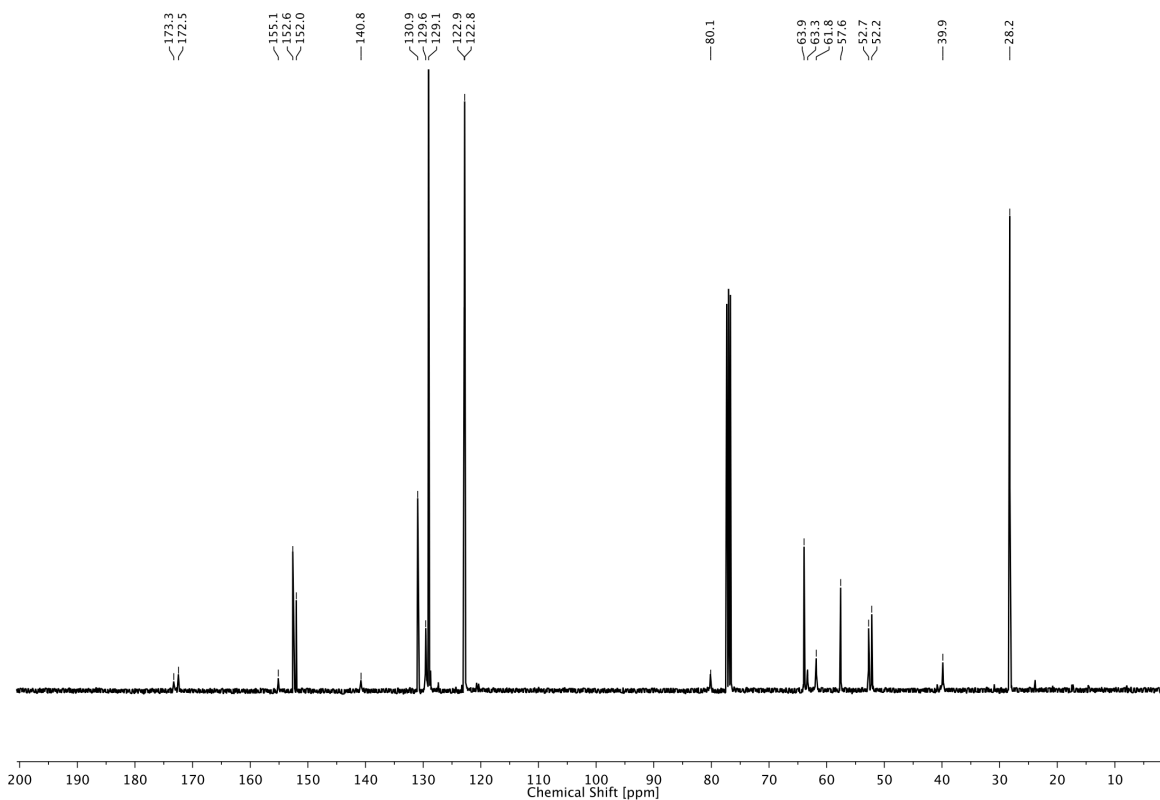
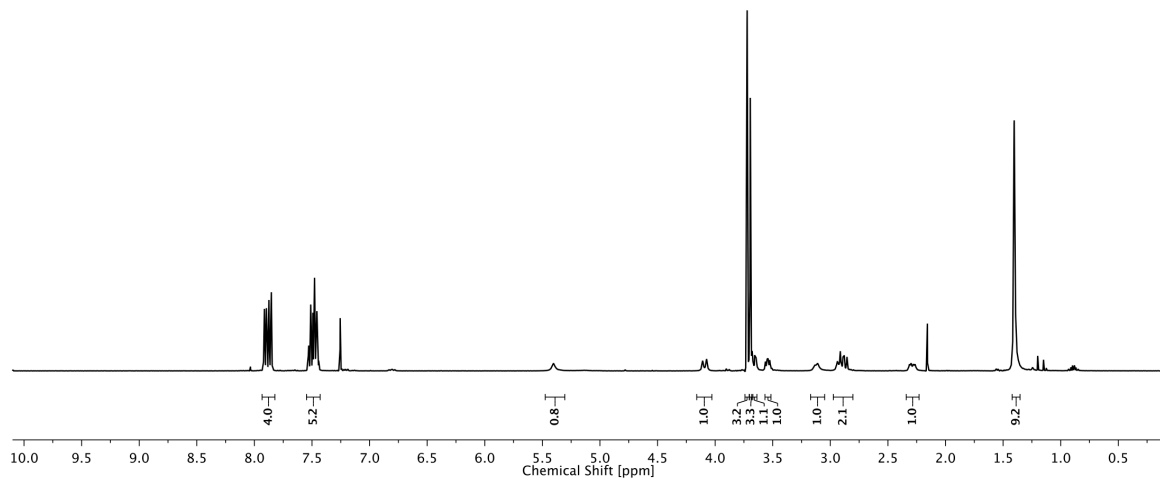
5 STUDIES TOWARD PHOTOSWITCHABLE mGLUR6 AGONISTS AS A POTENTIAL APPROACH TO VISION RESTORATION



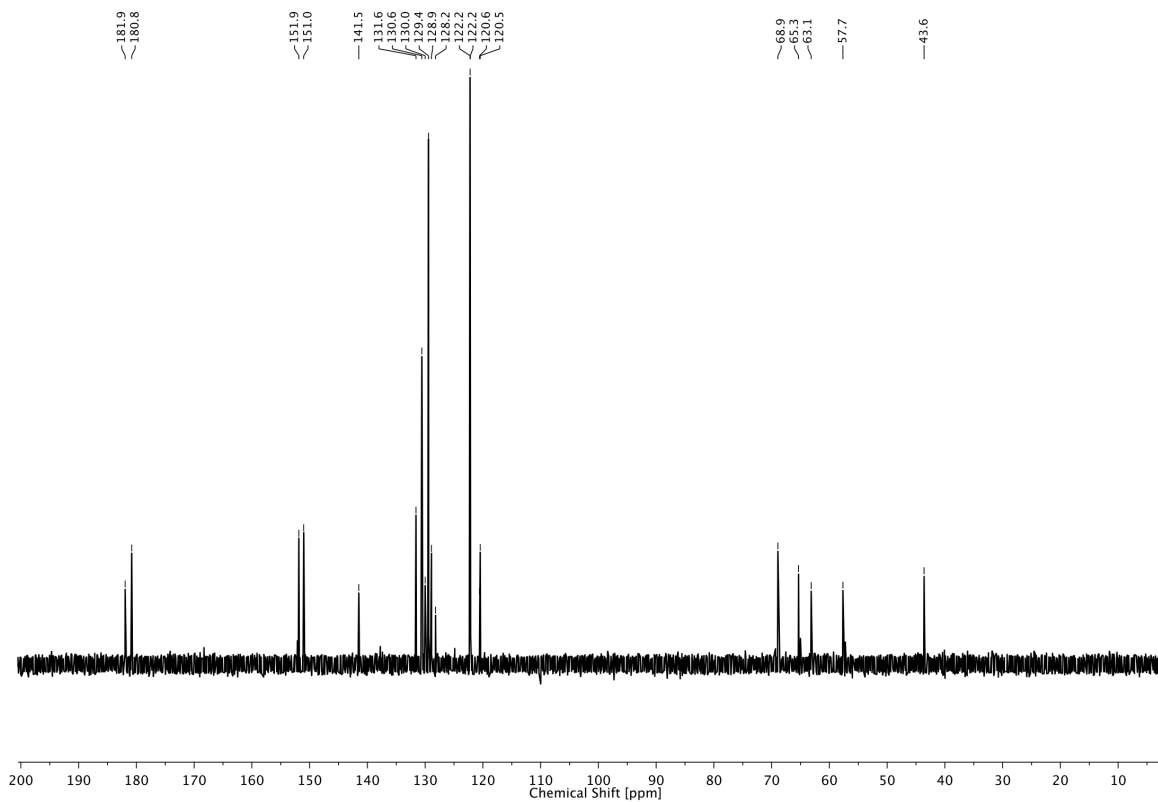
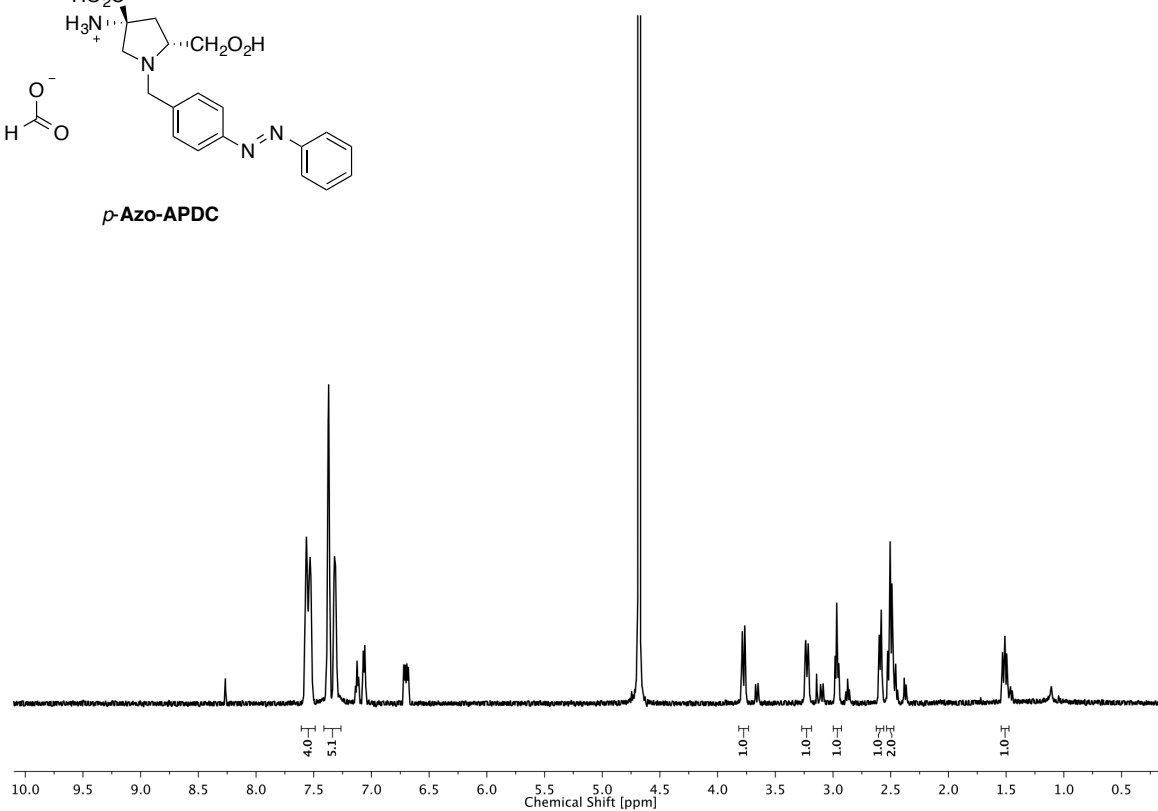
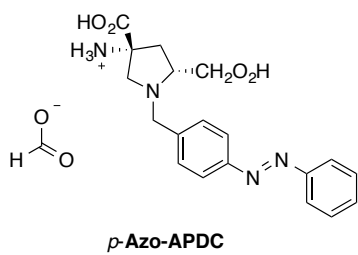
5 STUDIES TOWARD PHOTOSWITCHABLE mGLUR6 AGONISTS AS A POTENTIAL APPROACH TO VISION RESTORATION



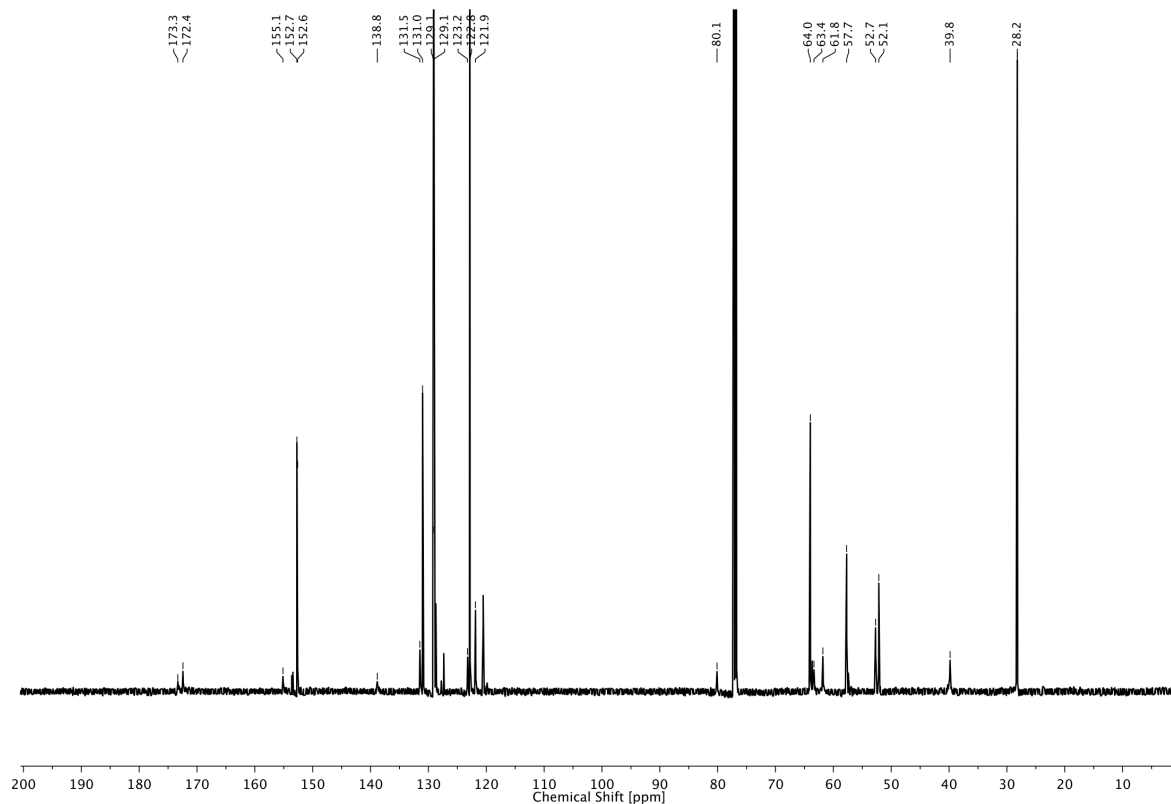
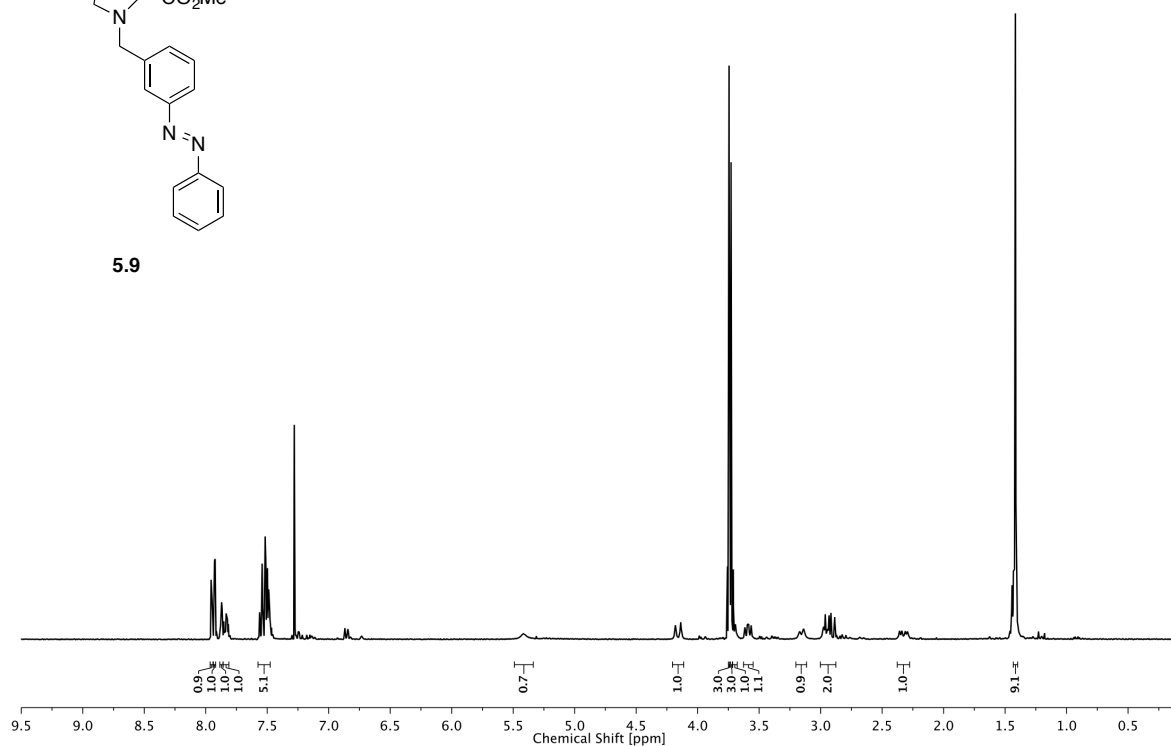
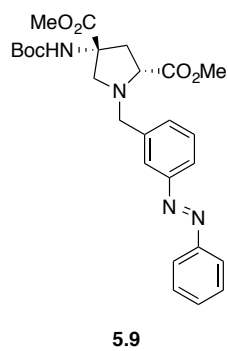
5.8



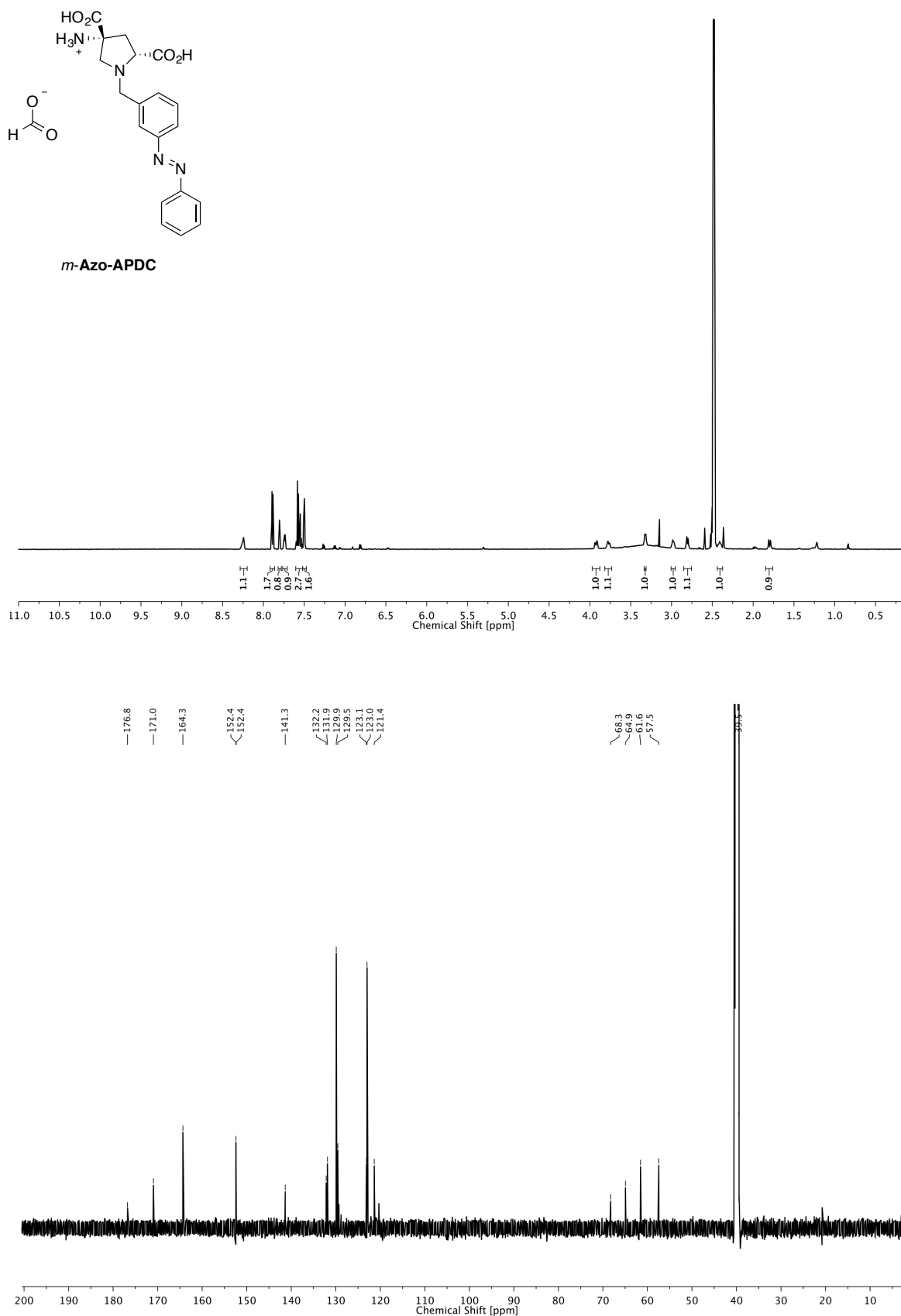
5 STUDIES TOWARD PHOTOSWITCHABLE mGLUR6 AGONISTS AS A POTENTIAL APPROACH TO VISION RESTORATION



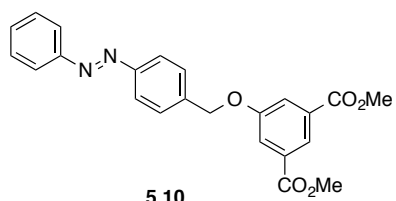
5 STUDIES TOWARD PHOTOSWITCHABLE mGLUR6 AGONISTS AS A POTENTIAL APPROACH TO VISION RESTORATION



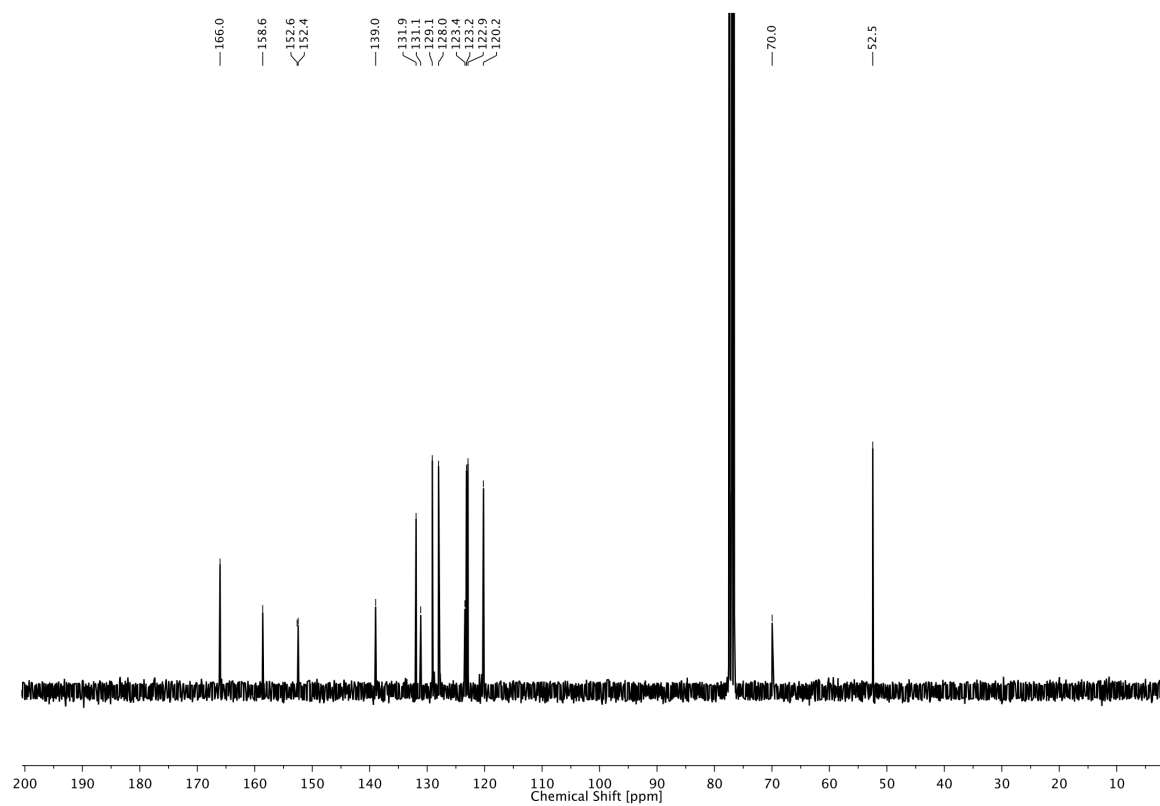
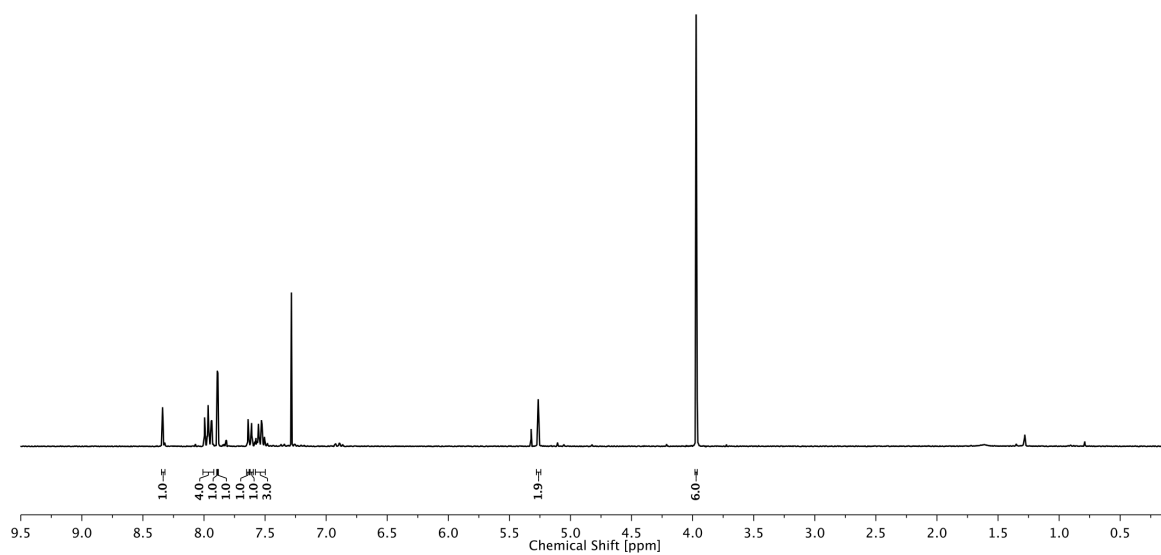
5 STUDIES TOWARD PHOTOSWITCHABLE mGLUR6 AGONISTS AS A POTENTIAL APPROACH TO VISION RESTORATION



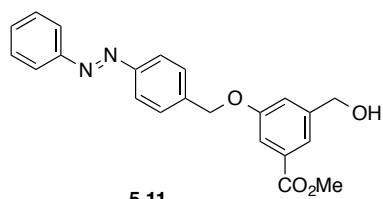
5 STUDIES TOWARD PHOTOSWITCHABLE mGLUR6 AGONISTS AS A POTENTIAL APPROACH TO VISION RESTORATION



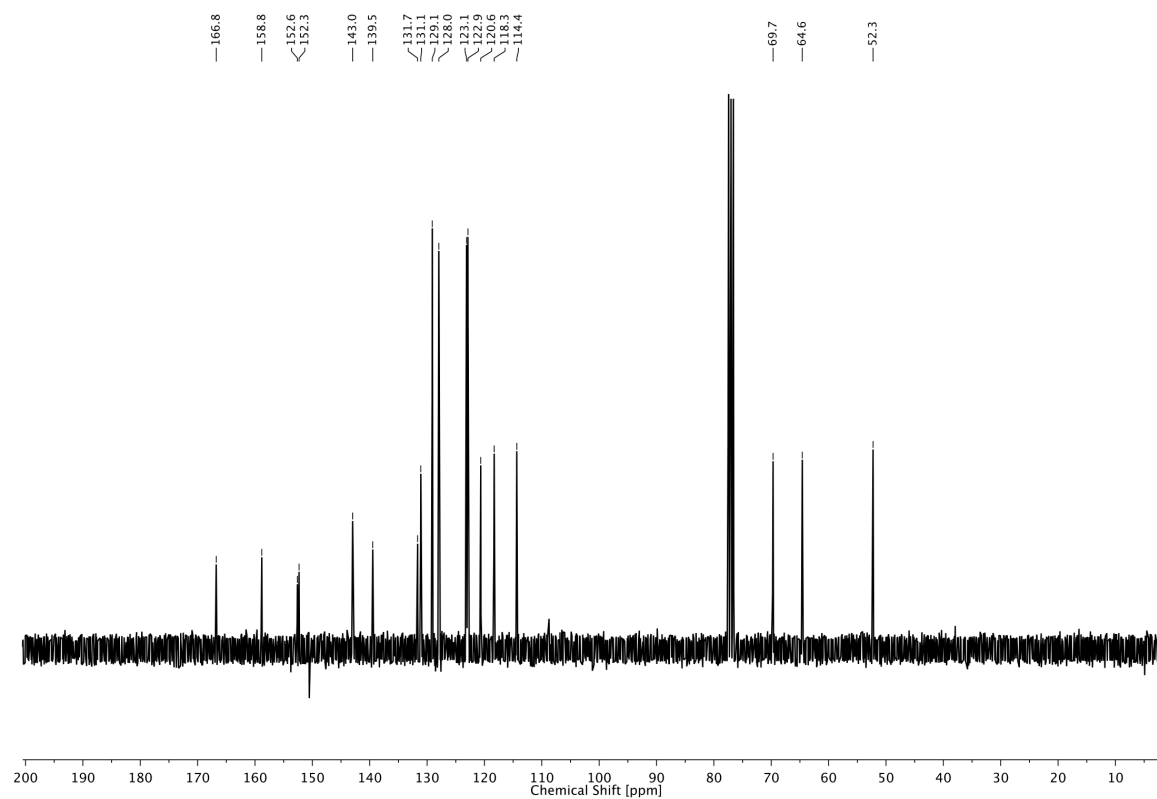
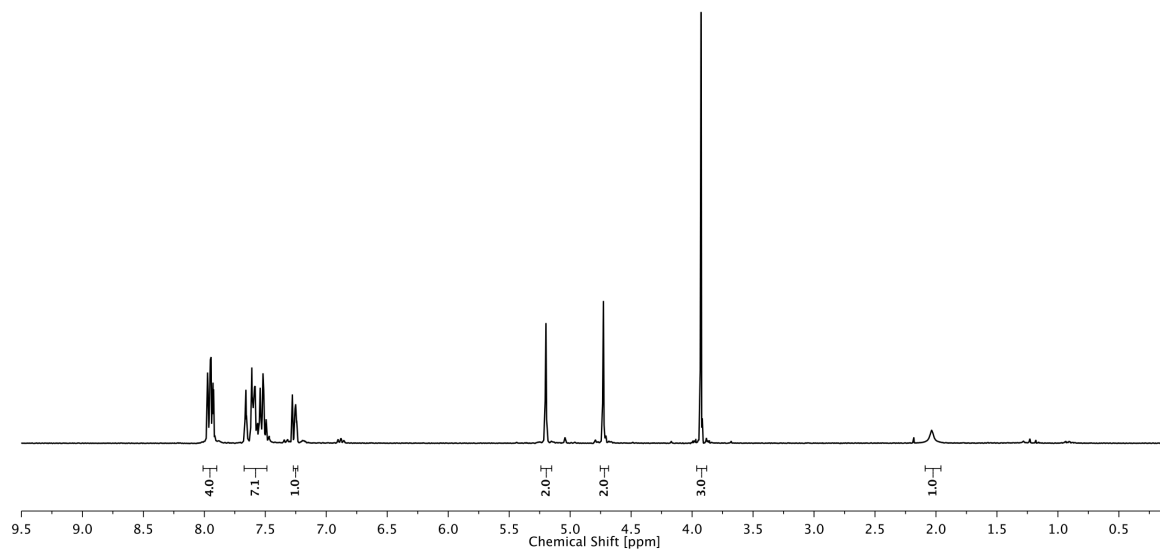
5.10



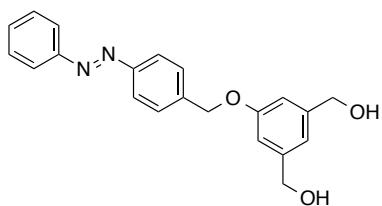
5 STUDIES TOWARD PHOTOSWITCHABLE mGLUR6 AGONISTS AS A POTENTIAL APPROACH TO VISION RESTORATION



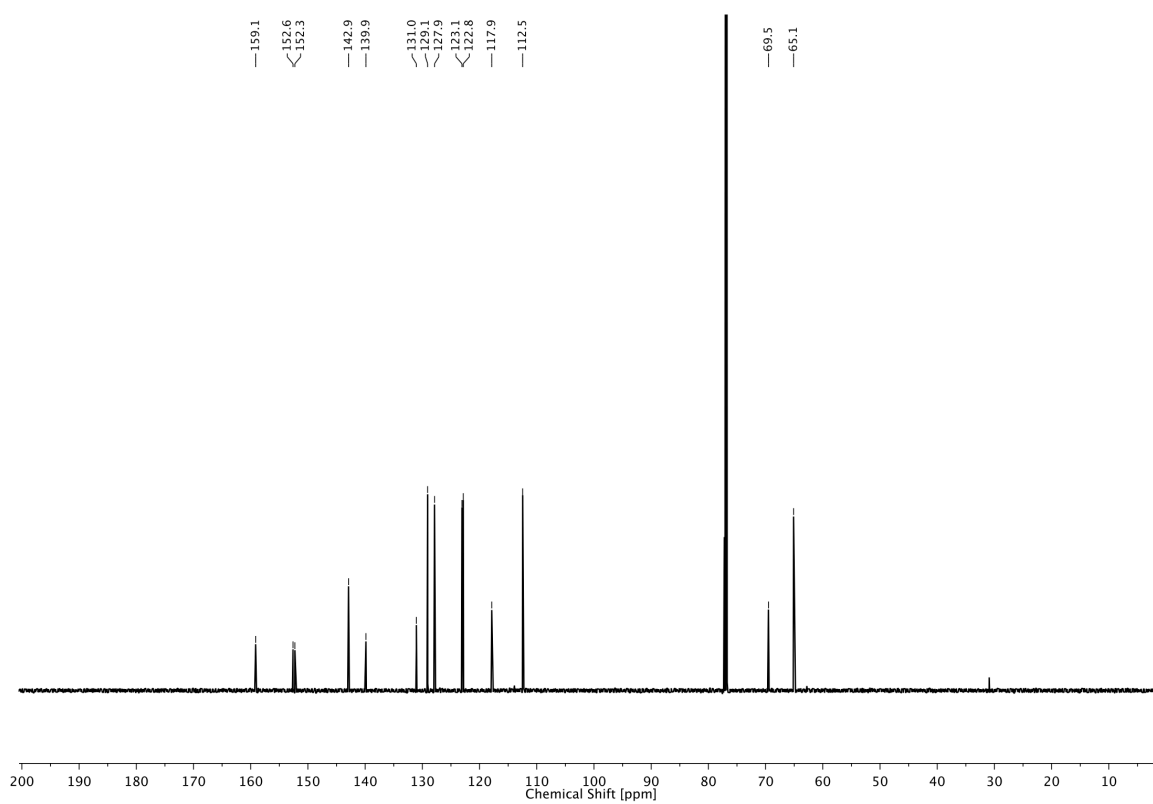
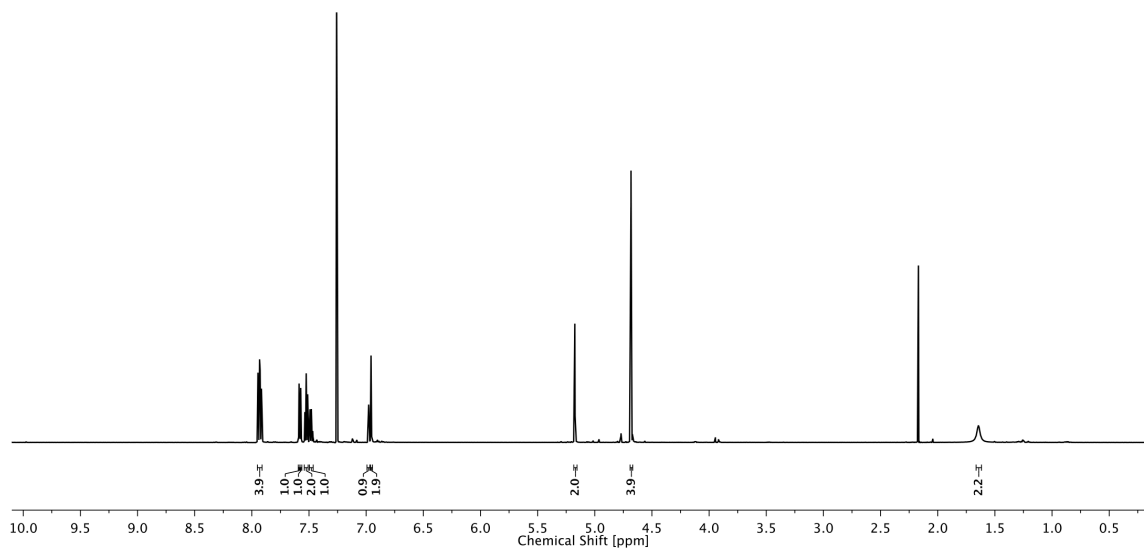
5.11



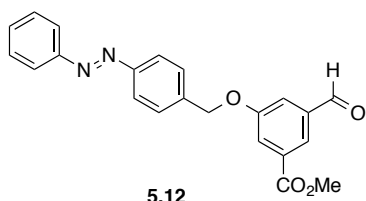
5 STUDIES TOWARD PHOTOSWITCHABLE mGLUR6 AGONISTS AS A POTENTIAL APPROACH TO VISION RESTORATION



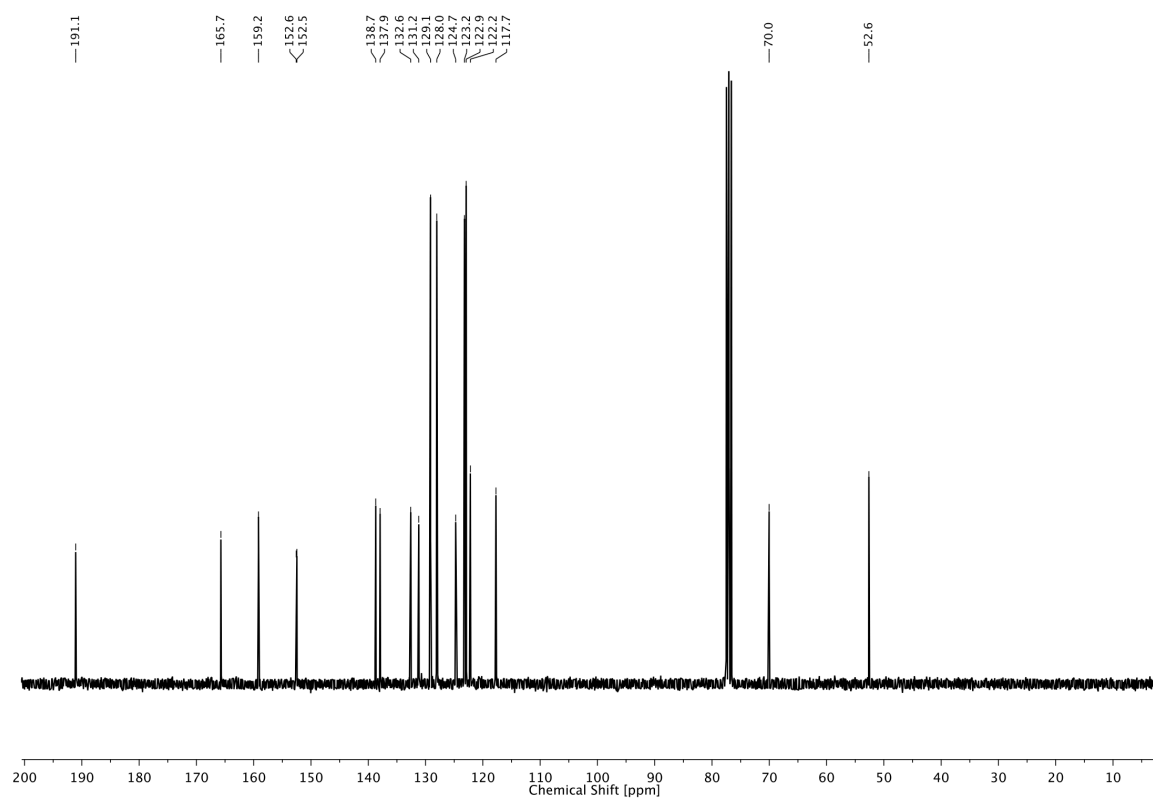
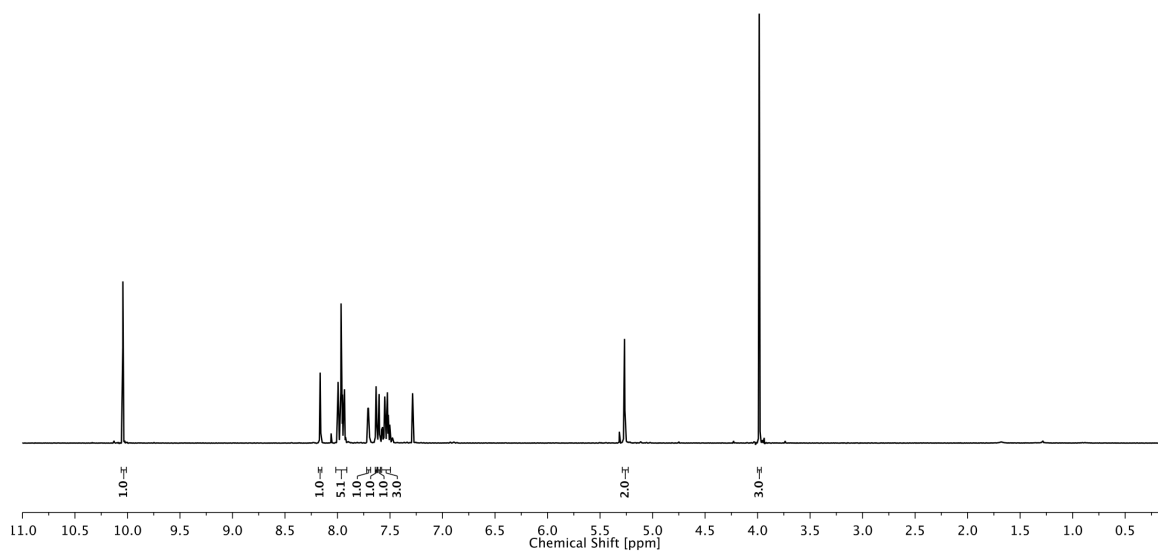
5.41



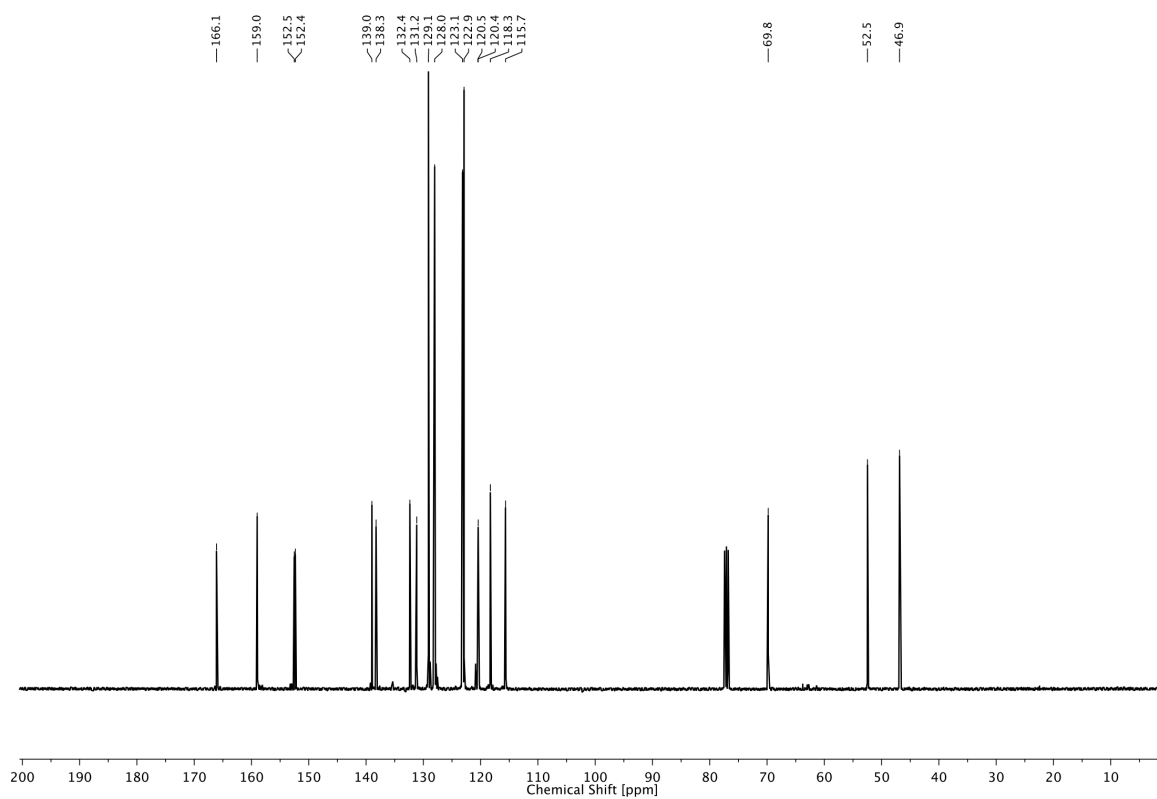
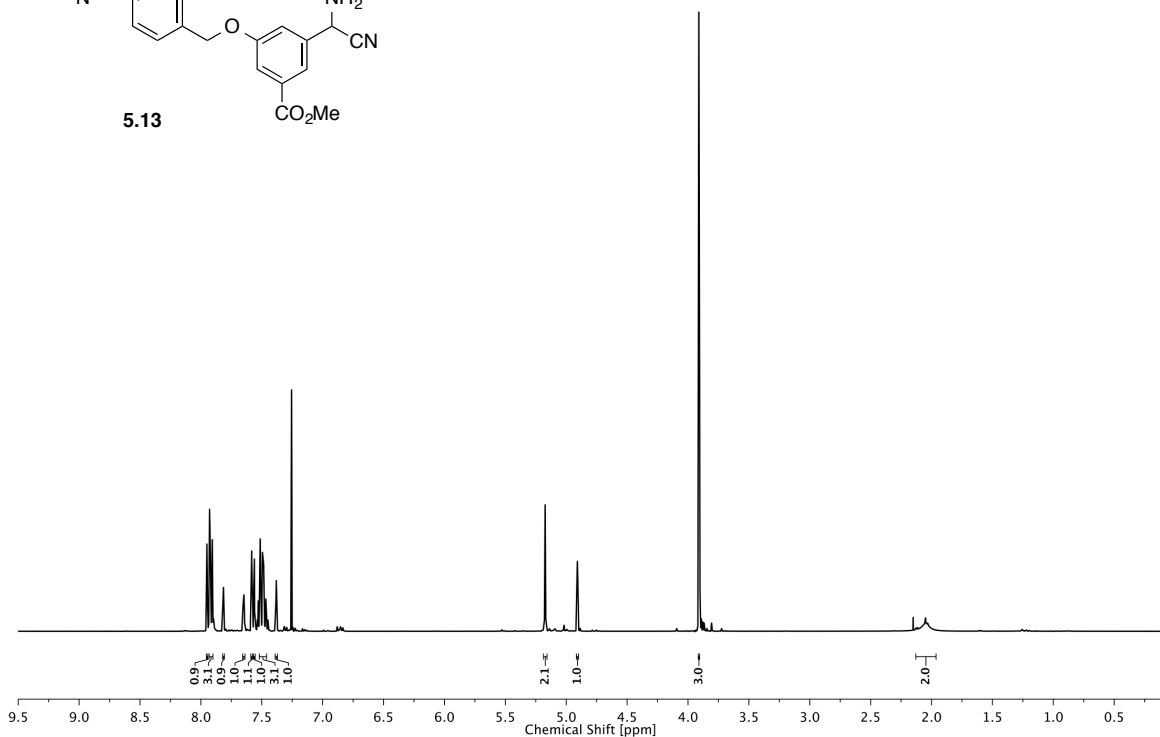
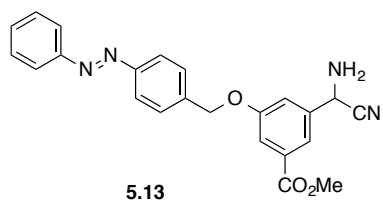
5 STUDIES TOWARD PHOTOSWITCHABLE mGLUR6 AGONISTS AS A POTENTIAL APPROACH TO VISION RESTORATION



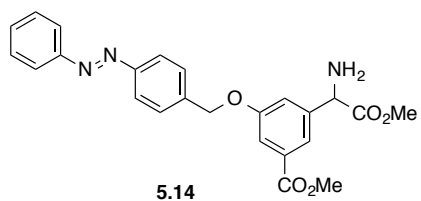
5.12



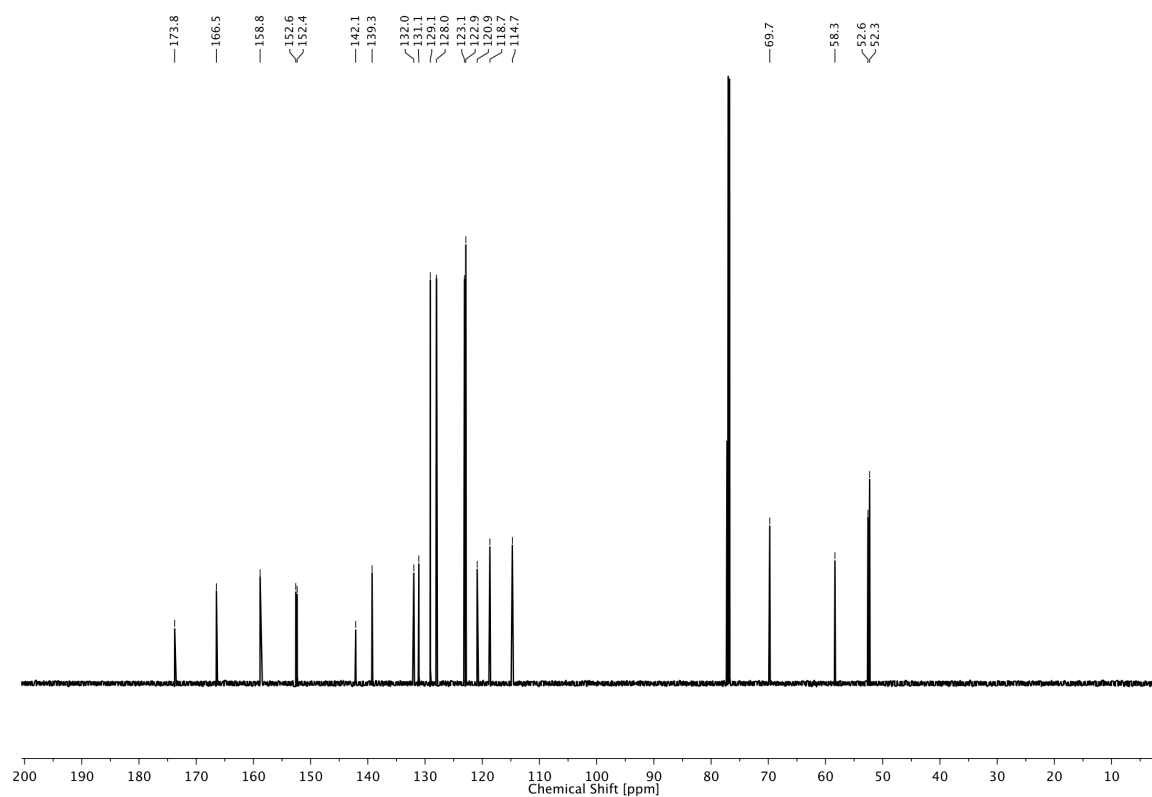
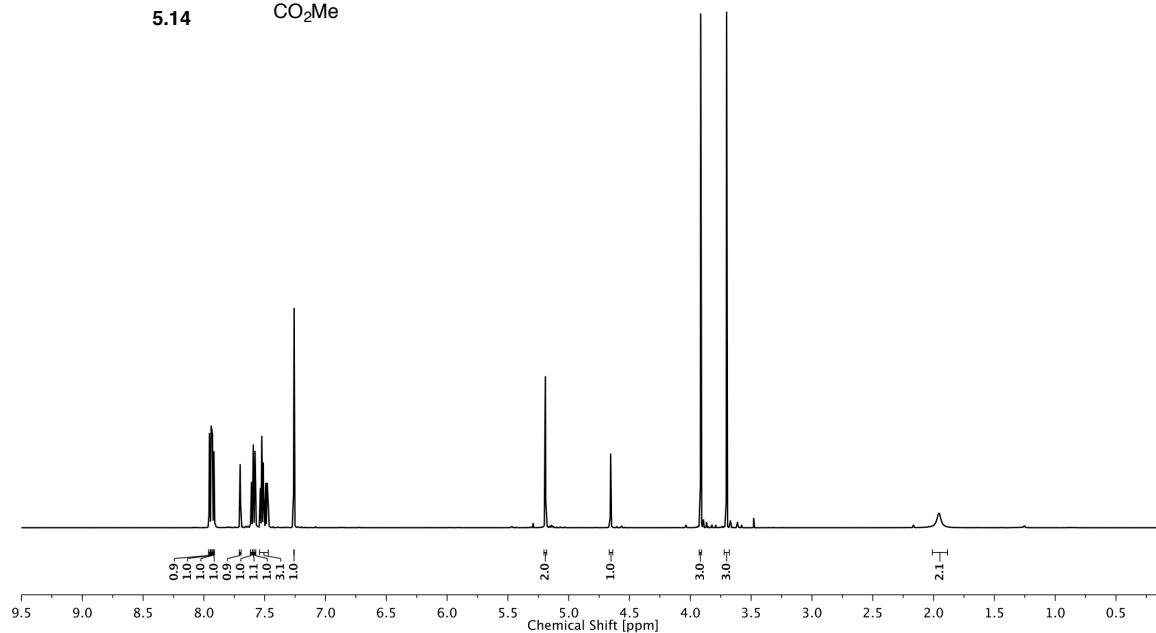
5 STUDIES TOWARD PHOTOSWITCHABLE mGLUR6 AGONISTS AS A POTENTIAL APPROACH TO VISION RESTORATION



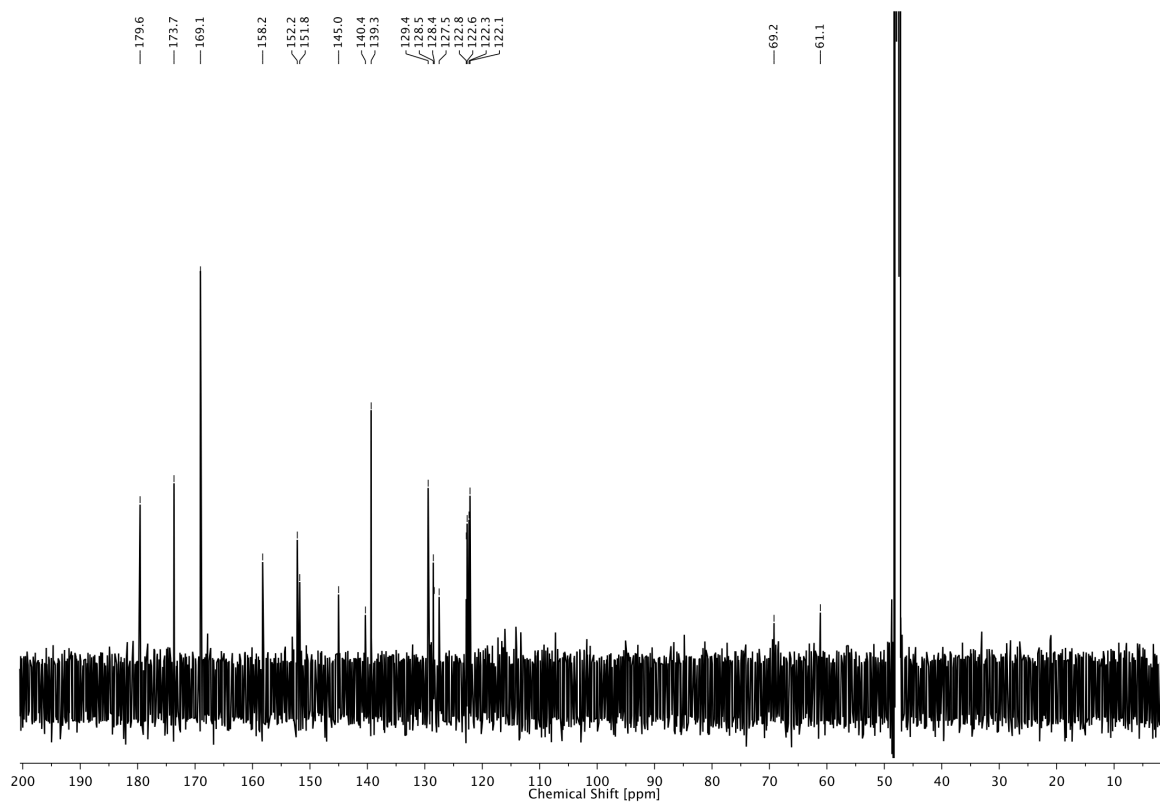
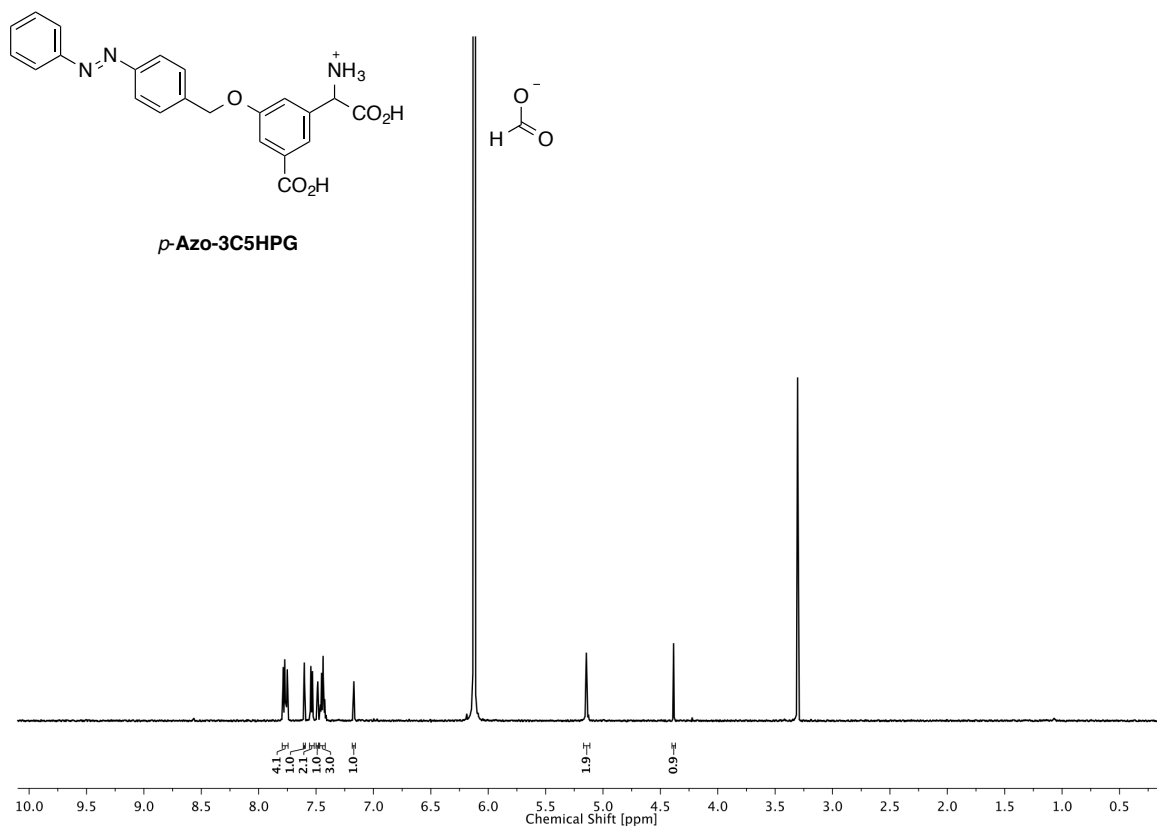
5 STUDIES TOWARD PHOTOSWITCHABLE mGLUR6 AGONISTS AS A POTENTIAL APPROACH TO VISION RESTORATION



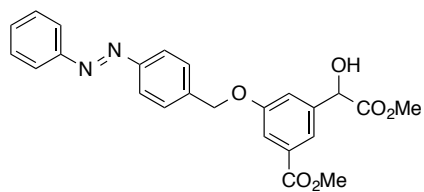
5.14



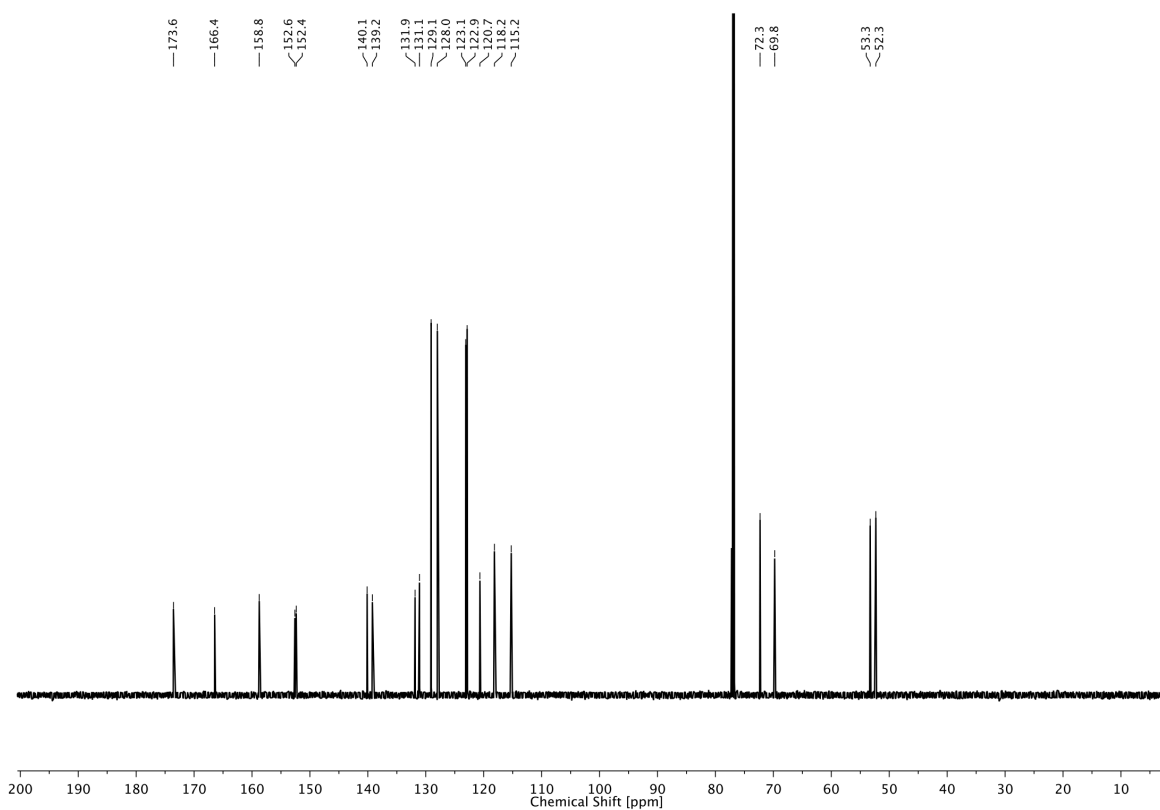
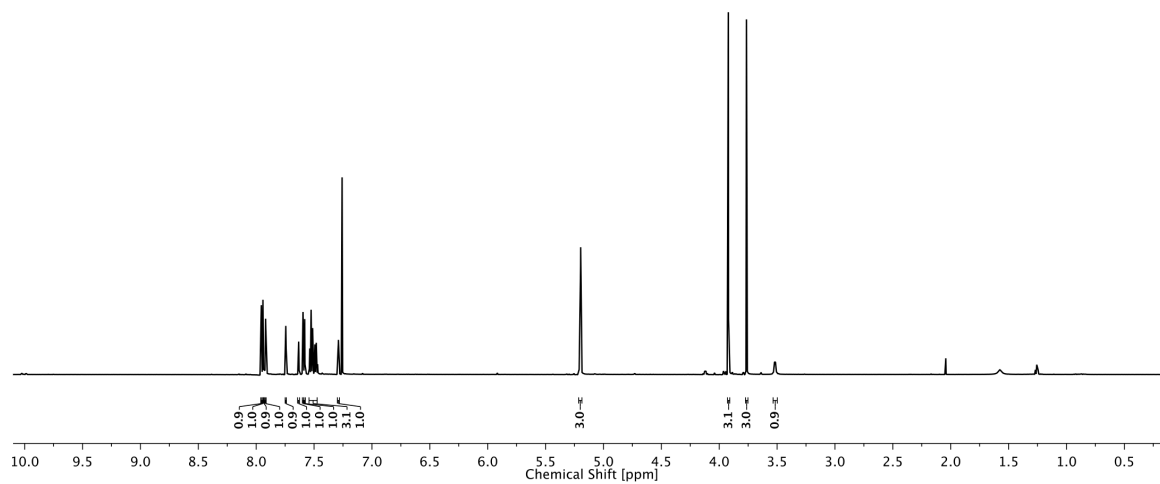
5 STUDIES TOWARD PHOTOSWITCHABLE mGLUR6 AGONISTS AS A POTENTIAL APPROACH TO VISION RESTORATION



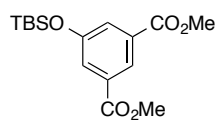
5 STUDIES TOWARD PHOTOSWITCHABLE mGLUR6 AGONISTS AS A POTENTIAL APPROACH TO VISION RESTORATION



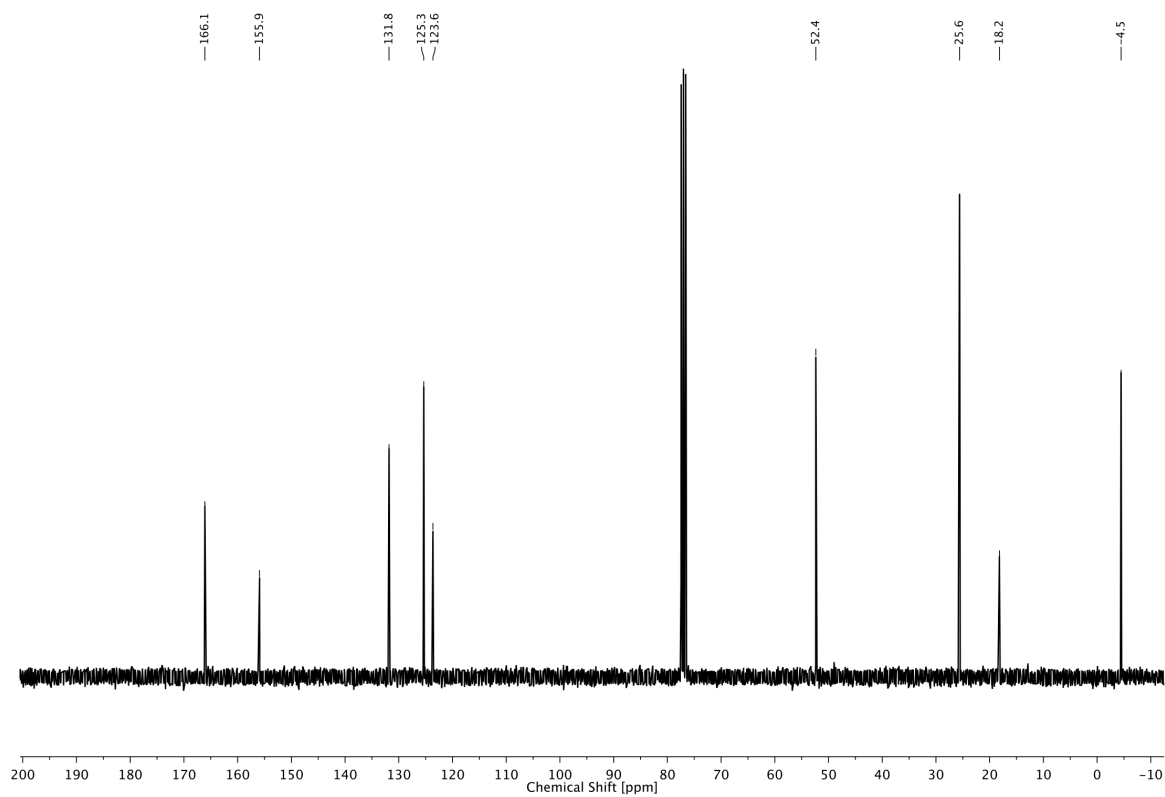
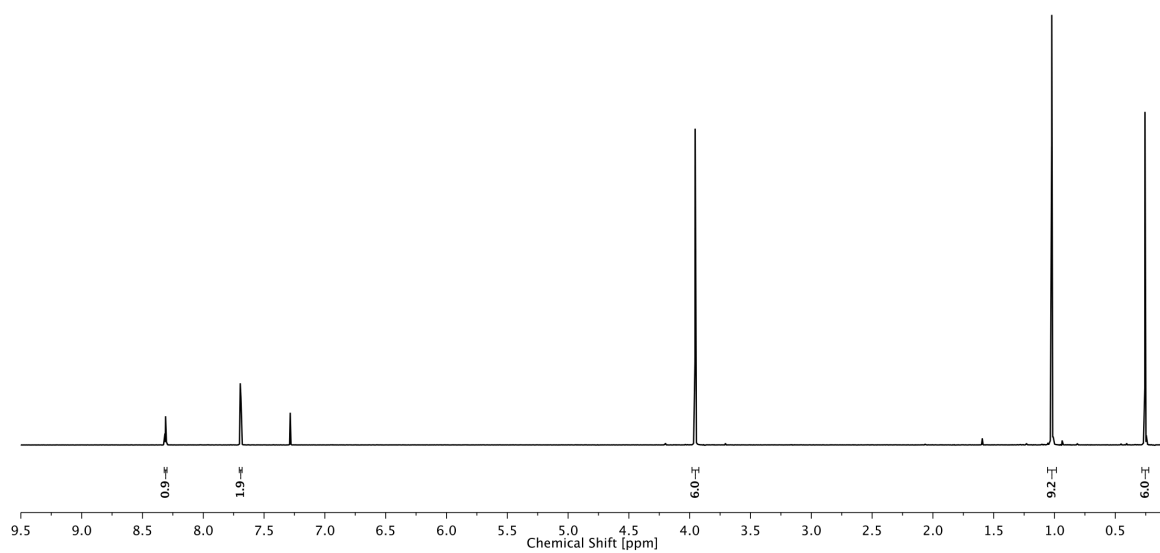
5.20



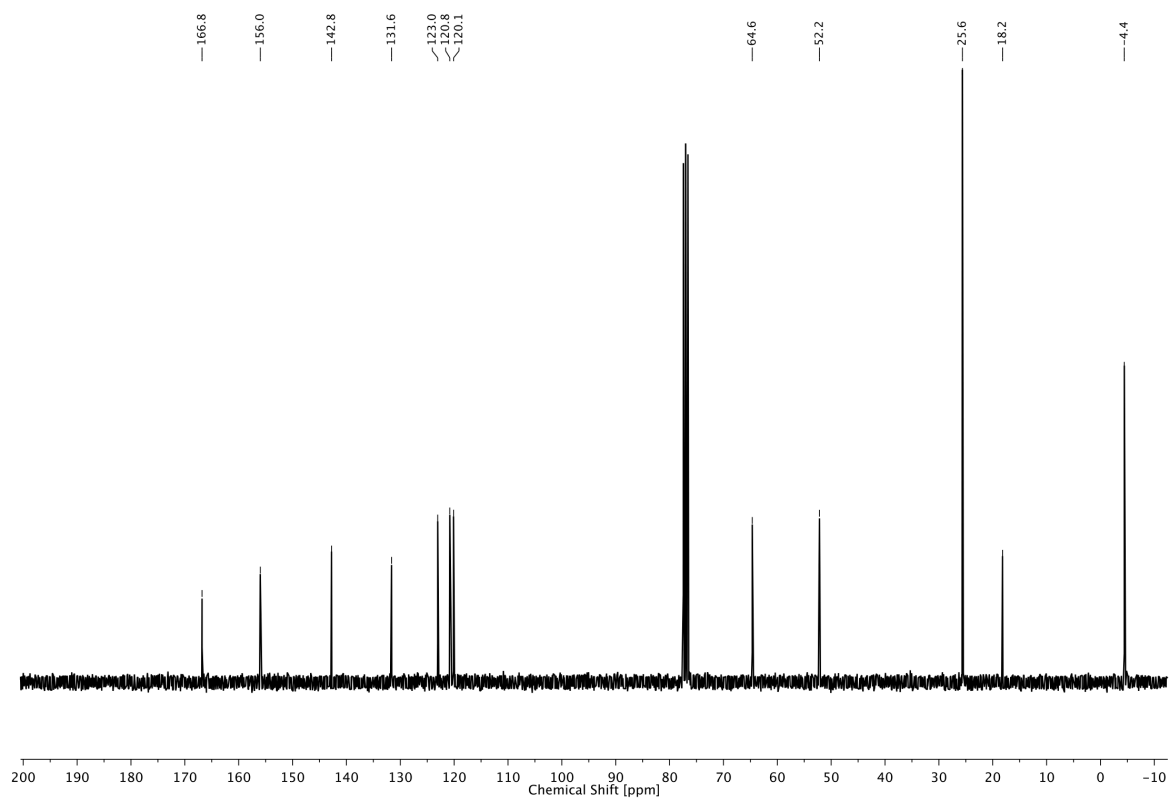
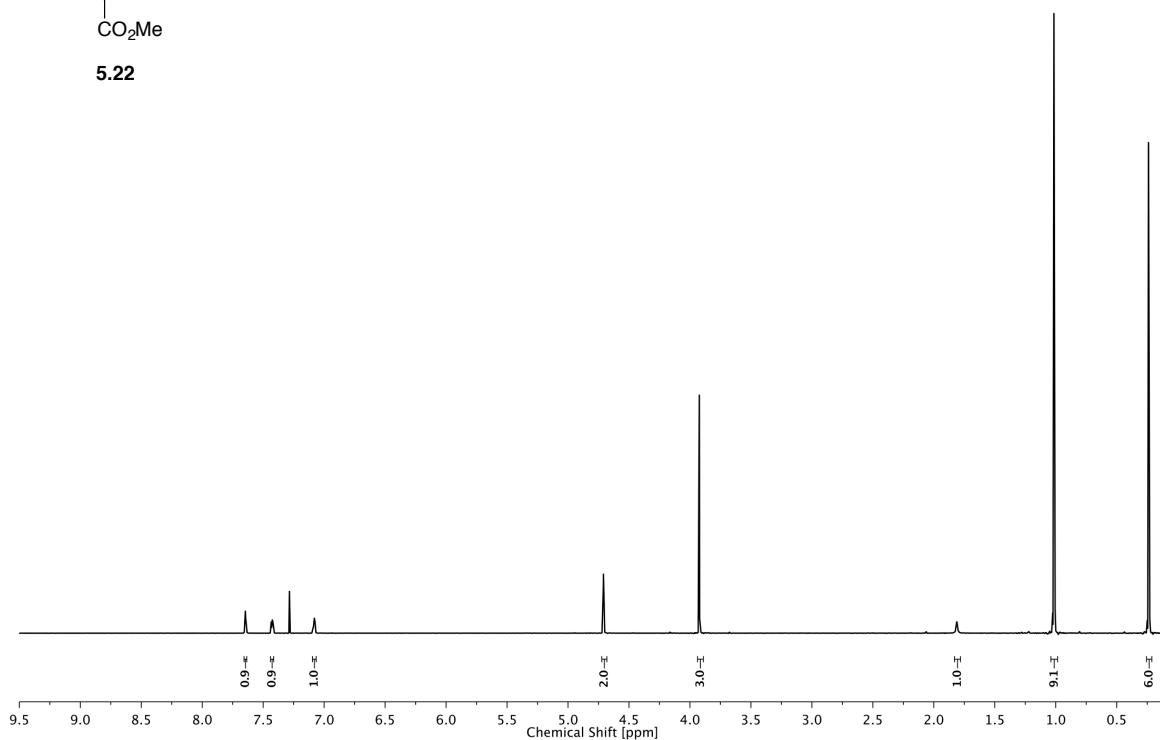
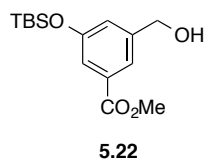
5 STUDIES TOWARD PHOTOSWITCHABLE mGLUR6 AGONISTS AS A POTENTIAL APPROACH TO VISION RESTORATION



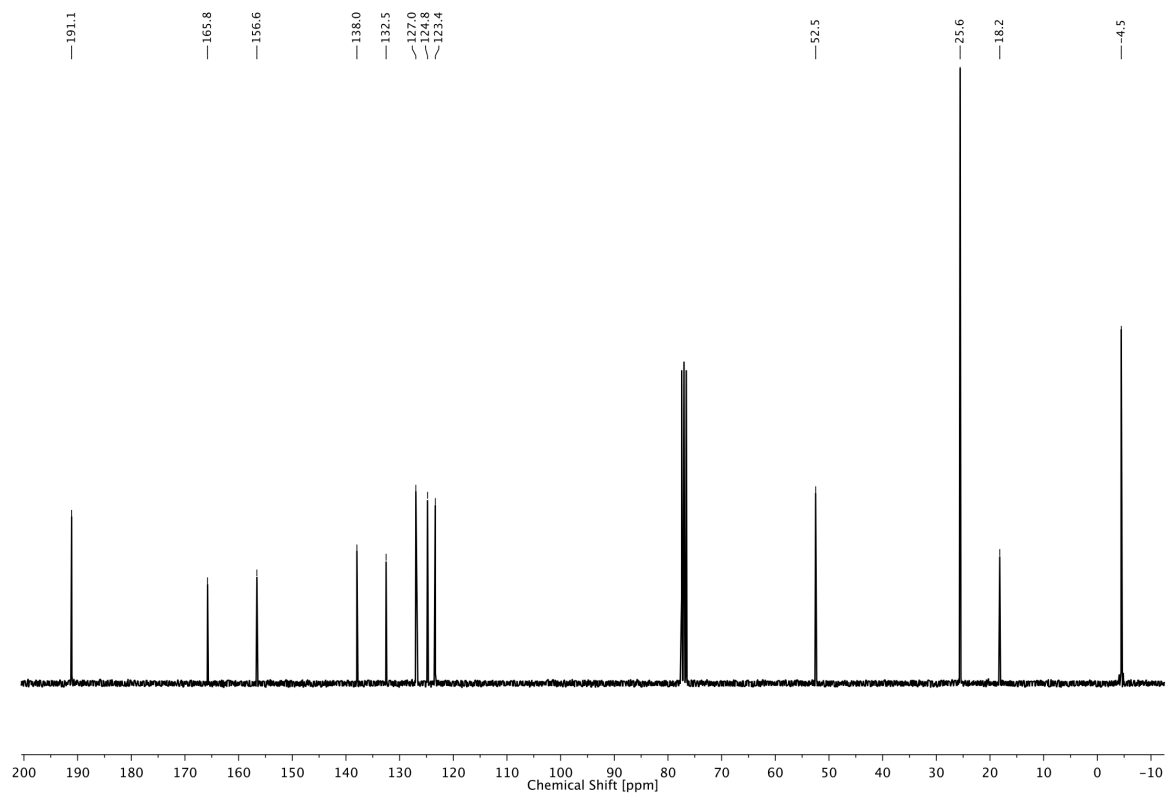
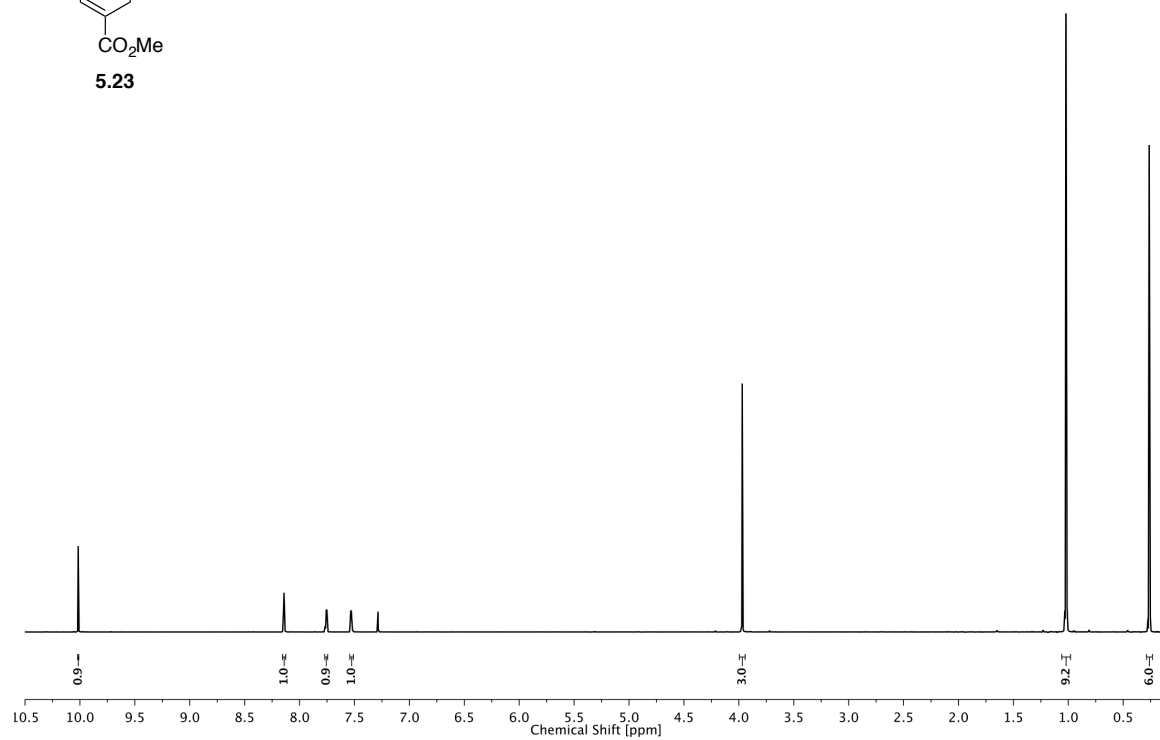
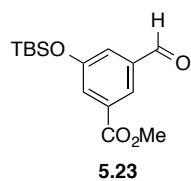
5.21



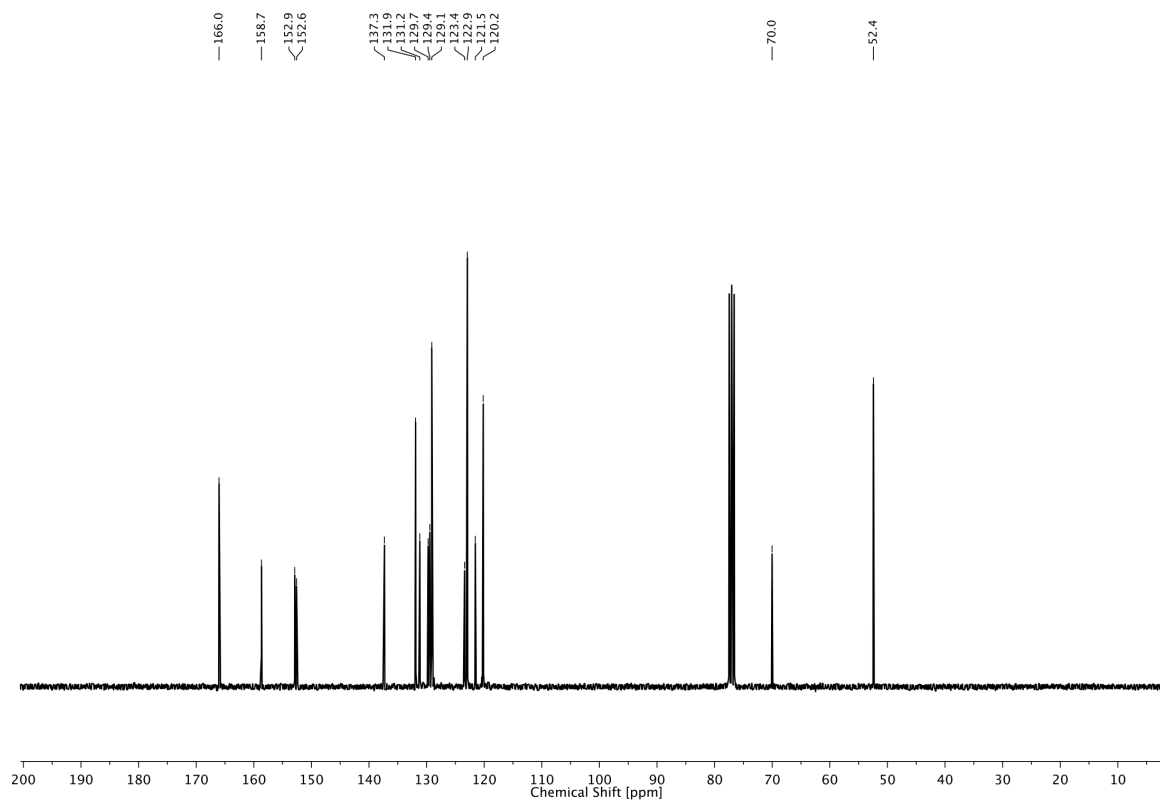
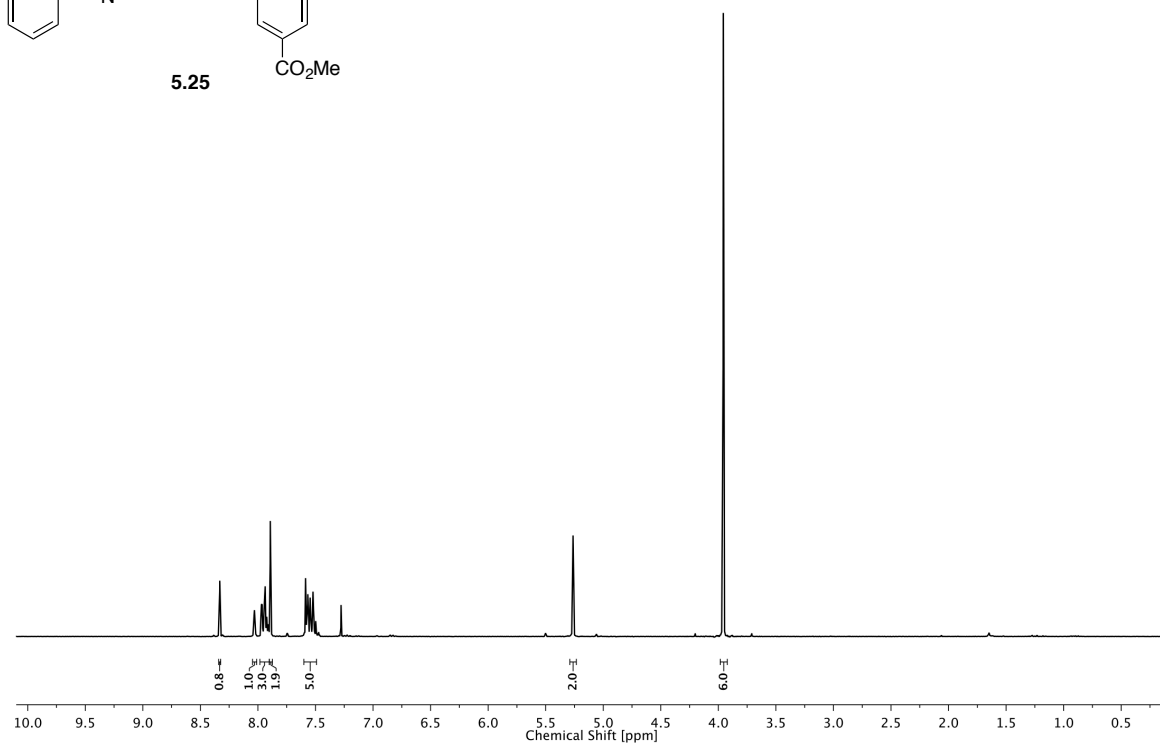
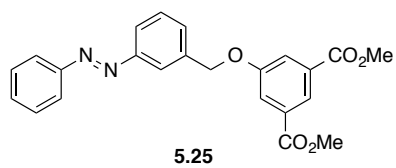
5 STUDIES TOWARD PHOTOSWITCHABLE mGLUR6 AGONISTS AS A POTENTIAL APPROACH TO VISION RESTORATION



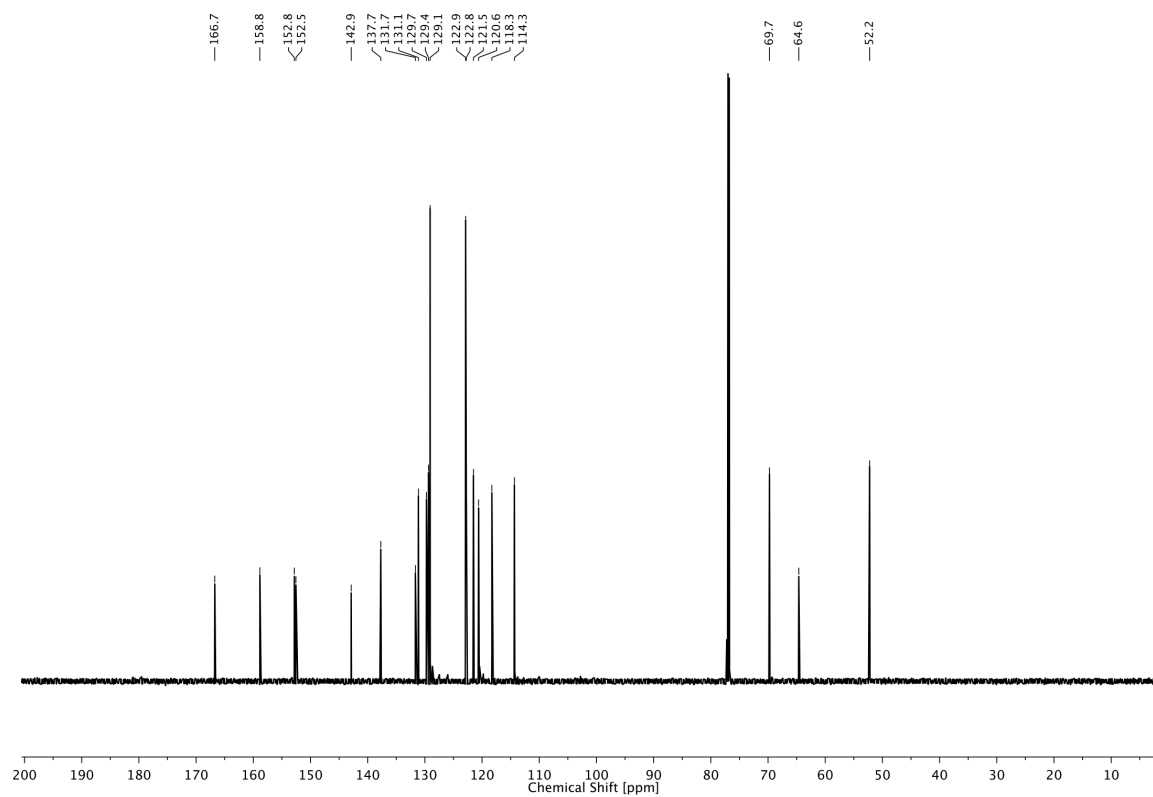
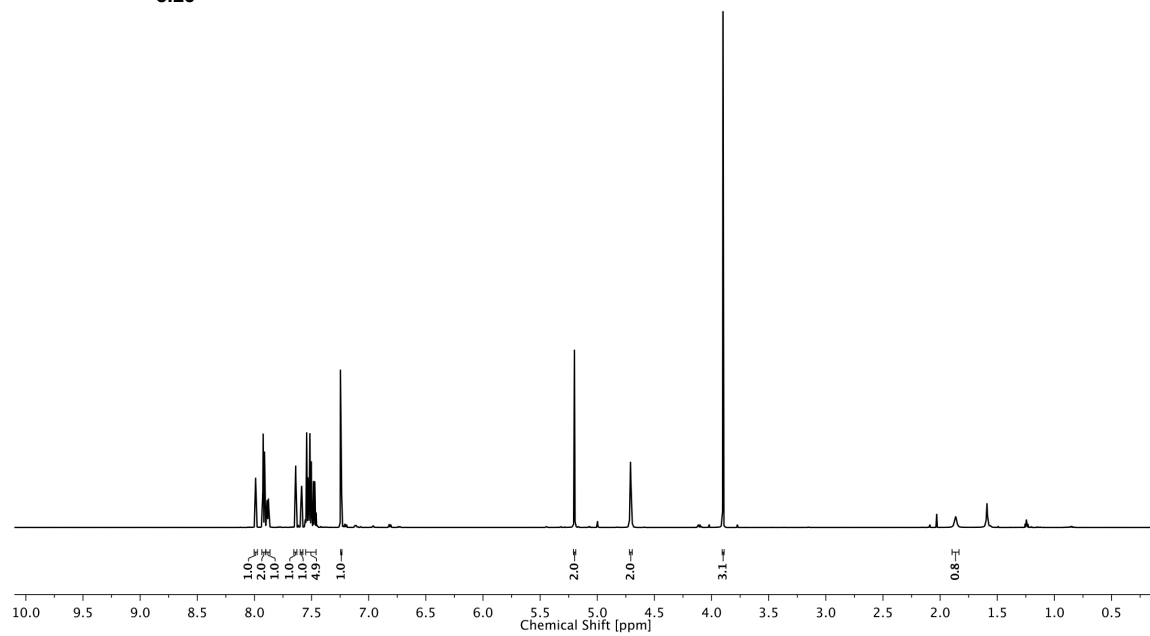
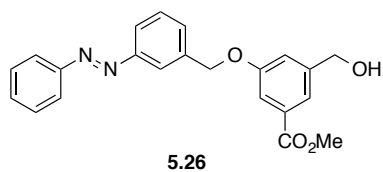
5 STUDIES TOWARD PHOTOSWITCHABLE mGLUR6 AGONISTS AS A POTENTIAL APPROACH TO VISION RESTORATION



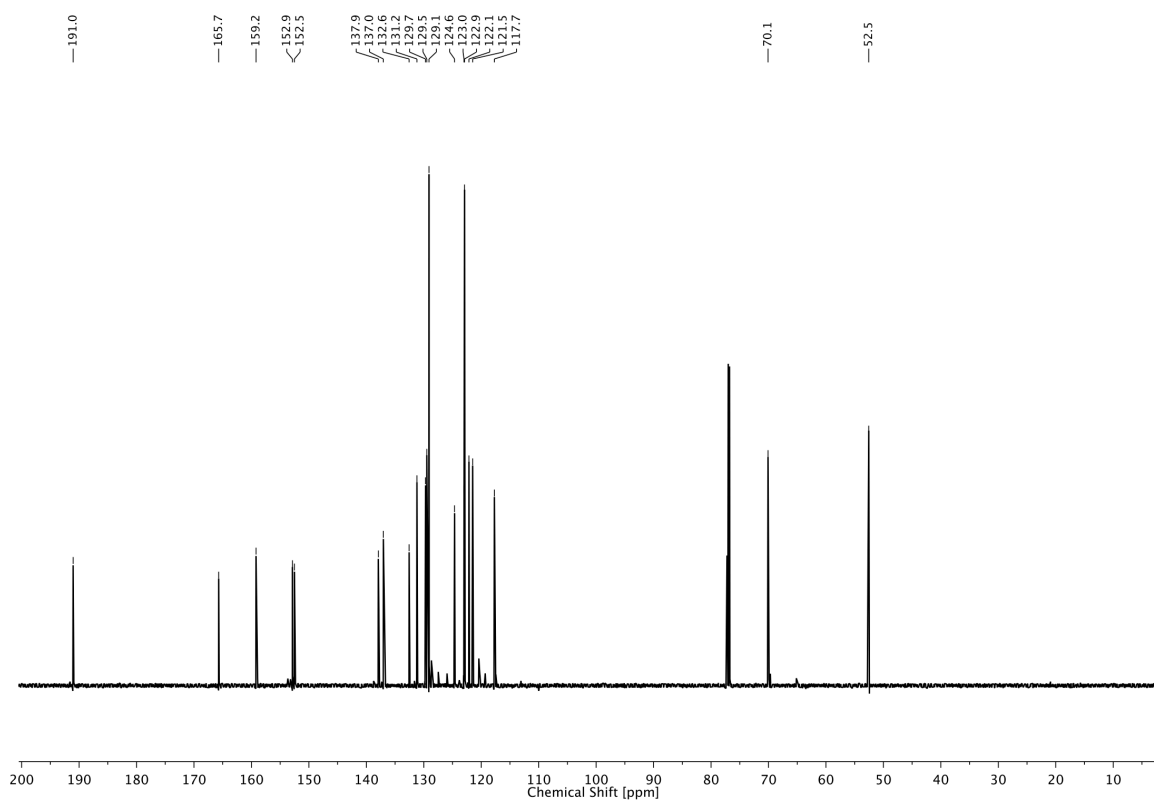
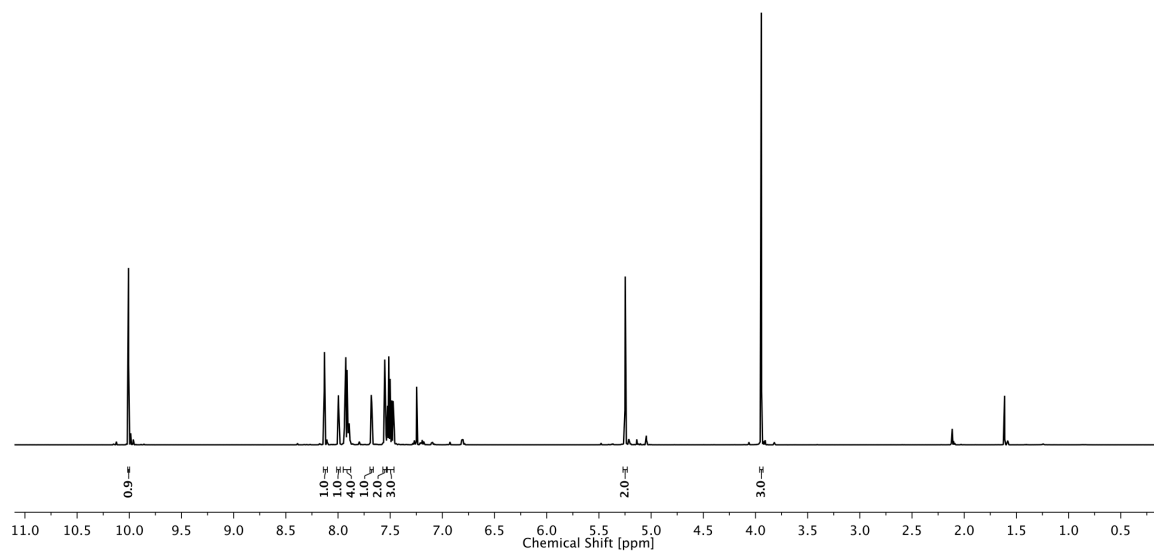
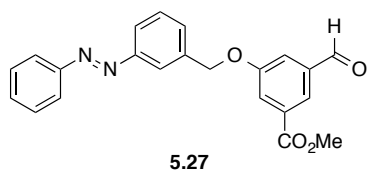
5 STUDIES TOWARD PHOTOSWITCHABLE mGLUR6 AGONISTS AS A POTENTIAL APPROACH TO VISION RESTORATION



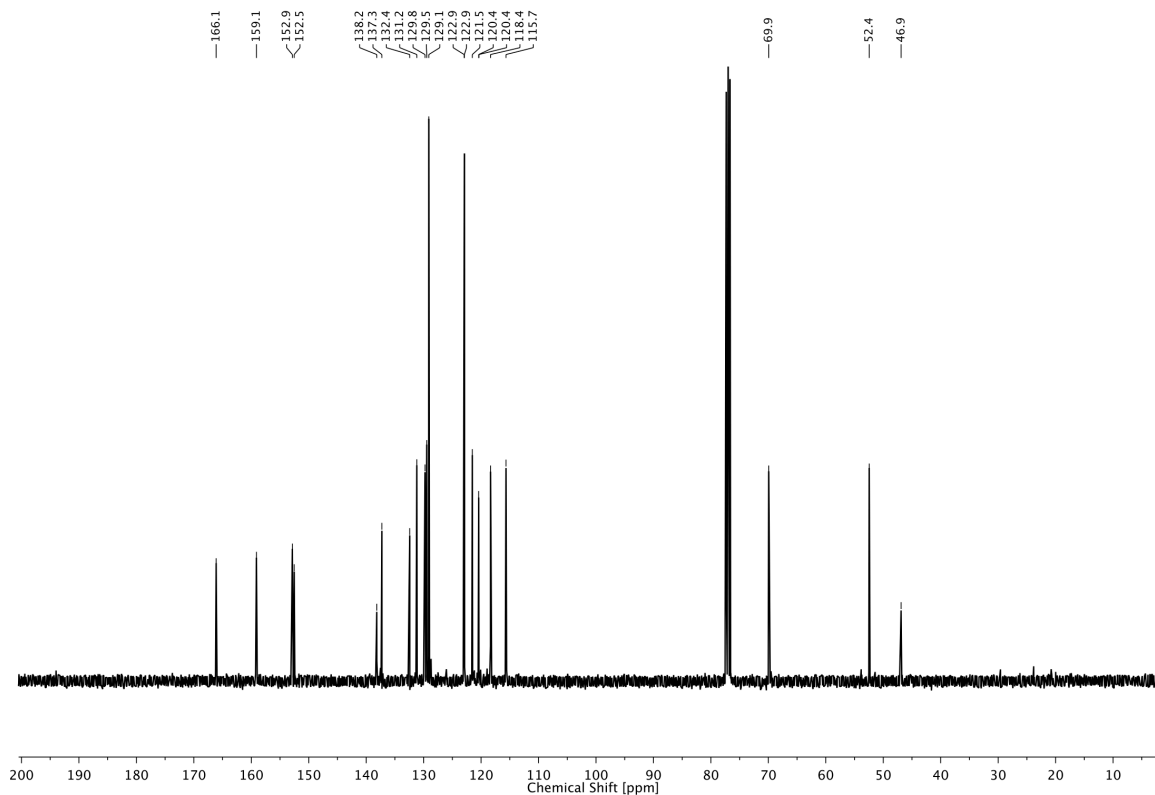
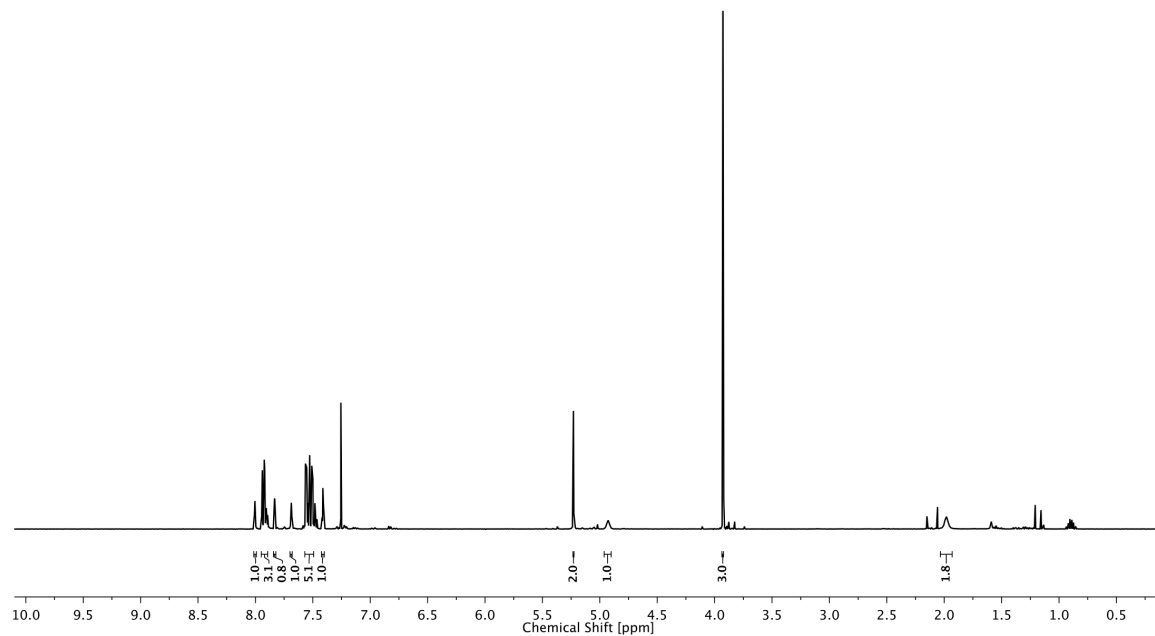
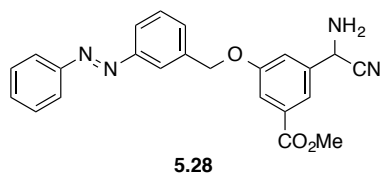
5 STUDIES TOWARD PHOTOSWITCHABLE mGLUR6 AGONISTS AS A POTENTIAL APPROACH TO VISION RESTORATION



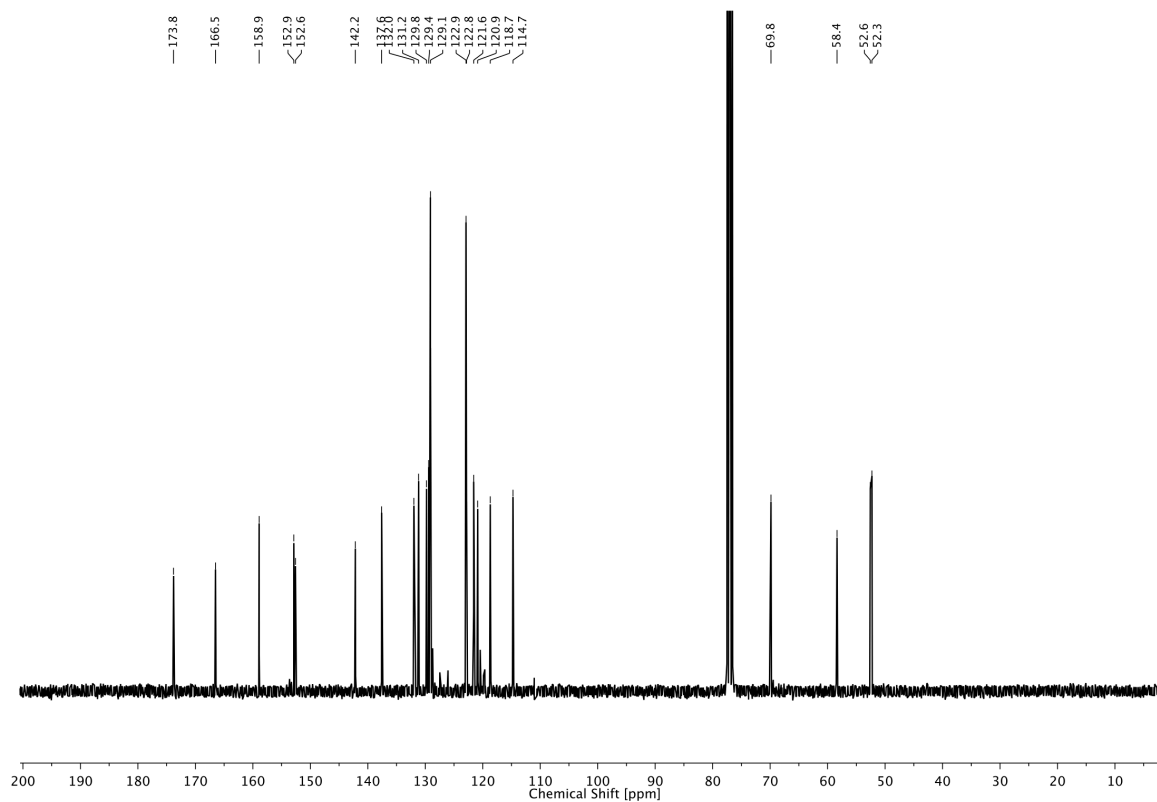
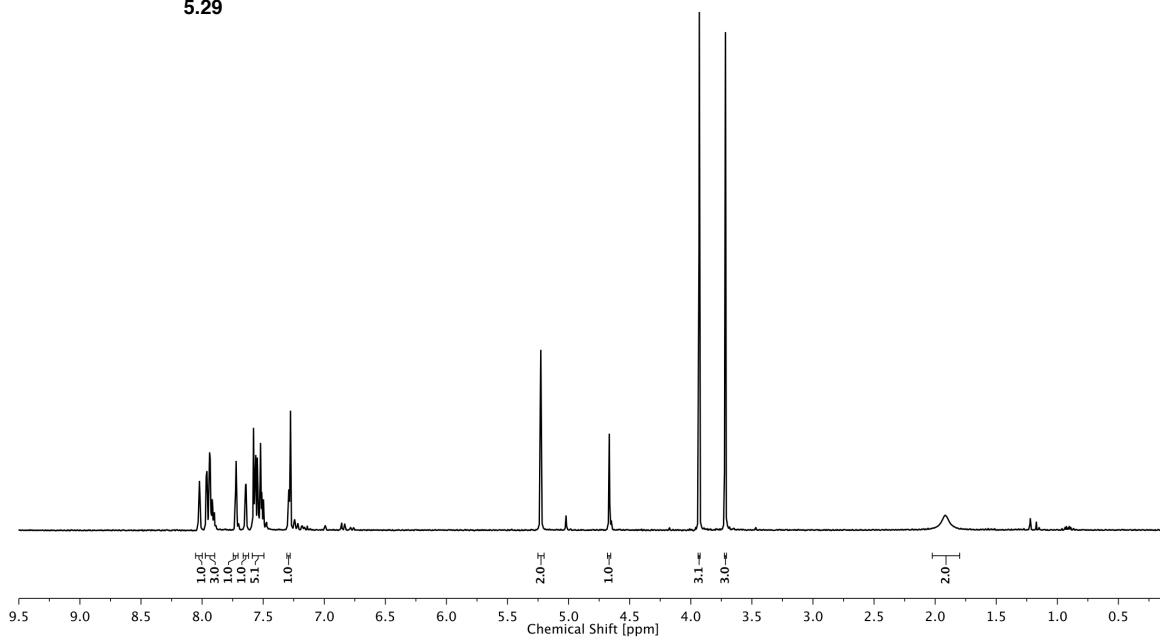
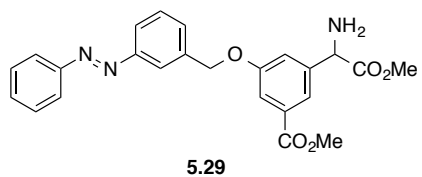
5 STUDIES TOWARD PHOTOSWITCHABLE mGLUR6 AGONISTS AS A POTENTIAL APPROACH TO VISION RESTORATION



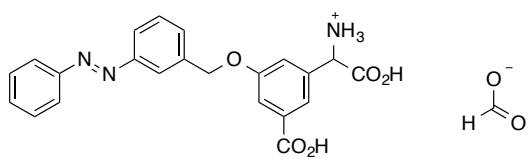
5 STUDIES TOWARD PHOTOSWITCHABLE mGLUR6 AGONISTS AS A POTENTIAL APPROACH TO VISION RESTORATION



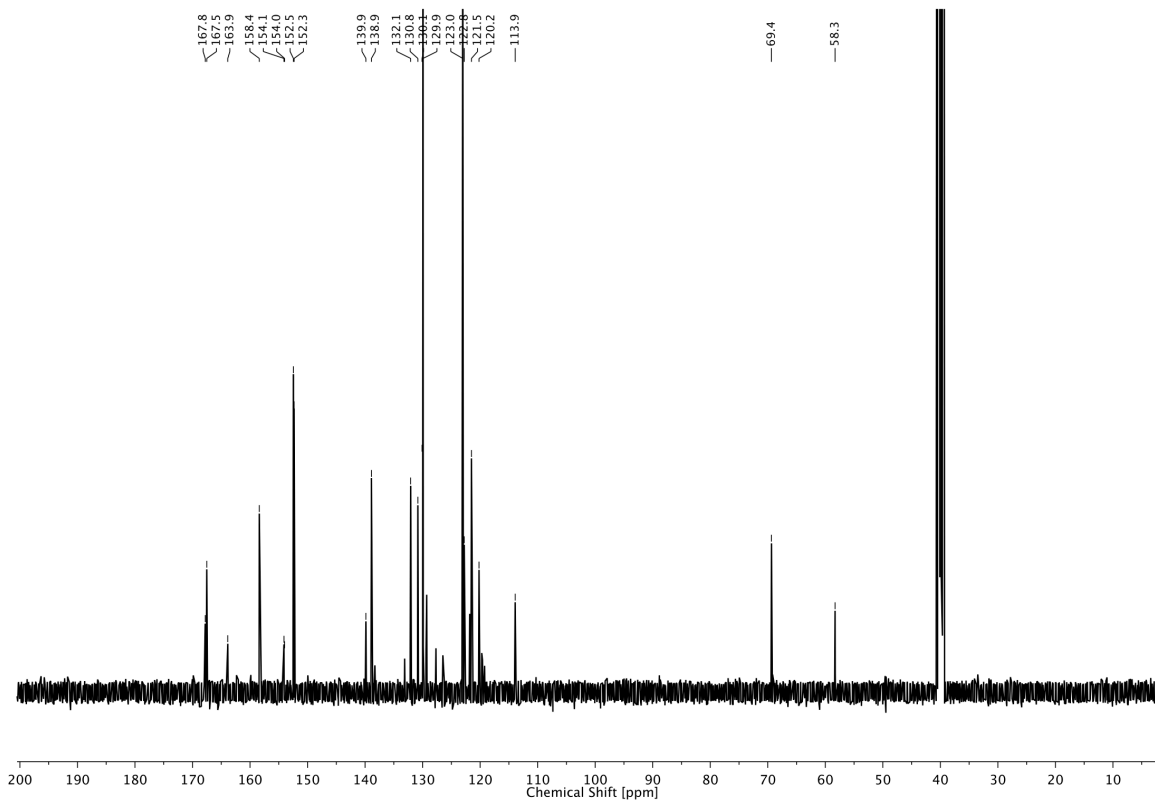
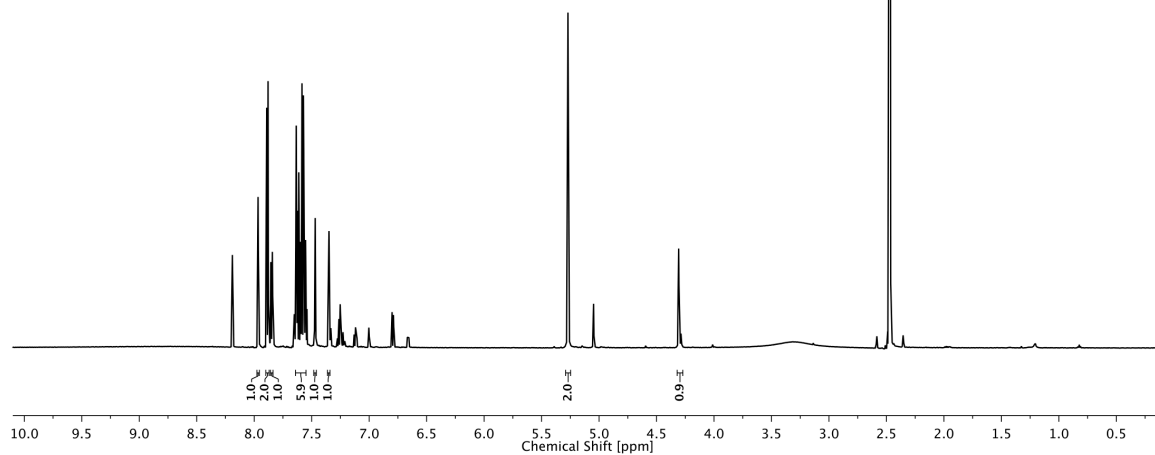
5 STUDIES TOWARD PHOTOSWITCHABLE mGLUR6 AGONISTS AS A POTENTIAL APPROACH TO VISION RESTORATION



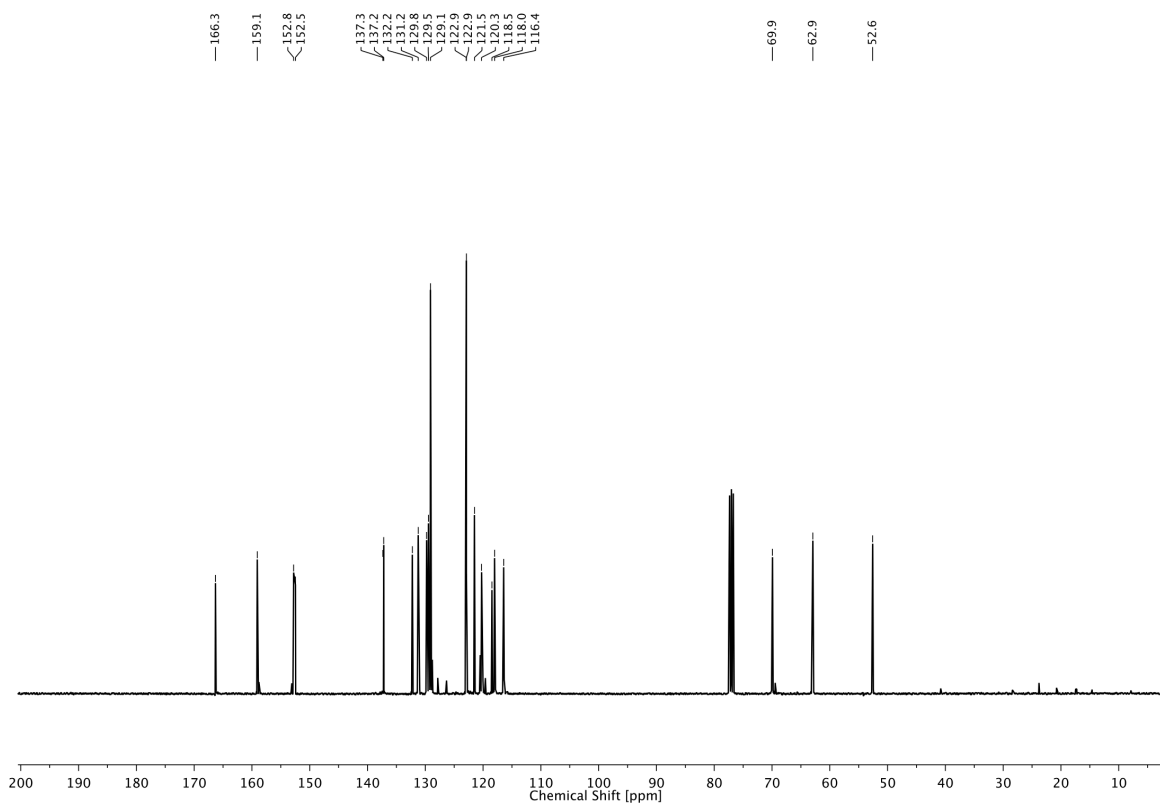
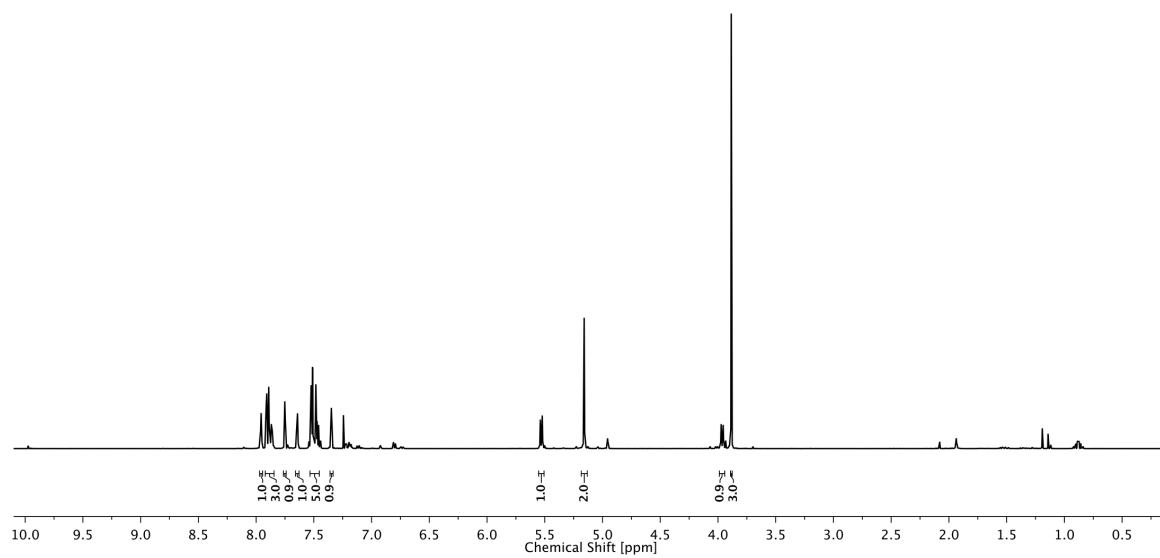
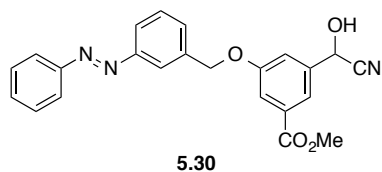
5 STUDIES TOWARD PHOTOSWITCHABLE mGLUR6 AGONISTS AS A POTENTIAL APPROACH TO VISION RESTORATION



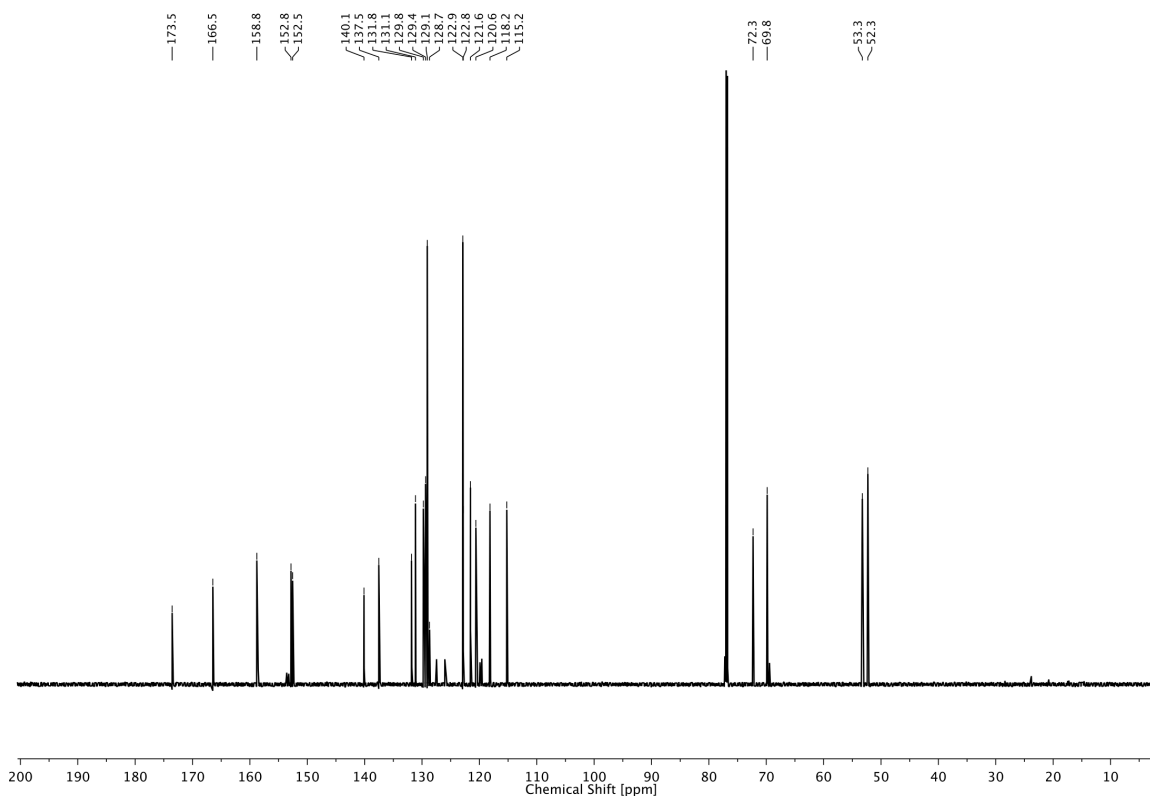
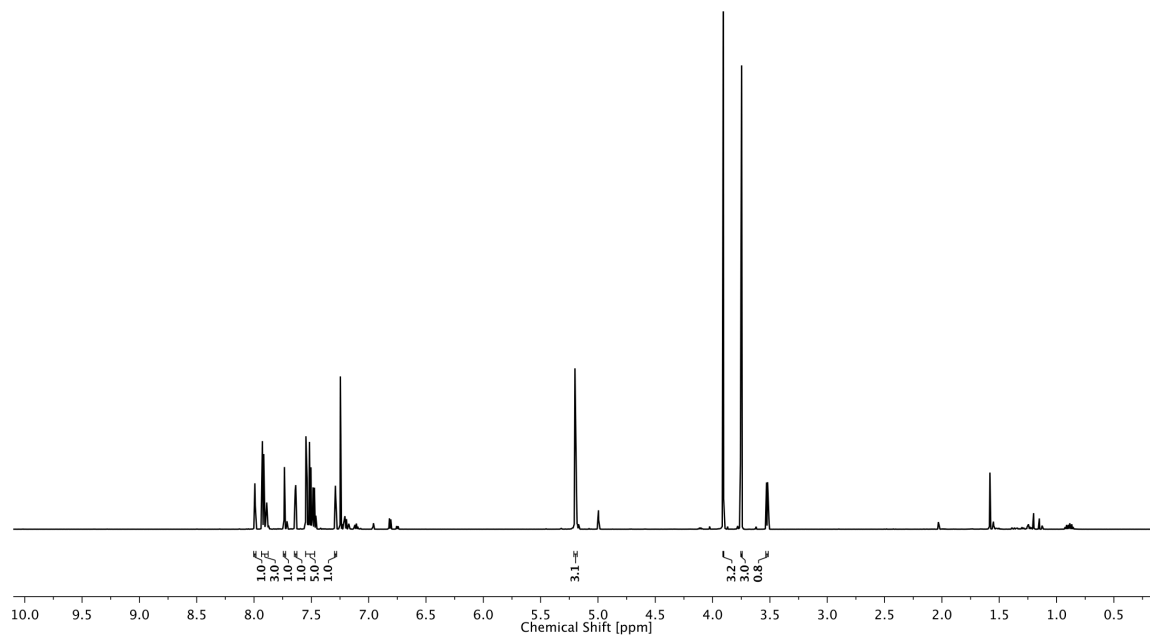
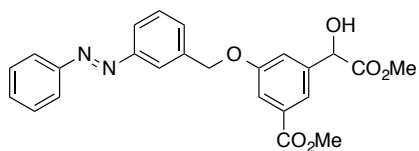
m-Azo-3C5HPG



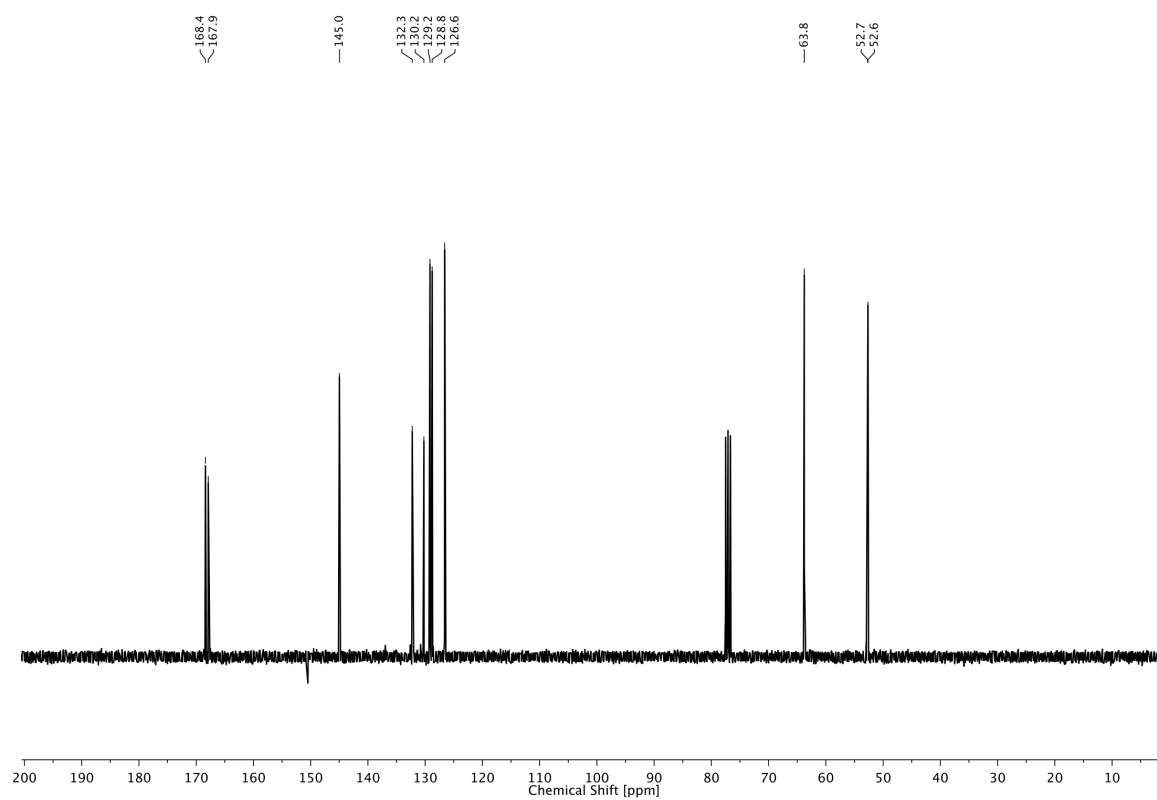
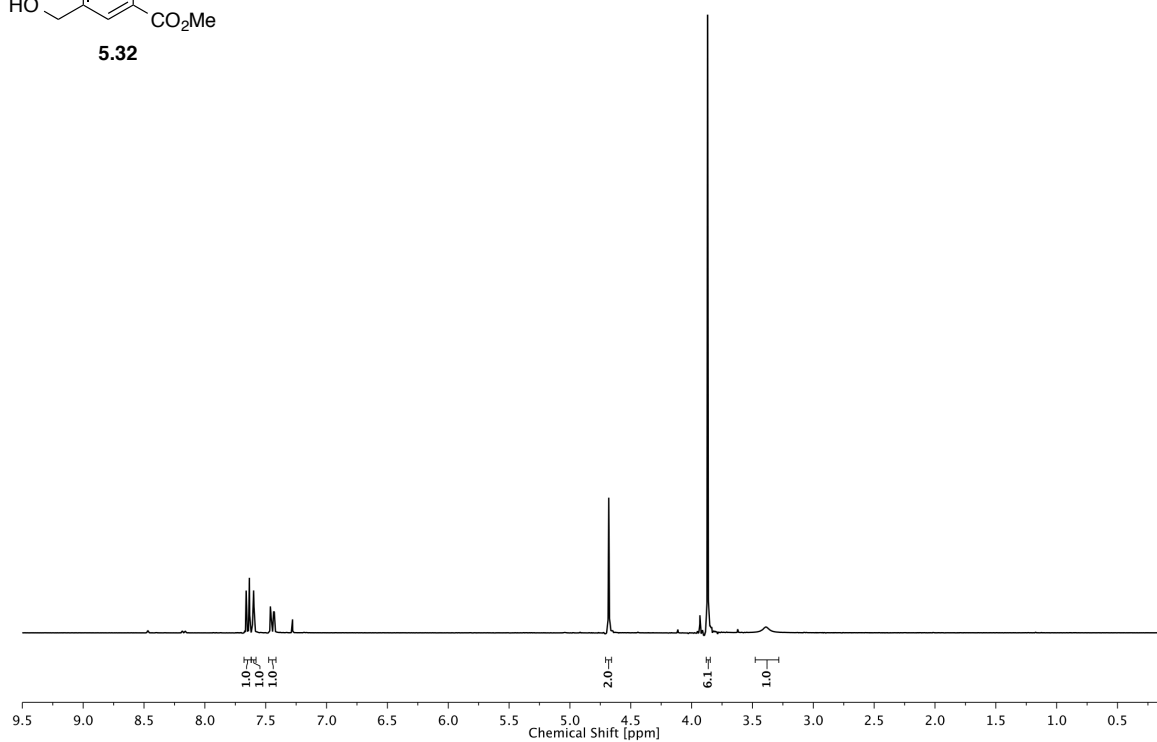
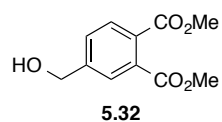
5 STUDIES TOWARD PHOTOSWITCHABLE mGLUR6 AGONISTS AS A POTENTIAL APPROACH TO VISION RESTORATION



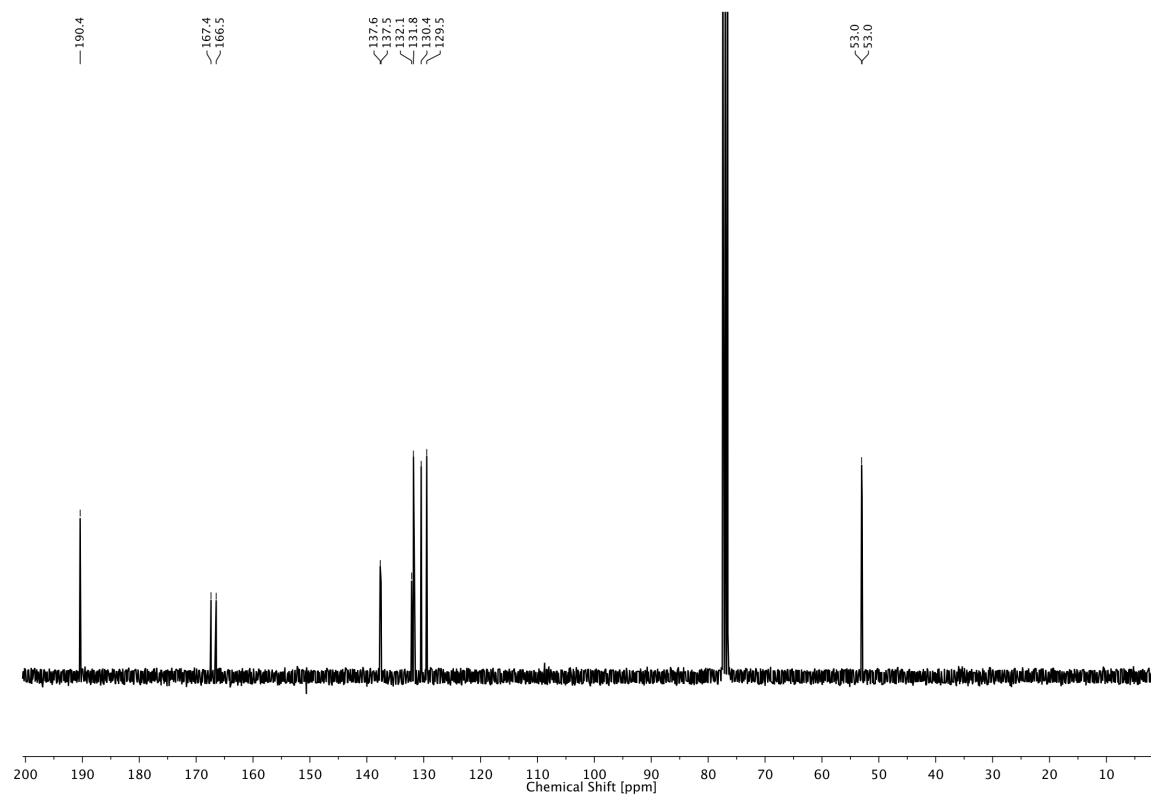
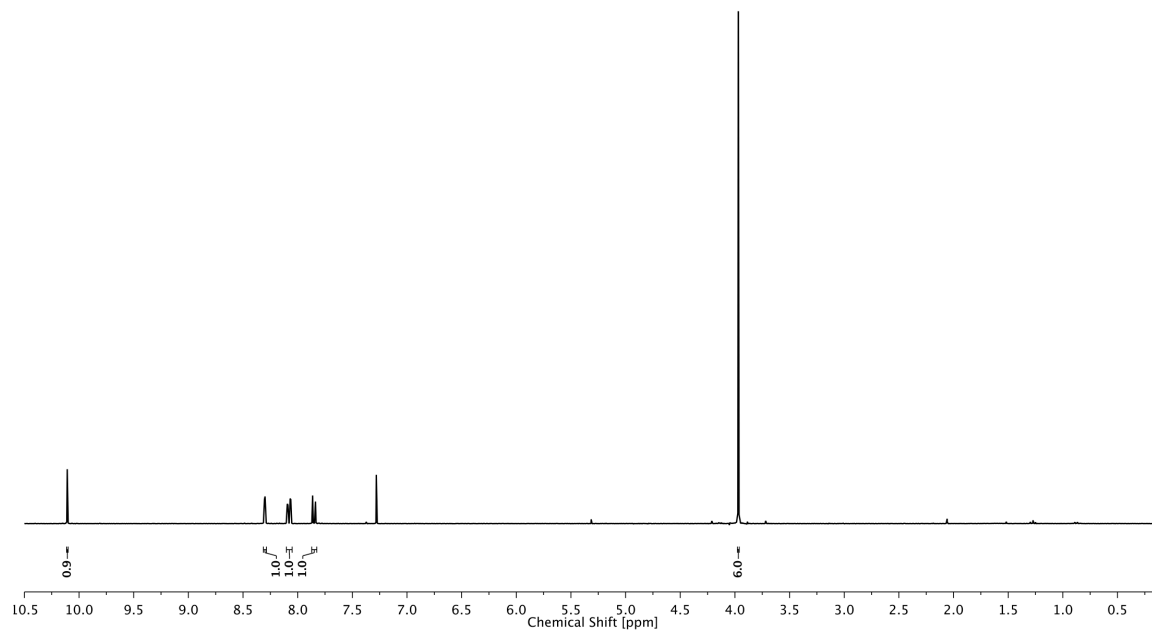
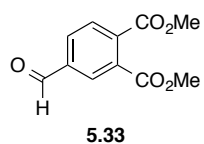
5 STUDIES TOWARD PHOTOSWITCHABLE mGLUR6 AGONISTS AS A POTENTIAL APPROACH TO VISION RESTORATION



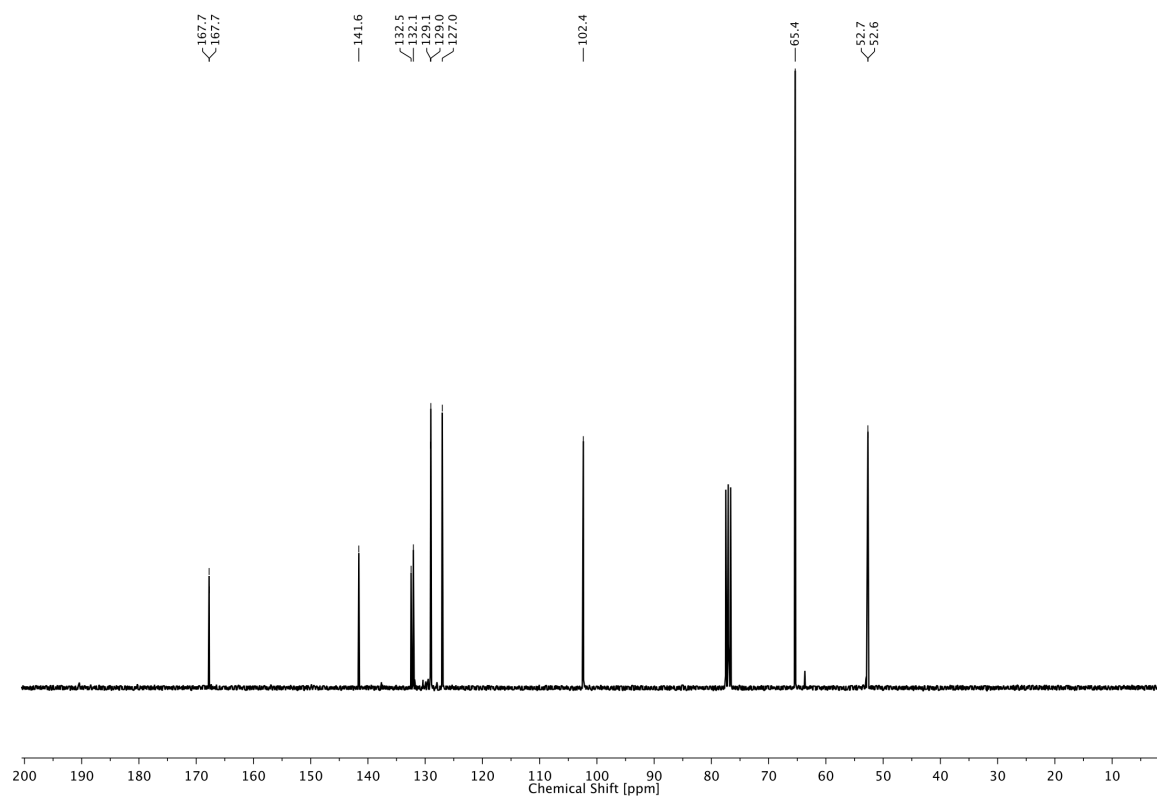
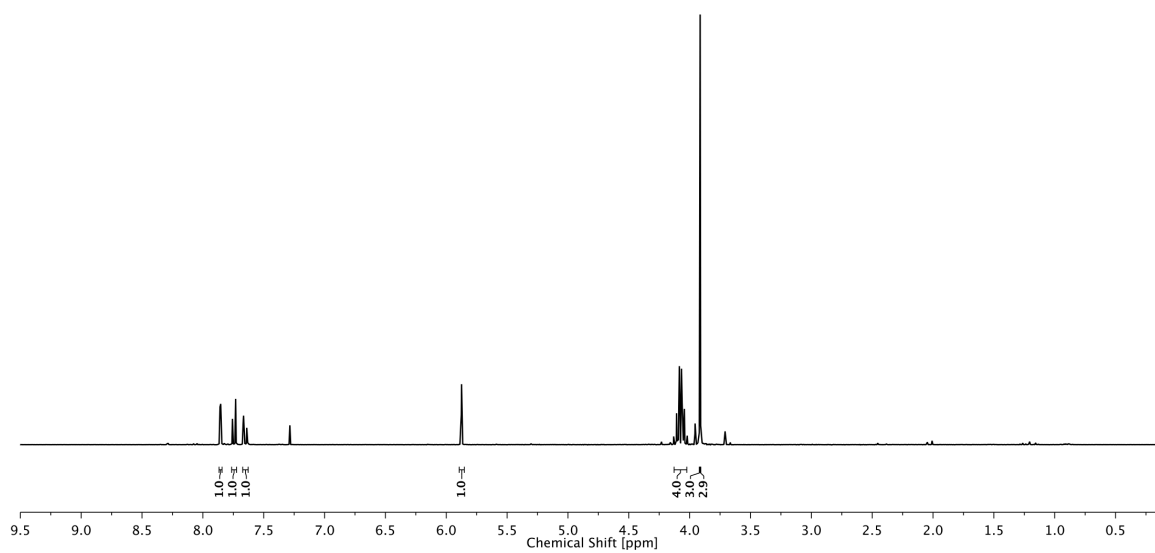
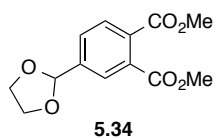
5 STUDIES TOWARD PHOTOSWITCHABLE mGLUR6 AGONISTS AS A POTENTIAL APPROACH TO VISION RESTORATION



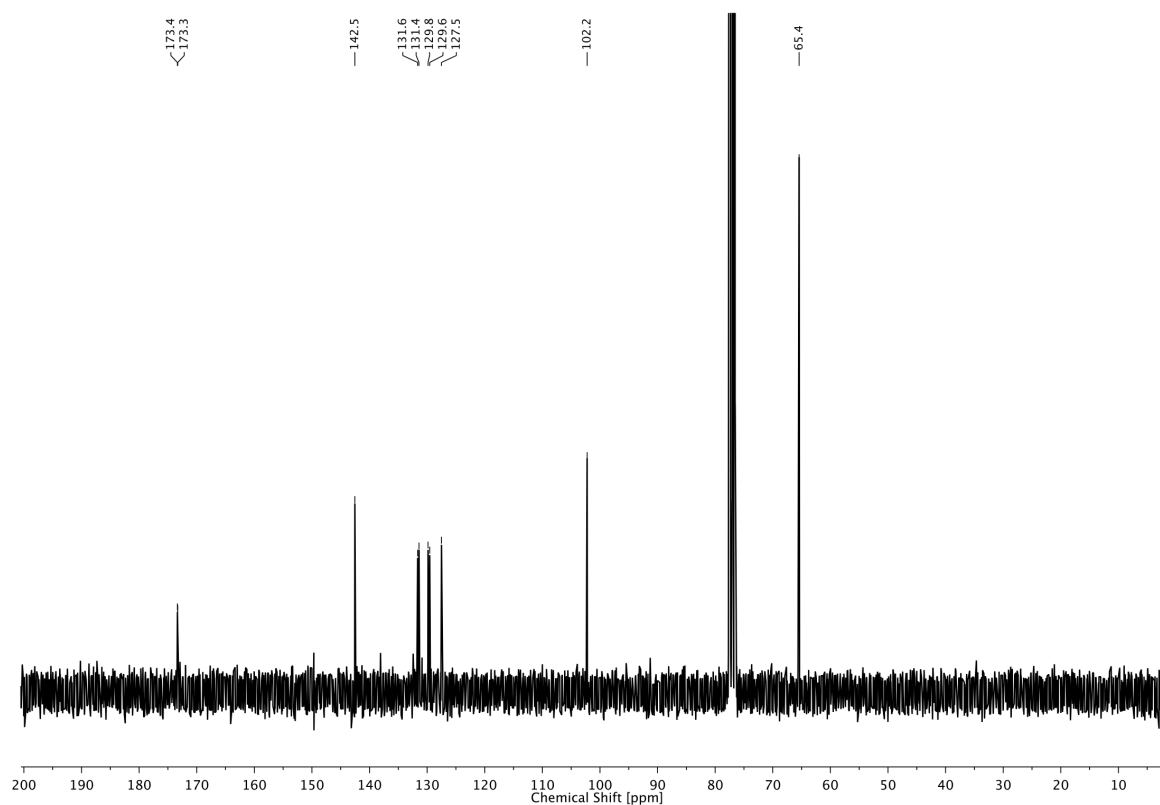
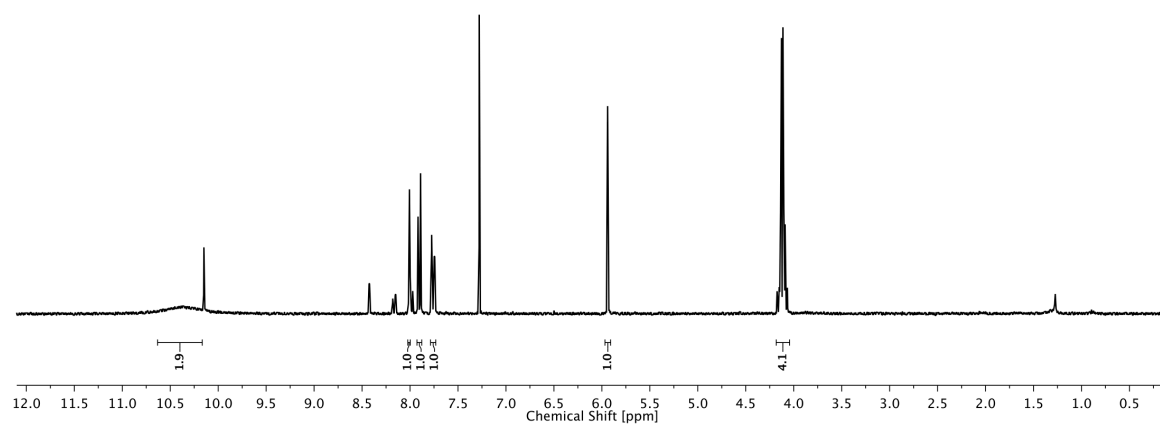
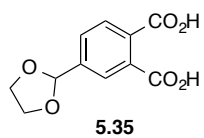
5 STUDIES TOWARD PHOTOSWITCHABLE mGLUR6 AGONISTS AS A POTENTIAL APPROACH TO VISION RESTORATION



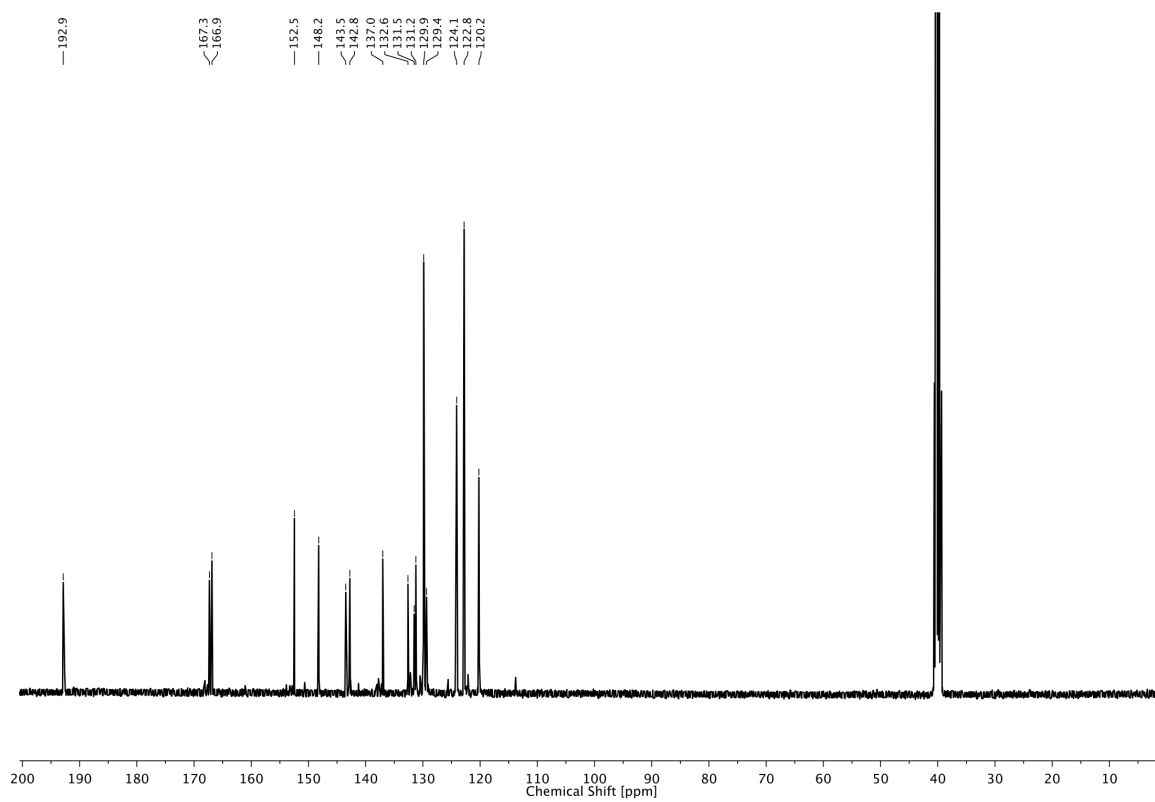
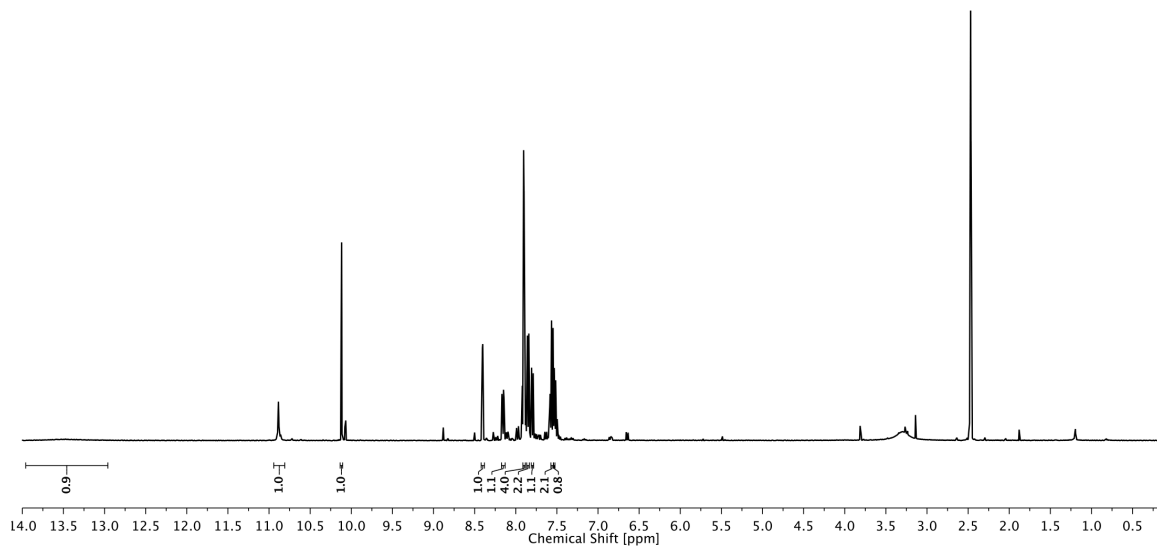
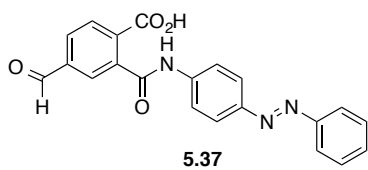
5 STUDIES TOWARD PHOTOSWITCHABLE mGLUR6 AGONISTS AS A POTENTIAL APPROACH TO VISION RESTORATION



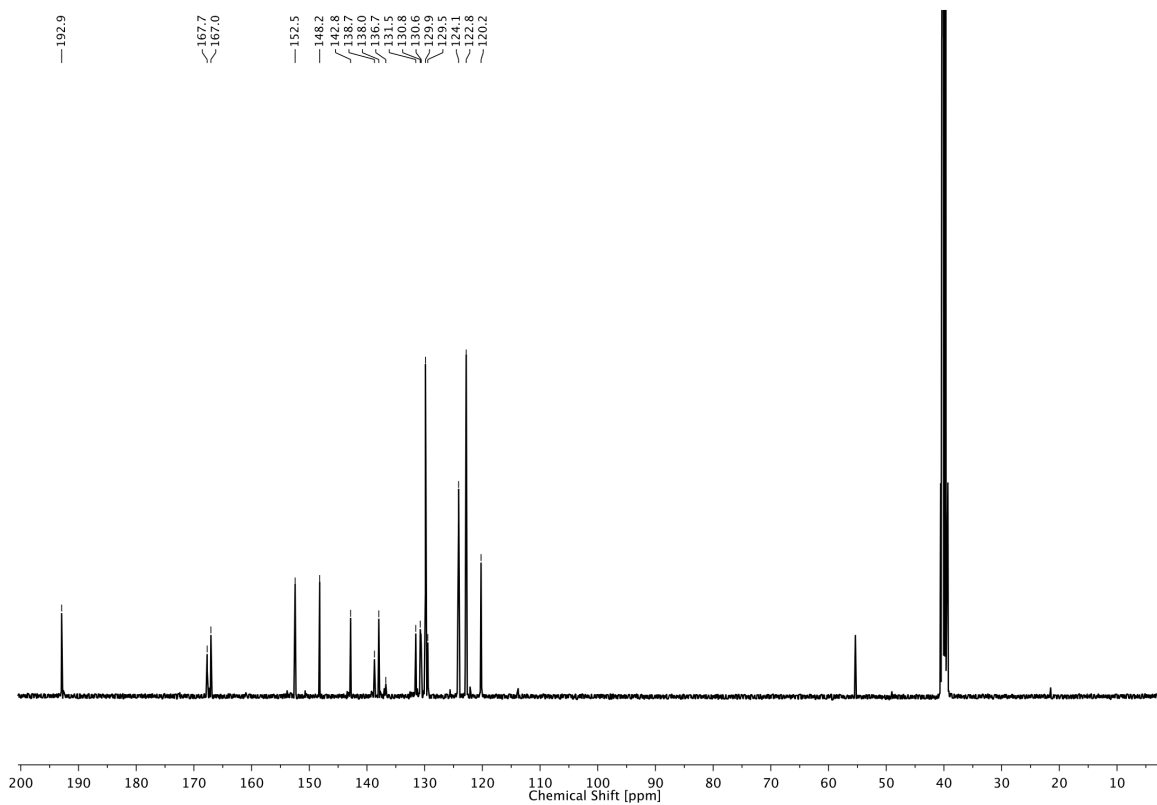
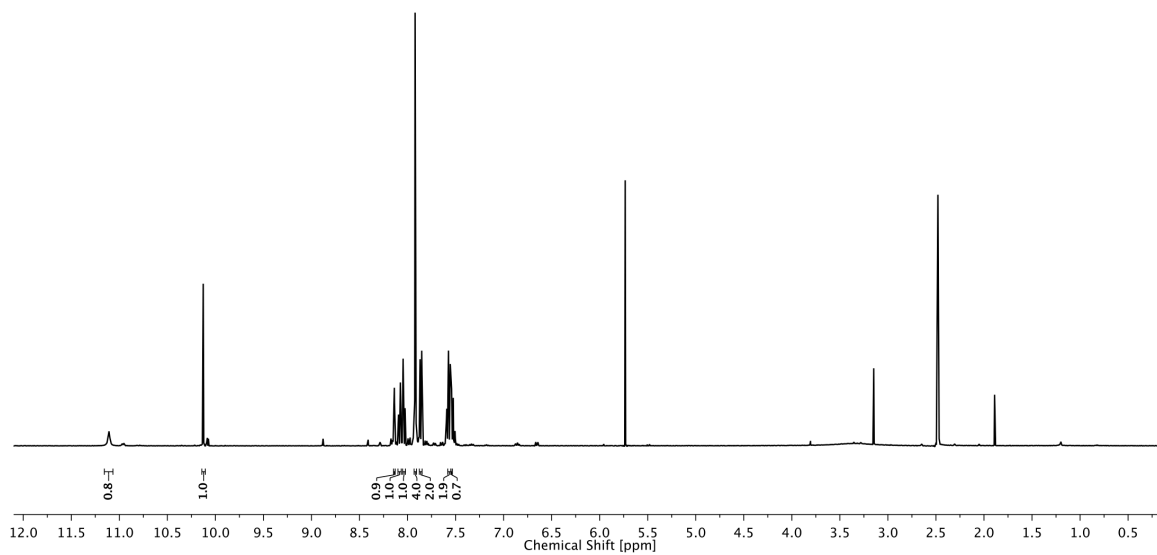
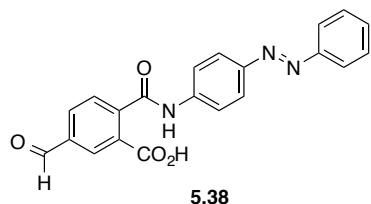
5 STUDIES TOWARD PHOTOSWITCHABLE mGLUR6 AGONISTS AS A POTENTIAL APPROACH TO VISION RESTORATION



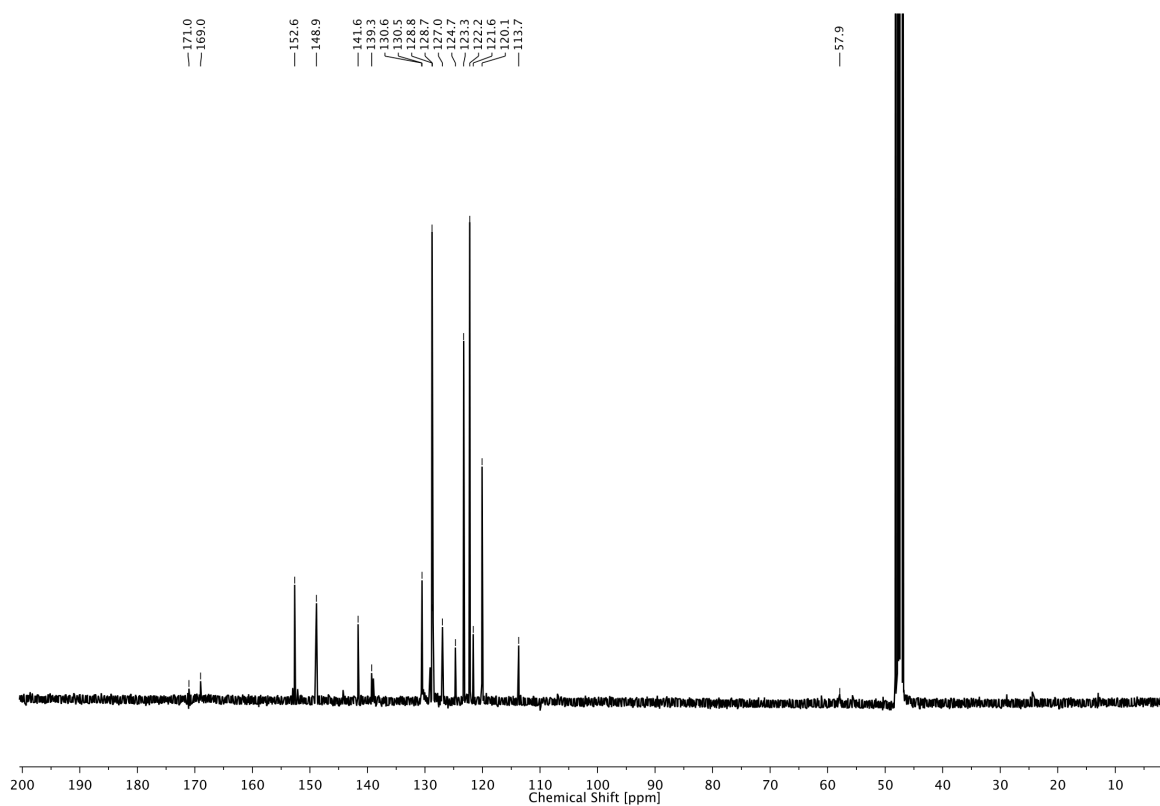
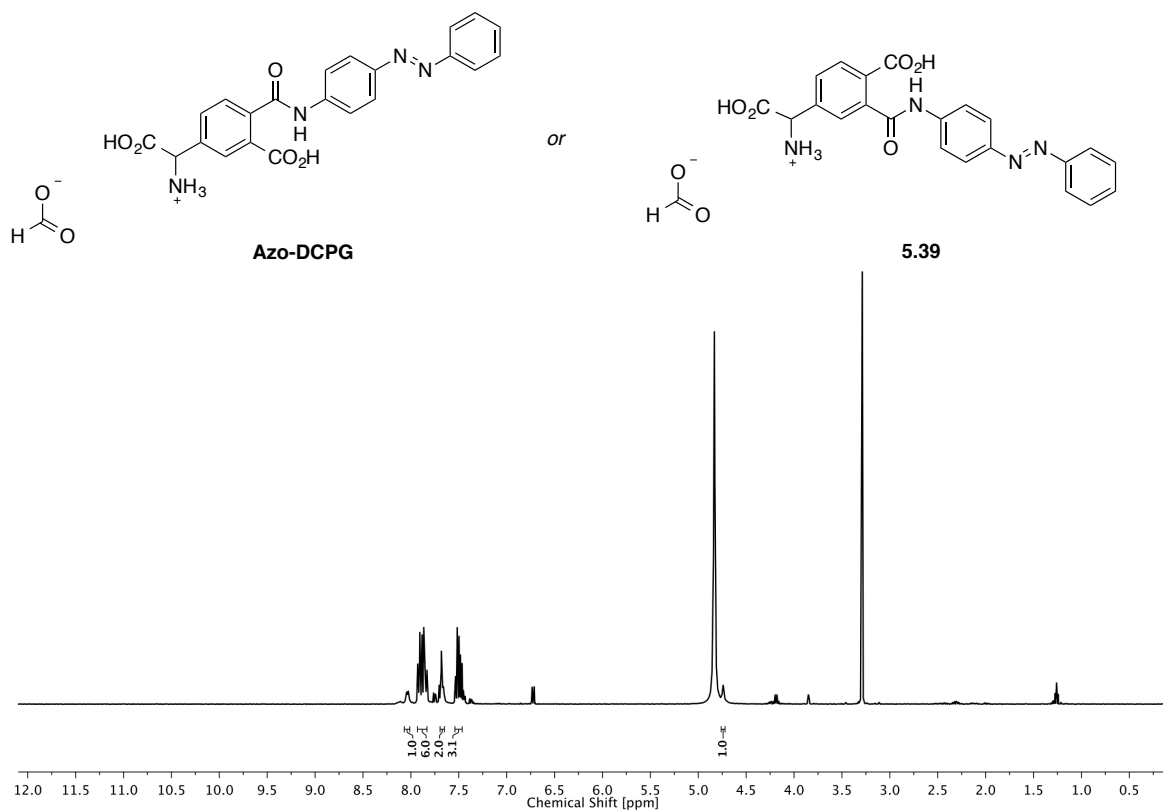
5 STUDIES TOWARD PHOTOSWITCHABLE mGLUR6 AGONISTS AS A POTENTIAL APPROACH TO VISION RESTORATION



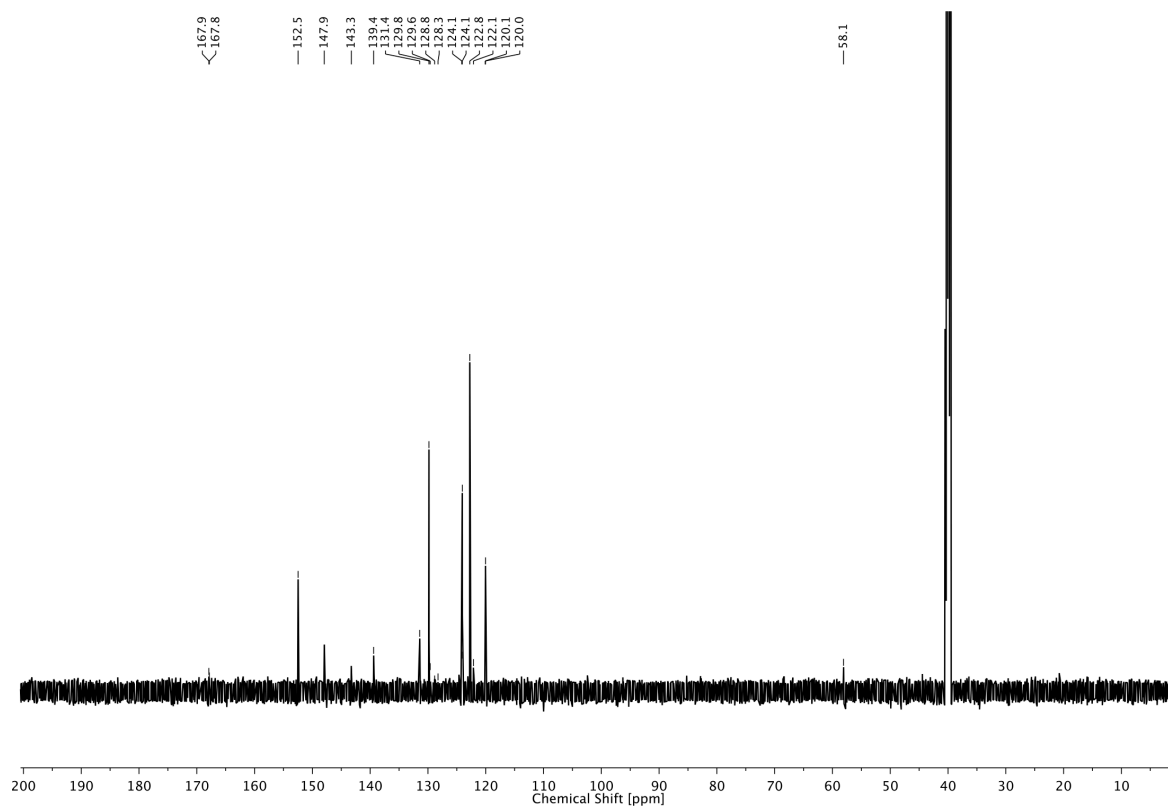
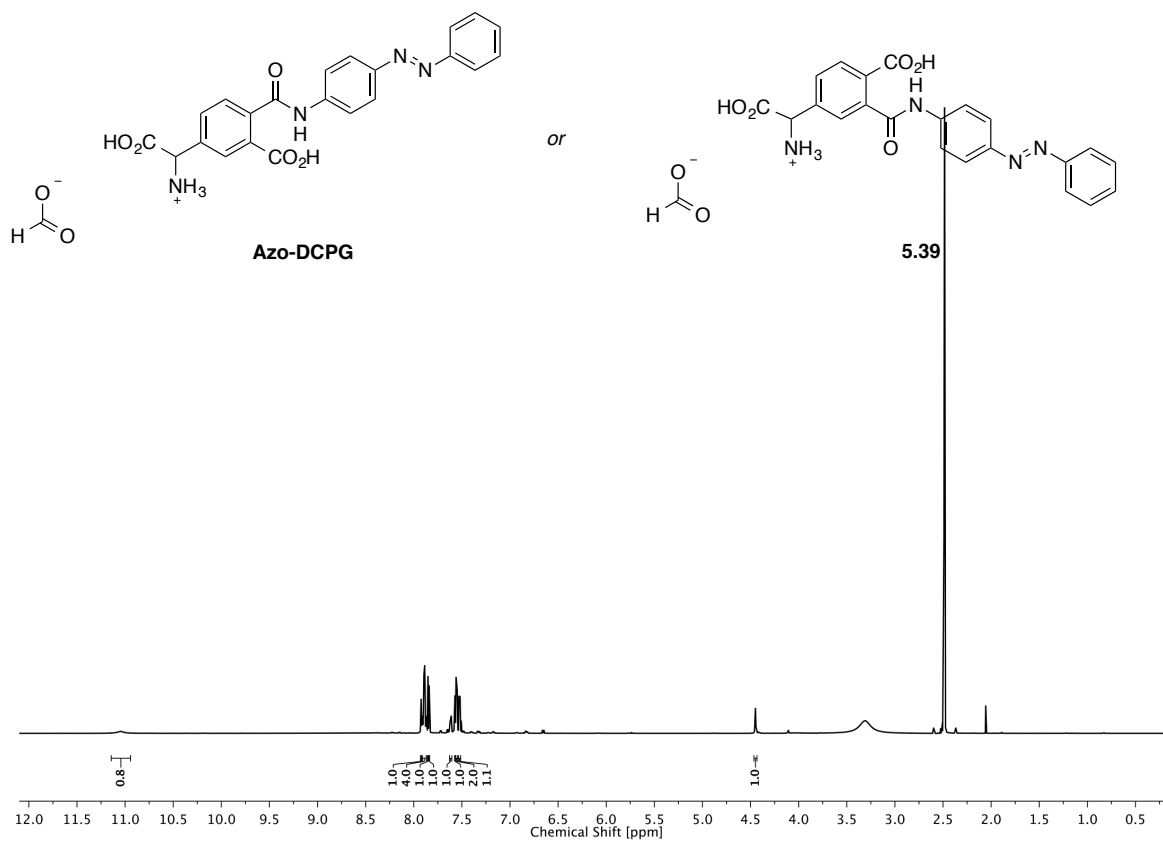
5 STUDIES TOWARD PHOTOSWITCHABLE mGLUR6 AGONISTS AS A POTENTIAL APPROACH TO VISION RESTORATION



5 STUDIES TOWARD PHOTOSWITCHABLE mGLUR6 AGONISTS AS A POTENTIAL APPROACH TO VISION RESTORATION



5 STUDIES TOWARD PHOTOSWITCHABLE mGLUR6 AGONISTS AS A POTENTIAL APPROACH TO VISION RESTORATION



5.7 LITERATURE

- [1] J.-P. Pin, F. Acher, *Curr. Drug Targets CNS Neurol. Disord.* **2002**, *1*, 297–317.
- [2] N. Kunishima, Y. Shimada, Y. Tsuji, T. Sato, M. Yamamoto, T. Kumasaka, S. Nakanishi, H. Jingami, K. Morikawa, *Nature* **2000**, *407*, 971–977.
- [3] H. Ahmadian, B. Nielsen, H. Bräuner-Osborne, T. N. Johansen, T. B. Stensbøl, F. A. Sløk, N. Sekiyama, S. Nakanishi, P. Krogsgaard-Larsen, U. Madsen, *J. Med. Chem.* **1997**, *40*, 3700–3705.
- [4] Y.-Y. Huang, M. F. Haug, M. Gesemann, S. C. F. Neuhauss, *PLoS ONE* **2012**, *7*, e35256.
- [5] S. Nakanishi, Y. Nakajima, M. Masu, Y. Ueda, K. Nakahara, D. Watanabe, S. Yamaguchi, S. Kawabata, M. Okada, *Brain Res. Rev.* **1998**, *26*, 230–235.
- [6] a) M. E. Burns, D. A. Baylor, *Annu. Rev. Neurosci.* **2001**, *24*, 779–805; b) G. L. Fain, H. R. Matthews, M. C. Cornwall, Y. Koutalos, *Physiol. Rev.* **2001**, *81*, 117–151; c) V. Y. Arshavsky, M. E. Burns, *J. Biol. Chem.* **2012**, *287*, 1620–1626; d) K. Palczewski, *J. Biol. Chem.* **2012**, *287*, 1612–1619.
- [7] W. Tückmantel, A. P. Kozikowski, S. Wang, S. Pshenichkin, J. T. Wroblewski, *Bioorg. Med. Chem. Lett.* **1997**, *7*, 601–606.
- [8] a) N. K. Thomas, R. A. Wright, P. A. Howson, A. E. Kingston, D. D. Schoepp, D.E. Jane, *Neuropharmacology* **2001**, *40*, 311–318; b) N. Sekiyama, Y. Hayashi, S. Nakanishi, D. E. Jane, H.-W. Tse, E. F. Birse, J. C. Watkins, *Br. J. Pharmacol.* **1996**, *117*, 1493–1503.
- [9] D. J. Laurie, P. Schoeffter, K. H. Wiederhold, B. Sommer, *Neuropharmacology* **1997**, *36*, 145–152.
- [10] H. Bräuner-Osborne, F. A. Sløk, N. Skjærbæk, B. Ebert, N. Sekiyama, S. Nakanishi, P. A. Krogsgaard-Larsen, *J. Med. Chem.* **1996**, *39*, 3188–3194.
- [11] T. Honore J. Lauridsen, P. Krogsgaard-Larsen, *J. Neurochem.* **1982**, *38*, 173–178.
- [12] It was found that *O*-alkylated AMPA derivatives were still active as agonists on ionotropic glutamate receptors (unpublished results).
- [13] M. Marinozzi, M. Serpi, L. Amori, M. Gavilan Diaz, G. Constantino, U. Meyer, P. J. Flor, F. Gasparini, R. Heckendorn, R. Kuhn, G. Giorhi, M. B. Hermit, C. Thomsen, R. Pellicciari, *Bioorg. Med. Chem.* **2007**, *15*, 3161–3170.
- [14] F. C. Acher, F. J. Tellier, R. Azerad, I. N. Brabet, L. Fagni, J.-P. Pin, *J. Med. Chem.* **1997**, *40*, 3119–3129.
- [15] K.-I. Tanaka, H. Sawanishi, *Tetrahedron Asym.* **1995**, *6*, 1641–1656.

- [16] J.-M. Bernardon, T. Biadatti (Galderma Research & Development, S.N.C.), US
6,831,106 B1, **2004**.
- [17] W. C. Still, M. Kahn, A. Mitra, *J. Org. Chem.* **1978**, *43*, 2923–2925.
- [18] H. E. Gottlieb, V. Kotlyar, A. Nudelman, *J. Org. Chem.* **1997**, *62*, 7512–7515.

6 MISCELLANEOUS PROJECTS

6.1 DEVELOPMENT OF AZO-SEN12333, A PCL FOR NICOTINIC ACETYLCHOLINE RECEPTORS

Alpha 7 nicotinic acetylcholine receptors ($\alpha 7$ nAChRs) are implicated in the modulation of many cognitive functions, such as attention, working memory and episodic memory. For this reason, $\alpha 7$ nAChR agonists are promising therapeutic candidates for the treatment of cognitive impairment associated with a variety of disorders including Alzheimer's disease and schizophrenia.^[1]

In a recent study by Wyeth Research (now part of Pfizer) novel $\alpha 7$ nAChR agonists were developed.^[1] Among various candidates, SEN12333 was found to be a selective agonist of $\alpha 7$ nAChRs ($EC_{50} = 1.65 \mu\text{M}$) with excellent *in vitro* and *in vivo* profiles, excellent brain penetration and oral bioavailability. Moreover, it demonstrated *in vivo* efficacy in multiple behavioural cognition models.^[1] The authors add that most $\alpha 7$ agonists are based on quinuclidine scaffolds which recently had often failed clinical trials due to toxicological reasons.^[1,2] Therefore, the $\alpha 7$ agonists developed by the authors based on a different class of compounds could avoid toxicity issues of quinuclidines.

The extensive SAR studies^[1] and two even more recent follow-up studies by the same authors^[3,4] suggested a relatively high tolerance toward substitution of the phenylpyridine amide anchor for large biaromatic substituents. Consequently, a photoswitchable azobenzene derivative of SEN12333 was designed (Fig. 6.1).

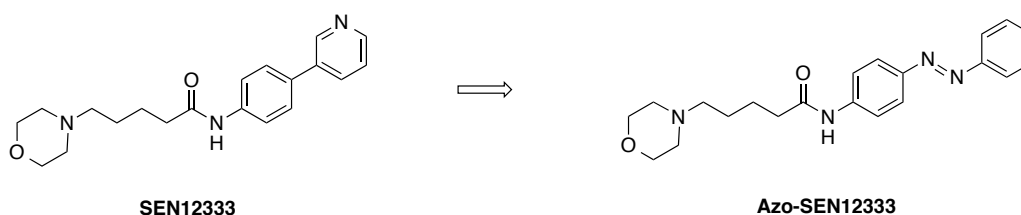
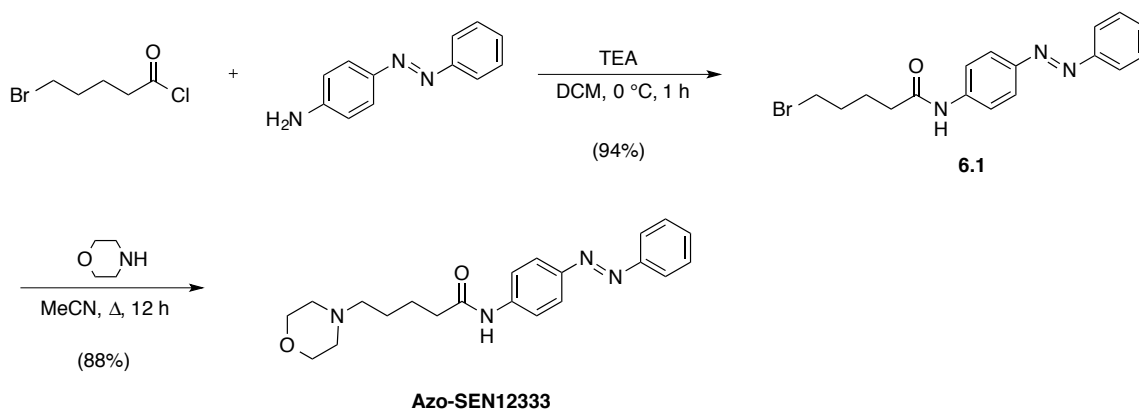


Figure 6.1. Structures of SEN12333 and **Azo-SEN12333**.

Synthesis of Azo-SEN12333

The synthesis of **Azo-SEN12333** commenced with an amide coupling of 5-bromovaleryl chloride with 4-aminoazobenzene to give amide **6.1** in 94% yield. Compound **6.1** was reacted with morpholine to furnish **Azo-SEN12333** in 88% yield (Scheme 6.1).



Scheme 6.1. Synthesis of **Azo-SEN12333**.

Biological Evaluation of Azo-SEN12333

Azo-SEN12333 (among other compounds) was tested in a quick screening assay on *Lymnaea stagnalis* (Ls), *Aplysia californica* (Ac) and *Aplysia californica* Y55W (AcY55W) for their ability to reduce epibatidine binding (Epi, a high-affinity nAChR agonist) to $\alpha 7$ nAChR (Fig. 6.2; Prof. Palmer Taylor, Skaggs School of Pharmacy and Pharmaceutical Sciences, La Jolla). In this assay, **Azo-SEN12333** reduced Epi binding by 20-40%.

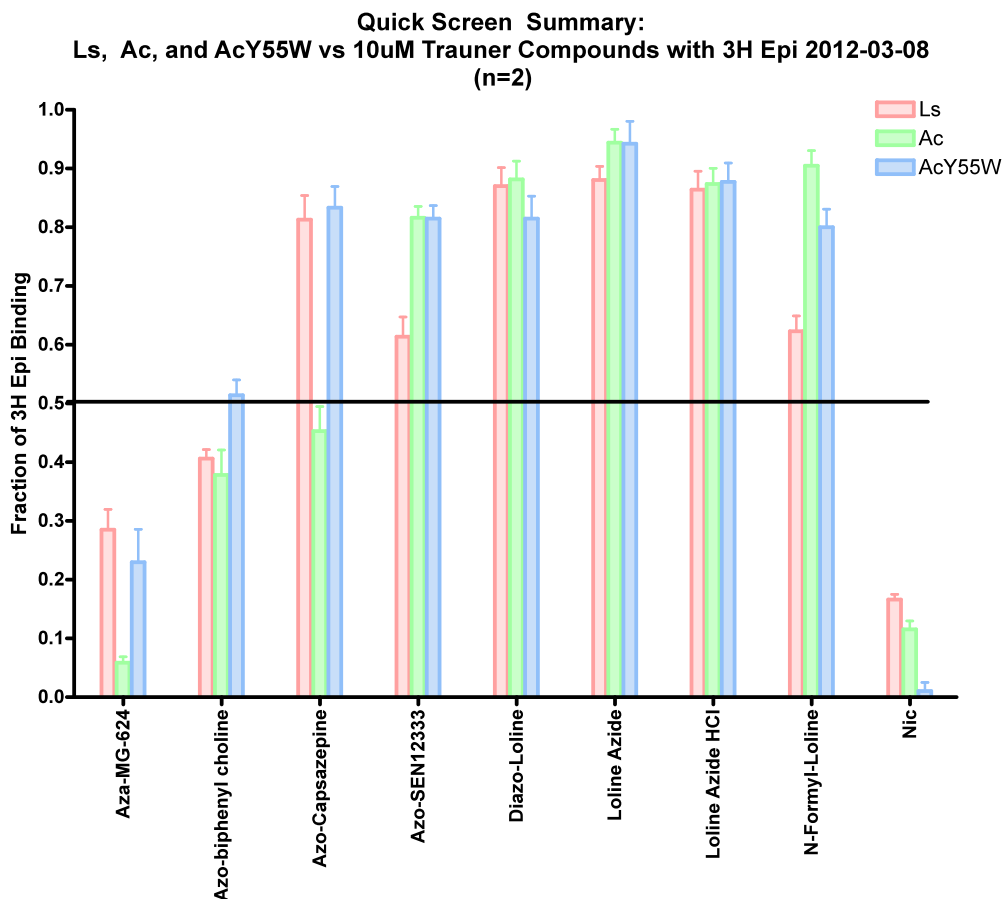


Figure 6.2. Binding studies of 10 μ M **Azo-SEN12333** (among other compounds) on Ls, Ac, and AcY55W. Nicotine (Nic; right) was used as an internal standard to verify proper functioning of the assay (Prof. Palmer Taylor, Skaggs School of Pharmacy and Pharmaceutical Sciences, La Jolla).

Analysis of the photoswitching properties by UV/Vis spectroscopy revealed maximum absorption peaks for **Azo-SEN12333** of $\lambda = 361$ nm and $\lambda = 446$ nm (Fig. 6.3a). The compound was then tested in HEK 293 cells transiently transfected with an $\alpha 7$ nAChR/glycine receptor chimera using the patch-clamp technique (Arunas Damijonaitis, LMU Munich). **Azo-SEN12333** turned out to be a potent agonist of $\alpha 7$ nAChRs, being slightly more active in its *trans* configuration. However, both isomers of **Azo-SEN12333** appear to be highly active, resulting in only limited amount of light-dependent current. The optimum photoswitching wavelengths were determined in a screening to be $\lambda = 367$ nm and $\lambda = 449$ nm (Fig. 6.3b and d). Kinetic measurements showed that photoswitching of nAChR currents with **Azo-SEN12333** occurs very rapidly ($\tau = 70$ ms at $\lambda = 449$ nm; Fig. 6.3c).

Despite these in part promising results, the limited amount of light-dependent current as well as a certain degree of receptor desensitization, which was observed during application of **Azo-SEN12333**, led to the conclusion to not follow up on these results.

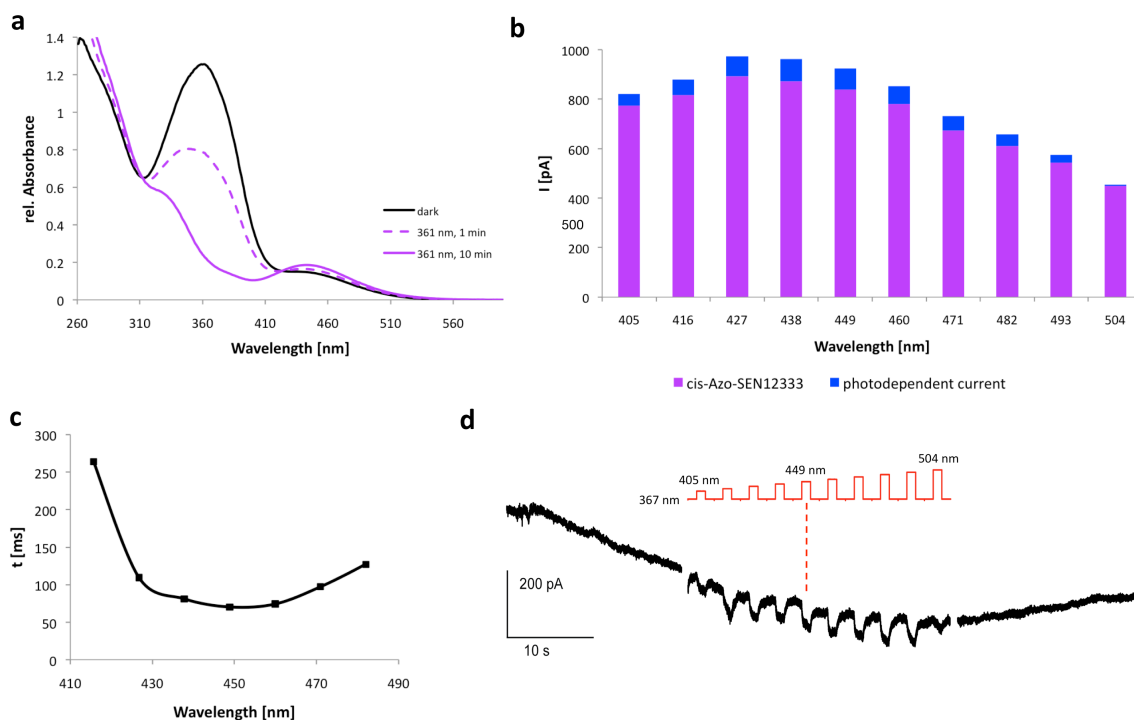


Figure 6.3. **a)** UV/Vis spectrum of **Azo-SEN12333**. The peak absorption wavelengths are $\lambda = 361$ nm and $\lambda = 446$ nm (DMSO). **b) – d)** Electrophysiological analysis of **Azo-SEN12333** (100 μ M) in HEK 293 cells transiently transfected with an $\alpha 7$ nAChR/glycine receptor chimera (Arunas Damijonaitis, LMU Munich). **b)** Wavelength screening. Irradiation with $\lambda = 367$ nm is used to generate the less active *cis* isomer, alternated by different wavelength pulses to isomerize **Azo-SEN12333** to the *trans* isomer. $\lambda = 449$ nm was obtained as the most efficient photoswitching wavelength. **c)** Determination of τ . The fastest photoswitching was observed for $\lambda = 449$ nm with $\tau = 70$ ms. **d)** Representative electrophysiological trace from **b)**.

6.2 DEVELOPMENT OF RED DAD, A RED-SHIFTED, NON-PERMANENTLY CHARGED PCL FOR VOLTAGE-GATED POTASSIUM CHANNELS

QAQ stands for a linear sequence of quaternary ammonium – azobenzene – quaternary ammonium and resembles the known local anesthetics lidocaine and its derivative QX-314 (Fig. 6.4). QAQ enables rapid and selective optical control of nociception and neuronal excitability.^[5] Due to its doubly charged nature, QAQ is membrane-impermeant but it is able to infiltrate pain-sensing neurons through TRPV1 channels. From the intracellular site QAQ blocks voltage-gated ion channels (Na_v , K_v , Ca_v) in the *trans* form but not the *cis* form.^[5] Whereas QX-314 is also charged and therefore unable to cross the membrane, lidocaine is a tertiary amine which is able to permeate the membrane in its neutral state but functions as a channel blocker for Na_v , K_v and Ca_v channels from the cytoplasmic side in its protonated state.^[6] Following this logic, a non-permanently charged and moreover red-shifted version of QAQ named **Red DAD** was designed and synthesized (Fig. 6.4). Having three basic nitrogen atoms in the molecule, **Red DAD** should exist in an equilibrium of positively charged and neutral molecules under physiological conditions and therefore be able to permeate membranes. Once **Red DAD** has crossed the membrane, it could be protonated and accumulate in the cytosol. Hence, it could function as photochromic blocker of voltage-gated ion channels, like QAQ does, without requiring noxious stimuli to open TRPV1 channels to allow the molecule to cross the membrane.

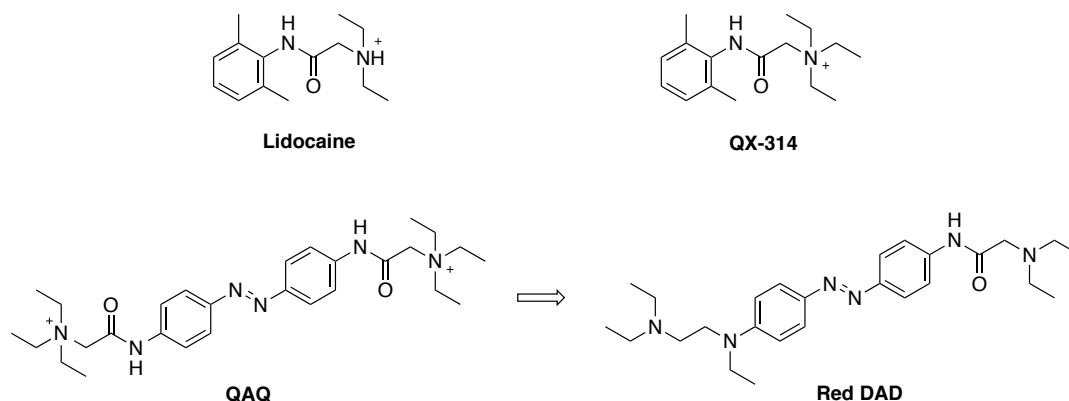
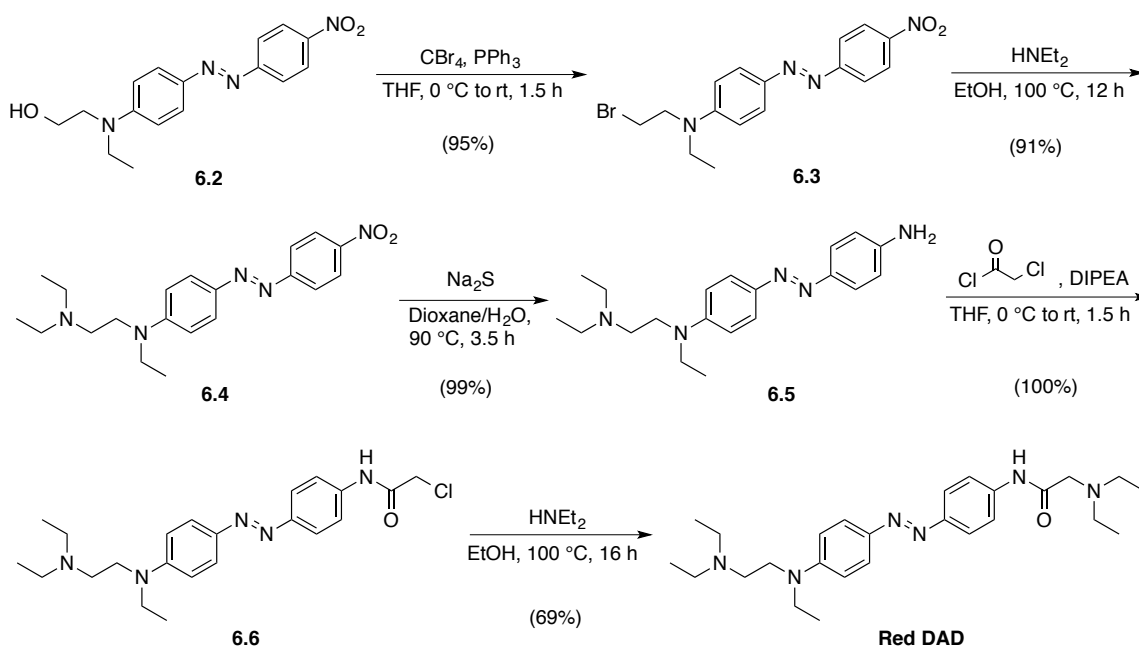


Figure 6.4. Structures of lidocaine (in its protonated form), QX-314, QAQ and **Red DAD**.

Synthesis of Red DAD

The synthesis of **Red DAD** is depicted in Scheme 6.2: The commercially available dye Disperse Red 1 (**6.2**) was treated under Appel conditions, affording bromide **6.3** in 95% yield. The

bromide was then replaced with diethyl amine by heating the two compounds together in a pressure tube. Thus, tertiary amine **6.4** was obtained in 91% yield. The nitro group was reduced using sodium sulfide, giving aniline **6.5** in 99% yield. Compound **6.5** was then converted to **6.6** following a protocol used for the synthesis of lidocaine:^[7] The aniline was reacted with chloroacetyl chloride which yielded α -chloro amide **6.6** quantitatively. The α -chloride was then replaced with diethyl amine by heating in a pressure tube, affording **Red DAD** in 69% yield.



Scheme 6.2. Synthesis of **Red DAD**.

The absorption maximum of **Red DAD** was determined by UV/Vis spectroscopy to be at $\lambda = 454$ nm (Fig. 6.5a). Whole-cell voltage-clamp recordings of layer 2/3 cortical neurons in an acute murine brain slice preparation (Laura Laprell, LMU Munich) revealed that **Red DAD** acts as a light-dependent blocker of K^+ currents. Intrinsic K_V channels were activated by voltage jumps from -70 mV to $+50$ mV in the presence of **Red DAD** ($200 \mu\text{M}$) while blocking Na_V channels using TTX ($1 \mu\text{M}$). Currents elicited in the dark (Fig. 6.5b, left) were significantly smaller than in the presence of light of different wavelengths ranging from $\lambda = 380$ nm to $\lambda = 520$ nm (Fig. 6.5b, right), indicating that *trans*-**Red DAD** is a more potent K_V channel blocker than *cis*-**Red DAD**. Statistical analyses showed that the highest relative change in current amplitude is obtained with $\lambda = 460$ nm (Fig. 6.5c) which is in good agreement with the absorption spectrum of **Red DAD** (Fig. 6.5a).

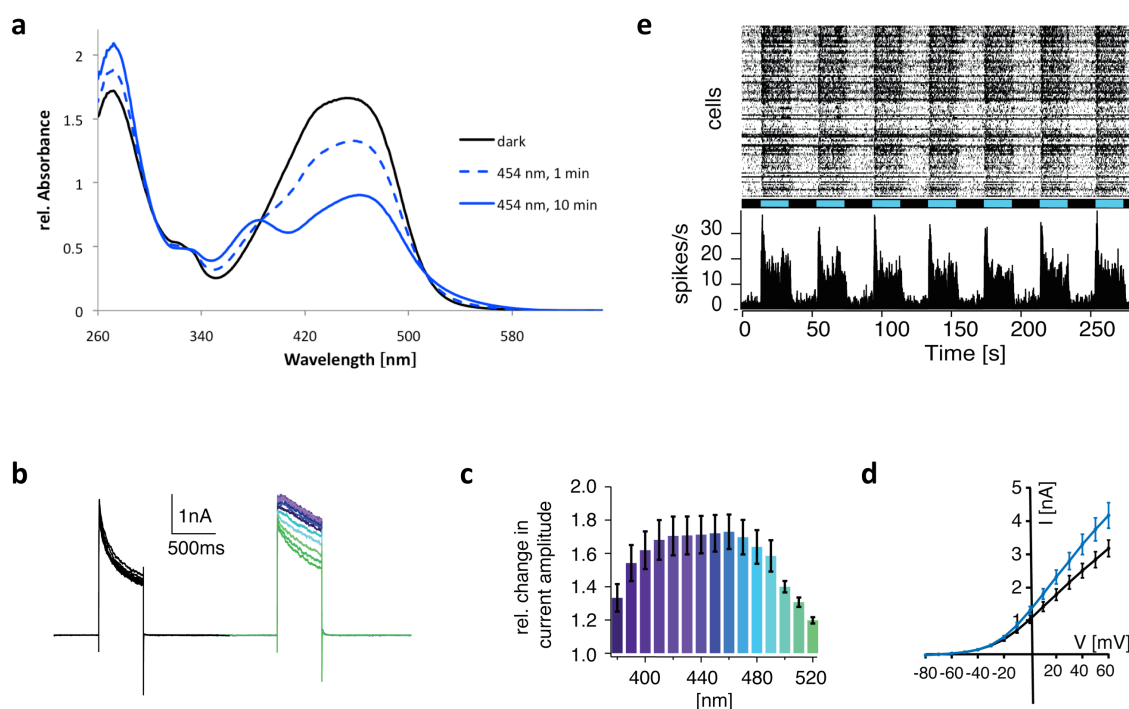


Figure 6.5. **a)** UV/Vis spectrum of **Red DAD** (DMSO). The maximum absorption peak is found at $\lambda = 454$ nm. **b)** Whole-cell voltage-clamp recording of layer 2/3 cortical neurons in presence of $200 \mu\text{M}$ **Red DAD** and $1 \mu\text{M}$ TTX. Voltage jumps from -70 mV to $+50$ mV induce large K^+ outward currents. Currents in darkness are compared to currents in the presence of light ($\lambda = 380\text{--}520$ nm). **c)** Quantification of experiments as performed in **b)**. Induced currents by voltage jump in darkness were normalized to 1. Note that all wavelengths induce larger currents compared to darkness. **d)** Current-voltage relationship in layer 2/3 cortical neurons in the presence of $200 \mu\text{M}$ **Red DAD** and $1 \mu\text{M}$ TTX compared in darkness and in the presence of light (black: dark, blue: $\lambda = 460$ nm). **e)** Top: Raster plot of a multi-electrode array (MEA) recording of a **Red DAD** treated blind retina (*cngA3*^{-/-}, *rho*^{-/-}, *opn4*^{-/-}) stimulated with light (black bars: dark, blue bars: $\lambda = 480$ nm). Retina was mounted on a $200 \mu\text{m}/30 \mu\text{m}$ MEA (Multichannel Systems) after short incubation with $200 \mu\text{M}$ **Red DAD**. During the experiment the retina was perfused with Normal Ringer's solution at $32\text{--}34$ °C at a flow rate of $2\text{--}3$ ml/min. Bottom: Average histogram of all cells detected with spiking rate in Hz (spikes/s; **b**) – **e)**: Laura Laprell, LMU Munich).

The current-voltage relationship in layer 2/3 cortical neurons in the presence of **Red DAD** and TTX confirmed that mostly outward rectifying currents are modulated by **Red DAD** in the presence of light ($\lambda = 460$ nm; Fig. 6.5d). Multi-electrode array (MEA) experiments in retinæ of blind mice (*cngA3*^{-/-}, *rho*^{-/-}, *opn4*^{-/-}; Laura Laprell, LMU Munich) revealed that short incubation with **Red DAD** ($200 \mu\text{M}$) prior to the recording leads to light-dependent spiking of retinal ganglion cells (RGCs). Illumination with light ($\lambda = 480$ nm) more than doubles the spiking rate in RGCs compared to darkness. This light-dependent change in spiking frequency occurs

relatively fast and is fully reversible (Fig. 6.5e). Taken together, **Red DAD** is the most promising tool for our vision restoration approach.

6.3 DEVELOPMENT OF A NEW DISULFIDE CONTAINING CLASS OF PTLs

Maleimide containing PTLs, such as MAQ or MAG, have been used in the past to optically control various functions such as neuronal activity,^[8-10] locomotor behavior in zebrafish^[11] and the restoration of visual responses.^[12] However, the usage of the highly reactive maleimides in *in vivo* experiments might be accompanied with various undesired side effects. Moreover, high concentrations of thiol containing molecules, such as serum albumin, might react with the maleimide moiety before it can reach its intended target. Therefore, new ways to covalently attach PTLs to ion channels or receptors are desired.

Sunesis Pharmaceuticals, Inc. has developed a concept called *Tethering*[®] for fragment-based drug discovery which is based on reversible covalent bond formation reactions between the protein target and the fragment(s) to be evaluated.^[13] It is based on sulfide exchange reactions of a fragment which contains a thiol functional group that is coupled to 2-aminothioethanol in order to increase solubility and a (genetically introduced) cysteine on the protein (Fig. 6.6).

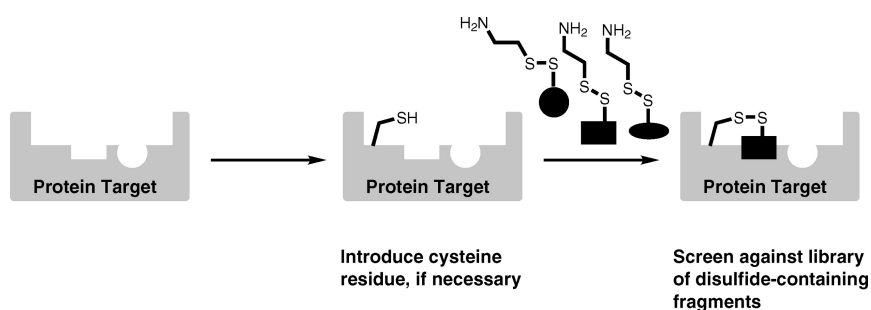


Figure 6.6. Schematic illustration of the concept of *Tethering*[®]. Illustration adapted from Erlanson *et al.*,^[13] reprinted with permission from ANNUAL REVIEWS. Copyright 2004.

Formation of the disulfide bond is extremely mild and occurs under equilibrium conditions, given a similar reduction potential of the thiol moieties engaged. As a result, a fragment with increased affinity to the target will lead to a thermodynamic sink and shift the equilibria toward this product (Fig. 6.7).

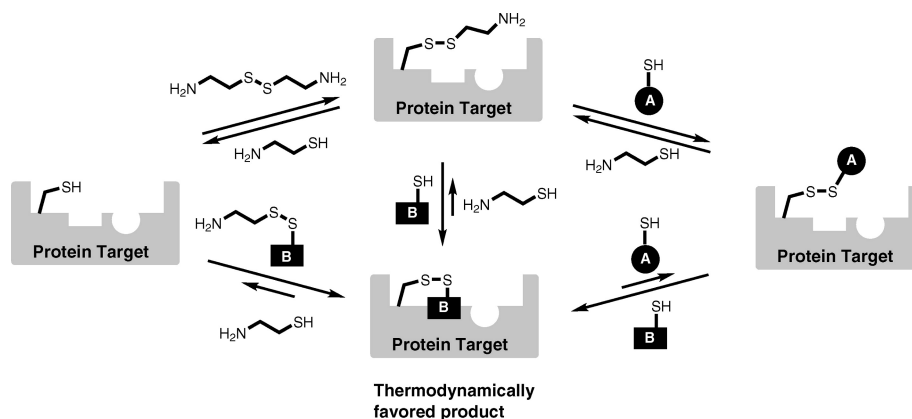


Figure 6.7. Schematic illustration of some equilibria reactions in *Tethering*[®]. If a fragment has inherent affinity for the target (here square B), equilibria will be shifted toward this complex. Illustration adapted from Erlanson *et al.*,^[13] reprinted with permission from ANNUAL REVIEWS. Copyright 2004.

Importantly, these disulfides are extracellularly stable and have no effect on other biological molecules. Therefore, they are potential candidates to replace the highly reactive maleimide moieties on previously used PTLs. Consequently, two disulfide analogues of the established PTL MAQ for voltage-gated potassium channels were designed which differ only in their distance between the azobenzene and the thiol moiety in order to screen for the optimum spacer length (Fig. 6.8).

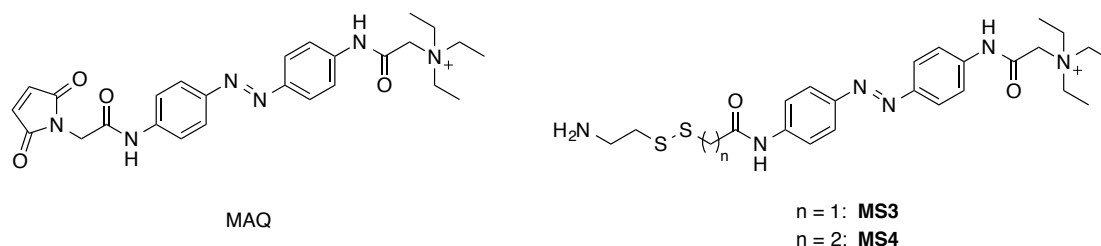


Figure 6.8. Structures of MAQ and **MS2** and **MS3**.

Synthesis of MS2 and MS3

Firstly, the Boc-protected disulfide precursors **6.10** and **6.11** were synthesized *via* a sulfide exchange reaction from commercially available di-Boc cystamine **6.7** and the corresponding mercaptocarboxylic acids thioglycolic acid (**6.8**) and 3-mercaptopropionic acid (**6.9**) in 56% and 30% yield, respectively (Scheme 6.3).

The maximum absorption wavelengths of **MS2** and **MS3** were determined to be at $\lambda = 377$ nm and $\lambda = 456$ nm (**MS2**, Fig. 6.9a), as well as at $\lambda = 376$ nm and $\lambda = 455$ nm (**MS3**, Fig. 6.9b). The compounds will be tested by Dr. Martin Sumser (LMU Munich) on their ability to act as PTLs on voltage-gated potassium channels in due time.

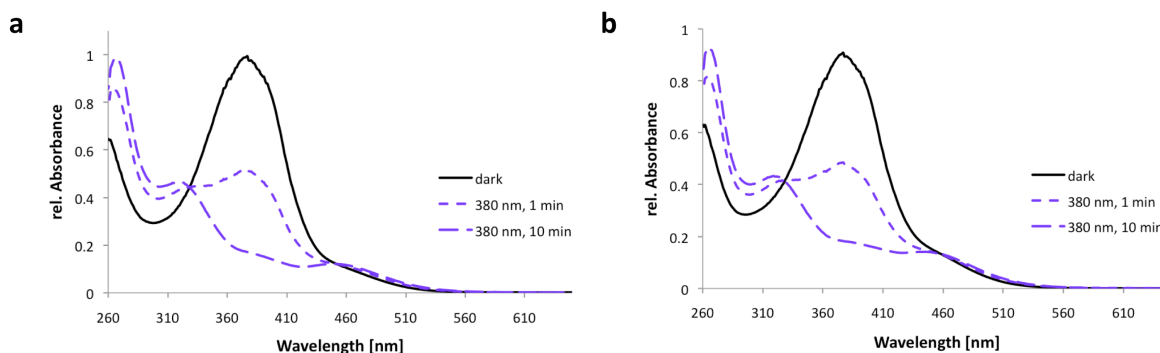


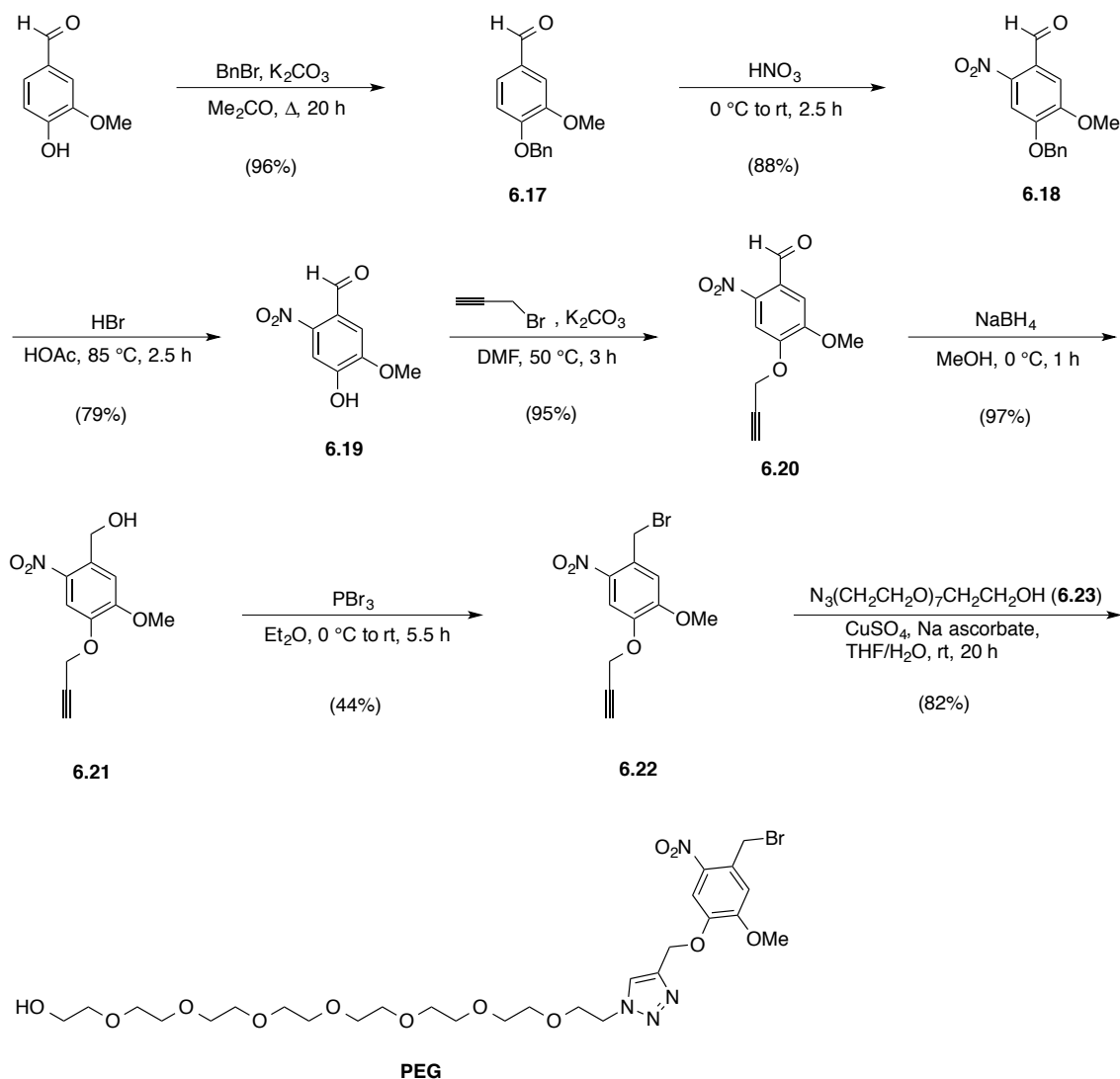
Figure 6.9. UV/Vis spectra (DMSO) of **a) MS2** and **b) MS3**. The maximum absorption wavelengths are $\lambda = 377$ nm and $\lambda = 456$ nm (**MS2**), as well as $\lambda = 376$ nm and $\lambda = 455$ nm (**MS3**).

6.4 SYNTHESIS OF A PEGYLATED PHOTOCLEAVABLE *o*-NITROBENZYL PROTECTING GROUP

In cooperation with the group of Prof. Herwig Baier (University of California, San Francisco, now Max-Planck-Institute Munich), a PEGylated photolytically cleavable *o*-nitrobenzyl protecting group (PG) was synthesized starting from vanillin (Scheme 6.5). The goal of this project was to increase the solubility of otherwise commercially available *o*-nitrobenzyl PGs (e.g. 4,5-dimethoxy-2-nitrobenzylbromide). The Baier group genetically engineered cysteine residues into a region on the cell surface which is responsible for cell-cell recognition and aggregation. By blocking these regions, interaction of cells would be prevented and therefore no cell aggregation could take place. If a photolytically cleavable PG is used, cell aggregation could be reinitiated by cleaving the PG with light in a high spatial and temporal precision.

Firstly, vanillin was reacted with benzyl bromide to give benzyl ether **6.17** in 96% yield. Nitration of **6.17** with 100% nitric acid yielded **6.18** in 88%. The benzyl ether was cleaved with HBr in acetic acid in 79% yield (**6.19**), followed by propargylation using propargyl bromide, affording alkyne **6.20** in 95% yield. Aldehyde **6.20** was then reduced to primary alcohol **6.21** with NaBH₄ (97% yield), followed by an Appel-type reaction with PBr₃, furnishing bromide **6.22** in 44% yield. Finally, the PEG azide **6.23** was attached *via* formation of a 1,2,3-triazole

using “click chemistry”.^[14] The PEGylated light-sensitive *o*-nitrobenzyl protecting group **PEG** was obtained in 82% yield.



Scheme 6.5. Synthesis of PEGylated *o*-nitrobenzyl PG **PEG** from vanillin.

First results in an N-Cadherin adhesion assay (Dr. Anna Lisa Lucido, University of California, San Francisco) showed that **PEG** appears to be effective in preventing cell aggregation, however lacks specificity for the D1C mutant (it also perturbs Ca^{2+} -mediated binding in the wildtype; Fig. 6.10 top). Illumination with UV light slightly increases the average particle size due to cell aggregation. However, the difference is relatively small compared to the particle size without **PEG**, suggesting that a significant proportion of PEG was not cleaved by UV illumination (Fig. 6.10 bottom). Since *o*-nitrobenzyl protecting groups are well established as light-cleavable PGs in biological systems,^[15] the conditions of UV illumination (wavelength, light intensity, duration of illumination) probably need to be further evaluated.

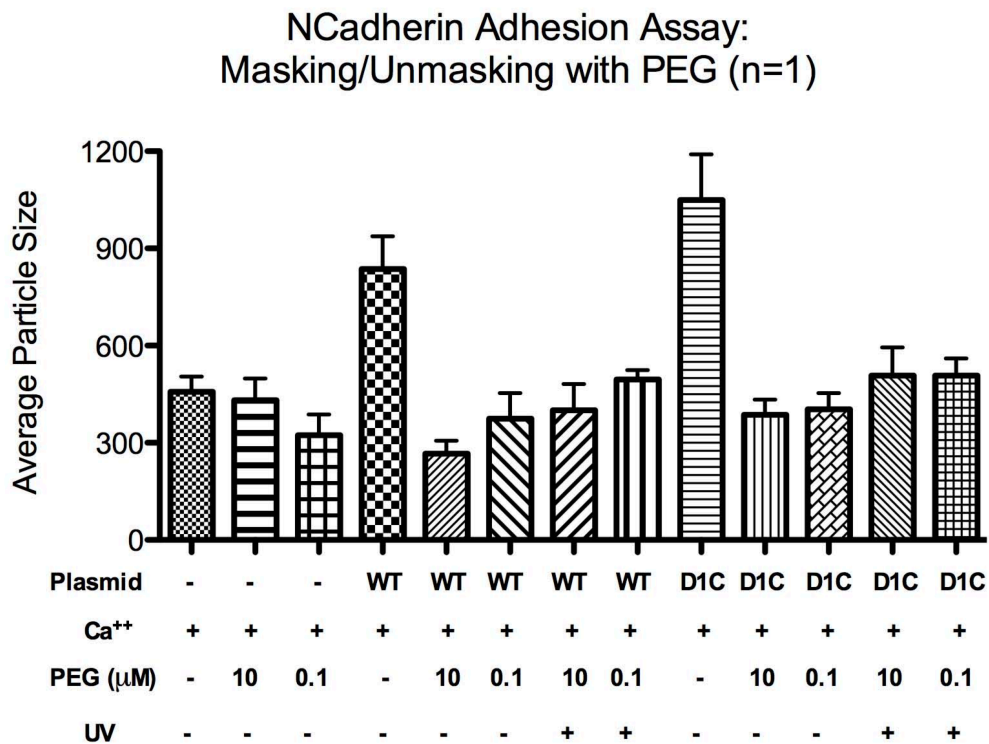
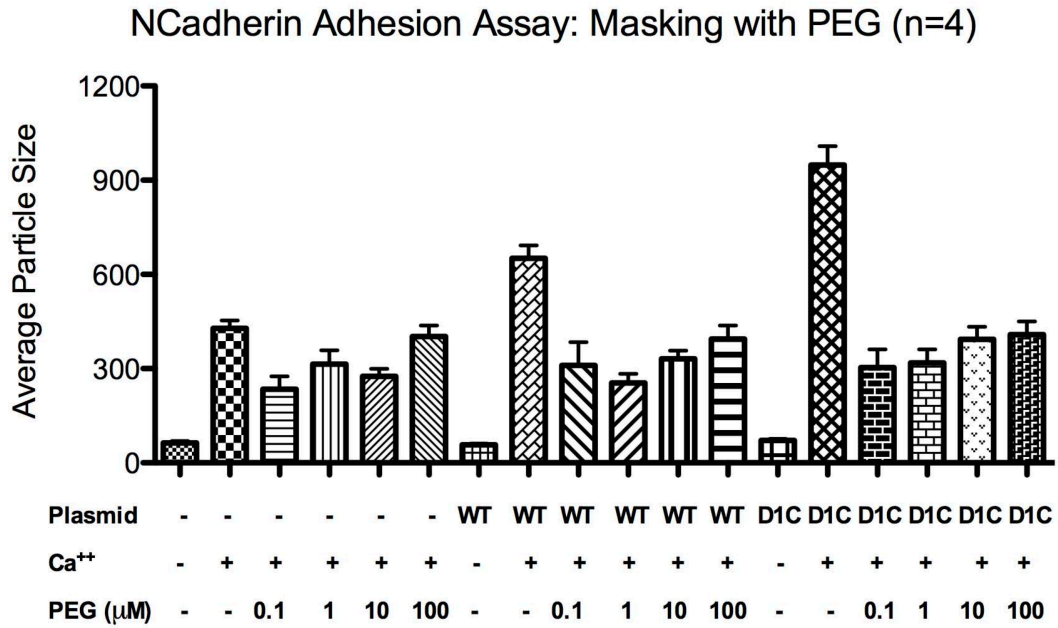


Figure 6.10. NCadherin adhesion assay of the PEGylated PG **PEG** (Dr. Anna Lisa Lucido, University of California, San Francisco). **PEG** appears to bind to the cell surface and therefore prevents cell aggregation. However, no significant specificity for the D1C mutant over the wildtype (top) was achieved. Illumination with light only led to a small increase in aggregation, suggesting that the PG was not removed completely (bottom).

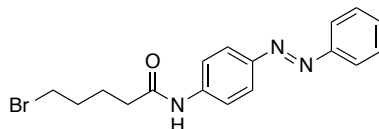
6.5 EXPERIMENTAL PROCEDURES AND ANALYTICAL DATA

6.5.1 GENERAL EXPERIMENTAL DETAILS AND INSTRUMENTATION

All reactions were carried out with magnetic stirring and if air or moisture sensitive in oven-dried glassware under an atmosphere of nitrogen or argon. Syringes used to transfer reagents and solvents were purged with nitrogen or argon prior to use. Reagents were used as commercially supplied unless otherwise stated. Thin layer chromatography was performed on pre-coated silica gel F₂₅₄ glass backed plates and the chromatogram was visualized under UV light and/or by staining using aqueous acidic vanillin or potassium permanganate, followed by gentle heating with a heat gun. Flash column chromatography was performed using silica gel, particle size 40–63 μm (eluants are given in parenthesis). The diameter of the columns and the amount of silica gel were calculated according to the recommendations of W. C. Still *et al.*^[16] IR spectra were recorded on a Perkin Elmer Spectrum Bx FT-IR instrument as thin films with absorption bands being reported in wave number (cm^{-1}). UV/Vis spectra were obtained using a Varian Cary 50 Scan UV/Vis spectrometer and Helma SUPRASIL precision cuvettes (10 mm light path).

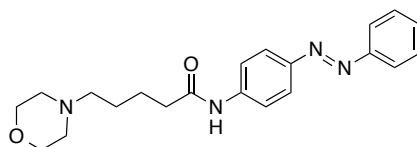
¹H and ¹³C NMR spectra were measured on Varian VNMRS 300, VNMRS 400, INOVA 400 or VNMRS 600 instruments. The chemical shifts are quoted as δ -values in ppm referenced to the residual solvent peak (CDCl_3 : δ_{H} 7.26, δ_{C} 77.2; CD_3OD : δ_{H} 3.31, δ_{C} 49.0; DMSO-d_6 : δ_{H} 2.50, δ_{C} 39.5).^[17] Multiplicities are abbreviated as follows: s = singlet, d = doublet, t = triplet, q = quartet, quint = quintet, sext = sextet, sept = septet, m = multiplet. High resolution mass spectra (EI, ESI) were recorded by LMU Mass Spectrometry Service using a Thermo Finnigan MAT 95, a Jeol MStation or a Thermo Finnigan LTQ FT Ultra instrument. Melting points were obtained using a Stanford Research Systems MPA120 apparatus and are uncorrected.

6.5.2 SYNTHESIS OF AZO-SEN12333

Synthesis of 5-bromo-*N*-(4-(phenyldiazenyl)phenyl)pentanamide (6.1)

4-Aminoazobenzene (2.00 g, 10.1 mmol, 1.0 equiv.) was dissolved in DCM (40 mL) at 0 °C and TEA (1.40 mL, 10.1 mmol, 1.0 equiv.) was added. To this solution, 5-bromovaleryl chloride (1.49 mL, 11.1 mmol, 1.1 equiv.) was added dropwise and the reaction mixture was stirred for 1 h at 0 °C. The organic phase was washed with sat. aqu. NaHCO₃ (100 mL) and brine (50 mL), dried over MgSO₄ and concentrated *in vacuo*. The crude product was purified by flash silica gel chromatography (DCM/MeOH, gradient from 100:0 to 4:1) to afford amide **6.1** (3.42 g, 9.49 mmol, 94%) as an orange solid.

TLC (DCM): R_f = 0.17. **M.p.:** 135–136 °C. **¹H NMR (CDCl₃, 300 MHz, 27 °C):** δ = 7.97–7.86 (m, 4H, ArH), 7.73–7.65 (m, 2H, ArH), 7.55–7.42 (m, 4H, ArH), 3.49–3.40 (m, 2H, CH₂), 2.49–2.39 (m, 2H, CH₂), 2.02–1.87 (m, 4H, 2 x CH₂) ppm. **¹³C NMR (CDCl₃, 75 MHz, 27 °C):** δ = 170.7, 152.6, 149.0, 140.3, 130.8, 129.0, 124.0, 122.7, 119.8, 36.6, 33.1, 32.0, 23.9 ppm. **IR (neat, ATR):** $\tilde{\nu}$ = 3320 (m), 3069 (w), 2948 (w), 2871 (w), 1669 (vs), 1594 (s), 1526 (vs), 1463 (m), 1442 (m), 1406 (m), 1384 (m), 1308 (m), 1266 (m), 1256 (m), 1211 (w), 1180 (m), 1152 (m), 1118 (w), 1106 (w), 1070 (w), 1020 (w), 962 (w), 920 (w), 888 (w), 853 (m), 836 (m), 768 (m), 732 (w), 718 (m), 685 (m), 668 (w) cm⁻¹. **HRMS (ESI⁺):** m/z calcd. for [C₁₇H₁₉N₃OBr]⁺: 360.0711, found: 360.0710 ([M+H]⁺).

Synthesis of 5-morpholino-*N*-(4-(phenyldiazenyl)phenyl)pentanamide (Azo-SEN12333)

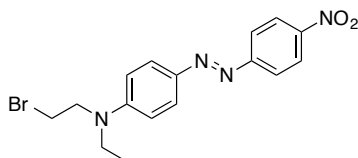
Bromide **6.1** (1.00 g, 2.78 mmol, 1.0 equiv.) was dissolved in MeCN (40 mL) and morpholine (0.51 mL, 5.8 mmol, 2.1 equiv.) was added. The mixture was heated to reflux for 12 h. The cooled suspension was diluted with EtOAc (50 mL), washed with sat. aqu. NaHCO₃ (100 mL), dried over MgSO₄ and concentrated *in vacuo*. The crude product was purified by flash silica gel

chromatography (CHCl₃/MeOH, 20:1 → 15:1), yielding **Azo-SEN12333** (896 mg, 2.45 mmol, 88%) as an orange solid.

TLC (DCM/MeOH, 10:1): R_f = 0.38. **M.p.:** 171–172 °C. **¹H NMR (CDCl₃, 300 MHz, 27 °C):** δ = 7.95–7.85 (m, 4H, ArH), 7.72–7.64 (m, 2H, ArH), 7.55–7.41 (m, 4H, ArH), 3.71 (t, J = 4.8 Hz, 4H, 2 x CH₂), 2.46–2.35 (m, 8H, 4 x CH₂), 1.86–1.72 (m, 2H, CH₂), 1.66–1.53 (m, 2H, CH₂) ppm. **¹³C NMR (CDCl₃, 75 MHz, 27 °C):** δ = 171.2, 152.6, 149.0, 140.4, 130.7, 129.0, 124.0, 122.7, 119.7, 66.9, 58.5, 53.7, 37.5, 26.0, 23.3 ppm. **IR (neat, ATR):** $\tilde{\nu}$ = 3341 (w), 2946 (w), 2853 (w), 2811 (w), 1700 (m), 1684 (m), 1670 (s), 1654 (m), 1601 (m), 1576 (m), 1559 (m), 1540 (s), 1522 (vs), 1507 (s), 1473 (m), 1458 (m), 1437 (m), 1407 (m), 1340 (m), 1302 (m), 1272 (m), 1247 (m), 1177 (w), 1155 (m), 1116 (m), 1068 (m), 1003 (m), 908 (w), 866 (w), 851 (w), 835 (w), 804 (w), 769 (w), 718 (w), 685 (w), 668 (w) cm⁻¹. **HRMS (ESI⁺):** m/z calcd. for [C₂₁H₂₇N₄O₂]⁺: 367.2134, found: 367.2131 ([M+H]⁺). **UV/Vis:** λ_{max} = 361, 446 nm.

6.5.3 SYNTHESIS OF RED DAD

Synthesis of *N*-(2-bromoethyl)-*N*-ethyl-4-((4-nitrophenyl)diazenyl)aniline (**6.3**)

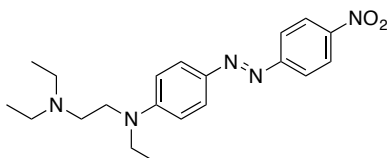


Disperse Red 1 (**6.2**; 2.00 g, 6.36 mmol, 1.0 equiv.) was dissolved in THF (40 mL) and CBr₄ (2.42 g, 7.31 mmol, 1.15 equiv.) and PPh₃ (1.92 g, 7.31 mmol, 1.15 equiv.) were added at 0 °C. The reaction mixture was warmed to room temperature and stirred for 1.5 h. The solvent was removed under reduced pressure and the crude product was purified by flash silica gel column chromatography (hexanes/EtOAc, 6:1), yielding bromide **6.3** (2.28 g, 6.04 mmol, 95%) as a deep red solid.

TLC (hexanes/EtOAc, 4:1): R_f = 0.60. **M.p.:** 142–143 °C. **¹H NMR (CDCl₃, 300 MHz, 27 °C):** δ = 8.38–8.29 (m, 2H, ArH), 7.98–7.87 (m, 4H, ArH), 6.82–6.72 (m, 2H, ArH), 3.81 (t, J = 7.8 Hz, 2H, CH₂), 3.62–3.45 (m, 4H, 2 x CH₂), 1.27 (t, J = 7.1 Hz, 3H, CH₃) ppm. **¹³C NMR (CDCl₃, 75 MHz, 27 °C):** δ = 156.6, 150.4, 147.6, 144.1, 126.3, 124.7, 122.7, 111.4, 52.3, 45.8, 27.6, 12.6 ppm. **IR (neat, ATR):** $\tilde{\nu}$ = 2974 (w), 1601 (m), 1559 (w), 1516 (vs), 1465

(w), 1424 (w), 1406 (w), 1390 (m), 1354 (m), 1340 (m), 1311 (w), 1271 (w), 1254 (w), 1218 (w), 1202 (w), 1155 (m), 1141 (m), 1106 (m), 1077 (w), 1002 (w), 858 (m), 823 (m), 756 (w), 724 (w), 686 (w), 668 (w) cm^{-1} . **HRMS (ESI⁺):** m/z calcd. for $[\text{C}_{16}\text{H}_{18}\text{N}_4\text{O}_2\text{Br}]^+$: 377.0613, found: 377.0610 ($[\text{M}+\text{H}]^+$).

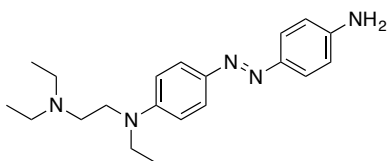
Synthesis of N^1,N^1,N^2 -triethyl- N^2 -(4-((4-nitrophenyl)diazenyl)phenyl)ethane-1,2-diamine (6.4)



Bromide **6.3** (300 mg, 0.800 mmol, 1.0 equiv.) was dissolved in EtOH (4 mL) in a pressure tube and diethyl amine (0.83 mL, 8.0 mmol, 10 equiv.) was added. The reaction mixture was heated to 100 °C for 12 h. The solvent was removed under reduced pressure and the crude product was purified by flash silica gel column chromatography (DCM/MeOH, gradient from 100:0 to 2:1) to give diamine **6.4** (268 mg, 0.730 mmol, 91%) as a deep red oil.

TLC (DCM/MeOH, 20:1): R_f = 0.30. **¹H NMR (CDCl₃, 400 MHz, 27 °C):** δ = 8.33–8.28 (m, 2H, ArH), 7.92–7.85 (m, 4H, ArH), 6.76–6.71 (m, 2H, ArH), 3.53–3.47 (m, 4H, 2 x CH₂), 2.68–2.61 (m, 2H, CH₂), 2.59 (q, J = 7.2 Hz, 4H, 2 x CH₂), 1.24 (t, J = 7.1 Hz, 3H, CH₃), 1.05 (t, J = 7.2 Hz, 6H, 2 x CH₃) ppm. **¹³C NMR (CDCl₃, 100 MHz, 27 °C):** δ = 156.9, 151.4, 147.2, 143.4, 126.3, 124.6, 122.5, 111.1, 50.4, 49.7, 47.6, 45.9, 12.4, 12.0 ppm. **IR (neat, ATR):** $\tilde{\nu}$ = 2969 (m), 1602 (s), 1557 (w), 1513 (vs), 1470 (w), 1423 (w), 1407 (w), 1390 (m), 1340 (m), 1255 (w), 1201 (w), 1156 (m), 1142 (m), 1105 (m), 1072 (w), 998 (w), 859 (m), 824 (m), 755 (w), 721 (w), 687 (w), 666 (w) cm^{-1} . **HRMS (ESI⁺):** m/z calcd. for $[\text{C}_{20}\text{H}_{28}\text{N}_5\text{O}_2]^+$: 370.2243, found: 370.2238 ($[\text{M}+\text{H}]^+$).

Synthesis of N^1 -(4-((4-aminophenyl)diazenyl)phenyl)- N^1,N^2,N^2 -triethylethane-1,2-diamine (6.5)

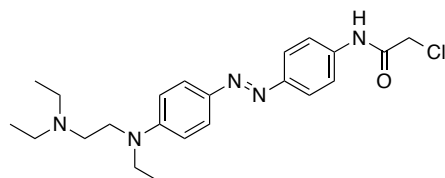


Nitroarene **6.4** (288 mg, 0.780 mmol, 1.0 equiv.) was dissolved in 1,4-dioxane (12 mL) and water (1 mL) and Na₂S (106 mg, 1.36 mmol, 1.7 equiv.) was added. The reaction mixture was

heated to 90 °C for 2 h. As TLC analysis indicated remaining starting material, more Na₂S (53 mg, 0.68 mmol, 0.9 equiv.) was added and the mixture was heated to 90 °C for another 1.5 h. Sat. aqu. NaHCO₃ (30 mL) was added and the aqueous phase was extracted with DCM (3 x 20 mL). The combined organic layers were washed with brine (50 mL), dried over MgSO₄ and the solvent was concentrated *in vacuo*. The crude product was purified by flash silica gel column chromatography (DCM/MeOH, gradient from 20:1 to 10:1) to give azoaniline **6.5** (260 mg, 0.770 mmol, 99%) as a deep red oil.

TLC (DCM/MeOH, 10:1): R_f = 0.30. **¹H NMR (CDCl₃, 300 MHz, 27 °C):** δ = 7.83–7.74 (m, 2H, ArH), 7.75–7.68 (m, 2H, ArH), 6.77–6.67 (m, 4H, ArH), 3.90 (br s, 2H, NH₂), 3.58–3.39 (m, 4H, 2 x CH₂), 2.73–2.55 (m, 6H, 3 x CH₂), 1.21 (t, *J* = 7.1 Hz, 3H, CH₃), 1.08 (t, *J* = 7.8 Hz, 6H, 2 x CH₃) ppm. **¹³C NMR (CDCl₃, 75 MHz, 27 °C):** δ = 149.3, 148.0, 146.1, 143.5, 124.5, 124.0, 114.8, 111.1, 50.2, 49.2, 47.6, 45.6, 12.5, 11.7 ppm. **IR (neat, ATR):** $\tilde{\nu}$ = 3337 (w), 3209 (w), 2968 (m), 2932 (w), 2811 (w), 1619 (m), 1591 (vs), 1561 (m), 1511 (m), 1468 (w), 1450 (w), 1395 (m), 1350 (m), 1294 (m), 1276 (m), 1245 (m), 1201 (w), 1149 (s), 1071 (w), 998 (w), 944 (w), 834 (m), 821 (m), 730 (w) cm⁻¹. **HRMS (ESI⁺):** *m/z* calcd. for [C₂₀H₃₀N₅]⁺: 340.2501, found: 340.2497 ([M+H]⁺).

Synthesis of 2-chloro-*N*-(4-((4-((2-(diethylamino)ethyl)(ethyl)amino)-phenyl)diazenyl)-phenyl)acetamide (**6.6**)

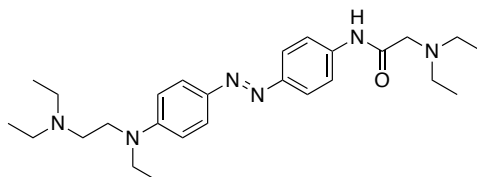


Aniline **6.5** (181 mg, 0.530 mmol, 1.0 equiv.) was dissolved in THF (25 mL) and cooled to 0 °C. DIPEA (0.11 mL, 0.64 mmol, 1.2 equiv.) and chloro acetylchloride (64 μ L, 0.80 mmol, 1.5 equiv.) were added. The reaction mixture was slowly warmed to room temperature and stirred for 1.5 h. The solvent was removed under reduced pressure and the crude product was purified by flash silica gel column chromatography (DCM/MeOH, gradient from 15:1 to 10:1) to yield amide **6.6** (226 mg, 0.530 mmol, 100%) as a deep red oil.

TLC (DCM/MeOH, 10:1): R_f = 0.34. **¹H NMR (CDCl₃, 400 MHz, 27 °C):** δ = 8.31 (br s, 1H, NH), 7.87–7.79 (m, 4H, ArH), 7.68–7.64 (m, 2H, ArH), 6.74–6.70 (m, 2H, ArH), 4.20 (s, 2H, CH₂), 3.54–3.43 (m, 4H, 2 x CH₂), 2.71–2.55 (m, 6H, 3 x CH₂), 1.21 (t, *J* = 7.1 Hz, 3H, CH₃), 1.07 (t, *J* = 7.1 Hz, 6H, 2 x CH₃) ppm. **¹³C NMR (CDCl₃, 100 MHz, 27 °C):** δ = 163.6, 150.3, 150.1, 143.2, 137.4, 125.2, 123.1, 120.1, 111.0, 50.2, 49.4, 47.6, 45.7, 42.9, 12.5, 11.8 ppm. **IR**

(neat, ATR): $\tilde{\nu}$ = 3249 (w), 2969 (m), 2810 (w), 1675 (m), 1596 (vs), 1541 (m), 1514 (s), 1446 (w), 1422 (m), 1393 (m), 1350 (m), 1313 (w), 1276 (w), 1248 (m), 1198 (w), 1154 (s), 1139 (s), 1073 (w), 998 (w), 844 (m), 821 (m), 731 (w), 696 (w) cm^{-1} . HRMS (ESI⁺): m/z calcd. for $[\text{C}_{22}\text{H}_{31}\text{ClN}_5\text{O}]^+$: 416.2217, found: 416.2215 ($[\text{M}+\text{H}]^+$).

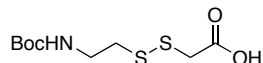
Synthesis of 2-(diethylamino)-*N*-(4-((4-((2-(diethylamino)ethyl)(ethyl)amino)-phenyl)-diazenyl)phenyl)acetamide (Red DAD)



Chloride **6.6** (218 mg, 0.520 mmol, 1.0 equiv.) was dissolved in EtOH (5 mL) in a pressure tube and diethyl amine (0.54 mL, 5.2 mmol, 10 equiv.) was added. The reaction mixture was heated to 100 °C for 16 h. The solvent was removed under reduced pressure and the crude product was purified by flash silica gel column chromatography (DCM/MeOH, 30:1 → 25:1) to give **Red DAD** (161 mg, 0.360 mmol, 69%) as a deep red oil.

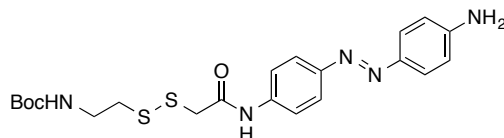
TLC (DCM/MeOH, 10:1): R_f = 0.41. **¹H NMR (CDCl₃, 600 MHz, 27 °C):** δ = 9.53 (br s, 1H, NH), 7.86–7.79 (m, 4H, ArH), 7.70–7.65 (m, 2H, ArH), 6.75–6.68 (m, 2H, ArH), 3.53–3.43 (m, 4H, 2 x CH₂), 3.16 (s, 2H, CH₂), 2.68–2.62 (m, 6H, 3 x CH₂), 2.59 (q, J = 7.0 Hz, 4H, 2 x CH₂), 1.21 (t, J = 7.1 Hz, 3H, CH₃), 1.09 (t, J = 7.2 Hz, 6H, 2 x CH₃), 1.06 (t, J = 7.1 Hz, 6H, 2 x CH₃) ppm. **¹³C NMR (CDCl₃, 150 MHz, 27 °C):** δ = 170.1, 150.0, 149.5, 143.3, 138.7, 125.0, 123.1, 119.3, 111.0, 58.2, 50.3, 49.4, 48.9, 47.6, 45.7, 12.5, 12.4, 11.9 ppm. **IR (neat, ATR):** $\tilde{\nu}$ = 3276 (w), 2967 (m), 2932 (w), 2813 (w), 1692 (m), 1597 (s), 1560 (m), 1510 (vs), 1447 (m), 1420 (m), 1393 (m), 1350 (m), 1299 (m), 1276 (m), 1247 (m), 1202 (m), 1152 (s), 1139 (s), 1070 (m), 998 (m), 905 (w), 845 (m), 820 (m), 730 (w), 668 (w) cm^{-1} . **HRMS (ESI⁺):** m/z calcd. for $[\text{C}_{26}\text{H}_{41}\text{ON}_6]^+$: 453.3342, found: 453.3337 ($[\text{M}+\text{H}]^+$). **UV/Vis:** λ_{max} = 454 nm.

6.5.4 SYNTHESIS OF MS2 AND MS3

Synthesis of 2-((2-((*tert*-butoxycarbonyl)amino)ethyl)disulfanyl)acetic acid (6.10)

Di-Boc-cystamine **6.7** (3.53 g, 10.0 mmol, 1.0 equiv.) was dissolved in CHCl_3 (60 mL) and TEA (8.73 mL, 63.0 mmol, 6.3 equiv.) was added. To this solution, thioglycolic acid **6.8** (0.69 mL, 10 mmol, 1.0 equiv.) was added in portions. The reaction mixture was stirred at room temperature for 2 h. The organic phase was washed with 0.5 M KHSO_4 (3 x 60 mL) and dried over MgSO_4 . The solvent was removed under reduced pressure and the residue was dissolved in Et_2O (300 mL). The organic phase was extracted with sat. aqu. NaHCO_3 (3 x 150 mL) and the combined aqueous phases were washed with Et_2O (200 mL), followed by acidification with 0.5 M KHSO_4 to pH = 3. The aqueous phase was extracted with CHCl_3 (3 x 150 mL), washed with brine (300 mL), dried over MgSO_4 and concentrated *in vacuo*. Disulfide **6.10** was obtained in 56% yield (1.49 g, 5.57 mmol) as colorless oil.

TLC ($\text{CHCl}_3/\text{MeOH}$, 9:1): $R_f = 0.49$. **$^1\text{H NMR}$** (DMSO-d_6 , 400 MHz, 27 °C): $\delta = 12.53$ (br s, 1H, CO_2H), 6.95 (t, $J = 5.5$ Hz, 1H, NH), 3.54 (s, 2H, CH_2), 3.21–3.15 (m, 2H, CH_2), 2.81–2.72 (m, 2H, CH_2), 1.35 (s, 9H, $\text{C}(\text{CH}_3)_3$) ppm. **$^{13}\text{C NMR}$** (DMSO-d_6 , 100 MHz, 27 °C): $\delta = 171.0$, 155.9, 78.2, 41.4, 39.6, 37.7, 28.7 ppm. **IR** (neat, ATR): $\tilde{\nu} = 3344$ (w), 2977 (m), 2929 (w), 1699 (s), 1516 (m), 1479 (w), 1454 (w), 1393 (m), 1366 (m), 1344 (w), 1272 (m), 1252 (m), 1162 (vs), 1050 (w), 1001 (w), 950 (w), 862 (m), 778 (w), 664 (w) cm^{-1} . **HRMS** (ESI): m/z calcd. for $[\text{C}_9\text{H}_{16}\text{NO}_4\text{S}_2]^-$: 266.0521, found: 266.0521 ($[\text{M}-\text{H}]^-$).

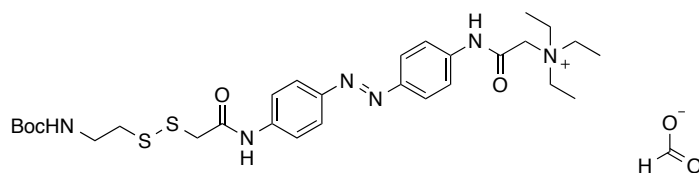
Synthesis of *tert*-butyl (2-((2-((4-((4-aminophenyl)diazenyl)phenyl)amino)-2-oxoethyl)disulfanyl)ethyl)carbamate (6.13)

4,4'-Azodianiline **6.12** (301 mg, 1.42 mmol, 1.0 equiv.), carboxylic acid **6.11** (380 mg, 1.42 mmol, 1.0 equiv.) and HBTU (1.61 g, 4.25 mmol, 3.0 equiv.) were dissolved in THF (19 mL) and TEA (0.59 mL, 4.3 mmol, 3.0 equiv.) was added. The reaction mixture was then heated to reflux for 20 h. EtOAc (40 mL) was added to the cooled mixture and the organic

phase was washed with sat. aqu. NaHCO₃ (2 x 30 mL), brine (30 mL), dried over MgSO₄ and concentrated *in vacuo*. The crude product was purified by reversed-phase flash column chromatography (H₂O/MeOH, gradient from 10:0 to 3:7) to yield amide **6.13** in 54% (349 mg, 0.760 mmol) as an orange oil.

TLC (DCM/MeOH/HOAc/H₂O, 90:10:0.6:0.6): R_f = 0.55. **¹H NMR (CD₃OD, 400 MHz, 27 °C):** δ = 7.77–7.67 (m, 6H, ArH), 6.74–6.70 (m, 2H, ArH), 3.37–3.31 (m, 4H, 2 x CH₂), 2.79–2.75 (m, 2H, CH₂), 1.43 (s, 9H, C(CH₃)₃) ppm. **¹³C NMR (CD₃OD, 100 MHz, 27 °C):** δ = 168.5, 156.9, 152.0, 149.4, 144.3, 139.4, 124.6, 122.4, 119.9, 113.7, 78.8, 39.3, 39.1, 37.6, 27.3 ppm. **IR (neat, ATR):** $\tilde{\nu}$ = 3355 (w), 2976 (w), 2930 (w), 2488 (w), 1677 (s), 1624 (m), 1597 (s), 1505 (m), 1477 (m), 1404 (m), 1365 (m), 1299 (m), 1248 (m), 1152 (vs), 1041 (w), 985 (w), 946 (w), 845 (m), 762 (vs), 666 (m) cm⁻¹. **HRMS (ESI⁺):** *m/z* calcd. for [C₂₁H₂₈N₅O₃S₂]⁺: 462.1639, found: 462.1634 ([M+H]⁺).

Synthesis of 2-((4-((4-(2-((*tert*-butoxycarbonyl)amino)ethyl)disulfanyl)acetamido)-phenyl)diazanyl)phenyl)amino)-*N,N,N*-triethyl-2-oxoethan-1-aminium formate (6.15**)**



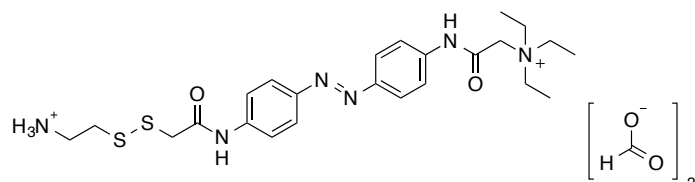
2-(Triethylammonio)acetate (239 mg, 1.50 mmol, 5.0 equiv.) was dissolved in MeCN (10 mL) and oxalyl chloride (0.75 mL, 2 M in DCM, 1.5 mmol, 5.0 equiv.) was added, followed by DMF (3 drops). The mixture was stirred for 1 h at room temperature. The solvent was removed *in vacuo* and dried under high vacuum for 30 min. The crude product was redissolved in DMF (7 mL) and slowly added to a solution of aniline **6.13** (138 mg, 0.300 mmol, 1.0 equiv.) and DIPEA (0.26 mL, 1.5 mmol, 5.0 equiv.) in DMF (13 mL) at 0 °C. The reaction mixture was slowly warmed to room temperature and stirred for 16 h. The solvent was removed under reduced pressure and the crude product was purified by reversed-phase flash column chromatography (H₂O/MeOH (+ 0.1% HCO₂H), gradient from 100:0 to 55:45) to yield amide **6.15** as its formate salt in 19% (35 mg, 0.058 mmol) as an orange oil.

¹H NMR (CD₃OD, 600 MHz, 27 °C): δ = 8.36 (br s, 1H, HCO₂⁻), 7.94–7.88 (m, 4H, ArH), 7.82–7.76 (m, 4H, ArH), 4.21 (s, 2H, CH₂), 3.69 (q, *J* = 7.2 Hz, 6H, 3 x CH₂), 3.62–3.57 (m, 2H, CH₂), 3.37–3.33 (m, 2H, CH₂), 2.87–2.83 (m, 2H, CH₂), 1.45–1.38 (m, 18H, C(CH₃)₃, 3 x CH₃) ppm. **¹³C NMR (CD₃OD, 150 MHz, 27 °C):** δ = 168.6, 166.5, 161.8, 156.9, 149.4, 148.9, 141.1, 139.8, 123.3, 123.3, 120.1, 119.8, 78.8, 56.1, 54.4, 43.0, 39.1, 37.6, 27.3, 6.5 ppm.

IR (neat, ATR): $\tilde{\nu}$ = 3263 (w), 2980 (w), 1691 (m), 1595 (vs), 1549 (s), 1501 (m), 1454 (w), 1413 (w), 1362 (w), 1326 (m), 1254 (m), 1158 (m), 1009 (w), 948 (w), 853 (m), 782 (w) cm^{-1} .

HRMS (ESI⁺): m/z calcd. for $[\text{C}_{30}\text{H}_{46}\text{N}_6\text{O}_4\text{S}_2]^+$: 604.2865, found: 604.2846 ($[\text{M}-\text{HCO}_2+\text{H}]^+$).

Synthesis of 2-((4-((2-((2-ammonioethyl)disulfanyl)acetamido)phenyl)diazenyl)phenyl)-amino)-*N,N,N*-triethyl-2-oxoethan-1-aminium formate (MS2)

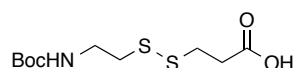


Boc-protected amine **6.15** (26 mg, 0.043 mmol) was dissolved in 1,4-dioxane (2 mL) and DMF (0.4 mL). A 4 M solution of HCl in 1,4-dioxane (2 mL) was added and the reaction mixture was stirred at room temperature for 16 h. The solvent was removed under reduced pressure and the crude product was purified by reversed-phase flash column chromatography (H₂O/MeOH (+ 0.1% HCO₂H), gradient from 10:0 to 8:2) to yield **MS2** as its formate salt in 67% (17 mg, 0.029 mmol) as an orange oil.

¹H NMR (CD₃OD, 400 MHz, 27 °C): δ = 8.43 (br s, 2H, 2 x HCO₂⁻), 7.93–7.86 (m, 4H, ArH), 7.81–7.76 (m, 4H, ArH), 4.27–4.14 (m, 2H, CH₂), 3.74–3.57 (m, 8H, 3 x CH₂, CH₂), 3.34–3.30 (m, 2H, CH₂), 3.07–2.99 (m, 2H, CH₂), 1.38 (t, J = 7.2 Hz, 9H, 3 x CH₃) ppm. **¹³C NMR (CD₃OD, 100 MHz, 27 °C):** δ = 168.4, 167.4, 161.8, 149.4, 149.0, 141.0, 139.9, 126.4, 123.3, 123.2, 122.7, 120.1, 119.8, 119.5, 119.2, 56.2, 54.4, 42.3, 37.8, 34.4, 6.5 ppm. **IR (neat, ATR):** $\tilde{\nu}$ = 2989 (m), 1687 (m), 1591 (vs), 1549 (s), 1500 (s), 1458 (m), 1412 (m), 1377 (m), 1329 (m), 1255 (m), 1156 (m), 1112 (w), 1010 (w), 953 (w), 900 (w), 852 (m), 764 (w), 732 (w) cm^{-1} . **HRMS (ESI⁺):** m/z calcd. for $[\text{C}_{24}\text{H}_{36}\text{N}_6\text{O}_2\text{S}_2]^+$: 504.2341, found: 504.2331 ($[\text{M}-2\text{HCO}_2+\text{H}]^+$).

UV/Vis: λ_{max} = 377, 456 nm.

Synthesis of 3-((2-((*tert*-butoxycarbonyl)amino)ethyl)disulfanyl)propanoic acid (6.11)

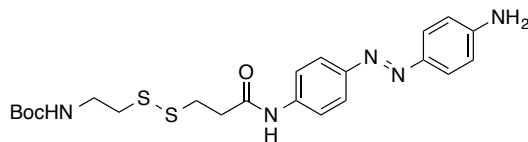


Di-Boc-cystamine **6.7** (1.76 g, 5.00 mmol, 1.0 equiv.) was dissolved in CHCl₃ (30 mL) and TEA (4.37 mL, 31.5 mmol, 6.3 equiv.) was added. To this solution, 3-mercaptopropionic acid **6.9** (0.44 mL, 5.0 mmol, 1.0 equiv.) was added in portions. The reaction mixture was stirred at

room temperature for 2.5 h. The organic phase was washed with 0.5 M KHSO₄ (3 x 30 mL) and dried over MgSO₄. The solvent was removed under reduced pressure and the residue was dissolved in Et₂O (100 mL). The organic phase was extracted with sat. aqu. NaHCO₃ (3 x 50 mL) and the combined aqueous phases were washed with Et₂O (100 mL), followed by acidification with 0.5 M KHSO₄ to pH = 3. The aqueous phase was extracted with CHCl₃ (5 x 30 mL), washed with brine (100 mL), dried over MgSO₄ and concentrated *in vacuo*. Disulfide **6.11** was obtained in 30% yield (419 mg, 1.49 mmol) as colorless oil.

TLC (DCM/MeOH/HOAc/H₂O, 90:10:0.6:0.6): R_f = 0.54. **¹H NMR (DMSO-d₆, 400 MHz, 27 °C):** δ = 12.36 (br s, 1H, CO₂H), 6.96 (t, *J* = 5.4 Hz, 1H, NH), 3.27–3.11 (m, 2H, CH₂), 2.94–2.83 (m, 2H, CH₂), 2.80–2.68 (m, 2H, CH₂), 2.66–2.55 (m, 2H, CH₂), 1.37 (s, 9H, C(CH₃)₃) ppm. **¹³C NMR (DMSO-d₆, 100 MHz, 27 °C):** δ = 173.1, 155.9, 78.2, 38.1, 34.1, 34.0, 33.5, 33.4, 28.7 ppm. **IR (neat, ATR):** $\tilde{\nu}$ = 3345 (w), 2978 (m), 2931 (w), 1708 (vs), 1517 (m), 1480 (w), 1454 (w), 1394 (m), 1367 (m), 1251 (s), 1164 (vs), 1046 (w), 1029 (w), 949 (w), 863 (w), 779 (w) cm⁻¹. **HRMS (ESI):** *m/z* calcd. for [C₁₀H₁₈NO₄S₂]: 280.0677, found: 280.0679 ([M-H]).

Synthesis of *tert*-butyl (2-((3-((4-((4-aminophenyl)diazenyl)phenyl)amino)-3-oxopropyl)disulfanyl)ethyl)carbamate (**6.14**)

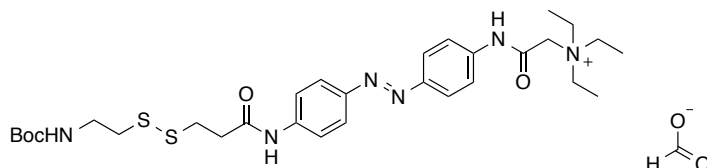


4,4'-Azodianiline **6.12** (189 mg, 0.890 mmol, 1.0 equiv.), carboxylic acid **6.11** (250 mg, 0.890 mmol, 1.0 equiv.) and HBTU (1.01 g, 2.67 mmol, 3.6 equiv.) were dissolved in THF (12 mL) and TEA (0.37 mL, 2.7 mmol, 3.6 equiv.) was added. The reaction mixture was then heated to reflux for 24 h. EtOAc (25 mL) was added to the cooled mixture and the organic phase was washed with sat. aqu. NaHCO₃ (2 x 20 mL), brine (20 mL), dried over MgSO₄ and concentrated *in vacuo*. The crude product was purified by reversed-phase flash column chromatography (H₂O/MeOH, gradient from 10:0 to 1:9) to yield amide **6.14** in 30% (130 mg, 0.270 mmol) as a red oil.

TLC (DCM/MeOH/HOAc/H₂O, 90:10:0.6:0.6): R_f = 0.74. **¹H NMR (CD₃OD, 400 MHz, 27 °C):** δ = 7.79–7.73 (m, 2H, ArH), 7.72–7.65 (m, 4H, ArH), 6.76–6.70 (m, 2H, ArH), 3.07–3.01 (m, 2H, CH₂), 2.85–2.78 (m, 4H, 2 x CH₂), 1.42 (s, 9H, C(CH₃)₃) ppm. **¹³C NMR (CD₃OD, 100 MHz, 27 °C):** δ = 170.7, 157.0, 151.9, 149.2, 144.3, 139.8, 124.6, 122.4, 119.8,

113.8, 78.8, 39.3, 37.7, 36.2, 33.6, 27.3 ppm. **IR (neat, ATR):** $\tilde{\nu}$ = 3354 (m), 3041 (w), 2977 (w), 2930 (w), 1680 (m), 1622 (m), 1597 (vs), 1534 (s), 1506 (s), 1456 (w), 1425 (m), 1402 (m), 1366 (m), 1300 (m), 1253 (m), 1160 (m), 1141 (m), 1045 (w), 950 (w), 844 (m), 780 (w), 754 (w) cm^{-1} . **HRMS (ESI):** m/z calcd. for $[\text{C}_{22}\text{H}_{28}\text{N}_5\text{O}_3\text{S}_2]^+$: 474.1634, found: 474.1633 ($[\text{M}-\text{H}]^+$).

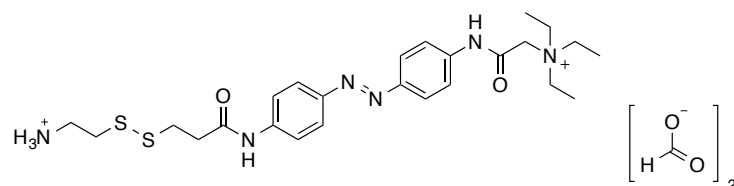
Synthesis of 2-((4-((4-(3-((2-((tert-butoxycarbonyl)amino)ethyl)disulfanyl)propanamido)-phenyl)diazenyl)phenyl)amino)-N,N,N-triethyl-2-oxoethan-1-aminium formate (6.16)



2-(Triethylammonio)acetate (215 mg, 1.35 mmol, 5.0 equiv.) was dissolved in MeCN (10 mL) and oxalyl chloride (0.68 mL, 2 M in DCM, 1.4 mmol, 5.0 equiv.) was added, followed by DMF (3 drops). The mixture was stirred for 1 h at room temperature. The solvent was removed *in vacuo* and dried under high vacuum for 30 min. The crude product was redissolved in DMF (13 mL) and slowly added to a solution of aniline **6.14** (130 mg, 0.270 mmol, 1.0 equiv.) and DIPEA (0.24 mL, 1.4 mmol, 5.0 equiv.) in DMF (7 mL) at 0 °C. The reaction mixture was slowly warmed to room temperature and stirred for 16 h. The solvent was removed under reduced pressure and the crude product was purified by reversed-phase flash column chromatography ($\text{H}_2\text{O}/\text{MeOH}$ (+ 0.1% HCO_2H), gradient from 100:0 to 55:45) to yield amide **6.16** as its formate salt in 52% (94 mg, 0.14 mmol) as an orange oil.

^1H NMR (CD_3OD , 600 MHz, 27 °C): δ = 8.34 (br s, 1H, HCO_2^-), 7.93–7.85 (m, 4H, ArH), 7.83–7.74 (m, 4H, ArH), 4.22 (s, 2H, CH_2), 3.68 (q, J = 7.2 Hz, 6H, 3 x CH_2), 3.37–3.34 (m, 2H, CH_2), 3.08–3.03 (m, 2H, CH_2), 2.87–2.83 (m, 2H, CH_2), 2.83–2.80 (m, 2H, CH_2), 1.43 (s, 9H, $\text{C}(\text{CH}_3)_3$), 1.39 (t, J = 7.2 Hz, 9H, 3 x CH_3) ppm. **^{13}C NMR (CD_3OD , 100 MHz, 27 °C):** δ = 170.8, 165.7, 161.8, 156.9, 149.4, 148.7, 141.3, 139.8, 123.2, 123.2, 120.1, 119.7, 78.8, 56.2, 54.4, 39.3, 37.8, 36.2, 33.5, 27.3, 6.6 ppm. **IR (neat, ATR):** $\tilde{\nu}$ = 3257 (w), 2979 (w), 1692 (m), 1594 (vs), 1546 (s), 1501 (m), 1455 (m), 1412 (m), 1366 (m), 1345 (m), 1302 (m), 1254 (m), 1210 (w), 1157 (m), 1011 (w), 982 (w), 950 (w), 853 (m), 784 (w) cm^{-1} . **HRMS (ESI $^+$):** m/z calcd. for $[\text{C}_{30}\text{H}_{46}\text{N}_6\text{O}_4\text{S}_2]^+$: 618.3022, found: 618.3001 ($[\text{M}-\text{HCO}_2+\text{H}]^+$).

Synthesis of 2-((4-((4-(3-((2-ammonioethyl)disulfanyl)propanamido)phenyl)diazenyl)-phenyl)amino)-*N,N,N*-triethyl-2-oxoethan-1-aminium formate (MS3)

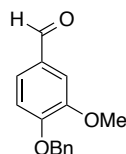


Boc-protected amine **6.16** (40 mg, 0.065 mmol) was dissolved in 1,4-dioxane (2.5 mL) and DMF (0.5 mL). A 4 M solution of HCl in 1,4-dioxane (2.5 mL) was added and the reaction mixture was stirred at room temperature for 16 h. The solvent was removed under reduced pressure and the crude product was purified by reversed-phase flash column chromatography (H₂O/MeOH (+ 0.1% HCO₂H), gradient from 100:0 to 85:15) to yield **MS3** as its formate salt in 66% (26 mg, 0.043 mmol) as an orange oil.

¹H NMR (CD₃OD, 400 MHz, 27 °C): δ = 8.43 (br s, 2H, 2 x HCO₂⁻), 7.93–7.83 (m, 4H, ArH), 7.83–7.69 (m, 4H, ArH), 4.21 (s, 2H, CH₂), 3.67 (q, *J* = 7.2 Hz, 6H, 3 x CH₂), 3.34–3.29 (m, 2H, CH₂), 3.14–3.05 (m, 2H, CH₂), 3.01–2.93 (m, 2H, CH₂), 2.90–2.81 (m, 2H, CH₂), 1.38 (t, *J* = 7.2 Hz, 9H, 3 x CH₃) ppm. **¹³C NMR (CD₃OD, 100 MHz, 27 °C):** δ = 170.7, 167.3, 161.8, 149.4, 148.7, 141.2, 139.8, 126.4 (*cis* isomer), 123.2, 123.2, 122.7 (*cis* isomer), 120.1, 119.7, 119.5 (*cis* isomer), 119.1 (*cis* isomer), 56.1, 54.4, 37.8, 36.0, 33.9, 32.9, 6.5 ppm. **IR (neat, ATR):** $\tilde{\nu}$ = 2990 (m), 1690 (m), 1593 (vs), 1501 (m), 1412 (m), 1375 (m), 1346 (m), 1302 (m), 1257 (m), 1156 (m), 852 (m), 766 (w) cm⁻¹. **HRMS (ESI⁺):** *m/z* calcd. for [C₂₅H₃₇N₆O₂S₂]⁺: 517.2419, found: 517.2416 ([M-2 HCO₂+H]⁺). **UV/Vis:** λ_{max} = 376, 455 nm.

6.5.5 SYNTHESIS OF PEG

Synthesis of 4-(benzyloxy)-3-methoxybenzaldehyde (6.17)

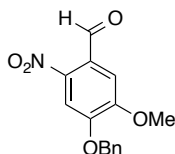


Vanillin (20.0 g, 131 mmol, 1.0 equiv.) was dissolved in acetone (300 mL) and K₂CO₃ (9.10 g, 65.5 mmol, 0.5 equiv.) and benzyl bromide (15.6 mL, 131 mmol, 1.0 equiv.) were added. The

mixture was heated under reflux for 20 h and then poured into water (300 mL). The resulting yellowish oil was extracted with DCM (3 x 75 mL). The combined organic layers were dried over MgSO₄ and concentrated *in vacuo*. The crude product was purified by flash silica gel column chromatography (hexanes/EtOAc, gradient from 20:1 to 6:1) to yield benzyl ether **6.17** (30.5 g, 126 mmol, 96%) as a colorless solid.

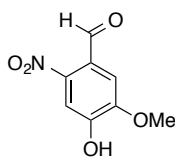
TLC (hexanes/EtOAc, 4:1): $R_f = 0.36$. **M.p.:** 63–64 °C. **¹H NMR (CDCl₃, 300 MHz, 27 °C):** $\delta = 9.86$ (s, 1H, CHO), 7.49–7.31 (m, 7H, ArH), 7.01 (d, $J = 8.2$ Hz, 1H, ArH), 5.27 (s, 2H, CH₂), 3.96 (s, 3H, OCH₃) ppm. **¹³C NMR (CDCl₃, 75 MHz, 27 °C):** $\delta = 190.8, 153.6, 150.1, 136.0, 130.3, 128.7, 128.2, 127.2, 126.6, 112.4, 109.4, 70.9, 56.1$ ppm. **IR (neat, ATR):** $\tilde{\nu} = 1680$ (s), 1585 (s), 1507 (s), 1464 (m), 1454 (m), 1424 (m), 1396 (w), 1340 (w), 1265 (vs), 1236 (m), 1194 (w), 1158 (m), 1135 (s), 1081 (w), 1022 (m), 919 (w), 866 (w), 809 (w), 782 (w), 733 (m), 698 (m), 658 (w) cm⁻¹. **HRMS (EI⁺):** m/z calcd. for [C₁₅H₁₄O₃]⁺: 242.0943, found: 242.0939 ([M]⁺).

Synthesis of 4-(benzyloxy)-5-methoxy-2-nitrobenzaldehyde (**6.18**)



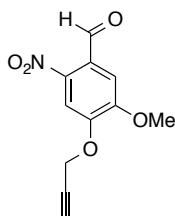
Compound **6.17** (14.6 g, 60.1 mmol) was added in 5 portions to aqu. 65% HNO₃ (75 mL) at 0 °C. The reaction mixture was stirred at 0 °C for 30 min, followed by 2 h at room temperature. The mixture was poured onto ice water (500 mL) and the solids were filtered and dried under high vacuum, yielding *ortho*-nitro aldehyde **6.18** (15.1 g, 52.6 mmol, 88%) as yellow crystals.

TLC (hexanes/EtOAc, 4:1): $R_f = 0.38$. **M.p.:** 122–124 °C. **¹H NMR (CDCl₃, 300 MHz, 27 °C):** $\delta = 10.46$ (s, 1H, CHO), 7.69 (s, 1H, ArH), 7.51–7.34 (m, 6H, ArH), 5.29 (s, 2H, CH₂), 4.04 (s, 3H, OCH₃) ppm. **¹³C NMR (CDCl₃, 75 MHz, 27 °C):** $\delta = 187.7, 153.7, 151.4, 143.6, 134.8, 128.9, 128.7, 127.6, 125.7, 110.0, 108.9, 71.6, 56.7$ ppm. **IR (neat, ATR):** $\tilde{\nu} = 1678$ (m), 1568 (m), 1511 (s), 1456 (w), 1402 (w), 1329 (m), 1281 (s), 1222 (m), 1165 (m), 1058 (vs), 978 (s), 872 (m), 849 (m), 802 (w), 752 (s), 699 (m) cm⁻¹. **HRMS (EI⁺):** m/z calcd. for [C₁₅H₁₃NO₅]⁺: 287.0794, found: 287.0802 ([M]⁺).

Synthesis of 4-hydroxy-5-methoxy-2-nitrobenzaldehyde (6.19)

Benzyl ether **6.18** (15.1 g, 52.6 mmol) was dissolved in a mixture of HOAc (100 mL) and aqu. 48% HBr (33 mL) at 85 °C. The mixture was stirred for 2.5 h at this temperature and then cooled to room temperature. The solids were filtered, washed with water and dried under high vacuum for 12 h. Phenol **6.19** (8.15 g, 41.3 mmol, 79%) was obtained as a yellow solid.

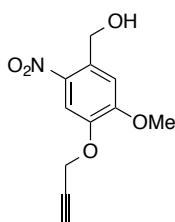
TLC (hexanes/EtOAc, 2:1): R_f = 0.33. **M.p.:** 206–208 °C. **^1H NMR (CDCl₃, 200 MHz, 27 °C):** δ = 10.40 (s, 1H, CHO), 7.68 (s, 1H, ArH), 7.45 (s, 1H, ArH), 6.20 (s, 1H, OH), 4.07 (s, 3H, OCH₃) ppm. **^{13}C NMR (CDCl₃, 75 MHz, 27 °C):** δ = 187.4, 150.3, 149.6, 144.8, 125.0, 111.2, 109.7, 56.9 ppm. **IR (neat, ATR):** $\tilde{\nu}$ = 3120 (m), 1670 (s), 1583 (s), 1512 (vs), 1460 (w), 1439 (w), 1421 (m), 1368 (m), 1326 (m), 1297 (vs), 1276 (vs), 1210 (s), 1180 (s), 1159 (s), 1056 (s), 990 (m), 914 (m), 900 (w), 883 (m), 809 (m), 735 (s), 720 (s), 681 (m) cm⁻¹. **HRMS (EI⁺):** m/z calcd. for [C₈H₇NO₅]⁺: 197.0324, found: 197.0304 ([M]⁺).

Synthesis of 5-methoxy-2-nitro-4-(prop-2-yn-1-yloxy)benzaldehyde (6.20)

Phenol **6.19** (1.55 g, 7.86 mmol, 1.0 equiv.) was dissolved in DMF (20 mL) and K₂CO₃ (1.41 g, 10.2 mmol, 1.3 equiv.) was added, followed by propargyl bromide (80% in toluene; 0.910 mL, 10.2 mmol, 1.3 equiv.). The mixture was heated to 50 °C for 3 h. Water (50 mL) was added and the mixture was extracted with EtOAc (3 x 30 mL). The combined organic layers were washed with aqu. 5% NaOH (3 x 50 mL) and brine (3 x 50 mL). The organic phase was dried over MgSO₄ and concentrated under reduced pressure. The crude product was purified by flash silica gel column chromatography (hexanes/EtOAc, 4:1) to give propargyl ether **6.20** (1.75 g, 7.44 mmol, 95%) as a yellow solid.

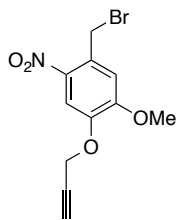
TLC (hexanes/EtOAc, 4:1): R_f = 0.33. **M.p.:** 133–136 °C. **^1H NMR (CDCl₃, 300 MHz, 27 °C):** δ = 10.49 (s, 1H, CHO), 7.82 (s, 1H, ArH), 7.46 (s, 1H, ArH), 4.94 (d, J = 2.4 Hz, 2H, CH₂), 4.05 (s, 3H, OCH₃), 2.68–2.61 (m, 1H, CH) ppm. **^{13}C NMR (CDCl₃, 75 MHz, 27 °C):** δ = 187.6, 153.7, 149.9, 143.4, 126.4, 110.3, 109.5, 77.7, 76.4, 57.2, 56.8 ppm. **IR (neat, ATR):** $\tilde{\nu}$ = 1688 (m), 1570 (m), 1508 (s), 1460 (m), 1396 (m), 1328 (m), 1284 (vs), 1222 (vs), 1168 (m), 1059 (s), 1012 (m), 972 (m), 880 (m), 814 (m), 765 (w), 738 (m), 710 (w), 688 (m) cm⁻¹. **HRMS (EI⁺):** m/z calcd. for [C₁₁H₉NO₅]⁺: 235.0481, found: 235.0482 ([M]⁺).

Synthesis of (5-methoxy-2-nitro-4-(prop-2-yn-1-yloxy)phenyl)methanol (6.21)



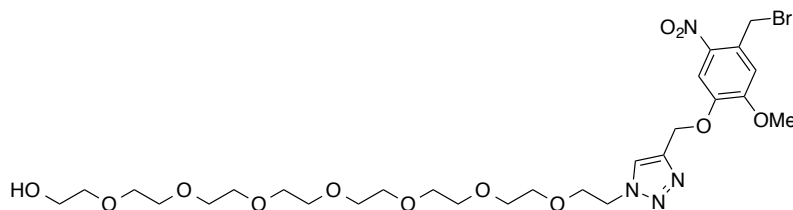
A solution of aldehyde **6.20** (1.73 g, 7.36 mmol, 1.0 equiv.) in MeOH (100 mL) at 0 °C was added to a solution of NaBH₄ in MeOH (50 mL) at 0 °C. The reaction mixture was stirred at this temperature for 1 h and then concentrated under reduced pressure. A sat. aqu. solution of NH₄Cl (100 mL) was added and the aqueous phase was extracted with DCM (5 x 30 mL). The combined organic layers were washed with brine (75 mL), dried over MgSO₄ and concentrated *in vacuo*, affording alcohol **6.21** (1.69 g, 7.12 mmol, 97%) as a yellow solid.

TLC (hexanes/EtOAc, 2:1): R_f = 0.42. **M.p.:** 137–138 °C. **^1H NMR (CDCl₃, 400 MHz, 27 °C):** δ = 7.87 (s, 1H, ArH), 7.20 (s, 1H, ArH), 4.96 (s, 2H, CH₂), 4.85–4.80 (m, 2H, CH₂), 3.99 (s, 3H, OCH₃), 2.68–2.47 (m, 2H, CH, OH) ppm. **^{13}C NMR (CDCl₃, 100 MHz, 27 °C):** δ = 154.5, 145.5, 139.5, 133.3, 111.4, 111.0, 77.1, 76.9, 62.8, 57.1, 56.5 ppm. **IR (neat, ATR):** $\tilde{\nu}$ = 3287 (m), 3264 (m), 1579 (w), 1515 (s), 1494 (m), 1453 (w), 1427 (w), 1383 (m), 1320 (m), 1254 (s), 1215 (m), 1164 (m), 1066 (vs), 1024 (w), 985 (w), 973 (w), 882 (m), 817 (m), 758 (w), 706 (w), 685 (w) cm⁻¹. **HRMS (EI⁺):** m/z calcd. for [C₁₁H₁₁NO₅]⁺: 237.0637, found: 237.0644 ([M]⁺).

Synthesis of 1-(bromomethyl)-5-methoxy-2-nitro-4-(prop-2-yn-1-yloxy)benzene (6.22)

Alcohol **6.21** (200 mg, 0.840 mmol, 1.0 equiv.) was suspended in Et₂O (30 mL) at 0 °C. PBr₃ (1 M in DCM; 2.02 mL, 2.02 mmol, 2.4 equiv.) was added and the mixture was stirred at 0 °C for 20 min, followed by 5 h at room temperature. The reaction was quenched by the addition of MeOH (2 mL) and then poured into water (100 mL). The aqueous phase was extracted with EtOAc (5 x 30 mL), dried over MgSO₄ and concentrated under reduced pressure. The crude product was purified by flash silica gel column chromatography (hexanes/EtOAc, gradient from 6:1 to 4:1) to give bromide **6.22** (111 mg, 0.370 mmol, 44%) as a yellowish solid.

TLC (hexanes/EtOAc, 2:1): R_f = 0.56. **M.p.:** 120 °C (dec.). **¹H NMR (CDCl₃, 300 MHz, 27 °C):** δ = 7.86 (s, 1H, ArH), 7.00 (s, 1H, ArH), 4.89 (s, 2H, CH₂), 4.86 (d, J = 2.4 Hz, 2H, CH₂), 4.01 (s, 3H, OCH₃), 2.62 (t, J = 2.4 Hz, 1H, CH) ppm. **¹³C NMR (CDCl₃, 75 MHz, 27 °C):** δ = 153.7, 146.5, 140.0, 128.4, 114.1, 111.2, 77.2, 76.9, 57.1, 56.6, 29.9 ppm. **IR (neat, ATR):** $\tilde{\nu}$ = 3286 (w), 1611 (w), 1581 (m), 1515 (vs), 1463 (m), 1398 (w), 1329 (s), 1271 (vs), 1212 (s), 1179 (m), 1123 (w), 1062 (s), 1024 (m), 987 (m), 928 (w), 871 (m), 817 (w), 793 (m), 760 (w), 732 (w), 676 (w) cm⁻¹. **HRMS (EI⁺):** m/z calcd. for [C₁₁H₁₀BrNO₄]⁺: 298.9793, found: 298.9768 ([M]⁺).

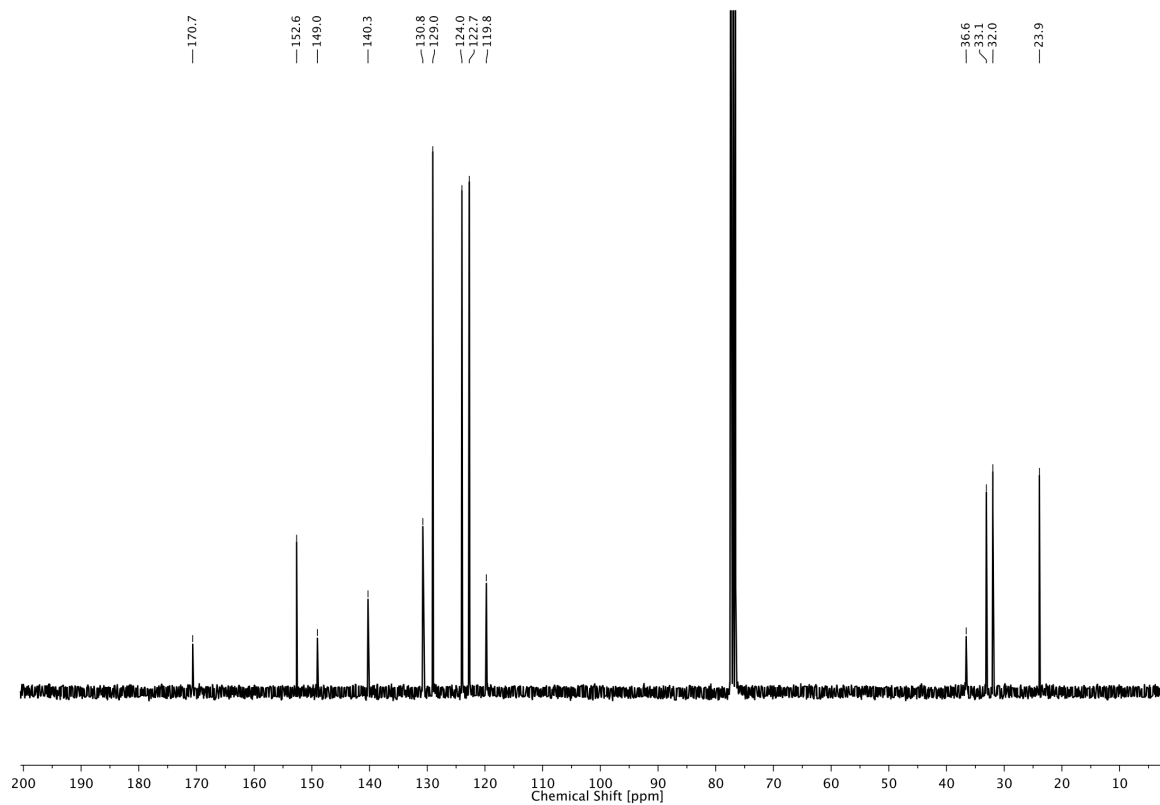
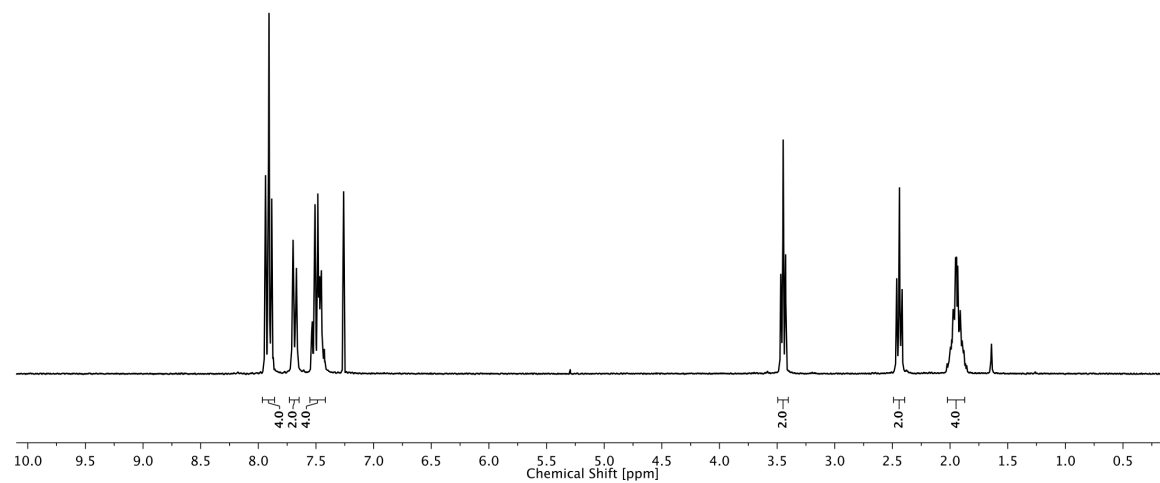
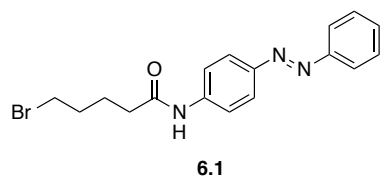
Synthesis of 23-(4-((4-(bromomethyl)-2-methoxy-5-nitrophenoxy)methyl)-1H-1,2,3-triazol-1-yl)-3,6,9,12,15,18,21-heptaooxatricosan-1-ol (PEG)

PEG azide **6.23** (26 mg, 0.066 mmol, 2.0 equiv.) was dissolved in THF (1 mL) and H₂O (1 mL). CuSO₄ • 5 H₂O (1.0 mg, 0.0040 mmol, 0.1 equiv.) and sodium ascorbate (1.6 mg, 0.0080 mmol, 0.2 equiv.) were added, followed by alkyne **6.22** (10 mg, 0.033 mmol, 1.0 equiv.). The mixture was stirred at room temperature for 16 h. H₂O (10 mL) was added and the aqueous phase was

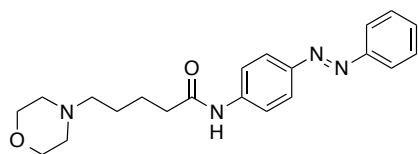
extracted with CHCl_3 (5 x 5 mL). The combined organic layers were washed with brine (20 mL), dried over MgSO_4 and concentrated under reduced pressure. The crude product was purified by flash silica gel column chromatography ($\text{CHCl}_3/\text{MeOH}$, 50:1 \rightarrow 25:1) to give triazole **PEG** (19 mg, 0.027 mmol, 82%) as a yellowish oil.

TLC (DCM/MeOH/H₂O/HOAc, 90:10:0.6:0.6): R_f = 0.37. **¹H NMR (CDCl₃, 600 MHz, 27 °C):** δ = 7.89 (s, 1H, ArH), 7.86 (s, 1H, ArH), 6.93 (s, 1H, ArH), 5.29 (s, 2H, CH₂), 4.83 (s, 2H, CH₂), 4.55–4.52 (m, 2H, CH₂), 3.94 (s, 3H, OCH₃), 3.87–3.83 (m, 2H, CH₂), 3.70–3.67 (m, 3H), 3.65–3.56 (m, 37H, CH₂), 2.68 (br s, 1H, OH) ppm. **¹³C NMR (CDCl₃, 150 MHz, 27 °C):** δ = 153.7, 147.5, 142.2, 140.1, 127.9, 124.7, 114.0, 110.9, 72.5, 70.6, 70.6, 70.6, 70.5, 70.5, 70.5, 70.5, 70.4, 70.3, 70.2, 70.0, 69.3, 63.1, 61.6, 56.5, 50.6, 50.4, 30.0 ppm. **IR (neat, ATR):** $\tilde{\nu}$ = 3434 (m), 2873 (m), 1581 (m), 1523 (vs), 1465 (m), 1346 (m), 1333 (m), 1280 (vs), 1217 (m), 1102 (s), 1063 (s), 986 (w), 949 (w), 829 (w) cm^{-1} . **HRMS (ESI⁺):** m/z calcd. for $[\text{C}_{27}\text{H}_{44}\text{BrN}_4\text{O}_{12}]^+$: 695.2139, found: 695.2134 ($[\text{M}+\text{H}]^+$).

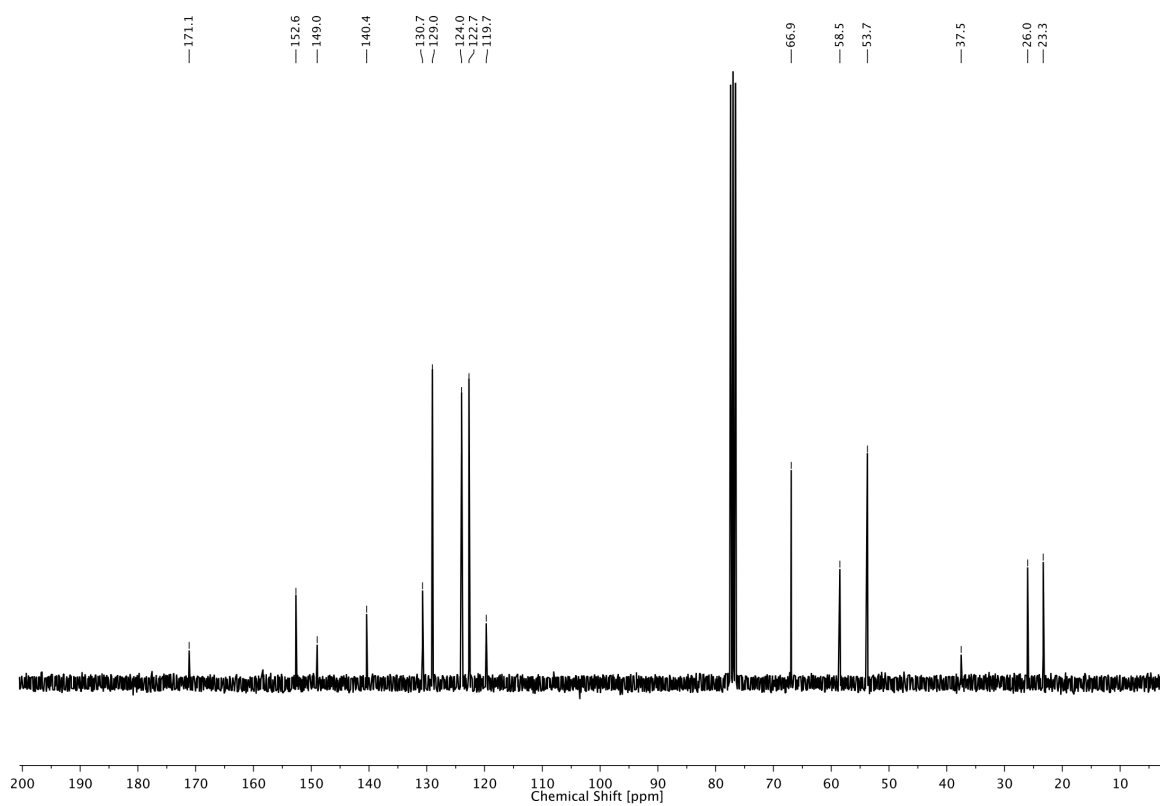
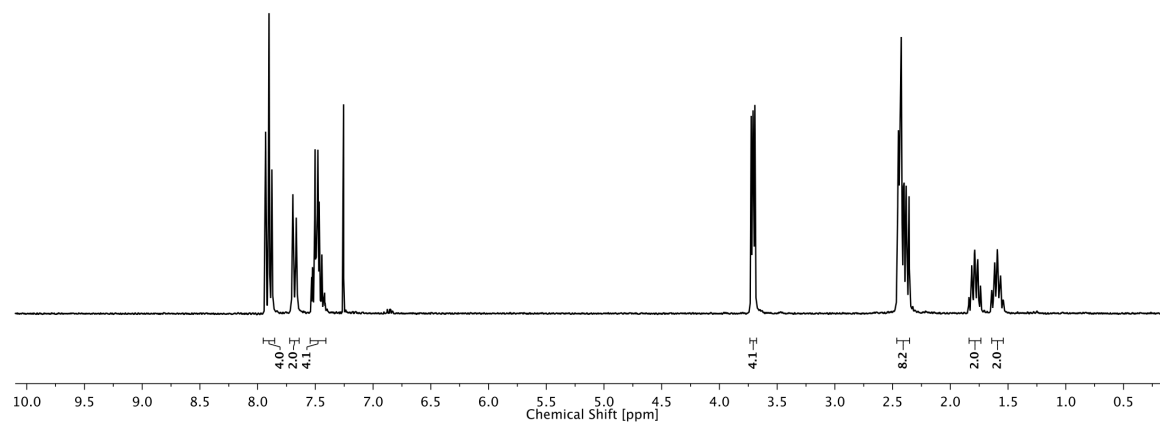
6.6 NMR SPECTRA



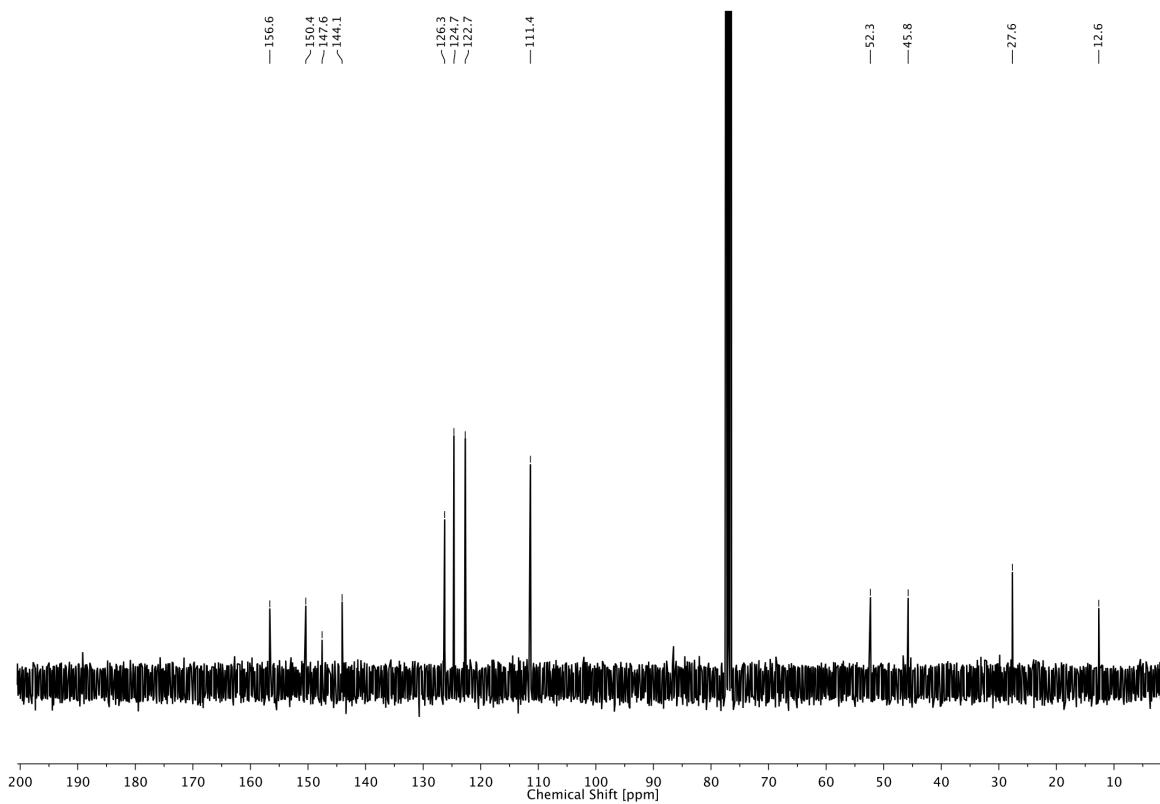
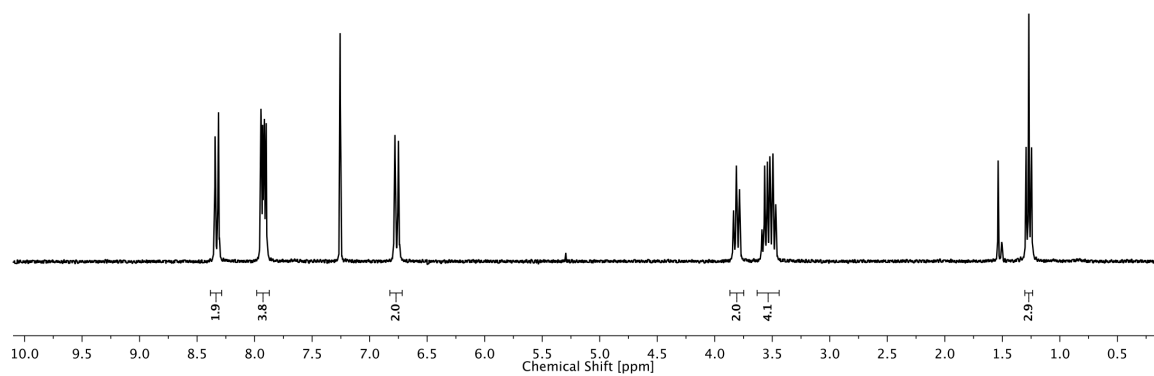
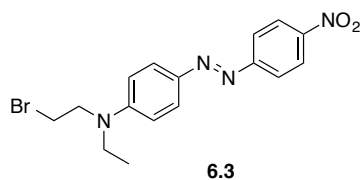
6 MISCELLANEOUS PROJECTS



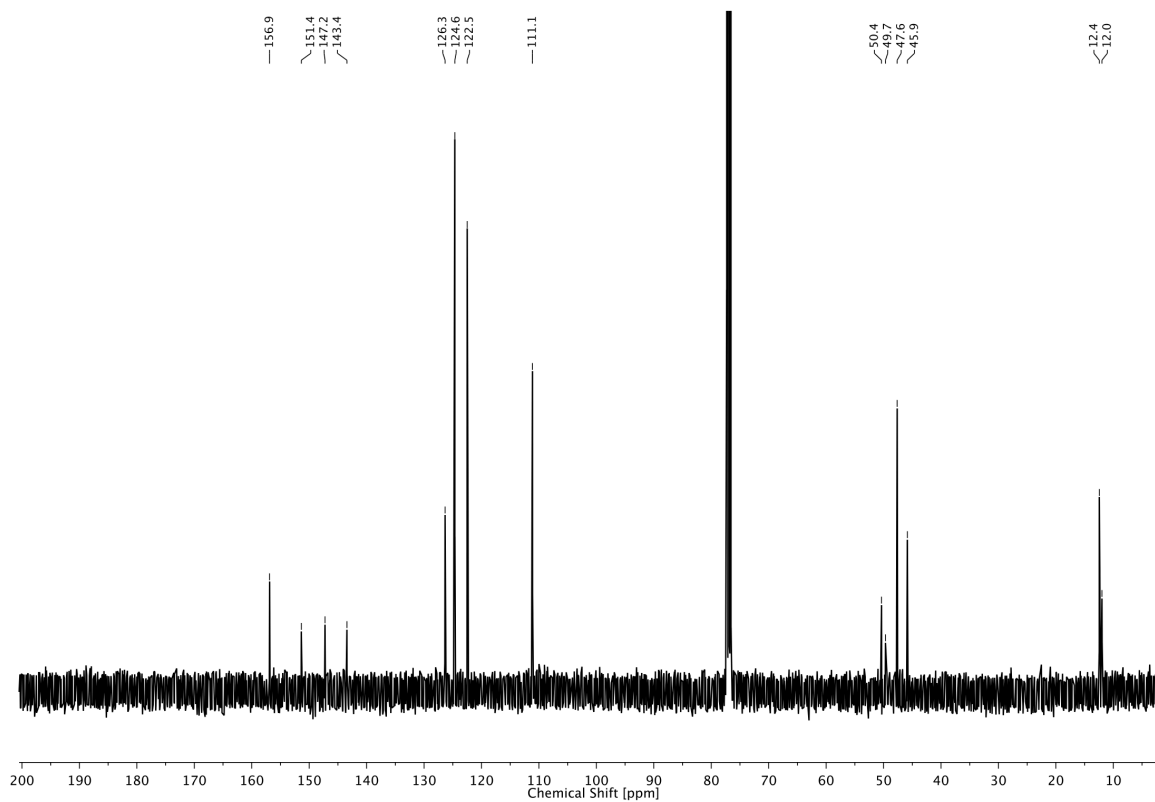
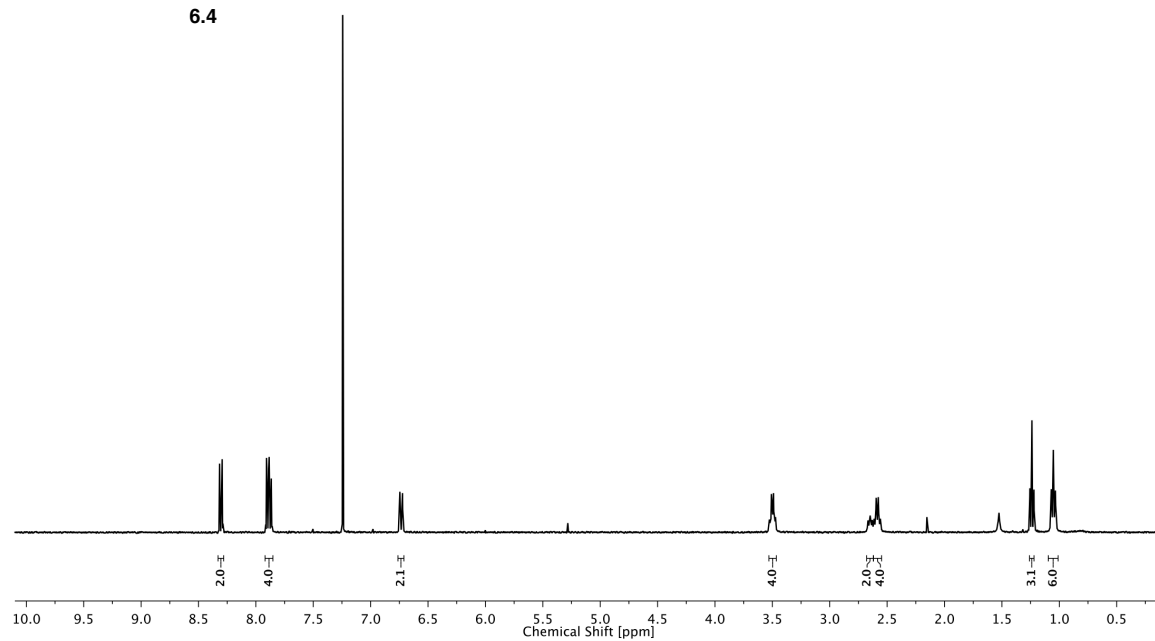
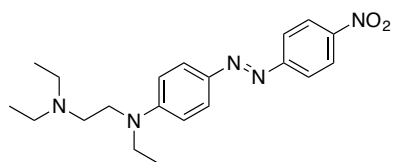
Azo-SEN12333



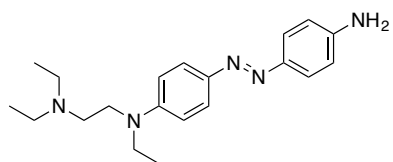
6 MISCELLANEOUS PROJECTS



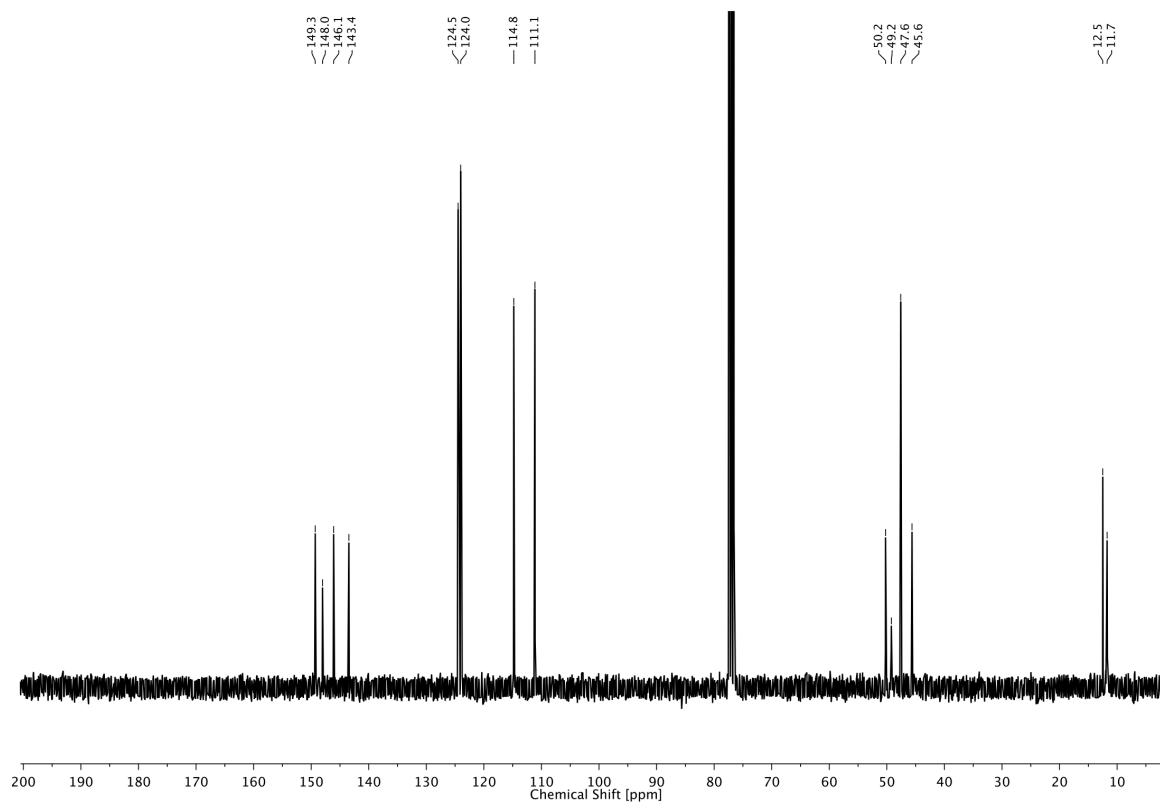
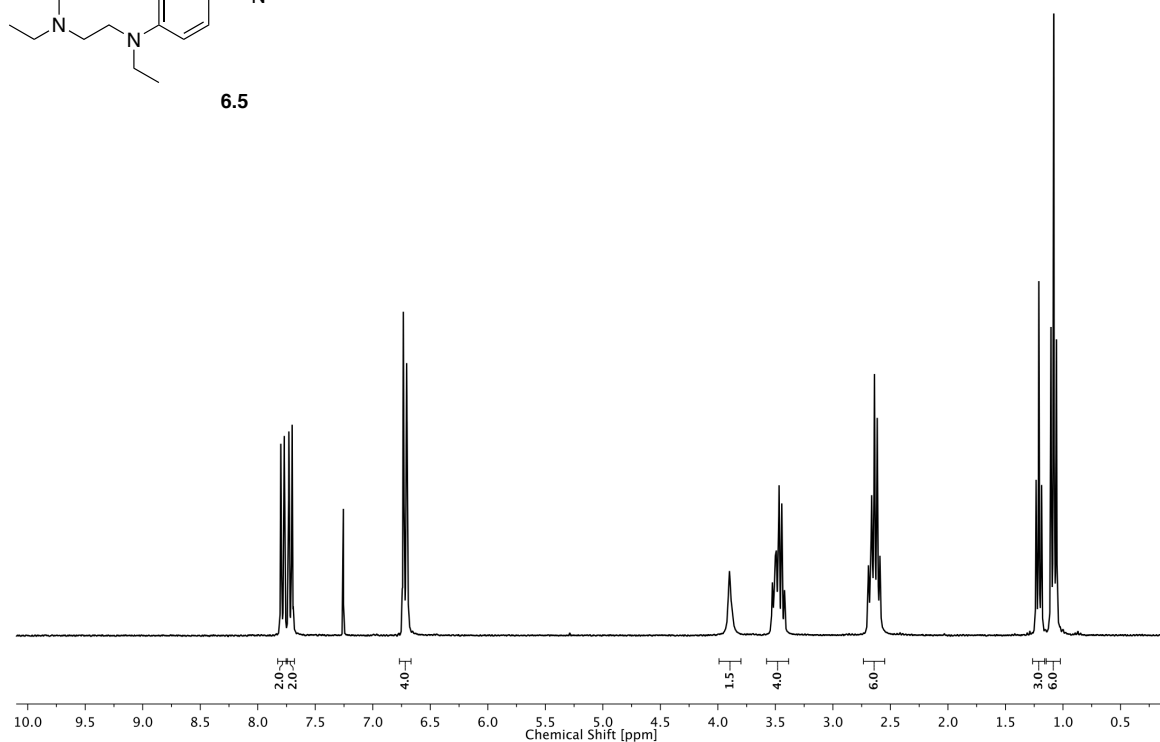
6 MISCELLANEOUS PROJECTS



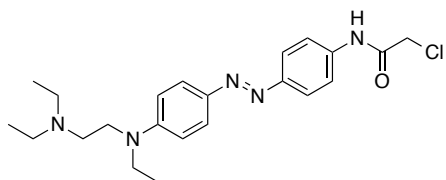
6 MISCELLANEOUS PROJECTS



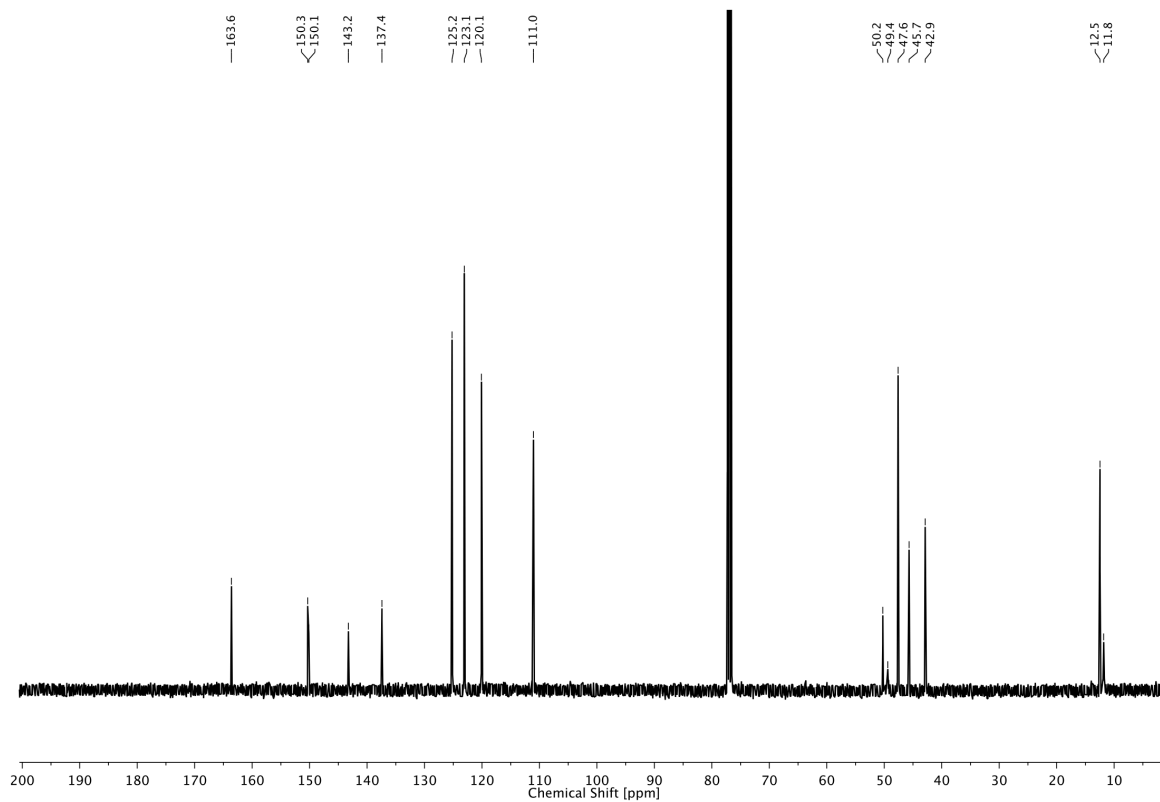
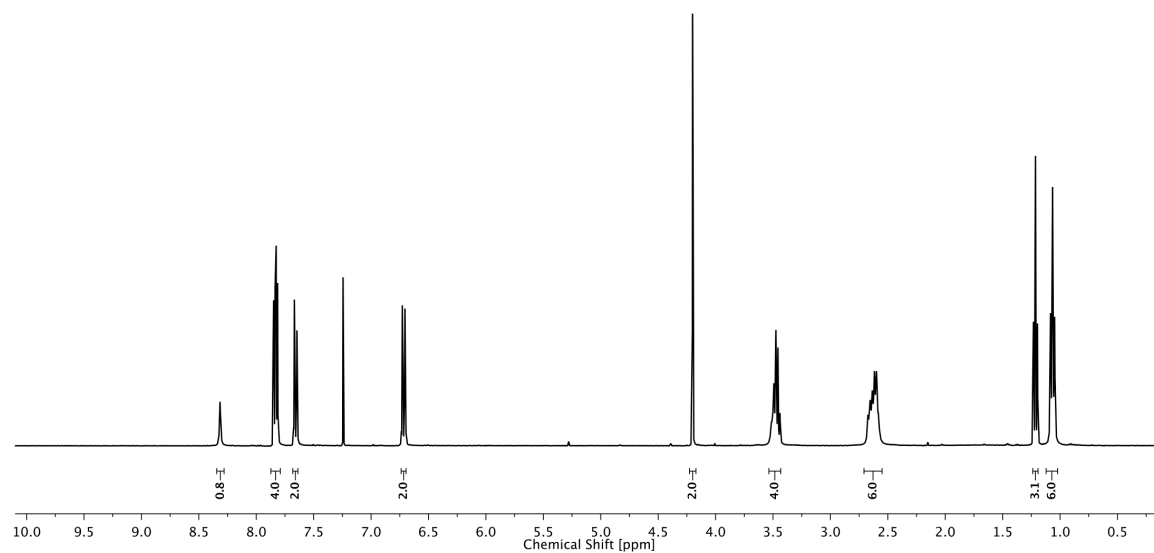
6.5

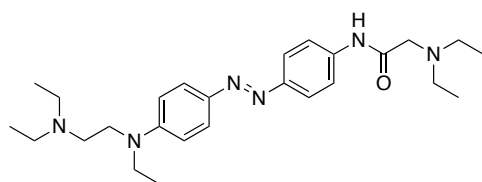


6 MISCELLANEOUS PROJECTS

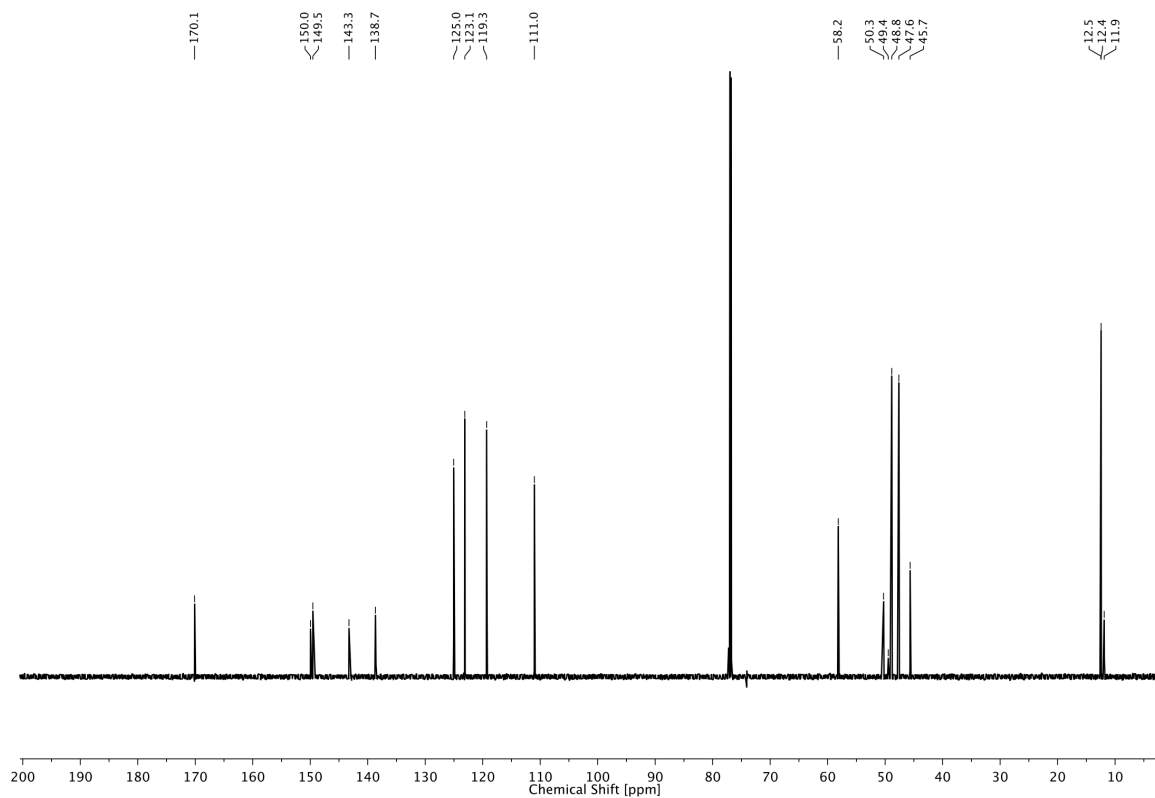
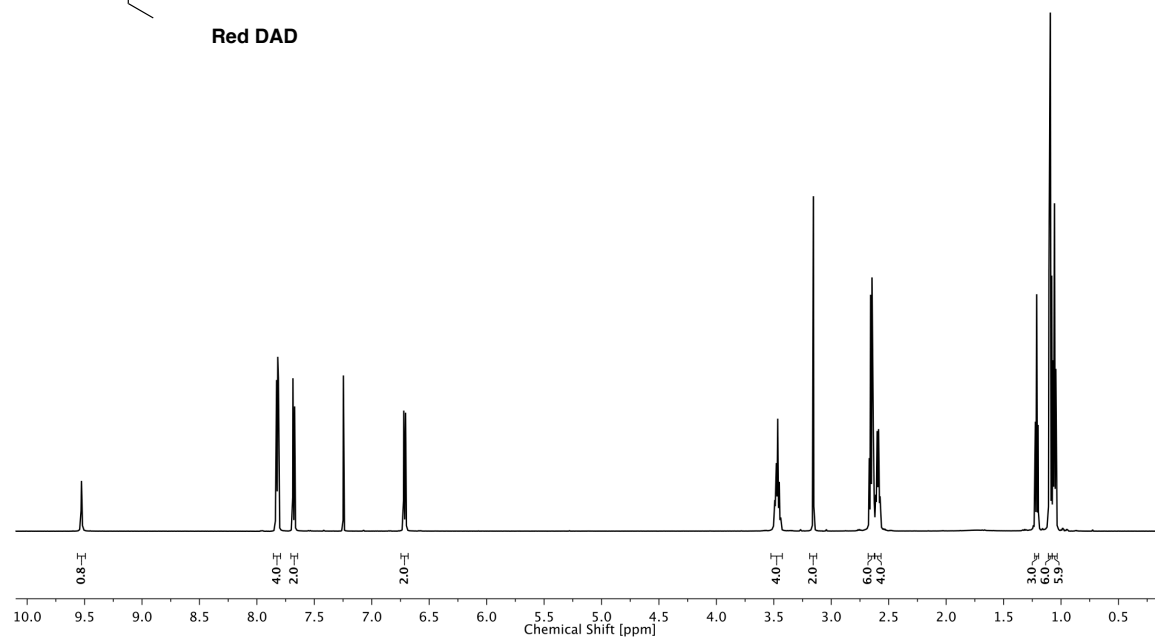


6.6

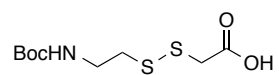




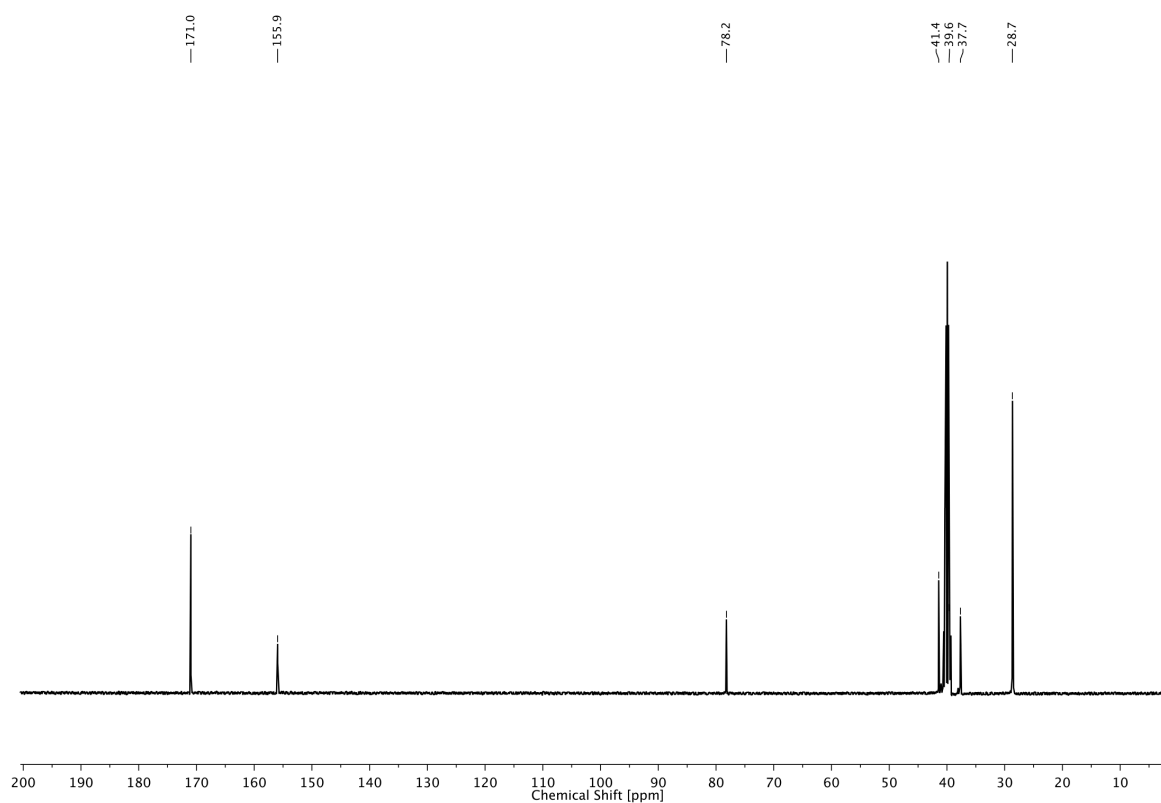
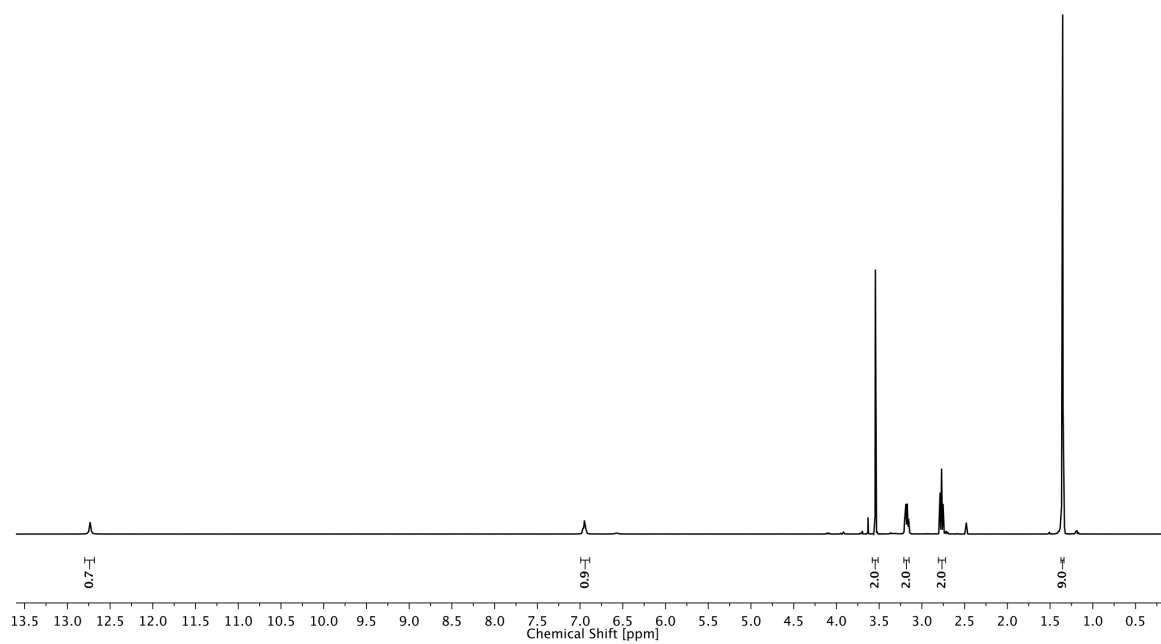
Red DAD

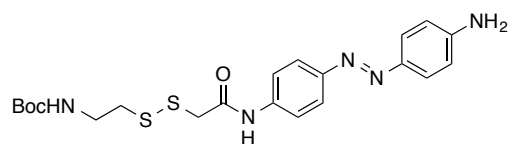


6 MISCELLANEOUS PROJECTS

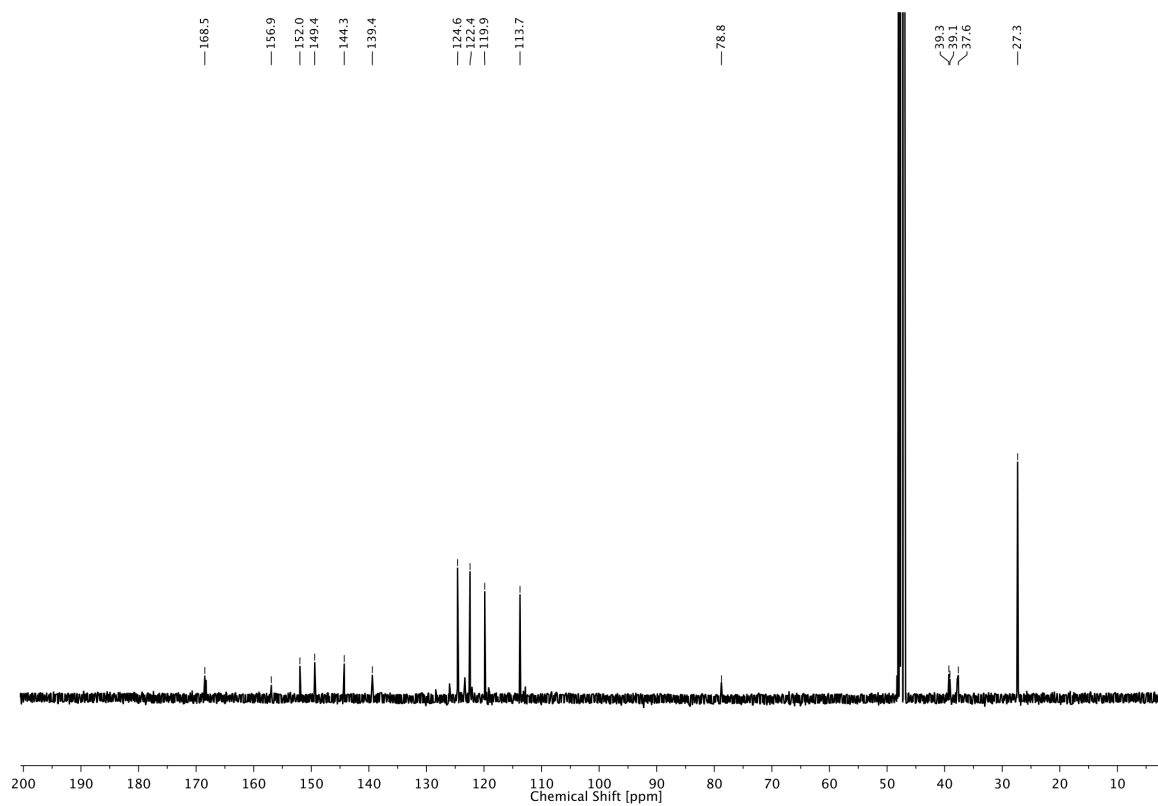
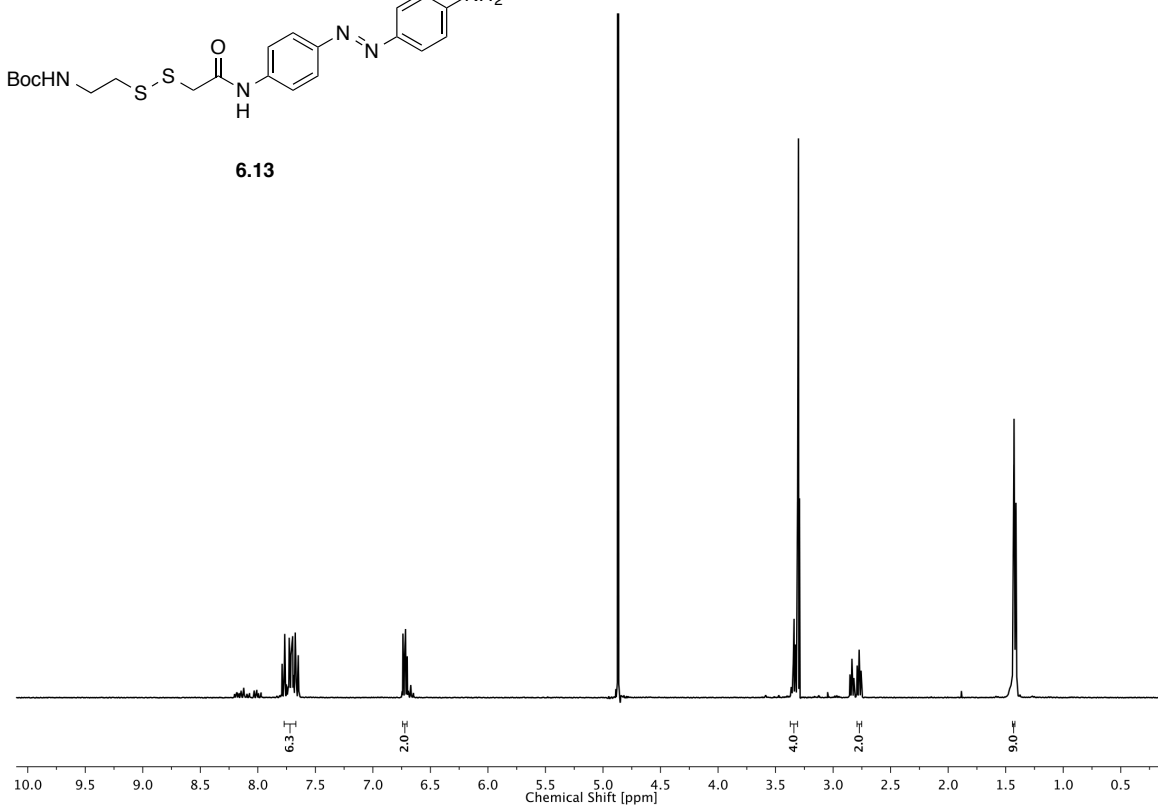


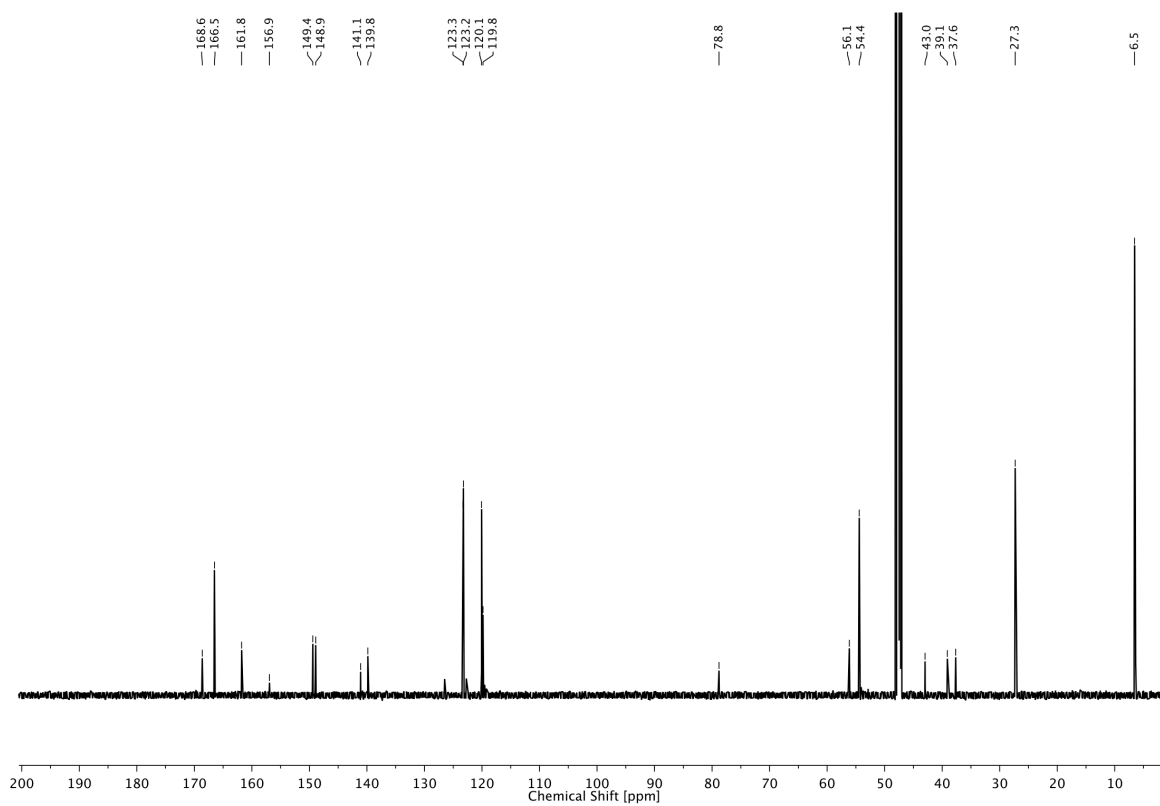
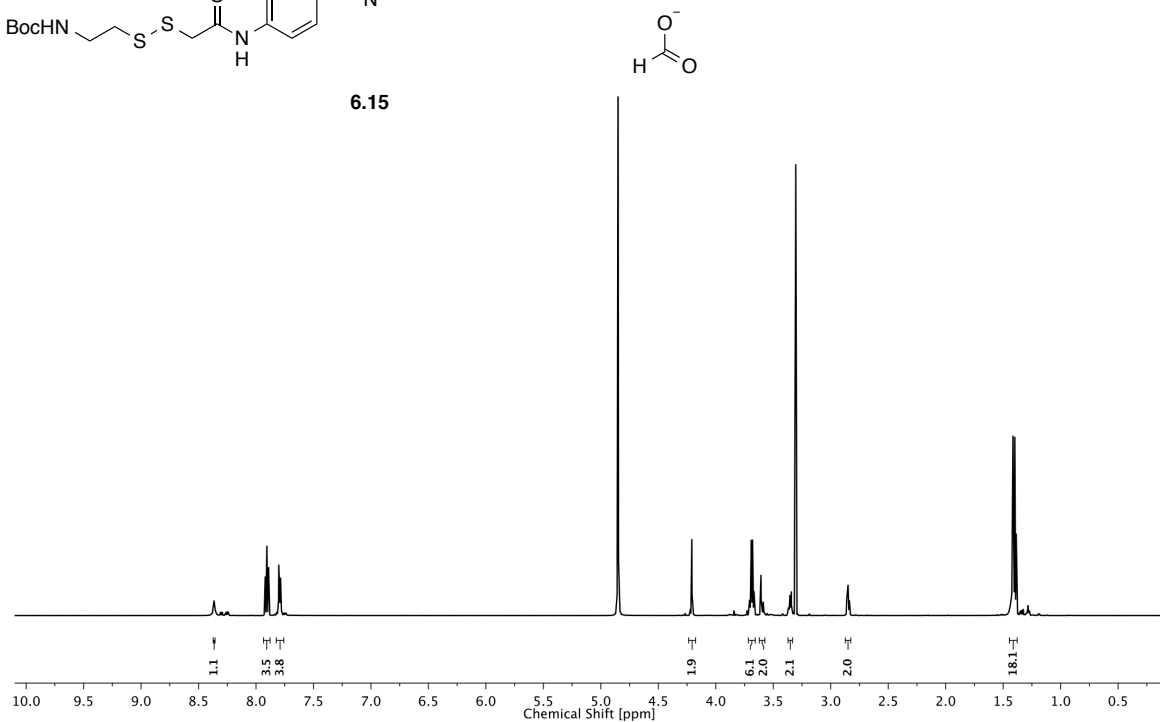
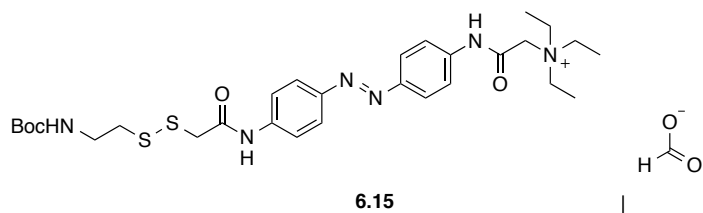
6.10

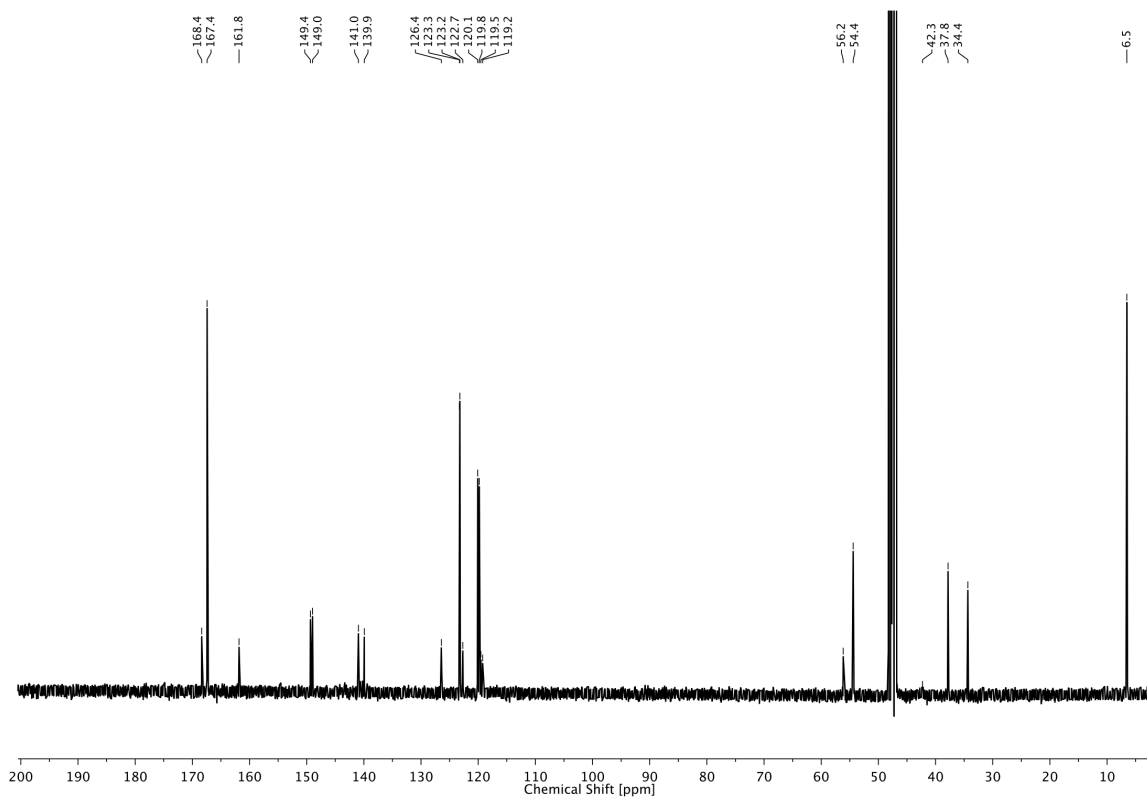
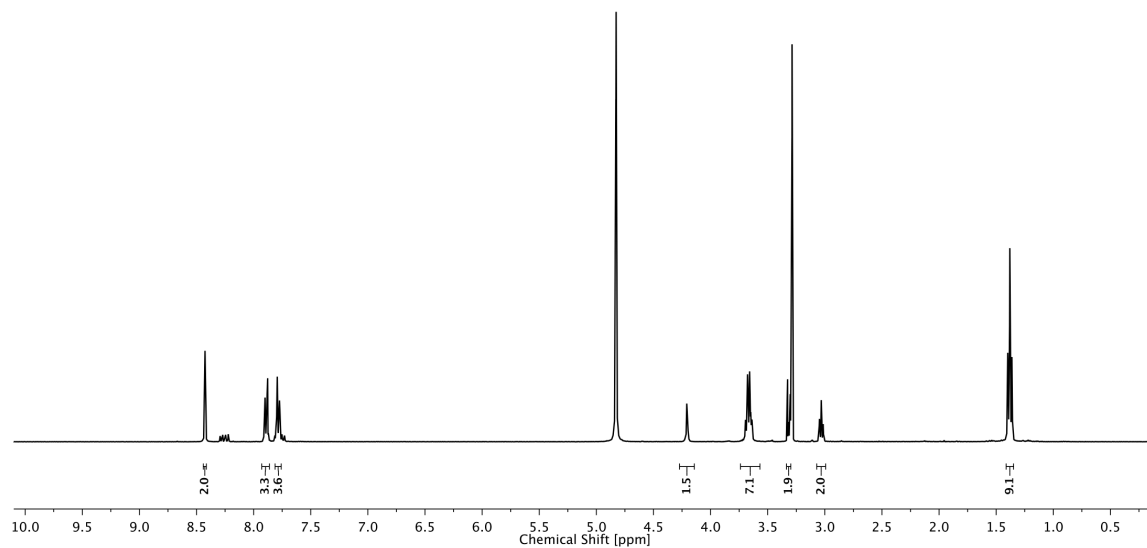
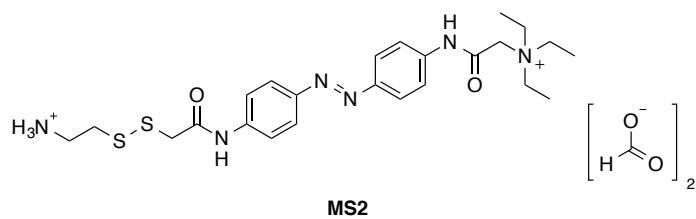




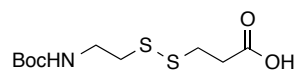
6.13



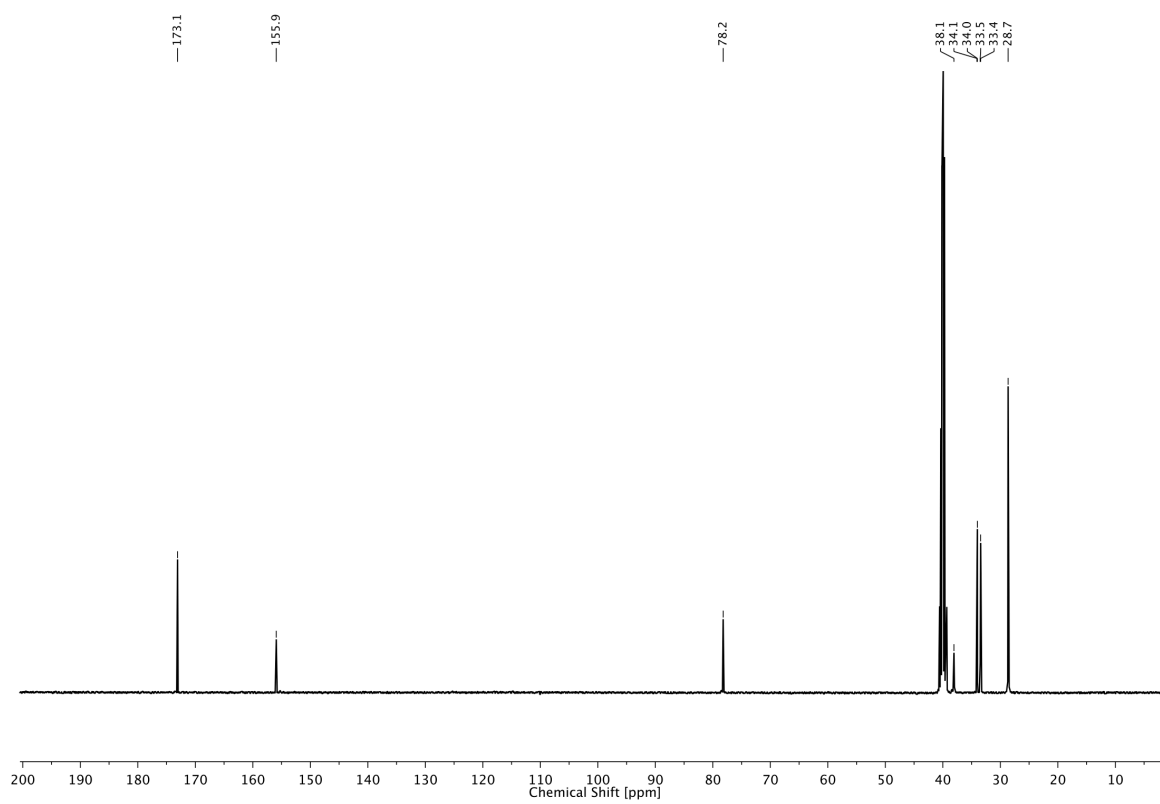
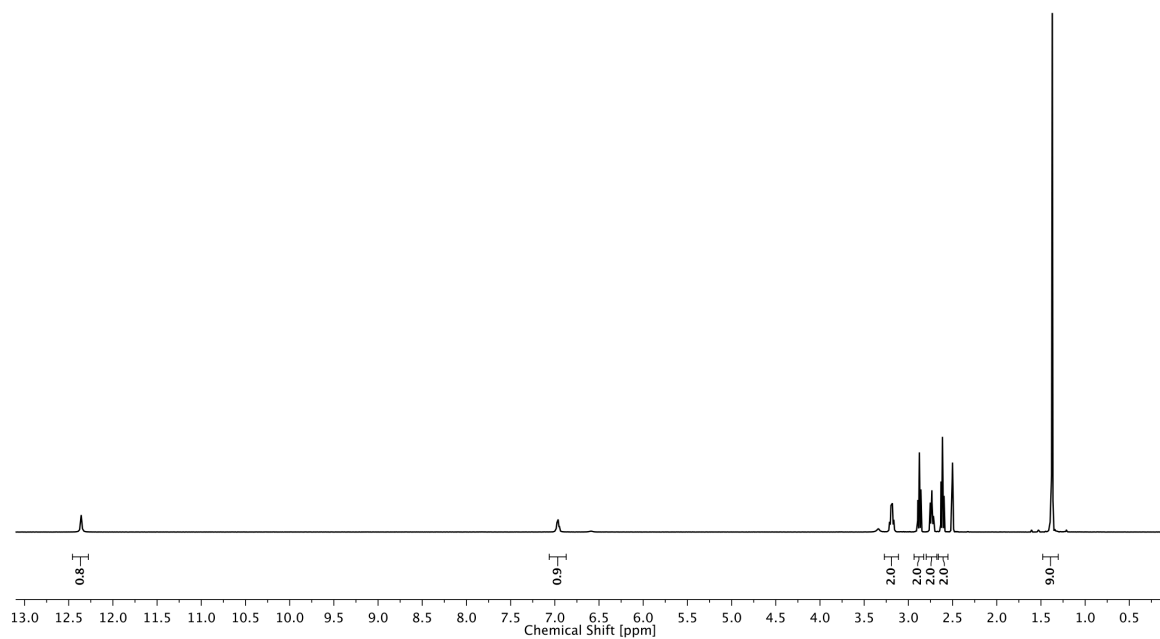


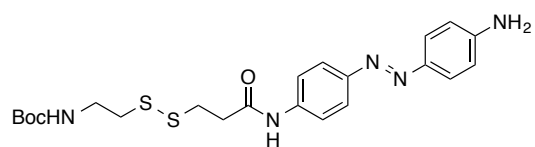


6 MISCELLANEOUS PROJECTS

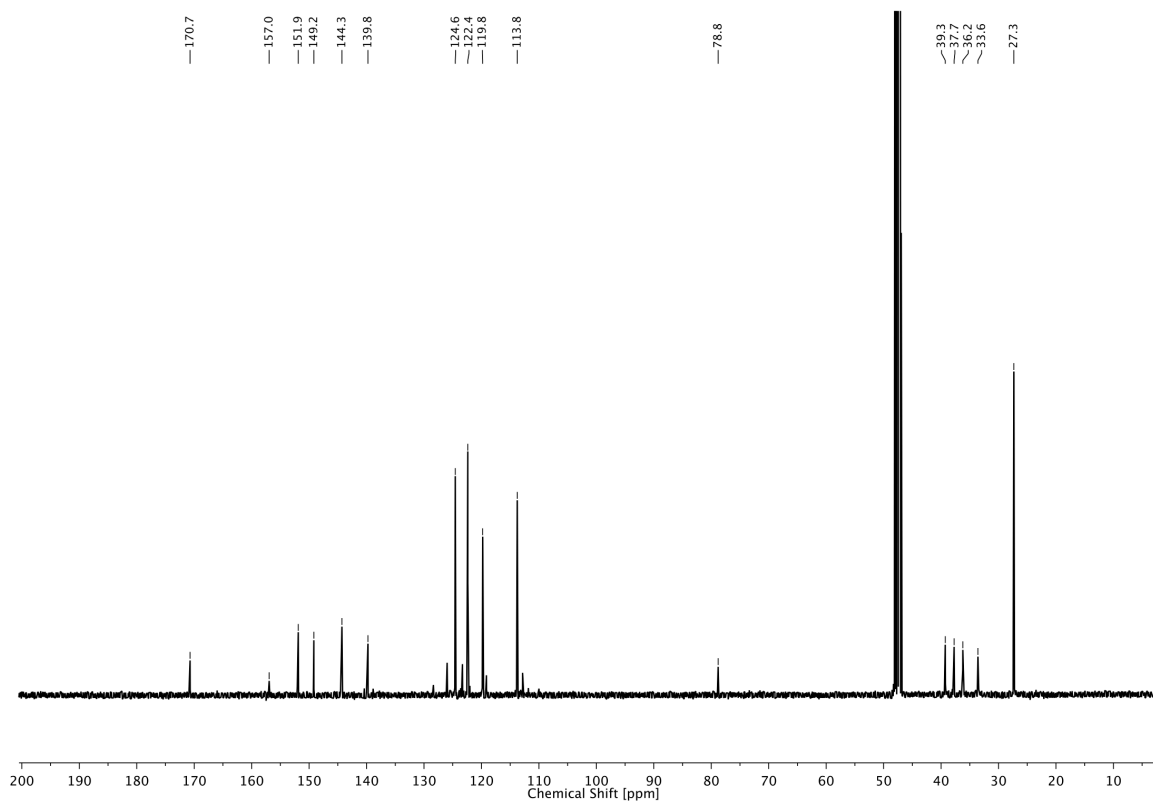
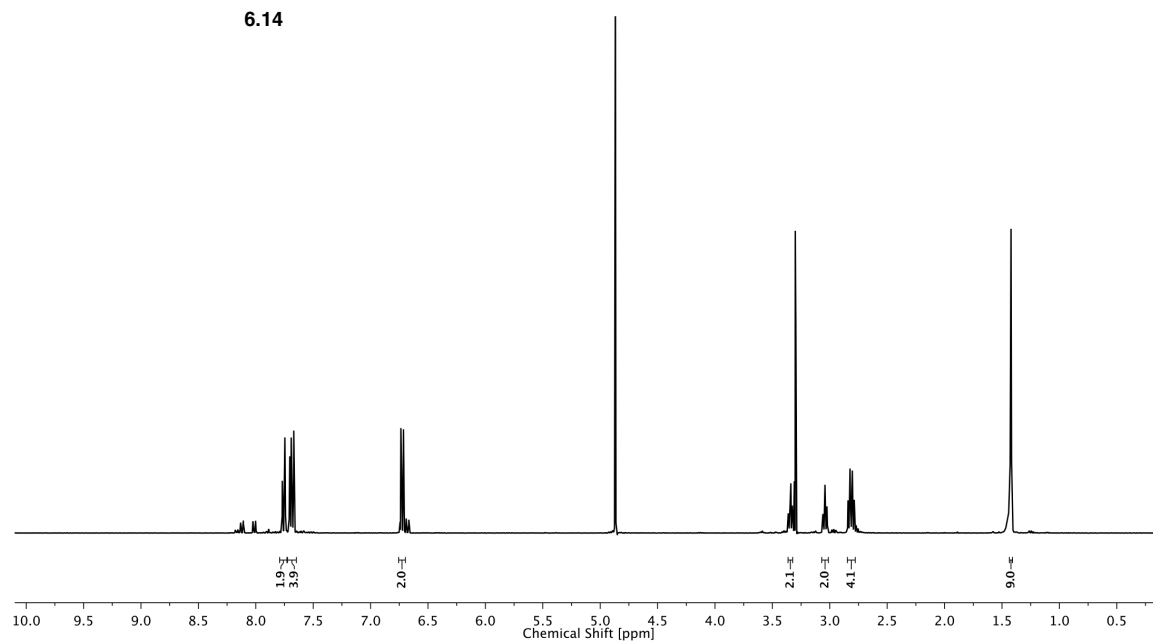


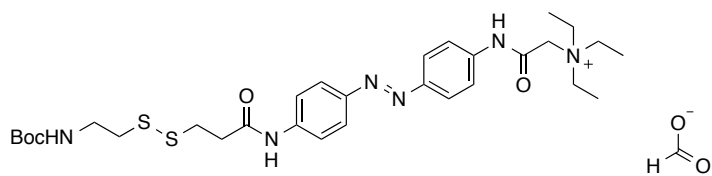
6.11



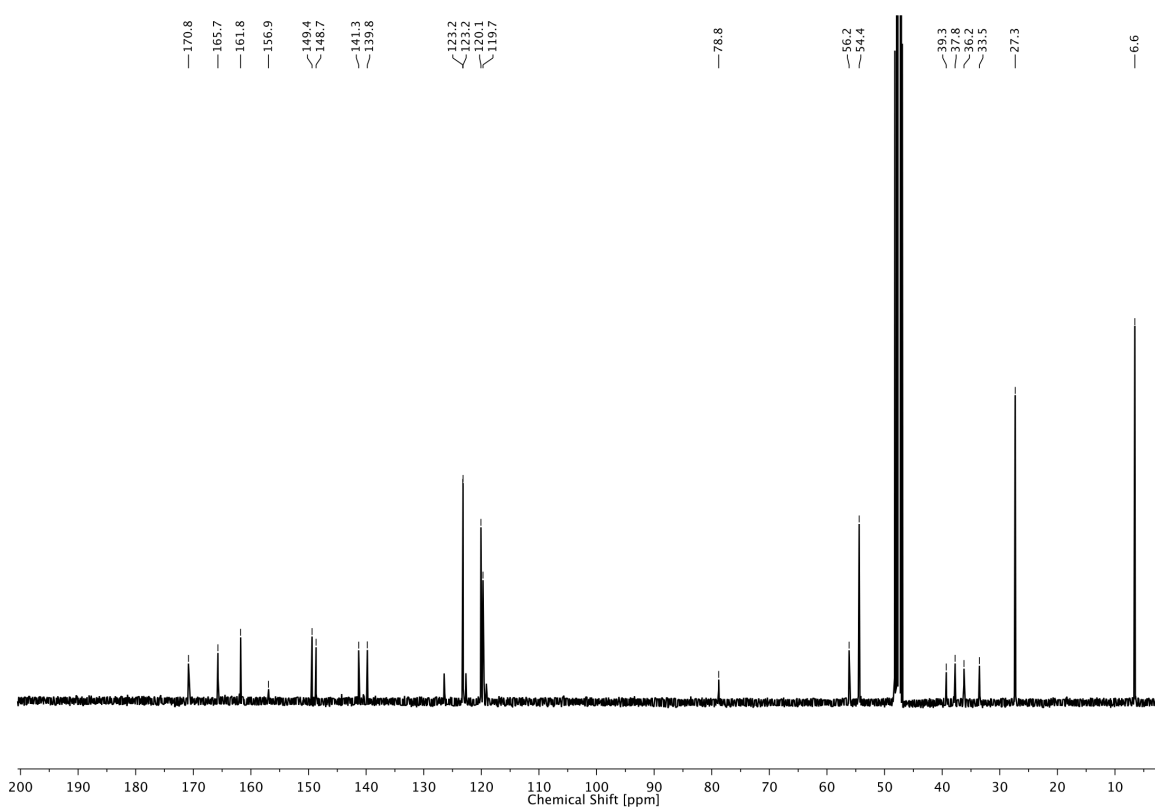
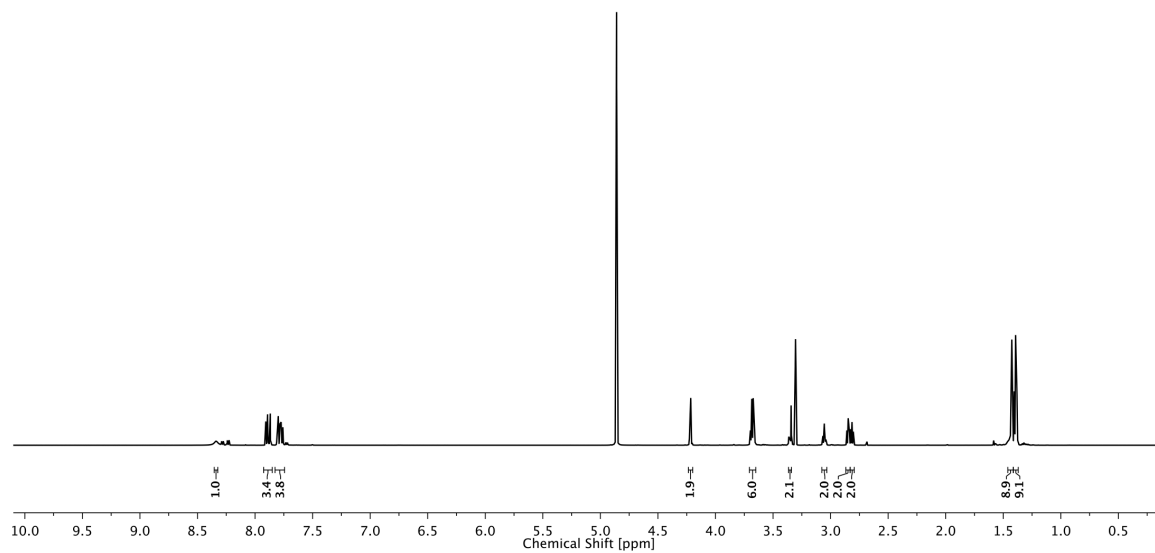


6.14

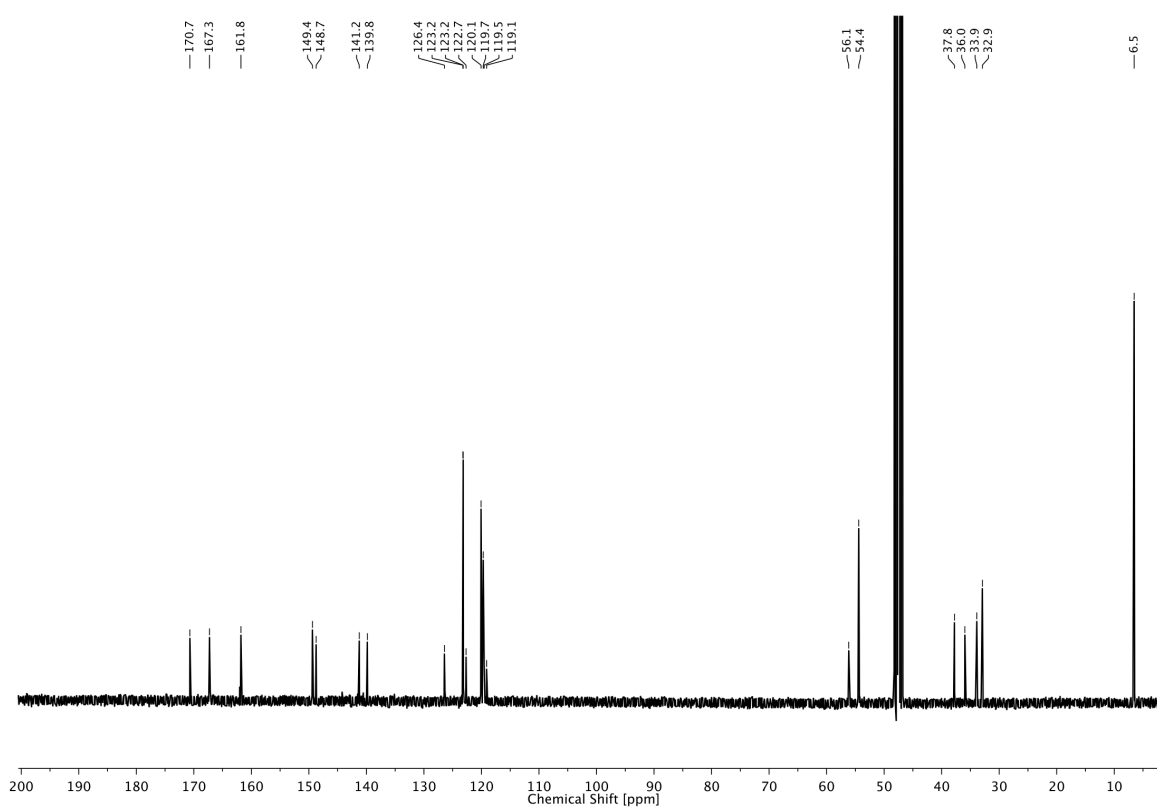
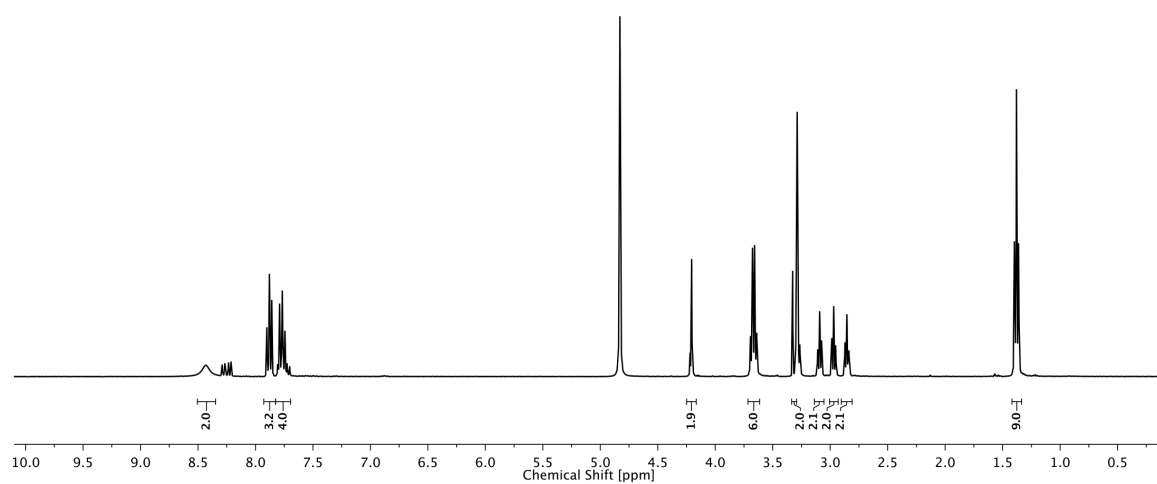
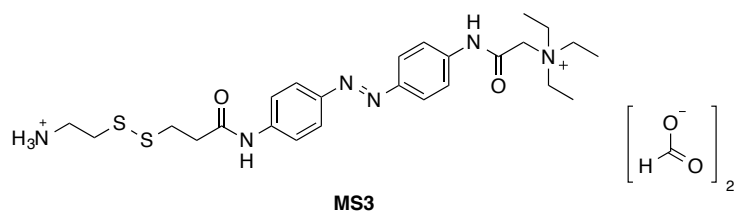




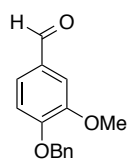
6.16



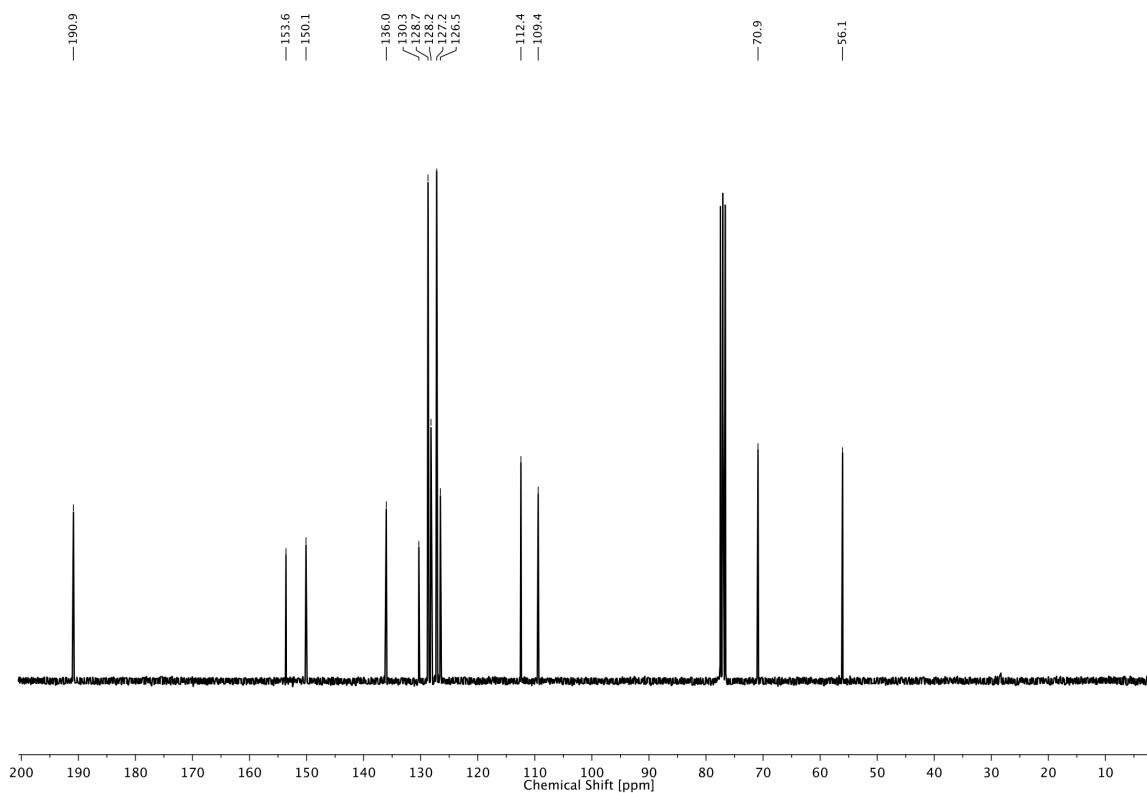
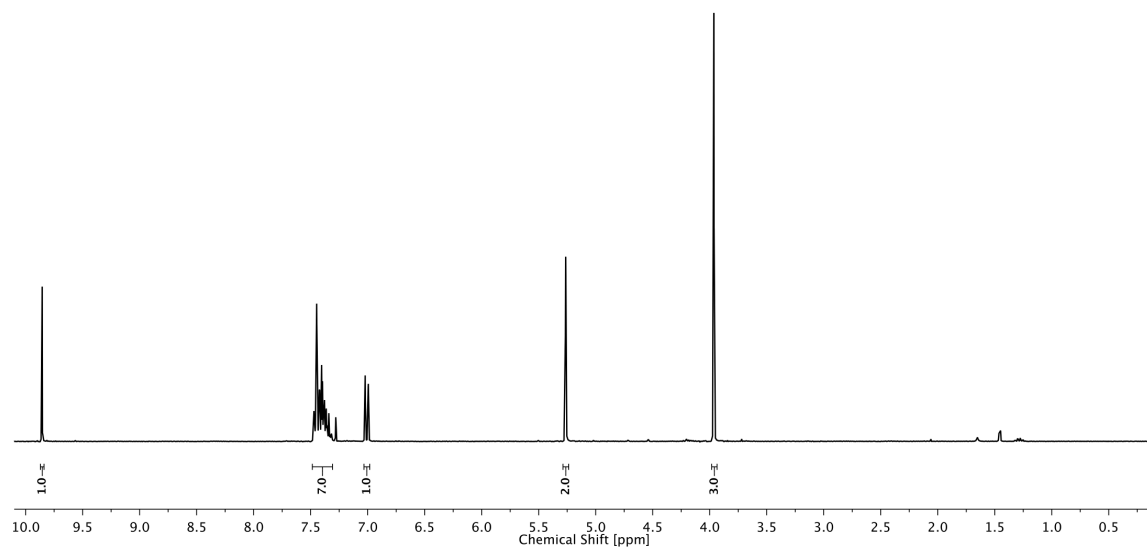
6 MISCELLANEOUS PROJECTS



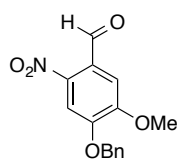
6 MISCELLANEOUS PROJECTS



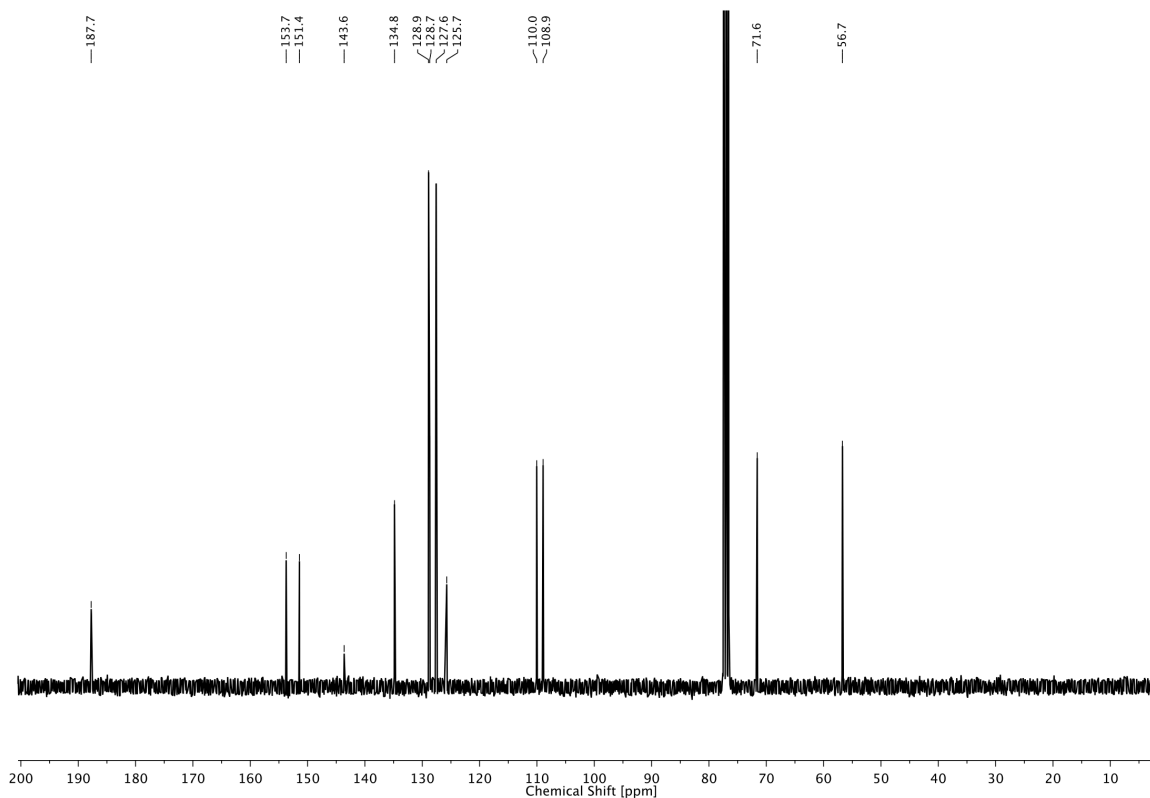
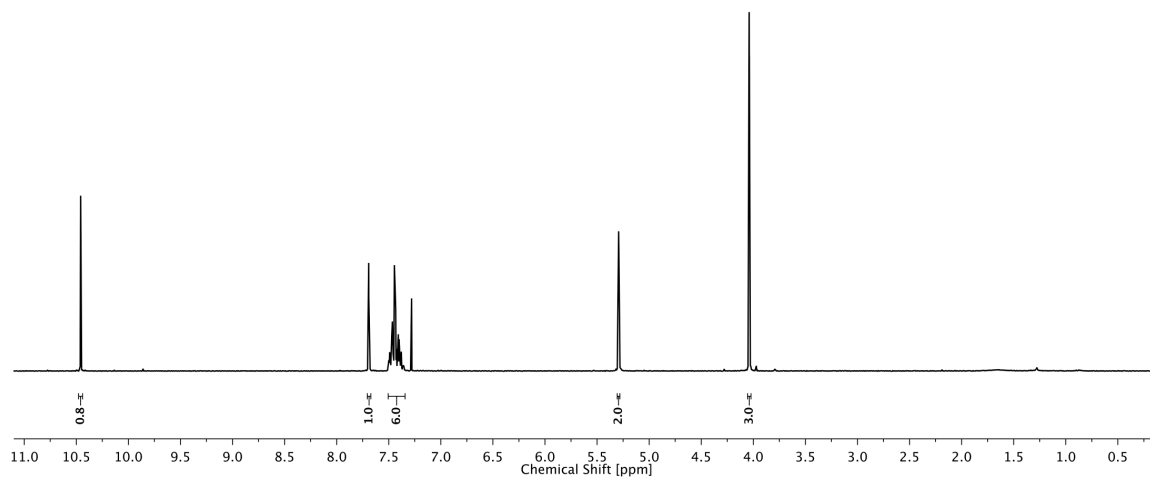
6.17



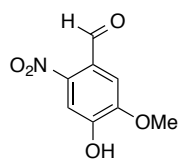
6 MISCELLANEOUS PROJECTS



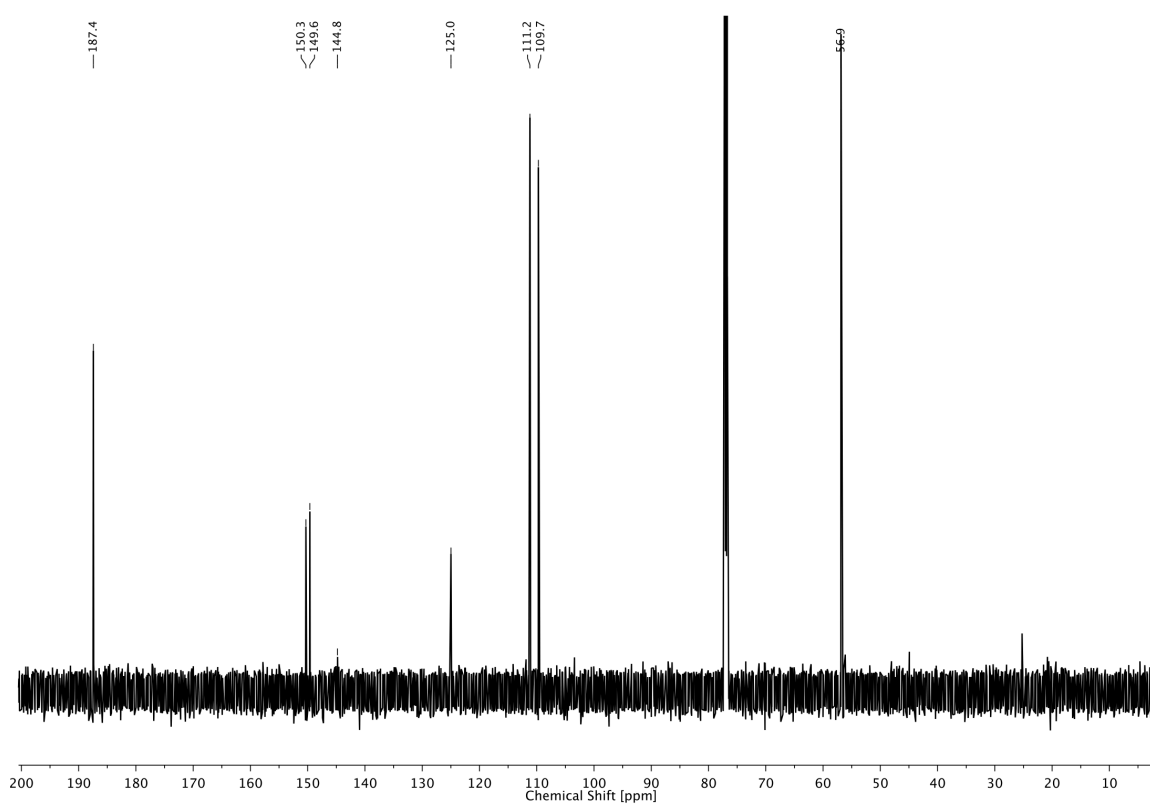
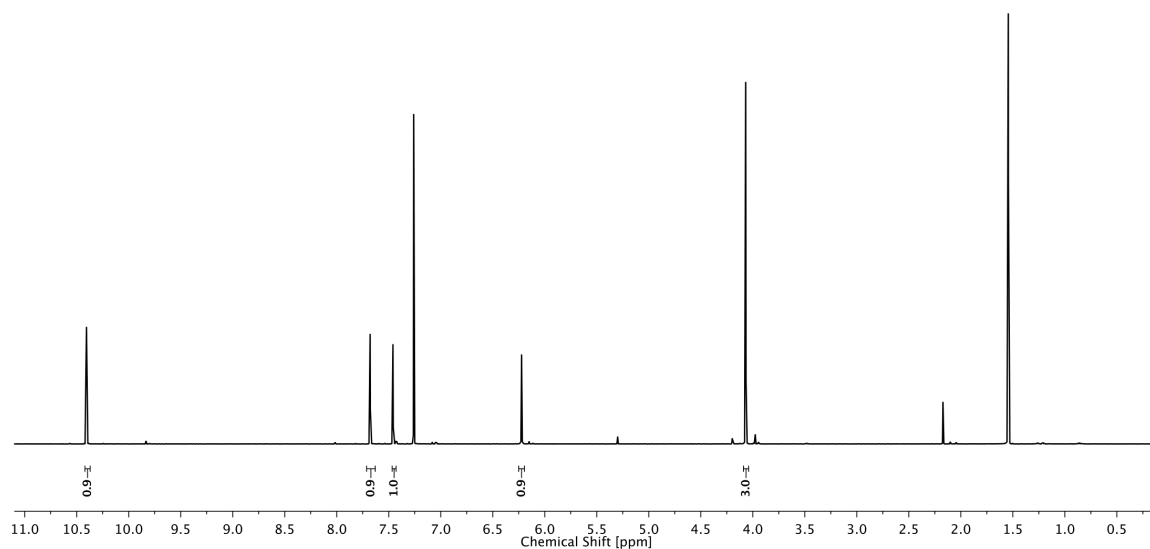
6.18



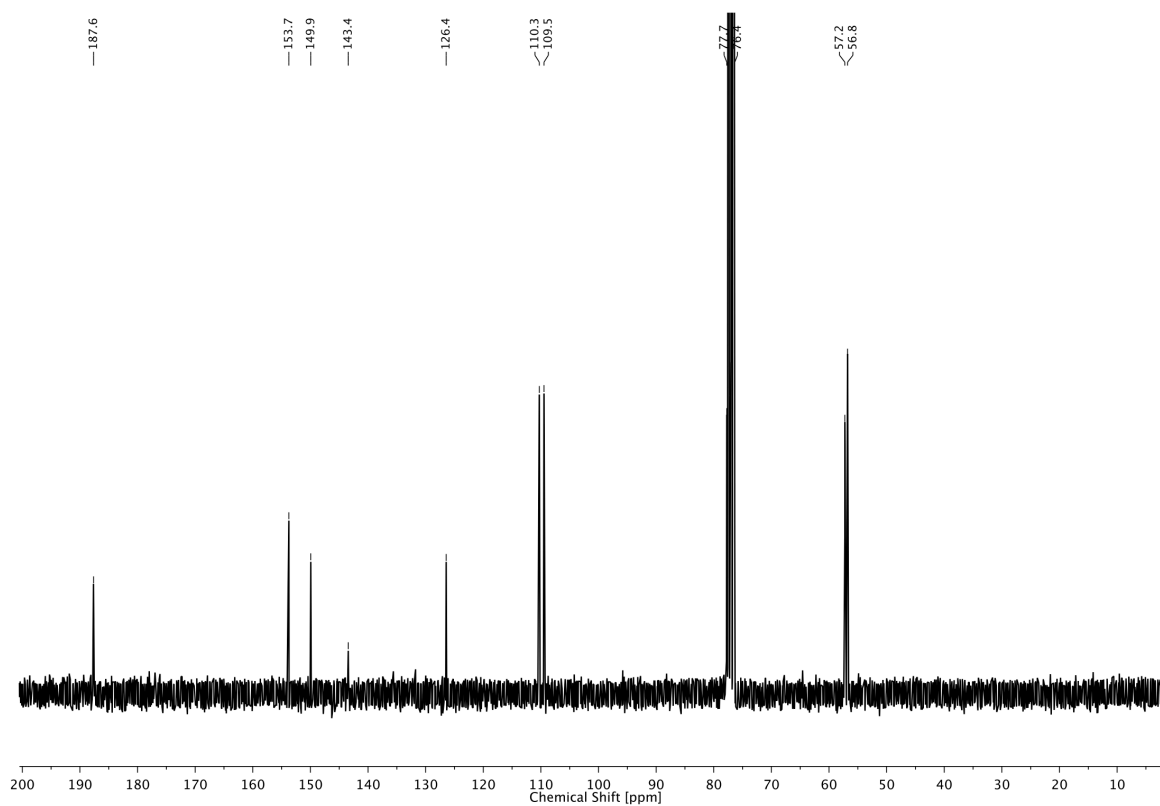
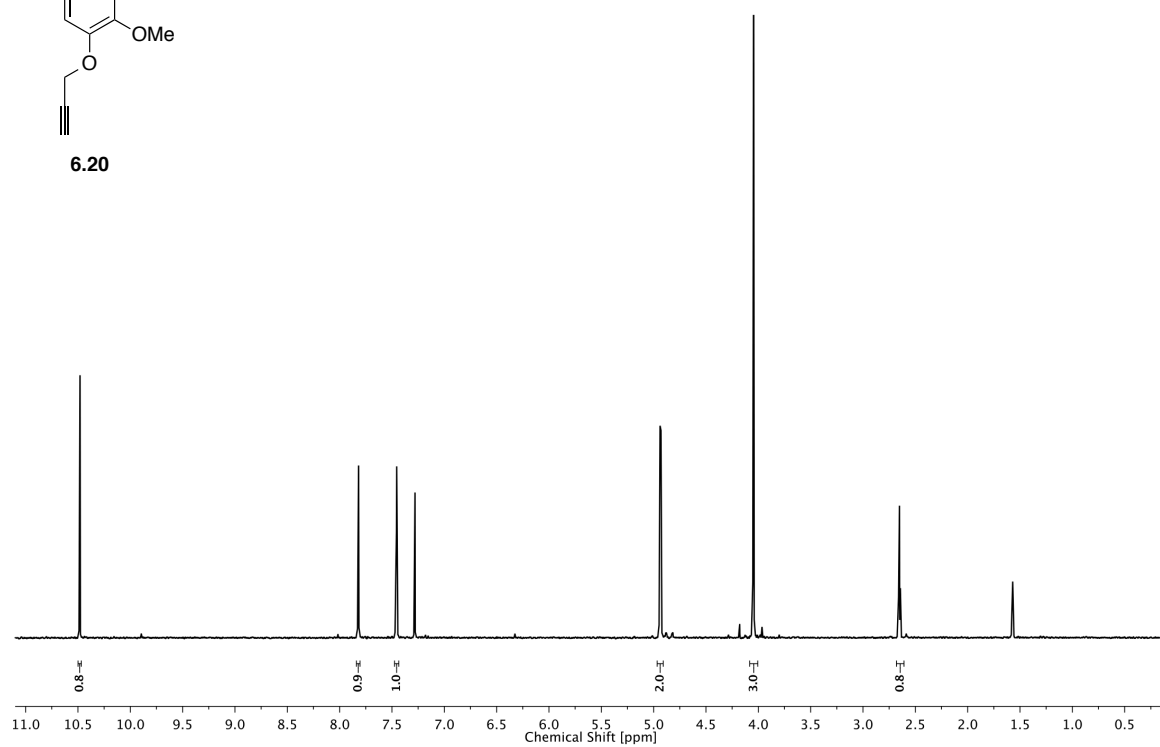
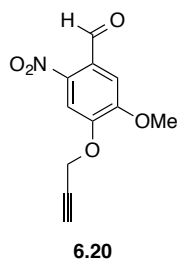
6 MISCELLANEOUS PROJECTS



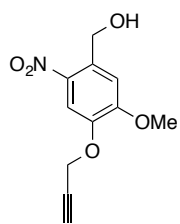
6.19



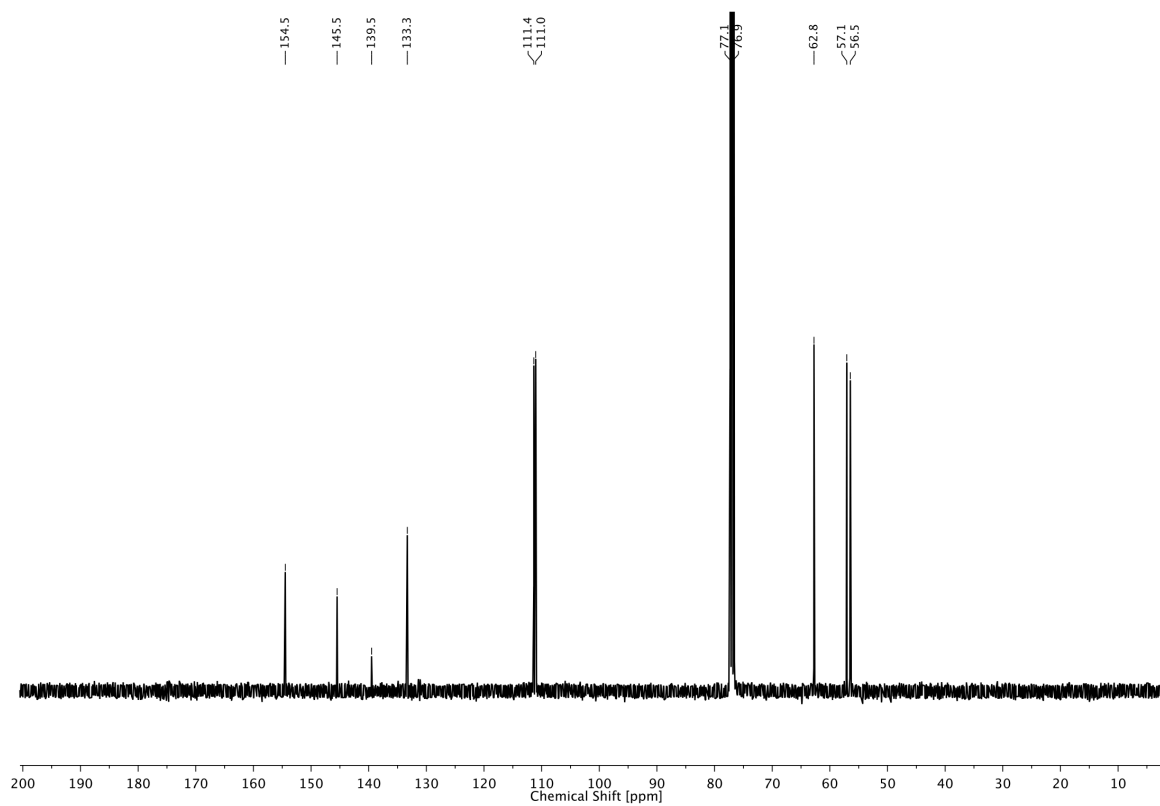
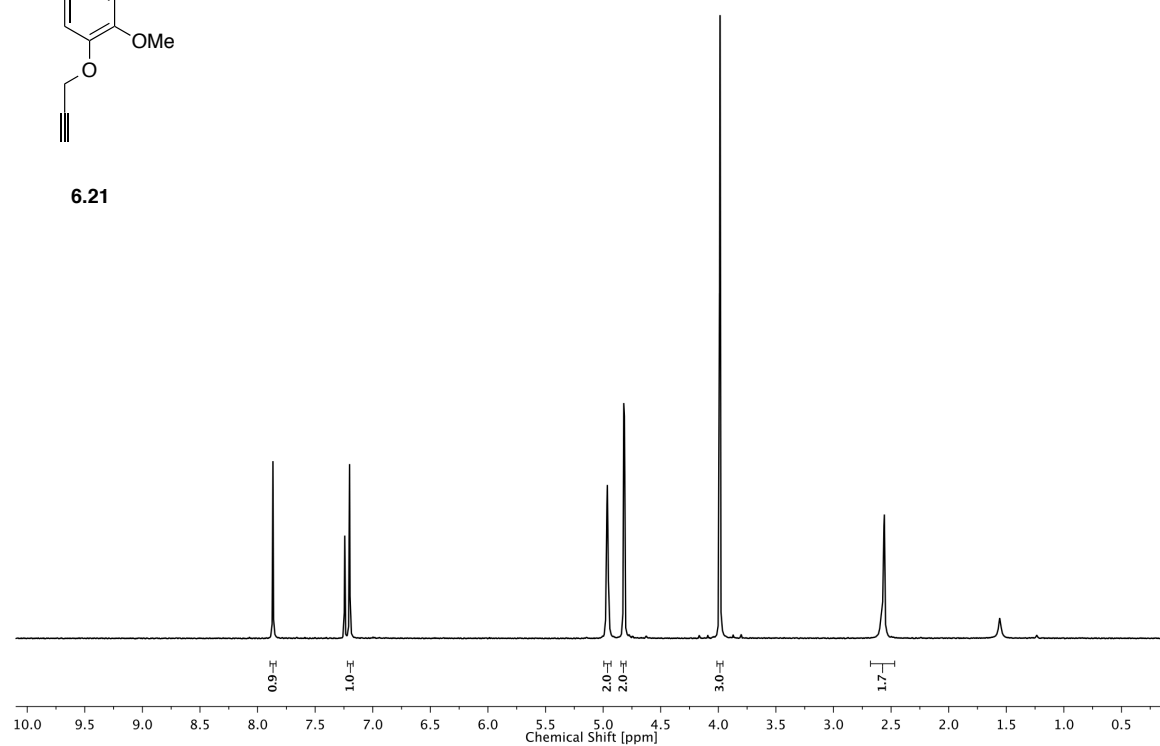
6 MISCELLANEOUS PROJECTS



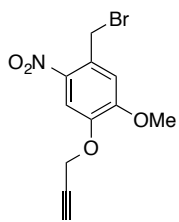
6 MISCELLANEOUS PROJECTS



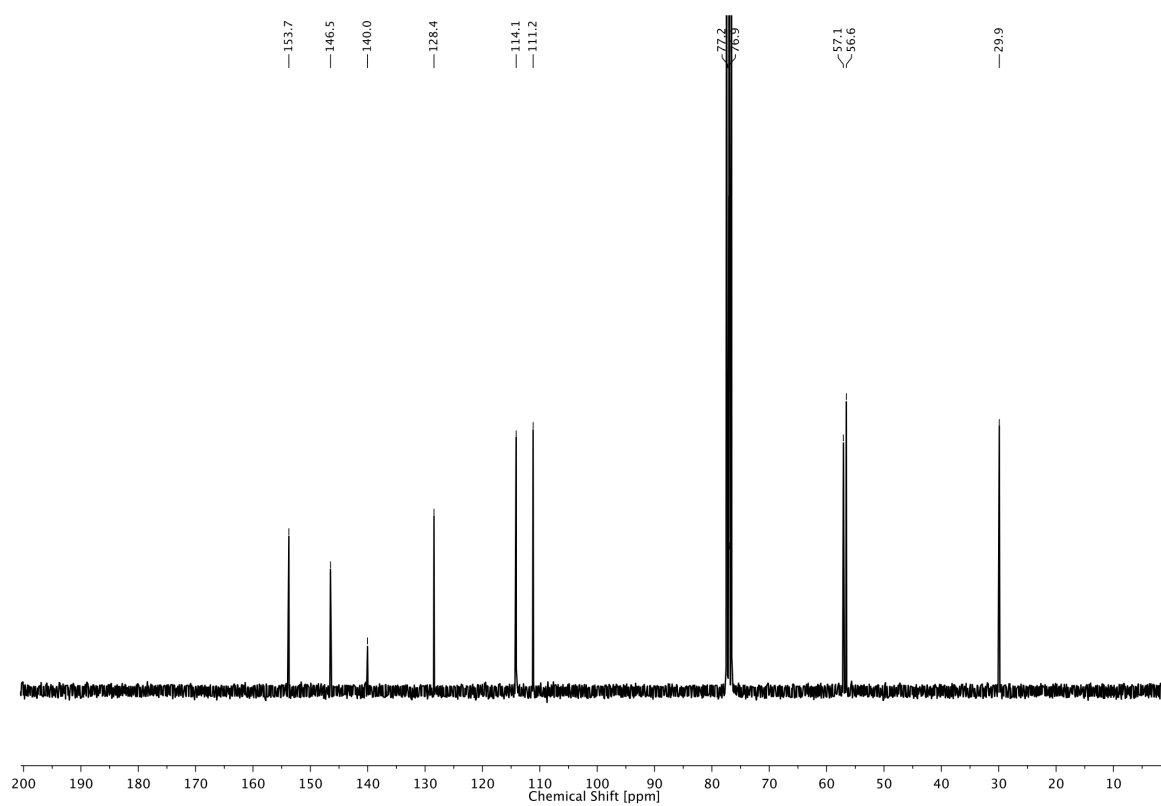
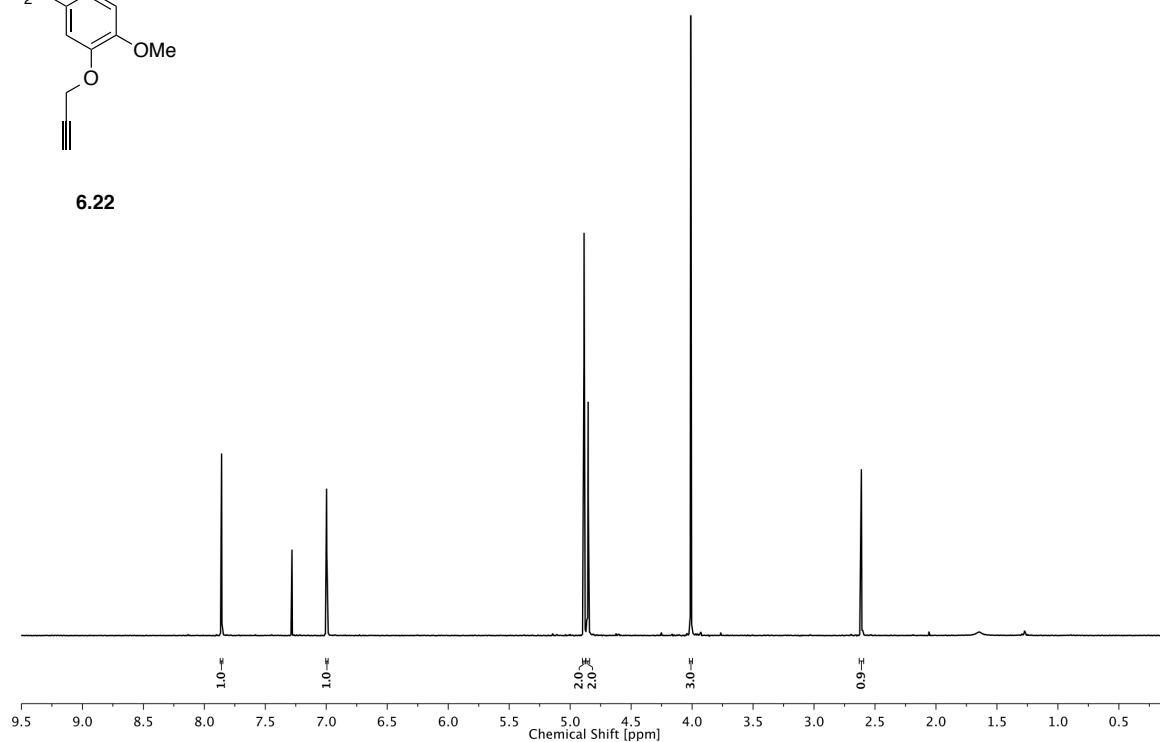
6.21



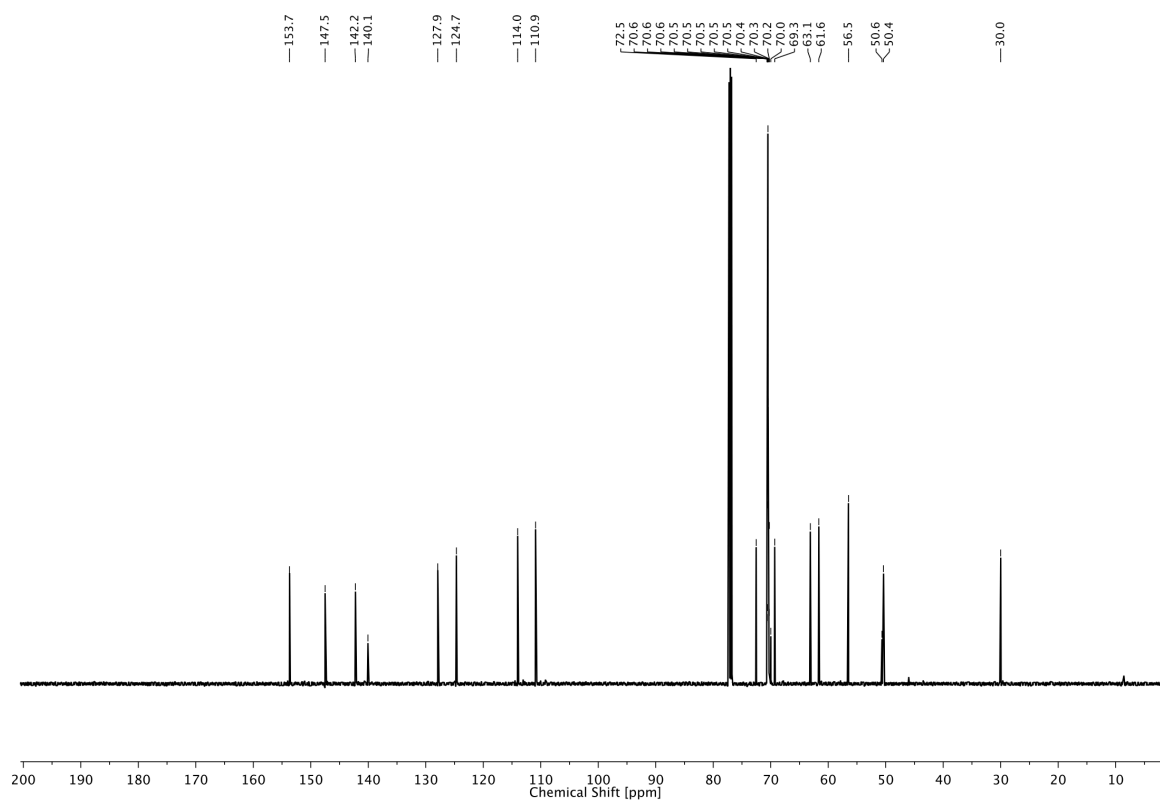
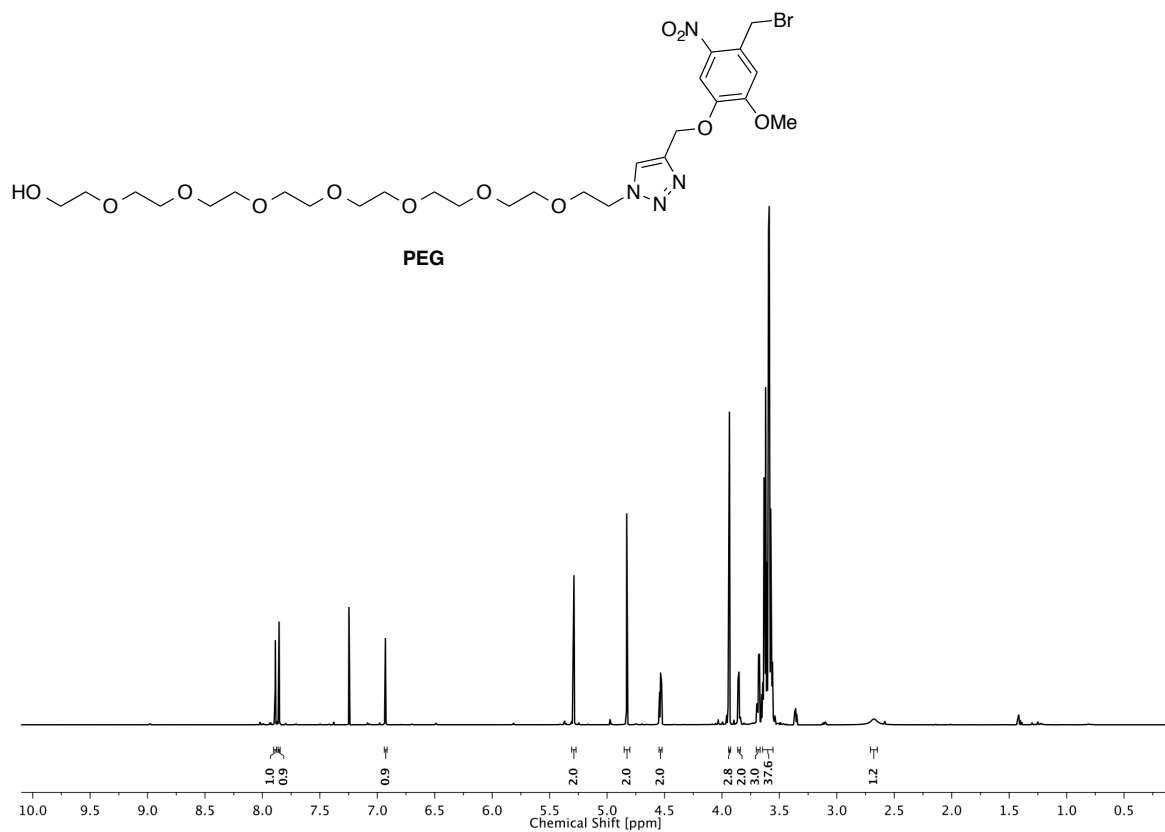
6 MISCELLANEOUS PROJECTS



6.22



6 MISCELLANEOUS PROJECTS



6.7 LITERATURE

- [1] S. N. Haydar, C. Ghiron, L. Bettinetti, H. Bothmann, T. A. Comery, J. Dunlop, S. La Rosa, I. Micco, M. Pollastrini, J. Quinn, R. Roncarati, C. Scali, M. Valacchi, M. Varrone, R. Zanaletti, *Bioorg. Med. Chem.* **2009**, *17*, 5247–5258.
- [2] C. J. O'Donnell, B. N. Rogers, B. S. Bronk, D. K. Bryce, J. W. Coe, K. K. Cook, A. J. Duplantier, E. Evrard, M. Hajos, W. E. Hoffmann, R. S. Hurst, N. Maklad, R. J. Mather, S. McLean, F. M. Nedza, B. T. O'Neill, L. Peng, W. Qian, M. M. Rottas, S. B. Sands, A. W. Schmidt, A. V. Shrikhande, D. K. Spracklin, D. F. Wong, A. Zhang, L. Zhang, *J. Med. Chem.* **2010**, *53*, 1222–1237.
- [3] R. Zanaletti, L. Bettinetti, C. Castaldo, G. Cocconcelli, T. A. Comery, J. Dunlop, G. Gaviraghi, C. Ghiron, S. N. Haydar, F. Jow, L. Maccari, I. Micco, A. Nencini, C. Scali, E. Turlizzi, M. Valacchi, *J. Med. Chem.* **2012**, *55*, 4806–4823.
- [4] R. Zanaletti, L. Bettinetti, C. Castaldo, I. Ceccarelli, G. Cocconcelli, T. A. Comery, J. Dunlop, E. Genesio, C. Ghiron, S. N. Haydar, F. Jow, L. Maccari, I. Micco, A. Nencini, C. Pratelli, C. Scali, E. Turlizzi, M. Valacchi, *J. Med. Chem.* **2012**, *55*, 10277–10281.
- [5] A. Mourot, T. Fehrentz, Y. Le Feuvre, C. M. Smith, C. Herold, D. Dalkara, F. Nagy, D. Trauner, R. H. Kramer, *Nat. Meth.* **2012**, *9*, 396–402.
- [6] A. Scholz, *Br. J. Anaesth.* **2002**, *89*, 52–61.
- [7] T. J. Reilly, *J. Chem. Ed.* **1999**, *76*, 1557.
- [8] T. Fehrentz, M. Schönberger, D. Trauner, *Angew. Chem. Int. Ed.* **2011**, *50*, 12156–12182.
- [9] S. Szobota, P. Gorostiza, F. Del Bene, C. Wyart, D. L. Fortin, K. D. Kolstad, O. Tulyathan, M. Volgraf, R. Numano, H. L. Aaron, E. K. Scott, R. H. Kramer, J. Flannery, H. Baier, D. Trauner, E. Y. Isacoff, *Neuron* **2007**, *54*, 535–545.
- [10] P. Gorostiza, M. Volgraf, R. Numano, S. Szobota, D. Trauner, E. Y. Isacoff, *Proc. Natl. Acad. Sci. USA* **2007**, *104*, 10865–10870.
- [11] C. Wyart, F. Del Bene, E. Warp, E. K. Scott, D. Trauner, H. Baier, E. Y. Isacoff, *Nature* **2009**, *461*, 407–410.
- [12] N. Caporale, K. D. Kolstad, T. Lee, I. Tochitsky, D. Dalkara, D. Trauner, R. H. Kramer, Y. Dan, E. Y. Isacoff, J. G. Flannery, *Mol. Ther.* **2011**, *19*, 1212–1219.
- [13] D. A. Erlanson, J. A. Wells, A. C. Braisted, *Annu. Rev. Biophys. Biomol. Struct.* **2004**, *33*, 199–223.
- [14] S. Cicchi, P. Fabbri, G. Ghini, A. Brandi, P. Foggi, A. Marcelli, R. Righini, C. Botta, *Chem. Eur. J.* **2009**, *15*, 754–764.

- [15] P. G. M. Wuts, T. W. Greene, in *Greene's Protective Groups in Organic Synthesis*, John Wiley & Sons, **2006**, p. 135–137.
- [16] W. C. Still, M. Kahn, A. Mitra, *J. Org. Chem.* **1978**, *43*, 2923–2925.
- [17] H. E. Gottlieb, V. Kotlyar, A. Nudelman, *J. Org. Chem.* **1997**, *62*, 7512–7515.

7 LIST OF ABBREVIATIONS

Δ	heating under reflux	ca.	circa
3C5HPG	3-carboxy-5-hydroxyphenyl-glycine	calcd.	calculated
ABCTC	Azo-BCTC	cat.	catalyzed/catalytic
Ac	acetyl	CAP	capsaicin
Ac	<i>aplysia californica</i>	CaM	calmodulin
AC	Azo-Capsazepine	CaMBD	calmodulin binding domain
AChBP	acetylcholine binding proteine	Ca _v	voltage-gated calcium (channel)
ACPT-I	(1 <i>S</i> ,3 <i>R</i> ,4 <i>S</i>)-1-aminocyclopentane-1,3,4-tricarboxylic acid	cDNA	complementary DNA
ACRO	Azo-Crobenetine	ChARGe	optochemical tool consisting of arrestin-2, rhodopsin and a G-protein
AETD	Azo-Etomidate	CHO	chinese hamster ovary
AFM	atomic force microscopy	ChR	channelrhodopsin
AI	Azo-Icilin	CL	caged ligand
ALCM	Azo-Lacosamide	conc.	concentrated/concentration
ALTG	Azo-Lamotrigine	CPZ	capsazepine
AMPA	2-amino-3-(3-hydroxy-5-methylisoxazol-4-yl)propanoic acid	cRNA	complementary RNA
AP	action potential	CSA	camphorsulfonic acid
AP	Azo-Propofol	Cys	cysteine
APDC	4-aminopyrrolidine-2,4-dicarboxylate	d	day(s)
aqu.	aqueous	d	doublet
Ar	aryl	DAG	diacyl glycerol
ATP	adenosine triphosphate	DCM	dichloromethane
ATR	attenuated total reflectance	DCPG	dicarboxyphenylglycine
AUC	area under curve	DHPG	dihydroxyphenylglycine
Bn	benzyl	DIC	<i>N,N</i> -diisopropylcarbodiimide
Boc	<i>tert</i> -butyloxycarbonyl	DIPEA	<i>N,N</i> -diisopropylethylamine
brsm	based on recovered starting material	DMAP	4-dimethylaminopyridine
Bt	benzotriazole	DMF	<i>N,N</i> -dimethylformamide
Bu	butyl	DMSO	dimethyl sulfoxide
BZ	benzodiazepine	DNA	deoxyribonucleic acid
		DRG	dorsal root ganglion
		E ⁺	electrophile
		e.g.	for example

EC ₅₀	half maximal effective concentration	HPLC	high-performance liquid chromatography
Ed.	editor	HRMS	high resolution mass spectrometry
ED ₅₀	median effective dose	i.e.	that is
EDCI	<i>N</i> -(3-dimethylaminopropyl)- <i>N'</i> -ethylcarbodiimide hydrochloride	I-RTX	iodoresiniferatoxin
EEG	electroencephalogram	IC ₅₀	half maximal inhibitory concentration
EGTA	ethylene glycol tetraacetic acid	ICK	inhibitor cysteine knot
EI	electron impact ionization	iGluR	ionotropic glutamate receptor
Epi	epibatidine	im	imidazole
equiv.	equivalent(s)	IR	infrared
ESI	electrospray ionization	<i>J</i>	coupling constant
Et	ethyl	k _B	Boltzmann constant
ETD	etomidate	KcsA	potassium crystallographically-sited activation (channel)
FBS	fetal bovine serum	K _v	voltage-gated potassium (channel)
FDA	Food and Drug Administration	LC	liquid crystal(s)
GABA	γ-aminobutyric acid	LCE	liquid crystal elastomer(s)
GIRK	G-protein-coupled inwardly-rectifying potassium (channel)	LCM	lacosamide
Glu	glutamate	LED	light-emitting diode
GPCR	G-protein-coupled receptor	LiGluR	light-gated ionotropic glutamate receptor
h	hour(s)	LimGluR	light-gated metabotropic glutamate receptor
HATU	<i>O</i> -(7-azabenzotriazol-1-yl)- <i>N,N,N',N'</i> -tetramethyluronium hexafluorophosphate	LORR	loss of righting reflex(es)
HBS	HEPES buffered saline	Ls	<i>lymnaea stagnalis</i>
HBTU	<i>O</i> -(benzotriazol-1-yl)- <i>N,N,N',N'</i> -tetramethyluronium hexafluorophosphate	LTG	lamotrigine
HCN1	hyperpolarization-activated cyclic nucleotide-gated channel 1	m	multiplet
HEK	human embryonic kidney	<i>m-</i>	<i>meta-</i>
HEPES	4-(2-hydroxyethyl)-1-piperazineethanesulfonic acid	m.p.	melting point
HMDS	hexamethyldisilazane	<i>m/z</i>	mass to charge ratio
		Me	methyl
		MES	maximum electroshock seizure
		mGluR	metabotropic glutamate receptor
		min	minute(s)

Ms	mesyl	rt	room temperature
MS	molecular sieves(s)	RTX	resiniferatoxin
nAChR	nicotinic acetylcholine receptor	s	second(s)
Nav	voltage-gated sodium (channel)	s	singlet
NavAb	voltage-gated sodium channel from <i>arcobacter butzleri</i>	SAR	structure–activity relationship(s)
Nic	nicotine	sat.	saturated
NMR	nuclear magnetic resonance	SD	standard deviation
NPC	4-nitrophenyl chloroformate	SEM	standard error of the mean
NpHR	halorhodopsin from <i>natronomonas</i>	sept	septet
Nu	nucleophile	sext	sextet
<i>o</i> -	<i>ortho</i> -	SHU	scoville heat unit(s)
P	pore	SM	starting material
<i>p</i> -	<i>para</i> -	T	temperature(s)
PCL	photochromic ligand	t	triplet
PEG	polyethylene glycol	TBS	<i>tert</i> -butyldimethylsilyl
PG	protecting group	TCDP	1,1'-thiocarbonyldi-2(1 <i>H</i>)- pyridone
Ph	phenyl	TEA	triethylamine
phen	phenantroline	Tf	triflyl
PIP ₂	phosphatidylinositol 4,5- biphosphate	THF	tetrahydrofuran
PKC	protein kinase C	TLC	thin layer chromatography
PLC	phospholipase C	TM	transmembrane
PPCG-2	(2 <i>S</i>)-2-(2'-phosphono-3'- phenylcyclopropyl)glycine	TMS	tetramethylsilyl/ or -silane
ppm	parts per million	TP	typical procedure
Pr	propyl	TRP	transient receptor potential
PTL	photoswitchable tethered ligand	TRPA	TRP ankyrin
py	pyridine	TRPC	TRP canonical or classical
q	quartet	TRPM	TRP melastatin
quint	quintet	TRPML	TRP mucolipin
R	organic rest	TRPN	TRP no mechanoreceptor potential C
R _f	retention factor	TRPP	TRP polycystin
RGC	retinal ganglion cell	TRPV	TRP vanilloid
RNA	ribonucleic acid	Ts	tosyl
		TTX	tetrodotoxin
		US	United States

UV	ultraviolet
VChR	<i>volvox</i> channelrhodopsin
Vis	visible
VSD	voltage-sensing domain
YFP	yellow fluorescent protein

*“Wir stehen selbst enttäuscht und sehn betroffen
Den Vorhang zu und alle Fragen offen.”*

*(Bertolt Brecht in *Der gute Mensch von Sezuan*)*